

# **REACTION KINETICS AND REACTOR DESIGN**

## CHEMICAL INDUSTRIES

A Series of Reference Books and Textbooks

*Consulting Editor*

**HEINZ HEINEMANN**

*Berkeley, California*

1. *Fluid Catalytic Cracking with Zeolite Catalysts*, Paul B. Venuto and E. Thomas Habib, Jr.
2. *Ethylene: Keystone to the Petrochemical Industry*, Ludwig Kniel, Olaf Winter, and Karl Stork
3. *The Chemistry and Technology of Petroleum*, James G. Speight
4. *The Desulfurization of Heavy Oils and Residua*, James G. Speight
5. *Catalysis of Organic Reactions*, edited by William R. Moser
6. *Acetylene-Based Chemicals from Coal and Other Natural Resources*, Robert J. Tedeschi
7. *Chemically Resistant Masonry*, Walter Lee Sheppard, Jr.
8. *Compressors and Expanders: Selection and Application for the Process Industry*, Heinz P. Bloch, Joseph A. Cameron, Frank M. Danowski, Jr., Ralph James, Jr., Judson S. Swearingen, and Marilyn E. Weightman
9. *Metering Pumps: Selection and Application*, James P. Poynton
10. *Hydrocarbons from Methanol*, Clarence D. Chang
11. *Form Flotation: Theory and Applications*, Ann N. Clarke and David J. Wilson
12. *The Chemistry and Technology of Coal*, James G. Speight
13. *Pneumatic and Hydraulic Conveying of Solids*, O. A. Williams
14. *Catalyst Manufacture: Laboratory and Commercial Preparations*, Alvin B. Stiles
15. *Characterization of Heterogeneous Catalysts*, edited by Francis Delannay
16. *BASIC Programs for Chemical Engineering Design*, James H. Weber
17. *Catalyst Poisoning*, L. Louis Hegedus and Robert W. McCabe
18. *Catalysis of Organic Reactions*, edited by John R. Kosak
19. *Adsorption Technology: A Step-by-Step Approach to Process Evaluation and Application*, edited by Frank L. Slejko
20. *Deactivation and Poisoning of Catalysts*, edited by Jacques Oudar and Henry Wise
21. *Catalysis and Surface Science: Developments in Chemicals from Methanol, Hydrotreating of Hydrocarbons, Catalyst Preparation, Monomers and Polymers, Photocatalysis and Photovoltaics*, edited by Heinz Heinemann and Gabor A. Somorjai
22. *Catalysis of Organic Reactions*, edited by Robert L. Augustine
23. *Modern Control Techniques for the Processing Industries*, T. H. Tsai, J. W. Lane, and C. S. Lin
24. *Temperature-Programmed Reduction for Solid Materials Characterization*, Alan Jones and Brian McNichol
25. *Catalytic Cracking: Catalysts, Chemistry, and Kinetics*, Bohdan W. Wojciechowski and Avelino Corma

26. *Chemical Reaction and Reactor Engineering*, edited by J. J. Carberry and A. Varma
27. *Filtration: Principles and Practices: Second Edition*, edited by Michael J. Matteson and Clyde Orr
28. *Corrosion Mechanisms*, edited by Florian Mansfeld
29. *Catalysis and Surface Properties of Liquid Metals and Alloys*, Yoshisada Ogino
30. *Catalyst Deactivation*, edited by Eugene E. Petersen and Alexis T. Bell
31. *Hydrogen Effects in Catalysis: Fundamentals and Practical Applications*, edited by Zoltán Paál and P. G. Menon
32. *Flow Management for Engineers and Scientists*, Nicholas P. Cheremisinoff and Paul N. Cheremisinoff
33. *Catalysis of Organic Reactions*, edited by Paul N. Rylander, Harold Greenfield, and Robert L. Augustine
34. *Powder and Bulk Solids Handling Processes: Instrumentation and Control*, Koichi Iinoya, Hiroaki Masuda, and Kinnosuke Watanabe
35. *Reverse Osmosis Technology: Applications for High-Purity-Water Production*, edited by Bipin S. Parekh
36. *Shape Selective Catalysis in Industrial Applications*, N. Y. Chen, William E. Garwood, and Frank G. Dwyer
37. *Alpha Olefins Applications Handbook*, edited by George R. Lappin and Joseph L. Sauer
38. *Process Modeling and Control in Chemical Industries*, edited by Kaddour Najim
39. *Clathrate Hydrates of Natural Gases*, E. Dendy Sloan, Jr.
40. *Catalysis of Organic Reactions*, edited by Dale W. Blackburn
41. *Fuel Science and Technology Handbook*, edited by James G. Speight
42. *Octane-Enhancing Zeolitic FCC Catalysts*, Julius Scherzer
43. *Oxygen in Catalysis*, Adam Bielanski and Jerzy Haber
44. *The Chemistry and Technology of Petroleum: Second Edition, Revised and Expanded*, James G. Speight
45. *Industrial Drying Equipment: Selection and Application*, C. M. van't Land
46. *Novel Production Methods for Ethylene, Light Hydrocarbons, and Aromatics*, edited by Lyle F. Albright, Billy L. Crynes, and Siegfried Nowak
47. *Catalysis of Organic Reactions*, edited by William E. Pascoe
48. *Synthetic Lubricants and High-Performance Functional Fluids*, edited by Ronald L. Shubkin
49. *Acetic Acid and Its Derivatives*, edited by Victor H. Agreda and Joseph R. Zoeller
50. *Properties and Applications of Perovskite-Type Oxides*, edited by L. G. Tejuca and J. L. G. Fierro
51. *Computer-Aided Design of Catalysts*, edited by E. Robert Becker and Carmo J. Pereira
52. *Models for Thermodynamic and Phase Equilibria Calculations*, edited by Stanley I. Sandler
53. *Catalysis of Organic Reactions*, edited by John R. Kosak and Thomas A. Johnson
54. *Composition and Analysis of Heavy Petroleum Fractions*, Klaus H. Altgelt and Mieczyslaw M. Boduszynski
55. *NMR Techniques in Catalysis*, edited by Alexis T. Bell and Alexander Pines
56. *Upgrading Petroleum Residues and Heavy Oils*, Murray R. Gray
57. *Methanol Production and Use*, edited by Wu-Hsun Cheng and Harold H. Kung

58. *Catalytic Hydroprocessing of Petroleum and Distillates*, edited by Michael C. Oballah and Stuart S. Shih
59. *The Chemistry and Technology of Coal: Second Edition, Revised and Expanded*, James G. Speight
60. *Lubricant Base Oil and Wax Processing*, Avilino Sequeira, Jr.
61. *Catalytic Naphtha Reforming: Science and Technology*, edited by George J. Antos, Abdullah M. Aitani, and José M. Parera
62. *Catalysis of Organic Reactions*, edited by Mike G. Scaros and Michael L. Prunier
63. *Catalyst Manufacture*, Alvin B. Stiles and Theodore A. Koch
64. *Handbook of Grignard Reagents*, edited by Gary S. Silverman and Philip E. Rakita
65. *Shape Selective Catalysis in Industrial Applications: Second Edition, Revised and Expanded*, N. Y. Chen, William E. Garwood, and Francis G. Dwyer
66. *Hydrocracking Science and Technology*, Julius Scherzer and A. J. Gruia
67. *Hydrotreating Technology for Pollution Control: Catalysts, Catalysis, and Processes*, edited by Mario L. Occelli and Russell Chianelli
68. *Catalysis of Organic Reactions*, edited by Russell E. Malz, Jr.
69. *Synthesis of Porous Materials: Zeolites, Clays, and Nanostructures*, edited by Mario L. Occelli and Henri Kessler
70. *Methane and Its Derivatives*, Sunggyu Lee
71. *Structured Catalysts and Reactors*, edited by Andrzej Cybulski and Jacob A. Moulijn
72. *Industrial Gases in Petrochemical Processing*, Harold Gunardson
73. *Clathrate Hydrates of Natural Gases: Second Edition, Revised and Expanded*, E. Dendy Sloan, Jr.
74. *Fluid Cracking Catalysts*, edited by Mario L. Occelli and Paul O'Connor
75. *Catalysis of Organic Reactions*, edited by Frank E. Herkes
76. *The Chemistry and Technology of Petroleum: Third Edition, Revised and Expanded*, James G. Speight
77. *Synthetic Lubricants and High-Performance Functional Fluids: Second Edition, Revised and Expanded*, Leslie R. Rudnick and Ronald L. Shubkin
78. *The Desulfurization of Heavy Oils and Residua, Second Edition, Revised and Expanded*, James G. Speight
79. *Reaction Kinetics and Reactor Design: Second Edition, Revised and Expanded*, John B. Butt

**ADDITIONAL VOLUMES IN PREPARATION**

# REACTION KINETICS AND REACTOR DESIGN

*Second Edition, Revised and Expanded*

**John B. Butt**

*Northwestern University  
Evanston, Illinois*



MARCEL DEKKER, INC.

NEW YORK • BASEL

**Library of Congress Cataloging-in-Publication Data**

Butt, John B.

Reaction kinetics and reactor design / J.B. Butt. – 2nd ed., rev. and expanded.

p. cm. – (Chemical industries ; v. 79)

Includes index.

ISBN 0-8247-7722-0 (alk. paper)

1. Chemical kinetics. 2. Chemical reactors. I. Title. II. Series.

QD502 .B87 1999

660'.2832-dc21

99-051459

The first edition was published by Prentice-Hall, Inc., 1980.

This book is printed on acid-free paper.

**Headquarters**

Marcel Dekker, Inc.

270 Madison Avenue, New York, NY 10016

tel: 212-696-9000; fax: 212-685-4540

**Eastern Hemisphere Distribution**

Marcel Dekker AG

Hutgasse 4, Postfach 812, CH-4001 Basel, Switzerland

tel: 41-61-261-8482; fax: 41-61-261-8896

**World Wide Web**

<http://www.dekker.com>

The publisher offers discounts on this book when ordered in bulk quantities. For more information, write to Special Sales/Professional Marketing at the headquarters address above.

**Copyright © 2000 by Marcel Dekker, Inc. All Rights Reserved.**

Neither this book nor any part may be reproduced or transmitted in any form or by any means, electronic or mechanical, including photocopying, microfilming, and recording, or by any information storage and retrieval system, without permission in writing from the publisher.

Current printing (last digit):

10 9 8 7 6 5 4 3 2 1

**PRINTED IN THE UNITED STATES OF AMERICA**

## Preface to the Second Edition

A lot of things have happened in chemical reaction engineering since the first edition of this book, and this second version is very much different from the first. The remarks here are confined mostly to pointing out the changes.

The first edition was designed to combine a thorough description of the origin and application of fundamental chemical kinetics all the way through to realistic reactor design problems. This is continued, although the present effort increases the applications to a much larger range of reactor design problems. The discussion of kinetics has been expanded in Chapter 1 to include material on chemical thermodynamics related to reaction systems and additional discussion of chain and polymerization reactions. New material on microbial and enzyme kinetics, and on adsorption–desorption theory, is given in Chapter 3. At the same time, some of the more deadly derivations arising from the kinetic theory of gases given in the original Chapter 2 have been streamlined and the presentation simplified in the present version. Hopefully this material, which is very important to the philosophy of this book, will now be more digestible.

Chapters 4–6 retain the general organization of the first edition, although the presentation has been expanded and brought up to date. After the first part of Chapter 7 on transport effects in catalytic reactions, the present book goes its own way. A discussion of gas–solid noncatalytic reactions is given, and the development of two-phase reactor theory based on plug flow, mixing cell, and dispersion models (including transport effects and nonisothermality) rounds out the presentation of the chapter. This then leads naturally into the detailed multiphase reactor design/analysis considerations of Chapter 8, which treats some specific types of multiphase reactors such as fluid beds and trickle beds. This material is generally oriented toward design considerations, but care has been taken to relate the presentation to the pertinent theoretical developments given in earlier chapters.

Finally, Chapter 9 deals with unsteady-state fixed-bed problems, including catalyst deactivation phenomena, adsorption, ion-exchange and chromatographic reactors. This chapter probably has less to do with chemical reactions *per se* than the others, but the foundations of the fixed-bed analyses employed are firmly established in the prior material, and it seems a waste not to make use of it here.

So much for the menu. The first edition was designed primarily as a text for an undergraduate course. This edition, as one might expect from the above, goes considerably beyond that. According to the desires of the instructor, portions can be used for undergraduate courses, other parts for graduate courses, or special topics selected for seminar or discussion purposes.



HORATIO SAYS

There are a number of major changes, in addition to the extent of coverage, to be found here. A major new feature is the inclusion of a large number of worked-out illustrations in the text as the narrative continues. These can be fairly comprehensive and are not always easy; hopefully they are indicative of what is to be expected in the “Exercises” at the end of each chapter. We also have a house pet mouse, “Horatio,” who appears at the end of almost all of the illustrations, asking further questions regarding the illustration—essentially giving another set of exercises at the choice of the instructor. They are effective in providing additional experience with specific topics as desired. Horatio also appears in several locations asking the reader to clarify for himself various points in the text. Thanks to Mr. David Wright for permission to use this figure.

Many references are given in the text, as we go along, to pertinent background material. It has been an objective here to go back to sources that presented the early, developmental work on a given topic, and to supplement those references with later ones presenting significant advances. A consequence of this is that one should not be surprised to see references from the 1950s, or even much earlier, from time to time. Another procedure that has been followed is to use the notation as generally employed in the source material to make it easier in reading those references. As a result, there is no set of standard notation in the book; however, all the notation used in each chapter is summarized as completely as possible, alphabetically, at the end of that chapter.

Computer literacy is assumed, and there are many problems that require computer solution, particularly as one becomes involved with nonisothermal reactors, boundary-value dispersion problems, the more advanced fixed-bed problems, and interpretation of kinetic data. We have not tried to get into the software business here, in view of the continuing rapid evolution of various aspects of that field. We have yielded to the temptation in a couple of instances to suggest, in outline, some algorithms for specific problems, but in general this is left up to the reader.

The indebtedness to colleagues, teachers, and students mentioned in the preface to the first edition remains unchanged. In addition, I would like to thank Professor James J. Carberry for his comments on the preparation of this second edition.

*John B. Butt*



## Preface to the First Edition

All I know is just what I read in the papers

— *Will Rogers*

It is probably obvious even to the beginning student that much of chemical engineering is centered on problems involving chemical transformation, that is, chemical reaction. It is probably not so obvious, at least in the beginning, that the rate at which such transformations occur is the determining factor in a great number of the processes that have been developed over the years to produce that vast array of goods that we consider an integral part of contemporary life. The study, analysis, and interpretation of the rates of chemical reactions is, itself, a legitimate field of endeavor. It ranges in scope from those problems concerned with the fundamentals of detailed mechanisms of chemical transformation and the associated rates to problems that arise during the development and implementation of procedures for chemical reactor and process design on a large scale. If we must give names to these two extremes, we might call the first “chemical kinetics,” and the second “chemical reaction engineering.”

In the following we shall range from one limit to the other, although our primary objective is the understanding of kinetic principles and their application to engineering problems. What will we find? For one thing, we will find that chemical reactions are not simple things; those fine, balanced equations which everyone has used in solving stoichiometry problems ordinarily represent only the sum of many individual steps. We will find that the rates of chemical transformation, particularly in engineering application, are often affected by rates of other processes, such as the transport of heat or mass, and cannot be isolated from the physical environment. We will find that the normal dependence of reaction rate on temperature is one of the most intractable of nonlinearities in nature, providing at the same time many of the difficulties and many of the challenges in the analysis of chemical rates. We will find that often it is not the absolute rate of a single reaction but the relative rates of two or more reactions that will be important in determining a design. We will find that space as well as time plays an important role in reaction engineering, and in the treatment of such problems it will be necessary to develop some facility in the use of rational mathematical models. Finally, we will find that the artful compromise is as important, if not more so, in our applications of reaction kinetics as it is in all the other areas of chemical engineering practice.

This may seem like a very short list of what is to be found if the topic is truly as important as we have indicated. It is intentionally short, because the essence should not be submerged in detail quite so soon, or, to paraphrase Thomas à Kempis, ... it is better not to speak a word at all than to speak more words than we should.

The material of this text is intended primarily to provide instruction at the undergraduate level in both chemical kinetics and reactor design. Of particular concern has been the detailing of reaction kinetics beyond phenomenological description. The rationale for the Arrhenius equation was a personal mystery to the author in earlier years, who hopes an appropriate solution is revealed in Chapter 2.

Numerous other aspects of classical theories of chemical kinetics are assembled in Chapter 2 and Chapter 3 to give some perception of the origin of phenomenological rate laws and an understanding of the differing types of elementary reaction steps. In Chapter 4 we swap the beret of the theoretician for the hard hat of the engineer, in pursuit of means for developing rational chemical reactor design and analysis models. A parallelism between mixing models and reactor models has been maintained in order to demonstrate clearly how reaction kinetic laws fit into reactor design. Chapters 4 through 6 are based on homogeneous models, and proceed from standard plug flow and stirred tank analysis to description of nonideal behavior via dispersion, segregated flow, mixing cell and combined model approaches. Phenomena associated with reaction in more than one phase are treated in Chapter 7 but no attempt is made to develop multiphase reactor models. The fact that reaction selectivity as well as reaction rate is an important and often determining factor in chemical reaction or reactor analysis is kept before the eyes of the reader throughout the text.

The exercises are an intentionally well-mixed bag. They range from simple applications of equations and concepts developed in the text to relatively open-ended situations that may require arbitrary judgement and, in some instances, have no unique answer. The units employed are equally well-mixed. Historically, multiple systems of measure have been a curse of the engineering profession and such is the case here particularly, where we range from the scientific purity of Planck's constant to the ultimate practicality of a barrel of oil. The SI system will eventually provide standardization, it is to be hoped, but this is not a short-term proposition. Because both author and reader must continue to cope with diverse sets of units, no attempt at standardization has been made here.

Symbols are listed in alphabetical order by the section of the chapter in which they appear. Only symbols which have not been previously listed or which are used in a different sense from previous listings are included for each section. Symbols used in equations for simplification of the form are generally defined immediately thereafter and are not listed in the Notation section found at the end of each chapter.

Each chapter is divided into more or less self-contained modules dealing with a unified concept or a group of related concepts. Similarly, the exercises and notation are keyed to the individual modules, so that a variety of possibilities exist for pursuit of the material presented.

Acknowledgment must be made to teachers and colleagues who, over the years, have had influence in what is to be found in this text. I am grateful to the late Charles E. Littlejohn and R. Harding Bliss, to Professors C. A. Walker, H. M. Hulburt, and R. L. Burwell, Jr., and especially to Professor C. O. Bennett, who offered many constructive and undoubtedly kind comments during preparation of this manuscript.

Thanks also to R. Mendelsohn, D. Casleberry and J. Pherson for typing various sections of the manuscript, and to the Northwestern chemical engineering students for detecting unworkable problems, inconsistent equations, and all the other gremlins waiting to smite the unwary author.

*John B. Butt*

# Contents

<i>Preface to the Second Edition</i>	<i>iii</i>
<i>Preface to the First Edition</i>	<i>v</i>
<b>1. Apparent Reaction Kinetics in Homogeneous Systems</b>	<b>1</b>
1.1 Mass Conservation and Chemical Reaction	1
1.2 Reaction Rate Equations: The Mass Action Law	6
1.3 Temperature Dependence of Reaction Rate	9
1.4 Rate Laws and Integrated Forms for Elementary Steps	12
1.5 Kinetics of “Nearly Complex” Reaction Sequences	25
1.6 Kinetics of Complex Reaction Sequences—Chain Reactions	35
1.7 Chemical Equilibrium	49
1.8 Reaction Rates and Conversion in Nonisothermal Systems	62
1.9 Interpretation of Kinetic Information	74
Exercises	93
Notation	104
<b>2. The Mechanisms of Chemical Reactions in Homogeneous Phases</b>	<b>107</b>
2.1 Elementary Kinetic Theory	107
2.2 Collision Theory of Reaction Rates	116
2.3 Transition-State Theory of Reaction Rates	133
2.4 Experimental Results on the Kinetics of Various Reactions	151
2.5 Some Estimation Methods	155
Exercises	160
Notation	165
<b>3. The Mechanisms of Chemical Reactions on Surfaces</b>	<b>169</b>
3.1 Adsorption and Desorption	170
3.2 Surface Reactions with Rate-Controlling Steps	187

3.3	Surface Reactions and Nonideal Surfaces	194
3.4	Enzyme and Microbial Kinetics	197
3.5	Interpretation of the Kinetics of Reactions on Surfaces	202
3.6	Decline of Surface Activity: Catalyst Deactivation	212
	Exercises	219
	Notation	226
<b>4.</b>	<b>Introduction to Chemical Reactor Theory</b>	<b>231</b>
4.1	Reaction in Mixed or Segregated Systems	232
4.2	Age Distributions and Macromixing	235
4.3	Mixing Models: Reactors with Ideal Flows	245
4.4	Applications of Ideal Reactor Models	252
4.5	Temperature Effects in Ideal Reactors	289
4.6	Catalyst Deactivation in Flow Reactors	301
4.7	Other Fixed Beds and Other Waves: Ion Exchange and Adsorption	308
	Exercises	315
	Notation	326
<b>5.</b>	<b>Modeling of Real Reactors</b>	<b>331</b>
5.1	Deviations from Ideal Flows	332
5.2	Modeling of Nonideal Flow or Mixing Effects on Reactor Performance	332
5.3	Combined Models for Macroscopic Flow Phenomena	356
5.4	Modeling of Nonideal Reactors	361
	Exercises	391
	Notation	395
<b>6.</b>	<b>Thermal Effects in the Modeling of Real Reactors</b>	<b>399</b>
6.1	Mixing-Cell Sequences	399
6.2	Some Reactor/Heat-Exchanger Systems	424
6.3	Gradients and Profiles	430
6.4	Temperature Forcing of Reactors with Catalyst Decay	445
	Exercises	451
	Notation	452
<b>7.</b>	<b>Reactions in Heterogeneous Systems</b>	<b>457</b>
7.1	Reactions in Gas/Solid Systems	457
7.2	Reactions in Gas/Liquid Systems	521
7.3	Two-Phase Reactor Models: The Dispersion Approach	537
	Exercises	560
	Notation	566

<b>8. Multiphase Reactors</b>	<b>571</b>
8.1 Fluidized-Bed Reactors	571
8.2 Slurry Reactors	592
8.3 Gas-Liquid Reactors	608
8.4 Trickle-Bed Reactors	635
Exercises	660
Notation	666
<b>9. Some More Unsteady-State Problems</b>	<b>673</b>
9.1 The Adsorption Wave	673
9.2 Chromatography	695
9.3 Deactivation Waves	709
Exercises	712
Notation	716
<i>Index</i>	<i>721</i>

# 1

---

## Apparent Reaction Kinetics in Homogeneous Systems

Gather ye rosebuds while ye may  
Old time is still a-flying

— *Robert Herrick*

### 1.1 Mass Conservation and Chemical Reaction

Certainly the most fundamental of laws governing the chemical transformations and separations with which chemical reaction engineering is involved is that of conservation of mass. Although this is surely not new to the readers of this text, it is worth the time here to revisit a simple example to make clear what specific functions in a typical mass balance might arise as a result of chemical reaction. The example may seem very elementary, but it is important that we all start at the same point. Consider then the steady-state separation process depicted in Figure 1.1. A stream,  $L$ , mass/time, containing two components, A and B, is fed to the process, which divides it into two product streams,  $V$  and  $W$ , mass/time, also containing components A and B. The mass fractions of components A and B in  $L$ ,  $V$ , and  $W$  are given as  $x_A$ ,  $x_B$ ,  $y_A$ ,  $y_B$ , and  $z_A$ ,  $z_B$ , respectively. Mass is conserved in this separation; we may express this mathematically with the following simple relations:

$$L = V + W \quad (1-1)$$

$$Lx_A = Vy_A + Wz_A \quad (1-2)$$

$$Lx_B = Vy_B + Wz_B \quad (1-3)$$

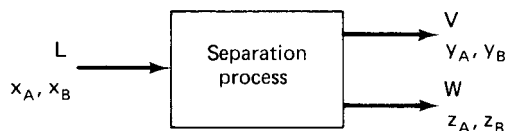


**Figure 1.1** Simple separation.

Now, since we also know that each stream consists of the sum of its parts, then

$$x_A + x_B = 1 \quad (1-4)$$

$$y_A + y_B = 1 \quad (1-5)$$

$$z_A + z_B = 1 \quad (1-6)$$

This, in turn, means that only two of the three mass balance relationships (1-1) to (1-3) are independent and can be used to express the law of conservation of mass for the separation. We are then left with a system of five equations and nine potential unknowns such that if any four are specified, the remaining five may be determined. Of course, all we have done is to say:

$$\text{Total mass in/time} = \text{total mass out/time}$$

$$\text{Mass A in/time} = \text{mass A out/time}$$

$$\text{Mass B in/time} = \text{mass B out/time}$$

Since the uniform time dimension divides out of each term of these equations, our result is the direct mass conservation law.

Now let us consider a slightly different situation in which the process involved is not a separation but a chemical transformation. In fact, we shall simplify the situation to a single input and output stream as in Figure 1.2 with the feed stream consisting of component A alone. However, within the process a chemical reaction occurs in which B is formed by the reaction  $A \rightarrow B$ . If the reaction is completed within the process, all the A reacts to form B and mass conservation requires that the mass of B produced equal the mass of A reacted. The material balance is trivial:

$$L = W \quad (x_A = 1, z_B = 1) \quad (1-7)$$

What happens, though, if not all of the A reacts to form B in the process? Then, obviously, the mass of B leaving is not equal to the mass of A entering, but rather

$$L = Wz_A + Wz_B \quad (1-8)$$

Comparison of the two processes illustrates in a simple but direct way the general concerns of this whole text. These are

1. To determine  $z_A$  and  $z_B$  given a certain type and size of reaction process
2. To determine the type and size of reaction process needed to produce a specified  $z_A$  and  $z_B$

Two factors enter into this problem. The first is the *stoichiometry* of the reaction transforming A to B. Chemical equations as normally written express the



**Figure 1.2** Chemical reaction process.



relationship between molal quantities of reactants and products, and it is necessary to transform these to the mass relationship in problems of mass conservation involving chemical reaction. The details of this are clear from the familiar combustion/mass balance problems, which seem so vexing the first time they are encountered. In our simple example reaction the stoichiometric relationship is 1 : 1, so mass conservation requires the molecular weight of B to equal that of A, and thus the mass of B produced equals the mass of A reacted. This particular type of transformation is called an *isomerization* reaction and is common and important in industrial applications.

The second factor is the *rate* at which A reacts to form B. Consider the problem in which we wish to determine  $z_A$  and  $z_B$ , given the type and size of process used in Figure 1.2. For the mass balance on component A, we want to write

$$\text{Mass A in/time} = \text{mass A out/time} + \text{mass A reacted/time} \quad (1-9)$$

and for B (recalling that there is no B in the feed)

$$\text{Mass B out/time} = \text{mass B formed/time} = \text{mass A reacted/time} \quad (1-10)$$

The last two terms of equation (1-10) incorporate the information concerning the stoichiometric relationship involved in the chemical reaction, since we have already seen that the mass relationship as well as the molal relationship in this particular example is 1 : 1. We can also paraphrase the statement of equation (1-10) to say that the rate at which B passes out of the system is equal to the rate at which it is formed, which is also equal to the rate at which A reacts. Thus, the rate of reaction is closely involved in this mass balance relationship—exactly how is what we are to learn—so for the moment our simple example must remain unsolved.

The most pressing matter at this point is to define what we mean by *rate of reaction*. This is by no means trivial. The definition of a reference volume for the rate sometimes gives trouble here. It should be clear that the magnitude of the rates involved in equation (1-10) depend on the magnitude of the process, so in principle we could have an infinite number of processes, as in Figure 1.2, each of different size and each with a different rate. Clearly this is an undesirable way to go about things, but if we define a reaction rate with respect to a unit volume of reaction mixture, the size dependency will be removed. Also, we should remember that the rate of reaction must be specified with respect to a particular component, reactant, or product. As long as the ratio of stoichiometric coefficients is unity, this presents no problem; however, if our example reaction were  $A \rightarrow 2B$ , then the rate (in mols/time) of A would always be one-half that of B, regardless of the reference volume employed. Finally, we must define the rate of reaction so that it will reflect the influence of state variables such as composition and temperature but will not be dependent on the particular process or reactor in which the reaction takes place. In accord with this, we can write:

$$\begin{aligned} r'_i &= (\text{change in mass of } i)/(\text{time-volume reaction}) \\ &= (1/V)(dM_i/dt) = \text{rate} \end{aligned} \quad (1-11a)$$

or

$$\begin{aligned} r_i &= (\text{change in mols of } i)/(\text{time-volume reaction}) \\ &= (1/V)(dN_i/dt) = \text{rate} \end{aligned} \quad (1-11b)$$

where  $i$  is reactant or product,  $V$  the volume of the reaction mixture and  $M$  and  $N$  are mass and mols, respectively. The rate is positive for change in product and negative for change in reactant. Most of our applications will deal with the use of molal quantities and, for the convenience of working with positive numbers, the rate of reaction of a reactant species is often encountered as  $(-r_i)$ .

There are a number of traps involved in even this straightforward definition. The use of the reference volume as that of the reaction mixture is necessary to account for the fact that in some cases the total volume will change in proportion to the molal balance between reactants and products. If the reaction were  $A \rightarrow 2B$  and involved ideal gases with no change in temperature or total pressure, the volume of product at the completion of the reaction would be twice that of initial reactant. To conserve our definition of reaction rate independent of the size of the system, the volume change must be accounted for. This is not difficult to do, as will be shown a little later. The problem is that one often sees reaction rates written in the following form:

$$r_i = (dC_i/dt) = d(N_i/V)/dt \quad (1-12)$$

where concentration  $C_i$  (mols/volume) is used in the rate definition. Equation (1-12) is in some sense embedded in the history of studies of chemical rates of reaction and dates from the very early physicochemical studies. These were mostly carried out in constant-volume batch reactors, for which, as we shall shortly see, equation (1-12) is valid. If one wishes to use concentrations (normally the case) but still conform to the definitions of equations (1-11), then

$$r_i = (1/V)[d(C_i V)/dt] \quad (1-13)$$

where  $N_i = C_i V$ . The problem with the use of equation (1-12) as a definition of rate is that it envisions no change in the reference volume as the reaction proceeds. Equations (1-11) and (1-13) resolve that particular difficulty, but we are still left with the fact that the proper formulation of a rate definition depends on the experimental system used to measure the rate, so there is really no single definition that is both convenient and universal [for further reading on the matter see A.E. Cassano, *Chem. Eng. Educ.*, 14, Winter Issue (1980)].

Related to the question of how to define the rate of chemical reaction is the use of the time derivative,  $dM_i/dt$  or  $dN_i/dt$ . This implies that things are changing with time and may tempt one to associate the appearance of reaction rate terms in mass conservation equations with unsteady-state processes. This is not necessarily true; in general, one must make a distinction between the ongoing time of operation of some process (i.e., that measured by an observer) and individual phenomena such as chemical reactions that occur at a *steady* rate in an operation that does not vary with time (steady-state). Later we will encounter both steady- and unsteady-state types of processes involving chemical reaction, to be sure, but this depends on the process itself; the reaction rate definition has been made without regard to a particular process.

Returning for a moment to the mass conservation equation, equation (1-9), we may now restate it in terms of a working definition of the rate of reaction.

For a specified volume element,  $\delta$  of reaction mixture within the process and under steady conditions:

$$(\text{mass A into } \delta/\text{time}) = (\text{mass A out of } \delta/\text{time} + \text{mass A reacted in } \delta/\text{time}) \quad (1-14)$$

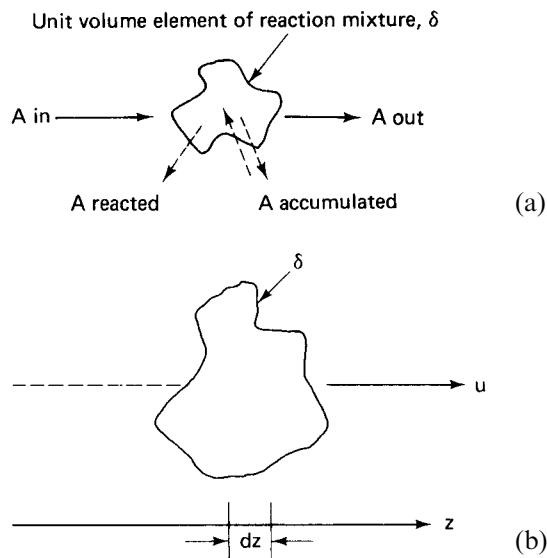


**Figure 1.3** (a) Mass balance with chemical reaction on a volume element of reaction mixture. (b) Traveling batch reactor.

as shown in Figure 1.3(a). The reaction term in equation (1-14) now conforms to the reaction rate definition; the left side of the equality is the *input* term and the right side the *output*. It is understood that A refers to a reaction or product species, not an element.

In the event of unsteady-state operation, the means of incorporating the rate expression in the mass balance are still the same, but the balance becomes

$$\begin{aligned}
 &(\text{Mass A into } \delta/\text{time}) - (\text{mass A out of } \delta/\text{time}) + (\text{mass A reacted in } \delta/\text{time}) \\
 &= (\text{change of mass of A in } \delta/\text{time})
 \end{aligned}
 \tag{1-15}$$

The input/output terms remain the same, but an *accumulation* term on the right side represents the time dependence of the mass balance.

From equation (1-15) we can immediately derive expressions relating the reaction rate to the type of process for two limiting cases. First, if the volume element  $\delta$  does not change as the reaction proceeds, and there is no flow of reactant into or out of  $\delta$ , equation (1-15) becomes (still in mass units)

$$(\text{A reacted in } \delta/\text{time}) = (\text{change of A in } \delta/\text{time})
 \tag{1-16}$$

The left-hand side is the definition of the reaction rate of A,  $r'_A$ , and the right-hand side (recall that  $\delta$  does not change) is given by the rate of change of concentration of A, so

$$r'_A = dC_A/dt
 \tag{1-12}$$

This is the equation for a *batch reactor*, a constant volume of reaction mixture, and we see that it corresponds to the rate definition given in equation (1-12). A similar expression, of course, would apply for molal units.

In the second case we also assume that the volume element  $\delta$  does not change and that there is no flow of A into or out of the element. However,  $\delta$  is now moving, with other like elements, in some environment such that the distance traversed from a reference point is a measure of the time the reaction has been occurring, as shown in Figure 1.3b. Now, for this little traveling batch reactor we may rewrite the time derivative in terms of length and linear velocity. For a constant velocity  $u$ , as the volume element moves through the length  $dz$

$$dt = dz/u$$

and equation (1-13) becomes

$$r'_A = u(dC_A/dz) \quad (1-16)$$

This is the equation for a *plug flow reactor*, or at least one form of it. Again, though, it is necessary to be careful. The time derivative above is based on constant velocity, which would not be the case, for example, in a gas reaction with differing net stoichiometric coefficients for reactants and products. Further, equation (1-16) as written employs a mass average velocity; if the rate definition is in molal units, then the molal average velocity must be used.

The batch reactor and plug flow reactor are two different types of reactors that are extremely important in both the analysis and implementation of chemical reaction processes. Much of the substance of what has been discussed above will be restated from a somewhat different perspective in Chapter 4.

## 1.2 Reaction Rate Equations: The Mass Action Law

Although a proper definition of the rate of reaction is necessary, we cannot do much with it until we find how the rate depends on the variables of the system such as temperature, total pressure, and composition. In general terms, we must set the rate definition equal to a mathematical expression that correlates properly the effects of such variables. That is,

$$r = \phi(C_i, C_j, \dots, T, P)$$

where  $\phi$  depends on the complexity of the reacting system. For the present we shall do this on the basis of observation and experience; good theoretical reasons for the results will be given in Chapter 2.

Again let us work through the example of a specific (but hypothetical) system, this time the irreversible reaction



The rate of this reaction can often be correlated by

$$r = k(C_A)^p(C_B)^q(C_C)^r \quad (1-17)$$

which form follows directly from the *law of mass action*. The rate constant  $k$  normally depends on the temperature, and the exponents  $p$ ,  $q$ , and  $r$  may also be temperature-dependent. The exponents are termed the order of the reaction; total order of the reaction is  $(p + q + r)$ , and order with respect to an individual reactant, say A, is  $p$ . The rate constant is a positive quantity, so if the rate expressed in equation (1-17) refers to disappearance of a reactant, it is necessary to include a minus sign on one side of the equality. If we rewrite equation (1-17) to refer specifically to the

disappearance of A, and use the definition of equation (1-12):

$$\begin{aligned} -k(C_A)^p(C_B)^q(C_C)^r \cdots &= -k(N_A/V)^p(N_B/V)^q(N_C/V)^r \cdots \\ &= r_A \quad \text{mols reacted/time-volume} \end{aligned} \quad (1-18)$$

If the total volume of the reaction system does not change, then

$$\begin{aligned} dC_A/dt &= -k(C_A)^p(C_B)^q(C_C)^r \cdots \\ &= r_A \quad \text{mols reacted/time-volume} \end{aligned} \quad (1-19)$$

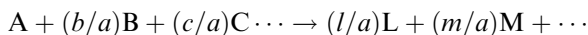
In many cases we shall see that the individual orders  $p$ ,  $q$ , and  $r$  have numerical values that are the same as the stoichiometric coefficients of the reaction,  $a$ ,  $b$ , and  $c$ . In this event it is said that *order corresponds to stoichiometry*; there is in general, however, no restriction on the numerical values of  $p$ ,  $q$ , and  $r$  determined on the basis of experimental observation, including negative values.

If the reaction is reversible, A, B, C, ... can be formed from the products L, M, ... and a corresponding form of the law of mass action applies. For this case equation (1-18) becomes

$$-k_f(C_A)^p(C_B)^q(C_C)^r + k_r(C_L)^u(C_M)^w = r_A \quad (1-20)$$

Here  $u$  and  $w$  are the orders of the reverse reaction with respect to L and M,  $k_f$  the forward rate constant, and  $k_r$  the reverse rate constant. The same comments as given earlier pertain to the relationship between the apparent orders and the stoichiometric coefficients  $l$  and  $m$ .

The rate constants here have been defined in molal terms and we will follow this convention for the time being, although there is no reason that mass units could not be used, following equation (1-11). The rate expression for the appearance or disappearance of a given component, however, implies a corresponding definition for the rate constant. In the preceding section we pointed out the general role of stoichiometric coefficients in determining relative rates. In more specific terms here,  $k$  in equation (1-18) defines the mols of A reacted per time per volume; whether the same number for  $k$  also gives mols of B reacted per time per volume depends on the relative values of the stoichiometric coefficients  $a$  and  $b$ ; yes only if  $a = b$ . Rewrite the reaction as



Clearly  $(b/a)$  mols of B react for each mol of A, and so on. The rate of reaction of any constituent  $i$  is then related to the rate of reaction of A by

$$r_i = r(\nu_i/\nu_A)$$

where  $\nu$  are the individual stoichiometric coefficients, positive for products and negative for reactants, and  $r = -r_A$ .

For reversible reactions it is sometimes convenient to consider the individual terms in rate expressions such as equation (1-20). The *forward* rate for A is

$$(r_A)_f = -k_f(C_A)^p(C_B)^q(C_C)^r \cdots \quad (1-20a)$$

and the reverse rate

$$(r_A)_r = k_r(C_L)^u(C_M)^w \cdots \quad (1-20b)$$

and the *net* rate the algebraic sum of the two:

$$r_A = (r_A)_f + (r_A)_r \quad (1-21)$$

When the forward and reverse rates are equal, the reaction is at equilibrium and we have the result

$$k_f(C_A)^p(C_B)^q(C_C)^r = k_r(C_L)^u(C_M)^w \quad (1-22)$$

or

$$(k_f/k_r) = [(C_L)^u(C_M)^w]/[(C_A)^p(C_B)^q(C_C)^r] \quad (1-23)$$

This equation is identical to that which defines a concentration-based equilibrium constant, so it is tempting to say that such a result leads us immediately to the equilibrium constant of the reaction. If the reaction under consideration is truly an *elementary step* in the sense we shall discuss later, this is so. But many, even most, chemical transformations that we observe on a macroscopic scale and that observe overall stoichiometric relationships as given by (I) consist of a number of individual or elementary steps that for one reason or another are not directly observable. In such cases observation of the stationary condition expressed by equation (1-22) involves rate constants  $k_f$  and  $k_r$  that are combinations of the constants associated with elementary steps. Further discussion of this and the relationship between rates and thermodynamic equilibria is given later in this chapter.

Mass action forms of rate correlation, often referred to as power law correlations, are widely applied, particularly for reactions in homogeneous phases. Table 1.1 gives a representative selection of correlations for various reactions. It is seen in several of the examples that the reaction orders are not those to be expected on the basis of the stoichiometric coefficients. Since these orders are normally established on the basis of experimental observation, we may consider them “correct” as far as the outside world is concerned, and the fact that they do not correspond to stoichiometry is a sure indication that the reaction is not proceeding the way we have written it on paper. Thus we will maintain a further distinction between the elementary steps of a reaction and the overall reaction under consideration. The direct application of the law of mass action where the orders and the stoichiometric coefficients correspond will normally pertain *only* to the elementary steps of a reaction, as will the dependence of rate on temperature to be discussed in the next section. Also,

**Table 1.1** Mass Action Law Rate Equations (II)

Reaction	Rate law
$\text{CH}_3\text{CHO} \rightarrow \text{CH}_4 + \text{CO}$	$k[\text{CH}_3\text{CHO}]^{1.5}$
$\text{N}_2 + 3\text{H}_2 \rightarrow 2\text{NH}_3$	$k[\text{N}_2][\text{H}_2]^{2.25}[\text{NH}_3]^{-1.5}$
$4\text{PH}_3 \rightarrow \text{P}_4 + 6\text{H}_2$	$k\text{PH}_3$
$\text{CH}_3\text{COCH}_3 + \text{HCN} \rightleftharpoons (\text{CH}_3)_3\text{C} \begin{array}{l} \text{OH} \\ \text{CN} \end{array}$	$k_f[\text{HCN}][\text{CH}_3\text{COCH}_3]$ $-k_r[(\text{CH}_3)_2\text{COHON}]$
$(\text{C}_2\text{H}_5)_2\text{O} \rightarrow \text{C}_2\text{H}_6 + \text{CH}_3\text{CHO}$	$k[\text{C}_2\text{H}_5\text{OC}_2\text{H}_5]$
$\text{CH}_3\text{OH} + \text{CH}_3\text{CHOHCOOH}$ $\rightarrow \text{CH}_3\text{CHOHCOOCH}_3 + \text{H}_2\text{O}$	$k[\text{CH}_3\text{OH}][\text{CH}_3\text{CHOHCOOH}]$

the theoretical background to be given in Chapter 2 concerning pressure, concentration, and temperature dependence of rate pertains to these elementary steps. Finally, for the forward and reverse steps of a reaction that is an elementary step, the principle of *microscopic reversibility* applies. This states that the reaction pathway most probable in the forward direction is most probable in the reverse direction as well. In terms of energy, one may say that the forward and reverse reactions of the elementary step are confronted with the same energy barrier.

### 1.3 Temperature Dependence of Reaction Rate

Mass action law rate equations are sometimes referred to as *separable* forms because they can be written as the product of two factors, one dependent on temperature and the other not. This can be illustrated by writing equation (1-18) as

$$-r_A = [k(T)](C_A)^p(C_B)^q(C_C)^r \quad (1-24)$$

where the rate constant  $k(T)$  is indicated to be a function of temperature and the concentration terms, aside from possible gas law dependencies, are independent of that variable. The possible dependence of  $p$ ,  $q$ , and  $r$  on temperature is small and normally arises from factors associated with the fitting of rate forms to kinetic data—not the problem we are concerned with here.

The temperature dependence of  $k$  associated with the rate of an elementary step is almost universally given by the awkward exponential form called the *Arrhenius equation*:

$$k(T) = k^\circ e^{-E/RT} \quad (1-25)$$

where  $E$  is the activation energy of the reaction,  $T$  the absolute temperature, and  $k^\circ$  the preexponential factor. In equation (1-25)  $k^\circ$  is written as independent of temperature; in fact, this may not be so, but the dependence is weak and the exponential term is by far the predominant one. Figure 1.4 illustrates the general form of dependence of reaction-rate constants obeying the Arrhenius law. Note that over a very wide range of temperatures this relation is sigmoid. The commonly expected exponential dependence of the rate constant on temperature is found only in a

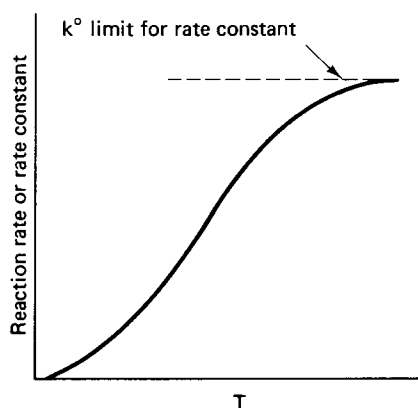


**Figure 1.4** Reaction-rate and rate-constant dependence on temperature according to the Arrhenius law.

certain region—depending on the value of the activation energy—and at very high temperature the response can be even less than linear.

### Illustration 1.1

The statement is sometimes made that the velocity of a reaction doubles for each 10°C rise in temperature. If this were true for the temperatures 298 K and 308 K, what would be the activation energy of the reaction? Repeat for 373 and 383 K. By what factor will the rate constant be increased between 298 and 308 K if the activation energy is 40,000 cal/gmol?

#### Solution

Writing equation (1-25) for two temperature levels  $T_1$  and  $T_2$ , we have as a ratio:

$$\ln(r_2/r_1) = (E/R)(1/T_1 - 1/T_2)$$

or

$$E = RT_1(1 + T_1/\Delta T) \ln(r_2/r_1)$$

$$\Delta T = T_2 - T_1$$

$$R = 1.98 \text{ for K, gmol, cal}$$

Now

$$(r_2/r_1) = 2; \quad \Delta T = 10 \text{ K}; \quad T_2 = 298 \text{ K}; \quad T_1 = 308 \text{ K}$$

so

$$E = 12,596 \text{ cal/gmol}$$

Repeating for  $T_1 = 373 \text{ K}$ ,  $T_2 = 383 \text{ K}$

$$E = 19,602 \text{ cal/gmol}$$

If the activation energy were 40,000 cal/gmol, then

$$(k_2/k_1) = [\exp(-40,000/1.98)][(1/298) - (1/308)]$$

$$(k_2/k_1) = 8.93$$



HORATIO SAYS

What if the true activation energy were only 15,000 cal/gmol? Would it then make so much difference?

The determination of activation energy from data on the temperature dependence of the velocity constant is often accomplished by a simple graphical analysis of



equation (1-25). Taking logarithms of both sides:

$$\ln[k(T)] = -(E/RT) + \ln(k^\circ) \quad (1-25a)$$

Thus, a plot of the logarithm of the rate constant versus the reciprocal of the temperature is linear with slope  $-(E/R)$  and intercept  $\ln(k^\circ)$ , as shown in Figure 1.5. In some cases the linear correlation may not be obtained. This may be due to several factors, the most frequent of which are:

1. The mechanism of the reaction changes over the temperature range studied.
2. The form of rate expression employed does not correspond to the reaction occurring (i.e., some composite rate is being correlated).
3. Other rate processes, such as mass diffusion, are sufficiently slow to partially obscure the reaction rates.
4. The temperature dependence of  $k^\circ$  becomes important (see problem 10).

In general, the Arrhenius correlation is probably one of the most reliable to be found in the kinetic repertoire if properly applied. There are sound theoretical reasons for this, as will be seen in Chapter 2. A problem of particular interest in chemical reaction engineering is that listed as factor 3 above; this shall be treated in Chapter 7.

Stated from a somewhat different point of view, the Arrhenius equation serves to define the activation energy  $E$ :

$$d[\ln(k)]/dT = (E/RT^2) \quad (1-26)$$

The form of equation (1-26) is reminiscent of the *van't Hoff relationship* for the temperature dependence of the equilibrium constant:

$$d[\ln(K)]/dT = (\Delta H^\circ/RT^2) \quad (1-27)$$

where  $\Delta H^\circ$  is the standard state heat of reaction. Consider the reaction  $A + B \leftrightarrow L + M$ , which is an elementary step. Then the ratio of forward to reverse

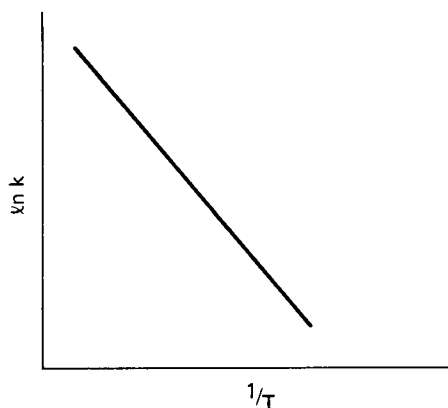


**Figure 1.5** Form of Arrhenius plot for determination of activation energy.

rate constants does give the equilibrium constant  $K$ , and we may write

$$d[\ln(K)]/dT = d[\ln(k_f/k_r)]/dT = (\Delta H^\circ/RT^2) \quad (1-28)$$

If we arbitrarily divide the total enthalpy change into the difference between two parts, one associated with the forward reaction,  $\Delta H_f^\circ$ , and the other with the reverse,  $\Delta H_r^\circ$ , then

$$\begin{aligned} d[\ln(k_f)]/dT - d[\ln(k_r)]/dT &= (\Delta H^\circ/RT^2) \\ &= (\Delta H_f^\circ/RT^2) - (\Delta H_r^\circ/RT^2) \end{aligned} \quad (1-29)$$

If, further, we arbitrarily associate corresponding terms on the two sides of equation (1-29), then

$$d[\ln(k_f)]/dT = (\Delta H_f^\circ/RT^2) \quad (1-30)$$

for example, and the enthalpy change  $\Delta H_f^\circ$  corresponds to what was called the activation energy in equations (1-25) and (1-26). This is a rather arbitrary way to associate some physical significance with the activation energy, but the thermodynamic argument above is that originally used to develop equation (1-25). We shall develop a more satisfying theoretical approach to both the form of the Arrhenius equation and the significance of the activation energy in Chapter 2. The exponential dependence of rate on temperature makes problems involving reaction kinetics in nonisothermal systems extremely nonlinear. They are among the most interesting and often the most challenging to be found in chemical reaction engineering.

## 1.4 Rate Laws and Integrated Forms for Elementary Steps

### 1.4.1 Individual and Overall Reactions

We have made a distinction between an overall reaction and its elementary steps in discussing the law of mass action and the Arrhenius equation. Similarly, the basic kinetic laws treated in this section can be thought of as applying primarily to elementary steps. What relationships exist between these elementary steps and the overall reaction? In Table 1.1 we gave as illustrations the rate laws that have been established on the basis of experimental observations for several typical reactions. A close look, for example, at the ammonia synthesis result is enough to convince one that there may be real difficulties with mass action law correlations. This situation can extend even to those cases in which there is apparent agreement with the mass action correlation but other factors, such as unreasonable values of the activation energy, appear. Let us consider another example from Table 1.1, the decomposition of diethyl ether:

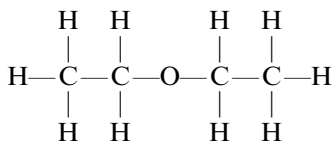


for which

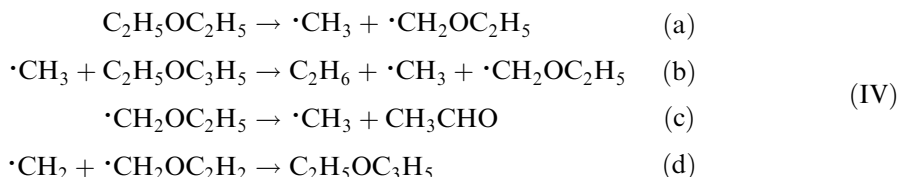
$$-r = k[\text{C}_2\text{H}_5\text{OC}_2\text{H}_5] \quad (1-31)$$

The overall reaction written in (III) does not indicate how the transformation from reactants to products actually occurs; indeed, (III) is quite misleading in this regard.

A little chemical intuition is helpful here; let us start by writing a simple two-dimensional structural formula for the ether:



and ask ourselves what must happen for the reaction to occur as in (III). Since ethane is a major product of the reaction, then a hydrogen would have to be shifted from one side of the molecule to the other at the same time that a C–O bond is being broken. Thus the single-step reaction of (III) implies a concerted action involving three bonds: breaking of one C–O and one C–H and formation of another C–H. For the suspicious among us it is not necessary to delve more deeply into the chemistry than this. A large number of events have to happen at essentially the same time (implying a substantial activation energy for the reaction, at least) so the question is whether it is not possible that some more chemically plausible, and energetically favorable, pathway might exist. Indeed it is the actual sequence of the reaction is



where each of the reactions (IVa) to (IVd) represents an elementary step in the overall decomposition. In practice, the intermediate species, such as  $\cdot\text{CH}_3$  and  $\cdot\text{CH}_2\text{OC}_2\text{H}_5$ , are very reactive and consequently have very short lifetimes and appear at very low concentrations. This will be discussed in detail later. These intermediates are, therefore, not readily observable, in contrast to the long-lived products of the reaction such as ethane. The reader may verify that the sum of the elementary steps of (IV) gives the overall reaction (III).

The ether decomposition is an example of a *chain reaction* in which elementary steps such as (IVb) and (IVc), involving the active intermediates in the chain, produce the final products. There are formal methods for treating the kinetics of such chain reactions that we shall encounter later; the important point here is to note the relationship between the overall reaction and the elementary steps and to note that even though the overall kinetics are apparently in accord with those for an elementary step, reaction (III) is not one.

As a second example consider a heterogeneous reaction—one occurring in two phases—rather than the homogeneous cases we have been discussing so far. The water gas reaction is a well-known example of one whose rate is influenced by the presence of a solid catalyst:



where the two phases involved are the gaseous reaction mixture and the solid catalytic surface. It is more apparent for (V) than for (III) that the overall reaction must consist of some sequence of elementary steps, since the scheme of (V) in no way

accounts for the influence of the catalyst on the reaction. If we let  $S$  represent some chemically active site on the catalytic surface, then one could envision writing (V) as



where  $[\text{SO}]$  is an oxide complex on the surface and plays the role of the intermediate in this reaction sequence.

When we compare (IV) and (VI), it is clear that much more detail concerning elementary steps is given in the former. The two reactions of (VI) provide a closer description of the water gas catalysis than does (V) but are not necessarily themselves the elementary steps. This is important in the applications of kinetics that we are concerned with, since frequently it is necessary to work with only partial information and knowledge of complicated reactions. The two-step sequence of (VI) is more desirable than (V), since it provides a means for incorporating the catalytic surface into the reaction scheme even though the two steps involved may not be elementary. We may summarize this by saying that the two-step sequence provides for an *essential feature* of the reaction, the involvement of the surface, which is absent in the overall reaction (V). Applied kinetics often requires the modeling of complicated reactions in terms of individual steps that incorporate the essential features of the overall reaction. As one develops more detailed information concerning a reaction, it will be possible to write in more depth the sequences of reaction steps involved, approaching (ideally) the actual elementary steps.

Boudart (M. Boudart, *Kinetics of Chemical Processes*, Prentice-Hall, Englewood Cliffs, N.J., 1968) has given a convenient means of classification of reaction sequences such as (IV) and (VI). The intermediates, such as  $\cdot\text{CH}_3$ ,  $\text{S}$ , and  $\text{SO}$ , are *active centers*, since the reaction proceeds via steps involving the reactivity of these species. In some cases, such as (IV) and (VI), the active centers are reacted in one step and regenerated in another [ $\cdot\text{CH}_3$  and  $\cdot\text{CH}_2\text{OC}_2\text{H}_5$  in (IV),  $\text{S}$  and  $\text{SO}$  in (VI)], so that a large number of product molecules can be produced through the action of a single active center. This is termed a *closed* sequence. In the case where this utilization and regeneration of active centers does not occur, the sequence is termed an *open* one and a single active center is associated with a single product-producing step. The gas-phase decomposition of ozone is an example of such an open sequence:



where the individual steps are



and oxygen atoms are the active centers for the reaction.

We shall ultimately be concerned with methods for establishing the rate laws for overall reactions such as (IV), (VI), and (VII) from a knowledge of (or speculation as to) the elementary steps. To do this we must certainly develop some facility with the simple rate laws that elementary reactions might be expected to obey. This is the topic of the following section.

### 1.4.2 Rates and Conversions for Simple Reactions

In this section we must be careful to respect our prior concern about the definition of rate with regard to the volume of reaction mixture involved. Further, since we wish to concentrate attention on the kinetics, we shall study systems in which the conservation equation contains the reaction term alone, which is the batch reactor of equation (1-12). It is convenient to view this type of reactor in a more general sense as one in which all elements of the reaction mixture have been in the reactor for the same length of time. That is, all elements have the same *age*. Since the reactions we are considering here occur in a single phase, the relationships presented below pertain particularly to *homogeneous batch* reactions, and the systems are isothermal.

The simplest of these is the class in which the reactions are irreversible and of constant volume. The most important here are zero, first, and second order with respect to the reactant(s), respectively.

*Zero Order.* It may seem somewhat at odds with the law of mass action to talk about rates that are independent of the concentration of reactant, but apparent zero-order reactions do occur, particularly in the description of the overall kinetics of some closed reaction sequences. We consider the model reaction,



with the zero-order rate law in molal units as

$$r_A = (1/V)(dN_A/dt) = -k = (dC_A/dt)$$

and in the batch reactor,  $C_A = C_{A0}$  at the start of the reaction  $t = 0$ . The concentration at any time is

$$\int_{C_{A0}}^{C_A} dC_A = - \int_0^t k dt \quad (1-32)$$

The rate constant  $k$  is a function only of temperature, so the integration of equation (1-32) gives directly:

$$C_A = C_{A0} - kt \quad (1-33)$$

*First Order.* The first-order case can be represented by the same model reaction,  $A \rightarrow B$ , with the rate law

$$r_A = (dC_A/dt) = -kC_A \quad (1-34)$$

For the same initial conditions as above,

$$\ln(C_A/C_{A0}) = -kt \quad (1-35)$$

or, if one is dealing with the course of the reaction between two specified time limits,  $C_{A1}$  at  $t_1$  and  $C_{A2}$  at  $t_2$ :

$$\ln(C_{A2}/C_{A1}) = -k(t_2 - t_1) \quad (1-36)$$

*Second Order.* Second-order reactions can be either of two general types:  $2A \rightarrow C + D$  or  $A + B \rightarrow C + D$ . In the first case,

$$r_A = (dC_A/dt) = -k(C_A)^2 \quad (1-37)$$

and

$$(1/C_A) - (1/C_{A0}) = kt \quad (1-38)$$

In the second case,

$$(dC_A/dt) = -kC_AC_B \quad (1-39)$$

For this system values for both  $C_A$  and  $C_B$  must be specified for some value of time, say  $t = 0$ . However, if we look to the integration of equation (1-39),

$$\int_{C_{A0}}^{C_A} (dC_A/C_AC_B) = - \int_0^t k dt \quad (1-40)$$

it is apparent that some relationship between  $C_A$  and  $C_B$  must be established before the integration can be carried out. This relationship is obtained from a combination of the specified values of  $C_A$  and  $C_B$  for a given time and the stoichiometry of the reaction. The stoichiometry of the reaction indicates that equimolal quantities of A and B react, so that if the reaction system is constant volume,

$$C_{A0} - C_A = C_{B0} - C_B \quad (1-41)$$

or

$$C_B = (C_{B0} - C_{A0}) + C_A$$

Then equation (1-40) becomes

$$\int_{C_{A0}}^{C_A} \frac{dC_A}{C_A[(C_{B0} - C_{A0}) + C_A]} = - \int_0^t k dt \quad (1-40a)$$

and

$$\ln(C_A/C_B) - \ln(C_{A0}/C_{B0}) = -(C_{B0} - C_{A0})kt \quad (1-42)$$

When the reactants A and B are initially present in stoichiometric proportion, that is  $C_{A0} = C_{B0}$ , equation (1-42) becomes indeterminate. The result, however, is given by equation (1-38), since the reaction stoichiometry requires that  $C_A = C_B$  for  $C_{A0} = C_{B0}$ .

*Nonintegral Order.* A nonintegral-order rate equation, such as that for acetaldehyde decomposition [the first reaction of Table 1.1], does not fit into the pattern expected for the rates of true elementary steps, but it is convenient to consider it here in succession with the other simple-order rate laws. Here we have, for example  $A \rightarrow B$ , where the reaction is  $n$ -order with respect to A:

$$r_A = (dC_A/dt) = -k(C_A)^n \quad (1-43)$$

The integrated result for  $C_A$  is

$$(C_A/C_{A0})^{1-n} - 1 = (n-1)(kt)(C_{A0})^{n-1} \quad (1-44)$$

*Half-Life, Conversion, and Volume Change Forms.* At this point we are going to break into the narrative of rate forms to discuss three particular aspects of kinetic formulations that pertain to most of the situations we discuss, at least for simple reactions.

The first of these are the concepts of *relaxation time* and reaction *half-life*. The rate equations we have written incorporate the constant  $k$  to express the proportionality between the rate and the state variables of the system, and, as such, it is some measure of a characteristic time constant for the reaction. For first-order reactions in particular, a convenient association may be made owing to the logarithmic time dependence of reactant concentration. If we rewrite equation (1-35) in exponential form, we see that the e-folding time of  $(C_A/C_{A0})$ , that is, the time at which  $-kt = -1$  and where  $(C_A/C_{A0})$  has decreased to 36.8% of its original value, occurs for  $t = 1/k$ . This value of time is referred to, for first-order processes, as the relaxation time  $\tau$  and gives directly the inverse of the rate constant. Since rate laws other than first order do not obey exponential relations, this interpretation of relaxation time is strictly correct for first-order reactions; however, a related concept, that of reaction half-life, can be used more generally. As indicated by the name, reaction half-life specifies the time required for reaction of half the original reactant. This is also a function of the rate constant and is obtained directly from the integrated equations where  $C_A = (1/2)C_{A0}$ , and  $t = t_{1/2}$ . For the cases of the previous section:

$$\begin{aligned} \text{Zero Order: } t_{1/2} &= \frac{C_{A0}}{2k} \\ \text{First Order: } t_{1/2} &= \frac{\ln 2}{k} \\ \text{Second Order (2A} \rightarrow \text{C + D): } t_{1/2} &= \frac{1}{kC_{A0}} \\ \text{Second Order (A + B} \rightarrow \text{C + D): } t_{1/2} &= \frac{1}{k(C_{A0} - C_{B0})} \ln \left[ \frac{(C_{B0})}{(2C_{B0} - C_{A0})} \right] \\ \text{Nonintegral Order: } t_{1/2} &= \frac{[(1/2)^{1-n} - 1](C_{A0})^{1-n}}{(n-1)k} \end{aligned} \quad (1-45)$$

The second of these aspects has to do with whether we wish to write kinetic expressions from the point of view of reactant remaining, as we have done so far, or from the point of view of product produced (reactant reacted). It is convenient in many instances to talk about the conversion in a reaction, which defines the amount of reactant consumed or product made. For constant-volume systems that can be represented in the rate equation as a concentration of material reacted,  $C_x$ ,  $C_A = C_{A0} - C_x$ . For a first-order example, then

$$(dC_A/dt) = d(C_{A0} - C_x)/dt = -k(C_{A0} - C_x)$$

and

$$\ln[1 - (C_x/C_{A0})] = -kt \quad (1-46)$$

corresponding to equations (1-34) and (1-35). The quantity  $(C_x/C_{A0})$  is a fraction varying between zero (no conversion) and unity (complete conversion) for this irreversible reaction and is ordinarily called the *fractional conversion* of reactant  $x$ . This

fractional-conversion definition in terms of concentration ratios applies only for constant-volume reaction systems, so we will define conversion more generally as the ratio of mols reactant remaining to initial mols of reactant. Hence

$$C_A = C_{A0}(1 - x) \quad (1-47)$$

Equation (1-47) is one of the few that should be committed to memory immediately. There are, of course, corresponding definitions of conversion on the basis of mass units, and in some cases fractional conversion to product (mols product made per mol reactant fed or reacted) is a useful measure. The important thing is always to be sure how the term *conversion* is defined. The integrated forms of simple irreversible rate laws written with conversion,  $x$ , from equation (1-47) are:

$$\text{Zero Order: } C_x = kt; \quad x = \frac{kt}{C_{A0}}$$

$$\text{First Order: } \ln\left(1 - \frac{C_x}{C_{A0}}\right) = \ln(1 - x) = -kt$$

$$\text{Second Order (2A} \rightarrow \text{C} + \text{D): } \frac{C_x}{C_{A0}} = x = \frac{ktC_{A0}}{1 + ktC_{A0}}$$

$$\begin{aligned} \text{Second Order (A} + \text{B} \rightarrow \text{C} + \text{D): } \ln \frac{(1 - C_x/C_{A0})}{(1 - C_x/C_{B0})} &= -(C_{B0} - C_{A0})kt \\ &= \ln\left(\frac{1 - x_A}{1 - x_B}\right) \end{aligned}$$

$$\begin{aligned} \text{Nonintegral Order: } \left(1 - \frac{C_x}{C_{A0}}\right)^{1-n} &= 1 + \frac{(n-1)}{C_{A0}^{1-n}} kt \\ &= (1 - x)^{1-n} \end{aligned}$$

An idea related to that of fractional conversion is the *molar extent of reaction*. If we return for a moment to the general irreversible reaction of (I) and replace the arrow with an equality, we can write



so that

$$\sum_I^n (\nu_i)(I) = 0 \quad (1-49)$$

where  $\nu_i$  is the stoichiometric coefficient for the species  $I$ , so defined that  $\nu_i$  is positive for products and negative for reactants. Now let us consider a reaction (not necessarily in a constant-volume system) with an initial number of mols of species  $I$  of  $N_{i,0}$  and mols at time  $t$  of reaction of  $N_i$ . Then the molar extent of reaction will be defined by

$$N_i = N_{i,0} + \nu_i X$$

or

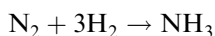
$$X = (N_i - N_{i,0})/(\nu_i) \quad (1-50)$$



A little thought about equation (1-50) will convince one that  $X$  defined in this way has the same value for each species. Thus, given  $N_{i,0}$  and  $X$ , all values of  $N_i$  may be calculated directly. Remember that the molar extent of reaction  $X$  is *not* the same as conversion  $x$ , but it is also a number that is constrained to be between zero and one. The use of  $X$  is particularly convenient in dealing with the mathematics that describe large numbers of reactions occurring simultaneously (see R. Aris, *Introduction to the Analysis of Chemical Reactors*, Prentice-Hall, Inc., Englewood Cliffs, NJ, 1965), and to problems in chemical equilibrium. Since the convention of fractional conversion is still most often encountered, however, we by and large use it in this book.

### Illustration 1.2

The ammonia synthesis reaction



is carried out in a reactor under conditions such that for an initial feed of 6 mols/time hydrogen and 7 mols/time nitrogen, 3 mols/time ammonia are measured coming out. What is a) the fractional conversion and b) the extent of reaction?

#### Solution

a. Fractional conversion: A molal balance according to reaction stoichiometry yields:

$$\text{Mols N}_2 \text{ reacted} = 1.5$$

$$\text{Mols H}_2 \text{ reacted} = 4.5$$

Now we need to specify the basis on which the fractional conversion is reported. For example, if we use mols of  $I$  converted per mol  $I$  fed as the basis, then there are two separate conversion measures, one for  $\text{H}_2$  and one for  $\text{N}_2$ :

$$x(\text{N}_2) = (1.5/7) = 0.214$$

$$x(\text{H}_2) = (4.5/6) = 0.750$$

and for this reaction with unequal mols of feed in the reactant and unequal stoichiometric coefficients there are always two measures of conversion.

b. Extent of reaction; use equation (1-50):

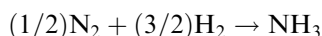
$$\nu(\text{NH}_3) = 2; \quad \nu(\text{N}_2) = -1; \quad \nu(\text{H}_2) = -3$$

$$\text{For NH}_3: \quad X = (3 - 0)/2 = 3/2$$

$$\text{For N}_2: \quad X = [(7)(3)(1/2) - 7]/(-2) = 3/2$$

$$\text{For H}_2: \quad X = [(6)(3)(3/2) - 6]/(-3) = 3/2$$

Obviously  $X$  is the same for any component. Note that if we decided to write the reaction in the stoichiometrically equivalent form



the coefficients would be changed to  $\nu(\text{NH}_3) = 1$ ,  $\nu(\text{H}_2) = (-3/2)$ , and  $\nu(\text{N}_2) = (-1/2)$ . The value of  $X$ , while still the same for all species, would now be 3.



HORATIO SAYS

If the reaction is reversible, what is the limiting value of  $X$  based on the two ways of writing the stoichiometric coefficients?

The *third* aspect of kinetic formulations is how to modify the rate equations when the reaction system volume is not constant. Volume changes can occur when there is a net change in the number of mols as the reaction proceeds. For most reactions that occur in the liquid phase, such changes in volume are small and normally can be neglected. Conversely, in gas-phase reactions the volume/molal relation is governed in the limit by the ideal gas law and volume changes must be taken into account. For the simple reactions we have been discussing, it is possible to write the volume change directly in terms of the amount of reaction in a convenient form using the fractional conversion. First define an expansion (or contraction) factor  $\epsilon$ , which represents the difference in reaction system volume at the completion of the reaction and at the start of the reaction divided by the initial value:

$$\epsilon = (V_{\infty} - V_0)/V_0 \quad (1-51)$$

where  $V_0$  is the initial volume and  $V_{\infty}$  the final volume. The relationship between the amount of reactant consumed and the reaction volume can now be determined from the stoichiometry of the particular reaction. As an example consider the irreversible first-order reaction  $A \rightarrow \nu B$ , where  $\nu$  is some stoichiometric coefficient other than unity and is a positive quantity for products of reaction. When the volume/molal relation is a direct proportionality, as in gas-phase reactions,

$$\epsilon = \nu - 1 \quad (1-52)$$

The number of mols of A at any time is

$$N_A = N_{A0}(1 - x)$$

the volume of the reaction system is

$$V = V_0(1 + \epsilon x) \quad (1-53)$$

and the concentration of reactant is

$$\begin{aligned} C_A &= (N_A/V) = [N_{A0}(1 - x)/V_0(1 + \epsilon x)] \\ &= (C_{A0})[(1 - x)/(1 + \epsilon x)] \end{aligned} \quad (1-54)$$

We can now use these relationships in the basic reaction-rate definition. For the first-order irreversible batch reaction,

$$(1/V)(dN_A/dt) = -k(N_A/V)$$

and on substitution for  $V$  and  $N_A$ ,

$$\frac{N_{A0}}{V_0(1+\epsilon x)} \frac{d(1-x)}{dt} = -k \left( \frac{N_{A0}}{V_0} \right) \frac{1-x}{1+\epsilon x}$$

or

$$\frac{1}{1+\epsilon x} \frac{dx}{dt} = k \frac{(1-x)}{1+\epsilon x} \quad (1-55)$$

To integrate equation (1-55) we must keep in mind that the use of fractional conversions changes the limits of integration:

$$\int_0^x \frac{dx}{1-x} = \int_0^t k dt \quad (1-56)$$

and

$$\ln(1-x) = -kt \quad (1-57)$$

Interestingly, the result obtained here is the same as that for the constant-volume system, equation (1-48), since the expansion factor does not appear. This is a peculiarity of first-order reactions only. (First-order reactions often do not follow the patterns anticipated from the behavior of other-order reactions. Another example is the first-order half-life, which is the only one independent of initial reactant concentration.) Keep in mind also that although fractional conversions are the same in the two systems, the concentrations will be different, as shown in equation (1-54). We can again give a listing, in terms of fractional conversion and expansion factors, of the equations for non-constant-volume systems.

Zero Order:  $C_{A0} \ln(1+\epsilon x) = \epsilon kt$

First Order:  $\ln(1-x) = -kt$

Second Order ( $2A \rightarrow \nu$  products):  $(1+\epsilon)x/(1-x) + \epsilon \ln(1-x) = C_{A0}kt$

Nonintegral Order:  $\int_0^x \frac{(1-\epsilon x)^{n-1}}{(1-x)^n} dx = (C_{A0})^{n-1}kt$

The integral in the last expression above is not a simple form and is best evaluated by numerical means. Use of the expansion factor is limited to reactions where there is a linear relationship between conversion and volume. For reactions that have complex sequences of steps, a linear relationship may not be true. Then we must rewrite the rate definition for a batch reactor:

$$\begin{aligned} r_A &= (1/V)(dN_A/dt) = (1/V)[d(C_A V)/dt] \\ &= (dC_A/dt) + (C_A/V)(dV/dt) \end{aligned} \quad (1-59)$$

and the volume terms must be evaluated from the detailed stoichiometry of the reaction steps.

### 1.4.3 Rates and Conversions for Some Reversible Reactions

The most important forms for reversible reactions are first order, forward and reverse, and second order, forward and reverse. If change in the number of mols occurs and order follows stiochiometry, the reversible reactions can also have forward and reverse steps of different order. Since in the following presentation we treat the reactions as elementary steps, the ratio of rate constants does define the equilibrium constant for the reaction,  $K = k_f/k_r$ .

*First-Order Forward and Reverse.* Here we have  $A \leftrightarrow B$ :

$$\begin{aligned} r_A &= (dC_A/dt) = -k_f C_A + k_r C_B \\ d(1-x)/dt &= -k_f(1-x) + k_r[(C_{B0}/C_{A0}) + x] \end{aligned} \quad (1-60)$$

where  $x$  is the conversion of A.

Equation (1-60) can be integrated to several possible forms; a convenient one is

$$(k_f + k_r)t = \ln[\alpha/(\alpha - x)] \quad (1-61)$$

where

$$\alpha = [k_f - (C_{B0}/C_{A0})k_r]/(k_f + k_r)$$

Sometimes one encounters first-order reversible kinetics treated by a rate equation that is written in terms of concentrations relative to the equilibrium position of the system. If we define  $x_\infty$  as the conversion of A at equilibrium, then

$$(dx/dt) = k'[(1-x) - (1-x_\infty)] \quad (1-62)$$

and

$$\ln[(x_\infty - x)/x_\infty] = -k't \quad (1-63)$$

The rate constant  $k'$  is equal to the sum of the forward and reverse rate constants,  $k_f + k_r$ , and one must exercise care in treating the temperature dependence of  $k'$ , since it does not follow an Arrhenius law. The usefulness of equation (1-63) depends on the availability of data on equilibrium conversion.

*Second-Order Forward and Reverse.* The reaction in this case is  $A + B \leftrightarrow C + D$  and

$$r_A = (dC_A/dt) = -k_f C_A C_B + k_r C_C C_D$$

or

$$\begin{aligned} C_{A0}[d(1-x)/dt] &= -k_f C_{A0}(1-x)(C_{B0} - C_{A0}x) \\ &\quad + k_r(C_{C0} + C_{A0}x)(C_{D0} + C_{A0}x) \end{aligned} \quad (1-64)$$

The right side of equation (1-64) yields a quadratic function that, with some manipulation, can be integrated to the following cumbersome form:

$$\ln \left[ \frac{2\gamma x/(\beta - q^{1/2}) + (1 + C_{A0})}{2\gamma x/(\beta + q^{1/2}) + (1/C_{A0})} \right] = q^{1/2}t \quad (1-65)$$

where

$$\begin{aligned}\gamma &= k_f - 1/K; & q &= \beta^2 - 4\alpha\gamma \\ \beta &= -k_f[C_{A0} + C_{B0} + (C_{C0} + C_{D0})/K] \\ \alpha &= k_f[C_{A0}C_{B0} - (C_{C0}C_{D0}/K)] \\ K &= (k_f/k_r)\end{aligned}$$

Often  $C_{C0}$  and  $C_{D0}$  will be zero (no products in the reaction mixture initially) and the preceding equations above can be simplified somewhat.

*First-Order Forward, Second-Order Reverse.* This scheme is often important in the kinetics of dissociation reactions in solution,  $A \leftrightarrow B + C$ , where volume changes are negligible. In that case

$$\begin{aligned}r_A &= (dC_A/dt) = -k_f C_A + k_r C_B C_C \\ d(1-x)/dt &= k_f(1-x) + C_{A0}k_r x^2\end{aligned}\tag{1-66}$$

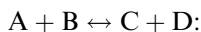
where we have taken  $C_{B0} = C_{C0} = 0$  for simplification. The conversion relationship is

$$2k_r\alpha t = \frac{1 + x(\beta - 1/2)}{1 - x(\beta + 1/2)}\tag{1-67}$$

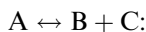
where

$$\begin{aligned}\alpha &= [(k_f/2k_r)^2 + C_{A0}(k_f/k_r)]^{1/2} \\ \beta &= K\alpha\end{aligned}$$

The integrated forms, equations (1-65) and (1-67), are as indicated, awkward to work with and are particularly inconvenient to use in the interpretation of conversion data. If data on the equilibrium conversion,  $x_\infty$ , are available, forms analogous to equation (1-63) may be written. These are, for the case of no products present initially:



$$\ln \left[ \frac{(1/C_{A0})(x_\infty + x) - 2x_\infty x}{(1/C_{A0})(x_\infty - x)} \right] = (2k_f)[(1/x_\infty) - 1]C_{A0}t\tag{1-65a}$$



$$\ln \left[ \frac{(x_\infty - x) + x}{x_\infty - x} \right] = k_f \left[ \frac{(2 - x_\infty)}{x_\infty} \right] t\tag{1-67a}$$

Equation (1-65a) is, in fact, one case of a general class of solutions for reversible reactions in terms of equilibrium conversion. If the right-hand side is written

$$\rho k_f [(1/x_\infty) - 1]C_{A0}t$$

then the following reactions are included:

Reaction	Value of $\rho$
$2A \leftrightarrow B + C$	1
$A + B \leftrightarrow C + D$	2
$2A \leftrightarrow 2B$	2
$A + B \leftrightarrow 2C$	4

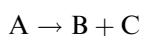
#### 1.4.4 Summary: Simple Reactions

The examples given here provide only an indication of the variety of rate forms and conversion relationships that exist even for simple reactions. Certainly there are many more combinations of reaction order and reversibility that could be included, but the tools for dealing with them have been established here. Some of these additional forms are involved in subsequent exercises and discussion without individual derivation. (See also J.W. Moore and R.G. Pearson, *Kinetics and Mechanism*, 3rd edition, John Wiley and Sons, New York, 1981, and S. W. Benson, *The Foundations of Chemical Kinetics*, McGraw-Hill, New York, 1960).

Although the formulation and integration of simple rate equations is not particularly troublesome, reflection on the nature of nonintegral and higher order (larger than unity) rate laws indicates much more difficult mathematics, since these are nonlinear in the concentration variables. Together with the exponential dependence of rate, the nonlinear concentration dependence of rate in these cases means that even apparently simple reactions may be difficult to analyze within the context of practical operation.

#### Illustration 1.3

An autocatalytic reaction is one in which a product of the reaction acts as a catalyst, so that the forward rate of reaction depends on the concentration of both reactants and products. Consider the reaction:



with rate constant  $k$ , where C acts as a catalyst for the decomposition of A. Derive the appropriate form for the concentration of A as a function of time of reaction in this isothermal, constant-volume reaction system. Under initial conditions the concentration of A is  $C_{A0}$  and that of C is  $C_{C0}$ .

#### Solution

Most autocatalytic reactions occur in liquid solutions where volume changes upon reaction are usually negligible, so the analysis using the constant-volume case here is reasonable. The normal kinetic formulation for this reaction is then

$$-r_A = kC_A C_C \quad \text{where } C_{C0} > 0$$

In terms of mols (for constant volume), let A be mols of reactant at time  $t$ , a be mols of reactant reacted at  $t$ , and  $A_0$  initial mols of reactant. Then

$$A = A_0 - a$$

$$B = B_0 + a$$

$$C = C_0 + a$$

Since the system is constant-volume the concentrations can be replaced by molar amount in the rate equation, and

$$(dA/dt) = -(da/dt) = -k(A_0 - a)(C_0 + a)$$

Upon integration from 0 to  $a$

$$[1/(A_0 + C_0)] \ln[A_0/(C_0 + a)]/[C_0/(A_0 - a)] = kt$$

The following properties of this autocatalytic reaction are also of interest:

At time zero (initially)

$$-r_A = kA_0C_0 \quad (\text{positive and finite})$$

At time  $\infty$  (completion of reaction)

$$-r_A = k(A_0 - A_0)(C_0 + A_0) = 0$$

Thus, the rate must pass through a maximum value at some time between  $0 < t < \infty$ . At the maximum of rate:

$$-(da/dt) = 0 = -k(A_0 - a)(C_0 + a)$$

$$-(d^2a/dt^2) = 0 = -kC_0 + kA_0 - 2ka$$

$$a = (A_0 - C_0)/2 \text{ at the maximum rate.}$$

This can be considered as a kind of fingerprint of autocatalytic reactions in that certain concentration constraints will pertain at the maximum of reaction rate.



HORATIO SAYS

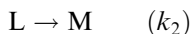
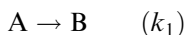
Watch out for autocatalysis in some biochemical reactions. Also, do not confuse product-catalyzed reactions with those requiring an initiator, as discussed later.

## 1.5 Kinetics of “Nearly Complex” Reaction Sequences

The fact that the kinetics of an overall reaction normally represent the net effects of the rates of a number of individual elementary steps means that one of our major concerns in analysis must be how to assemble the individual steps into the whole. There are systematic procedures for doing this, some of which will be discussed in detail for homogeneous reactions that occur by chain mechanisms. However, we have also pointed out that often, in the absence of detailed information, models that account for the essential features of the steps involved in an overall reaction can be of great utility. In this section we shall discuss three such schemes that have found useful application in a wide variety of reaction systems.

These are

*Type I.* Parallel reactions with separate reactants and products:



*Type II.* Parallel reactions with the same reactant:



*Type III.* Series reactions with a stable intermediate:



### 1.5.1 Yield, Selectivity, and Rates

In addition to the rate of consumption of reactant or appearance of product, two further quantities are of importance in the analysis of the kinetics of these schemes: the *yield* and the *selectivity*. These quantities serve to specify the relative importance of the reaction paths that occur and are ordinarily based on some product-to-reactant or product-to-product relationship. Here we shall define yield as the fraction of reactant converted to a particular product, so if more than one product is of interest in a reaction, there can be several yields defined. The yield of product  $j$  with respect to reactant  $i$ ,  $Y_j$ , is

$$Y_j = \frac{\text{mols of } i \rightarrow j}{\text{mols of } i \text{ present initially}}$$

Overall selectivity is defined by the following:

$$\text{Yield} = (\text{overall selectivity}) (\text{reactant conversion}) \quad (1-68)$$

Inserting the definitions for yield and conversion, we obtain

$$S_0 = \text{overall selectivity} = \frac{\text{mols } i \rightarrow j}{\text{mols } i \text{ reacted}}$$

For some types of reaction schemes this overall selectivity is a function of the degree of conversion, so often it is convenient to define in addition a *point* or *differential* selectivity referring to a particular conversion level:

$$S_d = \text{differential selectivity} = \frac{\text{rate of production of } j}{\text{rate of reaction of } i}$$

Application of these definitions to the three reaction sequences mentioned above will result in yield and selectivity values falling in the range from 0 to 1. If the stoichiometric coefficients of  $i$  and  $j$  differ, values outside this range may be obtained. In this case the preceding definitions can be normalized to the 0 to 1 range through multiplication by the ratio of the appropriate coefficients.

One should be careful in using these definitions in comparison with quantities given the same name elsewhere, since there is a considerable variation in the nomenclature found in the literature. Further, the present definitions are dimensionless, whereas yields and selectivities reported in various sources, particularly those



describing specific process results, may have mass or volume dimensions associated (e.g., grams product per liter of reactant).

The Type I, II, and II schemes have been termed “nearly complex” here since they incorporate features of selectivity and yield associated with reactions consisting of a number of elementary steps, but certainly do not approach the level of detail required to describe such systems completely. The analysis of rate, yield, and selectivity in such model systems is important in many chemical reaction engineering problems and is worth separate attention.

*Type I.* For parallel reactions with separate reactants, the analysis is easily handled, since the two steps are independent of each other. Indeed, the inclusion of Type I as a nearly complex scheme is not really necessary for the homogeneous batch reactions at constant volume treated here, since the yield and selectivity definitions are redundant in this case with rate and conversion. The system is important in heterogeneous systems, however, so we introduce it for later reference. For first-order, irreversible reactions:

$$r_A = (dC_A/dt) = -k_1 C_A \quad (1-69)$$

$$r_L = (dC_L/dt) = -k_2 C_L \quad (1-70)$$

$$\ln(C_A/C_{A0}) = -k_1 t \quad (1-71)$$

$$\ln(C_L/C_{L0}) = -k_2 t \quad (1-72)$$

We may define a yield for each of the two reaction paths, but since there is no interaction between the two, the fraction reacted to a particular product is equal to the conversion for each. That is,

$$Y_B(I) = Y_M(I) = x$$

where  $Y_B(I)$  and  $Y_M(I)$  are the yields of B and M, respectively, in the Type I reactions. The differential selectivity is unity for each reaction and the overall selectivity, according to equation (1-68), must be unity. Unfortunately, yet another definition of selectivity creeps into the discussion at this point, since for the Type I system it is possible that the relative rates of the two reactions will be of interest in some applications—particularly for some of the heterogeneous reactions to come. This we might term somewhat awkwardly a *parallel differential selectivity*, which would be given by

$$S_d(I) = -r_A/-r_L = (k_1/k_2)(C_A/C_L) \quad (1-73)$$

The rate constant ratio,  $k_1/k_2$ , appears in equation (1-73), and this is given yet another name, the intrinsic selectivity,  $S_i$ . The relationship between differential and intrinsic selectivity for the Type I system is shown in Figure 1.6. As expected, these are linear in  $S_i$ .

*Type II.* For parallel reactions with the same reactant the selectivity and yield definitions are more meaningful for homogeneous batch reactions. For the reactant the rates are additive, so

$$(dC_A/dt) = -(k_1 + k_2)C_A \quad (1-74)$$

and

$$\ln(C_A/C_{A0}) = -(k_1 + k_2)t \quad (1-75)$$

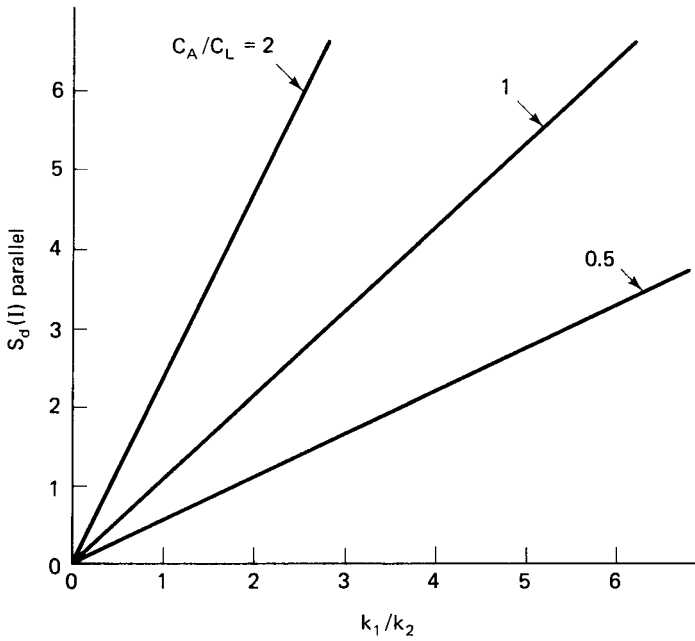


**Figure 1.6** Relationship between differential and intrinsic selectivities for a Type I reaction system.

The yield of product B is

$$\begin{aligned}
 Y_B(\text{II}) &= \frac{\text{reactant A} \rightarrow \text{B}}{\text{initial reactant A}} \\
 &= \frac{k_1}{(k_1 + k_2)} [1 - e^{-(k_1 + k_2)t}]
 \end{aligned} \tag{1-76}$$

From equation (1-68), the overall selectivity is

$$\begin{aligned}
 S_0(\text{II}) &= \frac{\text{yield}}{\text{conversion}} = \frac{(k_1)[1 - e^{-(k_1 + k_2)t}]}{(k_1 + k_2)[1 - e^{-(k_1 + k_2)t}]} \\
 S_0(\text{II}) &= \frac{k_1}{(k_1 + k_2)}
 \end{aligned} \tag{1-77}$$

The differential selectivity\* is given by the rate ratio:

$$\begin{aligned}
 S_d(\text{II}) &= \frac{\text{rate of production of B}}{\text{rate of consumption of A}} = \frac{k_1 C_A}{(k_1 + k_2) C_A} \\
 S_d(\text{II}) &= \frac{k_1}{(k_1 + k_2)}
 \end{aligned} \tag{1-78}$$

which in this case is identical to the overall selectivity.

---

\* Some define differential selectivity as the ratio of a rate of production to a rate of reaction, in which case the denominator is a negative quantity and the corresponding selectivities are negative numbers. Our definition in terms of the rate of consumption of reactant is purely for the convenience of working with positive quantities.

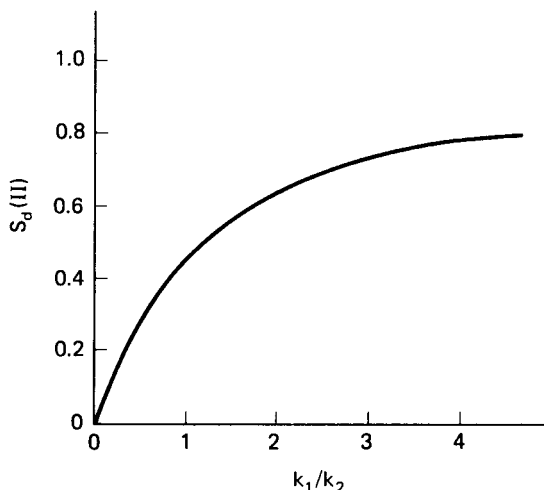


**Figure 1.7** Relationship between differential and intrinsic selectivities for a Type II reaction system.

For Type II, the differential or overall selectivity and intrinsic selectivity are simply related by taking the inverse of equation (1-78) and rearranging:

$$S_i(\text{II}) = \frac{S_d(\text{II})}{1 - S_d(\text{II})} \quad (1-79)$$

This is shown in Figure 1.7. Note that the relationship is independent of concentration (conversion). Similar yield and selectivity terms may be defined for product C.

*Type III.* The sequential reactions of a Type III system are probably the most widely encountered kind of nearly complex reaction model, since in many instances the desired product of a given reaction is able to participate in further reactions that remove it from the system.

For the reactant A we have the same relationships as before:

$$(dC_A/dt) = -k_1 C_A \quad (1-80)$$

$$\ln(C_A/C_{A0}) = -k_1 t \quad (1-81)$$

The net rate of reaction for the intermediate B depends on the concentrations of both A and B:

$$(dC_B/dt) = k_1 C_A - k_2 C_B \quad (1-82)$$

The instantaneous value of  $C_A$  as a function of time of reaction is available from equation (1-81), so substituting in equation (1-82) we have

$$(dC_B/dt) + k_2 C_B = k_1 C_{A0} \exp(-k_1 t) \quad (1-83)$$

For initial conditions  $C_A = C_{A0}$ , as employed in equation (1-81), and  $C_B = C_{B0}$ , the integration of equation (1-83) gives

$$C_B = C_{B0} e^{-k_2 t} + \frac{k_1 C_{A0}}{(k_2 - k_1)} (e^{-k_1 t} - e^{-k_2 t}) \quad (1-84)$$

provided that  $k_1 \neq k_2$ . For the final product C,

$$(dC_C/dt) = k_2 C_B \quad (1-85)$$

which on substitution from equation (1-84) and integration gives

$$C_C = (C_{A0} + C_{C0}) + C_{B0}(1 - e^{-k_1 t}) + \frac{C_{A0}}{(k_2 - k_1)} (k_1 e^{-k_2 t} - k_2 e^{-k_1 t}) \quad (1-86)$$

Since the stoichiometric coefficients are all unity in this example, we also have the material balance constraint for  $C_C$  to help us out:

$$C_C = (C_{A0} + C_{B0} + C_{C0}) - C_A - C_B \quad (1-87)$$

Now the intermediate B is both produced and consumed in the reaction by irreversible steps, so it will exhibit a maximum in concentration at some time after initiation of the reaction. The net rate for B is zero

$$(dC_B/dt) = 0$$

which occurs at the point where the concentrations are in the proportion of the rate constants per equation (1-82):

$$(C_B/C_A) = (k_1/k_2) \quad (\text{at maximum B}) \quad (1-88)$$

The time of reaction,  $t_m$ , at which the maximum of B occurs, and the value of  $C_B$  at that point are

$$t_m = \frac{\ln(k_2/k_1)}{k_1(k_2/k_1 - 1)} \quad (1-89)$$

$$(C_B)_{\max} = (w)[S_i(\text{III})^v - S_i(\text{III})^u] \\ u = -1/[1 - S_i(\text{III})], \quad v = -S_i(\text{III})/[1 - S_i(\text{III})] \quad (1-90)$$

where  $C_{B0} = 0$  and  $S_i(\text{III})$  is the intrinsic selectivity,  $(k_1/k_2)$ . The general behavior of the Type III system is shown in Figures 1.8a and b. Note in particular the "motion" of the intermediate curves in Figure 1.8b as the value of  $(k_2/k_1)$  is changed from a small value, smaller than 1, to 10. If we take  $k_1$  to be fixed here, then the magnitude of maximum intermediate concentration decreases and the time of maximum also decreases as the value of  $k_2$  increases. This trend has significance with regard to the discussion of chain reactions coming up soon.

The yield and selectivity factors are of particular interest in Type III reactions, since they will reflect the maximum of the intermediate. The yield of B for  $C_{B0} = 0$ :

$$Y_B(\text{III}) = \frac{k_1}{(k_2 - k_1)} (e^{-k_1 t} - e^{-k_2 t}) \quad (1-91)$$

and the overall selectivity for B is

$$S_0(\text{III}) = \frac{k_1(e^{-k_1 t} - e^{-k_2 t})}{[(k_2 - k_1)](1 - e^{-k_1 t})} \quad (1-92a)$$

The differential selectivity, defined analogously to that for the Type II reaction is

$$S_d(\text{III}) = 1 - (k_2/k_1)(C_B/C_A) \quad (1-92b)$$

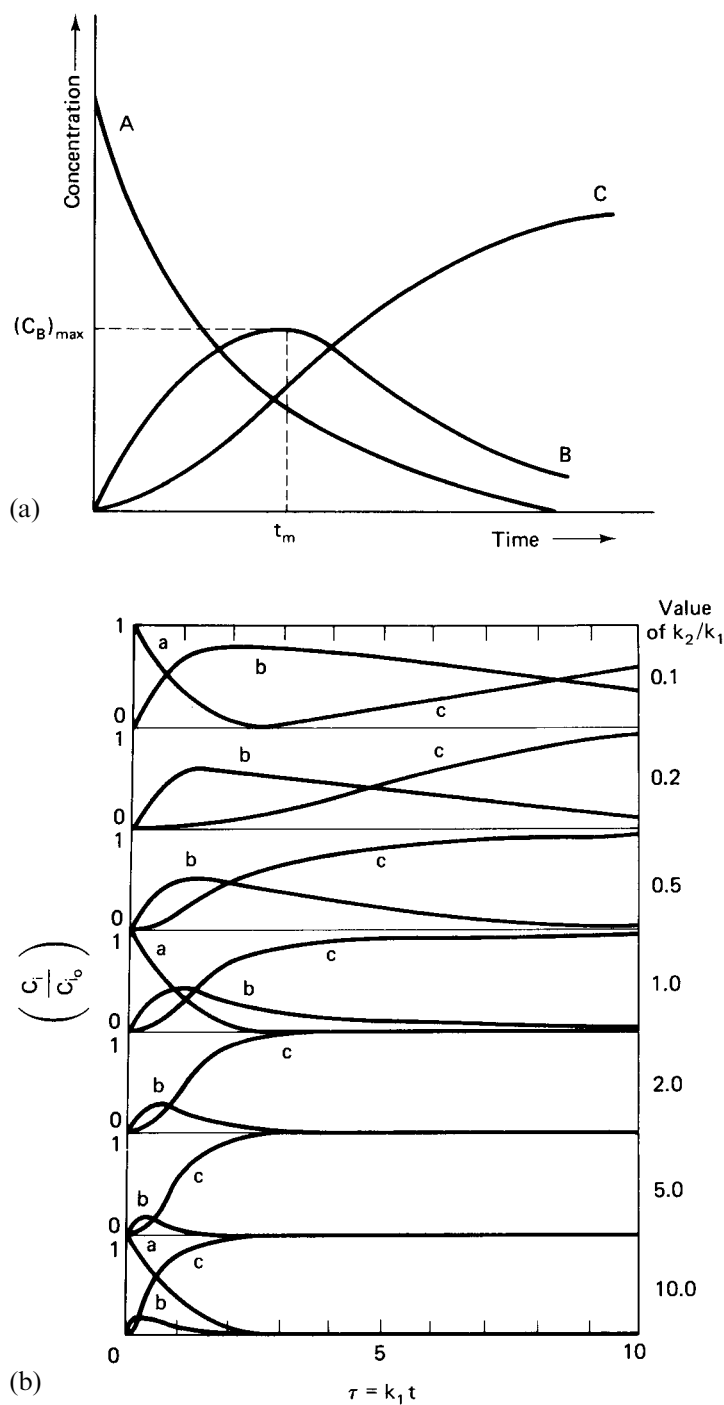


**Figure 1.8** (a) Typical concentration/time history for a Type III constant-volume reaction. (b) Variation of concentration/time behavior with kinetic parameters in a Type III reaction (after R. Aris, *Introduction to the Analysis of Chemical Reactors*, © 1965; reprinted by permission of Prentice-Hall, Inc., Englewood Cliffs, N.J.).

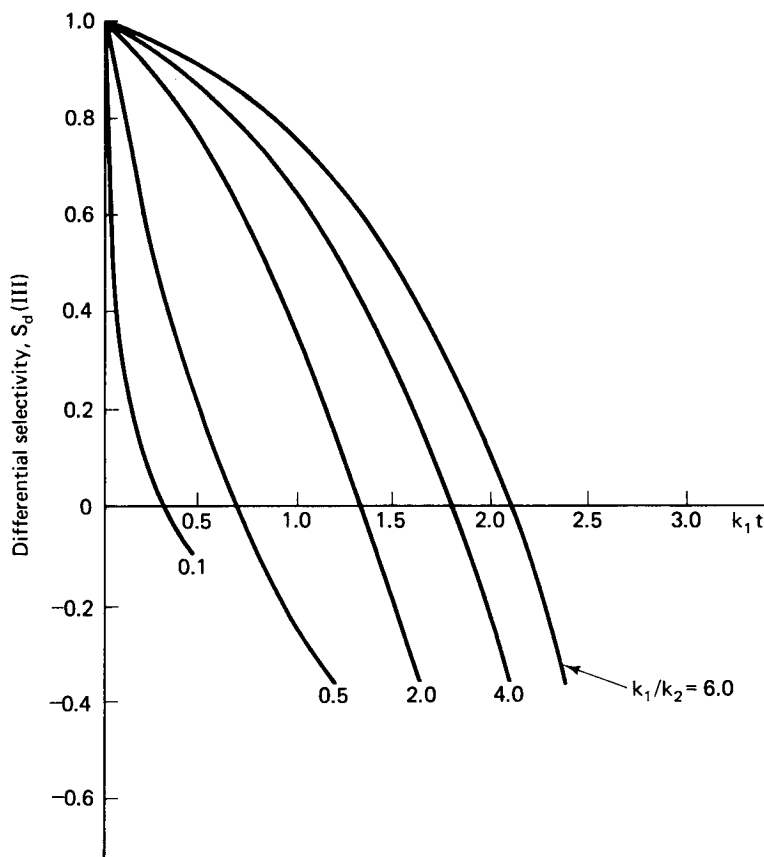


**Figure 1.9** Relationship between differential and intrinsic selectivities for a Type III reaction system.

The differential selectivity/intrinsic selectivity relationship here is shown in Figure 1.9.

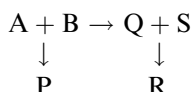
Many reactions of practical interest and importance can be represented by the Type III system; for example the oxidation of hydrocarbons proceeds through an intermediate stage of partial oxidation to the final products carbon dioxide and water. In chemical processing the partially oxidized intermediates are most often those of interest, such as ethylene oxide from the oxidation of ethylene. Thus, the maximization of the yield of B with respect to process operation is an important example of the application of the analysis of these nearly complex sequences.

### 1.5.2 Other Nearly Complex Reactions

Type I, II, and III reactions do not represent all the possible kinds of nearly complex sequences in which we may be interested. Series substitution reactions are often encountered, as in the formation of organic halides. In other instances the apparent kinetics of complicated reactions may be represented by higher-order series reactions somewhat analogous to Type III. Radioactive decay sequences are

represented by an extended Type III sequence involving as many intermediates as unstable isotopes in the sequence. Extensive discussions of a number of these reactions are given in the texts by Benson and Moore and Pearson cited in Section 1.4. Some examples are given in Table 1.2. In addition to the solution for conversion, definitions of selectivity and yield analogous to those discussed can be made for these reactions and will be of similar importance in definition of the relative efficiencies of the various reaction paths.

In addition to the chemical examples of Table 1.2, one further sequence, incorporating features of both series and parallel schemes should be mentioned here:



This is the so-called Denbigh sequence and will be treated further in Illustration 1.8.

**Table 1.2** Some Examples of Other Nearly Complex Reactions

$\left. \begin{array}{l} A \xrightarrow{k_1} C \\ B \xrightarrow{k_2} C \end{array} \right\}$	Radioactive decay to common product	$\begin{cases} C_A = C_{A_0} e^{-k_1 t} \\ C_B = C_{B_0} e^{-k_2 t} \\ C_C = C_{A_0} + C_{B_0} - (C_A + C_B) \end{cases}$
$A \xrightarrow{k_1} B \xrightarrow{k_2} C \xrightarrow{k_3} D \longrightarrow \dots$	Radioactive decay sequence	$C_i = a_{i1} e^{-k_1 t} + a_{i2} e^{-k_2 t} + \dots + a_{ii} e^{-k_i t}$ <p><math>a_{i1}, \dots =</math> constants dependent on initial concentrations</p>
$A \rightleftharpoons B \rightleftharpoons C \dots$	Series reversible reactions	Illustration 1.4
$\left. \begin{array}{l} A + B \rightarrow C + D \\ C + B \rightarrow D + E \end{array} \right\}$	Competitive second-order—series (saponification of esters)	Problem 23
$\left. \begin{array}{l} A + B \rightarrow D + E \\ A + C \rightarrow D + E \end{array} \right\}$	Competitive second-order—parallel (saponification of esters)	J.G. Van der Corput and H.S. Backer, <i>Proc. Acad. Sci. Amsterdam</i> , 41, 1508 (1938)
$\left. \begin{array}{l} A + B \rightarrow C + D \\ C + B \rightarrow E + D \\ E + B \rightarrow F + D \end{array} \right\}$	Series substitution	Problem 21
$\left. \begin{array}{l} A \rightarrow B \\ 2B \rightarrow C \end{array} \right\}$	Higher-order series reactions	J. Chien, <i>J. Amer. Chem. Soc.</i> , 70, 2256 (1948)
$2A \rightarrow B \rightarrow C$	Higher-order series reactions	$\left\{ \begin{array}{l} \text{Problem 22} \\ \text{V.W. Weekman, Jr., and D.M. Nace, } \textit{Amer. Inst. Chem. Eng. J.}, 16, 397 (1970) \end{array} \right.$
$\begin{array}{c} A \\ \swarrow \quad \searrow \\ C \rightleftharpoons B \end{array}$	General series and parallel reactions	J. Wei and C.D. Prater, <i>Amer. Inst. Chem. Eng. J.</i> , 9, 77 (1963)

**Illustration 1.4**

The Type III reaction system discussed consisted of irreversible individual steps; however, a more realistic model for many series reactions might be:



with  $k_1, k_3$  forward, and  $k_2, k_4$  reverse rate constants, respectively. Derive an expression for the concentration of B as a function of time of reaction under isothermal, constant-volume conditions.

*Solution*

The kinetic relationships are:

$$dC_A/dt = -k_1 C_A + k_2 C_B \quad (i)$$

$$dC_B/dt = k_1 C_A - (k_2 + k_3) C_B + k_4 C_C \quad (ii)$$

$$dC_C/dt = k_3 C_B - k_4 C_C \quad (iii)$$

The most convenient approach to obtaining a solution in the time domain for a sequence of reversible rate equations was detailed a long time ago [A. Rakowski, *Z. Physik. Chem.*, 57, 321 (1907)]. Basically, what we do is to work with the second derivative of the first reactant in the sequence

$$(d^2 C_A/dt^2) = -k_1(dC_A/dt) + k_2(dC_B/dt) \quad (iv)$$

The problem is then to express the term  $(dC_B/dt)$  in terms of  $C_A$ . From the material balance

$$C_A + C_B + C_C = C_{A0} \quad (v)$$

where  $C_{B0}$  and  $C_{C0}$  are zero. From (i)

$$C_B = [(dC_A/dt) + k_1 C_A]/(k_2) \quad (vi)$$

Now substitute (vi) and (ii) into (iv):

$$(d^2 C_A/dt^2) = -k_1(dC_A/dt) + k_2[k_1 C_A - (k_2 + k_3)(1/k_2)(dC_A/dt) + k_2 C_A + k_4 C_C]$$

and

$$C_C = C_{A0} - C_A - [(dC_A/dt) + k_1 C_A]/(k_2)$$

After considerable algebra, we can get

$$(d^2 C_A/dt^2) + R(dC_A/dt) + S C_A = k_2 k_4 C_{A0} \quad (vii)$$

where

$$R = k_1 + k_2 + k_3 + k_4$$

$$S = k_2 k_4 + k_1 k_4 + k_1 k_3$$

Following the normal procedure for the solution of second-order equations with constant coefficients, we obtain

$$C_A = C_1 e^{Mt} + C_2 e^{Nt} + k_1 k_4 C_{A0}/S$$



From (vi) we can obtain  $C_B$  after some effort as

$$C_B = (C_1/k_2)(k_1 - M)e^{Mt} + (C_2/k_1)(k_1 - N)e^{Nt} + k_1k_4C_{A0}/S$$

where:

$$M, N = [-R \pm (R^2 - 4S)^{1/2}]/2$$

$$C_1 = [k_1C_{A0} + N(C_{A0} - k_4C_{A0}/S)]/(N - M)$$

$$C_2 = [k_1C_{A0} + M(C_{A0} - k_4C_{A0}/S)]/(M - N)$$



HORATIO SAYS

What other reaction sequences of this sort are there that might have industrial importance?

## 1.6 Kinetics of Complex Reaction Sequences—Chain Reactions

### 1.6.1 Individual Steps and the Pseudo-Steady-State Hypothesis

In our previous discussion of the elementary steps involved in chemical reactions we used the decomposition of diethyl ether as an example of a chain reaction in which a cycle of elementary steps produces the final products. Many reactions are known to occur by chain mechanisms, and in the following discussion we refer primarily to those that generally correspond to the closed sequence in the classification of Boudart. Here active centers (also called *active intermediates* or *chain carriers*) are reacted in one step and regenerated in another in the sequence; however, if we look back to reaction (IV) a closer examination discloses that some of the steps have particular functions. In (IVa) active centers are formed by the initial decomposition of the ether molecule, and in (IVd) they recombine to produce the ether. The overall products of the decomposition,  $C_2H_6$  and  $CH_3CHO$ , however, are formed in the intermediate steps (IVb) and (IVc). In analysis of most chain reactions we can think of the sequence of steps as involving three principal processes:

1. *Initiation reactions*: reactions that provide the source of active intermediates in the chain
2. *Propagation reactions*: reactions that involve the consumption and regeneration of active intermediates and in which stable products are formed
3. *Termination or breaking reactions*: reactions that remove active intermediates from the chain (no regeneration)

The full analysis of the kinetics of a chain reaction such as this ether decomposition would require solution of the rate equations for each of the species involved, subject to material-balance restrictions. Except in special cases this cannot be done

analytically, and it has become customary to employ something called the *pseudo-steady-state hypothesis* (pssh) to simplify the mathematical problems encountered in solving the coupled rate equations for chain mechanisms. A commonly quoted version of this principle holds that since the concentrations of active centers are small, their rates of change are negligible throughout the course of the reaction. This idea gets at what is going on, but is inaccurate because low concentrations do not necessarily imply slow rates—remember, there is a rate constant too. Let us go back to Type III and the map outlined in Figure 1.8b to get a clearer picture of what the situation is. Write the Type III sequence in the form of an embryonic chain reaction as

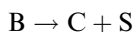
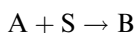


and think of the intermediate B now in the role of a potential chain carrier. Since carriers are very reactive intermediates, then it is likely that  $k_2 \gg k_1$  in this sequence and we proceed far beyond even what is shown at the bottom of Figure 1.8b. The curve for the intermediate B will become, to the naked eye at this scale, nearly flat and merged with the x-axis, in accord with a very low concentration. Indeed, the reaction sequence begins to look like



and the fact that two steps are actually involved is camouflaged by the large value of  $k_2$  with respect to  $k_1$ .

The message of this simple example is to focus attention on the fact that the success of the pssh depends largely on the requirement of a small ratio of active centers (low concentration) to initial reactant. This has been shown by Heineken and coworkers [F.G. Heineken, H.M. Tsuchiya and R. Aris, *Math-Biosciences*, **1**, 95 (1967)], and we can enlarge on our Type III discussion a bit more to show the requirement exactly. Consider then that the overall transformation from A to C is promoted by a catalytic surface, in which B represents a surface intermediate (the chain carrier). Thus



where S is an empty surface ‘site’ and both S and B are active centers. The rates of the elementary steps are

$$r_1 = k_1 C_A C_S \quad (1-93)$$

$$r_2 = k_2 C_B \quad (1-94)$$

and according to the pssh the rates of change of the active centers are zero; for a batch reactor we have

$$(dC_S/dt) = 0 = -k_1 C_A C_S + k_2 C_B \quad (1-95)$$

$$(dC_B/dt) = 0 = k_1 C_A C_S - k_2 C_B \quad (1-96)$$

Consistent with equations (1-95) and (1-96) is the invariance of total active center concentration:

$$C_{S0} = C_B + C_S \quad (1-97)$$

One of the pair (1-95) and (1-96) may be solved together with equation (1-97) to give the pssh concentration of the active center B:

$$C_B = (C_{S0})/[1 - (k_2/k_1)(1/C_A)] \quad (1-98)$$

The rate of formation of product is given by equation (1-94), so on substitution for  $C_B$ :

$$r_2 = (k_2 C_{S0} C_A)/[(k_2/k_1) + C_A] \quad (1-99)$$

Now let us examine this system to see what conditions are necessary to make the pssh valid. Write the rate equations for A and B

$$(dC_A/dt) = -r_1 = -k_1 C_A C_S \quad (1-100)$$

$$(dC_B/dt) = r_1 - r_2 = k_1 C_A C_S - k_2 C_B \quad (1-101)$$

with the initial conditions

$$t = 0, \quad C_A = C_{A0}, \quad C_S = C_{S0}, \quad C_B = 0$$

Now let us define the following dimensionless variables:

$$\begin{aligned} y &= (C_A/C_{A0}), & z &= (C_S/C_{S0}), & \mu &= (C_{S0}/C_{A0}) \\ \tau &= k_1 C_{S0} t, & \lambda &= (k_2/k_1 C_{A0}) \end{aligned} \quad (1-102)$$

When these definitions are substituted into equations (1-100) and (1-101), the following are obtained:

$$(dy/d\tau) = -yz \quad (1-103)$$

$$\mu(dz/d\tau) = -yz + (1 - z)\lambda \quad (1-104)$$

The quantity  $\mu$  is the key to the problem. For  $\mu = 0$  equation (1-104) reduces exactly to the pssh form for  $C_S$ . The success of the pssh requires that the value of  $\mu$  be small, not necessarily that the derivative  $(dz/d\tau)$  approach zero. Such a condition is ensured by maintaining a small ratio of total active centers to the reactant concentration. If a chain reaction is to be efficient, this condition should be approximated in the sense that relatively few active centers would be required to produce many molecules of product in the propagation reactions. Although the analysis here is for a heterogeneous reaction, the same principle applies to homogeneous reactions.

### 1.6.2 General Analysis of Kinetics

We may now apply the pssh to a general treatment of chain reactions. The following development is an adaptation of the excellent analysis originally given by Frost and Pearson (A.A. Frost and R.G. Pearson, *Kinetics and Mechanism*, 2nd ed, John Wiley, New York, 1961, ch. 8). Let us write the three parts of the chain reaction as follows:



In this sequence  $R$  represents the active center, which normally is an atom or radical in homogeneous reactions and a catalytic site in heterogeneous reactions. Other molecules in each step are not shown explicitly, and we let the product of their concentrations with the appropriate rate constants (requiring unit stoichiometric coefficient for  $R$ ) be designated by  $r_i$  for the initiation step,  $r_p$  for the propagation step, and  $r_t$  for the termination step. The rate equation for the active center  $R$  is

$$(dR/dt) = mr_i - Rr_p + Rr_p - 2r_tR^2 \quad (1-105)$$

If the pssh may be applied, equation (1-105) becomes

$$mr_i - 2r_tR^2 = 0 \quad (1-106)$$

$$R = (mr_i/2r_t)^{1/2} \quad (1-107)$$

Now if the formation of product in the chain occurs in the propagation step, the rate of product accumulation is given by

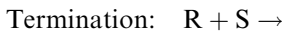
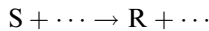
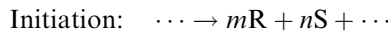
$$\text{propagation rate} = Rr_p = r_p(mr_i/2r_t)^{1/2} \quad (1-108)$$

The rates of other individual steps are:

$$\text{Initiation rate} = r_i$$

$$\text{Termination rate} = r_tR^2 = (mr_i/2)$$

It is convenient in the classification of general schemes such as (IX) to characterize the chain by both the number of active centers involved and the order of the chain termination step. Thus, (XI) would be referred to as a chain with a single active center and second-order termination. The ether decomposition reaction we have discussed is a chain with two active centers and second-order termination, first-order with respect to each of the active centers. In general notation:



$$\text{Initiation rate: } mr_i \text{ for } R \quad (X)$$

$$nr_i \text{ for } S$$

$$\text{Propagation: } Rr_{p1} \text{ for the first step}$$

$$Sr_{p2} \text{ for the second step}$$

$$\text{Termination rate: } RSr_t$$

Here we apply the pssh to both active centers  $R$  and  $S$

$$mr_i - Rr_{p1} + Sr_{p2} - RSr_t = 0 \quad (1-109)$$

$$nr_i + Rr_{p1} - Sr_{p2} - RSr_t = 0 \quad (1-110)$$

These may be solved for R and S and the result substituted into the propagation-rate expression. For the first step we have

$$\begin{aligned} \text{Propagation step 1 rate} &= Rr_{p1} \\ &= \frac{(m-n)}{4} r_i + \sqrt{\left[\frac{(m-n)}{4} r_i\right]^2 + \frac{(m+n)r_i r_{p1} r_{p2}}{2r_t}} \end{aligned} \quad (1-111)$$

This is a cumbersome expression and really of little use as it stands. Once again, however, we may make use of information concerning the relative magnitude of the quantities involved in the rate equations, much in the way that it was possible to verify the pssh. In this instance one looks to the relative magnitudes of the initiation rate,  $r_i$ , and the propagation rate,  $r_p$ . If the chain reaction is an efficient one, which it must be for the reaction to occur via a chain,  $r_i \ll r_p$ . Then all terms that contain only  $r_i$  are negligible compared to the others, and equation (1-111) becomes

$$Rr_{p1} = \sqrt{\frac{(m+n)r_i r_{p1} r_{p2}}{2r_t}} \quad (1-112)$$

The efficiency of a chain mechanism is often discussed in terms of the *chain length*. A number of definitions have been used for chain length, but all give some measure of the number of chain-propagation (product-yielding) steps resulting from a single active center. A reaction with long chain length produces many chain-propagation steps per active center and is correspondingly an efficient one. The analysis used to obtain equation (1-112) from (1-111) is called the *long-chain approximation*. We will define chain length,  $v$ , as the ratio of the rate of a particular propagation reaction to the rate of formation of the chain carriers involved in the propagation step. For the single-chain carrier with a second-order termination reaction, reaction (IX), we obtain

$$v = (r_p)/(2mr_i r_t)^{1/2} \quad (1-113)$$

and for the first propagation step of (X),

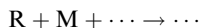
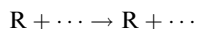
$$\nu_1 = \sqrt{\frac{r_{p1} r_{p2}}{2(m+n)r_i r_t}} \quad (1-114)$$

It is apparent that the analysis developed for the chain mechanisms illustrated in (IX) and (X) may be extended to various other types of chains. In Table 1.3 is given a summary of results for some of the more common types of chain mechanisms, together with examples of reactions that are known to conform to them. The specific propagation rate equations derived for examples A–D in Table 1.3 are special cases of the general proportionality given under E. The order of the chain termination step is important in determining the form of the overall kinetic expression, and in this sense the termination reaction is ultimately more important than the initiation reaction in its influence on the behavior of the chain. The reader may verify the general proportionality given in E for chain length before Horatio asks you to do it.

In summary, what we have done here is to identify the slow reaction steps (or, at least, those steps that are not very fast) and build up the kinetic model from that

**Table 1.3** Kinetics of Some Chain Reaction Mechanisms**A. Single Active Center with First-Order Termination**

Chain:



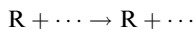
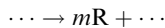
Propagation rate:

$$r_p R = r_o \left( \frac{mr_i}{r_t} \right)$$

Example: First-order termination steps are often associated with extraneous factors, for example, the adsorption of chain carriers on the walls of a reaction vessel.

**B. Single Active Center with Second-Order Termination**

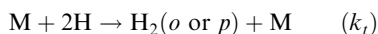
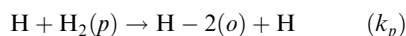
Chain:



Propagation Rate:

$$r_p R = r_o \left( \frac{mr_i}{2r_t} \right)^{1/2}$$

Example: Ortho-Para Hydrogen Conversion

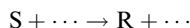
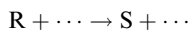


$$R = [H]$$

$$r_p R = k_p \left( \frac{k_i}{k_t} \right)^{1/2} [H_2]^{1/2} [H_2(p)]$$

**C. Two Active Centers with Second-Order Termination**

Chain:

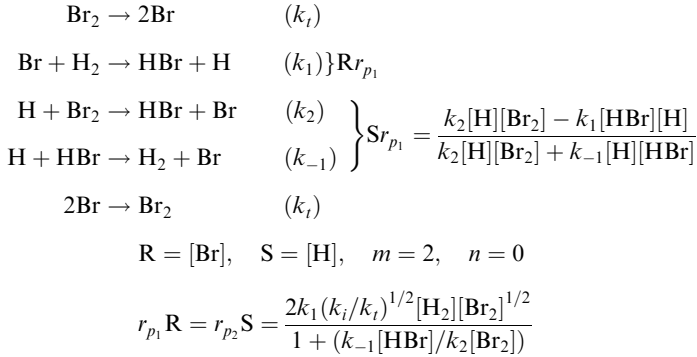


Propagation Rate (Long-Chain Approximation):

$$r_{p1} R = r_{p1} \left[ \frac{(m+n)r_i}{2r_t} \right]^{1/2}$$

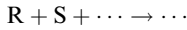
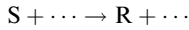
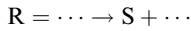
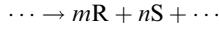
$$r_{p2} S = r_{p1} \left[ \frac{(m+n)r_i}{2r_t} \right]^{1/2}$$

Example:  $\text{H}_2 + \text{Br}_2 \rightleftharpoons 2\text{HBr}$



#### D. Two Active Centers with Second-Order Cross-Termination

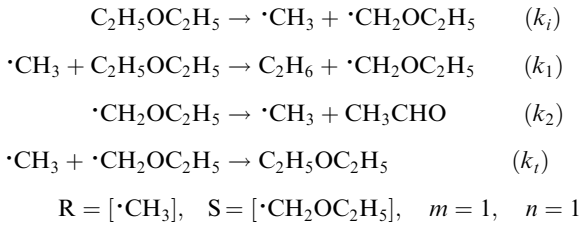
Chain:



Propagation Rate (Long-Chain Approximation):

$$\begin{aligned}
 r_{p_1} R &= \left[ \frac{(m+n)r_i r_{p_1} r_{p_2}}{2r_t} \right]^{1/2} \\
 r_{p_1} S &= \left[ \frac{(m+n)r_i r_{p_1} r_{p_2}}{2r_t} \right]^{1/2}
 \end{aligned}$$

Example:  $\text{C}_2\text{H}_5\text{OC}_2\text{H}_5 \rightarrow \text{C}_2\text{H}_6 + \text{CH}_3\text{CHO}$



$$r_{p_1} R + r_{p_2} S = 2 \left( \frac{k_i k_1 k_2}{k_t} \right)^{1/2} [\text{C}_2\text{H}_5\text{OC}_2\text{H}_5]$$

#### E. Some Generalized Results

$$1. \text{ Rate of propagation} \propto r_p \left( \frac{r_i}{r_t} \right)^{1/w}$$

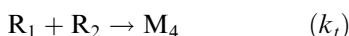
where  $w$  = order of chain termination step with respect to active center

$$2. \text{ Chain length} \propto \left( \frac{r_p}{r_i} \right) \left( \frac{r_i}{r_t} \right)^{1/w}$$

identification as a starting point. We shall do this over and over in the analysis of reaction sequences of all types.

### Illustration 1.5

The thermal decomposition of hydrocarbons in the gas phase occupies an important place both in industrial practice and in the development of the theory of chain reactions. A widely recognized approach to the kinetics of such reactions is that of Rice and Herzfeld [F.O. Rice and K.F. Herzfeld, *J. Am. Chem. Soc.*, **56**, 284 (1934)]. The chain steps proposed for these decompositions are



where the R's are radical chain carriers and the M's stable molecules. Derive an equation for the rate of reaction ( $dM_1/dt$ ).

#### Solution

Use of the pssh for the radical species gives

$$(dR_1/dt) = 0 = k_i M_1 - k_2 R_1 M_1 + k_3 R_2 - k_t R_1 R_2 \quad (i)$$

$$(dR_2/dt) = 0 = k_2 R_1 M_1 - k_3 R_2 - k_t R_1 R_2 \quad (ii)$$

Also, the kinetics of the overall disappearance of  $M_2$  is given by

$$(dM_2/dt) = k_i M_1 + k_2 R_1 M_1 \quad (iii)$$

Simultaneous solution of the two pssh equations gives

$$R_1 = (1/k_2) \{ (k_i/4) \pm [(k_i/4)^2 + (k_i k_2 k_3 / 2k_t)] \}^{1/2} \quad (iv)$$

If the long-chain approximation is valid, this becomes

$$k_2 R_1 = [k_i k_2 k_3 / (2k_t)]^{1/2} \quad (v)$$

and

$$-(dM_1/dt) = [k_i + (k_i k_2 k_3 / 2k_t)^{1/2}] M_1 \quad (vi)$$

Here, in spite of the chain sequence of steps, the reaction is apparent first-order. However, it can be seen that the apparent first-order rate constant is a combination of the rate constants of the individual elementary steps. A comparison of this example with the contents of Table 1.3 shows that the Rice-Herzfeld mechanism corresponds in this case to "Two Active Centers with Second-Order Cross-Termination Chain." The apparent first-order behavior here is a consequence of the particular kinetics of the initiation and termination steps. It is not difficult to show that various combinations of unimolecular or bimolecular initiation with bimolecular or even termolecular termination can result in apparent orders that range from 0 to 2 (M.F.R. Mulcahy, *Gas Kinetics*, John Wiley, New York, 1973, pp. 87-92).





HORATIO SAYS

What would happen in the preceding analysis if the first step were second order in  $M_1$ ? That is  $M_1 + M_1 \rightarrow \dots$ .

It is far safer to know too little than too much. (S. Butler)

### 1.6.2 Efficiency of Chain Mechanisms

The reason why so many chemical reactions proceed by a chain of individual steps involving active centers, rather than occurring directly, must have something to do with the fact that the chain mechanisms are more efficient in promoting the transformation. This efficiency can be translated directly into the energy requirement of the reaction; chain mechanisms (when they occur) have lower energy requirements than alternative direct reactions. Let us take for the moment the activation energy as a measure of the energy requirements of a reaction, and write the generalized rates in terms of their temperature dependence:

$$\begin{aligned} r_i &= (r_i)^\circ \exp(-E_i/RT) \\ r_p &= (r_p)^\circ \exp(-E_p/RT) \\ r_t &= (r_t)^\circ \exp(-E_t/RT) \end{aligned} \quad (1-115)$$

Now substitute these forms into the general expression for propagation rate from  $E$  in Table 1.3:

$$\begin{aligned} \text{Propagation rate} &\propto (r_p)^\circ \exp(-E_p/RT) \{[(r_i)^\circ/(r_t)^\circ] \\ &\quad \times [f(E_i, E_t)]\}^{1/w} \\ f(E_i, E_t) &= \exp[(E_t - E_i)/RT] \end{aligned}$$

and then

$$\text{Propagation rate} \propto \exp\{-[E_p + (1/w)(E_i - E_t)]RT\} \quad (1-116)$$

The apparent activation energy of the overall chain reaction is thus not the same as the activation energy for the propagation step, nor is it a direct function of the activation energy for the initiation step. In fact, the apparent activation energy can be considerably smaller than  $E_i$ , due either to  $E_t > 0$  or second-order termination where  $w = 2$ . For this reason, a chemical transformation may occur by a chain mechanism even if the chain involves an initiation step with higher activation energy than the alternative direct reaction.

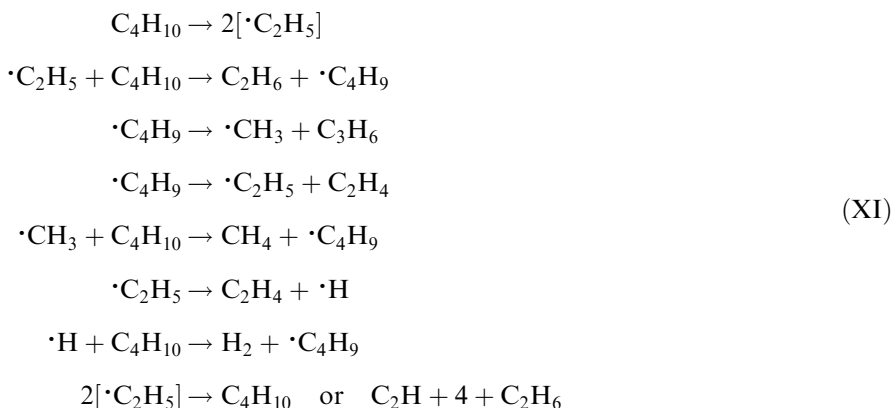
The preceding discussion may shed some light on why chain reactions occur, but the thoughtful reader will doubtless have asked by now how one determines which reactions are involved in a given chain. The answer is not simple, since reproduction of the form of a rate expression determined experimentally cannot

be taken as verification of a proposed chain mechanism ["It was beautiful and simple as all truly great swindles are."—(*O'Henry*)]. It is necessary to examine other plausible reaction steps and to show that their rates are negligibly slow compared to those in the proposed mechanism. This is a complicated task but can be accomplished by careful consideration of the activation energies of alternative reactions, of the bond energies involved in these reactions, and of the concentration levels of the various active centers appearing in the chain. These factors will be considered in detail in Chapter 2.

#### 1.6.4 Some Special Types of Chain Reactions and Their Analysis

Since chain reactions are so common, it would be unreasonable to expect all mechanisms to fit neatly into the four examples of Table 1.3. Illustration 1.5 has already given some further information on thermal decomposition reactions following Rice-Herzfeld mechanisms. Before going on to additional reaction systems, we should add a few comments on the two-active-center reaction illustrated by the combination of hydrogen and bromine in the gas phase. This is probably the first reaction for which a suitable chain sequence was identified. The kinetics of the reaction were carefully studied and reported as early as 1907 [M. Bodenstein and S.C. Lind, *Z. Physik. Chem.*, **57**, 168 (1907)] and the chain reaction interpretation of the reported kinetics, as shown in the tabulation of Table 1.3, was given over a decade later [J.A. Christiansen, *Kgl. Danske Videnskab. Selskab.*, **1**, 14 (1919); K.F. Herzfeld, *Ann. Physik. Chem.*, **59**, 635 (1919); M. Polanyi, *Z. Elektrochem.*, **26**, 50 (1920)]. A thorough discussion of this is given in the text by Frost and Pearson.

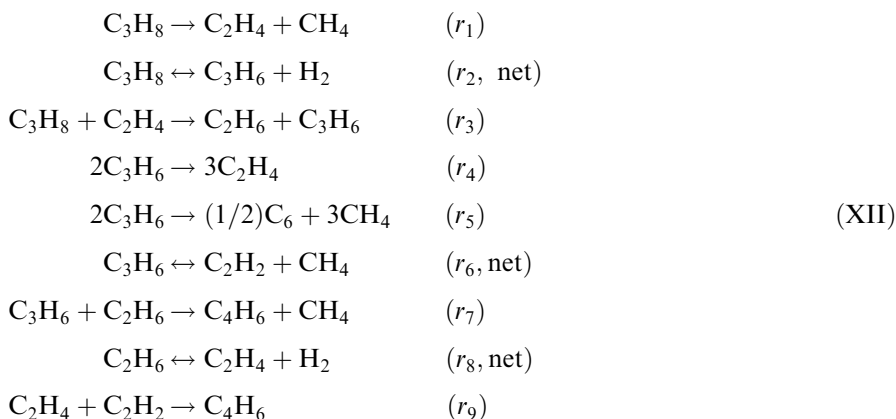
Because of their commercial importance, we still need to do more work on thermal cracking reactions, since their scope and complexity extend considerably beyond the world of Rice-Herzfeld mechanisms. For example, consider the pyrolysis of butane (K.J. Laidler, *Chemical Kinetics*, McGraw-Hill, New York, 1965). This molecule affords the formation of a number of radical chain-carrier species, and the number of elementary steps increases accordingly



It is not hard to envision that for a reaction of this complexity the application of the pssh is liable to rapidly become a labor of algebraic complexity.\* In such an event it

\* For a real introduction to the chamber of horrors of chain reactions, see, for example, E.W. Kaiser, C.K. Westbrook, and W.J. Pitz, *Int. J. Chem. Kinet.*, **18**, 655 (1986).

is probably easier to have recourse to the nearest available computer and solve the set of differential equations numerically. Even this may not be so easy if there are large differences in the magnitudes of the rate constants for the individual elementary steps. In some cases, practically speaking, trying to account for all the detailed elementary steps is not critical. Sundaran and Froment [K.M. Sundaran and G.F. Froment, *Chem. Eng. Sci.*, 32, 601 (1977)] have shown that the use of approximate molecular schemes that include all important products is convenient and often justifiable. They worked with another thermal decomposition reaction, that of propane. A list of reasonable overall reactions producing the observed products is



Here the rate equations are written as if they were for elementary steps (reaction order corresponds to stoichiometry) except for the more complex steps involved in 4 and 5 where first-order is assumed. The equilibrium constants for 2, 6, and 8 can be obtained from tabulated data; thus

$$r_2 = (k_2/K_2)([\text{C}_3\text{H}_8] - [\text{C}_3\text{H}_6][\text{H}_2]) \tag{1-117}$$

and so on. The net rate of reaction of propane and of propylene formation are

$$r(\text{C}_3\text{H}_8) = -(r_1 + r_2 + r_3) \tag{1-118}$$

$$r(\text{C}_3\text{H}_6) = (r_2 + r_3 - 2r_4 - 2r_5 - r_6 - r_7) \tag{1-119}$$

As implied by equations (1-117) to (1-119), no pssh is employed here, rather one uses direct numerical integration of the set. Since it is the stable species, reactant and products, that are of interest in practice, the set of describing equations is much more compact and easier to handle than the full set involving all possible chain carriers. The trick, of course, is deciding which set of molecular equations will give a reasonable approximation to reality. In essence this will depend upon a combination of intuition, observation, and prior experience; there are no general rules.

Another very important class of chain reactions, perhaps the most important from a commercial viewpoint, includes those involved in polymerization. Materials such as polyethylene and polystyrene are formed in chain reactions with free radical chain carriers. These addition polymerization chains are similar in substance to those we have been discussing, but differ in three important respects. *First*, the monomer, particularly when purified, is often quite unreactive and it is necessary to use small quantities of separate substances (initiators) that essentially trick the monomer into

forming a free radical and starting the polymer chain to grow. *Second*, once the growing polymer molecule has developed some size, there is little difference in the rate of addition of another monomer unit to a chain of, say  $N$  or  $(N + 1)$  units, so it is reasonable to assume that the propagation rate constant is the same for all addition steps. *Third*, the growing polymer molecule is its own chain carrier in these addition polymerizations. The termination step, which is typically a combination of two growing polymer units, produces the final product, sometimes called the “dead polymer.” With these points in mind, we can readily write out the chain scheme for addition polymerization:



where  $M_1$  is monomer,  $I$  initiator,  $P_n$  the growing polymer, and  $M_{n+m}$  the polymer product. The rate equations are:

$$d[M_1]/dt = -ar_i - k_p[M_1] \left( \sum_n [P_n] \right) \quad (1-120)$$

$$d[P_1]/dt = r_i - k_p[M_1][P_1] - k_t[P_1] \left( \sum_n [P_n] \right) \quad (1-121)$$

$$d[P_n]/dt = k_p[M_1][P_{n-1}] - k_p[M_1][P_n] - k_t[P_n] \left( \sum_n [P_n] \right) \quad (1-122)$$

where  $r_i$  is the initiation rate of free radical formation. The only ugly surprise in these equations is the appearance of the summation term; however, this can be handled by application of the pssh to the propagation step equations. Upon summation of these pssh balances we obtain

$$0 = r_i - k_t \left( \sum_n [P_n] \right)^2 \quad (1-123)$$

whence

$$\sum_n [P_n] = (r_i/k_t)^{1/2} \quad (1-124)$$

Substituting this result into the rate equation for monomer consumption and making the long-chain approximation ( $ar_i$  is small) yields

$$d[M_1]/dt = -k_p[M_1](r_i/k_t)^{1/2} \quad (1-125)$$

The precise form of the monomer reaction kinetics depends upon the kinetics of the initiation step,  $r_i$ . Here the possibilities are (i) second-order in monomer (thermal), (ii) first-order in monomer and first-order in initiator, and (iii) first-order in initiator

only. For addition reactions in which the first step employs only small concentrations of free radical initiator, the last possibility is the most likely; hence

$$r_i = k_i[\text{I}] \quad (1-126)$$

$$\sum_n [\text{P}_n] = (k_i/k_t)^{1/2} [\text{I}]^{1/2} \quad (1-127)$$

and the monomer rate is

$$d[\text{M}_1]/dt = -k_p(k_i/k_t)^{1/2} [\text{I}]^{1/2} [\text{M}_1] \quad (1-128)$$

It is seen that equation (1-128) also follows the general rule for reaction-propagation rate given in entry E of Table 1.3.

Now in polymerization it is probably not so much the monomer rate, but the product polymer rate and the properties of the product polymer that are of interest. The product polymer rate follows directly from equation (1-123) since, to the extent that the pssh is valid, the initiation and termination rates must be equal. The kinetic analysis also leads to some characterization norms for the product that are useful. The number-average degree of polymerization,  $\bar{P}_n$ , is the average number of monomer units in the polymer product. This is defined in a manner analogous to the chain length definition of equation (1-113) and is

$$\bar{P}_n = \frac{\text{rate of monomer molecules reacted}}{\text{rate of formation of chain carriers}} \quad (1-129)$$

or

$$\bar{P}_n = \frac{k_p[\text{M}_1] \sum_n P_n}{k_i[\text{I}]} = \frac{k_p[\text{M}_1]}{(k_i k_t [\text{I}])^{1/2}} \quad (1-129)$$

Additional parameters of use in description of the product are the number-average chain length and the weight-average chain length. Consider first the number average. For the free radical addition mechanism we can define the probability,  $p$ , of adding another monomer to a growing chain in terms of a simple ratio of rates

$$p = \frac{k_p[\text{M}_1][\text{P}_n]}{k_p[\text{M}_1][\text{P}_n] + k_t[\text{P}_n] \sum_n [\text{P}_n]}$$

which, upon substitution for the summation, is approximated by

$$p \approx 1 - (k_i k_t [\text{I}])^{1/2} / k_p [\text{M}_1] \quad (1-130)$$

The probability of a chain of length  $P$ , number distribution, when random addition occurs is given in terms of the monomer addition probability,  $p$ , as

$$N(P) = (1 - p)(p)^{p-1} \quad (1-131)$$

This is commonly referred to as the Schultz-Flory distribution [P.J. Flory, *J. Am. Chem. Soc.*, 58, 1877 (1936)] and is characteristic of random chain addition

processes.\* Since this is a normalized distribution:

$$\sum_{P=1}^{\infty} N(P) = 1$$

and the number-average chain length is a geometric progression

$$\bar{P}_n = \sum_{P=1}^{\infty} [PN(P)] = \frac{1}{(1-p)} \quad (1-132)$$

From equation (1-130), then, the number average is

$$P_N = k_p[M_1]/(k_i k_t[I])^{1/2} \quad (1-133)$$

which, we note, is identical to the working definition employed in presenting equation (1-129).

The weight-average distribution can also be defined in terms of the probability  $p$ . This is

$$W(P) = (1-p)^2(P)(p)^{P-1} \quad (1-134)$$

with the distribution given as

$$P_W = \sum_{P=1}^{\infty} [PW(P)] \approx \frac{2}{(1-p)} \quad (1-135)$$

Aside from texts on polymer chemistry, additional discussions of these and related topics of interest are given by Froment and Bischoff (G.F. Froment and K.B. Bischoff, *Chemical Reactor Design and Analysis*, John Wiley, New York, 1979) and in a review by Ray [W.H. Ray, *J. Macromolec. Sci., Rev. Macromolec. Chem.*, c8, 1 (1972)].

A final, interesting type of chain mechanism is the branching chain reaction. In this case one of the chain steps (branching) yields two active centers from the reaction of a single center:



The pssh gives for the concentration of R:

$$R = (mr_i)/(r_t - r_b) \quad (1-136)$$

where  $r_b$  is defined for the branching step in the same manner as  $r_i$  and  $r_t$  for initiation and termination. The propagation rate is

$$r_p R = (mr_i r_p)/(r_t - r_b) \quad (1-137)$$

---

\* The same distribution occurs in catalytic synthesis of hydrocarbons from CO and H<sub>2</sub> (Fischer-Tropsch synthesis). There are considerable similarities between polymerization chains and surface reactions.

which has the interesting property of approaching infinity as the magnitudes of  $r_t$  and  $r_b$  become the same. Physically this means an explosion, so  $r_t = r_b$  defines an explosion limit for the branching chain reaction. The branching chain theory has been used to interpret explosions in the low-pressure region for reactions such as  $\text{H}_2\text{--O}_2$  and  $\text{CO--O}_2$ . This sort of explosion is different from the normal thermal explosion in which the heat evolved in a reaction cannot be removed from the system, leading to increasing temperatures, rates of reaction, heat evolution, noise, and a puff of greasy blue smoke.



HORATIO SAYS

After you finish Chapter 3 come back here and show me how the chain-growth polymerization and the Fischer-Tropsch synthesis add up to about the same in terms of product distribution

## 1.7 Chemical Equilibrium

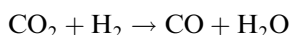
The logical joining point between the study of chemical kinetics and chemical thermodynamics is the point, in an elementary step, where the rate of the forward reaction is equal to the rate of the reverse reaction. This is the point of chemical equilibrium and is implied in the relationships of equations (1-22) and (1-23). While we cannot conduct a short course here on the thermodynamics of chemical equilibrium, some review will be useful. The reader may also wish to refer to a favorite text on thermodynamics for amplification of our condensed presentation.

### 1.7.1 Equilibrium in Single-Phase Systems

The criterion for chemical equilibrium in a single-phase, single-reaction system is stated in terms of the minimization of the free energy of the system. In terms of the reaction, then

$$\sum_i (v_i \bar{G}_i) = 0 \quad (1-138)$$

where  $v_i$  are the stoichiometric coefficients written in the same way as for equation (1-49), positive for products and negative for reactants, and  $\bar{G}_i$  are partial molar free energies. Following Sandler (S.I. Sandler, *Chemical Engineering Thermodynamics*, John Wiley, New York, 1989), let us follow the development for a typical reaction



occurring in a closed system (in the thermodynamic sense) at constant pressure and some suitable temperature. If the pressure is low enough to permit the assumption of

ideal gas behavior, the total free energy of the system is

$$G = \sum_i (N_i \underline{G}_i(T, P) + (RT) \sum_i (N_i) \ln(y_i)) \quad (1-139)$$

where  $N_i$  is the mols of  $i$ ,  $\underline{G}_i$  the free energy per mol, and  $y_i$  the mol fraction of  $i$ . The second term in equation (1-139) is that arising from the free energy of mixing. Using the molar extent of reaction as defined in equation (1-50), we may write for the illustrative reaction

$$X = -(N_{\text{CO}_2} - N_{\text{CO}_{2,0}}) = -(N_{\text{H}_2} - N_{\text{H}_{2,0}})$$

Substituting this into equation (1-139) we get

$$G = (1 - X)(\underline{G}_{\text{CO}_2} + \underline{G}_{\text{H}_2}) + X(\underline{G}_{\text{CO}} + \underline{G}_{\text{H}_2\text{O}}) + 2RT[(1 - X) \ln\langle(1 - X)/2\rangle + X \ln\langle X/2\rangle] \quad (1-140)$$

A plot of  $G$  vs  $X$  according to this equation for  $T = 1000^\circ\text{K}$  and  $P = 1$  atm is given in Figure 1.10. The equilibrium point is identified by  $X^*$  for minimum free energy, or clearly then

$$\left(\frac{\partial G}{\partial X}\right)_{T,P} = 0 \quad (1-141)$$

at equilibrium. Using this result in equation (1-140) gives

$$-\frac{(\underline{G}_{\text{CO}} + \underline{G}_{\text{H}_2\text{O}} - \underline{G}_{\text{CO}_2} - \underline{G}_{\text{H}_2})}{RT} = \ln \left[ \frac{(X^*)^2}{(1 - X^*)^2} \right]$$

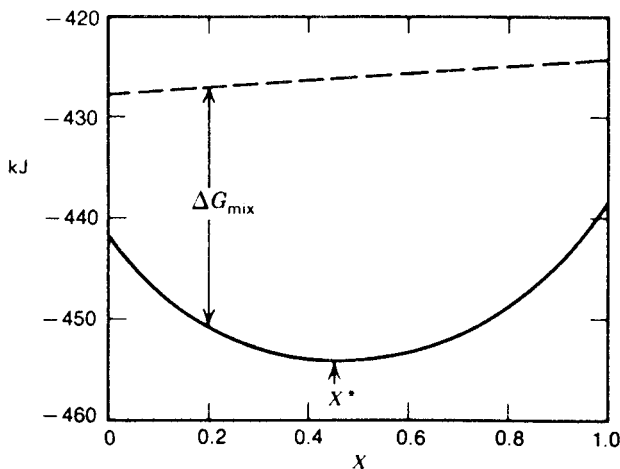


**Figure 1.10** Gibbs free energy for  $\text{CO}_2 + \text{H}_2$  at  $1000^\circ\text{K}$  and 1 atm relative to each atomic species at standard state of  $298^\circ\text{K}$ . [After S.I. Sandler, *Chemical and Engineering Thermodynamics*, reprinted by permission of John Wiley and Sons, New York, NY (1989).]



or, from stoichiometry

$$\frac{-(\underline{G}_{\text{CO}} + \underline{G}_{\text{H}_2\text{O}} - \underline{G}_{\text{CO}_2} - \underline{G}_{\text{H}_2})}{RT} = \ln \left[ \frac{y_{\text{CO}} y_{\text{H}_2\text{O}}}{y_{\text{CO}_2} y_{\text{H}_2}} \right] \quad (1-142)$$

For present purposes we will state without further derivation or proof that this may be generalized to

$$(1/RT) \left[ - \sum_i \nu_i \underline{G}_i \right] = \sum_i \ln(y_i)^{\nu_i} = \ln \left[ \prod_i (y_i)^{\nu_i} \right] \quad (1-143)$$

For nonideal gas mixtures describable by a fugacity function (ex equation of state or the principle of corresponding states):

$$(1/RT) \left[ - \sum_i (\nu_i \underline{G}_i) \right] = \ln \left[ \prod_i [x_i(\bar{f}_i/x_i P)/(f/P)_i]^{\nu_i} \right] \quad (1-144)$$

where  $\bar{f}_i$  is the fugacity of species  $i$  in the mixture,  $f$  is the pure component fugacity, and  $x_i$  the mol fraction. For liquid mixtures that can be described by an activity coefficient model

$$(1/RT) \left[ - \sum_i (\nu_i \underline{G}_i) \right] = \ln \left[ \prod_i (x_i \gamma_i)^{\nu_i} \right] \quad (1-145)$$

where  $\gamma_i$  is the activity coefficient of species  $i$ .

Now these expressions clearly define the composition-free energy relationships required to ensure adherence to the general equilibrium relationship of equation (1-138) and are useful for calculations if we know quantities such as  $\underline{G}_i$ ,  $\gamma_i$  or  $\bar{f}_i$ . However they are still somewhat far removed from the number that is normally of primary interest to us, which is the equilibrium constant. To get to this point in a practically useful way, we can define a reference or *standard state* for each species to define the partial molar free energy at a reference mol fraction,  $x_i^\circ$ , the temperature of interest,  $T$ , and a pressure of 1 atm. Following through with a little bit of thermodynamics, here is the following sequence of equations along the road to an equilibrium constant:

$$G_i(T, P, x_i) = G_i^\circ(T, P = 1, x_i^\circ) + (RT) \ln(a_i) \quad (1-146)$$

with  $a_i$  the activity of species  $i$  defined as

$$a_i = \left[ \frac{\bar{f}_i(T, P, x_i)}{\bar{f}_i^\circ(T, P = 1, x_i^\circ)} \right] \quad (1-147)$$

and equation (1-138) becomes

$$0 = \sum_i (\nu_i \bar{G}_i) = \sum_i \nu_i \bar{G}_i(T, P = 1, x_i^\circ) + (RT) \sum_i \nu_i (\ln a_i)$$

or

$$0 = \Delta G^\circ(rxn) + (RT) \sum_i \nu_i (\ln a_i) \quad (1-148)$$

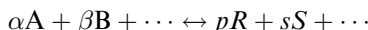
Obviously the operating variable above is  $a_i$  (we shall worry about  $\Delta G^\circ$  later). For engineering calculations this can be defined for several situations of interest as shown

in Table 1.4. What does one need to calculate  $a_i$  in a given situation? This is the practical question, and it is seen that as long as severe deviations from ideality are not encountered (normally this means that high pressures are not involved), the determination of  $a_i$  is not particularly difficult. For gas mixtures we have the familiar ideal gas result for partial pressure. In liquid mixtures it will generally be necessary to have a solution model or experimental data to determine values of the activity coefficient.

We can define the equilibrium constant,  $K_a$ , directly as

$$K_a = \exp[-\Delta G^\circ(\text{rxn})/RT] \quad (1-149)$$

Thus, for a reaction such as



$$K_a = [(a_R)^p (a_S)^s / (a_A)^\alpha (a_B)^\beta] \quad (1-150)$$

If we take the standard state of each component to be 25°C and 1 atm, then

$$\Delta G^\circ(\text{rxn}, 25^\circ\text{C}) = \sum_i [\nu_i (\Delta G_{f,i})^\circ(25^\circ\text{C})]$$

where  $(\Delta G_{f,i})^\circ(25^\circ\text{C})$  is the molar free energy of formation of  $i$  at 25°C. Extensive tabulations of values of  $(\Delta G_f)^\circ$  are to be found in handbooks and in most thermodynamic texts.

To compute  $K_a$  at any temperature given a value for  $(\Delta G_f)^\circ(25^\circ\text{C})$ , we make use of the van't Hoff equation:

$$\left( \frac{\partial \ln K_a}{\partial T} \right)_P = \frac{\Delta H^\circ(\text{rxn}, T)}{RT^2}$$

**Table 1.4** Activity of Species Based on Different Standard State Activities of Low and Moderate Pressures

State ( $T, P$ )	Standard State ( $T, P = 1 \text{ atm}$ )	Species Activity
1) Pure gas	$\bar{G}_i^\circ = G_i^v(T, 1 \text{ atm})$ pure gas	$a_i = P/(1 \text{ atm})$
2) Species in gas mixture	$\bar{G}_i^\circ = G_i^v(T, 1 \text{ atm})$ pure gas	$a_i = y_i P/(1 \text{ atm})$ $= P_i/(1 \text{ atm})$
3) Pure liquid	$\bar{G}_i^\circ = G_i^L(T, 1 \text{ atm})$ pure liquid	$a_i = 1$
4) Species in liquid mixture	$\bar{G}_i^\circ = G_i^L(T, 1 \text{ atm})$ pure liquid	$a_i = x_i \gamma_i$ $(\gamma_i, x_i \rightarrow 1)$
5) Pure solid	$\bar{G}_i^\circ = G_i^s(T, 1 \text{ atm})$	$a_i = 1$
6) Species in solid mixture	$\bar{G}_i^\circ = G_i^s(T, 1 \text{ atm})$	$a_i = 1$

$\bar{G}_i^\circ$  = partial molar standard state free energy

$G_i$  = free energy per mol

$\gamma_i$  = activity coefficient for species  $i$

$y_i, x_i$  = gas and liquid mol fractions, respectively

After S.I. Sandler, *Chemical and Engineering Thermodynamics*, reprinted by permission of John Wiley and Sons, New York, NY

where  $\Delta H^\circ(rxn, T)$  is the heat of reaction for each species in its standard state at the reaction temperature

$$\Delta H^\circ(rxn, T) = \sum_i [\nu_i (\Delta H_{f,i})^\circ(T)] \quad (1-152)$$

Heats of formation are also normally available in handbook or text references, tabulated for a reference of 25°C. To account for the effect of changes in reaction temperature recall that

$$\Delta H^\circ(rxn, T) = \Delta H^\circ(rxn, 25^\circ\text{C}) + \int_{25}^T (\Delta C_p)^\circ(T) dT \quad (1-153)$$

where

$$\Delta(C_p)^\circ = \sum_i [\nu_i (C_{p,i})^\circ]$$

All of this begins to seem a little discouraging because successive definitions depend upon each other and one appears to be only burrowing further and further down into more data required and computations needed. Take heart, however, since some simplification is often possible. Integrating equation (1-151) between any two temperatures  $T_1$  and  $T_2$  gives

$$\ln \left[ \frac{K_a(T_2)}{K_a(T_1)} \right] = \int_{T_1}^{T_2} \Delta H^\circ(rxn, T) (dT/RT^2) \quad (1-154)$$

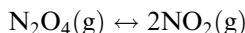
Now, if  $\Delta H^\circ(rxn)$  is temperature-independent, or nearly so, a number of problems evaporate and we have

$$\ln \left[ \frac{K_a(T_2)}{K_a(T_1)} \right] = -\frac{\Delta H^\circ(rxn)}{R} (1/T_2 - 1/T_1) \quad (1-155)$$

In fact, this is often the case, so equation (1-155) is an important working relationship in many situations associated with chemical equilibrium. In the more general case where  $\Delta H^\circ(rxn)$  is a function of temperature the thermal dependence of heat capacity must be stated explicitly. Often this is done in terms of a power series in temperature, the details of which (together with tabulations) are given in standard thermodynamics texts following the guide of equation (1-153).

### Illustration 1.6

Consider the decomposition of nitrogen tetroxide



- 1) Calculate the extent of decomposition at equilibrium at 25°C and 1 atm.
- 2) Determine the equilibrium extent of reaction over the temperature range 200–400° K at pressures of 0.1, 1.0 and 10.0 atmospheres.

#### Solution

1) First we have to look up the equilibrium relationship, equation (1-149), which in this case pertains to  $T = 25^\circ\text{C}$ . Then, from equation (1-150) we have

$$K_a = [a(\text{NO}_2)]^2/[a(\text{N}_2\text{O}_4)] = [y(\text{NO}_2)]^2/[y(\text{N}_2\text{O}_4)]$$

From a tabulation of free energies of formation we can calculate that

$$\begin{aligned}\Delta G^\circ(\text{rxn}, 25^\circ\text{C}, 1 \text{ atm}) &= 2\Delta G_f^\circ(\text{NO}_2) - \Delta G_f^\circ(\text{N}_2\text{O}_4) \\ &= (2)(12.26) - 23.41 = 1.11 \text{ kcal/mol} = 4644 \text{ J/mol}\end{aligned}$$

Then

$$K_a = \exp[-(4644 \text{ J/mol})/(8.314 \text{ J/mol}\cdot\text{K})(298.15^\circ\text{K})]$$

Note that the  $\Delta G^\circ$  calculated is a positive quantity. As a first estimate this will always mean that  $K_a$  is small and the corresponding equilibrium conversion will not be very large. In light of this let us look a little further into this question.

Write the material balances according to stoichiometry in terms of the extent of reaction variable,  $X$ . This gives us the following tabulation:

Initial	Mols Final	Mol fraction (Equilibrium)
$\text{N}_2\text{O}_4 = 1$	$(1 - X)$	$(1 - X)/(1 + X)$
$\text{NO}_2 = 0$	$2X/(1 - X)$	$2X/(1 + X)$
Total	$(1 + X)$	

Then the equilibrium constant is

$$K_a = 0.154 = \{[2X/(1 - X)]^2/[(1 - X)/(1 + X)]\}$$

so that

$$X = [K_a/(4 + K_a)] = 0.192$$

This gives the following for equilibrium mol fractions:

$$[y(\text{N}_2\text{O}_4)]_{\text{eq}} = 0.68$$

$$[y(\text{NO}_2)]_{\text{eq}} = 0.32$$

so the nitrogen tetroxide is about 19.2% decomposed under these conditions.

2) In order to solve this more complicated problem we will need to obtain thermal data from one of the tabulations mentioned before. Then we may calculate

$$\begin{aligned}\Delta H^\circ(\text{rxn}, 25^\circ\text{C}) &= (2)(7.96) - 2.33 \\ &= 13.7 \text{ kcal/mol} = 57,280 \text{ J/mol}\end{aligned}$$

and

$$\Delta C_p(T) = (2)[C_p(T, \text{NO}_2)] - [C_p(T, \text{N}_2\text{O}_4)]$$

Following equation (1-153) we eventually obtain

$$\begin{aligned}\Delta H^\circ(\text{rxn}, T) &= 56,271 - (12.80)T - (3.62 \times 10^{-2})T^2 \\ &\quad + (1.44 \times 10^{-5})T^3 + (3.93 \times 10^{-9})T^4\end{aligned}$$

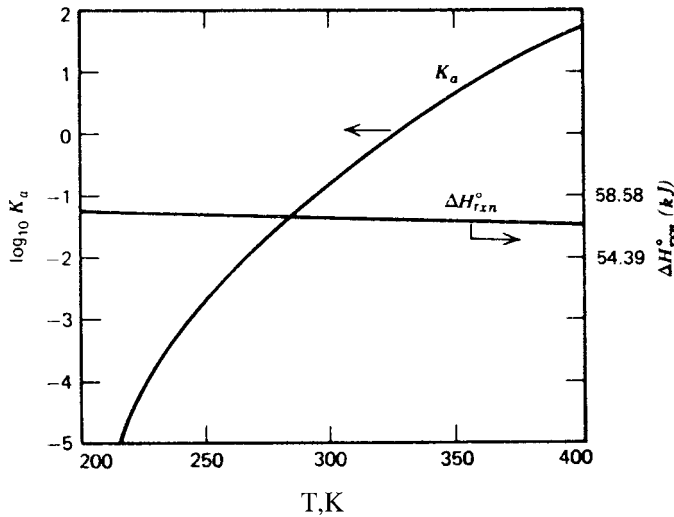


**Figure 1.11** Standard heat of reaction and equilibrium constant for nitrogen tetroxide decomposition. [After S.I. Sandler, *Chemical and Engineering Thermodynamics*, reprinted by permission of John Wiley and Sons, New York, NY (1989).]

This eventually, after integration of equation (1-151) gives the results shown in Figure 1.11. If the gas phase is ideal (still at relatively low pressure) then

$$K_a = \frac{[a(\text{NO}_2)]^2}{[a(\text{N}_2\text{O}_4)]} \\ = \frac{[y(\text{NO}_2)]^2}{[y(\text{N}_2\text{O}_4)]}, \quad [(P)/(1 \text{ atm})]$$

Substituting the extent of conversion relationship:

$$K_a = [(4X)^2/(1 - X^2)], \quad [(P)/(1 \text{ atm})]$$

or

$$X = [(K_a/P)/(1 + K_a/P)] \quad \text{for } P \text{ in atm}$$

The resulting extent of reaction and mol fraction of  $\text{NO}_2$  as a function of temperature are given in Figure 1.12. Also shown are results calculated in like manner for  $P = 0.1$  and 10 atm. These are displayed as characteristic S-shaped curves that tend to flatten out at higher pressure. Indeed, for the temperature range ca. 325–375°K at 10 atm the relationship is essentially linear.

There are a number of equilibrium constants, more easily measured than  $K_a$ , that are often met. First of these is the concentration equilibrium constant

$$K_c = \prod_i (C_i)^{v_i} \quad (1-156)$$

the mol fraction ratio

$$K_x = \prod_i (x_i)^{v_i} \quad (1-157)$$

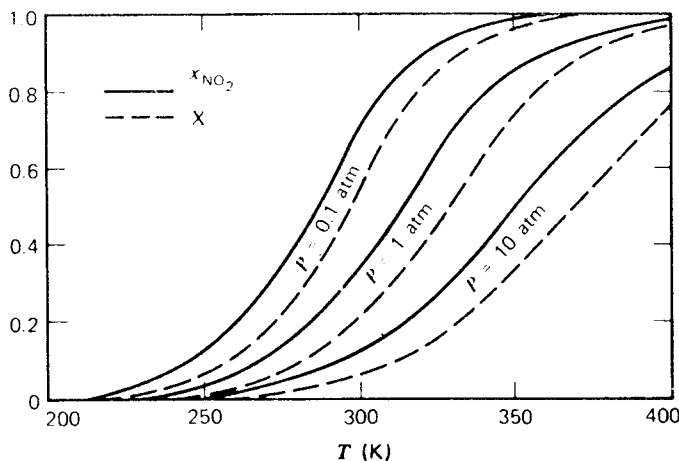


**Figure 1.12** Equilibrium mol fraction and extent of reaction for nitrogen tetroxide decomposition as a function of temperature and pressure. [After S.I. Sandler, *Chemical and Engineering Thermodynamics*, reprinted by permission of John Wiley and Sons, New York, NY (1989).]

or the partial pressure equilibrium ratio

$$K_p = \prod_i (P_i)^{v_i} \quad (1-158)$$

Table 1.5 gives some relationships among these quantities that will be useful in practical calculations. Finally, one may encounter somewhat less frequently the related constants  $K_V$  and  $K_\gamma$ , defined as

$$K_V = \prod_i (f_i/P)^{v_i} \quad (1-159)$$

$$K_\gamma = \prod_i (\gamma_i)^{v_i} \quad (1-160)$$

where the individual component fugacity,  $f_i$ , is often approximated by the Lewis–Randall rule

$$f_i = x_i f$$

### 1.7.2 Multiple Chemical Reactions

The equilibrium relations in a situation where there are  $M$  independent chemical reactions are written compactly as

$$K_{a,j} = \prod_{i=1}^R (a_i)^{\nu_{i,j}}; \quad j = 1, 2, \dots, M \quad (1-161)$$

with the accompanying stoichiometric relationships for the  $R$  components as follows

$$N_i = N_{i,0} + \sum_{j=1}^M (\nu_{i,j} X_j); \quad i = 1, 2, \dots, R \quad (1-162)$$

where  $X_j$  is the extent of reaction for the  $j$ th component.

**Table 1.5** Some Relationships Among Chemical Equilibrium Constants**Gaseous Mixture at Moderate or High Density***Standard state:* Pure gases at  $P = 1$  atm

$$K_a = \prod_i a_i^{\nu_i} = \prod_i \left[ \frac{y_i P \left( \frac{\bar{f}_i}{y_i P} \right)}{1 \text{ atm}} \right]^{\nu_i} = \prod_i \left[ \frac{P_i \left( \frac{\bar{f}_i}{y_i P} \right)}{1 \text{ atm}} \right]^{\nu_i}$$

$$= (1 \text{ atm})^{-\sum \nu_i} K_p K_\nu = \left( \frac{P}{1 \text{ atm}} \right)^{+\sum \nu_i} K_y K_\nu$$

**Gaseous Mixture at Low Density***Standard state:* State of unit activity

$$\left( \frac{f}{P} \right) \cong 1 \quad K_\nu \cong 1$$

and

$$K_a = (1 \text{ atm})^{-\sum \nu_i} K_p = \left( \frac{P}{1 \text{ atm}} \right)^{\sum \nu_i} K_y$$

**Liquid Mixture***Standard state:* State of unit activity\*

$$K_a = \prod_i a_i^{\nu_i} = \prod_i (x_i \gamma_i)^{\nu_i} = K_x K_\gamma$$

Using

$$x_i = C_i / C$$

where  $C_i$  is the molar concentration of species  $i$ , and  $C$  is the total molar concentration of the mixture, we have

$$K_a = \prod_i (x_i \gamma_i)^{\nu_i} = \prod_i \left( \frac{C_i}{C} \gamma_i \right)^{\nu_i} = C^{-\sum \nu_i} K_c K_\gamma$$

For an ideal mixture  $\gamma_i = 1$ , and

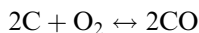
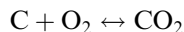
$$K_a = C^{-\sum \nu_i} K_c$$

\*The expressions here have been written assuming that the standard state of each component is the pure component state. Analogous expressions can be written using either of the Henry's law standard states for each component or, more generally, for the case in which the standard state of some species in the reaction is the pure component state and for others it is the infinite dilution or ideal 1 molal states.

*Source:* From S.I. Sandler, *Chemical and Engineering Thermodynamics*, reprinted by permission of John Wiley and Sons, New York, NY (1989).

Perhaps the key word in the above is “independent”, since the equilibrium analysis need consider only the independent reactions among the species involved, not all that can be written out on a piece of paper. (Note also that other simplifications are also often possible in a multiple reaction scheme, such as steps with very small equilibrium constants, or equilibrium constants that are small in comparison to those for other steps. “Comparisons are odious.”—*Christopher Marlowe*). An example will be useful here. Let us consider the following possible

reactions between carbon and oxygen:



Now, if we add the second and third we get twice the first, so not all three reactions are independent. This evaluation by inspection is easy to do if the number of reaction steps is limited, but what wisdom would guide us if the number of reactions becomes large? A simple procedure for systemization of this has been given by Denbigh [K. Denbigh, *Principles of Chemical Equilibrium*, 4th ed., Cambridge University Press, Cambridge, U.K., (1981)]. In this approach we first write out stoichiometric equations for the formation of all molecular species from their constituent atoms. This will ordinarily produce at least one equation containing an atomic species not actually present in the reaction set under consideration. This is then used to eliminate that species from the other equations, reducing the total set by one. The exercise is then repeated until all of the extraneous atomic species have been eliminated, at which point those relationships remaining form the desired independent set. A detailed application of this procedure is given in the following illustration.

### Illustration 1.7

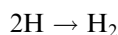
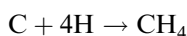
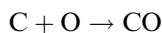
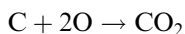
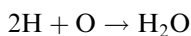
1) Determine the expressions needed to calculate the equilibrium in the reactions between steam and carbon given below:



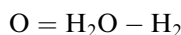
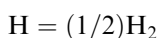
2) Calculate the equilibrium mol fractions as a function of temperature of reaction below 2000°K.

#### Solution

1) To start, we apply Denbigh's method by writing the following reaction steps



Since neither atomic O or H are present in the sequence of reactions (1)–(5), these may be eliminated as





Thus



are the independent reactions that need to be considered. The equilibrium expressions required are

$$K_{a,1} = [a(\text{CO}_2)][a(\text{H}_2)]^2/[a(\text{C})][a(\text{H}_2\text{O})]^2$$

$$K_{a,2} = [a(\text{CO})][a(\text{H}_2)]/[a(\text{C})][a(\text{H}_2\text{O})]$$

$$K_{a,3} = [a(\text{CH}_4)]/[a(\text{C})][a(\text{H}_2)]^2$$

2) The equilibrium constants above can be calculated from heat/free energy of formation data based on the pure component standard states at  $P = 1$  atm and the temperature of interest. These results are shown in Figure 1.13. As in Illustration 1.6, we make a table for the extent of reaction based on one mol of steam for the gaseous species. This gives the following set of coupled nonlinear

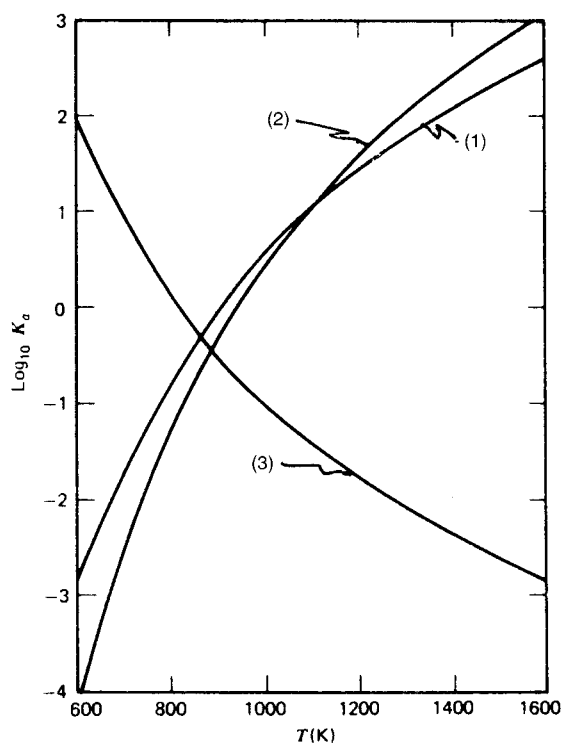


**Figure 1.13** Equilibrium constants for the reaction between steam and carbon.

	Number of moles in the gas phase		Equilibrium mole fraction
	Initial	Final	
H <sub>2</sub> O	1	$1 - 2X_1 - X_2$	$(1 - 2X_1 - X_2)/\Sigma$
CO <sub>2</sub>	0	$X_1$	$X_1/\Sigma$
CO	0	$X_2$	$X_2/\Sigma$
H <sub>2</sub>	0	$2X_1 + X_2 - 2X_3$	$(2X_1 + X_2 - 2X_3)/\Sigma$
CH <sub>4</sub>	0	$X_3$	$X_3/\Sigma$
Total	1	$\Sigma = 1 + X_1 + X_2 - X_3$	

equations to be solved

$$K_{a,1} = \frac{X_1(2X_1 + X_2 - 2X_3)^2}{(1 - 2X_1 - X_2)^2(1 + X_1 + X_2 - X_3)}$$

$$K_{a,2} = \frac{X_2(2X_1 + X_2 - 2X_3)}{(1 - 2X_1 - X_2)(1 + X_1 + X_2 - X_3)}$$

$$K_{a,3} = \frac{X_3(1 + X_1 + X_2 - X_3)}{(2X_1 + X_2 - 2X_3)^2}$$

This set requires a numerical solution that itself is not without pitfalls, since there are multiple values of  $X$  that satisfy the arithmetic requirements. We can add a little common sense chemistry to help out, though, since

$$2X_1 + X_2 \leq 1$$

This expression arises from the fact that no more steam can be used than is supplied (recall the basis for the calculation of one mol of steam). Using similar reasoning

$$0 \leq 2X_3$$

$$2X_3 \leq 2X_1 + X_2$$

because no more hydrogen can be used than is produced. Examination of the range of solutions for  $X$  in view of these inequalities allows the selection of reasonable values. The extent of conversion is, of course, readily translated into the corresponding equilibrium mol fractions for the individual components using the relations presented in the table. The final solution to the problem is shown in Figure 1.14. An interesting characteristic of the results is the invariance (and equality) of H<sub>2</sub> and CO mol fractions above about 1200°K. Note that, in addition to changes in the extent of reaction, the product distribution at equilibrium changes markedly over the range of temperatures, with CO<sub>2</sub> and CH<sub>4</sub> the major products at lower temperatures, and CO and H<sub>2</sub> predominating at higher temperatures. The total yield of any individual product will be given by the product (equilibrium conversion) (equilibrium mol fraction).

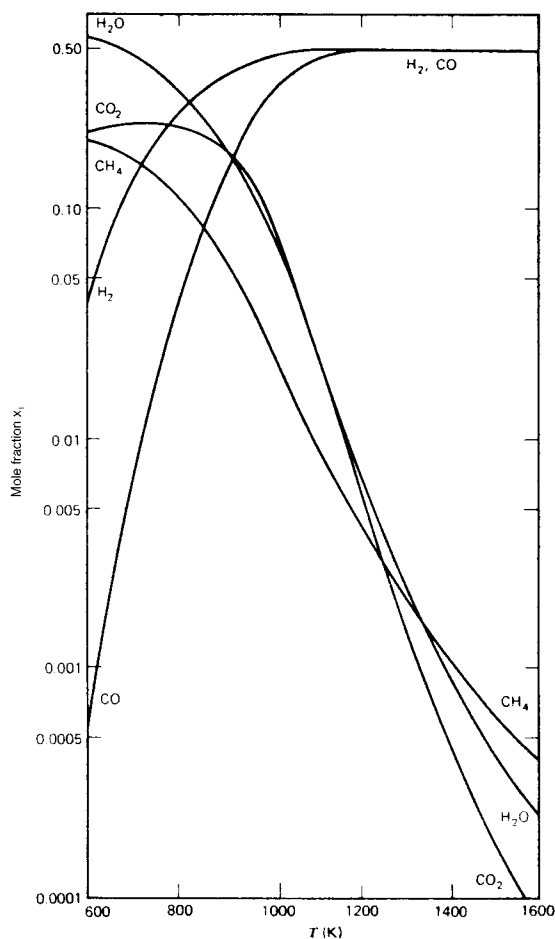


**Figure 1.14** Equilibrium mol fractions for the carbon-steam reaction as a function of temperature. [After S.I. Sandler, *Chemical and Engineering Thermodynamics*, reprinted by permission of John Wiley and Sons, New York, NY (1989).]



HORATIO SAYS

Are there any ways to estimate whether one (or more) of the reactions in the above set are not important in setting the equilibrium point?

### 1.8 Reaction Rates and Conversion in Nonisothermal Systems

Thus far in discussing kinetics we have confined our interests to analysis of expressions of the form

$$\int f(C_A, C_B, \dots) dC_A = \int k dt \quad (1-163)$$

for the example of a constant-volume batch system, where  $f(C_A, C_B, \dots)$  denotes the form of the concentration dependence of rate. In nonisothermal systems the temperature dependence of the rate, which is far more pronounced than its concentration dependence, becomes important and, on substitution of the Arrhenius form for  $k$  in equation (1-163), we end up with a much more formidable problem to solve

$$\int f(C_A, C_B, \dots) dC_A = \int k^\circ e^{-E/RT} dt \quad (1-164)$$

From one point of view, the solution depends on obtaining a relationship between temperature and composition, so the terms of equation (1-164) can be expressed in terms of a single dependent variable and, hopefully, integrated analytically. Alternatively, one could look for a temperature–time relationship. This may not be easy to do, however, since the time–temperature or composition–temperature history of a reaction in which heat is evolved or consumed is a function of the rate itself. Obviously, one must look to another relationship in addition to that of mass conservation in order to obtain this history.

#### 1.8.1 Coupling of the Energy–Conservation Equation to the Mass–Conservation Equation

In isothermal systems the general mass conservation–reaction rate expression of equation (1-15) is sufficient to describe the state of the system at any time. In nonisothermal systems this is not so, and expressions for both the conservation of mass and the conservation of energy are required. In reacting systems the energy balance most conveniently is written in terms of enthalpies of all the species entering and leaving a reference volume such as that of Figure 1.3a. Chemical reaction affects this balance by the heat that is evolved or consumed in the reaction. The balance that is required in addition to equation (1-15) is

$$\begin{aligned} & \left( \frac{\text{energy entering } \delta}{\text{time}} \right) - \left( \frac{\text{energy leaving } \delta}{\text{time}} \right) + \left( \frac{\text{energy produced in } \delta}{\text{time}} \right) \\ & = \left( \frac{\text{change of energy in } \delta}{\text{time}} \right) \end{aligned} \quad (1-165)$$

The second term above contains the items of most immediate interest. If the energy leaving  $\delta$  per time is associated only with effluent streams from the system, then there has been no heat loss and the reaction system is adiabatic. In general, however, one must account for heat transfer between the system and surroundings, and this term consists of two contributions: energy leaving in effluent streams and heat transfer with the surroundings. In this case the reaction system is both nonadiabatic and nonisothermal and the details of heat transfer with the surroundings become important in analysis. The energy produced in  $\delta$  per time is due to the heat of the reaction,

either exothermic or endothermic, and can be expressed in terms of the enthalpies of reactants and products relative to some reference temperature.

In the following we discuss some simple types of homogeneous adiabatic reactions to illustrate the application of the coupled conservation equations (1-15) and (1-165). Since the treatment of nonadiabatic reactions depends on the detail concerning heat transfer with the surroundings, a topic more conveniently associated with particular reactor types, we will for the moment be content with what can be learned from the limiting kinds of temperature behavior—isothermal and adiabatic.

### 1.8.2 Rates and Conversions in Some Simple Adiabatic Reactions

As we have done previously for isothermal reactions, let us first look at systems in which the conservation equations contain the reaction term alone, in order to concentrate on the kinetics. Then, we have for adiabatic reactions

$$\left( \frac{\text{mass A reacted in } \delta}{\text{time}} \right) = \left( \frac{\text{change of mass A in } \delta}{\text{time}} \right) \quad (1-15a)$$

$$\left( \frac{\text{change of energy in } \delta}{\text{time}} \right) = \left( \frac{\text{energy produced in } \delta}{\text{time}} \right) \quad (1-165a)$$

and, as stated before, these refer explicitly to a homogeneous, batch reaction.

*First-order Reaction.* The rate equation (1-34) must be written in terms of its temperature dependence, but otherwise is the same

$$r_A = (dC_A/dt) = -k^\circ e^{-E/RT} C_A \quad (1-166)$$

and the energy balance is

$$[d(\Delta H)/dt] = k^\circ e^{-E/RT} C_A (-\Delta H_R) \quad (1-167)$$

where  $(-\Delta H_R)$  is the heat of reaction. Again, keep clear the distinction between constant and nonconstant volume reaction systems and the equivalence of mass and molal formulations only if there is no change in total mols on reaction. For the constant volume system with no net change in the number of mols on reaction,  $\Delta H$  above is an enthalpy per unit volume, and  $(-\Delta H_R)$  is an heat of reaction per mol of A reacted. In accord with convention, a negative heat of reaction corresponds to an exothermic transformation. Now equation (1-167) is a total energy balance, so for the reaction  $A \rightarrow B$  it includes both reactant and product. If no phase changes are involved in the reaction and the heat capacities of A and B are constant, then  $\Delta H$  may be written with respect to reference temperature,  $T_0$ , as

$$\begin{aligned} \Delta H = \Delta H_A + \Delta H_B = C_{A0}(1-x)C_{pA}(T - T_0) \\ + (C_{B0} + C_{A0}x)C_{pB}(T - T_0) \end{aligned} \quad (1-168)$$

where  $\Delta H_A$  and  $\Delta H_B$  are individual enthalpies per unit volume and  $x$  is the conversion of A. Let us assume that the heat capacity of the reaction mixture,  $C_p$ , is independent of conversion. Then equations (1-167) and (1-168) can be combined:

$$C_p(C_{A0} + C_{B0}) \frac{dT}{dt} = \frac{dx}{dt} (-\Delta H_R) C_{A0} \quad (1-169)$$

from which

$$\frac{dT}{dx} = \frac{(-\Delta H_R)C_{A0}}{C_p(C_{A0} + C_{B0})} = \alpha \quad (1-170)$$

Equation (1-170) provides us with the temperature-conversion relationship that we need to solve problems of the general form of equation (1-164). Thus,

$$T - T_0 = \alpha x \quad (1-171)$$

Now, substituting in the rate equation (1-166)

$$\frac{1}{\alpha} \frac{dT}{dt} = k^\circ e^{-E/RT} (\beta - T/\alpha) \quad (1-172)$$

where  $\beta = 1 + T_0/\alpha$ .

Even though we have been successful in reducing the problem to a form containing one independent variable, the solution is not straightforward because of the nonlinearity of the Arrhenius equation. We can write equation (1-172) as

$$k^\circ t = \int_{T_0}^T \frac{e^{E/RT} dT}{\gamma - T} \quad (1-173)$$

where  $\gamma = \alpha\beta$ . Now make the variable substitution  $y = E/RT$ , which transforms the integral to

$$k^\circ t = - \int_{y_0}^y \frac{\exp y dy}{y[(R\gamma y/E) - 1]}$$

This may be expanded by partial fractions to give

$$k^\circ t = \int_{y_0}^y \frac{\exp y dy}{y} - \exp\left(\frac{E}{R\gamma}\right) \int_{z_0}^z \frac{\exp z dz}{z} \quad (1-174)$$

where

$$y_0 = E/RT_0; \quad z = y - E/R\gamma; \quad z_0 = y_0 - E/R\gamma$$

The integral terms in equation (1-174) are forms of the exponential integral, a tabulated function (M. Abramowitz and I.A. Stegun, *Handbook of Mathematical Functions*, Dover, New York, NY, (1965)] which is normally defined as

$$E_i(x) = \int_{-\infty}^x \frac{\exp x' dx'}{x'}$$

The final solution for the first-order adiabatic case is then

$$k^\circ t = E_i(y) - E_i(y_0) - \exp\left(\frac{E}{R\gamma}\right) [E_i(z) - E_i(z_0)] \quad (1-175)$$

which provides us with the time-temperature history of the reaction. Once this is determined, corresponding concentrations or conversions are obtained directly from equation (1-171).

*Solutions for Other Simple Orders.* The procedure just illustrated can be used to obtain  $t - T$  histories for other simple-order, irreversible reactions [J.M. Douglas and L.C. Eagleton, *Ind. Eng. Chem. Fundls.*, 1, 116 (1962)]. A tabulation of these

**Table 1.6** Solutions for Simple-Order, Irreversible Adiabatic Reactions1. Zero order:  $A \rightarrow B$ 

$$-r_A = k^\circ e^{-E/RT}$$

$$\alpha k^\circ t = T \exp\left(\frac{E}{RT}\right) - T_0 \exp\left(\frac{E}{RT_0}\right) - \left(\frac{E}{R}\right) \left[ E_i\left(\frac{E}{RT}\right) - E_i\left(\frac{E}{RT_0}\right) \right]$$

2. First order:  $A \rightarrow B$ 

$$-r_A = k^\circ e^{-E/RT} C_A$$

$$k^\circ t = E_i\left(\frac{E}{RT}\right) - E_i\left(\frac{E}{RT_0}\right) - \exp\left(\frac{E}{R\gamma}\right) [E_i(z) - E_i(z_0)]$$

3. Second order:  $2A \rightarrow B + C$ 

$$-r_A = k^\circ e^{-E/RT} C_A^2$$

$$k^\circ t = \frac{\alpha E}{R\gamma^2} \exp\left(\frac{E}{R\gamma}\right) \left[ \frac{\exp(z)}{z} - \frac{\exp(z_0)}{z_0} - E_i(z) + E_i(z_0) \right]$$

4. Second order:  $A + B \rightarrow C + D$ 

$$-r_A = k^\circ e^{-E/RT} C_A C_B$$

$$k^\circ t = \exp\left(\frac{E}{R\gamma}\right) (C_{B0} - C_{A0}) [E_i(z) - E_i(z_0)] \\ + \exp\left(\frac{E\alpha}{R\gamma'}\right) (C_{B0} - C_{A0}) [E_i(w) - E_i(w_0)]$$

where

$$\gamma = \alpha\beta = T_0 + \frac{C_{A0}(-\Delta H_R)}{C_p \sum C_{i_0}}$$

$$\gamma' = T_0 + \frac{C_{B0}(-\Delta H_R)}{C_p \sum c_{i_0}}$$

$$z = \frac{E}{RT} - \frac{E}{R\gamma}$$

$$z_0 = \frac{E}{RT_0} - \frac{E}{R\gamma}$$

$$w = \frac{E}{RT} - \frac{E}{R\gamma'}$$

$$w_0 = \frac{E}{RT_0} - \frac{E}{R\gamma'}$$

is given in Table 1.6. General analytical solutions of this type have not been obtained for reversible reactions or for the nearly complex reactions discussed earlier, and in general numerical procedures must be employed.

*Nonanalytical Methods and Approximations for Adiabatic Reactions.* A wide variety of techniques and associated numerical methods exist for the solution of non-isothermal reactions and reactor problems which are not tractable to analytical

procedures. In this section we will illustrate one simple technique for the example of the reaction  $A + B \leftrightarrow C$ , which involves volume change and reversibility. The equation for the rate of reaction of A is

$$\frac{1}{V} \frac{d(N_{A0} - N)}{dt} = - \frac{(k^\circ)_1 e^{-E_1/RT}}{V^2} (N_{B0} - N)(N_{A0} - N) + \frac{(k^\circ)_2 e^{-E_2/RT}}{V} N \quad (1-176)$$

or

$$V \frac{dN}{dt} = (k^\circ)_1 e^{-E_1/RT} (N_{A0} - N)(N_{B0} - N) - V(k^\circ)_2 e^{-E_2/RT} N \quad (1-176a)$$

where  $N$  is the number of mols of A and B reacted to product,  $V$  is the volume of the reaction system, and no product is present initially. Now for nonisothermal conditions,  $V$  will be a function of temperature as well as the net molal change. For the example of ideal gases, we can write

$$V = \frac{(N_{A0} + N_{B0} - N)RT}{P} \quad (1-177)$$

The energy balance is

$$N(-\Delta H_R) = (N_{A0} - N)(\Delta H_A) + (N_{B0} - N)(\Delta H_B) + N(\Delta H_C) \quad (1-178)$$

where  $\Delta H_A$ ,  $\Delta H_B$ , and  $\Delta H_C$  are enthalpy changes per mol. For the case of constant heat capacities, no phase change, and identical initial and enthalpy reference temperatures:

$$[(N_{A0} - N)C_{pA} + (N_{B0} - N)C_{pB} + NC_{pC}](T - T_0) - N(-\Delta H_R) = 0 \quad (1-179)$$

Combining equations (1-177) and (1-176a), and integrating, we obtain

$$t = \int_0^{N_{A0}, N_{B0}} \frac{dN}{f_1(T, P, N) - f_2(T, N)} \quad (1-180)$$

with

$$f_1(T, P, N) = \frac{(k^\circ)_1 e^{-E_1/RT} (N_{A0} - N)(N_{B0} - N)(P/RT)}{N_{A0} + N_{B0} - N}$$

$$f_2(T, N) = (k^\circ)_2 e^{-E_2/RT} N$$

where the upper limit refers to which of the two reactants is initially present in the smallest quantity (limiting reactant). Equations (1-179) and (1-180) can be solved simultaneously by the following iterative procedure:

1. Assume a value for the temperature for some time after the reaction has started. If the reaction is exothermic,  $T > T_0$ .
2. Knowing the value of  $T_0$  and  $T$ , together with  $N_{A0}$ ,  $N_{B0}$ , and the heat capacities, calculate the corresponding  $N$  from equation (1-179).
3. Calculate the corresponding value of  $t$  by numerical integration of equation (1-180).

As a result of the difficulties involved in obtaining general analytical solutions for these nonisothermal problems, one sometimes encounters approximations based on



simpler forms of the temperature dependence of the rate constant. The two most commonly used are

$$k = a + bT \quad (1-181)$$

$$k = a^\circ \left( \frac{T}{T_0} \right)^n \quad (1-182)$$

The dangers inherent in the linear approximation to an exponential function should be obvious and equation (1-181) is useful only when small changes in temperature are anticipated. Equation (1-182) is a more flexible approximation; however, in many cases it yields solutions in the form of series expansions which are ultimately no more convenient numerically than the simultaneous solution of equations (1-179) and (1-180). A comparison of these approximation methods for an example with an activation energy of 20,000 cal/mol and a constant of unity at 300°K is shown in Figure 1.15. The fit has been forced at 300 and 320°K in this illustration. For the linear approximation there are large deviations even within the range of the fit; the power-law form is much better, but only within the range of the fit.

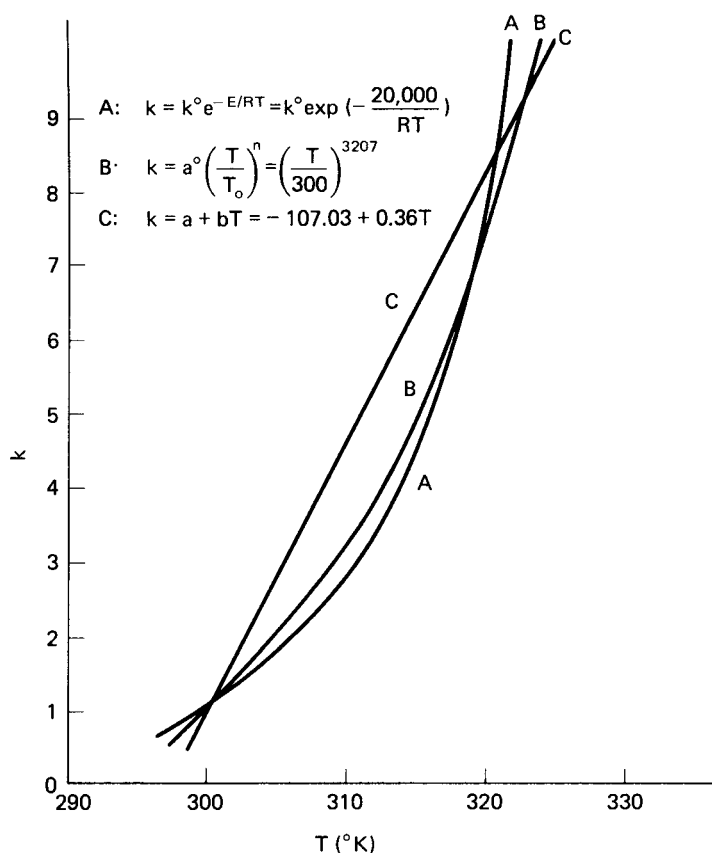


**Figure 1.15** Comparison of temperature dependence of rate-constant approximations:  $E = 20,000$  cal/mol,  $k = \text{unity}$  at 300 K.

### 1.8.3 Temperature Effects in Some Nonelementary Reaction Sequences

We have seen that one important reason for the efficiency of chain reaction mechanisms is the manner in which the combination of activation energies for initiation, propagation, and termination steps, equation (1-116), gives a net energy requirement less than that for the initiation step. In this sense, we should discuss the influence of temperature on the behavior of the examples of nearly complex reactions discussed previously. We shall not attempt solution of these systems for set adiabatic conditions now, but shall examine the results for conversion and selectivity in terms of how they are affected by temperature level.

Rewriting the differential selectivity definitions made previously for Types I, II, and III in terms of the temperature dependence:

$$S_d(\text{I}) = \left[ \frac{(k^\circ)_1}{(k^\circ)_2} \right] \exp\left(\frac{E_2 - E_1}{RT}\right) \frac{C_A}{C_L} \quad (1-183)$$

$$S_d(\text{II}) = \frac{1}{1 + \left[ \frac{(k^\circ)_2}{(k^\circ)_1} \right] \exp\left(\frac{E_1 - E_2}{RT}\right)} \quad (1-184)$$

$$S_d(\text{III}) = 1 - \left[ \frac{(k^\circ)_2}{(k^\circ)_1} \right] \exp\left(\frac{E_1 - E_2}{RT}\right) \frac{C_B}{C_A} \quad (1-185)$$

In each of these cases the differential selectivity will increase as the reaction temperature is increased if  $E_1 > E_2$ , and will decrease if  $E_2 > E_1$ . Of course, trends in selectivity with temperature are not always the same as for these three examples; it is entirely possible for selectivity to decrease with increasing temperature for some reactions.

One value of this sort of analysis is that it leads one to think of activation energy as a kind of temperature sensitivity parameter. Since the activation energy is conferred upon a reaction by nature, we cannot use this as a manipulated variable to obtain some desired yield or overall selectivity, but we can use such values as guides to indicate reaction temperature policies that might be advantageous. The outlines of such an approach have been given by Millman and Katz [M.C. Millman and S. Katz, *Ind. Eng. Chem. Proc. Design Devel.*, 6, 447 (1967)] and by Fournier and Groves [C.D. Fournier and F.R. Groves, *Chem. Eng.*, 77(3), 121; 77(13), 157 (1970)]. Consider the reaction sequence



where Q is the desired product. Now for  $E_3 > E_1$  and  $E_2 > E_1$  the optimal temperature policy would be that calling for a decrease in temperature with time of reaction, since the initial high temperature would promote production of Q but would need to be decreased shortly because the high temperature favors the high E reactions. On the other hand, for  $E_3 > E_1 > E_2$  the reverse reaction is endothermic so a high temperature is desirable from this point of view; however, this must be tempered by the high value of  $E_3$ . A suitable compromise might be to start at lower temperatures, when the concentrations of A and B are high, and then increase temperature. For a purely sequential scheme akin to Type III



again where Q is desired, if  $E_2 > E_1$  we would like to have a high temperature to get the reaction started and then lower the temperature to retard the further reaction of Q. If  $E_1 > E_2$  a uniformly high temperature might be desirable, although some decrease could be called for as the concentration of Q builds up.

Policies needed to optimize conversion (sometimes termed an *output objective*) are not always the same as those which improve selectivity or yield [K.G. Denbigh and J.C.R. Turner, *Chemical Reactor Theory*, Cambridge University Press, London, U.K., (1971)]. Such an equivocal case is given by the following variant of scheme (XVI):



where  $E_2 > E_1$ . For maximum conversion we would like to increase the temperature with time of reaction; the low temperature at the start will promote production of Q and the high temperature at the end will offset the lowered conversion rate which arises from the lowered concentration of reactants. This policy will indeed give more Q, but also more S. If the objective is to maximize Q, then a uniformly low temperature would be required, but the reactor would have to be large because of the low rates of reaction.

#### 1.8.4 Temperature-Scheduled Reactions

The examples above provide ample evidence that there can be significant advantages to temperature scheduling in batch reactors (temperature variation with time of reaction), and it will be seen later that these ideas can be carried over to continuous reactions as well. The implementation of such schemes normally implies nonadiabatic reactor operation which, as stated before, gets into details of reactor analysis beyond the scope of the present section. Let us then not look at the details but focus on the overall picture here. Assume, for the moment, that we can maintain by some means any desired level of temperature at any instant in the reaction/reactor system. Then, how might we proceed to a closer analysis of the temperature policies in the schemes given above, since “high temperature” and “low temperature” are only relative and qualitative terms?

The most important single class of reactions for which temperature scheduling can be beneficial are those which may be equilibrium limited. A classical case [O. Bilious and N.R. Amundson, *Chem. Eng. Sci.*, 5, 81 (1956)] is that of a reversible, first-order reaction



for which at low temperatures the equilibrium lies far to the right but the rate of reaction of A is slow, and for which at higher temperatures the rate of both forward and reverse reactions is large ( $E_2 > E_1$ ). What sort of temperature schedule can we impose on this reaction to obtain a given degree of conversion to B in the absolute minimum time? For a constant-volume reaction the rate equation is

$$(dC_A/dt) = -k_1 C_A + k_2 C_B \quad (1-60)$$

and the time of reaction is

$$t = \int_0^x \frac{C_{A0} dx}{k_1 C_{A0} - k_2 C_{B0} - (k_1 + k_2) C_{A0} x} \quad (1-186)$$

The problem is to define the path of  $x$  versus time which will minimize this integral. For this reaction, minimization of the integral corresponds to maximization of the rate of conversion to B at each instant. Mathematically we can state the requirement for this point maximization as

$$\frac{\partial}{\partial T} \left[ \frac{1}{k_1 C_{A0} - k_2 C_{B0} - (k_1 + k_2) x} \right] = 0 \quad (1-187)$$

This reduces to

$$C_{A0} \frac{\partial k_1}{\partial T} (1 - x) = \frac{\partial k_2}{\partial T} (C_{B0} + C_{A0} x) \quad (1-188)$$

From the Arrhenius equation

$$\begin{aligned} \frac{\partial k_1}{\partial T} &= k_1 (E_1 / RT^2) \\ \frac{C_{A0}(1 - x)}{C_{B0} + C_{A0} x} &= \frac{(k^\circ)_2 e^{-E_2/RT}}{(k^\circ)_1 e^{-E_1/RT}} \left( \frac{E_2}{E_1} \right) \end{aligned} \quad (1-189)$$

For a given conversion equation (1-188) defines a corresponding temperature maximizing the rate of reaction, which can then be used for the calculation of the time of reaction from equation (1-186). In this case the temperature schedule would call for very high temperatures at the start of the reaction, maximizing the conversion of A while its concentration is high and that of product low, with a subsequent rapid decrease in temperature to prevent the reverse reaction from occurring.

We shall see later that the time of reaction here corresponds to the size of chemical reactor required, so what we have accomplished is minimization of the size and cost of the reactor system required to accomplish a specified conversion. Of course, such absolute optimal temperature schedules may not always be accomplished practically, but they can serve at least as indicators for desirable design policies. The general aspects of the solution to the optimal scheduling problem of Bilous and Amundson are shown in Figure 1.16.

The results obtained above for the simple reversible reaction have been generalized by Fournier and Groves to the following schemes



again subject to the condition that

$$(\partial r_A / \partial T) = 0$$

is fulfilled at every point. The optimal temperature-conversion schedule is given by

$$T = \{[1/(-B_1)][\ln(B_2 B_3)]\}^{-1} \quad (1-190)$$

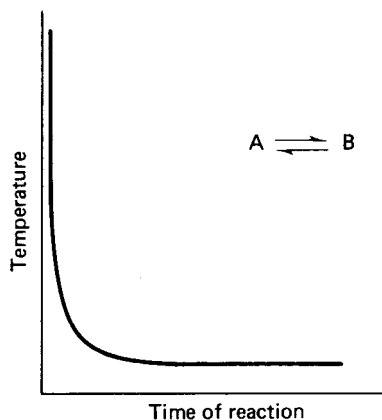


**Figure 1.16** Optimal temperature schedule for  $A \leftrightarrow B$ ,  $E_2 > E_1$

where

$$B_1 = (E_1 - E_2)/R$$

$$B_2 = [(k^\circ)_2(E_2)]/(k^\circ)_1$$

for all four schemes of (XIX), and

$$B_3 = x_A/(1 - x_A) \quad (\text{XIXa})$$

$$B_3 = (C_{A0}x_A)^2/(1 - x_A) \quad (\text{XIXb})$$

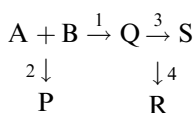
$$B_3 = x_A/[C_{A0}(1 - x_A)(M - x_A)] \quad (\text{XIXc})$$

$$B_3 = (x_A)^2/[(1 - x_A)(M - x_A)] \quad (\text{XIXd})$$

In the above  $E_1$  and  $E_2$  are activation energies for the forward and reverse reactions, respectively,  $(k^\circ)_1$  and  $(k^\circ)_2$  the corresponding Arrhenius preexponential factors, and  $M$  the ratio of initial concentrations,  $(C_{B0}/C_{A0})$ . In this analysis the initial product concentrations are taken to be zero.

### Illustration 1.8

1) A classical sequence of reactions involving most of the features of the Type I, II and III schemes is that proposed as a model by Denbigh:



Using the activation energy-temperature sensitivity analysis approach, determine possible temperature sequences for this scheme if S is the desired product.

2) With some small loss of generality from the Denbigh scheme, we may consider the first step to be first-order in A only. It is desired now to operate an isothermal batch reactor at a single temperature level to produce a maximum of the intermediate product Q in such a case. Aside from the first step, orders correspond to stoichiometry

and the following data are available for the rate constants:

$$k_1 = (10)^9 \exp(-6000/T) \text{ sec}^{-1}$$

$$k_2 = (10)^7 \exp(-4000/T) \text{ sec}^{-1}$$

$$k_3 = (10)^8 \exp(-9000/T) \text{ sec}^{-1}$$

$$k_4 = (10)^{12} \exp(-12000/T) \text{ sec}^{-1}$$

where  $T$  is in  $^{\circ}\text{K}$ . What temperature is required?

*Solution*

1) The best way to approach the solution to this part of the problem is by considering pairs of activation energies. There turn out to be four combinations of interest here (maximization of S):

- i)  $E_1 > E_2$  and  $E_3 > E_4$ , for which one would like a uniformly high temperature
- ii)  $E_1 < E_2$  and  $E_3 < E_4$ , for which one would like a uniformly low temperature
- iii)  $E_1 < E_2$  and  $E_3 > E_4$ , for which one would like the temperature increasing with time of reaction
- iv)  $E_1 > E_2$  and  $E_3 < E_4$ , for which one would like the temperature decreasing with time of reaction

You should examine these sequences in turn and write out why they would lead to overall behavior maximizing the production of S.

2) In this case we are not concerned with a time-temperature trajectory, but with the simpler problem of the optimum isothermal temperature. Also, we look here at the maximization of intermediate product Q rather than final product S. Writing the rate equations of interest we have

$$d[A]/dt = -(k_1 + k_2)[A] \quad (\text{i})$$

$$d[Q]/dt = k_1[A] - (k_3 + k_4)[Q] \quad (\text{ii})$$

so

$$[A] = [A_0] \exp[-(k_1 + k_2)t] \quad (\text{iii})$$

and

$$d[Q]/dt + (k_3 + k_4)[Q] = k_1[A_0] \exp[-(k_1 + k_2)t] \quad (\text{iv})$$

Equation (iv) has as its solution

$$\begin{aligned} [Q] = & k_1[A_0] \exp[-(k_1 + k_2)t/(k_3 + k_4 - k_1 - k_2)] \\ & - k_1[A_0] \exp[-(k_3 + k_4)t/(k_3 + k_4 - k_1 - k_2)] \end{aligned} \quad (\text{v})$$

provided that  $(k_3 + k_4) \neq (k_1 + k_2)$ . At the maximum of [Q] in the batch system

$$d[Q]/dt = 0 \quad (\text{vi})$$

which yields from equation (v)

$$\ln[(k_1 + k_2)/(k_3 + k_4)] = (k_1 + k_2 - k_3 - k_4)t \quad \text{at max } [Q] \quad (\text{vii})$$

Thus, for  $[Q]_{\max}$ :

$$t = (k_1 + k_2 - k_3 - k_4)^{-1} \ln[(k_1 + k_2)/(k_3 + k_4)] \quad (\text{viii})$$

The combination of equations (viii) and (v) in principle give the solution to the problem for  $[Q]_{\max}$  but not yet completely to the problem stated since we wish to know the temperature given the maximum of this maximum. Combining these two equations we get

$$\frac{[Q]_{\max}}{[A_0]} = \frac{k_1}{M - N} [(N/M)^{-p} - (N/M)^{-q}] \quad (\text{ix})$$

where

$$N = k_1 + k_2$$

$$M = k_3 + k_4$$

$$p = N/(N - M)$$

$$q = M/(N - M)$$

Following the analytical procedure for maximization, we then should obtain the derivative of the function of equation (ix) with respect to  $T$ , set that equal to zero, and solve for  $T_{\max}$ . However, in Section 1.3 we stated that the Arrhenius equation is an "...awkward exponential form...", and the reader can demonstrate this upon attempting the analytical differentiation of equation (ix)—spare time and Debussy on the radio are suggested. It is easier just to calculate the function in terms of  $T$  and see where the maximum falls (a one-dimensional search routine may be helpful).

The results of the numerical calculation are shown in Figure 1.17. From the figure it is seen that the function is well-behaved and that a well-defined optimum temperature exists, corresponding to a reaction temperature of 580°K.

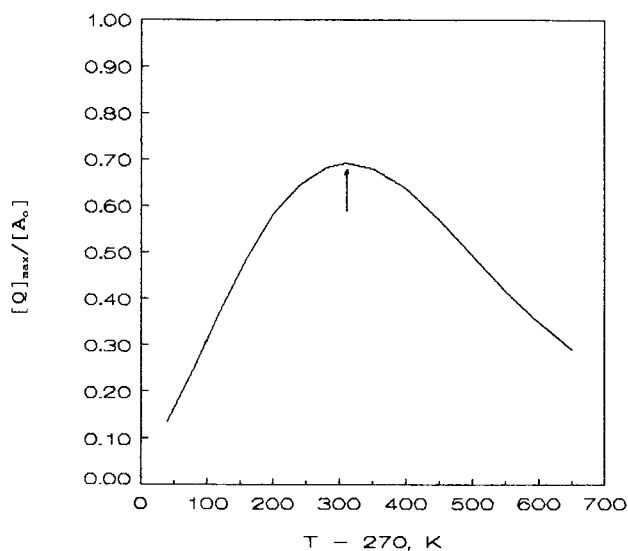


**Figure 1.17** Optimum isothermal temperature for production of maximum intermediate  $Q$ .



HORATIO SAYS

Remember that it is often convenient to think of the activation energy as a temperature sensitivity parameter.

## 1.9 Interpretation of Kinetic Information

A central problem in kinetics is the interpretation of laboratory data on rates of reaction. We have treated rates and selectivities to this point as if all the parameters such as reaction orders, rate constants, and activation energies were known. Suppose that this is not so [“None of them know the color of the sky,” *S. Crane*]. How does one go about the testing of rate or conversion information on a certain reaction in terms of the expressions we have been dealing with? Further, and importantly, what is the influence of experimental error on the parameters we determine from a given set of data? To what extent are the apparent kinetics of a reaction useful in providing information on the elementary steps of that reaction?

Answers to all these questions would make a good-sized book. Particularly in recent years there has been considerable interest in developing formalized statistical methods for planning experiments, determining the best models for representing apparent kinetics, and obtaining the “best” estimates of the associated parameters which we cannot begin to describe here. These are necessarily computer-based and generally are quite elegant. It is good to remember, though, that marvelous arithmetic cannot argue away poor data; “garbage in, garbage out” as the saying goes.

Fortunately there are a number of basic and very simple means for the interpretation of kinetic data which are sufficient to provide at least the first estimates of reaction order and the associated rate constants [R.G. Pearson, *Chemtech*, 552, September, (1978)]. These methods will provide a sound basis for visualization and some interpretation before proceeding to the more detailed analyses mentioned above. Before going further, however, it is fruitful to consider the practical matter of the influence of experimental error on the measurement of reaction kinetics.

### 1.9.1 Precision of Rate Measurements

Experimental results on reaction kinetics are sometimes characterized by a large amount of scatter in the measured information and corresponding uncertainty in associated rate constant and reaction orders. Such a situation is not necessarily the result of careless experimentation, because these quantities are generally very sensitive functions of the precision of experimental measurements. The following example [S.W. Benson, *The Foundations of Chemical Kinetics*, McGraw-Hill Book Co., New York, NY, (1960)] provides a clear illustration of this sensitivity.

Assume that we are engaged in study of the reaction  $2A \rightarrow B$  and have established it to be simple second-order and irreversible. We wish to investigate the effects



of random errors in the measurement of concentration, time, and temperature on the rate constant and the activation energy of the reaction. For measurements of concentration,  $C_A$ , at times  $t_1$  and  $t_2$ , equation (1-38) can be written

$$k = \frac{1}{t_2 - t_1} \left( \frac{C_{A1} - C_{A2}}{C_{A1} C_{A2}} \right) \quad (1-189)$$

Assume that the errors made in measuring the four data  $C_{A1}$ ,  $C_{A2}$ ,  $t_1$ , and  $t_2$  are independent of each other and are random. The expected error in the rate constant,  $\Delta k$ , is given by

$$\begin{aligned} (\Delta k)^2 = & \left( \frac{\partial k}{\partial t_1} \right)^2 (\Delta t_1)^2 + \left( \frac{\partial k}{\partial t_2} \right)^2 (\Delta t_2)^2 \\ & + \left( \frac{\partial k}{\partial C_{A1}} \right)^2 (\Delta C_{A1})^2 + \left( \frac{\partial k}{\partial C_{A2}} \right)^2 (\Delta C_{A2})^2 \end{aligned} \quad (1-190)$$

where equation (1-190) describes total error as the vector sum of the individual errors in the four measurements. Now rearrange in terms of the relative errors,  $(\Delta k/k)$ , and so on:

$$\begin{aligned} \left( \frac{\Delta k}{k} \right)^2 = & \left( \frac{\partial \ln k}{\partial \ln t_1} \right)^2 \left( \frac{\Delta t_1}{t_1} \right)^2 + \left( \frac{\partial \ln k}{\partial \ln t_2} \right)^2 \left( \frac{\Delta t_2}{t_2} \right)^2 \\ & + \left( \frac{\partial \ln k}{\partial \ln C_{A1}} \right)^2 \left( \frac{\Delta C_{A1}}{C_{A1}} \right)^2 + \left( \frac{\partial \ln k}{\partial \ln C_{A2}} \right)^2 \left( \frac{\Delta C_{A2}}{C_{A2}} \right)^2 \end{aligned} \quad (1-191)$$

The partial derivatives may be evaluated from equation (1-189):

$$\begin{aligned} \left( \frac{\Delta k}{k} \right)^2 = & \left( \frac{t_1}{t_2 - t_1} \right)^2 \left( \frac{\Delta t_1}{t_1} \right)^2 + \left( \frac{t_2}{t_2 - t_1} \right)^2 \left( \frac{\Delta t_2}{t_2} \right)^2 \\ & + \left( \frac{C_{A2}}{C_{A2} - C_{A1}} \right)^2 \left( \frac{\Delta C_{A1}}{C_{A1}} \right)^2 + \left( \frac{C_{A1}}{C_{A2} - C_{A1}} \right)^2 \left( \frac{\Delta C_{A2}}{C_{A2}} \right)^2 \end{aligned} \quad (1-192)$$

For a numerical example, select the following values:

$$t_2 - t_1 = 1000 \text{ sec}$$

$$\Delta t_1 = \Delta t_2 = \pm 1 \text{ sec}$$

$$C_{A2} = 0.9 C_{A1}$$

$$(\Delta C_{A1}/C_{A1}) = (\Delta C_{A2}/C_{A2}) = \pm 0.1\%$$

Substitution of these values in equation (1-192) gives the resulting error in  $k$ ,  $(\Delta k/k) = 1.4\%$ . If the analytical error is  $\pm 0.5\%$  rather than  $\pm 0.1\%$ , the error in  $k$  increases to  $\pm 7\%$ . If we state the problem conversely, one asks what precision would be required to determine  $k$  to within any given accuracy, say 1%. For the case above, our simple analysis shows that the relative errors in each of the quantities measured must be less than  $\pm 0.1\%$ , so in order to measure the rate constant to a specified accuracy, the individual time and concentration measurements must be considerably better. If the errors are completely random, the relative error in  $k$  may be reduced by making a large number of measurements. For  $n$  measurements

of equal estimated error, the error in the final mean will be decreased by a factor of  $(n - 1)^{1/2}$  and, in many cases, this represents the major hope for improvement. Thus, the replication of experiments is an important factor in measurement of kinetics.

Precision in the measurement of activation energies is even more difficult, since the Arrhenius equation acts as a sort of exponential amplifier for errors in temperature measurement. Substituting the Arrhenius form for  $k$ , we have for the results of measurements at two temperatures,  $T_1$  and  $T_2$ :

$$E = -\frac{RT_1T_2}{T_1 - T_2} \ln\left(\frac{k_2}{k_1}\right) \quad (1-193)$$

The error analysis gives

$$\begin{aligned} \left(\frac{\Delta E}{E}\right)^2 &= \left(\frac{T_2}{T_1 - T_2}\right)^2 \left(\frac{\Delta T_1}{T_1}\right)^2 + \left(\frac{T_1}{T_1 - T_2}\right)^2 \left(\frac{\Delta T_2}{T_2}\right)^2 \\ &\quad + \left[\frac{1}{\ln(k_2/k_1)}\right]^2 \left[\left(\frac{\Delta k_1}{k_1}\right)^2 + \left(\frac{\Delta k_2}{k_2}\right)^2\right] \end{aligned} \quad (1-194)$$

Here the precision of  $E$  depends strongly on the size of the temperature interval chosen and the error in measuring the individual rate constants. The latter is multiplied by the factor  $[\ln(k_2/k_1)]^{-2}$ , which can be a large number if  $k_2 \approx k_1$ .

Some examples given by Benson for the precision of activation energy measurements are:

1. If  $(T_1 - T_2) = 10^\circ\text{C}$  and the error in  $T_1$  and  $T_2$  is  $\pm 0.2^\circ\text{C}$ , the error in  $E$  is  $\pm 2\%$ .
2. If  $k_1$  and  $k_2$  are good to  $\pm 1\%$  and their ratio is about 2 for the  $10^\circ\text{C}$  interval, the error in  $E$  is also about  $\pm 2\%$ .
3. To measure  $E$  over a  $10^\circ\text{C}$  interval to  $\pm 0.5\%$  will generally require a temperature error of  $< \pm 0.03^\circ\text{C}$  and a measurement of  $k_1$  and  $k_2$  to within  $\pm 0.3\%$ .

The apparently simple task of precise temperature measurement (and control) is really not so at all, since tolerable temperature ranges become small, particularly at higher temperature levels. The Arrhenius definition:

$$\frac{d(\ln k)}{dT} = \frac{E}{RT^2}$$

can be rearranged to

$$\frac{\Delta k}{k} = \frac{E}{RT} \left(\frac{\Delta T}{T}\right) \quad (1-195)$$

where the derivatives have been approximated by finite differences. For many reactions under conditions where rates can be measured experimentally  $(E/RT) \sim 35$ , so to reduce the expected error in  $k$  to  $\pm 0.1\%$  the temperature must be known to about  $\pm 0.003\%$ . At  $300^\circ\text{K}$  this is  $\pm 0.01^\circ\text{C}$ , and at  $600^\circ\text{K}$  it is  $\pm 0.02^\circ\text{C}$ —a level that would be difficult to attain in practice.

In Table 1.7 some rules of thumb that can serve as a conservative guide for the precision of measurement are given, using as an example an hypothetical reaction

**Table 1.7** Effects of Errors in Measurement on Kinetic Parameters

To measure  $k$  with an estimated error of  $\pm x\%$ , it is necessary to:

1. Measure concentrations with an accuracy of

$$\pm \frac{\text{change in concentration}}{\text{largest concentration}} \frac{x}{1.4} \%$$

2. Measure time with an accuracy of

$$\pm \frac{\text{time interval}}{\text{largest time}} \frac{x}{1.4} \%$$

3. Measure temperature with an accuracy of

$$\pm \frac{x}{35} \% = \pm \frac{xT}{3500} ^\circ\text{K}$$

The resultant accuracy in  $E$  for two measurements of  $k$ , each of accuracy  $\pm x\%$  will be

$$\overline{\Delta^2(E)^{1/2}} = \pm \frac{\text{highest temperature}}{\text{temperature interval}} \frac{x}{18} \%$$

with a value of  $(E/RT) = 35$ . Variations from the example values may be estimated by the equations above.

Another view on this modifies the relationship to say that only the rate and the conversions are measured variables, which at a given temperature level is perhaps a reasonable view [J.M. Smith, *Chemical Engineering Kinetics*, 3rd ed., McGraw-Hill Book Co., New York, NY, (1981)]. This gives an expression corresponding to equation (1-192):

$$\left(\frac{\Delta k}{k}\right)^2 = \left(\frac{\Delta r}{r}\right)^2 + \left(\frac{\Delta C_{A1}}{C_{A1}}\right)^2 + \left(\frac{\Delta C_{A2}}{C_{A2}}\right)^2 \quad (1-196)$$

Here the rate,  $r$  is normally not a direct measurement but is calculated from variables such as time and concentration. Thus, equation (1-192) is probably the preferred analysis for a conservative estimate of error.

The overall message should be clear, however. In whatever method of preliminary screening of kinetics, as will be outlined below, or in more detailed computer analysis, one should be acutely aware of the experimental error associated with rate of reaction data. Realistic examination of the  $(\Delta C/C)$  terms in the above equations reveals their importance in the estimation of  $k$  and, thence, in the estimation of  $E$  via methods such as equation (1-193). Precise values of concentrations are often difficult to obtain.

## 1.9.2 Interpretation Methods and Graphs

It may seem a little quaint to discuss graphical means for the interpretation of kinetic data in the age of readily available personal computer software, but some discussion is worthwhile, particularly in view of the comments concerning experimental error above. We will assume that in general one has available data that give conversion level versus time of reaction at some set conversion level

(“integral conversion data”). Direct data on the rate of reaction at specified conditions of concentration and temperature (“differential conversion data”) are always desirable but often not available, and we will assume that to be the case here.

One does not need a road map to conclude that it is possible in most instances of simple-order reactions to evaluate both order(s) and rate parameter(s) by plotting a suitable linearized form of the particular rate law it is desired to test. For example, to test for first-order, irreversible kinetics, one would plot, according to equation (1-35),  $-\ln(C_A/C_{A0})$  versus time. If these kinetics are obeyed, the concentration data plot will be linear with a slope of  $k$ . Similarly, a second-order test according to equation (1-42) would require a plot of  $-\ln[(C_A/C_{A0})(C_{B0}/C_B)]$  versus time, yielding a straight line of slope  $(C_{B0} - C_{A0})k$ . Analogous forms employing the conversion can also be used in all cases.

If the order of the reaction being analyzed does not correspond to the kinetic law being tested, then presumably the desired linear plot will not result. There are some pitfalls here, however, because many rate laws appear to be first-order if the range of conversions is not too large. Further, if there is a significant amount of error in the data, the identification of reaction order becomes imprecise and, ultimately, impossible. An alternative approach to that of assuming reaction order and testing for linearity is to employ the  $n$ th-order form illustrated for an irreversible reaction by equation (1-44). Here we choose a value for  $n$  and test for linearity by plotting  $[(C_A/C_{A0})^{1-n} - 1]$  versus time. Illustration of these procedures for the various irreversible schemes are given in Figure 1.18.

For reversible reactions the problem of interpretation becomes more difficult since we have basically the same number of data, conversion versus time, but two rate constants to determine. If conversion data are available up to the point of equilibrium, we may use the equilibrium composition together with conversion-time data to solve for the two constants directly. Generally, however, we must assume that the experimenter does not have the time or patience to obtain true equilibrium information (bearing in mind that rates of reaction are very slow at this point) so that a simple trial procedure is probably most convenient. For the first-order forward and reverse case of equation (1-61) one would choose a value of  $\alpha$ , which is a function of both  $k_f$  and  $k_r$ , and test for linearity by plotting  $\ln[\alpha/(\alpha - x)]$  versus time. The correct choice of  $\alpha$  will result in a straight line of slope  $(k_f + k_r)$ , and then the values for  $\alpha$  and the slope may be used to solve for the individual constants. If equilibrium data are available, the rate of reaction is zero and the rate equation used directly to obtain the equilibrium constant:

$$K = \frac{k_f}{k_r} = \frac{C_{B0} + C_{A0}x_\infty}{C_{A0}(1 - x_\infty)} \quad (1-60a)$$

For the more complicated reversible reactions illustrated earlier involving second-order reverse reaction, the trial procedure is basically the same. One must essentially guess a value for the equilibrium constant, which defines the values of the constants  $\alpha$ ,  $\beta$ , and  $\gamma$  [equation (1-65)] or  $\alpha$  and  $\beta$  [equation (1-67)] and then test by plotting the data according to the indicated linear form. Graphical methods for these and other reversible reactions may be devised following the forms for irreversible reactions by casting the governing equations into linearized forms. These methods

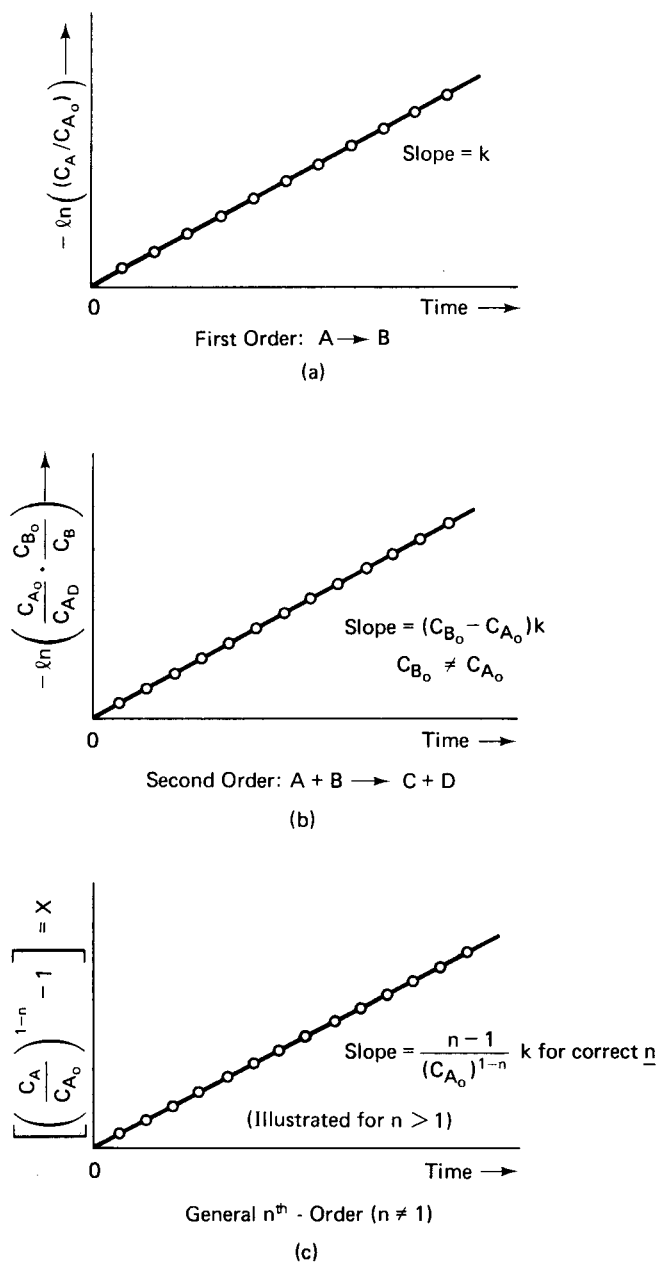


**Figure 1.18** Tests for irreversible reactions.

are described in many sources, starting with the equations in Section 1.5c. Tests for reversible reactions with and without equilibrium are illustrated in Figures 1.19 and 1.20. Overall, the procedures are direct, but sometimes tedious.

Now there is a little more fun available in the analysis of more complex reaction schemes (at least in part). Type I and Type II analyses follow from the

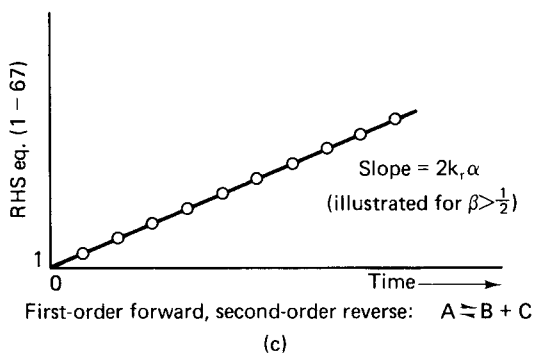
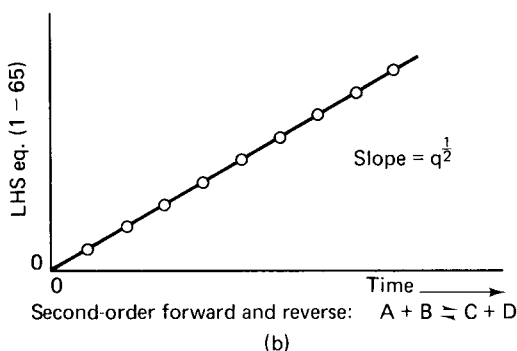
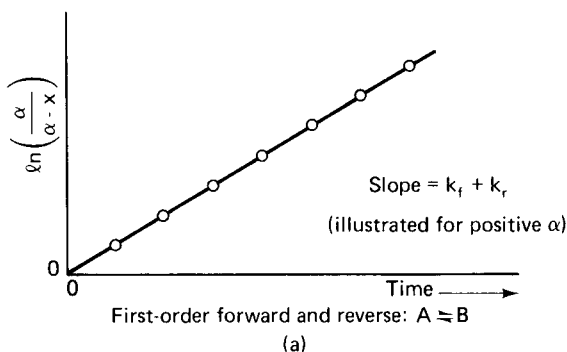
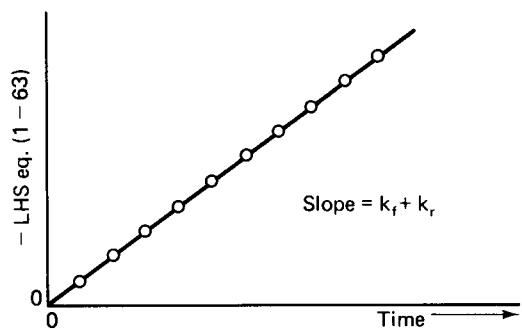


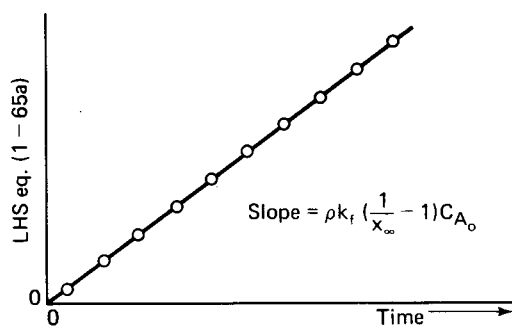
**Figure 1.19** Tests for some reversible reactions in the absence of equilibrium data.

procedures devised for irreversible reactions, provided that one has information concerning reactants A and L separately (Type I), and either A and B or A and C (Type II). Type III is more interesting. We have already pointed out that in this sequence the intermediate B will exhibit a maximum in concentration at some time after the initiation of the reaction in the case where  $C_{B0} = 0$ . The ratio of concentrations at this point ( $C_B/C_A$ ), at this maximum point defines directly the intrinsic selectivity of the system, ( $k_1/k_2$ ), by equation (1-88), and the time at which  $C_B$  is a maximum may then be used to solve for individual values of the rate constants, equation (1-89). Thus, all the kinetics constants of the Type III system can be

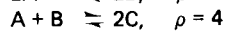
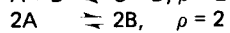
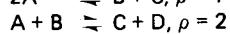
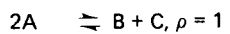


First-order forward and reverse:  $A \rightleftharpoons B$

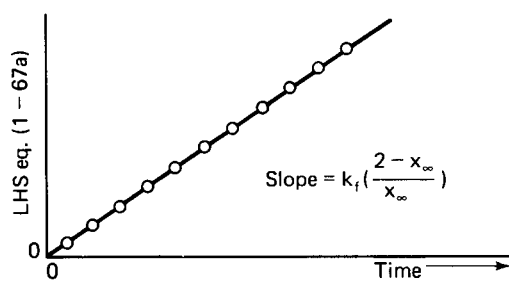
(a)



General second-order reversible:



(b)



First-order forward, second-order reverse:  $A \rightleftharpoons B + C$

(c)

**Figure 1.20** Tests for some reversible reactions employing equilibrium conversion data.

determined from data on the maximum concentration of the intermediate. An example of data interpretation for a simple system follows. Note the combination of intuition and analysis that is used.

### Illustration 1.9

Here are some data on the chlorination of toluene in 99.87% acetic acid at 25°C, as reported by Brown and Stock [H.C. Brown and L.M. Stock, *J. Amer. Chem. Soc.*, 79, 5175 (1957)]:

Molar Concentrations		
Time (s)	Toluene	Chlorine
0	0.1908	0.0313
2,790	0.1833	0.0238
7,690	0.1745	0.0150
9,690	0.1719	0.0123
14,000	0.1682	0.0086
19,100	0.1650	0.0055

Determine a reasonable kinetic sequence (reaction pathways) to explain these data and the value(s) of the appropriate rate constant(s).

#### Solution

For convenience in visualization of an approach to the analysis of these data, it is best to look at them graphically at first; this is provided in Figure 1.21. A first look at this would make one wonder if the reaction might be reversible. But—think a

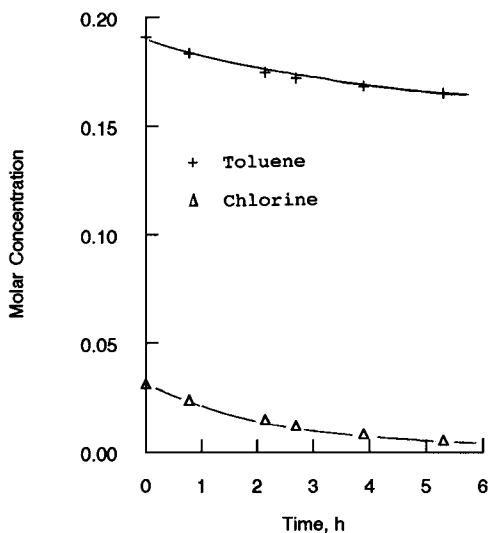


**Figure 1.21** Time plot of the data of Brown and Stock.



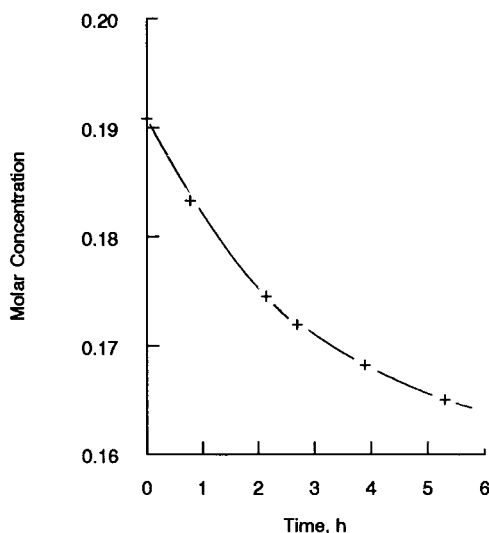
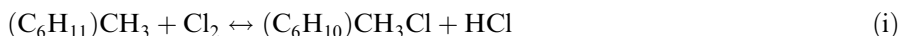


**Figure 1.22** Expanded scale plot for toluene.

moment. Write the overall chemistry involved as



Calculate the  $\Delta G^\circ$  for this reaction. Unless there are disturbing side-effects such as photochlorination (studiously avoided in the work of Brown and Stock), there is not much reason to believe it is reversible. Let us instead look in more detail at the data on the concentration of toluene. In an expanded scale (Figure 1.22) it can be seen that, at least over the time interval involved, the reaction really shows no sign of reversibility. Given this, let us test the most simple approach to correlation, that based on the overall chemistry of scheme (i). (This assumes that a similar scale expansion for chlorine also shows no definite trend toward reversibility, which is indeed so). Then, why not try second-order irreversible, something corresponding roughly to equation (1-39)? Ah, beware! Do not follow blindly the prescription of that derivation because all of the assumptions there may not apply to the experiment we are considering here. So, let's go through everything in detail as if no prior derivation were available. We will use the following notation:

$a$  = initial concentration of toluene

$b$  = initial concentration of chlorine

$x$  = amount of toluene reacted (in concentration units)

If we neglect distinctions among ortho-, meta- and para-products (no information given), then  $x$  is the total conversion variable. These reactions were carried out in the liquid phase, so volume changes associated with reaction are negligible. The rate equation to try first is second-order irreversible

$$dx/dt = k(a - x)(b - x) \quad (\text{ii})$$

where  $k$  is the apparent rate constant. Then, after integration and some algebra

$$\frac{dx}{[x^2 - x(a+b) + ab]} = \int_0^t dt \quad (\text{iii})$$

$$\ln [(a-x)/(b-x)] = (a-b)(kt) + \ln (a/b) \quad (\text{iv})$$

According to the suggestions concerning linearization given in the text a plot of  $\ln [(a-x)/(b-x)]$  versus  $t$  should be a straight line. Such a plot of the data available is shown in Figure 1.23. This is obviously a good straight line, so the assumption of second-order kinetics seems to be a good one but can be claimed only for the range of conversion data upon which it is based. The slope of the line in Figure 1.23 is  $3.6 \times 10^{-5}$ , so from (iv):

$$k = 5.2 \times 10^{-4} \text{ liters/mol-s}$$

Remember that we used a little intuition here to decide that the reaction was probably not reversible under the conditions investigated. This worked out, but it may not always be this easy. One should also note that, within the context of building interpolation models bounded by the data available, these results are for a case where  $a \gg b$ . It is also possible to obtain a satisfactory correlation of the data with a rate equation that is pseudo-first-order in toluene

$$dx/dt = k'(a-x) \quad (\text{v})$$

where  $k'$  is a function of chlorine concentration. One might also expect that a reversible reaction model would work as well, with a rather small value of the reverse rate constant to be expected. Any of these will be an acceptable solution to the problem as posed; there is no right or wrong as long as the model provides an acceptable fit to the data within the range investigated. More detailed statistical analysis of the data-fits may differentiate among differing degrees of "acceptable".

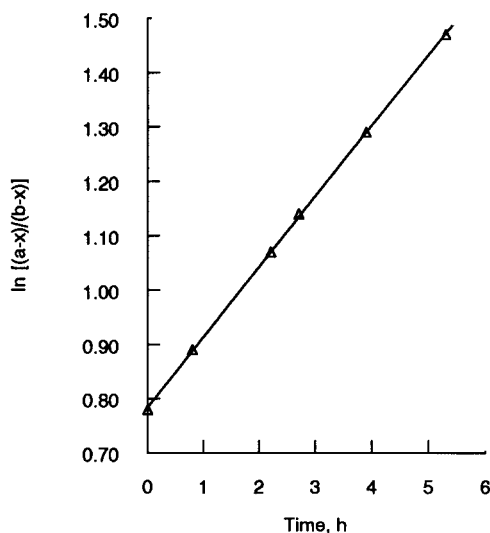


**Figure 1.23** Test of second-order kinetics for chlorination of toluene.



HORATIO SAYS

Remember that models such as those above are interpolation models and are no better than the data from which they are constructed. In the absence of further information they should not be extrapolated to other conditions.

### 1.9.3 Interpretation Methods: Additional Techniques

Most often for more complicated reactions than those discussed above, such as illustrated in Table 1.1b, direct methods of fitting conversion-time data become both tedious and difficult because of the convoluted form of the conversion equations and the number of rate constants incorporated in them. In such cases (and in the simpler ones also) the experimentalist can devise a number of special experiments which will simplify the subsequent task of interpretation. The most important of these are:

1. *Pseudo-order reactions*: When more than one component is involved in a reaction step (i.e., forward or reverse), one can identify separately the order with respect to the individual components by conducting experiments in which the initial concentration of one is set far in excess of the second. If we are considering the reaction  $aA + bB \rightarrow \text{products}$  in such a situation, for example

$$dC_A/dt = -k(C_A)^p(C_B)^q; \quad dC_B/dt = -v_B k(C_A)^p(C_B)^q \quad (1-197)$$

where  $v_B$  is the ratio of stoichiometric coefficients and the rate constant is based on the reaction rate of A. Now, if  $C_{A0} \gg C_{B0}$ , then the change in  $C_B$  is big compared to that in  $C_A$ , at least for small conversions, and the rate law effectively becomes

$$dC_B/dt = k'(C_B)^q \quad (1-198)$$

The values of  $k'$  and  $q$  can be obtained from conversion-time data by methods already discussed. Additionally, a second series of experiments is now run in which  $C_{B0} \gg C_{A0}$ , where:

$$dC_A/dt = k''(C_A)^p \quad (1-199)$$

The values of  $k''$  and  $p$  are evaluated, and thence the value of the true rate constant,  $k$ , from knowledge of  $p$ ,  $q$ ,  $v_B$  and the initial concentrations used. The kinetics given by equations (1-198) and (1-199) are said to be pseudo  $q$ th- or  $p$ th-order in B and A, respectively. An example of this procedure is given in Figure 1.24 for a simple second-order reaction and, indeed, has already been explored somewhat in Illustration 1.9. In the figure example  $p = q = 1$  the full process just described is not necessary; however, the two experiments provide replicate measurements of  $k$ .

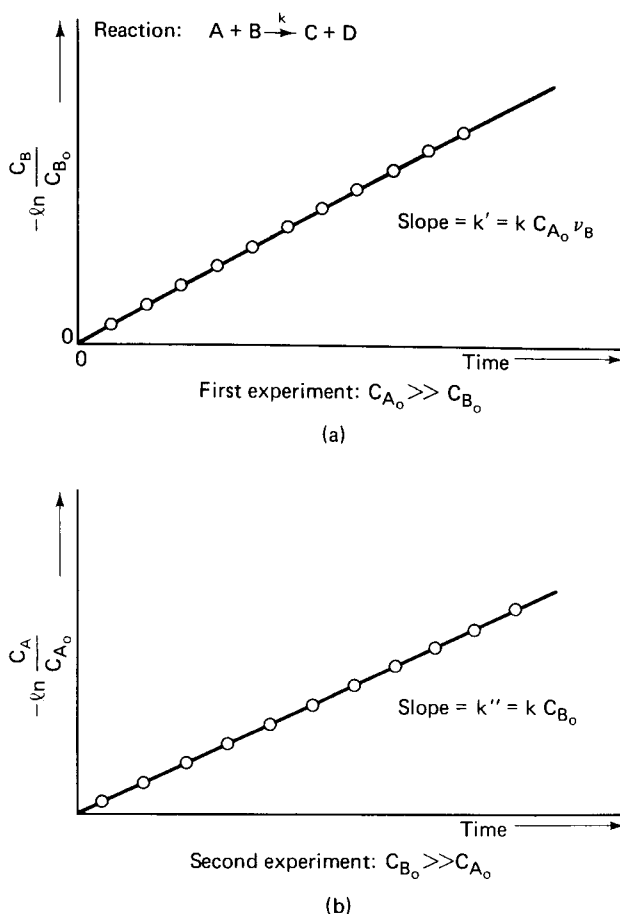


**Figure 1.24** Example of pseudo-order experiment for a second-order reaction.

Any deviation from the straight-line plot in either experiment would, of course, be indicative of  $p$  or  $q \neq 1$ . It is also wise to vary the levels of  $C_{A0}$  (for  $C_{A0} \gg C_{B0}$ ) and  $C_{B0}$  (for  $C_{B0} \gg C_{A0}$ ) to check the consistency of the interpretation of reaction order obtained from a single pair of experiments.

2. *Initial rates:* One of the requirements of the pseudo-order reaction was that the conversion be small, at least in the sense that the variation in one term be negligible compared to the other. Rates of reaction at low conversions (approaching zero) are called *initial rates* and correspond to the case depicted in Figure 1.25. Under these conditions great simplifications can be made in kinetic expressions for complex reactions, in particular for reversible reactions. Here we can consider a reaction  $aA + bB \leftrightarrow cC + dD$ , for which a general rate expression would be

$$dC_A/dt = -k_f(C_A)^p(C_B)^q + k_r(C_C)^u(C_D)^w \quad (1-200)$$

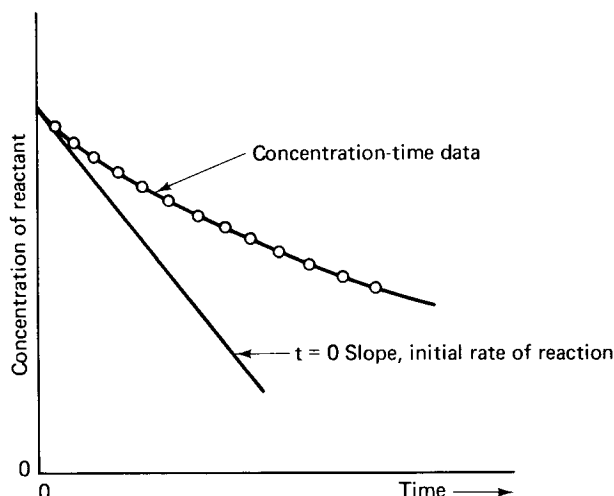


**Figure 1.25** Initial rate of reaction as determined from slope of tangent to conversion-time curve at zero conversion.

Now, if one conducts experiments under conditions such that  $C_{C0}$  and  $C_{D0}$  are zero, and the conversion of A is small, then

$$dC_A/dt = -k_f(C_A)^p(C_B)^q \quad (1-197)$$

and we have the same situation illustrated in the section above. A similar technique may be applied to the reverse reaction, of course. With no A or B initially,

$$dC_C/dt = -v_C k_r(C_C)^u(C_D)^w \quad (1-201)$$

where  $v_C = c/a$  and the rate constants  $k_f$  and  $k_r$  are based on the reaction of A.

3. *Definition of the maxima of intermediates:* Effectiveness of this method has already been demonstrated for the Type III system and arises from the fact that the net rate of reaction of intermediate is zero at the maximum, allowing one to work with the rate equation directly, rather than the integral time-conversion relationship. This is addressed in a number of the exercises given later.

By various combinations of these three methods, the kinetic constants of even very complex reactions can be obtained. At the least, one can expect to get preliminary values which can then be improved in obtaining a final fit to the conversion-time data.

There are also other techniques for treating experimental data, and other specific experiments possible, than the simple methods discussed here. Measurements of reaction half-life, as defined in equations (1-45), are directly related to rate constants and also provide a simple means for determination of reaction

order. From the expression for irreversible reaction of order  $n \neq 1$ :

$$t_{1/2} = \frac{2^{n-1} - 1}{k(n-1)(C_{A0})^{n-1}} \quad (1-45a)$$

$$t_{1/2} = \frac{\ln 2}{k} \quad (1-45b)$$

with  $n = 1$  in equation (1-45b). For all values of  $n$ ,  $t_{1/2}$  can be written generally as

$$t_{1/2} = \frac{f(n, k)}{C_{A0}^{n-1}} \quad (1-202)$$

or

$$\ln t_{1/2} = \ln f(n, k) - (n-1) \ln C_{A0} \quad (1-203)$$

where  $f(n, k)$  is some functional relationship pertaining to given kinetics and is a constant for constant temperature. Experimentally, we conduct two runs at the same temperature but different initial concentrations,  $(C_{A0})_1$  and  $(C_{A0})_2$ , measuring the half-life in each. For each of these a relationship of the form of equation (1-203) exists; if the two are subtracted,  $f(n, k)$  disappears since it is constant for the given temperature, and we may solve directly for  $n$ :

$$n = 1 + \frac{\ln (t_{1/2})_2 - \ln (t_{1/2})_1}{\ln (C_{A0})_1 - \ln (C_{A0})_2} \quad (1-204)$$

Graphically, a plot of  $\ln(t_{1/2})$  versus  $\ln(C_{A0})$  should be a straight line according to equation (1-203), and the order determined directly from the slope, as shown in Figure 1.26. Similar methods of interpretation may be devised employing other fractional-life periods with differing initial concentrations, or successive time intervals in a single run. Remember that half-life refers to the time required for half the initial reactant to be consumed, not to half the total time of reaction.

If direct information on rates of reaction is available, many of the tasks of interpretation are simplified, since one may work directly with the rate equations.

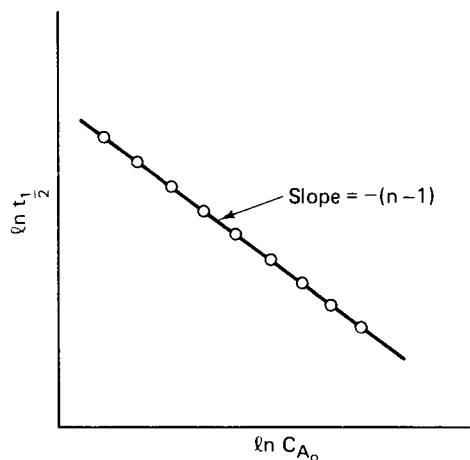


**Figure 1.26** Graphical analysis of half-life data for reaction order.

The information required here is not concentration versus time, but rate of reaction versus concentration. As will be seen later, some types of chemical reactors give this information directly, but the constant-volume, batch systems discussed here do not [“What does it profit you, anyway?”—*F. Villon*]. In this case it is necessary to determine rates from conversion-time data by graphical or numerical methods, as indicated for the case of initial rates in Figure 1.25. In Figure 1.27 a curve is shown representing the concentration of a reactant A as a function of time, and we identify the two points  $C_{A1}$  and  $C_{A2}$  for the concentration at times  $t_1$  and  $t_2$ . The mean value for the rate of reaction we can approximate algebraically by

$$\frac{d\bar{C}_A}{dt} \approx \frac{C_{A2} - C_{A1}}{t_2 - t_1} \quad (1-205)$$

or can determine graphically from the slope of the tangent to the curve at the midpoint of the interval. The two methods do not generally give the same result, as Figure 1.27 illustrates. The success of such approximation obviously depends critically upon the precision of the data and the size of the interval. However, assuming a satisfactory approximation can be obtained, we may analyze the rate expression directly. For example,

$$\frac{dC_A}{dt} = -k(C_A)^n \quad (1-43)$$

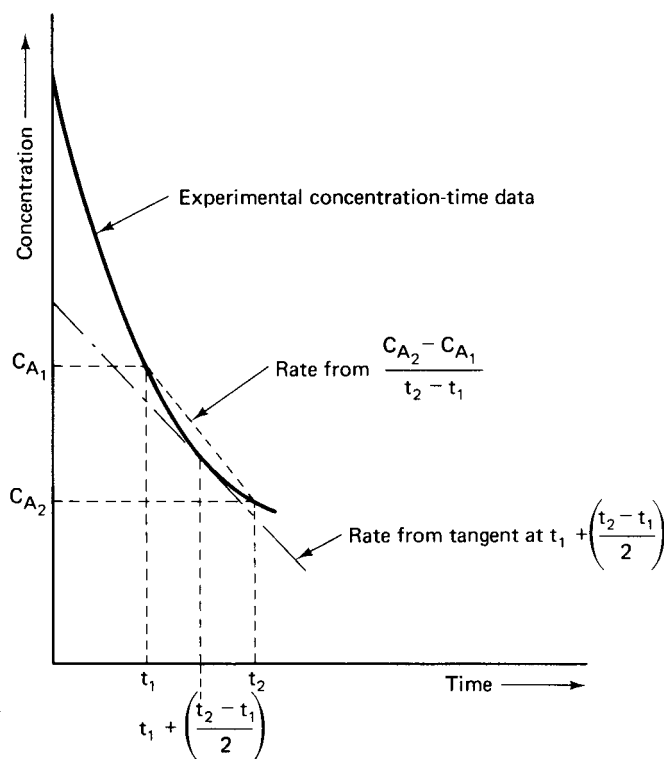


**Figure 1.27** Graphical evaluation of rate from concentration-time data.

can be written

$$\ln \left[ - \left( \frac{dC_A}{dt} \right) \right] = n \ln C_A + \ln k \quad (1-206)$$

and a series of rates with corresponding concentrations plotted on logarithmic coordinates should give a straight line of slope  $n$  (order) and intercept  $\ln k$  (rate constant). Similar methods for more complicated kinetics can easily be devised by the reader. It is important to keep in mind that the translation of data on concentration versus time to rate versus concentration is generally not an easy one. Differentiation of experimental data introduces noise in the result so that the advantages of working with simpler mathematics may be offset by the poorer quality of the information one has to work with. Such difficulties are particularly pronounced with respect to initial rates. A special warning applies to the procedure of making polynomial fits, by least squares or other means, to conversion-time data and then attempting to obtain rates by analytical differentiation of the resulting expressions.

#### 1.9.4 Patterns

Upon looking back at these sections on descriptive kinetics, one may be struck by the fact that all rate laws describe graphical patterns which, in fact, have been employed in the analysis of Section 1.9.2. There is one further thing we can do here to exploit this in interpretation of kinetics. Suppose we have a normal  $n$ th-order irreversible rate law

$$(dC/dt) = -kC^n \quad (1-43)$$

and define the conversion in the normal way

$$x = 1 - C/C_0$$

Now, let us define a scaled time variable,  $\tau$ , as

$$\tau = (x/t) \quad (1-207)$$

The solution of the corresponding equations in terms of  $\tau$  is very indicative of reaction order. Figure 1.28 shows how the values of  $(\tau)/(\tau)_0$  depend upon  $x$  for various reaction orders. For  $n = 0$  and 2 the lines are straight. Otherwise for  $n > 2$  the curvature is upward and for  $n < 2$  the curvature downward. For  $n \geq 1$ , the intercept at  $x = 1$  is zero, and for  $n < 1$  it is greater than zero. These curves are very distinct and allow one, given some intuition that the reaction in question is  $n$ th-order and irreversible, to estimate both the rate constant and the reaction order.

The detailed procedure is not complicated. First one plots  $\tau$  versus  $x$  from experimental data, keeping in mind the general shapes of the curves in Figure 1.28. This gives an indication of the order of reaction, thence the rate constant is evaluated as  $\tau_0/(C_0)^{1-n}$ , where  $\tau_0$  is the initial ( $x = 0$ ) intercept. For any order, the slope of the initial linear section of the plot ( $x \rightarrow 0$ ) is given by  $(-n\tau_0/2)$ . Thus the method provides a quick means for the estimation of reaction order and associated rate constant [E.M. Holleran, *Chemtech*, 500, August, (1981)]. A check on estimated order is provided by looking at the intercept at  $x = 1$ ,  $(\tau/\tau_0)_1$ . This should be equal to  $\tau_0/(1 - n/2)$ , as shown later.

In application, consider the hydrolysis of sucrose catalyzed by aqueous HCl. This is a single phase reaction with no volume change; experimental data are given in



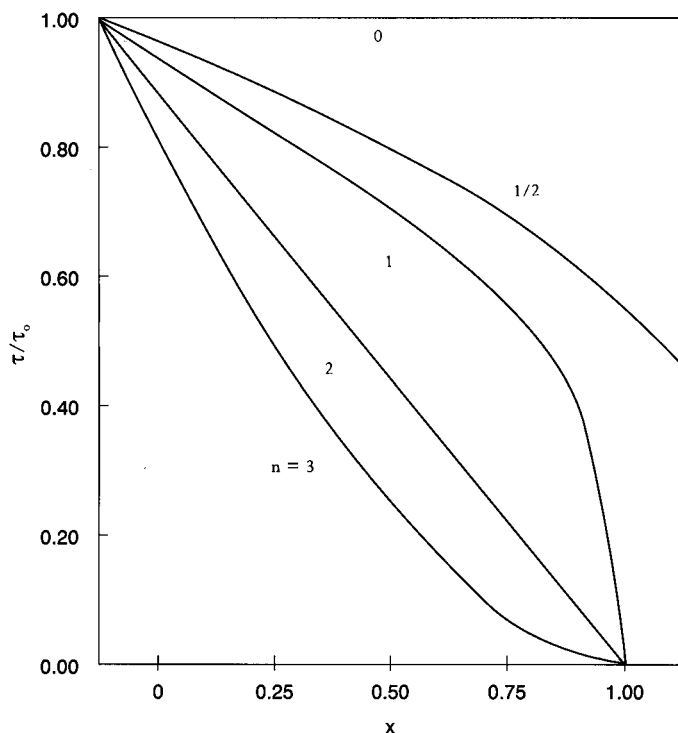


**Figure 1.28** Scaled time  $\tau$  for various orders of reaction  $n$ .

Table 1.8 [R. Alberty and F. Daniels, *Physical Chemistry*, 5th ed., John Wiley and Sons, New York, NY, (1978)]. A corresponding plot of  $\tau$  versus  $x$  is shown in Figure 1.29. A first-order law is strongly suggested by the shape of the curve upon comparison with Figure 1.28; however, if one is not convinced by this geometry it is still possible to look at extrapolation of the initial, linear portion of the plot. If  $n = 1/2$  the intercept at  $x = 1$  would be  $(\tau_0/4)$ ; if  $n = 3/2$  the intercept would be  $(3\tau_0/4)$ . It is apparent that one is too high and one is too low, thus  $n = 1$ . The  $k$  values corresponding are also given in Table 1.8. This is a reasonable analysis for engineering purposes, but it would be fruitful to see how sensitive the method is to experimental error.

**Table 1.8** Data for the Hydrolysis of Sucrose

$t$ , min	Sucrose remaining, %	$x$	$\tau \times 10^3$	$k$ , min <sup>-1</sup>
9.82	96.5	0.035	3.60	3.60
59.60	80.3	0.197	3.31	3.68
93.18	71.0	0.290	3.11	3.67
142.9	59.1	0.409	2.86	3.68
294.8	32.8	0.672	2.28	3.77
589.4	11.1	0.889	1.51	3.73

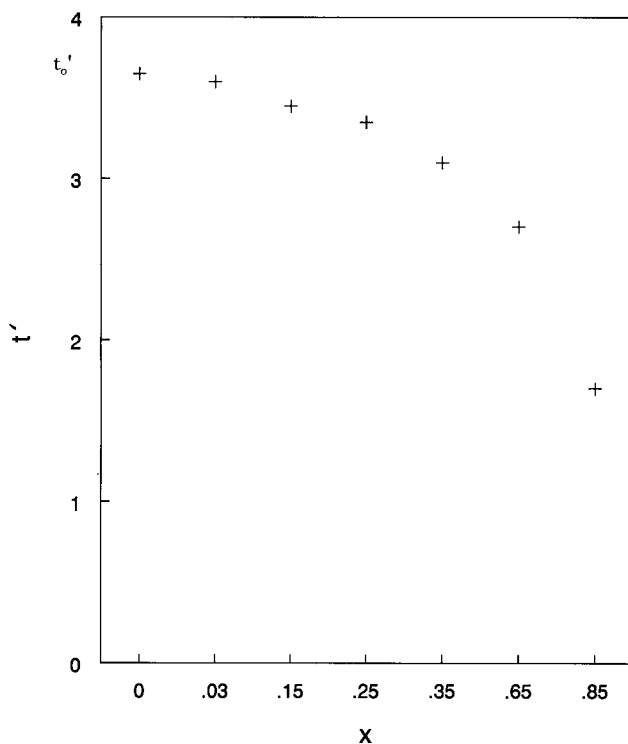


**Figure 1.29** Plot of  $t'$  versus  $x$  for the hydrolysis reaction;  $n = 1$ .

### Illustration 1.10

In the discussion of patterns many statements were made without justification as to the behavior of the function  $\tau = (x/t)$ . Show the origin of the analysis given, particularly as to the interpretation of slopes, intercepts and reaction orders.

#### Solution

Equation (1-43), as shown before, integrates to two forms depending upon whether  $n = 1$  or not. To start with the first-order form

$$\begin{aligned}\tau &= -(kx)/[\ln(1-x)] \\ &= k(1 - x/2 - x^2/12 - \dots)\end{aligned}\tag{i}$$

where (i) is obtained by expanding  $\ln(1-x)$  from equation (1-43) and eliminating  $t$ . From equation (i) we find the initial intercept,  $\tau_0$ , the initial slope,  $(\tau_0)'$ , and the final intercept,  $\tau_1$  at  $x = 1$ , to be

$$\begin{aligned}\tau_0 &= k \\ (\tau_0)' &= -(\tau_0/k) \\ \tau_1 &= 0\end{aligned}\tag{ii}$$

from which

$$\begin{aligned}\tau &= (n-1)k(C_0)^{n-1}x/[(1-x)^{1-n} - 1] \\ &= k(C_0)^{n-1}[1 + (n/2)x + n(n-2)x^2/12 + \dots]\end{aligned}\quad (\text{iv})$$

For  $n = 0$ ,  $\tau$  is independent of  $x$  and equal to  $(k/C_0)$ . For  $n = 2$ ,  $\tau$  is linear in  $x$  and equal to  $kC_0(1-x)$ . Also, from equation (iv) we find that

$$\tau_0 = k(C_0)^{n-1} \quad \text{and} \quad (\tau_0)' = -(n/2)\tau_0 \quad (\text{v})$$

The final intercept is, from equations (ii) and (iv)

$$\begin{aligned}\tau_1 &= 0 \quad \text{for } n \geq 1 \\ \tau_1 &= (1-n)\tau_0 \quad \text{for } n \leq 1\end{aligned}\quad (\text{vi})$$

For  $n > 1$ ,  $\tau_1$  is zero because the time to completion of reaction ( $x = 1$ ) is infinite. For  $n < 0$  the reaction is complete in a finite time,  $\tau_1 = 1/[(1-n)\tau_0]$ . For  $n = 0$  this is  $(C_0/k)$  and for  $n = 1/2$  it is  $(2C_0^{1/2}/k)$ .



HORATIO SAYS

All seems to be fair in love, war, and the fitting of kinetic data. "...may humanity after victory be the predominant feature..."—*Horatio Nelson*.

## Exercises

### Section 1.1

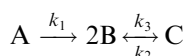
1. The chemical reaction  $A \rightarrow 2B + C$  involving ideal gases is carried out at constant temperature and pressure. Initially there is no B or C present and the rate is measured to be  $M$  mols of A reacted per time per liter. If the amount of A reacting per time does not change as the reaction proceeds, what would be the rate of this reaction when half the original A has disappeared?
2. In the reaction of Problem 1, what is the rate of appearance of B initially? After half the A has reacted?
3. What is the distinction between the time variable employed in the rate-of-reaction definition and that pertaining to the time of operation of a process in which a chemical reaction occurs?
4. Derive an analytical expression for the rate of disappearance of reactant in the ideal gas reaction



at constant temperature and pressure. No B is present initially and  $N_{A0}$  mols of A. The specific volume of the reaction mixture is  $v$  and does not change with conversion. Let  $x$  be the number of mols of A reacted at any time.

### Section 1.2

5. If the rate constant  $k$  for the disappearance of A in Problem 4 is  $M$  mols/volume-time at initial conditions, what is the corresponding constant for the appearance of B under the same conditions?
6. In which case(s) illustrated in Table 1.1a does the order of reaction correspond to stoichiometry?
7. A series of reactions



occurs in which order conforms to stoichiometry. Write the rate equation for the net rate of reaction of B. The individual rate constants are defined per mol of reactant in the separate steps.

### Section 1.3

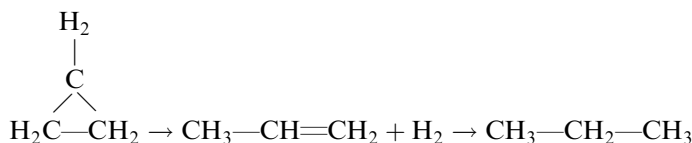
8. Suppose there is a reaction for which the activation energy is reported to be 45 kcal/mol. By what factor will the rate constant increase between 298 and 308°K? Suppose the activation energy is not 45 but 30 kcal/mol. What is the corresponding increase? Finally, suppose the activation energy is not really 45 kcal/mol, but is  $45 \pm 2$  kcal/mol. What then are realistic limits for the projection of rate from 298 to 308 K° (or maybe 328°K, for fun) compared to the base of 45 kcal/mol?
9. For a reversible elementary step, what relationship does the temperature dependence of the equilibrium constant have to the individual activation energies, forward and reverse?
10. For some reactions involving atoms or free radicals, the activation energies are very small and the temperature dependence of  $k^\circ$  in the Arrhenius equation is not negligible compared to the exponential term. A more accurate relationship is

$$k = (k^\circ) T^n e^{-E(fr)/RT}$$

What is the relationship between  $E(fr)$  and the activation energy employed in equation (1-25)?

11. The specific rate (turnover frequency) for hydrogenation of propene on a Pt/SiO<sub>2</sub> catalyst is 0.04 molecules reacted per surface Pt atom per second at -57°C when H<sub>2</sub>/C<sub>3</sub> is 14:1, and the activation energy is  $43.5 \times 10^6$  J/kmol. For cyclopropane hydrogenation the turnover frequency on the same catalyst is 0.15 at 0°C for the same feed concentration, and the activation energy is  $40.2 \times 10^6$  J/kmol [P.H. Otero-Schipper, W.A. Wachter, J.B. Butt, R.L. Burwell, Jr. and J.B. Cohen, *J. Catal.*, 50, 494 (1977)].
  - (a) What is the ratio of turnover frequencies for these reactions at -40°C under these conditions?

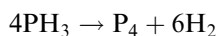
(b) It has been proposed that the hydrogenation of cyclopropane goes by the following reaction sequence on Pt/SiO<sub>2</sub> catalysts:



Based on the results of part (a), would you expect to be able to identify propene as an intermediate in this reaction at  $-40^\circ\text{C}$ ?

### Section 1.4

12. Verify that the sum of the elementary steps in reaction mechanism (IV) gives the overall reaction (III).
13. The decomposition of phosphine,

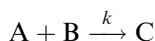


at  $650^\circ\text{C}$  is a gas-phase reaction and is irreversible. The dissociation is first-order and the reaction-rate constant is given by

$$\log_{10} k = -(18,963/T) + (2) \log_{10} T + 12.13$$

where  $k$  is in  $\text{sec}^{-1}$  and  $T$  is in  $^\circ\text{K}$ . Assuming that a closed vessel of constant volume is charged with the gas at 1 atm initially, what is the pressure at the end of 50, 100, 150 and 500 sec?

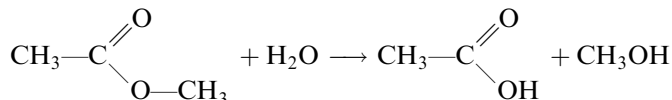
14. An irreversible reaction occurs as follows:



The order conforms to stoichiometry. Normally the reactants, preheated to reaction temperature, are charged in eqimolar proportions to a vessel and allowed to react for 10 h. This time is required to accomplish 99% conversion of B. Since it is quite easy to separate A from product C by physical means, it has been proposed that the charging proportions be changed to two A to one B in the hope of getting the reaction to go so much faster that the overall productivity will be improved. A 99% conversion of B is always necessary and the total volume of A and B charged is the same in the two cases. Is this proposal valid?

15. The fermentation of sucrose by yeast, one of man's most beloved reactions, is irreversible and zero-order in sucrose (yeast acts as a catalyst). When 4 g of sucrose ( $\text{C}_{12}\text{H}_{22}\text{O}_{11}$ ) in  $500\text{ cm}^3$  was fermented with 4 g catalyst, the half-life observed was 30 min.
  - (a) Determine the rate constant for the reaction; give the units.
  - (b) How long does it take to prepare a good jug of wine using 3 lb of sugar and 4 g of yeast? (For flavor, add three strawberries). The presiding oenologist knows half-lives, and says that two are about right. You may assume starting with the same sucrose concentration as in part (a), and that the rate constant is proportional to the weight ratio of yeast to sucrose.

16. The reaction



has been shown to be autocatalytic in acetic acid. The following data have been reported:

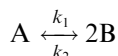
$$C_0 \text{ (acetate)} = 0.5 \text{ gmol/liter}$$

$$C_0 \text{ (acetic acid)} = 0.05 \text{ gmol/liter}$$

$$T = 40^\circ\text{C}$$

After 1 h the acetate concentration is 0.2 gmol/liter. At what time does the rate reach a maximum?

17. A group of workers investigating the reaction



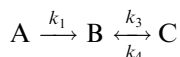
under isothermal, constant volume conditions report the equilibrium conversion to B as the following

$$(C_B)_{\text{eq}} = \frac{1}{2k_2} [-(2k_2C_{A0}) + k_1] + \sqrt{(2k_2C_{A0} + k_1)^2 + 8k_1k_2C_{A0}}$$

where  $C_{A0}$  is the initial concentration of A and no B was present initially. The statement is made that “order conforms to stoichiometry”; prove or disprove this statement.

### Section 1.5

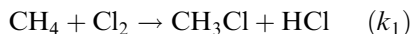
18. The following reaction is carried out under isothermal, constant-volume conditions:



Suppose that the starting charge to the reactor is  $(C_{A0} + C_{B0})$  with  $C_{B0}$  having the specific value  $(C_B)_{\text{eq}}$ , the equilibrium concentration. Thus, B starts and ends at the same concentration. What is the necessary value of  $C_{B0}$  in terms of the reaction velocity constants and  $C_{A0}$ ? What relationships among  $k_1$ ,  $k_3$ , and  $k_4$  are required for a maximum of B to exist during the course of the reaction? Order conforms to stoichiometry.

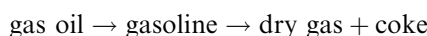
19. Successive substitution reactions are very important in some organic syntheses. A good example is the chlorination of methane, which can

be considered to go in four steps as follows:

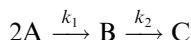


Derive the expressions that relate the concentrations of the mono- and dichloro intermediates to the amount of methane reacted in an isothermal, constant-volume system. The initial concentrations of methane and chlorine are  $C_{M0}$  and  $C_{C0}$ , respectively. There are no products present initially. (*Hint*: working with the rate equations directly is difficult. Eliminate the time variable.) At what conversion(s) do maxima in these intermediates occur if all the rate constants are the same?

20. A kinetic model for the catalytic cracking of gas oil cycle stocks has been proposed as follows [V.W. Weekman, Jr., *Ind. Eng. Chem. Proc. Design Devel.*, 7, 90 (1968); 8, 388 (1969); V.W. Weekman, Jr. and D.M. Nace, *Amer. Inst. Chem. Eng. J.*, 16, 397 (1970)]:

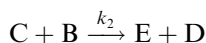
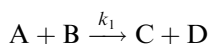


which can be represented roughly by the following sequence:



with order corresponding to stoichiometry, and  $k_1$  defined per mol of A reacted. Derive an expression for the yield and selectivity of gasoline formation according to this model. Assume isothermal reaction with constant volume.

21. Consider the successive reactions



Derive the expression by which the ratio  $(k_2/k_1)$  can be determined from experimental conversion data (i.e., products C and E versus A). The initial concentrations of C and E are zero. For the special case  $C_{A0} = 400$ ,  $C_{B0} = 300$ ,  $(k_2/k_1) = 0.5$ , what is the ratio of E to C at the completion of the reaction?

22. (a) It is stated in the text that differential selectivity for the Type II system is defined in terms of consumption of reactant in order to work with positive numbers. Yet, an analogously defined differential selectivity for a Type III reaction gives negative values for certain ranges of intrinsic selectivity and reaction mixture composition as shown in Figure 1.9. What is the significance of these negative values?
- (b) Derive equation (1-76) for the yield in a Type II system.

## Section 1.6

23. Using the pssh approach, derive the proagation rate equations shown in Table 1.2 for cases B, C and D.
- 24.\* The following mechanism has been proposed for the thermal decomposition of acetone:



Derive an expression for the overall rate of reaction,  $d[\text{CH}_3\text{COCH}_3]/dt$ , and calculate the corresponding activation energy.

- 25.\* In the polymerization reactions



if the rate constants are identical, the integrated rate equation has the form

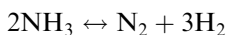
$$y = akt \left[ \frac{4 + kt}{(2 + kt)^2} \right]$$

where  $y$  represents the total amount of polymer:

$$y = \sum_{i=2}^n A_i$$

The initial amount of monomer A is  $a$ , the rate constant  $k$ , and  $t$  the time of reaction. What is the polymerization rate? Derive this rate equation.

26. The pseudo steady state hypothesis and the long chain approximation are encountered constantly in publications concerning chain reactions. Find in the recent literature a paper using this analysis. Describe the problem addressed by the authors, the reaction and chain mechanism proposed, and the analysis employed. Then see whether you agree with the result and the interpretation proposed in the paper.
27. Write a chain mechanism for the decomposition of ammonia:




---

\* Problems 24 and 25 from W.J. Moore, *Physical Chemistry*, 2nd ed., reprinted by permission of Prentice-Hall, Inc., Englewood Cliffs, NJ (1955).



Over a silica surface, the observed rate has been correlated by

$$-\frac{d[\text{NH}_3]}{dt} = \frac{kP_{\text{NH}_3}}{1 + K_1 P_{\text{H}_2} + (K_2 P_{\text{H}_2}/P_{\text{NH}_3})}$$

What might be the role of the surface in this chain?

### Section 1.7

- 28.\* The ammonia synthesis reaction is run in a suitable reactor at 450°K under conditions such that equilibrium is attained at the reactor outlet.
- (a) What are the mol fractions of N<sub>2</sub>, H<sub>2</sub>, and NH<sub>3</sub> exiting the reactor at 4 atm operating pressure?
  - (b) What will be the exit mol fractions if the reactor, again operated at 4 atm, is fed an equimolar amount of N<sub>2</sub>, H<sub>2</sub> and an inert diluent?
  - (c) The reaction is to be run in an isothermal, constant-volume reactor with a feed of stoichiometric amounts of N<sub>2</sub> and H<sub>2</sub>. Here the initial pressure is 4 atm. What are the species mol fractions and the pressure in the reactor when equilibrium is attained?
- 29.\* An equimolar mixture of benzene and ethylene at 370°K is fed into a reactor where ethylbenzene is formed. Separate experiments show that at 1 atm an equilibrium mixture is obtained. If the reactor is operated isothermally, what is the concentration of species at the reactor exit? What would you do with this analysis if the reactor were operated adiabatically?
30. What is the equilibrium of the ammonia synthesis reaction at the following conditions:
- a) 600°K, 1 atm
  - b) 600°K, 50 atm
  - c) 800°K, 1 atm
  - d) 800°K, 50 atm

Report concentrations on the basis of equimolar amounts of reactants. How does this relate to the question posed in problem 28?

### Section 1.8

31. A reaction that can be modeled by Type III kinetics is carried out in a batch reactor, and it is desired to obtain the maximum production of intermediate B per time. Operation at either 100 or 200°C is possible and which is chosen depends on the overall economics of the operation. The cost of heating is estimated to be \$0.01/°C\*-unit C<sub>B</sub>/C<sub>A0</sub>-h, where °C\* is the difference between the temperature of operation and room temperature, 20°C. Product value is \$5.00 per (C<sub>B</sub>/C<sub>A0</sub>) unit, and equal times are required for charging and discharging the reactor at both temperatures,

---

\* Problems 28 and 29 adapted from S.I. Sandler, *Chemical and Engineering Thermodynamics*, 2nd ed., reprinted by permission of John Wiley and Sons, New York, NY (1989).

0.5 h. No reaction occurs during this period. At 100°C,

$$(E_1/R) = 5560^\circ\text{K}$$

$$(E_2/R) = 7570^\circ\text{K}$$

$$k_1 = 1 \text{ h}^{-1}$$

$$k_2 = 0.1 \text{ h}^{-1}$$

32. Consider a first-order irreversible reaction for which  $k = 0.5 \text{ h}^{-1}$  at 200°C and  $10 \text{ h}^{-1}$  at 250°C. Suppose that this reaction is initiated by heating the charge from 30 to 230°C in 1 h at a constant rate of heating. Calculate the conversion when 230°C is reached. Compare the expression

$$k = k^\circ e^{-E/RT}$$

with the approximation

$$k = a^\circ (T/T_0)^n$$

for this problem.

33. Direct combination of nitrogen and oxygen is carried out at 4000°F until equilibrium is attained; then the gases are cooled quickly to retard the reverse reaction. The reaction is second order overall in both directions, with the rate equation

$$r = \frac{d(P_{\text{NO}})}{dt} = k_1 [P_{\text{N}_2} P_{\text{O}_2} - (P_{\text{NO}})^2 / K]$$

The rate constant is given as

$$\log_{10}(k_1/3) = [(T - 3800)/300]$$

$$T = ^\circ\text{F}$$

$$k_1 = \text{forward rate constant, (atm} - \text{sec)}^{-1}$$

Determine the mol fraction of NO present versus time and temperature for a cooling rate of 30,000°F/sec, starting at 4040°F and operating at atmospheric pressure. The following data are available for the equilibrium constant  $K$

$T(^{\circ}\text{F})$	1700	2060	2420	2780
$K = \frac{P_{\text{NO}}}{[P_{\text{O}_2} P_{\text{N}_2}]^{1/2}}$	$5.26 \times 10^{-4}$	$1.92 \times 10^{-3}$	$5.08 \times 10^{-2}$	$1.08 \times 10^{-2}$
$T(^{\circ}\text{F})$	3140	3500	3860	4040
$K = \frac{P_{\text{NO}}}{[P_{\text{O}_2} P_{\text{N}_2}]^{1/2}}$	$1.98 \times 10^{-2}$	$3.25 \times 10^{-2}$	$4.91 \times 10^{-2}$	$5.89 \times 10^{-2}$

34. While it is relatively simple to define the trends in point or differential selectivity with temperature in the examples discussed in the text, the trends of yield and overall selectivity are more complicated, since their expressions are not conveniently written in terms of rate-constant ratios.

In batch operation, however, these are more pertinent measures of efficiency than point selectivity. Demonstrate the dependence of the yield of B,  $Y_B(\text{III})$  [equation (1-91)] for systems in which  $E_1 > E_2$  and  $E_1 < E_2$  in the special case where  $(k^\circ)_1 = (k^\circ)_2$ .

35. Borchardt and Daniels [H.J. Borchardt and F. Daniels, *J. Amer. Chem. Soc.*, 79, 41 (1957)] were among the first to report a simple method for determining the kinetics of irreversible reactions using differential thermal analysis. Although specific designs of DTA equipment vary, generally the reactive substance (solution) to be studied is placed in a sample cell and an inert solution in a reference cell. The reference solution is selected to have approximately the same thermal conductivity and heat capacity as the reactant solution, and the two cells are so designed and agitated that equal heat transfer coefficients will be attained when the cells are immersed in a temperature bath. Within the bath, the temperature is normally changed such that the temperature of the reference cell,  $T_r$ , increases with time in a linear manner. In the absence of reaction the temperature of the sample cell,  $T$ , will also increase linearly and equal  $T_r$ . When an exothermic reaction occurs in the sample cell, the temperature  $T$  will be greater than  $T_r$ , and the difference  $\Delta T = T - T_r$  can be recorded, as well as the actual reference temperature. The outcome of the experiment is a record of  $\Delta T$  versus time, as shown in Figure 1.30.

(a) From a heat balance on the system, show how the heat of reaction can be determined from the DTA curve. Use the following notation:

$C_p$  = specific heat of reaction and reference mixture

$U$  = heat transfer coefficient for total cell area

$\alpha = (C_p/U)$

$k$  = rate constant in  $[d(N/V)/dt] = k(N/V)^n$

$N$  = mols reactant ( $N_0$  at  $t = 0$ )

$V$  = volume of reactant solution

$n$  = order of reaction

$t$  = time

(b) Using the result of the heat of reaction determination, eliminate this quantity and  $N$  (since this is not measured in DTA) from your heat balance. Derive an expression, making use of properties that can be observed or calculated from the DTA graph, which can be employed to determine the

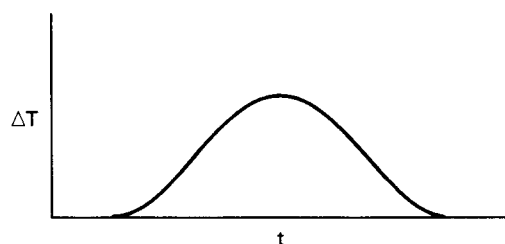


Figure 1.30 Typical DTA result for an irreversible exothermic reaction.

rate constant (expressed as a frequency factor and activation energy) and the order of reaction from a series of DTA experiments. Show how you would do this. (The final form of the equation will require assumption of one of the three parameters and subsequent checking for internal consistency.)

36. The following data pertain to the first-order reversible reaction  $A \leftrightarrow B$ :

$$k_f = (4 \times 10^{13}) \exp(-25,000/RT) \text{ days}^{-1}$$

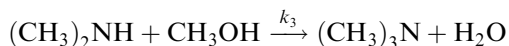
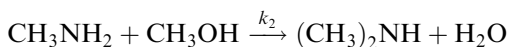
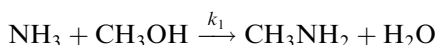
$$k_r = (6.67 \times 10^{14}) \exp(-30,000/RT) \text{ days}^{-1}$$

where  $T$  is in  $^{\circ}\text{K}$  and  $R = \text{cal/gmol} - \text{K}$ . Determine the equilibrium conversion at  $510^{\circ}\text{K}$  for an initial composition of 1 unit of A and 0.1 unit of B. A conversion of 99.1% of this equilibrium value is sought. What is the optimum isothermal temperature (minimum reaction time) for this conversion?

37. Calculate the optimal temperature program, including temperature versus conversion and the absolute minimum time, for the reaction of problem 36.

### Section 1.9

38. Consider the reactions

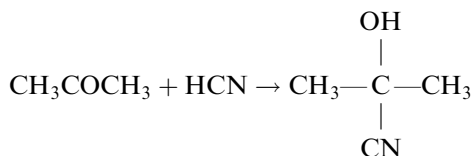


All are irreversible. Some laboratory data obtained under isothermal conditions are given below, where  $a$  is the initial concentration of  $\text{NH}_3$ ,  $y_1$  the concentration of  $\text{CH}_3\text{NH}_2$ ,  $y_2$  that of  $(\text{CH}_3)_2\text{NH}$ , and the corresponding fraction  $\text{NH}_3$  unconverted  $(a - x)/a$ . From these data determine the relative values  $(k_2/k_1)$  and  $(k_3/k_1)$ . How would you go about determining absolute values for  $k_1$ ,  $k_2$  and  $k_3$ ? Note that there are maxima in the concentrations of both intermediates, as expected, but that  $y_2$  occurs at a high value of ammonia conversion. A prudent accounting for the possible effects of experimental error will be important in the analysis of these data.

Experimental data for the ammonia-methanol reaction:

$\frac{a-x}{a}$	$\frac{y_1}{a}$	$\frac{y_2}{a}$
0.9	0.10	0.02
0.8	0.18	0.03
0.7	0.26	0.04
0.6	0.34	0.06
0.5	0.39	0.11
0.4	0.43	0.21
0.3	0.45	0.22
0.2	0.43	0.30
0.1	0.35	0.39
0.05	0.26	0.45
0.01	0.11	0.40

39. The reaction



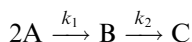
was carried out in aqueous solution by Svirbley and Roth [W.J. Svirbley and J.F. Roth, *J. Amer. Chem. Soc.*, 75, 3106 (1953)]. Typical data were as follows:

Time (min)	Concentration of HCN
4.37	0.0748 <i>N</i>
73.23	0.0710 <i>N</i>
172.5	0.0655 <i>N</i>
265.4	0.0610 <i>N</i>
346.7	0.0584 <i>N</i>
434.7	0.0557 <i>N</i>

Initial HCN concentration = 0.0758 *N*; initial acetone concentration = 0.1164 *N*

Determine a reasonable interpretation for the kinetics of this reaction with the values of the appropriate rate constants.

40. The series reaction:



has been studied in a constant-volume, batch reactor under isothermal conditions with the following results:

Time (h)	Concentration (mole/volume)		
	A	B	C
0	1.0	0	0
0.03	0.76	0.098	0.02
0.06	0.63	0.122	0.06
0.1	0.51	0.140	0.10
0.15	0.39	0.120	0.17
0.2	0.33	0.10	0.24
0.3	0.25	0.05	0.32

Assuming that the order conforms to stoichiometry, what are the values of  $k_1$  and  $k_2$ ?

41. The following data were obtained in an experiment to determine the rate constant of a half-order irreversible reaction (no volume change).

initial concentration = 0.78 M

concentration at  $t = 15 \text{ min} = 0.43 \text{ M}$

average error in time measurement =  $\pm 3 \text{ sec}$

average error in concentration measurement =  $\pm 0.01 \text{ M}$

What is the expected error in rate constant determination?

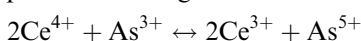
42. Gorin, Fontana and Kidder [E. Gorin, C.M. Fontana, and G.A. Kidder, *Ind. Eng. Chem.*, 40, 2135 (1948)] report data on methane chlorination in a KCl/CuCl<sub>2</sub> melt at 500°C. Individual runs were carried out with different reaction times and a significant amount of side-reaction products were observed. The individual yields are set so that their sum for a given time of reaction equals 100%.

Data for methane chlorination:

% Conversion of CH <sub>3</sub>	Yield of Product as % of CH <sub>2</sub> Reacted				
	CH <sub>3</sub> Cl	CH <sub>2</sub> Cl <sub>2</sub>	CHCl <sub>3</sub>	CCl <sub>4</sub>	Other
12.7	62.3	21.7	7.1	2.4	6.5
14.9	56.6	19.1	10.1	—	1.4
17.6	54.6	25.4	10.0	—	10.0
17.1	56.5	24.6	10.6	2.4	5.9
18.5	55.2	25.5	9.9	1.1	8.3
25.5	45.2	25.6	18.0	6.1	5.1
27.3	41.3	21.4	12.8	1.8	22.7
27.2	42.2	24.4	20.1	6.2	7.1
30.6	40.0	25.8	11.9	3.9	18.4
30.0	41.3	28.6	12.7	4.4	13.0

Use the results of problem 19 to estimate the ratios of the rate constants for the first three steps of the reaction to one significant figure.

43. What is the harm in differentiating polynomial fits of conversion-time data in order to obtain corresponding rate-conversion information?
44. From the conversion-time data of Problem 38, determine the corresponding rate-conversion information. Use this directly in the rate equation you postulated on the basis of the integral conversion data and compare the resulting rate constant with your previous values.
45. Below are data for the reaction of Ce<sup>4+</sup> and As<sup>3+</sup> in a homogeneous phase according to



<i>t</i> , min	[Ce <sup>4+</sup> ], mol/l	<i>x</i>	$\tau \times 10^3$
0	0.023	0	—
70	0.019	0.175	2.50
130	0.017	0.269	2.07
272	0.014	0.406	1.49
335	0.013	0.444	1.33
399	0.012	0.479	1.20

Initially [C<sup>4+</sup>] = 2[As<sup>3+</sup>]. Using the methods of Section 1.9.4, make an interpretation of these data.

### Notation

- a* stoichiometric coefficient; constant in equation (1-181)
- a<sub>i</sub>* activity; see equation (1-147)

$a^\circ$  constant in temperature correlation of equation (1-182)

$B_1, B_2, B_3$  constants defined after equation (1-190)

$b$  stoichiometric coefficient; constant in equation (1-181)

$C_{i,j}$  concentrations of  $i, j$ , mols/volume

$C_{i,x}$  concentration of  $i$  at conversion  $x$ , mols/volume

$C_{A0}, C_{B0}$  initial concentrations of A and B, mols/volume

$C_p$  heat capacity, typically kJ/mol or mass-K

$C_i$  mean value of concentration; see equation (1-205)

$E, E_1, E_2$  activation energy, normally kJ or kcal/mol

$$E_i(x) = \int_{-\infty}^x \exp(x')/(x') dx$$

$f_i$  fugacity of species  $i$ , atm

$G$  total free energy per mol, normally kJ or kcal/mol

$G_i^\circ, G_i$  partial molal free energies, standard state and at  $(T, P, x_i)$ , respectively

$\delta H^\circ$  standard state heat of reaction, normally kJ or kcal/mol

$\Delta H_f^\circ, \Delta H_r^\circ$  forward and reverse enthalpy changes, kJ or kcal/mol

$\delta H_1'$  enthalpy change per mol, kJ or kcal/mol

$\Delta H_r$  heat of reaction, kJ or kcal/mol

$I$  species I

$i$  species  $i$

$K$   $(k_f/k_r)$  or  $(k_1/k_2)$

$K_a, K_c, K_p, K_x$  equilibrium constants; see equations (1-149) and (1-156)–(1-158)

$K_f, K_r$  equilibrium constants; see Table 1.4

$k(T), k_i$  reaction rate constants, units depend upon reaction order

$k_f, k_r$  forward and reverse rate constants,  $\text{time}^{-1}$  for first-order

$k^\circ$  preexponential factor,  $\text{time}^{-1}$  for first-order

$L$  flow rate, mass/time

$l$  stoichiometric coefficient

$M$  ratio of initial concentrations; see (XIX) et seq.; sum of rate constants, Illustration 1.8

$M_i$  mass of  $i$

$m$  stoichiometric coefficient

$N$  sum of rate constants, Illustration 1.8

$N_{i,0}, N_i$  initial mols of  $i$ , mols of  $i$

$n$  nonintegral exponent, see equation (1-43); temperature constant in equation (1-182)

$P$  pressure, normally atm

$p$  stoichiometric coefficient; empirical reaction order; reaction factor in equation (1-67a)

$q$  stoichiometric coefficient; empirical reaction order; quadratic factor in equation (1-65)

$R$  gas constant, typically kcal/mol-K

$r$  general rate variable, mols/time-volume; order of exponent in equation (1-19); stoichiometric coefficient

$r_i$  mols  $i$  reacted, mols/time-volume

$r_A'$  mass A reacted, mass/time-volume

$r'_i$	mass $i$ reacted, mass/time/volume
$(r_i)_f, (r_i)_r$	forward and reverse rates, mols/time-volume
$S_0$	overall selectivity, mols $i$ to $j$ per mol reacted
$S_d$	differential selectivity, mols $i$ per mol $j$ ; $S_d(\text{I})$ , $S_d(\text{II})$ and $S_d(\text{III})$ refer to reactions of Type I, II and III
$S_i$	intrinsic selectivity, $(k_1/k_2)$
$T$	temperature, °C or °K
$t$	time, s or min
$u$	velocity, length/time; empirical reaction order
$V$	reaction mixture volume
$v$	flow rate, mass/time
$W$	flow rate, mass/time
$w$	empirical reaction order
$X$	overall conversion as in equation (1-50); molar extent of reaction, see equation (1-162)
$x_A, x_B$	mass fractions of A and B
$x_i$	fractional conversion of $i$ , see equation (1-47)
$x$	relation to concentration at equilibrium, see equation (1-62)
$Y_i$	yield of product $i$
$y_A, y_B$	mass fractions of A and B
$y_0, y$	functions of $(E/RT)$ , see equation (1-174)
$Z$	length
$z$	length element; $z$ and $z_0$ as in equation (1-174)
$z_A, z_B$	mass fractions of A and B
<i>Greek</i>	
$\alpha$	function defined in equation (1-67); see also equation (1-170)
$\beta$	quadratic factor, see equation (1-65); thermal parameter = $(1 + T_0/\alpha)$
$\gamma$	constant = $(\alpha\beta)$
$\gamma_i$	activity coefficient for species $i$
$\delta$	volume element
$\epsilon$	expansion factor, see equation (1-5)
$\tau$	scaled temperature variable, see equation (1-207)
$\nu, \nu_i$	stoichiometric coefficient, see equations (1-49) and (1-52)
$\nu_B$	ratio of stoichiometric coefficients, see equation (1-197)
$\phi$	reaction rate function

*Note:* Some additional notation is given and described in Table 1.6.



## 2

---

# The Mechanisms of Chemical Reactions in Homogeneous Phases

There is something fascinating about science. One gets such wholesale returns of conjecture out of such trifling investment of fact.

— *Mark Twain*

It was stated in Chapter 1 that theoretical justification for rate laws of the power-law form as applied to elementary steps could be provided. Our present purpose is to provide this justification in terms of several theories in sufficient detail to permit a basic comprehension of the origins and limitations of rate laws. Since we are not attempting a treatise on chemical kinetics, the presentation is selective, with much of the material relating specifically to reactions in the gaseous phase. The discussion is based on the fundamentals of the kinetic theory of gases with extensions to the transition-state theory of reaction rates. We shall follow the procedure of building a simple theory, criticizing it, building an improved theory, criticizing that, and so on—eventually reaching some reasonable level of theoretical background for ultimate engineering application.

### 2.1 Elementary Kinetic Theory

The simplest way in which to visualize a reaction between two chemical species is in terms of a collision between the two. Physical proximity is obviously a necessary condition for reaction, for there can be no interaction between two molecules that are well-separated from each other. In fact, though, collisions are rather difficult to define as discrete events, since the interaction between two molecules extends over a distance that depends on their individual potential energy fields. Fortunately, many useful results can be obtained by using simplified models; for gases the two most useful are the ideal gas (point particle) model and the hard-sphere model. In the *ideal gas model* a molecule is pictured as a point particle (i.e., dimensionless) of mass equal to the molecular weight with given position and velocity coordinates. For the *hard-sphere model* the normal analogy is to a billiard ball, a rigid sphere of given diameter and mass equal to the molecular weight. The potential-energy curves for intermolecular interactions according to the two models are shown in Figure 2.1a, and

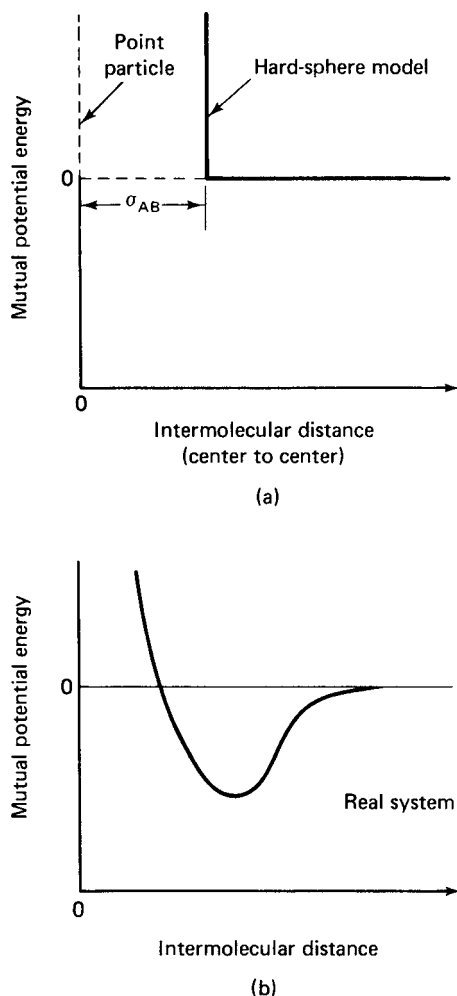


**Figure 2.1** Mutual-potential-energy diagrams for model and real systems.

for a representative real system in Figure 2.1b. A number of more detailed models have been devised to approximate the potentials corresponding to the interaction of real molecules; however, we shall be able to attain our major objectives here with the use of point-particle or hard-sphere models. It can be seen from Figure 2.1 that the major deficiency of the models is in ignoring the attractive forces (energy  $< 0$  on the diagrams) which exist in a certain range of intermolecular separation. However, the point-particle model will form the basis for our first try to produce a simple theory of reaction. Before doing this, though, let us take a look at the origin of the distribution laws that are so important in eventual application.

### 2.1.1 Distribution Laws

The properties of temperature, pressure, and composition which have been used in Chapter 1 to define rate laws refer to the averages of these quantities for the system

under consideration. To develop the idea of reaction as a result of intermolecular collision, it is necessary to look at individual molecular events and then assemble them into the overall, observable result. In this task we must be concerned with what average property arises from a distribution of individual properties. In the case of a gas, for example, the individual molecules are in constant motion as a result of their kinetic energy, and consequently are constantly colliding with one another. The velocities of individual molecules thus change continually, and the result is a distribution of velocities about an average value. How can we convince ourselves more quantitatively of the existence of such a distribution? Picture the collision between two hard-sphere molecules as shown in Figure 2.2. Before collision we have molecule A, mass  $m_A$ , diameter  $\sigma_A$ , and velocity  $v_A$  and molecule B, with mass  $m_B$ , diameter  $\sigma_B$ , and velocity  $v_B$ . If there are no tangential forces acting in the collision, which we shall assume, the velocities involved in energy transfer during collision are those parallel to the line of centers, as indicated on the figure. From momentum and energy conservation balances, one obtains the post-collision velocities in terms of the pre-collision values:

$$v'_A = \frac{2m_B v_B - v_A(m_B - m_A)}{m_A + m_B} \quad (2-1)$$

$$v'_B = \frac{2m_A v_A - v_B(m_A - m_B)}{m_A + m_B} \quad (2-2)$$

From equations (2-1) and (2-2) it can be shown that:

1. When  $m_A = m_B$ ,  $v'_A = v_B$ ,  $v'_B = v_A$ , the pre- and post-collision velocities are exchanged between molecules of equal mass.

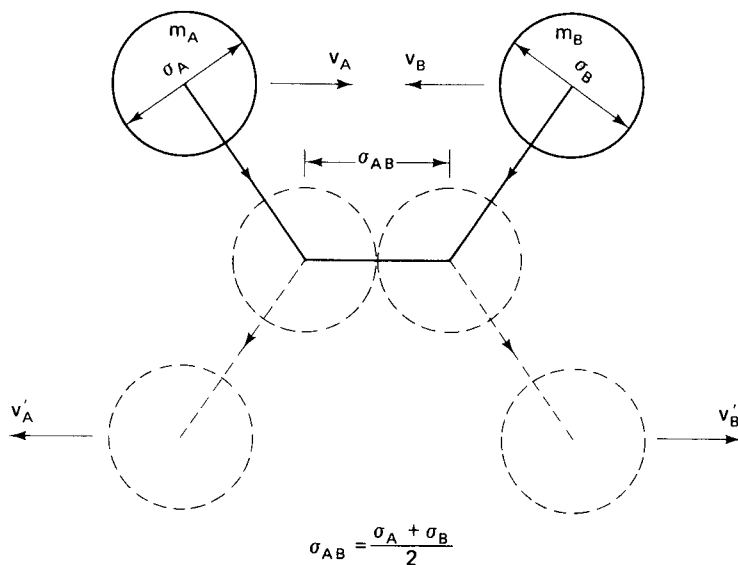


**Figure 2.2** Collision between two hard-sphere molecules. [After S.W. Benson, *The Foundations of Chemical Kinetics*, © 1960; with permission of McGraw-Hill Book Company, New York].

2. When  $m_A \gg m_B$ ,  $v'_A \approx v_A$ ,  $v'_B \approx 2v_A - v_B$ , the velocity of a light molecule is profoundly affected by collision with a heavy molecule, while the velocity of the heavy molecule remains essentially constant.

The exchange of kinetic energy, and thus velocity, as illustrated will ensure the existence of a distribution of velocities: energy is conserved in collisions where velocity is not conserved.

By making some rather general postulates concerning the nature of this distribution, we can derive its specific mathematical form. We shall suppose an isotropic medium at equilibrium such that the number of molecules in any region is the same and the velocities in any direction are equal, which requires that the components of velocity along any system of the coordinate directions are equal and independent of coordinate system. Also, we suppose that the velocities along any three coordinate axes are independent of each other, and that the change of a velocity lying between certain limits is a function only of the velocity and the limits considered. The details of the derivation are beyond the scope of our present discussion, but the important result is not:

$$P(v_x, v_y, v_z) dv_x dv_y dv_z = \frac{1}{\alpha^3 \pi^{3/2}} e^{-(v_x^2 + v_y^2 + v_z^2)/\alpha^2} dv_x dv_y dv_z \quad (2-3)$$

where  $P(v_x, v_y, v_z) dv_x dv_y dv_z$  is the fraction of all molecules having velocities in the range  $v_x$  to  $v_x + dv_x$ ,  $v_y$  to  $v_y + dv_y$ , and  $v_z$  to  $v_z + dv_z$  in the direction of the rectangular coordinate axes  $x$ ,  $y$ , and  $z$ , respectively. The quantity  $\alpha$  is the most probable speed, for which  $P(v_x, v_y, v_z) dv_x dv_y dv_z$  is a maximum (not the average speed) and is given by

$$\alpha = \left( \frac{2kT}{m} \right)^{1/2} \quad (2-4)$$

for an assembly of molecules of uniform molecular weight  $m$ , where  $k$  is Boltzmann's constant. Since the individual components of velocity are independent of each other, we may write from equation (2-3) the distribution of an individual component  $P(v_i)dv_i$ :

$$P(v_i)dv_i = \frac{1}{\alpha \pi^{1/2}} e^{-v_i^2/\alpha^2} dv_i$$

For our purposes it is most convenient to work with the velocity distribution without regard to individual component directions, since the medium is isotropic. This is expressed in terms of the speed,  $c$

$$c^2 = v_x^2 + v_y^2 + v_z^2 \quad (2-5)$$

as shown in Figure 2.3. Using the coordinate transformation as shown in Figure 2.4, equation (2-3) becomes

$$P(c, \theta, \phi) dc d\theta d\phi = \frac{c^2 \sin \theta}{\alpha^2 \pi^{1/2}} e^{-c^2/\alpha^2} dc d\theta d\phi \quad (2-6)$$

where  $P(c, \theta, \phi) dc d\theta d\phi$  represents the fraction of molecules with velocity vectors in the range  $c$  to  $c + dc$ ,  $\theta$  to  $\theta + d\theta$ , and  $\phi$  to  $\phi + d\phi$ . For an isotropic medium we

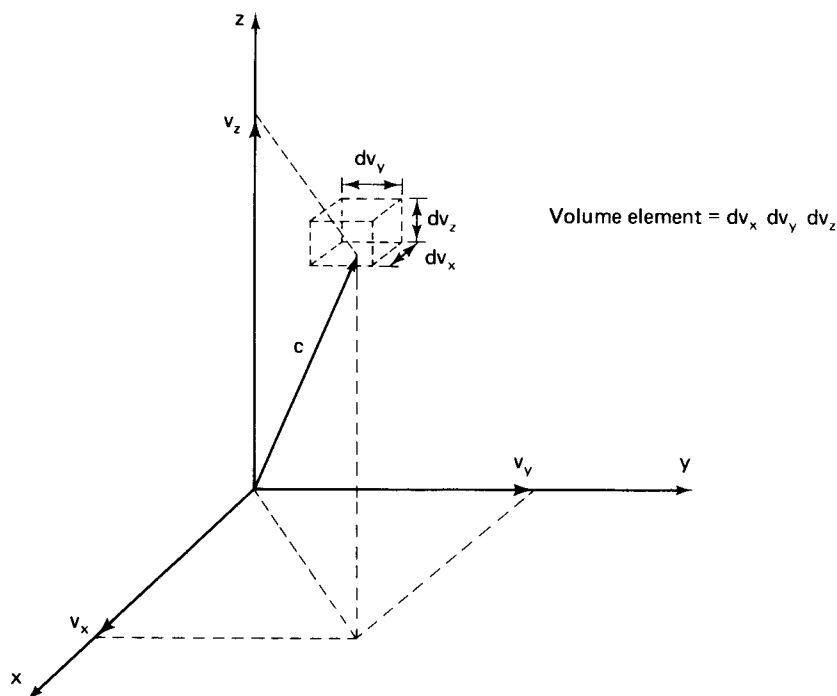


**Figure 2.3** Speed and individual velocity components in rectangular coordinates.

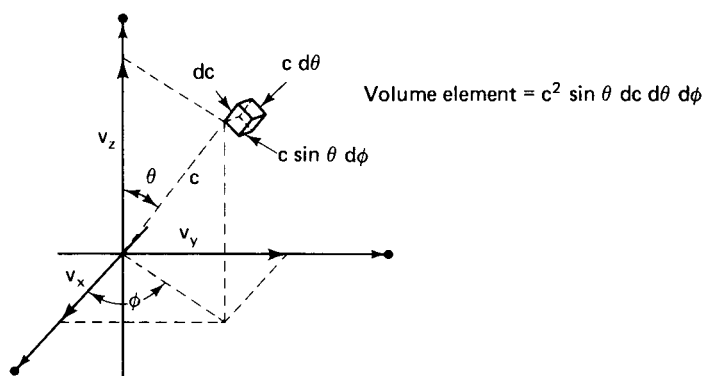


**Figure 2.4** Speed in terms of spherical coordinates. [After S.W. Benson, *The Foundations of Chemical Kinetics*, with permission of McGraw-Hill Book Company, New York, (1960).]

obtain the distribution of molecular speed by integrating equation (2-6) with respect to  $\theta$  (0 to  $\pi$ ) and  $\phi$  (0 to  $2\pi$ ). The result is

$$P(c) dc = \frac{4c^2}{\alpha^3 \pi^{1/2}} e^{-c^2/\alpha^2} dc \quad (2-7)$$

The nature of these distribution functions, for an individual Cartesian velocity component and for molecular speed, is shown in Figure 2.5. The velocity component

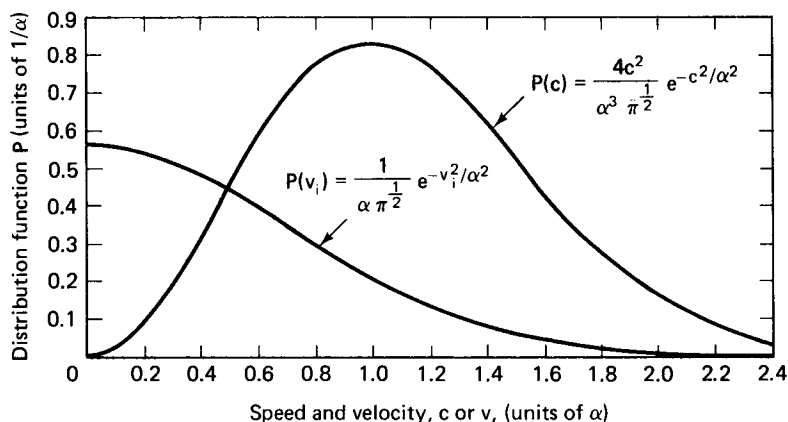


**Figure 2.5** Cartesian velocity component and speed distribution functions. [After S.W. Benson, *The Foundations of Chemical Kinetics*, with permission of McGraw-Hill Book Company, New York, (1960).]

distribution is symmetric about the origin since the range of a velocity component is  $-\infty$  to  $+\infty$ , while speed is a positive quantity. The  $P(v_i)$  distribution is Gaussian, while  $P(c)$  is no longer symmetric and is the Maxwell distribution law. From this Maxwell distribution we obtain other quantities of interest, such as the average velocity and the root-mean-square velocity. These are listed in Table 2.1. The translational energy distribution may also be obtained from the speed distribution (only kinetic energy here) as:

$$P(E) dE = \frac{4}{\alpha^3} \left( \frac{2E}{\pi m^3} \right)^{1/2} e^{-2E/m\alpha^2} dE \quad (2-8)$$

This equation will be of use later in connection with the analysis of energy requirements for chemical reactions [“... only a small percentage will profit by your most zealous energy.”—*George Gissing*].

**Table 2.1** Properties Derived from the Maxwell Distribution Law

Property	Description	Determination	Value
$\alpha$	Most probable speed	$P(c) dc$ is maximum	$\left( \frac{2kT}{m} \right)^{1/2}$
$\bar{c}$	Average speed	$\bar{c} = \int_0^\infty c P(c) dc$	$1.1284\alpha$
$c_m$	Median speed (speed exceeded by half the molecules)	$\int_0^{c_m} P(c) dc = \frac{1}{2}$	$1.088\alpha$
$\bar{c}^2$	Second moment of the distribution	$\bar{c}^2 = \int_0^\infty c^2 P(c) dc$	$1.5\alpha^2$
$(\bar{c}^2)^{1/2}$	Root-mean-square	$(\bar{c}^2)^{1/2} = \sqrt{1.5\alpha^2}$	$1.225\alpha$

## 2.1.2 Collision Numbers

With the distribution laws established, we can now attack the problem that is central to a collision theory of reaction: the number of collisions experienced per molecule per second in the Maxwellian gas. Clearly the magnitude of this collision number is a function of temperature (through the constant  $\alpha$ ), and if we define a total collision number, collisions of all molecules per second per volume, it will also depend on molecular density (i.e., concentration). Thus, the two independent variables of concentration and temperature used in power-law rate equations will appear in the total collision number.

Consider the simple situation illustrated in Figure 2.6. Here a single, hard-sphere molecule of A is moving through a gas composed of identical, stationary, hard-sphere B molecules. The speed of A is  $c_A$ , and in its path through the matrix of B molecules, A will follow a randomly directed course determined by collisions with B. Collisions are defined to occur when the distance between centers is smaller than:

$$\sigma_{AB} = (\sigma_A + \sigma_B)/(2)$$

If the matrix of B molecules is not too dense, we can approximate the volume in which collisions occur as that of a cylinder of radius  $\sigma_{AB}$ , developing a length of  $c_A$  per second. The number of collisions per second for the A molecule,  $Z(A, B)$  will then be the volume of this cylinder times the number of B molecules per unit volume,  $n_B$ :

$$Z(A, B) = n_B \pi \sigma_{AB}^2 c_A \quad (2-9)$$

This probably represents the first stop on the way to a collision theory of reaction rates. If, indeed, we have the passage of a single molecule through a dilute, fixed matrix of other molecules (sometimes called a “dusty gas”) with a known speed  $c_A$ , and with every collision resulting in reaction, then the reaction rate would in fact be given by equation (2-9). Yet, we know that we do *not* have a single molecule, we do *not* have a fixed speed, and we do *not* have a dusty gas, so this simple theory needs some cosmetics at this point.

One of the things we need to know is the collision number between molecule A, which is representative of a Maxwellian distribution of speeds of A molecules, and B molecules themselves possessing a Maxwellian distribution of speed. This can be done by defining a collision volume determined not by  $c_A$  but by a mean relative speed,  $c_r$ , between the Maxwellian populations of A and B. This approach has been discussed by Benson [S.W. Benson, *The Foundations of Chemical Kinetics*, McGraw-Hill Book Co.,

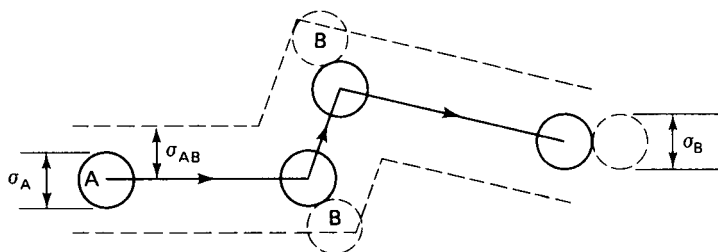


**Figure 2.6** Trajectory of single molecule A through a stationary matrix of B. [After S.W. Benson, *The Foundations of Chemical Kinetics*, with permission of McGraw-Hill Book Company, New York, (1960).]

New York, NY, (1960)]. The result, for identifiable molecular species A and B, is simply that

$$c_r = \left( \frac{8kT}{\pi\mu_{AB}} \right)^{1/2} \quad (2-10)$$

where  $\mu_{AB} = m_A m_B / (m_A + m_B)$  = reduced mass. For identical molecular species (A = B) we obtain the important result

$$C_r = \sqrt{2} \bar{c} \quad (2-11)$$

The collision number we are seeking may now be obtained by direct substitution into equation (1-8) using  $c_r$  instead of  $c_A$ . For the total number of collisions between Maxwellian molecules A and B, the collision number,  $\bar{Z}_{cT}(A, B)$  is determined by substitution of  $c_r$  from equation (2-10) and multiplication by the concentration of A molecules,  $n_A$ :

$$\bar{Z}_{cT}(A, B) = n_A n_B \pi \sigma_{AB}^2 \left( \frac{8kT}{\pi\mu_{AB}} \right)^{1/2} \quad (2-12)$$

A corresponding substitution for like molecules (A = B) into equation (2-12) gives

$$\bar{Z}_{cT}(A, A) = n_A^2 \pi \sigma_{AA}^2 \left( \frac{4kT}{\pi\mu_A} \right)^{1/2} \quad (2-13)$$

where the relative speed from equation (2-11) has been used. A summary of the various collision numbers, written in terms of temperature and concentration, is given in Table 2.2a, and a summary of some results for typical gases in Table 2.2b.

**Table 2.2a** Collision Numbers According to the Hard-Sphere Model

1. Single molecule of A moving at fixed speed  $c_A$  through a stationary matrix of B molecules of concentration  $n_B$ :

$$Z(A, B) = n_B \pi \sigma_{AB}^2 c_A$$

If  $c_A$  is taken to be the average speed from the Maxwell distribution:

$$Z(A, B) = n_B \pi \sigma_{AB}^2 \left( \frac{8kT}{\pi m_A} \right)^{1/2}$$

2. Single molecule of A with Maxwellian speed distribution moving through a matrix of B molecules, also with Maxwellian speed distribution:

$$\bar{Z}_c(A, B) = n_B \pi \sigma_{AB}^2 \left( \frac{8kT}{\pi\mu_{AB}} \right)^{1/2}$$

3. Total collision number between A and B, each with Maxwellian speed distribution:

$$\bar{Z}_{cT}(A, B) = n_A n_B \pi \sigma_{AB}^2 \left( \frac{8kT}{\pi\mu_{AB}} \right)^{1/2}$$

4. Total collision number for a gas containing only one molecular species, A:

$$\bar{Z}_{cT}(A, A) = n_A^2 \pi \sigma_{AA}^2 \left( \frac{4kT}{\pi m_A} \right)^{1/2}$$



**Table 2.2b** Speeds and Collision Numbers for Some Typical Gases<sup>a</sup>

Gas	Molecular Weight	Diameter (Å) (from viscosity data)	$\bar{c}$ at 25°C (km/sec)	Mean Free Path (Å) (STP)	Collision Number $\times 10^{-28}$ (number/cm <sup>3</sup> -sec)
H <sub>2</sub>	2.016	2.74	1.772	1180	20.4
He	4.002	2.18	1.257	1765	9.13
N <sub>2</sub>	28.02	3.75	0.475	596	10.22
C <sub>2</sub> H <sub>6</sub>	30.05	5.30	0.448	298	19.7
O <sub>2</sub>	32.00	3.61	0.434	644	8.87
Ar	39.94	3.64	0.3975	633	8.07
CO <sub>2</sub>	44.00	4.59	0.379	397	12.22
Kr	82.9	4.16	0.276	485	7.32

<sup>a</sup> Relative speed for like molecules:  $c_r = \sqrt{2} \bar{c}$

Average speed,  $\bar{c} = \left( \frac{8kT}{\pi\mu} \right)^{1/2}$

Ideal gas number density (STP) =  $2.687 \times 10^{19}$  molecules/cm<sup>3</sup>

Electronic mass =  $9.108 \times 10^{-28}$  g

Avogadro's number =  $6.025 \times 10^{23}$  molecules/mole

Planck's constant ( $h$ ) =  $6.625 \times 10^{-27}$  erg-sec/molecule

Gas constant ( $R$ ) =  $8.317 \times 10^7$  ergs/mole-°K

Boltzmann constant ( $k = R/N$ ) =  $1.38 \times 10^{-16}$  erg/molecule-°K

Source: [After S.W. Benson, *The Foundations of Chemical Kinetics*, Table VII. 2, p. 155; with permission of McGraw-Hill Book Company, New York, (1960).]

A final collision number, which will be of interest in future applications, is that between the molecules in a homogeneous gas and a solid surface. The details of this problem are left to the exercises at the end of this chapter, where it is seen that by considering the rate of effusion of molecules in a vessel through a small orifice such that the velocity distribution is not affected, one may derive that

$$\bar{Z}_{cT}(\text{surface}) = \frac{n_A}{4} \left( \frac{8kT}{\pi m_A} \right)^{1/2}$$

### Illustration 2.1

Compare the fraction of hydrogen molecules having a speed of 1 km/s at 30°C to that of oxygen molecules at the same temperature, atmospheric pressure in both cases. Is the energy distribution ratio the same as the speed distribution ratio?

#### Solution

This is simply asking to evaluate the value of  $P(c) dc$  for the two gases at 1 km/s, 303°K. Thus,

$$P(c) dc = \frac{4c^2}{(2kT/m_i)^{3/2} \pi^{1/2}} \exp(-c^2 m_i / 2kT) dc \quad (\text{i})$$

where  $i = \text{H}_2$  or  $\text{O}_2$ . The ratio is

$$\frac{P(c)\text{H}_2}{P(c)\text{O}_2} = \left( \frac{m_{\text{H}_2}}{m_{\text{O}_2}} \right)^{3/2} \exp[-(c^2 m_{\text{H}_2} / 2kT) + (c^2 m_{\text{O}_2} / 2kT)] \quad (\text{ii})$$

with numbers:  $c = 10^5 \text{ cm/s}$ ,  $m(\text{H}_2) = 3.32 \times 10^{-24}$ ,  $m(\text{O}_2) = 5.31 \times 10^{-23}$ ,  $k = 1.38 \times 10^{-16} \text{ g-cm}^2/\text{s}^2 - \text{K}$ ,  $T = 303^\circ\text{K}$ . From (ii) we obtain:

$$[P(c)\text{H}_2/P(c)\text{O}_2] = 6.034 @ 30; \quad 1.974 @ 100^\circ\text{C}$$

Obviously the  $P(c)$  fraction decreases with increasing temperature, and for set  $c$  at sufficiently high temperature will approach unity.

The analysis of energy distribution follows a similar path. Considering only kinetic energy, then

$$E_i = (1/2)m_i c^2 \quad (\text{iii})$$

and

$$P(E) dE = \frac{4}{\alpha_i^3} \left( \frac{2E}{\pi m_i^3} \right)^{1/2} \exp(-2E/m_i \alpha_i^2) dE \quad (\text{iv})$$

$$[P(E)\text{H}_2/P(E)\text{O}_2 = 384.7 @ 30; \quad 126.3 @ 100^\circ\text{C}$$

Again, the fraction decreases rapidly with temperature and the distribution sharpening with increasing temperature.



HORATIO SAYS

For some additional fun, derive the result of equation (iv) in the illustration from equation (i).

## 2.2 Collision Theory of Reaction Rates

### 2.2.1 Collision Numbers in Terms of Relative Kinetic Energy and Bimolecular Reactions

If we assume that every collision is effective in reaction, then  $\bar{Z}_{cT}(\text{A}, \text{B})$  from equation (2-12) gives us the rate of the reaction  $\text{A} + \text{B} \rightarrow \text{products}$  directly. Previously, we had written for the irreversible, second-order reaction between A and B, for constant-volume conditions,

$$r_A = (dC_A/dt) = -k' C_A C_B \quad (1-39)$$

For concentrations expressed as number densities (molecules/cm<sup>3</sup>),  $C_A = n_A$ , and so on, and the rate constant  $k'$  in molecular units from equation (2-12) is

$$k' = \pi \sigma_{AB}^2 \left( \frac{8kT}{\pi \mu_{AB}} \right)^{1/2}$$

It is now again time to compare the results of our theory with reality. We can see that there is something wrong with the indicated temperature dependence of the

rate constant, since measurements insist that there should be something like an Arrhenius temperature dependence of  $k'$ , yet indicated is only the factor of  $(T)^{1/2}$ . The difficulty here arises from the fact that we are still assuming that every collision is effective in the reaction. If we suppose that our colliding spheres must interact with a certain minimum relative energy before reaction occurs, the picture changes considerably.

In the new visualization consider a collision between hard-sphere molecules A and B with relative velocity  $v_r$ , and  $b$  as an impact parameter which can be related to, but is generally not equal to,  $\sigma_{AB}$ . The general view corresponds to Figure 2.7. Here  $v_{\parallel}$  and  $v_{\perp}$  are velocity components in the parallel and perpendicular directions to the line of flow. We can also write an energy expression in terms of these velocity components

$$E_r = \left( \frac{\mu_{AB}}{2} \right) (v_{\parallel}^2 + v_{\perp}^2)$$

The second term of this expression is the energy directed along the line of centers and, in the hard-sphere model, we assume that this is the component of energy involved in the reaction. Let us call this energy along the line of centers  $E_c$ . From Figure 2.7 we have

$$\left( \frac{E_c}{E_r} \right) = 0; \quad b > \sigma_{AB} \quad (2-14a)$$

$$\left( \frac{E_c}{E_r} \right) = 1 - \frac{b^2}{(\sigma_{AB})^2}; \quad b \leq \sigma_{AB} \quad (2-14b)$$

The adventuresome should try the geometric approach in derivation that leads to equation (2-14).

Now, we will further assume that there is an energy-dependent reaction probability and, in the most simple approach, that this is just an “on-off” switch such that the probability of reaction is zero if  $E_c < E^*$  and is unity if  $E_c > E^*$ , where  $E^*$  is

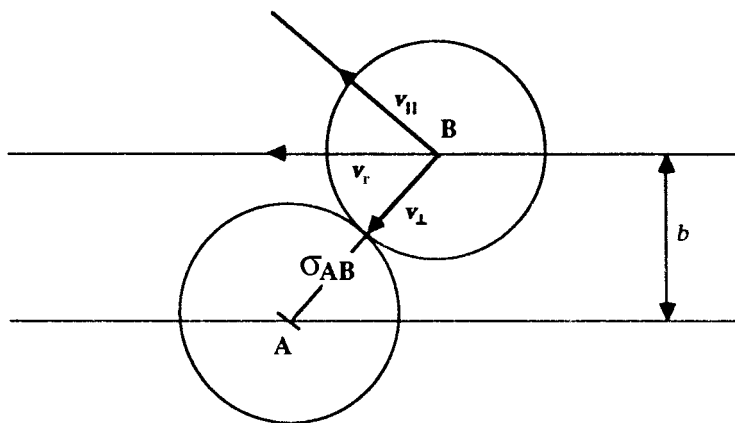


**Figure 2.7** The reactive hard-sphere model.

the minimum energy for reaction. If we write this out formally,

$$\begin{aligned}\delta(E_c) &= 0; & E_c &< E^* \\ \delta(E_c) &= 1; & E_c &> E^*\end{aligned}\quad (2-15)$$

The picture to this point then is the collision of hard spheres given in Figure 2.7, with energies as defined in equation (2-14) and probabilities as given in equation (2-15). How do we turn this into a reaction rate expression that is compatible with all the work done previously to get to equation (2-12)? This has been done over the years, following the terminology of the theorists, in terms of yet a new quantity that is generally called the *reactive cross-section*. For now, let us write down the definition and worry about the physical interpretation later. Thus, we define a reactive cross-section as

$$\sigma_R(E_r) = \int_0^\infty \sigma[E(b)] 2\pi b db \quad (2-16)$$

$$= 0; \quad (E_r < E^*); \quad = \pi \sigma_{AB}^2 (1 - E^*/E_r); \quad (E_r \geq E^*) \quad (2-17)$$

The energy dependence of  $\sigma_R$  is shown in Figure 2.8. This is essentially the collision area that the interacting molecules see as a function of the relative energy. Now in order to determine a reaction rate (or rate constant) from the result of equation (2-17) we need to integrate over the distribution of  $E_r$  and over the range of possible values of  $b < b_{\max}$  associated with each  $E_r$ . After some rather complex geometry one comes up with a collision number as a function of the relative energy that says:

$$Z(E_r) = \frac{2n_A n_B}{(kT)^{3/2}} \left( \frac{2}{\pi \mu_{AB}} \right)^{1/2} \int_{E^*}^\infty e^{-E_r/kT} \sigma_R(E_r) E_r dE_r \quad (2-18)$$

The quantities  $n_A$  and  $n_B$  in equation (2-18) are the number densities (molecules/volume) of A and B, and  $\sigma_R(E_r)$  is the reactive cross-section from equation (2-17).

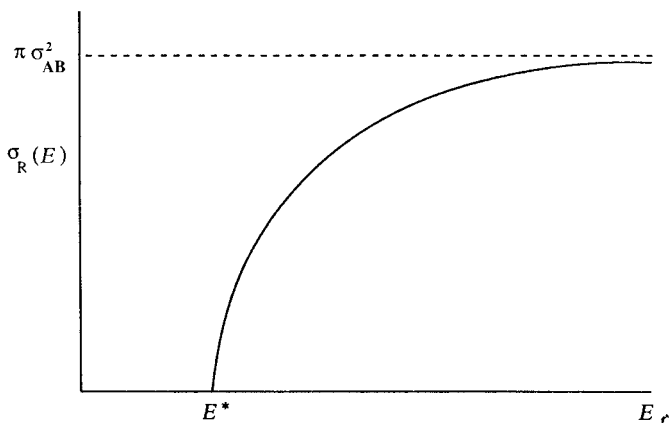


**Figure 2.8** Energy dependence of the reactive cross-section in the hard-sphere model.

The final integration yields

$$\bar{Z}_{E^*}(A, B) = \pi \sigma_{AB}^2 \left( \frac{8kT}{\pi \mu_{AB}} \right)^{1/2} e^{-E^*/kT} n_A n_B \quad (2-19)$$

where  $Z$  is the reactive collision number, and  $E^*$  (as shown on Figure 2.8) now appears as the activation energy. This, then, is the reactive collision number defined with activation energy  $E^*$  on the basis of the relative translational energy between reacting molecules. To ensure that the energy at  $E^*$  does not become confused with any other energy, let us call it  $\eta^*$ .

Often a steric factor,  $p$ , is introduced to account for all additional factors affecting the collision-reaction probability except for those directly associated with energy. Thus

$$\bar{Z}_\eta(A, B) = p \pi \sigma_{AB}^2 \left( \frac{8kT}{\pi \mu_{AB}} \right)^{1/2} e^{-\eta^*/kT} n_A n_B \quad (2-20)$$

We may now compare equation (2-20) with the bimolecular rate law, equation (1-39), to find what a corresponding rate constant would be. This is

$$k'(A, B) = p \sigma_{AB}^2 \left( \frac{8\pi kT}{\mu_{AB}} \right)^{1/2} e^{-\eta^*/kT} \quad (2-21)$$

and is the rate constant of a bimolecular reaction as determined from collision theory. It is essentially of the Arrhenius form, since the weak temperature dependence of the pre-exponential factor is generally negligible in comparison with the activation-energy term. For collisions between like molecules, equation (2-20) reduces to

$$\bar{Z}_\eta(A, A) = p \left( \frac{4\pi kT}{m_A} \right)^{1/2} \sigma_{AA}^2 e^{-\eta^*/kT} n_A^2 \quad (2-22)$$

and the collision-theory rate constant corresponding to the rate law of equation (1-37) is

$$k'(A, A) = p \sigma_{AA}^2 \left( \frac{4\pi kT}{m_A} \right)^{1/2} e^{-\eta^*/kT} \quad (2-23)$$

These equations can be converted to molecular units easily, since  $k = R/N_a$ , where  $N_a$  is Avogadro's number, and  $m$  would be defined as a molecular weight.

Our theory is done, then, except for some details concerning  $p$  and  $\sigma$ . In general these quantities can be only estimated, so that often an effective collision diameter,  $\sigma_e$ , is used. This is defined by

$$\begin{aligned} (\sigma_e)_{AB} &= \sigma_{AB}(p)^{1/2} \\ (\sigma_e)_{AA} &= \sigma_{AA}(p)^{1/2} \end{aligned} \quad (2-24)$$

and such quantities are determined experimentally.

A similar theory can be worked out for termolecular collisions by modifying the hard-sphere model slightly to permit interactions to occur over a specified distance rather than at a point. In the gas phase, however, termolecular collisions are relatively rare events, roughly one for every 10 million bimolecular collisions. Except for a few instances involving the reactions of NO and a group of atom recombination reactions, they play little role in gas-phase reaction kinetics. The termolecular collision theory requires that there be a finite time of interaction between two molecules, during which a third collides with the interacting pair. This requires, for example, in the triple collision between A, B, and C that there be a finite distance of approach,  $\delta$ , of the three molecules that defines the collision volume. The corresponding collision number [R.C. Tolman, *Statistical Mechanics*, Chemical Catalog Co., New York, NY, (1927)] is third-order and the rate constant is given by

$$k'(A, B, C) = (8p\delta)(2kT)^{1/2}\pi^{3/2}(\sigma_{AB}\sigma_{BC})^2[(\mu_{AB})^{-1/2} + (\mu_{BC})^{-1/2}]e^{-E/RT} \quad (2-25)$$

The distance of approach  $\delta$  is on the order of 1 Å.

While termolecular reactions are relatively uncommon, at the other end of the scale, unimolecular reactions are often encountered. The theory of the kinetics of such reactions is important for the detail it provides on the individual events that must occur in those reactions, which we have termed *elementary steps*, and we will treat it separately in the following section. First, however, let us take some time here for an example illustrating some additional aspects of binary collision theory via numerical calculations.

### Illustration 2.2

- Compute the binary collision numbers for hydrogen and oxygen at 100°C and 1 atm total pressure.
- What is the ratio of the mean collision times for the two gases under these conditions?
- What is the collision number for an equimolar mixture of hydrogen and oxygen at 400°C and 1 atm total pressure?

#### Solution

While the solution to this problem is straightforward, the numbers are informative. Since the author is lazy by nature, some computational effort has been avoided by using the results of Table 2.2b as a guide.

- The basic relationship to be used is equation (2-13). Numbers according to this, at 25°C, are given in Table 2.2b as

$$\bar{Z}_{cT}(\text{H}_2, \text{H}_2) = 20.4 \times 10^{28} \text{ collisions/cm}^3\text{-s}$$

$$\bar{Z}_{cT}(\text{O}_2, \text{O}_2) = 8.87 \times 10^{28} \text{ collisions/cm}^3\text{-s}$$

Following equation (2-13), we must correct these values to 100°C, which involves changes in both the square root term (relative velocity) and the number density,  $n_A$ . Thus

$$\bar{Z}_{cT}(T_2) = [\bar{Z}_{cT}(T_1)] \left( \frac{T_2}{T_1} \right)^{1/2} \left( \frac{T_1}{T_2} \right)^2 = [\bar{Z}_{cT}(T_1)] \left( \frac{T_1}{T_2} \right)^{3/2} \quad (i)$$

Substituting numbers and remembering that  $T$  is in  $^{\circ}\text{K}$ , we have at  $373^{\circ}\text{K}$

$$\bar{Z}_{cT}(\text{H}_2, \text{H}_2) = 14.6 \times 10^{28} \text{ collisions/cm}^3\text{-s}$$

$$\bar{Z}_{cT}(\text{O}_2, \text{O}_2) = 6.33 \times 10^{28} \text{ collisions/cm}^3\text{-s}$$

The ratio of collision numbers,  $(\text{H}_2/\text{O}_2) = 2.3$  at  $373\text{ K}$ . Note that the ratio obtained from Table 2.2b at  $298^{\circ}\text{K}$  is just about the same—even a little smaller. The weak dependence of collision number per unit volume on temperature is due to a compensation between collision frequency (increasing) and number density (decreasing). This should tell us that dramatic increases in reaction rate with temperature as observed in experiment surely cannot be explained solely on the basis of simple collision theory.

b) The ratio of collision times is informative in telling us the relative rates involved in interaction between molecules. Here we just assume that an appropriate mean collision time is given by the ratio of the number density to the collision number. For example, for  $\text{H}_2$ :

$$\text{Collision time} = t(\text{H}_2, T') = \frac{n_{\text{H}_2}(T')}{\bar{Z}_{cT}(\text{H}_2, \text{H}_2)(T')} \quad (\text{ii})$$

which gives

$$t(\text{H}_2, 373) = 1.35 \times 10^{-10} \text{ s}$$

$$t(\text{O}_2, 373) = 3.11 \times 10^{-10} \text{ s}$$

so the ratio of collision times is 0.435.

The message here is that collisions between larger molecules require more time to occur. Think about this for a moment. What would you expect, given relative velocities, for the time required to accomplish a collision between two Toyotas on a Los Angeles freeway compared to that between *THERMOPYLAE* and *CUTTY SARK* on one of their famous races? (We have data on the first but not the second.)

c) Since we have looked at hydrogen and oxygen separately, let us now look at them together. From Table 2.2a,

$$\bar{Z}_{cT}(\text{A}, \text{B}) = n_{\text{A}} n_{\text{B}} \pi \sigma_{\text{AB}}^2 \left( \frac{8kT}{\pi \mu_{\text{AB}}} \right)^{1/2} \quad (\text{iii})$$

Here  $T = 673^{\circ}\text{K}$  and  $n_{\text{A}}$  (say hydrogen)  $= n_{\text{B}}$  (oxygen)  $= 0.544 \times 10^{19}$  molecules/cm<sup>3</sup>. We will take from Table 2.2b the appropriate dimension of interaction to be

$$\sigma(\text{H}_2, \text{O}_2) = (2.74 + 3.61)/2 = 3.17 \times 10^{-8} \text{ cm}$$

The estimation of this dimension is always subject to some discussion, but for the present we will use the average. Also, from molecular weight data for hydrogen and oxygen, remembering that these equations are written in molecular units

$$\mu(\text{H}_2, \text{O}_2) = (1.88)/(6.02 \times 10^{23})$$

Finally, then

$$\bar{Z}_{cT}(\text{H}_2, \text{O}_2) = 2.56 \times 10^{28} \text{ cm}^{-3} \text{ s}^{-1}$$



HORATIO SAYS

I would like to know whether the result above is larger or smaller than the collision numbers for O<sub>2</sub> or H<sub>2</sub> at 298 or 373°K.

### 2.2.2 Unimolecular Reactions: The Lindemann Theory

At first glance it seems paradoxical to treat unimolecular reactions, in which a single molecule is apparently involved in reaction, in terms of a collision theory based on pairwise interactions. Indeed, we have developed a rather specific picture of a chemical reaction from the hard-sphere collision model, in which bonds are formed rather than broken and in which the energetics of reaction are represented in terms of relative kinetic energy.

The key phrase in the paragraph above is “apparently involved in reaction”. Let us look at a typical unimolecular reaction, for example the first step of the diethylether decomposition illustrated in Chapter 1:



Here the reaction process is one of spontaneous transformation, which requires sufficient energy to be present in the ether molecule to permit the rupture of a carbon-carbon bond. This energy is obviously internal to the molecule and cannot be represented as a translational-energy term. The pertinent question to ask is how a molecule acquires the required energy for the transformation to occur, and the answer lies in a consideration of the energy exchange from external (kinetic) to internal (rotational and vibrational) modes in polyatomic molecules.

We can obtain at least a qualitative picture of such an exchange by a modification of the hard-sphere approach. First, recall that in equations (2-1) and (2-2) we obtained expressions for the postcollision velocities of two hard spheres in terms of the precollision values. The change in kinetic energies for this process is

$$\Delta E_A = -\Delta E_B = \frac{m_A}{2} [v_A^2 - (v')_A^2] \quad (2-26)$$

and the fraction of the original energy of sphere A that is exchanged is

$$\frac{\Delta E_A}{E_A} = \frac{(m_A/2)[v_A^2 - (v')_A^2]}{(m_A/2)v_A^2} = 1 - \frac{(v')_A^2}{v_A^2} \quad (2-27)$$

In terms of the precollision values of  $v_A$  and  $v_B$ :

$$\frac{\Delta E_A}{E_A} = \frac{4\theta}{(1+\theta)^2} \left(1 - \frac{v_B}{v_A}\right) \left(1 + \frac{1}{\theta} \frac{v_B}{v_A}\right) \quad (2-28)$$



where  $\theta = m_A/m_B$ . Now let us consider this collision to be that shown in Figure 2.9, in which one of the hard spheres is an atom in a diatomic molecule and only the energy exchange along the line of centers is considered (i.e., a head-on collision). The same relationship, equation (2-28), pertains to energy exchange between the atom and the molecule, if we neglect any BC interactions. For the conservation of momentum in this collision, we can write

$$m_{BC}[(v')_B - v_{BC}] = m_A[v_A - (v')_A] \quad (2-29)$$

and in terms of precollision values

$$\frac{(v')_{BC}}{v_A} = \frac{2m_B m_A}{m_{BC} m_{AB}} \left(1 - \frac{v_B}{v_A}\right) + \frac{v_{BC}}{v_A} \quad (2-30)$$

The energy,  $\Delta E_v$ , transferred to the internal mode (vibrational) of BC is the difference between  $(\Delta E_A/E_A)$  and that appearing as a change in the translational energy of BC

$$\frac{\Delta E_v}{E_A} = \frac{\Delta E_A}{E_A} - \left(\frac{1}{2}\right) \frac{m_{BC}[(v')_{BC}^2 - v_{BC}^2]}{E_A} \quad (2-31)$$

Substituting from equation (2-30) for  $(v')_{BC}$ , we have

$$\frac{\Delta E_v}{\Delta E_A} = \frac{4m_C m_B m_A}{m_{AB}^2 m_{BC}} \left(1 - \frac{v_B}{v_A}\right) \left(1 + \frac{v_B}{v_A} \frac{m_{ABC} m_B}{m_C m_A} - \frac{v_{BC}}{v_A} \frac{m_{AB} m_{BC}}{m_C m_A}\right) \quad (2-32)$$

The value of  $(\Delta E_v/\Delta E_A)$  may be either positive or negative here, depending upon the relative signs of  $v_A$ ,  $v_B$ , and  $v_{BC}$ , since the picture of hard-sphere collisions requires an instantaneous interaction. For real molecules, however, we can think in terms of a "soft" collision taking place over a finite period of time in which several vibrational cycles of the molecule BC occur (i.e., B and C change directions with respect to each other), and we can time-average results such as that of equation (2-32).

The concept we are trying to illustrate from this simplified analysis is *collisional activation*, by which a polyatomic molecule through a series of favorable collisions is able to accumulate internal energy from kinetic-energy exchange. The concept of collisional activation was used by Lindemann [F.A. Lindemann, *Trans. Faraday*

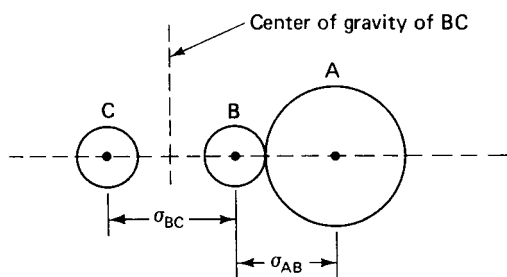


**Figure 2.9** Collisions between an atom and a diatomic molecule. [After S.W. Benson, *The Foundations of Chemical Kinetics*, with permission of McGraw-Hill Book Company, New York (1960).]

*Soc.*, 17, 598 (1922)] as the basis for his original development of a theory for unimolecular reactions.<sup>1</sup> Consider the unimolecular reaction  $A \rightarrow \text{products}$ , which we will write in two steps:



The first step involves the activation of the A molecule by collision with another A molecule, or in general with any other molecule, M, in the system to give  $A^*$ , and the reverse process of collisional deactivation of  $A^*$ . If the deactivation rate is large compared to the decomposition, we may apply the path for  $A^*$ :

$$(dC_A^*/dt) = 0 = k_1(C_A)^2 - k_{-1}C_A^*C_A - k_2C_A^* \quad (2-33)$$

from which

$$C_A^* = \frac{k_1 C_A^2}{k_2 + k_{-1} C_A}$$

and

$$\text{rate} = k_2 C_A^* = \frac{k_1 k_2 C_A^2}{k_2 + k_{-1} C_A} \quad (2-34)$$

This expression has two limits. At sufficiently high concentrations,  $k_{-1} C_A \gg k_2$  and

$$\text{rate} \approx \frac{k_1 k_2}{k_{-1}} C_A = k_\infty C_A \quad (2-35)$$

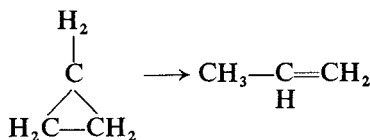
and at very low concentrations,  $k_{-1} C_A \ll k_2$ , and

$$\text{rate} \approx k_1 C_A^2 \quad (2-36)$$

The rate of the unimolecular reaction is thus first order at high pressure and second order at low pressure, or if one interprets the results wholly on the basis of a first-order form,

$$r = k^1 C_A \quad (2-37)$$

then the value of  $k^1$  decreases with pressure. This change has been observed experimentally for a number of reactions. A popular example is the data of Pritchard et al. for the isomerization of cyclopropane [H.O. Pritchard, R.G. Snowden and A.F. Trotman-Dickenson, *Proc. Roy. Soc. (London)*, 217A, 563 (1963)]:



<sup>1</sup> Looking at the dates associated with the development of bimolecular and unimolecular theories, respectively, reveals that it took at least two decades to go from two to one. "It was so slow it was like molasses drippin' through a bitty hole."—*Old Southern Saying*.

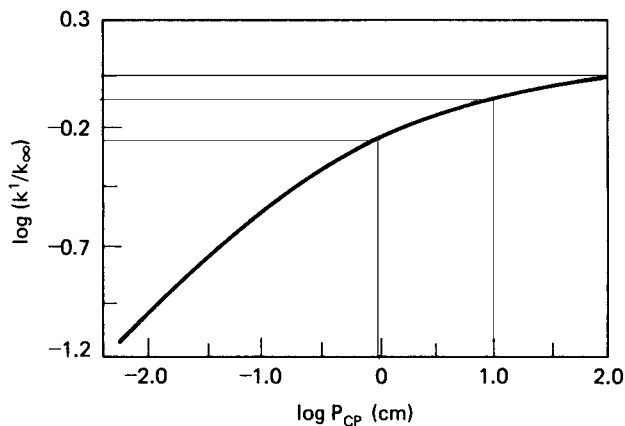


**Figure 2.10** Pressure dependence of the first-order rate constant for cyclo-propane isomerization. [After H.O. Pritchard, R.G. Sowden, and A.F. Trotman-Dickenson, *Proc. Roy. Soc. (London)*, *A217*, 563, with permission of The Royal Society, (1953).]

These data are shown in Figure 2.10, where the ratio of  $k_1$  to the limiting high-pressure rate constant,  $k_\infty$ , is plotted versus cyclopropane pressure. We can write  $k^1$  in terms of the individual rate constants of equation (2-34):

$$k^1 = \frac{k_1 k_2 C_A}{k_{-1} C_A + k_2} \quad (2-38)$$

which can be rearranged to

$$k^1 = \frac{k_\infty}{1 + (k_\infty/k_1)(1/C_A)} \quad (2-39)$$

According to simple collision theory we should be able to calculate  $k_1$  from simple collision theory via  $\bar{Z}_\eta(A, A)$ . If this is done, however, one finds only qualitative agreement with the pressure variation of rate constant. This is shown in a general way in Figure 2.11. As will be found in the exercises and later, the theoretical prediction tends to lie below the experiment over the pressure range. If  $k^1$  is decreasing from the high-pressure limit at too-large values of  $C_A$ , then in equation (2-39) the denominator is too large. This can occur because either  $k_\infty$  is too large or  $k_1$  is too small. Since  $k_\infty$  is the experimentally observed first-order rate constant at high pressure, however, we must take it at face value and conclude that the discrepancy can be due only to a value of  $k_1$  which is too small. The reason for this lies in the fact that  $k_1$  was computed from the collision-theory result for hard spheres,  $\bar{Z}_\eta(A, A)$  and even though an activation energy is involved, the true activation must occur more rapidly if we include the influence of energy transfer from external to internal modes in the calculation for  $k_1$ . In the following section we will discuss briefly several modifications of the Lindemann theory based on more realistic molecular models which lead ultimately to a workable theory for the kinetics of elementary steps.

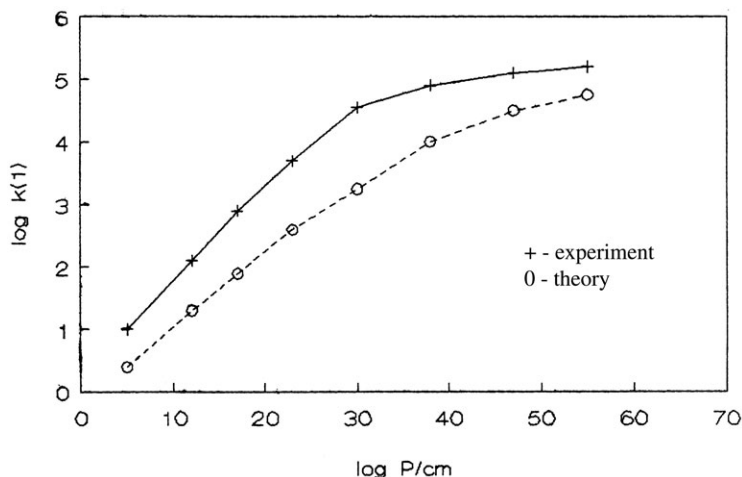


**Figure 2.11** Typical discrepancy between unimolecular reaction theory, equation (2-39), and experimental data.

### 2.2.3 Modifications of the Lindemann Theory

The first modification, due to Hinshelwood [C.N. Hinshelwood, *Proc. Roy. Soc. (London)*, 113A, 230 (1927)], is to abandon the hard-sphere collision theory result in favor of a more detailed consideration of energy exchange in complex molecules. We have seen from equation (2-32) that even the simplest picture of a polyatomic molecule indicates that a significant fraction of translational energy can be changed to vibrational energy on collision. Let us now assume that the molecules being activated consist of  $n$  weakly coupled harmonic oscillators (no interaction between the oscillators), and that we wish to determine the distribution of such molecules with total energy between  $E$  and  $E + dE$  with a fixed distribution  $E_1, E_2, \dots, E_n$  of energy between the oscillators, with  $E = \sum(E_i)$ . There exists a well-defined relationship between the number of oscillators,  $n$ , and the number of atoms in the molecule,  $N$ , since we can view  $n$  as representing the number of degrees of vibrational freedom in the molecule. For a molecule of  $N$  atoms,  $3N$  coordinates are required to locate the positions of individual atoms, and since the atoms of a molecule move through space as a coherent group the motion of the molecule as a whole can be represented by an additional three coordinates representing the motion of the center of mass. What remains,  $3N - 3$ , must represent the internal degrees of freedom, of which an additional three are required to represent rotational freedom (two if the molecule is linear), so

$$n = 3N - 6$$

for a nonlinear polyatomic molecule.

The total energy consists of a combination of potential- and kinetic-energy terms associated with each of the oscillators relative to the center of mass such that the sum of  $n$  terms for each type of energy,  $2n$  in all, defines  $E$ . This energy

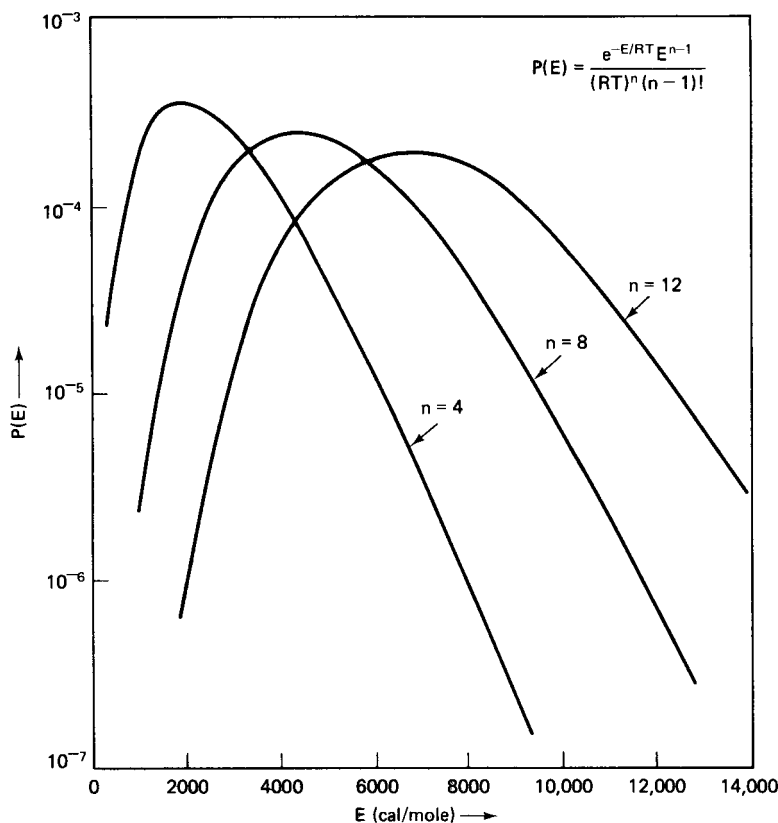


**Figure 2.12** Distribution function,  $P(E)$ , at 298°K.

distribution function is<sup>2</sup>

$$P(E)dE = \frac{e^{-E/kT} E^{n-1} dE}{(kT)^n (n-1)!} \quad (2-40)$$

Here  $P(E)dE$  is the fraction of molecules with total energy between  $E$  and  $E + dE$  distributed among  $n$  internal modes as  $E_1, E_2, \dots, E_n$ . This distribution is illustrated in Figure 2.12. The fraction of the total number of molecules with an energy of at least  $E^*$ ,  $f(E^*)$ , is obtained by integration of equation (2-40) from  $E^*$  to  $\infty$ . The result when  $E^* \gg (n-1)kT$  is

$$f(E^*) = \frac{e^{-E^*/kT} (E^*/kT)^{n-1}}{(n-1)!} \quad (2-41)$$

The distribution,  $P(E)dE$ , can be related to the equilibrium of the first step in the Lindemann scheme by the following argument. The equilibrium constant is

<sup>2</sup> Fortunately, perhaps, the details of this derivation are beyond the scope of this discussion. For a treatment the reader is referred to E.A. Moelwyn-Hughes, *Physical Chemistry*, pp. 34–35 and 43–44, Oxford University Press, New York, NY, (1960).

given by

$$\frac{k_1}{k_{-1}} = \frac{C_A^*}{C_A} \quad (2-42)$$

and we see that  $(C_A^*/C_A)$  is just the fraction of the total number of molecules with energy greater than  $E^*$ , as given directly by equation (2-41). Thus

$$\frac{k_1(E)}{k_{-1}} = f(E^*) = \frac{1}{(n-1)!} \left( \frac{E^*}{kT} \right)^{n-1} e^{-E^*/kT} \quad (2-43)$$

where we have written  $k_1$  as  $k_1(E)$  to emphasize the dependence of this quantity on energy level.

If  $k_{-1}$  is computed from the collision number,  $\bar{Z}_{cT}(A^*, A)$ , which is a reasonable assumption since no activation energy would be involved, then

$$k_1(E) = \frac{\bar{Z}'_{cT}(A^*, A)}{(n-1)!} \left( \frac{E^*}{kT} \right)^{n-1} e^{-E^*/kT} \quad (2-44)$$

where

$$\bar{Z}'_{cT}(A^*, A) = \frac{\bar{Z}_{cT}(A^*, A)}{C_A C_A^*} \quad (2-45)$$

Now  $P(E)$  or  $f(E^*)$  can be used to calculate the apparent  $k^1$  from equation (2-39), completely on the basis of theory.

We can see that  $k_1(E)$  is larger than  $k_1$  computed from collision theory (assuming  $\eta^*$  and  $E^*$  are the same) by the factor  $(E^*/kT)^{n-1}/(n-1)!$ . Subject to the conditions of the validity of equation (2-41), this is a large number and thus the Hinshelwood modification does predict higher activation rates than the original theory.

This cosmetology, however, deals only with the activation step of the Lindemann scheme. What about the decomposition step itself? Let us look at the rate constant  $k_2$ , then, in more detail. The equilibrium concentration of activated molecules contains species with energies from  $E^*$  to infinity, and certainly the individual rate of decomposition should be a function of the magnitude of energy in a given molecule. As a result of this, we must find a relationship between the magnitude of the true unimolecular rate constant,  $k_2$ , and the energy of the reacting molecule. Again we can solve the problem by determining an appropriate distribution. Here for a molecule of total energy between  $E$  and  $E + dE$ , where  $E > E^*$ , we require that  $E^*$  or greater be located in the bond that is being broken in the decomposition. In the model of the  $n$  oscillator polyatomic molecule, this requires that  $E^*$  or greater be located in a single oscillator. The problem can be solved in semiquantitative fashion (some faith is needed) by using a simplified quantum model. We postulate that a molecule consisting of a group of  $n$  oscillators decomposes when one oscillator has a critical energy equal to  $m$  quanta or more out of a total energy in the molecule of  $j$  quanta. Now the total number of ways of distributing  $j$  quanta among  $n$  oscillators (i.e.,  $j$  particles in  $n$  boxes) is

$$q(n, j) = \frac{(j+n-1)!}{(j)!(n-1)!} \quad (2-46)$$

If we require further that  $m$  of the  $j$  quanta be present in one of the oscillators, this total number is reduced to

$$q_m(n, j) = \frac{(j - m + n - 1)!}{(j - m)!(n - 1)!} \quad (2-47)$$

The probability of finding  $m$  or more quanta in the reactive oscillator for this molecule is the ratio

$$P_m(n, j) = \frac{q_m(n, j)}{q(n, j)} = \frac{(j - m + n - 1)!(j)!}{(j - m)!(j + n - 1)!} \quad (2-48)$$

This may be rearranged to the form

$$P_m(n, j) = \prod_{s=1}^{n-1} \left( 1 - \frac{m}{j + s} \right) \quad (2-49)$$

If we define  $\bar{\nu}_j$  as an average rate at which quanta of energy can be transferred among the oscillators of the molecule, a specific rate constant for decomposition would be defined by the product of this rate and the probability,  $P_m(n, j)$ :

$$\bar{k}(E_j) = \bar{\nu}_j P_m(n, j) \quad (2-50)$$

Recognizing that  $m$  in equation (2-49) represents the critical energy,  $E^*$ , and  $j$  the total energy ( $j \gg s$ ), it may be shown that equations (2-49) and (2-50) may be combined to give

$$\bar{k}(E_j) = \bar{\nu}_j \left( 1 - \frac{E^*}{E_j} \right)^{n-1} \quad (2-51)$$

where  $j \gg n$ .<sup>3</sup> The rate constant given in equation (2-51) was first derived in a more rigorous manner by Rice and Ramsperger, and Kassel [O.K. Rice and H.C. Ramsperger, *J. Amer. Chem. Soc.*, 49, 1617 (1927); *J. Amer. Chem. Soc.*, 50, 617 (1928); L.S. Kassel, *J. Phys. Chem.*, 32, 225 (1928)] and is often referred to as the *RRK rate constant*. In terms of the average energy of the reacting molecules, the RRK constant is given by

$$k_2(E_{av}) = \bar{\nu} \left( 1 - \frac{E^*}{nkT} \right)^{1-n} \quad (2-52)$$

Alternatively, for the decomposition rate of molecules of all energies, we may integrate with respect to the distribution function  $P(E)dE$ . This makes the apparent first-order rate constant,  $k^1$ , a function of  $E$ . Rewriting equation (2-38) to show this dependence,

$$k^1(E)dE = \frac{(k_1/k_{-1})k_2(E)}{1 + [k_2(E)/k_{-1}C_A]} dE$$

<sup>3</sup> This is not at all a rigorous approach to the problem. For more honesty see the text by Benson. The treatment here may satisfy physical intuition better, however. ["Keep out of snarls of every kind. They are perfectly abominable. . ." (J.E.B. Stuart)].

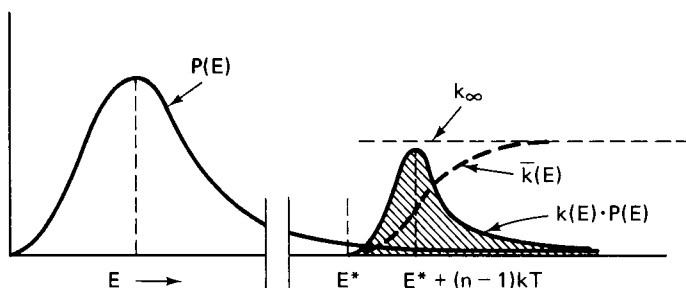


**Figure 2.13** The function  $\bar{k}(E)P(E)$ . The shaded area represents the population of reacting molecules. [After S.W. Benson, *The Foundations of Chemical Kinetics*, with permission of McGraw-Hill Book Company, New York, (1960).]

or

$$k^1(E)dE = \frac{k_2(E)P(E)dE}{1 + [k_2(E)/k_{-1}C_A]} \quad (2-53)$$

Although this result may seem rather unwieldy, it provides detail on all the individual steps involved in the reaction sequence. A major objective here is just to point out that each of the rate “constants” in the Lindemann scheme pertains to a different process, the overall result of which we would observe as a chemical reaction. The nature of the function  $\bar{k}(E)P(E)$  which appears in most applications of the theory (as below) is shown in Figure 2.13.

### Illustration 2.3

Demonstrate the application of the Lindemann theory to an isomerization reaction  $A \leftrightarrow B$  under conditions that might be encountered in practice.

*Solution*

Such a reaction would correspond to the Lindemann scheme under conditions where, for molecules that are not extremely complex, one may have

$$E^* \gg (n-1)kT \quad [\text{equation (2-41)}]$$

$$E^* \gg n \quad [\text{equation (2-51)}]$$

$$k_1C_A \gg k_2(E) \quad (\text{for higher pressures})$$

The apparent rate constant on integration of equation (2-53) is then

$$\bar{k}^1 = \frac{\bar{\nu}}{(n-1)!} \int_{E^*}^{\infty} \left(1 - \frac{E^*}{E}\right)^{n-1} \left(\frac{E}{kT}\right)^{n-1} e^{-E/kT} \left(\frac{dE}{kT}\right) \quad (\text{i})$$

Make the variable transformation  $x = (E - E^*)$ . This gives

$$\bar{k}^1 = \frac{\bar{\nu}}{(n-1)!} e^{-E^*/kT} \int_0^{\infty} \left(\frac{x}{kT}\right)^{n-1} e^{-x/kT} \left(\frac{dx}{kT}\right) \quad (\text{ii})$$

The integral function in equation (ii) is the gamma function, defined as

$$\Gamma(n) = \int_0^{\infty} y^{n-1} e^{-y} dy \quad (\text{iii})$$



which is a tabulated function via book or software. When  $n$  is an integer, however,  $\Gamma(n) = (n-1)!$ , and equation (ii) gives a familiar-looking result for the apparent rate constant  $k^1$ :

$$\bar{k}^1 = \bar{\nu} e^{-E^*/kT} \quad (\text{iv})$$

Since this corresponds to the high-pressure limit,  $k^1 = k_\infty$ .

At the low-pressure limit,  $k_{-1}C_A \ll k_2(E)$  and equation (2-53) becomes

$$\bar{k}^1 = \frac{\bar{Z}'_{cT}(A^*, A)C_A}{(n-1)!} \int_{E^*}^{\infty} \left(\frac{E}{kT}\right)^{n-1} e^{-E/kT} \left(\frac{dE}{kT}\right)$$

which gives (directly from the gamma function),

$$\bar{k}_1 = \bar{Z}'_{cT}(A^*, A)C_A = \pi\sigma_{AA}^2 \left(\frac{4kT}{\pi m_A}\right)^{1/2} c_A \quad (\text{v})$$

The interpretation of this result is that deactivating collisions between A and A\* are infrequent at low pressures, so the activated states have relatively long lifetimes and the apparent rate constant becomes equal to the rate of collisional deactivation of A.

It is seen that the theory also predicts the pressure effect on the apparent activation energy,  $E_{\text{app}}$ . At high pressure, from equation (iv),

$$E_{\text{app}} = kT^2 \frac{\partial \ln \bar{k}^1}{\partial T} = E^* \quad (\text{vi})$$

and at low pressure, from equation (v),

$$E_{\text{app}} = kT^2 \frac{\partial \ln \bar{k}^1}{\partial T} = \frac{1}{2} kT \quad (\text{vii})$$

Rarely does the combination of Mother Nature and mathematics choose an easy route, but the way from equation (ii) to (iv) seems to be one. All of this seems to be a lot of work to produce a well-known result, but it does hopefully produce some insight into the details of the collision process. Notice that we finally had to give up our treasured hard spheres.



HORATIO SAYS

Sometimes I find it hard to believe that getting a molecule to fall apart could be so complex. Somehow, putting them together seems easier. However, we've got a bit more for you coming up.

We may draw several conclusions from the illustration above—as already briefly mentioned. First, comparison of equation (iv) with the Arrhenius form

suggests that the pre-exponential factor of the latter is a frequency related to the vibrational frequency of the oscillators in the molecule (or, more correctly, some characteristic frequency at which energy can be exchanged intramolecularly). Such frequencies as evaluated from molecular spectra are generally in the range of  $10^{12}$  to  $10^{14} \text{ s}^{-1}$ . Arrhenius correlation of high-pressure rate constants yielding values much larger or smaller than this should be taken as indicative of large structural changes occurring in the reaction. The reason for this, and a more quantitative approach to such structural effects (basically entropy factors), will be given in the next section. Second, the RRK rate constant in terms of average energy, equation (2-52), approaches the Arrhenius form as  $n$  becomes large. An illustration for  $(E^*/kT) = 35$  is given in Figure 2.14. We also observe from Figure 2.14 that as the molecule under consideration becomes more complex ( $n$  increases), the ratio  $[k_2(E_{av})/\bar{\nu}]$  increases, meaning that the average lifetime of the molecule before decomposition increases with increasing molecular complexity. Finally, the different limiting forms for  $k^1$  and the associated activation energies clearly indicate the changing nature of the controlling or dominant step in the reaction as the conditions of reaction change.

It is possible to visualize a large number of additional reactions in terms of collisional activation/unimolecular reaction steps similar to those in the Lindemann scheme. For example, a fully detailed model of the isomerization reaction we have been discussing might be written as



where the first and last steps represent collisional activation and deactivation, and  $A^* \leftrightarrow B^*$  is a true RRK step. At the next level of complexity we might treat the

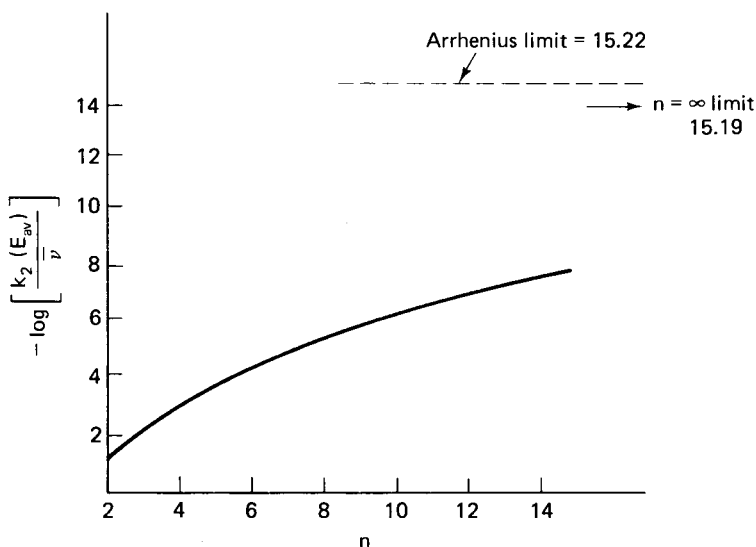


**Figure 2.14** Comparison of  $k_2(E_{avg})$  with the Arrhenius equation for  $(E^*/kT) = 35$ .

bimolecular association reaction  $A + B \leftrightarrow C$  as



where the unimolecular step involves  $(AB) \leftrightarrow C^*$  and all others involve collisional activation or deactivation. In (XXII),  $(AB)$  would represent an association complex of A and B without sufficient energy to react, and  $(AB)^*$  represents those complexes with sufficient energy for reaction, formed either from  $A^*$  and B, A and  $B^*$ , or collisional activation of  $(AB)$ . A number of cases like this have been treated by Benson and Axworthy [S.W. Benson and A.E. Axworthy, *J. Chem. Phys.*, 21, 428 (1953)], and their results are very illuminating insofar as giving one some intuitive feeling for the role individual steps play in the overall reaction process.

### 2.3 Transition-State Theory of Reaction Rates

In extending the collision theory to describe unimolecular reactions, we have seen that the concept of an activated state for a molecule arises quite naturally. This activated state in effect represents the molecule in transition from the reactant to the product, and it is the concentration of such activated molecules that determines the rate of formation of product. [“Always somebody goin’ away, somebody gettin’ home.”—*J.J. Bell*]. To obtain this concentration, we were required to determine the equilibrium constant defined by equation (2-42), which should immediately suggest that an alternative approach to the problem via thermodynamic arguments might be possible. In the *transition-state theory* (TST) we take such an approach, in which the reacting system is postulated to pass through a configuration of minimum potential energy as it goes from reactants to products, and the rate of passage through this configuration is the rate of reaction. Such a configuration is called the *transition state*, and a system in the transition state is termed the *activated complex*. The number of activated complexes, just as the energized molecules  $A^*$  in the Lindemann scheme, is determined by an equilibrium with the reactant molecules, and it is assumed that the generation of products by decomposition of the transition state complex does not affect this equilibrium.

Now, if we do this theory correctly, we can also address one of the major problems of the results developed so far.<sup>4</sup> The theory has dealt with molecular interactions at several levels, but basically has dealt with gas-phase reactions only. This is not to say that the correlation approaches such as those developed in Chapter 1 for general kinetics have no application to condensed phases (indeed, see Illustration 1.9), but we have not demonstrated any theoretical basis so far. There is no such restriction in TST, so the single-phase limitation will go away with no specific effort.

Since the transition state represents a minimum potential-energy configuration, one is tempted to conclude that complete information on potential energy for all configurations of the reacting system is required to implement the theory, and in the strictest sense this is true. Yet, the fact is such potential-energy information can be obtained only from quantum mechanical calculations of considerable precision

<sup>4</sup> One can hear the wails of anguish from afar, “After fifty or so pages, what possibly could have been left out?” It is simply the question of not seeing the forest because the trees are in the way.

for molecular binding energies, together with information concerning the shapes and dimensions of all molecules in the reacting system. Even from an optimistic point of view this is a near impossibility, and as a result, the most complicated system for which such calculations have been made in detail is on the order of the ortho-para hydrogen transformation, which involves only three electrons. How, then, can such a theory be of use if the basic information it requires is essentially nonexistent? We can answer this in part by saying that in many aspects the theory is more useful in its qualitative features than any exact results that might be computed. The perceptive reader will also note after following the development to be given in this section that TST has a lot to say concerning pre-exponential factors in rate constants, but not much about activation energies, since this is precisely the potential-energy information that is lacking. Nonetheless, since the application of TST requires definition of the transition state in some manner, as we shall see, one can obtain considerable insight into the nature of the reacting system, including all of the internal motions of

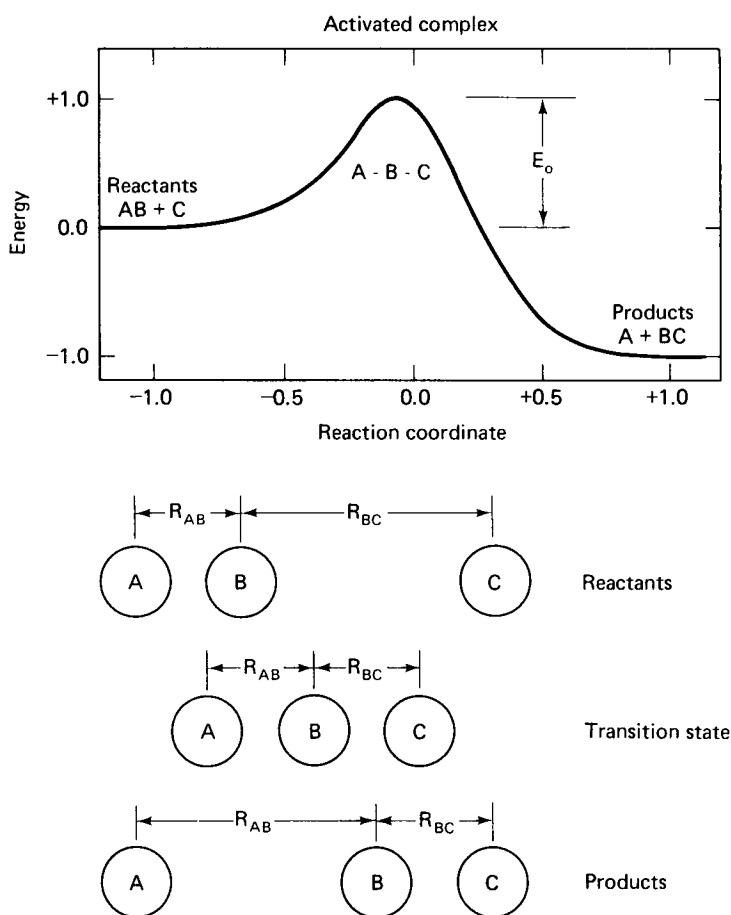


**Figure 2.15** Potential energy of the reaction  $AB + C$  as a function of the reaction coordinate. [From R.E. Watson, Jr., *Science*, 158, 332, by the American Association for the Advancement of Science, with permission, (1967).]

the molecules involved, from comparison of experimental and theoretical values, or even from comparison of predicted rate constants using different reaction models. These features will be appreciated best in their application.

### 2.3.1 Reaction Paths

The best way to illustrate the concept of a reaction according to TST is by examining the energy of the system as one proceeds from reactants to products. For an example we shall use a displacement reaction between the species A, B, and C, such that



The potential energy of this system as a function of some parameter indicating the progress of the reaction (reaction coordinate) would be as shown in Figure 2.15, where the barrier height between reactants and the transition state, (ABC), represents the classical activation energy of the reaction. Similarly, the difference in energy between reactants and products represents the heat of reaction, in this case exothermic for the illustration of Figure 2.15. Now, to simplify the problems of pictorial representation, let us assume for the moment that the molecules and the transition state are linear. Thus, of the  $3N$  coordinates specifying the positions of the individual

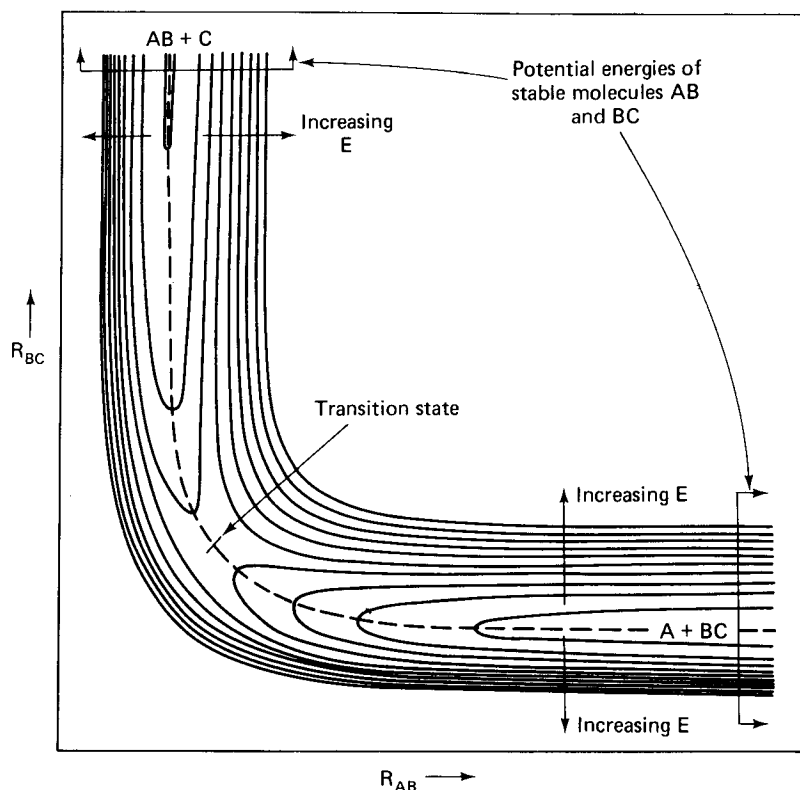


**Figure 2.16** Potential-energy surface for the reaction  $\text{AB} + \text{C} \rightarrow \text{A} + \text{BC}$  with linear geometry. [From R.E. Weston, Jr., *Science*, 158, 332, by the American Association for the Advancement of Science, with permission, (1967).]

molecules, nine total here, six are required to specify the location of the center of mass and its orientation in space, and an additional one to specify the linearity of the transition complex. This leaves us with two coordinates to specify the state of the reacting system (the reaction coordinate of Figure 2.15). For this simple example these two coordinates are obviously the intermolecular separations, A from B ( $R_{AB}$ ) and B from C ( $R_{BC}$ ), also shown in Figure 2.16. This implies that the potential energy of the reacting system can be represented by a two-dimensional diagram such as that of Figure 2.16, in which the contour lines represent differing energy levels. At the upper left, as indicated,  $R_{AB}$  is small and  $R_{BC}$  large, so a cross section drawn perpendicular to the energy contours would represent the potential energy of the stable molecule AB. Conversely, at the lower right one has the stable molecule BC. Now the stable reactant molecule AB with minimum potential energy will be located in the midst of the valley defined by the energy contours of Figure 2.16, as will the product BC, and according to the postulates of TST, the reacting system will move from AB + C to A + BC by the minimum-energy pathway. In this case the path is indicated by the dashed line on the figure, with the point of maximum energy along the path (minimum of the maxima) defining the transition state.

Such a potential energy surface and reaction path for the reaction  $H + H_2$  are shown in Figure 2.17. Obviously, the detailed knowledge required to construct such surfaces exists for only a few simple reactions. Another reaction that has been

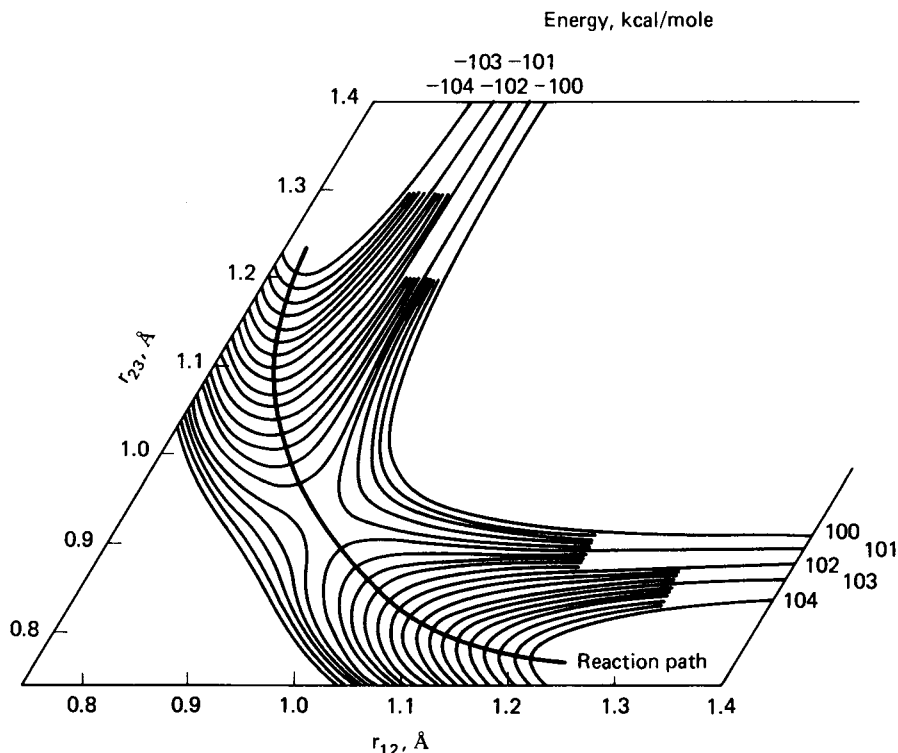


**Figure 2.17** Potential-energy surface and reaction path for  $H_2 + H$ . [From R.E. Weston, Jr., *J. Chem. Phys.*, 31, 892, with permission of the American Institute of Physics, (1959).]

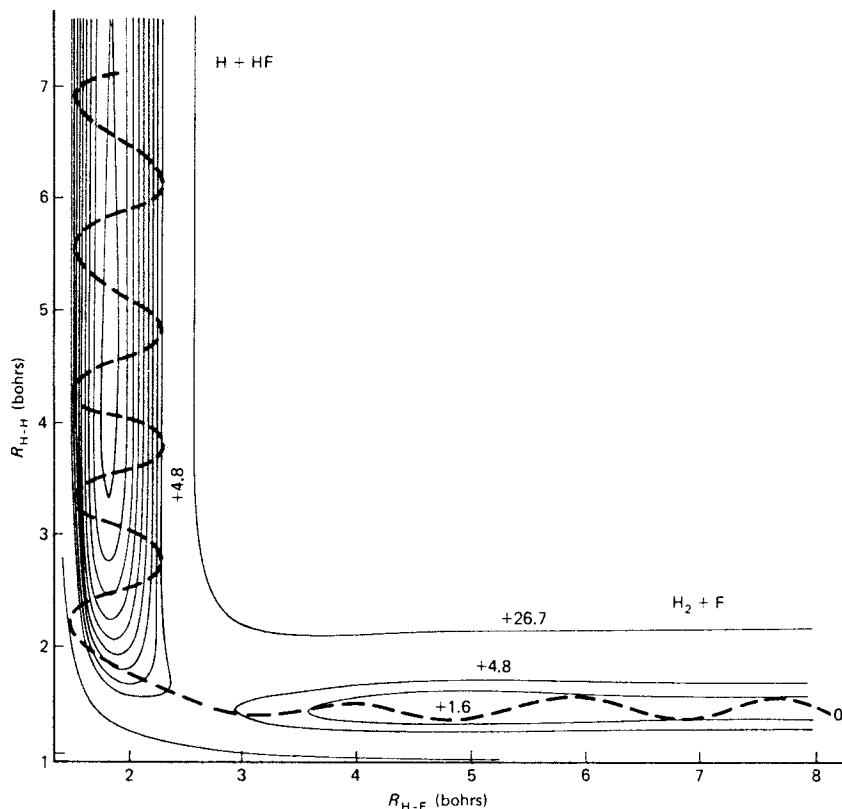


**Figure 2.18** Potential-energy surface and reaction path for the reaction  $F + H_2$ . [From J.I. Steinfeld, J.S. Francisco and W.L. Hase, *Chemical Kinetics and Dynamics*, with permission of Prentice-Hall, Englewood Cliffs, NJ, (1989).]

studied in some detail is  $F + H_2 \rightarrow HF + H$  [J.C. Polanyi and J.L. Schreiber, *Faraday Disc. Chem. Soc.*, 62, 267 (1977)], which is exothermic and involves dissimilar reactant molecules. The resultant potential energy surface, Figure 2.18, is quite assymmetric and the transition state occurs much closer to the reactant configuration than the product. It has been shown that for this reaction the exothermic energy is largely channeled into vibrational excitation of the product molecule, indicated by the pronounced waveform of the reaction trajectory at low values of  $R_{H-F}$  (reaction path from right to left in this case). As stated above, however, there are only a few reactions that we are privileged to know in so much detail, hence further developments here must lead back to the old reliables A, B and C.

### 2.3.2 Equilibrium of the Transition Complex

If the concentration of transition complexes is determined by an equilibrium with the reactant molecules, our example reaction (XXIII) must be viewed in terms of the following sequences:



where  $(ABC)^\ddagger$  is the transition state complex and its concentration,  $C_\ddagger$ , is determined from

$$K_C^\ddagger = \frac{C_\ddagger}{C_{AB}C_C} \quad (2-54)$$

From elementary statistical thermodynamics we know that the equilibrium constant can be written in terms of the partition functions of the individual molecules taking part in a reaction. These quantities represent the sum over all energy states in the system—translational, rotational, vibrational, and electronic. The probability that a molecule will be in a particular energy state,  $E_i$ , is given by the Boltzmann law,

$$P(E_i) \propto g_i e^{-E_i/kT} \quad (2-55)$$

in which  $g_i$  is a weighting factor associated with the degeneracy<sup>5</sup> of the energy state  $E_i$ . We have already derived a specific form of this law for the distribution of kinetic energies. Now the sum over all states,  $Q$ , is the partition function:

$$Q = \sum_i g_i e^{-E_i/kT} \quad (2-56)$$

and if we take the total energy to be composed of the sum of contributions from translation, rotation, vibration, and electronic factors,

$$Q = Q_t Q_r Q_v Q_e \quad (2-57)$$

since the energies are added in the argument of the exponential term.

The sum over all states defines a total probability, which if we write in terms of probability per unit volume will be (in ratio with other probabilities), the same as concentration ratios. Thus,

$$K_C^\ddagger = \frac{C_\ddagger}{C_{AB}C_C} = \frac{Q_\ddagger^\circ}{Q_{AB}^\circ Q_C^\circ} \quad (2-58)$$

Where the  $Q$ 's are partition functions per unit volume.

It is convenient to write these functions with respect to the lowest energy state of each molecule, taken to be zero for each, which means that we must account for the difference in energy between the lowest states of AB and C and the transition complex  $(ABC)^\ddagger$ . This is, in fact, the activation energy of the reaction as shown in Figure 2.15 (admittedly sort of entering through the back door here), so

$$K_C^\ddagger = \frac{Q_\ddagger^\circ}{Q_{AB}^\circ Q_C^\circ} e^{-E/kT} \quad (2-59)$$

where the partition functions are based on a zero value at the lowest energy level of the respective molecules. The generalization of equation (2-59) for any equilibrium step  $aA + bB + \cdots \leftrightarrow lL + mM + \cdots$  is

$$K_C = \frac{(Q_L^\circ)^p (Q_M^\circ)^q \cdots}{(Q_A^\circ)^r (Q_B^\circ)^s \cdots} e^{-E/kT} \quad (2-60)$$

<sup>5</sup> This is a term that often confuses. It has nothing to do with morality, rather it means the number of different configurations of individual energy states that lead to the same total energy,  $E_i$ . For more detail see, for example, T.L. Hill, *An Introduction to Statistical Mechanics*, Addison-Wesley, Reading, MA, (1960).



Values for the individual partition functions  $Q_i$ , and so on, for a given molecule can be computed from information on molecular weight, configuration, vibrational modes, and electronic levels of the molecule. For translation in three dimensions,

$$Q_t = \frac{(2\pi mkT)^{3/2}}{h^3} V \quad (2-61)$$

where  $V$  is the volume of the system considered,  $m$  the molecular weight, and  $h$  is Planck's constant.

In the calculation of chemical equilibrium, partition functions per unit volume are desired, so

$$Q_i^\circ = \frac{(2\pi mkT)^{3/2}}{h^3} \quad (2-62)$$

and

$$Q^\circ = Q_t^\circ Q_r Q_v Q_e \quad (2-63)$$

For a nonlinear molecule, three rotational degrees of freedom exist involving three principal moments of inertia,  $I_1$ ,  $I_2$ , and  $I_3$ :

$$Q_r = \frac{8\pi^2(8\pi^3 I_1 I_2 I_3)^{1/2} (kT)^{1/2}}{h^3 \sigma} \quad (2-64)$$

The quantity  $\sigma$  appearing in equation (2-64) is the molecular symmetry number and is determined by the number of spatial orientations of the subject molecule that are identical. For linear molecules there is only one principal moment of inertia,  $I$ , and two degrees of rotational freedom, so

$$Q_r = \frac{8\pi kTI}{h^3 \sigma} \quad (2-65)$$

For  $n$  degrees of vibrational freedom the partition function is

$$Q_v = \prod_{s=1}^n (1 - e^{-h\nu_s/kT})^{-1} \quad (2-66)$$

where  $\nu_s$  is the frequency of the  $s$ th mode.

Unless one is dealing with excited states of molecules, a problem considerably beyond the scope of our present interest, electronic energy does not contribute to the partition function. The lowest-energy state of a molecule is ordinarily a singlet state; hence  $Q_e = 1$ .

It is often convenient to represent these partition functions in terms of factors per degree of freedom. For an  $N$ -atom nonlinear molecule,

$$Q_t = f_t^3 \quad (2-67)$$

$$Q_r = f_r^3 \quad (2-68)$$

$$Q_v = f_v^{3N-6} \quad (2-69)$$

**Table 2.3** Estimated Partition Functions per Degree of Freedom<sup>a</sup>

Translation	$f_t$	$10^8$ – $10^9$
Rotation	$f_r$	$10^1$ – $10^2$
Vibration	$f_v$	$10^0$ – $10^1$

$$^a f_t = \frac{(2\pi mkT)^{1/2}}{h}$$

$$f_r = \left( \frac{8\pi^2}{\sigma} \right)^{1/3} \frac{(8\pi^3 I_1 I_2 I_3)^{1/6}}{h} (kT)^{1/2}$$

$$f_v = (1 - e^{h\nu_s/kT})^{-1}$$

Source: After A.A. Frost and R.G. Pearson, *Kinetics and Mechanism*, 2nd ed., with permission of John Wiley & Sons, Inc., New York, (1961).

and

$$Q^\circ = f_t^3 f_r^3 f_v^{3N-6} \quad (2-70)$$

Such representation is useful when it is impossible or impractical to make detailed calculations of partition functions, but when order-of-magnitude estimates would be helpful. Table 2.3 is a tabulation of representative values for these factors computed from equations (2-62), (2-64), or (2-65) and (2-66) using typical values for molecular constants in the temperature range from 300–500°K. The translational contribution per degree of freedom is much larger than rotation or vibration, however, in complicated polyatomic molecules it is possible for the total vibrational contribution to become large as  $(3N - 6)$  becomes a large number.

With these equations or estimates for the partition functions, we are now prepared to calculate the equilibrium constant,  $(K_c)^\ddagger$ , and thus in principle to determine  $C_\ddagger$  in terms of the observables  $C_{AB}$  and  $C_C$ , and what we know or are prepared to postulate concerning the nature of the reactants and the transition complex.

### 2.3.3 The Rate of Reaction

We have stated for the postulate of TST that the rate of reaction is the rate of passage of activated complexes through the transition state, that is, over the energy barrier shown in Figure 2.15. We can write this rate in terms of a frequency of passage over the barrier,  $v_\ddagger$ , such that

$$r = v_\ddagger C_\ddagger \quad (2-71)$$

where  $r$  is the rate of reaction.

For our example reaction, if we substitute for  $C_\ddagger$  from equation (2-58):

$$r = v_\ddagger \frac{Q_\ddagger^\circ}{Q_{AB}^\circ Q_C^\circ} e^{-E/RT} C_{AB} C_C \quad (2-72)$$

where we have used the molal constant  $R$  in place of  $k$ . Now we must examine in detail the nature of the partition functions  $Q_{AB}^\circ$ ,  $Q_C^\circ$ , and  $Q_\ddagger^\circ$ . The first two of these refer to the reactant molecules considered at equilibrium, and present no problem. However,  $Q_\ddagger^\circ$  refers to the complex in the transition state, and it is reasonable to assume that the configuration of this state as required for reaction to occur may

place some restriction on the degrees of freedom allowed, and this is indeed so. We have seen in Figure 2.15 that the relative values of  $R_{AB}$  and  $R_{BC}$  can serve as a measure of the extent of reaction (i.e., progress along the reaction coordinate, *not* conversion). If we view that passage through the transition state as a particular type of vibration, one in which C approaches B while A is departing (picture a dog, viewing a bone, pulling on a leash), we may consider that one of the vibrational degrees of freedom is fixed by this movement through the transition state. This is of low frequency compared to ordinary molecular vibrations and we may write equation (2-66) for this particular vibration as

$$(f_v^\ddagger)_t = (1 - e^{h\nu_t^\ddagger/kT})^{-1} \quad (2-73)$$

which for low frequency is

$$(f_v^\ddagger)_t = \frac{kT}{h\nu_t^\ddagger} \quad (2-74)$$

As the subscript in the equations above indicates, this frequency must also be identical with the frequency of passage through the transition state, so the rate equation becomes

$$r = \left( \frac{kT}{h} \right) \frac{(Q_\ddagger^\circ)'}{Q_{AB}^\circ Q_C^\circ} e^{-E/RT} C_{AB} C_C \quad (2-75)$$

in which

$$(f_v^\ddagger)_t (Q_\ddagger^\circ)' = Q_\ddagger^\circ \quad (2-76)$$

In evaluation of the partition function of the transition complex, then, one must subtract one degree of vibrational freedom to account for motion along the reaction coordinate. For a nonlinear transition state,

$$(Q_\ddagger^\circ)' = f_v^{3N-7} f_t^3 f_r^3 \quad (2-77)$$

or for the linear case, as involved in the example reaction we have been using:

$$(Q_\ddagger^\circ)' = f_v^{3N-6} f_t^3 f_r^2 \quad (2-78)$$

To generalize the result of equation (2-75), the TST predicts that the rate constant for a reaction is given universally by

$$k' = \left( \frac{kT}{h} \right) (K_c^\ddagger)' \quad (2-79)$$

where

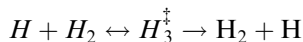
$$(K_c^\ddagger)' = \frac{(Q_\ddagger^\circ)'}{\prod_i (Q_i^\circ)} e^{-E/RT} \quad (2-80)$$

for  $i$  reactants. Pre-exponential factors may be calculated directly from equation (2-80) without the exponential factor.

In summary here, it can be seen that TST does include details of the internal molecular configurations in addition to the intermolecular interactions (collision). However as stated before, at this level of the theory we have nothing concerning  $E$ .

**Illustration 2.4**

Estimate a value for the frequency factor of the reaction



in terms of the appropriate partition functions using the approximations detailed in Table 2.3.

*Solution*

We can write the frequency factor as

$$k^\circ = \left( \frac{kT}{h} \right) \frac{(Q_3^\ddagger)'}{Q_H^\circ Q_{H_2}^\circ} \quad (\text{i})$$

Contributions to the partition functions will be:

$(Q_3^\ddagger)'$  = two rotational degrees of freedom for a linear molecule plus  
 $(3N - 5) - 1$  vibrational, plus three translational

$Q_H^\circ$  = three translational

$Q_{H_2}^\circ$  = two rotational plus one vibrational plus three translational

The order of magnitude estimate will then be

$$\left( \frac{kT}{h} \right) = 10^{13} \text{ s}^{-1}$$

and

$$k^\circ = (10)^{13} \left[ \frac{f_t^3 f_r^2 f_v^3}{f_t^3 f_t^3 f_r^2 f_v} \right] = \frac{(10^{13})(10^8)^3 (10)^2 (1)^3}{(10^8)^3 (10^8)^3 (10)^2 (1)} \quad (\text{ii})$$

thence

$$k^\circ = 10^{-10} \leftarrow \dots \rightarrow 10^{-11} \text{ cm}^3 \cdot \text{s}^{-1} \cdot \text{molecule}^{-1}$$

It is seen that the internal modes of the molecules have a large amount to say about the magnitude of the frequency factor even for this simple reaction.

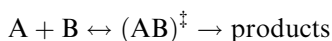


HORATIO SAYS

See the exercises at the end of the chapter. A detailed calculation of the above yields a value of about  $9 \times 10^{-11} \text{ cm}^3 \cdot \text{s}^{-1} \cdot \text{molecule}^{-1}$ , which is about as good as one can expect for a theory of this nature.

### 2.3.4 Some Applications of the Theory

Although this section may be a bit redundant after following the details enumerated in the illustration above, it is still probably worth the effort to find out what is obtained for the collision theory model that we have been using.<sup>6</sup> It will be recalled that two hard spheres, A and B, which possess only kinetic energy react upon collision when their relative energy exceeds  $\eta^*$ . In terms of TST we may write the reaction as



where the reactants are atoms and the transition state complex is a diatomic molecule of dimension  $\sigma_{AB}$  between centers. The rate is

$$r = \left( \frac{kT}{h} \right) \frac{(Q_\ddagger^\circ)'}{Q_A^\circ Q_B^\circ} e^{-\eta^*/kT} C_A C_B \quad (2-81)$$

and since atoms A and B have only kinetic energy the appropriate partition functions are

$$Q_i^\circ = \frac{2\pi m_i kT}{h^3}; \quad i = A, B$$

The transition state complex is linear and so will have  $(3N - 6)$  degrees of vibrational freedom (i.e., none in this case), two rotational, and three translational:

$$(Q_\ddagger^\circ)' = \frac{[2\pi(m_A + m_B)kT]^{3/2}}{h^3} \frac{8\pi^2 kT I_{AB}}{h^2 \sigma} \quad (2-82)$$

where

$$I_{AB} = \sigma_{AB}^2 \mu_{AB}$$

Substituting these expressions for  $Q_A^\circ$ ,  $Q_B^\circ$ , and  $(Q_\ddagger^\circ)'$

$$r = \left( \frac{8\pi kT}{\mu_{AB}} \right)^{1/2} \sigma_{AB}^2 e^{-\eta^*/kT} C_A C_B \quad (2-83)$$

which is the collision theory result obtained previously. Using the approximate values per degree of freedom given in Table 2.3, we can write

$$Q_A^\circ = Q_B^\circ = f_t^3$$

$$(Q_\ddagger^\circ)' = f_t^3 f_r^2 f_v^\circ$$

and after substitution in equation (2-81) and simplification

$$r = \left( \frac{kT}{h} \right) \left( \frac{f_r^2}{f_t^3} \right) e^{-\eta^*/kT} C_A C_B$$

<sup>6</sup> “You are old, Father William, the young man said, and your hair has become very white, yet you incessantly stand on your head. Do you think, at your age, it is right?”—*Lewis Carroll*

The preexponential factor for the binary collision is then

$$k^\circ = \left( \frac{kT}{h} \right) \left( \frac{f_r^2}{f_t^3} \right)$$

which for values of  $T \approx 300$  to  $500^\circ\text{K}$ , and  $f_t$  and  $f_r$  (as given in Table 2.3), gives

$$r \approx (10^{-10}) e^{-\eta^*/kT} C_A C_B \quad (2-84)$$

The steric factor,  $p$ , of equation (2-20) can be estimated directly from TST using either exact or approximate methods. This is satisfying, since in the manner in which it was introduced  $p$  seemed to be yet another adjustable parameter. In general the steric factor is given by the ratio of the pre-exponential factor of the reaction in question to that for the binary collision model:

$$p = \frac{[(Q_\ddagger^\circ)'] \prod_i (Q_\ddagger^\circ)_i}{(f_r^2/f_t^3)}$$

or, substituting for individual degrees of freedom,

$$p = \frac{(f_t^3 f_r^2 f_v^{3N_\ddagger-7}) / \prod_i (f_t^3 f_r^3 f_v^{3N_i-6})_i}{(f_r^2/f_t^3)} \quad (2-85)$$

A listing of typical estimates of this sort is given in Table 2.4. It can be seen that as the reaction becomes more complex in relation to the hard-sphere collision model, the steric factor decreases. In practice, then, one might be able to use the magnitude of experimentally determined steric factors as the basis for more detailed hypotheses concerning the nature of a given reaction.

For unimolecular reactions, the transition state and reactant can differ by only one degree of vibrational freedom, thus

$$r = \left( \frac{kT}{h} \right) \left( \frac{1}{f_v} \right) e^{-E/RT} C_A \approx (10^{13}) e^{-E/RT} C_A \quad (2-86)$$

Now, let us find a little flaw in the theory: equation (2-86) predicts only first-order behavior for the unimolecular reaction, something we know in fact is not true at low pressures. The reason for this failure in TST is the assumption of universal equilibrium between reactants and the transition state complex. At low pressures the collisional deactivation process becomes very slow, since collisions are infrequent, and the rate of decomposition becomes large compared to deactivation. In such an event, equilibrium cannot be established; nearly every molecule which is activated will decompose to product. However, the magnitude of the rate of decomposition of the transition complex is much larger than the decomposition of the activated molecule in the collision theory scheme, so one must resist the temptation to equate the two. Since the transition state complex represents a configuration of the reacting molecule on the way from reactants to products, the activated molecule must be a precursor of the transition state complex.

In numerical application of the equations of this section, one must be careful of the units involved. Rate constants such as those defined by equation (2-75) are

**Table 2.4** Approximate Expressions and Values for Biomolecular Rate Constants for Different Types of Reactants and Complexes

Frequency factor			Steric factor	
Formula	Value (cm <sup>3</sup> /molecule-sec)	<i>T</i> Exponent	Formula	Value
1. Two atoms				
$\frac{kT}{h} \frac{f_r^2}{f_i^3}$	10 <sup>-10</sup> – 10 <sup>-9</sup>	$\frac{1}{2}$	1	1
2. Atom + linear molecule, linear complex				
$\frac{kT}{h} \frac{f_v^2}{f_i^3}$	10 <sup>-12</sup> – 10 <sup>-11</sup>	$-\frac{1}{2}$ to $\frac{1}{2}$	$\left(\frac{f_v}{f_r}\right)^2$	10 <sup>-2</sup>
3. Atom + linear molecule, nonlinear complex				
$\frac{kT}{h} \frac{f_v f_r}{f_i^3}$	10 <sup>-11</sup> – 10 <sup>-10</sup>	0 to $\frac{1}{2}$	$\left(\frac{f_v}{f_r}\right)$	10 <sup>-1</sup>
4. Atom + nonlinear molecule, nonlinear complex				
$\frac{kT}{h} \frac{f_v^2}{f_i^3}$	10 <sup>-12</sup> – 10 <sup>-11</sup>	$-\frac{1}{2}$ to $\frac{1}{2}$	$\left(\frac{f_v}{f_r}\right)^2$	10 <sup>-2</sup>
5. Two linear molecules, linear complex				
$\frac{kT}{h} \frac{f_v^4}{f_i^3 f_r^2}$	10 <sup>-14</sup> – 10 <sup>-13</sup>	$-\frac{3}{2}$ to $\frac{1}{2}$	$\left(\frac{f_v}{f_r}\right)^4$	10 <sup>-4</sup>
6. Two linear molecules, nonlinear complex				
$\frac{kT}{h} \frac{f_v^3}{f_i^3 f_r}$	10 <sup>-13</sup> – 10 <sup>-12</sup>	-1 to $\frac{1}{2}$	$\left(\frac{f_v}{f_r}\right)^3$	10 <sup>-3</sup>
7. One linear + one nonlinear molecule, nonlinear complex				
$\frac{kT}{h} \frac{f_v^4}{f_i^3 f_r^2}$	10 <sup>-14</sup> – 10 <sup>-13</sup>	$-\frac{3}{2}$ to $\frac{1}{2}$	$\left(\frac{f_v}{f_r}\right)^4$	10 <sup>-4</sup>
8. Two nonlinear molecules, nonlinear complex				
$\frac{kT}{h} \frac{f_v^5}{f_i^3 f_r^3}$	10 <sup>-15</sup> – 10 <sup>-14</sup>	-2 to $\frac{1}{2}$	$\left(\frac{f_v}{f_r}\right)^5$	10 <sup>-5</sup>
Unimolecular reaction				
$\frac{kT}{h}$	10 <sup>13</sup> sec <sup>-1</sup>	1		

Source: After A.A. Frost and R.G. Pearson, *Kinetics and Mechanism*, 2nd ed., with permission of John Wiley & Sons, Inc., New York, (1961).

molecular values, as is the activation energy.<sup>7</sup> Consistent units, molecules/volume, must then be used for concentration terms. For activation energies in molal units, *k* is replaced by the gas constant  $R = N_a k$ , and the rate constant must be multiplied by Avagadro's number,  $N_a$ . All this may seem a bit messy, and it is, however, if the solutions to the problems begin to differ from the correct answer by a factor of 10<sup>24</sup> the locus of the difficulty is not hard to identify.

<sup>7</sup>Actually, we may have been a little carefree in interchanging  $E/RT$  and  $E/kT$ . The former implies molal units and the latter molecular units for *E*, and *R* or *k*.

### 2.3.5 Thermodynamic Analysis of Transition-State Theory

From the way that the reaction sequence (XXIV) is written, one might suppose that it is possible to look at the overall problem also in terms of macroscopic thermodynamic functions defined on a molal basis. Certainly this is so; the equilibrium between transition state and reactants can be expressed in terms of a classical free energy of activation as

$$(\Delta G^\circ)^\ddagger = -RT \ln (K^\ddagger) \quad (2-87)$$

where  $K^\ddagger$  would be an equilibrium constant defined via activities in the usual way, and the change in free energy is per mol between reactants and the transition state complex. At constant temperature we know that

$$(\Delta G^\circ)^\ddagger = (\Delta H^\circ)^\ddagger - T(\Delta S^\circ)^\ddagger \quad (2-88)$$

so then

$$K^\ddagger = e^{-(\Delta H^\circ)^\ddagger/RT} e^{(\Delta S^\circ)^\ddagger/R} \quad (2-89)$$

The corresponding rate equation, following equation (2-75), is

$$r = \left( \frac{kT}{h} \right) \frac{e^{-(\Delta H^\circ)^\ddagger/RT} e^{(\Delta S^\circ)^\ddagger/R}}{C^\circ} C_{AB} C_C \quad (2-90)$$

in which  $(\Delta H^\circ)^\ddagger$  and  $(\Delta S^\circ)^\ddagger$  are standard enthalpies and entropies of activation (formation of the transition state complex), and  $C^\circ$  is a reference concentration. Numerical evaluation of equation (2-90) can give difficulties unless one is careful about  $C^\circ$ ; this may be chosen as  $(P/RT)$  at 1 atm and  $T$  for gases, or as the molal concentration of pure components for liquids. The inclusion of  $C^\circ$  in equation (2-90) arises from the fact that the term  $\exp[(\Delta S^\circ)^\ddagger/R]/C^\circ$  will be independent of the choice of reference state. Thus, for tabulated or calculated values of  $(\Delta H^\circ)^\ddagger$  and  $(\Delta S^\circ)^\ddagger$  for a given reaction we can directly determine the rate constant. Such tabulations are, in effect, another way of reporting kinetic parameters.

A question that immediately comes to mind is what might be the relationship between this enthalpy of activation and the quantity we have been calling activation energy. If we let the latter play the role of internal energy in classical thermodynamics, then

$$(\Delta H^\circ)^\ddagger = (\Delta E^\circ)^\ddagger + P(\Delta V^\circ)^\ddagger \quad (2-91)$$

for reactions at constant pressure. In general, for reactions in the liquid or solid phase, the second term is small, so that

$$E_{\text{app}} = RT^2 \left( \frac{\partial \ln(k)}{\partial T} \right) = (\Delta H^\circ)^\ddagger + RT \quad (2-92)$$

A look at the data given in Chapter 1 will further convince one that  $RT$  is generally much smaller than  $(\Delta H^\circ)^\ddagger$ , so the apparent activation energy for these reactions is often approximately equal to the enthalpy of formation of the transition state. For ideal gases, on the other hand, we have

$$P(\Delta V^\circ)^\ddagger = (\Delta n)^\ddagger RT \quad (2-93)$$



where  $\Delta n^\ddagger$  is the difference in mols between reactant and complex (complex *minus* reactant) and then

$$E_{\text{app}} = (\Delta H^\circ)^\ddagger - [(\Delta n)^\ddagger - 1]RT \quad (2-94)$$

In many instances the value of  $[(\Delta n)^\ddagger - 1]$  is such that  $E_{\text{app}}$  and  $(\Delta H^\circ)^\ddagger$  differ only by several multiples of  $RT$  at most (consider our example of  $A + BC$ ). While such differences do not appear to be large in absolute value, one must remember that  $E_{\text{app}}$  appears in an exponential term in most calculations, and therefore factors on the order of  $RT$  can be significant numerically.

From a conceptual point of view, the thermodynamic formulation of TST is probably of most use in pointing out that it is a *free energy* barrier that must be overcome in reaction. The entropy change associated with formation of the transition state is separate from the enthalpy change. It is quite possible for a reaction with a large energy requirement to go at a respectable rate because of a compensating large positive value for  $(\Delta S^\circ)^\ddagger$ . This would mean that the reaction exhibits a larger than normal frequency factor, compensating for the large energy requirement.

The steric factor we have discussed previously is closely related to the entropy of activation. Small values of the steric factor will generally be associated with large changes in the structure as the system moves to the configuration of the transition state, involving large entropy changes. As a qualitative example, compare cases 2 and 3 of Table 2.3. The linear complex of 2 is a more ordered structure than the nonlinear complex of 3, both for the same reactant, and the steric factor for 2 is an order of magnitude smaller than that of 3. This is directly the result of the larger entropy change required for formation of the transition complex of case 2. A crude generalization of this would associate small steric factors with reactions in which the transition complex is far removed in configuration from the reactants with larger values for those in which the transition complex is similar in structure to the reactants.

Benson [S.W. Benson, *Thermochemical Kinetics: Methods for the Estimation of Thermochemical Data and Rate Parameters*, Second ed., John Wiley and Sons, New York, NY, (1976)] has presented ways for determining Arrhenius parameters in some detail using methods derived from the TST-thermodynamic approach. Although the specifics of this are beyond the scope of the presentation here, the methods are relatively rapid and reliable, and of considerable utility for those who may have further interest. Extensive compilations of data and examples are given for a large number of gas-phase reactions classified as to unimolecular fission, isomerization, bimolecular, metathesis, atom recombination, and so on.

### 2.3.6 Reactions in Nonideal Systems

So far the theories considered have treated only reactions in ideal systems, where the rate constant  $k'$  is given by equation (2-79):

$$k' = \left( \frac{kT}{h} \right) (K_c^\ddagger)' \quad (2-79)$$

However, we know that the use of equilibrium constants based on concentration is correct only for ideal systems. For reactions at high pressure or in solution, the nonideality of the reaction mixture becomes important and equilibrium constants

must be written in terms of activity rather than concentration. If we define activity in the normal way

$$a_i = \frac{\gamma_i C_i}{C_T} \quad (2-95)$$

where  $a_i$  is the activity and  $\gamma_i$  the activity coefficient for species  $i$  of concentration  $C_i$ . The activity-based equilibrium constant corresponding to equation (2-80) is

$$K^\ddagger = \frac{a_F}{a_{AB}a_C} = \frac{C_\ddagger C_T}{C_{AB}C_C} \frac{\gamma_\ddagger}{\gamma_{AB}\gamma_C} \quad (2-96)$$

If this modification is incorporated into the TST development, equation (2-79) becomes, for the example of reaction (XXIV),

$$k' = \left( \frac{kT}{h} \right) (K_c^\ddagger)' \frac{\gamma_{AB}\gamma_C}{\gamma_\ddagger} \quad (2-97)$$

and application of the theory involves the dual problem of determination of  $(K_c^\ddagger)'$  and the activity coefficients. The troubles involved in application of this result lie in estimation of activity coefficients for transition complexes, so that, again, the picture we have is qualitative rather than quantitative. The correctness of the approach, though, has been verified in application to ionic reactions in dilute electrolyte solutions, for which the Debye-Hückel theory can be used to compute activity coefficients. For a concise discussion of this application, the reader is referred to the text by Laidler [K.J. Laidler, *Chemical Kinetics*, 2nd ed., Ch 5, McGraw-Hill Book Company, New York, NY, (1965)]. The importance of such verification is in the use of concentration rather than the expression of reaction rates. In the present example the correct rate expression for the nonideal system states that

$$r = \left( \frac{kT}{h} \right) (K_c^\ddagger)' e^{-E/RT} \left( \frac{\gamma_{AB}\gamma_C}{\gamma_\ddagger} \right) C_{AB}C_C \quad (2-98)$$

If one uses activity instead of concentration in the rate equation, which in some places seems a popular idea but is *incorrect*,

$$r = \left( \frac{kT}{h} \right) (K_c^\ddagger)' e^{-E/RT} (\gamma_{AB}\gamma_C) C_{AB}C_C \quad (2-99)$$

Other important applications of TST to nonideal reactions have been made for ion/molecule reactions in solution, for reactions in thermodynamically nonideal solutions, and for the effect of pressure on the rates of reaction in solution. These applications are also discussed in detail by Laidler.

### Illustration 2.5

Using the collision theory expression for the rate constant of a bimolecular reaction and the thermodynamic form of the TST result (in molecular units), show that, approximately:

$$p = e^{[(\Delta S^\ddagger)/R]} \quad (i)$$

where  $p$  is the collision theory steric factor.

*Solution*

From collision theory we have

$$k' = pA(T)^m e^{-E_0/RT} \quad (\text{ii})$$

with

$$A = \sigma_{AB}^2 \left( \frac{8\pi k}{\mu_{AB}} \right)^{1/2}$$

From the thermodynamic formulation of TST we have

$$k' = \left( \frac{kT}{h} \right) e^{(\Delta S^\ddagger)/R} e^{-(\Delta H^\ddagger)/RT} \quad (\text{iii})$$

Further, the apparent activation energy via the Arrhenius correlation appears as

$$k' = Ze^{-E_{\text{app}}/RT} \quad (\text{iv})$$

where  $Z$  is some general pre-exponential factor. We know the relationship between  $E_{\text{app}}$  and  $(\Delta H^\ddagger)$  from equation (2-94) to be

$$E_{\text{app}} = (\Delta H^\ddagger) + 2RT \quad (\text{v})$$

Now, what is the relationship between  $E_{\text{app}}$  and  $E_0$ ? Recall that the activation energy is formally defined as

$$\frac{d(\ln k')}{d(1/T)}$$

so

$$\frac{d(\ln k')}{d(1/T)} = \frac{E_{\text{app}}}{RT^2} \quad \text{via (iv)}$$

$$\frac{d(\ln k')}{d(1/T)} = \frac{E_0}{RT^2} + \frac{m}{T} \quad \text{via (ii)}$$

and

$$\begin{aligned} E_0 &= E_{\text{app}} - mRT; & m &= (1/2) \text{ via collision theory} \\ E_0 &= E_{\text{app}} - 0.5(RT) \end{aligned} \quad (\text{vi})$$

In terms of  $(\Delta H^\ddagger)$ :

$$(\Delta H^\ddagger) = E_0 - 1.5(RT) \quad (\text{vii})$$

Substituting for  $(\Delta H^\ddagger)$  in the TST expression

$$\begin{aligned} \left( \frac{kT}{h} \right) e^{(\Delta S^\ddagger)/R} e^{-(E_0 - 1.5RT)/RT} &= pA(T)^{1/2} e^{-E_0/RT} \\ \left( \frac{kT}{h} \right) e^{(\Delta S^\ddagger)/R} e^{1.5} &= pA(T)^{1/2} \end{aligned} \quad (\text{viii})$$

Now, order of magnitude values are

$$(kT/h) = 10^{13} \text{ s}^{-1}$$

$$\exp(1.5) = 10$$

$$A(T)^{1/2} = 10^{14} - 10^{15} \text{ cm}^3\text{-mol-s}^{-1}$$

and we have

$$(10^{13})(10) \exp[(\Delta(S^\circ)^\ddagger/R)] = (10^{14})p$$

or, finally

$$p = e^{[(\Delta S^\circ)^\ddagger/R]} \quad (\text{ix})$$

### Illustration 2.6

From the concepts of transition state theory and the thermodynamic relationship given by

$$V = \left( \frac{\partial G}{\partial P} \right)_T \quad (\text{i})$$

derive an expression for correlating the effect of pressure on the rate constant of a chemical reaction. This will be expressed most conveniently in terms of an activation volume,  $(\Delta V^\circ)^\ddagger$ , corresponding to the free energy of activation of the transition state complex,  $(\Delta G^\circ)^\ddagger$ .

*Solution*

From equation (2-87) we have that

$$(\Delta G^\circ)^\ddagger = -RT \ln K^\ddagger \quad (\text{ii})$$

and we may write (i) above as

$$(\Delta V^\circ)^\ddagger = \left[ \frac{\partial (\Delta G^\circ)^\ddagger}{\partial P} \right]_T \quad (\text{iii})$$

for establishment of the transitions state. Also, from equation (2-79) the rate constant is defined as

$$k' = \left( \frac{kT}{h} \right) (K_c^\ddagger)' \quad (\text{iv})$$

From these relationships we have directly that

$$\begin{aligned} \left( \frac{\partial \ln K^\ddagger}{\partial P} \right)_T &= - \frac{(\Delta V^\circ)^\ddagger}{RT} \\ \left( \frac{\partial \ln k'}{\partial P} \right)_T &= - \frac{(\Delta V^\circ)^\ddagger}{RT} \end{aligned} \quad (\text{v})$$

Over a range of pressures  $k'$  then becomes a log-linear function of pressure:

$$\ln k' = \ln k'_0 - \frac{(\Delta V^\ddagger)}{RT} P \quad (\text{vi})$$

Here  $k'_0$  would presumably be the value of the rate constant as  $P \rightarrow 0$ , however, the precise physical significance of this may be a little hard to grasp (i.e., is there a reaction at  $P = 0$ ?). It is probably just as well to view  $\ln k'_0$  as a constant that follows from the linear relationship.



HORATIO SAYS

A group of questionably qualified chemical explorers have decided that the best way to correlate reaction equilibrium is directly through the change in mols via

$$(\Delta G^\circ)^\ddagger = -RT(K^\ddagger) + \Delta n^\ddagger(RT/P)$$

Where did this ever come from?

## 2.4 Experimental Results on the Kinetics of Various Reactions

While we have been concerned primarily with generalized reaction models and a few specific examples, there is a vast amount of literature available concerned with studies of the kinetics of individual reactions, and new work appears literally almost every day. Tables 2.5(a–h) present a selection of experimental results for various types of gas- and liquid-phase reactions. The data in Tables 2.5(a–g) are taken from the text of Frost and Pearson, and those in Table 2.5h from Laidler. Extensive compilations of kinetic parameters for gas-phase reactions are also given by Benson, as mentioned in the previous section.

The reaction order as given in some of these tables may not correspond to the true molecularity of the reaction, so in general we cannot claim to be quoting results

**Table 2.5a** First-Order Gaseous Decompositions;  $(\Delta S^\circ)^\ddagger$  Calculated at 285°C

Compound	$k^\circ$ (sec <sup>-1</sup> )	$E$ (kcal/mole)	$(\Delta S^\circ)^\ddagger$ (eu)
Cyclobutane	$4.0 \times 10^{15}$	62.5	2
Toluene	$2.0 \times 10^{13}$	77.5	1
<i>p</i> -Xylene	$5.0 \times 10^{13}$	76.2	4
Propylene oxide	$1.2 \times 10^{14}$	58.0	6
Ethyl peroxide	$5.1 \times 10^{14}$	31.5	8
Azomethane	$3.5 \times 10^{16}$	52.5	17
Nitrogen tetroxide	$8.0 \times 10^{14}$	13.9	9
Methyl azide	$3.0 \times 10^{15}$	43.5	12
Nitromethane	$4.1 \times 10^{13}$	50.6	2
Ethyl chloride	$1.6 \times 10^{14}$	59.5	6

Source: After A.A. Frost and R.G. Pearson, *Kinetics and Mechanism*, 2nd ed., with permission of John Wiley & Sons, Inc., New York, (1961).

**Table 2.5b** First-Order Isomerizations;  $(\Delta S^\ddagger)$  Calculated at 285°C

Compound	$k^\circ$ (sec <sup>-1</sup> )	$E$ (kcal/mole)	$(\Delta S^\ddagger)$ (eu)
Methylmaleic acid to methyl fumaric acid	$6.8 \times 10^5$	26.5	-32
Dimethylmaleic ester to dimethylfumaric ester	$1.3 \times 10^5$	26.5	-36
Vinyl allyl ether to allylacetalddehyde	$5.0 \times 10^{11}$	30.6	-5
Cyclopropane to propylene	$1.5 \times 10^{15}$	65.0	11

Source: After A.A. Frost and R.G. Pearson, *Kinetics and Mechanism*, 2nd ed., with permission of John Wiley & Sons, Inc., New York, (1961).

**Table 2.5c** Radical Recombination Reactions

Reaction	$k^\circ$ liters/mole-sec	$E$ (kcal/mole)
$2\text{CH}_3\cdot \rightarrow \text{C}_2\text{H}_6$	10.3	0
$2\text{C}_2\text{H}_5\cdot \rightarrow \text{C}_4\text{H}_{10}$	11.2	2
$2\text{CF}_3\cdot \rightarrow \text{C}_2\text{F}_6$	10.3	0
$2\text{NO}_2\cdot \rightarrow \text{N}_2\text{O}_4$	8.7	0
$\text{CH}_3\cdot + \text{NO}\cdot \rightarrow \text{CH}_3\text{NO}$	8.3	0
$\text{COCl}\cdot + \text{Cl}\cdot \rightarrow \text{COCl}_2$	11.6	1

Source: After A.A. Frost and R.G. Pearson, *Kinetics and Mechanism*, 2nd ed., with permission of John Wiley & Sons, Inc., New York, (1961).

**Table 2.5d** Second-Order Reactions of Atoms or Radicals

Reaction	$p$	$E$ (kcal/mole)
$\text{H} + \text{H}_2 \rightarrow \text{H}_2 + \text{H}$	1	7.5
$\text{Br} + \text{H}_2 \rightarrow \text{HBr} + \text{H}$	$10^{-1}$	17.6
$\text{H} + \text{HBr} \rightarrow \text{H}_2 + \text{Br}$	$10^{-1}$	1.2
$\text{Cl} + \text{C}_2\text{H}_6 \rightarrow \text{HCl} + \text{C}_2\text{H}_5$	1	1.0
$\text{CH}_3\cdot + \text{CH}_2\text{OCH}_2$	$2 \times 10^{-4}$	9.0
$\text{CH}_3\cdot + \text{C}_2\text{H}_6$	$5 \times 10^{-4}$	10.4
$\text{CH}_3\cdot + n\text{-C}_4$	$3 \times 10^{-4}$	8.3
$\text{CH}_3\cdot + n\text{-C}_5$	$2.5 \times 10^{-4}$	8.1
$\text{CF}_3\cdot + \text{C}_2\text{H}_6 \rightarrow \text{CF}_3\text{H} + \text{C}_2\text{H}_5$	$10^{-3}$	7.5
$\text{CF}_3\cdot + \text{H}_2 \rightarrow \text{CF}_3\text{H} + \text{H}$	$10^{-3}$	8.8

Source: After A.A. Frost and R.G. Pearson, *Kinetics and Mechanism*, 2nd ed., with permission of John Wiley & Sons, Inc., New York, (1961).

for true elementary steps. However, order is a convenient means of classification, and in at least some cases (Tables 2.5c and 2.5d), a fair argument may be made that the results do pertain to elementary steps. The activation energy and pre-exponential factor values given are from the Arrhenius correlation, and where  $(\Delta S^\ddagger)$  values depend on the choice of standard state. As for second-order reactions, a condition of 1 mol/cm<sup>3</sup> has been used.

**Table 2.5e** Second-Order Gas Reactions of Stable Molecules

Reaction	$k^\circ$ (cm <sup>3</sup> /mole-sec)	$E$ (kcal/mole)	$(\Delta S^\circ)^\ddagger$ (eu)
H <sub>2</sub> + I <sub>2</sub> → 2HI	$1 \times 10^{14}$	40.0	2
2HI → H <sub>2</sub> + I <sub>2</sub>	$6 \times 10^{13}$	44.0	0
HI + CH <sub>3</sub> I → CH <sub>4</sub> + I <sub>2</sub>	$1.6 \times 10^{15}$	33.4	8
HI + C <sub>2</sub> H <sub>5</sub> I → C <sub>2</sub> H <sub>6</sub> + I <sub>2</sub>	$4 \times 10^{14}$	29.8	5
2NOCl → 2NO + Cl <sub>2</sub>	$9 \times 10^{12}$	24.0	-3
NO + O <sub>3</sub> → NO <sub>2</sub> + O <sub>2</sub>	$8 \times 10^{11}$	2.5	-8
2C <sub>2</sub> H <sub>4</sub> → C <sub>4</sub> H <sub>8</sub>	$7.1 \times 10^{10}$	37.7	-12
2C <sub>3</sub> H <sub>6</sub> → C <sub>6</sub> H <sub>12</sub>	$1.6 \times 10^{10}$	38.0	-15
C <sub>2</sub> H <sub>4</sub> + H <sub>2</sub> → C <sub>2</sub> H <sub>6</sub>	$4 \times 10^{13}$	43.2	0

Source: After A.A. Frost and R.G. Pearson, *Kinetics and Mechanism*, 2nd ed., with permission of John Wiley & Sons, Inc., New York, (1961).

**Table 2.5f** Third-Order Gas Reactions of Various Types

Reaction	$k^\circ$ (cm <sup>6</sup> /mole <sup>2</sup> -sec)	$E$ (kcal/mole)
2NO + O <sub>2</sub> → 2NO <sub>2</sub>	$8 \times 10^9$	0
2NO + Cl <sub>2</sub> → 2NOCl	$\sim 1 \times 10^9$	$\sim 4$
H + H + M → H <sub>2</sub> + M	$2 \times 10^{16}$	0
Br + Br + M → Br <sub>2</sub> + M	$1 \times 10^{16}$	0
I + I + He → I <sub>2</sub> + He	$0.34 \times 10^{16}$	0
I + I + CO <sub>2</sub> → I <sub>2</sub> + CO <sub>2</sub>	$2.7 \times 10^{16}$	0

Source: After A.A. Frost and R.G. Pearson, *Kinetics and Mechanism*, 2nd ed., with permission of John Wiley & Sons, Inc., New York, (1961).

**Table 2.5g** Ionic Reactions in Aqueous Solution

Reaction	$k^\circ$ (liters/mole-sec)	$(\Delta S^\circ)^\ddagger$ (eu)
Cr(H <sub>2</sub> O) <sub>6</sub> <sup>3+</sup> + CNS <sup>-</sup>	$1.3 \times 10^{14}$	0.7
Co(NH <sub>3</sub> ) <sub>5</sub> Br <sup>2+</sup> + OH <sup>-</sup>	$4.2 \times 10^{17}$	20.1
ClO <sup>-</sup> + ClO <sup>-</sup>	$9.6 \times 10^8$	-19.6
ClO <sup>-</sup> + ClO <sub>2</sub> <sup>-</sup>	$8.5 \times 10^8$	-19.8
CH <sub>2</sub> BrCOO <sup>-</sup> + S <sub>2</sub> O <sub>3</sub> <sup>2-</sup>	$1.2 \times 10^7$	-28.3
CH <sub>2</sub> ClCOO <sup>-</sup> + S <sub>2</sub> O <sub>3</sub> <sup>2-</sup>	$2.3 \times 10^9$	-17.7
Co(NH <sub>3</sub> ) <sub>5</sub> Br <sup>2+</sup> + Hg <sup>2+</sup>	$1.3 \times 10^8$	-23.6
S <sub>2</sub> O <sub>4</sub> <sup>2-</sup> + S <sub>2</sub> O <sub>4</sub> <sup>2-</sup>	$1.8 \times 10^4$	-41.2
S <sub>2</sub> O <sub>3</sub> <sup>2-</sup> + SO <sub>3</sub> <sup>2-</sup>	$2.3 \times 10^6$	-31.4

Source: After A.A. Frost and R.G. Pearson, *Kinetics and Mechanism*, 2nd ed., with permission of John Wiley & Sons, Inc., New York, (1961).

The first-order reactions of Tables 2.5a and 2.5b are most probably not elementary steps, but many of them likely do involve some type of unimolecular rearrangement as the first, slow, step. The values of  $(\Delta S^\circ)^\ddagger$  are evaluated by the procedure suggested in the exercises, with positive or negative values corresponding

**Table 2.5h** Volumes and Entropies of Activation

Reaction	$(\Delta V^\ddagger)$ (cm <sup>3</sup> /mole)	$(\Delta S^\ddagger)$ (cal/°K-mole)
CH <sub>2</sub> BrCOOCH <sub>3</sub> + S <sub>2</sub> O <sub>3</sub> <sup>2-</sup>	3.2	6
CH <sub>2</sub> (S <sub>2</sub> O <sub>3</sub> <sup>-</sup> )COOCH <sub>3</sub> + Br <sup>-</sup>		
Sucrose + H <sub>2</sub> O $\xrightarrow{H^+}$	2.5	8
Glucose + Fructose		
CH <sub>2</sub> ClCOO <sup>-</sup> + OH <sup>-</sup>	-6.1	-12
CH <sub>2</sub> OHCOO <sup>-</sup> + Cl <sup>-</sup>		
CH <sub>3</sub> CONH <sub>2</sub> + H <sub>2</sub> O $\xrightarrow{OH^-}$	-14.2	-34
CH <sub>3</sub> COOH + NH <sub>3</sub>		

Source: After K.J. Laidler, *Chemical Kinetics*, 2nd ed., with permission of McGraw-Hill Book Company, New York, (1965).

to rates greater or less than the “norm,”  $(kT/h) = 10^{13}$ , respectively. A number of the reactions in Table 2.5a have pre-exponential factors quite comparable to the norm, given the precision of most kinetic measurements<sup>8</sup>, and hence are in good agreement with order-of-magnitude theoretical results. On the other hand, note the very large negative values of  $(\Delta S^\ddagger)$  for the first two isomerizations in Table 2.5b.

The radical recombination results of Table 2.5c are based on the data given for the methyl-radical recombination. This reaction requires no activation energy and has a steric factor of unity, so the rate is given by the collision number for the system. Very little activation energy is required for any of these recombination reactions and, again taking into account the precision of measurement, it would appear that the rates are all about the same order of magnitude. In Table 2.5d the steric factors reported are also determined from the collision theory development of Section 2.2; some of these will be recognized as the elementary steps of the chain reaction examples of Chapter 1. The precision of this data is severely limited by the difficulties associated with determining free-radical concentrations, since they can be determined only indirectly.

The values for  $(\Delta S^\ddagger)$  in Table 2.5e are obtained from pre-exponential factor measurements, values for  $p$  determined from equation (2-33a) or (2-34a), and the estimation procedure suggested in Illustration 2.5. In general, these are not elementary steps, although for many years it was believed that the hydrogen/iodine reaction was a true bimolecular reaction, since both collision theory and TST estimates of pre-exponential factors were in good agreement with experiment. This view, however, has changed (J.H. Sullivan, *J. Chem. Phys.*, 46, 73 (1967)).<sup>9</sup>

As mentioned earlier, the termolecular reactions, shown in Table 2.5f, are either NO reactions or atom recombinations involving a third-body collision. The activation energies in these reactions are all essentially zero and, indeed, one would not expect to observe termolecular reactions with significant activation energies. Since the collision numbers are very low compared with bimolecular values, the

<sup>8</sup> To be conservative, it is safe to figure that most activation energies are not determined to better than kilocalorie accuracy and pre-exponential factors to better than within a factor of 5. [“It is better to have a little than nothing.”—*Publilius Syrus*].

<sup>9</sup> Alas, alas, was it ever so; the more we learn, the less we know.—*Anonymous*



existence of a large activation energy, further decreasing the rate, would probably mean that some other mechanism of reaction would be favored.

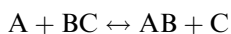
In Tables 2.5g and 2.5h some kinetics of reactions are reported in which non-idealities are important; the former gives some information on a number of ionic reactions in aqueous solution, and the latter gives the effect of pressure on the rates of liquid-phase reactions. The large negative values for  $(\Delta S^\ddagger)^\ddagger$ , corresponding to reaction between like-charged ions in solution, is often the result of an effect known as *electrostriction*. The charge on the transition complex is the algebraic sum of the charge on reactants; when these do not counteract each other, strong electrostatic forces are established in the solvent molecules surrounding the transition state complex and the freedom of motion of that complex is severely restricted. Thus, one thus sees a large decrease in entropy associated with formation of the transition state. The activation volume data of Table 2.5h is representative; the rate constant increases with pressure for negative  $(\Delta V^\ddagger)^\ddagger$ , meaning that the transition state has a smaller volume than the reactants, and vice versa. It has been observed [M.W. Perrin, *Trans. Faraday Soc.*, 34, 144 (1938)] that entropies and volumes of activation tend to correspond in sign, although solvent interactions may vary in the exact relationship for the same reaction carried out in different solvents.

## 2.5 Some Estimation Methods

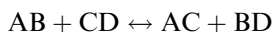
### 2.5.1 Estimation of Activation Energies

At several points in this chapter it has been stated to the effect that, while the theory considered has much to say about the pre-exponential factors of the Arrhenius correlation, it is relatively mute concerning activation energies. This is not surprising. How does one leave with the kinetic equivalent of earth, air, fire, and water and manage to come home with potential-energy surfaces such as those of Figures 2.17 and 2.18? Not easily, to be sure. There are, though, many semi-empirical methods that have been proposed over the years for estimation of activation energy, mostly based on the correlation of very specific experimental results.

Some of the early correlation efforts are still of use, at least as a place to start, although they approach historical interest as well. Early on, Hirschfelder [J.O. Hirschfelder, *J. Chem. Phys.*, 9, 645 (1941)] suggested that if a reaction is exothermic the activation energy should somehow be related to the dissociation energy of the bond being broken. Specifically, for metathesis reactions of the form



when written in the exothermic direction,  $E$  is approximately 5.5% of this dissociation energy (B-C). In the endothermic direction,  $E$  is this amount plus the heat of reaction,  $\Delta H_R$ . For displacement reactions of the type



it was proposed that  $E$  would be approximately 28% of the sum of the energies of the bonds being broken (exothermic direction), or this amount plus the heat of reaction (endothermic direction). A second correlation was proposed by Semenov [(N.N. Semenov, *Some Problems in Chemical Kinetics and Reactivity*, Vol. I, Princeton University Press, Princeton, NJ, (1958)] for addition or abstraction reactions of

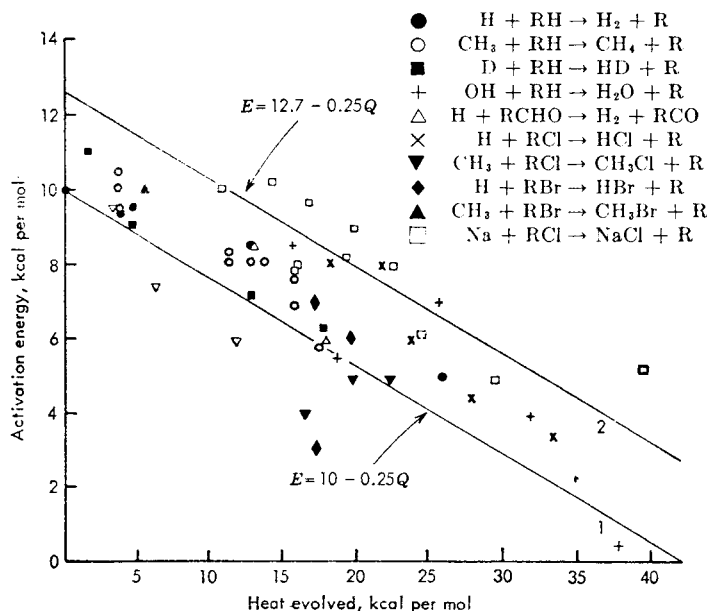


**Figure 2.19** Activation energy versus heat of reaction,  $Q$ , for a number of exothermic atom/radical reactions. [From K.J. Laidler, *Chemical Kinetics*, 2nd ed., with permission of McGraw-Hill Book Co., New York, NY, (1965)].

atoms or small radicals. This comes in two parts, depending upon whether the reaction (as written) is exothermic or endothermic:

$$\begin{aligned} E &= 11.5 - 0.25(-\Delta H_R); & \text{exothermic} \\ E &= 11.5 + 0.75(-\Delta H_R); & \text{endothermic} \end{aligned} \quad (2-100)$$

where  $E$  is in kcal/mol for the values of the constants given. The correlations of equations (2-100) are particularly useful in the estimation of energy requirements for the screening of candidate reactions as elementary steps in chain reactions.

An impression of the reliability of such correlations is given in Figure 2.19, which presents the data used for the correlation of Semenov. There is quite a bit of scatter apparent, such that the rather generous  $\pm$  limits indicated in the figure should be kept in mind. Benson reports also that neither of the two Hirschfelder rules is better than about  $\pm 5$  kcal/mol, which is enormous when one is concerned with activation energies, and that occasionally much larger discrepancies are encountered<sup>10</sup>. Hence we take these as qualitative norms to provide guidance rather than quantitative numbers to provide definition. [see also Z.G. Szabó, *Chem. Soc. (London) Spec. Publ.*, 16, 113 (1962)].

Of course, much more can be done on a theoretical basis in the calculation of activation energies via computer. Most current methods have as a distant ancestor the treatment of Eyring and Polanyi [H. Eyring and M. Polanyi, *Z. Physik. Chem.*, B12, 279 (1931)]. They considered the problem in terms of the coulombic and

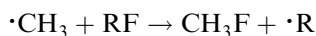
<sup>10</sup> Truth is rarely pure, and never simple.—Oscar Wilde

exchange energies of individual atom pairs for a triatomic molecule. Values of the total energy were obtained from the Morse curves (based on analysis of spectroscopic data for the H—H—H system) and an arbitrary percentage assigned to each type of energy. In this way an approximate energy surface for  $\text{H}_2 + \text{H}$  was obtained. While the details of that paper do not fit into the technical program of this text, those with an historical bent will find it of interest.



HORATIO SAYS

Figure 2.19 looks “sort-of” good but certainly not convincing. I’ll try it anyway to estimate the activation energy for



What range of values might result from this exercise? Does the result lend any confidence to the method?

## 2.5.2 Linear Free-Energy Relationships: Hammett and Taft Correlations

Some useful correlations for both rate and equilibrium constants have been obtained for homologous series of reactions involving related compounds. The best known of these, due to Hammett [L.P. Hammett, *Physical Organic Chemistry*, McGraw-Hill Book Co., New York, NY, (1940); see also H.H. Jaffe, *Chem. Rev.*, 53, 191 (1953)], deals with the reactions of various meta- and para-substituted benzene derivative compounds. The correlation proposes that for a similar series there is a linear logarithmic relationship between either the rate or equilibrium constants of a given reaction and some reference reaction for the series. Hence

$$\log(k') = \log(k'_0) + \sigma\rho \quad (2-101)$$

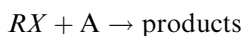
$$\log(K) = \log(K_0) + \sigma\rho \quad (2-102)$$

where  $k'$  and  $k'_0$  are rate constants for the given and reference reactions, respectively, and similarly for the equilibrium constants  $K$  and  $K_0$ . In the sense of the original correlation, these relationships pertain specifically to compounds with the same reactive group as a side-chain with a series of substituents meta- or para- attached to it. The constants  $\sigma$  and  $\rho$  depend upon different factors;  $\sigma$  on the substituent group and  $\rho$  on the conditions of reaction and the solvent.

Such a correlation actually implies a linear relationship between the free energies of the reactions in the series. This can be seen as follows. From the thermodynamic formulation of TST we have

$$k' = \left(\frac{kT}{h}\right) e^{-(\Delta G^\ddagger)/RT}$$

Thus, we consider a series of reactions



where  $R$  is the reactive fraction of the molecule and  $X$  is not directly involved in the chemical transformation. As indicated above, what is done is to plot  $\log(k')$  versus  $\log(K)$  for the series that differs only by the substituent  $X$ . In TST terminology we will have

$$\log(k') = \log\left(\frac{kT}{h}\right) = \frac{(\Delta G^\ddagger)}{2.3(RT)} \quad (2-103)$$

Equating (2-101) and (2-103) gives

$$\log(k'_0) + \sigma\rho = \log\left(\frac{kT}{h}\right) - \frac{(\Delta G^\ddagger)}{2.3(RT)} \quad (2-104)$$

$$(\Delta G_1^\ddagger) = (\Delta G_1^\circ)^\ddagger - 2.3(RT\rho_1\sigma_1) \quad (2-105)$$

$$(\Delta G_2^\ddagger) = (\Delta G_0^\circ G_2^\circ)^\ddagger - 2.3(RT\rho_2\sigma_2)$$

where the subscripts 1 and 2 refer to reaction series 1 and 2, respectively. The free-energy relationships for the two series can be combined to give

$$(\Delta G_1^\ddagger) - \left(\frac{\rho_1}{\rho_2}\right)(\Delta G_2^\ddagger) = (\Delta G_1^\circ)^\ddagger - \left(\frac{\rho_1}{\rho_2}\right)(\Delta G_2^\circ)^\ddagger \quad (2-106)$$

which is the linear relationship sought.

In application of the Hammett correlation a value of unity is commonly assigned to the ionization constant for benzoic acid in aqueous solution at 25°C. From this we can write a relationship for  $\sigma$

$$\sigma = \log \left[ \frac{K_i(\text{substituted benzoic acid})}{K_i(\text{benzoic acid})} \right] \quad (2-107)$$

Now, from  $\sigma$  defined by equation (2-107) values of  $\rho$  can be determined for other reactions. Some typical values of  $\sigma$  and  $\rho$  are given in Table 2.6. The linear free-energy

**Table 2.6** Substituent and Reaction Constants of the Hammett Relationship for Some Reactions

Substituent group	$\sigma(\text{meta})$	$\sigma(\text{para})$
CH <sub>3</sub>	-0.07	-0.17
C <sub>2</sub> H <sub>5</sub>	-0.04	-0.15
OH	0.00	-0.46
Cl	0.37	0.23
NO <sub>2</sub>	0.71	0.78
Reaction series	$\rho$	
Benzoic acids ionization (aq), equilibrium	1.000	
Phenols ionization (aq), equilibrium	2.113	
Benzoylation of aromatic amines in benzene, rate	-2.781	

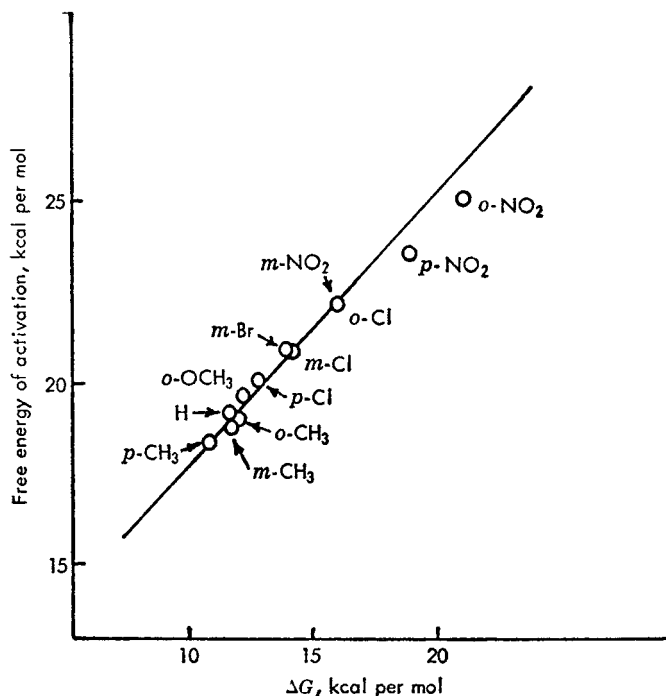


**Figure 2.20** Example of a linear free-energy correlation. Free energy of benzylation of substitute anilines versus free energy of dissociation of the aniline. [Data of F.J. Stubbs and C.N. Hinshelwood, *J. Chem. Soc.*, 571 (1949); from K.J. Laidler, *Chemical Kinetics*, 2nd ed., with permission of McGraw-Hill Book Co., New York, NY, (1965)].

relationship envisioned in deriving the Hammett correlation is not the result of guesswork; an example of experimental correlation is given in Figure 2.20.

The Hammett relation does run into difficulties in some instances, however. A prominent example of this is provided by ortho-substituted compounds because steric hinderance is often important in their reactions; this is a factor not accounted for in the linear free-energy relationship. A similar procedure, though, has been devised by Taft [R.W. Taft, *J. Amer. Chem. Soc.*, 74, 2729, 3120 (1952)] to overcome some of these difficulties. For aliphatic compounds we have

$$\log(k') = \log(k'_0) + \sigma^* \rho^* \quad (2-108)$$

where  $k'$  is a rate (or equilibrium) constant for a particular member of a reaction series,  $k'_0$  normally the value for the parent methyl compound,  $\rho^*$  the reaction constant, and  $\sigma^*$  a constant indicative of the electron-attracting capacity of the substituent. The  $\sigma^*$  values of the Taft correlation were originally derived on the basis of rate constant comparisons for the acidic and basic hydrolysis of esters with the substituent adjacent to the carbonyl group. The defining relationship is

$$\sigma^* = (1/2.5) \left[ \log \left( \frac{k'}{k'_0} \right)_{\text{basic}} - \log \left( \frac{k'}{k'_0} \right)_{\text{acidic}} \right] \quad (2-109)$$

**Table 2.7** Some Values for Taft  $\sigma^*$  and  $\rho^*$  Constants

Substituent group	$\sigma^*$
CH <sub>3</sub>	0.00
C <sub>2</sub> H <sub>6</sub>	-0.10
i-C <sub>3</sub> H <sub>7</sub>	-0.19
t-C <sub>4</sub> H <sub>9</sub>	-0.30
H	0.49
C <sub>4</sub> H <sub>5</sub>	0.60
C <sub>4</sub> H <sub>5</sub> CH <sub>2</sub>	0.22
CH <sub>3</sub> CHO	1.65
CCl <sub>3</sub>	2.65
Reaction	$\rho^*$
RCOOH + H <sub>2</sub> O $\leftrightarrow$ RCOO <sup>-</sup> + H <sub>3</sub> O <sup>+</sup>	1.72 (equil)
RCH <sub>2</sub> OH + H <sub>2</sub> SO <sub>4</sub> $\leftrightarrow$ RCH <sub>2</sub> OSO <sub>3</sub> H + H <sub>2</sub> O	4.60 (rate)
C <sub>6</sub> H <sub>5</sub> COCHR <sub>2</sub> + Br <sub>2</sub> $\rightarrow$ C <sub>6</sub> H <sub>5</sub> COCR <sub>2</sub> Br + Br <sup>-</sup>	1.59 (rate) <sup>a</sup>
(RCH—CH <sub>2</sub> )O + H <sub>2</sub> O $\rightarrow$ RCHOHCH <sub>2</sub> OH	-1.83 (rate) <sup>b</sup>

<sup>a</sup> In the presence of OH<sup>-</sup>.<sup>b</sup> In the presence of HClO<sub>4</sub>.

where the factor of 2.5 is set to scale  $\sigma^*$  values to correspond to the Hammett  $\sigma$ s. Values of  $\sigma^*$  and  $\rho^*$  are given in Table 2.7.

A number of correlations involving linear relationships between pre-exponential factors and activation energy are widely quoted for reactions on surfaces, as we shall see in the next chapter. This behavior, commonly termed the *compensation effect* implies a linear relationship between  $\Delta H^\ddagger$  and  $\Delta S^\ddagger$ . An exact linear relationship between  $\Delta H^\ddagger$  and  $T\Delta S^\ddagger$  means that there is no variation in  $\Delta G^\ddagger$  for the series. An example of this for a liquid-phase reaction is given by Fairclough and Hinshelwood for ethyl benzoate hydrolysis [R.A. Fairclough and C.N. Hinshelwood, *J. Chem. Soc.*, 1573 (1937)].

## Exercises

### Section 2.1

1. Molecules A and B are characterized by Boltzmann velocity distributions with different temperatures,  $T_A$  and  $T_B$ , respectively. If  $d$  is the A–B collision diameter, show that the average rate of bimolecular collision per unit volume is

$$\pi d^2 \left[ \frac{8kT_A}{\pi m_A} + \frac{8kT_B}{\pi m_B} \right]^{1/2} C_A C_B$$

2. Consider the problem of determining the collision number between the molecules of a homogeneous gas and a solid surface. This is equivalent to calculating the rate of effusion of molecules contained in a vessel through an orifice sufficiently small that the effusion rate does not disturb the velocity distribution of the molecules remaining in the vessel. For a gas of number density  $n_A$  and average speed  $c$ , the geometry may be visualized

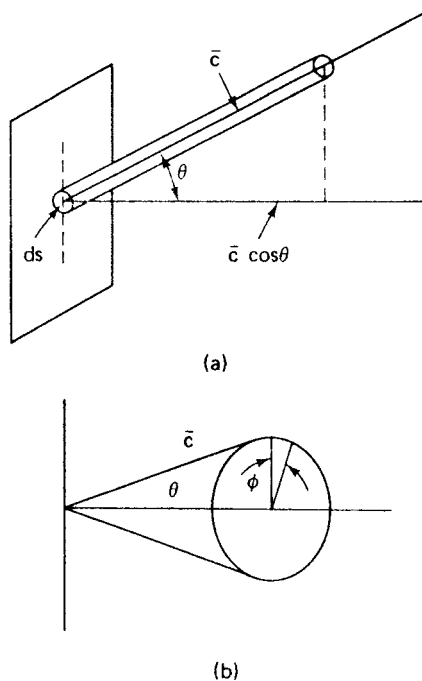


**Figure 2.21** Geometry of the molecular effusion problem. [After W.J. Moore, *Physical Chemistry*, 2nd ed., reprinted by permission of Prentice-Hall, Inc., Englewood Cliffs, NJ, (1955).]

as shown in Figure 2.21a, where the distance from the orifice of area  $ds$  is  $\bar{c}$ , and the angles  $\theta$  and  $\phi$  represent its direction. The differential solid angle containing molecules of speed between  $\bar{c}$  and  $\bar{c} + d\bar{c}$  at positions between  $\theta$  and  $\theta + d\theta$  and  $\phi$  and  $\phi + d\phi$  is, in polar coordinates (Figure 2.21b),  $\sin \theta d\theta d\phi$ . The fraction of the total number of molecules is given by  $(\sin \theta d\theta d\phi / 4\pi)$ , where  $4\pi$  is the total solid angle subtended by the spherical surface of radius  $\bar{c}$ . From this information, derive equation (2-14).

3. The molecular diameter is variously reported as the following:

Diameter (Å)	Method of determination
2.96	Gas viscosity
2.90	van der Waals constant
2.34	Molecular refraction
3.75	Closest packing

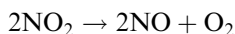
How much difference is there in the minimum and maximum estimates of collision number at 373°K and 1 atm corresponding to these values?

4. Using the collision number result for a diameter of 3.75 Å in Problem 3, and assuming a collision time of  $10^{-13}$  s for  $O_2$  molecules and a molecular diameter of 4 Å for  $O_4$  complexes, calculate the number of triple collisions

in  $O_2$  at 373°K and 1 atm. What conclusion might one draw from this result concerning the importance of third-order processes?

## Section 2.2

5. The decomposition of nitrogen dioxide,



obeys second-order kinetics. The following rate constant data was reported by Bodenstein [M. Bodenstein, *Z. Physik. Chem.*, 100, 106 (1922)]:

$T(^{\circ}K)$	592	603.2	627	651.5	656
$k(\text{cm}^3/\text{mol}\cdot\text{s})$	522	755	1700	4020	5030

Using the appropriate collision-theory rate constant, determine the effective collision diameter for this reaction based on the data above. Is this quantity a function of temperature?

6. In a binary collision between hard-sphere molecules, what ratio of molecular masses results in the maximum transfer of translational energy?
7. What is  $(\Delta E_A/E_A)$  for collision between hydrogen (A) and oxygen (B), each with a line-of-center velocity equal to one-half the average speed at 25°C (given in Table 2.2b)?
- 8a. The gas-phase kinetics of cyclopropane isomerization have been studied by Chambers and Kistakowsky [T.C. Chambers and G.B. Kistakowsky, *J. Amer. Chem. Soc.*, 56, 399 (1934)], who report the limiting high-pressure rate constant  $k_{\infty}$  to be represented by an Arrhenius form

$$k_{\infty} = (k^{\circ})_{\infty} e^{-E/RT}$$

where

$$\log(k^{\circ})_{\infty} = 15.17; \quad (k^{\circ})_{\infty} \text{ in } \text{s}^{-1}$$

$$E = 65.0 \text{ kcal/mol}$$

In terms of the Lindemann theory, what must be the effective collision number ( $k_1$ ) if the calculation is to agree with the experimental results shown in Figure 2.10? Use  $(k^1/k_{\infty}) = 0.525$  at  $\log P(\text{cm}) = 0$  as a basis. The temperature is 492°C.

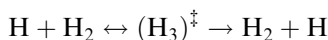
- 8b. From this value, compute the dependence of  $(k^1/k_{\infty})$  over the pressure range shown in Figure 2.10 and compare it with the experimental curve.
9. What energy corresponds to the maximum of the  $P(E)$  distribution? What energy corresponds to the average?
10. A certain molecule is nonlinear and contains six atoms. At 400°C what fraction of these molecules will have an energy of at least 20 kcal/mol? How much does this fraction increase if the temperature is 700°C? What are the corresponding figures for a linear six-atom molecule?
11. For a specified energy level and comparable values of  $\bar{\nu}$ , what can one conclude concerning the mean lifetime of reacting molecules as the complexity of the molecule increases?



12. Using collision theory, estimate a rate constant for the recombination of oxygen atoms at 200°C, with  $\sigma_{\infty} = 3 \text{ \AA}$ .
13. Write a detailed kinetic sequence describing all the individual processes involved in the RRK theory for decomposition reactions. From this derive the general expression for the decomposition rate.

### Section 2.3

14. Formulate the expression for the rate constant of the reaction



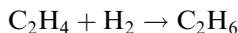
in terms of the appropriate detailed partition functions. Assume that the transition state is linear and symmetric and ignore electronic contributions. Compute the frequency factor for this reaction at 300°K. The moment of inertia of  $\text{H}_2$  is  $0.459 \times 10^{-40} \text{ g-cm}^2$  and its fundamental vibrational frequency corresponds to a wave number of  $4395.2 \text{ cm}^{-1}$ . The moment of inertia of  $(\text{H}_3)^{\ddagger}$  is estimated to be  $3.34 \times 10^{-40} \text{ g-cm}^2$  and its fundamental frequencies are stretching at  $3650 \text{ cm}^{-1}$  and doubly degenerate bending at  $670 \text{ cm}^{-1}$  [H. Eyring and M. Polanyi, *Z. Physik. Chem.*, *B12*, 279 (1931)].

15. The rate constant for the reaction of Problem 14 has been determined experimentally by Farkas and Farkas [A. Farkas and L. Farkas, *Proc. Roy. Soc. (London)*, *A152*, 124 (1935)]. Their result is

$$k = (10)^{8.94} (T)^{1/2} e^{-5500/RT} \text{ liters/mol-s}$$

Compare this experimental value for the frequency factor with that computed in Problem 14. Would you consider the agreement to be exceptional, good, average or poor?

16. The specific rate constant for the homogeneous gas-phase reaction



has the following values:

$$T = 500^\circ\text{K} \quad k = 6.98 \times 10^{-9} \text{ liters/mol-s}$$

$$T = 600^\circ\text{K} \quad k = 4.16 \times 10^{-6} \text{ liters/mol-s}$$

at a temperature of 500°K, what is:

- (a) The experimental activation energy?
  - (b) The enthalpy and entropy of activation?
  - (c) The concentration of transition-state complexes in equilibrium with  $\text{C}_2\text{H}_4$  and  $\text{H}_2$ , each at a concentration of 0.05 mol/liter? Assume a linear transition complex.
  - (d) The steric factor for this reaction?
17. For unimolecular reactions, using the approximation that  $(kT/h) \approx 10^{13} \text{ s}^{-1}$ , and that  $(E/RT) \approx (\Delta H^\circ)^\ddagger/RT$ , show that  $(\Delta S^\circ)^\ddagger \approx R \ln(k^\circ \times 10^{-13})$

where  $k^\circ$  is the experimentally determined pre-exponential factor of an Arrhenius correlation.

18. The symmetry number,  $\sigma$ , that appears in the expression for the rotational partition function is sometimes troublesome. Basically,  $\sigma$  can be defined as the number of equivalent arrangements that can be obtained by rotating the molecule (not really as simple as all that, but it will have to do for now). For example, in  $\text{Cl}_2$  there are two equivalent orientations,  $\text{Cl}(1)\text{--Cl}(2)$  and  $\text{Cl}(2)\text{--Cl}(1)$ . Following this reasoning and using any other data on geometry that may be necessary, determine the symmetry numbers for HF, planar  $\text{NO}_3$ ,  $\text{H}_2\text{O}$ ,  $\text{CH}_4$ ,  $\text{CH}_2=\text{CH}_2$ ,  $\text{CHD}=\text{CH}_2$  and neopentane.
19. Determine the value of the activation volume for the hydrolysis of ethyl acetate from the following data:

Pressure (atm)	$k$ (liters/mol-s)	$T$ ( $^{\circ}\text{C}$ )
1	0.080	25
272	0.089	25
544	0.098	25
816	0.107	25

20. Consider the simplified model for a reaction between two ions in solution given in Figure 2.22. The reactants are conducting spheres of radii  $r_A$  and  $r_B$  with charge  $z_A e$  and  $z_B e$ , respectively. The electronic charge is  $e$ , and  $z_A$  and  $z_B$  whole numbers corresponding to the ionic charges. Initial and transition states are as shown on the figure. At a distance  $x$ , the force between them is

$$f = \frac{Z_A z_B e^2}{\epsilon x^2}$$

Solution dielectric constant =  $\epsilon$

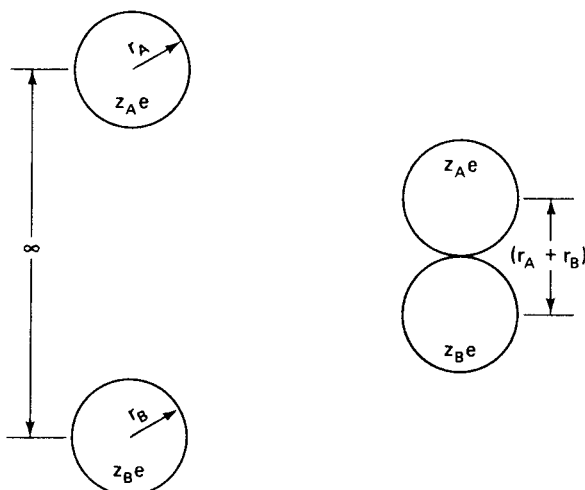


**Figure 2.22** Transition state model for an ionic reaction between species A and B in solution.

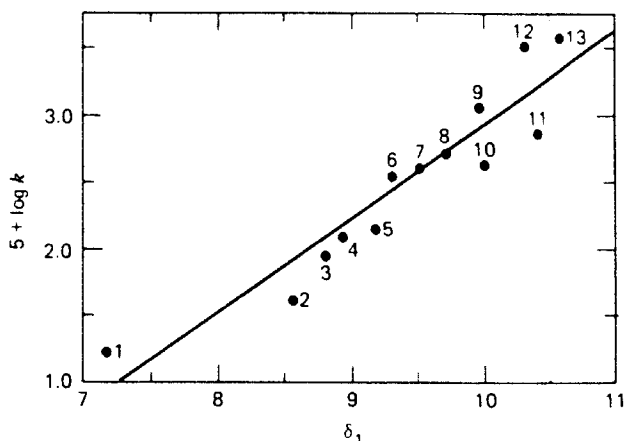


**Figure 2.23** Reaction of pyridine with methyl iodide:  $\log k$  versus the square root of the internal pressure of the solvent. Solvents are (1) isopropyl ether, (2) carbon tetrachloride, (3) mesitylene, (4) toluene, (5) benzene, (6) chloroform, (7) chlorobenzene, (8) bromobenzene, (9) iodobenzene, (10) dioxane, (11) anisole, (12) benzonitrile, and (13) nitrobenzene. [Reproduced with permission from A.P. Stefani, *J. Amer. Chem. Soc.*, 90, 1694, American Chemical Society, (1968).]

where  $\epsilon$  is the dielectric constant of the solution. Determine the electrostatic contribution to the free energy of activation. Show that the rate constant for reaction between ions in solution is log-linear with respect to the reciprocal of the dielectric constant.

21. Consider the bimolecular reaction of  $A + B$  to products as it is carried out in a series of different solutions that are nonideal. Now, regular solution theory predicts that the activity coefficient of a solute (reference to pure liquid) in dilute solution is given by

$$RT \ln a_2 = V_2(\delta_2 - \delta_1)^2$$

where  $V_2$  is the molar volume of the pure liquid solute, and  $\delta_{1,2}$  are parameters of the solvent and solute, respectively, called the internal pressure. Derive a linear relationship between  $(k/k_0)$ , the ratio of rate constants in the nonideal (regular) solutions to that in a reference ideal solution, and the internal pressure  $\delta_1$  of the solvent used. You will find equation (2-98) useful. This approach provides a valuable correlation of solvent effects in many liquid-phase reactions; Figure 2.23 gives an example.

## Notation

- $A$  constant defined after equation (ii), Illustration 2.5  
 $a_i$  concentration coefficients or activities; see equation (2-95)  
 $b$  impact parameter; see Figure 2.7  
 $b_{\max}$  maximum impact parameter associated with  $E_r$   
 $C_{AB}$  concentration of the pair AB, mols or molecules/volume

$C_i$	concentration of $i$ , mols/volume
$C_A^*$	concentration of activated complex, mols or molecules/volume
$C^\ddagger$	transition complex concentration, mols or molecules/volume
$c$	speed function, length/time; see equation (2-5)
$\bar{c}$	average velocity, length/time
$c_A$	length/time of molecule A
$c_r$	relative velocity, length/time
$E$	activation energy, kJ or kcal/mol
$E_A$	original kinetic energy, kcal/mol
$E_{app}$	apparent activation energy, kJ or kcal/mol
$E_C$	energy along line of centers; derived activation energy, kJ or kcal/mol; see Illustration 2.5
$E^*$	minimum energy for reaction, kJ or kcal/mol; see also $\eta^*$
$E_j$	activation energy for species $j$ , kJ or kcal/mol
$E_{AV}$	average activation energy, kJ or kcal/mol
$E_r$	relative energy, kcal/mol
$\Delta E_A, \Delta E_B$	changes in kinetic energy of A and B, kcal/mol
$\Delta E_v$	energy transferred to internal mode
$f(E^*)$	function defined by equation (2-43)
$f_i$	individual degree of freedom for component $i$
$(f_v^\ddagger)_t$	degree of freedom as defined in terms of internal vibrational
$f_r, f_t, f_v$	individual degrees of freedom for rotation, translation, and vibration
$(\Delta G^\circ)^\ddagger$	free energy change between reactants and transition complex, standard state, kJ or kcal/mol
$(\Delta G_{1,2}^\circ)^\ddagger$	free energy change for Hammett series, kcal/mol
$g_i$	correlation factor in equation (2-55)
$(\Delta H^\circ)^\ddagger$	enthalpy change between reactants and transition complex, standard state, kJ or kcal/mol
$h$	Planck's constant
$I_j$	moment of inertia in $j$ th rotational degree of freedom
$i$	component $i$
$j$	number of quanta; see equation (2-46)
$K, K_0$	equilibrium constants for given and reference reactions, Hammett correlation
$K^\ddagger$	equilibrium constant between reactants and transition state based on activities; see equation (2-87)
$K_c^\ddagger$	equilibrium constant based on partition functions
$(K_c^\ddagger)'$	equilibrium constant; see equation (2-80)
$k$	Boltzmann constant
$k^\circ$	frequency factor, equation (i), Illustration 2.4
$k'$	rate constant in molecular units
$k', k'_0$	rate constants for given and reference reactions; Hammett [equation (2-01)], Taft [equations (2-108), (2-109)]
$k'(A, A), k'(A, B)$	rate constants based on equations (2-15) and (2-16)
$k'(A, B, C)$	termolecular rate constant
$k^1$	overall rate constant in Lindemann scheme
$k_1, k_{-1}$	forward and reverse rate constants in Lindemann scheme; see equation (2-33)

- $k_2$  decomposition rate constant in Lindemann scheme; see equation (2-33)  
 $k_\infty$  high pressure rate constant; see equation (2-39)  
 $\bar{k}_1$  rate constant defined in equation (i), Illustration 2.3  
 $\bar{k}(E_j)$  average rate constant for  $E_j$ ; see equation (2-51)  
 $k_2(E_{av})$  average rate constant for decomposition of RRK molecules  
 $m$  molecular mass; quanta in  $j$  oscillators; constant from collision theory in Illustration 2.5  
 $m_A, m_B$  molecular masses of A and B  
 $m_i$  molecular weight of  $i$   
 $N$  atoms in a molecule  
 $N_a$  Avogadro's number  
 $n$  degrees of freedom; number of groups of oscillators; exponent in equation (2-51) et seq.  
 $n_i$  number of  $i$  molecules/volume  
 $(\Delta n)^\ddagger$  change in mols between reactants and transition state  
 $P$  pressure, normally atm  
 $P(c)$  speed distribution; see equation (2-7)  
 $P(E), P(E_i)$  energy distribution; see equation (2-8)  
 $P(v_i)$  velocity distribution of species  $i$   
 $P(v_x, v_y, v_z)$  fraction of molecules in velocity range from  $v_x$  to  $v_x + dv_x$ ,  $v_y$  to  $v_y + dv_y$ ,  $v_z$  to  $v_z + dv_z$   
 $P_m(n, j)$  total probability function; see equations (2-48) and (2-49)  
 $p$  steric factor; stoichiometric coefficient; see also equation (i), Illustration 2.5  
 $Q$  overall partition function, sum of states  
 $Q_r, Q_t, Q_v, Q_e$  partition functions for rotation, translation, vibration and electronic states  
 $Q_i$  partition function per unit volume  
 $Q_i^\circ$  overall partition function for  $i$   
 $Q_\ddagger^\circ$  partition function defined in equation (2-76)  
 $(Q_\ddagger^\circ)'$  partition function defined in equation (2-77)  
 $q$  stoichiometric coefficient  
 $q(m, j)$  distribution function among  $(m, j)$ ; see equation (2-47)  
 $q(n, j)$  distribution function among  $(n, j)$ ; see equation (2-46)  
 $R$  gas constant, kJ or kcal/mol-K  
 $r$  rate of reaction, mols or molecules/volume-time; stoichiometric coefficient  
 $r_A$  rate of reaction of A, molecules/cm<sup>3</sup>-time; see equation (1-39)  
 $(\Delta S^\circ)^\ddagger$  entropy change between reactants and transition state, kJ or kcal/mol  
 $s$  variable defined in equation (2-49); stoichiometric coefficient  
 $T$  temperature, °C or °K  
 $V$  volume, cm<sup>3</sup> or liters  
 $(\Delta V^\circ)^\ddagger$  volume change on formation of transition state  
 $v_A, v_B$  line of centers velocity for A-B, length/time  
 $v_r$  relative velocity, length/time  
 $v_x, v_y, v_z$  velocities in  $x, y$  and  $z$  directions, length/time  
 $v_\parallel, v_\perp$  parallel and perpendicular velocity components  
 $v_A$  post-collision velocity of A, length/time; see equation (2-26)  
 $v'_A, v'_B$  molecular velocities of A and B, length/time; see equations (2-1) and (2-2)  
 $x$  scaled energy =  $(E - E^*)$

$Z(A, B)$	collisions of A with $n_B$ , number/volume-time
$Z(E_r)$	collision number at relative energy $E_r$ , number/volume-time
$Z_\eta(A, A), Z_\eta(A, B)$	reactive collision numbers for AA or AB based on $\eta$ , number/volume-time
$\bar{Z}_{cT}$	general collision number, number/volume-time
$\bar{Z}_{E_r}(A, B)$	reactive collision number as per equation (2-19), number/volume-time
$\bar{Z}'_{cT}$	limiting low pressure collision number, number/volume-time
$\bar{Z}_{cT}(A, A), Z_{cT}(A, B)$	Maxwellian collisions for AA and AB, number/volume-time; see equations (2-12) and (2-13)
$\bar{Z}_{cT}(\text{surface})$	surface collision number, number/area-time; see equation (2-14)
<i>Greek</i>	
$\alpha$	constant = $(2kt/m)^{1/2}$
$\Gamma(n)$	Gamma function of $n$ ; see equation (iii), Illustration 2.3
$\gamma_i$	activity coefficient of $i$
$\delta$	distance of approach in equation (2-23)
$\delta(E_c)$	reaction function; see equation (2-15)
$\eta^*$	general activation energy, kJ or kcal/mol
$\theta$	angle in Figure 2.4; constant = $(m_A/m_B)$
$\mu_{i,j}$	reduced mass of $i, j = [m_i m_j / (m_i + m_j)]$
$\nu_i \nu_s$	frequency of the $i$ th or $s$ th mode, $(\text{time})^{-1}$
$\bar{\nu}$	average overall decomposition frequency, $(\text{time})^{-1}$
$\bar{\nu}_j$	average frequency of transfer of energy quanta, $(\text{time})^{-1}$
$\rho$	Hammett correlation constant
$\rho^*$	Taft correlation constant
$\sigma_A, \sigma_B$	molecular diameters of A and B, Å or cm
$\sigma_R$	reactive crosssection from integration of equation (2-16)
$\sigma_{i,j}$	constant = $(\sigma_i + \sigma_j)/2$
$\sigma_r(E_r)$	reactive crosssection; see equation (2-16)
$(\sigma_e)_{AA}, (\sigma_e)_{BB}$	effective collision diameters, Å or cm
$\phi$	angle in Figure 2.4

*Note:* Some additional notation is described in Tables 2.1, 2.2, 2.4, and 2.5.

### 3

---

## The Mechanisms of Chemical Reactions on Surfaces

Who durst be so bold with a few crooked  
boards nailed together, a stick standing  
upright, and a rag tied to it, to adventure  
into the ocean

— *Thomas Fuller*

Probably the single case of reactions most important in chemical reaction engineering application are those which occur on solid surfaces when an heterogeneous catalyst is used to promote the rate of reaction (catalysis). Catalysts for various reactions are found among a wide variety of metals, metal oxides, and metals on various support materials such as carbon and metal oxides. One property of most catalysts is that they provide a large amount of surface per unit volume on which reaction can occur, which normally requires the effective surface to be contained within a porous matrix of some sort. This particular characteristic leads to a number of interesting and important problems arising from the interaction of the rates of transport of mass and energy through such porous matrices, which we shall discuss in detail later. Further, since we wish to discuss the more general aspects of the theory of surface reactions, we shall not be involved with the details of the mechanisms of too many specific reactions, although the ubiquitous A and B will be transformed into real chemical entities in the exercises associated with this chapter.

Another characteristic of catalytic reactions is that it cannot in general be assumed, once reaction is established at a certain rate under given conditions, that the rate will remain constant with the passage of chronological time. Catalysts normally lose some or all of their specific activity for a desired chemical transformation with time of utilization. This effect, normally referred to as *deactivation*, can come from a number of different sources and is often very important in the analysis and/or design of catalytic processes and reactors.

Our concern also includes reactions that are catalyzed by enzymes, and we will have the opportunity to see the parallel development of the topics of chemical catalysis and enzyme catalysis as set forth by two related scientific communities (physical chemistry and biochemistry) with little apparent intercommunication but with essentially the same results.

It is most convenient to consider surface reactions as a series of several steps, in essence a type of chain reaction, which (as we have seen in Chapter 1) employs the active centers of reaction in a closed sequence. Let us again turn to the simple example of an isomerization reaction,  $A \leftrightarrow B$ , now taking place on a surface containing one type of active center, S. The individual reaction steps are:



The first step in this sequence, which we have written as a chemical reaction, represents the adsorption of A on the surface; the second is the reaction of the surface-adsorbed A species,  $A \cdot S$ , to the corresponding B species on the surface,  $B \cdot S$ ; and third is the desorption of product B from the surface. We will have to develop our ideas concerning surface reactions by considering each of three steps individually, much as we did in examining the Lindemann scheme. The development is based mostly on gas/solid systems, which comprise the most common types of heterogeneous catalytic reactions, however the analysis is also generally valid for liquid/solid systems. Normally for gas/solid systems the expressions for adsorption equilibrium and reaction rate are written in terms of partial pressures of reactant and product species, whereas in liquid/solid systems concentrations are employed. This is the first time that we have considered kinetics in heterogeneous (i.e., more than one phase) reaction systems. This transition is not particularly painful, although one must prepare for a few concepts of “two-dimensional chemistry” that are relatively new, such as concentrations based on area rather than volume.

### 3.1 Adsorption and Desorption

#### 3.1.1 Ideal Surfaces

According to the first step of reaction (XXV) given above, an essential feature of catalysis is the adsorption of the reacting species on the active surface prior to reaction. As indicated, this type of adsorption is generally a very specific interaction between surface and adsorbate which is a chemical reaction in itself and is called *chemisorption*. *Desorption* is just the reverse of this, so it is logical to discuss the two together.

To begin with, let us consider the rate at which A molecules in a homogeneous gas will strike a solid surface. For once, this is a problem we have already solved.

$$\bar{Z}_{cT} = \frac{1}{4} n_A \left( \frac{8kT}{\pi m_A} \right)^{1/2} \tag{2-14}$$

This would give us the maximum possible rate of adsorption in any system if every molecule striking the surface was adsorbed. Now, just as in collision theory, to proceed further we must decide upon a more detailed model of what we mean by adsorption. Molecules we already know something about, so in the present instance we need more detail on the nature of the surface. The simplest model of a surface, the



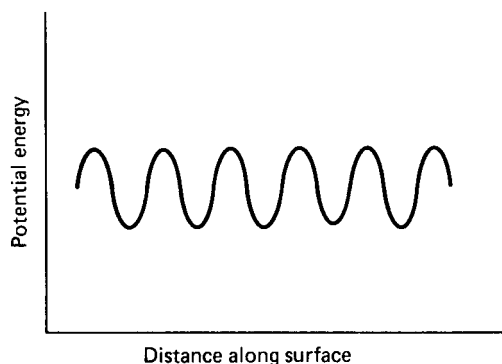


**Figure 3.1** Representation of an energetically homogeneous surface.

*ideal* surface.<sup>1</sup>, is one in which each adsorption site, S, has the same energy of interaction with the adsorbate, which is not affected by the presence or absence of sorbate molecules on adjoining sites, and in which each site can accommodate only one adsorbate molecule or atom. We might represent the energy contours of each a surface qualitatively as shown in Figure 3.1. Adsorption would occur when a molecule or atom of adsorbate with the required energy strikes an unoccupied site, and the energy contours would be unaffected by the extent of adsorption.

These requirements for reaction (adsorption) to occur look very similar to those we imposed on the bimolecular collision number in order to derive the reactive collision number,  $Z_\eta(A, B)$ , of equation (2-20). If we designate  $E$  as the activation energy required for chemisorption,  $C_s$  as the concentration of sites available for chemisorption,  $n_s$  the site density per unit area of surface, and  $f(\theta)$  some function of the fraction of surface covered by the adsorbate,  $\theta_A$ , the following analog to equation (2-20) may be written as

$$C_s = n_s \cdot f(\theta)$$

$$\bar{Z}_{cT}(ads) = \frac{1}{4} n_A \left( \frac{8kT}{\pi m_A} \right)^{1/2} n_s \cdot \frac{f(\theta)}{n_s} e^{-E/kT} \quad (3-1)$$

Expressing  $n_A$  in terms of the ideal gas law,  $n_A = P_A/kT$ :

$$\bar{Z}_{cT}(ads) = \frac{P_A}{\sqrt{2\pi m_A kT}} n_s \cdot \frac{f(\theta)}{n_s} e^{-E/kT} \quad (3-2)$$

We may also include a term analogous to the steric factor to be used as a measure of the deviation of chemisorption rates from this ideal limit.

$$\bar{Z}_{cT}(ads) = \frac{\sigma P_A}{\sqrt{2\pi m_A kT}} n_s \cdot \frac{f(\theta)}{n_s} e^{-E/kT} \quad (3-3)$$

where  $\sigma$  is such a factor and is commonly termed the *sticking probability*. The adsorption rate constant,  $k_a^\circ$ , is thus seen to be  $[\sigma/(2\pi m_A kT)^{1/2}]$ . Estimates of  $k_a^\circ$  or  $\sigma$  for various models of the chemisorption process may be made by using TST in a

<sup>1</sup> "Ideals are like stars; you will not succeed in touching them."—C. Schurz

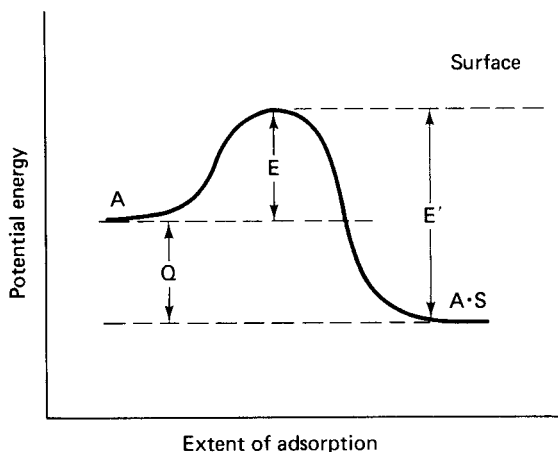


**Figure 3.2** Potential-energy diagram for adsorption-desorption.

manner similar to that employed for the steric-factor calculations reported in Table 2.4. Some problems of this sort are included in the exercises.

A potential-energy diagram for the adsorption-desorption process  $A + S \leftrightarrow A \cdot S$  is shown in Figure 3.2. As illustrated, the chemisorption is exothermic, which is, in general, the case. Also, since adsorption results in a more ordered state compared to the gas, we can argue in thermodynamic terms that entropy changes on chemisorption are negative. This fact will be of use later in testing the reasonableness of rate expressions for reactions on surfaces.

The development of an expression for desorption rates can be made along somewhat more qualitative lines. The rate will be proportional to the concentration of adsorbed species on the surface,  $C_{As}$ , which we will express as  $f'(\theta) \cdot n_s$ , and will require the activation energy  $E'$ , is shown in Figure 3.2. Thus, a reasonable form for the rate of desorption is

$$\bar{Z}(des) = k_d^\circ n_s \cdot \frac{f'(\theta)}{n_s} e^{-E'/kT} \quad (3-4)$$

where  $k_d^\circ$  is a desorption rate constant per unit surface area. Here again, some more quantitative arguments as to the nature of  $k_d^\circ$  can be made in terms of TST, as shown in the problems.

An important step in the consideration of surface reactions is the equilibrium level of adsorption on a surface. In terms of the example  $A + S \leftrightarrow A \cdot S$ , the rate is shown to be reversible and equilibrated, so the rate of adsorption equals the rate of desorption. It is convenient to think of this as a process of dynamic equilibrium, where the net rate of change is zero. From equations (3-3) and (3-4) we have

$$\frac{\sigma P_A}{\sqrt{2\pi m_d kT}} n_s \cdot f(\theta) e^{-E/kT} = k_d^\circ n_s \cdot f'(\theta) e^{-E'/kT} \quad (3-5)$$

This expression is extraordinarily useful, since it permits us to obtain some information concerning the surface coverage factors,  $f(\theta)$  and  $f'(\theta)$ , about which we have been rather vague. The point is that these factors cannot be measured conveniently,

while macroscopic quantities such as  $P_A$  and the heat of adsorption can. Equation (3-5) provides a link between the two. Solving for the ratio  $f'(\theta)/f(\theta)$

$$\frac{f'(\theta)}{f(\theta)} = \frac{\sigma P_A e^{Q/kT}}{k_d^\circ \sqrt{2\pi m_A kT}} \quad (3-6)$$

it can be seen that the surface coverage at equilibrium (or at least some function of it), is determined by the temperature of the system and the partial pressure of adsorbate. Such an equation for fixed temperature and varying partial pressure expresses the *adsorption isotherm* for the adsorbate, or, for fixed partial pressure and varying temperature, the *adsorption isobar*. The heat of adsorption,  $Q$ , appears in equation (3-6) since in solving for the ratio of surface coverage functions the difference  $(E' - E)$  appears in the exponential; from Figure 3.2 we see that this is equal in magnitude to the heat of adsorption.

Equation (3-6) is a form of the Langmuir isotherm [I. Langmuir, *J. Amer. Chem. Soc.*, 40, 1361 (1918)], which we may write in more general notation as

$$\frac{f'(\theta)}{f(\theta)} = K_A P_A = K_A^\circ e^{Q/kT} P_A \quad (3-6a)$$

where

$$K_A = \frac{\sigma e^{Q/kT}}{k_d^\circ \sqrt{2\pi m_A kT}} \quad (3-7)$$

Specific forms of this equation will depend on what  $f'(\theta)$  and  $f(\theta)$  are. For the example we have been using, the surface concentration of sites available for chemisorption,  $C_s$ , is obviously equal to the total number of sites per area times the fraction that are not occupied by A,

$$C_s = n_s(1 - \theta_A) \quad (3-7)$$

where  $\theta_A$  is the fraction of sites occupied by A. The surface concentration of adsorbate,  $C_{As}$  is

$$C_{As} = n_s \theta_A \quad (3-8)$$

so that

$$\begin{aligned} f'(\theta) &= \theta_A \\ f(\theta) &= 1 - \theta_A \end{aligned} \quad (3-9)$$

Inserting these values into equation (3-6a) and solving for  $\theta_A$  gives

$$\theta_A = \frac{K_A P_A}{1 + K_A P_A} \quad (3-10)$$

which is the Langmuir isotherm equation for the nondiassociative adsorption of a single species on a surface (i.e., single molecule on a single site).

In many cases of practical importance, the adsorbate molecule will dissociate on adsorption [ $H_2$  on many metals is probably the most well-known example; see J. R. Roberts, *Proc. Roy. Soc. London*, A152, 445 (1935); O. Beeck and A.W. Ritchie, *Disc. Faraday. Soc.*, 8, 159 (1950)], or occupy two sites by bonding at two

points in the molecule [ethylene on nickel; G.H. Twigg and E.K. Rideal, *Proc. Roy. Soc. (London)*, *A171*, 55 (1939)]. In such cases,

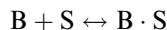
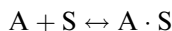
$$\begin{aligned} f'(\theta_A) &= \theta_A^2 \\ f(\theta_A) &= (1 - \theta_A)^2 \end{aligned} \quad (3-11)$$

and the corresponding isotherm equation is

$$\theta_A = \frac{(K_A P_A)^{1/2}}{1 + (K_A P_A)^{1/2}} \quad (3-12)$$

If the adsorbate molecule is immobile on the surface, the occupancy of nearest-neighbor sites should be accounted [A.R. Miller, *Proc. Cambridge Phil. Soc.*, *43*, (1947)]. This is not a large refinement, however, and equations (3-11) will be employed without reference to the detailed nature of the adsorbate layer.

A second modification of practical importance is when more than one adsorbate species is present on the surface. For example, consider the adsorption equilibrium (no surface reaction)



where A and B are chemisorbed on the same type of surface site, S; that is, they are competitively adsorbed on the surface. It will be seen in a subsequent exercise that the corresponding isotherm equations for the surface coverages of A and B are

$$\begin{aligned} \theta_A &= \frac{K_A P_A}{1 + K_A P_A + K_B P_B} \\ \theta_B &= \frac{K_B P_B}{1 + K_A P_A + K_B P_B} \end{aligned} \quad (3-13)$$

A major property of the Langmuir isotherm is that of saturation. In equation (3-10), for example when  $K_A P_A \gg 1$ ,  $\theta_A \rightarrow 1$ , and no further adsorption occurs. This is a result of the surface model, in which each adsorption site can accommodate only one adsorbate molecule. Saturation of the surface, then, corresponds to the occupancy of all sites and is called *monolayer coverage*. At low pressures,  $K_A P_A \ll 1$  and equation (3-10) assumes a linear form in  $P_A$  corresponding to Henry's law of adsorption. These general features are shown in Figure 3.3. Experimentally, one measures either the weight or volume of material adsorbed, and the ratio of this quantity at a given partial pressure to that at saturation can be taken as a direct measure of surface coverage. This is indicated in the figure, where  $\theta_A = V/V_M$ , in which  $V$  is the volume adsorbed and  $V_M$  the volume adsorbed at saturation.

The interpretation of data on adsorption in terms of the Langmuir isotherm is most easily accomplished using the procedure previously described for reaction rate data, that is examination of the results first through a linear form of the isotherm equation. Rearrange equation (3-10) to

$$\frac{1}{V} = \left( \frac{1}{P_A} \right) \left( \frac{1}{K_A V_M} \right) + \frac{1}{V_M} \quad (3-14)$$

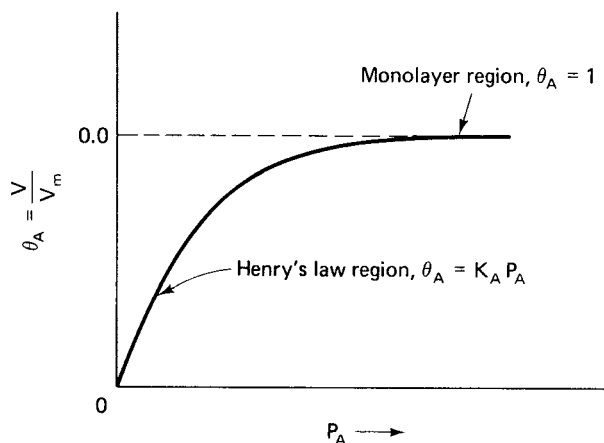


**Figure 3.3** Typical Langmuir adsorption isotherm.

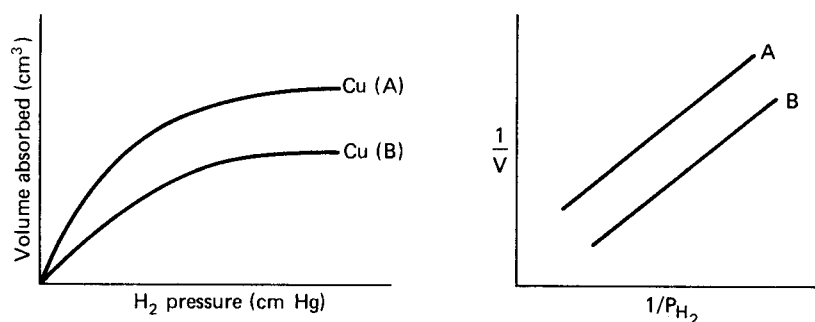


**Figure 3.4** Langmuir interpretation of  $H_2$  adsorption on copper powder. [After A.F.H. Ward, *Proc. Roy. Soc. (London)*, A133, 506 with permission of The Royal Society, (1931).]

which indicates that a plot of  $(1/V)$  versus  $(1/P_A)$  should be linear with slope  $(1/K_A V_M)$ . Figure 3.4 gives a representation of some results of the adsorption of hydrogen on copper and a corresponding Langmuir interpretation that provides a satisfactory correlation of the data.<sup>2</sup>

Examples of false obedience to the Langmuir isotherm abound. These usually arise when adsorption data have not been obtained over a sufficiently wide range of partial pressures; a good test is to see if value of  $V_M$  evaluated from isotherm data at different temperatures are equal, since within the framework of the Langmuir surface model the saturation capacity should not vary with the temperature. It can be difficult to tell, however, in view of experimental error.

<sup>2</sup> In some sources it is recommended to plot according to the alternative linear form:

$$(P_A/V) = (P_A/V_M) + (1/K_A V_M)$$

This has the disadvantage of involving  $P_A$  on both axes and may result in some loss of sensitivity of the test. "Seek simplicity and distrust it."—A.N. Whitehead

**Illustration 3.1**

The following data were reported by Taylor and Williamson [H.S. Taylor and A.T. Williamson, *J. Amer. Chem. Soc.*, 53, 2168 (1931)] for the chemisorption of hydrogen on a mixed manganous/chromic oxide powder at 305 and 444 °C.

$T = 305\text{ }^{\circ}\text{C}$		$T = 444\text{ }^{\circ}\text{C}$	
Pressure (mm Hg)	Vol. ads. (cm <sup>3</sup> )	Pressure (mm Hg)	Vol. ads. (cm <sup>3</sup> )
44	156.9	3	57.1
51	160.8	22	83.3
63	163.6	48	95.0
121	167.0	77	98.1
151	169.6	165	100.9
230	171.1		
269	171.6		

Test these data for adherence to the Langmuir isotherm. What is the monolayer volume in each case? Are these results consistent?

*Solution*

According to equation (3-14), we must test the data for a linear fit to  $(1/P)$  versus  $(1/V)$ .

305 °C		444 °C	
(1/P)	(1/V)	(1/P)	(1/V)
0.0227	0.00640	0.333	0.0175
0.0196	0.00622	0.045	0.0120
0.0159	0.00611	0.020	0.0105
0.0083	0.00600	0.013	0.0102
0.0066	0.00590	0.006	0.0099
0.0044	0.00584		
0.0037	0.00583		

The units are  $P$  (in mm Hg) and  $V$  (in cm<sup>3</sup>). The plotted data is shown in Figure 3.5. A reasonable straight-line fit is obtained in both cases, so we can proceed with the analysis via

$$\text{Slope} = (1/KV_M)$$

$$\text{Intercept} = (1/V_M)$$

The results of this give, for the monolayer volume,

$$V_M(305\text{ }^{\circ}\text{C}) = 181.8\text{ cm}^3$$

$$V_M(444\text{ }^{\circ}\text{C}) = 101.0\text{ cm}^3.$$

As stated before, for true Langmuir adsorption the value of  $V_M$  is not a function of temperature hence, while there is apparent conformity to the Langmuir isotherm at each temperature, the results are internally inconsistent.

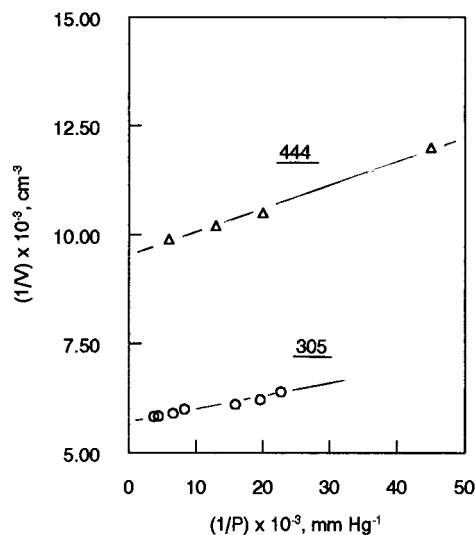


**Figure 3.5** Langmuir test plot of data for chemisorption of hydrogen on manganous/chromic oxide powder.



HORATIO SAYS

What if hydrogen and oxygen were simultaneously adsorbed on the mixed oxide surface? What data would we need and how would we interpret it?

### 3.1.2 Nonideal Surfaces

If once again we are to criticize a theory<sup>3</sup> it would be that no real surface could have the potential-energy contour depicted in Figure 3.1, nor is it reasonable to expect that adsorbate molecules on the surface would not interact with each other. Somewhat more plausible, but still possibly distant from reality in many situations, is the limitation of monolayer adsorption. In any of these events, one would expect to observe some distribution of energies of interaction with the surface which might be correlated with surface coverage. Since the strongest interactions would occur on the nearly-unoccupied surface, the experimental observation would be that of decreasing heat of chemisorption with increasing coverage. It is not possible to distinguish from this information alone whether energetic inhomogeneity of the surface or adsorbate interactions are the cause, but in most of the practical applications with which we are concerned, this amount of detail is not necessary. In the

<sup>3</sup>“Critics are like the brushers of Noblemen’s clothes.”—*F. Bacon*

following discussion, the case of an inhomogeneous surface shall be considered, using the specific example of nondissociative adsorption of a single species for illustration.

Consider that the surface may be divided into a number of groups of sites, each characterized with a similar heat of chemisorption, and so capable of being represented by a Langmuir isotherm. The fractional coverage of each of these for a single sorbate A is

$$\theta_{Ai} = \frac{K_{Ai}P_A}{1 + K_{Ai}P_A} \quad (3-10a)$$

and the total coverage is

$$\theta_A = \sum_i \theta_{Ai} n_i \quad (3-15)$$

where  $n_i$  is the number of adsorption sites belonging to group  $i$  and can be represented by an appropriate distribution function. It is reasonable to write this distribution function in terms of the heat of chemisorption,  $Q$ , and in one of the major isotherm expressions for nonideal surfaces, the *Freundlich isotherm*, this distribution is taken to be an exponential one. That is,

$$dn_i = n_0 e^{-Q/Q_M} dQ \quad (3-16)$$

where  $n_0$  and  $Q_M$  are scaling constants and  $dn_i$  the fraction of sites with heats of chemisorption between  $Q$  and  $Q + dQ$ . If we further assume, as indicated by the form of equation (3-16), that the groups of sites do not differ greatly in energy level as one goes from one level to the next, the summation may be replaced by integration with respect to the distribution function.

$$\theta_A = \int_0^\infty n_0 e^{-Q/Q_M} \frac{K_{Ai}P_A}{1 + K_{Ai}P_A} dQ \quad (3-17)$$

Recalling from equation (3-6a) that  $K_{Ai}$  is also a function of  $Q$ , we have:

$$\theta_A = \int_0^\infty n_0 e^{-Q/Q_M} \frac{K_A^\circ e^{Q/kT} P_A}{1 + K_A^\circ e^{Q/kT} P_A} dQ \quad (3-18)$$

which, for  $Q \gg kT$  can be integrated to

$$\theta_A = (K_A^\circ P_A)^{kT/Q_M} (n_0 Q_M) \quad (3-19)$$

It can be shown that the product of the scaling constants,  $n_0 Q_M$ , is unity, so that

$$\theta_A = (K_A^\circ P_A)^{kT/Q_M} \quad (3-20)$$

This is the basic expression of the Freundlich isotherm, which we see is just a power law of the form

$$\theta = cP^m \quad (3-20a)$$

The exponential distribution law employed defines the nature of the change of the heat of chemisorption with surface coverage. The Clausius-Clapeyron equation is the thermodynamic relation defining the heat effect accompanying a change of



phase, which we may certainly consider adsorption to be. This is

$$-Q = k \left[ \frac{d \ln P_A}{d(1/T)} \right]_{\theta_A} \quad (3-21)$$

Substituting from the isotherm equation and carrying out the indicated differentiation gives

$$Q = -Q_M \ln \theta_A \quad (3-22)$$

so that the heat of chemisorption is logarithmically dependent on surface coverage.

Testing experimental data for obedience to the isotherm is accomplished by a log-log plot of volume adsorbed versus adsorbate partial pressure, in accordance with the linearized form of equation (3-20):

$$\log V = \log V_M + \frac{kT}{Q_M} \log K_A^\circ + \frac{kT}{Q_M} \log P_A \quad (3-23)$$

where  $V$  and  $V_M$  are the volume adsorbed and the monolayer volume, respectively. In Figure 3.6 is a representation of some data for the adsorption of hydrogen on tungsten powder and the corresponding Freundlich interpretation.

A second type of isotherm that has been employed for nonideal surfaces is that of Temkin, which postulates that the heat of chemisorption decreases linearly with surface coverage:

$$Q = Q_0(1 - \alpha\theta) \quad (3-24)$$

where  $Q_0$  is the heat of chemisorption at zero surface coverage and  $\alpha$  the linear scaling constant. By a derivation similar to that for the Freundlich isotherm, we obtain

$$\theta_A = \frac{kT}{Q_0\alpha} \ln (K_A^\circ e^{-Q_0/kT} P_A) \quad (3-25)$$

in which the correlation is limited to the midrange of surface coverage ( $0.25 < \theta_A < 0.75$ ). This isotherm is best known for its correlation of the important system of nitrogen and hydrogen on iron involved in ammonia synthesis. For an extensive discussion of various isotherm expressions and many experimental results for both ideal and nonideal systems, see the monograph by Hayward and Trapnel [D.O. Hayward and B.M.W. Trapnell, *Chemisorption*, 2nd ed., Butterworth, Washington, D.C., (1964)].

### 3.1.3 Physical Adsorption and the BET Theory

Thus far we have examined only the process of chemisorption, in the sense of it being the first step on the road to chemical reaction on a surface. If we summarize to this point, chemisorption is a chemical interaction between the adsorbate and the surface. The heats and activation energies of chemisorption are typical of those of a chemical reaction, and that is exactly what it is: a chemical reaction, albeit three-dimensional on one side of the arrow and two-dimensional on the other side. The activation energies are such that the species involved have sufficient energy to cross the activation energy barrier at temperature levels that are experimentally accessible and of practical importance.

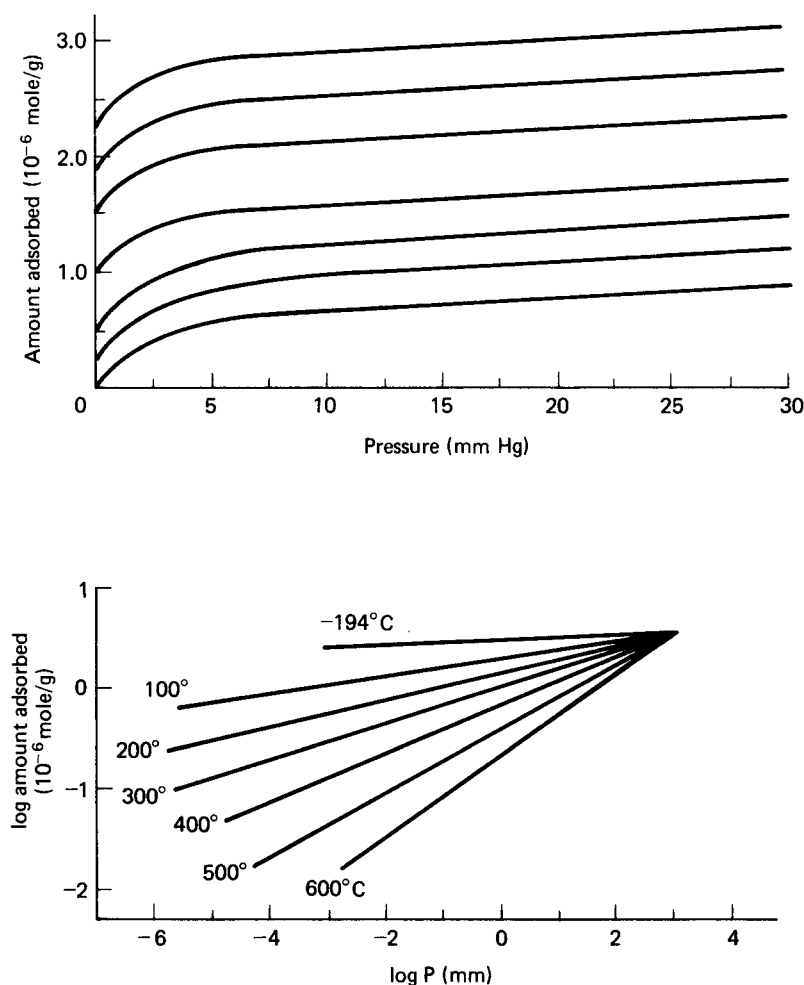


**Figure 3.6** Freundlich interpretation of  $H_2$  adsorption on tungsten powder. [Reprinted with permission from W.G. Frakennberg, *J. Amer. Chem. Soc.*, 66, 1827, copyright by the American Chemical Society, (1944).]

Now we need to talk about physical adsorption, which, though it is not generally considered to be a crucial factor in surface reactions, is of importance in relation to the topic as a whole. One might say that physical adsorption does things a bit differently from chemisorption, as is shown in Table 3.1. The analysis of physical adsorption can be complicated, even more so than for chemisorption, because attractive–repulsive interactions are involved that may be more complex than direct chemisorptive interactions.

We need to examine a particular model for physical adsorption that has been extremely useful over the years in the characterization of the porous materials that are often employed as catalyst support structures or as catalysts in their own right. The basic question is how to measure the internal (pore) surface area of a material that is perhaps 50% void and has an average pore diameter on the order of 5 nm (see

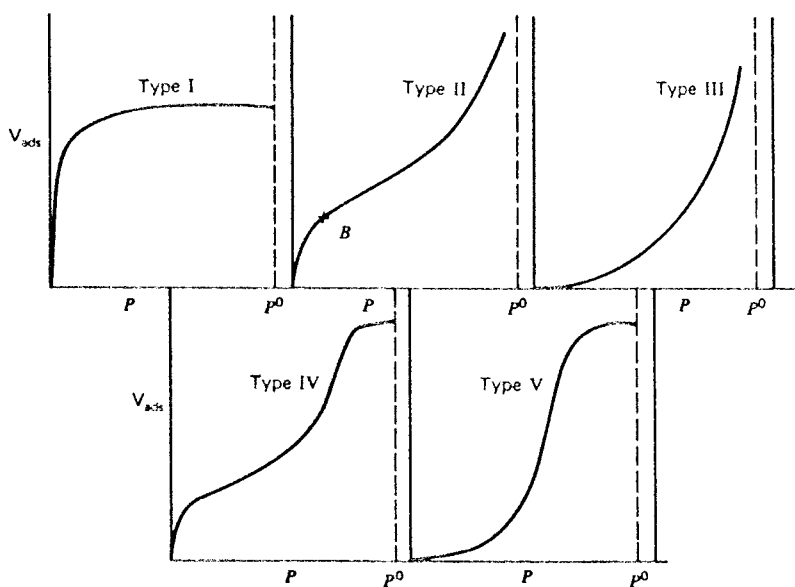
**Table 3.1** Characteristics of Physical and Chemical Adsorption

Physical Adsorption	Chemisorption
Low heat of adsorption ( $< 2$ or $3$ times latent heat of evaporation.)	High heat of adsorption ( $> 2$ or $3$ times latent heat of evaporation.)
Non specific	Highly specific
Monolayer or multilayer. No dissociation of adsorbed species. Only significant at relatively low temperatures.	Monolayer only. May involve dissociation. Possible over a wide range of temperature.
Rapid, non-activated, reversible.	Activated. May be slow and irreversible.
No electron transfer although polarization of sorbate may occur	Electron transfer leading to bond formation between sorbate and surface.

Source: After D.M. Ruthven, *Principles of Adsorption and Adsorption Processes*, with permission of John Wiley and Sons, New York, NY (1984).

Chapter 7 for further elucidation of such structural characteristics). We want to know this surface area because it is presumably important in determining the overall rate of reaction per unit volume of catalyst in a given application.

The analysis of physical adsorption in general, and that used to approach this particular problem, derives from a classification later summarized by Brunauer [S. Brunauer, *The Adsorption of Gases and Vapors*, Princeton University Press, Princeton, NJ, (1945)]. He classified the isotherms for physical adsorption of gases on surfaces into five general types, as shown in Figure 3.7. Isotherm I is already

**Figure 3.7** Classification of physical adsorption isotherms.

recognizable as a typical Langmuir isotherm. Isotherms II–IV show the various complexities of physical adsorption; it is isotherm II that is of most interest. Early work showed that this was typical for adsorption of nitrogen (at liquid nitrogen temperatures) on a large number of porous adsorbents. The result of that observation was the derivation of an appropriate analytical theory to describe this type of adsorption and to use it for physical characterization, in terms of internal surface area of the adsorbent [S. Brunauer, P.H. Emmett and E.J. Teller, *J. Amer. Chem. Soc.*, 60, 309 (1938)]. From the last initials of the authors comes the name “BET theory”. To begin our consideration of this theory, let us once again recall the Hertz-Knudsen equation for the collision of gas molecules (atoms) with surfaces:

$$Z(\text{surface}) = (n\bar{c}/4) \quad (3-26)$$

where  $n$  is the number density of colliding molecules and  $\bar{c}$  is the proper relative velocity. From Chapter 2,

$$Z(\text{surface}) = \left(\frac{n}{4}\right) \left(\frac{8kT}{\pi m}\right)^{1/2} \quad (3-27)$$

This is how fast collisions occur. Now we also have to make up a little picture of the surface and adsorbed layer(s) that the collisions are involved with, as in Figure 3.8.

In each layer there is a dynamic equilibrium. Consider adsorption in the first layer.

$$\text{Adsorption rate} = \frac{NP}{(2\pi MRT)^{1/2}} (\sigma_1 \theta_0) = u_1 \quad (3-28)$$

where  $\theta_0$  is the vacant fraction of the surface and  $\sigma_1$  is the sticking coefficient. For desorption

$$\text{Desorption rate} = (\nu')_1 n_s \theta_1 e^{-E_1/RT} = (u')_1 \quad (3-29)$$

where  $\theta_1$  is the fraction covered by the first layer. At equilibrium

$$u_1 = (u')_1 \quad (3-30)$$

and if we define  $K$  as

$$K = N/(2\pi MRT)^{1/2}$$

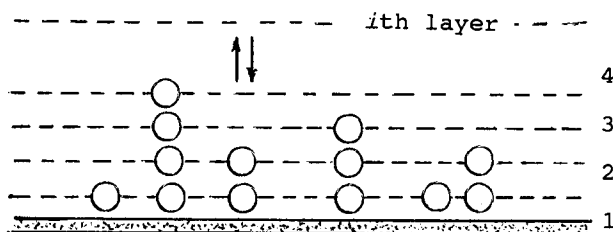


**Figure 3.8** Multilayer surface adsorption model for the BET isotherm.

then we can write for the first, second and  $i$ th layers:

$$KP\sigma_1\theta_0 = n_s\theta_1(\nu')_1 e^{-E_1/RT} \quad (3-31)$$

$$KP\sigma_2\theta_1 = n_s\theta_2(\nu')_2 e^{-E_2/RT} \quad (3-32)$$

$$KP\sigma_i\theta_{i-1} = n_s\theta_i(\nu')_i e^{-E_i/RT} \quad (3-33)$$

The total number of molecules adsorbed per unit surface area of adsorbent is

$$n = n_s(\theta_1 + 2\theta_2 + 3\theta_3 + \cdots + i\theta_i) \quad (3-34)$$

If we let  $s$  be the surface area per weight of adsorbent, then  $(s)$  is the number per weight. Further, let us make  $x_M$  the monolayer capacity in weight of adsorbate per weight of adsorbent. Then

$$\left(\frac{x}{x_M}\right) = \left(\frac{sn}{sn_s}\right) = \left(\frac{n}{n_s}\right) \quad (3-35)$$

$$\left(\frac{x}{x_M}\right) = (\theta_1 + 2\theta_2 + 3\theta_3 + \cdots + i\theta_i) \quad (3-36)$$

In order to get something out of the series here we must make some assumptions about the relationships among  $(\nu')_i$ ,  $E_i$ , and  $\sigma_i$  in the different layers. The two major BET assumptions are

1. The activation energy for desorption in all layers above the first is equal to the latent heat of condensation. Hence  $E_2 = E_3 \cdots = E_i = \lambda$ , where  $\lambda$  is the latent heat of condensation.
2. Ratios of desorption frequencies to sticking probabilities in all layers above the first, are the same. Thus,

$$\frac{(\nu')_2}{\sigma_2} = \frac{(\nu')_3}{\sigma_3} \cdots = \frac{(\nu')_i}{\sigma_i}$$

Now, what do we have? *First*,

$$\left(\frac{\theta_1}{\theta_0}\right) = \left(\frac{\sigma_1 KP}{n_s(\nu')_1}\right) e^{E_1/RT} = \alpha \quad (3-37)$$

$$\theta_1 = \alpha\theta_0 \quad (3-38)$$

*Second*,

$$\left(\frac{\theta_2}{\theta_1}\right) = \left(\frac{\sigma_2 KP}{n_s(\nu')_2}\right) e^{E_2/RT} = \left(\frac{\sigma_2 KP}{n_s(\nu')_2}\right) e^{\lambda/RT} = \beta \quad (3-39)$$

$$\theta_2 = \beta\theta_1 = \alpha\beta\theta_0 \quad (3-40)$$

Since the ratios of  $[\sigma_i/(\nu')_i]$  are the same for all layers beyond the first,

$$\theta_i = \beta\theta_{i-1} \quad (i > 2) \quad (3-41)$$

We will now designate a constant,  $C$ , as

$$C = \left( \frac{\alpha}{\beta} \right) = \left[ \frac{\sigma_1(\nu')_2}{\sigma_2(\nu')_1} \right] e^{(E_1 - \lambda)/RT} \quad (3-42)$$

Then

$$\begin{aligned} \theta_i &= C\beta^i\theta_0 \\ n &= Cn_s\theta_0(\beta + 2\beta^2 + \cdots + i\beta^i) \end{aligned} \quad (3-43)$$

This last equation can be written more compactly as

$$n = Cn_s\theta_0 \sum_{i=1}^{\infty} (i\beta^i) \quad (3-44)$$

Now, note that

$$i\beta^i = \beta \frac{d(\beta^i)}{d\beta} \quad (3-45)$$

which immediately reduces the problem posed by equation (3-44), since we now have an infinite geometric series with known sum  $\beta/(1 - \beta)$ . Hence

$$n = Cn_s\theta_0\beta \frac{d}{d\beta} \left[ \frac{\beta}{(1 - \beta)} \right] = Cn_s\theta_0 \frac{\beta}{(1 - \beta)^2} \quad (3-46)$$

This essentially solves the problem, since we know already that

$$\theta_0 = 1 - \sum_{i=1}^{\infty} (\theta_i)$$

and from equation (3-42)

$$\theta_0 = 1 - C\theta_0 \left( \frac{\beta}{1 - \beta} \right)$$

This gives

$$\begin{aligned} \theta_0 &= \frac{1}{1 + C\beta/(1 - \beta)} \\ \left( \frac{n}{n_s} \right) &= \frac{C\beta}{(1 - \beta)(1 - \beta + C\beta)} \end{aligned} \quad (3-47)$$

Now  $\beta$  contains the ratio  $[\sigma_i/(\nu')_i]$  which is not immediately accessible to experimental determination. However, we have the limit that when the adsorbate reaches its saturated vapor pressure it will condense as a liquid and there will be an infinite number of layers. This means that

$$P \rightarrow P_0; \quad (n/n_s) \rightarrow \infty$$

which requires that  $\beta = 1$  at  $P = P_0$ . Thus we have

$$\text{At } P = P; \quad \beta = \left( \frac{\sigma_i K P}{n_s(\nu')_i} \right) e^{\lambda/RT} \quad (3-48)$$

$$\text{At } P = P_0; \quad 1 = \left( \frac{\sigma_i K P_0}{n_s(\nu')_i} \right) e^{\lambda/RT} \quad (3-49)$$

These two equations state simply that  $b$  is identical to  $(P/P_0)$ . Substituting this into equation (3-47) we have

$$\left( \frac{n}{n_s} \right) = \left( \frac{x}{x_M} \right) = \frac{C(P/P_0)}{(1 - P/P_0)[1 + (C - 1)(P/P_0)]} \quad (3-50)$$

This can be arranged into a more convenient form that is generally termed the BET equation.

$$\frac{P}{x(P_0 - P)} = \frac{1}{x_M C} + \frac{C - 1}{x_M C} \left( \frac{P}{P_0} \right) \quad (3-51)$$

The units of  $x$  and  $x_M$  are typically  $\text{cm}^3(\text{STP})/\text{g}$ , and  $C$  is a nondimensional constant. As in the case of the rearrangement of the Langmuir isotherm, equation (3-14), this is a pseudo-linear form of equation which, given experimental data on  $P$  versus  $x$ , can be used to extract the parameters  $x_M$  and  $C$  from the slope and intercept in the usual way.

Of these parameters the most informative is probably  $x_M$ , the capacity at monolayer coverage. We stated earlier that the physical adsorption of nitrogen on many surfaces resembled Type II in the classification of Brunauer (as it turns out, Type III is also seen in a number of instances). Nonetheless, the idea is that if equation (3-51) is obeyed we can obtain a value for  $x_M$  and, following some judicious assumptions, a value of the internal surface area. Let us look at the specifics associated with the adsorption of nitrogen at liquid nitrogen temperatures. If we propose that the surface area of a nitrogen molecule (as adsorbed) can be calculated from the density of the adsorbate in the normal liquid phase, then

$$A_M = f(M/\rho N)^{2/3} \times 10^{16} \quad (3-52)$$

where  $A_M$  is in  $\text{\AA}^2$ ,  $M$  is the molecular weight,  $N$  Avagadro's number,  $\rho$  density, and  $f$  is a packing factor for the arrangement on the surface. Inserting the appropriate constants for liquid nitrogen and assuming a packing factor slightly greater than unity ( $f = 1.091$  for HCP structures), we get a very useful working relationship

$$A_M = 16.2 \text{ \AA}^2 \quad \text{for } N_2 \quad (3-53)$$

where the density has been taken as  $0.81 \text{ g/cm}^3$  at 78K. The surface area is then

$$S = (4.35 \times 10^4) V_M \quad (3-54)$$

with  $S$  in  $\text{cm}^2/\text{g}$ , and  $x_M$  has been converted into a volumetric measurement in  $\text{cm}^3/\text{g}$ .

The shape of the isotherm predicted by the BET equation depends on the value of  $C$ . In short, if  $C > 2$  there is a Type II isotherm, and if  $C < 2$  there is a Type III isotherm.  $C$  is related to the heat of adsorption via equation (3-42). Sometimes the

approximation is made (which may be very poor) that the pre-exponential factor in equation (3-42) is unity, and a net heat of adsorption can be estimated from

$$E_1 - \lambda + RT[\ln(C)]$$

The shape of the isotherm, thus, is related to this heat of adsorption,  $\lambda$ . From the approximation

$$C = 2; \quad E_1 \text{ slightly} > \lambda$$

$$C = 1; \quad E_1 = \lambda$$

$$C < 1; \quad E_1 < \lambda$$

### Illustration 3.2

Figure 3.9 indicates that for a Type II isotherm a point of inflection exists. What information can be obtained from this?

#### Solution

Let us modify equation (3-51) to the following

$$X = \frac{1}{1-Y} - \frac{1}{1+(C-1)Y} \quad (i)$$

where  $X = (x/x_M)$  and  $Y = (P/P_0)$ . The second derivative of this is

$$\frac{d^2X}{dY^2} = 2C \left[ \frac{(C-1)^2 Y^3 + 3(C-1)Y - C + 2}{\{(1-Y)[1+(C-1)Y]\}^3} \right]$$

Solving for  $Y$  at  $(d^2X/dY^2) = 0$  gives the pressure corresponding to the inflection point,  $Y_y$ :

$$Y_y = \frac{(C-1)^{2/3} - 1}{(C-1) + (C-1)^{2/3}} \quad (ii)$$

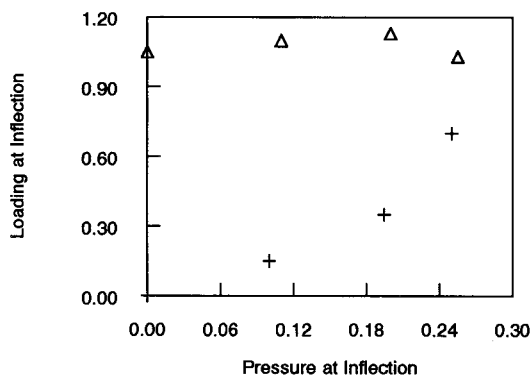


**Figure 3.9** Locus plot for inflection points from the BET equation.



with the corresponding value of  $X_y$  as

$$X_y = (1/C)[(C-1)^{2/3} + 1][(C-1)^{2/3} - 1] \quad (\text{iii})$$

From these relations one can obtain the value of  $C$ , given the locus of the inflection point. One may also construct a locus plot as shown below with each point associated with a particular value of  $C$ .



HORATIO SAYS

The basic BET result is very useful, as shown, but obviously holds only for lower values of  $(P/P_0)$ . What happens when the pores begin to fill with condensate?

### 3.2 Surface Reactions with Rate-Controlling Steps

At the beginning of this chapter it was stated that reaction sequences involving surface steps [such as (XXV)], could be visualized as a type of chain reaction. This is indeed so, and we shall have more to say concerning the analysis of surface reactions via the pssh a little later on. However, also associated with the development of the theory of surface reaction kinetics has been the concept of the rate-limiting or rate-controlling step. This presents a rather different view of sequential steps than does pure chain reaction theory, since if a single step controls the rate of reaction then all other steps must be at equilibrium. This is a result that is not a consequence of the general pssh.

In fact, pursuing the example of (XXV) a bit further in this regard, if the surface reaction is rate-limiting, we can express the net rate of reaction directly in terms of the surface species concentrations,  $C_{As}$  and  $C_{Bs}$ :

$$\text{rate} = k_{s1}C_{As} = k_{s2}C_{Bs} \quad (3-55)$$

where  $k_{s1}$  and  $k_{s2}$  are velocity constants for the forward and reverse surface reaction steps. This represents a considerable simplification from the normal chain reaction analysis, because the first and third steps of (XXV) are at equilibrium and the surface species concentrations are entirely determined by their adsorption/desorption equilibrium on the surface. If we write, as previously, the surface concentrations in terms of surface coverage and total site density

$$\begin{aligned} C_{As} &= n_s \cdot \theta_A \\ C_{Bs} &= n_s \cdot \theta_B \end{aligned} \quad (3-56)$$

Substitution of equations (3-13) and (3-56) into (3-55) gives the rate of reaction in terms of the partial pressures of the reacting species.

$$r = \frac{k_{s1}n_sK_AP_A}{1 + K_AP_A + K_BP_B} - \frac{k_{s2}n_sK_BP_B}{1 + K_AP_A + K_BP_B} \quad (3-57)$$

In fact, the value of  $n_s$  may be a somewhat elusive quantity, so that in practice this is often absorbed into the rate constant as, say,  $k'_{S1} = (k_{S1}n_s)$ .

The rates of catalytic reactions are usually expressed in terms of unit mass or unit total surface (not external surface) of the catalyst. An appropriate working form of equation (3-57) for the disappearance of A in (XXV) is

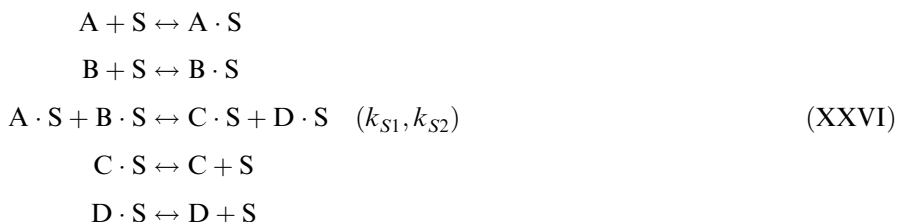
$$-\frac{1}{W_c} \frac{dN_A}{dt} = -r_A = \frac{k'_{S1}K_A P_A - k'_{S2}K_B P_B}{1 + K_A P_A + K_B P_B} \quad (3-57a)$$

or

$$-\frac{1}{A_c} \frac{dN_A}{dt} = -r_A = \frac{k'_{S1}K_A P_A - k'_{S2}K_B P_B}{1 + K_A P_A + K_B P_B} \quad (3-57b)$$

where  $W_c$  is the weight of catalyst,  $A_c$  the total surface area, and the specific rate constants  $k'_{S1}$  and  $k'_{S2}$  defined accordingly as per unit mass or area. Since there is a wide variation in surface area per unit mass in various catalysts, rate definitions based on mass may be misleading as to the true activity of a catalyst. If information on  $A_c$  is available, specific area rates are preferable. This is why we spent so much effort on learning how to measure it in the previous section.)

As a second example of surface-reaction-rate control, consider the slightly more complicated case of a bimolecular reaction occurring on the same sites, S, of a surface. Overall,  $A + B \leftrightarrow C + D$ , and the individual steps are



and the rate of reaction of A is

$$-r_A = k_{S1}C_{As}C_{Bs} - k_{S2}C_{Cs}C_{Ds} \quad (3-58)$$

The appropriate form of equation (3-13) for the competitive adsorption of A, B, C, and D on the surface is

$$\theta_i = \frac{K_i P_i}{1 + K_A P_A + K_B P_B + K_C P_C + K_D P_D} \quad (i = A, B, C, D)$$

and the rate equation is

$$-r_A = \frac{k'_{S1}K_A K_B P_A P_B - k'_{S2}K_C K_D P_C P_D}{(1 + K_A P_A + K_B P_B + K_C P_C + K_D P_D)} \quad (3-59)$$

where the  $K$ 's represent the adsorption equilibrium constants for the individual species on the surface.

It is clear from equations (3-57) and (3-58) that when a surface reaction step is rate-controlling, one needs only information concerning adsorption equilibria of reactant and product species in order to write the appropriate rate equation for

the overall transformation. It also often occurs that the products of a reaction are much less strongly bound to the surface than are the reactants, or that the surface reaction step is essentially irreversible, or both. In such cases the product terms disappear from equations such as (3-57) or (3-59), and in much of the literature equations of this form (referring to surface-reaction steps rate controlling), are termed *Langmuir-Hinshelwood (LH) rate equations*. A bewildering array of such equations may be derived for various types of reactions, depending on specific assumptions concerning the magnitude of adsorption equilibrium constants, dissociative or nondissociative adsorption of species, type of sites involved in adsorption and surface reaction, and so on. Some examples of these are given in Table 3.2. In each of these the active centers or sites form a closed sequence in the overall reaction. According to this view, when the stoichiometry between reactants and products is not balanced, the concentration of vacant active centers also enters the rate equation [reaction (2), Table 3.2]. In formulation of the overall rate equation, this concentration may be written in terms of active centers through the relationship

$$C_s = \frac{n_s}{1 + \sum_i (K_i P_i)} \quad (3-60)$$

where the summation is with respect to all species adsorbed on the surface. The denominator of all LH rate equations consists of a summation of the adsorption terms for species on the surface; these are sometimes called *adsorption inhibition terms* (particularly with reference to product adsorption) since they decrease the magnitude of the rate as given by the power-law functions that make up the numerator of LH equations. The bimolecular reaction involving one reactant non-adsorbed [reaction (6), Table 3.2] is sometimes referred to as a *Rideal* or *Eley-Rideal mechanism*. It is encountered primarily in interpretation of catalytic hydrogenation kinetics.

The analysis of rate-controlling steps other than surface reaction on ideal surfaces has been developed in detail by Hougen and Watson [O.A. Hougen and R.K. Watson, *Chemical Process Principles*, Vol. III, John Wiley and Sons, New York, NY, (1947); see also R.H. Yang and O.A. Hougen, *Chem. Eng. Progr.*, 46, 146 (1950)]. If, for example, the rate of adsorption of a reactant species on the surface is slow compared to other steps, it is no longer correct to suppose that its surface concentration is determined by adsorption equilibrium. Rather, there must be chemical equilibrium among all species on the surface, and the surface concentration of the species involved in the rate-limiting step is determined by this equilibrium. The actual partial pressure of the rate-limiting adsorbate consequently will not appear in the adsorption terms of the rate equation, but is replaced by that pressure corresponding to the surface concentration level established by the equilibrium of other steps. This is the *virtual pressure* of the species in equation. Again consider the isomerization example of (XXV), this time in which the rate of adsorption of A is controlling. From equations (3-3) and (3-4) we may write the net rate of reaction as the difference between rates of adsorption and desorption of A:

$$-r_A = k_a P_A C_s - k_d C_{A_s} \quad (3-61)$$

**Table 3.2** Some Examples of Langmuir-Hinshelwood Rate Equations

Reaction Description	Individual Steps	Equation, $(-r_A)$	Constants
(1) Isomerization: $A \rightleftharpoons B$	$A + S \rightleftharpoons A \cdot S$ $A \cdot S \rightleftharpoons B \cdot S$ $B \cdot S \rightleftharpoons B + S$	$-r_A = k_{S1}C_{AS} - k_{S2}C_{BS}$ $= \frac{k'_{S1}K_A P_A - k'_{S2}K_B P_B}{1 + K_A P_A + K_B P_B}$	$k'_{S1} = k_{S1}n_s$ $k'_{S2} = k_{S2}n_s$
(2) Decomposition: $A \rightleftharpoons B + C$	$A + S \rightleftharpoons A \cdot S$ $A \cdot S + S \rightleftharpoons B \cdot S + C \cdot S$ $B \cdot S \rightleftharpoons B + S$ $C \cdot S \rightleftharpoons C + S$	$-r_A = k_{S1}C_{AS}C_S - k_{S2}C_{BS}C_C$ $= \frac{k'_{S1}K_A P_A - k'_{S2}K_B K_C P_B P_C}{(1 + K_A P_A + K_B P_B + K_C P_C)^2}$	$k'_{S1} = k_{S2}n_s^2$ $k'_{S2} = k_{S2}n_s^2$
(3) Bimolecular: $A + B \rightleftharpoons C + D$	$A + S \rightleftharpoons A \cdot S$ $B + S \rightleftharpoons B \cdot S$ $A \cdot S + B \cdot S \rightleftharpoons C \cdot S + D \cdot S$ $C \cdot S \rightleftharpoons C + S$ $D \cdot S \rightleftharpoons D + S$	$-r_A = k_{S1}C_{AS}C_{BS} - k_{S2}C_{CS}C_{DS}$ $= \frac{k'_{S1}K_A K_B P_A P_B - k'_{S2}K_C K_D P_C P_D}{(1 + K_A P_A + K_B P_B + K_C P_C + K_D P_D)^2}$	$k'_{S1} = k_{S1}n_s^2$ $k'_{S2} = k_{S2}n_s^2$
(4) Bimolecular, different sites: $A + B \rightleftharpoons C + D$	$A + S_1 \rightleftharpoons A \cdot S_1$ $B + S_2 \rightleftharpoons B \cdot S_2$ $A \cdot S_1 + B \cdot S_2 \rightleftharpoons C \cdot S_1 + D \cdot S_2$ $C \cdot S_1 \rightleftharpoons C + S_1$ $D \cdot S_2 \rightleftharpoons D + S_2$	$-r_A = k_{S1}(C_{AS})_1(C_{BS})_2 - k_{S2}(C_{CS})_1(C_{DS})_2$ $= \frac{k'_{S1}(K_A)_1(K_B)_2 P_A P_B - k'_{S2}(K_C)_1(K_D)_2 P_C P_D}{[1 + (K_A)_1 P_A + (K_C)_1 P_C][1 + (K_B)_2 P_B + (K_D)_2 P_D]}$	$k'_{S1} = k_{S1}n_{s1}n_{s2}$ $k'_{S2} = k_{S2}n_{s1}n_{s2}$
(5) Bimolecular with dissociation of one reactant: $\frac{1}{2}A_2 + B \rightleftharpoons C + D$	$A_2 + 2S \rightleftharpoons 2A \cdot S$ $B + S \rightleftharpoons B \cdot S$ $A \cdot S + B \cdot S \rightleftharpoons C \cdot S + D \cdot S$ $C \cdot S \rightleftharpoons C + S$ $D \cdot S \rightleftharpoons D + S$	$-r_A = k_{S1}C_{AS}C_{BS} - k_{S2}C_{CS}C_{DS}$ $= \frac{k'_{S1}(K_A P_A)^{1/2} K_B P_B - k'_{S2}K_C K_D P_C P_D}{[1 + (K_A P_A)^{1/2} + K_B P_B + K_C P_C + K_D P_D]^2}$	$k'_{S1} = k_{S1}n_s^2$ $k'_{S2} = k_{S2}n_s^2$
(6) Bimolecular with one reactant not adsorbed: $A(g) + B \rightleftharpoons C$	$B + S \rightleftharpoons B \cdot S$ $A(g) + B \cdot S \rightleftharpoons C \cdot S$ $C \cdot S \rightleftharpoons C + S$	$-r_A = k_{S1}C_{BS}C_A - k_{S2}C_{CS}$ $= \frac{k'_{S1}(K_B P_B(P_A/RT) - k'_{S2}K_C P_C}{1 + K_B P_B + K_C P_C}$	$k'_{S1} = k_{S1}n_s$ $k'_{S2} = k_{S2}n_s$

in which  $k_s$  and  $k_d$  are adsorption and desorption rate constants (i.e.,  $k_s = k_s^\circ e^{-E/RT}$ ) and  $C_{As}$  is the surface concentration of A as determined by the equilibrium of all other steps. We define a surface reaction equilibrium constant,  $K_s$ , as in the normal way,

$$K_s = \frac{C_{Bs}}{C_{As}}$$

and

$$C_{As} = \frac{C_{Bs}}{K_s} \quad (3-62)$$

According to the discussion above, we can define  $C_{As}$  also from the normal isotherm equation where the virtual pressure,  $P_A^*$ , is used in place of the actual partial pressure  $P_A$ :

$$C_{As} = n_s \theta_A = \frac{n_s K_A P_A^*}{1 + K_A P_A^* + K_B P_B} \quad (3-63)$$

and similarly for  $C_{Bs}$ :

$$C_{Bs} = n_s \theta_B = \frac{n_s K_B P_B}{1 + K_A P_A^* + K_B P_B} \quad (3-64)$$

Substituting (3-63) and (3-64) into the expression for  $K_s$  and solving for  $P_A^*$  gives

$$P_A^* = \frac{K_B P_B}{K_A K_s} \quad (3-65)$$

Employing these expressions for  $C$ ,  $C_{Bs}$ ,  $P_A^*$  and equation (3-60) for  $C_s$  gives the final rate equation from (3-61).

$$-r_A = \frac{k'_A P_A - (k'_d K_B P_B / K_s)}{1 + (K_B P_B / K_s) + K_B P_B} \quad (3-66)$$

An entirely analogous procedure may be used for a desorption-rate-controlling step in this example, with  $(-r_A)$  determined by

$$(-r_A) = k_d C_{Bs} - k_a P_B C_s \quad (3-67)$$

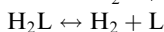
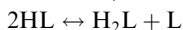
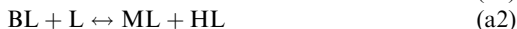
with the appropriate surface concentrations defined in terms of the virtual pressure of B. Application of these procedures to more complicated reaction schemes is left to the exercises.

The equations shown in Table 3.2 deal with variants on monomolecular or bimolecular reaction rate equations in general A to D terms. For a more concrete example in terms of chemical species, let us consider the specific case of the dehydrogenation of butene to butadiene over a chromia/alumina catalyst as detailed by Dumez and Froment [F.J. Dumez and G.F. Froment, *Ind. Eng. Chem. Proc. Design Devel.*, 15, 291 (1976)]. In Table 3.3a is a number<sup>4</sup> of reaction schemes for dehydrogenation classified as to atomic or molecular with the various possibilities listed as to the nature of the hydrogen recombination, (a)-(e), and with subdivisions as to

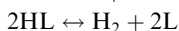
<sup>4</sup> "Nobody goes to that restaurant anymore; it's too crowded."—Y. Berra

**Table 3.3a** Reaction Schemes for Butene Dehydrogenation

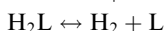
## (a) Atomic Dehydrogenation: Surface Recombination of Hydrogen



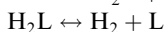
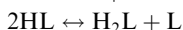
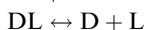
## (b) Atomic Dehydrogenation: Gas-Phase Recombination of Hydrogen



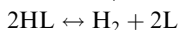
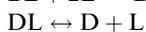
## (c) Molar Dehydrogenation



## (d) Atomic Dehydrogenation: Intermediate Complex with Short Lifetime and Surface recombination of Hydrogen



## (e) Atomic Dehydrogenation: Intermediate Complex with Short Lifetime and Gas-Phase Recombination of Hydrogen



B = n-butene; D = butadiene; H<sub>2</sub> = hydrogen; M = intermediate complex; L = surface site.

Source: From F.J. Dumez and G.F. Froment, *Ind. Eng. Chem. Proc. Design Devel.*, 15, 291 (1976). With permission of the American Chemical Society.

potential rate-controlling steps, (a1), (a2), (a3) . . . , etc. As one can see, consideration of all the possibilities leads to a large group of reaction possibilities. These give rise to the rate equations shown in Table 3.3b. This is quite a menu of kinetic fare, approaching the indigestible unless we can devise some way to sort among them. The task of discrimination, which we can state simply as finding out which equation provides the best fit to experimental data, is not simple. The most complicated is not always the best, though it may sometimes seem so, and the best may not arise from a reaction scheme as chemically plausible as some others. One feels almost like apologizing for the length of the entries in Table 3.3b, but the magnitude of the situation is best appreciated visually.

**Table 3.3b** Rate Equations for Butene Dehydrogenation

$$r_{\text{H}}^0 = \frac{k_1 C_{\text{tL}} \left( p_{\text{B}} - \frac{p_{\text{H}} p_{\text{D}}}{K} \right)}{\left( 1 + \frac{p_{\text{H}} p_{\text{D}}}{K_2 K_3 K_4 K_5 K_6} + \frac{p_{\text{D}} \sqrt{p_{\text{H}}}}{K_3 K_4 \sqrt{K_5 K_6}} + \frac{p_{\text{D}}}{K_4} + \frac{\sqrt{p_{\text{H}}}}{\sqrt{K_5 K_6}} + \frac{p_{\text{H}}}{K_6} \right)} \quad (\text{a1})$$

$$r_{\text{H}}^0 = \frac{k_1 K_1 C_{\text{tL}}^2 \left( p_{\text{B}} - \frac{p_{\text{H}} p_{\text{D}}}{K} \right)}{\left( 1 + K_1 p_{\text{B}} + \frac{p_{\text{D}} \sqrt{p_{\text{H}}}}{K_3 K_4 K \sqrt{K_5 K_6}} + \frac{p_{\text{D}}}{K_4} + \frac{\sqrt{p_{\text{H}}}}{\sqrt{K_5 K_6}} + \frac{p_{\text{H}}}{K_4} \right)^2} \quad (\text{a2})$$

$$r_{\text{H}}^0 = \frac{k_1 K_1 K_2 \sqrt{K_5 K_6} C_{\text{tL}}^2 \left( p_{\text{B}} - \frac{p_{\text{H}} p_{\text{D}}}{K} \right)}{\sqrt{p_{\text{H}}} \left( 1 + K_1 p_{\text{B}} + K_1 K_2 \sqrt{K_5 K_6} \frac{p_{\text{B}}}{\sqrt{p_{\text{H}}}} + \frac{p_{\text{D}}}{K_4} + \frac{\sqrt{p_{\text{H}}}}{\sqrt{K_5 K_6}} + \frac{p_{\text{H}}}{K_6} \right)^2} \quad (\text{a3})$$

$$r_{\text{H}}^0 = \frac{k_1 K_1 K_2 K_3 K_5 K_6 C_{\text{tL}} \left( p_{\text{B}} - \frac{p_{\text{A}} p_{\text{D}}}{K} \right)}{\left( p_{\text{A}} + K_1 p_{\text{B}} p_{\text{H}} + K_1 K_2 \sqrt{K_5 K_6} p_{\text{B}} \sqrt{p_{\text{H}}} + K_1 K_2 K_3 K_5 K_6 p_{\text{B}} + \frac{p_{\text{H}}^{3/2}}{\sqrt{K_5 K_6}} + \frac{p_{\text{H}}^2}{K_6} \right)} \quad (\text{a4})$$

$$r_{\text{H}}^0 = \frac{k_1 C_{\text{tL}} \left( p_{\text{B}} - \frac{p_{\text{H}} p_{\text{D}}}{K} \right)}{\left( 1 + \frac{p_{\text{H}} p_{\text{D}}}{K_2 K_3 K_4 K_5} + \frac{p_{\text{D}} \sqrt{p_{\text{H}}}}{K_3 K_4 \sqrt{K_5}} + \frac{p_{\text{D}}}{K_4} + \frac{\sqrt{p_{\text{H}}}}{\sqrt{K_5}} \right)} \quad (\text{b1})$$

$$r_{\text{H}}^0 = \frac{k_1 K_1 C_{\text{tL}}^2 \left( p_{\text{B}} - \frac{p_{\text{H}} p_{\text{D}}}{K} \right)}{\left( 1 + K_{\text{B}} p_{\text{B}} + \frac{p_{\text{D}} \sqrt{p_{\text{H}}}}{K_3 K_4 \sqrt{K_5}} + \frac{p_{\text{D}}}{K_4} + \frac{\sqrt{p_{\text{H}}}}{\sqrt{K_5}} \right)^2} \quad (\text{b2})$$

$$r_{\text{H}}^0 = \frac{k_1 K_1 K_2 \sqrt{K_5} C_{\text{tL}}^2 \left( p_{\text{B}} - \frac{p_{\text{H}} p_{\text{D}}}{K} \right)}{\sqrt{p_{\text{H}}} \left( 1 + K_{\text{B}} p_{\text{B}} + \frac{p_{\text{D}}}{K_4} + \frac{\sqrt{p_{\text{H}}}}{\sqrt{K_5}} + K_1 K_2 \sqrt{K_5} \frac{p_{\text{B}}}{\sqrt{p_{\text{H}}}} \right)^2} \quad (\text{b3})$$

$$r_{\text{H}}^0 = \frac{k_1 K_1 K_2 K_3 K_5 C_{\text{tL}} \left( p_{\text{B}} - \frac{p_{\text{H}} p_{\text{D}}}{K} \right)}{\left( p_{\text{H}} + K_1 p_{\text{B}} p_{\text{H}} + K_1 K_2 K_3 K_5 p_{\text{B}} + K_1 K_2 \sqrt{K_5} p_{\text{B}} \sqrt{p_{\text{H}}} + \frac{p_{\text{H}}^{3/2}}{\sqrt{K_5}} \right)} \quad (\text{b4})$$

$$r_{\text{H}}^0 = \frac{k_1 C_{\text{tL}} \left( p_{\text{B}} - \frac{p_{\text{H}} p_{\text{D}}}{K} \right)}{\left( 1 + \frac{p_{\text{D}} p_{\text{H}}}{K_2 K_3 K_4} + \frac{p_{\text{D}}}{K_3} + \frac{p_{\text{H}}}{K_4} \right)} \quad (\text{c1})$$

$$r_{\text{H}}^0 = \frac{k_1 K_1 C_{\text{tL}}^2 \left( p_{\text{B}} - \frac{p_{\text{H}} p_{\text{D}}}{K} \right)}{\left( 1 + K_1 p_{\text{B}} + \frac{p_{\text{D}}}{K_3} + \frac{p_{\text{H}}}{K_4} \right)^2} \quad (\text{c2})$$

Table 3.3b Continued

$$r_H^0 = \frac{k_1 K_1 K_2 K_4 C_{tL} \left( p_B - \frac{p_H p_D}{K} \right)}{\left( p_H + K_1 p_B p_H + K_1 K_2 K_4 p_B + \frac{p_H^2}{K_4} \right)} \quad (c3)$$

$$r_H^0 = \frac{k_1 C_{tL} \left( p_B - \frac{p_H p_D}{K} \right)}{\left( 1 + \frac{p_B p_D}{K_1 K_3 K_4 K_5} + \frac{p_D}{K_3} + \frac{\sqrt{p_H}}{\sqrt{K_4 K_5}} + \frac{p_H}{K_5} \right)} \quad (d1)$$

$$r_H^0 = \frac{k_1 K_1 C_{tL}^2 \left( p_B - \frac{p_H p_D}{K} \right)}{\left( 1 + K_1 p_B + \frac{p_D}{K_3} + \frac{\sqrt{p_H}}{\sqrt{K_4 K_5}} + \frac{p_H}{K_5} \right)^2} \quad (d2)$$

$$r_H^0 = \frac{k_1 C_{tL} \left( p_B - \frac{p_H p_D}{K} \right)}{\left( 1 + \frac{p_H p_D}{K_1 K_3 K_4} + \frac{p_D}{K_3} + \frac{\sqrt{p_H}}{\sqrt{K_4}} \right)} \quad (e1)$$

$$r_H^0 = \frac{k_1 K_1 C_{tL}^2 \left( p_B - \frac{p_H p_D}{K} \right)}{\left( 1 + K_1 p_B + \frac{p_D}{K_3} + \frac{\sqrt{p_H}}{\sqrt{K_4}} \right)^2} \quad (e2)$$

### 3.3 Surface Reactions and Nonideal Surfaces

The development presented for rates of surface reactions has thus far involved only the theory for ideal surfaces, quite directly in the treatment of surface-reaction rate-determining steps and a little more implicitly using the chain reaction analysis. Yet we have made a special effort in the discussion of adsorption and desorption to point out that ideal surfaces are rare; in fact, when one is concerned with the applications of catalysis in reaction engineering it is probably fair to say that ideal surfaces are never involved. Nonetheless, LH rate forms or modifications of it are widely used and accepted, particularly in chemical engineering practice, for the correlation of rates of catalytic reactions. This is so even though it has been shown in many instances that the adsorption equilibrium constants appearing in the denominator of the kinetic expressions do not agree with adsorption constants obtained in adsorption experiments. There are many reasons for this, but the skeptic will note from the voluminous illustrations of Tables 3.2 and 3.3 that such equations are of a very flexible mathematical form, with separate product and summation terms in numerator and denominator, and are richly endowed with constants that become adjustable parameters when correlating rate data.<sup>5</sup>

The form of the Freundlich isotherm suggests immediately that simple, power-law forms might be applied successfully to surface reaction kinetics. Since the

<sup>5</sup> “With two adjustable parameters, I can fit an elephant. With three, a running elephant.”—Anonymous. For more detail on the art of elephant fitting, see J. Wei, *Chemtech*, 128, (February, 1975).



Freundlich isotherm pertains to a type of nonideal surface, one might argue in favor of power-law equations on the basis of the dual advantages of mathematical simplicity compared to LH equations with some relation to the theory of nonideal surfaces. To develop this point in detail, though, is at the same time both beyond the scope of this section and also telling the reader more than one needs to know anyway. Fortunately, the topic is well-treated in two contrasting papers by Weller and Boudart [S.W. Weller, *Amer. inst. Chem. Eng. J.*, 2, 59 (1956); M. Boudart, *Amer. Inst. Chem. Eng. J.*, 2, 62 (1956)], who discuss within the framework of rate data on a number of catalytic reactions the pros and cons of various forms of rate equations. The arguments are developed roughly as follows.

1. Given that rate expressions are nonunique to the kinetic sequence, and that
2. Forms which bear resemblance to LH equations may actually represent situations far from that model, then why not
3. Admit that what we have is an empirical rate equation, and
4. For purposes of design and analysis use the simplest rate equation that will adequately fit the experimental data, that is,  $r = k(P_A)^M(P_B)^n \dots$ ,
5. Keeping in mind that the representation will be valid only for a limited range of operating conditions.

In Table 3.4 is a summary of some comparisons provided by Weller on the basis of this argument. The power-law correlations generally provide an adequate representation of the rate data, although they are not (nor do they propose to be) strongly based on any fundamental consideration of nonideal surfaces. In fact, the adequacy of both power-law and LH equations can be explained, in part, by the fact that the general LH form,

$$r = \frac{aP}{1 + bP}$$

can be approximated by the general power-law form,

$$r = cP^n$$

In addition to the skeptic's view of LH correlations, however, there must be additional reasons why this model has been used successfully for the correlation of kinetics in so many different types of catalytic reactions. Two factors seem to be most important. First is the fact that the expressions are fairly insensitive to the precise sort of kinetic scheme involved. Many widely differing types of reaction sequences can be shown to give approximate LH forms, as given in Tables 3.2 and 3.3 [see also a further good example based on the ammonia synthesis reaction by G. Buzzi Ferraris, G. Donati, F. Rejna and S. Carrà, *Chem. Eng. Sci.*, 29, 1621 (1974)]. Second is the fact that for reasonable assumptions concerning the nature of typical nonuniform surfaces it can be shown that they tend to look like uniform surfaces in overall behavior. This second point can be illustrated by an example scheme in which the heat of formation of surface complexes is a linear function of surface coverage. Consider the two-step sequence

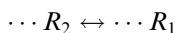
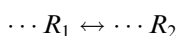


**Table 3.4** Comparison of Power-Law and Langmuir-Hinshelwood Rate Equations

I. SO <sub>2</sub> Oxidation <sup>a</sup>	
LH Form:	Power-Law Form:
$r = \frac{k(P_{\text{SO}_2} P_{\text{O}_2}^{1/2} - P_{\text{SO}_3}/K)}{[1 + (K_{\text{O}_2} P_{\text{O}_2})^{1/2} + K_{\text{SO}_2} P_{\text{SO}_2}]^2}$	$r = k[P_{\text{SO}_2} P_{\text{SO}_3}^{-1/2} - P_{\text{SO}_2}^{-1/2} P_{\text{O}_2}^{1/2}/K]$
% deviation = 15.4 (average of 12 experiments on variation of $P_{\text{SO}_2}$ and $P_{\text{SO}_2}$ )	% deviation = 13.3 (average of 12 experiments on variation of $P_{\text{SO}_2}$ and $P_{\text{SO}_3}$ )
II. Hydrogenation of Codimer <sup>b</sup>	
LH Form:	Power-Law Form:
$r = \frac{kP_{\text{H}}P_{\text{U}}}{(1 + K_{\text{H}}P_{\text{H}} + K_{\text{U}}P_{\text{U}} + K_{\text{S}}P_{\text{S}})^2}$	$r = kP_{\text{U}}^{1/2}P_{\text{H}}^{1/2}$
H = hydrogen\deg U = codimer S = product	
% Deviation	% Deviation
20.9 (200°C)	19.6 (200°C)
19.6 (275°C)	32.9 (275°C)
19.4 (325°C)	21.4 (325°C)
III. Phosgene Synthesis <sup>c</sup>	
LH Form:	Power-Law Form:
$r = \frac{kK_{\text{CO}}K_{\text{Cl}_2}P_{\text{CO}}P_{\text{Cl}_2}}{(1 + K_{\text{Cl}_2}P_{\text{Cl}_2} + K_{\text{COCl}_2}P_{\text{COCl}_2})^2}$	$r = kP_{\text{CO}}P_{\text{Cl}_2}^{1/2}$
% Deviation	% Deviation
3.4 (30.6°C)	13.0 (30.6°C)
5.6 (42.7°C)	9.1 (42.7°C)
2.6 (52.5°C)	13.9 (52.5°C)
7.0 (64.0°C)	3.0 (64.0°C)

<sup>a</sup> References: W.K. Lewis and E.D. Ries, *Ind. Eng. Chem.*, 19, 830 (1927); O.A. Uyehara and K.M. Watson, *Ind. Eng. Chem.*, 35, 541 (1943).

<sup>b</sup> References: J.L. Tschernitz, S. Bornstein, R.B. Beckmann, and O.A. Hougen, *Trans. Amer. Inst. Chem. Eng.*, 42, 883 (1946).

<sup>c</sup> Reference: C. Potter and S. Baron, *Chem. Eng. Progr.*, 47, 473 (1951).  
Source: From S.W. Weller, *Amer. Inst. Chem. Eng.*, 2, 59 (1956).

The normal result corresponding to an ideal surface is

$$r = \frac{n_s(r_1 r_2 - r_{-1} r_{-2})}{(r_1 + r_{-1} + r_2 + r_{-2})} \quad (3-68)$$

where  $r_1, r_2 \dots$  are rate factors that contain all quantities except the active center concentrations (see reaction scheme IX in Chapter 1). The derivation of this

equation has been described by Christiansen [J.A. Christiansen, *Adv. Catal.*, 5, 311 (1953)]. The corresponding result for a nonideal surface with linear variation of heats of chemisorption is

$$r = \frac{\alpha n_s (r_1 r_2 - r_{-1} r_{-2})}{(r_1 + r_2 + r_{-1} + r_{-2})^\beta} \quad (3-69)$$

The slight differences in these two forms due to the exponent in the denominator of equation (3-69) would, in practice, not strongly affect the results of an overall correlation of rates, so the comparison suggests that ignoring the nonideality of the surface still leads to rate forms that are qualitatively correct.



HORATIO SAYS

Is this an elephant?

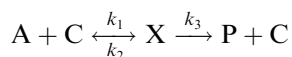


### 3.4 Enzyme and Microbial Kinetics

An important class of surface reactions that needs to be considered is that involving enzymes. These materials are macromolecules composed largely or entirely of protein, and act as biological catalysts by increasing the rate of individual highly specific reactions. “Selectivity” is a very important term in enzyme kinetics because in many cases a given enzyme is specifically related to only one (or one class of) reaction. They are also extraordinarily active, yielding rates on the order of  $10^{10}$  to  $10^{19}$  times those of the corresponding noncatalyzed reactions [for an overview see W.P. Jencks, *Catalysis in Chemistry and Enzymology*, McGraw-Hill Book Co., New York, NY (1969)].

It should be recognized that the analysis of enzyme kinetics grew up in a related but different branch of science—largely biological—than the surface reaction kinetics we have been discussing, which comes largely from physical chemistry. As a result, one will see that the results are strikingly similar to many of those already seen, but the names and nomenclature are completely different.

A very simple enzymatic sequence can be represented by



where A is the reactant (“substrate” in the enzymatic vocabulary), C is the catalyst (the enzyme), and X is some intermediate species bound to a finite amount of the catalyst. We mentioned above the high activities typical of enzymatic catalysis, so within this context the decomposition of X should be rapid and we can think immediately of analysis of the kinetics via the pssh. First, define a total enzyme

concentration as that of the free enzyme,  $C$ , plus that associated with the intermediate,  $X$ .

$$C_t = C + X$$

and for  $X$

$$\frac{dX}{dt} = 0 = k_1 AC - (k_2 + k_3)X \quad (3-70)$$

Combination of the two equations gives

$$X = \frac{k_1 AC_t}{k_1 A + k_2 + k_3} \quad (3-71)$$

The overall rate of reaction is

$$r = -\frac{dA}{dt} = k_3 X$$

Thus we end up quickly with a familiar-looking form for the rate equation

$$r = \frac{(k_3 C_t) A}{[(k_2 + k_3)/k_1] + A} \quad (3-72)$$

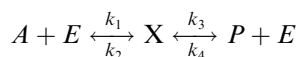
In the form, and with the nomenclature most often used in the biochemical literature, this is

$$r = \frac{VA}{K + A} \quad (3-73)$$

where  $V = k_3 C_t$  and  $K = (k_2 + k_3)/k_1$ . This particular form of equation is called the *Michaelis-Menton* equation [L. Michaelis and M.L. Menton, *Biochem. Z.*, 49, 333 (1913)]. Here  $V$  has the interpretation as the maximum rate (when  $A \gg K$ ), and  $K$  is known as the Michaelis constant. Note that  $K$  is numerically equal to  $A$  when the rate is at one-half the maximum value.

### Illustration 3.3

The procedure used in deriving the Michaelis-Menton equation is readily generalized. Equation (3-73) supposes that the decomposition of complex  $X$  is reversible, but suppose that it is not; that is



where  $E$  represents the free enzyme. What are the equations corresponding to equation (3-73), and what is the significance of the associated constants?

#### Solution

The pssh for  $X$  yields

$$(k_1 A + k_4 P)E - (k_2 + k_3) = 0 \quad (i)$$

and the enzyme balance is

$$E + X = E_t \quad (ii)$$

so that

$$X = \frac{(k_1 A + k_4 P) E_t}{(k_1 A + k_4 P + k_2 + k_3)} \quad (\text{iii})$$

$$E = \frac{(k_2 + k_3) E_t}{(k_1 A + k_4 P + k_2 + k_3)} \quad (\text{iv})$$

The rate in terms of product formation,  $(dP/dt)$ , is

$$r = \frac{(k_1 k_3 A - k_2 k_4 P) E_t}{(k_2 + k_3 + k_1 A + k_4 P)} \quad (\text{v})$$

It is apparent that we must define more than one Michaelis constant, and more than one value of  $V$ . Considering only the forward rate ( $P = 0$ ),

$$r = \frac{(k_3 E_t) A}{[(k_2 + k_3)/k_1 + A]} \quad (\text{vi})$$

where we now will define  $V_1 = k_3 E_t$  and  $K_a = (k_2 + k_3)/k_1$ . Similarly for the reverse reaction ( $A = 0$ ),  $V_2 = k_2 E_t$  and  $K_p = (k_2 + k_3)/k_4$ . The kinetic constants in terms of these values are

$$k_2 = \frac{V_2}{E_t}; \quad k_3 = \frac{V_1}{E_t}$$

$$k_1 = \frac{V_1 + V_2}{K_a E_t}; \quad k_4 = \frac{V_1 + V_2}{K_p E_t}$$

It is clear that there is a rather complex relationship between the kinetic constants on the one hand and the  $K$ s and  $V$ s on the other. For a generalization of this approach, see the paper by Cleland [W.W. Cleland, *Biochim. Biophys. Acta*, 67, 104 (1963)].



HORATIO SAYS

What would be the form of the rate equation (appearance of final product) in a system of two reactions each catalyzed by a different enzyme and where the product of the first reaction is the substrate for the second with all steps reversible?

One can probably guess that in relation to reality, the reaction examples of the illustration or of equation (3-73) are much simplified. Many enzymes of known function catalyze reactions involving more than one substrate. The mechanisms can be quite complex, however, the rate laws do generally follow the form of equation (3-73) if the composition of only one substrate is varied at one time. A good discussion of such multisubstrate enzyme-catalyzed reactions is given by Plowman [K.M. Plowman, *Enzyme Kinetics*, McGraw-Hill Book Co., New York, NY, (1972)]. There is a strong family resemblance between these enzymatic sequences and those encountered in the detailed collision theory of Benson and Axworthy in Chapter 1.

Somewhat similar to enzyme kinetics, but definitely not the same, is the area of microbial kinetics. Here one is concerned with “reactions” between entities that may not be of the same level of organization (i.e., not atom-atom, atom-molecule, etc.). Indeed, microbial kinetics is more concerned with interactions between populations of living organisms, and some of the problems seem more akin to population dynamics than to chemical kinetics. In fact, in much of the discussion below we are concerned with population-changing processes. First, we need to define a few terms.

1. *Growth*      Production of a new biomaterial by a population when it absorbs living or nonliving material and converts part of it into its own substance.
2. *Reproduction*      Production of new individual organisms of a population.
3. *Maintenance*      Consumption of energy-yielding materials by a population for purposes other than growth or reproduction.
4. *Death*      Loss of the ability to reproduce when placed in a favorable environment.
5. *Biomass concentration, c*      Amount of biomass per unit volume of culture (abiotic liquid plus biomass).
6. *Population density,  $\mu$*       Number of individuals in a population per unit volume of culture.
7. *Specific growth rate,  $\mu$*       Growth rate divided by biomass concentration.
8. *Specific reproduction rate,  $\nu$*       Reproduction rate divided by the population density.

A primary interest is to determine and to model the specific growth rate of a population that consumes a single (“rate-limiting”) substrate. The starting point for most treatments of microbial growth is based on a model suggested by Monod [J. Monod, *Ann. Rev. Microbiol.*, 3, (1949)]. It is essentially a restatement of the Michaelis-Menton equation.

$$\mu = \frac{\mu_m s}{K_s + s} \quad (3-74)$$

where  $s$  is the substrate concentration,  $\mu_m$  the maximum specific growth rate, and  $K_s$ , the Michaelis constant associated with the substrate. Further, there will be a relationship between this specific growth rate and the rate of consumption of the substrate defined by a yield coefficient,  $Y$ , such that

$$\frac{dc}{dt} = -Y \frac{ds}{dt} = \frac{\mu_m cs}{K_s + s} \quad (3-75)$$

Monod showed that a large number of bacterial growth systems could be described by this pair of equations so long as there was a single rate-limiting substrate. It will be seen later that these forms have large implications on reactor dynamics.

Work concerned with other aspects of biomass conversion normally start with equations (3-74) and (3-75). For example, a number of models for maintenance have been proposed. [(D. Herbert, *Proc. Symp. Continuous Cultivation of Micro-organisms*, (I. Malek, ed.), Czech. Academy of Sciences, Prague, (1958)] suggested that the source of energy for maintenance was oxidation of the cell

substance itself, so

$$\frac{dc}{dt} = \frac{\mu_m cs}{K_s + s} - \mu_c c \quad (3-76)$$

$$\frac{ds}{dt} = -\left(\frac{1}{Y}\right) \frac{\mu_m cs}{K_s + s} \quad (3-77)$$

where  $\mu_c c$  is the maintenance term. An alternative model [A.G. Marr, E.H. Nilson and B.J. Clark, *Ann. N.Y. Acad. Sci.*, 102, 536 (1963)] proposes that the energy for maintenance comes directly from the substrate that supports growth, thus

$$\frac{dc}{dt} = \frac{\mu_m cs}{K_s + s} \quad (3-75)$$

$$\frac{ds}{dt} = -\left(\frac{1}{Y}\right) \frac{\mu_m cs}{K_s + s} - \mu'_c c \quad (3-78)$$

where  $\mu'_c$  is the substrate-related maintenance term. Both the models of Herbert and Marr et al. have been used with apparent success in correlation of maintenance in biomass growth.

A final point of importance here is the production of substances other than biomass, since microbial growth processes are used to produce a number of products such as alcohols, antibiotics, vitamins, and so on. A typical model is that of Luedeking and Piret [R. Luedeking and E.L. Piret, *J. Biochem. Microbiol. Tech. Eng.*, 1, 393 (1959)]. Here

$$\frac{dc}{dt} = \frac{\mu_m cs}{K_s + s} \quad (3-75)$$

$$\frac{ds}{dt} = -\left(\frac{1}{Y}\right) \frac{\mu_m cs}{K_s + s} \quad (3-77)$$

$$\frac{dp}{dt} = \frac{\alpha \mu_m cs}{K_s + s} + \beta c \quad (3-79)$$

where  $p$  is the product of interest and  $\alpha$  and  $\beta$  are constants at constant temperature and pH. The first term in equation (3-79) is said to be “growth-associated” product formation, and the second “nongrowth associated”. Note that this model does not include any term for maintenance.

Another important factor often associated with product formation is the inhibition of growth by the product. This is prominent in one of the most important processes, alcohol formation via fermentation of sugar by yeast. Here the anaerobic growth of brewer's yeast is inhibited by alcohol. A time-tested model for this case replaces equation (3-75) with

$$\frac{dc}{dt} = \frac{\mu_m cs}{K_s + s} - kpc \quad (3-80)$$

where  $kpc$  is the inhibition term. Equation (3-77) is retained from the Luedeking-Piret model, but the non-growth-associated term is dropped from equation (3-79).

One can see throughout this section the importance of the Michaelis-Menton formulation, both for enzymatic and microbial processes. A good review is given by Fredrickson and Tsuchiya [A.G. Fredrickson and H.M. Tsuchiya, *Chemical Reactor*

*Theory*, (L. Lapidus and N.R. Amundson, eds.), p. 405, Prentice-Hall, Inc., Englewood Cliffs, NJ, (1977)].



HORATIO SAYS

What's the difference between the Michaelis constant and a typical adsorption constant appearing in the denominator of a LH rate equation?

---

### 3.5 Interpretation of the Kinetics of Reactions on Surfaces

While we have devoted considerable effort in Chapter 1 to discussion of means for the interpretation of kinetic data, surface reactions present a particular challenge. The application of statistical techniques<sup>6</sup> to interpretation of catalytic rate data has been the subject of considerable investigation over the years, but a detailed exposition of this goes beyond our present interests. For a thorough description, see Frocaent and Bischoff [G.F. Froment and K.B. Bischoff, *Chemical Reactor Analysis and Design*, 2nd ed., John Wiley and Sons, New York, NY, (1990)]. What we will do next is a little more intuitive.

The fundamental problems in the interpretation of heterogeneous rate data are the same as for homogeneous reactions: selecting the rate form that best correlates the measured information and determining the values of the associated constants. Therefore, much of the general philosophy remains the same. Special difficulties arise because of the more cumbersome form of potential rate equations for surface reactions (assuming now that we are dealing with general LH or related forms and not power-law forms), in evaluation of the relative degree of correlation provided by rival models (discrimination), and in evaluation of the multiple parameters that may be involved from a limited amount of experimental information (estimation). The design of experiments to measure the kinetics of reactions on surfaces is, as a result, much more of an individual affair, differing from one system to another and depending in large measure on what the investigator knows or suspects about the nature of the reaction from other sources or from preliminary experiments. By way of contrast to the interpretation of homogeneous kinetics, there are, for example, no conveniently applicable general procedures for testing reaction order or for the use of reaction equilibrium information in the determination of kinetic constants.

From the typical forms illustrated in Table 3.2 it can be seen that a number of different relationships are indicated between the partial pressure of various reactants and products and the rate of reaction. As a result, pressure or concentration is an important variable in experimentation on the kinetics of surface reactions. Conversely, the constants appearing in these equations are all strong functions of

---

<sup>6</sup>“Everything that deceives may be said to enchant.”—*Plato*



temperature, and their appearance in both products and ratios makes interpretation of the temperature dependence of rate in terms of individual constants a sometimes troublesome problem. Related to the use of pressure or concentration as an experimental variable is the use of conversion level as a means for separately determining reactant and product adsorption effects on rate. In particular, the use of initial rate experiments is a convenient method to use when starting a study of the kinetics of a given surface reaction.

To illustrate the use of initial rate data, consider the bimolecular reaction  $A + B \leftrightarrow C + D$ . The rate equation for a rate-limiting surface reaction in the sequence is

$$-r_A = \frac{k'_{S1}K_AK_BP_AP_B - k'_{S2}K_CK_DP_CP_D}{(1 + K_AP_A + K_BP_B + K_CP_C + K_DP_D)^2} \quad (3-81)$$

Under initial rate conditions there are no products present and  $P_C = P_D \approx 0$ . Equation (3-81) becomes

$$(-r_A)_0 = \frac{k'_{S1}K_AK_BP_AP_B}{(1 + K_AP_A + K_BP_B)^2}$$

where  $(-r_A)_0$  is the initial rate of reaction of A.

Now let us consider a particular type of initial rate experiment, one in which  $P_A = P_B = (1/2)P_T$ . The initial rate becomes

$$(-r_A)_0 = \frac{k'_{S1}K_AK_B(P_T)^2}{4[1 + 0.5(K_A + K_B)P_T]^2} \quad (3-82)$$

Writing equation (3-82) in terms of the combined constants  $a$  and  $b$ :

$$(-r_A)_0 = \frac{a(P_T)^2}{(1 + bP_T)^2} \quad (3-83)$$

where  $a = k'_{S1}K_AK_B/4$  and  $b = 0.5(K_A + K_B)$ .

Similar derivations using the Hougen and Watson procedure give, for the adsorption of A rate-controlling,

$$(-r_A)_0 = \frac{a'P_T}{(1 + b'P_T)} \quad (3-84)$$

or for an Eley-Rideal mechanism with one of the reactants not adsorbed [reaction (6), Table 3.2],

$$(-r_A)_0 = \frac{a''(P_T)^2}{(1 + b''P_T)} \quad (3-85)$$

where  $a' \cdots b''$  are combined constants similar to  $a$  and  $b$ .

There is quite a different dependence of initial rate on total pressure according to the three equations above, the general form of which is shown in Figure 3.10. Curves of this type for a number of reaction schemes with various rate controlling steps have been given in many sources, following Hougen [O.A. Hougen, *Reaction Kinetics in Chemical Engineering*, Chem. Eng. Prog. Monograph Ser., 1, (1951)]. Many authors include, in addition to the above, an expression for the initial rate corresponding to a product-desorption controlling step. The result gives  $(-r_A)_0$

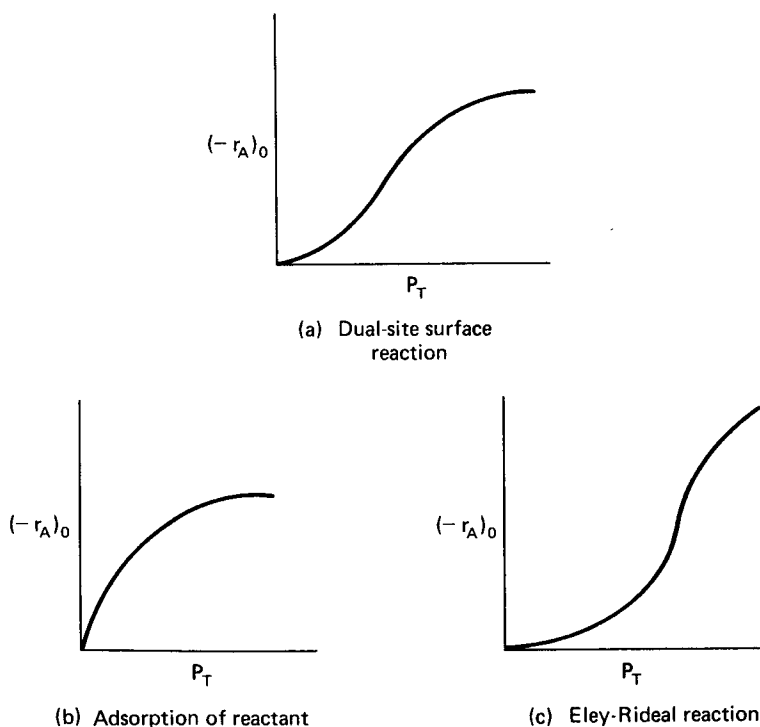


**Figure 3.10** Comparison of initial rate dependence on total pressure for various controlling steps in the reaction  $A + B \leftrightarrow C + D$ .

independent of  $P_T$ , which seems intuitively correct. The interpretation of initial rate data in terms of a product step, however, seems a contradiction, and it is best to study product steps with specific experiments involving variation of conversion level or with product added to the reactant.

It can be seen that such initial rate experiments are useful for screening purposes in rejection of obviously inappropriate rate forms. Not much more than this can be expected realistically, however, since the difference in the shape of the curves among the various cases is sometimes rather subtle granted the experimental range of  $P_T$  and the precision of the measured rate data. Distinguishing between cases (a) and (c) in Figure 3.10, for example, depends on being able to distinguish between a rate proportional to  $P_T$  at high values of  $P_T$ , and a rate approaching zero-order in  $P_T$  in this region. Distinguishing between (a) and (b) depends on being able to define experimentally the presence or absence of the characteristic inflection of (a).

In biochemical reactions rate dependencies of the form of Figure 3.10b are often encountered. These are normally interpreted by the Michaelis-Menton correlation, using a linearization procedure. Here, equation (3-73) is rewritten as

$$\frac{1}{r} = \frac{K}{V} \left( \frac{1}{A} \right) + \frac{1}{V} \quad (3-86)$$

which is now linear in  $(1/r)$  versus  $(1/A)$ . Typical data of this form are shown in Figure 3.11, and the linear plot resulting is shown in Figure 3.12. This type of plot is

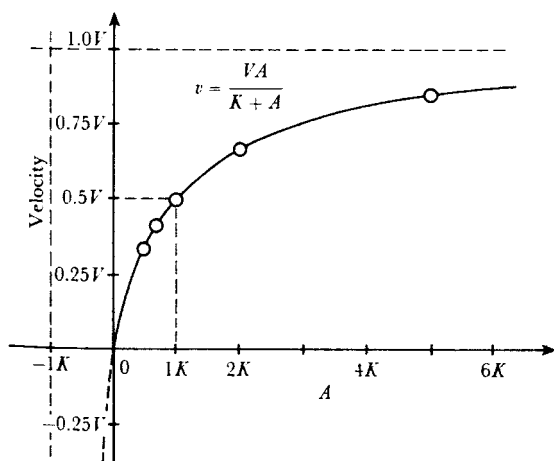


**Figure 3.11** Typical form of Michaelis-Menten kinetic results.

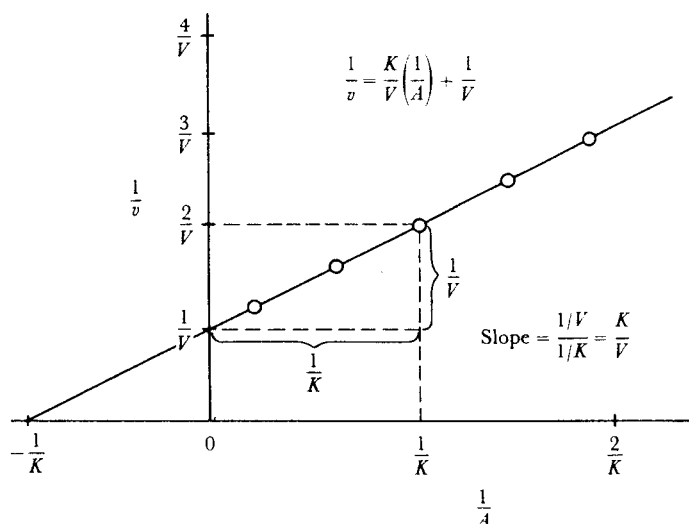


**Figure 3.12** Lineweaver-Burke plot corresponding to Figure 3-11. [From K.M. Plowman, *Enzyme Kinetics*, with permission of McGraw-Hill Book Co., New York, NY (1972).]

commonly known as a Lineweaver-Burke, or reciprocal plot [H. Lineweaver and D. Burke, *J. Amer. Chem. Soc.*, 58, 658 (1934)]. In such a plot the slope is  $(K/V)$  and the ordinate intercept is  $(1/V)$ , with the abscissa intercept at  $(-1/K)$ . In this interpretation  $K$  must have the same units of concentration as  $A$ .

From the results of such rate experiments (either chemical or biochemical) and preliminary interpretation, one hopefully will have gained sufficient insight into the reaction system to permit intelligent planning of further experiments from which the best values of the constants of correlating equations (or rival correlating equations) can be obtained. The same sort of overall comparison of the individual equations based on goodness of fit to the experimental data (and chemical reasonableness), can

be used as a final choice. It should *always* be kept in mind that any such model, regardless of how good it is, is an interpolation model that is valid only for the range of experimental results from which it was determined. Extrapolation should not be attempted without adult supervision.

There are any number of different means for evaluating constants corresponding to best-fit models and for comparing goodness of fit, and even for using ongoing parameter estimation for the design of future experiments. Books have been written on this topic. These approaches generally involve nonlinear methods, and a good example is provided by the work of Dumez and Froment cited earlier. Approaches using linear least-squares fitting, however, are also useful for parameter evaluation and comparative fit, at least as a first estimate, and are convenient to use. By now there are dozens of linear least-square software programs available, and sometimes it is all too easy to plug in the numbers without a good appreciation of what is going on. Let's take a moment then, to go through some of the innards of least-squares fitting of one of these rate equations.

### Illustration 3.4

Develop a procedure using linear least-squares for estimating the parameters of the initial-rate form of equation (3-57).

#### Solution

We may first write this in a form convenient for parameter estimation by rearranging to

$$y = \sqrt{\frac{P_A P_B}{(r_A)_0}} = \frac{1 + K_A P_A + K_B P_B}{(k'_{S1} K_A K_B)^{1/2}} = C_1 + C_2 P_A + C_3 P_B \quad (\text{i})$$

$$C_1 = (k'_{S1} K_A K_B)^{-1/2}; \quad C_2 = (K_A / k'_{S1} K_B)^{1/2}; \quad C_3 = (K_B / k'_{S1} K_A)^{1/2}$$

If we have  $n$  measurements of  $y$  for various conditions of  $P_A$  and  $P_B$  equation (i) becomes the set

$$\begin{aligned} y_1 &= C_1 + C_2(P_A)_1 + C_3(P_B)_1 \\ y_2 &= C_1 + C_2(P_A)_2 + C_3(P_B)_2 \\ &\vdots \\ y_n &= C_1 + C_2(P_A)_n + C_3(P_B)_n \end{aligned} \quad (\text{ii})$$

and by least squares we wish to find the values of the constants  $C_1$ ,  $C_2$ , and  $C_3$  which minimizes the sum of squares of residuals  $v_1, v_2, \dots, v_n$  expressing the difference between the observed values  $y_1, y_2, \dots, y_n$  and what would be calculated from the estimate, which is the RHS of equation (i). This gives us another set of relationships that may be written as

$$\begin{aligned} v_1 &= C_1 + C_2(P_A)_1 + C_3(P_B)_1 - y_1 \\ v_2 &= C_1 + C_2(P_A)_2 + C_3(P_B)_2 - y_2 \\ &\vdots \\ v_n &= C_1 + C_2(P_A)_n + C_3(P_B)_n - y_n \end{aligned} \quad (\text{iii})$$

The condition for minimization is

$$\frac{\partial \left( \sum_{i=1}^n v_i^2 \right)}{\partial C_1} = \frac{\partial \left( \sum_{i=1}^n v_i^2 \right)}{\partial C_2} = \frac{\partial \left( \sum_{i=1}^n v_i^2 \right)}{\partial C_3} = 0 \quad (\text{iv})$$

yielding the following equations, called the *normal* equations for the set:

$$\begin{aligned} C_1 n + C_2 \sum_{i=1}^n (P_A)_i + C_3 \sum_{i=1}^n (P_B)_i - \sum_{i=1}^n y_i &= 0 \\ C_1 \sum_{i=1}^n (P_A)_i + C_2 \sum_{i=1}^n (P_A)_i^2 + C_3 \sum_{i=1}^n (P_A)_i (P_B)_i - \sum_{i=1}^n (P_A)_i y_i &= 0 \\ C_1 \sum_{i=1}^n (P_B)_i + C_2 \sum_{i=1}^n (P_A)_i (P_B)_i + C_3 \sum_{i=1}^n (P_B)_i^2 - \sum_{i=1}^n (P_B)_i y_i &= 0 \end{aligned} \quad (\text{v})$$

In the equations (v), the only unknowns are the constants, which can be evaluated by any convenient method for solving simultaneous linear algebraic equations. Individual values for  $k'_{s1}$ ,  $K_A$  can  $K$  can then be computed. An obvious method for comparing the fit afforded a given set of data by various rate forms is then to use the least-squares constants so determined to calculate the sum of squares residuals corresponding to the different forms and to compare their magnitudes.

For a given rate expression the choice of a form of equation for least-squares evaluation, such as equation (i), is largely a matter of convenience. For example, we could have chosen  $y = [1/(r_A)_0]^{1/2}$ , which would give an entirely different expression for the sum of squares of residual minimization. The constants so evaluated would not be the same as those from equation (i). Another important point to remember is that since we have not worked with the residuals of the rate directly but with some function of the rate, the least-squares constants so determined do not in general correspond to the best fit of the rate itself. These comments apply also to the Lineweaver-Hurke analysis in biochemical kinetics, since the original rate equation is transformed into a linear expression, equation (3-86).

There have been many suggestions made concerning methods by which the meaningfulness of the constants determined in an LH interpretation of rates can be evaluated. Certainly, negative values for any of the constants cast doubt on the validity of the rate equation being examined, although in such an event one must be sure that the negative value is not an artifact created by a fit to experimental data with considerable scatter. This can happen particularly in the evaluation of adsorption constants contained in the denominator of the rate equation when the species in question is not strongly adsorbed and the true value of the constant is small.

A very useful method for determining the reasonableness of constants estimated by LH analysis has been advanced by Boudart et al. [M. Boudart, D.E. Mears and M.A. Vannice, *Ind. Chim. Belge*, 32, 281 (1967)]. The method is based on the compensation effect, often noted in the kinetics of catalytic reactions on a series of related catalysts, in which there is observed a linear relationship between the logarithm of the pre-exponential factor of the rate equation and the activation energy. Explanations for such behavior abound. Perhaps the most reasonable is

that in many cases an increase in the activation energy is accompanied by an increase in active sites [H.M.C. Sosnovsky, *J. Phys. Chem. Solids*, 10, 304 (1959); E. Cremer, *Adv. Catal.*, 7, 75 (1955)]. The effect was first noted by Constable [F.H. Constable, *Proc. Roy. Soc. (London)*, A108, 355 (1925)] for ethanol dehydration on a series of copper catalysts reduced at different temperatures. This correlation is shown in Figure 3.13.

Compensation effects have been reported for the rates of a large number of catalytic reactions and adsorption-desorption processes. Our present interests focus in particular on the study of such effects in physical adsorption equilibria by Everett [D.H. Everett, *Trans. Faraday Soc.*, 46, 942 (1950)], who reported a linear relationship between the entropy and enthalpy changes on adsorption. Thus,

$$(\Delta S_a)^\circ = m(\Delta H_a)^\circ + b \quad (3-87)$$

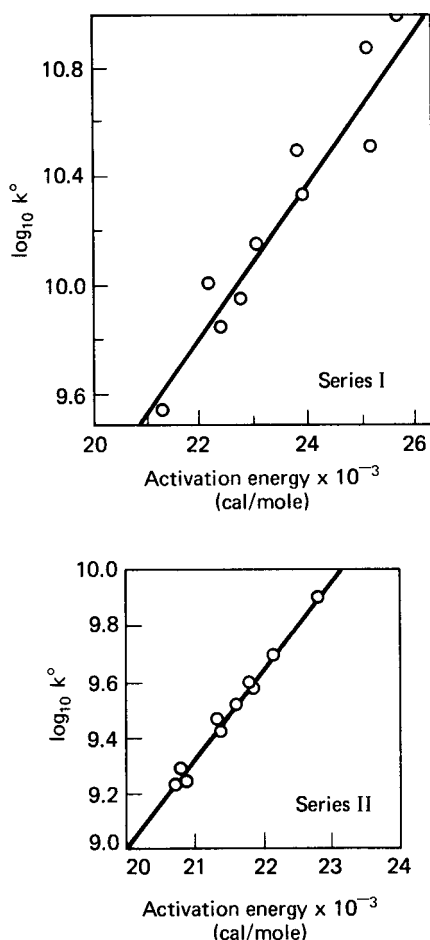


**Figure 3.13** Data of Constable for compensation in ethanol dehydration on Cu reduced at different temperatures. [After F.H. Constable, *Proc. Roy. Soc. (London)*, A108, 355, with permission of The Royal Society, (1925).]

where  $(\Delta S_a)^\circ$  is the entropy change on adsorption, most conveniently referred to a standard state of 1 atm at the temperature of adsorption, and  $(\Delta H_a)^\circ$  the corresponding enthalpy change. From experimental data on the physical adsorption of a large number of gases at less than monolayer coverage on charcoal, Everett obtained the correlation

$$(\Delta S_a)^\circ = 0.0014(\Delta H_a)^\circ - 12.2 \quad (3-87a)$$

for units of cal, g-mol, and  $^\circ\text{K}$ . Following these ideas, Boudart et al. reported the results of a  $(\Delta S_a)^\circ - (\Delta H_a)^\circ$  analysis based on a large number of chemisorbed systems, using adsorption constant data reported from LH interpretations in the literature that were deemed to be reasonable results. Writing these equilibrium constants in thermodynamic terminology

$$K = e^{(\Delta S_a)^\circ / R} e^{-(\Delta H_a)^\circ / RT} \quad (3-88)$$

we have an expression that permits calculation of  $(\Delta S_a)^\circ$  from experimental information on  $K$  and values of  $-(\Delta H)^\circ$ , which may be determined for the particular chemisorption involved. The results of this analysis, in comparison with Everett's correlation, are shown in Figure 3.14. While it would appear that the chemisorption data are not linearly correlated, it seems reasonable to establish the Everett correlation as a limiting case for the entropy-enthalpy relationship, since almost all the data falls below the line. The result of Figure 3.14 thus provides some guide as to reasonable values of  $(\Delta S_a)^\circ$  in chemisorbed-reacting systems and can be used as a further test of the meaningfulness of the adsorption constants appearing in LH correlations of reaction rates, and indeed of the correlations themselves. We can, in fact, establish some rules concerning reasonable values for  $(\Delta S_a)^\circ$ . First, since the chemisorbed layer is a more ordered state than the gas phase,  $(\Delta S_a)^\circ$  should be negative. Second,

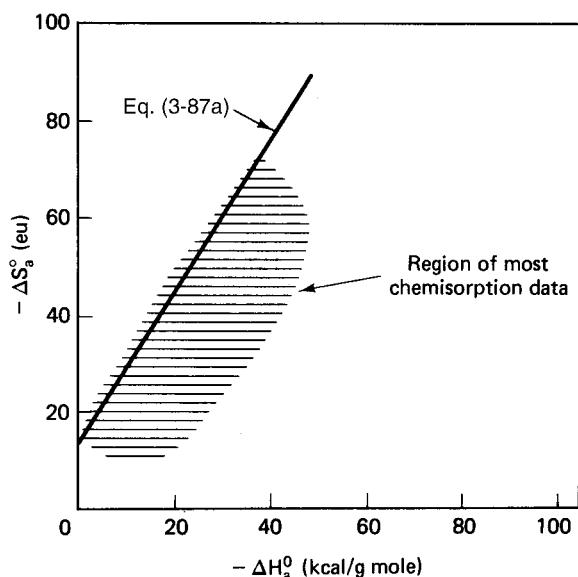


**Figure 3.14** Correlation of  $(\Delta S_{aa})^\circ$  and  $(\Delta H_{aa})^\circ$  results for chemisorption.

$(\Delta S_a)^\circ$  should be smaller than the standard-state entropy of the gas phase,  $(\Delta S_g)^\circ$ , since the entropy change on adsorption cannot be larger than the entropy of the nonadsorbed state. These two rules are rather obvious ones, which can be termed “strong rules.” A “weak rule,” based on the calculation

$$(\Delta S_a)^\circ = R \ln \left( \frac{V_g}{V_c} \right) \quad (3-89)$$

where  $V_g$  is the molar volume of gas at 1 atm and adsorption temperature and  $V_c$  the critical volume of the liquid (adsorbed state), states that  $(\Delta S_a)^\circ$  should be of the order of  $-10$  eu.

### Illustration 3.5

The dehydrogenation of methylcyclohexane to toluene was studied by Sinfelt et al. [J.H. Sinfelt, H. Hurwitz and R.A. Shulman, *J. Phys. Chem.*, **64**, 1559 (1960)], over a 0.3% Pt on  $\text{Al}_2\text{O}_3$  catalyst. The temperature range from 315 to 372°C was investigated, with methylcyclohexane partial pressures varying from 1.1 to 4.1 atm. Experimental rate data were well correlated by an equation of the form

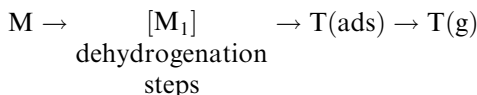
$$r = \frac{k' b P_M}{1 + b P_M}$$

where  $r$  is the rate of the dehydrogenation reaction and  $P_M$  the pressure of methylcyclohexane. The following values were obtained for the constants.

$T$ (°C)	$k'$	$b$ (atm <sup>-1</sup> )
315	0.013	27
344	0.043	11
372	0.154	3

There are difficulties in associating the rate correlation with a Langmuir-Hinshelwood mechanism, however, since the temperature dependence of the adsorption constant  $b$  corresponds to a heat of adsorption of about 30 kcal/mol, which is far too high for this reaction in light of independent information on adsorption. Further, the absence of any product adsorption term in the denominator is suspicious, since aromatics are known to be more strongly adsorbed on the catalyst than are saturated compounds.

Show that a similar form of equation may be derived assuming the reaction scheme to be



with  $k_1$  the rate constant for M to  $[\text{M}_1]$  and  $k_2$  that for T(ads) to T(g). The dehydrogenation steps are very rapid and the adsorbed toluene intermediate is at steady state. The rate of desorption of toluene is controlling. Show that the temperature dependence of the constants of the scheme above also provides a much more reasonable interpretation of the results.



*Solution*

Based on the problem statement we will assume that

1. Dehydrogenation steps are very rapid.
2. Adsorbed toluene intermediate is at steady state.
3. The rate of adsorption of toluene is slow.

Then,

$$\text{rate} = k_2 C_T(\text{ads}) \quad (\text{i})$$

and

$$\frac{dC_T(\text{ads})}{dt} = 0 = k_1 P_M \theta - k_2 C_T(\text{ads})$$

where  $\theta$  is the concentration of empty sites. Then,

$$\theta = n_s [1 - \theta_T(\text{ads})]$$

$$C_T(\text{ads}) = n_s \theta_T(\text{ads})$$

We have from (i)

$$k_1 P_M n_s [1 - \theta_T(\text{ads})] = k_2 n_s \theta_T(\text{ads}) \quad (\text{ii})$$

$$\theta_T(\text{ads}) = k_1 P_M / (k_2 + k_1 P_M) \quad (\text{iii})$$

Substituting in equation (i)

$$\begin{aligned} r &= k_2 n_s \theta_T(\text{ads}) = k_2 k_1 n_s P_M / (k_1 P_M + k_2) \\ r &= \frac{k_1 n_s P_M}{(k_1/k_2) P_M + 1} \end{aligned} \quad (\text{iv})$$

Comparison with the experimental correlation gives

$$b = (k_1/k_2) \quad \text{and} \quad k' = k_2$$

The procedure is now to evaluate  $k_2$  from data on  $k'$ , then evaluate  $k_1$  (the adsorption rate constant) and see if the heat of adsorption so derived is reasonable. As an example, take two points to evaluate  $k_2$ ;  $k' = 0.154$  and  $0.043$  at  $T = 645$  and  $617$  K, respectively. Then

$$\ln(0.154/0.043) = -(E_2/R)(645 - 617)^{-1}$$

$$E_2 = 36 \text{ kcal/mol}$$

Now we can calculate the activation energy associated with  $b$ , and from that calculate the heat of adsorption from  $k_1$ . From the results  $b = 11$  and  $3$  at  $617$  and  $645$  K, respectively. Then

$$\ln(3/11) = -(E_b/R)(645 - 617)^{-1}$$

$$E_b = -34.7 \text{ kcal/mol}$$

Since  $b = (k_1/k_2)$

$$\exp(-E_b/RT) = \exp(-E_1/RT)/\exp(-E_2/RT)$$

$$E_1 = 1.3 \text{ kcal/mol} = Q$$

This approach gives results much more in accord with the experimental data than those obtained with a standard Langmuir-Hinshelwood analysis. Note that we have invoked both a rate-controlling step and a pssh (for the adsorbed toluene) in the overall analysis. No one said they could not happen at the same time.



HORATIO SAYS

This illustration should serve as an example that, while many rate equations appear as though they have Langmuir-Hinshelwood origins, their ancestry can be quite a bit different.

### 3.6 Decline of Surface Activity: Catalyst Deactivation

One particular aspect of reactions on surfaces that is not encountered in reactions that are not catalytic is a progressive decrease in the activity of the surface with its time of utilization. The reasons for this are numerous, but we will divide them into three general categories.

1. *Poisoning*: loss of activity due to strong chemisorption of a chemical impurity on the active sites of the surface, denying their access by reactant molecules. This should not be confused with inhibition as expressed by adsorption terms in the denominator of LH rate expressions.
2. *Coking* or *fouling*: loss of activity, normally in reactions involving hydrocarbons, due to reactant or product degradation, producing a carbonaceous residue on the surface which is inactive for catalysis.
3. *Sintering*: loss of activity due to a decrease in active surface per volume of catalyst, normally the result of excessively high temperatures.

A vast effort has been expended over the years in investigation of these types of deactivation as they are encountered in catalytic reactions and catalysts of technological importance. The uninitiated are often amazed at the fact that many reaction-system process designs are dictated by the existence of catalyst deactivation, as are process operation and optimization strategies. In some cases the deactivation behavior is so pronounced as to make detailed studies of intrinsic kinetics of secondary importance.

In Table 3.5 are some examples of the three major categories of deactivation. The literature cited there generally refers to earlier work that has become definitive of the classifications used. Further detail is available in texts by Butt and Petersen [J.B. Butt and E.E. Petersen, *Activation, Deactivation and Poisoning of Catalysts*,

**Table 3.5** Some Examples of Catalyst Deactivation

Reference	System	Activity/Time	Comments
1	Poisoning of Pt by metals, S, N, hydrogenation reactions	Linear, exponential	First systematic investigation of impurity poisoning effects on noble metals
2	Poisoning of SiO <sub>2</sub> and SiO <sub>2</sub> /Al <sub>2</sub> O <sub>3</sub> by organic bases, cracking reactions	Exponential	Demonstrated acidic nature of these oxides, developed activity correlation based on poisoning behavior
3	Poisoning of different types of Al <sub>2</sub> O <sub>3</sub> with various alkali metals, isomerization and dehydration reactions	Linear, exponential	Showed specificity of poisoning behavior to both chemical nature of poison and reaction
4	Coking of metal-oxide cracking catalysts	Power law, time on stream	Developed correlation for coke on catalyst versus time of reaction
5	Coking of SiO <sub>2</sub> /Al <sub>2</sub> O <sub>3</sub> and zeolite cracking catalysts	Exponential time on stream	Deactivation and kinetic models for catalytic cracking
6	Sintering in reforming on Pt/Al <sub>2</sub> O <sub>3</sub>	Hyperbolic	Preferential deactivation of one function of a bifunctional catalyst
7	Sintering, primarily supported Pt	Many	Review paper

1, E.B. Maxted, *Advan. Catalysis*, 3, 129 (1951).

2, G.A. Mills, E.R. Boedeker, and A.G. Oblad, *J. Amer. Chem. Soc.*, 72, 1554 (1950).

3, H. Pines and W.O. Haag, *J. Amer. Chem. Soc.*, 82, 2471 (1960).

4, A. Voorhies, Jr., *Ind. Eng. Chem.*, 37, 318 (1945).

5, V.W. Weekman, Jr., *Ind. Eng. Chem. Proc. Design Devel.*, 7, 90 (1968); 8, 388 (1969); V.W. Weekman, Jr., and D.M. Nace, *Amer. Inst. Chem. Eng. J.*, 16, 397 (1970); D.M. Nace, S.E. Voltz, and V.W. Weekman, Jr., *Ind. Eng. Chem. Proc. Design Devel.*, 10, 530, 538 (1971).

6, H.J. Maat and L. Moscou, *Proc. Int. Congr. Catalysis*, 3rd, p. 1277, North-Holland, Amsterdam, 1965.

7, S.E. Wanke and P.C. Flynn, *Cat. Rev.—Sci. Engr.*, 12, 92 (1975).

Academic Press, Inc., San Diego, CA, (1989)] and by Hughes (R. Hughes, *Deactivation of Catalysts*, Academic Press, Inc., London, UK, (1984)].

Closely related to catalyst deactivation is regeneration, which generally refers to any process or procedure employed to restore a deactivated catalyst to its original (or a substantial fraction of its original) activity. In practice the term is most often used in reference to catalysts which have been deactivated by coking, where the carbonaceous deposits can be removed by oxidation (burning) under suitable conditions. This leads to some interesting problems in reactor operations, since one is literally setting a fire (hopefully controlled) in the reactor. In a similar vein, the regeneration of poisoned catalysts is often termed detoxification, and the regeneration of sintered catalysts redispersion. Regeneration via oxidation ordinarily is able to produce the recovery of a substantial portion of lost activity for coked catalysts; the success of detoxification or redispersion of poisoned or sintered catalysts is

often much more elusive and is very much dependent on the specific chemistry of the catalyst and reaction involved.

The simplest approach to a quantitative analysis of deactivation phenomena is to treat the overall reaction/catalyst/deactivation assembly in terms of reaction pathways very similar to the Type I and Type III “nearly complex” reactions of Chapter 1. If we let  $S$  be an active site on the surface, independent chemical poisoning in the simplest example can be represented by

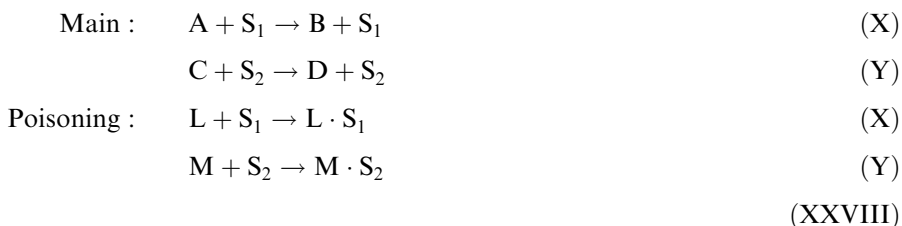


where in this case  $L$  is the poison that removes active sites from the surface via irreversible chemisorption. It can be seen that this is very similar to the Type I scheme. Networks describing deactivation via coking may be more complex than this, because in many hydrocarbon reactions both reactants and products are capable of forming the carbonaceous deposits. A simple example of this is



where  $A \cdot S$  and  $B \cdot S$  represent the deactivated surface. This is reminiscent of the Type III scheme, with  $A$  the reactant,  $B$  the intermediate desired product, and  $A \cdot S$  and  $B \cdot S$  corresponding to  $C$  of Type III. Sintering does not fall easily into either of these reaction type categories, since it is normally a thermally activated process and generally independent of reactants or products; another way to think of it is that sintering is a physical phenomenon and so is not properly described by chemical reaction networks.

There is an important variation on these mechanisms of deactivation when one is dealing with bifunctional catalysts, that is, surfaces that possess more than one type of catalytic function. (An example of this is given in the exercises for  $n$ -pentane isomerization on  $\text{Pt}/\text{Al}_2\text{O}_3$ ). Here it can be envisioned that one reaction is carried out on, say, the  $X$  function of the catalyst, and a second reaction on the  $Y$  function, and the reactions may be either independent (parallel) or sequential. Again there is a resemblance to Types I and III, but the representation is more complex. For the parallel sequence:



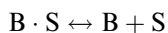
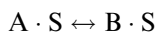
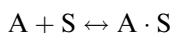
and for the series sequence:



(XXIX)

The basic importance of these schemes is that they indicate clearly how deactivation may seriously interfere with the selectivity as well as the activity of the surface. Consider (XXIX); if the *Y* function is poisoned to a greater extent than the *X* function, there will obviously come a time when product *C* is no longer observed. If the converse holds true, the reaction will eventually shut down completely, even though *Y* activity remains, since there is no *B* intermediate to react. In supported metal catalysts the metal is often preferentially deactivated by sintering over a long period and there is a gradual change in the product selectivity. Such a situation is illustrated in the work of Maat and Moscou cited in Table 3.5, and is an example of a process result ultimately being dictated by deactivation. In that work, when the product selectivity for dehydrocyclization drops below a certain level, operation must be discontinued and a fresh charge of catalyst introduced into the reactor.

Some approaches to the modeling of the kinetics of catalyst deactivation are also suggested by the results given in Table 3.5. We see there observations of the variations of catalyst activity with time, which in some cases are linear, exponential, or hyperbolic. Hopefully we remember from Chapter 1 that these types of temporal variations are the fingerprints of zero-, first-, and second-order reactions, respectively, so the suggestion is that catalyst deactivation kinetics may be represented by simple power-law forms. Now, how might this variation be incorporated into the rate law for a surface reaction? Let us reconsider the isomerization scheme of (XXV) on an ideal surface but with the surface reaction step slow and rate-controlling:



The surface sites, represented by *S*, will be considered to be at an activity level *s*, lower than that of the undeactivated surface. Indeed, we will let *s* represent a scaled activity variable, with *s* = 1 for the fresh surface and *s* = 0 for the completely deactivated surface. In this case the kinetics of the three steps of the reaction are

$$k_{dA}P_A(1 - \theta_A - \theta_B) = k_{dA}\theta_A s \quad (3-90)$$

$$(-r_s) = k'_s\theta_A s \quad (3-91)$$

$$k_{dB}\theta_B s = k_{dB}(1 - \theta_A - \theta_B)s \quad (3-92)$$

As shown before, the development of a rate equation depends on the development of an expression for  $\theta_A$ . If we follow the procedures detailed for equations (3-6) to (3-10), it is clear that the net adsorption and desorption rate constants, such as

$k_{dA}s$  and  $k_{dA}s$ , will always appear in ratio, and the activity variable  $s$  will divide out. The resulting overall rate equation then becomes

$$(-r_A) = \frac{k'_s s K_A P_A}{1 + K_A P_A + K_B P_B} \quad (3-93)$$

The effect of deactivation on the kinetics of the main reaction is thus modeled by the single activity factor which multiplies the surface reaction rate constant. The rate of deactivation, as suggested by the data of Table 3.5, would be represented in a separate rate equation with the precise form depending on the mechanism of deactivation. For example, if poisoning were the mechanism of deactivation in a scheme such as (XXVI), then

$$-\frac{ds}{dt} = (-r_d) = k_d s P_L \quad (3-94)$$

This approach is termed separable *deactivation*, since the activity factor  $s$  is carried along as separable in the formulation of equation (3-93), and was originally proposed by Szepé and Levenspiel [S. Szepé and O. Levenspiel, *Proc. European Fed., 4th Chem. Reaction Eng.*, Brussels, Pergamon Press, London, (1970)].

An alternative approach to the correlation of catalyst deactivation kinetics has been widely employed for coking mechanisms. Here the precise reactions that cause deactivation may be more complex or difficult to identify than in chemical poisoning, and one may not write such precise expressions as equation (3-94) for  $(-r_d)$ . The practice generally has been to relate activity to the time of utilization or “time-on-stream”, and a number of mathematical forms have been employed. The best known is the *Voorhies correlation* [A. Voorhies, Jr., *Ind. Eng. Chem.*, 37, 318 (1945)], which relates the weight of coke on the catalyst to a power of time on stream,

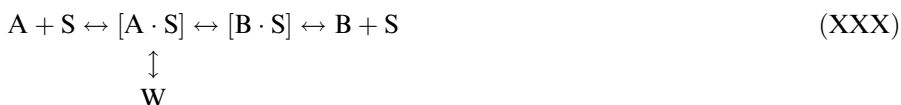
$$C_c = A(t_c)^n \quad (3-95)$$

where  $A$  and  $n$  are experimentally determined constants. Other forms that have been used are exponential and hyperbolic. It is of note that these correlations generally refer to the amount of coke,  $C_c$ , not the activity factor,  $s$ , so that it is normally necessary to develop additional information of the form

$$s = f(C_c) \quad (3-96)$$

to complete the correlation for activity.

Reaction-deactivation schemes such as (XXVII) are useful limiting cases, but such simplification may sacrifice important information. To illustrate this point, let us consider scheme (XXVII) for reactant deactivation more thoroughly. Thus



with  $k_1, k_{-1} \cdots k_3, k_{-3}$  rate constants for the three steps of the main reaction, and  $k_4, k_{-4}$  for formation of the carbonaceous residue  $W$ . As usual,  $S$  is an empty site, and the surface intermediate  $[A \cdot S]$  is the coke precursor. Following LH procedure we will postulate a rate-limiting step, in this case the conversion of adsorbed reactant to

adsorbed product. Mathematically this implies an ordering of the rate constants as

$$k_{-2} \ll k_2 \ll k_1, k_{-1}, k_3, k_{-3} \quad (3-97)$$

In many instances the rate of deactivation is small compared to the rate of reaction, which we take as the case here, so

$$k_1 < k_{-4} \ll k_2$$

If the initial concentration of active sites is  $X_0$ , then

$$X_1 + X_2 + X_3 + X_4 = X_0 \quad (3-98)$$

From the Langmuir-Hinshelwood analysis we obtain

$$(-r) = k_2 X_2 \quad (3-99)$$

$$X_2 = K_1 C_A X_1 \quad (3-100)$$

$$X_3 = K_3 C_B X_1 \quad (3-101)$$

Combining these with equation (3-98) yields

$$X_1 = \frac{X_0 - X_4}{1 + K_1 C_A + K_3 C_B} \quad (3-102)$$

Equation (3-102) has the familiar LH adsorption terms in the denominator, but differs by the appearance of  $X_4$  in the numerator. The difference  $(X_0 - X_4)$  corresponds to the undeactivated surface; accordingly equation (3-102) shows that the concentration of unoccupied sites is proportional to the number of undeactivated sites, and the reaction rate is also proportional to  $(X_0 - X_4)$ . However, we know that  $X_4$  grows with chronological time during the course of the reaction, and we are obliged to write some form of additional rate equation to express this. Following scheme (XXX),

$$\frac{dX_4}{dt} = k_4 X_2 - k_{-4} X_4 \quad (3-103)$$

Neglecting the  $k_{-4}$  term and combining equation (3-103) with equations (3-100) and (3-102)

$$\frac{dX_4}{dt} = \frac{k_4 K_1 C_A (X_0 - X_4)}{1 + K_1 C_A + K_3 C_B} \quad (3-104)$$

We can now define the activity variable  $s$  as

$$s = \frac{(X_0 - X_4)}{X_0} \quad (3-105)$$

and

$$\frac{ds}{dt} = -\left(\frac{1}{X_0}\right) \left(\frac{dX_4}{dt}\right) \quad (3-106)$$

Substituting this result into equation (3-104)

$$\frac{ds}{dt} = \frac{sk_4 K_1 C_A}{1 + K_1 C_A + K_3 C_B} = K'_s \quad (3-107)$$

Under conditions of constant temperature and reactant and product concentration this leads to the exponential decay function

$$s = \exp(-K't) \quad (3-108)$$

which might be considered a kind of cousin of the Voorhies correlation, but one which relates activity directly to time. The assumption of constant concentration implies that the activity variable, according to this view at least, is independent of conversion.

An important modification of the deactivation step of (XXX) would have that



in which the deactivation could be considered a kind of polymerization or condensation reaction. Following the analysis above we obtain

$$-\frac{ds}{dt} = k_4 X_0^2 \left( \frac{s K_1 C_A}{1 + K_1 C_A + K_3 C_B} \right)^2$$

which can be written simply as

$$-\frac{ds}{dt} = K'' s^2 \quad (3-109)$$

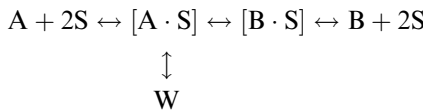
This leads to an hyperbolic form of activity variation

$$s = \frac{1}{(1 + K''t)} \quad (3-110)$$

which again assumes constant temperature and concentrations. This form of correlation has been investigated extensively by Wojciechowski [B.W. Wojciechowski, *Catal. Rev.*, 9, 79 (1974)].

### Illustration 3.6

Consider the reaction scheme



again with  $k_1, k_{-1} \cdots k_3, k_3, k_{-3}$ , the rate constants for the sequence of main reactions, and  $k_4, k_{-4}$  the constants for the formation of W.

- Derive an expression for the rate of reaction under deactivating conditions.
- Does this result correspond to the form of a separable deactivation formulation?

*Solution*

a) Assume that the rate of surface reaction is rate-determining and that deactivation is slow compared to the main reaction. We then have inequalities as shown before:

$$\begin{aligned} k_{-2} &\ll k_2 \ll k_1, k_{-1}, k_3, k_{-3} \\ k_{-4} &< k_4 \ll k_2 \end{aligned}$$

The reaction rate is

$$(-r) = k_2 X_2 \quad (i)$$



where  $X_2$  is the concentration of  $A \cdot S$ . The active site balance is as before

$$X_0 = \sum_{i=1}^4 (x_i) \quad (\text{ii})$$

From the equilibrium assumptions

$$X_2 = K_1 C_A X_1^2; \quad X_3 = K_3 C_B X_1^2 \quad (\text{iii}), (\text{iv})$$

Substituting for  $X_2$  and  $X_3$  in (ii), the site balance becomes

$$X_0 = X_1 + 2K_1 C_A X_1^2 + 2K_3 C_B X_1^2 + 2X_4 \quad (\text{v})$$

Solving for the concentration  $X_1$ ,

$$X_1 = \frac{-1 + [1 - 8(K_1 C_A + K_3 C_B)(2X_4 - X_0)]^{1/2}}{4(K_1 C_A + K_3 C_B)} \quad (\text{vi})$$

On the basis of the site balance, we must define the activity variable  $s$  as

$$s = \frac{X_0 - 2X_4}{X_0} \quad (\text{vii})$$

Substituting (vi) and (vii) back into the rate equation gives

$$(-r) = K_1 K_3 C_A \{-1 + [1 + 8(sKX_0/4K)]^{1/2}\} \quad (\text{viii})$$

where  $K = K_1 C_A + K_3 C_B$ .

b) The activity variable  $s$  is buried deeply within the RHS of equation (viii), so it is not possible to write a simple separable form for deactivation kinetics.



HORATIO SAYS

The result here concerning separability seems to be rather pessimistic in fact. Maybe a curve-fit variable of  $s$  would serve just as well. How might we be able to test this? Would it really be worth the effort? Also, the appearance of  $2S$  in the main reaction makes the rate equation nonlinear. Does this mean that separable kinetics for deactivation will not work for nonlinear kinetics?

## Exercises

### Section 3.1

1. Calculate the rate at which nitrogen molecules at 1 atm and 100 °C strike an exposed surface.
2. Compare the rate computed in problem 1 with the rate of chemisorption of nitrogen molecules, at the same conditions of temperature and pressure, on an hypothetical surface with site density,  $n_s$ , of  $10^{13} \text{ cm}^{-2}$  at half-monolayer surface coverage. The activation energy for chemisorption is 5 kcal/mol, and  $\sigma = 0.1$ .

3. Calculate the equilibrium surface coverage according to the Langmuir isotherm for the nitrogen example of problems 1 and 2. The heat of adsorption is 10 kcal/mol, the sticking probability is unity, and  $k_d^0 \approx 10^{30} \text{ sec}^{-1}$ .
4. Derive the Langmuir isotherm expressions for the equilibrium surface coverages,  $\theta_A$  and  $\theta_B$ , of two gases competitively adsorbed on the same surface [equations (3-13)].
5. Using a procedure akin to that employed to derive the Freundlich isotherm, obtain the Temkin isotherm equation (3-25).
6. Below are the data of Emmett and Brunauer [P.H. Emmett and S. Brunauer, *J. Amer. Chem. Soc.*, 56, 35 (1934)] for the adsorption of nitrogen on powdered iron catalyst at 396 °C.

Pressure (mm Hg)	Vol. ads. (cm <sup>3</sup> )(STP)
25	2.83
53	3.22
150	3.69
397	4.14
768	4.55

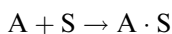
From these data can you distinguish which of the three isotherms—Langmuir, Freundlich, or Temkin—is best obeyed?

### Section 3.2

7. Following the procedure described in Section 3.2, derive the rate equations for reactions (2) and (6) in Table 3.2.
8. Derive a rate equation for reaction scheme (XXVI) if the rate of adsorption of reactant A is rate-controlling. Repeat for the rate of desorption of C rate-controlling.

### Section 3.3

9. Using the general pssh approach, derive the rate equation for reaction (2) in Table 3.2
10. We wrote for the path of chemisorption of an atom or molecule A on a surface,



with S the surface site. The following expression was used to express the rate of chemisorption

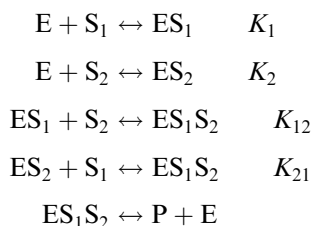
$$r(ads) = \sigma(2\pi m_A kT)^{-1/2} f(\theta) \exp(-E/RT) P_A$$

where the sticking coefficient,  $\sigma$ , was considered to be a kind of correlation parameter to fit the data in a given case. Transition state theory, however, can provide additional insight into this matter. Consider that the adsorption follows



where the transition state complex,  $(A \cdot S)^\ddagger$ , is immobile on the surface, although it can retain vibrational modes. On this basis, derive an analytical expression for  $\sigma$ . Assume that for the surface site the function consists only of vibrational modes of very high frequency.

11. The apparent first-order conversion from A to P occurs more rapidly in the acidic range of pH, with an observed half-life (303 K) of 0.437 min at pH = 6 and 0.099 min at pH = 5. Compute the corresponding rate constants.
12. In many two-substrate reactions it appears that a tertiary complex may be formed with both substrates attached to the enzyme. One possible sequence for such a scheme is



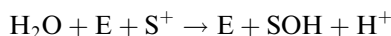
so that

$$(-r) = k[ES_1S_2]$$

a) Show that the overall rate equation for this sequence is given by

$$(-r) = \frac{k[E]_0}{1 + K_{21}/[S]_1 + K_{12}/[S]_2 + \frac{(1/2)(K_2K_{21} + K_1K_{12})}{[S]_1[S]_2}}$$

- b) What happens if  $K_1K_{12} = K_2K_{21}$ ?
- 13.<sup>7</sup> An enzyme-catalyzed reaction irreversibly generates protons according to the scheme



where E is the enzyme and  $S^+$  is the substrate. If the active form of the enzyme is  $E^-$ , and if  $(E^-/E) = 1$  at pH = 6.0 ( $= pK_1$ ), and  $(E^{-2}/E^-) = 1$  as pH = 10.0 ( $= pK_2$ ), show that the reaction velocity at a pH of 7.0 is given approximately by

$$(-r) = (-r_{\max}) \left( \frac{s}{K_s + s} \right) \left( \frac{K_1}{K_1 + h} \right)$$

where  $h = [H^+]$  and  $s = [S]$ . Be sure to define exactly what is meant by  $(-r)_{\max}$ .

- 14.<sup>7</sup> Some data for the initial rates of an enzyme-catalyzed reaction for various substrate concentrations are listed below. Evaluate the rate maximum and the Michaelis constant via a Lineweaver-Burke plot, and then

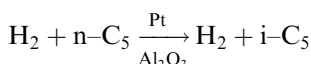
<sup>7</sup> Problems 13 and 14 from J.E. Bailey and D.F. Ollis, *Biochemical Engineering Fundamentals*, reprinted by permission of McGraw-Hill Book Co., New York, NY., (1977).

devise a simple graphical method to evaluate the consistency of the Michaelis constant evaluated from the data.

[S], mol/l	$(-r)$ , mol/l – min $\times 10^6$
$4.10 \times 10^{-3}$	177
$9.50 \times 10^{-4}$	173
$5.20 \times 10^{-4}$	125
$1.03 \times 10^{-4}$	106
$4.90 \times 10^{-5}$	80
$1.06 \times 10^{-5}$	67
$5.10 \times 10^{-6}$	43

### Section 3.5

15. Sinfelt, Hurwitz, and Rohrer [J.H. Sinfelt, H. Hurwitz and J.C. Rohrer, *J. Phys. Chem.*, 64, 892 (1960)] studied the kinetics of the isomerization of n-pentane over a platinum-on-alumina catalyst in the presence of excess hydrogen. Overall,

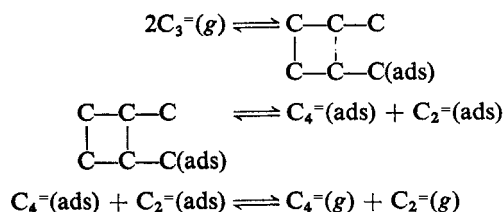


They postulated a mechanism whereby the n-C<sub>5</sub> is chemisorbed on the Pt, simultaneously being dehydrogenated to the n-C<sub>5</sub> olefin. The chemisorbed n-pentene species then desorbs from the Pt sites and is reabsorbed on the acidic sites of the alumina, where isomerization to i-pentene occurs. The i-pentene is then desorbed and reabsorbed on the Pt site, where it is rehydrogenated to i-pentane and desorbed.

Assuming that the isomerization is rate-controlling and irreversible, write the reaction scheme representing the mechanism above. Derive the rate equation for the rate of n-pentane isomerization if all species obey the Langmuir isotherm.

What might be the role of hydrogen in this reaction, aside from its participation in the hydrogenation/dehydrogenation steps?

16. The disproportionation of propylene on supported tungsten oxide catalysts is thought to proceed via a cyclobutane intermediate as follows.



In this view the decomposition of the cyclobutane intermediate would be the rate-determining step. Alternative views hold that the first step above should be broken into two steps, adsorption of C<sub>3</sub><sup>=</sup> and surface reaction of 2C<sub>3</sub><sup>=</sup>(ads) to form the intermediate, or that the formation of intermediate

is via reaction of  $C_3^-(g)$  with  $C_3^-(ads)$ . In both of these cases the decomposition of intermediate is rapid.

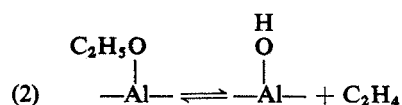
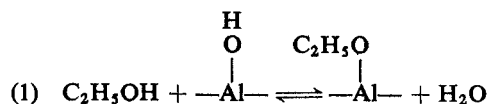
a) Develop rate equations for all three of these views of the reaction mechanism.

b) Simplify your results for the initial rates of reaction (product partial pressures are small).

c) Examine the three rate equations in view of the following results [U. Hattikudur and G. Thodos, *Advan. Chem.*, 133, 80 (1974)]:

T(°F)	$P_{C_3} = (atm)$	Initial rate (g moles/g cat-hr)
650, 750, 850	2.17, 2.09, 2.06	0.58, 2.40, 6.80
	6.98, 2.52, 9.41	2.30, 2.48, 11.39
	9.67, 6.89, 17.58	2.98, 5.30, 12.29
	35.86, 17.82, 34.37	5.13, 7.46, 12.92
	50.85, 34.86, 48.91	5.42, 8.14, 13.37
	65.24, 49.55, —	5.86, 8.60, —

17. The mechanism proposed by Topchieva [K.V. Topchieva, R. Yun-Pun and I.V. Smirnova, *Advan. Catalysis*, 9, 799 (1957)] for ethanol dehydrogenation over  $Al_2O_3$ , is



The designated active site,  $\begin{array}{c} OH \\ | \\ -Al- \end{array}$ , is consumed in the first step and regenerated in the second, thus forming a closed sequence. Derive a rate equation for the rate of dehydration of alcohol assuming that:

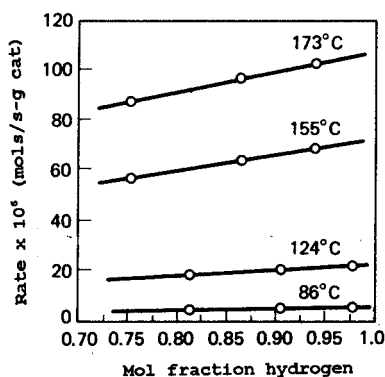
- a) Both reactions occur at the same rate.  
b) Reaction (1) is at equilibrium and (2) is rate-controlling and irreversible.
18. The following initial rates (lb mols A reacted/h-lb cat) have been reported for the reaction



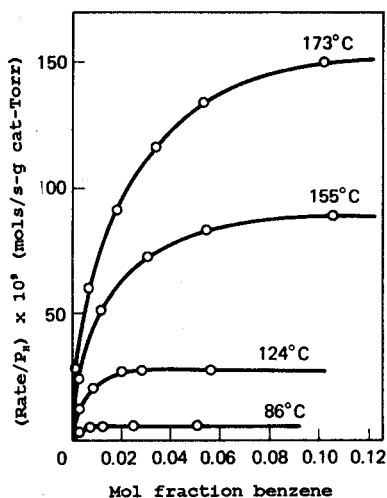
T(°F)	$P_A(atm)$											
	0.5	1.0	2.0	2.5	3.0	4.0	5.0	7.0	8.0	9.0	13.0	
550	0.008	0.012	0.015	—	0.017	0.017	—	0.014	—	0.013	0.011	
575	0.016	0.024	—	—	0.028	—	0.026	0.022	—	0.019	—	
600	0.041	0.042	—	—	0.043	0.042	0.042	0.042	—	0.036	0.027	
650	0.113	—	—	—	0.114	—	—	0.116	—	0.109	0.098	
700	0.192	0.195	0.190	0.189	0.193	0.188	0.183	—	0.195	0.197	0.190	

Determine a consistent explanation for these data, giving the rate equations applicable with all pertinent constants. The desorption of D is slower than that of C under all conditions reported here.

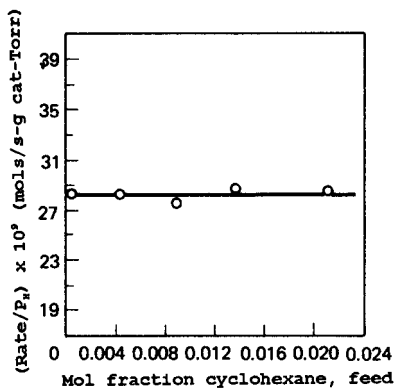
19. In Figure 3.15 are some experimental results of Kehoe and Butt [J.P.G. Kehoe and J.B. Butt, *J. Appl. Chem. Biotechnol.*, 23, (1972)] on the initial rates of the hydrogenation of benzene over a nickel-kieselguhr catalyst in an excess of hydrogen at low temperatures. Determine a consistent form of Langmuir-Hinshelwood expression to correlate these data, and obtain the values of the associated rate and equilibrium constants and their temperature dependence.
20. Synthesis gas, primarily methane and hydrogen, produced by the steam reforming of hydrocarbons still contains about 0.5 mol% CO<sub>2</sub> after



(a)



(b)



(c)

**Figure 3.15** Initial rate data of benzene hydrogenation over Ni-kieselguhr. (a) rate of hydrogenation as a function of hydrogen concentration,  $P = 760$  Torr; (b) rate of hydrogenation as a function of benzene concentration,  $P = 760$  torr; (c) product inhibition effects at low conversions,  $P = 760$  Torr,  $T = 124^\circ\text{C}$ . [After J.P.G. Kehoe and J.B. Butt, *J. Appl. Chem. Biotechnol.*, 23, with permission of the Society of Chemical Industry, (1972).]

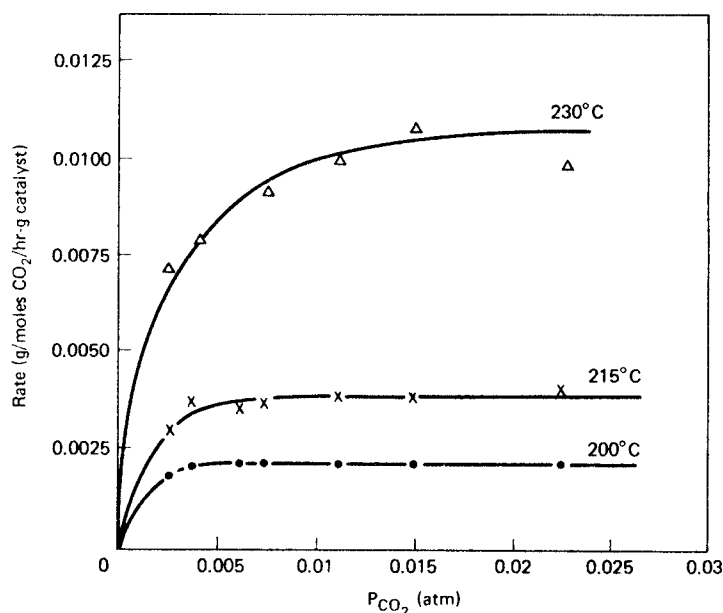


**Figure 3.16** Rate of methanation of  $\text{CO}_2$  on supported nickel. [From T. Van Herwinjnen, H. Van Doesburg, and W.A. de Jong, *J. Catalysis*, 28, 391 with permission of Academic Press, Inc., New York, NY (1973).]

scrubbing to remove CO and  $\text{CO}_2$ . It is important to remove this impurity before using the gas in subsequent processes (i.e., ammonia synthesis), and this is often accomplished by hydrogenation of the  $\text{CO}_2$  to methane on a  $\text{Ni}/\text{Al}_2\text{O}_3$  catalyst.

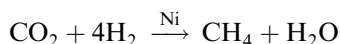


Figure 3.16 gives some data for the rate of methanation of  $\text{CO}_2$ . Hydrogen is present in great excess in these experiments.

- Suggest a reasonable interpretation of these kinetics, and describe in detail the methods required for determination of all the associated constants.
- Carry out numerically your suggestions from part (a). You may use numerical values from the curves presented for this purpose. It is suggested that you solve this part of the problem with a partner, each estimating the required numerical values independently, to obtain some idea of the error involved in such an estimation procedure.

### Section 3.5

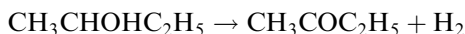
- The following expression, known as the Elovich equation, is often encountered in the correlation of data on rates of chemisorption,

$$\theta = A \ln \left[ \frac{(t + t_0)}{t} \right]$$

where  $\theta$  does not  $\rightarrow 1$ . Here  $A$  and  $t_0$  are experimental parameters, dependent upon temperature, pressure, and molecular weight, and  $\theta$  is the fractional surface coverage.

What does this correlation imply concerning the relationship between activation energy for chemisorption and fractional surface coverage? (*Hint*: Start your derivation with the Hertz-Knudsen equation as given in the text).

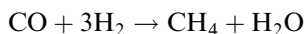
22. In a study of the dehydrogenation of sec-butyl alcohol to methyl-ethyl ketone over a metal catalyst



data were obtained that appeared to show the existence of two rate-controlling steps, depending upon the temperature level. At low temperatures it seemed that surface reaction was rate-controlling, while at high temperature desorption of  $\text{H}_2$  (perhaps) was rate-controlling. Using the LH approach, show how these two possibilities might be distinguished on the basis of initial rate data from experiments in which the total (reactant) pressure is varied.

### Section 3.6

23. Christoph and Baerns [R. Christoph and M. Baerns, *Chem-Ing-Tech.*, 58, 494 (1968)] have conducted extensive studies of the methanation of CO,



using supported Ni catalysts in the presence of a large excess of  $\text{H}_2$  ( $\text{H}_2/\text{CO} > 25$ ), low concentrations of CO, and temperatures of about 500 K. A correlation proposed for the reaction kinetics under these conditions is

$$(-r)_{\text{CO}} = \frac{a(C_{\text{CO}})^{0.5}(s)}{[d + b(C_{\text{CO}})^{0.5}]^2}$$

where  $r$  is (mols CO/h-vol cat),  $C_{\text{CO}}$  is the CO concentration,  $a$  and  $d$  are rate/equilibrium factors,  $b$  is an adsorption coefficient for CO, and  $s$  is the current activity. The rate of deactivation is correlated by

$$\left(\frac{ds}{dt}\right) = -k_d(C_{\text{CO}})(s)$$

Outline an experimental program that will allow you to determine values for both kinetic and deactivation constants, assuming that all experiments will be carried out at 500 K.

### Notation

- $A$  substrate concentration in enzymatic sequence; coking constant in equation (3-101)  
 $A_c$  total surface of catalyst, typically  $m$   
 $A_m$  surface area/molecule; for nitrogen see (3-53)  
 $a, a', a''$  constants defined in equations (3-83) to (3-85)



- $b, b', b''$  constants defined in equations (3-92) and (3-83) to (3-85)  
 $C$  constant defined in equation (3-42); free enzyme concentration  
 $C_A, C_B$  concentrations of A and B in (XXX)  
 $C_c$  wt% coke on catalyst  
 $C_s$  concentration of surface sites for chemisorption, sites/area  
 $C_t$  total enzyme concentration, mass/volume  
 $C_{AS}$  surface concentration of adsorbate, sites/area  
 $C_{is}$  surface concentration of i, typically molecules or mols/area  
 $C_1 \cdots C_3$  constants defined in equation (ii), Illustration 3.4  
 $c$  constant defined in equation (3-20a); biomass concentration, mass/volume culture  
 $\bar{c}$  relative velocity between colliding molecules and surface, length/time  
 $E$  activation energy; activation energy for adsorption, kJ or kcal/mol  
 $E_i$  energy of desorption from  $i$ th layer, kcal/mol  
 $E_1$  energy of desorption from first layer, kcal/mol  
 $E'$  activation energy for desorption, kJ or kcal/mol  
 $f$  surface packing factor  
 $f(\theta), f'(\theta)$  functions of surface coverage  
 $(\Delta H_a)^\circ$  enthalpy change on adsorption at standard state, cal or kcal/mol  
 $K$  physical adsorption constant after eqn (3-30); Michaelis constant =  $(k_2 + k_3)/k_1$ ; defined in equation (3-88)  
 $K_A$  adsorption equilibrium constant for A,  $\text{atm}^{-1}$ ; see equation (3-6a)  
 $K_{Ai}$  adsorption equilibrium constant on surface element  $i$ ,  $\text{atm}^{-1}$   
 $K_A$  adsorption equilibrium constant; see equation (3-6a)  
 $K_B$  adsorption equilibrium constant for B,  $\text{atm}^{-1}$   
 $K_i$  general Langmuir adsorption constant,  $\text{atm}^{-1}$ ; see after equation (3-58)  
 $K_s$  surface reaction equilibrium constant =  $(C_{BS}/C_{AS})$ ; Michaelis constant associated with substrate  
 $K'$  constant in exponential decay function  
 $K'_s$  deactivation rate; see equation (3-107)  
 $K''$  constant in hyperbolic decay function  
 $k$  Planck's constant; product inhibition constant in equation (3-80)  
 $k_a, k_d$  adsorption and desorption rate constants,  $\text{time}^{-1}$   
 $k'_a, k'_d$   $k_a n_s, k_d n_s$   
 $k_d^\circ$  adsorption rate constant, molecules or mols/times-atm  
 $k_d^\circ$  desorption rate constant, molecules or mols/time  
 $k_{da}$  deactivation rate constant,  $\text{time}^{-1}$   
 $k_1 \cdots k_4$  rate constants in (XXX)  
 $k_{S1}, k_{S2}$  rate constants for forward and reverse surface reactions  
 $k'_{S1}, k'_{S2}$   $k_{S1} n_s, k_{S2} n_s$   
 $M$  molecular weight  
 $m$  constant defined in equation (3-20a); molecular weight or mass; empirical reaction order; constant in equation (3-87)  
 $m_A$  molecular weight or mass of A  
 $N$  factor Avogadro's number  
 $n$  number density, number/volume; total molecules adsorbed per area; empirical reaction order; population density, number of individuals per volume of culture, coking power dependence in equation (3-95)

$n_A$	number density of A, number/volume
$n_i$	fraction of total adsorption sites belonging to class $i$
$n_0$	scaling constant in Freundlich isotherm
$n_s$	site density on surface, number/area
$P$	pressure, typically atm; product concentration in enzymatic sequence, mass/volume
$P_A$	partial pressure of A, atm
$P_A^*$	virtual pressure of A, atm
$P_L$	partial pressure of poison L, atm
$P_0$	saturated vapor pressure, atm or mm Hg
$P_T$	total pressure, atm
$p$	product concentration, product/volume culture
$Q$	heat of adsorption, $= E' - E$ , kJ or kcal/mol
$Q_M$	scaling constant in Freundlich isotherm
$Q_0$	heat of adsorption at zero coverage, kJ or kcal/mol
$R$	gas constant, kJ or kcal/mol-K
$r$	overall rate of reaction; see equation (3-72)
$r_A$	rate of adsorption of A, mols/time
$(-r_A)_0$	initial rate of reaction of A, mols/volume-time
$(-r_s)$	rate of change of activity, $\text{time}^{-1}$
$S$	surface area, $\text{cm}^2$ or $\text{m}^2/\text{g}$
$(\Delta S_a)^\circ$	entropy change on adsorption at standard state, cal or kcal/mol-K
$s$	surface area per unit weight of adsorbent; substrate concentration, mass/volume culture; scaled activity variable for deactivation
$s(n)$	number of molecules adsorbed per weight of adsorbate
$T$	temperature, $^\circ\text{C}$ or K
$t$	time
$u_1$	physical adsorption rate; see equation (3-28)
$u_1'$	physical desorption rate; see equation (3-29)
$V$	volume adsorbed, volume per volume or weight of adsorbent; factor $= k_3 C_t$ in equation (3-73)
$V_c$	critical volume of liquid, volume/mol
$V_g$	molar volume of gas, volume/mol at 1 atm and adsorption temperature
$V_M$	volume adsorbed at saturation, monolayer volume
$v_i$	residual functions, equations (iii), Illustration 3.4
$W_c$	weight of catalyst, typically g
$X$	function $= (x/x_M)$ ; intermediate enzyme concentration
$X_i$	occupied active sites; see equation (3-98)
$X_0$	initial concentration of active sites in (XXX)
$X_y$	value of $X$ at $X = Y_y$
$x$	weight of adsorbate/weight of solid; see equation (3-35), or volume adsorbate (STP)/g
$x_M$	monolayer capacity, weight of adsorbate/weight of solid or volume adsorbate (STP)/g
$Y$	$(P/P_0)$ ; yield coefficient in equation (3-75)
$Y_y$	inflection point; see equation (ii), Illustration 3.2
$y_i$	functions defined in equations (ii), Illustration 3.4
$Z_{cT}(ads)$	adsorption collision number, number/sites or area

$Z_{cT}$  (*surface*),  $Z$  (*surface*)      surface collision number, number/area

*Greek*

$\alpha$       linear scaling constant in equation (3-24); constant in equation (3-37); constant in product rate, equation (3-79)

$\beta$       constant in equation (3-39); constant in product rate, equation (3-79)

$\theta, \theta_A, \theta_B$       fractional surface coverages

$\theta_i$       fraction covered in  $i$ th layer; see equation (3-33)

$\theta_0$       vacant fraction on surface

$\theta_1$       fraction covered by first layer

$\theta_A$       fractional coverage of A on surface element  $i$

$\lambda$       latent heat of condensation, kJ or kcal/mol

$\mu$       specific growth rate, growth rate/biomass concentration

$\mu_c$       maintenance constant; see equation (3-76)

$\mu_m$       maximum specific growth rate, rate/biomass concentration

$\mu'_c$       substrate-related maintenance constant; see equation (3-78)

$\nu$       specific reproduction rate, reproduction rate/population density

$\nu'_i$       desorption frequency from  $i$ th layer,  $\text{time}^{-1}$ ; see equation (3-33)

$\nu'_1$       desorption frequency from first layer,  $\text{time}^{-1}$

$\rho$       liquid phase density, mass or mols/volume

$\sigma$       sticking probability

$\sigma_i$       sticking probability in  $i$ th layer; see equation (3-33)

$\sigma_1$       sticking probability in first layer

*Note:* Additional notation given in Tables 3.2, 3.3b, 3.4, and Illustrations 3.3, 3.5, and 3.6

# 4

---

## Introduction to Chemical Reactor Theory

We must all hang together, or assuredly  
we shall all hang separately

— *Benjamin Franklin*

In the first three chapters we have presented the equations relating rates of chemical reaction to observable quantities such as, temperature and composition, demonstrated the origin of these equations, and shown how they may be used in the interpretation of experimental information on kinetics. We now turn our attention to analysis of the devices in which chemical reactions are conducted, both in the laboratory and in large-scale operation, and we shall see that to a great extent such analysis hinges on physical as well as chemical factors.

The rate equations of Chapter 1 were given, for the most part, as they pertain to homogeneous batch *reactions*. While the purpose there was to treat descriptive kinetics, the results obtained pertain also to the operation of homogeneous batch *reactors*. One of the features of such a reactor was said to be that all the molecules in the reactor at a given time of reaction had been there for the same amount of time; in other words, they had the same age. A second feature implied in the treatment was the intimate association, on a molecular scale, of all species contained in the reactor.

Both of these features are associated with the degree of mixing in the reactor, although the concept of age as related to mixing has more meaning for flow than for batch systems. Mixing effects in chemical reactors are very, very important in determining exactly what goes on. They are often divided into the separate contributions of two distinct mechanisms; *micromixing*, which determines the extent of mixing on a molecular level, and *macromixing*, which is the result of different flow paths, channeling, and bypass flows within the reactor. The two contributions must be considered independent of each other, in that definition of a state of macromixing does not, for example, define a corresponding level of micromixing.

Well-defined limits of macro- and micromixing can be obtained in a number of instances, and these serve to define corresponding ideal reactor types. Deviations of mixing from these limits are sometimes termed *nonideal flows*. Since it is difficult to define a measure for quantities such as the degree of micromixing or, indeed, to make measurements on the hydrodynamic state of the internals of a reactor system, extensive use has been made of models that describe the observable behavior in terms of external measurements. As in any other kind of modeling, these models may not be

correct in every detail and a number of different forms, each possessing different degrees of reality with respect to the phenomena being modeled, may be equally well used over a sufficiently small range of operating conditions. As with kinetic models, these are based on experimentally determined parameters for the most part, and extrapolation is hazardous.<sup>1</sup> Mixing models for both ideal and nonideal flows lead directly to chemical reactor models. However, before treating these let us examine in a more general way the concepts involved in micro- and macromixing.

#### 4.1 Reaction in Mixed or Segregated Systems

In order to visualize physically what is meant by molecular-level or micromixing, consider a “point” volume element of fluid within the reactor that is just large enough to possess the average value of an intensive property such as concentration at the particular location considered [P.V. Danckwerts, *Chem. Eng. Sci.*, 8, 93 (1958)]. All molecules within a point-volume element have zero age when entering the reactor, and all have zero time to remain within the reactor (life expectancy) when the element exits. The degree of micromixing defines what happens to the individual molecules within a point-volume element in the time between its entrance and exit from the reactor.

We can readily envision two extremes. First, all the molecules within the point element on its entrance to the reactor remain within it until exit, as if the element were surrounded by a molecularly impermeable barrier. This is termed segregated flow. Second, complete mixing on the molecular level occurs immediately on entrance, which is termed a state of *maximum-mixedness* [T.N. Zweitering, *Chem. Eng. Sci.*, 11, 93 (1958)]. We may define segregated flow more precisely by saying that the variance of the age distribution of molecules within the point element is zero, which may be a good definition but may not eventually lead to a good night’s sleep. The detailed analysis of intermediate degrees of micromixing requires the use of various models that we shall be discussing later.

Now just what is the importance of micromixing in chemical reaction systems? The question is perhaps best answered using a famous example from the paper of Danckwerts cited above. Consider the isothermal, second-order irreversible reaction  $A + B \rightarrow C$ , carried out homogeneously and at constant volume. The initial concentrations of A and B,  $C_{A0}$  and  $C_{B0}$ , are set in the ratio

$$C_{B0} = C_{A0}(1 + x) \quad (4-1)$$

If the system is in a state of maximum mixedness, after a fraction  $f$  of A is reacted, the concentrations are

$$C_A = C_{A0}(1 - f); \quad C_B = C_{B0}(1 - f + x) \quad (4-2)$$

At the opposite end of the spectrum of micromixing, let us consider the same system, but now consisting of two segregated portions having differing degrees of conversion of A,  $f_1$ , and  $f_2$ , with the volumes of the two portions in the ratio  $\alpha$  to  $(1 - \alpha)$ . The concentrations of A in the two portions are,

$$C_{A1} = C_{A0}(1 - f_1); \quad C_{A2} = C_{A0}(1 - f_2) \quad (4-3)$$

<sup>1</sup> “Don’t look back; something may be gaining on you.” — S. Page

and for B:

$$C_{B1} = C_{A0}(1 - f_1 + x); \quad C_{B2} = (1 - f_2 + x) \quad (4-4)$$

The rate of reaction, averaged over the two portions is

$$\begin{aligned} r_1 &= k\alpha C_{A0}^2(1 - f_1)(1 - f_1 + x) \\ &\quad + k(1 - \alpha)C_{A0}^2(1 - f_2)(1 - f_2 + x) \end{aligned} \quad (4-5)$$

Now let us mix the two fractions, so the resulting concentrations are

$$\begin{aligned} C_A &= C_{A0}[\alpha(1 - f_1) + (1 - \alpha)(1 - f_2)] \\ C_B &= C_{A0}[\alpha(1 - f_1 + x) + (1 - \alpha)(1 - f_2 + x)] \end{aligned} \quad (4-6)$$

and the resulting rate is

$$\begin{aligned} r_2 &= kC_{A0}^2[\alpha(1 - f_1) + (1 - \alpha)(1 - f_2)] \\ &\quad \cdot [\alpha(1 - f_1 + x) + (1 - \alpha)(1 - f_2 + x)] \end{aligned} \quad (4-7)$$

These two rates are not the same. Comparing equations (4-5) and (4-7) gives

$$r_2 = r_1 - \alpha(1 - \alpha)(f_2 - f_1)^2 \quad (4-8)$$

and, since  $\alpha < 1$ ,  $r_2 < r_1$ , the effect of segregation is to increase the point rate of this second-order reaction.

There are two important points illustrated by this example. First is the obvious one that the extent of micromixing can affect the rate of reaction through its influence on the local concentration of reactants. Second is that the magnitude of such effects is also affected by the degree of macromixing. Recall that in the example above we allowed the two volume portions to have differing degrees of conversion of A; if segregation of the two volumes had existed from the beginning of the reaction, differing conversions could be the result only of differing times of reaction for the two elements or, in present terminology, differing ages of the two. This latter is determined by macromixing in the system. Thus we see that while physically the two types of mixing are independent processes, there can be interaction between them which is apparent from the point of rates of reaction.

It is important to generalize the example to an  $n$ th-order reaction. We let  $r_0$  be the initial rate of reaction for a mixture of reactants in stoichiometric proportion, so that

$$r = r_0(1 - f)^n$$

when fraction  $f$  of the reactants has disappeared. Again, consider two portions with  $f_1$ , and  $f_2$  fractions and volumes in the ratio of  $\alpha$  and  $(1 - \alpha)$ . Rates before and after mixing are

$$\begin{aligned} \frac{r_1}{r_2} &= \alpha(1 - f_1)^n + (1 - \alpha)(1 - f_2)^2 \\ \frac{r_2}{r_0} &= [\alpha(1 - f_1) + (1 - \alpha)(1 - f_2)]^n \end{aligned} \quad (4-9)$$

Let  $\alpha$  and  $f_1$  be held constant and define

$$\gamma = \frac{1 - f_2}{1 - f_1}$$

Then

$$\frac{dr_1}{dr_2} = \frac{(dr_1/d\gamma)}{(dr_2/d\gamma)} = \left[ \frac{\gamma}{\alpha + (1 - \alpha)\gamma} \right]^{n-1} \quad (4-10)$$

which is  $> 0$  when  $\gamma > 0$  and  $\alpha < 1$ . Also, the second derivative,

$$\begin{aligned} \frac{d^2r_1}{dr_2^2} &= \frac{d(dr_1/dr_2)/d\gamma}{(dr_2/d\gamma)} \\ &= \frac{n-1}{n} \frac{\alpha\gamma^{n-2}}{(1-f_1)^n(1-\alpha)[\alpha + (1-\alpha)\gamma]^{2n-1}} \end{aligned} \quad (4-11)$$

is  $> 0$  if  $n > 1$ , and  $< 0$  if  $n < 1$ . Two additional properties of these equations are of interest.

$$\begin{aligned} \gamma &= 1; & r_1 &= r_2; & \text{and} & & (dr_1/dr_2) &= 1 \\ \gamma &= 0; & (r_1/r_2) &= \alpha^{1-n} \\ \alpha^{1-n} &> 1 & \text{for } n > 1; & \alpha^{1-n} < 1 & \text{for } n < 1 \end{aligned} \quad (4-12)$$

A graphical summary of the requirements attached to equations (4-10) to (4-12) is given in Figure 4.1 in terms of the rates  $r_1$  and  $r_2$ . The requirement from equation (4-12) establishes for  $\gamma$  of 0 or 1 and  $n = 1$  that the two rates be equal. Further,  $dr_1/dr_2 = 1$  for  $\gamma = 1$ , and  $(d^2r_1/dr_2^2) = 0$  for  $n = 1$ ; thus  $r_1 = r_2$  for  $\gamma > 1$ . This

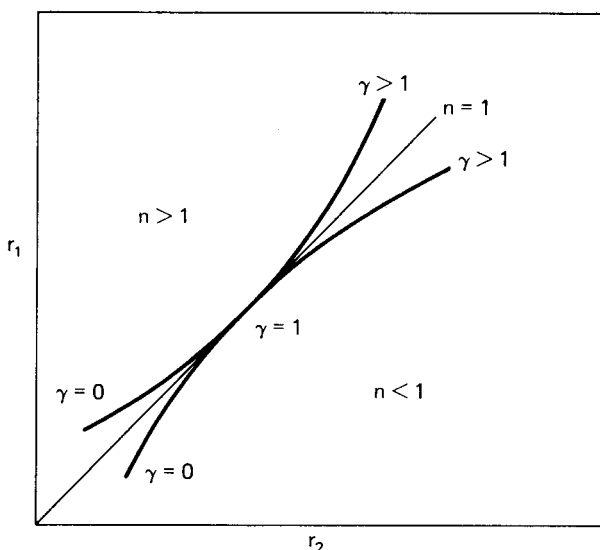


**Figure 4.1** Effect of segregation on rates of  $n^{\text{th}}$ -order reactions. [After P.V. Danckwerts, *Chem. Eng. Sci.*, 8, 93, with permission of Pergamon Press, Ltd., London, (1958).]

establishes the equality of rates for all values of  $\gamma$  when  $n = 1$ . *The degree of micromixing has no effect on the rate of a first-order reaction.* Similar reasoning leads to the conclusions that  $r_1 > r_2$  for  $n > 1$ , and  $r_1 < r_2$  for  $n < 1$ , save at the point  $\gamma = 1$ , where  $r_1 = r_2$ . The magnitude of the difference in rates depends on  $\gamma$ , which one can see is a function of the degree of macromixing since age distribution effects are contained in the differing fractions reacted  $f_1$  and  $f_2$  and  $\alpha$ , the micromixing parameter.

As mentioned before, quantitative measures for the degree of micromixing intermediate to the extremes of maximum mixedness and complete segregation are difficult to establish on an *a priori* basis. Thus, aside from the demonstration given here to demonstrate the potential effects of micromixing on reactions of differing kinetic order, a more quantitative treatment must await the development of various models that can describe the mixing process.

## 4.2 Age Distributions and Macromixing

Macromixing is concerned only with the history of individual point-volume elements during their residence in a given system. For example, consider the case of laminar flow through a length of cylindrical tube. We know that when the laminar flow is fully developed, there exists a parabolic profile of velocities in the direction of flow across the radius of the tube, with maximum velocity at the center and zero at the wall. Hence, a point element with radial position near the wall will require a larger amount of time to traverse a given length of tubing than will a point element near the center. If the flow is segregated (which is a reasonable assumption for laminar flow at normal temperatures), there will exist a distribution of times required for elements at various radial positions to traverse the given length, which is dictated by the parabolic velocity profile. The time required is called the *residence time* and the distribution is the *residence-time distribution* (RTD). In this example, owing to the existence of segregation at the micromixing level, the RTD is a direct measure of the extent of macromixing in the system.

Now, consider a second example, that of turbulent flow through the tube. Again there exists some sort of velocity profile, but in addition there is some level of micromixing due to eddy motion among the elements. In this case it is possible to identify a distribution of residence times for individual molecules within the system, not volume elements, and the RTD is a measure of the combined effects of macro- and micromixing.

In the most general case, then, measurements of residence-time distribution by the methods to be discussed here *cannot* define micromixing. In spite of this limitation, knowledge of the residence-time distribution is most valuable because it provides us with as much information on the state of mixing as we can obtain short of detailed measurements on the microscopic level.

In addition to the residence-time distribution, there are a number of other age distributions which are of importance and which sound just a little like something from a life-insurance brochure. The distribution of ages of elements or molecules within the system at a given time is called the *internal-age* distribution, and the distribution of ages on exit from the system is the *exit-age distribution*. Finally, corresponding to the internal-age distribution there is a residual lifetime or *life-expectancy distribution*, which is a measure of time remaining before exit from the



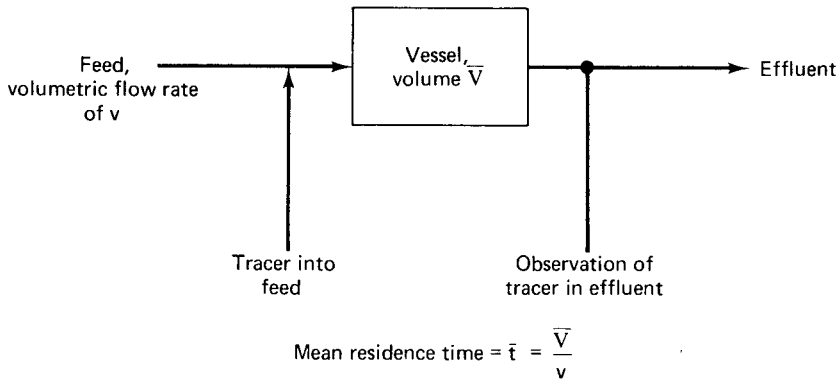


**Figure 4.2** Experiment for measurement of residence time distribution.

system. We shall be most concerned with the residence-time, internal, and exit-age distributions.

It is most convenient to define these distributions quantitatively within the context of the experimental methods normally used for the determination of the residence-time distribution. Once again we base the vocabulary and the development on the pioneering work of Danckwerts [P.V. Danckwerts, *Chem. Eng. Sci.*, 2, 1 (1953)].

Consider, then, the simple experiment shown in Figure 4.2. Fluid is flowing through a vessel of volume  $\bar{V}$  at a steady-state volumetric flow rate of  $v$ . Immediately at the entrance there is a means for injecting a trace substance at a certain concentration level,  $C_0$ , and immediately at the outlet a means for detecting instantaneously and continuously the concentration of this tracer leaving the vessel. Introduction of the tracer does not affect the steady-state flow rate. The *mean residence time* in the vessel, which is the average over all elements of the fluid, is given by

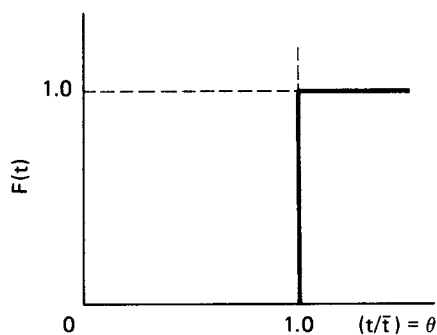
$$\bar{t} = \frac{\bar{V}}{v} \quad (4-13)$$

Now let us perform the following experiment. Initially we set the feed to flow at steady-state through the vessel and no tracer is introduced. Then, at a set time, a step change in the concentration of tracer from zero to  $C_0$  (mixed concentration of tracer with the feed) is introduced into the feed and is subsequently maintained at that level, while simultaneously the concentration of tracer in the effluent is observed and recorded. What sort of response might one observe in the concentration of tracer at the exit to this step-function change? Three plausible results are illustrated in Figure 4.3, termed an *F-diagram* by Danckwerts, in terms of the variables

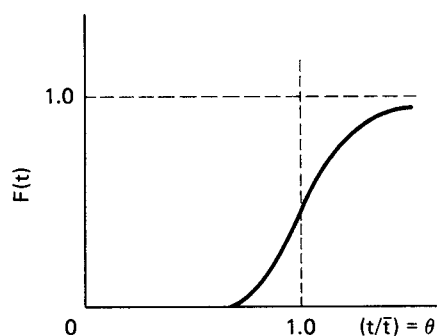
$$F(t) = \frac{C_{exit}}{C_0}, \quad \theta = \frac{t}{\bar{t}} \quad (4-14)$$

$$(4-15)$$

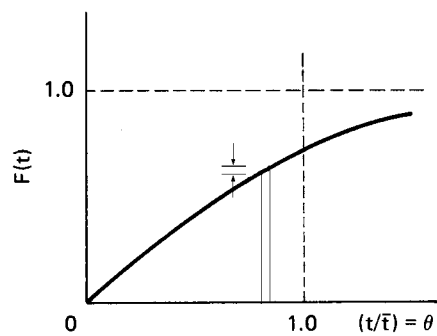
where  $F(t)$ , the concentration breakthrough, is the residence-time distribution and  $\theta$  the number of residence times. In Figure 4.3a, we see that all tracer molecules exit from the vessel at the same time, therefore they have identical exit ages. In Figure 4.3b, there is some distribution of ages about  $\theta = 1$ , with some molecules exiting



(a)



(b)



(c)

**Figure 4.3** Plausible responses to a step function introduction of tracer into a flow system.

before one residence time and some after, while in Figure 4.3c some molecules exit immediately upon introduction of the tracer and others remain for times  $\theta \gg 1$ . One might infer correctly from the shapes of the curves that (a) and (c) represent some sort of limiting cases for mixing behavior, with (b) intermediate. We will discuss these limits in a moment, but first let us determine what relationships exist among such an experimentally-determined response and the various age distribution. We

make the following definitions:

1. Elements of material in the vessel for  $t$  have the “age”  $t$ .
2. The fraction of material with ages between  $t$  and  $t + dt$  in the system is  $I(t) dt$ .
3. The fraction of materials with ages between  $t$  and  $t + dt$  on leaving the system is  $E(t)dt$ .

$I(t)$  and  $E(t)$  are the internal- and exit-age distribution functions, respectively. Now let us write a material balance on the tracer for a step change in its concentration from zero to 1 (the arbitrary concentration units will not affect the results here) at  $t = 0$ . After time  $t$  we have

$$\text{entered system} = vt$$

$$\text{within system} = \bar{V} \int_0^t I(t') dt'$$

$$\text{departed system} = v \int_{t''=0}^t \int_{t'=0}^{t''} E(t') dt' dt''$$

The last equality comes from the fact that the rate of flow of tracer out of the system at any time  $t''$  after the concentration step is given by the integral of the exit-age distribution for all ages up to  $t''$ ; that is,

$$\text{leaving at } t'' = v \int_{t'=0}^{t''} E(t') dt'$$

The material balance is

$$\theta = \frac{vt}{\bar{V}} = \int_0^t I(t') dt' + \frac{v}{\bar{V}} \int_{t''=0}^t \int_{t'=0}^{t''} E(t') dt' dt'' \quad (4-16)$$

The residence-time distribution,  $F(t)$ , including the contributions of all elements or molecules up to the time considered, must then be the time integral of the exit-age distribution

$$F(t) = \int_0^t E(t') dt' \quad (4-17)$$

Taking the time derivative of equation (4-16), we have

$$1 - \int_0^t E(t') dt' = \frac{\bar{V}}{v} I(t) \quad (4-18)$$

and from (4-17), then

$$1 - F(t) = \frac{\bar{V}}{v} I(t) \quad (4-19)$$

which relates the measured residence-time distribution  $F(t)$  to the internal age distribution,  $I(t)$ . Further, from the time derivative of equation (4-17) we have

$$\frac{d}{dt} [F(t)] = E(t) \quad (4-20)$$

It is also convenient to remember from the definitions of internal- and exit-age distributions that

$$\int_0^\infty I(t) dt = \int_0^\infty E(t) dt = 1 \quad (4-21)$$

since the integral for all ages from 0 to  $\infty$  represents the total amount of material (fraction = 1) in the system.

A second type of experiment often used in the determination of RTD is the response to a pulse input of tracer rather than a step function. Here a total quantity,  $Q$ , of the tracer is injected into the feed stream at a concentration of  $C_0$  over a small time period  $\Delta t$ . Differing residence times of molecules in the system will lead to a dispersion of the pulse with typical response curves shown in the *C-diagram* of Figure 4.4, corresponding to those illustrated in Figure 4.3. The response of the  $C(t)$  curves of Figure 4.4 is just the derivative of the  $F(t)$  curves in Figure 4.3.

$$\frac{d}{dt} [F(t)] = E(t) \quad (4-22)$$

where

$$E(t) = \frac{C(t)}{Q} \quad (4-23)$$

Thus, either pulse-response or step-function response experiments give sufficient information to permit evaluation of exit-age, internal-age, and residence-time distributions. The average age or mean residence time, which we have defined intuitively in equation (4-13), can be more precisely stated in terms of the time average of the exit-age distribution.

$$\bar{t} = \frac{\int_0^\infty tE(t) dt}{\int_0^\infty E(t) dt} = \int_0^\infty tE(t) dt \quad (4-24)$$

From equation (4-20) we may write this as

$$\frac{v\bar{t}}{\bar{V}} = \int_0^1 (vt/\bar{V}) d[F(t)] = 1 \quad (4-25)$$

so that

$$\bar{t} = \frac{\bar{V}}{v}$$

The average age of material in the system at any time,  $t_1$ , is most easily evaluated graphically or

$$\bar{t}_1 = \int_0^{t_1} tI(t) dt = \frac{v}{2\bar{V}} \int_0^{F(t_1)} t^2 d[F(t)] \quad (4-26)$$

numerically from  $F(t)$  diagram<sup>2</sup>.

<sup>2</sup>“By hook or crook.”—*J. Wycliffe*.

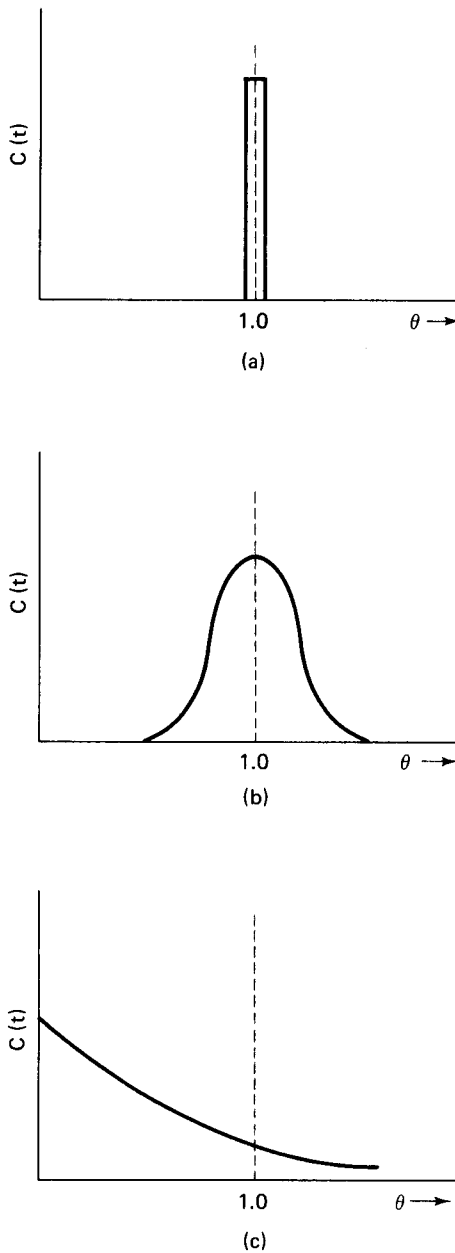


**Figure 4.4** Responses to a pulse input of tracer into a flow system.

Pulse-response and step-function-response experiments are perhaps the easiest to carry out and analyze; however, any perturbation-response technique can be used to determine age distributions. Kramers and Alberda [H. Kramers and G. Alberda, *Chem. Eng. Sci.*, 2, 173 (1953)] describe a frequency-response analysis, and a general treatment of arbitrary input functions. Errors associated with input and

measurement, and other factors are discussed in a review by Levenspiel and Bischoff [O. Levenspiel and K.B. Bischoff, *Advan. Chem. Engr.*, 4, 95 (1963)].

While the concepts involved in the definition of these distributions are relatively simple, practical application is sometimes confusing because of the differing time measures used. There are two time variables and one time constant that we must consider:

1.  $t$  = real time, in seconds, minutes, and so on. This is the time variable employed in the age-distribution definitions up to this point.
2.  $\bar{t}$  = the nominal residence time in the system, also in seconds, minutes, and so on, defined in equation (4-13).
3.  $\theta$  = the number of residence times,  $t/\bar{t}$ , a dimensionless quantity.

Experimental data on exit-age or residence-time distributions most often take the form of discrete values of tracer concentration measured at successive time intervals after introduction of the tracer. Thus, the integrals involved can be replaced by summations in the analysis of actual data. We will illustrate the procedure for the analysis of a pulse-response experiment. Available are tracer concentrations in the effluent,  $C(t)$  and corresponding times, and from these data we would like to determine the exit-age distribution, or  $E(\theta)d\theta$ , the distribution in terms of the residence-time variable  $\theta$ . First determine  $E(t)$  from  $C(t)$  versus  $t$  by

$$E(t) = \frac{C(t)}{\sum C(t)\Delta t} = \frac{C(t)}{Q} \quad (4-27)$$

Division by  $Q = \sum C(t)\Delta t$  in equation (4-27) ensures the normalization of the distribution required by equation (4-21); graphically, the area under a plot of  $E(t)$  versus  $t$  must be unity. Next, determine the value of  $\bar{t}$ . This can be done in either of two ways:

$$\bar{t} = \frac{\sum tC(t)\Delta t}{\sum C(t)\Delta t} \quad (4-28)$$

$$\bar{t} = \sum tE(t)\Delta t \quad (4-29)$$

Now, with values for  $E(t)$  and  $\bar{t}$  determined,  $E(\theta)$  can be evaluated from the simple relationship

$$E(\theta) + \bar{t}[E(t)] = \frac{\sum tC(t)\Delta t}{\sum C(t)\Delta t} \cdot \frac{C(t)}{\sum C(t)\Delta t} \quad (4-30)$$

It will be shown later that it is the exit-age distribution (or the derivative of the  $F$ -curve) that is important in determining the efforts of nonideal flow on actual chemical reactor performance.

### Illustration 4.1

Show analytically that

$$E(\theta) = \bar{t}[E(t)]$$

*Solution*

From the definition of the various distributions we can write

$$\int_0^{\infty} E(t) dt = \int_0^{\infty} E(\theta) d\theta = 1$$

and

$$\theta = \frac{t}{\bar{t}}$$

$$dt = \bar{t} d\theta$$

Then

$$\int_0^{\infty} E(\theta) d\theta = \int_0^{\infty} \bar{t} E(t) d\theta$$

$$\bar{t} E(t) = E(\theta)$$



HORATIO SAYS

What about  $I(t)$  and  $E(t)$ ?

Let us return finally to a more thorough analysis of the limiting types of response indicated by Figures 4.3 and 4.4a and c. In case (a), all molecules have an identical residence time in the system and the residence-time distribution is given by

$$\begin{aligned} F(t) &= 0 & t < \bar{t} \\ F(t) &= 1 & t > \bar{t} \end{aligned} \quad (4-31)$$

or

$$\begin{aligned} F(\theta) &= 0 & \theta < 1 \\ F(\theta) &= 1 & \theta > 1 \end{aligned}$$

This type of RTD is normally associated with the terms “plug flow” or (misleading) “no mixing”, since the characteristics of plug flow through a tube—uniform velocity across the radius and no macromixing in the direction of flow—require a unique residence time. Once again, let it be stated that such a response does not define the state of micromixing.

The response in case (c) is at the opposite end of the spectrum from plug flow and is the limit established when the internal-age distribution and the exit-age distribution are identical. The consequence of this is an exponential RTD, as shown by the following. Rewrite the material balance, equation (4-16), subject to

$$\int_0^t E(t') dt' = \int_0^t I(t') dt' = F(t) \quad (4-32)$$

This then produces a material balance expressed in terms of  $F(t)$

$$\frac{vt}{\bar{V}} = F(t) + \frac{v}{\bar{V}} \int_{t''=0}^t F(t'') dt'' \quad (4-33)$$

Taking the derivative with respect to time and rearranging yields

$$\frac{d[F(t)]}{dt} + \frac{v}{\bar{V}} F(t) = \frac{v}{\bar{V}} \quad (4-34)$$

Solving for  $F(t)$ ,

$$\int_0^{F(t)} d[F(t)] = e^{-(v/\bar{V})t} \int_0^t \frac{v}{\bar{V}} e^{(v/\bar{V})t} dt$$

and then

$$\begin{aligned} F(t) &= 1 - e^{-(v/\bar{V})t} \\ F(\theta) &= 1 - e^{-\theta} \end{aligned} \quad (4-35)$$

The corresponding exit-age distribution is

$$\begin{aligned} E(t) &= \frac{d[F(t)]}{dt} = \frac{v}{\bar{V}} e^{-(v/\bar{V})t} \\ E(\theta) &= e^{-\theta} \end{aligned} \quad (4-36)$$

The exponential RTD is associated with the term “perfect mixing”, although this may or may not be the case on both the macroscopic and microscopic levels.

A summary of the possible limiting combinations of macro- and micromixing, and the result in terms of a residence-time distribution result for the step-function experiment that we have described, is given in Figure 4.5.

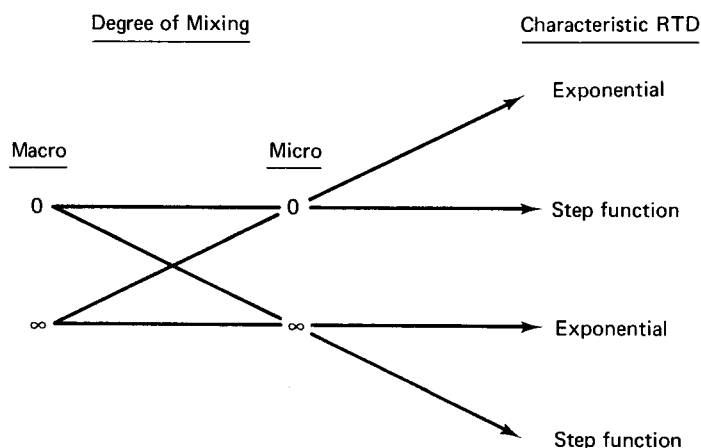


**Figure 4.5** Residence-time distributions for limiting combinations of macro- and micro-mixing.



**Illustration 4.2**

The flow patterns in a reactor are to be investigated by determining the residence-time distribution. Below are the results obtained for the concentration of tracer in the effluent after introduction of a step function input at a concentration of 0.05 M.

Time (min)	1	3	5	10	15	20	25	30
Conc. (M)	0.002	0.011	0.016	0.022	0.031	0.038	0.040	0.041

Determine the exit-age distribution function for this reactor. What type of ideal reactor model does this most closely resemble?

*Solution*

For a step input:

$$F(t) = [C_{exit}/C_0] \quad (i)$$

$$E(t) = d[F(t)]/dt \quad (ii)$$

From the data given we can determine the following

Time, min	$F(t)$	$E(t), \text{min}^{-1}$
1	0.04	0.057
3	0.22	0.075
5	0.32	0.055
10	0.44	0.032
15	0.62	0.024
20	0.76	0.015
20	0.80	0.006
30	0.82	0.002

where  $E(t)$  has been determined from  $F(t)$ . These results are shown in Figure 4.6.

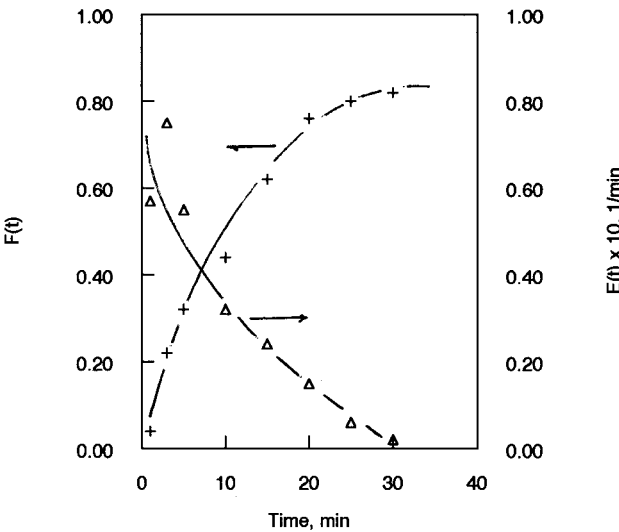


**Figure 4.6** Residence-time and exit-age distributions for Illustration 4.2.

The patterns displayed above conform to the general shapes shown in Figures 4.3c and 4.4c, which will be seen to be characteristic, according to Figure 4.5, of combinations  $(\infty, 0)$  or  $(\infty, \infty)$  macro-micromixing.



HORATIO SAYS

Calculate the mean residence time from these distributions.

### 4.3 Mixing Models: Reactors with Ideal Flows

The step-function and exponential residence-time distributions of Figure 4.5 can be modeled by two different types of flow systems. For the step-function response we have already alluded to the model of plug flow through a tube, which is, indeed, a standard model for this response. The exponential response, described previously as the result of the equality of the internal- and exit-age distributions, requires a bit more thought. In the following we will derive the equations for the mixing models and then the corresponding reactor models for these two limits.

#### 4.3.1 Plug Flow: The Mixing Model

Consider a differential length,  $dz$ , of cylindrical conduit as shown in Figure 4.7. Fluid with a uniform velocity  $u$  in the axial direction is passing through the differential volume  $Adz$ , where  $A$  is the cross section of the tube. At a time  $t = 0$ , a step input of tracer is introduced uniformly across the cross section at the entrance to the tube at a concentration  $C_0$ . We write the general unsteady-state mass balance for the differential volume in the normal fashion:

$$\text{input} - \text{output} = \text{accumulation}$$

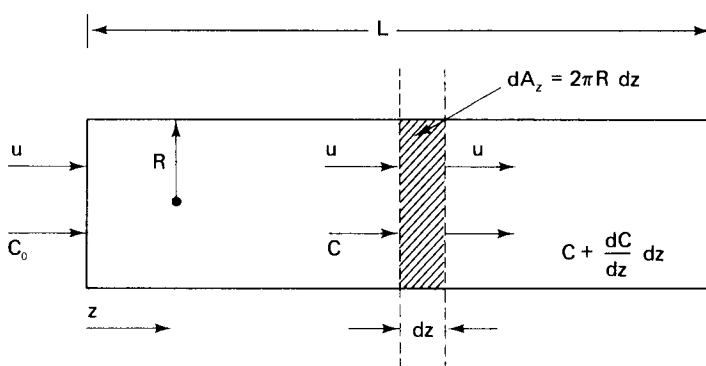


Figure 4.7 Plug-flow model.

where

$$\text{tracer input} = uCA$$

$$\text{tracer output} = uA \left( C + \frac{dC}{dz} \cdot dz \right)$$

$$\text{tracer accumulation} = A \, dz \, \frac{dC}{dt}$$

Equating the terms,

$$uCA - uA \left( C + \frac{dC}{dz} \cdot dz \right) = A \, dz \, \frac{dC}{dt}$$

or

$$-u \frac{dC}{dz} = \frac{dC}{dt} \quad (4-37)$$

with the initial and boundary conditions

$$t < 0; \quad z = 0; \quad C = 0$$

$$t > 0; \quad z = 0; \quad C = C_0$$

$$t = 0; \quad z > 0; \quad C = 0$$

$$t = 0; \quad z < 0; \quad C = C_0$$

Now it may be reasonable on the basis of the assumptions above to consider that this model conforms to the response illustrated in Figure 4.3a. Indeed, this is so; thus, following up on equation (4-37) we can say that

$$C(t, z) = C_0[t - (z/u)] \quad (4-38)$$

$$C_{out}(t) = C(t, L) = C_0(t - \bar{t}) \quad (4-39)$$

From the boundary condition at the entrance

$$C_0(t) = \delta(t) \quad (4-40)$$

where  $\delta(t)$  is just the step-function representing the condition. The outlet response must then be  $\delta(t - \bar{t})$ , and the solution for tracer at the exit is

$$C = 0; \quad t < \frac{L}{u}; \quad C = C_0; \quad t > \frac{L}{u} \quad (4-41)$$

which is the step-function response of Figure 4.3.

The specific mixing assumptions involved in this model are the absence of mixing in the axial direction, and uniformity of concentration and velocity in the radial direction.

#### 4.3.2 Plug Flow: The Reactor Model

We must make several modifications to the plug-flow mixing model in order to turn it into the corresponding reactor model. First, since our primary interest will be in the steady-state behavior of the reactor, the time-dependent accumulation term need not be included and the corresponding initial condition disappears. Second, since

there is now a chemical reaction occurring in the reactor, a term expressing the disappearance of reactants (or appearance of products) due to reaction must be added. Third, we are not dealing with a tracer experiment here, so the concentration  $C$  will refer to that of the reactant or product to which the chemical rate pertains and for which the mass balance is written. Thus,

$$\begin{aligned} \text{input} &= uCA \\ \text{output} &= uA \left( C + \frac{dC}{dz} \cdot dz \right) + (-r)A dz \end{aligned}$$

where  $C$  is the concentration of reactant or product, and  $(-r)$  is the rate of reaction per unit volume. Equating input to output for steady-state operation,

$$uCA - uA \left( C + \frac{dC}{dz} \cdot dz \right) - (-r)A dz = 0$$

which, upon simplification becomes

$$-u \frac{dC}{dz} = -r \quad (4-42)$$

The rate of reaction term,  $(-r)$ , as employed in equation (4-42) is a net positive quantity if  $C$  refers to reactant, negative if  $C$  refers to product. Note that the rate equations of Chapter 1 were written as  $(r)$  or  $(-r) = \dots$ , so that for specified kinetics these may be substituted directly into the conservation expression of equation (4-42). The reactor balance inlet condition specifies  $C = C_0$  (normally reactant) at  $z = 0$ . The rate of reaction is a function of  $C$ , so it is convenient to rearrange (4-42) to

$$\frac{dC}{(-r)} = -\frac{dz}{u} \quad (4-43)$$

which can be partially integrated to

$$\int_{C_0}^C \frac{dC}{(-r)} = -\frac{L}{u} \quad (4-44)$$

The integrated form of the left-hand side of this equation depends of course on the form of the rate equation expressing  $(-r)$ . Equation (4-41) is the basic design equation of the *plug-flow reactor* (PFR) model and may be encountered in a number of different forms. The most familiar of these employs the reactor volume,  $\bar{V}$ , instead of length; total mass or molal flow rate,  $F$ ; conversion,  $x$ . This is commonly written

$$\int_{x_0}^x \frac{dx}{(-r)} = \frac{\bar{V}}{F} \quad (4-45)$$

Remember that the rate equation must be consistent with the measure of the extent of reaction employed; if conversion is used,  $(-r)$  must be expressed in terms of  $x$ ; if concentration is used,  $(-r)$  is in terms of  $C$ . If  $F$  is mass flow rate,  $(-r)$  and  $C$  must be in mass units, and so on. Also, equation (4-45) is often used as a pseudo-homogeneous model for two-phase PFR catalytic reactors. In such cases the rate constant contained in  $(-r)$  is usually expressed in terms per volume or weight of catalyst. In the former case,  $\bar{V}$  would refer to catalyst volume and a value for bed porosity would be required to obtain reactor volume. In the latter case, catalyst weight would be

used and we would require the catalyst bulk density to obtain  $V$ . Finally, it is important to remember that  $F$  and  $(-r)$  are keyed to each other not only as to dimension but also as to component. Thus, if a mixture of two reactants is fed to the reactor,  $(-r)$  represents the rate of reaction in terms of one of the reactants and  $F$  is the feed rate of that reactant, not the total feed rate. A good way to keep these details straight is to remember that the reactor design equation is nothing more than a mass balance over the system.

If the feed rate is converted to volumetric units, the inverse of the ratio on the right-hand side of equation (4-45) is termed the *space velocity*,  $SV$ ,

$$\frac{\nu F}{V} = \frac{v}{V} = SV \quad (4-46)$$

with units of reciprocal time. For some unknown reason<sup>3</sup> this inverse measure of things is widely used. It gives the maximum feed rate which can be used per unit volume of reactor in order that a stated conversion level can be attained. If the feed contains material in addition to that for which the reactor mass balance is written, the total feed rate and corresponding density must be used in equation (4-46). Small space velocities mean slow reactions and a corresponding large reactor volume to attain the specified conversion.

The reciprocal of space velocity, the *space time*, is also sometimes employed. One's first thought is to associate this with the residence time. This can be misleading, however, since the space time (defined in terms of inlet conditions) is, in general, equal to the actual residence or contact time within the reactor only if the temperature, pressure, and reaction mixture density are constant throughout the reactor. A generalized expression for the residence time in a PFR can be derived as follows, in terms of molar flow rates:

$$dt = \frac{d\bar{V}}{F[\nu(z)]}$$

where  $\nu(z)$  is the specific volume. The total volumetric flow rate  $F\nu(z)$  may vary along the reactor length (but not across the radius in the PFR model), owing to a change in mols on reaction or variations in temperature or pressure. In this formulation, then, the specific volume is that based on an inlet total feed rate of  $F$  mols/time. If we substitute for  $d\bar{V}$  from the derivative of equation (4-45),

$$d\bar{V} = \frac{F dx}{(-r)}$$

and

$$dt = \frac{dx}{(-r)\nu(z)} \quad (4-47)$$

The true residence time is then

$$t_R = \int_0^x \frac{dx}{(-r)\nu(z)} \quad (4-48)$$

<sup>3</sup> Conversion or concentration, and length or volume should be enough entities to satisfy anyone; why introduce another one? Ah well, "Theirs not to reason why ..."—*Lord Tennyson*.

### 4.3.3 Perfect Mixing: The Mixing Model

The equality of internal- and exit-age distributions for this case implies that each molecule within the system at a given instant has a past history indistinguishable from any other. Its life expectancy within the system is thus independent of when it entered the system, and all molecules or elements have an equal chance of leaving. This can be so only if there is a uniform concentration within the system, which is equal to the concentration at the exit. A working model for this situation is that given in Figure 4.8, consisting of a very well agitated vessel of volume  $\bar{V}$  with a steady volumetric flow rate  $v$ . Again, at time  $t = 0$  a step input of tracer at concentration  $C_0$  is introduced to the system. The unsteady-state mass balance of the tracer is

$$\text{tracer input} = vC_0$$

$$\text{tracer output} = vC$$

$$\text{tracer accumulation} = \bar{V} \frac{dC}{dt}$$

where  $C$  is the uniform tracer concentration within the vessel. Equating the terms,

$$\begin{aligned} \bar{V} \frac{dC}{dt} &= v(C_0 - C) \\ \frac{dC}{dt} + \frac{1}{\bar{t}} C &= \frac{1}{\bar{t}} C_0 \end{aligned} \quad (4-49)$$

where  $\bar{t}$  is the residence time ( $\bar{V}/v$ ) and the limits of integration are  $0 \leq t' \leq t$  and  $0 \leq C' \leq C$ . Carrying out this integration we obtain

$$C = C_0(1 - e^{-t/\bar{t}}) \quad (4-50)$$

which is the exponential response of Figure 4.3. The specific mixing assumptions involved in this model are the spatial uniformity of concentration within the vessel and the equality of exit and internal concentrations. It is seen from Figure 4.5 that

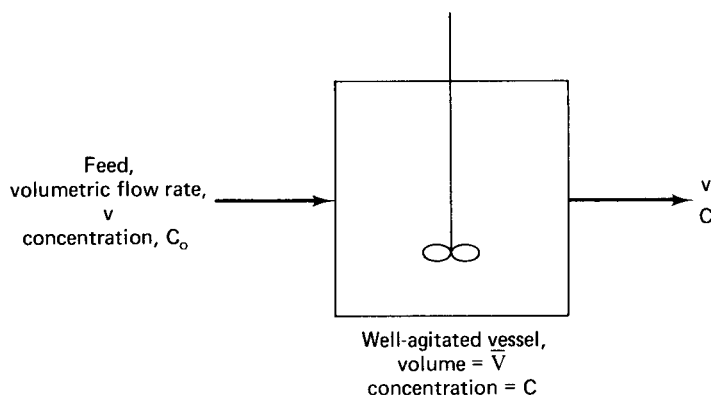


**Figure 4.8** Perfect mixing model.

either combination of macro- and micromixing,  $(\infty, 0)$  or  $(\infty, \infty)$  can lead to the characteristic exponential response of “perfect” mixing.

#### 4.3.4 Perfect Mixing: The Reactor Model

Again we make modifications to the mixing model to obtain the reactor model. These are the assumptions of steady state, the inclusion of a reaction term in the mass balance, and the reference of concentration to that of a reactant or product corresponding to the rate term rather than that of a tracer. The mass balance now becomes

$$\begin{aligned} \text{input} &= vC_0 \\ \text{output} &= vC + (-r)\bar{V} \end{aligned}$$

where the rate of reaction per unit volume,  $(-r)$ , is defined as for the PFR. The result is very simple, since the assumption of concentration uniformity results in an algebraic relationship between inlet and exit compositions.

$$vC_0 = vC + (-r)V$$

or

$$C = C_0 - (-r)\bar{t} \quad (4-51)$$

Equation (4-51) is the basic design equation for what is popularly called a *continuously stirred tank reactor* (CSTR). The derivation assumes equality of volumetric flow rate of feed and effluent; as in the case of the PFR, the residence-time definition must be changed if this is not so. In most applications of the CSTR, however, reactions in the liquid phase are involved and volume changes with reaction are not important.

#### 4.3.5 Some Additional Ideal Reactor Models

The PFR and CSTR models encompass the extremes of the residence-time distributions shown in Figure 4.3; however the batch reactor and the laminar-flow reactor, both of which we have already mentioned in this chapter, are also types exhibiting a well-defined mixing behavior. The batch reactor is straightforward, since it is simply represented by the perfect mixing model with no flow into or out of the system, and has been treated extensively in Chapter 1.

The laminar-flow reactor with segregation and negligible molecular diffusion of species has a residence-time distribution which is the direct result of the velocity profile in the direction of flow of elements within the reactor. To derive the mixing model of this reactor, let us start with the definition of the velocity profile.

$$u(r_p) = \frac{2v}{\pi R^2} \left[ 1 - \left( \frac{r_p}{R_0} \right)^2 \right] \quad (4-52)$$

where  $R_0$  is the radius of the tube,  $r_p$  the radial position at which the velocity  $u(r_p)$  is determined, and  $v$  again the volumetric flow rate. For length  $L$  of tubing the residence time  $t(r_p)$  corresponding to  $u(r_p)$  is

$$t(r_p) = \frac{L}{u(r_p)} \quad (4-53)$$

and the average residence time  $\bar{t}$  is

$$\bar{t} = \frac{L}{\bar{u}}$$

with the average velocity  $\bar{u} = (v/\pi R_0^2)$ . Solving equations (4-52) and (4-53) for  $r_p$ ,

$$r_p = R_0 \sqrt{1 - L/\bar{u}t} = R_0 \sqrt{1 - \bar{t}/2t}$$

Now

$$F(t) = \frac{C}{C_0} = \frac{\int_0^{r_p} 2\bar{u}[1 - (r_p/R_0)^2](C)2\pi r_p dr_p}{\int_0^{R_0} uC(2\pi r_p) dt_p} \quad (4-54)$$

or

$$F(t) = \frac{1}{\pi R_0^2 \bar{u}} \int_0^{f(t)} 2\bar{u}[1 - (r_p/R_0)^2](2\pi r_p) dr_p$$

where  $f(t) = R_0[1 - \bar{t}/2t]^{1/2}$ . Evaluation of this integral yields the residence-time and exit age distribution functions as

$$F(t) = 1 - 0.25(\bar{t}/t)^2 \quad (4-55)$$

$$E(t) = d[F(t)]/dt = (\bar{t})^2/2t^3 \quad (4-56)$$

A comparison of the laminar-flow residence time distribution with corresponding plug flow and perfect mixing results is shown in Figure 4.9.

The reactor model for laminar flow is similar to that for plug flow, except for the radial dependence of velocity. The analog of equation (4-42) is

$$-u(r_p) \frac{dC(r_p)}{dz} = (-r)$$

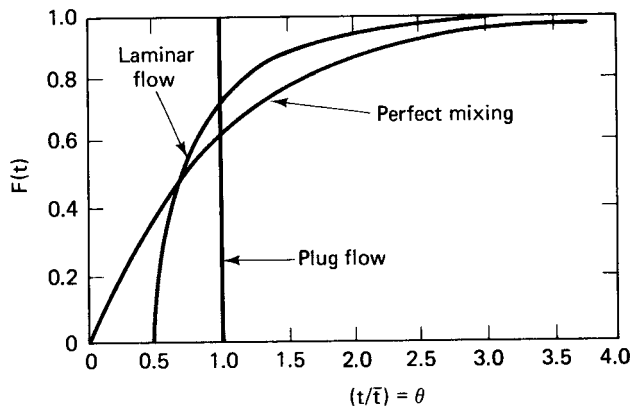


**Figure 4.9** Comparison of plug flow, perfect mixing, and laminar flow residence-time distributions.



This is integrated for the position-specific concentration  $C(r_p)$  as

$$\begin{aligned} \int_{C_0}^C \frac{dC(r_p)}{(-r)} &= \frac{L}{u(r_p)} = \frac{\pi R_0^2 L}{2v[1 - (r_p/R_0)^2]} = \int_0^x \frac{dx(r_p)}{(-r)} \\ &= \frac{\bar{V}}{2v[1 - (r_p/R_0)^2]} \end{aligned} \quad (4-57)$$

The solution of equation (4-57) explicitly for exit concentration depends on the form of the rate law. When an explicit solution is obtained the value of  $C(r_p)$  must be averaged over the exit cross section to determine the average exit concentration  $\langle C \rangle$ :

$$\langle C \rangle = \frac{\int_0^{r_0} u(r_p) C(r_p) r_p dr_p}{\int_0^{R_0} u(r_p) r_p dr_p} \quad (4-58)$$

#### 4.4 Applications of Ideal Reactor Models

In each case of Section 4.3 the reactor models obtained on the basis of the mixing models were left in general form, with specific results for concentration or conversion versus reactor size depending on the type of rate law to be used. In the following we shall derive a number of expressions for particular rate laws which relate conversion, reactor size, and residence time for the particular case of homogeneous, isothermal ideal reactors.

##### 4.4.1 Plug-Flow Reactors

For the plug-flow reactor there is a formal analogy with the batch reactor equations derived in Chapter 1 if there is no volume change on reaction. As an example, consider the PFR design equation, (4-45), written for first-order irreversible kinetics ( $A \rightarrow B$ ).

$$\frac{\bar{V}}{F_A^\circ} = \int_0^x \frac{dx}{-r}$$

with  $(-r) = kC_A$  in mols A/time-volume.  $F_A^\circ$  is the entering molal feed rate of A, no B is present in the feed, and  $x$  is the conversion defined as the ratio of mols reacted to mols fed. Thus,

$$x = \frac{F_A^\circ - F_A}{F_A^\circ} = 1 - \frac{F_A}{F_A^\circ} \quad (4-59)$$

Now we have the following relationships among the various molal flow rates and the constant total flow

$$\begin{aligned} F_A &= F_A^\circ(1 - x) \\ F_T &= F_A + F_B = F_A^\circ(1 - x) + F_A^\circ x = F_A^\circ \end{aligned}$$

where  $F_T$  is total molal flow. If the specific volume of the reaction mixture is  $\nu$  volume/mol, the reactant concentration at any point can be written in terms of the conversion.

$$C_A = \frac{F_A}{F_A^\circ \nu} = \frac{1-x}{\nu} \quad (4-60)$$

and

$$(-r) = \frac{k(1-x)}{\nu} \quad (4-61)$$

Substitution into the PFR equation gives

$$\frac{\bar{V}}{F_A^\circ} = \int_0^x \frac{\nu dx}{k(1-x)}$$

which integrates directly to

$$\frac{\bar{V}}{F_A^\circ} = -\frac{1}{k} \ln(1-x) \quad (4-62)$$

The left side of equation (4-62) is just the residence time,  $t_R$ , so that

$$t_R = -\frac{1}{k} \ln(1-x) \quad (4-63)$$

which is identical to the result given in Chapter 1 for a homogeneous batch reactor.

Corresponding derivations for the second-order irreversible cases  $2A \rightarrow C + D$  or  $A + B \rightarrow C + D$  yield (assuming equimolal amounts of A and B in the feed in the second case)

$$t_R = \frac{\nu}{k} \cdot \frac{x}{1-x} \quad (4-64)$$

which is again directly comparable to the batch results of Chapter 1.

Volume changes on reaction can be accounted for by writing explicitly the dependence of concentration on conversion. As an example, consider the first-order reaction  $A \rightarrow C + D$ . Here total mols are

$$F_T = F_A^\circ(1-x) + 2F_A^\circ x = F_A^\circ(1+x)$$

assuming no C or D in the feed. The corresponding concentration of reactant A is

$$C_A = \frac{F_A^\circ(1-x)}{F_A^\circ(1+x)\nu}$$

and

$$\int_0^x \frac{dx}{(-r)} = \int_0^x \frac{\nu(1+x)dx}{k(1-x)} \quad (4-65)$$

$$t_R = \frac{1}{k} [-2\ln(1-x) - x] \quad (4-66)$$

**Table 4.1** Plug-Flow Reactor Conversion/Residence-Time Relationships

---

 1.  $n$ th-order irreversible reaction:  $A \rightarrow \beta$  products

$$t_R = \frac{1}{\nu} \int_0^x \frac{dx}{k C_A^n} = \frac{v^{n-1}}{k} \int_0^x \frac{(1 + \epsilon x)^n dx}{(1 - x)^n}$$

2. Zero-order irreversible reaction:

$$t_R = \frac{1}{\nu} \int_0^x \frac{dx}{k} = \frac{x}{k\nu}$$

3. First-order irreversible reaction:

$$t_R = \frac{1}{\nu} \int_0^x \frac{dx}{k C_A} = -\frac{1 + \epsilon}{k} \ln(1 - x) - \frac{\epsilon x}{k}$$

4. Second-order irreversible reactions:

$$t_R = \frac{1}{\nu} \int_0^x \frac{dx}{k C_A^2} \text{ or } \frac{1}{\nu} \int_0^x \frac{dx}{k C_A C_B} \quad (C_{A0} = C_{B0})$$

$$= \frac{2\nu\epsilon}{k} (1 + \epsilon) \ln(1 - x) + \frac{\nu\epsilon^2 x}{k} + \frac{\nu(\epsilon + 1)^2}{k} \left( \frac{x}{1 - x} \right)$$

5. First-order reversible reaction:  $A \rightleftharpoons \beta B$  ( $k_1$  forward,  $k_2$  reverse)

$$t_R = \frac{\epsilon x}{k_1 \alpha} - \frac{\alpha + \epsilon}{k_1 \alpha^2} \ln(1 - \alpha x)$$

$$\alpha = 1 + \frac{k_2}{k_1} (1 + \epsilon)$$

6. General  $n$ th-order irreversible reaction with no volume change:

$$1 - x = [1 + (n - 1) C_0^{n-1} k t_R]^{1/(1-n)}$$


---

General expressions for PFR  $t_R - x$  relationships, in terms of the volume change factor  $\epsilon$  defined in Chapter 1, are summarized in Table 4.1 for a number of rate expressions.

Plug-flow reactors are often employed in the laboratory for the measurement of reaction rates. Most often, such application is made for heterogeneous gas/solid catalytic reactions; however, the general methods of the procedure do not differ substantially between homogeneous and heterogeneous systems. The experiments normally consist of measuring in a series of runs the conversion of reactant (and product distribution in complex reactions) as a function of residence time or space velocity in the reactor. Each run is made at constant temperature, total pressure or composition and inlet reactants ratio. Similar experiments are repeated until the entire range of temperature, composition, and pressure of interest have been investigated. If the conversions are high, conversion-time data may be interpreted in terms of relationships such as those of Table 4.1, or corresponding forms written for space velocity, according to the convenience of the experimenter, using procedures analogous to those described in Chapter 1. The PFR is then described as an *integral reactor*, since the measured conversions are the integral result of the reaction kinetics over a range of reaction mixture compositions. If the conversion is kept at a very low

level in experimentation,  $dx$  may be approximated by the small  $\Delta x$ , and equation (4-45), for example, becomes

$$\frac{\Delta x}{(-r)} = \frac{\bar{V}}{F}$$

which can be solved directly for the rate of reaction:

$$(-r) = \left( \frac{F}{\bar{V}} \right) \Delta x \quad (4-67)$$

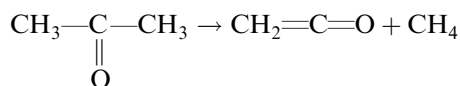
In this application the PFR is termed a *differential reactor*.

Direct rate measurements are always preferable if one is trying to determine the form of reaction kinetics, reaction orders, rate constants, and so on, as pointed out in Chapter 1. There are, though, a number of practical operational difficulties in the utilization of differential reactor techniques which somewhat limit their utility. A primary difficulty is the precise measurement of very small differences in concentration required by the “differential” conversion level—a consideration that also requires one to define what conversion level is satisfactory in approximating “differential”. If the form of the rate equation has been established and one is merely trying to determine values for the kinetic constants, the errors involved in the differential conversion approximation may be estimated by comparison of results from the differential and integral forms of the appropriate PRF equation. A second operational difficulty, which is also involved in integral reactor applications, is the experimental balance act required to vary independently  $t_R$  or  $(\bar{V}/F)$  while maintaining convenient or required conversion levels and ensuring the ideal flows required for analysis of the data in terms of the PFR model. This last strictly refers only to integral operation, for at sufficient low conversions the effects of nonideal flows, as will be seen, become small. Further problems with integral reactor operation may arise from the appearance of gradients of temperature or pressure associated with low or high space velocities.

When these considerations are appended to other restrictions that we shall discuss later concerning inter- and intraphase gradients of temperature and concentration in heterogeneous reactions, it is clear that successful utilization of the laboratory PFR for measurement of intrinsic kinetics is often a delicate matter. There exist a large number of kinetic data, particularly in the older literature, which are unreliable because the experimental compromises required were not recognized. It may seem surprising that many difficulties have been with the most obvious symptoms, such as temperature gradients. This is not surprising, however, after one has had some experience with reactions of, say,  $(-\Delta H_R) = 50 \text{ kcal/mol}$ .

### Illustration 4.3

The following conversion data were obtained in a tubular flow reactor for the pyrolysis of acetone at 520 °C and 1 atm to form ketene:



Flow rate (g/hr)	Fraction decomposed at exit
130	0.05
50	0.13
21	0.24
10.8	0.35

The tubular reactor employed in the investigation was 3.3 cm in inside diameter and 80 cm long. What rate equation would you propose for this reaction based on this data?

*Solution*

Reactor dimensions are i.d. 3.3 cm with a length of 80 cm. The volume is

$$\bar{V} = (\pi/4)d^2L = 685 \text{ cm}^3$$

Now for the reaction kinetic analysis the procedure is not much different from that illustrated in Chapter 1. We have to assume a reasonable rate equation and see if the data interpretation according to that equation is internally consistent. Starting with the simplest logical assumption here, we use  $A \rightarrow B + C$ , rate constant  $k$ , as the prototype. This will be first-order irreversible, but with a volume change on the conversion of acetone (A).

$$\frac{\bar{V}}{F_A^\circ} = \int_0^x \frac{dx}{kC_A} \quad (\text{i})$$

At time  $t$  a molal balance gives, on the basis of one mol of feed,

$$A = 1 - x$$

$$B = x$$

$$C = x$$

$$\text{Total mols} = (1 + x)$$

$$\text{Total volume} = \nu(1 + x)$$

where  $\nu$  is the molal volume of the reaction mixture. The concentration of A at time  $t$  is

$$C_A = \frac{(1 - x)}{[\nu(1 + x)]}$$

so in equation (i) we have

$$\frac{\bar{V}}{F_A^\circ} = \int_0^x \frac{\nu(1 + x) dx}{k(1 - x)} \quad (\text{ii})$$

$$\frac{\bar{V}}{F_A^\circ} = \left(\frac{\nu}{k}\right)[-2 \ln(1 - x) - x] \quad (\text{iii})$$

Thus, we should expect linearity in a plot of  $(V/F_A^\circ)$  versus  $[-2\ln(1-x) - x]$ . From the data,

$F_A^\circ$	$(V/F_A^\circ)$	$x$	$[-2\ln(1-x) - x]$
2.24	306	0.05	0.053
0.66	795	0.13	0.148
0.36	1892	0.24	0.309
0.19	3685	0.35	0.512

where the units of  $F_A^\circ$  are mols/h and the molecular weight of the feed, acetone, is 58 g/gmol.

A plot of these results is shown in Figure 4.10. The first-order plot is given in Figure 4.10a, and one can see that there is an approximate correlation to the values obtained from the experiment. However, look at Figure 4.10b. This is a least-squares polynomial fit to the data, and it obviously shows a trend with the logarithmic function of equation (iii). The question is whether we go back and reformulate the rate equation to test another form, or do we leave the interpretation as is, admitting

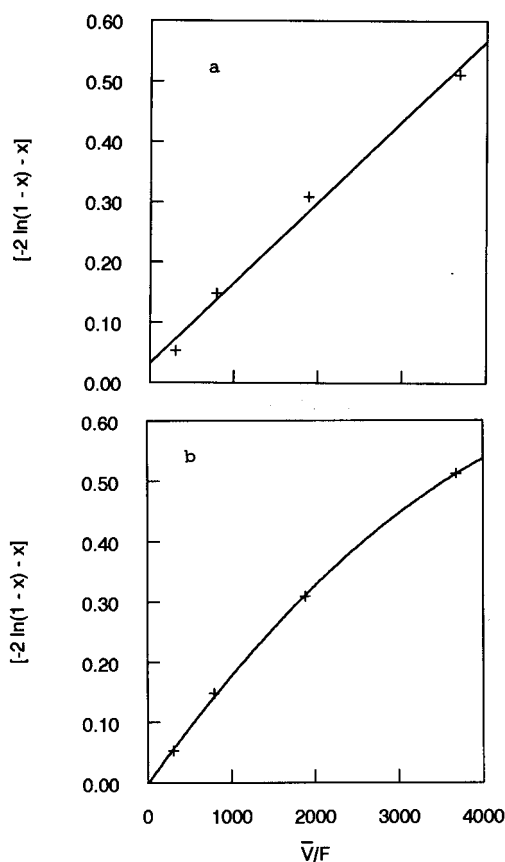


**Figure 4.10** Data analysis for acetone pyrolysis. (a) First order; (b) curve fit.

that the reaction is probably not first-order irreversible, but also being willing to tolerate a little  $\pm$ ? The first thought might be to leave the matter as is, within the range considered and *forbidding extrapolation*.

The trouble is that people *love to extrapolate*. It is dead certain that sooner or later someone is going to want to know how the reactor will operate at  $(\bar{V}/F)$  of, say, 6000. It is sure that the first-order model won't work, and even extrapolation of the polynomial fit is dangerous. The only safe thing to do is rework the model, including an experimental result at  $(\bar{V}/F)$  of 6000.

With the data given here, one finds indeed that a correlation based on second-order irreversible kinetics, with a rate constant of about  $8.7 \times 10^5 \text{ cm}^3/\text{gmol}\cdot\text{h}$  gives a satisfactory fit over the range investigated. This is not surprising, since the reaction goes by a thermal chain mechanism, which, as seen in Chapter 1 can lead to a variety of kinetic possibilities. Even at that, one would hesitate to extrapolate the interpretation to 6000 without some additional evidence.

This rather verbose discussion has to do with saying that, in such interpretations, there is really no right or wrong answer. The answer to this question lies in the use in which the result will be employed.



HORATIO SAYS

Derive the appropriate second-order irreversible reaction result (don't forget volume change) and show that it gives a better fit than first-order. In fact, write out a plausible chain-reaction mechanism that gives second-order fit with respect to acetone.

#### 4.4.2 Continuously stirred tank reactors

The analysis of the CSTR is simpler than for the PFR, since the basic relationship between concentration or conversion and rate is an algebraic rather than a differential one. Utilization of the CSTR also offers some advantages over the PFR in terms of ease of control and steady operation resulting from the well-mixed state within the reactor. There is also a significant disadvantage, however; for positive-order kinetics the reaction occurring always goes at the slowest possible rate, that is, at the rate corresponding to the concentration level of the reactant in the product stream. This disadvantage can be compensated by putting several CSTR in series rather than using a single reactor of larger volume. In view of this, the analysis of CSTR sequences, as well as that of the single reactor, is important.

For a first-order irreversible reaction  $A \rightarrow B$ , equation (4-51) becomes

$$C = C_0 - kC\bar{t}$$

and solving for the exit concentration  $C$ ,

$$\frac{C}{C_0} = \frac{1}{1 + k\bar{t}} \quad (4-68)$$

The substitution of  $(-r) = kC$ , with  $C$  the exit concentration, is the result of the mixing state within the reactor.

For second-order kinetics,  $2A \rightarrow C + D$ , a similar treatment yields

$$C = C_0 - kC^2\bar{t}$$

and

$$C = \frac{-1 + \sqrt{1 + 4k\bar{t}C_0}}{2k\bar{t}} \quad (4-69)$$

A summary of results for several simple-order rate equations is given in Table 4.2. The effect of volume changes on reaction is presumed negligible in these results. Note that in the general  $n$ th-order case and the second-order reaction between different reactants, it is not possible to obtain an explicit solution for the exit concentration. This leads to some difficulty in the analysis of CSTR sequences, as seen below.

CSTR are often employed for polymerization reactions, and owing to the special nature of the kinetics of the chain reactions involved, the analysis is changed somewhat from the above. Let us consider the following chain for the conversion of monomer  $M$  into a series of polymeric products  $R_j$ , similar to a

**Table 4.2** CSTR Conversion/Residence-Time Relationships—Single Reactors

- 
1.  $n$ th-order irreversible reaction:  $A \rightarrow \beta$  products

$$\frac{C}{C_0} = \frac{1}{1 + kC^{n-1}\bar{t}}$$

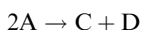
2. Zero-order irreversible reaction:

$$C = C_0 - k\bar{t}$$

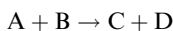
3. First-order irreversible reaction:

$$\frac{C}{C_0} = \frac{1}{1 + k\bar{t}}$$

4. Second-order irreversible reactions:



$$C = \frac{1 - 1 + \sqrt{1 + 4k\bar{t}C_0}}{2k\bar{t}}$$



$$\frac{C_A}{C_{A_0}} = \left( 1 + \frac{kC_{B_0}\bar{t}}{(1 + kC_A\bar{t})} \right)^{-1}$$

$$\frac{C_B}{C_{B_0}} = \frac{1}{(1 + kC_A\bar{t})}$$

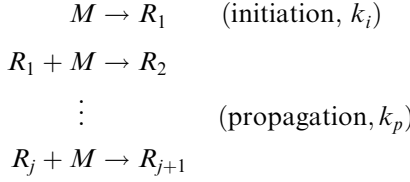
5. First-order reversible reaction:  $A \rightleftharpoons B$  ( $k_1$  forward,  $k_2$  reverse)

$$C_A = \frac{C_{A_0}}{1 + k_1\bar{t} + k_2\bar{t}} + \frac{k_2\bar{t}(C_{A_0} + C_{B_0})}{1 + k_1\bar{t} + k_2\bar{t}}$$


---



chain transfer reaction



The rates of initiation and propagation are, respectively,

$$\begin{aligned}
 -r_i &= k_i C_M \\
 -r_j &= k_p C_{R_j} C_M
 \end{aligned}$$

where the propagation rate constants are the same for each step. For the monomer, the rate of reaction to be substituted into equation (4-51) is

$$-r_M = k_i C_M + k_p C_M \sum_{j=1}^{\infty} C_{R_j}$$

and the CSTR material balance is

$$\frac{C_{M_0} - C_M}{\bar{t}} = k_i C_M + k_p C_M \sum_{j=1}^{\infty} C_{R_j} \quad (4-70)$$

In order to calculate the conversion of monomer, we must determine a value for  $\sum C_{R_j}$  in equation (4-70). This can be done by writing balances for each of the  $R_j$  and determining their sum. For  $R_1$ ,

$$-r_1 = -k_i C_M + k_p C_{R_1} C_M \quad (4-71)$$

Substitution in equation (4-51) gives

$$k_i C_M = \frac{C_{R_1}}{\bar{t}} + k_p C_{R_1} C_M \quad (4-72)$$

and in general

$$k_p C_M C_{R_{j-1}} = \frac{C_{R_j}}{\bar{t}} + k_p C_{R_j} C_M \quad (j = 2, \dots, \infty) \quad (4-73)$$

Upon adding the balances for all individual species, equations (4-72) and (4-73) give

$$k_i C_M = \sum_{j=1}^{\infty} \frac{C_{R_j}}{\bar{t}} \quad (4-74)$$

Substituting equation (4-74) into (4-70) gives the final expression for concentration of monomer

$$\begin{aligned}
 C_{M_0} - C_M &= k_i \bar{t} C_M + k_i k_p \bar{t}^2 C_M^2 \\
 C_M &= \frac{-(k_i \bar{t} + 1) + \sqrt{(k_i \bar{t} + 1)^2 + 4k_i k_p \bar{t}^2 C_{M_0}}}{2k_i k_p \bar{t}}
 \end{aligned} \quad (4-75)$$

By sequential substitution for  $C_{R_{j-1}}$  in the series of CSTR balance equations (4-72) and (4-73), we can also determine the concentrations of the individual products,  $C_{R_j}$ , as

$$C_{R_j} = \frac{k_i}{k_p} \left[ 1 + \frac{1}{k_p \bar{t} C_M} \right]^{-j} \quad (4-76)$$

The weight distribution,  $d_j$ , of the total polymeric product may be calculated from the ratio of the amount of  $R_j$  produced to the amount of monomer reacted

$$d_j = \frac{C_{R_j}(jW_M)}{(C_{M_0} - C_M)W_M} \quad (4-77)$$

where  $W_M$  is the molecular weight of the monomer and  $jW_M$  the molecular weight of polymer molecule,  $R_j$ .

Another specific but important application of the CSTR is in biochemical reactor systems, for both evaluation of kinetic parameters in the laboratory and in commercial operation. The CSTR in such applications is most often referred to as a *chemostat*. Let us consider, then, the analysis for a typical unstructured culture of micro-organisms. Recall the general form of mass balance, equation (4-51),

$$C = C_0 - (r_x)\bar{V}$$

where now  $C_0$  represents a concentration of viable cells in the feed,  $C$  is the concentration in the chemostat and in the exit stream, and  $r_x$  is the rate of cell formation in cells/time-volume. Then

$$v(C_0 - C) + \bar{V}r_x = 0 \quad (4-78)$$

Now if we consider only cell growth processes with no change for maintenance or death, equation (4-78) becomes

$$DC_0 = (D - \mu)C \quad (4-79)$$

where  $D$  is the *dilution rate*  $= v/\bar{V}$  and  $\mu$  is the specific growth rate,  $r_x/C$ . The dilution rate is the number of reactor volumes that pass through the reactor per unit time, and we recognize this parameter as just the inverse of the holding time  $\bar{t}$ . Often the value of  $C_0 = 0$ , and the feed (containing nutrient) is referred to as *sterile*. In such an event,

$$DC_0 = 0 = (D - \mu)C \quad (4-80)$$

which is satisfied only when  $D \geq 0$  if there is to be a finite cell concentration in the effluent. This is an interesting result, since it doesn't appear that  $C$  can be well-defined from equation (4-79). This has been observed experimentally, but also has been shown to occur only when the specific growth rate is independent of cell concentration  $C$  and the substrate (nutrient) concentration  $S$ . If a particular substrate is growth-limiting, then we get rid of the intermediate  $C$ . For example, recall Monod's model, equations (3-74) and (3-75)

$$\mu = \frac{\mu_m S}{K_s + S} \quad (3-74)$$

and

$$\frac{dS}{dt} = -\left(\frac{1}{Y}\right) = \frac{\mu_m CS}{K_s + S} \quad (3-75)$$

where the yield coefficient,  $Y$ , is defined as the mass of cells formed per mass of substrate consumed. Then equation (4-79) becomes

$$\left(\frac{\mu_m S}{K_s + S} - D\right)C + DC_0 = 0 \quad (4-81)$$

The substrate mass balance is

$$D(S_0 - S) - \frac{\mu_m SC}{Y(K_s + S)} = 0 \quad (4-82)$$

For the common case of sterile feed,  $C_0 = 0$ , these equations give

$$C = Y\left(S_0 - \frac{DK_s}{\mu_m - D}\right) \quad (4-83)$$

$$S = \left(\frac{DK_s}{\mu_m - D}\right) \quad (4-84)$$

and there is obviously a well-defined steady state of operation.

The kinetics employed in the Monod model, however, lead to some interesting behavior. For low flow rate  $D \rightarrow 0$ , one obtains the expected result that nearly all the nutrient is consumed and thus  $C \rightarrow (S_0/Y)$ . Conversely, as the dilution rate  $D \rightarrow \mu_m$ ,  $C \rightarrow 0$ . In this latter case  $D$  is greater than the maximum growth rate; this condition is termed *washout*. The governing condition is easily determined from equation (4-83) with  $C = 0$ ,

$$D_{max} = \frac{\mu_{max} S_0}{K_s + S_0} \quad (4-85)$$

An informative example of the general patterns of behavior of the chemostat upon variation of  $D$  has been given by Bailey and Ollis [J.E. Bailey and D.F. Ollis, *Biochemical Engineering Fundamentals*, McGraw-Hill Book Co., New York, NY, (1977)] and is shown in Figure 4.11 for a typical set of parameters. Note that the reactor is very sensitive to changes in  $D$  when operation is at conditions near wash-out. This sensitivity becomes particularly important if one wishes to maximize the amount of biomass effluent from the reactor,  $CD$ . Here of course the requirement is

$$\frac{d(CD)}{dD} = 0 \quad (4-86)$$

which yields

$$D_{max} = \mu_m \left[ 1 - \left( \frac{K_s}{K_s + S_0} \right)^{1/2} \right] \quad (4-87)$$

Often  $S_0 \gg K_s$ , under which condition  $D_{max} \rightarrow \mu_s$  and the operation is near wash-out. This is a very good example of the parametric sensitivity of the reactor(s), which is a topic we will explore in more detail later.

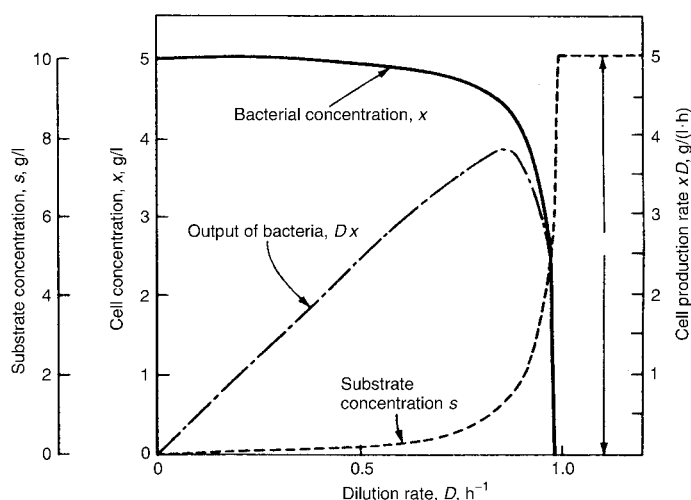


**Figure 4.11** Dependence of  $S$ ,  $C$  and  $(CD)$  on continuous culture dilution rate according to the Monod model for  $\mu_m = 1 \text{ h}^{-1}$ ,  $K_s = 0.2 \text{ g/l}$ ,  $Y = 0.5$ . (From J.E. Bailey and D.F. Ollis, *Biochemical Engineering Fundamentals*, with permission of McGraw-Hill Book, Co., New York, NY, (1977).)

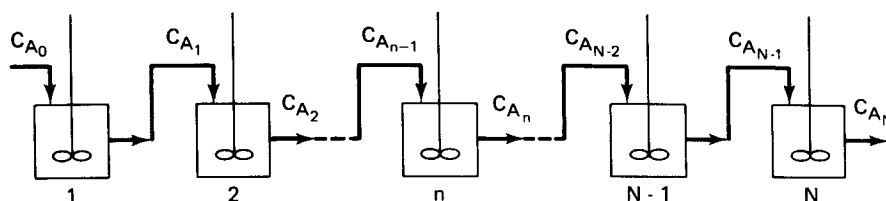
### 4.3.3 CSTR Sequences

Let us now consider a series sequence of CSTR of equal volumes ( $\bar{t}$  uniform) and operating at the same temperature (rate constants uniform), as shown in Figure 4.12.

For the first-order irreversible reaction, the relationship of equation (4-68) applies to each reactor of the sequence, where we will now include a subscript on the concentration denoting position in the sequence. Thus,

$$\frac{C_{A1}}{C_{A0}} = \frac{1}{1 + k_1 \bar{t}} = \frac{1}{1 + k \bar{t}}$$

$$\frac{C_{A2}}{C_{A1}} = \frac{1}{1 + k \bar{t}}$$



$$k_1 = k_2 = \dots k_n = \dots = k_N$$

$$r_i = k_1 C_{A_i}$$

$$\bar{t}_1 = \bar{t}_2 = \dots \bar{t}_n = \dots = \bar{t}_N$$

**Figure 4.12** CSTR sequence for the reaction  $A \rightarrow B$ .

and so on. Obviously, the exit concentration from vessel 2 can be related to the feed concentration to the CSTR series by multiplication of the equations above.

$$\frac{C_{A_2}}{C_{A_0}} = \frac{1}{(1 + k\bar{t})^2} \quad (4-88)$$

Or, in general

$$\frac{C_{A_n}}{C_{A_0}} = \frac{1}{(1 + k\bar{t})^n} \quad (4-89)$$

Conversion in the sequence is

$$x_n = 1 - \frac{C_{A_n}}{C_{A_0}} = 1 - \frac{1}{(1 + k\bar{t})^n} \quad (4-90)$$

If the restriction of equal residence times and rate constants is removed, then

$$x_n = 1 - \frac{1}{\prod_{j=1}^n (1 + k_j \bar{t}_j)} \quad (4-91)$$

The difficulties of this type of analysis for reactions other than first order can be illustrated by the following example for the second-order reaction  $2A \rightarrow C + D$ . We can generalize the result of Table 4.2 to the form

$$\frac{C_{A_{n-1}}}{C_{A_n}} = 1 + k\bar{t}C_{A_n}$$

leading, for example, to

$$\frac{C_{A_0}}{C_{A_2}} = (1 + k\bar{t}C_{A_2})(1 + k\bar{t}C_{A_1})$$

Now, we would like to eliminate  $C_{A_1}$  in terms of the feed concentration,  $C_{A_0}$ :

$$\frac{C_{A_0}}{C_{A_2}} = (1 + k\bar{t}C_{A_2})[1 + k\bar{t}C_{A_2}(1 + k\bar{t}C_{A_2})]$$

If we continue for  $C_{A_3}$ ,

$$\begin{aligned} \frac{C_{A_0}}{C_{A_3}} &= \{1 + k\bar{t}C_{A_3}(1 + k\bar{t}C_{A_3})[1 + k\bar{t}C_{A_3}(1 + k\bar{t}C_{A_3})]\} \\ &\quad \cdot \{1 + k\bar{t}C_{A_3}(1 + k\bar{t}C_{A_3})\}(1 + k\bar{t}C_{A_3}) \end{aligned} \quad (4-92)$$

The unwieldy form of such telescoping functions precludes the development of general  $n$ th reactor expressions for higher-order rate laws, so that step-by-step algebraic calculations, or the graphical method described below, are normally employed. In Table 4.3 are given in general form the stepwise mass-balance relationship for a number of rate laws. Further discussion is given in the original derivations [R. B. MacMullen and M. Weber, Jr., *Trans. Amer. Inst. Chem. Eng.*, 31, 409 (1935)] and by Piret and coworkers [J. W. Eldridge and E. L. Piret, *Chem. Eng. Progr.*, 46, 290 (1950) and R. W. MacDonald and E. L. Piret, *Chem. Eng. Progr.*, 47, 363 (1951)]. Also, for a graphical solution to some of these relationships, see Schoenemann [K. Schoenemann, *Dechema Monographien*, 21, 203 (1952)].

**Table 4.3** Recursion Formula for Series CSTR

---

<i>Irreversible reactions</i>	
1. Zero order: $A \rightarrow \text{products}$	$\frac{C_{A_{n-1}}}{C_{A_n}} = 1 + \frac{k\bar{t}_n}{C_{A_n}}$
2. First order: $A \rightarrow \text{products}$	$\frac{C_{A_{n-1}}}{C_{A_n}} = 1 + k\bar{t}_n$
3. Second order: $2A \rightarrow \text{products}$ or $A + B \rightarrow \text{products}$	$\frac{C_{A_{n-1}}}{C_{A_n}} = 1 + k\bar{t}_n C_{A_n}$
4. Second order: $A + B$ (stoichiometric excess) $\rightarrow \text{products}$	$\frac{C_{A_{n-1}}}{C_{A_n}} = 1 + k(E + C_{A_n})\bar{t}_n$ $C_{B_n} = (E + C_{A_n}), \quad E = C_{B_0} - C_{A_0}$
<i>Reversible reactions</i>	
1. First order: $A \rightleftharpoons B$	$\frac{C_{A_{n-1}}}{C_{A_n}} = 1 + \left[ k_1 + k_2 \left( 1 - \frac{C_{A_0}}{C_{A_n}} \right) \right] \bar{t}_n$
2. Second order/first order: $2A \rightleftharpoons B$	$\frac{C_{A_{n-1}}}{C_{A_n}} = 1 + \left[ k_1 C_{A_n} + \frac{k_2}{2} \left( 1 - \frac{C_{A_0}}{C_{A_n}} \right) \right] \bar{t}_n$
3. Second order/first order: $A + B \rightleftharpoons C$	$\frac{C_{A_{n-1}}}{C_{A_n}} = 1 + \left[ k_1(E + C_{A_n}) + k_2 \left( \frac{1 - C_{A_0}}{C_{A_n}} \right) \right] \bar{t}_n$ $C_{B_n} = (E + C_{A_n})$
4. Second order/second order: $A + B \rightleftharpoons C + D$	$\frac{C_{A_{n-1}}}{C_{A_n}} = 1 + \left[ k_1(E + C_{A_n}) - k_2 \frac{(C_{A_0} - C_{A_n})^2}{C_{A_n}} \right] \bar{t}_n$
<i>Some useful general expressions</i>	
1. Zero order: $A \rightarrow \text{products}$	$\frac{C_{A_n}}{C_{A_0}} = 1 - \frac{nk\bar{t}}{C_{A_0}}$
2. First order: $A \rightarrow \text{products}$	$\frac{C_{A_n}}{C_{A_0}} = \frac{1}{(1 + k\bar{t})^n}$
3. First order/first order: $A \rightleftharpoons B$	$C_{A_n} = \alpha^n C_{A_0} + k_2\bar{t}(C_{A_0} + C_{B_0}) \left( \frac{\alpha}{1 - \alpha} - \frac{\alpha^{n+1}}{1 - \alpha} \right)$ $\alpha = (1 + k_1\bar{t} + k_2\bar{t})^{-1}$

---

**Illustration 4.4**

A Type III reaction has been studied in the liquid phase at 150 °C and each step determined to be first-order and irreversible, with  $k_1 = 1.0 \text{ h}^{-1}$  and  $k_2 = 0.6 \text{ h}^{-1}$  at this temperature. A process consisting of three CSTRs of equal volume is contemplated, in which it is wished to maximize the concentration of intermediate leaving the system. What residence time per reactor is required? There is no intermediate or product in the feed.

*Solution*

The reaction sequence here is



and the concentration of A leaving the  $n$ th CSTR, shown in Table 4.3, is

$$\frac{C_{A_n}}{C_{A_0}} = \frac{1}{(1 + k_1 \bar{t})^n} \quad (\text{i})$$

For B in vessel  $n$ ,

$$C_{B_n} - C_{B_{n-1}} = -(-r) \bar{t}$$

$$(-r) = k_1 C_{A_n} + k_2 C_{B_n}$$

In general

$$C_{B_n} - C_{B_{n-1}} = (k_1 C_{A_n} - k_2 C_{B_n}) \bar{t} \quad (\text{ii})$$

In the first CSTR, if we substitute in (ii) the value of  $C_{A_n}$  from (i)

$$C_{B_1} = \frac{C_{B_0}}{1 + k_2 \bar{t}} + \frac{k_1 \bar{t} C_{A_0}}{1 + k_1 \bar{t}} \quad (\text{iii})$$

Applying the recursion relationship of (ii) we obtain for  $C_{B_3}$

$$C_{B_3} = \frac{k_1 C_{A_0}}{(k_2 - k_1)(1 + k_1 \bar{t})^3} - \frac{k_1 C_{A_0}}{(k_2 - k_1)(1 + k_2 \bar{t})^3} \quad (\text{iv})$$

where  $k_1 \neq k_2$ ,  $C_{B_0} = 0$  and  $n = 3$ . For a maximum

$$\frac{dC_{B_3}}{d\bar{t}} = 0$$

$$\frac{k_1 C_{A_0}}{k_2 - k_1} \left[ \frac{3k_2}{(1 + k_2 \bar{t})^4} - \frac{3k_1}{(1 + k_1 \bar{t})^4} \right] = 0$$

Solving for  $\bar{t}$

$$\bar{t} = \frac{(k_1/k_2)^{0.25} - 1}{k_1 - k_2(k_1/k_2)^{0.25}} \quad (\text{v})$$

For  $k_1 = 1 \text{ h}^{-1}$ ,  $k_2 = 0.6 \text{ h}^{-1}$ ,  $C_{B_0} = 0$ , we obtain

$$\bar{t} = 0.426 \text{ h}; \quad (C_{B_3}/C_{A_0}) = 0.393$$

*Note:*

A related problem is: *given a* value for  $\bar{t}$  in each CSTR, what is the value of  $n$  to give a maximum B? The solution to this one is not as simple as one might think. It is incorrect to state that

$$(dC_B/dn) = 0$$

defines a maximum because  $C_B$  is not a continuous function of the number  $n$ ; it is defined only for integer values of  $n$ . Rather, one must use an inequality analysis,

$$C_{B_{n-1}} < C_{B_n} > C_{B_{n+1}}$$

This will be discussed in more detail later on.



HORATIO SAYS

Suppose we set the feed rate and the conversion requirement, but let the vessel volume be a variable. How can this problem be solved for the maximum conversion to intermediate?

The conversion sequence in a series of CSTRs is illustrated in Figures 4.13 and 4.14 for first- and second-order reactions, respectively. The dimensions of the rate constants and of the holding times,  $\bar{t}_n$ , in these figures must correspond, and the inlet concentration, which must be specified for the second order reaction, is set at 3 gmol/l. Otherwise, the results presented are general.

Figure 4.13 also serves to illustrate the answer to a common problem in the design of a CSTR sequence, namely, for a given total residence time how much improvement in conversion can be obtained by increasing the number of units in the sequence. The answer is clearly seen to be dependent upon the relative magnitudes of the rate constant and the total holding time. We see that for  $k \sim 0.1\bar{t}$ , that is, a difference of about one order of magnitude, there is virtually no change in conversion between a single reactor with  $\bar{t} = 1$  and a series of 10 with  $\bar{t}$  in each of 0.1. As the rate constant approaches the total residence time in magnitude, there will be a certain number of reactors for which the conversion may be improved, but with little change beyond this point (for results with  $k = 1.2$  and 1.6 see Figure 4.13).

Qualitatively similar results pertain to the second-order case of Figure 4.14, where the solid line at the top corresponds to the results illustrated in Figure 4.13. For second-order kinetics, however, the conversions within the series depend on the number of reactors (dotted lines), whereas for first-order the conversions within the series are independent of the total number of units.

It might be asked at this point why so much emphasis has been placed on the analysis of CSTR series with equal individual holding times. The reasons turn out to be both economic and, on occasion, esthetic. The equality of residence times does not, in general, maximize conversion for reactions with kinetics other than first order. The analysis of variable residence time, and the more general one of determining both optimal temperature and holding-time sequences can be found elsewhere [R. Aris, *The Optimal Design of Chemical Reactors*, Academic Press, New York, NY (1971); O. Levenspiel, *Chemical Reaction Engineering*, 2 ed., John Wiley and Sons, New York, NY (1972); D. Luss, *Chem. Eng. Sci.*, 20, 17, (1965)].

There are some other points, however, to be considered in determining the length of a CSTR sequence. Obviously, any given conversion can be obtained in a single large reactor as well as in a series of smaller ones (think of irreversible



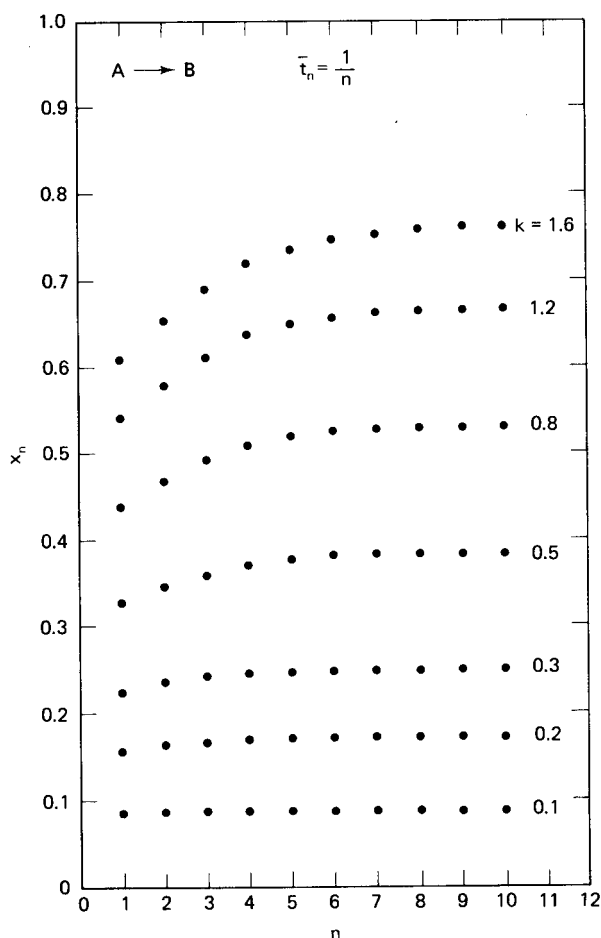


**Figure 4.13** Illustration of the conversion in a series of CSTR for a first-order irreversible reaction with a constant total residence time and a variable number of units in the series. The total residence time is 1 (arbitrary units) and the rate constant is in the same time units.

reactions). The total volume decreases with  $n$ , as indirectly shown by Figures 4.13 and 4.14, but the cost per reactor will change. If we use the 0.6 power scaling law, beloved of design engineers, as a rough guide, the cost per reactor is proportional to  $(\bar{V})^{0.6}$ , and for an  $n$ -unit sequence, proportional to  $n(\bar{V})^{0.6}$ . The total cost for an  $n$ -unit sequence may well have a minimum with respect to  $n$  that can differ from the optimum obtained from an analysis such as that of Illustration 4.4, which is devoid of economics. In practice it is found that most of the decrease in total volume requirement occurs for  $n$  of maybe 3–5, so that long CSTR sequences are infrequently encountered.

The algebraic sequences involved in the computation of series CSTR are also well-suited for simple graphical analysis. If we solve equation (4-51) for the reciprocal of residence time,

$$\frac{1}{\bar{t}} = \frac{(-r)}{(C_0 - C)} \quad (4-93)$$

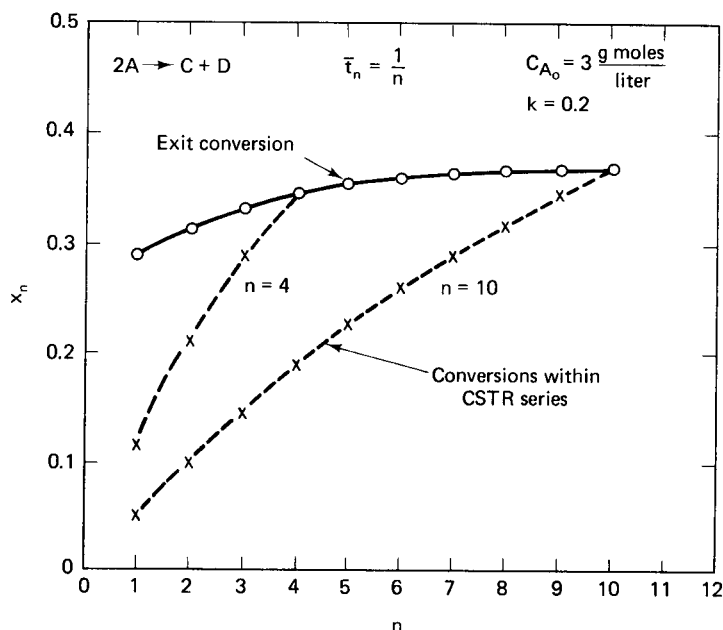


**Figure 4.14** Conversion in a series of CSTR for a second-order irreversible reaction with constant total residence time.

and suppose that we have available information on the dependence of  $(-r)$  on  $C$ , we may then construct a plot as shown in Figure 4.15a. The graphical interpretation of equation (4-93) is shown in Figure 4.15b. Here the quantity  $(-r)/(C_0 - C)$  is the tangent of the angle included between  $(C_0 - C)$ , on the abscissa, and the straight line between the locus of  $C_0$  on the abscissa and  $(-r)$  corresponding to the exit concentration  $C$ , located on the  $(-r) - C$  curve. Thus,  $(1/\bar{t})$  is also the tangent of this angle. For the construction, we start at  $C_0$  on the abscissa a draw a straight line at an angle,  $\arctan(1/\bar{t})$ , from this point to the  $(-r) - C$  curve. The intersection defines the corresponding value of  $(-r)$ , and a vertical line from the intersection to the abscissa determines  $C$ . The extension of this procedure to a sequence of CSTR is easily visualized. In Figure 4.15c the method is illustrated for a sequence of 4 CSTR of differing residence times. If the sequence is not an isothermal one, then a number of  $(-r) - C$  curves for the individual temperature levels involved will be required. This approach is probably not to be recommended for detailed design, but it surely has attractions for rapid preliminary estimates. It does not require a kinetic model, since  $(-r)$  is used directly, and as shown can be used for sequences of variable  $\bar{t}_n$  and  $T_n$  if the necessary data is available.

The single CSTR has been used for many years in the laboratory for the study of kinetics of liquid phase reactions, and is now increasingly being employed for the measurement of gas/solid heterogeneous catalytic kinetics as well [early developments in the latter application are described by J.J. Carberry, *Ind. Eng. Chem.*, 56, 39 (1964); D.J. Tajbl, J.B. Simons and J.J. Carberry, *Ind. Eng. Chem. Fundls.*, 5, 171 (1966). A number of related designs based on internal recirculation of the reaction mixture through a small fixed bed of catalysts may also be treated conceptually as

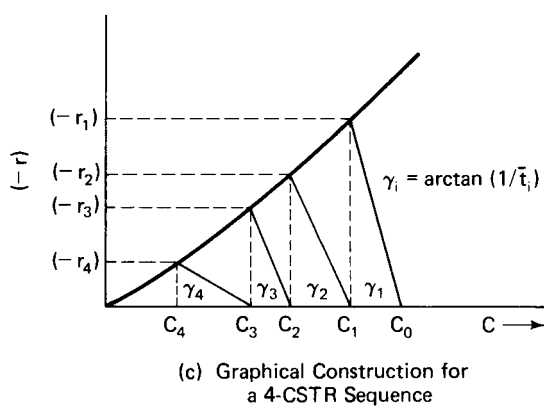
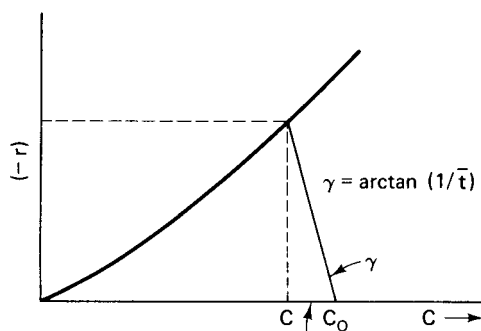
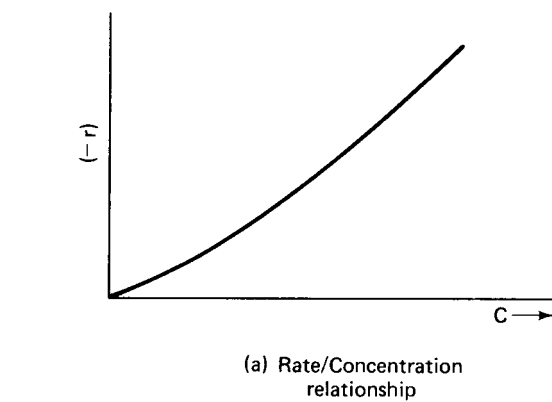


**Figure 4.15** A graphical construction for a sequence of CSTRs.

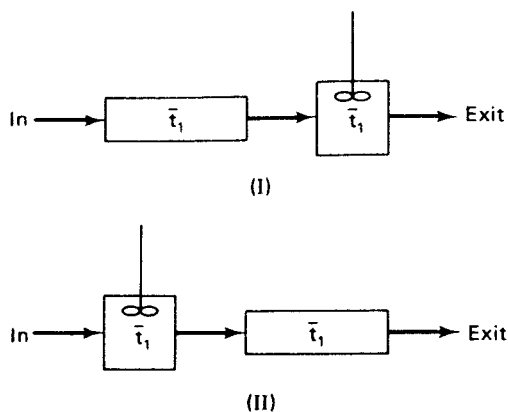
CSTRs. Solving equation (4-51) for the rate,

$$(-r) = \frac{C_0 - C}{\bar{t}} \quad (4-94)$$

Measurements of inlet and outlet concentrations corresponding to the residence time  $\bar{t}$  then yield rate data directly. This  $\Delta C$ , unlike the PFR, does not need to approach differential levels for a direct measurement of rate. The measured rate is that corresponding to  $C$ , and the relation between rate and concentration can be obtained over the desired range of  $C$  by variation of the residence time in the reactor. Except at very low residence times there will be substantial differences between  $C_0$  and  $C$ , so the difficult analytical problems encountered in measuring rates with a differential PFR are, by and large, absent in the CSTR. In addition, owing to the mixing within the CSTR, gradients that obscure kinetic measurements are easily controlled. The same general experimental procedure is used with the CSTR as for the PFR. Each series of runs in which residence time is varied is carried out at a constant temperature and inlet reactants ratio; then another series at a different inlet reactants ratio and the same temperature and continuing until the desired range of all variables has been investigated. The advantage of the CSTR is that direct rate data is provided under all conditions. For additional details on CSTR and PFR laboratory applications, see Weekman [V.W. Weekman, Jr., *Amer. Inst. Chem. Eng. J.*, 20, 833 (1974)].

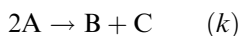
#### Illustration 4.5

Consider the two different reactor sequences of I and II below.



In each, the CSTR exhibits perfect mixing and the tubular reactor acts as a PFR. The mean residence time,  $\bar{t}_1$ , is the same in each reactor.

- Draw the  $F(t)$  versus  $t$  curves for I and II.
- Consider the two reactor sequences above to be used for the homogeneous second-order reaction



which is irreversible. The temperatures in the two reactors are the same, and the

following parameters apply.

$$k = 0.1 \text{ ft}^3/\text{mol}\cdot\text{min}$$

$$\bar{t}_1 = 4 \text{ min}$$

$$C_{A_0} = 1 \text{ lb mol/ft}^3$$

$$v = 1 \text{ ft}^3/\text{lb mol} \quad (\text{independent of conversion})$$

Determine the ratio of  $(C_{A(\text{II})})_{\text{exit}}$  to  $(C_{A(\text{I})})_{\text{exit}}$  for these two sequences. The exit concentrations will differ. Provide a reasonable explanation for the observed difference.

*Solution*

(a) In case I, a step-function input to the PFR will be translated through that vessel with a dead-time lag of  $t_1$ , thus forming a step-function input to the CSTR, which will in turn give us its characteristic exponential response with time constant of  $(1/\bar{t}_1)$ . In case II the step function to the CSTR emerges as an exponential with time constant  $(1/\bar{t}_1)$ , which then passes through the PFR without further change, emerging after a lag of  $\bar{t}$ . In both cases we have the same characteristic response, as shown in Figure 4.16.

The two reactor sequences are, thus, indistinguishable from each other on the basis of the  $F$ -diagram.

(b) (i): For the PFR-CSTR sequence,

*PFR second order*

$$t_R = (v/k)[x/(1-x)]$$

$$x/(1-x) = 0.4$$

$$x = 0.286$$

$$C_A(\text{exit}, \text{PFR}) = 0.714 \text{ lb mol/ft}^3$$

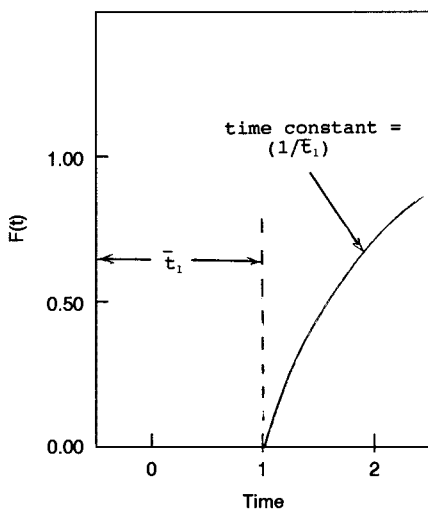


**Figure 4.16**  $F$ -diagram for the reactor sequences I and II.

*CSTR second order*

$$[C_A(in)/C_A(exit, CSTR)] = 1 + kt_1[C_A(exit, CSTR)]^2$$

$$kt_1[C_A(exit, CSTR)]^2 + C_A(exit, CSTR) - C_A(in) = 0$$

Straightforward application of the quadratic formula yields

$$C_A(exit, CSTR) = 0.580 \text{ lb mol/ft}^3$$

The overall conversion is

$$x_{overall} = 0.420$$

(ii): For the CSTR-PFR sequence,

*CSTR second order*

$$C_A(in) = 1.0 \text{ lb mol/ft}^3$$

Again, application of the quadratic formula gives

$$C_A(exit, CSTR) = 0.766 \text{ lb mol/ft}^3$$

*PFR second order*

In the PFR the initial conversion is 0.234, so

$$\int_{x_1}^{x_2} \frac{dx}{(-r)} = \frac{1}{k[C_A(PFR)]^2} \int_{x_1}^{x_2} \frac{dx}{(1-x)^2} \quad (i)$$

$$t_R = \frac{1}{\nu k[C_A(PFR)]^2} \int_{x_1}^{x_2} \frac{dx}{(1-x)^2} = \frac{1}{kC_A(PFR)} \int_{x_1}^{x_2} \frac{dx}{(1-x)^2}$$

Therefore,

$$t_R = \frac{1}{kC_A(PFR)} \left[ \frac{1}{(1-x_0)} - \frac{1}{(1-x_1)} \right] \quad (ii)$$

Inserting numerical values and solving for  $x_2$  gives

$$x_{overall} = x_2 = 0.413$$

$$C_A(exit, PFR) = 0.587 \text{ lb mol/ft}^3$$

*Moral:* As predicted, the conversions differ for the two sequences even though their overall  $F$ -diagrams are the same. The important lesson from this result is that combined models predicting the same apparent overall mixing behavior do not imply the same reaction conversions for reaction orders other than one. The differences shown here are, to be sure, not large, but they would increase for higher conversions or if the holding times in each unit were different. The mixing occurring in the early stages of reaction in sequence II means that the reaction goes at a lower rate (corresponding to the exit concentrations from the CSTR) compared to the PFR in sequence I, and therein lies the ultimate difference in total conversion between the two. Considerable literature on this and related issues is available [J.G. Van de Vusse, *Chem. Eng. Sci.*, 19, 994 (1964); J.D. Paynter and D.E. Haskins, *Chem. Eng. Sci.*, 25, 1415 (1970); H. Kramers and K.R. Westerterp, *Elements of Chemical Reactor Design and Operation*, Academic Press, New York, NY, 1963; K. Denbigh and J.C.R. Turner, *Chemical Reactor Theory*, 2nd ed., Cambridge University Press, London, (1971)]. The application of such combined models, meaning models which include various combinations of series and parallel CSTRs and PFRs—with or without other ornaments such as recycle and bypass flows, and dead volumes with no chemical reaction—is of utility in approaching the analysis of reactors which lie outside the realm defined by the

limits of perfect mixing and plug flow (which, indeed, includes many large-scale commercial units). More discussion on these topics is in Chapter 5.



HORATIO SAYS

What would be the result if the reaction were half-order? Repeat the analysis for half-order kinetics, using the same values of the parameters in appropriate units.

#### 4.4.4 Semibatch Reactors

*Semibatch reactors* are stirred tank reactors used for liquid-phase reactions in which there is a nonsteady flow through the system. In their most normal application, treated here, one reactant is contained initially in the tank and a second continuously added to it, with no flow out of the vessel, as shown schematically in Figure 4.17. Other applications may involve withdrawal of a product stream but at a different rate from the addition of a reactant, or even two reactants premixed in the vessel with no further feed and continuous withdrawal of product. The model of the ideal semibatch reactor assumes perfect mixing, as in the CSTR and batch reactor, but the reaction volume changes with time of operation due to the introduction of the reactant. The overall process, thus, is an unsteady-state one. A common utilization of the semibatch reactor is for reactions that are highly exothermic; the net rate of heat generation can be controlled through regulation of the rate of introduction of the second reactant.

Consider the process illustrated in Figure 4.17, where the second-order irreversible reaction  $A + B \rightarrow C$  is carried out in a semibatch reactor. Since there is a large excess of A present within the reactor, we may take the kinetics of the reaction to be pseudo-first-order in B, and since this is not a constant-volume operation let us write a molal balance on B.

$$\text{input} = F_B \quad \text{mols B added/time (constant)}$$

$$\text{reaction} = (-r_B)V \quad \text{mols B reacted/time}$$

$$\text{accumulation} = \frac{dN_B}{dt}$$

where  $V$  is the reaction mixture volume,  $(-r_B)$  the rate of reaction in mols per unit volume, and  $N_B$  the mols of B. Equating these terms,

$$\frac{dN_B}{dt} = F_B - (-r_B)V \quad (4-95)$$

If  $C_B$  is the concentration of B at any time, then

$$N_B = VC_B$$

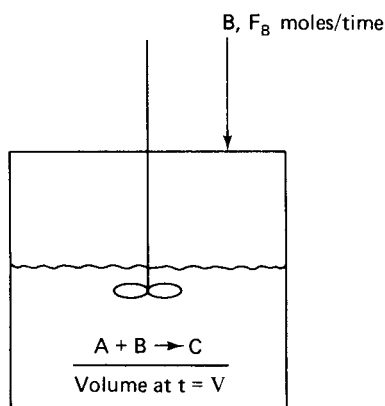


**Figure 4.17** A semibatch reactor.

and

$$\frac{dN_B}{dt} = V \frac{dC_B}{dt} + C_B \frac{dV}{dt}$$

Inserting this into equation (4-95), together with the first-order rate equation for B, we have

$$V \frac{dC_B}{dt} + C_B \frac{dV}{dt} = F_B - kC_B V \quad (4-96)$$

The volume of the reaction mixture (we must keep this distinct from the reactor volume) is included in equations (4-95) and (4-96), and this is given as a function of time by

$$V = V_A + F_B \nu_B t \quad (4-97)$$

where  $V_A$  is the volume of A initially present,  $\nu_B$  is the molal specific volume of B, and  $t$  is the time of the filling period, identical to the time of reaction. Substituting for  $V$  and  $dV/dt$  in equation (4-96),

$$(V_A + F_B \nu_B t) \frac{dC_B}{dt} + F_B \nu_B C_B = F_B - kC_B (V_A + F_B \nu_B t)$$

This can be recognized as a simple first-order differential equation, which, with some rearrangement, becomes

$$\frac{dC_B}{dt} + C_B \left( \frac{1}{(m+t)} + k \right) = \frac{(1/\nu_B)}{m+t} \quad (4-98)$$

with  $m = (V_A/F_B \nu_B)$ . The solution for  $C_B$ , with the initial condition that  $C_B = 0$  at  $t = 0$ , is

$$C_B = \frac{1 - e^{-kt}}{k\nu_B(m+t)} \quad (4-99)$$

In a similar manner we obtain for the concentration of product,  $C_C$ ,

$$C_C = \frac{t}{\nu_B(m+t)} + \frac{e^{-kt} - 1}{k\nu_B(m+t)} \quad (4-100)$$

where  $C_C = 0$  at  $t = 0$ .



For a reversible first order reaction,  $A + B \leftrightarrow C$ , under the same conditions and assumptions just treated, we obtain

$$C_B = \frac{1}{\nu_B(m+t)} \left[ \frac{1 - e^{-(k_1+k_2)t} + k_2 t}{k_1 + k_2} + \frac{k_2 e^{-(k_1+k_2)t}}{(k_1 + k_2)^2} - \frac{k_2}{(k_1 + k_2)^2} \right] \quad (4-101)$$

$$C_C = \frac{1}{\nu_B(m+t)} \left[ \frac{k_1 t}{k_1 + k_2} + \frac{k_1}{(k_1 + k_2)^2} (e^{-(k_1+k_2)t} - 1) \right] \quad (4-102)$$

It is interesting to see, for a typical case, how well the assumption of pseudo-first-order kinetics (based on  $C_A \gg C_B$ ) stands up. Figure 4.18 gives some results in terms of the ratio of mols of A present to mols of B present for the reversible case. The results are specific to the particular parameters used, of course but should illustrate that for the time near the end of the filling period the assumption may break down. This depends ultimately on what is to be the total charge of B in comparison to the amount of A present initially.

For more complex kinetics than those illustrated, a general numerical procedure based on equation (4-95) is easily implemented. Software routines are widely available for solution of the simple differential equations encountered here, but it is perhaps of use to discuss one typical approach to see what is involved. Accordingly, let us write the governing molal balance in finite-difference form,

$$\Delta N_B = [F_B(-r_B)V]\Delta t \quad (4-103)$$

At the time of reaction,  $t$ , considered,

$$V = V_A + F_B \nu_B(t + \Delta t)$$

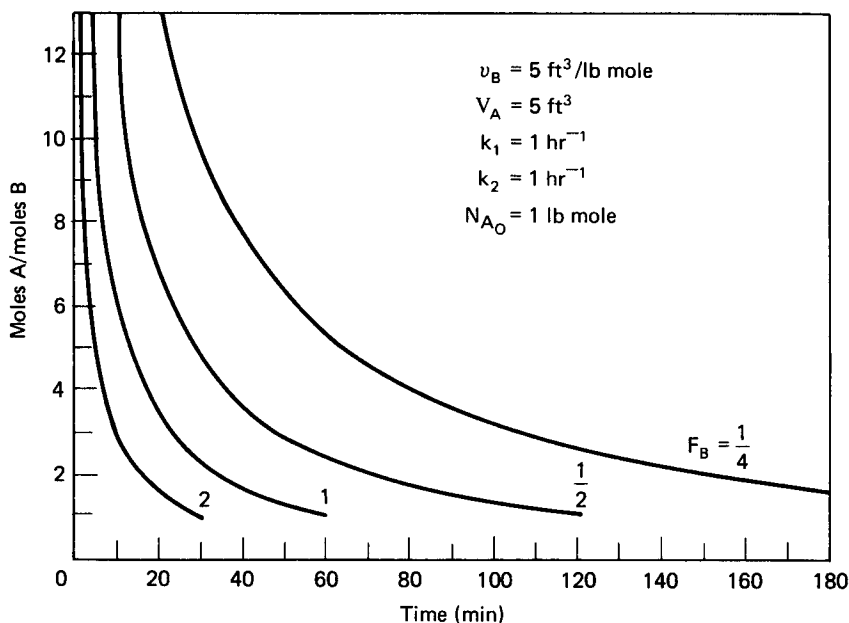


Figure 4.18 Reactants molal ratio for an example semibatch reactor.

so that

$$\Delta N_B = \{F_B - (-r_B)[V_A + F_B \nu_B(t + \Delta t)]\} \Delta t \quad (4-104)$$

The problem is an initial value one, so we use the following procedure, starting at  $t = 0$ :

- (a) Select a suitable small time increment  $\Delta t$  and calculate the corresponding  $\Delta N_B$ . The rate of reaction,  $(-r_B)$ , which in all likelihood will be a function of  $C_B$  (and hence  $\Delta N_B$ ) is not known, so one must estimate its value for this calculation.
- (b) After  $\Delta N_B$  has been calculated using the estimated value for  $(-r_B)$ , the concentration of B can be determined and a new value of  $(-r_B)$  then used to recalculate  $\Delta N_B$  for the initial  $\Delta t$ .
- (c) The calculation of (b) is then repeated until there is no further change in  $(-r_B)$  from one iteration to the next.
- (d) Calculations for successive time intervals follow the same procedure. The value of  $(-r_B)$  will be known at the beginning of the interval, and the corresponding  $\Delta N_B$  determined. The resulting  $C_B$  is used to check the estimated  $(-r_B)$  at the end of the time interval and the calculation continued with successive values of  $C_B$  until there is no further change in the rate.
- (e) For a more precise method, one can average  $(-r_B)$  over the time interval and use the check with  $C_B$  to determine a proper average rate over the interval considered.
- (f) Remember that it is always prudent to check the approximation  $\Delta t \rightarrow dt$  by repeating the calculation for differing values of  $\Delta t$  to ensure there is no variation.

#### 4.4.5 Laminar-Flow Reactors

In general, analytical solutions to the laminar-flow reactor are not convenient to work with because of the awkward forms that arise from the concentration averaging of equation (4-58). For first-order irreversible kinetics, the design equation (4-57), becomes

$$\frac{1}{k} \int_{C_{A_0}}^{C_A} \frac{dC_A}{C_A} = - \frac{L}{u_0 [1 - (r_p/R_0)^2]}$$

where  $u_0$  is the central streamline velocity,  $2v/\pi R_0^2$ . Integrating the above we obtain the exit concentration as a function of radial position

$$C_A = C_{A_0} \exp\left(-\frac{\lambda}{1 - U^2}\right) \quad (4-105)$$

where

$$\lambda = \frac{kL}{u_0} \quad U = \frac{r_p}{R_0}$$

Substituting this result into equation (4-58) for the average exit concentration, we have

$$\begin{aligned}\langle C_A \rangle &= C_{A_0} \frac{\int_0^1 U(1 - U^2)e^{-\lambda/(1-U^2)} dU}{\int_0^1 U(1 - U^2) dU} \\ &= 4C_{A_0} \int_0^1 U(1 - U^2)e^{-\lambda/(1-U^2)} dU\end{aligned}\quad (4-106)$$

The substitution  $X = \lambda/(1 - U^2)$  allows partial integration of equation (4-106) to

$$\frac{\langle C_A \rangle}{C_{A_0}} = e^{-\lambda}(1 - \lambda) + \lambda^2 \int_{\lambda}^{\infty} \frac{e^{-X} dX}{X} \quad (4-107)$$

The integral in the second term is a form of the exponential integral, normally tabulated as  $E_1(z)$  [M. Abramowitz and I.A. Stegun, *Handbook of Mathematical Functions*, Dover, New York, NY, (1965)]. Further discussion of the ideal laminar-flow reactor with a first-order reaction is given by Cleland and Wilhelm [F.A. Cleland and R.H. Wilhelm, *Amer. Inst. Chem. Eng. J.*, 2, 489 (1956)].

A similar derivation for the second-order irreversible reaction  $2A \rightarrow B$  has been given by Denbigh [K.G. Denbigh, *J. Appl. Chem.* (London), 1, 227 (1951)]. The result corresponding to equation (4-107) is

$$\frac{\langle C_A \rangle}{C_{A_0}} = 1 - 2\lambda' \left( 1 - \lambda' \ln \frac{1 + \lambda'}{\lambda'} \right) \quad (4-108)$$

where  $\lambda' = C_{A_0} kL/u_0$  and  $k$  is the appropriate second-order rate constant. The conversions for these two cases are illustrated in Figure 4.19.

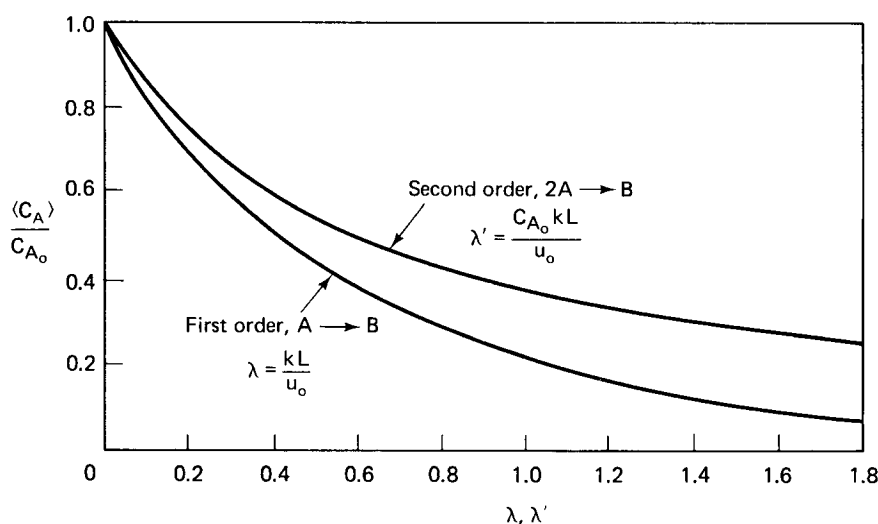


**Figure 4.19** Conversion in a laminar-flow reactor for first- and second-order irreversible

#### 4.4.6 Some Comparisons of Conversion and Selectivity in Ideal reactors

Since the CSTR and PFR represent the extremes in mixing behavior in terms of residence-time distributions, it is of interest to examine their relative performance characteristics for both single and multiple reactions. However, comparison solely on the basis of the mathematical results of the reactor analysis is often not the full story. Many factors associated with the operation, the nature of the process stream, the reaction conditions, and so on, are important in determination of the type of reactor to be used in a given situation. Stirred tank reactors are used most often for liquid-phase reactions, generally at low or moderate pressures. The nature of the economics of stirred tank reactors normally dictates that they will have relatively large volumes and corresponding long average residence times; and as mentioned earlier, the spatial uniformity of concentrations and temperature in this type of reactor allows an inherent ease of control for reactions with large heat effects that is not possible with the tubular flow type. The heat transfer rates in stirred tank reactors, however, are generally lower than in tubular reactors, since their surface area/volume ratio is smaller, so that in spite of the inherent ease of control in the stirred tank, tubular reactors are still very often employed for reactions with large heat-supply or heat-removal requirements. Gas-phase reactions are also not often carried out in stirred tanks because of mechanical problems (stirrer seals effective at higher temperatures and pressures) and because it is simply harder to obtain well-mixed conditions in the gas phase. Most reactions employing heterogeneous catalysts are conducted in tubular reactors containing a fixed bed of the catalyst. (There are important exceptions; fluidized-bed reactors, discussed in Chapter 8, are one.) Such reactions generally involve gas-phase process streams at moderate or high pressures and the reactions have substantial heat supply or removal requirements. Various types of mixed-phase reactions—gas/liquid or gas/liquid/solid—are conducted in either stirred reactors (slurry reactors) or fixed beds (trickle beds). These will also be discussed in Chapter 8. An extensive discussion of the utilization of stirred tank reactors has been given in the papers of MacMullen and Weber and Piret and coworkers, previously cited, and by Denbigh and coworkers [R.G. Denbigh, *Trans. Faraday Soc.*, 40, 352 (1944); 43, 648 (1947); R.G. Denbigh, M. Hicks and F.M. Page, *Trans. Faraday Soc.*, 44, 479 (1948)].

In terms of a comparison between PFRs and CSTRs, a little reasoning plus common sense should tell us that for well-behaved kinetics of the reaction(s) involved (positive power law), the PFR will always be more efficient than a corresponding CSTR on a per-volume basis. For such reactions the rate increases with the concentration level of the reactant, and since the CSTR always operates at the lowest level of reactant concentration (i.e., the reactor exit concentration), the PFR will always win. We can support this conclusion more precisely by comparing the residence times required by each to attain the same conversion level, which for a set feed rate then determines the reactor volume required. As an example, for a first-order reaction at constant density, we have

$$t_{PFR} = -\frac{1}{k} \ln(1-x)$$

and

$$\bar{t}_{CSTR} = \frac{1}{k} \frac{x}{1-x}$$

so that

$$\frac{t_{PFR}}{\bar{t}_{CSTR}} = \frac{(1-x) \ln(1-x)}{x} \quad (4-109)$$

Corresponding results for zero-order and second-order reactions at constant density are

$$\text{zero order} \quad \frac{t_{PFR}}{\bar{t}_{CSTR}} = 1 \quad (4-110)$$

$$\text{second order} \quad \frac{t_{PFR}}{\bar{t}_{CSTR}} = 1 - x \quad (4-111)$$

where the second-order results are for  $2A \rightarrow \text{products}$ . A comparison of these is given in Figure 4.20, where it is shown that the PFR is more efficient in this regard than the CSTR. The difference is not large at low conversions, but for higher-order reactions the difference becomes substantial even for conversions well below 50 percent.

The comparisons above are for simple, positive power-law kinetics. What about more complex kinetics such as Langmuir-Hinshelwood (alias Michaelis-Menton) or negative-order power laws? Here the problem of comparison becomes

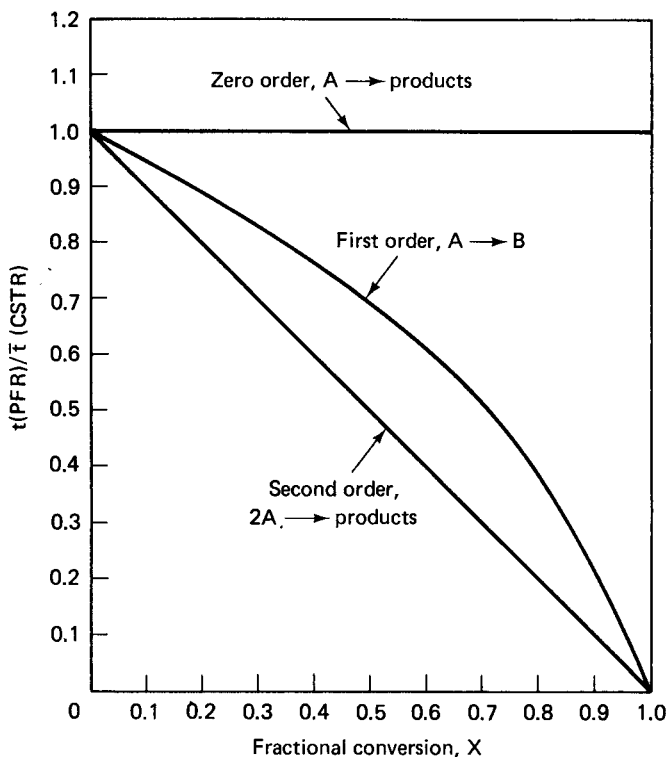


**Figure 4.20** Comparison of residence-time requirements of PFR and CSTR single reactors for some simple irreversible reactions.

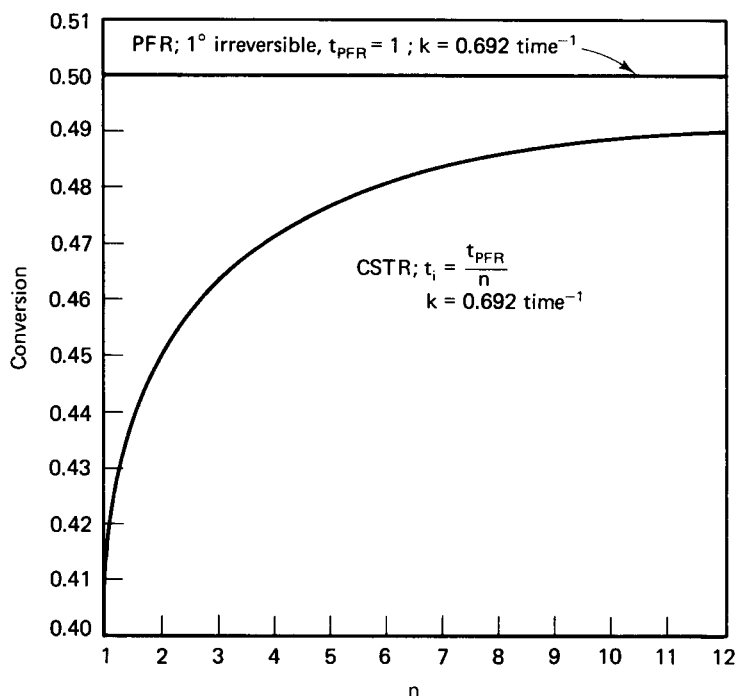


**Figure 4.21** Comparison of a PFR and a CSTR sequence: conversion for a first-order reaction at the same total residence time.

more complicated. In many of these cases the combined volume of a CSTR-PFR sequence is less than that required by either of the reactor types alone. An interesting analysis of this was given by Bischoff [R.B. Bischoff, *Can. J. Chem. Eng.*, 44, 281 1966)] for the case of Michaelis-Menton kinetics; the topic is also discussed in further detail in the text of Levenspiel.

Now let us turn to some aspect of the yield and selectivity obtained in PFR and CSTR systems for the Type II and Type III “nearly complex” reactions discussed in Chapter 1.<sup>4</sup> The specific results here are of interest in themselves, but just as important are the methods used for the analysis of the comparative yield and selectivities of the different reactors.

A comparison in terms of CSTR sequences rather than individual reactors is given in Figure 4.21, where we show the conversion obtained in a single PFR of set residence time with various CSTR sequences, differing in the number of reactors but with the same total residence time as the PFR, that is,  $t_{CSTR} = t_{PFR}/n$ , with  $n$  the number of CSTR. For the first-order example illustrated, the conversion steadily increases as  $n$  increases in the CSTR sequence, and indeed will approach the PFR value in the limit of very large  $n$ . This can be shown quantitatively by comparison of the series expansions of the conversion expressions for the two types of

<sup>4</sup> As pointed out in Chapter 1, the Type I scheme has significance mainly in heterogeneous reactions, so it is not included here.

reactors. For the PFR

$$1 - x = e^{-kt} = 1 - kt + \frac{(kt)^2}{2} - \frac{(kt)^3}{6} + \dots$$

and for the CSTR

$$1 - x = (1 + k\bar{t}_i)^{-n} = 1 - k(n\bar{t}_i) + \frac{k^2(n)(n+1)\bar{t}_i^2}{2} - \frac{k^3(n+1)(n+2)\bar{t}_i^3}{6} + \dots$$

These expansions approach each other term by term as  $n$  becomes large.

The similarity of the behavior of the sequence of a large number of CSTRs to that of a PFR has important applications in the modeling of nonideal reactors, since from the illustration above it is apparent that for  $1 < n < \infty$  we have obtained a conversion result corresponding to something intermediate between the ideal limits of the single CSTR and the PFR. However, since the example we have given is a very specific one and since this type of modeling is sufficiently important to be the topic of a subsequent section, we will not pursue the matter further at this point.

To return to the yield/selectivity analysis, first let us recall the definitions of those quantities as they were given in Chapter 1.

$$\text{Yield} = (\text{mols } i \text{ to } j) / (\text{mols } i \text{ initial})$$

$$\text{Selectivity} = (\text{mols } j \text{ produced}) / (\text{mols } i \text{ reacted})$$

For the PFR the expressions for these quantities are the same as given in Chapter 1 for the batch reactor with no volume change, with the time of reaction given by the residence time in the reactor. For product B of a Type II reaction

$$Y_B(II)_{PFR} = \frac{k_1}{k_1 + k_2} [1 - e^{-(k_1 + k_2)t_R}] \quad (1-76)$$

and

$$S_B(II)_{PFR} = \frac{k_1}{k_1 + k_2} \quad (1-77)$$

where  $t_R$  is the PFR residence time and possible volume expansion is neglected.

For an  $n$ -unit equally sized CSTR sequence we may obtain  $C_{A_n}$  by modification of equation (4-89)

$$\frac{C_{A_n}}{C_{A_0}} = \frac{1}{[1 + (k_1 + k_2)\bar{t}]^n} \quad (4-112)$$

where  $\bar{t}$  is the average residence time per unit. The concentration of B is given by

$$C_{B_n} = C_{B_{n-1}} + k_1 C_{A_0} \bar{t} \quad (4-113)$$

Combination of equations (4-112) and (4-113) gives

$$\frac{C_{B_n}}{C_{A_0}} = k_1 \bar{t} \sum_{i=1}^n [1 + (k_1 + k_2)\bar{t}]^{-i} \quad (4-114a)$$

$$\frac{C_{B_n}}{C_{A_0}} = k_1 \bar{t} \left( \frac{\gamma}{1 - \gamma} - \frac{\gamma^{n+1}}{1 - \gamma} \right) \quad (4-114b)$$

where the parenthetical term in equation (4-114b) is the sum of the geometric progression of (4-114a),  $\gamma = [1 + (k_1 + k_2)\bar{t}]^{-1}$ , and  $C_{B_0}$  is taken to be zero. Substitution of these results into the yield and selectivity definitions gives

$$Y_B(II)_{CSTR} = k_1 \bar{t} \left( \frac{\gamma}{1 - \gamma} - \frac{\gamma^{n+1}}{1 - \gamma} \right)$$

or, simplifying a bit,

$$Y_B(II)_{CSTR} = \frac{k_1}{k_1 + k_2} \frac{\gamma^{n-1}}{\gamma^n} \quad (4-115)$$

$$S_B(II)_{CSTR} = \frac{k_1 \bar{t}}{1 - \gamma^n} \left( \frac{\gamma}{1 - \gamma} - \frac{\gamma^{n+1}}{1 - \gamma} \right) = \frac{k_1}{k_1 + k_2} \quad (4-116)$$

An item of interest in the above is that PFR and CSTR selectivities are the same for the Type (II) reaction. This equality must pertain for the relative yields as well, as long as the comparison is made for the *same conversion level*, and follows from the definition

$$\text{yield} = (\text{selectivity})(\text{conversion})$$

Now, if the comparison is not made at equal conversion levels far different results will be obtained. We have seen in Figure 4.21 that for first-order kinetics, the conversion in the CSTR lags behind that of a PFR of comparable total residence time. Since both PFR and CSTR Type II selectivities are equal and independent of conversion, a comparison of yields based on *equivalent total residence times* would show the CSTR Type II yield always to be inferior up to the limit of  $n = \infty$ , where, of course, the conversions in the two reactor systems are equal.

For a Type III system the PFR selectivity is given by equation (1-92)

$$S_B(III)_{PFR} = \frac{k_1}{k_2 - k_1} \frac{e^{-k_1 t_R} - e^{-k_2 t_R}}{1 - e^{-k_1 t_R}} \quad (1-92)$$

For the  $n$ -unit, equally sized CSTR sequence, we may derive the following results.

$$C_{A_n} = C_{A_0} \alpha^{-n} \quad (4-89)$$

$$C_{B_n} = \frac{k_1 \bar{t} C_{A_0}}{\alpha \beta^n} \sum_{p=0}^{n-1} \left( \frac{\beta}{\alpha} \right)^p \quad (4-117)$$

Combining these two expressions for the condition that  $C_{B_0} = 0$  gives

$$C_{B_n} = \frac{k_1 C_{A_0}}{k_2 - k_1} \left( \frac{1}{\alpha^n} - \frac{1}{\beta^n} \right) \quad (4-117a)$$

where  $\alpha = (1 + k_1 \bar{t})$  and  $\beta = (1 + k_2 \bar{t})$ . The corresponding expression for selectivity is

$$S_B(III)_{CSTR} = \frac{k_1}{k_1 - k_2} \frac{(\alpha/\beta)^n - 1}{\alpha^n - 1} \quad (4-118)$$

Now, to compare the PFR and CSTR selectivities at the same conversion, we require that

$$1 - e^{-k_1 t_R} = 1 - (1 + k_1 \bar{t})^{-n}$$



so

$$t_R = \frac{n}{k_1} \ln(1 + k_1 \bar{t}) = \frac{n}{k_1} \ln \alpha \quad (4-119)$$

Substituting this value for  $t_R$  in the PFR selectivity equation, we obtain

$$S_B(III)_{PFR} = \frac{k_1}{k_2 - k_1} \frac{\alpha^{-n} - \alpha^{-n/S_i}}{1 - \alpha^{-n}} \quad (4-120)$$

where  $S_i$  is the intrinsic selectivity,  $k_1/k_2$ . The ratio of the PFR and CSTR selectivities is then

$$\frac{S_B(III)_{PFR}}{S_B(III)_{CSTR}} = \frac{1 - \alpha^{(1-1/S_i)n}}{1 - (\alpha/\beta)^n} \quad (4-121)$$

Some results computed from equation (4-121) for Type III reactions with intrinsic selectivities both greater and less than unity are shown in Figure 4.22. The comparison is made for a series of  $n$  reactors ( $n$  variable) with  $\bar{t} = 0.1$  and  $k_1 = 1.0$  in consistent time units, and conversion changed by allowing  $n$  to vary. The PFR selectivity is greater regardless of the intrinsic selectivity. Although we note that the ratio PFR/CSTR decreases with increasing conversion for  $S_i < 1$  and increases for  $S_i > 1$  (solid lines), this is an artifact due to the manner in which conversion is made to vary in the comparison. The dashed line in Figure 4.22 gives a corresponding calculation in which conversion is varied by fixing  $n$  and allowing  $\bar{t}$  to change. Regardless of the manner in which the conversion is made to vary in this comparison, however, the PFR selectivity is greater.

Several interesting problems arise in the analysis of Type III reactions in both PFR and CSTR systems that are concerned with maximizing the intermediate B in the reactor effluent. The considerations involved extend to more complex reactions as well, so we will provide a little detail in such analysis. For the PFR, we have already shown in Chapter 1 that the residence time that maximizes B is

$$t_R = \frac{\ln(k_2/k_1)}{k_1(k_2/k_1 - 1)} \quad (1-89)$$

where  $C_{B_0} = 0$ . In the CSTR sequence, however, the problem is more complicated, as mentioned in Illustration 4.4. We have just seen that the total residence time in a CSTR sequence can be varied either by fixing  $\bar{t}$  and varying  $n$ , or by fixing  $n$  and varying  $\bar{t}$ . In terms of maximizing the intermediate, the two procedures are not the same. Consider the first alternative. The value of  $C_{B_n}$  is given by equation (4-117), however, we cannot follow the normal maximization procedure via evaluation of the first derivative for the reasons given in Illustration 4.4. Use the inequality condition

$$C_{B_{n-1}} < C_{B_n} > C_{B_{n+1}} \quad (4-122)$$

It can be shown that for the right-hand side of the constraint to be satisfied,

$$(\alpha^{-n} - \beta^{-n}) > (\alpha^{-(n+1)} - \beta^{-(n+1)}) \quad (4-123)$$

which, after rearrangement, can be cast in the form

$$\frac{\ln(1/S_i)}{\ln(\beta/\alpha)} < n + 1 \quad (4-124)$$



The differentiation, under this condition only, gives the lower limit of the inequality analysis.

If we are dealing with fixed  $n$  and wish to maximize  $C_{B_n}$  by variation of  $\bar{t}$ , the inequality analysis is not required. Carrying out the differentiation of equation (4-117) with respect to  $\bar{t}$ , we obtain (after considerable algebra),

$$\left(\frac{\partial C_{B_n}}{\partial \bar{t}}\right)_n = 0 = -\frac{k_1 C_{A_0} n}{(k_2 - k_1)} \left(\frac{k_1}{\alpha^{n+1}} - \frac{k_2}{\beta^{n+1}}\right) \quad (4-127)$$

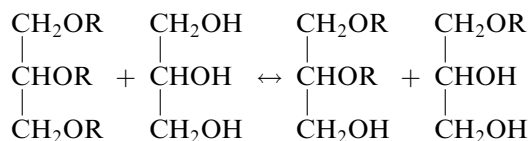
and

$$\bar{t}_{C_{B_n}=\max} = \frac{(S_i)^{1/(n+1)} - 1}{k_1 - k_2(S_i)^{1/(n+1)}}$$

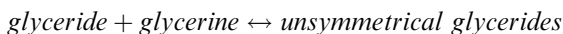
Similar methods may be used for analysis of selectivity, yield, and concentration maxima in other types of parallel or sequential reaction schemes with either reversible or irreversible steps. However, when the kinetics involve other than first-order rate laws, convenient analytical solutions cannot be obtained, in general, and step-by-step calculations are probably more convenient. Also, the graphical method illustrated in Figure 4.15 is not applicable for parallel or sequential schemes because normally the rate of appearance or consumption of intermediates of interest depends on the concentration of more than one species and representation of rate in a single  $(-r)$  versus  $C$  relationship is not possible.

### Illustration 4.6

The first stage in the manufacture of alkyl resins may be represented by



That is,



The glycerine is most often present in considerable excess, since it, along with the unsymmetrical glycerides, is later esterified with a dibasic acid. The reaction in the forward direction may thus be considered pseudo-first-order. Below are some data at 240 and 280 °C obtained with a 50 liter batch reactor. There were no products present initially.

240 °C		280 °C	
$t, h$	$x, \%$	$t, h$	$x, \%$
0	0	0	0
1	29	0.5	47
2	53	1	65
3	67	1.5	71
4	76	2	73
5	85		

- (a) Compare the conversion obtained with a series of 6 CSTRs at 240 and 280 °C, with each vessel to hold 500 liters and the feed rate to be 1000 l/h.
- (b) Compare the conversion obtained in part (a) for six CSTRs at 240 °C with that obtained in a single PFR of the same total volume and at the same feed rate.

### Solution

The first thing to be done is to extract the kinetic constants that are associated with some reasonable rate correlation. The experimental data on conversion versus time of reaction are shown graphically in Figure 4.23. From the shape of this plot one would tend to view this reaction as irreversible at 240 °C but perhaps reversible at 280 °C.

The best strategy in interpretation is to base the approach on a reversible reaction model, seeking simplification when possible. Furthermore, start with first-order kinetics as a base. This puts us on very familiar ground, with  $A \leftrightarrow B$  ( $k_1, k_2$ ) for which

$$(k_1 + k_2) = \ln[\alpha/(\alpha - x)] \quad (i)$$

For batch reactions at constant volume (this is a liquid phase reaction)

$$\frac{C_A}{C_{A_0}} = \left( \frac{k_2}{k_1 + k_2} \right) + \left( \frac{k_1}{k_1 + k_2} \right) e^{[-(k_1 + k_2)t]} \quad (ii)$$

as shown in Chapter 1. The reversible reaction analysis works well, with the following results.

$$240^\circ\text{C} : \quad k_1 = 0.39 \text{ h}^{-1}; \quad k_2 = 0 \text{ h}^{-1}$$

$$280^\circ\text{C} : \quad k_1 = 1.68 \text{ h}^{-1}; \quad k_2 = 0.57 \text{ h}^{-1}$$

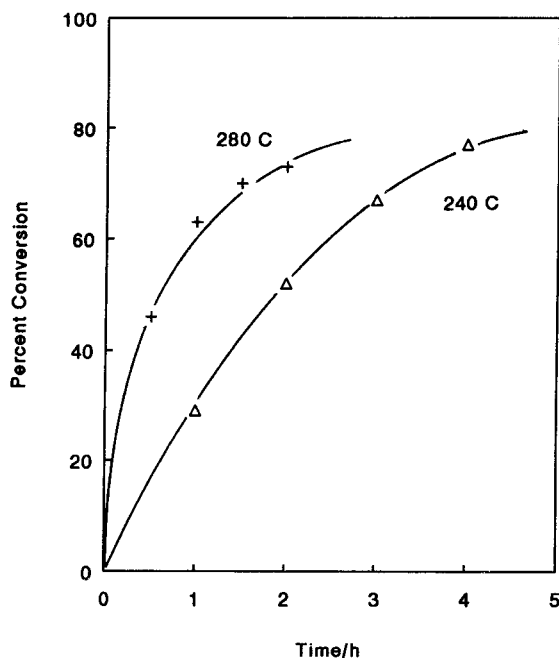


**Figure 4.23** Conversion-time data for the glyceride-glycerine reaction.

(a)

*At 240 °C*

Since the reaction is essentially irreversible at this temperature, we have for the CSTR sequence

$$\frac{C_{A_n}}{C_{A_0}} = \frac{1}{(1 + k_1 \bar{t})^6} \quad (\text{iii})$$

with

$$\bar{t} = 500/10000 \text{ h} = 0.5 \text{ h}$$

and

$$\left( \frac{C_{A_n}}{C_{A_0}} \right) = 0.340$$

Conversion at 240 °C = 66.0% for six CSTRs.

*At 280 °C*

We can rewrite equation (ii) as

$$\frac{C_{A_n}}{C_{A_0}} = \alpha^n + k_2 \bar{t} \left[ \frac{\alpha}{(1 - \alpha)} - \frac{\alpha^{n+1}}{(1 - \alpha)} \right] \quad (\text{iv})$$

$$\alpha = \frac{1}{(1 + k_1 \bar{t} + k_2 \bar{t})}$$

From the data given we calculate under these conditions a value of  $\alpha = 0.476$ . From equation (iv) we derive

$$\left( \frac{C_{A_n}}{C_{A_0}} \right) = 0.269$$

Conversion at 280 °C = 73.1% for six CSTRs.

(b) For the irreversible reaction at 240 °C the appropriate PFR design equation is simply

$$\ln(1 - x) = -k_1 t_R \quad (\text{v})$$

Now remember that the holding time per vessel in the CSTR sequence, 0.5 h, must be multiplied by the number of vessels to give the PFR residence time. Thus,

$$t_R = 3 \text{ h}$$

$$k_1 = 0.39 \text{ h}^{-1}$$

and from equation (v)

$$x = 0.690 = 69.0\% \text{ in the PFR}$$

The PFR does give a small increase in the conversion compared to the CSTR sequence. Keep in mind that according to Figure 4.21, however, the six-tank sequence is already well along the path to where CSTR series  $\sim$  PFR.



HORATIO SAYS

Excited by all this? Then for a further exercise derive equation (iv) above. Also, what would the PFR be at 280 °C?

## 4.5 Temperature Effects in Ideal Reactors

The treatment of reactor theory so far has dealt exclusively with isothermal systems. In practice, however, the majority of important reactions are accompanied by significant heat effects which must be recognized and must be incorporated into the analysis or design of the reactor. In Chapter 1 we developed some theories for adiabatic reactions in batch, homogeneous reactors by simultaneous solution of the mass and energy conservation equations. The problem of reaction systems that are both nonisothermal and nonadiabatic was put off then as being a topic more suitable for discussion when considering particular reactor types.<sup>5</sup> This is where we are now, so in the following we will present some analysis of PFR and CSTR systems in cases of both adiabatic and nonisothermal/nonadiabatic operation.

### 4.5.1 Adiabatic or Nonisothermal Plug-Flow Reactors

The plug-flow model for nonisothermal operation is shown in Figure 4.24. We assume in writing the enthalpy terms that there are no phase changes occurring, that the temperature, as well as the reaction mixture concentration, is uniform across the radius at any given axial position, and that heat transfer at the wall may be represented by a uniform overall heat-transfer coefficient,  $U$ . Since the nonisothermal analysis will normally lead to nonlinear problems that frown upon analytical

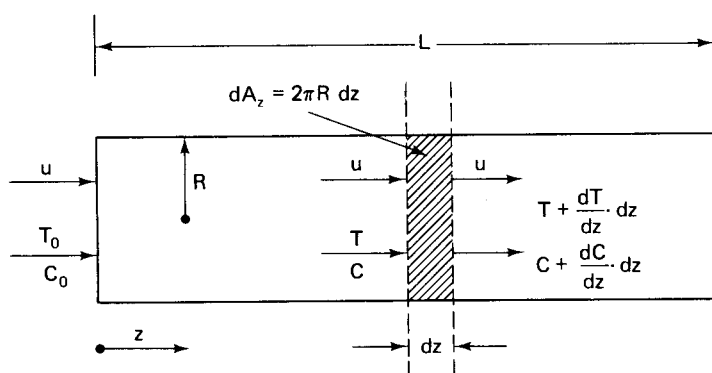


**Figure 4.24** Plug-flow reactor in a nonisothermal reaction.

<sup>5</sup> “‘Lord save us!’ cried the duck. ‘How does it make up its mind?’” —*H. Lofting*

solution, much of the strategy here will be to set up the analysis in a general form suitable for numerical procedures, as was done in Chapter 1. The energy balance is developed to relate the degree of conversion to the temperature, which can then be checked from the mass balance.

Consider the heat transfer occurring at the wall along a small length of external area,  $dA_z = 2\pi R dz$ , as indicated in the figure.

$$Q = U(T - T_M) dA_z = U(T - T_M)(2\pi R) dz \quad (4-128)$$

where  $T_M$  is a constant external temperature and  $T$  is the uniform temperature across the reactor cross section. Now, following the general approach outlined in Chapter 1, we may write the following energy balance on the reactor using the reaction  $A + B \rightarrow C + D$  as an example.

$$\begin{aligned} \int_{T^*}^{T_0} (N_{A_0} C_{pA} + n_{B_0} C_{pB}) dT &= \int_{T^*}^T N_{A_0} (1 - x) C_{pA} dT \\ &+ \int_{T^*}^T (N_{B_0} - N_{A_0} x) C_{pB} dT \\ &+ \int_{T^*}^T (N_{A_0} x) C_{pC} dT \\ &+ \int_{T^*}^T (N_{A_0} x) C_{pD} dT + N_{A_0} x (-\Delta H)_{T^*} \\ &- \int_0^z U(T - T_M) 2\pi R dz \end{aligned} \quad (4-129)$$

where  $N_{A_0}$  and  $N_{B_0}$  are molal feed rates of A and B,  $x$  the conversion of A (mols A reacted/mols A fed),  $T^*$  a reference temperature,  $T_0$  the inlet temperature,  $(-\Delta H)_{T^*}$  the heat of reaction per mol of A, and  $C_{pi}$  the various heat capacities. In addition we have the mass balance

$$\int_0^x \frac{dx}{(-r)} = \frac{1}{N_{A_0}} \int_0^z \pi R^2 dz \quad (4-130)$$

Solution of the nonisothermal problem then consists of utilizing equations (4-129) and (4-130) to obtain the relationship among  $x$ ,  $T$  and  $z$  along the length of the reactor.

There are many numerical approaches that one may take to solve the problem, depending to some extent on what simplifying assumptions one is willing to make, and, again, many software routines are available for conducting the integration. As in the case of the batch filling reactor, however, it is worth giving a detailed description of one possible approach. A simplification often valid is that the heat capacities of reactants and products are constant, in which case equation (4-129) becomes

$$\begin{aligned} (N_{A_0} + N_{B_0}) C_{pR} (T_0 - T^*) &= (N_{A_0} + N_{B_0} - 2N_{A_0} x) C_{pR} (T - T^*) \\ &+ 2N_{A_0} x C_{pP} (T - T^*) \\ &+ N_{A_0} x (-\Delta H)_{T^*} \\ &- 2\pi R \int_0^z U(T - T_M) dz \end{aligned} \quad (4-131)$$

where  $C_{pR}$  and  $C_{pP}$  are heat capacities of reactants and products, respectively. To solve these equations one might pursue the following courses.

- (a) Pick an increment of reactor length,  $\Delta z$ .
- (b) Assume a value of  $T = T_{\Delta z}$  for the temperature at the end of the increment.
- (c) Evaluate  $T_0$  and  $T_{\Delta z}$  to obtain an average value for the increment. The concentrations corresponding to  $\Delta z$  are not known at this point, so use the inlet concentrations at both  $z = 0$  and  $z = \Delta z$ .
- (d) Determine the conversion directly from equation (4-130).
- (e) For the set  $\Delta z$ , assumed  $T_{\Delta z}$ , and conversion, see if equation (4-131) is satisfied.
- (f) Adjust the value of  $T_{\Delta z}$  according to the result (e) and repeat steps (c) to (e).
- (g) When  $T_{\Delta z}$  and  $x$  corresponding to  $\Delta z$  are obtained such that equation (4-131) is satisfied, go to the second length increment and repeat the procedure for  $T_{\Delta z}$  (known) and  $T_{2\Delta z}$  (assumed). Equation (4-131) will have to be modified slightly to account for the fact that conversion is not zero at the beginning of the second increment. For this step  $T_0$  of equation (4-131) is  $T_{\Delta z}$  and  $T = T_{2\Delta z}$ .
- (h) This procedure is then repeated along the entire length of the reactor.

A wide-range of specific numerical techniques may be employed in this solution, the selection of which architecture is often up to the individual. The only specific comment we offer here is to say that the computation time and precision is strongly dependent on the magnitude of  $\Delta z$ . A small value of  $\Delta z$  permits reasonably precise evaluation of the integrals in the two equations by a simple method such as the trapezoidal rule, but of course requires more steps across a given interval. An acceptable  $\Delta z$  depends on the magnitude of the heat of reaction; an interval size that is quite adequate for a reaction with a small heat of reaction may be unacceptable for one with a large heat of reaction. Testing the sensitivity of any solution with respect to the magnitude of  $\Delta z$  is always necessary.

Various modifications of the approach above have been discussed [J.M. Smith, *Chemical Engineering Kinetics*, 3rd ed., McGraw-Hill Book Co., New York, NY, (1970); A.R. Cooper and G.V. Jeffries, *Chemical Kinetics and Reactor Design*, Prentice-Hall, Inc., Englewood Cliffs, NY, (1971); S.M. Walas, *Reaction Kinetics for Chemical Engineers*, McGraw-Hill Book Co., New York, NY, (1959); C.G. Hill, Jr., *Chemical Engineering Kinetics and Reactor Design*, John Wiley and Sons, New York, NY, (1977)].

As an alternative to the procedure above, where the energy balance was written explicitly in terms of the conversion, we may derive the balance in differential terms.

$$\text{output} = A\rho u C_p \left( T + \frac{dT}{dz} \cdot dz \right) - (-r)(-\Delta H)A dz$$

$$\text{input} = A\rho u C_p T$$

$$\text{heat transfer} = U(T - T_M)2\pi R dz$$

Equating these terms gives

$$-\rho\pi R^2 u C_p \frac{dT}{dz} \cdot dz + (-r)(-\Delta H)\pi R^2 dz - U(T - T_M)2\pi R dz = 0$$



in which the cross-sectional area,  $A$ , has been replaced by  $\pi R^2$ . On dividing out the area terms, the energy balance becomes

$$\rho u C_p \frac{dT}{dz} = (-r)(-\Delta H) - \frac{2U}{R} (T - T_M) \quad (4-132)$$

which is to be solved simultaneously with the mass balance

$$-u \frac{dC}{dz} = (-r) \quad (4-42)$$

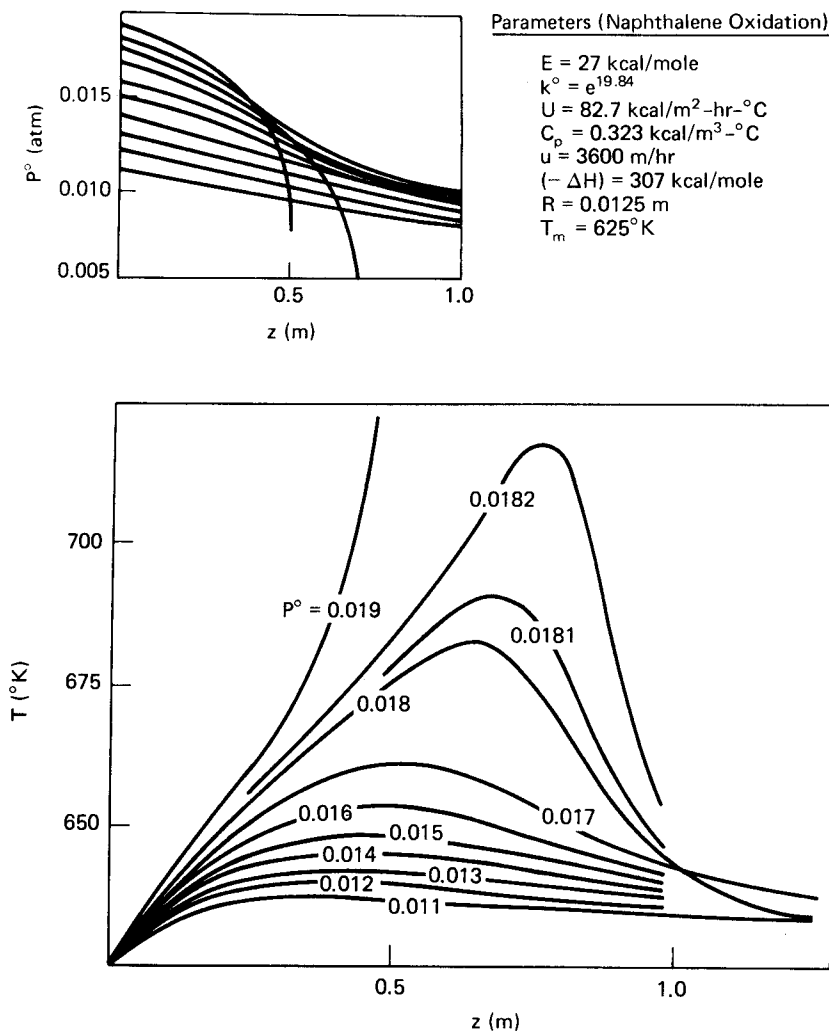


**Figure 4.25** Typical temperature and partial pressure profiles for nonisothermal reactor operation with the highly exothermic naphthalene oxidation reaction. (After R.J. Van Welsenaere and G.F. Froment, *Chem. Eng. Sci.*, 25, 1503, with permission of Pergamon Press, Ltd., London, (1970).]

A very nice example of the application of equations (4-42) and (4-132) to the analysis of a nonisothermal reactor problem is provided by the work of Van Welsenaere and Froment [R.J. Van Welsenaere and G.F. Froment, *Chem. Eng. Sci.*, 25, 1503 (1970)) on naphthalene oxidation. This is a highly exothermic reaction that in commercial operation involves nonisothermal, nonadiabatic reactor operation. Some typical results obtained, in terms of temperature and partial pressure profiles along the reactor length, are illustrated in Figure 4.25 for a number of different inlet naphthalene partial pressures. It is seen that a prominent feature of such reactor operation is the existence of a temperature maximum, or “hot spot,” along the axis of the reactor. Also illustrated by these results is the extreme sensitivity of the locus and magnitude of this hot spot to relatively small changes in inlet conditions. Such behavior, termed *parametric sensitivity*, can be a major concern in reactor stability and control. This will be discussed in more detail in Chapter 6.

Adiabatic reactor problems may be handled by the same procedures and techniques developed for nonisothermal reactors simply by deleting the external heat transfer term from the energy balance. Also, Table 1.3 presented some analytical solutions for simple-order, irreversible adiabatic reactions in batch systems: these solutions apply as well to the adiabatic plug-flow reactor if the system can be considered to be at constant density. In this event, time,  $t$  (in the relationships of Table 1.3) then becomes the PFR residence time,  $t_R$ . The analytical method has also been applied to the more practical problem of reactor operation at constant pressure. In Table 4.4 are two examples for zero- and first-order reactions. Additional solutions are given in the original paper by Douglas and Eagleton [J.M. Douglas and L.C. Eagleton, *Ind. Eng. Chem. Fundls.*, 1, 116 (1962)]. For the two types of second-order reaction, however, they are rather unwieldy.

### Illustration 4.7

In commercial operation of fixed-bed reactors in which the catalyst is deactivating, it is often necessary to maintain constant conversion by increasing the temperature of the reactor to compensate for catalyst decay. One can think of this as a “constant activity” policy in which the bed may be considered isothermal at any given time with the overall temperature level increasing with time of operation.

Consider the case in which the deactivation rate is taken to be concentration-independent (a common industrial model), i.e.,

$$\frac{ds}{dt} = -k_d s^n \quad (\text{i})$$

where  $s$  is the activity variable scaled between 0 and 1, and

$$k_d = A_d \exp(-E_d/RT) \quad (\text{ii})$$

A separable form has been taken to relate the influence of deactivation on the main reaction, which is first order and irreversible with no volume change, intrinsic rate constant  $k$ . Thus, at any time the net rate constant for the main reaction is the product  $ks$ , with

$$k = A_A \exp(-E_A/RT) \quad (\text{iii})$$

**Table 4.4** Example Analytical Solutions for Adiabatic Plug-Flow Reactors at Constant Pressure<sup>a,b</sup>1. Zero order:  $A \rightarrow \nu P$ 

$$-r_A = k$$

$$\frac{\bar{V}}{F} = \frac{C_p}{k(-\Delta H)} \left[ T \exp\left(\frac{E}{RT}\right) - T_0 \exp\left(\frac{E}{RT_0}\right) \right]$$

$$- \frac{EC_p}{Rk(-\Delta H)} \cdot \left[ E_i\left(\frac{E}{RT}\right) - E_i\left(\frac{E}{RT_0}\right) \right]$$

2. First order:  $A \rightarrow \nu$  products

$$\epsilon = \nu - 1 \quad \delta = T_0 + \frac{(-\Delta H)n_{A_0}}{C_p}$$

$$-r_A = k_1 P \left( \frac{n_A}{n_t} \right)$$

$$\frac{\bar{V}}{F} = \frac{-\epsilon C_p}{k_1^0(-\Delta H)P} \left[ T \exp\left(\frac{E}{RT}\right) - T_0 \exp\left(\frac{E}{RT_0}\right) \right] + \left[ n_0 + \epsilon n_{A_0} + \frac{\epsilon EC_p}{R(-\delta H)} \right] (k_1^0 P)^{-1}$$

$$\times \left[ E_i\left(\frac{E}{RT}\right) - E_i\left(\frac{E}{RT_0}\right) \right] - \frac{(n_0 + \epsilon n_{A_0}) \exp(E/R\delta)}{k_1^0 P} [E_i(Z) - E_i(Z_0)]$$

where

$$Z = \frac{E}{R} \left( \frac{1}{T} - \frac{1}{\delta} \right) \quad E_i(x) = \int_{-\infty}^x \frac{\exp x' dx'}{x'}$$

$$Z_0 = \frac{E}{R} \left( \frac{1}{T_0} - \frac{1}{\delta} \right)$$

$$n_t = n_0 + \epsilon x_A$$

<sup>a</sup> In the original reference the following dimensions are employed: $C_p$  = average heat capacity, Btu/mass-°F $F$  = feed rate, mass/time $(-\Delta H)$  = heat of reaction, Btu/mole of A converted $k$  = zero order rate constant, moles A/ft<sup>3</sup>-sec $k_1^0$  = first order frequency factor, moles A/atm-ft<sup>3</sup>-sec $n_{A_0}$  = initial moles of A per unit mass of feed $n_0$  = total moles of feed per unit mass of feed $n_t$  = total moles of reacting system per unit mass of feed $x_A$  = moles of A converted per unit mass of feed $P$  = pressure, atm<sup>b</sup> Any self-consistent set of dimensions may be employed. For example, the zero-order result may be expressed in  $F$  = moles fed/time if  $C_p$  is determined as a molar heat capacity.

For a start-of-run temperature  $T_0$ , where  $k = k_0$ , derive an expression for the relationship between time-on-stream and reactor temperature.

$$t = f(A_i, E_i, n, T, T_0) \quad i = A, d$$

The activity variable, not measurable during operation, should not appear in this expression. Note that while it would be nice to have the relationship the other way around, that is  $T = f(t, \dots)$ , the algebra is uncooperative.

*Solution*

The constant conversion requirement is met by

$$(k)(s) = k_0 \quad (\text{iv})$$

with  $k_0$  the rate constant at  $t = 0$ ,  $T = T_0$  and  $s = 1$ . From equations (iii) and (iv) we can derive a relationship between catalyst activity and temperature as

$$\frac{1}{T} = \left( \frac{R}{E_A} \ln s + \frac{1}{T_0} \right) \quad (\text{v})$$

Substituting equations (v) and (ii) into (i) and integrating, we obtain

$$t = \frac{\exp(E_d/RT_0)}{\kappa} [1 - s^{(E_d/E_A - n + 1)}] \quad (\text{vi})$$

$$\kappa = A_d[(E_d/E_A) - n + 1]$$

Rearrangement of equation (v) and subsequent substitution into (vi) gives the required time-temperature relationship.

$$t = \frac{\exp(E_d/RT_0)}{\kappa} \left\{ 1 - \exp \left[ \frac{E_d - (n)E_A + E_A}{R} - \left( \frac{1}{T} - \frac{1}{T_0} \right) \right] \right\}$$

Further details on the application of equation (vii) with respect to both reactor analysis and the interpretation of data are given by Krishnaswamy and Kittrell [S. Krishnaswamy and J.R. Kittrell, *Ind. Eng. Chem. Proc. Design Devel.*, 18, 399 (1979)]. We shall also revisit this type of reactor operation in Chapter 9.



HORATIO SAYS

Always remember that whenever there is a reactor with a deactivating catalyst there will be an unsteady state to deal with.

## 4.5.2 Stirred-Tank Reactors

Adiabatic or nonisothermal operation of a stirred tank reactor presents a different physical situation from that for plug flow, since spatial variations of concentration and temperature do not exist. Rather, reaction heat effects manifest themselves by establishing a temperature level within the CSTR that differs from that of the feed. Thus, when we use the terms “adiabatic” or “nonisothermal” in reference to CSTR systems, it will be understood to imply analysis where thermal effects are included in the conservation equations but not to imply the existence of thermal gradients.

Since spatial variations are absent, the analysis of thermal effects in the CSTR is much more straightforward than that for a PFR. Consider the steady-state CSTR operation depicted in Figure 4.26. Once again we consider a first-order irreversible reaction, this time exothermic, occurring within the reactor. The

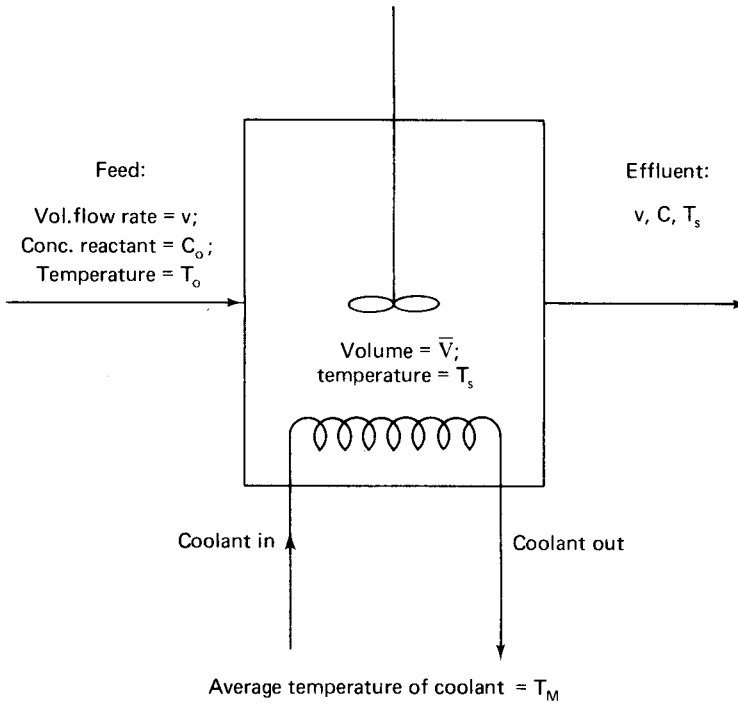


**Figure 4.26** A CSTR in steady-state operation with heat effects.

vessel is cooled by heat transfer to an internal coil of surface area  $A$ , with coolant at an average temperature of  $T_M$  and a constant heat-transfer coefficient,  $U$ . The mass balance is

$$vC_{A_0} - vC_A - k\bar{V}C_A = 0$$

from which, as before,

$$C_A = \frac{vC_{A_0}}{v + k\bar{V}} \quad (4-133)$$

The steady-state heat balance corresponding is

$$vC_p\rho(T_0 - T_s) + kC_A\bar{V}(-\Delta H) - UA(T_s - T_M) = 0 \quad (4-134)$$

We may eliminate  $C_A$  in equation (4-134) from the expression of (4-133) to obtain a relation in terms of the kinetic parameters and  $(-\Delta H)$

$$v\rho C_p(T_0 - T_s) - UA(T_s - T_M) = \frac{-\bar{V}(-\Delta H)k_0e^{-E/RT_s}vC_{A_0}}{v + \bar{V}k_0e^{-E/RT_s}} \quad (4-135)$$

where  $k = k_0e^{E/RT_s}$ . Equation (4-135) establishes the temperature of operation for any given set of operating parameters. For adiabatic operation the heat-transfer term disappears from the expression.

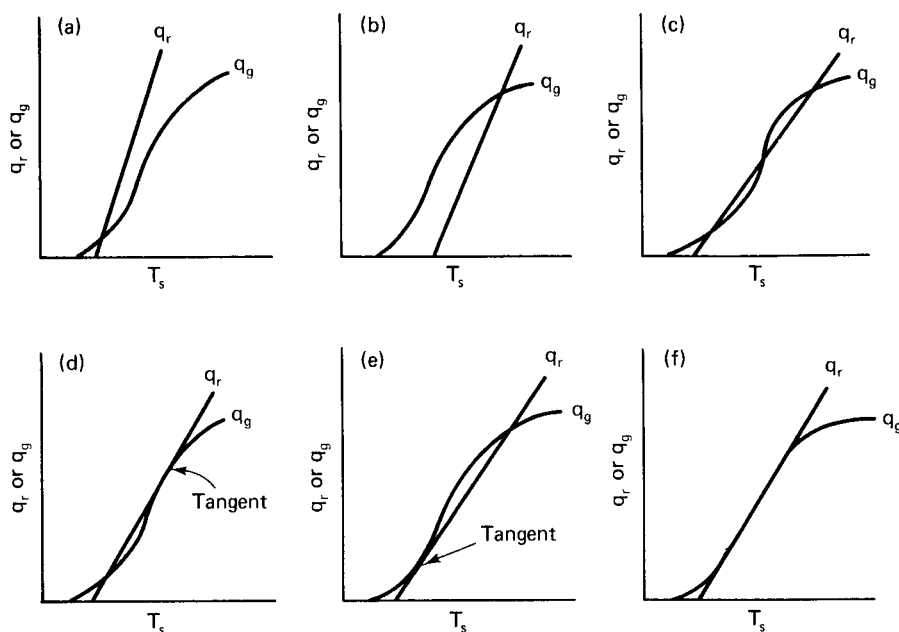
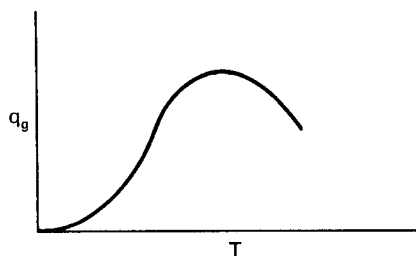


**Figure 4.27** Various operating states for a CSTR with heat effects.

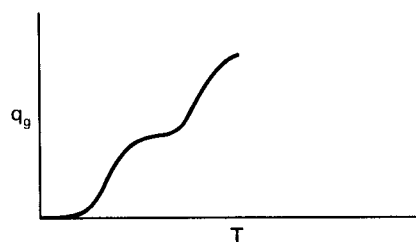
We may also visualize equation (4-135) in the following interesting way: all the terms on the left-hand side, which we shall call  $q_r$ , refer to the rate of heat removal from the system (convective transport and heat transfer to the cooling coil). Conversely, those terms on the right-hand side, which we denote as  $q_g$ , refer to the rate of heat generation in the system by chemical reaction for  $(-\Delta H) > 0$ . We see also that the heat removal rate,  $q_r$ , is a linear function of temperature if  $\rho C_p$  is not sensitive to  $T_s$ , while the heat generation rate,  $q_g$ , is a nonlinear function of  $T_s$ . If these heat-generation and heat-removal functions are plotted individually as a function of  $T_s$ , we can envision a number of different results, depending on operating parameters, as shown in Figure 4.27 for an exothermic, irreversible reaction.

The intersection of the  $q_r$  and  $q_g$  plots sets the temperature of operation, and we see in (a) and (b) the establishment of a single, steady temperature of operation. In case (a) this is a low temperature, with corresponding low conversion, while in (b) is a high temperature with higher conversion. It is apparent from plots (c)-(f) in the figure, however, that a number of other possibilities exist involving either multiple intersections or points of tangency between the  $q_r$  and  $q_g$  curves. Such multiple intersections or points of tangency have significance as to the stability or parametric, sensitivity of the CSTR operation, and these problems will be considered in Chapter 6. The shape of the  $q_g$  curves given in Figure 4.27 is specific to the first-order irreversible kinetics invoked in equation (4-135); some other possibilities are illustrated in Figure 4.28 (see also Section 6.1).

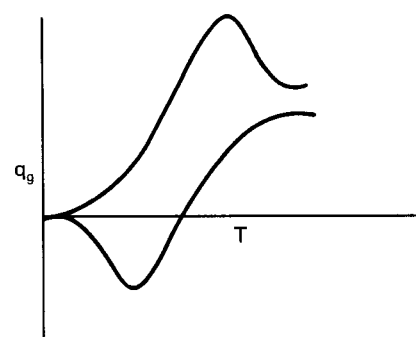
The transcendental nature of equation (4-135) for  $T_s$  precludes the development of any generalized treatment of nonisothermal or adiabatic CSTR sequences as



(a) Reversible Single Reaction



(b) Series (Type III),  
Both Steps Exothermic



(c) Series (Type III),  
1.  $(-\Delta H_1) > 0$ ;  $(-\Delta H_2) < 0$   
2.  $(-\Delta H_1) < 0$ ;  $(-\Delta H_2) > 0$

**Figure 4.28** Heat-generation curves for some more complex reactions.

was possible in the isothermal case. For example, the following general recursion formulas may be developed for the first-order irreversible, adiabatic sequence (which is about as simple as we can make it).

$$C_{A_n} = \frac{C_{A_0}}{\sum_{i=1}^n [1 + k(T_i)\bar{t}]} \quad (4-136)$$

$$\rho C_p (T_n - T_{n-1}) + \frac{k(T_n)C_{A_0}\bar{t}(-\Delta H)}{\prod_{i=1}^n [1 + k(T_i)\bar{t}]} = 0 \quad (4-137)$$

The denominators of both of these equations involve the temperature of all stages up to the  $n$ th in the sequence; thus, individual solutions for each stage, in order, will be required.

A bit more discussion of Figure 4.27c is appropriate. Let us magnify the picture at each of the intersections of the intersections of the  $q_r$  and  $q_g$  curves as shown in Figure 4.29.

Each intersection represents a possible steady-state operating temperature, but the reactor behavior in cases (a) and (c) differs from that in (b). Consider case (a): if there is a small perturbation of reactor temperature from  $T_s$  [say an increase as shown by the arrow in (a)], then both  $q_r$  and  $q_g$  are increased; however, the increase in  $q_r$  is greater than that in  $q_g$  and the excess heat removal capacity will make the

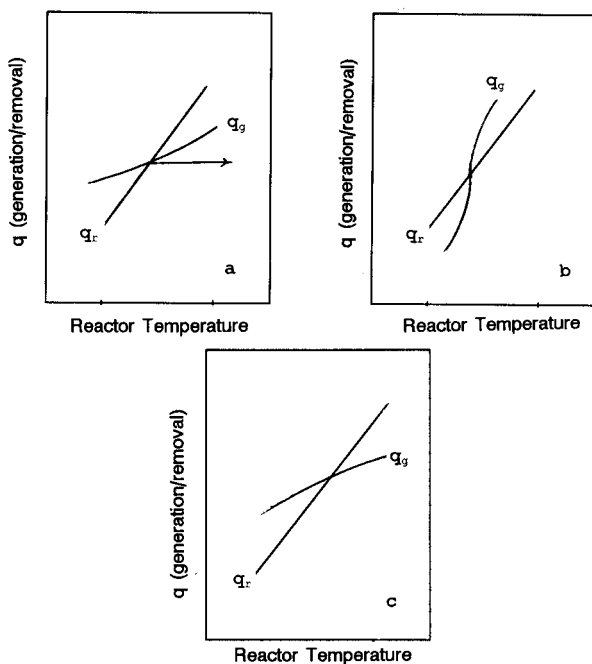


**Figure 4.29** Detail of  $q_r$  and  $q_g$  intersections.



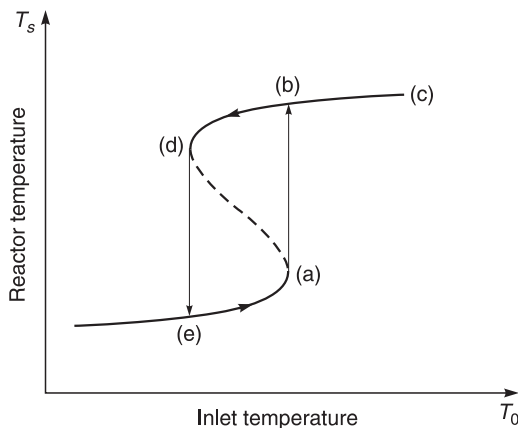


**Figure 4.30** Hysteresis loop for a CSTR with multiple steady states; variation of inlet temperature  $T_0$ .

reactor return to the original  $T_s$ . If we go the opposite way, with a perturbation decrease in reactor temperature from  $T_s$ , then  $q_g$  is greater than  $q_r$ , heat generation exceeds heat removal, and again the system will return to  $T_s$ . One can see that this behavior is also exhibited at the upper intersection shown in case (c), but with the opposite behavior of  $q_r$  and  $q_g$  on either side of  $T_s$ . These types of operating points are stable, or *self regulating*. The behavior in case (b) is completely different: a perturbation increase in reactor temperature from  $T_s$  gives us  $q_g > q_r$  and the reactor will move to the upper steady state. Decrease in temperature from  $T_s$  will remove the reactor to the lower steady state. In actual operation of a reactor of this sort, with no external control, one would never see the intermediate steady state of (b), only operation at point (a), quenched, or point (c), ignited.<sup>6</sup>

Another way to visualize this multiplicity is to follow the reactor operating temperature,  $T_s$ , as a function of the inlet temperature,  $T_0$ . The “S” curve of Figure 4.30 is typical. Increasing  $T_0$  along the lower branch of the curve yields a monotonic increase in  $T_s$  to point (a), at which point the reactor operating temperature jumps to position (b). Further increase in  $T_0$  again results in a monotonic increase in  $T_s$  in the direction toward (c). If we now decrease  $T_0$  there is a smooth decline in  $T_s$  to (d), thus a sudden drop in temperature to (e). This represents the trajectory from quenched, to ignited, to quenched states. The interior region (dotted line) represents the zone of the middle (unstable) steady state. A very nice example of such behavior, more than a mathematical curiosity, is provided by the results of Vejtassa and Schmitz [S.A. Vejtassa and R.A. Schmitz, *Amer. Inst. Chem. Engr. Jl.*, 16, 410, (1970)] on the reaction of sodium thiophosphate and hydrogen peroxide in an adiabatic CSTR and is shown in Figure 4.31.

Multiple steady states are not associated exclusively with temperature-dependent reactor operations. For some types of more complex reaction kinetics, steady-state multiplicity can exist under isothermal conditions. For example, Matsura and Rato [T. Matsura and M. Rato, *Chem. Eng. Sci.*, 22, 171 (1967)]

<sup>6</sup> “Somewhere a place for us.”—From “West Side Story”

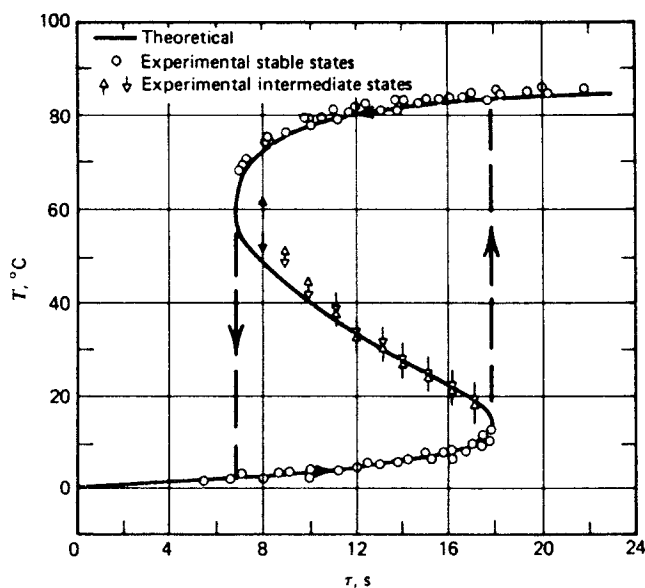


**Figure 4.31** Measured hysteresis for reaction of sodium thiophosphate and hydrogen peroxide in an adiabatic CSTR. In this experiment reactor temperature was measured as a function of holding time. [After S.A. Vejtassa and R.A. Schmitz, *Amer. Inst. Chem. Engrs. J.*, 16, 410, with permission of the American Institute of Chemical Engineers, (1970).]

have shown that the isothermal CSTR with

$$(-r) = \frac{kC_A}{(1 + kC_A)^2}$$

exhibits multiplicity for certain ranges of reactor and reaction parameters. Such behavior is also commonly encountered in biological systems which follow the Monod model. Note that the concepts of multiplicity and parametric sensitivity seem to be paired, but the existence of one does not automatically imply the other. More discussion of all this will be found in Chapter 6.

## 4.6 Catalyst Deactivation in Flow Reactors

### 4.6.1 Plug-Flow Reactors

An important application of ideal reactor models is with reference to actual reactors involving two phases (reaction mixture plus catalyst), or even three phases (trickle beds). In such applications the multiple phases are often lumped together, and the combination treated as a pseudo-homogeneous entity, with transport and reaction parameters appropriate to this particular approach. The pseudo-homogeneous assumption becomes more apparent, and critical, when we begin to think about events in the solid phase, normally a catalyst, having a course differing from those in the fluid phase. Nothing is more typical of this than the situation in which a catalyst is being deactivated under conditions that otherwise would define just typical steady-state reactor operation. This situation is important from both the general

concerns of this chapter—definition and application of ideal reactor models—and from the fact that it is quite important in practice.

This much said, let us now examine the behavior of a PFR in this predicament. The classical example was provided by Froment and Bischoff [G.F. Froment and K.B. Bischoff, *Chem. Eng. Sci.*, 10, 189; 17, 105 (1962)] for isothermal conditions, with catalyst deactivation by either parallel or series reaction steps (see Chapter 3), and our favorite imaginary reaction  $A \rightarrow B$ . Thus we deal with overall sequences such as (XXVI) or (XXVII) of Chapter 3.

If the time scales for deactivation and of the main reaction are of the same order of magnitude (this is not normally the case, but we retain it for the time being), a reactor balance for reactant A (mol fraction  $x$ ) is

$$\frac{\partial x}{\partial \tau} + \frac{\partial x}{\partial z} = \left( \frac{\Omega \rho_B d_p}{F} \right) (-r_A) \quad (4-138)$$

in which the nondimensional variables are defined as

$$\tau = \left( \frac{F}{\epsilon \rho_A \Omega d_p} \right) \theta; \quad z = \frac{w}{d_p}; \quad Z = \frac{W}{d_p}$$

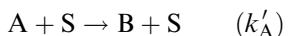
For convenience in reference, we will use here the original notation of Froment and Bischoff, with  $F$  the feed rate in mass/time,  $\epsilon$  the bed void fraction,  $d_p$  the catalyst particle diameter,  $\Omega$  the reactor total cross section,  $\rho_A$  the mass density of reactant A,  $\rho_A$  the bulk density of the catalyst,  $W$  the reactor length,  $\theta$  the time, and  $(-r_A)$  the rate of reaction of A in consistent units. Now, assuming that the deactivation is via coke formation, we can write for the rate of accumulation of coke on the catalyst,

$$\frac{\partial C_c}{\partial \tau} = \left( \frac{\epsilon \rho_A \Omega d_p}{F} \right) (r_c) \quad (4-139)$$

where  $C_c$  is coke-on-catalyst in weight per total weight. By a change of variables to  $\eta' = \tau - z$  [ $\eta'$  is a variable along the characteristic of equation (4-139)] equations (4-138) and (4-139) are simplified to

$$\begin{aligned} \frac{\partial x}{\partial z} &= - \left( \frac{\Omega \rho_B d_p}{F} \right) (r_A) \\ \frac{\partial C_c}{\partial \eta'} &= \left( \frac{\Omega \rho_A \epsilon d_p}{F} \right) (r_c) \end{aligned}$$

For the moment let us further assume that the coke-forming molecule is also the reactant A in the main reaction. Then, for parallel reaction pathways



where S is an available surface reaction site and  $A \cdot S \downarrow$  is a deactivated site. We may now write the rate equations as

$$r_A = k'_A(P)(x) + k'_{A,d}(P)(x) \quad (4-140)$$

$$r_c = k'_{A,d}(P)(x) \quad (4-141)$$

One additional step is required to complete the model: note that equation (4-139) does not give an expression for catalyst activity, only the amount of coke on the catalyst,  $C_c$ . Various relationships between  $C_c$  and  $s$ , the activity variable, have been reported over the years. For the moment let's say this is exponential,

$$s = e^{-\alpha_2 C_c} \quad (4-142)$$

If  $k'_{A,d}$  is independent of  $s$ , then

$$\frac{\partial x}{\partial z} = -a[\exp(-\alpha_2 C_c) + \nu]x \quad (4-143)$$

$$\frac{\partial C_c}{\partial \eta'} = bx \quad (4-144)$$

The constants in equations (4-143) and (4-144) are

$$a = \left( \frac{\Omega \rho_B d_p P}{F} \right) k'_{A_0}$$

$$b = \left( \frac{\Omega \rho_A \epsilon d_p P}{F} \right)$$

$$\nu = \frac{k'_{A,d_0}}{k'_{A_0}}$$

The boundary conditions, expressed for this set of variables, are

$$x(0, \eta') = 1 \quad (4-145)$$

$$C_c(z, 0) = 0 \quad (4-146)$$

stating that the inlet mol fraction of reactant A is unity, and that there is initially no coke deposition within the reactor.

There is one important simplification possible. If the rate of coke deposition is slow compared to the rate of the main reaction or, more precisely, if

$$k'_{A,d} \ll k'_A$$

then the quantity  $\nu$  in equation (4-143) is small and we have as an approximation

$$\frac{\partial x}{\partial z} = -a[\exp(-\alpha_2 C_c)]x \quad (4-143a)$$

Analytical solutions to equations (4-134a) and (4-144) with the boundary and initial conditions as stated may be obtained as

$$x = \{1 + \exp(-\alpha_2 b \eta') [\exp(az) - 1]\}^{-1} \quad (4-147)$$

$$\exp(-\alpha_2 C_c) = \{1 + \exp(-az) [\exp(\alpha_2 b \eta') - 1]\}^{-1} \quad (4-148)$$

Keep in mind that inclusion of the catalyst decay expression has changed the problem from a routine steady-state reactor analysis into a more difficult unsteady-state formulation. The assumption that  $\nu \ll 1$  means simply that within one residence time of a reactant molecule inside the reactor nothing noticeable

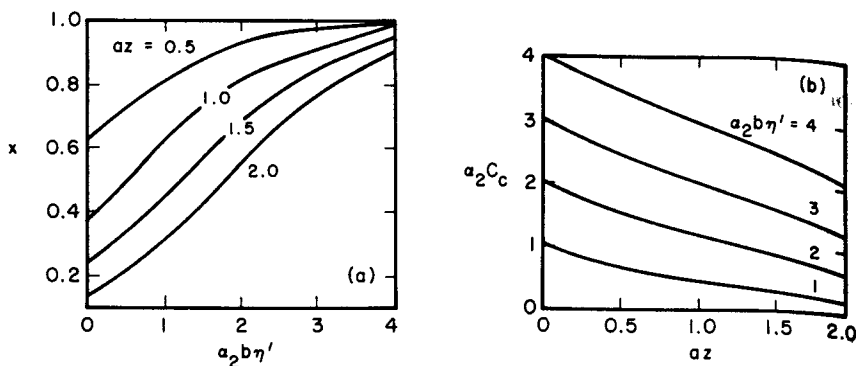
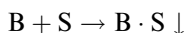
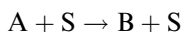


**Figure 4.32** (a) Reactant mol fraction versus time parameter at different positions in the bed; (b) corresponding coke profiles. Parallel deactivation by coke formation with an exponential decay function. [After G.F. Froment and K.B. Bischoff, *Chem. Eng. Sci.*, 10, 189, with permission of Pergamon Press, Ltd., London, (1961).]

happens to the catalyst activity; however, this time-dependent change will manifest itself over characteristic periods of several residence times.

Now let us take a look at some of the results of the analysis. Figure 4.32 shows the reactant composition and carbon deposition profiles computed from equations (4-147) and (4-148). Note that these are nonlinear and time-variant in shape as well as magnitude. Note also that the coke profiles show a decrease in content from bed inlet to bed outlet. This is directly the result of the fact that the reactant is the coke precursor so that, all other factors being the same, the maximum rate of coke deposition (and deactivation) will occur where the precursor is present in the greatest concentration, that is, at the bed inlet. Changing the nature of the  $C_c$  versus  $s$  relationship, for example from exponential to linear, does not affect the general form of these trends.

Now let us go back and reformulate the problem for the case in which the product is the coke precursor.



In this case the rate equations become

$$r_A = k'_A P x \quad (4-149)$$

$$r_c = k'_{B,d} P (1 - x) \quad (4-150)$$

The reactant and coke profiles for this situation are shown in Figure 4.33. The general behavior of the reactant profiles is the same as in the case of parallel deactivation, however the situation with respect to the coke profiles is just the opposite in that the coke concentration increases with reactor length. Here no coke can be formed at the bed entrance in the absence of product, and increasing amounts are produced only as the reaction product concentration increases.

An important consequence of some of this behavior that is probably not apparent from the discussion so far is the formation of moving reaction zones in the reactor, and the way in which they move. This is most clearly illustrated for the parallel deactivation

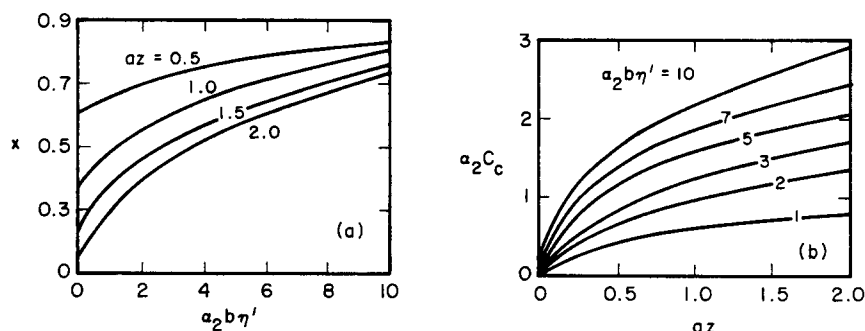


**Figure 4.33** (a) Reactant mol fraction versus time parameter at different positions in the bed; (b) corresponding coke profiles. Series deactivation by coke formation with an exponential decay function. (Ref.: see Figure 4.32.)

shown in Figure 4.32. For this system, where coke concentration and activity both decline with increasing bed length, it is implied that the locus of maximum reactivity may change with chronological time since the reactor inlet—normally the most reactive portion of the bed because the reactant concentration is highest—is preferentially deactivated. The rate of reaction relative to that in the fresh catalyst is

$$\left(\frac{r_A}{r_A^0}\right) = \left(\frac{k_A' P x}{k_{A_0}' P}\right) = x \exp(-\alpha_2 C_c) \quad (4-151)$$

This can be evaluated as a function of time and position upon substitution for  $x$  and  $C_c$  from equations (4-147) and (4-148) into the expression above. The result is quite profound, as shown in Figure 4.34. The development of a maximum in the reaction

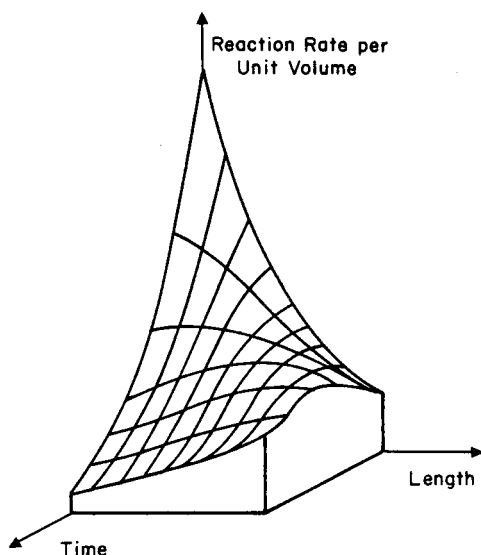


**Figure 4.34** Rate surface for parallel deactivation with an exponential activity function. (Ref.: see Figure 4.32.)

rate is clearly demonstrated here; the maximum passes along the length of the bed and eventually out the end. One thus has an activity wave within the reactor and, if the operation is not isothermal as has been assumed here, the activity wave will also give rise to a thermal wave in the form of continuously varying temperature profiles within the bed. The activity wave shown in Figure 4.34 is a result of the opposing trends of reactant concentration profile and carbon concentration profile within the reactor on the rate of deactivation and, ultimately, on the net rate of reaction per unit volume of reactor as a function of position. Such behavior, then, would be observed only for the descending carbon concentration with reactor length.

If we apply the same reasoning to the carbon profiles shown in Figure 4.33, we would anticipate a progressive narrowing of the zone of activity progressing backwards from the exit, which is preferentially deactivated in this case, to the inlet. There the reaction zone is literally squeezed out of the front of the bed at a sufficiently long time of reaction.

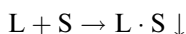
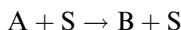
We can summarize these effects of moving zones by saying that for the reactant precursor mechanism (either poisoning or coking), the bed is deactivated from front to back, and for the product precursor mechanism deactivated from back to front. The similarity of such behavior to some corresponding reaction schemes involving individual catalyst particles is striking, as will be shown in Chapter 7.

#### 4.6.2 Stirred-Tank Reactors

The analysis of the effects of catalyst deactivation on CSTR performance is straightforward and there is really not too much to write about; however, this can be of considerable importance in the design of slurry reactors, which will be discussed in Chapter 8. We can start with the familiar relationship for a first-order reaction given in equation (4-68)

$$\frac{C_A}{C_{A_0}} = \frac{1}{(1 + k\bar{t})} \quad (4-68)$$

Since we have used coke formation as the example of the previous section, let us consider here deactivation by the uptake of an irreversible poison  $L$ , so that the overall reaction scheme is that of XXII in Chapter 3.



A mass balance for the poison  $L$  is

$$\frac{C_L}{C_{L_0}} = \frac{1}{(1 + k_d \bar{t})} \quad (4-152)$$

Following the analysis of the previous section, we will define a scaled activity variable,  $s$ , pertaining to both reactant  $A$  and poison  $L$  as

$$s = \left( \frac{S}{S_0} \right) \quad (4-153)$$

and write the kinetic relationships for deactivation

$$\frac{ds}{dt} = (-r_s) = k_d^\circ(s)C_L \quad (4-154)$$

$$k = k^\circ(s) \quad (4-155)$$

Here  $k^\circ$  and  $k_d^\circ$  refer to the initial values of the rate constants (fresh catalyst), and are not to be confused with pre-exponential factors. Now, from equation (4-154)

$$\left(\frac{ds}{s}\right) = k_d^\circ(C_L) \quad (4-156)$$

There are two ways to go from here. One is to combine equations (4-156) and (4-152) and then solve the problem rigorously [note that equation (4-156) will define a logarithmic function of  $s$ ]. The second is to use a correlation, similar to that of equation (4-142) based upon experience with activity versus time-on stream such as

$$s = \exp(-\alpha_p t) \quad (4-157)$$

We will use the second approach here for illustration. In this way we combine equation (4-157) with (4-68)

$$\left(\frac{C_A}{C_{A_0}}\right) = \frac{1}{[1 + k^0 \exp(-\alpha_p t)\bar{t}]} \quad (4-158)$$

Figure 4.35 shows the time-on-stream behavior for a single CSTR at three levels of holding time according to the exponential decay function. It can be seen that the reactor performance is very sensitive to the relative magnitudes of the decay constant  $\alpha$  and the residence time  $t$ . Use of the empirical time-on-stream correlation of equation (4-157) amounts to disregarding the kinetics expressed in equation (4-156). Just as a reminder we will repeat that the nature of the deactivation function—exponential, linear, hyperbolic, etc.—will not change the qualitative nature of the results

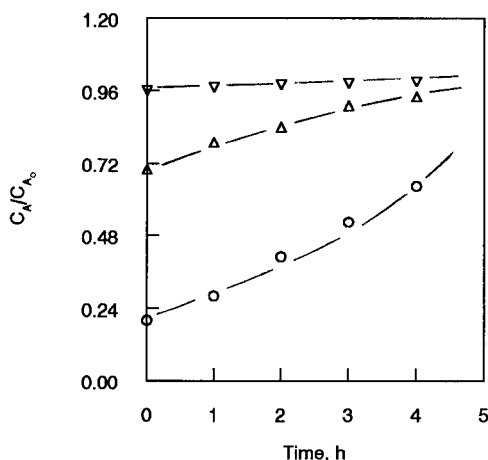


**Figure 4.35** Effect of deactivation on the performance of a single CSTR.  $\alpha = 0.5 \text{ h}^{-1}$ ;  $\nabla - \bar{t} = 0.04 \text{ h}$ ;  $\triangle - \bar{t} = 0.4 \text{ h}$ ;  $\circ = 4 \text{ h}$ .



illustrated in this section. In general, it is seen that if decay is significant, be it via coking, poisoning or whatever, it will control the long-term behavior of the reactor.<sup>7</sup>

#### 4.7 Other Fixed Beds and Other Waves: Ion Exchange and Adsorption

Wave motion similar to that examined in the previous section occurs in other applications of fixed-bed technology. Important among these are processes involving ion exchange or selective adsorption. While these are for the most part separation processes and may or may not include chemical reactions, the analysis is too closely related to what we have been discussing to allow it to pass by now. The nature of the equilibrium between fluid and solid phases plays a more direct and obvious role than in pseudo-homogeneous reactor models, and provides a convenient means for classification.

##### 4.7.1 Favorable Equilibrium with Interphase Mass Transport Rate Controlling

As indicated by the title above we are going to do something a little new here by abandoning the strictly pseudo-homogeneous models that have been used so far, at least to the extent of considering mass transfer between the fluid and solid (adsorbent or ion-exchange resin) phases to be of importance in the overall rate process. All the systems treated will be isothermal.

To begin with, we shall specify a *favorable* equilibrium. In this case, if  $q$  is the concentration of some transferred component in the solid phase, and  $C$  the corresponding fluid-phase concentration, the favorable equilibrium implies a relationship of the sort shown in Figure 4.36. The precise shape of the  $q - C$  curve is not important, only that it reflects the fact that a high loading of transferred component can be attained on the solid phase even at rather low concentrations in the fluid phase—hence the term “favorable”.

A visualization of the wave-like nature of what is going on in the bed is shown qualitatively in Figure 4.37. After some time of operation a zone or “band” of activity develops and passes down the bed as shown in the figure. One can think of this picture as a kind of snapshot showing the bed in action after some time of operation. Upstream of the band the solid phase has been saturated ( $q_\infty$ ) and, since

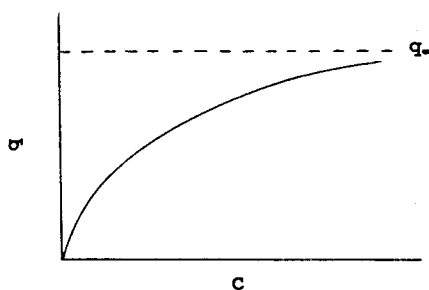


**Figure 4.36** Example of a favorable equilibrium in an adsorption or ion exchange process.

<sup>7</sup> All things are poison and nothing is without a poison, the dose alone makes a thing not a poison.”—*Paracelsus*

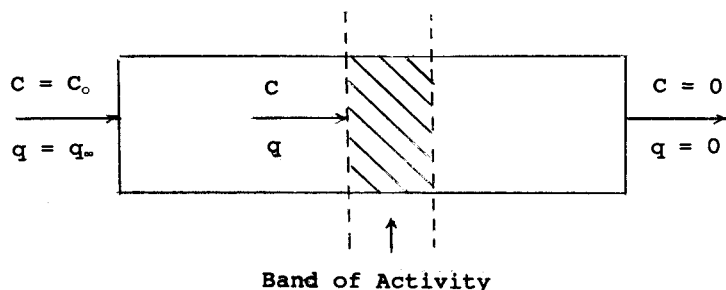


**Figure 4.37** Qualitative sketch of the fixed bed in mid-operation showing the active zone or band of activity.

there is no capacity for further transfer, the fluid phase concentration in this region also remains constant at  $C_0$ . In the band one finds active transport between fluid and solid phases with the concentrations ranging from  $C_0$  to zero and  $q_\infty$  to zero in fluid and solid phases, respectively. Downstream from the band all the transferred component has been removed from the fluid phase, so that  $q = 0$ . This suggests overall that nothing is happening either upstream or downstream from the band, so our analysis need be concerned only with the band itself. From a material balance around the band

$$\frac{C}{q} = \frac{C_0}{q_\infty} \quad (4-159)$$

We will also assume that the band does not change in length as it passes through the bed, which has been verified by experiment for the favorable equilibrium case. As a result, inside the band we may write an equation for the rate of transfer from fluid to solid which is valid wherever the band is located within the bed during operation,

$$\frac{dq}{dt} = (k_D S)(C - 0); \quad q < q_\infty \quad (4-160)$$

$$\frac{dq}{dt} = 0; \quad q = q_\infty \quad (4-161)$$

The significance of the zero value in equation (4-160) is that of an approximation to the equilibrium curve in Figure 4.36, where we state in effect that the equilibrium  $C \rightarrow 0$  for the entire range of  $q$  values, i.e.,  $q \rightarrow q_\infty$  for even very small values of  $C$ . Obviously the validity of this assumption will depend very much on the particular fluid-solid system considered and how sharp the  $C - q$  curve is. The mass-transfer coefficient  $k_D S$  is a volume-based quantity, where  $S$  is the specific surface area per volume for interphase transport. Now, let us make a simple change of variables

$$dt = \left( \frac{dy}{v} \right) = \frac{\text{volume of fluid through bed}}{\text{volumetric flow rate}}$$

We will find it convenient to work with this downstream volume,  $y$ , in the direct determination of total bed capacity and therefore bed life.

From equation (4-159),

$$\left(\frac{dC}{dt}\right) = \left(\frac{C_0}{q_\infty}\right) \left(\frac{dq}{dt}\right)$$

or

$$\left(\frac{dq}{dt}\right) = \left(\frac{q_\infty}{C_0}\right) \left(\frac{dC}{dt}\right) \quad (4-162)$$

Going back to the rate equation (4-160), and substituting from equation (4-162),

$$\left(\frac{dC}{C}\right) = \left(\frac{k_D S C_0}{q_\infty}\right) dt$$

Or, in terms of the downstream volume variable

$$\left(\frac{dC}{C}\right) = \left(\frac{k_D S C_0}{q_\infty v}\right) dy \quad (4-163)$$

This comes from combining the rate equation with the material balance in the band.

The only place we have direct information on  $C$  and  $y$  is from the *breakthrough curve*, that is, when the band exits from the bed, as shown in Figure 4.38. For the overall material balance to be satisfied we must account for the transferred component that escapes the bed as breakthrough is occurring. Integrating along the breakthrough curve we have, from equation (4-163),

$$\ln\left(\frac{C}{C_0}\right) = \left(\frac{k_D S C_0}{q_\infty v}\right) (y - y_{C_0}) \quad (4-164)$$

To obtain the value of  $y$  corresponding to  $C_0$ , let us look at the physical picture when the band has just passed out of the bed (the end of the breakthrough curve). The

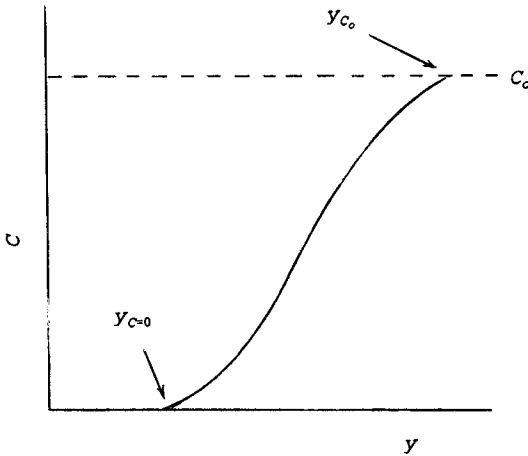


**Figure 4.38** Breakthrough curve as observed when the active band exits from the bed.

overall material balance is

$$y_{C_0} C_0 = q_\infty x + \int_{y_{C=0}}^{y_{C_0}} C dy \quad (4-165)$$

where  $x$  is the weight of the bed utilized. The left-hand side of the equation represents the total amount of material that has entered the bed, the first term on the right-hand side is the amount adsorbed or exchanged, and the integral term is the amount of material escaping as the band is eluted from the bed. Following equation (4-163) it is possible to express the integral term as

$$\int_{y_{C=0}}^{y_{C_0}} C dy = \frac{v q_\infty}{k_D S C_0} \int_{C=0}^{C=C_0} dC = \frac{v q_\infty}{k_D S} \quad (4-166)$$

Thus, in the material balance,

$$y_{C_0} = \frac{q_\infty x}{C_0} + \frac{v q_\infty}{k_D S C_0} \quad (4-167)$$

Substituting this result back into equation (4-164) and rearranging gives [I.M. Klotz, *Chem. Rev.*, 39, 241 (1946)]

$$\ln\left(\frac{C}{C_0}\right) = \left(\frac{k_D S C_0}{q_\infty v}\right) y - \left(\frac{k_D S}{v} x\right) - 1 \quad (4-168)$$

which is the desired relationship among  $C$ ,  $y$  and  $x$ . This form suggests that a logarithmic plot of  $(C/C_0)$  should be linear with

$$\begin{aligned} \text{slope} &= \left(\frac{k_D S C_0}{q_\infty v}\right) \\ \text{intercept} &= -\left(\frac{k_D S}{v} x - 1\right) \end{aligned} \quad (4-169)$$

The analysis is vague only to the extent that nowhere is it obvious that the boundary condition

$$\left(\frac{dq}{dt}\right) = 0; \quad q - q_\infty$$

is included.

The constant size of the bandwidth is a clear fingerprint of the combination of favorable equilibrium and boundary layer mass transfer control of rate. This can be investigated experimentally by making runs at two or more values of  $x$  and comparing the breakthrough curves. Further detail on this, also called *constant-pattern elution*, has been given by Cooney and Lightfoot [D.O. Cooney and W.N. Lightfoot, *Ind. Eng. Chem. Fundls.*, 4, 233 (1965)].

#### Illustration 4.8

The data given below were obtained for the ion exchange of violet chromium with Amberlite IR-100<sup>®</sup> resin in the hydrogen form. All runs were with 20-50 mesh resin and in columns of 1.08 cm internal diameter. The exchange was isothermal at 23.5°C

	Run 14A	Run 16A
Weight (g)	11.0	11.0
$C_0$ (meq/l)	8.08	7.85
$v$ (cm <sup>3</sup> /min)	20.0	20.0

$y$	$C/C_0$	$y$	$C/C_0$
2.1	0.018	1.8	0.010
2.4	0.078	2.1	0.030
2.7	0.241	2.4	0.138
3.0	0.558	2.7	0.462
3.3	0.819	3.0	0.795
3.6	0.931	3.3	0.900
		3.6	0.940

	Run 25A	Run 28A
Weight (g)	11.0	5.5
$C_0$ (meq/l)	7.39	8.00
$v$ (cm <sup>3</sup> /min)	39.0	19.6

$y$	$C/C_0$	$y$	$C/C_0$
1.99	0.049	0.88	0.068
2.15	0.065	1.02	0.143
2.31	0.135	1.12	0.220
2.47	0.261	1.22	0.304
2.63	0.338	1.32	0.469
2.79	0.445	1.40	0.540
2.95	0.574	1.56	0.700
3.11	0.677	1.68	0.770
3.31	0.797		
3.51	0.855		

	Run 29A
Weight (g)	11.0
$C_0$ (meq/l)	14.8
$v$ (cm <sup>3</sup> /min)	19.9

$y$	$C/C_0$
0.90	0.008
1.04	0.021
1.12	0.036
1.20	0.091
1.28	0.193
1.44	0.525
1.52	0.665
1.60	0.775
1.68	0.814

Are this data consistent with an interpretation based on equation (4-168)?

*Solution*

As stated in the text, a semi-log plot of  $\ln (C/C_0)$  versus  $y$  should be linear if equation (4-168) is obeyed. For brevity, we will select Runs 14A and 16A as examples for the interpretation. A semi-log plot of these data is shown in Figure 4.39. It is shown that the data lies fairly close together, which is reasonable since the two runs differ only by a minor amount in  $C_0$ . A reasonable straight line can be drawn through the two sets for  $y \leq 3.0$ . Breakthrough values for  $y \geq 3.0$  are well away from the linear correlation, even in the most optimistic view. Thus, there is reasonable doubt as to whether this analysis is valid.

We will pursue the analysis, however, in the sense that it is more important to fit the initial portion of the breakthrough curve than the end (certainly so in design applications). One should also recognize that end-of-breakthrough data can be less reliable because they are more susceptible to influences of extraneous factors such as nonideal flow patterns, the sensitivity of the chemical analysis, and instrumental uncertainty. Continuing then

Run	Slope	Intercept	$k_s S$	$q_\infty$
14A	1.94	-5.83	22.6	2.04
16A	1.87	-5.40	20.8	1.90

where the units of  $k_D S$  are  $\text{cm}^3/\text{g-min}$  and of  $q$  meq/g. Following the same procedure for the other runs we obtain

Run	Slope	Intercept	$k_D S$	$q_\infty$
25A	1.47	-4.29	31.6	1.76
28A	2.18	-3.15	22.3	1.83
29A	3.46	-5.24	20.1	1.88

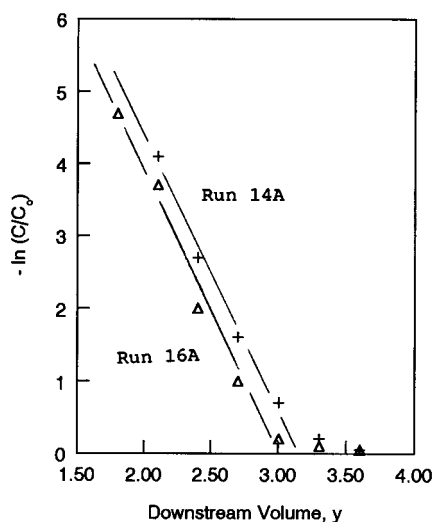


**Figure 4.39** Breakthrough data for Runs 14A and 16A plotted according to equation (4-168).

The numerical values for  $k_D S$  and  $q_\infty$  jump around a bit, but seem generally consistent. The average values are  $21.5 \text{ cm}^3/\text{g-min}$  for  $k_D S$  (excluding Run 25A) and  $1.88 \text{ meg/g}$  for  $q_\infty$ . The effect of flow rate can be estimated by a simple power-law correlation,

$$\frac{(k_D S)_1}{(k_D S)_2} = \left( \frac{v_1}{v_2} \right)^n \quad (\text{i})$$

Using the average  $k_D S$  of 21.5 at an average velocity of  $19.9 \text{ cm}^3/\text{min}$  and the specific values for Run 25A of 31.6 and 39, respectively we obtain  $n = 0.6$ , which is a reasonable value according to mass transfer theory.

Let us now go back to see how well these parameter values do in predicting breakthrough behavior. Using the averaged parameter values in equation (4-168), for run 14A we have

$$\left( \frac{C}{C_0} \right) = \frac{(21.5)(8.09)}{(1.88)(20)} y - \frac{(21.5)(11)}{(20)} - 1 \quad (\text{ii})$$

or

$$\ln \left( \frac{C}{C_0} \right) = 4.62y - 12.82 \quad (\text{iii})$$

The result is

$y$	$C/C_0$
2.1	0.044
2.4	0.179
2.7	0.690
3.0	0.990
3.3	1.0
3.9	1.0

Another way is to check the values of  $y$  corresponding to a given  $(C/C_0)$ . Thus

$$y = \frac{\ln(C/C_0) + 12.82}{4.62} \quad (\text{iv})$$

The results from this type of evaluation are as follows.

$C/C_0$	$y$
0.1	2.28
0.3	2.51
0.5	2.62
0.7	2.70
0.9	2.75

A comparison of experimental data versus calculated values from equation (iv) for Run 14A is given in Figure 4.40. With the exception of the initial breakthrough point, the two seem to have little to do with each other. However, as mentioned before, the prediction of initial breakthrough is no mean accomplishment and may be satisfactory in many instances for design purposes. To be sure, though, one would

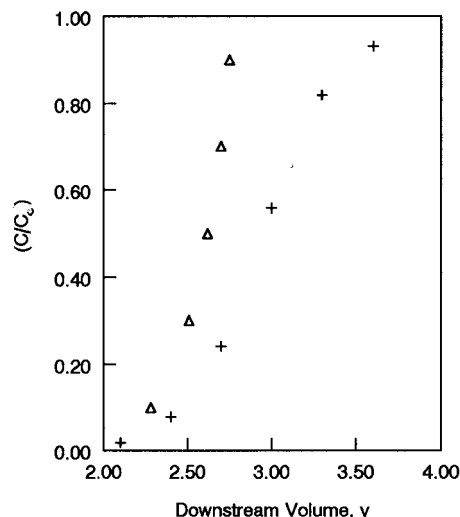


**Figure 4.40** Comparison of experimental and calculated breakthrough for Run 14A;  $\Delta$ -calculated; + -experimental.

certainly not wish to extrapolate for runs of other conditions, and the parameters  $k_D S$  and  $q_\infty$  may not have too much physical significance here.



HORATIO SAYS

I can't help thinking that the person who solved this illustration is either lazy or less than satisfied with the best. Can't we get a better fit, at least up to about  $(C/C_0) = 0.5$ ? Or is the physical model incorrect? Try it anyway, in light of the fact that there are many other possibilities.

This presentation may be viewed as a sampler of a whole group of fixed-bed problems that are concerned with the combination of transport rates with various types of fluid-solid equilibrium. Some of these cases involve chemical reactions, but generally they do not.

## Exercises

### Section 4.2

- Below are two sets of data from tracer experiments to determine residence time in fixed beds. Determine for each case the internal- and exit-age distributions, and the corresponding average holding time.



t, s (sec)	Concentration (ml tracer/ml solution)	t, s	Concentration of tracer
100	0.008	12	0
150	0.050	14	0.04
155	0.070	16	0.12
160	0.090	18	0.20
170	0.106	20	0.18
185	0.090	22	0.09
190	0.080	24	0.04
200	0.060	26	0.02
210	0.046	28	0
220	0.038		
250	0.028		
300	0.019		
400	0.0005		
500	0.000		

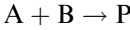
**Sections 4.3 and 4.4**

2. An author has written the following equation for the volume of a PFR to be used for a second-order irreversible reaction

$$\bar{V} = \int_{x_1}^{x_2} \frac{M}{f(x)} d\left(\frac{x}{Cx + D}\right)$$

where

$x$  = mol fraction of reactant A in the reaction



$M$  = mass flow rate, g/s

$f(x)$  = reaction rate

$Cx + D$  = linear relationship for the molecular weight of the mixture in terms of  $x$

For the case considered he wrote

$$f(x) = Kx^3 \quad \text{g mols A reacted/cm}^3\text{-s}$$

For the further specialized case with  $C = -108$  and  $D = 108$ , he wrote the result of the integration as

$$\bar{V} = K_1 \left[ -\frac{3}{2x^2} + 4 \ln \frac{x}{1-x} - \frac{1-2x}{x(1-x)} \right]_{x_1}^{x_2}$$

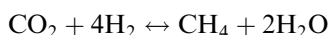
$K_1$  is related but not equal to  $K$ . Comment critically upon this development.

3. The following experimental data were obtained for a first-order irreversible reaction occurring in the liquid phase in a laminar-flow tubular reactor.

$\lambda$	$\langle C_A \rangle / C_{A_0}$
0	1.0
0.05	0.910
0.10	0.835
0.30	0.608
0.70	0.330
1.40	0.119
2.00	0.060

Compare the experimental  $\langle C_A \rangle / C_{A_0}$  data with the predictions of equation (4-107) for the laminar-flow reactor.

4. Dew, White, and Sliepcevich [J.N. Drew, R.R. White and C.M. Sliepcevich, *Ind. Eng. Chem.*, 47, 140 (1955)] present data for the kinetics of the reaction



carried out in a differential reactor. Initial rates were correlated by

$$(-r)_0 = -\frac{kP_{\text{CO}_2}(P_{\text{H}_2})^4}{(1 + K_1P_{\text{H}_2} + K_2P_{\text{CO}_2})^5}$$

where  $(-r)_0$  is in (lb mols methane)/h-lb catalyst, and pressures are in atm. At 596°F and 30 atm the values of the constants are  $k = 7$ ,  $K_1 = 1.73$ , and  $K_2 = 0.29$ . If a stoichiometric feed is introduced at the rate of 100 lb mols  $\text{CO}_2/\text{h}$ , how much catalyst is needed to attain 20% conversion, assuming no product inhibition?

5. The second-order irreversible reaction  $2\text{A} \rightarrow \text{B} + \text{C}$  is being carried out in the gas phase in a laminar-flow reactor, 1 in. in internal diameter and 8 ft long. The feed rate of A is 0.1 lb mol-h at 1 atm, and conversion of A is 53%. In an attempt to increase conversion at the same temperature and molar flow rate it proposed to increase operating pressure to 10 atm. Determine the conversion under the new conditions.
6. The thermal cracking of a petroleum feedstock was studied experimentally at 800°C in a furnace coil 42.5 m long and 0.53 cm internal diameter. The feed rate was 94 g/min and under the experimental conditions it could be assumed that the reactor was isothermal. The measured conversion to the major products (gas and gasoline) was 42.2 wt%. Hydrocarbon cracking of this sort is a first-order irreversible reaction, however, the density of the reaction mixture is a function of the weight fraction conversion,  $x_W$  according to

$$\rho = \frac{1}{0.0014 + 0.0196x_W} \quad \text{g/l}$$

Determine the rate constant for this reaction.

7. The rate of oxidation of CO in an automobile exhaust catalytic converter has been approximated by the expression

$$(-r) = k_0 e^{-E/RT} \left( \frac{C_{\text{O}_2}}{C_{\text{CO}}} \right)$$

where

$$k_0 = 3.47 \times 10^{-3} \text{ mol CO/h-volume}$$

$$E = 12 \text{ kcal/mol}$$

and the concentrations are in mols per volume at standard conditions. In normal operation the converter operates essentially as a PFR at a modified space velocity of  $10^{-5}$  mols CO/h-volume.

What operating temperature is required to attain 90% conversion of CO under these conditions if the reactor inlet composition is 1% CO, 10% O<sub>2</sub>, and the remainder inert. Neglect volume changes of the reaction.

8. Sinfelt, Burwitz and Rohrer [J.B. Sinfelt, S. Hurwitz and J.C. Rohrer, *J. Phys. Chem.*, 64, 892 (1960)] report the following rate equation for the isomerization of *n*-pentane in a hydrogen atmosphere.

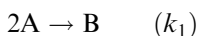
$$(-r) = k \left( \frac{P_{n-C_5}}{P_{H_2}} \right)^n \frac{\text{g mols } C_5 \text{ converted}}{\text{h-g catalyst}}$$

At 372 °C, they report  $k = 0.04$  and  $n = 0.5$ . It is desired to carry out additional investigations at this temperature and 100 psia total pressure with an available laboratory reactor 1 in. in diameter and 1 ft long. The catalyst used, Pt on Al<sub>2</sub>O<sub>3</sub>, has a bulk density of 187.5 lb/ft<sup>3</sup>. The volumetric feed rate to the reactor is limited to a value of 12.5 ft<sup>3</sup>/min (SC). What conversion can be attained with feeds of

- (a) 5% *n*-pentane, 95% hydrogen?
  - (b) 20% *n*-pentane, 80% hydrogen?
9. (a) The gas-phase reaction  $A \rightarrow 2B$  is conducted at 400 K in a tubular reactor (PFR) of diameter 6 cm. The feed contains 50 mol% A and the balance is inert gases. The molecular weight of A is 50 and the inert gases 20. The total feed rate is 400 kg/h, inlet pressure 5 atm, and the reaction rate constant is  $2 \times 10^3 \text{ h}^{-1}$ .
- 1. Determine the reaction length required for 35 % mol conversion of A.
  - 2. If the reactor diameter was 9 cm, what length would be required? Is this the same total volume as needed in case one?
- (b) Obtain the integrated form of the PFR design equation

$$\frac{\bar{V}}{F} = \int_0^x \frac{dx}{(-r)}$$

with the order corresponding to stoichiometry for



10. A dilute aqueous solution of maleic anhydride is to be continuously hydrolyzed at 25 °C. Because of the dilution the reaction is pseudo-first-order, and the rate constant is  $0.143 \text{ min}^{-1}$  at this temperature. A

volumetric feed rate of  $530 \text{ cm}^3/\text{min}$  is to be processed with an anhydride concentration of  $1.5 \times 10^{-4} \text{ g mol/cm}^3$ . There are two 2.5-liter and one 5-liter well-stirred reactor vessels available.

- (a) Would conversion be greater if the one 5-liter vessel or the two 2.5-liter vessels (used as a CSTR sequence) were used for the reaction?
  - (b) What would be the conversion if the two 2.5-liter vessels were operated in parallel, with half the total feed to each?
  - (c) Compare the results of parts (a) and (b) with the conversion in a PFR of 5 liters.
  - (d) Would it be a valid proposition for increasing conversion to place a 2.5-liter PFR after a 2.5-liter CSTR?
11. As a designer, you are confronted with the following dilemma. You have available  $N$  CSTR of equal individual volume  $\bar{V}$ . These are to be used under isothermal conditions (same temperature in each vessel) to carry out an irreversible first-order reaction with rate constant  $k$ . You wish to process the maximum volume per time of feed,  $F_T$ , and would like to decide whether the  $N$  reactors should be placed  $N$  in parallel, or in  $m$  parallel processing lines, each with  $n$  reactors (i.e.,  $N = mn$ ). A specified fractional conversion,  $x$ , of reactant is always required. Show that the allowable feed rate is given by

$$F_T = \frac{kN\bar{V}}{n(1-x)^{-1/n} - n}$$

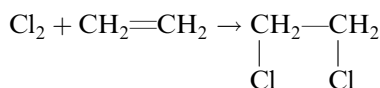
This in general will lead to the policy  $m = 1$ ,  $n = N$ , as giving maximum feed volume per time.

12. Consider the successive irreversible reactions



which are first order. They are to be carried out in a series of CSTR. If we assume that  $k_1 = k_2$  and that the initial concentrations of B and C in the feed are zero, derive a general expression from which the required number of reactors in series to give maximum concentration of B in the product may be found. What is the number of reactors required for the particular case of  $k = 0.1 \text{ h}^{-1}$  and 1-h holding time in each of the vessels?

13. A first-order irreversible reaction is being carried out in a sequence of three CSTRs of equal volume and the same temperature is maintained in each unit. A fraction of the product stream is recycled to the feed of the first reactor. Derive an equation relating to  $C_3$  to  $C_0$ , where  $v$  is the total volumetric feed rate,  $f$  the fraction recycle,  $k$  the rate constant and  $C_i$  the concentration in vessel  $i$ .
14. A characteristic reaction of alkenes is the addition of halogens across the double bond, as



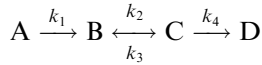
Consider this reaction carried out at  $100^\circ\text{C}$  in a PFR. The feed rate of

each reactant is 10 g mol/min and the rate constant under these conditions is  $6 \times 10^5 \text{ cm}^3/\text{g mol}\cdot\text{h}$ . Molar volume is  $1.64 \times 10^4 \text{ cm}^3/\text{g mol}$  at  $100^\circ\text{C}$

(a) What reactor volume is required for conversion of 60%?

(b) If the linear velocity is to be 500 m/h, what length reactor is required?

15. The reaction



is to be carried out in a series of CSTRs of equal holding time. In the design of these reactors the conversion of A to B in the first unit must be limited to 3% owing to a high rate of heat generation and limited cooling surface. Subsequent stages are not restricted. Reactant A alone is fed to the system at a concentration of  $1 \text{ lb mol/ft}^3$ . All reactions are first order and the rate constants under the contemplated operating conditions are

$$k_1 = 1 \text{ h}^{-1} \quad k_3 = 1 \text{ h}^{-1}$$

$$k_2 = 2 \text{ h}^{-1} \quad k_4 = 2 \text{ h}^{-1}$$

(a) Derive an expression for the concentration of B leaving the  $n$ th reactor in terms of the inlet concentration of A to the first vessel. It is not necessary to write this expression in general form, but indicate how each of the terms in your result can be related to the inlet concentration of A in terms of the rate constants and the holding time alone.

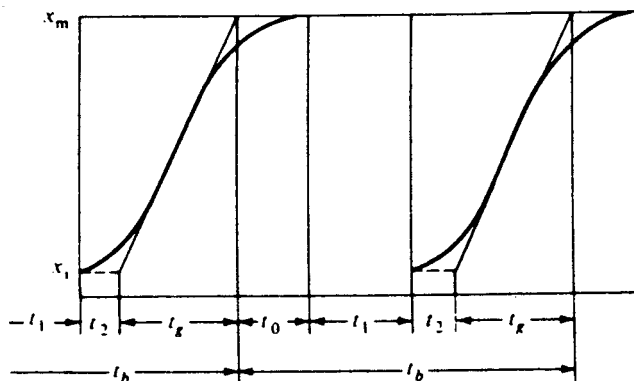
(b) Under these conditions of operation, will it be possible to attain 10% conversion of A to B in two vessels? If not, what conversion is possible?

16. Consider an organism that follows the Monod equation with  $\mu_{\max} = 0.5 \text{ h}^{-1}$  and  $K_s = 2 \text{ g/l}$ .

(a) In a chemostat at steady state and with no cell death, if  $S_0 = 50 \text{ g/l}$  and  $Y = 1 \text{ g cells/g substrate}$ , what dilution rate,  $D$ , will give the maximum total rate of cell production?

(b) For the same value of  $D$ , using tanks of the same size in series, how many units will be required to reduce the substrate concentration to  $1 \text{ g/l}$ ?

17. The figure below gives a typical time cycle involved in the production of biomass.



Here  $t_b$  is total cycle inoculation time,  $t_1$  is preparation and inoculation time,  $t_2$  is induction time for growth phase,  $t_g$  is time of cell growth, and  $t_0$  is the time of cell harvest, Thus we have

$$t_b = t_g + t_0 + t_1 + t_2$$

with a total batch turnaround time of

$$t_d = t_0 + t_1 + t_2$$

We will assume an exponential growth during  $t_g$ , with  $\mu$  the specific growth rate. If  $t_c$  is the holding time to achieve the same amount of cell growth in a CSTR culture, show that

$$\left(\frac{t_b}{t_c}\right) = \frac{\ln(x_f/x_0) + \mu t_0}{1 - (x_0/x_f)}$$

Also show why you would expect this quantity always to be  $> 1$ .

18. Using any method of approach you wish, make a comparison of PFR and CSTR selectivities at equivalent conversions for a Type III reaction in which the kinetics of the first step are half-order. Repeat the analysis for second-order first-step kinetics.
19. A series of CSTRs is being used to carry out a Type III reaction with rate constants  $k_1$  and  $k_2$  for the first and second steps, respectively. It is desired to derive a general expression for the concentration of B leaving vessel  $n$  in terms of the concentrations of A and B in the feed to the first vessel, holding time  $\bar{t}$ , and the rate constants. For the case of  $k_1 = 1 \text{ h}^{-1}$ ,  $k_2 = 0.8 \text{ h}^{-1}$ ,  $\bar{t} = 1 \text{ h}$ ,  $C_{A_0} = 1 \text{ M}$  and  $C_{B_0} = 0.1 \text{ M}$ , determine the vessel for which the exit concentration of B is a maximum.
20. Consider the batch-filling case with the reversible reaction  $A + B \leftrightarrow C$  in which the stoichiometry is as written and first-order kinetics with respect to B (the substance separately charged to the reactor) is assumed. With  $m = (1/3)$ ,  $k_1 = k_2 = 1 \text{ t}^{-1}$ , and  $\nu_B = 5$ , determine the time-history of the concentration of B in the reactor.
21. The reaction  $A + B \rightarrow C$  involves a very high rate of heat generation, and it is proposed that this problem be addressed by charging A to the vessel at reaction temperature and then adding B to it, also at reaction temperature. Under these conditions the reaction is approximately first-order in B. The volume change on reaction is negligible, so the only volume variation is due to the addition of B. The original charge is 1.0 lb mol of A, the specific volumes of A and B are the same,  $1 \text{ ft}^3/\text{lb mol}$ ,  $k$  is  $10 \text{ h}^{-1}$ , and the heat of reaction is  $1.5 \times 10^5 \text{ Btu/lb mol C formed}$ . The estimated maximum rate of heat removal from the reactor is  $5 \times 10^4 \text{ Btu/h}$ . What is the maximum permissible rate of feed of B if a stoichiometric amount of B is to be added? Note that two approaches to this problem may be considered; one would base the feed rate on the maximum instantaneous rate of heat generation, the other would be based on a time average. Which would be preferred, and why?
22. Repeat problem 21 for the case of a reversible first-order reaction (forward with respect to the added component B and reverse with respect to C);  $k_1 = 10$  and  $k_2 = 5 \text{ h}^{-1}$ .

23. A Type III reaction is being carried out in the liquid phase in a stirred tank reactor. Pure A (no B or C) is fed to the reactor, and it is desired to maximize the production of desired intermediate B. The following operating data apply

$$k_1 = 4.0 \times 10^{13} \exp(-25,000/RT); \quad k_1 = 0.0837 \text{ h}^{-1} \text{ at } 100^\circ\text{C}$$

$$k_2 = 6.7 \times 10^{14} \exp(-29,000/RT); \quad k_2 = 0.0064 \text{ h}^{-1} \text{ at } 100^\circ\text{C}$$

$$T = ^\circ\text{K}; R = 1.98 \text{ cal/g mol} \cdot \text{K}; \quad t = 0.5 \text{ h}$$

minimum operating temperature =  $50^\circ\text{C}$

At what temperature is the yield a maximum and what is its value? Does this temperature also maximize the *selectivity* for the production of B?

24. Compare the total recovery of C in the two methods shown below for operation of batch-filling reactors for the reaction  $A + B \rightarrow C$ . The following parameters apply in both cases.

$$R_B = 2700 \text{ g mols B/h}; \quad \text{filling time} = 2 \text{ h}$$

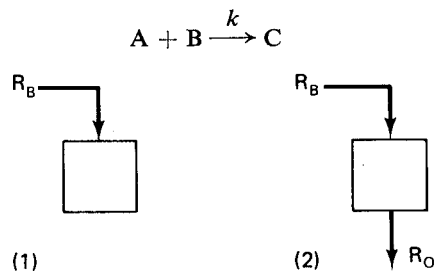
$$k = 0.75 \text{ h}^{-1}$$

$$N_A = \text{pure A present initially} = 5400 \text{ g mols}$$

$$\nu_A = \nu_B = \nu_C = 0.06 \text{ l/g mol}$$

$$R_0 = (R_B/4) \quad \text{g mols mixture/h}$$

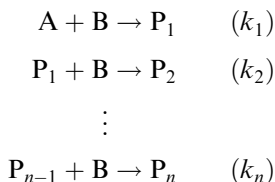
Tank 2 is initially charged with A, and the withdrawal of material begins as soon as B is added. The product fraction is immediately cooled so that no further reaction occurs between A and B after they have been removed from the reactor.



Determine expressions for  $C_B$  and  $C_C$  in tank 2 as a function of time and for the amount of C removed from tank 2 over the 2 h filling period. Compare the two methods on the basis of total mols of C produced. You may assume that C may be completely recovered from the reaction mixture in both cases.

25. A class of homogeneous, competitive-consecutive reactions frequently encountered in commercial processes can be represented by the following

elementary steps:



Included in this sequence are reactions such as the hydration of ethylene oxide to mono-, di-, and triethylene glycol, chlorination of benzene to mono-, di-, and trichlorobenzene (similarly with nitration), etc. Since we are going to consider these as elementary steps, order corresponds to stoichiometry and the rate constants follow the Arrhenius law.

Derive a general expression for a single CSTR that will relate the concentration of product  $P_i$  leaving the reactor,  $C_i$ , to the inlet concentration of reactant A. It will be convenient to represent the result in terms of the rate constant ratio of reaction  $i$  to reaction 1,  $\alpha_i$ , and A remaining in the product,  $\gamma = (C_A/C_{A0})$ . For a full analysis of this see Russell and D.T. Buzzelli [T.W.F. Russell and D.T. Buzzelli, *Ind. Eng. Chem. Proc. Design Devel.*, 8, 2 (1969)].

## Section 4.5

26. Towell and Martin [G.D. Towell and J.J. Martin, *Amer. Inst. Chem. Eng. J.*, 7, 693 (1961)] write the following differential expression for a first-order reaction in a PFR under nonisothermal conditions.

$$\left(\frac{F}{S}\right) \frac{R[F(1+x) + N_D]}{PF(1-x)} dx = \left(\frac{k}{T}\right) dZ$$

where  $F$  is the reactant feed rate in g mols/s,  $S$  reactor cross section in  $\text{cm}^2$ ,  $N_D$  feed rate of diluent in g mols/s,  $R$  the gas constant,  $P$  pressure in atm,  $x$  fractional conversion of reactant,  $T$  temperature in  $^\circ\text{K}$ ,  $k$  the rate constant in  $\text{s}^{-1}$ , and  $Z$  reactor position in cm ( $L$  = total length).

Now let us examine the irreversible first-order decomposition of ethylene to acetylene and hydrogen in view of this, for which the following parametric values apply

$$\begin{aligned} F &= 5.34 \times 10^{-4} \\ N_D &= 2.39 \times 10^{-3} \\ S &= 0.138 \\ P &= 1.008 \\ L &= 66 \end{aligned}$$

The following temperature profile was measured in a steady-state experiment



$Z$ (cm)	$T$ ( $^{\circ}\text{C}$ )
10.2	780
20.4	990
30.5	1050
40.6	1110
50.8	1130
61.0	1040

For this reaction

$$k = (1.03 \times 10^{11}) \exp(-61,900/RT) \text{ s}^{-1}$$

with  $R$  in cal/g mol-K.

Using as input data the experimental values of the temperature versus length reported above, and the parametric values reported by Towell and Martin, compute the conversion of ethylene at the reactor exit.

27. Van Welsenaere and Froment [R.J. Van Welsenaere and G.F. Froment, *Chem. Eng. Sci.*, 25, 1503 (1970)] propose the following model for a one-dimensional tubular reactor with constant wall temperature, a single reaction, and a fluid phase of constant density.

$$u \frac{dp}{dz'} = - \frac{MP\rho_b}{\rho_g} \cdot r$$

$$u \frac{dT}{dz'} = \frac{(-\Delta H)\rho_b}{C_p} \cdot r - \frac{2U}{C_p R} (T - T_M)$$

$$r = (pP_B^{\circ}) \exp \left[ - \left( \frac{a}{T} \right) + b \right]$$

At  $z' = 0$ ,  $p = p^0$ ,  $T = T_M$ , where  $z'$  is the length along the reactor. Their particular study was concerned with the oxidation of naphthalene, a very exothermic reaction, for which the following values of reaction and operating parameters applied.

$$\rho_g = 1.293 \text{ kg/m}^3$$

$$m = \text{molecular weight} = 29.48 \text{ kg/k mol}$$

$$p^{\circ} = \text{inlet partial pressure of naphthalene, atm}$$

$$\rho_b = \text{bulk density of catalyst} = 1300 \text{ kg/m}^3$$

$$(-\Delta H) = 307,000 \text{ kcal/k mol}$$

$$P = \text{total pressure} = 1 \text{ atm}$$

$$C_p = 0.323 \text{ kcal/m}^3\text{-}^{\circ}\text{C}$$

$$U = \text{heat transfer coefficient} = 82.7 \text{ kcal/m}^2\text{-h-}^{\circ}\text{C}$$

$$P_B^{\circ} = \text{constant} = 0.208 \text{ k mol/atm-kg-h}$$

$$a = 13,636 \text{ K}$$

$$b = 19.837$$

$$u = \text{linear velocity} = 3600 \text{ m/h}$$

$$R = \text{reactor radius} = 0.0125 \text{ m}$$

$$T_M = \text{wall temperature} = 625 \text{ K}$$

For an inlet and wall temperature of 625 K, compute the partial pressure and temperature profiles along the reactor length up to 1 m for naphthalene inlet partial pressures of 0.011, 0.013, 0.015, 0.017, 0.018 and 0.019 atm. Use any numerical method you wish but be prepared to encounter sharp gradients that change significantly with inlet conditions.

28. Repeat problem 27 for adiabatic operation,  $U = 0$ .
29. A batch-filling reaction is being carried out under nonisothermal conditions. The reaction occurring is that of the text example,  $A + B \rightarrow C$ , with rate constant  $k$  and heat of reaction  $(-\Delta H) = Q \text{ J/g mol B}$ . The initial charge of A is  $V_A$  liters at temperature  $T_0$  and the rate of addition of B is  $R_B \text{ g mol/time}$ , also at temperature  $T_0$ . The density of the reaction mixture in the vessel is  $\rho$ , and the heat capacities of A, B, and C are equal and  $= C_p$ . It may be assumed that
  1. Reaction is first order in B.
  2.  $k = k_0(T/T_0)^n$
  3. Both  $\rho$  and  $C_p$  are independent of temperature.

Derive the equations describing the process and obtain expressions for the behavior of  $T$  and  $N_B$  with time.

## Section 4.6

30. A reaction that has been shown to be first order and irreversible with  $k = 1 \text{ h}^{-1}$  at a temperature of 250 °C is to be carried out in a sequence of three CSTRs with equal holding times of 3 h. The reaction is promoted by a contained catalyst in the form of small granules intimately mixed together with the liquid reaction mixture. However, the catalyst loses its activity,  $s$ , according to the experimentally determined time-on-stream correlation

$$s = \exp(-0.3t)$$

where  $t$  is in h. Calculate the conversion-time history in each reactor of the sequence from initial operation until the catalyst is completely useless. It may be assumed that initial conversions may be determined via the normal steady-state relationships.

31. Equation (4-158) for CSTR deactivation was derived on the basis of a time-on-stream model for catalyst decay, equation (4-157). Suppose, however, that it is necessary to account for the concentration dependence of the decay rate, as given in equation (4-156). Derive an equation on this basis for  $(C_A/C_{A_0})$  as a function of time-on-stream.
32. Consider cases (a) and (b) of problem 8. Some separate studies of deactivation in this system indicate that the rate of deactivation is independent of the concentration of reactants or products, but is proportional to the second power of activity itself, with a half-life of 20 h. (Second-order kinetics, independent of concentrations, are often a sign of decay via sintering of the metallic component of the catalyst—here Pt on  $\text{Al}_2\text{O}_3$ ).

Derive an expression for the conversion of  $n$ -pentane in the reactor as a function of time of operation for both cases (a) and (b). From this

calculate a time-conversion history from initial operation to a catalyst residual activity of 10%.

33. The reaction system described in problem 9, case (1), is being run under conditions such that the rate of deactivation of the catalyst is a significant factor in the long-term operation. This deactivation is due to coke formation, where the rate of decay is first order in  $C_A$  and is irreversible, so

$$\left(\frac{ds}{dt}\right) = -k_D C_A$$

with  $k_D = 5 \times 10^2$  in appropriate units. This reactor is to be operated at a time-invariant conversion of 35%, so the reactor temperature must be increased with time of operation to counterbalance the decline in the activity of the catalyst. Determine the time temperature schedule that would be required to maintain this constant conversion operation up to a final temperature limit of 650 °K. What would be the extent of deactivation of the catalyst at this point, expressed as a fraction of the activity at 400 °K? Consider two cases.

1.  $E_A = 20$  kcal/mol;  $E_D =$  kcal/mol
2.  $E_A = 10$  kcal/mol;  $E_D = 20$  kcal/mol

34. Equations (4-147) and (4-148) describe the conversion and coke profiles in an isothermal reactor subject to deactivation by coke formation via a parallel mechanism. Derive the corresponding equations for deactivation via a series mechanism.

#### Section 4.7

35. On the basis of the results obtained in Illustration 4.8, establish the weight of resin needed to obtain 98% utilization (i.e., 98% of the total capacity of the bed) at a breakthrough of 0.01. The flow is to be 30 cm<sup>3</sup>/min, the column diameter the same as in the illustration, and the inlet concentration 10 meq/l. Note that a full-scale bed can be designed in this manner; one would change only the diameter to keep the linear velocity the same.
36. Following the hint given at the end of the problem above, let us design a bed that is capable of treating 10,000 l of feed to a specified breakthrough of 0.01. Give the dimensions (diameter and length) and the weight of resin required. Suppose the resin capacity was only one-half of that specified. How would this change the design?

#### Notation

- $A$  cross sectional area, cm<sup>2</sup> or m<sup>2</sup>; heat transfer surface area; see equation (4-134).
- $A_z$  cross sectional area at axial position  $z$
- $a$  constant defined after equation (4-144)
- $b$  constant defined after equation (4-144)
- $C$  concentration of reactant, product, or tracer, mass or mols/volume

- $C_A, C_c$  concentration of A or C, mols/volume  
 $C_c$  coke on catalyst, wt/wt  
 $C_L$  concentration of poison, mass or mols/volume  
 $C_M$  concentration of monomer, mols/volume  
 $C_{A_0}, C_{B_0}, C_{L_0}, C_{M_0}$  initial concentrations of A, B, poison or monomer, mols/volume  
 $C_0$  inlet concentration of tracer, mass or mols/volume  
 $C_{Pi}$  molal heat capacity of  $i$ , typically kcal/m<sup>3</sup>·°C  
 $C_{Rj}$  concentration of polymer product in  $j$ th step, mols/volume  
 $C_{out}, C_{exit}$  exit concentration of tracer, mass or mols/volume  
 $C(t)$  concentration response; see Figure 4.4  
 $C(r_p)$  concentration at  $r_p$ , mols/volume  
 $\langle C_A \rangle$  average exit concentration of A in laminar-flow reactor, mols/volume  
 $D$  reactor diameter, cm or m; dilution rate =  $(v/V), t^{-1}$   
 $D_{max}$  maximum dilution rate,  $t^{-1}$   
 $d_j$  weight distribution of polymer product; see equation (4-77)  
 $d_p$  catalyst particle diameter, cm or m  
 $E$  activation energy, kJ or kcal/mol  
 $E(t)$  exit-age distribution; see equation (4-20)  
 $E_1(z)$  exponential integral; see equation (4-107)  
 $F$  total flow rate, mass or mols/time; feed rate, mass/time; see equation (4-138)  
 $F_A, F_B, F_T$  mols A or B/time at conversion  $x$ ; see equation (4-59) ; also for  $F_B$  feed of B, mols/time; total mols/time  
 $F_A^\circ$  entering feed rate of A, mols/time  
 $F(t)$  residence-time distribution  
 $Fv(z)$  total volumetric flow rate, volume/time  
 $f_1, f_2, f_3$  fractions of A reacted  
 $(-\Delta H_i)$  heat of reaction for step  $i$ , kcal/mol  
 $(-\Delta H)_{T^*}$  heat of reaction at reference  $T^*$  kcal/mol  
 $I(t)$  internal age-distribution function; see equation (4-19)  
 $K_s$  Michaelis constant; see equation (3-74)  
 $k$  reaction rate constant,  $t^{-1}$  for first order  
 $k_d$  deactivation rate constant; see equation (4-152)  
 $k_i$  initiation rate constant, normally second order  
 $k_0$  pre-exponential factor,  $t^{-1}$  for first order  
 $k_p$  propagation rate constant  
 $k_D S$  volumetric mass-transfer coefficient, cm<sup>3</sup>/g·min  
 $k_d^\circ$  initial deactivation rate constant  
 $k_A, k_{A,d}$  rate constants in coke deposition scheme  
 $k^\circ$  rate constant for initial operation; see equation (4-155)  
 $k_1, k_2$  rate constants for  $A \rightarrow B \rightarrow C$  or  $A \leftrightarrow B$   
 $L$  reactor length, cm or m  
 $m$  constant =  $(V_A/F_B \nu_B)$ ; see equation (4-98)  
 $N_B$  mols of B  
 $n$  reaction order; number of CSTRs in a sequence  
 $P$  pressure, normally atm  
 $Q$  total tracer input, mols or mass; heat transferred, kcal/h  
 $q$  concentration of transferred component in solid phase, meq/g in ion exchange

$q_g, q_r$	heat generation and removal rates, kcal or kJ/t
$q_\infty$	equilibrium concentration in solid phase, meq/g
$R_0, R$	reactor radius, l; gas constant, kcal/mol-K
$r_0$	initial rate of reaction, mols/volume- $t$
$r_p$	radial position, l
$r_1$	rate averaged over segregated elements, mass or mols/volume- $t$
$r_2$	rate in mixed elements, mass or mols/volume- $t$
$(-r_B)$	reaction rate of B, mols/volume- $t$
$(r_c)$	rate of coke deposition; see equation (4-139)
$(-r_i), (-r_j)$	initiation or propagation rate, mols/volume- $t$
$(-r_s)$	rate of deactivation, nondimensional
$(-r_x)$	rate of cell formation, mass/volume- $t$
$r_A^\circ$	initial rate of A; see equation (4-151)
$S$	substrate concentration, typically mass/volume
$S_i$	intrinsic selectivity, $(k_1/k_2)$
$S_0$	inlet substrate concentration, mass/volume
$SV$	space velocity, $t^{-1}$
$S_B(\text{II})_{CSTR}, S_B(\text{III})_{CSTR}$	selectivity for B in Type II or III reaction in a CSTR
$S_B(\text{II})_{PFR}, S_B(\text{III})_{PFR}$	selectivity for B in Type II or III reaction in a PFR
$s$	activity; see equations (4-142) and (4-153)
$T$	temperature °C or °K
$T_M$	coolant or external temperature, °C or °K
$T_0$	inlet temperature, °C or °K
$T_s$	steady operating temperature in a CSTR; see Figure 4.24
$t$	time, s, min, h
$\Delta t$	time increment
$t_R$	residence time; see equation (4-63)
$t_{PFR}$	residence time in a PFR for conversion $x$
$\bar{t}$	mean or average residence time; residence time in a CSTR
$\bar{t}_{CSTR}$	residence time in a CSTR for conversion $x$
$\bar{t}_i$	residence time in CSTR unit $i$
$t_1$	specified time; see equation (4-26)
$t(r_p)$	residence time corresponding to radius $r_p$
$U$	nondimensional radius $= (r_p/R_0)$ ; overall heat transfer coefficient, kcal/m <sup>2</sup> -h-°C
$u$	axial flow velocity, length/ $t$
$u_0$	central streamline axial velocity, length/ $t$
$\bar{u}$	average velocity, length/ $t$
$u(r_p)$	axial velocity at radius $r_p$ , length/ $t$
$V$	volume of reaction mixture
$V_A$	volume of A initially present; see equation (4-97)
$V$	vessel volume
$v$	volumetric flow rate, volume/ $t$ ; specific volume, volume/mol
$W$	reactor length
$W_M$	molecular weight of monomer
$jW_M$	molecular weight of polymer molecule in step $j$
$w$	axial length variable

$x$	ratio of initial conversions; conversion; mol fraction of reactant A in coke deposition scheme; weight of bed utilized
$\Delta x$	increment in conversion
$x_n$	conversion leaving CSTR unit $n$
$x_{overall}$	total conversion; see Illustration 4.5
$x(r_p)$	conversion at radius $r_p$
$Y$	yield coefficient, mass cells formed/mass substrate consumed
$Y_B(\text{II})_{CSTR}$	yield of B in Type II reaction in a CSTR
$Y_B(\text{II})$	yield of B in Type II reaction in a PFR
$Y$	downstream volume at time $t$
$y_{Co}$	downstream volume at end of breakthrough
$y_{C=0}$	downstream volume at starts of breakthrough
$Z$	constant = $(W/d_p)$ ; see equation (4-138)
$z$	reactor length variable; nondimensional variable = $(w/d_p)$ ; see equation (4-138)
$\Delta z$	increment of reactor length

*Greek*

$\alpha$	ratio of volumes segregated elements: micromixing parameter; constant = $(1 + k_1 \bar{t})$ in equation (4-89)% reversible rate factor on Illustration 4.6
$\alpha_p$	poisoning-activity correlation constant; see equation (4-157)
$\alpha_2$	coke-activity correlation constant
$\beta$	constant = $(1 + k_2 \bar{t})$ in equation (4-117)
$\gamma$	constant = $[(1 - f_2)/(1 - f_1)]$ ; constant = $[1 + (k_1 + k_2) \bar{t}]^{-1}$ ; see equation (4-114b)
$\delta(t)$	input function for tracer introduction
$\epsilon$	volume change factor; void fraction
$\eta'$	variable = $(\tau - z)$ ; see equation (4-138)
$\theta$	number of residence times = $(t/\bar{t})$ ; time; see equation (4-138)
$\lambda$	constant = $(kL/u_0)$ with $k$ first-order rate constant
$\lambda$	constant = $(C_{A_0} kL/u_0)$ , with $k$ second order
$\mu$	specific growth rate = $(r_x/C)$
$\mu_m$	maximum specific growth rate; see equation (3-74)
$\nu$	constant defined after equation (4-144)
$\nu_B$	specific volume of B, volume/mol B
$\nu(z)$	specific volume of reaction mixture at axial position $z$ , volume/mol
$\rho$	density, g/cm <sup>3</sup> or kg/m <sup>3</sup>
$\rho_A$	mass density of A; see equation (4-138)
$\rho_B$	bulk density of catalyst; see equation (4-138)
$\tau$	specific volume of reaction mixture, cm <sup>3</sup> /mol
$\Omega$	reactor cross section; see equation (4-138)

---

## Modeling of Real Reactors

Cauliflower is nothing  
but cabbage with a college education

—Mark Twain

The first section of Chapter 4 gave considerable attention to the development of mixing models for several types of “ideal” cases—ideal in the sense that they represent extremes of mixing behavior that are well-defined and can be treated analytically. The residence-time, internal- and exit-age distributions were shown to provide some means for characterization of mixing within a given system, though the distinction between macro- and micromixing was not resolved completely. From a working point of view, however, we were able to define a PFR as exemplary of the case in which all elements of fluid leaving the system have identical exit ages, and the CSTR as that in which the internal- and exit-age distributions are identical. Further, we were able to show how such distributions could be determined from experimental information on  $F(t)$  or  $C(t)$ .

Figures 4.3(b) and 4.4(b) gave some response curves intermediate between the ideal mixing limits, which obviously reflect the effects of some type of deviation from well-characterized mixing. Two questions arise:

1. What factors may be responsible for such deviations?
2. How can we use age distribution information to predict the influence of such deviations on actual reactor performance?

As will be seen, a number of alternative approaches have been developed which provide a considerable degree of flexibility in the modeling of nonideal reactors.

One of these approaches is to use the exit-age distribution directly. For ideal reactors this will allow determination of limits between which the actual conversion must lie. These two limits are, of course, those of complete segregation and maximum mixedness as described in Chapter 4. For nonideal reactors one follows the same procedure employing the experimentally determined exit-age distribution.

A second approach is to use various combinations of the ideal reactor models in simulation of nonideal behavior. This may seem a bit contradictory at first, but hopefully our later discussion will be sufficient to illuminate the reasoning behind this method. A hint of this approach is given by the discussion in Chapter 4 on the comparisons between the conversions in PFR and CSTR sequences of the same total

residence time. Figure 4.21 shows clearly that the conversion attained in a sequence of CSTRs approaches that of a PFR of equivalent residence time as the number of units in the CSTR sequence becomes large. Hence, such sequences may be useful in modeling deviations from PFR behavior and in giving some insight as to the role of mixing phenomena in such deviations.

Yet another approach is based on the following simple notion. The characteristic  $C(t)$  curve of Figure 4.4(b) for responses intermediate to the ideal limits is broader and more diffuse than that of the pulse input response for the plug-flow limit. This suggests that some type of diffusion or dispersion term might be incorporated into the basic plug-flow model to represent the effects of nonideal flows on reactor performance.

The concepts involved in the development and application of these differing approaches are themselves quite different, and their successful application may well vary from case to case. To understand this better, let us first examine some of the kinds of deviation commonly encountered from ideal flow.

### 5.1 Deviation from Ideal Flows

The possible sources of deviation from ideal flow are both numerous and diverse in nature. Three major problems are *channeling* of fluid in the reactor, *dead volume* within the reactor, or *bypassing* of fluid through the reactor. In channeling, a path of least resistance through the reactor exists such that a major portion of the fluid passes through the channel leading to local inhomogeneities in concentration. Dead volumes indicate regions of stagnation in which there is no fluid motion and thus loss of contact with the surrounding reaction mixture. Bypassing means that a significant amount of fluid enjoys a much abbreviated residence time in the reactor. As one might expect, these three are not mutually exclusive and may in certain situations be related—particularly in the case of channeling and bypass flows. Schemata of these types of nonideal flow phenomena are given in Figure 5.1 together with typical  $F(t)$  and  $C(t)$  curves.

Aside from these large-scale, macroscopic deviations from ideal flow patterns, nonideal  $F(t)$  responses can arise from diffusion within the reactor, from velocity profiles in tubular reactors that deviate from the plug-flow pattern, or from combinations of the two effects. It is the sum combination of all such processes that constitute what we have called “mixing effects” on chemical reactor performance. In what follows, we will first attempt to develop a model adequate for the types of  $F(t)$  and  $C(t)$  behavior illustrated in Figures 4.3(b) and 4.4(b), then attempt to extend these ideas to modeling some of the more pathological behavior illustrated in Figure 5.1.

### 5.2 Modeling of Nonideal Flow or Mixing Effects on Reactor Performance

In this section we will develop the techniques for modeling mixing effects on reactor performance. As pointed out above, three approaches have received the most attention (1) direct use of RTD information, (2) mixing-cell approximations, and (3) dispersion-plug-flow models.



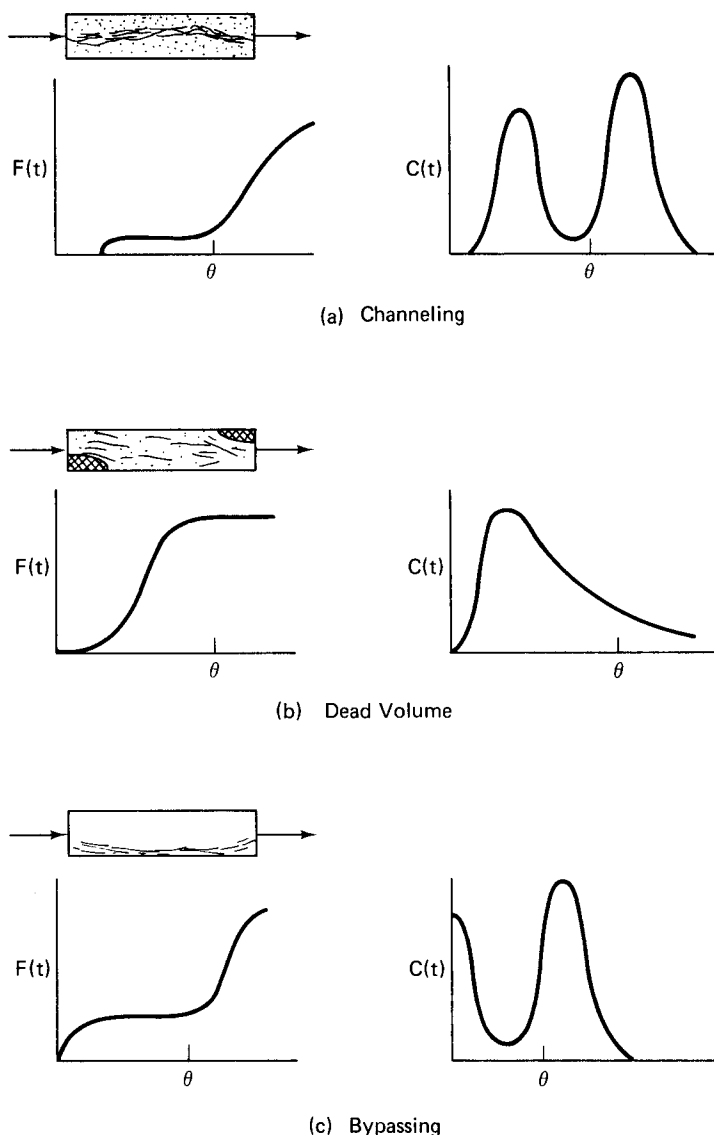


**Figure 5.1** Response diagrams for channeling, dead volume, and bypassing.

### 5.2.1 Direct Use of RTD Information: The Segregated-Flow Model

If we assume that the flow in a given reactor is completely segregated, that is, with no communication between the individual volume elements as they pass through the reactor, then for whatever kinetics applicable the conversion in each element is uniquely determined by the length of time the element has spent in the reactor.<sup>1</sup> To obtain the average conversion in the effluent from the reactor, we

<sup>1</sup> Oh the wasted hours of life that have drifted by. Oh, the good that might have been.”—*S. Doudney*

integrate the appropriate conversion expression with respect to the exit-age distribution.

$$\bar{x} = \int_0^{\infty} x(t) E(t) dt \quad (5-1)$$

This integration can be carried out analytically if a suitable expression for  $E(t) dt$  exists for the reactor under consideration.

Let us consider, for example, the second-order reaction  $2A \rightarrow C + D$ , for which the conversion is given by

$$x = \frac{ktC_{A_0}}{1 + ktC_{A_0}}$$

Now, let us assume that this reaction is being carried out in a CSTR in which segregated flow exists. The residence-time distribution function is

$$F(t) = 1 - e^{-t/\bar{t}} \quad (4-35)$$

and the exit-age distribution is

$$E(t) = \frac{dF(t)}{dt} = \frac{e^{-t/\bar{t}}}{\bar{t}} \quad (4-36)$$

Conversion in the segregated flow CSTR will then be

$$\bar{x} = kC_{A_0} \left( \frac{1}{\bar{t}} \right) \int_0^{\infty} \frac{te^{-t/\bar{t}} dt}{1 + kC_{A_0}t} \quad (5-2)$$

This can be integrated to

$$\bar{x} = 1 - \frac{e^{(1/kC_{A_0}\bar{t})}}{kC_{A_0}\bar{t}} E_1(1/kC_{A_0}\bar{t}) \quad (5-3)$$

where

$$E_1(x) = \int_x^{\infty} \frac{\exp(-x')}{x'} dx'$$

The result of a corresponding derivation for first-order reactions can be written as

$$x = 1 - e^{-kt}$$

$$\bar{x} = \int_0^{\infty} (1 - e^{-kt}) \frac{e^{-t/\bar{t}}}{\bar{t}} dt \quad (5-4)$$

$$\bar{x} = \frac{k\bar{t}}{1 + k\bar{t}} \quad (5-5)$$

The result here is identical in form to the result obtained for perfect mixing, which is in agreement with the discussion early in Chapter 4 showing that first-order reactions are unaffected by the extent of micromixing.<sup>2</sup>

<sup>2</sup>“Plus ça change, c’est plus la même chose.”—Anonymous

For half-order kinetics we may derive

$$x = 1 - \left( 1 - \frac{kt}{2\sqrt{C_{A_0}}} \right)^2$$

for  $0 < t < 2(C_{A_0}/k)^{1/2}$ . Then

$$\bar{x} = \int_0^{2\sqrt{C_{A_0}/k}} \left[ 1 - \left( 1 - \frac{kt}{2\sqrt{C_{A_0}}} \right) \right] \frac{e^{-t/\bar{t}}}{\bar{t}} dt \quad (5-6)$$

which gives

$$\bar{x} = \frac{k\bar{t}}{\sqrt{C_{A_0}}} \left[ 1 - \frac{k\bar{t}}{2\sqrt{C_{A_0}}} (1 - e^{-2\sqrt{C_{A_0}/k}\bar{t}}) \right] \quad (5-7)$$

Corresponding expressions for the case of complete mixing are given in Table 4.2. A comparison of typical conversion results for complete mixing and complete segregation for half-, first-, and second-order kinetics is shown in Figure 5.2. It is

- Curve: 1 — perfectly mixed,  $n = \frac{1}{2}$   
 2 — segregated,  $n = \frac{1}{2}$   
 3 — perfectly mixed or segregated,  $n = 1$   
 4 — segregated,  $n = 2$   
 5 — perfectly mixed,  $n = 2$

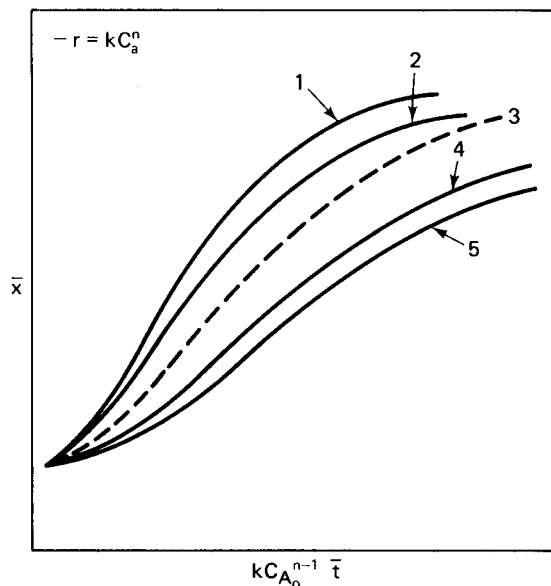


**Figure 5.2** Comparison of conversions in a segregated-flow STR with a perfectly mixed STR for half-, first-, and second-order reactions.

seen that segregation *increases* average conversion for reaction orders  $> 1$  and *decreases* conversion for reaction orders  $< 1$ , with no effect for first order, as suggested previously. The difference in the curves for segregated and perfectly mixed cases indicates the magnitude of effects due to micromixing. If some extent of micromixing exists in an actual situation, actual conversions will lie between the two limits.

Direct use of the age distribution in this manner, then, amounts to a segregated-flow model, not micromixing, which is able to predict for simple kinetics either the upper or lower bound of the effects of nonideality, depending on the order of the reaction.

According to this view, then, the conversion in any sort of reactor can be estimated if we know the exit-age distribution function, and indeed this is so. For a further illustration, let us reconsider the laminar-flow reactor results of Chapter 4. There we stated

$$E(t) = \frac{\bar{t}^2}{2t^3} \quad (4-56)$$

For a first-order reaction, then

$$\bar{x} = \frac{\bar{t}^2}{2} \int_{1/2}^{\infty} \frac{1 - e^{-kt}}{t^3} dt$$

and for a second-order case,

$$\bar{x} = \frac{kC_{A_0}\bar{t}^2}{2} \int_{1/2}^{\infty} \frac{dt}{t^2(1 + ktC_{A_0})}$$

The demonstration that these forms reduce to the corresponding equations given previously [equations (4-107) and (4-108)], is left to the exercises.

Now, in many applications in practice, such as shown in Figure 5.1, one will not have available analytical expressions for the exit-age distribution but rather a set of concentration-response data from either pulse- or step-input experiments. The brave may wish to curve-fit such data and then integrate the resulting expression. In general, the integral of equation (5-1) can always be replaced by the corresponding summation and the average conversion can be determined from

$$\bar{x} = \sum x(t)E(t) \Delta t \quad (5-8)$$

using the general techniques discussed in Chapter 4.

### Illustration 5.1

Compare the conversion obtained for the second-order reaction  $2A \rightarrow C + D$  in a single CSTR with that determined from the segregated flow result of equation (5-3). The parameter  $k\bar{t}C_{A_0} = 0.079$  liter/g mol. Is this result consistent with the postulated effects of micromixing on reactions of order  $> 1$ ?

*Solution*

For the reaction  $2A \rightarrow C + D$ ,

$$k\bar{t}C_{A_0} = 0.079 \text{ liters/g mol}$$

$$C_{A_0} = 1 \text{ mol/liter}$$

We have from equation (5-3) for segregated flow:

$$\bar{x} = \left( \frac{1}{k\bar{t}C_{A_0}} \right) \exp(1 - k\bar{t}C_{A_0}) \cdot E_1(1/k\bar{t}C_{A_0}) \quad (i)$$

with  $(1/k\bar{t}C_{A_0}) = 12.66 = y$ . Interpolation from tabulated values for  $E_1(y)$  gives

$$y[\exp(y)]E_1(y) = 0.928$$

$$E_1(y) = 2.33 \times 10^{-7}$$

Using these values in (i) we obtain

$$\bar{x} = 1 - (3.98 \times 10^6)(2.33 \times 10^{-7})$$

$$x = 0.071 \text{ for segregated flow.}$$

For the CSTR, the mass balance is

$$C_{A_0} = C_{A_1} + k\bar{t}(C_{A_1})^2 \quad (ii)$$

with  $k\bar{t} = 0.079$ . Solving for  $C_{A_1}$  gives

$$(C_{A_1}/C_{A_0}) = 0.931$$

$$x = 0.068 \text{ for the CSTR}$$

Segregation thus does indeed increase conversion for reaction orders  $> 1$ , even at these low levels.



HORATIO SAYS

I think the author is trying to show that his derivations are correct. It will be interesting to see how large the changes can be.

### 5.2.2 Mixing-Cell Approximations

The thought of using mixing cells to approximate deviations from ideal behavior originates from studying the transient response of CSTR sequences. Let us run a tracer experiment, as in Chapter 4, for determining the RTD of a sequence of CSTRs as shown in Figure 4.12. Initially, there is a steady flow of fluid throughout the sequence, and at a given time a step function of tracer is introduced. For any unit in the sequence, we have

$$\bar{V}_n \frac{dC_n}{dt} = v(C_{n-1} - C_n) \quad (5-9)$$

where  $\bar{V}_n$  is the volume of the unit,  $C$  is the tracer concentration, and  $v$  is the steady volumetric flow rate. This can be rearranged, for equal volumes in all

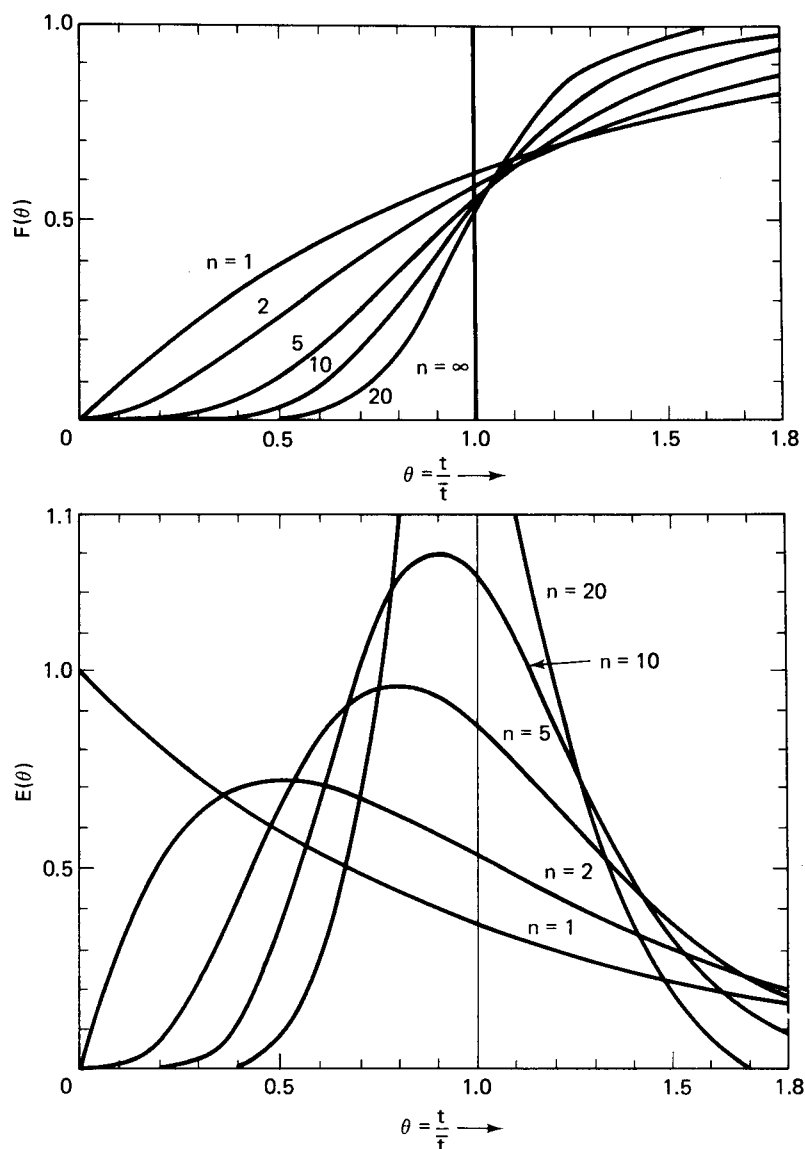


**Figure 5.3**  $F(\theta)$  and  $E(\theta)$  as determined from mixing cells in series model. [After A.R. Cooper and G.V. Jeffreys, *Chemical Kinetics and Reactor*.]

units, to

$$\frac{dC_n}{dt} + \frac{C_n}{\bar{t}} = \frac{C_{n-1}}{\bar{t}} \quad (5-10)$$

where  $\bar{t}$  is the nominal average residence time per unit,  $\bar{V}/v$ . For  $n=1$ ,

$$\frac{dC_1}{dt} + \frac{C_1}{\bar{t}} = \frac{C_0}{\bar{t}} \quad (5-11)$$

This is identical to equation (4-49), with the same limits of integration, and with the result

$$C_1 = C_0(1 - e^{-t/\bar{t}}) \quad (5-12)$$

Now, for  $n = 2$ ,

$$\frac{dC_2}{dt} + \frac{C_2}{T} = \frac{C_0(1 - e^{-t/\bar{t}})}{\bar{t}} \quad (5-13)$$

which has as its solution

$$C_2 = C_0 \left[ 1 - e^{-2t/\bar{t}_t} \left( 1 + \frac{2t}{\bar{t}_t} \right) \right] \quad (5-14)$$

where  $\bar{t}_t$  is the mean residence time of the two-unit sequence.

Following this procedure systematically through the entire  $n$ -unit sequence, one can obtain the general expression for concentration response as

$$F_n(t) = F(\theta) = \frac{C_n}{C_0} = 1 - e^{-nt/\bar{t}_t} \left[ \sum_{i=1}^n \frac{(nt/\bar{t}_t)^{i-1}}{(i-1)!} \right] \quad (5-15)$$

where  $\bar{t}_t$  is the total residence time,  $n\bar{t}$ .

The exit-age distribution,  $E_n(t)$ , for the  $n$ -unit CSTR sequence is

$$E_n(t) = \frac{n^n}{\bar{t}_t} \left( \frac{t}{\bar{t}_t} \right)^{n-1} \frac{e^{-nt/\bar{t}_t}}{(n-1)!} \quad (5-16)$$

The  $F(\theta)$  and  $E(\theta)$  [ $E(\theta) = t_t E(t)$ ] curves computed from these two expressions are shown in Figure 5.3. It is clear that as  $n$  increases in the sequence the shapes of the response curves assume the character of the intermediate situations illustrated in Figures 4.3 and 4.4. For very large  $n$ , the response becomes essentially that of the plug-flow case.

### Illustration 5.2

When experimental data on  $F(t)$  or  $E(t)$  are available, one can model the effects of nonideal behavior by fitting the response using  $n$  as an adjustable parameter. Then integral expressions conforming to equation (5-1) may be set up in terms of  $E(t)$  from equation (5-16) for computing conversions in the nonideal reactor. Derive the appropriate equations for a second-order reaction using this approach.

#### Solution

From equation (5-1) we may write

$$\bar{x} = \int_0^\infty \frac{kC_{A_0}t}{1 + kC_{A_0}t} \cdot \frac{n^n}{\bar{t}_t} \left( \frac{t}{\bar{t}_t} \right)^{n-1} \frac{e^{-nt/\bar{t}_t}}{(n-1)!} dt$$

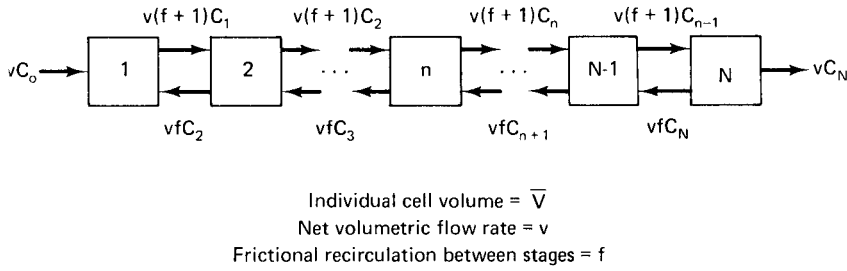


**Figure 5.4** Mixing-cell sequence with micromixing effects.

This may be rearranged to

$$\bar{x} = \frac{n^n}{(\bar{t}_t)^n (n-1)!} \int_0^\infty \frac{t^n e^{-nt/\bar{t}_t}}{(1/kC_{A_0}) + t} dt$$

$$\bar{x} = \frac{n^n}{(\bar{t}_t)^n (n-1)!} \left[ (-1)^{n-1} \left( \frac{1}{kC_{A_0}} \right) \exp \left( \frac{nt}{kC_{A_0} \bar{t}_t} \right) \right.$$

$$\cdot \left[ E_i \left( -\frac{nt}{kC_{A_0} \bar{t}_t} \right) + \sum_{i=1}^n (i-1)! \left( -\frac{1}{kC_{A_0}} \right)^{n-i} \left( \frac{nt}{\bar{t}_t} \right)^{-i} \right]$$

As seen from this example, for most types of kinetics the integrals are a bit messy for analytical evaluation, but numerical evaluation is simple. Again, we point out that this amounts to a segregated-flow model which has the capability of predicting upper or lower bounds on conversion depending on whether the kinetics, assuming simple orders, are  $>$  or  $<$  first order, respectively.

A simple modification of the mixing-cell sequence has been proposed which would provide for the incorporation of micromixing effects into the model. In this modification we view that there is some circulation between individual cells, as shown in Figure 5.4. This flow in the reverse direction, or *backmixing*, is equivalent to a micromixing effect in the reactor model. Let us denote  $f$  as the fraction of fluid involved in recirculation expressed in terms of the net volumetric flow  $v$ . Then, for the first cell in the series, the tracer experiment material balance is

$$\bar{V} \frac{dC_1}{dt} = vC_0 - v(f+1)C_1 + vfC_2 \quad (5-17)$$

and for the  $n$ th cell

$$\bar{V} \frac{dC_n}{dt} = v(1+f)(C_{n-1} - C_n) + vf(C_{n+1} - C_n) \quad (5-18)$$

One can see immediately that there is trouble. The generation of analytical  $F(t)$  or  $E(t)$  responses is not going to be a fruitful exercise, since the concentration of tracer downstream,  $C_{n+1}$ , appears in the equation for the determination of  $C_n$ .<sup>3</sup> However, there is an interesting relationship between these CSTR sequence mixing models, both with and without backmixing, and the dispersion models to be discussed in the following, so we shall keep both in mind for the present.

<sup>3</sup> “No good deed shall go unpunished.”—Anonymous



### 5.2.3 Dispersion Models

We have already called attention to the fact that the spreading observed in pulse-response experiments is reminiscent of diffusional phenomena, so it is reasonable to expect that a “diffusional correction” term appended to the plug-flow model would also afford a means for modeling nonideal flows. Consider the one dimensional dispersion model as illustrated in Figure 5.5. For the mass balance around the differential length  $dz$ :

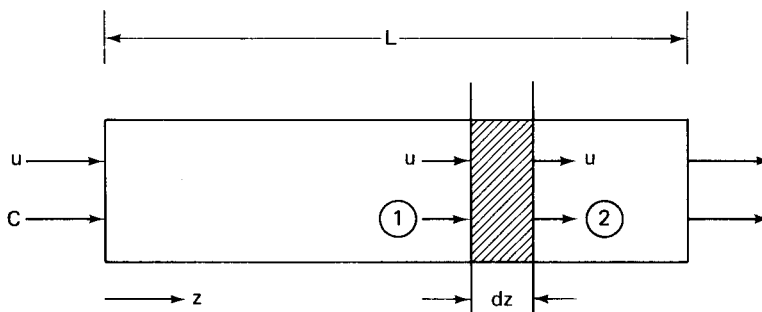
$$\begin{aligned}
 \text{enter:} \quad & \text{convection:} \quad uCA \\
 & \text{dispersion:} \quad -D \frac{dC}{dz} \cdot A \\
 \text{exit:} \quad & \text{convection:} \quad u \left( C + \frac{dC}{dz} \cdot dz \right) A \\
 & \text{dispersion:} \quad -D \left[ \frac{dC}{dz} + \frac{d}{dz} \left( \frac{dC}{dz} \right) dz \right] A \\
 \text{accumulation:} \quad & \frac{dC}{dt} \cdot A \cdot dz
 \end{aligned}$$

Equating the difference in input/output terms to accumulation in the volume element gives

$$\frac{dC}{dt} dz = -u \frac{dC}{dz} dz + D \frac{d}{dz} \left( \frac{dC}{dz} \right) dz \quad (5-19)$$

which on rearrangement becomes

$$D \frac{d^2 C}{dz^2} - u \frac{dC}{dz} = \frac{dC}{dt} \quad (5-20)$$



$$\text{At (1):} \quad uCA + \left( -D \frac{dC}{dz} + \frac{d}{dz} \cdot A \right)$$

$$\text{At (2):} \quad u \left( C + \frac{dC}{dz} \cdot dz \right) A + \left[ -D \frac{dC}{dz} + \frac{d}{dz} \frac{dC}{dz} \cdot dz \right] A$$

$A$  = cross-sectional area

**Figure 5.5** One-dimensional dispersion model.

Here  $D$ , the *axial dispersion* (or *diffusion*) *coefficient*, is the parameter used to describe the deviations from ideal flow. If  $u$  is taken to be constant in the radial direction, the rightmost terms in equation (5-20) constitute the plug-flow mixing model and  $D(d^2C/dz^2)$  is a Fickian form of a diffusional correction term.

Now let us see what this model gives us in terms of  $F(t)$  or  $E(t)$  responses. To solve this equation (which, incidentally, is no longer of the form of an initial-value problem but is a boundary-value problem), it is convenient to make a change of variables. We let  $v$  represent the position of the moving interface represented by all elements of fluid introduced into the reactor at some given time, analogous to the downstream volume  $y$  used in Chapter 4. In terms of the length variable, this transformation is

$$v = z - ut \quad (5-21)$$

Substituting for  $z$  in terms of  $v$  in equation (5-20)

$$D \frac{d^2C}{dv^2} = \frac{dC}{dt} \quad (5-22)$$

The boundary conditions for a step function in inlet concentration of tracer are<sup>4</sup>

$$\begin{aligned} C &= 0 & (\nu > 0, t = 0) \\ C &= 1 & (\nu < 0, t = 0) \\ C &= 0 & (\nu = \infty, t > 0) \\ C &= 1 & (\nu = -\infty, t > 0) \end{aligned} \quad (5-23)$$

The corresponding solution is

$$C = \frac{1}{2} \left[ 1 - \operatorname{erf} \left( \frac{\nu}{2\sqrt{Dt}} \right) \right] \quad (5-24)$$

where

$$\operatorname{erf}(y) = \frac{2}{\sqrt{\pi}} \int_0^y \exp(-v^2) dv$$

and is a tabulated function. The  $F(t)$  response computed from the one-dimensional dispersion model is

$$F(t) = \frac{1}{2} - \frac{1}{2} \operatorname{erf} \left( \frac{L - ut}{2\sqrt{Dt}} \right) \quad (5-25)$$

$$F(t) = F(\theta) = \frac{1}{2} - \frac{1}{2} \operatorname{erf} \left[ \frac{1 - t/t_R}{2\sqrt{(t/t_R)(D/Lu)}} \right] \quad (5-26)$$

The dimensionless grouping,  $(Lu/D)$ , appearing in equation (5-26) has commonly been used to represent the magnitude of dispersion effects, since it represents the ratio of the characteristic time constants for convective and dispersive effects. It is termed the *axial Peclet number*,  $N_{Pe}$ . Now equations (5-25) or (5-26) can be fit to experimental  $F(t)$  data to determine the value of  $D$  or  $N_{Pe}$  applicable to a given

<sup>4</sup> Considerable energy has been expended debating the proper form for these boundary conditions. The question will be addressed in more detail in a later section. "Now we see through a glass, darkly."—*I Corinthians XIII, 12*

situation. This can be done either with a least squares procedure or, at least as a first approximation, by determining the midpoint slope of the  $F(t)$  data. The latter method derives from the fact that

$$\left[ \frac{d[F(t)]}{d(t/t_R)} \right]_{t/t_R=1} = \frac{1}{2} \sqrt{\frac{Lu}{\pi D}} = \frac{1}{2} \sqrt{\frac{N_{Pe}}{\pi}} \quad (5-27)$$

so numerical evaluation of  $\Delta F(t)/\Delta(t/t_R)$  at the point  $(t/t_R) = 1$  yields a value for  $N_{Pe}$  directly.

Solution of the dispersion equation for the impulse response, using a slightly different set of boundary conditions for equation (5-20), gives

$$E(\theta) = \frac{\exp\{-[1 - (t/t_R)]^2/4(D/Lu)(t/t_R)\}}{2\sqrt{\pi(D/Lu)(t/t_R)}} \quad (5-28)$$

In the case where dispersion effects are small but not negligible, the expression for  $E(\theta)$  given above can be reasonably approximated by the following Gaussian form of the exponential

$$E(\theta) = \frac{1}{2\sqrt{\pi(D/Lu)}} \exp\left[-\frac{(1 - t/t_R)^2}{4(D/Lu)}\right] \quad (5-29)$$

Examples of  $F(\theta)$  and  $E(\theta)$  curves computed from equations (5-26) and (5-28) are given in Figures 5.6a and 5.6b. It is seen that their shapes are quite similar to

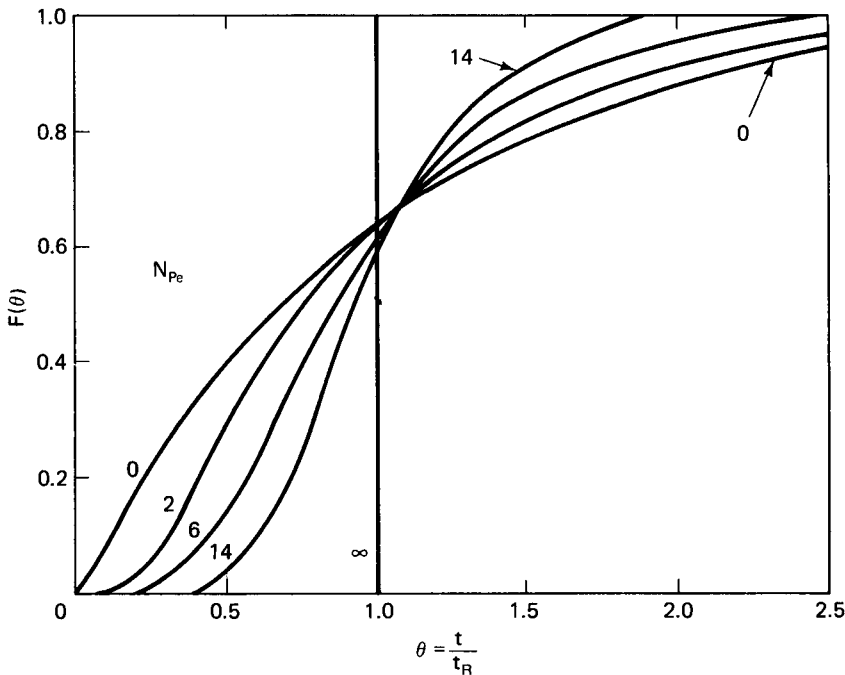


**Figure 5.6** (a)  $F(\theta)$  as determined from the one-dimensional dispersion model with the Peclet number as the parameter.

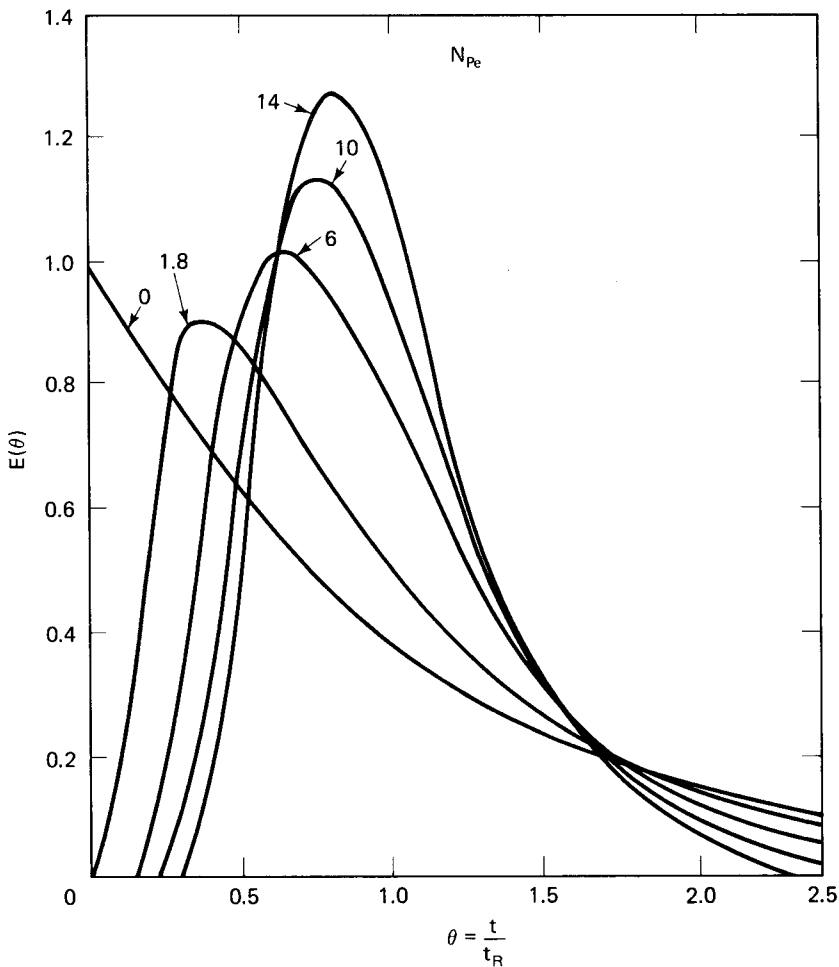


**Figure 5.6** (b)  $E(\theta)$  as determined from the one-dimensional dispersion model with the Peclet number as the parameter.

those obtained from the mixing cell in series approach, but in this case the Peclet number rather than the number of mixing cells is the parameter determining the shape.

The way we have presented the one-dimensional dispersion model so far has been as a modification of the plug-flow model. Hence,  $u$  is treated as uniform across the tubular cross section. In fact, the general form of the model can be applied in numerous instances where this is not so. In such situations the dispersion coefficient  $D$  becomes a more complicated parameter describing the net effect of a number of different phenomena. This is nicely illustrated by the early work of Taylor [G.I. Taylor, *Proc. Roy. Soc. (London)*, *A219*, 186 (1953); *A223*, 446 (1954); *A224*, 473 (1954)], a classical essay in fluid mechanics, on the combined contributions of the velocity profile and molecular diffusion to the residence-time distribution for laminar flow in a tube.

It is worth a short detour into fluid mechanics to explore some details of this approach and how it fits into the reactor conservation equations. For moderate flow velocities the dispersion of a tracer in laminar flow will occur by axial and radial diffusion from the flow front of the tracer and, in the absence of eddy motion, this will be via a *molecular* diffusion mechanism. However, the net contribution of diffusion in the axial direction can be taken as small in comparison to the contribution of the flow velocity profile. This leaves us with a two-dimensional problem with diffusion in the radial direction and convection in the longitudinal direction; the situation is considered in illustrated in Figure 5.7.

Following the procedures outlined for equation (5-20), we may derive the following

$$\frac{\partial C}{\partial t} = D_M \left( \frac{\partial^2 C}{\partial r^2} + \frac{1}{r} \frac{\partial C}{\partial r} \right) - u(r) \frac{\partial C}{\partial z} \quad (5-30)$$

where  $D_M$  is the molecular diffusivity of the tracer and  $u(r)$  represents the laminar velocity profile. Now equation (5-30) is a nonsteady-state partial differential equation, and the details of its solution is tangential to our main line of interest. However, as engineers and opportunists we often look for rational approximations or equivalent representations in models that can save us some work. This is precisely what Taylor was able to do. He showed that an exactly equivalent representation in one dimension of equation (5-30) is given by

$$\frac{\partial C_m}{\partial t} = D_e \frac{\partial^2 C_m}{\partial z^2} - \bar{u} \frac{\partial C_m}{\partial z} \quad (5-31)$$

where  $C_m$  is a mean radial concentration;  $\bar{u}$  the average velocity independent of  $r$ , and  $D_e$  an effective dispersion coefficient. In terms of the parameters of equation (5-30),  $D_e$  is given by

$$D_e = \frac{R^2 \bar{u}^2}{48 D_M} \quad (5-32)$$

where  $R$  is the tubular radius. Of course, this representation is valid only under the conditions stated with molecular diffusion in the axial direction being negligible. Taylor further showed that for this condition to exist it is necessary that

$$\frac{4L}{R} > \frac{\bar{u}R}{D_M} \gg 6.9 \quad (5-33)$$

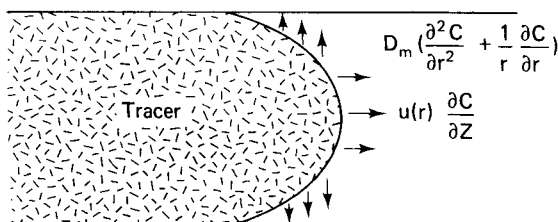


**Figure 5.7** Convective and molecular diffusion contributions to dispersion in laminar flow.

Note that in the inequality of (5-33) that the quantity  $(\bar{u}R/D_M)$  can be considered a radial Peclet number defined analogously to the longitudinal quantity defined previously. It has been suggested that the right inequality is a little tight, and that  $(\bar{u}R/D_M) > 50$  is a more comfortable approximation [V. Ananthakrishnan, W.N. Gill and A.I. Barduhn, *Amer. Inst. Chem. Eng. J.*, 11, 1063 (1965)].

Subsequent to this development, Aris [R. Aris, *Proc. Roy. Soc. (London)*, A235, 67 (1956)] showed that the effects of molecular diffusion in the axial direction could be included in the one-dimensional representation of equation (5-31) and that, in fact, the correction is a simple additive term.

$$D_e = D_M + \frac{R^2 \bar{u}^2}{48 D_M} \quad (5-34)$$

The analysis was also generalized to include all types of velocity distributions in flow vessels of any geometry.

These one-dimensional dispersion models for laminar flow are of importance for two reasons: (1) much industrial processing involving polymers, oils, colloids, pastes, and the like involve laminar flow and, in many cases, non-Newtonian fluids; and (2) the fact that a true two-dimensional problem can be reduced to an equivalent one-dimensional problem—although admittedly for a special set of circumstances—lends credibility to the extensive use of the one-dimensional dispersion model reported in the literature and reflected in upcoming discussions of reactor modeling here. This does not mean that one-dimensional models are always adequate, though.<sup>5</sup> Some rigorous solutions and one-dimensional approximations are reviewed by Wen and Fan [C.Y. Wen and L.T. Fan, *Models for Flow Systems and Chemical Reactors*, Marcel Dekker, New York, N.Y., (1975)] for the following cases involving laminar flow:

1. Molecular diffusion negligible compared to the contribution of the velocity profile (for Reynolds numbers in the upper range of the laminar flow regime).
2. Both radial and axial molecular diffusion effects comparable to the contribution of the velocity profile (midrange of Reynolds numbers).

The analysis presented here pertains to case 2 above; the derivation of the  $F(t)$  relationship for laminar-flow reactors given in Chapter 4 pertains to case 1, which is a segregated-flow model.

## 5.2.4 Comparison of Mixing-Cell and Dispersion Models

In Chapter 4 it was pointed out that the performance of a CSTR sequence approached that of a single PFR of equivalent total residence time as the number of units in a sequence approached infinity. This result is also obeyed by the  $F(\theta)$  and  $E(\theta)$  curves computed from the mixing-cell model reported in Figure 5.3. Since the plug-flow model represents one limit of the dispersion model (that when  $D \rightarrow 0$ ), it is reasonable to assume that there is an interrelationship between mixing-cell and dispersion models that can be set forth for the more general case of finite values

<sup>5</sup> “Drowsiness shall clothe a man with rags.”—*Proverbs, XXIII, 21*

for  $D$ . Starting again with the one-dimensional mass balance for the dispersion model,

$$D \frac{\partial^2 C}{\partial z^2} - u \frac{\partial C}{\partial z} = \frac{\partial C}{\partial t} \quad (5-20)$$

If a central finite-difference approximation is used to represent the spatial derivatives in equation (5-20), the following is obtained for point  $n$

$$D \left[ \frac{C_{n-1} - 2C_n + C_{n+1}}{(\Delta z)^2} \right] - \frac{u}{2\Delta z} (C_{n+1} - C_{n-1}) = \frac{dC_n}{dt} \quad (5-35)$$

On the other hand, the mass balance for the mixing cells in series model is

$$v(C_{n-1} - C_n) = \bar{V}_n \frac{dC_n}{dt} \quad (5-9)$$

Now let us view the dispersion model in terms of a series of mixing cells, of as-yet-unspecified dimension, and determine the conditions required for equivalence between the two. Thus, we may rewrite equation (5-9) as

$$\frac{dC_n}{dt} = \frac{\bar{u}C_{n-1} - \bar{u}C_n}{2\Delta z} \quad (5-36)$$

where  $\Delta z$  represents some length over which perfect mixing occurs, and  $\bar{u}$  is  $(1/\bar{t})$ . If we add and subtract the term  $(\Delta z \bar{u} C_{n+1})/2(\Delta z)^2$  to equation (5-36)

$$\frac{dC_n}{dt} = \frac{\bar{u}\Delta z}{2(\Delta z)^2} (C_{n+1} - 2C_n + C_{n-1}) - \frac{\bar{u}\Delta z}{2(\Delta z)^2} (C_{n+1} - C_{n-1}) \quad (5-37)$$

Term-by-term comparison of equations (5-37) and (5-35) discloses the following requirement for the equivalence of the two models:

$$\frac{\mu\Delta z}{2} = D; \quad (C_n \approx C_{n-1}) \quad (5-38)$$

Thus, the correct axial Peclet number for defining the equivalent length of a perfect mixing cell is 2. This, in turn, provides the relationship between the number of mixing-cell parameters of the mixing-cell model and the corresponding axial dispersion parameters of the dispersion model.

A similar comparison may be made between the dispersion model and the forward/reverse flow mixing-cell model of Figure 5.4. This is perhaps even a physically more meaningful comparison, although we were unable to use the model to derive analytical expressions for the age distributions, because the forward/backward communication provided is more similar to the physical nature of the diffusion process. In this case the expression corresponding to equation (5-37) is

$$\frac{dC_n}{dt} = \frac{f\bar{u}}{\delta z} (C_{n-1} - 2C_n + C_{n+1}) - \frac{\bar{u}}{2\Delta z} (C_{n+1} - C_n) \quad (5-39)$$

The equivalence condition is

$$\frac{f\bar{u}}{\Delta z} \approx \frac{D}{(\Delta z)^2} = \frac{(L/\Delta z)}{N_{Pe}} \quad (5-40)$$

It is clear that the parameters  $\Delta z$  and  $f$  are interrelated through the equivalence condition.

The fact that such equivalences between the mixing-cell and dispersion models exist makes the task of correlating information on nonideal flows somewhat more simple. In the following we will refer to the Peclet number as the measure of the influence of nonideal flow with the understanding that modeling can be accomplished interchangeably with either dispersion or mixing-cell approaches.

### 5.2.5 Evaluation of the Peclet Number as a Parameter in Nonideal Flow Modeling

Over the years a considerable body of experimental information has been built up concerning values of the Peclet number, or the corresponding dispersion coefficient, for various types of flow situations. These include laminar and turbulent flow of both gases and liquids in empty tubes, fixed and fluidized beds, and adsorption and extraction columns. The bulk of available data deals with axial dispersion, but there have also been a number of studies of radial dispersion, primarily for liquids and gases in fixed beds. A number of these results have been summarized some time ago in the monograph of Wen and Fan cited earlier. The attraction of this approach is that if one succeeds in correlating the Peclet number in terms of fluid mechanical quantities, the dispersion coefficient, and thus the influence of nonideal flow can be determined via correlation and does not require separate experimentation. This does not include instances where there is severe channeling or bypass flow, where the fragility of the dispersion model becomes very apparent.

We recall that for laminar flow the analysis of Taylor and Aris led to the result

$$D_e = D_M + \frac{R^2 \bar{u}^2}{48 D_M} \quad (5-34)$$

which can be rewritten in terms of the Reynolds, Schmidt, and Peclet numbers as

$$\frac{1}{N_{Pe}} = \frac{1}{N_{Re} N_{Sc}} + \frac{N_{Re} N_{Sc}}{192} \quad (5-41)$$

where  $N_{Pe} = \bar{u}d/D_e$ ,  $N_{Re} = d\bar{u}\rho/\mu$ , and  $N_{Sc} = \mu/\rho D_M$ . The Peclet number has been written in terms of the tube diameter,  $d$ , rather than radius in order to make it consistent with the normal definition of the Reynolds number. Available laminar flow data in empty tubes, indicated by the cross-hatched region, are plotted in comparison with equation (5-41) in Figure 5.8a for the range  $1 < N_{Re} < 2000$  and for  $0.23 < N_{Sc} < 1000$ ; it is clear that the agreement is excellent. For turbulent flow in empty tubes, an approximate relationship between  $N_{Pe}$  and  $N_{Re}$  is

$$\frac{1}{N_{Pe}} = \frac{1}{(N_{Re})^{0.125}} \quad (5-42)$$

This leads to the following empirical correlation

$$\frac{1}{N_{Pe}} = \frac{(3 \times 10^7)}{(N_{Re})^{2.1}} + \frac{1.35}{(N_{Re})^{0.125}} \quad (5-43)$$



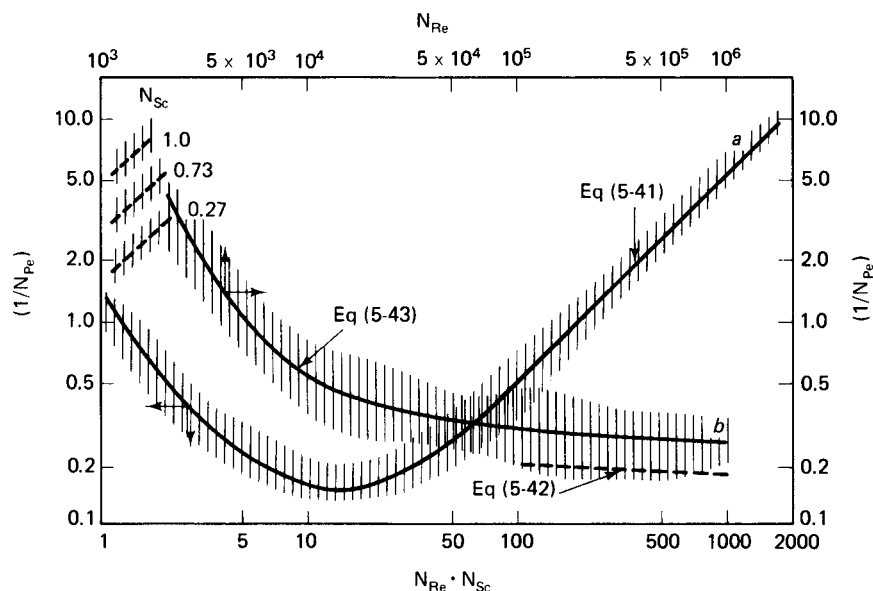


**Figure 5.8** (a) Correlation of axial dispersion coefficient for flow of fluids through pipes in laminar flow region ( $N_{Re} < 2000$ ); (b) Correlation of axial dispersion coefficient for flow of fluids through pipes for  $N_{Re} > 2000$  (shaded area represents approximate range of experimental data).

The fit to experiment afforded by equation (5-43) together with the limiting value of  $(N_{Re})^{-0.125}$  is given in Figure 5.8b. It is seen that  $N_{Pe}$  is not a function of  $N_{Sc}$  in the region of well-developed turbulence.

Flow of liquids or gases through fixed beds is very important in chemical reaction engineering, since many commercially important processes involve reactors that contain beds of catalyst used to promote a desired reaction. The axial dispersion model has been used extensively to model these flows, even though two phases, fluid and solid, are present. Such a pseudo-homogeneous model assumes the same form we have described in the preceding section if the Peclet number is based on particle dimension and the interstitial fluid velocity is used. In this event

$$N_{Pe} = \frac{\bar{u}d_p}{D_e} \quad (5-44)$$

where  $\bar{u} = u_0/\epsilon$ ,  $\bar{u}$  is the interstitial velocity,  $u_0$  the superficial velocity, and  $\epsilon$  is the bed porosity. Similar types of models have also been applied to the description of fluidized beds, although with somewhat less success, owing to the far more complex mixing patterns associated with these beds. Chung and Wen [S.F. Chung and C.Y. Wen, *Amer. Inst. Chem. Eng. J.*, 14, 857 (1968)] have given a correlation for liquids based on the pseudo-homogeneous model of both fixed and fluidized bed data, as shown in Figure 5.9a. Though the correlation is based on data for both types of beds, much of the scatter arises from the fluid-bed cases and we will regard the correlation primarily of use for fixed beds. Further details on the modeling of fluidized beds is given in Chapter 8.

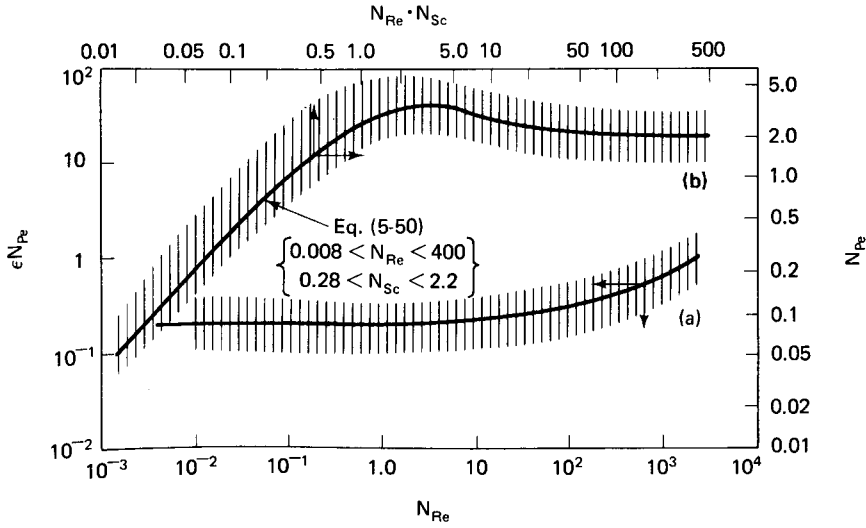


**Figure 5.9** (a) Correlation of axial dispersion coefficients in liquid phase fixed and fluidized beds; (b) correlation of axial dispersion coefficient for gases flowing through fixed beds.

The correlation equation corresponding to the curve of Figure 5.9a is

$$\epsilon N_{Pe} = 0.2 + 0.011(N_{Re})^{0.48} \quad (5-45)$$

Note that  $N_{Pe}$  in the figure and in equation (5-45) is defined on the basis of superficial velocity, thus  $N_{Re} = d_f v_0 \rho / \mu$ . Owing to the small values of the molecular diffusion coefficient in liquids, the Schmidt number is not an important contributor to  $N_{Pe}$  in this case.

For gaseous flows in fixed beds, we can develop an approximate form of correlation based on the following arguments. First, because of the larger magnitude of diffusion coefficients in the gas phase, it is reasonable to expect that this will be a contributing factor at low  $N_{Re}$ . This can be expressed in terms of the molecular diffusion coefficient via a *tortuosity factor*,  $\tau$ , which accounts in some overall sense for the reduction of diffusivity occasioned by the nondirect flow paths characteristic of the fixed bed. Thus, at very low flow velocities through a bed of porosity  $\epsilon$ , we may expect

$$D_e = \frac{D_M \epsilon}{\tau} \quad (5-46)$$

On the other hand, it has been shown that for large values of  $N_{Re}$ , the following occurs

$$N_{Pe} = \frac{\bar{u} d_p}{D_e} = \frac{2}{\eta} \quad (5-47)$$

where the distance between successive layers of particles is given by  $\eta d_p$  and  $\eta$  is between approximately 0.8 and 1 for various types of packing geometry. For our

present purposes, if we take  $\eta = 1$ , then at high  $N_{Re}$ ,

$$D_e = \frac{\bar{u}d_p}{2} \quad (5-47a)$$

Combining low- and high-velocity contributions to  $D_e$  additively gives

$$D_e = \frac{D_M \epsilon}{\tau} + \frac{\bar{u}d_p}{2} \quad (5-48)$$

In terms of the corresponding dimensionless numbers

$$\frac{1}{N_{Pe}} = \frac{\epsilon(\epsilon/\tau)}{N_{Re}N_{Sc}} + \frac{1}{2} \quad (5-49)$$

The experimental data shown in Figure 5.9b exhibit a slight maximum for values of  $N_{Re}N_{Sc}$  in the range 1 to 10, which is a feature not to be expected from the form of equation (5-49). Aside from this, however, the limiting behavior expected is observed and an empirical correlation based on equation (5-49) is

$$\frac{1}{N_{Pe}} = \frac{0.3}{N_{Re}N_{Sc}} + \frac{0.5}{1 + 3.8(N_{Re}N_{Sc})^{-1}} \quad (5-50)$$

where  $N_{Re}$  is again based on the superficial fluid velocity.

Thus far the emphasis has been on one-dimensional dispersion models, for reasons we have discussed previously. In some cases, however, particularly in the modeling of large-scale nonisothermal reactors, the one-dimensional approach is not sufficient. Indeed, the evaluation of conditions corresponding to the adequacy of a given model is a delicate art, as was shown some time ago by Froment [G.F. Froment, *Ind. Eng. Chem.*, 59, 18 (1967)] and in subsequent literature. In nonisothermal operation, the existence of significant radial temperature gradients will induce corresponding radial concentration gradients and we must resort to a two-dimensional dispersion representation. In terms of a mixing model only (no reaction), this is

$$\frac{\partial C}{\partial t} = D_r \left( \frac{\partial^2 C}{\partial r^2} + \frac{1}{r} \frac{\partial C}{\partial r} \right) + D_e \frac{\partial^2 C}{\partial z^2} - \bar{u} \frac{\partial C}{\partial z} \quad (5-51)$$

Values of the radial dispersion coefficient, or the corresponding radial Peclet number,  $(\bar{u}d_p/D_r)$ , in packed beds have been determined for both liquids and gases by a number of researchers; they are definitely not the same as those in the axial direction. These results are shown in Figure 5.10a and b for liquids and gases, respectively. The corresponding empirical equations fitting these data are

$$N_{Pe_r} = \frac{17.5}{(N_{Re})^{0.75}} + 11.4 \quad \text{liquids} \quad (5-52)$$

$$\frac{1}{N_{Pe_r}} = \frac{0.4}{(N_{Re}N_{Sc})^{0.8}} + \frac{0.09}{1 + (10/N_{Re}N_{Sc})} \quad \text{gases} \quad (5-53)$$

As with the results for axial  $N_{Pe}$ , the value of  $N_{Sc}$  is important only for dispersion in gaseous systems.

A convenient fact to keep in mind is the limiting values of  $N_{Pe}$  for axial and radial directions in fixed beds, particularly for gases. At the higher values of

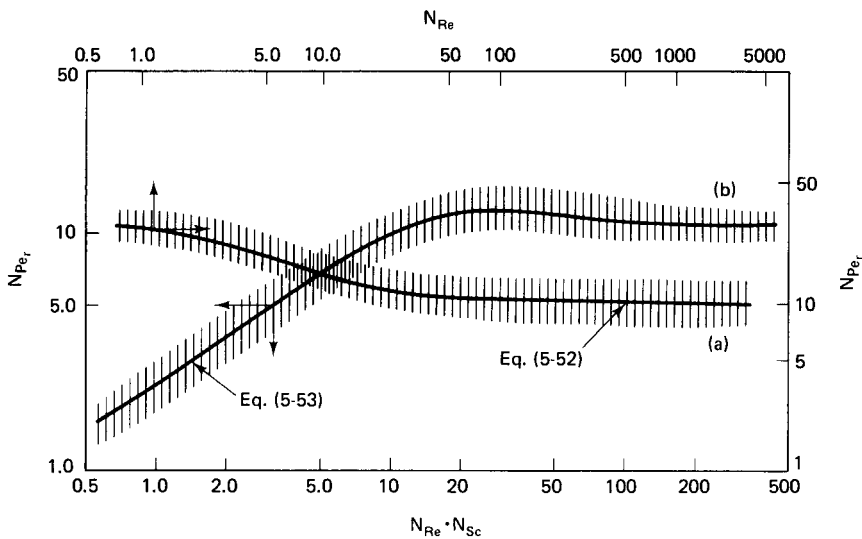


**Figure 5.10** (a) Correlation of radial dispersion coefficient for liquids in fixed beds; (b) correlation of radial dispersion coefficient for gases in fixed beds.

Reynolds number, which in general are more typical of industrial processing conditions, the axial Peclet number approaches 2, while the radial Peclet number is approximately 10. It is easy to show, at least for the one-dimensional dispersion model, that this represents only a small deviation from plug-flow results. For example, the axial Peclet number appearing in equation (5-26) for the  $F(t)$  of the one-dimensional dispersion model for flow in an empty tube is defined on the basis of the total length  $L$ . The axial Peclet numbers we have just been considering for flow in packed beds are defined on the basis of some representative particle diameter,  $d_p$ . In most applications of fixed-bed reactors the bed consists of many hundreds or even thousands of layers of catalyst particles. If there are, say,  $j$  layers of particles, then the Peclet number based on total length is  $2j$  in the limit of higher  $N_{Re}$ . This would approach the plug-flow response for sufficiently large  $j$  (Figure 5.6a).

In spite of this consideration, however, we will not dismiss these deviations from ideality out of hand as being of little importance in practical application. It will be seen later that even if the conversion in a given reactor is little affected by dispersion, the selectivity may well be. Further, in nonisothermal reactors analogous mechanisms for the dispersion of energy significantly affect the shape of temperature profiles within the reactor. Since temperature is the single most significant variable affecting kinetics and selectivity, this will have a profound effect on reactor performance.

### 5.2.6 Recycle Flow Reactors

Consider a tubular flow reactor with recycle as shown in Figure 5.11. Here a portion of the product stream is recycled to the feed. By changing the recycle rate,  $Q_R$ , with respect to the feed rate,  $Q_F$ , it seems logical that the degree of mixing can be adjusted

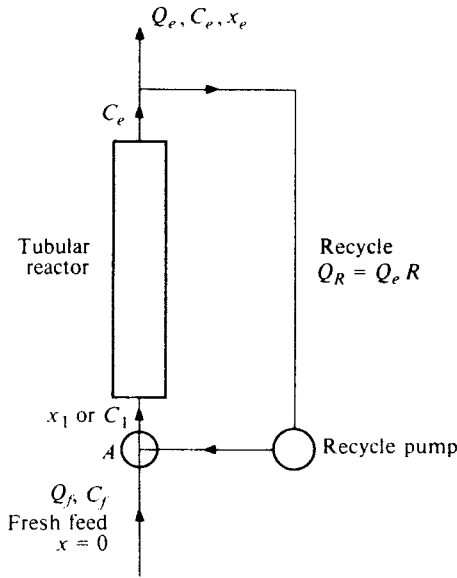


**Figure 5.11** A continuous flow reactor with partial recycle of the product stream.

to any level desired. In this case, the recycle ratio  $R$ , defined as

$$R = \frac{Q_r}{Q_e} \quad (5-54)$$

becomes the mixing parameter, playing the same role as  $n$  for the CSTR sequence or  $N_{Pe}$  for the dispersion model. An overall mass balance corresponding to Figure 5.11 gives

$$Q_f C_f + Q_e C_e + \int_0^{V_R} (-r) dV_R = 0 \quad (5-55)$$

with  $V_R$  the vessel total volume and the other notation corresponding to that in Figure 5.11. For small changes in concentration,  $C_e \approx C_f$  and the reactor acts as a differential reactor,  $(-r)$  is nearly invariant with position (i.e., entrance, exit) and

$$(-r) = -\frac{Q_f C_f - Q_e C_e}{V_R} \quad (5-56)$$

In cases where  $Q_f = Q_e$ , such as liquid-phase reactions or gas-phase reactions with no mols change, then

$$(-r) = -\left(\frac{Q_f}{V_R}\right)(C_f - C_e) \quad (5-57)$$

The concentration  $C_1$  is the result of combining the recycle and fresh feed, and is given by

$$(Q_f + Q_R)C_1 + (Q_R + Q_e)C_e + \int_0^{V_R} (-r) dV_R = 0 \quad (5-58)$$

For low conversions with  $Q_f = Q_e$

$$C_1 = C_e - \left( \frac{V_R}{Q_R - Q_e} \right) (-r) \quad C_1 = C_e - \frac{V_R (-r)}{Q_e (R + 1)} \quad (5-59)$$

where  $R$  is the parameter to be used to obtain any desired value of  $(C_1 - C_e)$ .

When there is a significant change in the concentration or concentration gradients, we can formulate such balances more conveniently using the PFR design equation based on a particular reactant or product. For example, let the key component be species A, for which we can designate  $F_{A_0}$  as the feed rate of A derived from the sum of that in the fresh feed plus that in the recycle. When  $Q_f = Q_e$ , the balance is

$$F_{A_0} = Q_R C_{A_f} + Q_f C_{A_f} = C_{A_f} (Q_R + Q_f)$$

In terms of  $R$ ,

$$F_{A_0} = Q_{A_f} Q_f (R + 1) \quad (5-60)$$

The plug-flow design equation, (4-45), now becomes

$$\left( \frac{V_R}{Q_f} \right) = -C_f (R + 1) \int_{x_1}^{x_2} \frac{dx}{(-r)} \quad (5-61)$$

where  $x$  represents both inlet and outlet conversions and again is a function of the recycle ratio. It is convenient to write equation (5-61) in terms of the concentrations of A, so we have

$$x = \left( \frac{C_f - C}{C_f} \right); \quad dx = \left( \frac{dC}{C_f} \right)$$

where the subscript A has been deleted. With this substitution equation (5-61) becomes

$$\left( \frac{V_R}{Q_f} \right) = (R + 1) \int_{C_1}^{C_e} \frac{dC}{(-r)} \quad (5-62)$$

and the total feed concentration including both fresh feed and recycle, is

$$(Q_R + Q_f) C_1 + Q_f C_f + Q_R C_e \quad (5-63)$$

and

$$C_1 = \frac{C_f + R C_e}{R + 1} \quad (5-64)$$

Limiting cases of equation (5-64) depend upon the value of  $R$ . For example, with  $R = 0$  we have a once-through reactor and equation (5-62) reduces to the familiar PFR form. When  $R$  is large equation (5-62) becomes

$$\frac{V_R}{Q_f} = \frac{(R + 1)(C_e - C_1)}{(-r)} \quad (5-65)$$

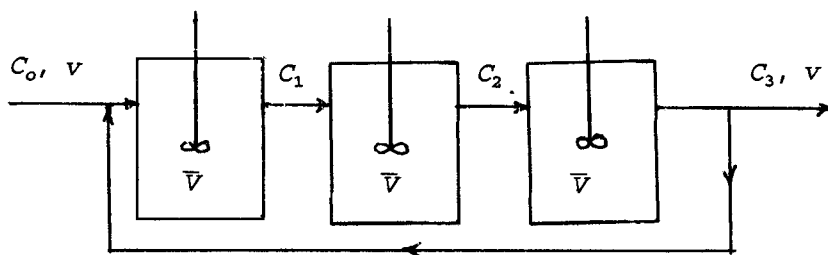
and substitution for  $C_1$  from equation (5-64) gives finally

$$\frac{V_R}{Q_f} = \frac{(C_e - C_1)}{(-r)} \quad (5-66)$$

which we recognize as the CSTR equation for a single unit.

**Illustration 5.3**

Following Figure 5.4 it was stated that the attempt to model micromixing in a sequence of CSTRs with reverse flows was not particularly fruitful (at least for the configuration shown) because of the complexity of the resulting equation. However, a variant on the problem would include only one feedback loop (recycle), as shown below.



Here  $v$  is the volumetric flow rate and each reactor has the same volume,  $\bar{V}$ . A certain fraction of the output from vessel 3, equal to  $fv$ , is recycled, but the holding time in each vessel is the same. Derive an expression relating  $C_3$  to  $C_0$  for the case of a first-order irreversible reaction.

*Solution*

It helps to work this problem backwards. Thus, the material balance around vessel 3 is

$$C_2(v + fv) = C_3(v + fv) + kC_3\bar{V} \quad (i)$$

This is easily rearranged to

$$\left(\frac{C_3}{C_2}\right) = \frac{(1 + f)}{(1 + f) + k\bar{t}} \quad (ii)$$

A similar balance around vessel 2 gives

$$\left(\frac{C_2}{C_1}\right) = \frac{(1 + f)}{(1 + f) + k\bar{t}} \quad (iii)$$

Thus

$$C_3 = \frac{C_1(1 + f)^2}{[(1 + f) + k\bar{t}]^2} \quad (iv)$$

An overall balance is

$$C_0v + C_3fv = C_1(v + fv) + kC_1\bar{V} \quad (v)$$

Substitution for  $C_1$  and doing some algebra leads us to

$$\left(\frac{C_3}{C_0}\right) = \frac{(1 + f)^2}{[(1 + f) + k\bar{t}]^3 - f(1 + f)^2} \quad (vi)$$

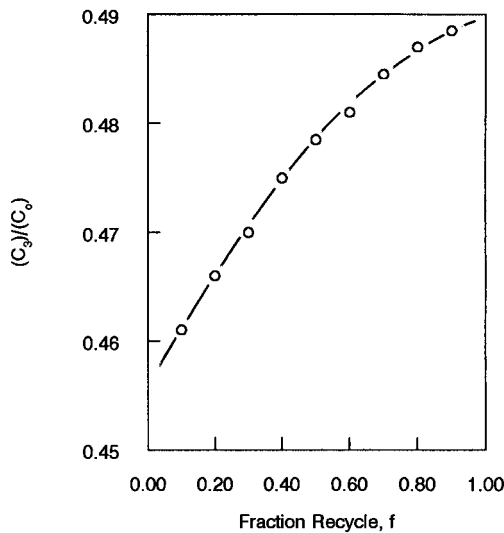


**Figure 5.12** Variation of conversion with recycle ratio in a three CSTR sequence.

The variation of  $(C_3/C_0)$  for a representative case with  $k\bar{t} = 0.3$  is shown in Figure 5.12.



HORATIO SAYS

What would be the physical significance in the model of this illustration if one allowed the recycle ratio  $f$  to approach unity?

### 5.3 Combined Models for Macroscopic Flow Phenomena

The mixing-cell approximations or dispersion models have the ability to reproduce  $F(t)$  or  $E(t)$  responses intermediate to the limiting PFR and CSTR models, as shown in Figures 4.4a and b. They are, though, clearly incapable of dealing with some of the very anomalous behavior induced by problems such as channeling or bypassing shown in Figure 5.1 because they implicitly assume some type of symmetry along the direction of flow. We can remove this restriction if we use combined models consisting of assemblies of individual (and differing) mixing models in various sequences. An original proposal was that of Cholette and Cloutier [A. Cholette and L. Cloutier, *Can. J. Chem. Eng.*, 37, 105 (1959)], who envisioned three basic combinations, to a given flow: (1) plug flow, (2) short-circuiting, and (3) complete mixing. We may conveniently add to this dead volume as well.



Now by assembling various combinations of plug flow, complete mixing, short-circuiting, and dead volume, we may simulate a very large number of different types of macroscopic flow phenomena. Derivation of the appropriate response functions for such models is not difficult, since the procedure consists mostly of the simple assembly of components from the types of analysis we have carried out previously. In Table 5.1 are several examples of combined flow models together with their  $F(t)$  responses. Consider the CSTR with short-circuiting and dead volume, which is number 5 in the table. The contribution of the perfect mixing section to  $F(t)$  would be that of a CSTR of effective volume  $f\bar{v}$ , where  $f$  is the fraction of total volume perfectly mixed, multiplied by the fraction of total flow passing through the mixing circuit,  $v_1/v$ . Thus

$$F(t)(\text{mixing} + \text{dead volume}) = \frac{v_1}{v} \left[ 1 - \exp \left( -\frac{v_1}{f\bar{v}} \cdot \frac{t}{\bar{t}} \right) \right]$$

where the residence time  $\bar{t}$  is based on total reactor volume,  $\bar{V}$ . The contribution of the short circuit is direct transfer of the volume fraction of feed ( $v_2/v$ ) to the outlet, effective at time zero. Thus,

$$F(t)(\text{short circuit}) = \frac{v_2}{v}$$

and the net residence-time distribution for the combined model is simply

$$F(t) = \frac{v_1}{v} \left[ 1 - \exp \left( -\frac{v_1}{f\bar{v}} \cdot \frac{t}{\bar{t}} \right) \right] + \frac{v_2}{v} \quad (5-67)$$

Most of these models involve exponential functions in their  $F(t)$  responses as shown in the table, so tests of their possible application in interpretation of  $F(t)$  data are conveniently carried out via simple log-linear plots of the response data. If linearity is attained, the model parameters are readily evaluated.

Obviously, many such combinations can be assembled and the intelligent application of a given combined model to interpretation of nonideal flows in a particular reactor must rely on additional information concerning geometric properties such as stirrer placement, feed inlet and product withdrawal placement, corners or internal structural elements leading to dead volumes, and so on. A certain amount of intuition is also a useful commodity in each modeling.<sup>6</sup>

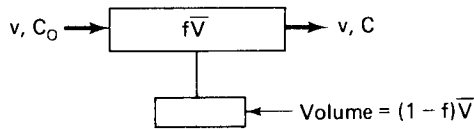
It is apparent from the illustrations given in Table 5.1, for example, that none of them will be able to reproduce the  $F(t)$  or  $C(t)$  response typical of channeling shown in Figure 5.1. Examination of this response indicates a bimodal  $C(t)$ , each peak of which is generally characteristic of a mixing-cell response with different residence times.

One possible model for this situation would be that shown in Figure 5.13. Two parallel lines are employed, one consisting of a pure mixing-cell sequence and the second a plug flow/mixing cell sequence, in series. Total feed is split between the two parallel trains. The number of mixing cells in sequence in each train would be determined by individual fit to the two peaks of the  $C(t)$  or  $E(t)$  response, while the residence time in the plug-flow section would be determined by the difference of the average residence times of the two peaks. Inclusion of the plug-flow

<sup>6</sup> "How long halt ye between two opinions?"—*I Kings, XVIII, 21*

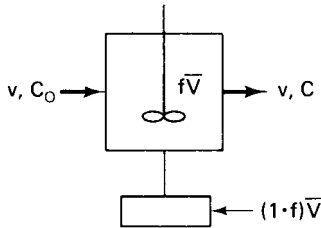
**Table 5.1** Some Typical Combined Flow Models

1. Plug flow with dead space:



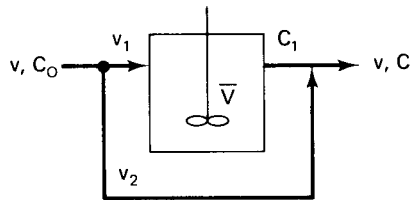
$$F(t) = \delta\left(\frac{t}{t_R} - f\right) \quad \delta(x) = \text{step function at } x = 0$$

2. CSTR with dead space:



$$F(t) = 1 - \exp\left[-\frac{t}{f\bar{t}}\right]$$

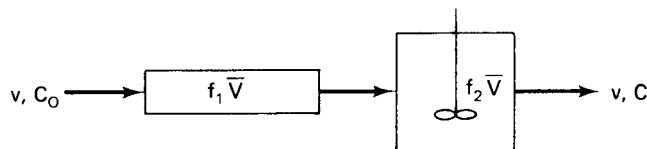
3. CSTR with short-circuiting:



$$F(t) = \frac{v_1}{v} \left\{ 1 - \exp\left[-\left(\frac{v_1}{v}\right)\left(\frac{t}{\bar{t}}\right)\right] + \frac{v_2}{v} \delta\left(\frac{t}{\bar{t}} = 0\right) \right\}$$

$$\bar{t} = \frac{\bar{V}}{v}$$

4. PFR-CSTR sequence:



$$f_1 + f_2 = 1; \bar{V} = \text{combined PFR - CSTR volume}$$

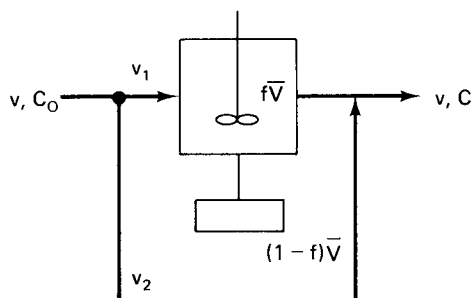
$$t_R = \frac{f_1 \bar{V}}{v}, \quad \bar{t} = \frac{f_2 \bar{V}}{v}$$

$$F(t) = 1 - \exp\left[\left(\frac{f_1}{f_2}\right) - \frac{t}{f_2(t_R + \bar{t})}\right] \delta\left(\frac{t}{t_R + \bar{t}} - f_1\right)$$

This expression applies for either PFR-CSTR or CSTR-PFR sequence.

Table 5.1 Continued

5. CSTR with short-circuiting and dead volume:



$$F(t) = \frac{v_1}{v} \left[ 1 - \exp \left( -\frac{v_1}{f\bar{V}} \cdot \frac{t}{\bar{t}} \right) \right] + \frac{v_2}{v} \delta \left( \frac{t}{\bar{t}} = 0 \right)$$

$$\bar{t} = \frac{\bar{V}}{v}$$

section ensures a lag in the appearance of the  $E(t)$  response of the top train in comparison with that of the bottom, thus producing the characteristic bimodal response.

More complex versions of these combination models have been proposed by various researchers [D. Wolf and W. Reanick, *Ind. Eng. Chem. Fundls.*, 2, 287 (1962); J.G. van de Vusse, *Chem. Eng. Sci.*, 17, 507 (1962)]; B.A. Buffham and L.G. Gibilarco, *Amer. Inst. Chem. Engr. JI.*, 14, 805 (1968)]. These have been shown to be useful in a number of practical applications in extension of the ideas above.

A class of what is essentially combined models can also be used to represent micromixing effects in reaction systems. We will not try to present them here as a separate class of mixing models, for in essence they duplicate much of the formalism given in the present development, although their interpretation is rather different. This is more clearly illustrated when applications to chemically reacting systems are involved, as will be discussed later.

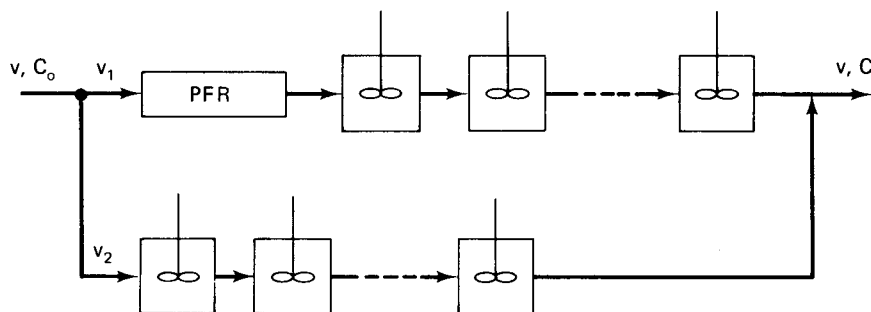
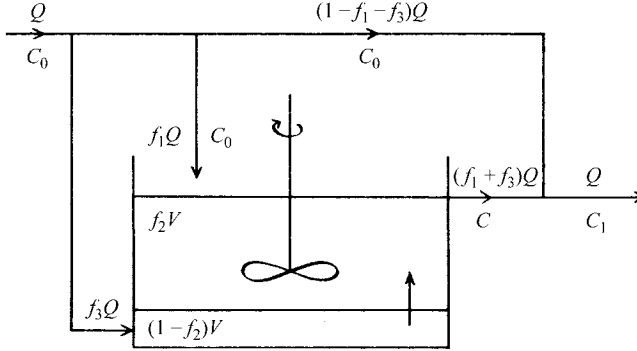


Figure 5.13 A possible combined model for channeling.

**Illustration 5.4**

As can be seen in Table 5.1, there are many combinations using the concepts of PFR and CSTR, with additional trinkets such as dead volume and recycle thrown in just to keep things interesting. In this light, consider the arrangement below consisting of series/parallel plug flow with additional short-circuiting.



As shown, the well-mixed region has a fraction,  $f_1$ , of the feed entering directly, while a fraction,  $f_3$ , enters it only after traversing the plug-flow region. Derive an expression for  $F(t)$ , i.e.  $(C_1/C_0)$ , of this unit.

*Solution*

It is convenient to use Laplace transform methods for solution of these response problems. Accordingly, the Laplace transform of the concentration leaving the plug flow region is

$$\frac{C_0}{s} \left[ 1 - \exp \left\{ -\frac{s(1-f_2)V}{f_3Q} \right\} \right] \quad (i)$$

and the transform of the equation representing the well-mixed region is

$$f_2V[s\bar{c} - C_0] + (f_1 + f_3)Q\bar{c} = f_3Q \frac{C_0}{s} \left[ 1 - \exp \left\{ -\frac{s(1-f_2)V}{f_3Q} \right\} \right]$$

or

$$\bar{c} = \frac{C_0}{s + \frac{(f_2+f_3)Q}{f_2V}} + \frac{f_3QC_0}{f_2V} \left[ \frac{1}{s \left( s + \frac{(f_1+f_3)Q}{f_2V} \right)} \right] \times \left[ 1 - \exp \left\{ -\frac{s(1-f_2)V}{f_3Q} \right\} \right] \quad (ii)$$

Thus, for  $0 < t < [(1-f_2)V/f_3Q]$

$$\frac{C}{C_0} = \exp \left\{ -\frac{(f_1+f_3)Qt}{f_2V} \right\} + \frac{f_3}{f_1+f_3} \left[ 1 - \exp \left\{ \frac{(f_1+f_3)Qt}{f_2V} \right\} \right] \quad (iii)$$

and since

$$QC_1 = (f_1 + f_3)QC$$

$$\frac{C_1}{C_0} = f_3 + f_1 \exp \left\{ -\frac{(f_1 + f_3)Qt}{f_2 V} \right\} \quad (\text{iv})$$

Similarly for  $t > [(1 - f_2)V/f_3Q]$

$$\frac{C_1}{C_0} = \left[ f_1 + f_3 \exp \left\{ \frac{(f_1 + f_3)(1 - f_2)}{f_2 f_3} \right\} \right] \exp \left\{ -\frac{(f_1 + f_3)Qt}{f_2 V} \right\}. \quad (\text{v})$$



HORATIO SAYS

Is the result of the illustration above unique? What other kinds of flow models can you think of that might give the same type of residence-time distribution result?

## 5.4 Modeling of Nonideal Reactors

The reader may very well wonder what happened to the chemical reaction, since we have mostly discussed mixing models in this chapter without reference to reaction. In review of the various approaches to modeling nonideal flow effects on reactor performance, however, we find that in fact a number of these have already been treated, although perhaps with different applications in mind. The classes of reactor models we have treated are

1. Those making direct use of exit-age distribution information—segregated-flow models.
2. Those employing mixing-cell sequences.
3. Those employing a diffusion/dispersion term in the continuity equation.
4. Those employing combinations of ideal reactor models with dead volume, short circuiting, or channeling components.

Direct application of the residence-time/exit-age data has been treated in application to chemical reactor design in Section 5.2a. In terms of the net effect of the exit-age distribution on conversion, we wrote

$$\bar{x} = \int_0^\infty x(t)E(t) dt \quad (5-1)$$

There is little further to be said concerning the application of this method. One interesting approach, however, that seems not to have been explored very much, is incorporation of the mixing-cell model representation for  $E(t)$  in equation (5-1), as shown in Section 5.2.2.

Mixing-cell models were discussed extensively in Chapter 4 under the guise of the analysis of CSTR sequences. It is a good time to revisit some of this analysis from the specific point of view of modeling nonideal reactors.

#### 5.4.1 Mixing-Cell Sequences as Reactor Models

As discussed in Section 5.2.2, the number of cells in sequence becomes the parameter used to model deviations from the ideal PFR  $F(t)$  or  $E(t)$  responses. In terms of conversion alone, such deviations can be evaluated from comparison of the results computed from PFR and CSTR conversion/residence time relationships, as detailed in Chapter 4. Because of the difficulties in deriving general  $(C_n/C_0)$  relationships for CSTR sequences involving nonlinear kinetics [see equation (4-92)], a generalized mixing-cell model for nonideal reactors is not conveniently obtained. The following analysis for the specific and by-now familiar example of first-order kinetics is offered with some apologies for possible duplication. The analysis is adequate to illustrate the direction and magnitude of deviations from ideal reactor behavior, however, and as long as trends rather than *numbers* are considered, we should remain healthy.<sup>7</sup>

Consider the PFR conversion given by

$$x = 1 - e^{-kt_R} \quad (5-67)$$

to be the limit obtained for the ideal reactor. For the CSTR series model we have seen that conversion is given by

$$x = 1 - \frac{1}{\alpha^n} \quad (5-68)$$

where  $\alpha = 1 + k\bar{t}$  and  $\bar{t}$  is the (uniform) residence time per individual cell. In both equations (5-67) and (5-68),  $k$  is a first-order rate constant. Deviations from the ideal reactor conversion limit then are given by equation (5-68), in which  $n$  typically is determined by fit to experimental  $F(t)$  or  $E(t)$  results obtained for the actual reactor. The value of  $t$  is determined from the nominal PFR residence time of the actual reactor by

$$\bar{t} = \frac{t_R}{n} \quad (5-69)$$

The procedure is thus far entirely analogous to that discussed for the comparisons between CSTR and PFR in Chapter 4. In Figure 5-14a is an example of the effect of a nonideal exit-age distribution on conversion in a tubular reactor modeled by equation (5-68). The PFR residence time is fixed, so in the representation of Figure 5.14a increasing deviations from ideal behavior are illustrated as  $n$  decreases. The values of  $\delta$  shown on the figure are determined from

$$\delta = \frac{(x_{PFR} - x_{model})(100)}{x_{PFR}} \quad (5-70)$$

It is shown that these deviations do not become large until  $n$  approaches, say, 2 to 4. From Figure 5.3 it is clear that for  $n = 20$  there are significant differences already between the residence-time and exit-age distributions of the nonideal reactor and the plug-flow case, yet the deficit in conversion is only 1.5%. The reason for this is a

<sup>7</sup>“The buyer needs a hundred eyes, the seller not one.”—G. Herbert

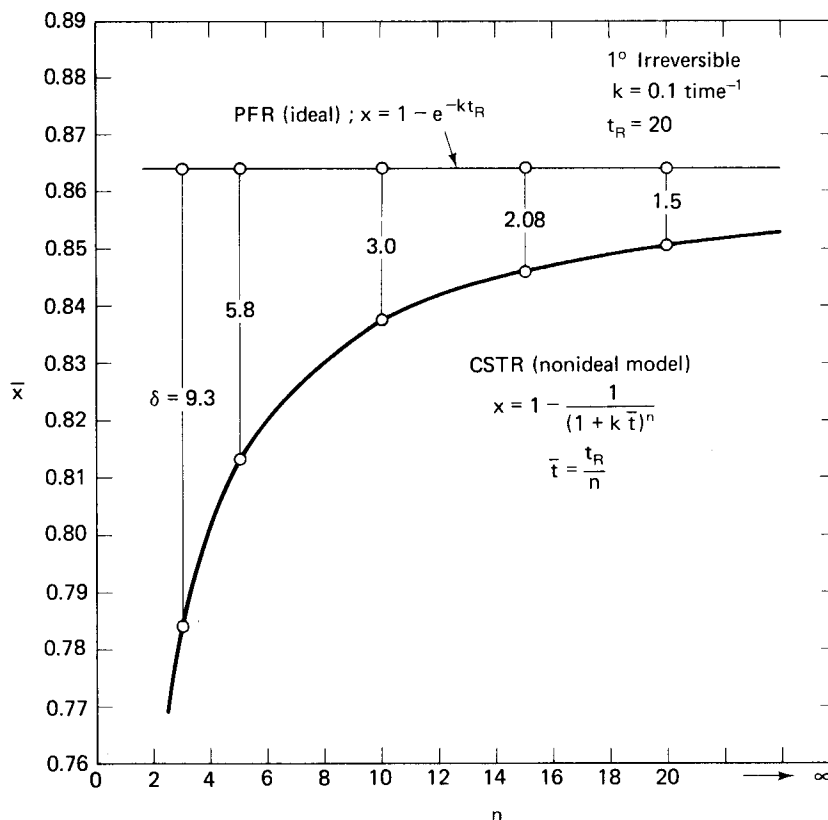


**Figure 5.14** (a) Effect of nonideal exit-age distribution on conversion as modeled by a CSTR sequence.

compensation between those elements having shorter residence times and lower conversion, and those with longer residence times and higher conversion. We will also keep in mind that the deviations may be larger for nonlinear kinetics. Inspection of the response curves in Figure 5.3, however, shows that both are skewed to the left of  $(t/\bar{t}) = 1$ ; that is, there is a preferential weighting of elements of shorter residence time, and thus the net conversion will be reduced.

Now, it may seem that we are belaboring the point of nonideality to account for a tax of only 2 or 3% on net conversion. One needs only to reflect on the magnitude of many process streams to realize, however, that while the percentage amounts here may be relatively small, the absolute magnitude of the quantities of the materials involved can be large.

Perhaps more important than conversion deficits in nonideal reactors are the associated changes in selectivity and yield in more complex reactions. Let us look at a Type III system ( $A \rightarrow B \rightarrow C$ ) to illustrate this. For selectivity in a PFR, Type III reaction, we had previously derived

$$S_{B(III)PFR} = \left( \frac{k_1}{k_2 - k_1} \right) \frac{e^{-k_1 t_R} - e^{-k_2 t_R}}{1 - e^{-k_1 t_R}} \quad (5-71)$$

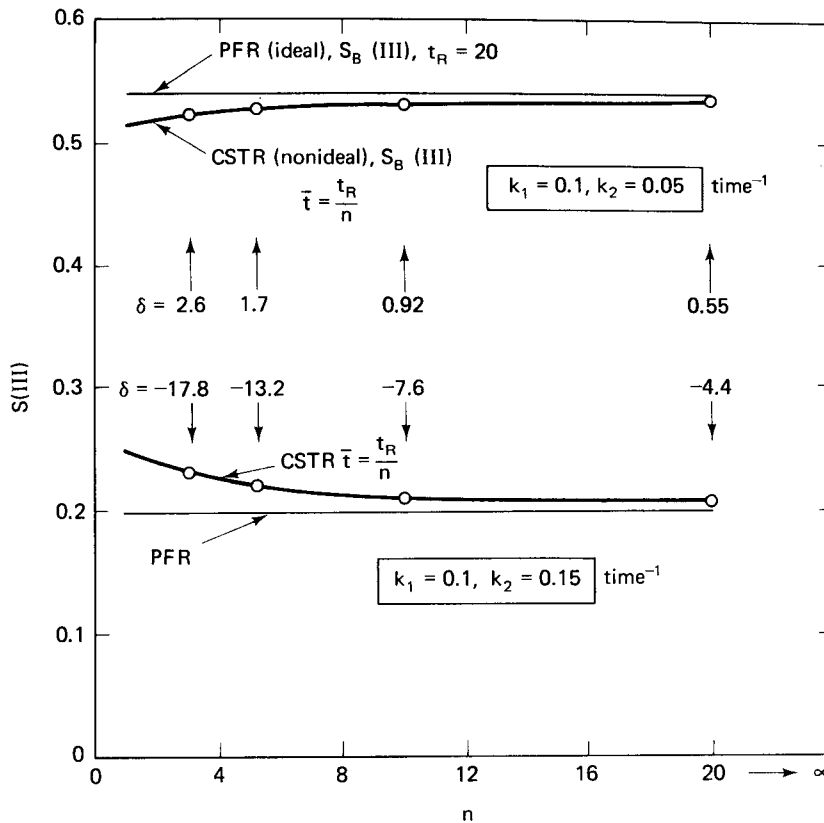


**Figure 5.14** (b) Effect of nonideal exit-age distribution on Type III selectivity in a tubular flow reactor (mixing-cell model).

and for the CSTR sequence consisting of  $n$  equally sized units at the same temperature

$$S_{B(III)CSTR} = \left( \frac{k_1}{K_1 - k_2} \right) \frac{(\alpha/\beta)^n - 1}{\alpha^n - 1} \quad (5-72)$$

where  $k_1$  and  $k_2$  are the rate constants for the first and second steps, respectively, and  $\alpha = 1 + k_1 t$ , and  $\beta = 1 + k_2 t$ . Again, in comparison between the two selectivities,  $t$  is determined from  $t_R$  according to equation (5-69). Figure 5.14b shows results for selectivity variation in nonideal reactors according to the CSTR model for  $(k_1/k_2)$  both  $> 1$  and  $< 1$ . As in the case of comparisons of conversion, the parameter  $n$  represents the magnitude of deviation from ideality. Here we see a decrease in selectivity with respect to the PFR limit for  $(k_1/k_2) > 1$ , but again of relatively small magnitude. For  $(k_1/k_2) < 1$  the selectivity is actually enhanced by a small amount for reasons that will be described next.

Now let us recall the definition of selectivity

$$\text{selectivity} = \frac{\text{mols } j \text{ produced}}{\text{mols } i \text{ reacted}}$$

As pointed out previously, this defines a measure of the efficiency of a particular



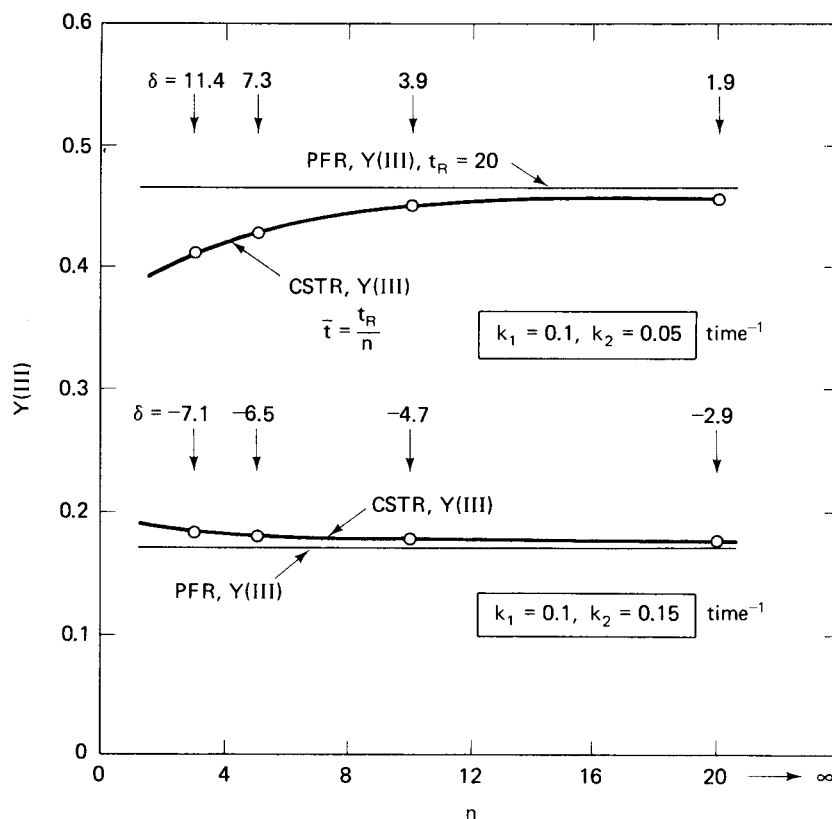


**Figure 5.14** (c) Yield results corresponding to conversion/selectivity computations.

reaction for production of a specified intermediate or product,  $j$ , from the reactant  $i$ . Just a moment ago we were discussing, relative to conversion, that small deviations might in fact represent large absolute amounts of product. In this regard, the yield obtained in a complex reaction is the item of ultimate importance. Recall also the definition

$$\text{yield} = (\text{selectivity})(\text{conversion})$$

This is not a particularly desirable result for the nonideal reactor, since it indicates that the individual effects on conversion and selectivity are multiplied together in determination of the net loss in yield. For  $S_i(\text{III}) > 1$ , unfortunately, the decrease in yield due to nonideality is then greater than individual losses in either conversion or selectivity; a given loss in conversion may show up as two or three times that amount in the yield of a desired product. On the other hand, trends in conversion and selectivity tend to compensate each other for  $S_i(\text{III}) < 1$ ; this is shown in Figure 5.14c for the same reaction parameters used in Figures 5.14a and b. Plotted are the product of conversion and selectivity for the two reaction systems (intrinsic selectivity  $>$  and  $< 1$ ) as a function of  $n$ . It is clear that for  $S_i(\text{III}) > 1$ , the  $\delta$ -value decrease for yield is larger in each case than the corresponding decreases for conversion or selectivity.

The results above are obviously specific to the particular set of kinetic parameters employed. Yield and selectivity comparisons for the Type III system as

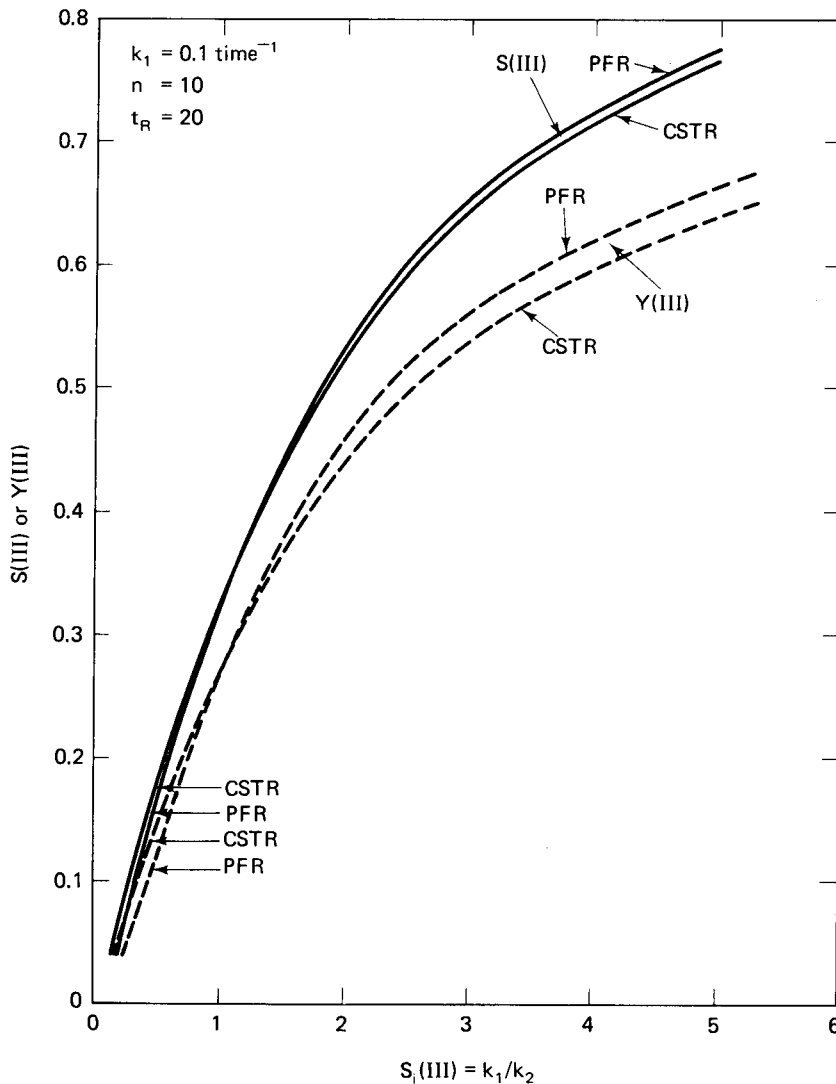


**Figure 5.14** (d) Selectivity and yield variations with Type III kinetic parameters in a nonideal reactor (10 CSTR units in series).

a function of the kinetic parameters are shown in Figure 5.14d, where the nonideal reactor model is a CSTR sequence with  $n = 10$ . The magnitude of the deviation from PFR performance is sensitive to the relative values of  $k_1$  and  $k_2$ , increasing as the intrinsic selectivity  $[S_i(III) = k_1/k_2]$  increases. There exists a region for  $S_i(III) < 1$  where the selectivity for the nonideal reactor is actually greater than the PFR value, while the yields are essentially the same. This is the result of compensation between elements of longer and shorter residence time. Here  $k_1 < k_2$ , so that longer residence times tend to promote the faster reaction  $B \rightarrow C$ , removing the desired intermediate. Conversely, shorter residence times do not provide as much opportunity for the intermediate to react away and, as we see here, for this range of  $k_1$  and  $k_2$  the

skew toward shorter residence time in the nonideal reactor is sufficient to result in an enhancement in the selectivity.

Overall the analysis here should convey the message that generalizations concerning selectivity or yield performance in nonideal reactors with reference to an ideal model are slippery; conversion, however, is perhaps somewhat more predictable. We may normally expect modest taxes on conversion as the result of nonideal exit-age distributions; if the reaction system involves selectivity/yield functions these will also be influenced by the exit-age distribution, but the direction is not certain. Normally nonideality is reflected in a decrease in yield and selectivity, but there are possible interactions between the reactor exit-age distribution and the reaction kinetic parameters that can force the deviation in the opposite direction. Keep in mind that the comparisons being offered here are *not* analogous to those for PFR-CSTR Type III selectivities given in Chapter 4, which were based on the premise of equal conversion in the two reactor types.

To complete this discussion of conversion, selectivity, and yields in nonideal reactors, let us consider a similar set of illustrations for a Type II system. Recall that

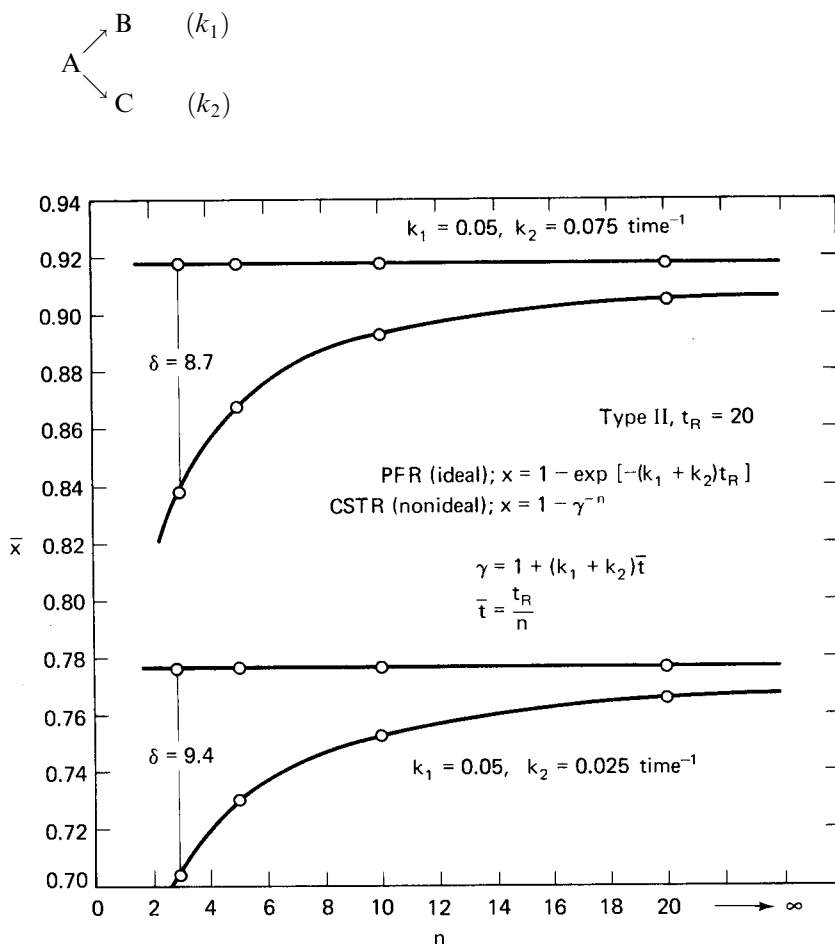


**Figure 5.15** (a) Conversion in a nonideal reactor for a Type II reaction system.

The pertinent relationships are, for the PFR model,

$$x = 1 - e^{-(k_1+k_2)t_R} \quad (5-73)$$

$$S_B(II)_{PFR} = \frac{k_1}{k_1 + k_2} \quad (5-74)$$

and for the CSTR sequence,

$$x = 1 - \gamma^{-n} \quad (5-75)$$

$$S_B(II)_{CSTR} = \frac{k_1}{k_1 + k_2} \quad (5-76)$$

where  $\gamma = 1 + (k_1 + k_2)\bar{t}$ . In both cases yield is calculated as before from the product of conversion and selectivity. Now it is apparent that since the selectivity in both cases is the same and is constant, the effects of nonideality on yield will be in the same direction as those on conversion, and in fact will be of the same magnitude. This is illustrated in Figure 5.15a for conversion, and 5.15b for yield, using the same kinetic parameters employed for the Type III reaction.

A comparison of conversion and yield for the Type II reaction in terms of the kinetic parameters using a nonideal reactor model ( $n = 10$ ) is shown in Figure 5.15c. Here as the value of  $(k_1/k_2)$  decreases, yield and conversion in the nonideal reactor approach the ideal value; in this case this is a limiting value owing to the equality of the selectivity in the two reactor models.

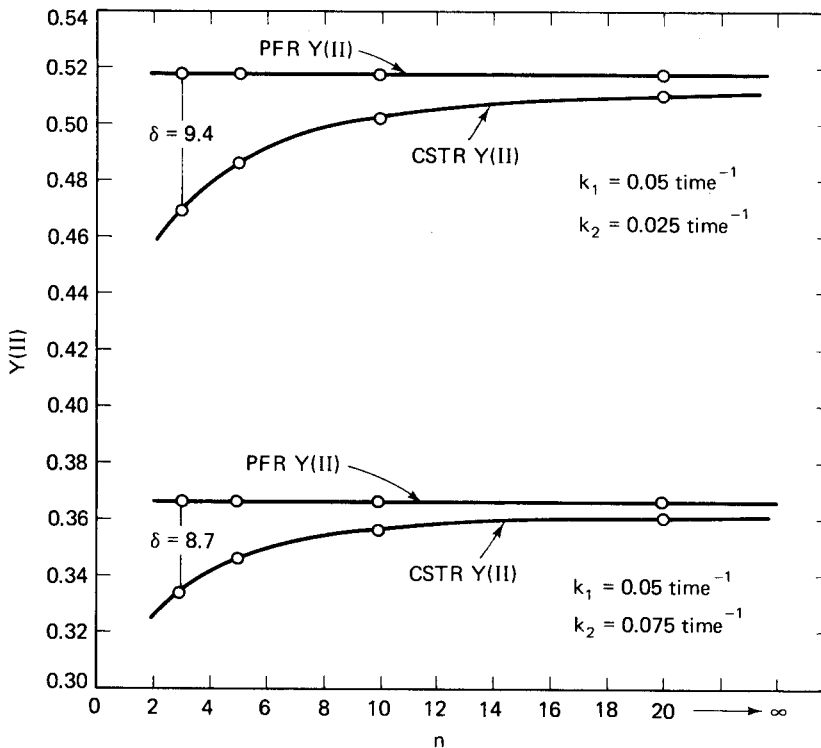
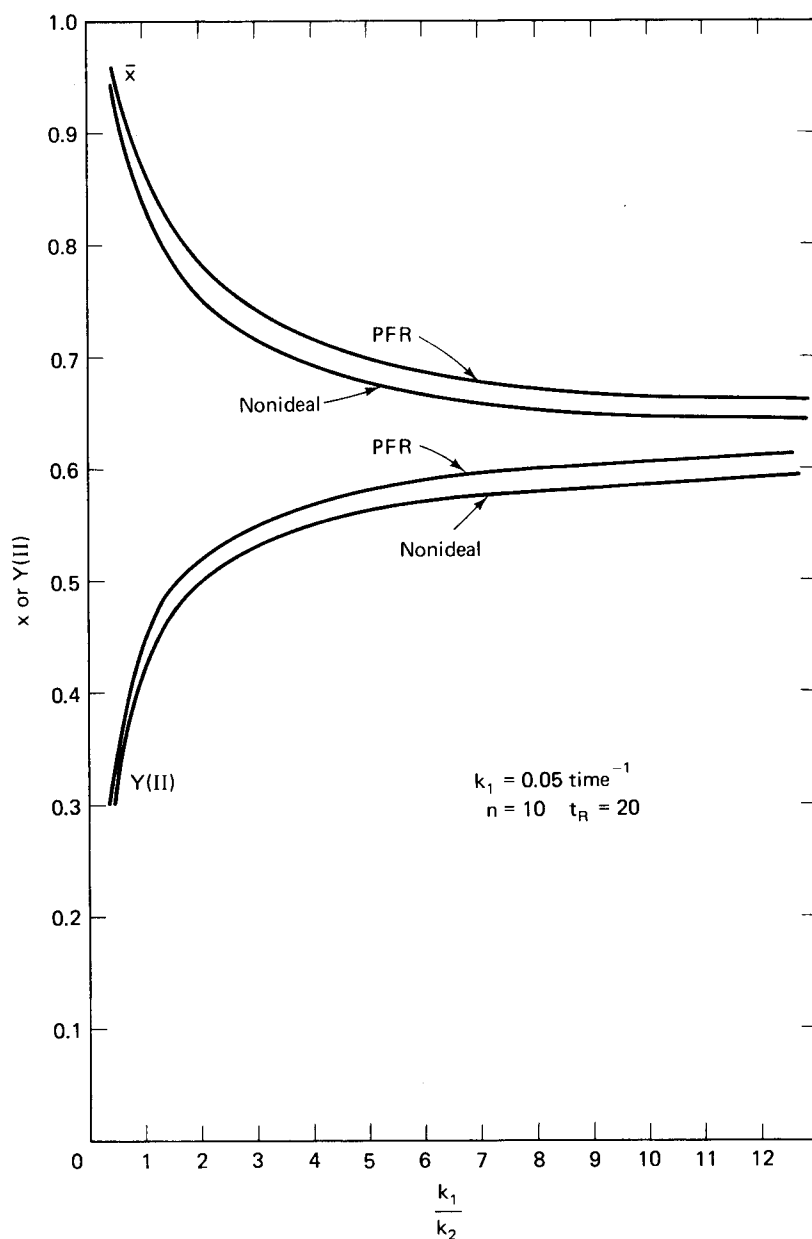


Figure 5.15 (b) Yield in a nonideal reactor for a Type II reaction system.



**Figure 5.15** (c) Conversion and yield, Type II, in a nonideal reactor.

Use of the CSTR sequence as a model for nonideal reactors has been criticized on the basis that it lacks certain aspects of physical reality, such as the absence of backward communication between the individual mixing cell units. Such may be the case; nonetheless the mathematical simplicity of the approach makes it very attractive, particularly for systems with complex kinetics, nonisothermal effects, or other complicating factors.

### 5.4.2 Axial Dispersion Models

A nonideal reactor model based on the axial dispersion (one-dimensional) equation is readily written down following the procedure used in deriving the PFR relationship. Thus, equation (5-20) becomes, for steady-state conditions,

$$D \frac{d^2 C}{dz^2} - u \frac{dC}{dz} - (-r) = 0$$

where  $C$  now refers to the concentration of a reactant or product of interest. Again, following the convention adopted for the PFR equation,  $(-r)$  is a net positive quantity if  $C$  refers to the reactant, negative if  $C$  refers to the product.

We have previously pointed out that the use of the dispersion model changes the reactor analysis from an initial-value (PFR) to a boundary-value problem. As a result, we should worry about the form of the boundary conditions to use for equation (5-77). This is illustrated in Figure 5.16, where several possible configurations of inlet and outlet conditions are shown. Hopefully, this is not to make a

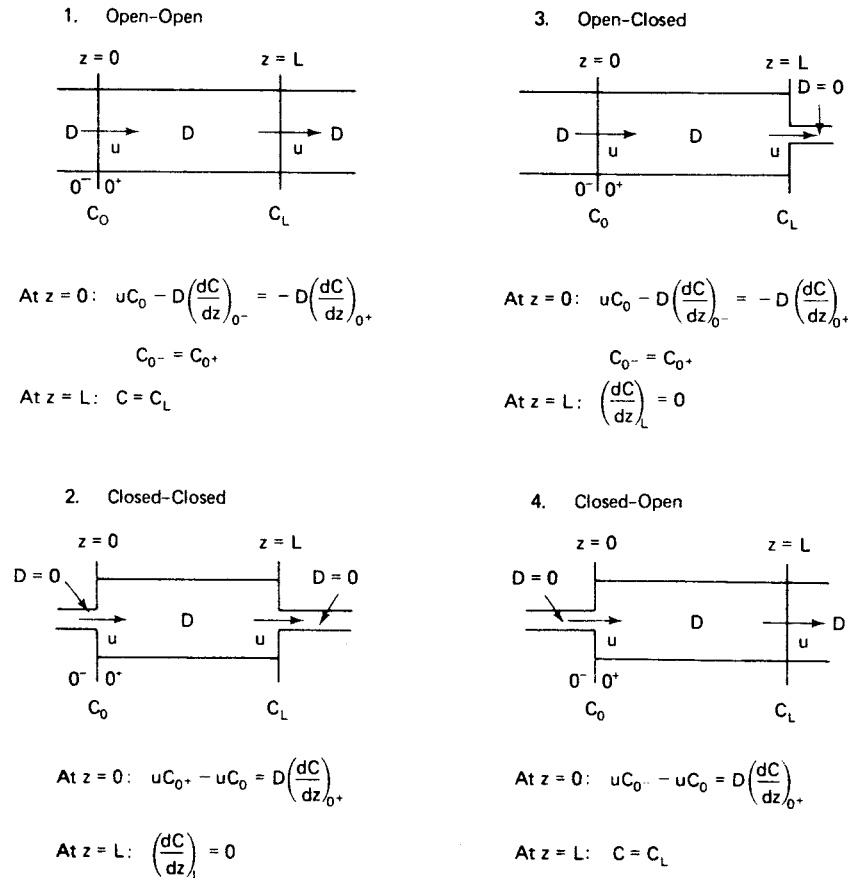


**Figure 5.16** Different inlet/outlet configurations with corresponding boundary conditions for the one-dimensional dispersion reactor model.

complicated mess out of something relatively simple, however the “correct” form of the boundary conditions is not intuitively obvious. In the *open–open* configuration, for example, we consider that dispersion in both fore and aft sections, outside the reactor proper, is possible. In the *closed–closed* configuration only convective transport occurs external to the reactor. Intermediate cases such as *open–closed* and *closed–open* configuration might also more closely conform to particular instances of flow patterns associated with various types of reactor assemblies. Certainly the complexity of the solution to equation (5-65) will depend on the complexity of the boundary conditions employed, so often some compromise may be required between the realities of nonideal flow patterns and realistic boundary condition approximations. It is legitimate to ask whether the boundary conditions used really make much difference in the numerical solution to most problems; read further to find the answer to this exciting question.

Three sets of conditions have been employed in most work dealing with one-dimensional dispersion reactor models. These are

$$\begin{aligned} \text{Type A: } (z = 0) \quad uC_0 &= uC_{0+} - D\left(\frac{dC}{dz}\right)_{0+} \\ (z = L) \quad \left(\frac{dC}{dz}\right) &= 0 \end{aligned} \quad (5-77)$$

$$\begin{aligned} \text{Type B: } (z = 0) \quad uC_0 &= uC_{0+} \\ (z = L) \quad \left(\frac{dC}{dz}\right) &= 0 \end{aligned} \quad (5-78)$$

$$\begin{aligned} \text{Type C: } (z = 0) \quad uC_0 &= uC_{0+} \\ (z \rightarrow \infty) \quad \lim C(z) &= 0 \end{aligned} \quad (5-79)$$

Typical references concerning these three types are found in the writings of Danckwerts [P.V. Danckwerts, *Chem. Eng. Sci.*, 2, 1 (1953)], Hulburt [H.M. Hulburt, *Ind. Eng. Chem*, 36, 1012 (1944)], and Levenspiel and Smith [O. Levenspiel and W.K. Smith, *Chem. Eng. Sci.*, 6, 227 (1957)], for A, B, and C, respectively. The notation employed in equations (5-77) to (5-79) is illustrated in Figure 5.16. It is seen that the Type A conditions correspond to the closed–closed configuration, which is case 2 in Figure 5.16. The reasoning involved in writing this set of boundary conditions is roughly as follows. At the entrance to the reactor the concentration is established by convective transport from the region  $z < 0$  across the plane  $z = 0$ , which must be balanced by the combination of convective transport and dispersion occurring within the reactor,  $z = 0^+$ . No dispersion occurs for  $z < 0$ , so this term is absent from the left side of equation (5-70) for  $z = 0$ . A similar balance may be written for the exit of the reactor, with convection plus dispersion at  $z = L$  balance by convection at  $z = L^+$ , so that

$$uC_{out} = uC_L - D\left(\frac{dC}{dz}\right)_L$$

Now if  $(dC/dz)_L$  is negative, the concentration in the exit stream must be greater than that within the reactor, whereas if  $(dC/dz)_L$  is positive, the concentration of

reactant would have to pass through a minimum somewhere in the reactor. Neither one of these alternatives is physically reasonable, so we are left with

$$uC_{out} = uC_L$$

or

$$\left(\frac{dC}{dz}\right)_L = 0$$

To evaluate which among the alternative or conditions presented by A, B, or C is most correct in an absolute sense, we might establish as a criterion that the solution with the correct boundary conditions should reduce to the PFR limit for  $D \rightarrow 0$ , and to the CSTR limit for  $D \rightarrow \infty$ . Fan and Ahn [L-T. Fan and Y-R. Ahn, *Ind. Eng. Chem. Proc. Design Devel.*, 1, 190 (1962)] have shown that the Type A conditions, as proposed by Danckwerts, is the only one of the three that yields this proper limiting behavior. We will illustrate this for first-order irreversible kinetics, for which an analytical solution is exhausting but possible.<sup>8</sup> It is first convenient to render equations (5-76) and (5-77) into nondimensional form by substitution of the following dimensionless variables.

$$f = \frac{C}{C_0} = 1 - x \quad \zeta = \frac{z}{L}$$

$$N_{Pe} = \frac{Lu}{D} \quad R' = \frac{kL}{u} = \frac{L}{uC} (-r)$$

then

$$\frac{1}{N_{Pe}} \frac{d^2 f}{d\zeta^2} - \frac{df}{d\zeta} - R' f = 0 \quad (5-80)$$

$$(\zeta = 0): \quad \frac{df(0^+)}{d\zeta} = N_{Pe}[f(0^+) - 1]$$

$$(\zeta = 1): \quad \frac{df(1)}{d\zeta} = 0 \quad (5-81)$$

The solution obtained by Danckwerts is reported for the nondimensional concentration  $f$  as a function of the nondimensional length  $\zeta$

$$f(\zeta) = \exp\left(\frac{N_{Pe}}{2} \zeta\right) \cdot \left[ \frac{2(1+\beta) \exp\left[\frac{N_{Pe}\beta}{2} (1-\zeta)\right] - 2(1-\beta) \exp\left[\frac{N_{Pe}\beta}{2} (\zeta-1)\right]}{(1+\beta)^2 \exp\left(\frac{N_{Pe}}{2} \beta\right) - (1-\beta)^2 \exp\left(\frac{-N_{Pe}}{2} \beta\right)} \right] \quad (5-82)$$

where

$$\beta = \left(1 + \frac{4R'}{N_{Pe}}\right)^{1/2}$$

<sup>8</sup> Results for other kinetics are reported by Fan and Balie [L-T. Fan and R.C. Balie, *Chem. Eng. Sci.*, 13, 63 (1960)] and by Burghardt and Zaleski [A. Burghardt and T. Zaleski, *Chem. Eng. Sci.*, 23, 575, (1968)] "A mighty maze! but not without a plan."—A. Pope



Conversion at the reactor exit is obtained from evaluation of  $(1 - f)$  at  $\zeta = 1$

$$x(1) = 1 - \frac{4\beta}{(1 + \beta)^2 \exp\left[-\frac{N_{Pe}}{2}(1 - \beta)\right] - (1 - \beta)^2 \exp\left[-\frac{N_{Pe}}{2}(1 + \beta)\right]} \quad (5-83)$$

Now let us examine the limiting forms of equation (5-83) for  $D \rightarrow 0$  and  $D \rightarrow \infty$ . As  $D \rightarrow 0$ ,  $4R'/N_{Pe}$  must also approach zero, so that  $\beta \rightarrow 1$  and

$$\exp\left[-\frac{N_{Pe}}{2}(1 - \beta)\right] \rightarrow \exp[-R']$$

from equation (5-83) if we make the approximation that

$$1 - \left(1 + \frac{4kD}{u^2}\right)^{1/2} \approx \frac{2kD}{u^2}$$

for small  $D$ . Then

$$x(1) = 1 - \exp[-R'] \quad (5-84)$$

which is the proper PFR result for these kinetics. For  $D \rightarrow \infty$  we can expand the exponential terms in the denominator linearly.

$$x(1) = 1 - \frac{4\beta}{(1 + \beta)^2 \left(1 - \frac{N_{Pe}}{2} + \frac{N_{Pe}\beta}{2}\right) - (1 - \beta)^2 \left(1 - \frac{N_{Pe}}{2} - \frac{N_{Pe}\beta}{2}\right)}$$

Algebraic simplification of the expression yields

$$x(1) = \frac{1}{(1 + 1/R')} \quad (5-85)$$

which is the proper CSTR limit.

For very small but not vanishing values of  $D$ , the following result can be obtained.

$$x(1) = 1 - \left(1 + \frac{k^2 DL}{u^2}\right) \exp(-R') \quad (5-86)$$

So the deviation from PFR behavior is given by the magnitude of  $(1 + k^2 DL/u^2)$ . Thus, a criterion for negligible dispersion effects is given by

$$\frac{k^2 DL}{u^2} \ll 1$$

or

$$\frac{(\ln f)^2}{N_{Pe}} \ll 1 \quad (5-87)$$

The solutions of equation (5-80) for the other types of boundary conditions, B and C, are given in Table 5.2. The result for Type B is almost as complicated as for Type A; however, the Type C result is a simple exponential form which is obviously very easy to determine. We may now approach the answer to the exciting question posed previously, which is now more specifically stated as when significant deviations may be expected from the Danckwerts solution. Such a comparison has been reported by Fan and Ahn, and is shown in Figure 5.17. Here are plotted deviations of the solutions obtained with Types B and C boundary conditions

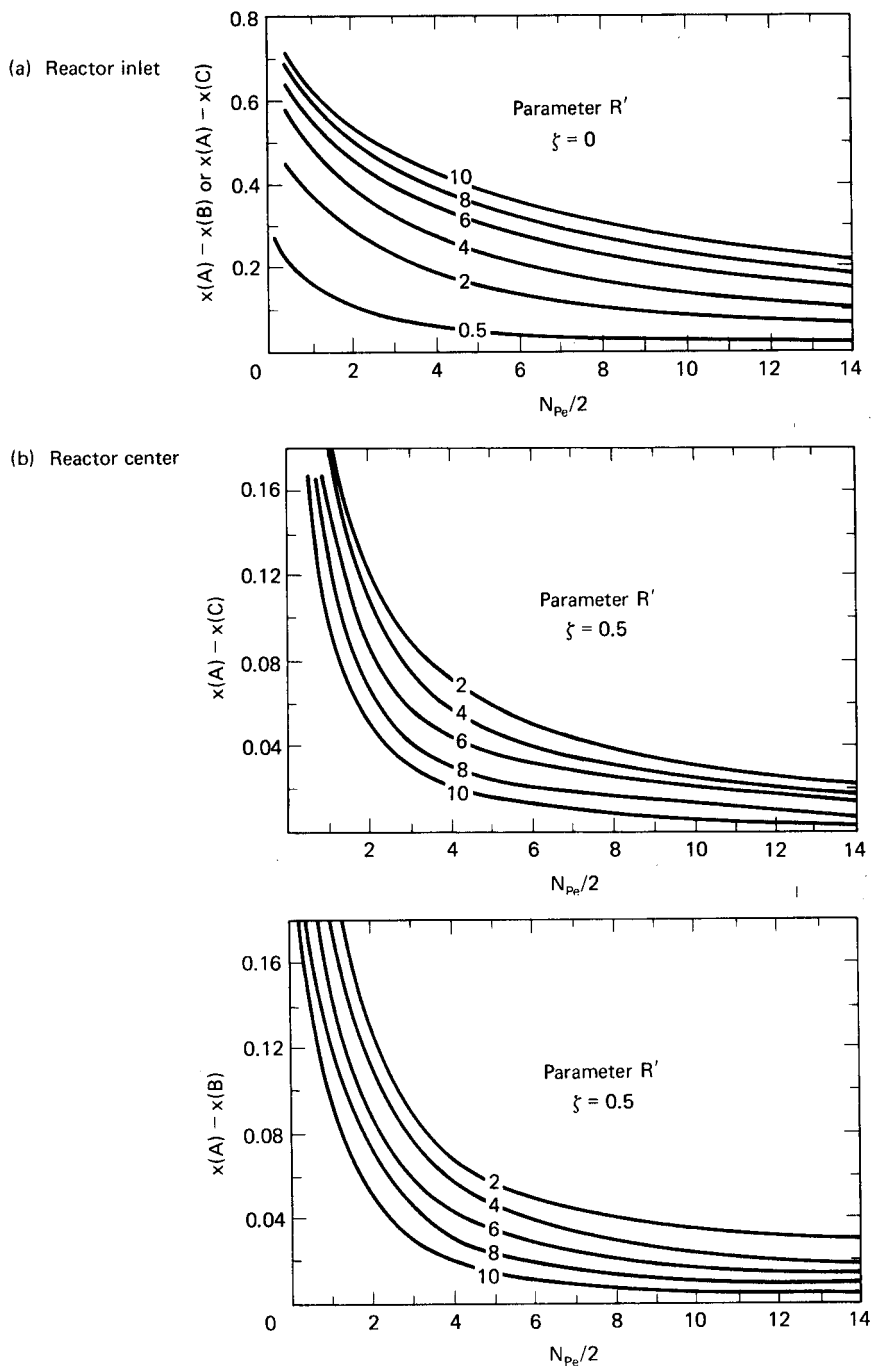


**Figure 5.17** Differences in conversion computed from boundary conditions A, B, and C for reactor inlet, center, and exit. [From L-T. Fan and Y-K. Ahn, *Ind. Eng. Chem. Process Design Devel.*, 1, 190 copyright by the American Chemical Society, (1962).]

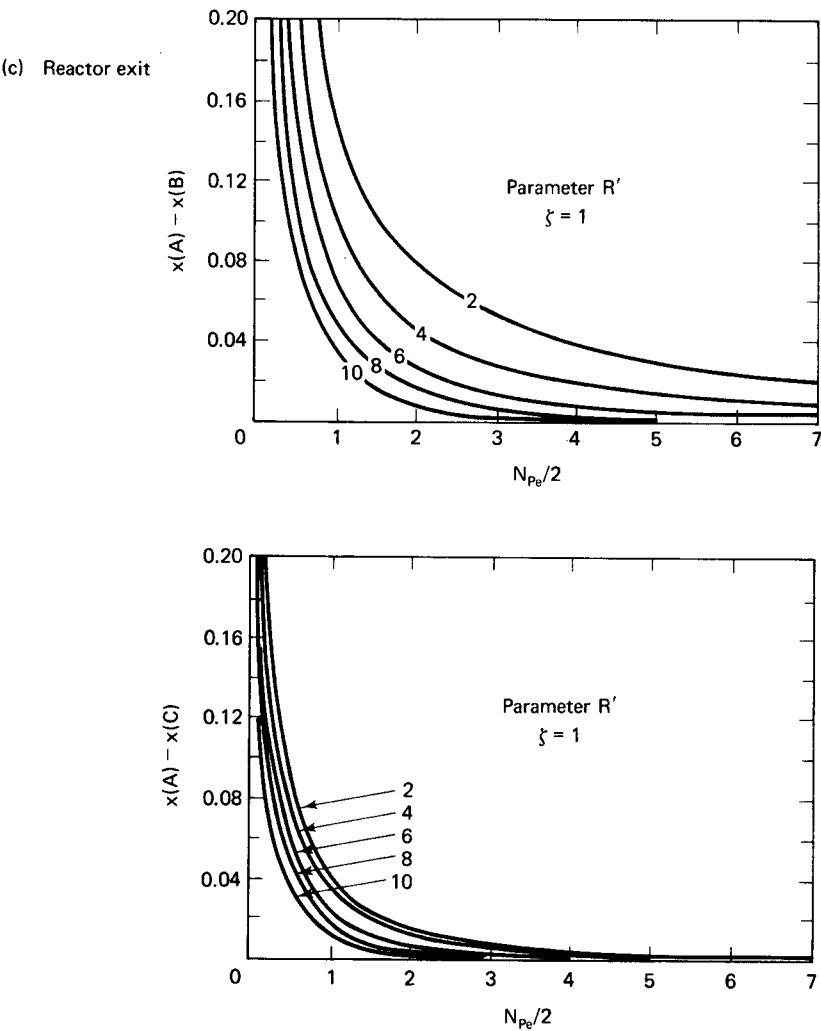
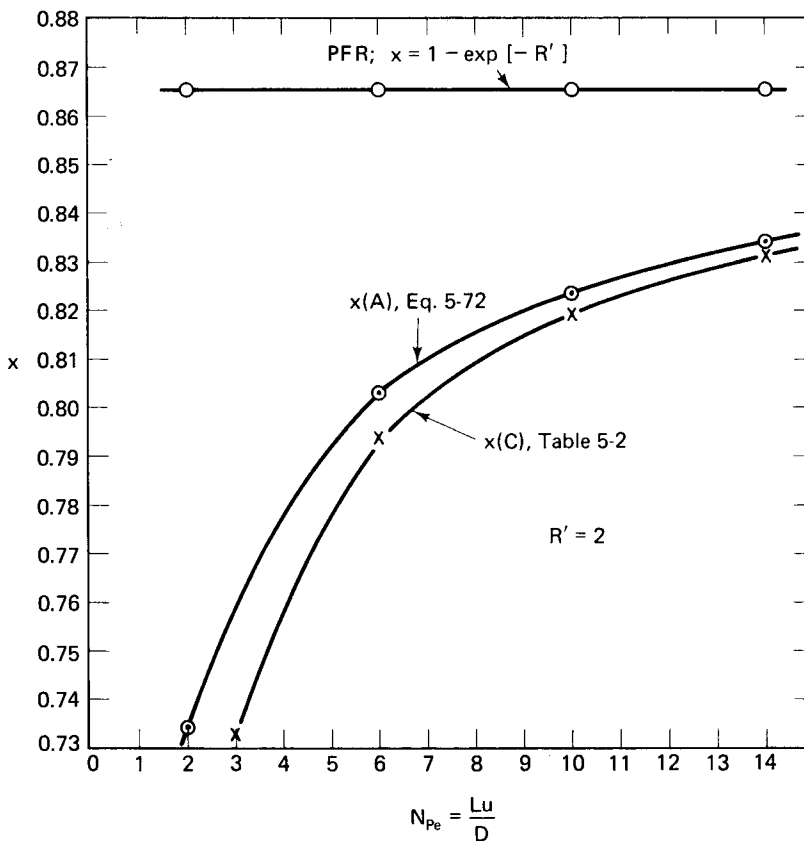


Figure 5.17 Continued.

**Table 5.2** Solutions to the One-Dimensional Dispersion Model for Types B and C Boundary Conditions: Irreversible First-Order Kinetics

Type B
$f(\zeta) = \frac{(1 + \beta) \exp \left[ \frac{N_{Pe}}{2} (1 + \beta) + \frac{N_{Pe}}{2} (1 - \beta) \zeta \right] - (1 - \beta) \exp \left[ \frac{N_{Pe}}{2} (1 + \beta) \zeta + \frac{N_{Pe}}{2} (1 - \beta) \right]}{(1 + \beta) \exp \left[ \frac{N_{Pe}}{2} (1 + \beta) \right] - (1 - \beta) \exp \left[ \frac{N_{Pe}}{2} (1 - \beta) \right]}$
Type C
$f(\zeta) = \exp \left[ \frac{N_{Pe}}{2} (1 - \beta) \zeta \right]$
$\beta = \left( 1 + \frac{4R'}{N_{Pe}} \right)^{1/2}$



**Figure 5.18** Some conversion results computed by the axial dispersion model.

from those of Type A at the entrance, midsection, and exit of the reactor. Such deviations can be expressed entirely in terms of the parameters  $R'$  and  $N_{Pe}$ , as shown. The differences are most pronounced for small values of  $R'$  and  $N_{Pe}$ , a condition which we can visualize qualitatively as corresponding to a sluggish reaction in a reactor with large nonideal flow effects. Also evident from the figure is that Type B conditions give results that are generally inferior to Type C.

The magnitude of nonideality in the dispersion model is given by the value of  $N_{Pe}$ , as we have discussed previously. In Figure 5.18 are presented the results of calculations for two of the axial dispersion models in terms of  $N_{Pe}$  as compared with the PFR result. The value of  $R'$  employed in this calculation corresponds to the kinetic parameters employed for the CSTR model comparison given in Figure 5.14a, so the results in the two figures are directly comparable. As an example, consider the conversion of 0.833 determined from the axial dispersion model for  $N_{Pe} = 14$ . The same conversion level corresponds to  $n \approx 9$  from Figure 5.14a, indicating that the residence-time distributions generated by the two models should be equivalent. This comparison of  $F(t)$  for the CSTR series model,  $n = 9$ , and the axial dispersion model,  $N_{Pe} = 14$ , is shown in Figure 5.19. The point of this figure is to give some numerical support with corresponding visual effects to what has been said all along:

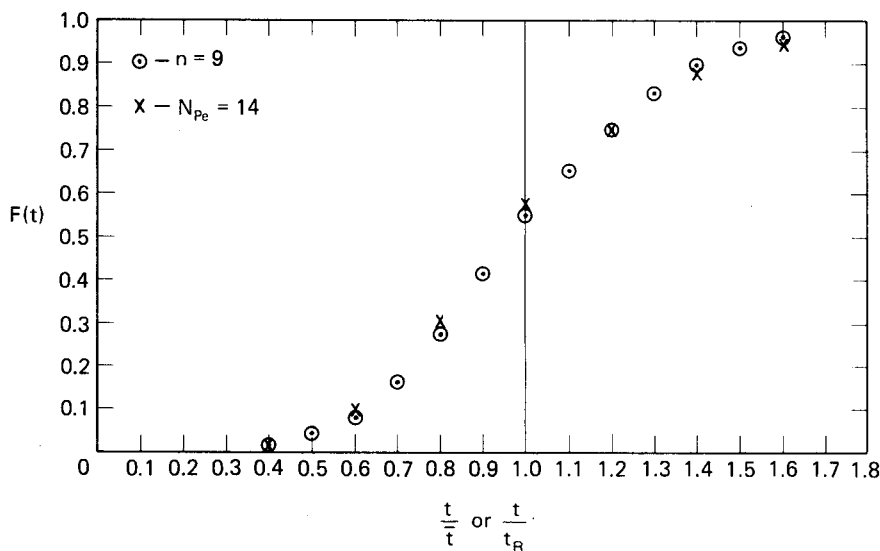


**Figure 5.19**  $F(t)$  curves for CSTR and axial dispersion models demonstrating identical effects on conversion in a first-order reaction.

both mixing-cell and dispersion models provide essentially the same capabilities in representation of nonideal flows short of channelling, bypassing, or similar macroscopic phenomena.



HORATIO SAYS

The results given in Figure 5.17 look good enough, but suppose there was an uncertainty of  $\pm 1$  in determination of  $R'$  and the same for  $(N_{pe}/2)$ ? Then for  $\zeta$  of 0.5, how much would be the uncertainty in estimation of  $[x(A) - x(B)]$  and  $[x(A) - x(C)]$ ?

The most general solution to the one-dimensional axial dispersion model has been given by Wehner and Wilhelm [J.F. Wehner and R.H. Wilhelm, *Chem. Eng. Sci.*, 6, 89 (1956)]. It is formulated in a way such that a variety of the cases illustrated in Figure 5.16 can be obtained as particular solutions of the general model. There are no assumptions in the boundary conditions concerning the role of dispersion in the sections fore and aft of the reactor proper, and the overall formulation is designed to obviate the need for the testing of Types A, B, and C.<sup>9</sup> The overall system extends from  $-\infty$  to  $+\infty$  with the reaction system located from  $0 \leq \zeta \leq 1$ , as shown in Figure 5.20. The external boundary conditions then apply at  $\pm\infty$ , and a total

<sup>9</sup> "It ain't over 'till it's over."—Y. Berra

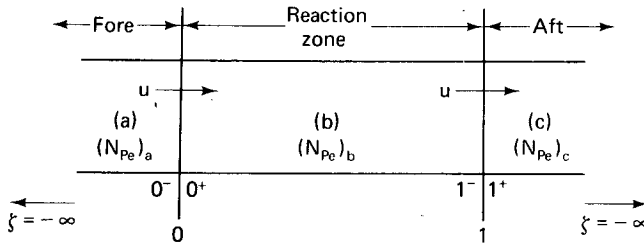


**Figure 5.20** The general axial dispersion model.

mass flux balance including both dispersion and convection can be written between sections *a* and *b* and *b* and *c*. Using the nondimensional variables defined for equation (5-80), the conservation equations for the three sections are

$$(a) \quad \frac{1}{(N_{Pe})_a} \frac{d^2 f}{d\zeta^2} - \frac{df}{d\zeta} = 0; \quad \zeta \leq 0 \quad (5-88)$$

$$(b) \quad \frac{1}{(N_{Pe})_b} \frac{d^2 f}{d\zeta^2} - \frac{df}{d\zeta} - R'f = 0; \quad 0 \leq \zeta \leq 1 \quad (5-89)$$

$$(c) \quad \frac{1}{(N_{Pe})_c} \frac{d^2 f}{d\zeta^2} - \frac{df}{d\zeta} = 0; \quad \zeta \geq 1 \quad (5-90)$$

There are now three boundary value problems involved in the description of the overall reactor, so six boundary conditions are required. These are

$$\begin{aligned} (1) \quad & f(-\infty) = 1 & \zeta = -\infty \\ (2) \quad & f(0^-) - \frac{1}{(N_{Pe})_a} \frac{df(0^-)}{d\zeta} = f(0^+) - \frac{1}{(N_{Pe})_b} \frac{df(0^+)}{d\zeta} & \zeta = 0 \\ (3) \quad & f(0^-) = f(0^+) & \zeta = 0 \\ (4) \quad & f(1^-) - \frac{1}{(N_{Pe})_b} \frac{df(1^-)}{d\zeta} = f(1^+) - \frac{1}{(N_{Pe})_c} \frac{df(1^+)}{d\zeta} & \zeta = 1 \\ (5) \quad & f(1^-) = f(1^+) & \zeta = 1 \\ (6) \quad & f(\infty) = \text{finite} & \zeta = \infty \end{aligned} \quad (5-91)$$

The general solutions obtained for the three reactor sections with these boundary conditions are

$$(a) \quad \frac{1-f}{1-f(0)} = \exp[(N_{Pe})_a \zeta] \quad \zeta \leq 0 \quad (5-92)$$

$$\begin{aligned} (b) \quad & f = g_0 \exp\left[\frac{(N_{Pe})_b \zeta}{2}\right] \left\{ (1 + \beta) \exp\left[\frac{\beta(N_{Pe})_b(1-\zeta)}{2}\right] \right. \\ & \left. - 1(1 - \beta) \exp\left[\frac{\beta(N_{Pe})_b(\zeta-1)}{2}\right] \right\} \quad 0 \leq \zeta \leq 1 \end{aligned} \quad (5-93)$$

$$(c) \quad f = f(1) = 2\beta g_0 \exp\left[\frac{(N_{Pe})_b}{2}\right] \quad \zeta \geq 1 \quad (5-94)$$

where

$$\beta = \left[ 1 + \frac{4R'}{(N_{pe})_b} \right]^{1/2}$$

$$g_0 = 2 \left\{ (1 + \beta)^2 \exp \left[ \beta \frac{(N_{pe})_b}{2} \right] - (1 - \beta)^2 \exp \left[ -\beta \frac{(N_{pe})_b}{2} \right] \right\}^{-1} \quad (5-95)$$

$$f(0) = g_0 \left\{ (1 + \beta) \exp \left[ \beta \frac{(N_{pe})_b}{2} \right] - (1 - \beta) \exp \left[ -\beta \frac{(N_{pe})_b}{2} \right] \right\} \quad (5-96)$$

We see from the above that the  $(f - \zeta)$  profile in the fore section depends on the  $a - b$  boundary concentration,  $f(0)$ , which in turn is a function only of the parameters in the reaction section,  $(N_{pe})_b$  and  $R'$ , while the profile in the reaction section does not depend on the parameters of the fore section. The magnitude of  $(N_{pe})_a$  controls the shape of the concentration profile in the vicinity of the  $a - b$  boundary. As  $(N_{pe})_a$  increases, the profile in the vicinity of  $z = 0$  becomes increasingly steep and approaches the limit of the Type A boundary condition of Danckwerts.

Reference was made earlier to some specific numerical studies reported for the axial dispersion model employing rate expressions other than first order. Some results given by Fan and Balie for half-, second-, and third-order kinetics are illustrated in Figure 5.21. In these results the parameter  $R'_n$  is defined as

$$R'_n = \frac{2knL}{u} C_0^{n-1} \quad (5-97)$$

where  $n$  is the order of the reaction. Conversions for these cases can be compared with the corresponding PFR values, which are conveniently computed from

$$x = 1 - \left[ 1 - \frac{R'_n(1 - n)}{2n} \zeta \right]^{1/(1-n)} \quad (5-98)$$

It is apparent from the shapes of the curves given in Figure 5.21 that interpolation or extrapolation for various orders and values of  $N_{pe}$ , is difficult. Indeed, if any degree of accuracy is required, individual numerical solutions, will probably be needed. Again, the numerical convenience of the CSTR sequence beckons.

### Illustration 5.5

- Given the residence-time data of Figure 5.22 below, determine the corresponding Peclet number based on overall reactor length.
- Evaluate the conversion for a first-order irreversible reaction, rate constant  $k = 0.0796 \text{ s}^{-1}$  in this reactor using the one-dimensional dispersion model. Average residence time is 17.4 s.
- Compare this result with a plug-flow reactor, and with the solution of Wehner and Wilhelm for equal Peclet numbers in sections  $a$ ,  $b$ , and  $c$ .

#### Solution

- Follow the suggestion of equation (5-27) and evaluate the derivative of  $F(t)$  with respect to  $(t/t_R)$  at unity of the latter. This value comes out to be about 0.85, with the corresponding Peclet number about 9.1. Remember, though, that this procedure

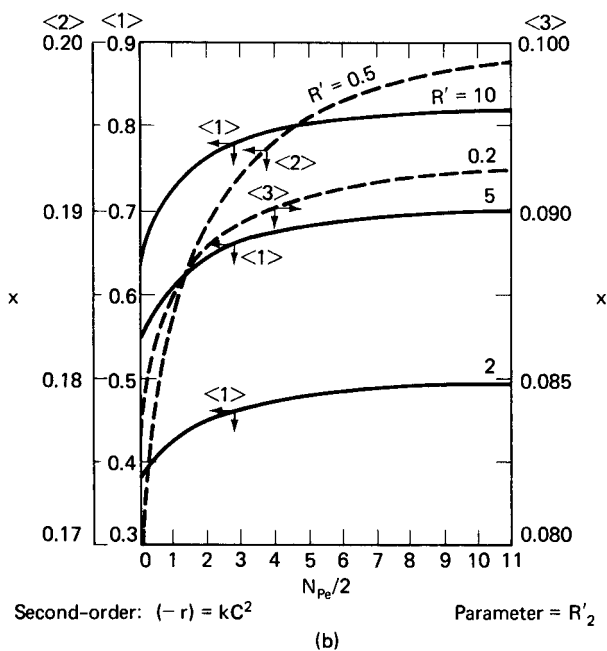
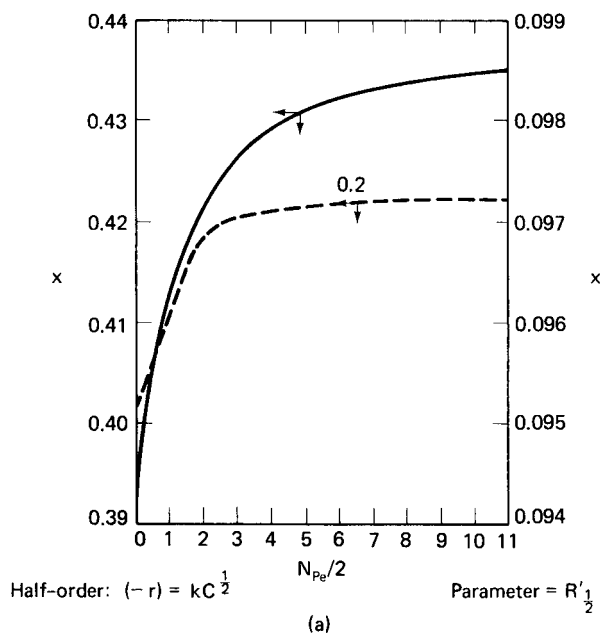


**Figure 5.21** Conversion according to the axial dispersion model for nonlinear kinetics. [After L-T. Fan and R.C. Balie, *Chem. Eng. Sci.*, 13, 63, with permission of Pergamon Press, Ltd., London, (1963).]



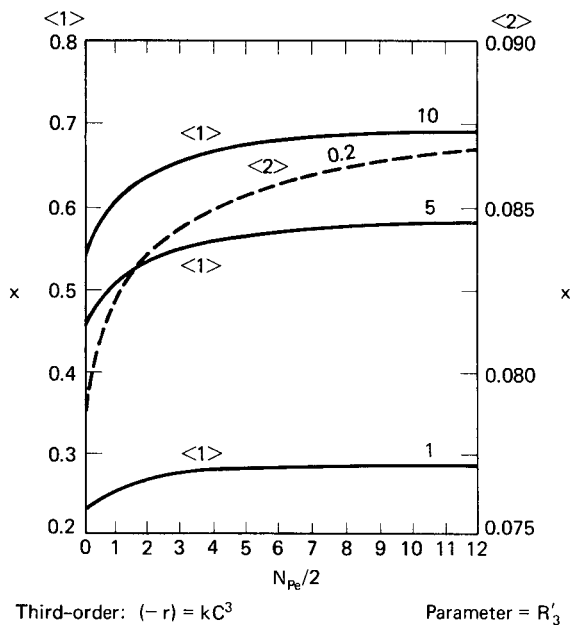


Figure 5.21 Continued.

amounts to taking the derivative of experimental data, which is usually not the most precise way of going about things. The value of  $N_{Pe}$  is probably good to  $\pm 10\%$ .

b) Following the solution according to Danckwerts, equation (5-83), we have

$$\beta = (1 + 4R'/N_{Pe})^{1/2} \tag{i}$$

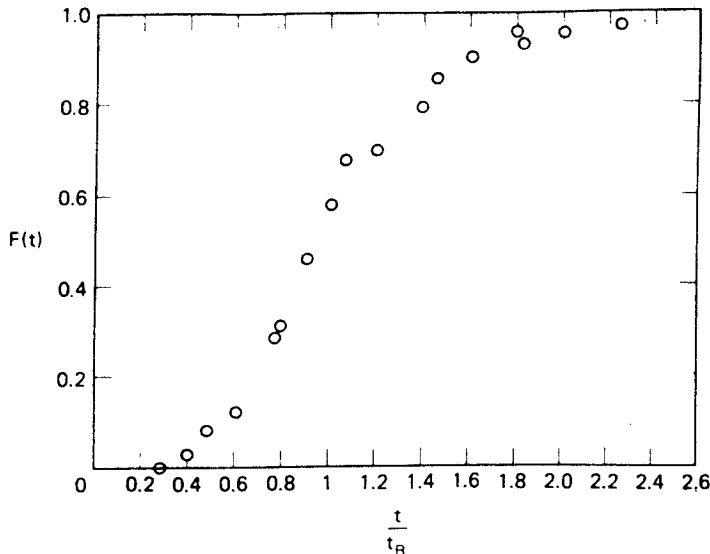


Figure 5.22 Residence-time distribution data for Illustration 5.5.

where

$$R' = k(L/u) = kt_R$$

$$R' = (0.0796)(17.4) + 1.385 \quad (\text{ii})$$

thus

$$\beta = (1 + 0.609)^{1/2} = 1.27 \quad (\text{iii})$$

Inserting the appropriate numerical values derived from the parameters of the system into the Danckwerts relationship, we find

$$x(1) = 0.711 \quad (\text{iv})$$

c) The conventional PFR solution is

$$x = 1 - \exp(-R') = 1 - \exp(-1.385)$$

$$x(1) = 0.750 \quad (\text{v})$$

For the Wehner and Wilhelm solution, we use equations (5-94) and (5-95).

$$1 - x(1) = (2\beta g_0)\{\exp[(N_{Pe})_b/2]\} \quad (\text{vi})$$

where

$$g_0 = 1.20 \times 10^{-3}$$

$$\beta = 1.27$$

$$(N_{Pe})_b = 9.1$$

This yields the result

$$x(1) = 0.712$$

which is essentially the same as that obtained using the Danckwerts relationship [in part (b)].



HORATIO SAYS

In general there is not too much numerical difference between the results from Wehner and Wilhelm and those of Danckwerts. The message is not to make the problem more complicated than it needs to be, in spite of what the learned men may say.

### 5.4.3 Combined Models

Conversion equations for the combined models are easily derived by the same general procedures demonstrated for the mass-balance equations of CSTR and PFR systems. Consider the CSTR with short-circuiting illustrated in Table 5.1. If we write, for steady-state conditions, a mass balance around the vessel of volume  $\bar{V}$ ,

**Table 5.3** Solutions to Example Combined Models<sup>a</sup>

1. Plug flow with dead space:

$$\frac{C}{C_0} = \exp(-fk t_R)$$

2. CSTR with dead space:

$$\frac{C}{C_0} = \frac{1}{1 + f k \bar{t}}$$

3. CSTR with short-circuiting:

$$\frac{C}{C_0} = \frac{v_1/v}{1 + (v/v_1)k\bar{t}} + \frac{v_2}{v}$$

4. PFR-CSTR sequence:

$$\frac{C}{C_0} = \frac{\exp[-f_1 k(\bar{t} + t_R)]}{1 + f_2 k(\bar{t} + t_R)}$$

5. CSTR with short-circuiting and dead volume:

$$\frac{C}{C_0} = \frac{v_1/v}{1 + f(v/v_1)k\bar{t}} + \frac{v_2}{v}$$

<sup>a</sup> See Table 5.1 for notation.

for first-order kinetics,

$$v_1 C_0 = v_1 C_1 + k C_1 \bar{V}$$

$$\frac{C_1}{C_0} = \frac{1}{1 + k \bar{t}_1} \quad (5-99)$$

where  $t_1 = \bar{V}/v_1$ . Now, at the exit the short-circuit stream combines with the reactor effluent so that

$$vC = v_1 C_1 + v_2 C_0 \quad (5-100)$$

Substituting in equation (5-99) for  $C_1$  and rearranging yields

$$\left(\frac{C}{C_0}\right) = \frac{(v_1/v)}{1 + k \bar{t}_1} + \frac{v_2}{v}$$

and, since  $\bar{t} = (v_1/v)\bar{t}_1$ , according to the definitions employed in Table 5.1, we obtain

$$\left(\frac{C}{C_0}\right) = \frac{(v_1/v)}{1 + (v/v_1)k\bar{t}} + \frac{v_2}{v} \quad (5-101)$$

Similar relationships for the steady-state conversions (according to the combined models given previously) are reported in Table 5.3. See Hooper [W.B. Hooper, *Chemtech*, 20, 54 (1990)] for an interesting discussion.

#### 5.4.4 Mixing-Cell, Axial Dispersion, and Combined Models: The Unsteady State

The models as presented and analyzed in the three previous sections are steady state and thus yield no information as to how the state was attained. Reactor startup and

shutdown operations, however, are often an important, even critical, factor in actual processing operations. This is particularly so with stirred tank reactors, in which one reactor or series of reactors may be used for a variety of reactions on some time-shared basis. Operation during startup often results in the production of products that do not meet quality standards, so it is of interest to be able to analyze such an operation. The mixing models presented in Section 5.2 provide the foundation for this. Because of their unsteady-state nature, each model is able to provide an interpretation of the  $F(t)$  and  $E(t)$  responses.

Let us begin here with the PFR and, once again,  $A \rightarrow B$ , first-order and irreversible (otherwise known as Academic Reaction #1). The unsteady-state form of equation (4-42) is

$$-u\left(\frac{\partial C}{\partial z}\right) + (-r) = \left(\frac{\partial C}{\partial t}\right) \quad (5-102)$$

and the following change of variables is useful

$$Y = \frac{(C_A - C_{A_0})}{C_{A_0}}; \quad X = \frac{z}{L}$$

so that

$$\left(\frac{\partial Y}{\partial X}\right) + \left(\frac{\partial Y}{\partial t}\right) = -k(1 + Y) \quad (5-103)$$

for  $t > 0$  and  $0 < X < X_f$ , where  $X_f = (L/u)$ . The initial and boundary conditions are

$$\begin{aligned} Y(0, t) &= 0 \\ Y(X, 0) &= 0 \end{aligned} \quad (5-104)$$

This equation is amenable to solution via Laplace transforms, so transforming with respect to  $t$  we obtain

$$\mathcal{L}[Y(X, t)] = \int_0^\infty e^{-st} Y(X, t) dt = y(X, s) \quad (5-105)$$

The transform of equation (5-103) yields a linear, first-order ordinary differential equation for the transform variable,  $y$ , in terms of the nondimensional length,  $X$ , as

$$\left(\frac{dy}{dX}\right) + sy = -k\left(\frac{1}{s} + y\right) \quad (5-106)$$

with the conditions given in equation (5-104) transformed to

$$\begin{aligned} y(X, 0) &= 0 \\ y(0, s) &= 0 \end{aligned} \quad (5-107)$$

The solution to this is obtained by separation of variables in a straightforward manner.

$$y(X, s) = -\left(\frac{1}{s}\right) + (e^{-Xs} e^{-kX}) + \frac{1}{(s+k)} - \frac{e^{-(s+k)X}}{(s+k)} \quad (5-108)$$

The inverse transform of this equation is

$$Y(X, t) = -1 + (e^{-kX} - e^{-kt})S_X(t) + e^{-kt} \quad (5-109)$$

where  $S_X(t)$  is a step-function input defined as

$$S_X(t) = 0 \quad (0 < t < X)$$

$$S_X(t) = 1 \quad (t > X)$$

Restatement of equation (5-109) in terms of the original variables gives us

$$C_A = C_{A_0}[e^{-kX} - e^{-kt}]S_X(t) + C_{A_0}e^{-kt} \quad (5-110)$$

The solution here actually comes in two parts, depending upon the relative magnitudes of  $t$  and the normalized length

$$\text{i) } C_A = C_{A_0}e^{-kt}; \quad 0 < t < X \quad (5-111)$$

$$\text{ii) } C_A = C_{A_0}e^{-kt_R}; \quad t > X \quad (5-112)$$

where  $t_R = (L/u)$ .

For the CSTR sequence, the general mass balance with chemical reaction in the unsteady-state becomes

$$\frac{dC_n}{dt} + \frac{C_n}{\bar{t}} + (-r) = \frac{C_{n-1}}{\bar{t}}$$

which for an irreversible first-order reaction in a single unit becomes

$$\frac{dC_{A_1}}{dt} + C_{A_1} \left( \frac{1 + k\bar{t}}{\bar{t}} \right) = \frac{C_A(t)}{\bar{t}} \quad (5-113)$$

where  $C_A(t)$  is the time-dependent feed concentration. This equation may be solved via Laplace transforms for a step change from an initial value, say  $C_{A_0}$ , to a new value,  $C_{A_0} + \Delta C_{A_0}$ . The result is

$$C_{A_1}(t) = \frac{C_{A_0} + \Delta C_{A_0}}{1 + k\bar{t}} + \exp \left[ (1 + k\bar{t}) \frac{t}{\bar{t}} \right] \left( A_1 - \frac{C_{A_0} + \Delta C_{A_0}}{1 + k\bar{t}} \right) \quad (5-114)$$

where  $A_1$  is the initial value of  $C_{A_1}$  as obtained from the steady-state solution with feed of  $C_{A_0}$ . The first-order case may be generalized to a  $n$ -unit sequence, provided that equal temperatures and volumes pertain for each unit, to the following.

$$C_{A_0} = \frac{C_{A_0}}{Q^n} + e^{-Q\bar{t}/t} \left\{ A_n + A_{n-1} \left( \frac{t}{\bar{t}} \right) + \cdots + \frac{A_1}{(n-1)!} \left( \frac{t}{\bar{t}} \right)^{n-1} \right. \\ \left. - \frac{C_{A_0}}{Q^n} \left[ 1 + \frac{Q\bar{t}}{\bar{t}} + \cdots + \frac{1}{(n-1)!} \left( \frac{Q\bar{t}}{\bar{t}} \right)^{n-1} \right] \right\} \quad (5-115)$$

where  $C_{A_0}$  at time zero is given by  $A_0$ , and  $Q = 1 + k\bar{t}$ .

An approximate solution for second-order irreversible kinetics in a single CSTR can be obtained by linearization of the rate term. The solution is the same as equation (5-114), except the term  $(1 + k\bar{t})$  is replaced by  $(1 + 2k\bar{t}C_{A_0})$ , where  $C_{A_0}$  is the initial feed concentration. This result depends on the fact that  $C_{A_1}(t)$  does not differ greatly from  $C_{A_1}(0)$ , or more specifically that

$$2C_{A_1}(0)[C_{A_1}(t) - C_{A_1}(0)] \approx [C_{A_1}(t)^2 - C_{A_1}(0)^2]$$

In many cases this can prove to be a very restrictive assumption, so that in general the evaluation of transients for CSTR sequences with non-first-order kinetics is a numerical problem. Various other cases of unsteady-state operation are summarized in the papers of Piret and coworkers cited in Chapter 4, and in the text by Cooper and Jeffries [A.R. Cooper and G.V. Jeffries, *Chemical Kinetics and Reactor Design*, Prentice-Hall, Inc., Englewood Cliffs, NJ, (1973)].

### Illustration 5.6

A reaction that has been shown to correspond to Academic Reaction #1 with  $k = 0.8 \text{ h}^{-1}$  at  $250^\circ\text{C}$  is to be carried out in a sequence of three CSTRs, each with  $\bar{t} = 1 \text{ h}$ . Compare these two techniques of starting the reaction.

- Charging to each reactor the raw feed at  $250^\circ\text{C}$ , running them batchwise until the proper conversions are reached, and then starting flow.
- Charging to each reactor the raw feed at  $250^\circ\text{C}$ , and starting flow immediately.

Which of these procedures would you endorse, and why?

#### Solution

We have a series of CSTRs,  $k = 0.8 \text{ h}^{-1}$ , and  $\bar{t} = 1 \text{ h}^{-1}$ . Let us look at the batch startup first.

- a) *Batch startup*. The steady-state operating condition we are aiming for is

$$\left(\frac{C_{A_1}}{C_{A_0}}\right) = (1 + k\bar{t})^{-1} = 0.555 \quad (\text{i})$$

Similarly,

$$\left(\frac{C_{A_2}}{C_{A_0}}\right) = 0.308; \quad \left(\frac{C_{A_3}}{C_{A_0}}\right) = 0.172 \quad (\text{ii})$$

Obviously, conversion in the third vessel will control startup time for the sequence, so

$$\left(\frac{C_{A_3}}{C_{A_0}}\right) = e^{-kt}; \quad \ln(0.172) = -0.8t \quad (\text{iii})$$

and

$$t = 2.2 \text{ h for batch startup.}$$

- b) *Transient startup*. Here we start with initial concentrations of  $C_{A_0}$ . For the sequence of three CSTRs, equation (5-115) becomes

$$\begin{aligned} \left(\frac{C_{A_3}}{C_{A_0}}\right) = \frac{1}{Q^3} - e^{-Q\bar{t}/\bar{t}} \left\{ \frac{A_3}{C_{A_0}} + \frac{A_2}{C_{A_0}} \left(\frac{t}{\bar{t}}\right) + \frac{A_1}{2C_{A_0}} \left(\frac{t}{\bar{t}}\right)^2 \right. \\ \left. - \frac{1}{Q^3} \left[ 1 + \frac{Qt}{\bar{t}} + \frac{1}{2} \left(\frac{Qt}{\bar{t}}\right)^2 \right] \right\} \end{aligned} \quad (\text{iv})$$

$$Q = 1 + k\bar{t} = 1.8$$

$$A_n = C_{A_0} \quad \text{so} \quad (A_n/C_{A_0}) = 1$$

Evaluating this expression

$$\left(\frac{C_{A_3}}{C_{A_0}}\right) = (1.8)^{-3} - e^{-1.8t} \left\{ 1 + t + \frac{t^2}{2} - (1.8)^{-3} \cdot \left[ 1 + 1.8t + \frac{(1.8t)^2}{2} \right] \right\} \quad (v)$$

Now, for

$$t = 1 \text{ h} \quad C_{A_3}/C_{A_0} = 0.458$$

$$t = 2 \text{ h} \quad C_{A_3}/C_{A_0} = 0.275$$

$$t = 3 \text{ h} \quad C_{A_3}/C_{A_0} = 0.196$$

At  $t = 3 \text{ h}$  the value of  $(C_{A_3}/C_{A_0})$  here has still not attained the level of conversion required for steady-state operation, hence the batch startup is preferred.



HORATIO SAYS

Would the batch startup procedure always be preferable if the main reaction is irreversible? Even for negative-order kinetics? What if the reaction is reversible?

A transient solution for step-change in the inlet concentration for the axial dispersion model, using Type A boundary conditions, has been given by Fan and Ahn [L-T. Fan and Y-R. Ahn, *Chem. Eng. Progr. Symp. Ser.*, 46(59), 91 (1963)]. For a step of  $C_{A_0}$

$$\begin{aligned} \frac{C(t)}{C_{A_0}} = 1 - 4 \sum_{n=1}^{\infty} \frac{M \delta_n (M \sin \delta_n + \delta_n \cos \delta_n)}{(M^2 + 2M + \delta_n^2)(M^2 + \delta_n^2 + 2MR')} \\ \cdot \exp \left[ M - \left( \frac{M^2 + \delta_n^2 + 2MR'}{2M} \right) \left( \frac{t}{t_R} \right) \right] \end{aligned} \quad (5-116)$$

where

$$M = (N_{Pe}/2)$$

$$\delta_n = n\text{th root of:} \quad \cot \delta = (1/2)[(\delta/M) - (M/\delta)]$$

$$R' = kt_R$$

Some examples of transients computed from equation (5-116) are shown in Figure 5.23 for  $R' = 0.1$ .

A comparison of these transient forms for first-order kinetics, equation (5-115) for the CSTR sequence and (5-116) for the axial dispersion model, on the basis of their steady-state equivalence in terms of  $n$  and  $N_{Pe}$ , is suggested in the exercises. The basic equation to be answered is whether the equivalence of the two models in the

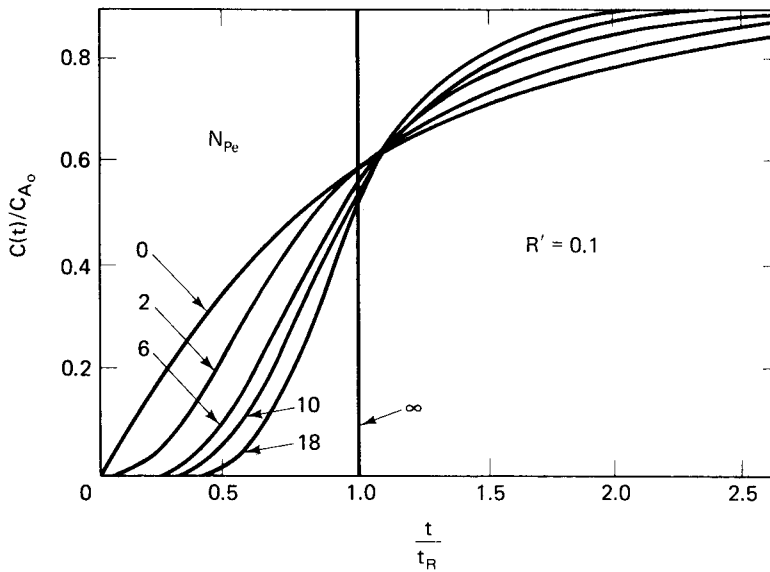


**Figure 5.23** Response of axial dispersion model with reaction to step-function concentration input,  $0 \rightarrow C_{A_0}$ .

steady state is sufficient to ensure their equivalence in modeling the unsteady-state (startup) operation.

The transient forms of the combined models, corresponding to those shown in Tables 5.1 and 5.3, are given in Table 5.4.

**Table 5.4** Unsteady-State Solutions for Combined Models, First-Order Reaction

1. Plug flow with dead space:

$$\frac{C(t)}{C_0} = \exp(-fk t_R) \delta\left(\frac{t}{t_R} - f\right)$$

2. CSTR with dead space:

$$\frac{C(t)}{C_0} = \frac{1}{1 + fk\bar{t}} - \frac{1}{1 + fk\bar{t}} \exp\left[-(1 + fk\bar{t}) \frac{t}{f\bar{t}}\right]$$

3. CSTR with short-circuiting:

$$\frac{C(t)}{C_0} = \frac{(v_1/v)^2}{(v_1/v) + k\bar{t}} \left\{ 1 - \exp\left[-\left(k\bar{t} + \frac{v_1}{v}\right) \frac{t}{\bar{t}}\right] + \frac{v_2}{v} \delta\left(\frac{t}{\bar{t}} - 0\right) \right\}.$$

4. PFR-CSTR sequence:

$$\frac{C(t)}{C_0} = \left\{ \frac{\exp[-f_1 k(\bar{t} + t_R)]}{1 + f_2 k(\bar{t} + t_R)} - \frac{\exp\{f_1/f_2 - [1 + f_2 k(\bar{t} + t_R)]t/f_2\bar{t}\}}{1 + f_2 k(\bar{t} + t_R)} \right\} \delta\left(\frac{t}{\bar{t}} - f_1\right)$$

5. CSTR with short-circuiting and dead volume:

$$\frac{C(t)}{C_0} = \frac{(v_1/v) + (fv_1^2/v)k\bar{t}}{(v_1/v) + fk\bar{t}} - \frac{(v_1/v)^2}{(v_1/v) + fk\bar{t}} \exp\left[-\left(\frac{v_1}{v} + fk\bar{t}\right) \frac{t}{f\bar{t}}\right]$$



**Illustration 5.7**

Deactivation reactions introduce transients into reactors (and their analysis), which may be misleading. We have seen some aspects of this already in Chapter 4. Consider here a slurry reactor that can be modeled as a CSTR with a contained solid catalyst phase and which is used in the hydrogenation of a high molecular weight aromatic compound. The catalyst in the slurry deactivates at a rate dependent upon the hydrogen concentration, and in experiments at fixed hydrogen concentration there have been identified two catalysts of interest in the region of operating conditions. Both have the same initial activity for the reaction  $A \rightarrow B$ , which is first-order and irreversible. Catalyst 1 is defined by its rate of decay

$$\left(\frac{k}{k_0}\right) = e^{-\alpha t} \quad (\text{i})$$

where  $\alpha = (s/s_0)$  is the catalyst activity corresponding to time-on-stream  $t$ . Catalyst 2 is also defined by its rate of decay, in this case correlated linearly.

$$\left(\frac{k}{k_0}\right) = 1 - \beta t \quad (\text{ii})$$

Make a comparison of these two catalysts and report which you would select for what kind of service. There are four cases to compare.

$$\begin{array}{ll} \text{Catalyst 1} & \alpha = 0.2 \text{ h}^{-1}; \quad 0.5 \text{ h}^{-1} \\ \text{Catalyst 2} & \beta = 0.2 \text{ h}^{-1}; \quad 0.5 \text{ h}^{-1} \end{array} \quad (\text{iii})$$

For the reaction under consideration the rate constant with the fresh catalyst,  $k_0$ , is  $1 \text{ h}^{-1}$ , and the reactor has a nominal holding time,  $\bar{t}$ , of  $0.4 \text{ h}$ .

*Solution*

As a first evaluation it might be wise to look just at the basic deactivation results in chronological time. Thus, the four cases are

$$\begin{array}{ll} \text{Catalyst 1} & k = \exp(-0.2t) \\ & k = \exp(-0.5t) \end{array} \quad (\text{iv})$$

$$\begin{array}{ll} \text{Catalyst 2} & k = 1 - 0.2t \\ & k = 1 - 0.5t \end{array} \quad (\text{v})$$

The results of this straightforward comparison are shown in Figure 5.24. As can be seen, the exponential decay case of Catalyst 1 wins with no question in this comparison.

What happens, however, when we translate this to the slurry reactor? Now, we also have to make the comparison on the basis of chronological time, but with the holding time  $\bar{t}$  in the reactor as a consideration. Here we have, for example,

Catalyst 1

$$(1 - x) = \frac{1}{1 + \exp(-0.2\bar{t})} \quad (\text{vi})$$

Catalyst 2

$$(1 - x) = \frac{1}{1 + (1 - 0.2\bar{t})} \quad (\text{vii})$$

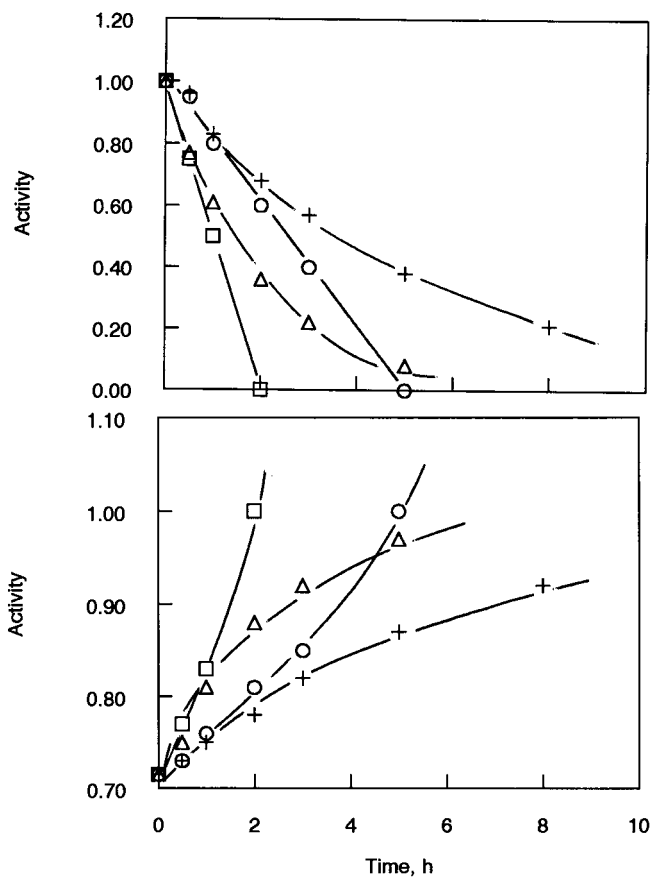


**Figure 5.24** (Top) Comparison of the four combinations of deactivation based on chronological time; (bottom) comparison based on slurry reactor results. Catalyst 1,  $+$  =  $\alpha$  of  $0.2 \text{ h}^{-1}$ ,  $\Delta$  =  $\alpha$  of  $0.5 \text{ h}^{-1}$ ; catalyst 2,  $\circ$  =  $\beta$  of  $0.2 \text{ h}^{-1}$ ,  $\square$  =  $\beta$  of  $0.5 \text{ h}^{-1}$ .

This comparison is shown on the bottom of Figure 5.24. It is clear in this case that there is no disguise of the superior catalyst by the slurry reactor. Note, though, that the slurry reactor indicates a smaller difference in the performance between Catalyst 1 and Catalyst 2 than might have been expected on the basis of the chronological time comparison.



HORATIO SAYS

The PFR is much better at disguising catalyst activity in direct, comparisons such as the above. This is all seen in the sensational expose of Weekman [V.W. Weekman, Jr., *Amer. Inst. Chem. Engr. Symp. Ser.*, 75, 11 (1979)].

**Exercises****Section 5.2.1**

1. Compare the result of the integration of the segregated-flow model for first-order reaction in a laminar flow reactor with the result presented in Chapter 4.
2. Using the residence-time distribution function for a laminar-flow reactor, compare the yield of B in n Type III reaction with that obtained in a PFR of the same average residence time. There is no B or C in the feed, and  $k_1 = 2k_2$  with  $k_2\bar{t} = 1$ .

**Section 5.2.2**

3. What is the ratio of the  $F(t)$  function for two CSTR sequences, one of five units and one of nine units, at  $(t/\bar{t})$  of 0.5, 1.0 and 1.5? Repeat for  $E(t)$ .
4. Derive an expression for the response of an  $n$ -unit CSTR sequence to a step-function decrease in inlet concentration.
5. Determine the proper CSTR mixing model to fit the response data of Problem 1, Chapter 4.

**Section 5.2.3**

6. Determine the proper dispersion model to fit the response data of problem 1, Chapter 4.
7. What is the ratio of the  $F(t)$  and  $E(t)$  functions for two dispersion models, of  $N_{Pe} = 15$  and  $N_{Pe} = 5$ , at  $t/t_R = 0.5, 1.0$  and  $1.5$ ?
8. Determine  $N_{Pe}$  according to the Taylor-Aris model for a component of a solution in laminar flow in a tube of 0.5 cm radius at an average velocity of 10 m/h. The molecular diffusivity is  $2.3 \times 10^{-5} \text{ cm}^2/\text{s}$ . What would the  $F(t)$  curve look like for this situation?

**Section 5.2.4**

9. Demonstrate by calculation that the results obtained in problems 5 and 6 indeed produce the exit-age distribution of problem 1b in Chapter 4.

**Section 5.3**

10. The results illustrated in Figure 5.25 were obtained for  $F(t)$  in a given system. Determine an appropriate combined mixing model and the associated parameters that will provide a reasonable representation of this response. [*Hint*: The mixing may be more easily visualized in terms of  $E(t)$  determined from this data.]

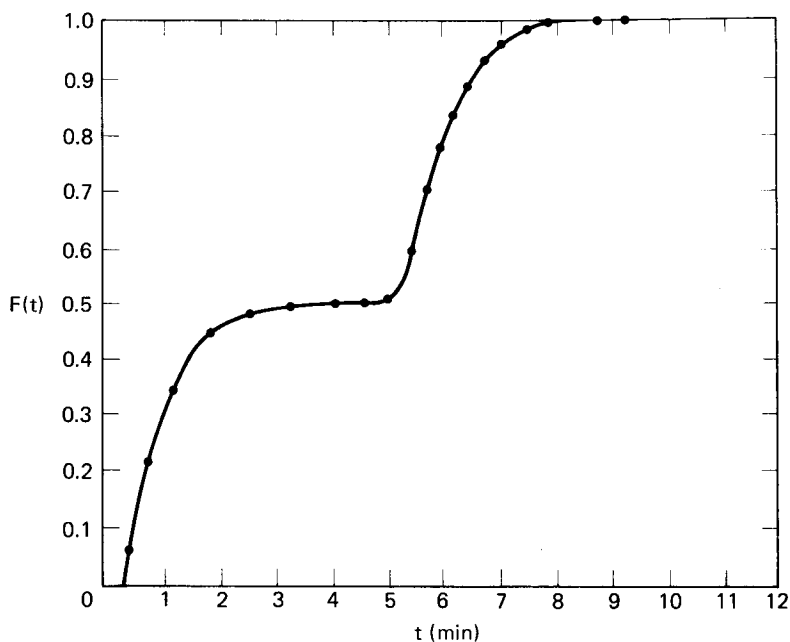


**Figure 5.25** Response data for problem 10.

### Section 5.4.1

11. The reactor described in problem 1b, Chapter 4, is to be used for the reaction  $A + B \rightarrow C + D$ , with order corresponding to stoichiometry. Predict the conversion at the outlet under isothermal conditions and compare it with that for a PFR of the same average residence time. The following parameters apply

$$C_{A_0} = 0.01211 \text{ M}$$

$$C_{B_0} = 0.02578 \text{ M}$$

$$C_{C_0} = C_{D_0} = 0$$

$$k = 0.57 \text{ liter/mol-s}$$

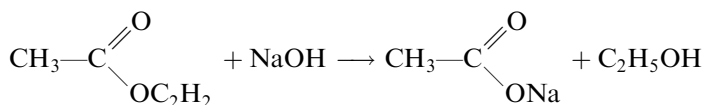
$$L = 15.3 \text{ cm}$$

12. A tubular flow reactor exhibits a residence-time distribution which can be modeled by a sequence of CSTRs in series, all of the same volume. The nominal residence time in the tubular reactor is 20 s. Compare, for a Type III reaction, the conversion, selectivity, and yield obtained in the reactor (as modeled by the CSTR sequence) with that which would be obtained in a true PFR of the same residence time. The rate constants are  $k_1 = 0.1 \text{ s}^{-1}$  and  $k_2 = 0.05 \text{ s}^{-1}$ .
13. In Figure 5.14a the effect of nonideal flow on conversion in a tubular flow reactor was presented in terms of the CSTR model for a first-order reaction. Repeat this calculation for a second-order reaction and

- a half-order reaction with the same numerical value of the rate constant and an inlet concentration of reactant of  $1.0 M$ . Compare the magnitude of the effect on conversion among the three different types of kinetics.
14. Make a comparison of the selectivity behavior of a CSTR sequence and approach to PFR behavior, similar to that of Figure 5.14b, for a Type III system in which
    - (a) The kinetics of the first reaction are half order.
    - (b) The kinetics of the first reaction are second order.
  15. What is the ratio between elements of residence time  $(t/\bar{t}) \leq 1$  and  $(t/\bar{t}) \geq 1$  in the CSTR model for  $n = 5, 10$  and  $25$ ?

### Section 5.4.2

16. Compare the conversion for a first-order reaction as predicted by the dispersion model for Types A, B, and C boundary conditions. The parameters are  $L = 3.2$  m,  $u = 1.6$  m/s,  $k = 1.34$  s $^{-1}$ , and  $N_{Pe} = 10$ .
17. Consider the rate investigations of Sinfelt et al. in problem 8, Chapter 4. If the catalyst particle diameter is 1/16 in. (spherical), what would be the influence of axial dispersion on conversion for a 5% n-pentane/95% hydrogen feed at the conditions indicated? A value for  $N_{Pe}$ , may be determined from Figure 5.9b.
18. Evaluate the results obtained in problems 8 and 14, Chapter 4, in terms of the criterion developed by Mears for freedom from axial dispersion effects in tubular reactors [D.E. Mears, *Ind. Eng. Chem. Proc. Design Devel.*, 10, 541 (1971)].
19. The saponification of ethyl acetate in aqueous solution,



is a second-order, irreversible reaction with a rate constant at  $25^\circ\text{C}$  that has been measured as  $8.0 \times 10^{-2}$  liter/mol-s [K.J. Laidler and D. Chen, *Trans. Faraday Soc.*, 54, 1026 (1958)]. A tubular reactor, 3 in. in length and 1 cm in radius is available. Determine the total amount of feed (in cm $^3$ /s) that can be processed for

- (a) 60% conversion at exit
- (b) 98% conversion at exit

using  $1 M$  concentrations of each reactant in the feed. Use a PFR model first, then repeat for a one-dimensional dispersion model. In the latter case  $N_{Pe}$  may be determined from Figure 5.8b. Is the use of either of these models consistent with the required flow rates?

- (c) The activation energy is 15 kcal/mol. Repeat the calculation above for  $T = 85^\circ\text{C}$ . Neglect density changes with temperature.
20. A certain first-order reaction is being carried out in a fixed-bed reactor in which the axial dispersion coefficient has been determined to be

$3 \times 10^{-3} \text{ cm}^2/\text{s}$ . The linear velocity within the reactor is  $5 \text{ cm/s}$  and the rate constant is  $0.25 \text{ s}^{-1}$ .

- (a) How long should the reactor be in order to have negligible effects of dispersion on the conversion? (Judgement is required here.)
- (b) What is the conversion?

21. The flow characteristics of a continuous reactor have been studied using the tracer step-response method. The concentrations of tracer in the effluent at various times after the instant of addition are reported as

Time (min)	Concentration (mg/liter)
0.1	0.20
0.2	0.17
1.0	0.15
2.0	0.125
5.0	0.07
10.0	0.02
30.0	0.001

- (a) What type of ideal reactor does the actual vessel most closely approach?
  - (b) If an isothermal first-order reaction ( $k_1 = 0.15 \text{ min}^{-1}$ ) occurs in the vessel, what conversion may be expected?
22. Another first-order reaction is to be studied at the same flow rate in the vessel characterized in problem 21. Measurements for this reaction in a PFR, operating at the same mean residence time, give a conversion of 75.2%.
- (a) Calculate the value of the rate constant for this reaction.
  - (b) Calculate the conversion expected for this reaction in the reactor of problem 21.
  - (c) Are any assumptions made in obtaining the answer to part (b)? If the reaction were second order, would additional assumptions be necessary to use the same procedure for part (b)?
23. As a source of ethylene for petrochemicals, propane is thermally cracked to ethylene and methane. In one plant propane is passed through 16 ft-long sections of tubes. Each section is connected to the next with U-bends, and the whole array is contained within a furnace.

The possible influence of nonideal flow is to be estimated. For this approximate study assume that the temperature in the tubes is constant and that the reaction gases are completely mixed in the U-bend at the end of each tube section. The cracking reactions are approximately first order and kinetic data indicate that three tube sections would be required to obtain 96% conversion of the propane for plug flow in each section. The flow rate is such that the Reynolds number in the tubes is 10,000. For these conditions the axial dispersion parameter,  $D/ud_t$ , where  $d_t$ , the tube

diameter, is about 100. If the effect of nonideal flow is accounted for with the dispersion model, calculate

- (a) the conversion at the end of three sections, and
  - (b) the number of sections required to attain 96% conversion.<sup>9</sup>
24. Derive an equation for the conversion in a first-order, irreversible reaction using the combined model you proposed to fit the  $E(t)$  data of problem 10.
  25. Consider the combined flow model of Illustration 5.4.
    - (a) For reasonable values of  $f_1$ ,  $f_2$ , and  $f_3$  sketch what you think the  $F(t)$  curve would look like and explain your reasoning.
    - (b) For  $f_1 = 0.2$  and  $f_2 = 0.3$ , what would be the conversion of the second-order reaction  $2A \rightarrow B + C$ . Use the parameters from problem 11 with  $C_{A0} = 0.036$  mol/liter.
  26. Consider the solution for the transient response of the dispersion model to a step-function input in concentration as given in Figure 5.23 for the particular case of  $N_{Pe} = 10$  and  $R' = 0.1$ . Is the transient response of a comparable CSTR series model the same?
  27. Let us reconsider Illustration 5.6, but with the reaction  $2A \rightarrow B + C$ , second-order in A,  $k = 0.8$  liter/mol-h, still carried out in the three CSTRs with  $\bar{t} = 1$  h. Again, compare the two modes of startup, (a) and (b) as described in the illustration, and compare with values for the first-order reaction. Repeat for half-order kinetics in A.

## Notation

$A$	reactor cross sectional area
$A_1$	initial value of $C_{A1}$ , mols/volume
$A_n$	concentration of A in $n$ at $t = 0$ , mols/volume
$C_e$	exit concentration from recycle reactor, mass or mols/volume
$C_f$	feed concentration to recycle reactor, mass or mols/volume
$C_i$	concentration of reactant in stage $i$ , mols/volume
$C_m$	mean radial concentration, mass or mols/volume
$C_n$	concentration of tracer in $n$ th CSTR, mass/volume; concentration at grid point $n$ , mols/volume
$C_0$	inlet concentration of tracer, mass/volume
$C_{A0}$	inlet concentration of A, mols/volume
$C_{Af}$	concentration defined in equation (5-60), mols/volume
$C_1$	mixed feed and recycle concentration, mass or mols/volume
$C_{out}$	concentration of reactant immediately beyond reactor exit, mols/volume
$\Delta C_{A0}$	magnitude of step input of $C_{A0}$ mols/volume; see equation (5-114)
$C(t)$	experimental response to pulse input of tracer
$D$	axial dispersion coefficient, area/time
$D_e$	effective dispersion coefficient, area/time
$D_M$	molecular diffusion coefficient, area/time

<sup>9</sup> Problems 21–23 courtesy of J.M. Smith, *Chemical Engineering Kinetics*, 3ed., with permission of McGraw-Hill Book Co., New York, NY, (1981).

$d$	tube or reactor diameter, length
$d_p$	particle diameter, length
$d_t$	tube diameter, length
$E$	activation energy, kcal or kJ/mol
$E(t)$	exit-age distribution function
$E(\theta)$	$E(\theta) = \bar{t}_t E(t)$
$E_n(t)$	exit-age distribution for $n$ -unit CSTR sequence
$E_1(x)$	exponential integral of $x$
$\text{erf}(y)$	error function integral of $y$
$F(t)$	residence-time distribution function
$F(\theta)$	residence-time distribution function
$F_{A_0}$	feed rate of A based on sum of A in fresh feed plus recycle, mass or mols/time
$f$	fractional recirculation between stages; nondimensional concentration = $(C/C_0)$
$k$	rate constant, units dependent upon reaction order
$L$	reactor length
$\mathcal{L}(x)$	Laplace transform of $x$
$M$	constant = $(N_{Pe}/2)$
$N_{Pe}$	Peclet number = $(Lu/D)$ or $(d\bar{u}/D_e)$
$(N_{Pe})_i$	$i = a, b, c$ for Peclet number in fore-, reaction-, and aft-sections of reactor
$N_{Re}$	Reynolds number = $(d\bar{u}\rho/\mu)$
$N_{Sc}$	Schmidt number = $(\mu/\rho D_M)$
$(N_{Pe})_r$	radial Peclet number = $(d_p \bar{u}/D)$
$n$	reaction order; stage of CSTR sequence
$Q$	constant = $(1 + k\bar{t})$ ; see equation (5-115)
$Q_e$	exit rate from recycle reactor, volume/time
$Q_F$	feed rate to recycle reactor, volume/time
$Q_R$	recycle rate, volume/time
$R$	reactor radius, length; recycle ratio = $(Q_R/Q_e)$ ; gas constant
$R'$	reaction parameter = $(kL/u)$
$R'_n$	reaction parameter = $(2knL/u)(C_0)^{n-1}$ , with $k$ the $n$ th-order rate constant
$r$	radial distance variable, length
$(-r)$	rate of reaction, mass or mols/volume-time
$S_{B(\text{II, III})_{CSTR}}$	selectivity for B in Type II or III reaction in a CSTR
$S_{B(\text{II, III})_{PFR}}$	selectivity for B in Type II or III reaction in a PFR
$S_i(\text{III})$	intrinsic selectivity in Type III reaction = $(k_1/k_2)$
$S_x$	step-function input
$s$	Laplace transform parameter
$t$	time
$\Delta t$	time increment
$t_R$	residence time in a PFR
$\bar{t}$	mean residence time
$t_t$	total residence time = $n\bar{t}$
$u$	axial velocity, length/time
$u_0$	superficial velocity, length/time
$u(r)$	axial velocity as a function of $r$ , length/time
$\bar{u}$	average axial velocity = $(1/\bar{t})$ ; see equation (5-36); interstitial velocity = $(u/\epsilon)$ , length/time



$\bar{V}$	individual vessel volume
$V_R$	vessel total volume
$V_n$	volume of $n$ th unit in CSTR sequence
$v$	volumetric flow rate, volume/time
$X$	nondimensional length = $(z/L)$
$x$	conversion
$x(t)$	conversion as a function of time
$x_1, x_2$	inlet and outlet conversions, recycle reactor
$\bar{x}$	average conversion
$Y$	nondimensional concentration = $(C_A - C_{A_0})/C_{A_0}$
$Y(\text{III})$	yield in Type (III) reaction
$Y$	constant = $(1/kC_{A_0}\bar{t})$ ; Illustration 5.1
$z$	axial length variable
$\Delta z$	axial length increment

*Greek*

$\alpha$	parameter = $(1 + k\bar{t})$ or $(1 + k_1\bar{t})$ for Type III reaction; catalyst activity
$\beta$	parameter = $(1 + k_2\bar{t})$ for Type III reaction; parameter = $(1 + 4R'/N_{pe})$ , see equation (5-82); linear decay constant
$\gamma$	parameter = $[1 + (k_1 + k_2)\bar{t}]$ for Type III reaction
$\delta$	deviation factor; see equation (5-70); parameter of equation (5-116)
$\epsilon$	bed porosity
$\zeta$	nondimensional length = $(z/L)$
$\eta$	geometric constant; see equation (5-47)
$\theta$	number of residence times = $(t/\bar{t})$
$\mu$	viscosity, mass/length-time
$v$	transformed variable = $(z - ut)$ ; see equation (5-21)
$\rho$	fluid density, mass/volume
$\tau$	tortuosity factor

*Note:* Additional notation in Tables 5.1 and 5.4, Illustration 5.4, and Figure 5.16.

# 6

## Thermal Effects in the Modeling of Real Reactors

Round numbers are always false

— Samuel Johnson

As we have seen in Chapter 4, the analysis of nonisothermal reactors in any general way, even for the ideal PFR and CSTR, is not possible to the same degree of elegance as for nonisothermal reactors because of the intractable nonlinearity of the Arrhenius equation. When we graduate to the more complicated models of nonideal reactors, the problem is of course compounded. For example, while the CSTR-sequence model retains its algebraic structure, the energy balance requires solution of an equation implicit in temperature for each unit; stagewise computation is required and much of the convenience of that model is lost. Similarly, dispersion models require numerical solution. The result of this will be a slight change in emphasis in the chapter, with more attention being given to the strategies and procedures involved in the solution of nonisothermal models. Hopefully, the justifications for the choice of models for nonideal reactors has been sufficiently established so that we can take care of some more practical business.

### 6.1 Mixing-Cell Sequences

The mass and energy balances for an individual unit in the mixing-cell sequence may be written in general form as

$$v(C - C_0) + \bar{V}(-r) = 0 \quad (6-1)$$

and

$$v(\theta_0 - \theta) + \bar{V}(-r) - \frac{U'}{C_p} (\theta - \theta_M) = 0 \quad (6-2)$$

where  $\theta$  is the reduced temperature,  $C_p T / (-\Delta H)$ ,  $U'$  is the total heat-transfer coefficient ( $U' = UA$ ), and  $C_p$  is in a volumetric basis. When written in this form, the similarity of the two equations in the limit of adiabatic operation is evident. The

remainder of the nomenclature here is as defined in Figure 4.24. Now the sum of equations (6-1) and (6-2) may be written as follows.

$$v(C_0 - C) + v(\theta_0 - \theta) - \frac{U'}{C_p} (\theta - \theta_M) = 0 \quad (6-3)$$

or

$$C = C_0 + (\theta_0 - \theta) + \frac{U'}{vC_p} (\theta_M - \theta) \quad (6-4)$$

If we specify the concentration in the unit, then the reaction rate is fixed according to

$$(-r) = (C_0 - C) \frac{v}{\bar{V}} = \frac{C_0 - C}{\bar{t}} \quad (6-5)$$

Parametric values:

$$k_0 \bar{t} = 1.0 \times 10^{-11}$$

$$\frac{C_p (E/R)}{(-\Delta H)C_0} = 75$$

$$\frac{C_p T_M}{(-\Delta H)C_0} = 2.5$$

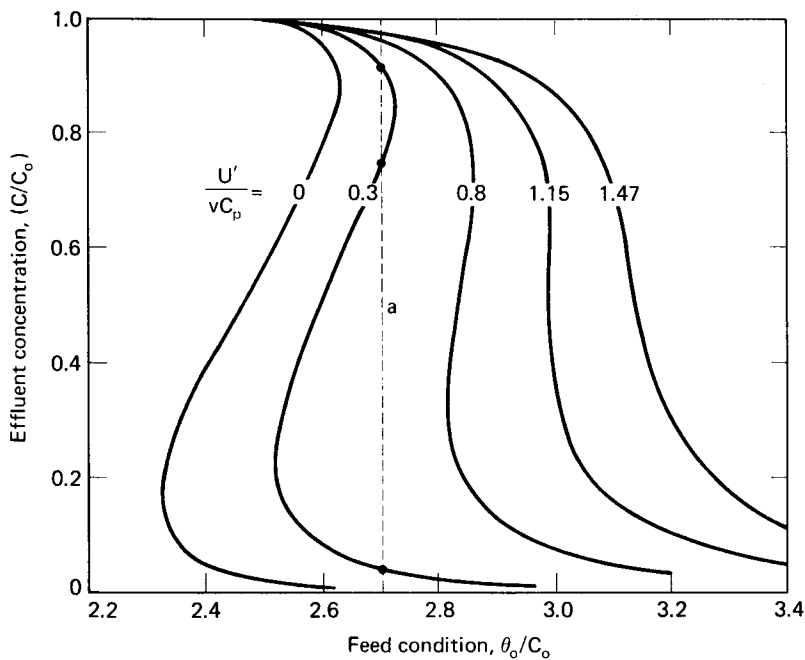


**Figure 6.1** Operating diagram for temperature effects on CSTR (single-unit) operation. [After D.D. Perlmutter, *Stability of Chemical Reactors*, reprinted by permission of Prentice-Hall, Inc., Englewood Cliffs, NJ, (1972).]

and the temperature is fixed by the form of temperature dependence of  $(-r)$ . For a first-order irreversible reaction, thus

$$T = \frac{E/R}{\ln [k_0 \bar{t} C / (C_0 - C)]} \quad (6-6)$$

Equations (6-4) to (6-6) may be used to establish an *operating diagram* for this CSTR unit [C.R. McGowan and D.D. Perlmutter, *Amer. Inst. Chem. Eng. J.*, 17, 831 (1971)] of the type shown in Figure 6.1 for this first-order case. The operating temperature is not shown explicitly on these curves and needs to be determined separately. The condition of steady-state multiplicity is indicated on the diagram, for example, by line *a*, at the three points of intersection with the operating curve for  $U'/vC_p = 0.3$ .

The type of multiplicity illustrated in Figure 6.1 is not just a theoretical construct, referring to a situation which might rarely (or never) be encountered in practice. Rather, the possibility of CSTR multiplicity is very real, as shown in Figure 6.2. These are the results of Vejtassa and Schmitz [S.A. Vejtassa and R.A. Schmitz, *Amer. Inst. Chem. Eng. J.*, 16, 410 (1970)] for the exothermic reaction between sodium thiosulfate and hydrogen peroxide in the liquid phase, carried out in an adiabatic CSTR. The hysteresis demonstrated in Figure 6.2 is obtained from steady-state operating conditions resulting from a progressive increase or decrease in the holding time. Operation of the unconstrained reactor would be possible only at the lower steady state (line segment *abc*) or the upper steady state (line segment *def*). Which steady state the reactor operates at depends on how it is started up, as we will see later in this discussion.

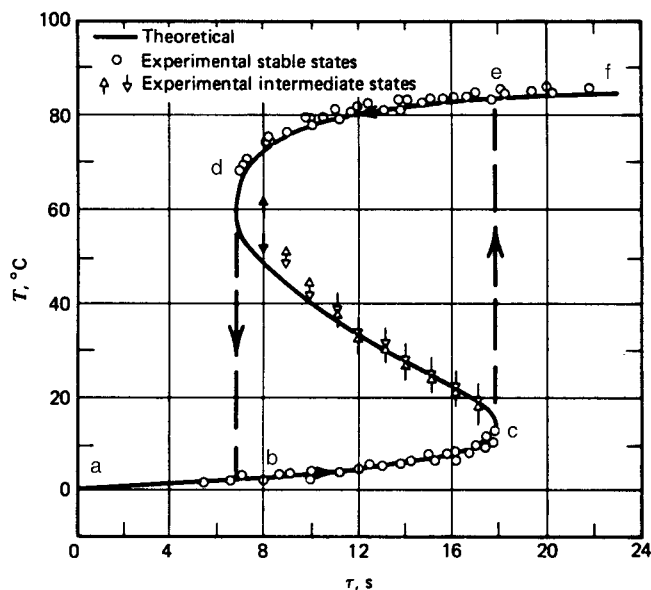


**Figure 6.2** CSTR hysteresis in the liquid-phase reaction between sodium thiosulfate and hydrogen peroxide. [After S.A. Vejtassa and R.A. Schmitz, *Amer. Inst. Chem. Eng. J.*, 16, 410, with permission of the American Institute of Chemical Engineers.]

The operating diagram of Figure 6.1 demonstrates an overall picture of temperature effects on CSTR operation, but does not take us very far in terms of modeling these thermal effects in nonideal reactors using mixing-cell sequences. The reason for this is because the model turns out to be set up backwards from the way we would like; that is to say we specify conversion, normally the quantity we are seeking, to define the conditions of operation. In fact, the coupling between mass- and energy-conservation relationships makes it rather inconvenient to use the CSTR sequence as a model for nonisothermal operation. The crux of the problem may be illustrated by using equations (6-1) and (6-2) for the simplest case, that of adiabatic operation and our normal irreversible first-order kinetics. Thus,

$$v(C_0 - C) - \bar{V}kC = 0 \quad (6-1a)$$

$$v(\theta_0 - \theta) - \bar{V}kC = 0 \quad (6-1b)$$

Solving for  $C$  from equation (6-1a) gives, in the usual fashion,

$$C = \frac{C_0}{1 + k\bar{t}}$$

Replacing this in equation (6-2a) yields the general relationship to be satisfied by temperature and concentration

$$\theta_0 - \theta - \frac{k\bar{t}C_0}{1 + k\bar{t}} = 0 \quad (6-7)$$

The problem of “backwardness” alluded to above resides in the fact that  $k$  in both of these equations depends on  $\theta$ , not  $\theta_0$ .

### 6.1.1 A Two-dimensional Mixing-Cell Model for Nonisothermal Reactors

Since nonisothermality in tubular reactors often leads to radial as well as axial gradients, and since the mixing-cell model in its one-dimensional form is not very convenient anyway, it seems logical to see what a two-dimensional mixing-cell model might entail.

The basic geometrical formulation of such a model is shown in Figure 6.3. Each cell, perfectly mixed, is fed from two cells and feeds two cells in turn, thus allowing for radial as well as axial mixing. We can define a characteristic cell dimension in terms of a packing or catalyst particle dimension,  $d_p$ , which in turn defines a cell holding time,  $t$ , as

$$t = (d_p/v) \quad (6-8)$$

where  $v$  is used here as the interstitial fluid velocity. At a given level in the bed,  $i$ , a general material balance, is

$$C_{i-1} - C_i = \frac{DC_i}{dt} \left( \frac{d_p}{v} \right) \quad (6-9)$$

where, in general,

$$C_i(0) = f(i) \quad 1 \leq i \leq N \quad (\text{function of position})$$

$$C_0(t) = g(t) \quad t > 0 \quad (\text{function of time})$$

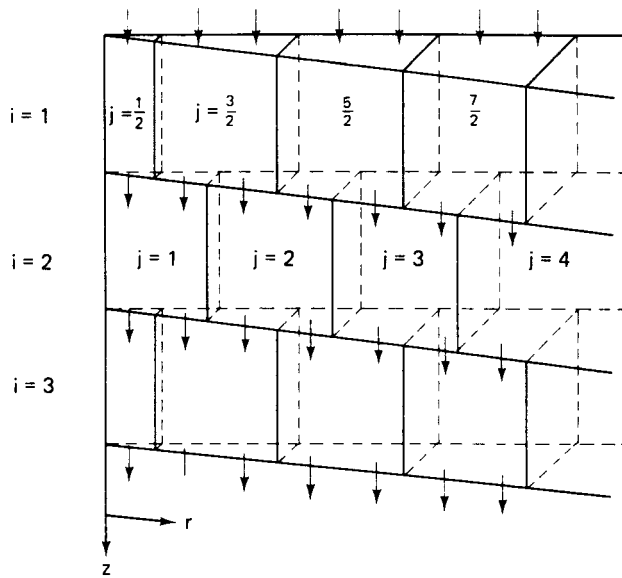


**Figure 6.3** Mixing-cell sequence in the model of Deans and Lapidus. [After H.A. Deans and L. Lapidus, *Amer. Inst. Chem. Eng. J.*, 6, 656, with permission of the American Institute of Chemical Engineers, (1960).]

At each level,  $i$ , the horizontal stage is bounded by a plane of length  $id_p$  and  $(i-1)d_p$  from the entrance to the bed. Radial stages are bounded at  $j$  by concentric cylindrical surfaces, radius  $K(j-1)d_p$  and  $Kjd_p$ . The index  $i$  is an integer, but  $j$  assumes non-integer values (multiples of  $1/2$ ) for odd values of  $i$ . The radius, in terms of particle diameters,  $M$ , is also taken to be an integer

$$M = \frac{D_B}{(2d_p)K} \quad (6-10)$$

where  $D_B$  is bed diameter and  $K$  is a scaling factor on the radial dimension such that  $Kd_p$  is the mixing length in the radial direction. Basically, the  $K$  factor is introduced to bring the model into agreement with experimental values for the radial Peclet number. A correlation for  $K$  is

$$K = \left( \frac{8.2}{N_{pe_g}} \right)^{1/2}$$

For well-developed turbulence, the radial Peclet number is about 10, and  $K$  corresponding is 0.905. The volume per cell is

$$\bar{V}_{i,j} = \epsilon A_j d_p \quad (6-11)$$

where  $\epsilon$  is bed porosity and  $A_j$  the cell interface area. In terms of the dimensions given,

$$\begin{aligned} A_j &= \pi[K(j)d_p]^2 - \pi[K(j-1)d_p]^2 \\ A_j &= \pi K^2 d_p^2 (2j-1) \end{aligned} \quad (6-12)$$

Substituting this into equation (6-11)

$$\bar{V}_{i,j} = \bar{V}_j = \epsilon \pi K^2 d_p^3 (2j - 1) \quad (6-13)$$

Now at the centerline when  $j = 1/2$ ,  $(j - 1) = 0$ ,

$$\bar{V}_{1/2} = \epsilon \pi K^2 d_p^3 (1/2)^2 \quad (6-14)$$

The total volumetric flow at  $(i, j)$  is

$$Q_{ij} = A_j \epsilon v \quad (6-15)$$

Now let us consider in detail an individual mixing cell as depicted in Figure 6.4. Concentration in the cell is  $C_{i,j}$  and, in accordance with the perfect mixing assumption, is also the concentration in streams 3 and 4 leaving the cell. The problem is to determine the concentrations of streams 1 and 2 entering the cell. Let the total throughput in this stage be  $Q_j$ ; then

$$\text{Stream 1} \quad C_{i-1,j-1/2}$$

$$\text{Stream 2} \quad C_{i-1,j+1/2}$$

The average concentration is

$$\phi_{i-1,j} = \frac{Q_1 C_{i-1,j-1/2} + Q_2 C_{i-1,j+1/2}}{Q_j} \quad (6-16)$$

where

$$Q_j = Q_1 + Q_2 = \epsilon \pi K^2 d_p^3 v [j - (j - 1)^2] \quad (6-17)$$

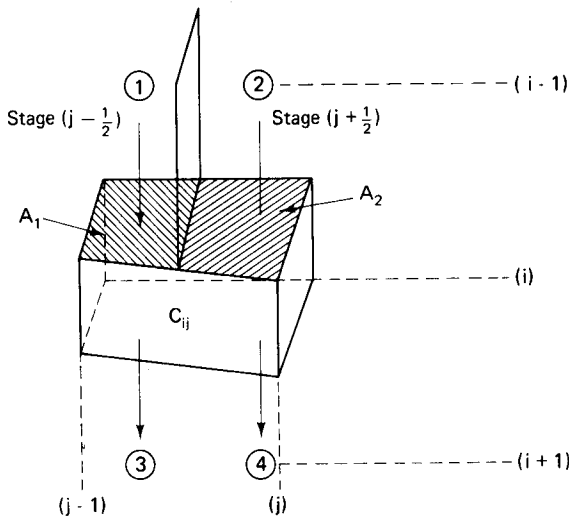


**Figure 6.4** Individual mixing cell in the matrix. [After H.A. Deans and L. Lapidus, *Amer. Inst. Chem. Eng. J.*, 6, 656, with permission of the American Institute of Chemical Engineers, (1960).]

Now we form the ratio ( $Q_1/Q_2$ ),

$$\frac{Q_1}{Q_2} = \frac{A_1}{A_2} = \frac{(j-1/2)^2 - (j-1)^2}{j^2 - (j-1/2)^2} = \frac{j-3/4}{j-1/4} \quad (6-18)$$

Solving equations (6-17) and (6-18) for  $Q_1$  and  $Q_2$  and resubstituting in equation (6-16) gives

$$\phi_{i-1,j} = \frac{(j-3/4)C_{i-1,j-1/2} + (j-1/4)C_{i-1,j+1/2}}{2j-1} \quad (6-19)$$

For the case where  $j = 1/2$ , we are again involved with symmetry about the center-line. Here we say that  $(j-3/4) = 0$ , and the value of  $\phi_{i-1,1/2}$  is

$$\phi_{i-1,1/2} = C_{i-1,1} \quad (6-20)$$

At the wall

$$\phi_{i-1,M} = C_{i-1,M-1/2} \quad (6-21)$$

which is required by the continuum argument that insists  $(dC/dr) = 0$  at the wall.

The heat balance may be written in a similar manner, for which in our pseudo-homogeneous model the solid and fluid temperatures are taken to be the same. Thus, corresponding to  $\phi_{i-1,j}$  we may define an average temperature  $\psi_{i-1,j}$  as

$$\psi_{i-1,j} = \frac{(j-3/4)T_{i-1,j-1/2} + (j-1/4)T_{i-1,j+1/2}}{2j-1}$$

The entire mixing-cell model can then be represented by the following simultaneous equations

$$\phi_{i-1,j} - C_{i,j} = \frac{dC_{i,j}}{dt} \left( \frac{d_p}{v} \right) \quad (6-23)$$

$$\psi_{i-1,j-t_{i,j}} = \beta \frac{dT_{i,j}}{dt} \left( \frac{d_p}{v} \right) \quad (6-24)$$

$$\beta = 1 + \frac{C_s \rho_s (1 - \epsilon)}{C_p \rho_f \epsilon}$$

with  $C_s$  the heat capacity of the solid phase (mass),  $\rho_s$  the density of the solid phase (mass),  $C_p$  the heat capacity of the gas phase (molal), and  $\rho_f$  the density of the gas phase (molal). As written above,  $C_{i,j}$  and  $T_{i,j}$  are dimensionless variables, normalized with reference to inlet conditions.

If the bed is adiabatic, these definitions must be slightly modified, as shown in the derivation of Deans and Lapidus [H.A. Deane and L. Lapidus, *Amer. Inst. Chem. Eng. J.*, 6, 656 (1960)]. For non-zero time derivatives the determination of concentration as a function of time and position is an initial value problem with the starting conditions of

$$C_{i,j} = C_{i,j}(0)$$

$$T_{i,j} = T_{i,j}(0)$$

A solution procedure is developed as follows.



1. Inlet conditions  $C_{0,j}(t)$  and  $T_{0,j}(t)$  determine the values of  $\phi_{0,j}$  and  $\psi_{0,j}$  as a function of time.
2.  $\phi_{0,t}$  and  $\psi_{0,j}(t)$  together with initial conditions  $C_{i,j}(0)$  and  $T_{i,j}(0)$  [or  $C_{1,j}(0)$  and  $T_{1,j}(0)$  here, since we refer to the first row] allow solution of equations (6-23) and (6-24) for  $C_{1,j}$  and  $T_{1,j}$  for all  $t > 0$  [ $j$  is fractional, since  $i$  is odd on the first row].
3. The first row solutions  $C_{1,j}(t)$  and  $T_{1,j}(t)$  determine  $\phi_{1,t}(t)$  and  $\psi_{1,t}(t)$ , which in turn allow computation of the next row elements  $C_{2,j}(t)$  and  $T_{2,j}(t)$  according to the procedures of step 2.
4. This computation is repeated for successive values of the index  $i$  to the bed exit.

If it is assumed that variations in density and other physical parameters are small, equations (6-23) and (6-24) are readily modified to include reaction-rate terms. For component  $m$  of the reaction mixture in the  $(i, j)$ th stage

$$\phi_m - C_m - [-r_m(C_m, \dots T)] = \frac{dC_m}{dt} \quad (6-25)$$

$$\psi - T - [-r_T(C_m, \dots T)] = \beta \frac{dT}{dt} \quad (6-26)$$

Here subscripts  $i$  and  $j$  have been omitted for clarity.

Let us simplify the model of equations (6-25) and (6-26) to the steady state and consider their detailed form for first-order kinetics. Then

$$(-r_m) = -kCe^{-E/T}$$

$$(-r_T) = k\lambda Ce^{-E/T}$$

where

$$\lambda = -\frac{(\Delta H_r)C_0}{C_p\rho_f T_0}; \quad E = \frac{E_a}{RT_0}; \quad k = k_0 \left( \frac{d_p}{v} \right)$$

with  $E_a$  the activation energy and  $k_0$  the pre-exponential factor. The balance equations then become

$$\frac{dC_{i,j}}{dt} = \phi_{i-1,j} - C_{i,j}(1 + ke^{-E/T_{i,j}}) \quad (6-27)$$

$$\beta \frac{dT_{i,j}}{dt} = \psi_{i-1,j} - T_{i,j} + \lambda C_{i,j} ke^{-E/T_{i,j}} \quad (6-28)$$

for  $1 \leq i \leq N$  and  $0 \leq j \leq M$ . Now, at the point where  $j = M$ , the effect of heat transfer at the wall must be considered<sup>1</sup> To do this we can write equation (6-28) in the modified form

$$\beta' \frac{dT_{i,M}}{dt} = \psi'_{i-1,M} - T_{i,M} + \lambda' C_{i,M} ke^{E/T_{i,M}} \quad (6-29)$$

<sup>1</sup> Including wall heat transfer at this point is a little premature, since we will not discuss this in any detail until Chapters 8 and 9. "If ye have faith as a grain of mustard seed . . ."—*Matthew, XIII, 20*

where the modified quantities  $\psi'$ ,  $\lambda'$ , and  $\beta'$  are defined as

$$\begin{aligned}\psi'_{i-1,M} &= \frac{\psi_{i-1,M} + N_{St_w} \bar{T}_{w_i}}{1 + N_{St_w}} \\ \lambda' &= \frac{\lambda}{1 + N_{St_w}} \\ \beta' &= \frac{\beta}{1 + N_{St_w}} \\ N_{St_w} &= \frac{h_w A_{wI}}{Q_M C_p \rho_f}; \quad \bar{T}_{w_i} = \text{wall temperature}\end{aligned}$$

Typical inlet and initial conditions are

$$\begin{aligned}\phi_{0,j} &= \phi_0(t) && \text{inlet concentration} \\ \psi_{0,j} &= \psi_0(t) && \text{inlet temperature} \\ T_{wi} &= T_{wi}(t) && \text{wall temperature} \\ C_{i,j}(0) &= C(i,j) && \text{initial concentration} \\ T_{i,j}(0) &= T(i,j) && \text{initial temperature}\end{aligned}$$

In the steady state we may write equations (6-27) and (6-28)

$$\phi_{i-1,j} - C_{i,j}(1 + ke^{-E/T_{i,j}}) = 0 \quad (6-27a)$$

$$\psi_{i-1,j} - T_{1,j} + C_{i,j}\lambda e^{-E/T_{i,j}} = 0 \quad (6-28a)$$

Eliminating  $C_{i,j}$  between this pair gives

$$\psi_{i-1,j} - T_{i,j} + \frac{\lambda\phi_{i-1,j}}{(1/k)e^{-E/T_{i,j}} + 1} = 0 \quad (6-30)$$

This is essentially the same form of expression as equation (6-7) derived for an adiabatic example. If we recall that  $\psi_{i-1,j}$  and  $\phi_{i-1,j}$  are numbers from previous row solutions, we can then obtain  $T_{i,j}$  from equation (6-30). Once this is determined,  $C_{i,j}$  is computed directly from equation (6-27a). For values of  $j = M$  the same procedure applies using equations (6-27a) and (6-29).

### Illustration 6.1

Establish the equations for the concentration response to a step function input in concentration, uniform across the radius, using the generalized model.

*Solution*

1. Following the above analysis, we obtain

$$\phi_{0,j} = \frac{(j-3/4)C_{0,j-1/2} + (j-1/4)C_{0,j+1/2}}{2j-1} \quad (i)$$

but  $C_{0,j-1/2} = C_{0,j+1/2}$ , therefore  $\phi_{0,j} = C_0$ .

2. For the first row:

$$C_{0,j} - C_{1,j} = \frac{dC_{1,j}}{dt}$$

or

$$\frac{dC_{1,j}}{dt} + C_{1,j} = C_0 = \phi_0 \quad (\text{ii})$$

with  $C_j = 0$  at  $t = 0$ . Thus,

$$C_{i,j} = C_0(1 - e^{-t})$$

3. For the second row:

$$\phi_{1,j} = \frac{(j-3/4)C_{1,j-1/2} + (j-1/4)C_{1,j+1/2}}{2j-1} \quad (\text{iii})$$

Taking some values of  $j$  ( $j$  integer for  $i$  even),

$$j = 1$$

$$\phi_{1,1} = \frac{(1/4)C_0(1 - e^{-t}) + (3/4)C_0(1 - e^{-t})}{1} = C_0(1 - e^{-t})$$

$$j = 2$$

$$\phi_{1,2} = \frac{(5/4)C_0(1 - e^{-t}) + (7/4)C_0(1 - e^{-t})}{3} = C_0(1 - e^{-t})$$

$$j = 3$$

$$\phi_{1,3} = \frac{(9/4)C_0(1 - e^{-t}) + (11/4)C_0(1 - e^{-t})}{5} = C_0(1 - e^{-t})$$

and so on. Thus,

$$\frac{dC_{2,j}}{dt} = \phi_{1,j} - C_{2,j} \quad (\text{iv})$$

$$\frac{dC_{2,j}}{dt} + C_{2,j} = C_0(1 - e^{-t})$$

4. Similar procedures yield differential equations giving higher-order responses for each stage  $i$ . The model here is formally analogous to the CSTR-sequence mixing model.

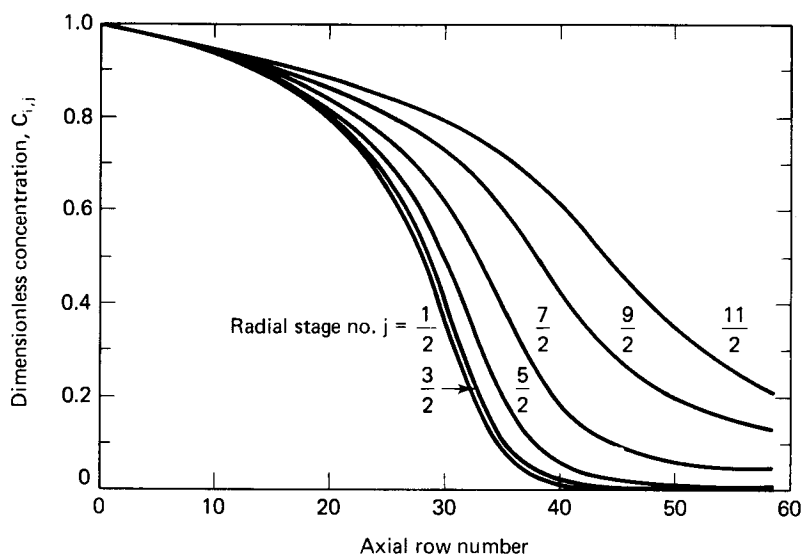
The results of a calculation of the nonisothermal steady state is shown in Figure 6.5 for the following typical parametric values.

$$2M = 11 \quad N = 60$$

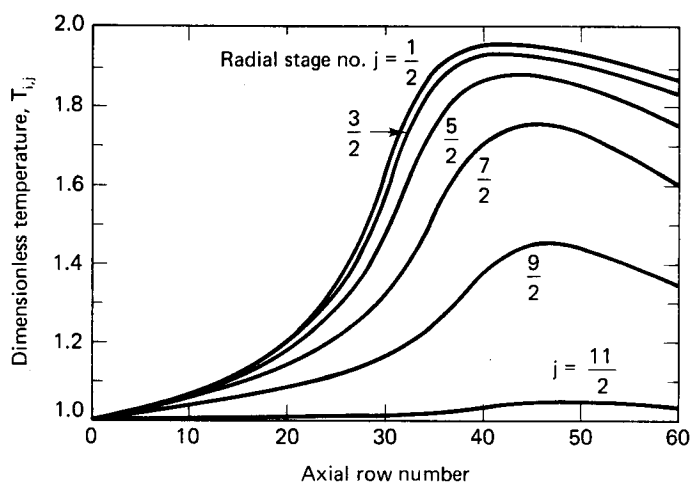
$$\lambda = 1 \quad [\exp(E)]/k = 250$$

$$\beta = 2.5 \quad (N_{St})_w = 2$$

$$E = 10$$



(a) Longitudinal Concentration Profiles at Various Radial Positions, Static System



(b) Longitudinal Temperature Profiles at Various Radial Positions, Static System

**Figure 6.5** Results of a typical steady-state simulation with the mixing-cell model of Deans and Lapidus. [After H.A. Deans and L. Lapidus, *Amer. Inst. Chem. Eng. J.*, 6, 663, with permission of the American Institute of Chemical Engineers, (1960).]

The results shown are for longitudinal temperature and concentration profiles at various radial positions. In addition to demonstrating the capabilities of the model in terms of the typical shapes of the profiles generated, the figures also show that significant radial as well as longitudinal gradients may be encountered in nonisothermal operation. This is reasonable; for an exothermic reaction we are transferring heat out of the reactor at the wall—there has to be a temperature gradient somewhere. It may be, then, often important to incorporate the two-dimensional approach in nonideal reactor models, or at least to determine what level of approximation is involved in using a one-dimensional approach.



HORATIO SAYS

We have an adiabatic reactor. How would this alter the heat balance presented in the text? Can you think of any simplifications in the calculation method for this case?

### 6.1.2 Stability of CSTR

Figure 6.1 illustrates the fact that for various ranges of kinetic and reactor parameters it is possible for the mass and energy conservation relations for a CSTR to be in stable balance at more than one condition. This may imply that there are other balance conditions that are unstable<sup>2</sup>; the point needs to be examined. Which of the stable balances is attained in actual operation may be dependent on the details of startup procedure, for example, which are not subject to the control of the designer. Thus, it is important to investigate reactor stability using unsteady-state rather than steady-state models.

In the case of the CSTR, we have previously derived the relationship

$$v\rho C_p(T_0 - T_s) - UA(T_s - T_M) = \frac{-\bar{V}(-\Delta H)k_0 e^{-E/RT_s} v C_{A_0}}{v + \bar{V}k_0 e^{-E/RT_s}} \quad (4-135)$$

to describe the steady-state operating temperature,  $T_s$ , of the reactor (notation as in Section 4.5.2). For the unsteady state the individual mass and energy balances are

$$vC_{A_0} - vC_A - \bar{V}k_0 e^{-E/RT} C_A = \bar{V} \frac{dC_A}{dt}$$

$$vC_p\rho(T_0 - T) + \bar{V}(-\Delta H)k_0 e^{-E/RT} C_A - UA(T - T_M) = \bar{V}C_p\rho \frac{dT}{dt}$$

This set of equations is nonlinear, as usual, so we will base the stability analysis on a linearization about the steady-state position [O. Bilous and N.R. Amundson, *Amer. Inst. Chem. Eng. J.*, 1, 513 (1955)].

<sup>2</sup>“Unstable as water; thou shalt not excell it . . .”—*Genesis XLIX, 4*

Let

$$\begin{aligned} x_1 &= C_{A_0} - C_A \\ x_2 &= T_s - T \end{aligned} \quad (6-31)$$

where  $T_s$ , and  $C_{A_0}$  are steady-state variables. Using a Taylor series expansion of the general form

$$f(x_0 + h, y_0 + k) = f(x_0, y_0) + h \left( \frac{\partial f}{\partial x} \right)_{x_0, y_0} + k \left( \frac{\partial f}{\partial y} \right)_{x_0, y_0}$$

for estimation of a function  $f(x_0 + h, y_0 + k)$  in terms of the fixed dependent variables  $x_0$  and  $y_0$ , we may linearize the balance equations about  $C_{A_0}$  and  $T_s$ . The result of this is

$$\frac{dx_1}{dt} = -a_{11}x_1 - a_{12}x_2 \quad (6-32)$$

$$\frac{dx_2}{dt} = -a_{21}x_1 - a_{22}x_2 \quad (6-33)$$

where the  $a$  coefficients are rather complex functions of the system parameters,

$$a_{11} = \frac{v}{\bar{V}} + k_0 e^{-E/RT_s}$$

$$a_{12} = k_0 C_{A_0} \left( \frac{E}{RT_s^2} \right) e^{-E/RT_s}$$

$$a_{21} = k_0 \frac{(-\Delta H)}{\rho C_p} e^{-E/RT_s}$$

$$a_{22} = \frac{v}{\bar{V}} + k_0 \frac{(-\Delta H)}{\rho C_p} C_{A_0} \left( \frac{E}{RT_s^2} \right) e^{-E/RT_s} + \frac{UA}{\rho C_p \bar{V}}$$

It is not necessary to solve equations (6-32) and (6-33) for the stability analysis, although this can be done if one wishes. One can make use of the fact that if the system is stable, the small perturbations  $h$  and  $k$  must approach zero as time increases. In matrix form we can write the above as

$$\frac{d\mathbf{x}}{dt} = \mathbf{A}\mathbf{x} \quad (6-34)$$

with the coefficient matrix  $\mathbf{A}$  given by

$$\mathbf{A} = \begin{bmatrix} -a_{11} & -a_{12} \\ -a_{21} & -a_{22} \end{bmatrix}$$

We know from matrix theory that the solution to equation (6-34) is given by a sum of exponential terms in time in which the coefficients of time in the exponentials are the eigenvalues,  $\lambda$ , of the problem. Stability may be expected only if these eigenvalues contain real negative parts, so that the exponential terms will die out as time increases. The values of  $\lambda$  are obtained from the characteristic equation

$$\det \begin{bmatrix} (-a_{11} - \lambda) & -a_{12} \\ -a_{21} & (-a_{22} - \lambda) \end{bmatrix} = 0 \quad (6-35)$$

Expanding the determinant,

$$\lambda^2 + (a_{11} + a_{22})\lambda + a_{11}a_{22} - a_{12}a_{21} = 0 \quad (6-36)$$

thus

$$\lambda_1, \lambda_2 = \frac{-(a_{11} + a_{22}) \pm [(a_{11} + a_{22})^2 - 4(a_{11}a_{22} - a_{12}a_{21})]^{1/2}}{2} \quad (6-37)$$

From examination of equation (6-37) it can be determined that the following conditions are required for the eigenvalues to have negative real parts.

$$a_{11} + a_{22} > 0$$

$$a_{11}a_{22} - a_{12}a_{21} > 0$$

or

$$\begin{aligned} \frac{2v}{\bar{V}} + k_0 e^{-E/RT_s} + \frac{UA}{\rho C_p \bar{V}} &> k_0 e^{-E/RT_s} \frac{(-\Delta H)}{\rho C_p} C_{A_s} \left( \frac{E}{RT_s^2} \right) \\ \frac{v}{\bar{V}} + k_0 e^{-E/RT_s} + \frac{UA}{\rho C_p \bar{V}} + \frac{U A k_0 e^{-E/RT_s}}{v \rho C_p} &> k_0 e^{-E/RT_s} \left( \frac{-\Delta H}{\rho C_p} \right) C_{A_s} \left( \frac{E}{RT_s^2} \right) \end{aligned} \quad (6-38)$$

It is clear that these thermal criteria for stability are given in terms of steady-state values; no transients need be calculated. Since the problem may be formulated in terms of a linear matrix, it is easily generalized to chemical reactions involving  $n$  species, in either simultaneous or sequential kinetic schemes. While probably obvious, it is worth remarking that there is very little that is intuitive about the criteria of equations (6-38). One cannot rely on a guessing game for such rules.

Now the stability criteria above refer to small perturbations, a consequence of the curtailed Taylor series expansion used. At the other end, for “large perturbations” substitute “startup”, where we wish to follow the approach to steady state and, where multiplicity exists, to determine which steady state is approached. A qualitative treatment of this problem can be constructed as follows. Rewrite the balance equations as

$$\frac{dC_A}{dt} = A_1 - B_1 C_A - D_1 C_A e^{-E/RT} \quad (6-39)$$

$$\frac{dT}{dt} = A_2 - B_2 T + D_2 C_A e^{-E/RT} \quad (6-40)$$

where  $A_i$ ,  $B_i$ , and  $D_i$  are constants  $> 0$ . When multiplicity exists, two lines may be plotted in the  $C_A - T$  plane corresponding to  $(dC_A/dt) = 0$  and  $(dT/dt) = 0$ , lines 1 and 2, respectively, as shown qualitatively in Figure 6.6. For a fixed value of  $T$  as  $C_A$  increases, the following must be true:

1.  $A_1 - B_1 C_A - D_1 C_A e^{-E/RT}$  decreases
2.  $A_2 - B_2 T + D_2 C_A e^{-E/RT}$  increases

Thus,

<i>Above curve 1</i>	$(dC_A/dt) < 0$
<i>Below curve 1</i>	$(dC_A/dt) > 0$
<i>Above curve 2</i>	$(dT/dt) > 0$
<i>Below curve 2</i>	$(dT/dt) < 0$

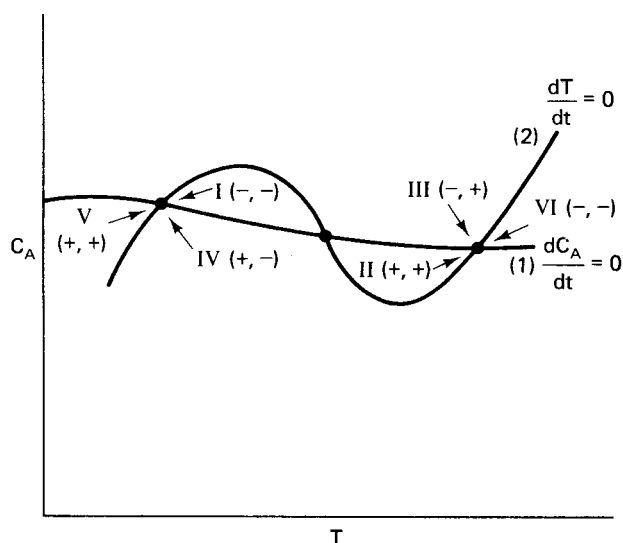


**Figure 6.6** Phase-plane diagram ( $C_A - T$ ) for a CSTR exhibiting steady-state multiplicity.

The phase-plane diagram of Figure 6.6 is divided into regions I to VI, each corresponding to a particular combination of the signs on the concentration and temperature derivatives. In region I, for example, according to the above inequalities ( $dC_A/dt$ ) is negative and ( $dT/dt$ ) negative as well, indicated by  $I(-, -)$  on the figure. Corresponding signs of the derivatives in the other sections are also indicated. Each combination of signs shows the direction of motion of the concentration/temperature behavior of the reactor in the unsteady state as shown by the arrows.

In the phase plane the intersections of curves 1 and 2 determine potential steady-state operating points ( $dC_A/dt = dT/dt = 0$ ); it is seen that regardless of the precise location of a ( $C_A, T$ ) coordinate representing a starting condition in the six regions, only the two outer steady states are approached. Whether the upper or lower state is the one attained in steady operation is strictly a function of the signs of the concentration and temperature derivatives. The middle “steady-state” is an unstable one; the reactor will not spontaneously move to this condition on startup. The consequences of this have already been illustrated for an experimental system in Figure 6.2.

The unstable nature of the intermediate steady state can also be envisioned through the response to temperature perturbations of the heat generation and heat removal terms,  $q_g$  and  $q_r$ . These have been defined in the discussion of Chapter 4; here we return for some further examination of the steady-state multiplicity corresponding to the phase-plane plot of Figure 6.6. Consider the operating curves of Figure 6.7 and the intersection of  $q_g$  and  $q_r$  at point A. As the temperature is increased a small amount above the steady-state operating temperature  $T_A$ , the rate of heat removal,  $q_r$ , increases more rapidly than the rate of heat generation,  $q_g$ . Hence, the natural tendency of the system in response to this perturbation is to return to the steady-state condition,  $T_A$ . Conversely, as the temperature is decreased a small amount below  $T_A$ ,  $q_g$  becomes greater than  $q_r$  and the reactor will also return to  $T_A$ . Precisely the same situation pertains to the upper steady state at point C. For



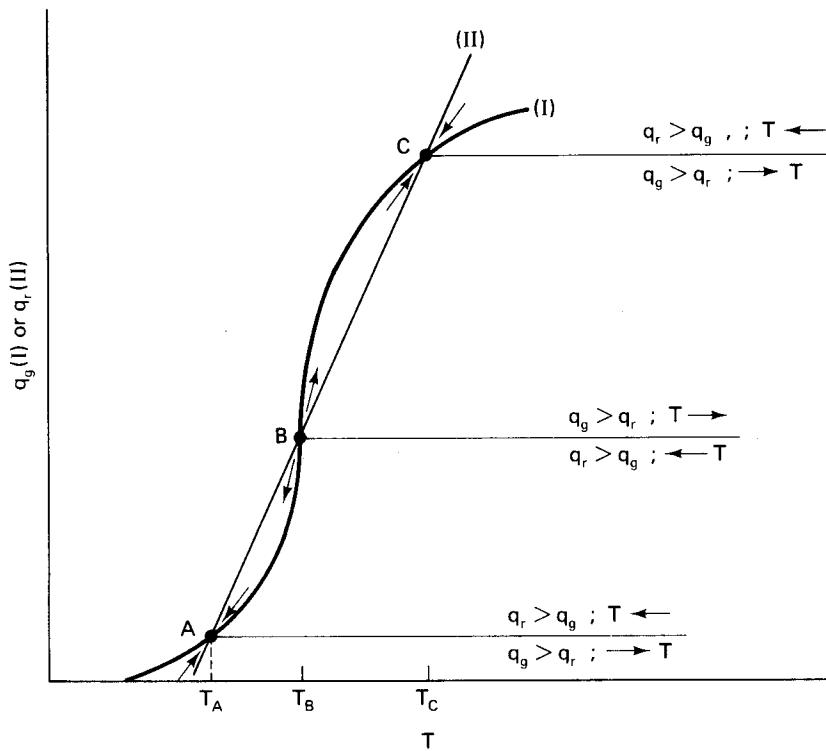


**Figure 6.7** Heat generation-removal plot for a case of CSTR multiplicity.

the midpoint B, however, things are reversed. In the event of a positive perturbation about  $T_B$ ,  $q_g$  becomes greater than  $q_r$ , and the system will move spontaneously to a point where heat-generation and heat-removal rates are in balance (i.e., point C). Similarly for negative perturbations about  $T_B$ ,  $q_r > q_g$  and the reactor will move to point A. Keep in mind that these are unconstrained steady states. In practice it would be quite possible to operate the reactor at point B, however, an external control system would be required.

### 6.1.3 Uniqueness of a CSTR

Let us now, having considered the question of multiple steady states, look at the opposite situation, that of a reactor with a single (unique) steady state. More particularly, can we define a criterion that would ensure the uniqueness of the steady-state operation of a CSTR? This indeed can be done in a number of ways; here we will start with the sum of the steady-state balances given by equation (6-4)

$$C = C_0 + (\theta_0 - \theta) + \frac{U'}{vC_p} (\theta_M - \theta) \quad (6-4)$$

where in this initial case we assume that there is external heat transfer to cooling coils at a relative temperature of  $\theta_M$ . Substitution of this relationship into equation (6-2),

the heat balance, gives

$$f(\theta) = 0 = v(\theta_0 - \theta) + \bar{V}[-r(\theta)] - \frac{U'}{C_p} (\theta - \theta_M) \quad (6-41)$$

where  $[-r(\theta)]$  is now a function of the temperature variable  $\theta$  only. In order for there to be only a single solution to equation (6-41), the function  $f(\theta)$  can be zero at only one point. Since  $f(\theta)$  is a continuous function, if it is zero at more than one point, the mean value theorem will insist that  $[df(\theta)/d\theta]$  must be zero at some point. Hence, if we can define conditions that ensure this derivative will never be zero, uniqueness is assured. We can seek these conditions through differentiation of equation (6-41) and determine if any equality/inequality constraints may apply. We then have

$$\frac{df(\theta)}{d\theta} = -v + \bar{V} \frac{d(-r)}{d\theta} - \frac{U'}{C_p} \quad (6-42)$$

From this expression it is apparent that the derivative cannot be zero if  $[d(-r)/d\theta] \leq 0$ , or since  $\theta = C_p T / (-\Delta H)$ , if

$$\frac{d(-r)}{dT} \leq 0 \quad (6-43)$$

The specific form of the uniqueness criterion will then depend on the kinetics of the reaction. For  $n$ th-order irreversible kinetics,

$$(-r) = k_0 C^n e^{-E/RT}$$

$$\frac{d(-r)}{dT} = (-r) \left( \frac{E}{RT^2} + \frac{n}{C} \frac{dC}{dT} \right) \quad (6-44)$$

From equation (6-44) we obtain

$$\frac{d(-r)}{dT} \leq 0 \quad \text{if} \quad \left( \frac{E}{RT^2} + \frac{n}{C} \frac{dC}{dT} \right) \leq 0 \quad (6-45)$$

The derivative of concentration with respect to temperature may be obtained from equation (6-4) as

$$\frac{dC}{dT} = -\frac{C_p}{(-\Delta H)} \left( 1 + \frac{U'}{vC_p} \right)$$

Substituting equation (6-46) into (6-45) gives

$$\frac{E(-\Delta H)C}{nRC_p T^2} \leq 1 + \frac{U'}{vC_p}$$

This is more useful if written in terms of the feed conditions,  $C_0$  and  $T_0$ , for which the criterion must also apply.

$$\frac{E(-\Delta H)C_0}{nRC_p T_0^2} \leq 1 + \frac{U'}{vC_p} \quad (6-47)$$

The treatment of the inequalities is based on the assumption that the reaction is exothermic with  $T_0 > T_M$ . If  $T_M > T_0$ ,  $(T_M)^2$  should be substituted for  $(T_0)^2$  in equation (6-47).

In fact, the criterion of equation (6-47) is quite a conservative one because of some approximations involved in defining the conditions required for  $[df(\theta)/d\theta] \leq 0$ . The use of  $[d(-r)/dT] \leq 0$  will indeed ensure this, but a more precise definition of the required inequality from equation (6-42) would state that

$$\frac{d(-r)}{d\theta} < \frac{v}{\bar{V}} + \frac{U'}{\bar{V}C_p}$$

or, in terms of temperature,

$$\begin{aligned} \frac{d(-r)}{dT} &< \alpha \frac{v}{\bar{V}} \\ \alpha &= \frac{C_p}{(-\Delta H)} + \frac{U'}{v(-\Delta H)} \end{aligned} \quad (6-48)$$

In the language of those concerned with such criteria,  $[d(-r)/dT] \leq 0$  forms a sufficient but not a necessary condition for steady-state uniqueness. The criteria that may be derived from the condition of equation (6-48) depends on whether the temperature range involved in the reactor operation includes a possible maximum of  $[d(-r)/dT]$ , as defined by  $[d^2(-r)/dT^2] = 0$ , or whether  $[d(-r)/dT]$  is monotonic in reactor operation. In the former case,

$$\text{One of } T_0, T_M \leq \frac{(E/R)}{2 + \psi}$$

and uniqueness is established, for first-order kinetics, by

$$\frac{v}{k_0 \bar{V}} > \left( \frac{\psi + 4}{\psi} \right) e^{(-\psi-2)} \quad (6-49)$$

In the latter case,

$$\text{Both } T_0, T_M \geq \frac{(E/R)}{2 + \psi}$$

and uniqueness is established by

$$\frac{v}{k \bar{V}} > \left[ \frac{E}{RT_0^2} \left( \frac{E}{R\psi} - T_0 \right) - 1 \right] e^{E/RT_0} \quad (6-50)$$

where

$$\psi = \frac{(\alpha E/R)}{C_0 + [C_p T_0 / (-\Delta H)] + [U' T / v(-\Delta H)]}$$

A more quantitative feeling for what is expressed in the analysis above can be obtained by another look at the sodium thiosulfate-hydrogen peroxide reaction illustrated in Figure 6.2. Consider the relationships possible between  $q_g$  and  $q_r$  for this reaction (computed for a feed mixture of 0.8M sodium thiosulfate and 1.2M hydrogen peroxide) shown in Figure 6.8. The only variable here is  $\bar{t}$ , the holding time in the reactor. Steady-state operation corresponds to the intersection of the  $q_g$  and  $q_r$  curves, so it is apparent that three steady states are possible between  $\bar{t} = 6.8$  and 17.8 s. From the analysis of the previous section we would expect the intermediate steady state to be inherently unstable and not observable in unconstrained operation.

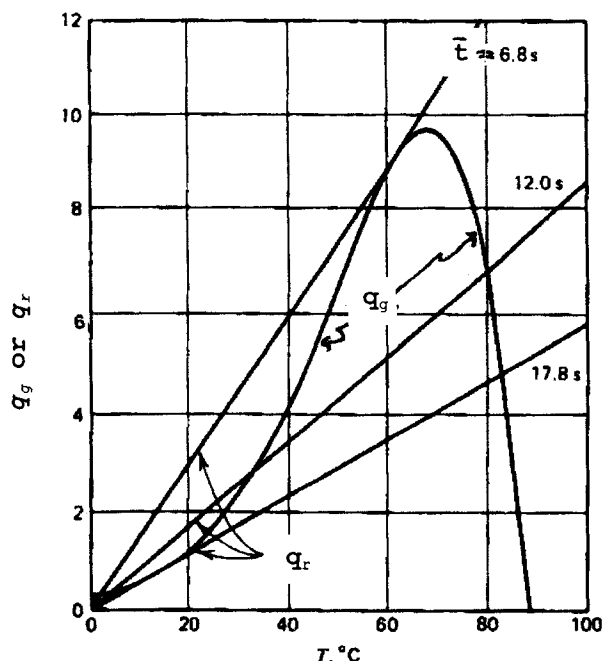


**Figure 6.8** Heat generation and heat removal curves for the thiosulfate-peroxide reaction in a CSTR at different holding times. [After S.A. Vejtassa and R.A. Schmitz, *Amer. Inst. Chem. Eng. J.*, 16, 410, with permission of the American Institute of Chemical Engineers, (1970).]

### Illustration 6.2

The derivation of equation (6-50) was carried out for a reactor with heat exchange. What if the reactor is isothermal? Would the form of the kinetics of the reaction have any significant influence on this type of operation?

#### Solution

For the steady-state reactor with no heat exchange we have

$$0 = f(C) = v(C_0 - C) - \bar{V}[-r(C)] \quad (\text{i})$$

We may again use the requirement of a non-zero derivative of  $f(C)$  to establish the needs of a unique solution. Hence, from (i),

$$\left(\frac{df}{dC}\right) = -v - \bar{V} \frac{d[-r(C)]}{dC} \quad (\text{ii})$$

This requires, for non-zero values of the derivative, that

$$\frac{d[-r(C)]}{dC} \geq 0 > \left(\frac{v}{\bar{V}}\right) \quad (\text{iii})$$

This last inequality can be combined with equation (i) to give

$$\frac{(C - C_0)}{[-r(C)]} \cdot \frac{d[-r(C)]}{dC} = (C - C_0) \frac{d\{\ln[-r(C)]\}}{dC} < 1 \quad (\text{iv})$$

For general power-law kinetics

$$[-r(C)] = kC^n \quad (\text{v})$$

$$\frac{d[-r(C)]}{dC} = nkC^{n-1} \geq 0 \quad (\text{vi})$$

Then, comparison with the uniqueness criterion, equation (iii), indicates that this type of reactor with power-law kinetics has a unique steady state regardless of the operating conditions or the magnitudes of the kinetic parameters.

The form of the kinetic expression can be of importance, however. For example, we can consider the CSTR system with a rate equation of more complex form than simple power law, such as

$$[-r(C)] = \frac{kC}{(1 + KC)^2} \quad (\text{vii})$$

which has been shown by Matsura and Kato [T. Matsura and M. Kato, *Chem. Eng. Sci.*, 22, 171 (1967)] to have multiple steady states in certain regions of parameter space. The picture of multiplicity that arises here, though, depends to some extent on the interests of the designer. If a primary factor in design is the nature of the feed condition to be handled, then combination of the rate equation (vii) with the criterion established by equation (iv) yields

$$2KC^2 - KC_0C + C_0 > 0 \quad (\text{viii})$$

It can be shown that if the discriminant of this equation is negative, then uniqueness is ensured, in this case requiring that  $KC_0 < 8$ . On the other hand, if the size of the reactor is the design concern, then it is of more use to note that the derivative of the rate equation is a minimum at the point  $C = 2/K$ . Then

$$\min \left\{ \frac{d[-r(C)]}{dC} \right\} = \min \left[ \frac{k(1 - KC)}{(1 + KC)^3} \right] = \left( -\frac{k}{27} \right) \quad (\text{ix})$$

Combining this with equation (iv) establishes the condition for uniqueness as

$$\left( \frac{v}{\bar{V}k} \right) > \frac{1}{27} \quad (\text{x})$$



HORATIO SAYS

What would be the uniqueness condition in a CSTR with Michaelis-Menton rates

$$-r(C) = [kC]/(K + C)?$$

Systems with multiple reactions can also be analyzed using the methods above. Here, however, we are concerned with possible multiple selectivities corresponding to the various steady states. For an illustration of this, consider two components of an

overall reaction, A and B, in which separate rate equations can be written for each. Then, for an isothermal CSTR

$$0 = -vC_A + \bar{V}(-r_1) \quad (6-51)$$

$$0 = -vC_B + \bar{V}(-r_2) \quad (6-52)$$

Eliminating  $C_B$  from the above,

$$f(C_A) = 0 = -vC_A + \bar{V}[-r_1(C_A)] \quad (6-53)$$

For the reactor system without heat effects, equation (6-53) is just a balance between the reaction-rate term and the convective term for A. Then we let

$$M_g = \bar{V}[-r_1(C_A)]; \quad M_r = vC_A \quad (6-54)$$

Figure 6.9 shows the type of multiplicity of this sort involved for a typical oxidation chain reaction, the liquid-phase oxidation of isopropanol. The overall kinetics are given by

$$\begin{aligned} -r_1(C_A) &= k_1 C_B - k_2 C_A^2 \\ -r_2(C_B) &= k_2 C_A^2 - k_3 C_B^2 \end{aligned} \quad (6-55)$$

where in this case A is hydrogen peroxide and B is the free radical  $[(CH_3)_2COH]$ . Following the analysis of the illustration, we have for the derivative of the mass balance

$$\frac{d[f(C_A)]}{dC_A} = -v + \bar{V} \frac{d[-r_1(C_A)]}{dC_A} \quad (6-56)$$

giving the uniqueness condition

$$\frac{d[-r_1(C_A)]}{dC_A} < \left( \frac{v}{\bar{V}} \right); \quad \max \frac{d[-r_1(C_A)]}{dC_A} < \left( \frac{v}{\bar{V}} \right)$$

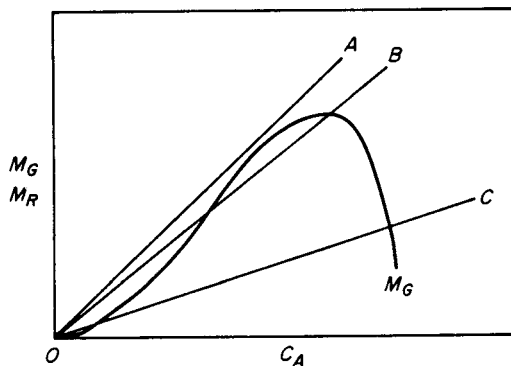


**Figure 6.9** Operating conditions for a CSTR with multiple reactions. Different steady-state possibilities are illustrated by lines A, B, and C.

The same statement can be related to the slopes of the  $M_g$  or  $M_r$  curves in Figure 6.9 as

$$\frac{dM_g}{dC_A} < \frac{dM_r}{dC_A} \quad (6-57)$$

Combining equations (6-55) and (6-52),

$$[-r_1(C_A)] = \left( \frac{k_1}{2\bar{V}k_3} \right) \left( v + \sqrt{v^2 + 4\bar{V}^2 k_2 k_3 C_A^2} \right) - k_2 C_A^2 \quad (6-58)$$

$$\frac{d(-r_1)}{dC_A} = 2k_2 C_A \left[ \frac{k_1 \bar{V}}{(v^2 + 4\bar{V}^2 k_2 k_3 C_A^2)^{1/2}} - 1 \right] \quad (6-59)$$

This is a maximum at

$$C_A = \frac{v}{2\bar{V}} \sqrt{\frac{1}{k_2 k_3} \left[ \left( \frac{k_1 \bar{V}}{v} \right)^{2/3} - 1 \right]}^{1/2} \quad (6-60)$$

and

$$\max \left[ \frac{d(-r_1)}{dC_A} \right] = \left( \frac{v}{\bar{V}} \right) \left( \frac{k_2}{k_3} \right)^{1/2} \left[ \left( \frac{k_1 \bar{V}}{v} \right)^{2/3} - 1 \right]^{3/2} \quad (6-61)$$

Combining equation (6-61) with the uniqueness condition of equation (6-56a) gives the final result

$$\left( \frac{k_2}{k_3} \right)^{1/2} \left[ \frac{k_1 \bar{V}}{v} - 1 \right]^{3/2} < 1 \quad (6-62)$$

#### 6.1.4 CSTR Uniqueness: Another Method

In the analysis of thermal effects on CSTR uniqueness (given at the beginning of the last section), it was seen that different criteria resulted depending on the nature of the condition selected [i.e., equation (6-43) or equation (6-48)]. This suggests the inverse question, are there any other approaches to such an analysis and, if so, are their results subject to the same variability?

Consider a reaction for which we again write Academic Reaction #1 with the rate

$$(-r) = (k_0 e^{-E/RT}) C \quad (6-63)$$

Combining this with the conventional CSTR mass balance gives

$$C = \frac{vC_0}{v + \bar{V}k_0 \exp(-E/RT)} \quad (6-64)$$

Now we can use this expression instead of equation (6-4) to develop the analog of equation (6-41),

$$(-r) = \frac{vC_0 k_0 \exp(-E/RT)}{v + \bar{V}k_0 \exp(-E/RT)} \quad (6-65)$$

and

$$\frac{d(-r)}{dt} = \frac{k_0 v^2 C_0 (E/R) \exp(-E/RT)}{T^2 [v + \bar{V} k_0 \exp(-E/RT)]^2} \quad (6-66)$$

$$\frac{d(-r)}{dt} = \frac{(-r)(E/R)}{T^2} \left( \frac{C}{C_0} \right) \quad (6-67)$$

The derivative given by equation (6-67) is positive for all  $T$ ,  $C$ , and the  $[-r(T)]$  curve corresponding cannot have any maximum. There is, however, an inflection point of equation (6-65) corresponding to an inflection temperature,  $T_i$ , defined by

$$\left[ \frac{(E/2RT_i) + 1}{(E/2RT_i) - 1} \right] \exp(-E/RT_i) = \frac{v}{\bar{V} k_0} \quad (6-68)$$

and at this point

$$\max \frac{d(-r)}{dT} = \frac{C_0 v}{(E/R) \bar{V}} \left\{ \left[ \frac{(E/R)}{2T_i} \right]^2 - 1 \right\} \quad (6-69)$$

$$\max \frac{d(-r)}{dT} < \beta \left( \frac{v}{\bar{V}} \right) \quad (6-70)$$

where equation (6-70) is the uniqueness criterion for this case. Following this, then

$$\frac{\beta(E/R)}{C_0} > \left[ \frac{(E/R)}{2T_i} \right]^2 - 1 \quad (6-71)$$

In terms of the parameter  $\psi$  of equation (6-50) this can be written as

$$\frac{\psi(E/RT_0)}{(E/RT_0) - \psi} > \left[ \frac{(E/R)}{2T_i} \right]^2 - 1 \quad (6-72)$$

A comparison of the criterion of equation (6-72) with that of equation (6-49) is shown in Figure 6.10. We see that the criterion via equation (6-72) is parameterized with respect to  $(E/RT_0)$ , while that via equation (6-49) is not. The more conservative criterion is the one giving the highest  $\psi$  for a given value of  $(v/\bar{V}k_0)$ . Obviously, which is more conservative depends on the specific values of these two groups.

### Illustration 6.3

The stability of a fluidized-bed reactor has been examined under the assumption that both phases were well-mixed. For the steady state of this reactor the following balances apply.

*Overall Mass*

$$0 = v(C_0 - C_1) + k_G(C - C_1) \quad (i)$$

*Overall Heat*

$$0 = vC_p(T_0 - T_I) + h_G(T - T_1) + U(T_w - T_1) \quad (ii)$$

*Mass Transfer*

$$k_G(C_1 - C) - \bar{V}[-r(C, T)] \quad (iii)$$



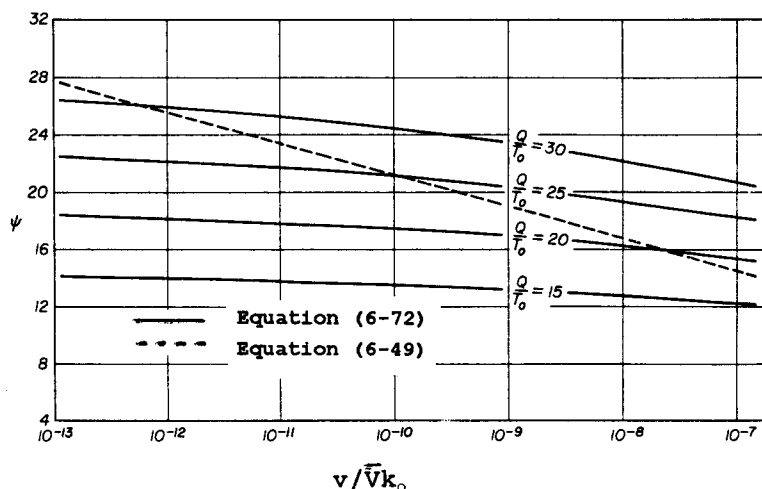


**Figure 6.10** Comparison of the results for two uniqueness criteria for a CSTR. [From D.D. Perlmutter, *Stability of Chemical Reactors*, reprinted by permission of Prentice-Hall, Inc, Englewood Cliffs, NJ, (1972).]

### Heat Transfer

$$h_G(T_1 - T) + (-\Delta H)\bar{V}[-r(C, T)] \quad (\text{iv})$$

(Chapter 8 will reveal that this is one version of a well-known fluidized-bed reactor model due to Davidson and Harrison). Using this, make an analysis of the uniqueness of steady-state operation.

### Solution

We may first define the heat generation and heat removal functions,  $q_g$  and  $q_r$  respectively, as

$$q_g = (-\Delta H)\bar{V}[-r(C, T)] \quad (\text{v})$$

$$q_r = h_G(T - T_1) \quad (\text{vi})$$

Rearranging equation (ii)

$$T_1 = \frac{vC_p T_0 + UT_W + h_G T}{vC_p + U + h_g} \quad (\text{vii})$$

and from equations (i) and (iii)

$$\frac{kG}{\alpha\bar{V}}(C_0 - C) = [-r(C, T)] \quad (\text{viii})$$

where  $\alpha = 1 + (k_G/v)$ . Inserting the rate equation and solving for  $C$ ,

$$C = \frac{C_0}{1 + \alpha(k_0\bar{V}/k_G)\exp(-E/RT)} \quad (\text{ix})$$

Here we have uniqueness determined via the derivative of rate with respect to temperature; thus

$$\frac{d(-r)}{dT} = \frac{h_G}{(-\Delta H)\bar{V}} \left( 1 - \frac{dT_1}{dT} \right) \quad (\text{x})$$

From equation (vii)

$$\frac{dT_1}{dT} = \frac{h_G}{vC + U + h_G}$$

and substituting this into equation (x)

$$\frac{d(-r)}{dT} = \frac{h_G(vC_p + U)}{(-\Delta H)\bar{V}(vC_p + U + h_G)}$$

From the form of the rate equation

$$\frac{d(-r)}{dT} = (-r) \left[ \frac{(E/R)}{T^2} + \left( \frac{1}{C} \right) \frac{dC}{dT} \right] \quad (\text{xii})$$

Combining with equation (x) and its derivative, we then directly obtain

$$\frac{d(-r)}{dT} = \frac{(-r)(E/R)}{T^2} \left( \frac{C}{C_0} \right) \quad (\text{xiii})$$

Also, from equation (viii), if we substitute directly for  $(-r)$ ,

$$\frac{d(-r)}{dT} = \frac{k_G(E/R)(C_0 - C)C}{\alpha \bar{V} C_0 T^2} \quad (\text{xiv})$$

An upper bound on this derivative may be established by recalling that for an exothermic, irreversible reaction the following inequalities are *always* observed.

$$\frac{d(-r)}{dC} \leq 0; \quad \frac{d(-r)}{dC} > -\frac{v}{\bar{V}}$$

Then an upper bound may be established by

$$\max \frac{d(-r)}{dT} < \frac{k_G C_0 (E/R)}{\alpha \bar{V} T_0^2} \quad (\text{xv})$$

and, upon substitution of (xv) into inequality (xi),

$$\frac{(-\Delta H)C_0(E/R)}{C_p T_0^2} < \frac{\alpha G_2}{(\alpha - 1) + G_2 G_3}$$

where

$$G_2 = 1 + (U/vC_p); \quad G_3 = (k_G C_p / h_G)$$

Equation (xvi) is a sufficient uniqueness condition.

Now, there is another way to establish a bound for  $[d(-r)/dT]$ , via analysis of its maximum. In this case we can write

$$\max \frac{d(-r)}{dT} = \frac{k_G C_0}{\alpha (E/R) \bar{V}} \left[ \left( \frac{E/R}{2T} \right)^2 - 1 \right] \quad (\text{xvii})$$

where  $(E/RT)$  is determined from the solution of

$$\left( \frac{E/2RT + 1}{E/2RT - 1} \right) \exp(-E/RT) = \frac{k_G}{\alpha \bar{V} k_0} \quad (\text{xviii})$$

For values of  $(E/RT) > 10$  equation (xviii) can be approximated by

$$(E/RT) = -\ln \left( \frac{k_G}{\alpha \bar{V} k_0} \right)$$

and equation (xvii) simplified to

$$\max \frac{d(-r)}{dT} = \frac{k_G C_0}{\alpha (E/R) \bar{V}} \left( \frac{E/R}{2T} \right)^2$$

Combining these two equations gives

$$\max \frac{d(-r)}{dT} = \frac{k_G C_0}{4\alpha (E/R) \bar{V}} \left[ \ln \left( \frac{k_G}{\alpha \bar{V} k_0} \right) \right]^2 \quad (\text{xix})$$

If we now use equation (xix) in place of the inequality (xv), the criterion for uniqueness becomes

$$\frac{(-\Delta H) C_0}{4(E/R) C_p} \left[ \ln \left( \frac{k_G}{\alpha \bar{V} k_0} \right) \right]^2 < \frac{\alpha G_2}{(\alpha - 1) + G_2 G_3} \quad (\text{xx})$$

It is not unreasonable if one begins to wonder if the effort of all the above is worth it, given the wonderful combinations of parameters involved and how precisely we know them. The best that can be said is to wait for some inspiration from the discussion in Chapter 8.



HORATIO SAYS

Which of the two criteria above is the more conservative, and why? Considering that the fluid bed consists of two well-mixed phases, would you think that nonuniqueness is liable to be a problem in these reactors?

## 6.2 Some Reactor/Heat-Exchanger Systems

### 6.2.1 Autothermal Reactors

A system in which some of the heat produced in an exothermic reaction is used to preheat the feed stream, or to heat other streams associated with the overall process, is termed an autothermal reactor<sup>3</sup>. A simplified diagram for the case of feed preheat using the reactor effluent is given in Figure 6.11.

<sup>3</sup> “I remember your name perfectly, I just can’t think of your face.”—*W.A. Spooner*

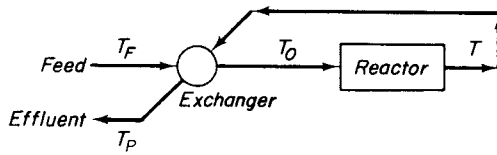


**Figure 6.11** An autothermal reactor system with feed preheat. [After J.M. Smith, *Chemical Engineering Kinetics*, 3rd ed., with permission of McGraw-Hill Book Co., New York, NY, (1981).]

We consider the reactor here to be operated adiabatically, with  $T > T_0 > T_F$ . A measure of the heat-exchange capacity of the system is given by

$$\epsilon_H = (T - T_F)/(T - T_0) \quad (6-73)$$

where  $\epsilon_H$  is the capacity measure, and the temperatures are shown in Figure 6.11. If it is assumed that the reactor in question is a CSTR, then a steady-state heat balance around the reactor is

$$vC_p(T_0 - T) = -\bar{V}(-\Delta H)(-r) \quad (6-74)$$

Inserting the capacity measure into equation (6-74) gives

$$\left( \frac{vC_p}{\epsilon_H} \right) (T_F - T) + \bar{V}(-\Delta H)(-r) = 0 \quad (6-75)$$

Substituting from the above for the rate term in the mass balance equation for the reactor

$$C = C_0 - \frac{C_p}{\epsilon_H(-\Delta H)} (T - T_F) \quad (6-76)$$

The combined mass and energy balance for the CSTR given in equation (6-4) can be written for adiabatic operation as

$$C = C_0 + \frac{C_p}{(-\Delta H)} (T_F - T) \quad (6-77)$$

Given the similarity between equations (6-76) and (6-77), one may conclude that the analysis of multiplicity for the autothermal system is similar (which is indeed the case), where the parameter  $\epsilon_H$  is found in place of the heat-transfer coefficient. Note that  $\epsilon_H$  can also be written as a function of the operating conditions  $C$  and  $T$ .

$$\epsilon_H = \frac{C_p(T - T_F)}{(-\Delta H)(C_0 - C)} \quad (6-78)$$

Now if we assume that the reactor in the autothermal scheme is a PFR rather than a CSTR, the mass balance is

$$v \left( \frac{dC}{dz} \right) = (1 - \epsilon_B)(-r) \quad (6-79)$$

where  $\epsilon_B$  is the reactor bed porosity and  $(-r)$  is based on unit volume of catalyst. The energy balance is

$$vC_p \left( \frac{dT}{dz} \right) = (1 - \epsilon_B)(-\Delta H)(-r) \quad (6-80)$$

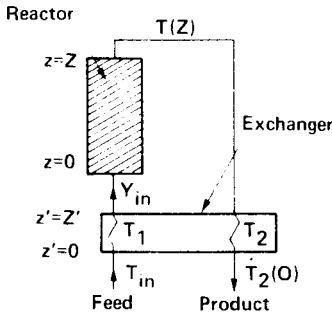


**Figure 6.12** An autothermal reactor system with details on external heat exchange from product to feed. [After J.M. Smith, *Chemical Engineering Kinetics*, 3rd ed., with permission of McGraw-Hill Book Co., New York, NY, (1981).]

A schematic of the overall system, somewhat more detailed than Figure 6.11 with respect to the external heat exchange, is given in Figure 6.12. In addition to the balances of equations (6-79) and (6-80), we have for external heat exchange

$$(vC_p)_1 \frac{dT_1}{dz'} = UA(T_2 - T_1) \quad (6-81)$$

and

$$(vC_p)_1 dT_1 = (vC_p)_2 dT_2 \quad (6-82)$$

where  $v$  is molar flow rate,  $z$  reactor length variable,  $z'$  heat exchanger length variable,  $U$  overall heat-transfer coefficient, and  $A$  heat exchange area. The following initial/boundary conditions apply.

$$\begin{aligned} z = 0 \quad C &= C_{in}; \quad T = T_1(z') \\ z' = 0 \quad T_1(0) &= T_{in} \\ z = Z, \quad z' = Z' \quad T_2(Z') &= T(Z) \end{aligned} \quad (6-83)$$

Combining equations (6-79) and (6-80) and integrating the result over  $z$  gives

$$y(Z) - y_{in} = \frac{vC_p}{(-\Delta H)(F_{in})} [T(Z) - T(Z')] \quad (6-84)$$

where  $v$  is superficial velocity and  $F_{in}$  is the inlet molar flow rate. If  $(vC_p)_1 = (vC_p)_2$ , we have [also from equation (6-82)],

$$T_{in} - T_1(z') = T_2(0) - T_2(z') \quad (6-85)$$

$$T_{in} - T_1(Z') = T_2(0) - T_2(Z') \quad (6-86)$$

Now, from equation (6-85) it can be seen that  $(T_2 - T_1)$  in equation (6-81) is a constant, so after integration

$$T_1(Z') - T_{in} = \frac{UAZ'}{(vC_p)_1} [T_2(0) - T_{in}] \quad (6-87)$$

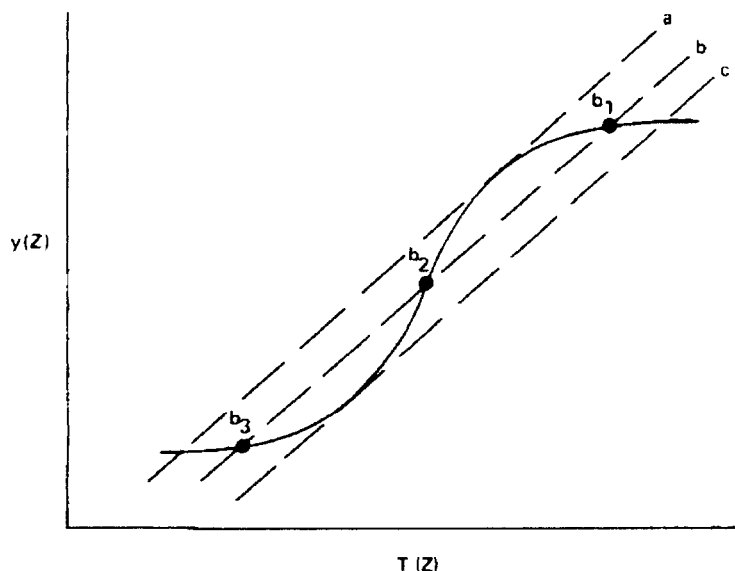


**Figure 6.13** General form of multiplicity in an autothermal reactor system with heat exchange between feed and product. [After H.H. Lee, *Heterogeneous Reactor Design*, with permission of Butterworth Publishers, Boston, MA, (1985).]

This can be manipulated to give

$$T(Z) - T_{in} = \left[ 1 + \frac{UAZ'}{(vC_p)_1} \right] [T(Z) - T_1(Z')] \quad (6-88)$$

Combining this with equation (6-84) finally gives

$$\begin{aligned} y(Z) - y_{in} &= \frac{T(Z) - T_{in}}{\left[ 1 + \frac{UAZ'}{(vC_p)_1} \right] \left[ \frac{F_{in} - (-\Delta H)}{(vC_p)_1} \right]} \\ &= \gamma [T(Z) - T_{in}] \end{aligned} \quad (6-89)$$

On an operating diagram of  $y - T$ , equation (6-89) is given by a straight line of slope  $\gamma$ , as seen in Figure 6.13. We observe from this figure that it is again possible to have three steady states, at  $b_1$ ,  $b_2$ , and  $b_3$ , and the relative stability of these is as found for the three states in a nonunique CSTR; thus,  $b_2$  is unstable to small perturbations.

## 6.2.2 Countercurrent Operation

An even closer coupling of the reactor-heat exchange combination is obtained by the countercurrent operation illustrated in Figure 6.14. This problem was first studied by Grens and McKean [E.A. Grens and R.A. McKean, *Chem. Eng. Sci.*, 18, 291 (1963)] who obtained an analytical solution for the temperature profiles of both reactant and coolant fluids in the (somewhat artificial) case where the reaction rate is independent of concentration and temperature. While not too realistic for practical application,

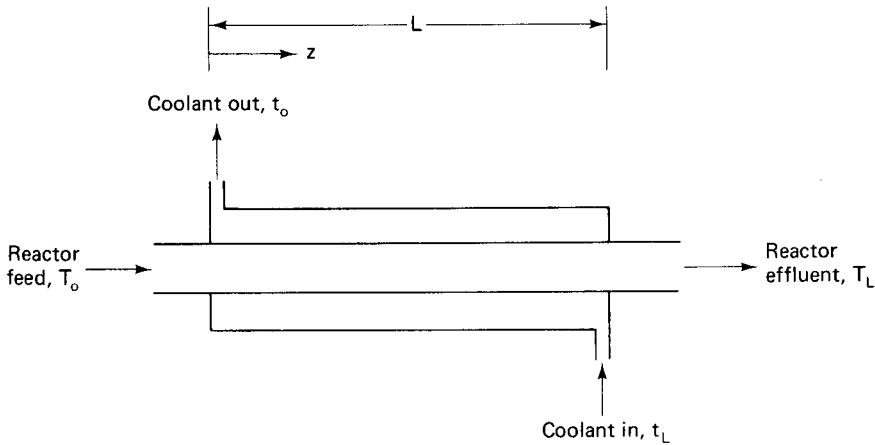


**Figure 6.14** A counter current reactor/heat exchanger. [After E. A. Grens and R. A. McKean, *Chem. Eng. Sci.*, 18, 291, with permission of Pergamon Press, Inc., London, England, 1963.]

the results are of use as a “base case” for evaluation of more complex kinetics, where a numerical solution is normally required. With this caveat, we proceed.

Two heat balances are required: one for reactant and one for coolant. For the reactant in a PFR

$$\rho u C_p \frac{dT}{dz} = (-r)(-\Delta H) - \frac{2U}{R} (T - t) \quad (6-90)$$

and for coolant

$$\rho_c u_c C_{p_c} \frac{dt}{dz} + \frac{2U}{R} (T - t) = 0 \quad (6-91)$$

with the boundary conditions  $T = T_0$  at  $z = 0$ , and  $t = t_L$  at  $z = L$ , as shown in Figure 6.14. A convenient set of nondimensional variables is

$$\zeta = \frac{z}{L}; \quad \phi = \frac{T - T_0}{\Delta T_0}; \quad \chi = \frac{t - T_0}{\Delta T_0}$$

where

$$\Delta T_0 = \frac{(-r)(-\Delta H)L}{\rho u C_p}$$

The two heat balance equations then become

$$\frac{d\phi}{d\zeta} + \alpha(\phi - \chi) = 1 \quad (6-90a)$$

$$\frac{d\chi}{d\zeta} + \alpha\gamma(\phi - \chi) = 0 \quad (6-91a)$$

with the parameters defined as

$$\alpha = \frac{2UL}{R\rho u C_p}; \quad \gamma = \frac{\rho u C_p}{\rho_c u_c C_{p_c}}$$

The boundary conditions transform to

$$\phi = 0 \quad \text{at} \quad \zeta = 0; \quad \chi = \theta = \frac{t_L - T_0}{\Delta T_0} \quad \text{at} \quad \zeta = 1 \quad (6-92)$$

The temperature profiles obtained upon solution are

$$\begin{aligned} \phi &= \theta \frac{[1 - e^{\alpha(\gamma-1)\zeta}]}{[1 - \gamma e^{\alpha(\gamma-1)}]} + \frac{\gamma}{(\gamma-1)\zeta} + \frac{(1/\alpha + \gamma)[1 - e^{\alpha(\gamma-1)\zeta}]}{(1-\gamma)[1 - \gamma e^{\alpha(\gamma-1)}]} \\ \chi &= \theta \frac{[1 - \gamma e^{\alpha(\gamma-1)\zeta}]}{[1 - \gamma e^{\alpha(\gamma-1)}]} + \frac{\gamma}{(\gamma-1)\zeta} + \frac{(\gamma/\alpha)[e^{\alpha(\gamma-1)} - e^{\alpha(\gamma-1)\zeta}] + \gamma[1 - \gamma e^{\alpha(\gamma-1)\zeta}]}{(1-\gamma)[1 - \gamma e^{\alpha(\gamma-1)}]} \end{aligned} \quad (6-93)$$

Equating the derivative of the length from equation (6-93) to zero and solving reveals the maximum temperature to be

$$\begin{aligned} \phi_{max} &= \frac{\theta(1-\gamma) + (1/\alpha) + \gamma}{(1-\gamma)[1 - \gamma e^{\alpha(\gamma-1)}]} \\ &+ \frac{\gamma}{\alpha(1-\gamma)^2} \cdot \left\{ \ln \left[ \frac{\gamma[1 - \gamma e^{\alpha(\gamma-1)}]}{\alpha(1-\gamma)[\theta(1-\gamma) + (1/\alpha) + \gamma]} \right] - 1 \right\} \end{aligned} \quad (6-95)$$

and to be located at

$$\zeta_{max} = \frac{1}{\alpha(\gamma-1)} \ln \left\{ \frac{\gamma[1 - \gamma e^{\alpha(\gamma-1)}]}{\alpha(\gamma-1)[\theta(1-\gamma) + (1/\alpha) + \gamma]} \right\} \quad (6-96)$$

Clearly, this maximum temperature is a function only of the two parameters  $\alpha$  and  $\gamma$ , which then assume the role of design or process variables if  $\phi_{max}$  is specified. The heat of reaction would also be a major contributor through  $\Delta T_0$ . A characteristic of this type of reactor is a temperature crossover located in the region where the reaction stream temperature is increasing, shown in Figure 6.15, so there is heat transfer

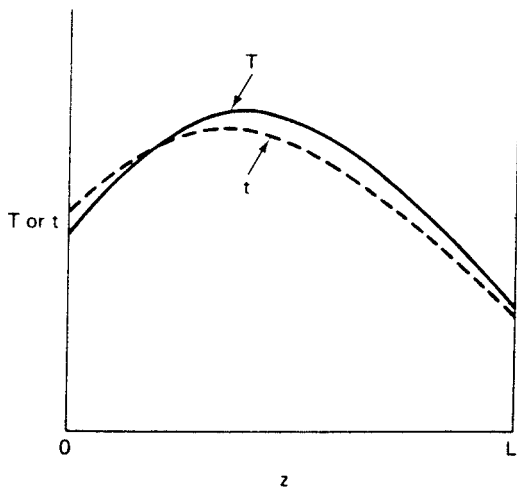


**Figure 6.15** Typical temperature crossover in a countercurrent reactor/heat exchanger. [After E. A. Grens and R. A. McKean, *Chem. Eng. Sci.*, 18, 291, with permission of Pergamon Press, Inc., London, England, 1963.]



to streams entering at either end of the reactor/heat exchanger. The result of this is that internal temperature profiles can be quite sensitive to process or design parameters. As stated above, the quantitative results here pertain only for  $(-r)$  independent of concentration and temperature, but numerical solution of the model with a concentration functionality and Arrhenius temperature dependence of rate should not be difficult. One can imagine that parametric sensitivity, however, would become even more pronounced in that case.

### 6.3 Gradients and Profiles

By and large we can describe the results of the analysis of distributed parameter systems (i.e., flow reactors other than CSTRs) in terms of the gradients or profiles of concentration and temperature they generate. To a large extent, the analysis we shall pursue for the rest of this chapter is based on the one-dimensional axial dispersion model as used to describe both concentration and temperature fields within the nonideal reactor. The mass and energy conservation equations are coupled to each other through their mutual concern about the rate of reaction and, in fact, we can use this to simplify the mathematical formulation somewhat. Consider the adiabatic axial dispersion model in the steady state.

$$D \frac{d^2 C}{dz^2} - u \frac{dC}{dz} - (-r) = 0 \quad (6-97)$$

and

$$\alpha \frac{d^2 \theta}{dz^2} - u \frac{d\theta}{dz} + (-r) = 0 \quad (6-98)$$

where  $D$  is the axial dispersion coefficient,  $\alpha$  the corresponding thermal dispersion coefficient, and  $\theta$  is a reduced temperature,  $C_p T / (-\Delta H)$ . Following the discussion of boundary conditions given in Chapter 5, we have

$$\frac{d\theta}{dz} = \frac{u}{\alpha} (\theta - \theta_0); \quad \frac{dC}{dz} = \frac{u}{D} (C - C_0); \quad z = 0 \quad (6-99)$$

$$\frac{d\theta}{dz} = 0; \quad \frac{dC}{dz} = 0; \quad z = L \quad (6-100)$$

Adding equations (6-97) and (6-98) gives

$$\alpha \frac{d^2 \theta}{dz^2} + D \frac{d^2 C}{dz^2} = u \left( \frac{d\theta}{dz} + \frac{dC}{dz} \right) \quad (6-101)$$

If it is assumed that  $(D/\alpha) = 1$  (a popular but suspect procedure in general), then we can define a new variable

$$\omega = \theta + C \quad (6-102)$$

which takes equation (6-101) to the much simplified form

$$\frac{d^2 \omega}{dz^2} = \left( \frac{u}{D} \right) \frac{d\omega}{dz} \quad (6-103)$$

The boundary conditions now appear as

$$\begin{aligned}\frac{d\omega}{dz} &= \left(\frac{u}{D}\right)(\omega - \omega_0); & z = 0 \\ \frac{d\omega}{dz} &= 0; & z = L\end{aligned}\quad (6-104)$$

A general solution to the set (6-103) and (6-104) is

$$\omega(z) = A + B[\exp(uz/D)] \quad (6-105)$$

where, for the specific boundary conditions here,  $B = 0$  and  $A = \omega_0$ . Thus,

$$\omega(z) = \omega_0 = C_0\theta_0 = \text{constant} \quad (6-106)$$

and

$$C = C_0 + \theta_0 - \theta \quad (6-107)$$

The original balance equation now becomes a function of a single dependent variable.

$$\alpha \frac{d^2\theta}{dz^2} - u \frac{d\theta}{dz} + [-r(\theta)] = 0 \quad (6-108)$$

where

$$[-r(\theta)] = k_0 \exp[-EC_p/R\theta(-\Delta H)](C_0 + \theta_0 - \theta)$$

While all this simplifies the problem, we still need a numerical solution.

### 6.3.1 Uniqueness of a PFR

For the steady state of a nonisothermal PFR we have, via the simplification of equations (6-97) and (6-98), and adding a heat-transfer term,

$$-u \frac{dC}{dz} = (-r) \quad (6-109)$$

$$-u \frac{d\theta}{dz} = -(-r) + \left(\frac{h}{C_p}\right)(\theta - \theta_w) \quad (6-110)$$

where  $h$  is an appropriate wall heat transfer coefficient (see Chapter 7 for more on this), and  $\theta_w$  is a constant wall temperature parameter. An operating diagram for the PFR, akin to that of Figure 6.1 for the CSTR, is given in Figure 6.16 [parameters as in F.S. Wang and D.D. Perlmutter, *Amer. Inst. Chem. Eng. Jl.*, 16, 934 (1968)]. No multiplicity, but pronounced parametric sensitivity (in the region where the curves are nearly vertical) is observed in this case. The operating diagram corresponds directly to the construction of Figure 6.1 for the CSTR: the output function ( $C/C_0$ ) is given as a function of the feed condition ( $\theta_0/C_0$ ) in terms of an operating parameter, ( $hL/uC_p$ ).

The immediate question is whether it is possible for the PFR to demonstrate multiplicity in the same way as for the CSTR. Intuitively, we can approach this question by going all the way back to the visualization of the little traveling batch reactors discussed in Chapter 1. Thus we can replace the PFR with an assembly of traveling batch reactors and ask whether it is possible for a batch reactor to

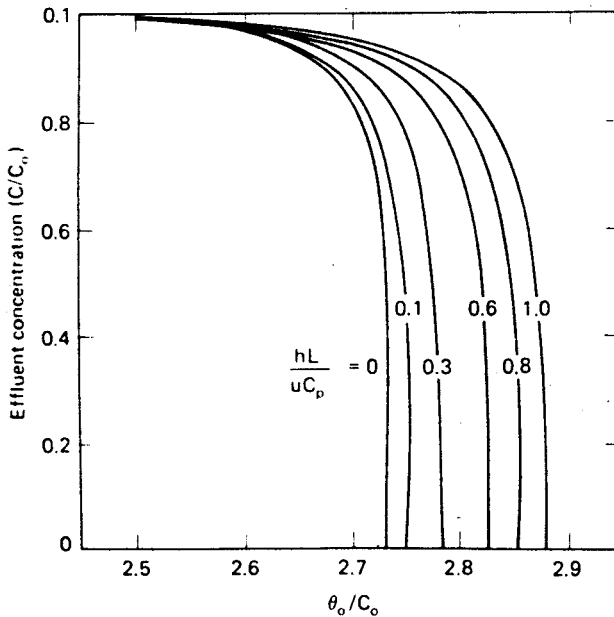


**Figure 6.16** Steady-state operating diagram for a PFR. [After D.D. Perlmutter, *Stability of Chemical Reactors*, reprinted by permission of Prentice-Hall, Inc., Englewood Cliffs, NJ, (1972).]

follow more than one conversion-time trajectory for a specified set of feed (initial) conditions. The short form of the answer is no. A short formal treatment follows from the generalized set of two differential equations, first order, as follows.

$$\frac{d\eta}{d\tau} = f_1(C, \eta); \quad \eta(0) = \eta_0 \quad (6-111)$$

$$\frac{dC}{d\tau} = f_2(C, \eta); \quad C(0) = C_0 \quad (6-112)$$

This conforms to the initial-value problem posed by the nonisothermal PFR, and the solution is always unique if  $f_1$  and  $f_2$  have continuous first partial derivatives. Functions such as the reaction rate and heat-transfer terms appearing in equations (6-109) and (6-110) normally satisfy this requirement.

### 6.3.2 Uniqueness of the Axial Dispersion Model

Here let us consider the nonisothermal axial dispersion model in extension of equations (6-97) and (6-98) as

$$D \frac{d^2 C}{dz^2} - u \frac{dC}{dz} - (-r) = 0 \quad (6-97)$$

$$(\rho C_p E') \frac{d^2 T}{dz^2} - (\rho u C_p) \frac{dT}{dz} + (-r)(-\Delta H) - \left( \frac{2U}{R} \right) (T - T_M) = 0 \quad (6-113)$$

where  $E'$  is a transport coefficient for energy analogous to  $D$  for mass,  $u$ ,  $\rho$ , and  $C_p$  are independent of position and conversion,  $R$  is the reactor radius, and  $U$  is an

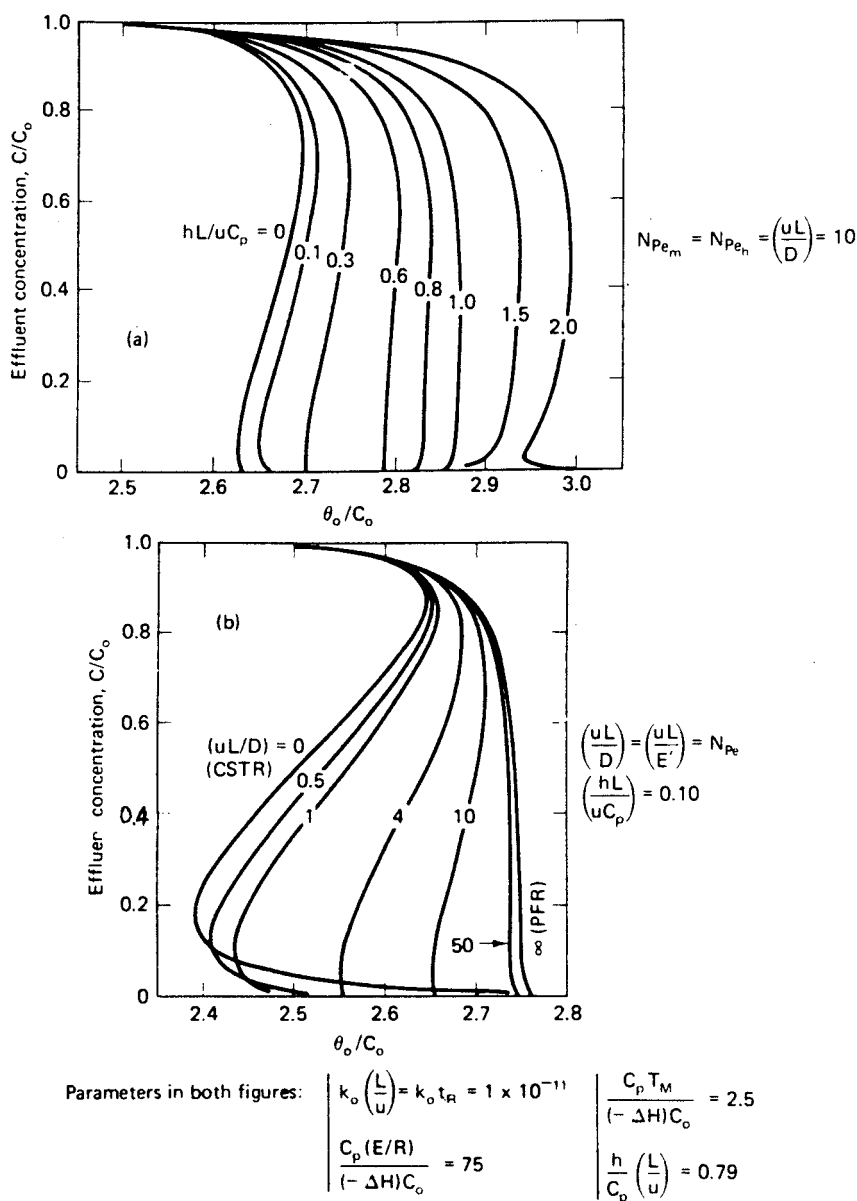


**Figure 6.17** Steady-state operating diagram for one-dimensional axial dispersion model. [After D.D. Perlmutter, *Stability of Chemical Reactors*, reprinted by permission of Prentice-Hall, Inc., Englewood Cliffs, NJ, (1972).]

overall heat-transfer coefficient. Multiple steady states for this model were determined in the computational studies of Raymond and Amundson [L.R. Raymond and N.R. Amundson, *Can. J. Chem. Eng.*, 42, 173 (1964)] and of McGowan and Perlmutter [C.R. McGowan and D.D. Perlmutter, *Amer. Inst. Chem. Eng. J.*, 17, 831 (1971)]. Typical results from the latter work are shown in Figures 6.17. For the

purposes of comparison, the same kinetic and heat-transfer parameters are used as for the PFR of Figure 6.16. Figure 6.17 shows the effect of the magnitude of the heat-transfer term for a Peclet number of 10, based on reactor length and equivalent for both heat and mass dispersion mechanisms. It is seen that external heat transfer has a signal effect on the operation of the reactor. Two features are striking: first is the existence of steady-state multiplicity for all conditions of heat transfer except for a narrow range in the vicinity of  $(hL/uC_p) = 0.6$ . Second, the nearly vertical plot of  $C/C_0$  versus feed condition,  $\theta_0/C_0$ , for a wide range of the heat-transfer parameter is indicative of extreme parametric sensitivity of the reactor, as indeed was the case for the PFR. Figure 6.17b employs the axial Peclet number as a parameter for a fixed value of the heat-transfer term, spanning the range from CSTR to PFR behavior. It is seen that for the parameters employed in the calculation the range of feed conditions over which multiplicity occurs decreases markedly as one proceeds from CSTR to PFR limits, although the parametric sensitivity appears as the latter limit is approached.<sup>4</sup>

The computational results illustrated in Figure 6.17 are based on the assumption that  $D = E'$ . For homogeneous reactors with fluids in turbulent flow this is probably not a bad assumption in view of what we know about the analogies between heat and mass transfer. If one is using the model as a pseudo-homogeneous representation of a fixed-bed catalytic reactor, however, the problem is rather different. (A discussion of what to do with the parameters of the axial dispersion model will be given in Chapter 7.) If one thinks that these results on tubular reactor multiplicity are only computational bric-a-brac, see the classical experimental work of Wicke and associates [for example, G. Padberg and E. Wicke, *Chem. Eng. Sci.*, 22, 1035 (1967); E. Wicke, G. Padberg and H. Arens, *Proc. 4th European Symp. on Chem. Reaction Eng., Brussels 1968*, Pergamon Press, Oxford, England, (1971).]

#### Illustration 6.4

Develop a computational procedure for the solution of the nonisothermal, one-dimensional axial dispersion reactor model.

##### Solution

We will start with the equations for the model given as (6-97) and (6-113), which we shall refer to as (i) and (ii) here. Now define a normalized temperature variable as done for the CSTR previously.

$$\theta = \frac{C_p T}{(-\Delta H)} \quad (\text{iii})$$

Upon substitution into equation (ii) we obtain

$$E' \frac{d^2 \theta}{dz^2} - u \frac{d\theta}{dz} + (-r) + Q_T = 0 \quad (\text{iv})$$

<sup>4</sup> The parameters employed in Figures 6.16 and 6.17 differ in units from those we have used in the development of the isothermal and nonisothermal one-dimensional dispersion models. In particular,  $h$  is a volumetric heat-transfer coefficient, typically kcal/volume-K-time, and  $C_p$  is a volumetric heat capacity, typically kcal/volume-K. The concentrations and heats of reaction are consistent with this in units of mols/volume and kcal/mol, respectively. "It is difference of opinion that makes horse races."—*M. Twain*

where  $Q_T$  is the external heat-transfer term. It is convenient to write the mass and energy balances in terms of the reduced variables for concentration and temperature, defined as,

$$f = (C/C_0); \quad \tau = (T/T_0)$$

This leads to the mass balance

$$\frac{1}{N_{Pe_m}} \frac{d^2 f}{d\zeta^2} - \frac{df}{d\zeta} - (-r) \left( \frac{L}{u} \right) = 0 \quad (v)$$

with the corresponding heat balance

$$\frac{1}{N_{Pe_h}} \frac{d^2 \tau}{d\zeta^2} - \frac{d\tau}{d\zeta} + \frac{(-r)(-\Delta H)}{\rho C_p T_0} \left( \frac{L}{u} \right) C_0 - \frac{2U}{\rho C_p R} \left( \frac{L}{u} \right) (\tau - \tau_M) = 0 \quad (vi)$$

with the boundary conditions

$$\begin{aligned} \frac{df(0^+)}{d\zeta} &= N_{Pe_m} [f(0^+) - 1]; & \zeta &= 0 \\ \frac{d\tau(0^+)}{d\zeta} &= N_{Pe_h} [\tau(0^+) - 1]; & \zeta &= 0 \\ \frac{d\tau}{d\zeta} = \frac{df}{d\zeta} &= 0; & \zeta &= 1 \end{aligned} \quad (vii)$$

In general, regardless of the form of  $(-r)$ , these equations require numerical solution. We present a scheme ( $u$ ,  $\rho$ ,  $C_p$  independent of position and conversion) based on a combination of central- and forward-difference approximations which has proven to be well-suited for the solution of diffusional-type boundary-value problems [J.J. Carberry and M.M. Wendel, *Amer. Inst. Chem. Eng. J.*, **9**, 129 (1963)].

Consider the mass balance, equation (v). Let us introduce the following finite-differences.

$$\begin{aligned} \frac{df}{d\zeta} &= \frac{f_{p+1} - f_p}{\Delta\zeta} \\ \frac{d^2 f}{d\zeta^2} &= \frac{f_{p+1} - 2f_p + f_{p-1}}{\Delta\zeta^2} \end{aligned}$$

where  $p$ ,  $p-1$ , and  $p+1$  are points along an axial grid of  $N$  points separated by  $\Delta\zeta$  from each other such that  $N\Delta\zeta = 1$ . Thus equation (v) becomes

$$\left( \frac{1}{N_{Pe}} \right) \frac{f_{p+1} - 2f_p + f_{p-1}}{\Delta\zeta^2} - \frac{f_{p+1} - f_p}{\Delta\zeta} - (-r)_p \left( \frac{L}{u} \right) = 0 \quad (viii)$$

where subscript  $m$  has been dropped from  $N_{Pe}$  because of laziness. If we include our familiar Academic Reaction #1 as an example, then

$$(-r)_p = kf_p$$

Note, though, that the method here is *not* restricted to linear rate equations. Equation (viii) may now be written as

$$\left(\frac{1}{N_{Pe}}\right)f_{p-1} + \left(\Delta\zeta - \frac{2}{N_{Pe}} - R'\Delta\zeta^2\right)f_p + \left(\frac{1}{N_{Pe}} - \Delta\zeta\right)f_{p+1} = 0 \quad (\text{ix})$$

with

$$R' = k_p \left(\frac{L}{u}\right) = \left(\frac{L}{u}\right)e^{-\gamma/\tau_p}; \quad \gamma = \frac{E}{RT_0}$$

Now, let us put the reaction-rate terms of equation (ix) on the right-hand side such that, after some rearrangement, we obtain

$$f_{p-1} + (N_{Pe}\Delta\zeta - 2)f_p + (1 - N_{Pe}\Delta\zeta)f_{p+1} = N_{Pe}\left(\frac{L}{u}\right)\Delta\zeta^2 k_0 e^{-\gamma/\tau_p} f_p \quad (\text{x})$$

This equation is of the form

$$f_{p-1}A_p + f_pB_p + f_{p+1}C_p = D_p \quad (\text{xi})$$

for point  $p$  in the axial grid. The coefficients are

$$\begin{aligned} A_p &= 1; & B_p &= N_{Pe}\Delta\zeta - 2 \\ C_p &= 1 - N_{Pe}\Delta\zeta; & D_p &= N_{Pe}\left(\frac{L}{u}\right)\Delta\zeta^2 k_0 e^{-\gamma/\tau_p} f_p \end{aligned}$$

For the whole reactor, then, with the exception of the entrance point,  $p = 1$ , and the exit point,  $p = N$ , we have a set of equations following the form of equation (xi) for each of the internal grid points  $p$ ,

$$\begin{aligned} f_1A_2 + f_2B_2 + f_3C_2 &= D_2 \\ f_2A_3 + f_3B_3 + f_4C_3 &= D_3 \\ &\vdots \\ f_{p-1}A_p + f_pB_p + f_{p+1}C_p &= D_p \\ &\vdots \\ f_{N-2}A_{N-1} + f_{N-1}B_{N-1} + f_NC_{N-1} &= D_{N-1} \end{aligned} \quad (\text{xii})$$

At the inlet we may write

$$f_0A_1 + f_1B_1 + f_2C_1 = D_1 \quad (\text{xiii})$$

but the boundary condition requires that

$$f_0 = 1 + \frac{1}{N_{Pe}} \left(\frac{df}{d\zeta}\right)_0 \quad (\text{xiv})$$

Initial gradients are best estimated by higher-order difference formulas such as

$$\left(\frac{df}{d\zeta}\right)_0 = \frac{-3f_0 + 4f_1 - f_2}{2\Delta\zeta} \quad (\text{xv})$$

Substituting equations (xiv) and (xv) for  $f_0$  in equation (xiii) and rearranging,

$$f_1 B_1 + f_2 C_1 = D_1 - A_1 \left[ \frac{(2N_{Pe})\Delta\zeta + 4f_1 - f_2}{(2N_{Pe})\Delta\zeta + 3} \right] \quad (\text{xiiia})$$

or

$$f_1 B_1 + f_2 C_1 = D'_1$$

At the exit we have

$$f_{N-1} A_N + f_N B_N + f_{N+1} C_N = D_N \quad (\text{xvi})$$

The derivative of concentration at the exit is zero, so this boundary condition requires that

$$\frac{f_{N-1} - f_N}{\Delta\zeta} = 0$$

$$f_{N+1} = f_N$$

Substituting this into equation (xvi) gives

$$f_{N-1} A_N + f_N (B_N + C_N) = D_N$$

or

$$f_{N-1} A_N + f_N B'_N = D_N \quad (\text{xiva})$$

The full set of finite-difference equations for the mass balance on the reactor, with boundary conditions built in, consists of equations (xii) plus (xiii) and (xiva):

$$\begin{aligned} f_1 B_1 + f_2 C_1 &= D'_1 \\ f_1 A_2 + f_2 B_2 + f_3 C_2 &= D_2 \\ &\vdots \\ f_{p-1} A_p + f_p B_p + f_{p+1} C_p &= D_p \\ &\vdots \\ f_{N-2} A_{N-1} + f_{N-1} B_{N-1} + f_N C_{N-1} &= D_{N-1} \\ f_{N-1} A_N + f_N B'_N &= D_N \end{aligned} \quad (\text{xvii})$$

Now some of the manipulations that have been employed to this point in arranging the finite-difference form of this mass conservation equation may seem rather arbitrary, however, there was a good reason for the procedure. If we write out the set of equations (xvii) in matrix form we find that the matrix of coefficients on the left-hand side is tridiagonal, that is, all elements off the three main diagonals are zero. The overall set of equations can then be solved directly by a Gaussian elimination method for the set of  $f_1 \cdots f_N$  (recalling that  $f_0$  is fixed). Thus, writing the set out



in matrix formulation gives

$$\begin{bmatrix} B_1 & C_1 & & & & \\ A_2 & B_2 & C_2 & & & \\ & A_3 & B_3 & C_3 & & \\ & & & \ddots & \ddots & \ddots \\ & & & & C_{N-1} & \\ & & & & A_N & B'_N \end{bmatrix} \begin{bmatrix} f_1 \\ f_2 \\ f_3 \\ \vdots \\ f_{N-1} \\ f_N \end{bmatrix} = \begin{bmatrix} D'_1 \\ D_2 \\ D_3 \\ \vdots \\ D_{N-1} \\ D_N \end{bmatrix} \quad (\text{xviii})$$

Using the elimination method, let us determine

$$w_1 = B_1$$

$$w_r = B_r - A_r q_{r-1} \quad (r = 2, 3, \dots, N \text{ and } B_N = B'_N)$$

where

$$q_{r-1} = (C_{r-1})/(w_{r-1}) \quad (\text{xix})$$

Also,

$$g_1 = \frac{D'_1}{w_1} = \frac{D'_1}{B_1}$$

$$g_r = \frac{D_r - A_r g_{r-1}}{w_r} \quad (r = 2, 3, \dots, N) \quad (\text{xx})$$

The solution to the set of equations is

$$f_N = g_N$$

$$f_r = g_r - q_r f_{r+1} \quad (r = 1, 2, \dots, N-1) \quad (\text{xxi})$$

Following this method we calculate values of  $w$  and  $g$  for increasing values of the index  $r$ , starting at 1. Then we compute values of  $f$  starting at  $f_N$  and going back to  $f_1$ .

The way these equations have been set up, the values of the coefficients  $D_p$  depend upon the values of  $f_p$  and  $\tau_p$ , that is, on what the temperature and concentration profiles are. In addition, remember that equation (xviii) is for the material balance only. Thus we have two tasks left at this point: 1) what of the energy balance and, 2) what of the coefficients  $D_p$ ?

The answer to the first task is fairly straightforward. We must construct a corresponding tridiagonal system for the energy balance and solve the two sets of equations simultaneously. The same procedures may be used to construct the matrix of energy equations as for the mass balance; some of the coefficients in the resultant matrix may also be dependent on  $f_p$  and  $\tau_p$ .

The answer to the second task is a little more complicated. In using the elimination procedure to solve the matrix, we are assuming that all coefficients  $A$ ,  $B$ ,  $C$ , and  $D$  are constants; however, we know from the above that this is not so. The result of this, for purposes of solution, requires the equivalent of the childhood game "Let's Pretend". We must use an iterative procedure for solution, and for each

iteration we will pretend that the coefficients are constant, computed with the current value of  $f_p$  and  $\tau_p$ . The iterative procedure is relatively simple: since we are dealing with normalized variables, start the computation with an initial assumption of  $f_p$  and  $\tau_p$  at each grid point; then solve the resultant matrices via equations (xix) to (xxi); use the resulting sets of  $f_p$  and  $\tau_p$  to determine new values for the matrix elements that require it; and iterate on this resubstitution procedure. In principal, arbitrary sets of  $f_p$  and  $\tau_p$  can be used to start the iteration; in practice, it is helpful to get the solution started in the right direction (remember that a forward-difference formula is used for the inlet boundary condition) with  $f_p$  decreasing with reactor length and  $\tau_p$  either increasing or decreasing depending upon whether the reaction is exothermic or endothermic. Final solution is indicated when the variation between  $f$  and  $\tau$  profiles from one iteration to the next is less than some specified minimum. Selection of an appropriate minimum,  $\epsilon$ , may require some computational experiments, since there can be a wide variation from one set of parameters to another. The following types of convergence criteria are typical.

$$\sum_{p=1}^N (\tau_{i-1} - \tau_i)_p \leq \epsilon_1 \quad (\text{xxii})$$

$$\sum_{p=1}^N (f_{i-1} - f_i)_p \leq \epsilon_1 \quad (\text{xxiii})$$

or

$$\text{Max}(\tau_{i-1} - \tau_i) \leq \epsilon_2$$

$$\text{Max}(f_{i-1} - f_i) \leq \epsilon_2$$

where  $i - 1$  and  $i$  are the next-to-last and last iteration steps, respectively. Equations (xxii) propose that the sum of the deviations of both profiles in the last two iterations be  $\leq \epsilon_1$ , while equation (xxiii) proposes that the maximum differences in iteration for the two profiles be  $\leq \epsilon_2$ . For comparable conditions of convergence  $\epsilon_2$  will be roughly 0.01 to  $0.1\epsilon_1$  dependent on the number of grid points. Both types of convergence criteria have been used successfully in published reports. The number of grid points required for effective solution depends upon the parametric values. In general, large heat of reaction or rate constants (leading to steep gradient) will require correspondingly finer grid spacing. Brave people blanch at the prospect of having to give quantitative rules for this. One should, of course, always carry out the solution with more than one (or several) grid spacings until the solution is invariant with this factor. Grids that are too coarse can lead to instability (nonconvergence) of this method, particularly for nonisothermal reactions.

The particular form of the coefficients  $D_p$ , and their cousins in the energy balance equations, depends on the form of kinetics under consideration. A more general derivation not restricted to the first-order case would carry the corresponding expression for  $R'$  into the right-hand term, giving a different form for  $D_p$ . For power-law kinetics, for example, an appropriate nondimensional form of equation (5-97) may be used. With this modification to the coefficients, the procedure may be used to obtain numerically the solutions previously discussed for the isothermal, one-dimensional dispersion model (see Figure 5.17).

Finally, we can make the observation that, while the iterative resubstitution method of solution is not particularly elegant, it is very effective and, indeed, rather rapid, because of the algebraic equations of the Gaussian elimination procedure.



HORATIO SAYS

This example uses the tridiagonalization procedure because it is relatively straightforward and is readily rendered into a computer program with considerable flexibility. However, this is not the only way that sets of equations like these can be solved. Your well-read mouse suggests the possibility of alternative approaches in works such as those of Douglas [J. Douglas, Jr., *A Survey of Numerical Methods for Parabolic Differential Equations*, *Advan. Computers*, 2 (1961)]; von Rosenberg [D.U. von Rosenberg, *Methods for the Solution of Partial Differential Equations*, G. Farrar, Tulsa, OK, (1984)]; and Finlayson [B.A. Finlayson, *The Method of Weighted Residuals and Variational Principles*, Academic Press, New York, NY, (1972)] among others. See also Chapter 7 for additional applications of these methods.

### 6.3.3 Parametric Sensitivity of a PFR

The illustration of nonisothermal PFR behavior at the end of Chapter 4, in Figure 4.25, showed extreme responses of temperature and partial pressure profiles to small changes in operating conditions in certain regions. Similarly, small changes in reactor parameters may result in such changes for fixed operating conditions. Such behavior has been termed the *parametric sensitivity* of the reactor; the phenomenon is distinctly different from reactor stability or multiplicity in the sense that we have discussed so far, though the terms are sometimes used interchangeably in the literature.

The basic model that has been used in most studies of parametric sensitivity is the nonisothermal PFR, for which we have seen in Chapter 4

$$-u \frac{dC}{dz} = (-r) \quad (4-42)$$

$$\rho u C_p \frac{dT}{dz} = (-r)(-\Delta H) - \frac{2U}{R} (T - T_M) \quad (4-132)$$

with initial conditions  $C_0$  and  $T_0$  specified at the inlet, and with constant heat-transfer coefficient,  $U$ , and wall temperature,  $T_M$ .<sup>5</sup>

<sup>5</sup> In fact, this corresponds relatively well to an important class of reactors in industrial practice that are subject to parametric sensitivity. Hydrocarbon oxidation reactions, highly exothermic, are often carried out in reactors resembling large shell-and-tube heat exchangers, with the tube side containing catalyst and the shell side some heat-transfer medium which serves to maintain an essentially constant tube wall temperature. "They ought to give medals to those who dare to oxidize unsaturated hydrocarbons."—J.J. Carberry

Obviously, the most important practical problem associated with parametric sensitivity is to identify conditions under which this condition is to be expected and to determine what criteria may be established to ensure its absence. In 1959, Barkelew [C.H. Barkelew, *Chem. Eng. Progr. Symp. Ser.*, 55(25), 37 (1959)] reported the results of a study aimed at determining regions of operating conditions where parametric sensitivity might exist. The analysis was based on the systematic numerical integration of equations (4-42) and (4-132) for many, many sets of parameters and the results were presented in the form of correlations in terms of kinetic and operating parameters, as illustrated in Figure 6.18. For each type of kinetics, the line indicates a region where parametric sensitivity may exist. In addition, the region surrounding the solid line for the first-order case indicates the magnitude of variation in the region of parametric sensitivity as the inlet temperature is allowed to vary from the wall temperature within the range  $T_M \pm (T_M^2 R/E)$ . The regions indicated for zero-order and second-order kinetics pertain to  $T_0 = T_M$ . These regions of parametric sensitivity indicated on the Barkelew diagram indicate only potential problems, in particular where the "hot spot" temperature may vary greatly with system parameters. The magnitude of this sensitivity or its relationship to individual parameters is not indicated and should be evaluated on a case-to-case basis. As such,

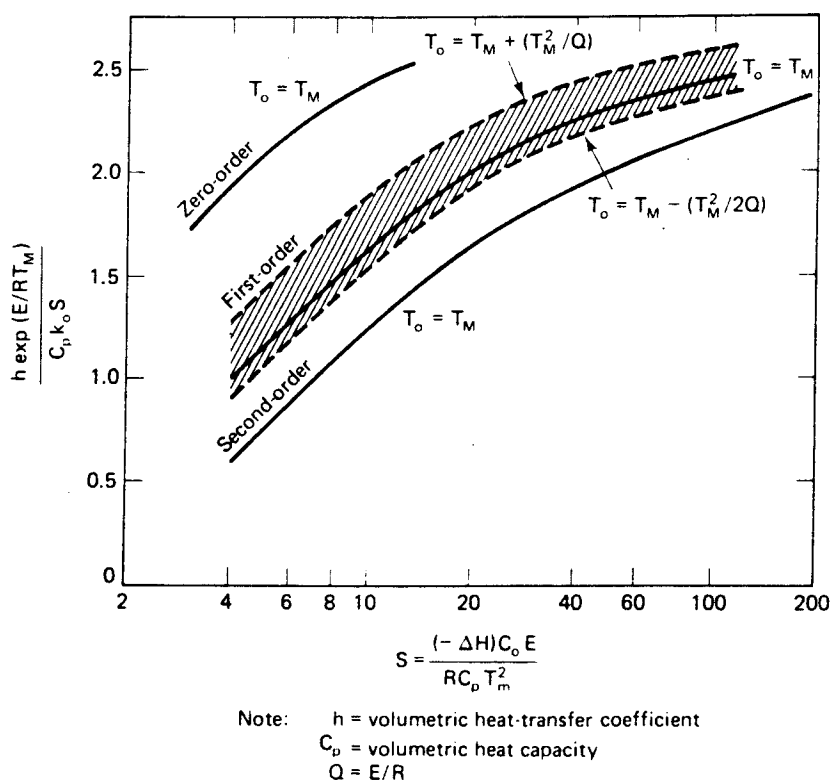


**Figure 6.18** Barkelew diagram: regions of parametric sensitivity in nonisothermal PFR operation. [After D.D. Perlmutter, *Stability of Chemical Reactors*, reprinted by permission of Prentice-Hall, Inc., Englewood Cliffs, NJ, (1972).]

the criteria established by diagrams such as Figure 6.18 tend to be conservative, and alternative approaches have been developed to produce more precise *a priori* criteria defining parametric sensitivity.

To approach the problem more quantitatively, let us focus attention on the *hot spot temperature*, that is, the maximum of the temperature profile along the length of the reactor (exothermic reactions are the subject of examination here). At this point,  $(dT/dz) = 0$ , so the rate of heat generation is equal to the rate of heat removal. From equation (4-132)

$$(-r)(-\Delta H) = \frac{2U}{R} (T_{max} - T_M) \quad (6-114)$$

where  $T_{max}$  is the maximum temperature along the reactor length. The left-hand side of equation (6-114) is a heat-generation term and the right-hand side a heat-removal term. We can thus establish some control over sensitivity by specification of some allowable  $T_{max}$  and manipulation of the heat-transfer coefficient and/or wall temperature such that

$$[-r(T_{max}, C_{max})] \leq \frac{2U}{(-\Delta H)R} (T_{max} - T_M) \quad (6-115)$$

where  $[-r(T_{max}, C_{max})]$  is the rate of reaction at the temperature maximum and  $C_{max}$  is the reactant concentration at this point. In fact, equation (6-115) is still not very much help, since if we are to know the rate at  $(T_{max}, C_{max})$  we must solve the full problem. If we are willing, however, to accept a degree of conservatism in this analysis, we can note that

$$[-r(T_{max}, C_{max})] < [-r(T_{max}, C_0)]$$

where  $C_0$  is the reactor inlet concentration. If  $T_{max}$  is specified, then  $[-r(T_{max}, C_0)]$  is known and we may use the following as design basis.

$$[-r(T_{max}, C_0)] = \frac{2U}{(-\Delta H)R} (T_{max} - T_M) \quad (6-116)$$

This analysis is shown in Figure 6.19. Two rate curves are shown,  $-r(T_{max}, C_0)$ , which we know, and  $-r(T_{max}, C_{max})$ , which we do not know but can be assured that for any temperature will be smaller than the value for  $-r(T_{max}, C_0)$ . Heat removal is represented by a straight line with a location and slope determined by  $T_M$  and  $U$ .  $T_{max}(2)$  is the design specified maximum based on  $-r(T_{max}, C_0)$ , while  $T_{max}(1)$  is actually obtained. Since the actual rate is smaller than  $-r(T_{max}, C_0)$ , the conservative result  $T_{max}(2) > T_{max}(1)$  is obtained. Artful compromise is required in such procedures, since overly conservative policies on  $U$  or  $T_M$  can result in quenching the reaction; on the other hand, the analysis is based on steady-state balances and therefore does not anticipate dynamic effects produced by the perturbation of operating conditions. It has been suggested that maximum security in design can be obtained by making the straight line for heat transfer tangent to  $-r(T_{max}, C_0)$  at the specified value for  $T_{max}$ . This yields the following specification, assuming Arrhenius temperature dependence of rate,

$$(T_{max} - T_M) = \frac{RT_{max}^2}{E} \quad (6-117)$$

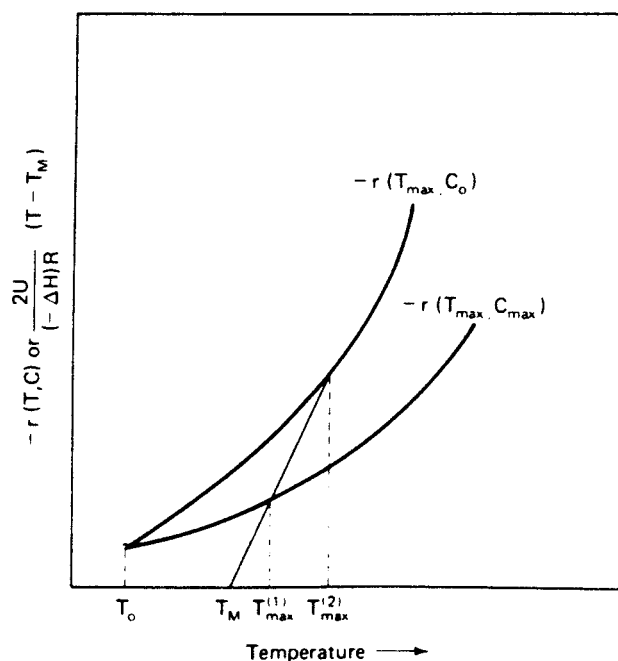


**Figure 6.19** A less conservative parametric sensitivity analysis for a nonisothermal PFR. [After P. Harriot, *Chem. Eng.*, 68(10), 165, with permission of McGraw-Hill, Inc., New York, NY, (1961).]

Further discussion of these approaches to parametric sensitivity has been given by Harriot [P. Harriot, *Chem. Eng.*, 68(10), 165 (1961)].

Now the procedure described above, although avoiding extreme conservatism, has been criticized because it requires one to specify *a priori* some allowable maximum temperature. How does one know what this is? An overly conservative guess can yield performance inferior to that allowed by the Barkelew diagram, and an overly optimistic one can lead to disaster. In the work of Van Welsenaere, which we discussed in Chapter 4, an attempt was made to eliminate this arbitrariness from the analysis and base the approach on the nature of the concentration/temperature trajectories within the reactor. For first-order kinetics let us write the heat-balance equation at the locus of the hot spot.

$$u \frac{dT}{dz} = 0 = \frac{(-\Delta H)k_0 e^{-E/RT}}{\rho C_p} C - \frac{2U(T - T_M)}{\rho R C_p}$$

from which we may obtain

$$C_{max} = \frac{T_{max} - T_M}{[(-\Delta H)R/2u]k_0 e^{-E/RT_{max}}} \quad (6-118)$$

This equation relates the concentration and temperature at the hot spot, and for a given reaction and reactor is a function of the wall temperature. The general shape of these curves is illustrated in Figure 6.20; these are called *maxima curves*. The

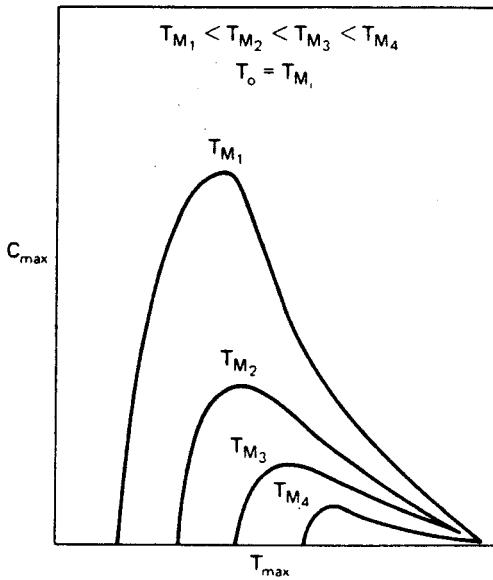


**Figure 6.20** Shapes of a series of typical maxima curves. [After R.J. Van Welsenaere and G.F. Froment, *Chem. Eng. Sci.*, 25, 1503, with permission of Pergamon Press, Inc., London, England, (1970).]

temperature corresponding to the maximum of a maxima curve, obtained from  $(dC_{max}/dT_{max}) = 0$ , is

$$(T_{max})_{max} = \frac{1}{2} \left[ \frac{E}{R} - \sqrt{\frac{E}{R} \left( \frac{E}{R} - 4T_M \right)} \right] \quad (6-119)$$

The particular importance of  $(T_{max})_{max}$  is that  $C$ - $T$  trajectories that intersect the maximum of the maxima curve are associated with parametrically sensitive behavior. One criterion proposed by Van Welsenaere and Froment for parametric sensitivity is that the “trajectory going through the maximum of the maxima curve is considered as critical and therefore as the locus of the critical inlet conditions for concentration and temperature corresponding to a given wall temperature...” In many cases  $T_0 = T_M$ , so the specification of a “critical” inlet condition means the critical inlet concentration. A lower limit (conservative) for this may be established on the basis of an adiabatic trajectory from the maximum curve, since this will automatically ensure an inlet concentration less than that which could be tolerated when heat transfer occurs. Thus,

$$\begin{aligned} [C_0(\text{critical}) - (C_{max})_{max}](-\Delta H) &= \rho C_p [(T_{max})_{max} - T_0] \\ C_0(\text{critical}) &= (C_{max})_{max} + \frac{\rho C_p}{(-\Delta H)} [(T_{max})_{max} - T_0] \end{aligned} \quad (6-120)$$

where  $(C_{max})_{max}$  is determined from equation (6-115) with  $T_{max} = (T_{max})_{max}$ , and  $(T_{max})_{max}$  is obtained from equation (6-119).

As pointed out at the beginning of this section, these analyses are limited to reactor models for which  $T_M$  is constant and independent of position. In other situations the reactor may be cooled by a countercurrent flow of coolant, and we would have a reactor/heat exchanger, as discussed in Section 6.2.

#### 6.4 Temperature Forcing of Reactors with Catalyst Decay

In previous sections we have dealt with nonisothermal effects arising from the thermochemistry of the reactions involved. There is another type of thermal effect that appears in the operation of large-scale reactors such as those used in hydrotreating. These reactors are normally subject to slow catalyst deactivation, and constant conversion operation is required in order not to upset subsequent processing units. Here the reactor temperature is used to cope with the loss of intrinsic catalyst activity and the thermal parameters of the main and deactivation reactions, particularly the activation energies, have a great influence on the operation. Further, it has been common practice in many industrial laboratories for many years to evaluate catalyst activity and activity maintenance for such processes in laboratory experiments which are also conducted under constant-conversion conditions. In this procedure, catalyst deactivation effects are manifested in the rate of temperature increase needed to maintain constant conversion, that is, a temperature increase required (TIR).

To simulate this type of operation a mixing-cell sequence is quite useful [J.B. Butt and D.M. Rohan, *Chem. Eng. Sci.*, 23, 489 (1968)]. Let us start with the familiar case of first-order kinetics for the main reaction and first-order kinetics for the deactivation, where coke deposition occurs via a reactant precursor mechanism [see scheme (XXVII) in Chapter 3]. For the main reaction we may write

$$\frac{C_0}{C_n} = \prod_1^n (1 + k_i s_i \theta) \quad (6-121)$$

where  $k_i$  is the rate constant for the main reaction,  $s_i$  the scaled activity variable ( $0 \leq s_i \leq 1$ ), and  $\theta$  is the holding time, equal in each of the  $n$  cells. We will neglect the consumption of reactant in the coke formation reaction. Now

$$\ln \left( \frac{C_0}{C_n} \right) = \sum_i^n \ln (1 + k_i s_i \theta) \quad (6-122)$$

and we require the conversion to be constant, thus,

$$\frac{d[\ln (C_0/C_n)]}{dt} = 0 = \sum_i^n \frac{d[\ln (1 + k_i s_i \theta)]}{dt} \quad (6-123)$$

Now,

$$\frac{d}{dt} [\ln (1 + k_i s_i \theta)] = \frac{\theta}{1 + k_i s_i \theta} \left( s_i \frac{dk_i}{dt} + k_i \frac{ds_i}{dt} \right) \quad (6-124)$$

so, for the sequence of mixing cells, the combination of equations (6-123) and (6-124) gives us

$$\sum_i^n \left[ \frac{s_i (dk_i/dt) + k_i (ds_i/dt)}{(1 + k_i s_i \theta)} \right] = 0 \quad (6-125)$$



where  $k_i = k_i^\circ e^{-E/RT}$ . We may write

$$\frac{dk_i}{dt} = \frac{dk_i}{dT_i} \frac{dT_i}{dt} = \frac{k_i}{RT_i^2} \frac{dT_i}{dt} \quad (6-126)$$

so

$$\sum_i^n \left[ \frac{s_i(k_i/RT_i^2)(dT_i/dt) + k_i(ds_i/dt)}{(1 + k_i s_i \theta)} \right] = 0 \quad (6-127)$$

Now for the deactivation kinetics we have

$$\frac{ds_i}{dt} = k_{di} s_i C_i \quad (6-128)$$

where  $k_{di}$  is the deactivation rate constant in cell  $i$ . Substituting this into equation (6-127) and rearranging gives

$$\sum_i^n \frac{s_i(k_i/RT_i^2)(dT_i/dt)}{(1 + k_i s_i \theta)} = \sum_i^n \frac{k_i k_{di} s_i C_i}{(1 + k_i s_i \theta)} \quad (6-129)$$

For isothermal conditions,  $(dT_i/dt) = (dT/dt)$  and we may solve for the TIR directly.

$$\frac{dT}{dt} = \frac{\sum_i^n k k_{di} s_i C_i}{\sum_i^n s_i (k/RT^2)} \quad (6-130)$$

with the concentrations of reactant as

$$\frac{C_i}{C_0} + (1 + k s_i \theta)^{-i} \quad (6-131)$$

The simplifications realized in equation (6-130) arise from the isothermality, hence  $T_i = T$ , and so on. If it is wished to retain generality in the model where the mechanism (and kinetics) of deactivation is concerned, then

$$\frac{dT}{dt} = \frac{\sum_i^n k(ds_i/dt)}{\sum_i^n s_i (k/RT^2)}; \quad s_i = 1 \quad t = 0 \quad (6-132)$$

$$\quad (6-133)$$

Now for the restriction to a constant conversion operation, in addition to the initial condition above, the temperature must satisfy the following requirement.

$$\ln \left( \frac{C_0}{C_n} \right) = \text{specified constant} = \sum_i^n \ln(1 + \theta k_i^\circ e^{-E/RT}) \quad (6-134)$$

Let us now turn to the construction of a similar analysis for constant-conversion operation in an adiabatic reactor, ignoring the effects of axial thermal

conductivity. The conservation equations about cell  $i$  are

$$FC_{i-1} - FC_i = \bar{V}k_i s_i C_i \quad (6-135)$$

$$FC_p T_i - FC_p T_{i-1} = (-\Delta H) \bar{V}k_i s_i C_i \quad (6-136)$$

where  $F$  is the volumetric flow rate,  $\bar{V}$  the reactor volume, and  $C_p$  a volumetric heat capacity. The direction of  $T_i > T_{i-1}$  is implied in the energy balance, assuming an exothermic reaction. Then

$$C_{i-1} - C_i = k_i s_i \theta C_i \quad (6-137)$$

$$T_i - T_{i-1} = k_s s_i \beta C_i \quad (6-138)$$

where  $\theta = \bar{V}/F$  and  $\beta = \bar{V}(-\Delta H)/FC_p$ . As before

$$\frac{C_n}{C_0} = \frac{1}{\prod_i^n (1 + k_i s_i \theta)} \quad (6-139)$$

and since temperature varies throughout the sequence,  $k_i = k^\circ \exp(-E/RT_i)$ . Substituting for  $C_i$  in the energy balance of equation (6-138)

$$T_i - T_{i-1} = \frac{k^\circ s_i \beta e^{-E/RT_i}}{\prod_i (1 + k^\circ s_i \theta e^{-E/RT_i})} \quad (6-140)$$

The difficulty in this is the awkward form of equation (6-140) with respect to  $T_i$ . One likes to compute in sequence through the series of cells, but here we face the implicit form of  $T_i$  as a function of  $T_{i-1}$ . This is the same basic difficulty that limits the utility of the CSTR sequence as an analytical model for nonisothermal reactors. For the case here though, where we employ a relatively large value of the index  $n$  in approximation of a plug-flow reactor, and where the solution will be via numerical methods anyway, we will strong-arm the problem with the approximation  $T_i \approx T_{i-1}$  in the exponentials, so that

$$T_i = T_{i-1} + \frac{k^\circ \beta e^{-E/RT_{i-1}}}{\prod_i (1 + s_i k^\circ \theta e^{-E/RT_{i-1}})} \quad (6-141)$$

with the requirement that

$$\frac{C_n}{C_0} = \text{constant} = \frac{1}{\prod_i^n (1 + k^\circ \theta e^{-E/RT_i})} \quad (6-142)$$

to establish the initial adiabatic profile [ $s_i = 1$  in equation (6-141) for initial operation]. After computation of the initial set of  $T_i$ , we increment  $s$

$$\frac{ds_i}{dt} = -k_d^\circ e^{-E_d/RT_i} s_i C_i \approx \frac{\Delta s_i}{\Delta t} \quad (6-143)$$

If  $j$  is a time index, with  $j = 0$  initially, then we solve for  $(s_i)_{j+1}$  and the temperature profile for  $t_{j+1}$

$$(s_i)_{j+1} = (s_i)_j - [k_d^\circ(s_i)_j(C_i)_j e^{-E_d/RT_j}](t_{j+1} - t_j) \quad (6-144)$$

$$T_{i,j+1} = T_{i-1,j+1} + \frac{k^\circ \beta e^{-E/RT_{i-1,j+1}} s_{i,j+1}}{\prod_i (1 + k^\circ e^{-E/RT_{i-1,j+1}} s_{i,j+1})} \quad (6-145)$$

with the requirement

$$\frac{C_n}{C_0} = \text{constant} = \frac{1}{\prod_i^n (1 + k^\circ \theta e^{-E/RT_{i,j+1}} s_{i,j+1})} \quad (6-146)$$

As an example concentration profiles for A in a Type II reaction, isothermal, are given by

$$[a]_n = \frac{1}{\prod_1^n [1 + (k_A^\circ \Phi_{A,n} + k_{A,d}^\circ \Phi_{d,n}) S_0 \theta(s)_n]} \quad (6-147)$$

where  $\Phi_{m,n} = \exp[\gamma_m(1 + 1/\phi_n)]$ ,  $n$  is the mixing cell number,  $\theta$  the holding time per cell,  $\gamma_m$  is the temperature sensitivity of reaction  $m$ ,  $E_m/RT_0$ ,  $k_A^\circ S_0$  are specific rate constants for the undecivated catalyst; and  $T_0$  is a reference temperature, normally the initial operating temperature. For slow deactivation

$$(-r) = \frac{d(s)}{d\beta} = \tau(A_0/S_0) k_{A,d}^\circ S_0 \Phi_{d,n} [a]_n [s]_n \quad (6-148)$$

where  $\tau$  is the total residence time in the reactor and  $\beta$  the total time of operation in terms of number of residence times. The kinetics of the main reaction incorporated into equation (6-147) include loss of reactant due to coke formation. The quantity  $S_0$ , which has not appeared our previous discussion, is a scaling constant that essentially refers to the total number of active sites per unit area on the fresh catalyst surface.

Some characteristics of reactor behavior are shown in Figure 6.21, where reactor temperature versus time of operation is illustrated for operation with constant conversion of 60% for the Type II reactant fouling case. The parameter  $X$  of the figure is the residence time-concentration grouping appearing in the deactivation rate equation,  $X = \tau(A_0/S_0) k_{A,d}^\circ S_0$ . The exponential nature of the increase is evident, representing the “activated” reaction process, though one obtains a near-linear correlation over a certain range of processing time, depending on the parameters of the reaction system-principal. These parameters are the intrinsic selectivity  $\psi$  between main and deactivation reactions, given by  $(k_A^\circ/k_{A,d}^\circ)$ , and the relative temperature sensitivity of the two reactions, given by  $(\gamma_A/\gamma_{A,d})$ . The initial temperature of operation indicated in Figure 6.21 is determined wholly by the intrinsic activity of the catalyst for the main reaction; deactivation, reasonably enough, has no effect on initial operation. In these examples the reduced temperature  $\phi$  is defined with respect to the reference temperature  $T_0$  used in the definition of  $\gamma$ , so  $\phi = T/T_0$ . Operation

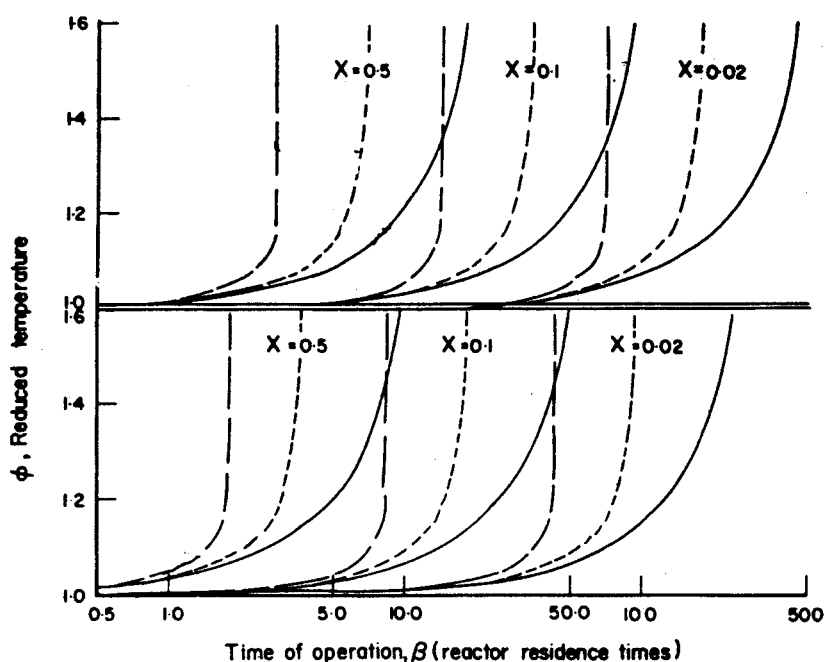


**Figure 6.21** Effect of catalyst deactivation on reactor operation: temperature increase at constant conversion for type II reactant deactivation. Top:  $\psi = 20$ ,  $\gamma_A = 10$ ; bottom:  $\psi = 10$ ,  $\gamma_A = 10$ . Left curves:  $\gamma_{A,d} = 3\gamma_A$ ; middle curves:  $\gamma_{A,d} = \gamma_A$ ; right curves:  $\gamma_{A,d} = 0.2\gamma_A$ . [After J.B. Butt and D.M. Rohan, *Chem. Eng. Sci.*, 23, 489, with permission of Pergamon Press, Ltd., London, England, (1968).]

at  $\phi = 1$  implies catalyst activity at a level just sufficient to meet the specified conversion with  $T = T_0$ .

An appealing theoretical approach for reactor behavior in the case when deactivation rates are functions of the activity level alone (often the case in deactivation by sintering of supported metals) was given by Krishnaswamy and Kittrell [S. Krishnaswamy and J.R. Kittrell, *Ind. Eng. Chem. Proc. Design Devel.*, 18, 399 (1979)]. Thus, we write for the rate of deactivation

$$(-r_d) = -\frac{ds}{dt} = k_d s^n \quad (6-149)$$

where  $s$  is the usual activity variable and  $n$  any arbitrary power of the deactivation kinetics. The relationship between temperature and time-on-stream is obtained in the following way, assuming that conversion is time-independent. We have that

$$k_d = A_d \exp(-E_d/RT) \quad (6-150)$$

and the normal conversion requirement that

$$k \cdot s = k_0 \quad (6-151)$$

where  $k_0$  is the value of the rate constant at the start of run temperature,  $T_0$ , and

$$k = A_A \exp(-E_A/RT) \quad (6-152)$$

Combining the last two expressions gives

$$\frac{1}{T} = \left(\frac{R}{E_A}\right) \ln s + \left(\frac{1}{T_0}\right) \quad (6-153)$$

as the requirement for constant conversion. If we then substitute equations (6-153) and (6-150) into the activity expression and integrate with respect to time, a time-activity relationship is obtained directly

$$t = \frac{\exp(E_d/RT_0)}{A_d(E_d/E_A - n + 1)} (1 - s^{(E_d/E_A) - n + 1}) \quad (6-154)$$

Substitution of equation (6-153) into (6-154) gives the desired time-temperature relationship

$$t = \frac{\exp(E_d/RT_0)}{A_d(E_d/E_A - n + 1)} \left\{ 1 - \exp \left[ \frac{E_d - E_A n + E_A}{R} \left( \frac{1}{T} - \frac{1}{T_0} \right) \right] \right\}$$

In the case that  $n = 2$  (often the case for sintering) and  $E_d = E_A$ , this expression is rewritten as

$$t = \frac{\exp(E_d/RT_0)}{A_d} \left( \frac{E_A}{R} \right) \left( \frac{1}{T_0} - \frac{1}{T} \right) \quad (6-156)$$

The central point of the analysis is to recognize that equation (6-155) is of the form

$$t = C(1 - e^{AY})$$

where

$$C = \frac{\exp(E_d/RT_0)}{A_d(E_d/E_A - n + 1)}; \quad A = \frac{(E_d - E_A n + E_A)}{R} \quad (6-157)$$

$$Y = \left( \frac{1}{T} - \frac{1}{T_0} \right)$$

Thus, if one plots data of  $t$  versus  $(1/T)$  and subdivides the reciprocal temperature axis into four equal segments, that is,

$$\left( \frac{1}{T_0} - \frac{1}{T_1} \right), \left( \frac{1}{T_1} - \frac{1}{T_2} \right), \left( \frac{1}{T_2} - \frac{1}{T_3} \right), \left( \frac{1}{T_3} - \frac{1}{T_4} \right)$$

then

$$C = \frac{(t_1 t_4 - t_2 t_3)}{(t_1 + t_4) - (t_2 + t_3)} \quad (6-158)$$

where  $t_1$  is the time corresponding to  $(1/T_1)$ . Now, having obtained an estimate of the value of  $C$ , let us rearrange equation (6-157) to the form

$$\ln(1 - t/C) = AY \quad (6-159)$$

It is then possible to plot the left-hand side of equation (6-159) versus  $Y$  and, of course, if the result is linear to conclude that the model provides a valid representation of the TIR data.

The application of this analysis to experimental data on both hydrocracking and reforming reactions was demonstrated by Krishnaswamy and Kittrell. In the

case of hydrocracking, for example, a simple deactivation model with  $n = 1$  provided an excellent correlation of the data, although the analysis is not limited to linear deactivation kinetics. Once values of the constants  $A$  and  $C$  are known one can extract values of the individual activation energies from the definition of  $A$

$$E_d = AR + E_A(n - 1) \quad (6-160)$$

A further discussion of the analysis of constant conversion policies in reactions with catalyst deactivation was given by Ho [T.C. Ho, *J. Catal.*, 86, 48 (1984)], and an excellent experimental example was provided in the work of Tamm, et al. [P.W. Tamm, H.F. Harnsberger, and A.G. Bridge, *Ind. Eng. Chem. Proc. Devel.*, 20, 262 (1981)].

## Exercises

### Section 6.1

1. Determine the number of CSTR steady-state operating temperature and their values for the following two sets of parametric values and equation (4-135).\*

Case I	Case II
$\rho CP = 50 \text{ Btu/ft}^3 \cdot F$	$(-\Delta H_R / \rho C_p) = 200^\circ \text{K-liter/gmol}$
$T_0 = T_M = 530 \text{ R}$	$T_0 = T_M = 350^\circ \text{K}$
$UA = 500 \text{ Btu/h} - F$	$UA / v \rho C_p = 1$
$\bar{V} = 100 \text{ ft}^3$	$v / \bar{V} = 1 \text{ min}^{-1}$
$(-\Delta H) = 10^4 \text{ Btu/lbmol}$	$k_0 = e^{25} \text{ min}^{-1}$
$k_0 = 10^8 \text{ h}^{-1}$	$E/R = 10^4 \text{ }^\circ \text{K}$
$E/R = 10^4 \text{ R}$	$C_{A0} = 1 \text{ gmol/liter}$
$v = 200 \text{ ft}^3/\text{h}$	
$C_{A0} = 0.270 \text{ lmol/ft}^3$	

2. Examine Case II above in view of the stability criteria of equation (6-38).
3. Consider the case of a reversible reaction  $A \leftrightarrow B$  as carried out in a CSTR. Thus, we have as mass balances

$$\bar{V}(dC_A/dt) = v(C_{A0} - C_A) - \bar{V}[r(C_A, C_B)]$$

$$\bar{V}(dC_B/dt) = v(C_{B0} - C_B) + \gamma \bar{V}[r(C_A, C_B)]$$

where  $\gamma$  is a stoichiometric ratio. This reaction is conducted under conditions where thermal effects are not important, but the reaction rate written in general form is given by

$$r(C_A, C_B) = k_1(C_A)^n - k_2(C_B)^m$$

It may be assumed in the kinetic correlation that  $n$  and  $m$  are both  $> 0$ . Using the procedures outlined in Section 6.1, determine a simple uniqueness criterion for this system.

\* Case I is from J.S. Berger and D.D. Perlmutter, *Amer. Inst. Chem. Eng. J.*, 10, 233 (1964); Case II is from R. Aris and N.R. Amundson, *Chem. Eng. Sci.*, 7, 121 (1958).

## Section 6.3

4. (a) Using the nonisothermal one-dimensional dispersion model, solve for conversion and temperature as a function of length along the reactor for a reaction system with the following parameters.

$$\begin{array}{ll}
 N_{Pe} = 10 & U = 0.15 \text{ cal/cm}^2\text{-s-K} \\
 T_0 = 768^\circ\text{K} & \tau_M = 1 \\
 u = 1000 \text{ cm/s} & \rho C_p = 8.12 \times 10^{-5} \text{ cal/cm}^3\text{-K} \\
 L = 100 \text{ cm} & (-\Delta H) = 7000 \text{ cal/gmol} \\
 R = 3 \text{ cm} & E = 3500 \text{ cal/gmol} \\
 (-r) = kf; \quad k_0 = 35 \text{ s}^{-1} & C_0 = 0.5 \text{ mol/liter}
 \end{array}$$

(b) Once a converged solution is obtained for case (a), explore the sensitivity of the profiles to the value of  $N_{Pe}$ . The range  $2 < N_{Pe} < 20$  is reasonable.

5. Determine the range of exit temperatures corresponding to adiabatic operation ( $hL/aC_p = 0$ ) shown in Figure 6.17a.
6. (a) Using the parameters for naphthalene oxidation given in Figure 4.23, estimate the critical inlet concentration (lower limit) for runaway according to the procedure of Van Welsenaere and Froment.

(b) What is the sensitivity of  $C_0$  (critical) to the inlet temperature if it is greater than  $T_M$ ? That is, what is the value of  $[dC_0 \text{ (critical)}/dT_0]$  for this case?

## Notation

$A$	coefficient matrix, after equation (6-34); heat transfer area
$A, B, C, Y$	constant defined after equation (6-157)
$A_A$	pre-exponential factor for main reaction, $\text{time}^{-1}$
$A_d$	pre-exponential factor for deactivation reaction $\text{time}^{-1}$
$A_1, B_1, D_1$	constants associated with $(dC_A/dt)$ in equation (6-39)
$A_2, B_2, D_2$	Constants associated with $(dT/dt)$ in equation (6-40)
$[a]_n$	concentration profile for A
$a_{11}, a_{12}, a_{21}, a_{22}$	coefficients of $x$ in linearized balance equations, after equation (6-33)
$C$	reactant concentration, mols/volume
$C_A, C_B$	concentration of A, B, mols/volume
$C_n$	reactant concentration leaving sequence of $n$ CSTR, mols/volume
$C_i$	reactant concentration in CSTR unit $i$ , mols/volume
$C_0$	inlet reactant concentration, mols/volume
$C_p$	volumetric heat capacity, $\text{kcal/volume-}^\circ\text{C}$ ; molal heat capacity, $\text{kcal/mol-}^\circ\text{C}$ ; see equation (6-74)
$C_{A0}$	inlet concentration of A, mols/volume
$C_{As}$	steady-state concentration of A, mols/volume
$C_{pc}$	coolant heat capacity, $\text{kcal/volume-}^\circ\text{C}$
$C_{max}$	reactant concentration at $T_{max}$ , mols/volume
$(C_{max})_{max}$	concentration corresponding to $(T_{max})_{max}$ , mols/volume

- $D$  axial dispersion coefficient, area/time  
 $d_p$  catalyst dimension, length  
 $E, E_A$  activation energy for main reaction, kJ or kcal/mol  
 $E_d$  activation energy for deactivation reaction, kJ or kcal/mol  
 $E'$  energy dispersion coefficient; see equation (6-113)  
 $F$  volumetric flow rate, volume/time  
 $F_{in}$  inlet molar flow rate, mols/time  
 $f(C)$  concentration function; see equation (i), Illustration 6.2  
 $f(C_A)$  concentration function for A; see equation (6-53)  
 $f(x_0, y_0)$  function at  $x_0, y_0$  in Taylor series expansion  
 $f(x_0 + n, y_0 + k)$  function at increment of  $h, k$  in Taylor series expansion  
 $f(\theta)$  function of reduced temperature; see equation (6-41)  
 $f_1(C, \eta), f_2(C, \eta)$  general functions of  $C, \eta$ ; see equations (6-111) and (6-112)  
 $G_1, G_2$  constants in equation (xvi), Illustration 6.3  
 $(-\Delta H)$  heat of reaction, kcal/mol or kJ/mol  
 $h$  wall heat-transfer coefficient, kJ or kcal/time-°C, K  
 $h_G$  heat-transfer coefficient, energy/time-K; see Illustration 6.3  
 $K$  adsorption parameter of equation (vii), Illustration 6.2  
 $k$  rate constant, units depend upon reaction order  
 $k_d$  deactivation rate constant, time<sup>-1</sup>  
 $k_{di}$  deactivation rate constant in CSTR unit  $i$  time<sup>-1</sup>; see equation (6-128)  
 $k_G$  mass-transfer coefficient, volume/time; see Illustration 6.3  
 $k_i$  rate constant in CSTR unit  $i$   
 $k_0$  pre-exponential factor, time<sup>-1</sup>  
 $k_i^\circ$  pre-exponential factor for  $k_i$ , time<sup>-1</sup>  
 $k_A S_0, k_{A,d}^\circ S_0$  rate constant for fresh catalyst  
 $k_1, k_2, K_3$  rate constant for oxidation chain reaction; see equation (6-55)  
 $L$  reactor length  
 $M_g, M_r$  rate and concentration factors; see equations (6-54a,b)  
 $n$  reaction order  
 $Q$  constant =  $(E/R)$   
 $q_g, q_r$  heat generation and removal functions, energy/time  
 $R$  gas constant; kJ or kcal/mol-K; reactor radius, length  
 $(-r)$  rate of reaction, mole/volume-time  
 $-r_1(C_A), (-r_1)$  rate of reaction of A, mols/volume-time  
 $-r_2(C_B), (-r_2)$  rate of reaction of B, mols/volume-time  
 $(-r_d)$  rate of deactivation  
 $[-r(T_{max}, C_0)]$  rate at  $T_{max}, C_0$ , mols/volume-time  
 $[-r(T_{max}, C_{max})]$  rate at  $T_{max}, C_{max}$ , mols/volume-time  
 $s$  scaled activity variable  $0 < s < 1$   
 $s_i$  activity variable in CSTR unit  $i$   
 $\Delta s_i$  activity increment  
 $T$  temperature, °C or °K  
 $T_A, T_B, T_C$  temperature operating points, Figure 6.7  
 $T_F$  feed temperature, °C, °K  
 $T_i$  inflection temperature; see equation (6-68); temperature in CSTR unit  $i$ , °C, °K  
 $T_L$  reactor outlet temperature, °C



$T_M$	reactor wall or coolant temperature, °C
$T_0$	inlet temperature; temperature after inlet heat exchanger; initial operating temperature, °C, °K
$\Delta T_0$	constant = $[(-r)(-\Delta H)L/\rho u C_p]$
$T_s$	reactor steady-state operating temperature, °C, °K
$T_w$	wall temperature, °C, °K
$T_1, T_2$	heat exchanger inlet and outlet temperatures, °C, °K
$T_{max}$	maximum temperature, along reactor length, °C, °K
$(T_{max})_{max}$	temperature maximum of a maxima curve, °C, °K; see equation (6-119)
$t$	time; coolant temperature, °C
$\Delta t$	time increment
$t_L, t_0$	inlet and outlet coolant temperatures, °C; see Figure 6.14
$t_1 \cdots t_4$	times corresponding to $(1/T_1) \dots (1/T_4)$ ; see equation (6-158)
$\bar{t}$	CSTR residence time
$U$	heat-transfer coefficient, energy/area-time-°C, °K, or energy/time-°C, °K; see Illustration 6.3
$U'$	UA, kcal/time-°C
$u$	axial velocity, length/time
$u_c$	axial velocity of coolant, length/time
$\bar{V}$	reactor volume
$v$	volumetric flowrate, volume/time; molar flow rate, mols/time; see equation (6-81)
$X$	operating parameter = $\tau(A_0/S_0)k_{A,d}^\circ S_0$
$\mathbf{x}$	$x$ matrix
$x_1$	deviation variable = $(C_{As} - C_A)$
$x_2$	deviation variable = $(T_s - T)$
$y(z), y(Z)$	mol fraction reactant at $z$ and $Z$
$y_{in}$	mol fraction reactant in
$Z, Z'$	reactor length; heat exchanger length
$z, z'$	reactor and heat exchanger length variable

### Greek

$\alpha$	heat of reaction factor after equation (6-48); constant = $(1 + k_G/v)$ ; parameter of equation (6-90a); energy dispersion term in equation (6-98)
$\beta$	parameter in equations (6-70) and (6-71); constant = $[V(-\Delta H)/FC_p]$ ; see equation (6-138)
$\gamma$	slope of $y(z)$ versus $T(z)$ ; see equation (6-89) and Figure 6.13; parameter in equation (6-91a)
$\gamma_i$	constant = $(E_i/RT_0)$
$\epsilon_H$	heat exchange capacity; see equation (6-73)
$\zeta$	nondimensional length variable
$\zeta_{max}$	quantity defined in equation (6-96)
$\eta, \eta_0$	dependent variable in equation (6-116); initial value of $\eta$
$\theta, \theta_0, \theta_M$	reduced temperature = $[C_p T_j/(-\Delta H)]$ , with $T_j = T, T_0, T_M$
$\theta_w$	reduced wall temperature = $(T/T_w)$
$\lambda_1, \lambda_2$	eigenvalues defined in equation (6-37)
$\rho, \rho_c$	density, mols/volume; coolant density

$\tau$	independent variable in equations (6-111) and (6-112); total residence time in reactor; see equation (6-148)
$\phi_{i,n}$	function = $\exp[\gamma_i(1 + 1/\phi_n)]$
$\phi$	nondimensional temperature = $(T - T_0)/\Delta T_0$ or $(T/T_0)$
$\phi_{max}$	maximum of $\phi$ ; see equation (6-95)
$\chi$	nondimensional temperature = $(t - T_p)/\Delta T_0$
$\phi$	uniqueness factor, after equation (6-56)
$\omega, \omega_0$	combined variable = $(\theta + C)$ ; constant = $(\theta_0 + C_0)$

# 7

---

## Reactions in Heterogeneous Systems

Though it be honest, it is never good  
to bring bad news

— *William Shakespeare*  
(Antony and Cleopatra)

With the exception of the discussion of reactions on surfaces in Chapter 3 and some references to fixed-bed reactors in Chapters 5 and 6, we have largely been concerned with reactions in homogeneous phases (or pretended so) and corresponding reactor models. Although those models are not completely restricted to reactions in homogeneous phases, there are a number of properties of reactions in heterogeneous systems, particularly when we get down to more detailed analysis, which are sufficiently important that they must be treated separately.

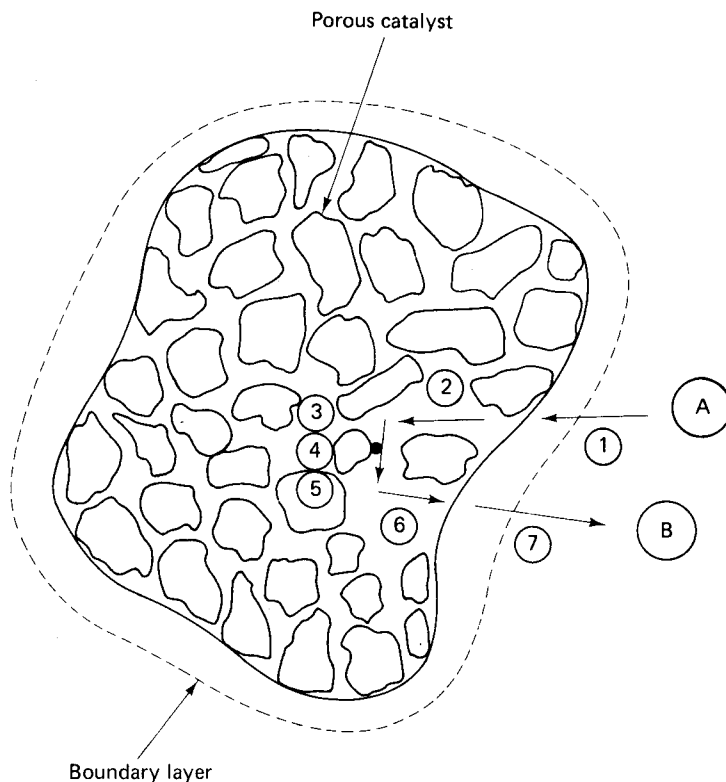
Ordinarily two phases are involved: gas/solid, gas/liquid, or liquid/solid. Other important applications can involve three phases, and some of these will be treated in Chapter 8. The most important case of heterogeneous reaction must be the gas/solid system, which is typical of most catalytic processes; fortunately, the same general principles pertain to the analysis of all two-phase systems of interest here, so separate developments on a case-by-case basis are not required.

The primary feature of heterogeneous systems is that the purely physical problem of transporting reactants and products between phases is appended to the chemical transformation. Stated alternatively, a physical rate process (transport) occurs in series with a chemical rate process (reaction). As nature would have it, often these rates are of similar magnitudes and the overall behavior of the reaction system depends on their relative magnitude, not only in terms of the net kinetics of transformation but also with regard to the product selectivity in complex reactions.

In this chapter we shall develop the theory at a basic level for reactions in some two-phase systems, then discuss applications to reactor modeling and design some specific examples.

### 7.1 Reactions in Gas/Solid Systems

Heterogeneous catalytic reactions by their nature involve a serial transport/reaction rate process, since the reaction species must be transported to and removed from the surface site where the chemical transformation occurs. Much of the theory rests on the simplified picture of the combined reaction and transport process shown in



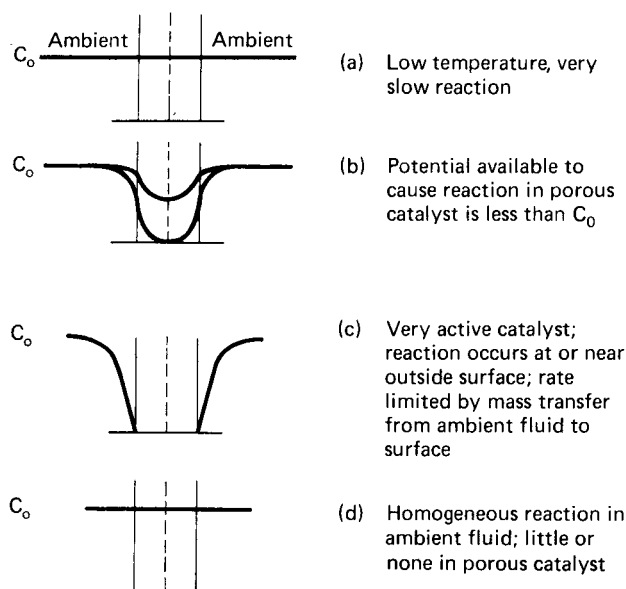
**Figure 7.1** Sequential steps involved in a catalytic reaction.

Figure 7.1. The catalyst particle, containing a large surface area per unit volume, is bathed in reaction mixture as illustrated for a reactant molecule A and a product molecule B. For the overall transformation, the following sequence is necessary:

1. Diffusion of A through a boundary layer or “film” adjacent to the external surface of the catalyst.
2. Diffusion of A through the porous interior of the catalyst to the point at which adsorption/reaction occurs.
- 3., 4., and 5. Sequence of adsorption, surface reaction, and desorption, the details of which determine the intrinsic kinetics of the catalytic reaction.
6. Diffusion of B through the porous structure to the external surface.
7. Diffusion of B through the external boundary layer into the bulk gas phase.

Note that there is nothing in the above sequence that is specific to the gas phase, thus these concepts, and the developments below, are valid for liquid/solid systems as well.

If the intrinsic rate of the surface reaction steps 3 to 5 is slow, the rate of transport through the surrounding media would easily be great enough to supply instantaneously a molecule of A as needed for reaction and to remove the product B molecule when it was formed. Thus, when the intrinsic kinetics are slow, the overall



**Figure 7.2** Concentration profiles in a porous catalyst under different reaction regimes. [After C.N. Satterfield, *Mass Transfer in Heterogeneous Catalysis*, with permission of MIT Press, Cambridge, MA, (1970).]

transport/reaction process occurs without the establishment of significant concentration gradients within the porous catalyst particle or in the surrounding boundary layer. However, when the intrinsic reaction kinetics are of similar magnitude to the mass transport rates, gradients in concentration will be necessary to produce the required rate of supply and removal of reactants and products. It is convenient to visualize relative mass transfer and reaction rates in terms of these *intraparticle* gradients as, indeed, they have a profound effect on the behavior of the catalyst as a whole.

In Figure 7.2 is a simple representation of gradients for several cases of relative mass transfer/reaction rates. Since these gradients are established when transport rates become finite, the net effect is to reduce the overall rate of reaction due to the lower incident concentration of reactant within the catalyst as compared to external surface (or bulk) concentration. The net activity of the catalyst is diminished, and it is common to define this quantitatively in terms of the catalytic *effectiveness factor*, given by

$$\eta = \frac{\text{observed rate of reaction}}{\text{rate of reaction at surface concentration}} \quad (7-1)$$

The definition of equation (7-1) does not envision differences between bulk and external surface concentrations, a point that will be discussed later. We will first treat the problem of transport limitations within the porous matrix (intrapphase), then the combination of boundary-layer (interphase) transport with the intrapphase effects.<sup>1</sup>

<sup>1</sup>“Two gifts perforce he has given us yet.”—A.C. Swinburne

Except for the discussion of some specific forms of complex rate equations and references to several specific studies of various reactions, we must again be content in the following with those ubiquitous reaction species A and B, and occasionally C, for purposes of selectivity. The rationale for this approach is that while there are tangible chemical objectives ultimately involved, mass- and energy-transport processes are basically physical and illustration of their effects is best served by using the conventions of “nonchemical” kinetics.

Comprehensive treatments of the theory and application of diffusion and chemical reaction have been given in the following classical works [D.A. Frank-Kamenetskii, *Diffusion and Heat Transfer in Chemical Kinetics*, 2nd ed., Plenum Press, NY, (1969); C.N. Satterfield, *Mass Transfer in Heterogeneous Catalysis*, MIT Press, Cambridge, MA, (1970); R. Aris, *The Mathematical Theory of Diffusion and Reaction in Permeable Catalysts*, Clarendon Press, Oxford, England, (1975)].

### 7.1.1 Steady-State Diffusion and Chemical Reaction in Porous Catalysts Under Isothermal Conditions

Some of the first considerations of the problem of diffusion and reaction in porous catalysts were reported independently by Thiele [E.W. Thiele, *Ind. Eng. Chem.*, 31, 916 (1939)]; Damköhler [G. Damköhler, *Der Chemie-Ingenieur*, 3, 430 (1937)] and Zeldovich [Ya.B. Zeldovich, *Acta Phys.-Chim. USSR*, 10, 583 (1939)]; although the first solution to the mathematical problem was given by Jüttner in 1909 [F. Jüttner, *Z. Phys. Chem.*, 65, 595 (1909)]. Consider the porous catalyst in the form of a flat slab of semi-infinite dimension on the surface, and of half-thickness  $W$  as shown in Figure 7.3. The first-order, irreversible reaction  $A \rightarrow B$  is catalyzed within the porous matrix with an intrinsic rate  $(-r)$ . We assume that the mass-transport process is in one direction though the porous structure and may be represented by a normal diffusion-type expression, that there is no net convective transport contribution, and that the medium is isotropic. For this case, a steady-state mass balance over the differential volume element  $dz$  (for unit surface area) (Figure 7.3), yields

$$D_{eff} \frac{d^2 C_A}{dz^2} - (-r) = 0 \quad (7-2)$$

This model represents the catalyst as a pseudo-homogeneous medium in which the effective transport coefficient for the reactant,  $D_{eff}$ , is in general a complex function

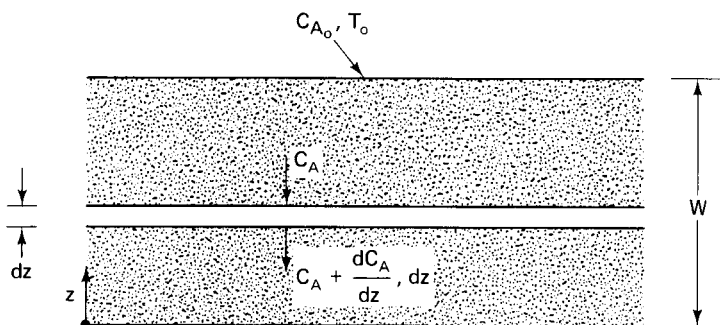


**Figure 7.3** Diffusion and reaction in a semi-infinite slab of porous catalyst.

of the porous structure and composition, some aspects of which we will consider in more detail later. It is normally a sufficient approximation, however, to treat  $D_{eff}$  as a constant. The boundary conditions corresponding to equation (7-2) specify conditions at the external surface and have a symmetry at the center

$$C_A = C_{A_0}, \quad z = W; \quad \frac{dC_A}{dz} = 0, \quad z = 0 \quad (7-3)$$

For first-order kinetics,  $(-r) = kC_A$  and equation (7-2) may be written in nondimensional form as

$$\frac{d^2 f}{d\zeta^2} - W^2 \left( \frac{k}{D_{eff}} \right) f = 0 \quad (7-4)$$

with

$$f = \frac{C_A}{C_{A_0}}, \quad \zeta = \frac{z}{W}$$

The quantity  $W^2(k/D_{eff})$  relates the relative magnitudes of the rate parameters for chemical reaction and mass transport and hence is a characteristic property of the overall system. It is most often called the *Thiele modulus*,  $\phi$ , defined by

$$\phi^2 = W^2 \left( \frac{k}{D_{eff}} \right) \quad (7-5)$$

The solution of equation (7-4) for the concentration profile of reactant A through the slab is

$$f = \frac{C_A}{C_{A_0}} = \frac{\cosh(\phi\zeta)}{\cosh \phi} \quad (7-6)$$

The total rate of reaction can be obtained via Fick's law for the mass flux at the external surface (for steady state this is equal to the rate of reaction), using the concentration gradient evaluated at that point from equation (7-6). For unit surface area,

$$N_A = \text{total rate} = -D_{eff} \left( \frac{dC_A}{dz} \right)_W \quad (7-7)$$

This result is

$$N_A = \frac{D_{eff} C_{A_0}}{W} \phi \tanh \phi$$

We recall that the net effect on the intrinsic activity of the catalyst caused by the presence of a concentration gradient is defined in terms of the effectiveness factor of equation (7-1). The overall rate in the absence of gradients is  $kC_{A_0}W$  (for unit surface area), so

$$\eta = \left( \frac{1}{kC_{A_0}W} \right) \left( \frac{D_{eff} C_{A_0}}{W} \phi \tanh \phi \right) = \frac{\tanh \phi}{\phi} \quad (7-8)$$

The net rate of reaction per unit volume of catalyst is then given by

$$(-r)_{net} = \eta k C_{A_0} = \frac{\tanh \phi}{\phi} k C_{A_0} \quad (7-9)$$

When the diffusional influence is very pronounced, that is, when  $D_{eff} \ll k$ ,  $\phi$  becomes large and  $\tanh \phi$  approaches unity. The effectiveness factor for this *strong diffusion limit* is

$$\eta = \frac{1}{\phi}$$

The results above are very specific to the geometry employed in Figure 7.3. For spherical coordinates the corresponding solution is

$$\eta = \frac{3}{\phi_S^2} (\phi_S \coth \phi_S - 1) \quad (7-10)$$

with  $\phi_S = R_p(k/D_{eff})^{1/2}$ . For cylindrical geometry (infinite in extent along the axis),

$$\eta = \frac{2I_1(\phi_C)}{\phi_C I_0(\phi_C)} \quad (7-11)$$

with  $\phi_C$  defined similarly to  $\phi_S$ ,  $R_p$  being the radius in both cases. In equation (7-11)  $I_0$  and  $I_1$ , are modified Bessel functions of the first kind. The apparent dependence of these results for  $\eta$  on geometry can be removed for most engineering applications by defining a characteristic dimension of the particular geometry involved as the ratio of volume  $V$  to external surface area,  $S_A$  [R. Aris, *Chem. Eng. Sci.*, 6, 292 (1957)]. For a sphere ( $V/S_A$ ) is  $(R_p/3)$ , while for the slab it is  $W$ ; hence the values of  $\phi$  employed in equations (7-8) and (7-10) differ by a factor of 3 if one wishes to compare corresponding conditions in the two geometries. Figure 7.4 gives some solutions for effectiveness factors plotted in accord with the  $(V/S_A)$  rule. The maximum difference in the two geometries shown is about 10% in  $\eta$  for  $2 \leq \phi_S \leq 6$ . In subsequent discussion we shall present various results, some for spherical and some for slab

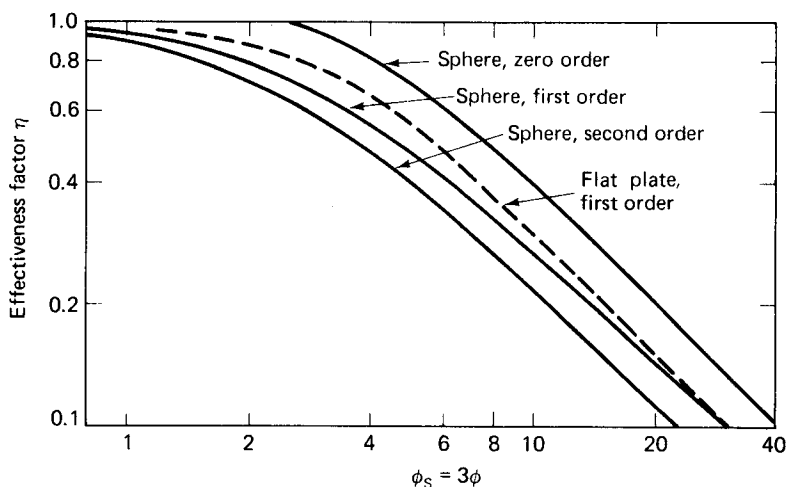


**Figure 7.4** Effectiveness factors for power-law kinetics and various geometries:  $\phi_S$  (sphere) =  $3\phi$  (slab). [After C.N. Satterfield, *Mass Transfer in Heterogeneous Catalysis*, with permission of MIT Press, Cambridge, MA, (1970).]



geometries, without making any special distinction between the two. As one might infer, cylindrical geometry gives results intermediate to these two limits.

When  $(-r)$  is given as an integer power law, results analogous to equations (7-8) to (7-11) may be obtained with the Thiele modulus defined as

$$\phi + W \left( \frac{n+1}{2} \cdot \frac{kC_{A_0}^{n-1}}{D_{eff}} \right)^{1/2} \quad (7-12)$$

where  $n$  is the order of reaction. The results of calculations using this definition are also depicted in Figure 7.4. One point of interest (and caution) is the behavior of a zero-order reaction; in this case there are two regions of solution, one in which  $C_A$  is finite at  $z = 0$  and the second in which  $C_A$  becomes zero at some point  $z < W$ . In the former case  $\eta = 1$ , effectiveness is independent of  $\phi$ , and although gradients exist, they do not affect the rate of reaction. When  $C_A$  becomes zero at some interior point, the effectiveness must decrease since a portion of the catalyst is not contacted with the reactant [V.W. Weekman, Jr. and R.L. Goring, *J. Catalysts*, 4, 260 (1965)]. The analysis of reaction systems in which the kinetics are not simple order, Langmuir-Hinshelwood for example, extends beyond elementary methods and has been treated by Chu and Hougen [C. Chu and O.A. Hougen, *Chem. Eng. Sci.*, 17, 1 (1962)] and Roberts and Satterfield [G.W. Roberts and C.N. Satterfield, *Ind. Eng. Chem. Fundls.*, 4, 288 (1965); 5, 317 (1966)].

Finally, while much of the work concerned with effectiveness factors has dealt with irreversible reactions, there is a useful simple result for the reversible first-order reaction as given in equation (1-60), with the modulus of the form

$$\phi = W \left[ \frac{(k_f + k_r)}{D_{eff}} \right]$$

or, in terms of the equilibrium constant  $K$ ,

$$\phi = W \left[ \frac{k_f(K+1)}{KD_{eff}} \right]$$

### Illustration 7.1

The discussion above leaves the impression that there is a separate Thiele modulus and corresponding effectiveness factor for every specific form of reaction kinetics. Unfortunately, this is indeed so, and for most complex kinetic laws the mathematics is not tractable to direct analytical solution. Is it reasonable to see if we can pose the problem in more general form to get around this? If so, how can this be done?

#### Solution

For simplicity we will assume slab geometry for equation (7-2), and employ the boundary conditions of equation (7-3). However, to preserve the generality of the approach we will assume for the moment that  $D_{eff}$  is a function of  $C_A$  (or  $z$ ). Thus, for reaction within a volume element the catalyst we have

$$\frac{d}{dz} \left( D_{eff} \frac{dC_A}{dz} \right) = (-r) \quad (i)$$

or, upon integration

$$D_{eff} \frac{dC_A}{dz} = \left[ 2 \int_{C_{Aw}}^{C_A} D_{eff}(-r) dC_A \right]^{1/2} \quad (ii)$$

where  $C_{Aw}$  is the centerline concentration of reactant A. We do not know *a priori* what this concentration is, but we can, in effect, go through the back door here in terms of a quantity we do know, the dimension  $W$ . Thus, from equation (ii)

$$W = \int_{C_{Aw}}^{C_A} \frac{D_{eff} dC}{2 \int_{C_{Aw}}^{C_A} D_{eff}(-r) dC} \quad (iii)$$

Again we can define the effectiveness factor in terms of the flux of reactant A at the particle surface, so that

$$\eta = \frac{D_{eff} \left( \frac{dC_A}{dz} \right)_W}{W(-r)_W} \quad (iv)$$

Combining this result with equation (iii) gives

$$\eta = \frac{\sqrt{2}}{W(-r)_W} \left[ \int_{C_{Aw}}^{C_A} D_{eff}(C_A)(-r) dC_A \right]^{1/2} \quad (v)$$

where  $(-r)_W$  is the reaction rate at  $W$ , and where  $C_{Aw}$  can be calculated from equation (iii). Now, we also have to ensure that the effectiveness factor computed from equation (v) will obey what we know about the limiting behavior required. Thus,  $\eta \rightarrow 1$  as  $C_A \rightarrow C_{A0}$  and  $\eta \rightarrow 1/\tanh \phi$  in the limit of strong diffusion. The

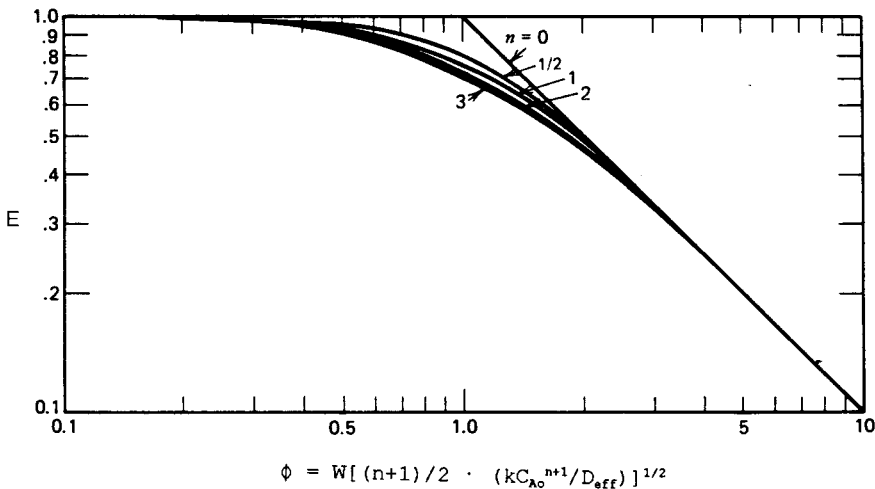


**Figure 7.5** Effectiveness factor versus generalized modulus for power law reaction kinetics.

second of these requirements forces equation (v) to the form

$$\eta = \frac{1}{\phi} = \frac{\sqrt{2}}{W(-r)_W} \left[ \int_{C_{A_e,0}}^{C_{A_0}} D_{eff}(C_A)(-r) dC_A \right]^{1/2} \quad (\text{vi})$$

where the lower limit of integration will be either the equilibrium concentration of A,  $C_{A_e}$ , if the reaction is reversible, or zero if it is irreversible.

We may take equation (vi) as defining a generalized modulus, compatible with any kinetics.

$$\phi = \left( \frac{\bar{V}}{S} \right) \frac{(-r)_W}{\sqrt{2}} = \left[ \int_{C_{A_e,0}}^{C_{A_0}} D_{eff}(C_A)(-r) dC_A \right]^{1/2} \quad (\text{vii})$$

Use of this generalized modulus brings effectiveness factor curves that are nearly superimposed upon each other for  $n$ th-order power law kinetics. The results of this are shown in Figure 7.5 for slab geometry.



HORATIO SAYS

Show me that the generalized modulus reduces to the form of equation (7-5) for a first-order irreversible reaction with constant  $D_{eff}$ . Further, what about equation (7-12)?

### 7.1.2 Implications with Respect to Temperature and Reaction Order: Diffusional Camouflage

We have previously defined the apparent activation energy of a chemical reaction as

$$\frac{E_a}{RT^2} = \frac{d \ln k}{dT}$$

or, more generally, as

$$E_a = R \frac{d \ln (-r)}{d(1/T)} \quad (7-13)$$

where  $(-r)$  is the observed reaction rate. Now the effectiveness factor is defined so that the observed rate can be written as

$$(-r) = \eta \cdot f(T_0, C_0) \quad (7-14)$$

where  $f(T_0, C_0)$  is the functional form of the correlation for intrinsic kinetics. For a rate constant obeying the Arrhenius equation,

$$(-r) = \eta \cdot k^\circ \exp(-E/RT) \cdot f'(C_0) \quad (7-15)$$

substituting into equation (7-14) and performing the indicated differentiation gives

$$\begin{aligned} \frac{d \ln(-r)}{d(1/T)} &= \frac{d \ln k}{d(1/T)} + \frac{d \ln \eta}{d(1/T)} \\ E_a &= E - R \frac{d \ln \eta}{d \ln \phi} \cdot \frac{d \ln \phi}{d(1/T)} \end{aligned} \quad (7-16)$$

For small values of  $\phi$ ,  $(d \ln \eta / d \ln \phi) = 0$  and the apparent and Arrhenius activation energies are the same. For large values of  $\phi$  this derivative approaches  $(-1)$  and, assuming  $D_{eff}$  can also be approximately represented by an Arrhenius form,

$$D_{eff} = D_{eff}^{\circ} \exp(-E_D/RT) \quad (7-17)$$

This is not the theoretical temperature dependence of  $D_{eff}$ , as will be shown later, however the approximation is useful and often used. Equation (7-16) then gives

$$E_a = \frac{E + E_D}{2} \quad (7-18)$$

Normally  $E \gg E_D$ , since diffusion is not very temperature-sensitive, so the apparent activation energy is about one-half the true value when pronounced concentration gradients are present.

Figure 7.6 shows in Arrhenius form what might be observed for the reaction rate in a catalytic reaction (porous catalyst) as one continues to increase the temperature. At low temperatures the reaction is slow, mass transport is no limitation, and one observes the true activation energy. As the temperature increases, the rate of reaction increases more rapidly than the rate of mass transport, transport limitations appear, and the observed activation energy begins to fall off toward the ultimate limit given by equation (7-18). When both intra and interphase gradients occur, the limits predicted by equations (7-16) and (7-18) are considerably modified. This will be treated later, as well as the details of the calculations shown in Figure 7.6 for the combination of mass- and heat-transfer effects.

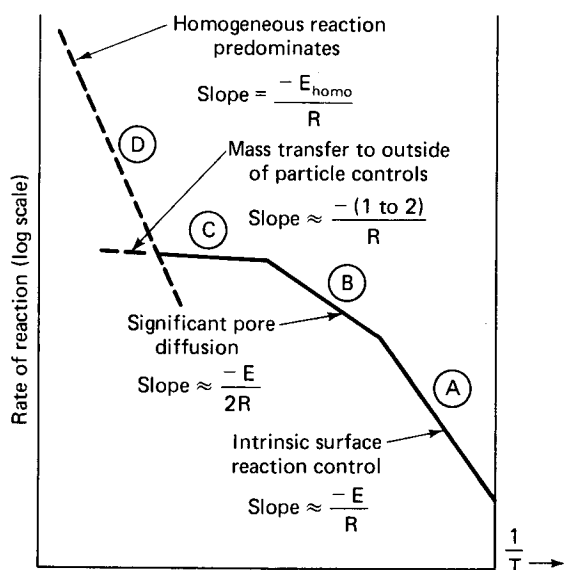
Figure 7.7 gives some experimental results, obtained for the cracking of cumene on silica/alumina catalysts, in which the diffusional modulus has been changed by variation of the catalyst pellet dimension [P.B. Weisz and C.D. Prater, *Advan. Catalysis*, 6, 144 (1954)]. It is seen that the slope of the  $\ln r$  versus  $1/T$  plot for the severely diffusionally limited pellets of 0.175-cm radius is approximately one-half that of the smaller 0.0056-cm pellets.

A similar analysis can be conducted for the influence of mass transport on the apparent reaction order. For a reaction with intrinsic  $n$ th-order kinetics,

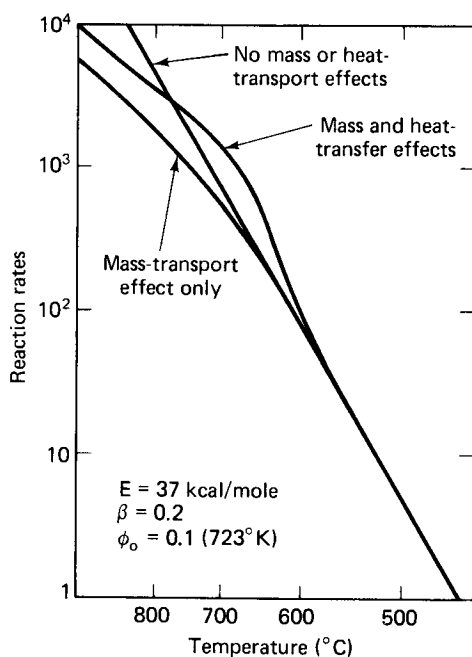
$$(-r) = \eta k C_0^n \quad (7-19)$$

The apparent order with respect to  $C_0$  is

$$\frac{d \ln(-r)}{d \ln C_0} = n_a \quad (7-20)$$



(a) Possible Kinetic Regimes in a Gas-Phase Reaction Occurring on a Porous Solid Catalyst



(b) Modification of the Arrhenius Plot of Activity Due to Mass-Transport Effect, and Due to Both Mass and Heat-Transport Effect

**Figure 7.6** Differing regimes of diffusion as they might affect an Arrhenius correlation. [(a), after C.N. Satterfield, *Mass Transfer in Heterogeneous Catalysis*, with permission of MIT Press, Cambridge, MA, (1970); (b) after P.B. Weisz and J.S. Hicks, *Chem. Eng. Sci.*, 17, 265, with permission of Pergamon Press, Ltd, London, England, (1962).]

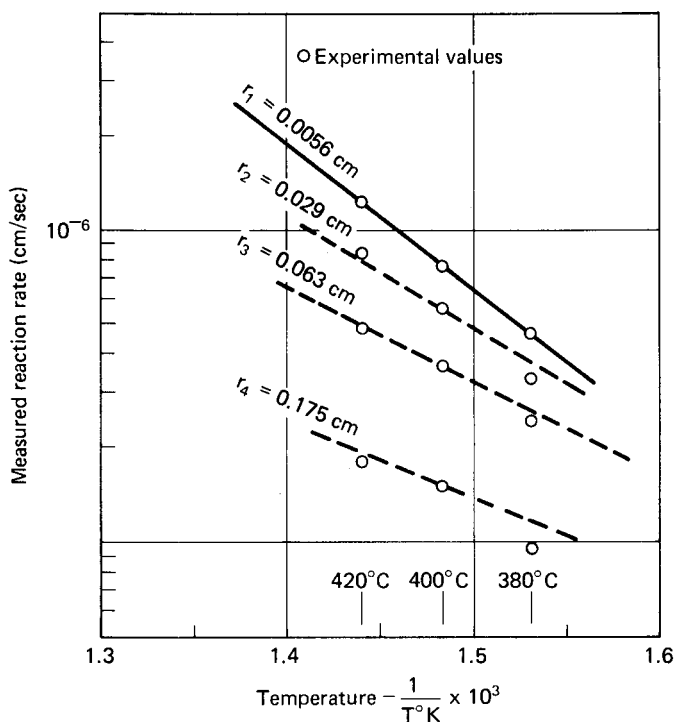


**Figure 7.7** Variation in apparent activation energy with extent of diffusion for cumene cracking on silica/alumina. [After P.B. Weisz and C.D. Prater, *Advan. Catalysis*, 6, 144, with permission of Academic Press, Inc., New York, NY, (1954).]

Combination of equations (7-19) and (7-20) gives

$$n_a = n + \frac{d \ln \eta}{d \ln \phi} \cdot \frac{d \ln \phi}{d \ln C_0} \quad (7-21)$$

with  $\phi$  defined as in equation (7-12) and  $D_{eff}$  independent of concentration. This gives

$$n_a = n + \frac{n-1}{2} \cdot \frac{d \ln \eta}{d \ln \phi} \quad (7-22)$$

The apparent reaction order will lie somewhere between the true order and unity. For first-order reactions the diffusion process will have no effect on order, as is apparent from equation (7-22). It is convenient sometimes to recall that, kinetically, diffusion rates are first-order in concentration.

These modifications of kinetics, with respect to both activation energy and reaction order when mass transfer becomes rate-limiting, have profound implications in many aspects of catalytic reaction engineering and have quite justifiably been referred to in summation as the diffusional “falsification” or “camouflage” of chemical kinetics. It is important for the experimentalist to be aware of such effects when investigating a reaction in the laboratory, and for the designer to account for them in formulating kinetic models pertinent to actual process conditions. Certainly, no one with any interest in job security would wish to misestimate a value of activation energy by a factor of two.

**Illustration 7.2**

A first-order reaction is carried out using a catalyst of characteristic dimension 0.2 cm and effective diffusivity of  $0.015 \text{ cm}^2/\text{s}$ . At  $100^\circ\text{C}$  the intrinsic rate constant was measured to be  $0.93 \text{ s}^{-1}$  with an activation energy of 20 kcal/mol.

(a) For a reactant concentration of  $3.25 \times 10^{-2} \text{ mol/liter}$ , what is the rate of reaction at  $100^\circ\text{C}$ ?

(b) For the same reactant concentration, what is the rate of reaction at  $150^\circ\text{C}$ ? Assume that  $D_{\text{eff}} \neq f(T)$ .

(c) What is the apparent activation energy of the reaction?

(d) Compare values of the Thiele modulus at 100 and  $150^\circ\text{C}$ .

*Solution*

(a) The rate of reaction at  $100^\circ\text{C}$  and the concentration given is

$$(-r) = (0.93)(3.25 \times 10^{-2}) = 3.02 \times 10^{-2} \text{ mols/liter-s}$$

However, let us check the catalytic effectiveness at this condition. The diffusional modulus is

$$\phi_S = \Lambda(k/D_{\text{eff}})^{1/2}, \quad \text{with } \Lambda \text{ the characteristic dimension}$$

$$\phi_S = (0.2)(0.93/0.015)^{1/2} = 1.57$$

The corresponding effectiveness factor estimated from Figure 7.5 is approximately 0.7, so

$$(-r)_{\text{apparent}} = (0.7)(3.02 \times 10^{-2})$$

$$(-r)_{\text{apparent}} = 2.11 \times 10^{-2} \text{ mols/liter-s}$$

(b) the rate of reaction at  $150^\circ\text{C}$

$$\frac{k_{150}}{k_{100}} = \frac{k_{150}}{0.93}$$

$$k_{150} = (0.93) \exp \left[ \frac{-20,000}{(1.98)(423)} + \frac{(20,000)}{(1.98)(373)} \right]$$

so

$$k_{150} = 22.82 \text{ s}^{-1}$$

and

$$\phi = (0.2)(22.82/0.015) = 7.80$$

Again, estimating from Figure 7.5,

$$\eta = 0.12$$

and

$$(-r)_{\text{apparent}} = (0.12)(22.82)(3.02 \times 10^{-2})$$

$$(-r)_{\text{apparent}} = 8.27 \times 10^{-2} \text{ mols/liter-s}$$

(c) The apparent activation energy from these results.

$$(-r)_{100} = 2.11 \times 10^{-2} \text{ mols/liter-s}$$

$$(-r)_{150} = 8.27 \times 10^{-2} \text{ mols/liter-s}$$

$$\frac{8.27}{2.11} = \exp \left[ -\frac{E_a}{(1.98)(423)} + \frac{E_a}{(1.98)(373)} \right]$$

from which we obtain

$$E_a = 8537 \text{ cal/mol}$$

(d) The comparative values of the Thiele modulus are

$$\phi_{S(100)} = 1.57$$

$$\phi_{S(150)} = 7.80$$

Thus, the modulus increases by a factor of 4.97, while the actual rate of reaction changes by a factor of 3.92 over the 50 °C temperature range. The apparent activation energy is somewhat less than 1/2 the true value. This is due to approximations in graph reading; the activation energy value is quite sensitive to the rate ratio—a fact which should be well known to us by now.



HORATIO SAYS

I'm still worried about that  $E_a$  value. Aside from graphical estimation, what would be the results of the analysis above if there were a 10% uncertainty in the values of both the effective diffusivity and the rate constant?<sup>2</sup>

### 7.1.3 Nonisothermal Theory

Since a large number of catalytic reactions are accompanied by thermal effects due to the heat of reaction (in the majority of cases these are exothermic reactions), it may not be realistic to pursue expectations based on isothermal analysis. In the development below, a direct proportion between temperature and concentration gradients is indicated [C.D. Prater, *Chem. Eng. Sci.*, 8, 284 (1958)]; thus, in instances where significant concentration gradients exist and the reactions are not thermally neutral, it is reasonable to expect that thermal gradients will also exist. Under steady-state conditions we may write for the mass balance,

$$D_{eff} \frac{d^2 C}{dz^2} - (-r) = 0 \quad (7-23)$$

<sup>2</sup> "... in short, I was afraid."—*T.S. Eliot*



and for the heat balance,

$$k_{eff} \frac{d^2 T}{dz^2} + (-\Delta H)(-r) = 0 \quad (7-24)$$

in which  $(-\Delta H)$  is the heat of reaction per mol of reactant, and  $k_{eff}$  is an effective thermal conductivity in the porous matrix. Since  $(-r)$  is the same in both balances, we can write

$$-\frac{(-\Delta H)(D_{eff})}{k_{eff}} \frac{d^2 C}{dz^2} = \frac{d^2 T}{dz^2} \quad (7-25)$$

For surface conditions of  $C_0$  and  $T_0$ , integration of equation (7-25) twice gives

$$T - T_0 = \frac{(-\Delta H)(D_{eff})}{k_{eff}} (C_0 - C) \quad (7-26)$$

showing that the relationship between temperature and concentration is linear and independent of geometry and reaction kinetics. The largest possible difference is when  $C = 0$ .

$$(\Delta T)_{\max} = \frac{(-\Delta H)(D_{eff})}{k_{eff}} C_0 \quad (7-27)$$

Obviously, then, the magnitude of  $(\Delta T)_{\max}$  will depend upon the values of the parameters  $D_{eff}$ ,  $k_{eff}$ , and  $(-\Delta H)$ . Anticipating some results to be discussed later in this chapter, we can say that the relative values of the two effective transport coefficients lead to estimates of intraphase temperature gradients on the order of tens of degrees or so for very exothermic (or endothermic) reactions. Anticipating another forthcoming result, we can also say that it is generally accepted that boundary-layer temperature gradients (interphase) are normally more important than the intraphase gradients [see, for example, C. McGreavy and D.L. Cresswell, *Chem. Eng. Sci.*, 24, 608 (1969), or J.P.G. Kehoe and J.B. Butt, *Amer. Inst. Chem. Eng. J.*, 18, 347 (1972)]. Nonetheless, the solution to this nonisothermal diffusion/reaction problem is important. This will require simultaneous solution of equations (7-23) and (7-24) using boundary conditions for temperature and concentration analogous to equation (7-3), and a general treatment requires numerical methods. If equations (7-23) and (7-24) are cast into nondimensional form, two additional parameters appear.

$$\beta = \text{reaction heat parameter} = \frac{(\Delta T)_{\max}}{T_0} = \frac{(-\Delta H)D_{eff}}{k_{eff} T_0} C_0$$

$$\gamma = \text{activation energy parameter} = \frac{E}{RT_0}$$

An example of typical results was given by Weisz and Hicke [P.B. Weisz and J.S. Hicks, *Chem. Eng. Sci.*, 17, 265 (1962)] for the case of first-order reaction in spherical geometry. Some of these are shown in Figure 7.8 for a range of the parameters  $\beta$ ,  $\gamma$ , and  $\phi_S$ . The isothermal theory is embedded as a special case ( $\beta = 0$ ) of this nonisothermal analysis. The increased parameterization required here presents additional complexity in the presentation of the results, since the entire display of Figure 7.8 is for a single value of the parameter  $\gamma$ . However, it has been shown

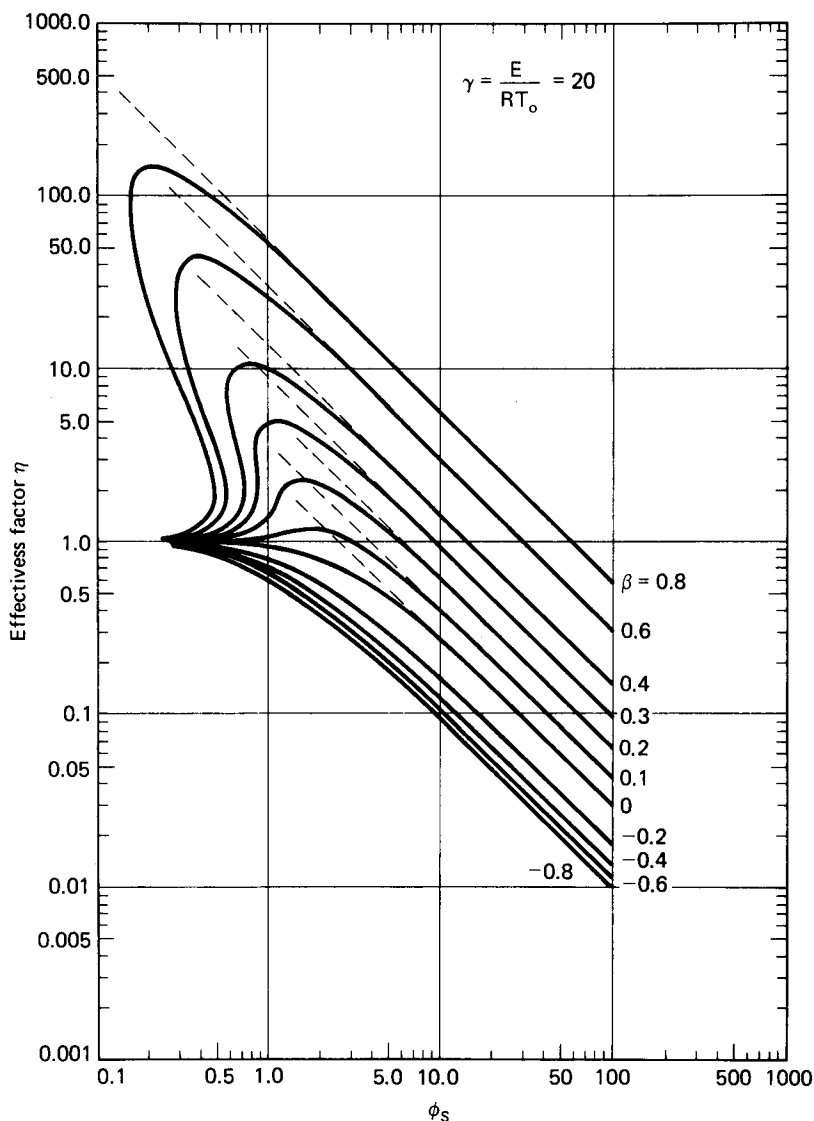


**Figure 7.8** Nonisothermal effectiveness factor for first-order reaction in a sphere;  $\phi_S = (k/D_{eff})^{1/2}$ . [After P.B. Weisz and J.S. Hicks, *Chem. Eng. Sci.*, 17, 265, with permission of Pergamon Press, Ltd., London, England, (1962).] Dotted lines are the asymptotic solution given by Petersen [E.E. Petersen, *Chem. Eng. Sci.*, 17, 1987 (1962).]

that a set of plots for differing  $\gamma$  may be reduced to a single diagram by plotting  $\eta$  versus  $\phi_S$  using  $\beta\gamma$  as a parameter rather than  $\beta$  alone [J.J. Carberry, *Am. Inst. Chem. Engr. J.*, 7, 350 (1961)]. Liu [S.L. Liu, *Am. Inst. Chem. Engr. J.*, 15, 337 (1971)] has further shown that the nonisothermal results are nicely mapped over a range of  $\phi_S$  by

$$\eta = (1/\phi_S) \exp(\beta\gamma/5) \quad (7-28)$$

Both of these results would seem to decrease the complexity of the nonisothermal results in relation to practical problems.

A little further attention to the results of Figure 7.8 reveals the possible presence of two familiar characteristics of nonisothermal systems already explored in Chapter 6—parametric sensitivity and multiplicity. Consider, for example, the curve shown for a  $\beta$  value of 0.3. This indicates that for a small range of  $\phi_S$ , around 0.85, there is a corresponding range of  $\eta$  from about 1.1 to 4.0, demonstrating a pronounced parametric sensitivity. Further, for  $\beta$  values greater than about 0.3, the existence of multiple steady states is indicated for  $\phi_S \leq 0.5$ . This multiplicity has been worried about from time to time by various people and, as in the parameterization of Figure 7.8, the implications in practice are not quite as fierce as the figure would imply. Luss [D. Luss, *Chem. Eng. Sci.*, 23, 1249 (1968)] showed that an appropriate criterion for uniqueness is given by

$$\beta\gamma < 4(1 + \beta) \quad (7-29)$$

Further, from the inequality of (7-29), one sees that multiplicity would be associated only with large values of  $\beta$  (already obvious from the figure), and similarly also for parametric sensitivity. Some estimates of  $\beta$  for catalytic reactions have been reported by Hlavacek et al. [V. Hlavacek, M. Kubicek and M. Marek, *J. Catal.*, 15, 17, 31 (1969)] and a few typical values are given in Table 7.1. It would seem from these data that many reactions of industrial significance are characterized by rather small values of  $\beta$  and the nasty behavior located in the northwest quadrant of Figure 7.8 is not too important in reality. We should not forget, however, that there is a region, even for moderate values of  $\beta$ , where the effectiveness factor is greater than 1. In this situation the increase in rate resulting from the increase in intraparticle temperature overbalances the decrease in rate due to the decrease in intraparticle concentration. This is a good example, by the way, to remind one that temperature is the most important kinetic variable. This behavior is shown, for example, in the region of about  $0.9 > \phi_S > 3.5$  for  $\beta = 0.1$  in Figure 7.8, which, upon reflection, is a fairly substantial range of  $\phi_S$ .

One further effect is implied by these curves but is not directly shown. Since the plots of  $\eta$  versus  $\phi_S$  are not uniformly decreasing for  $\beta > 0$  the derivative in the relationship between observed and actual activation energies becomes greater than zero in certain temperature ranges and the apparent activation energy is greater than the actual value. An example of this is shown on the lower part of Figure 7.6 for the curve labeled “Mass- and heat-transfer effects.”

**Table 7.1** Thermal Parameters for Some Exothermic Catalytic Reactions

Reaction	$\beta$	$\gamma$
Ammonia synthesis	$6.1 \times 10^{-5}$	29.4
Methanol oxidation	$1.1 \times 10^{-2}$	16.0
Ethylene hydrogenation	$6.6 \times 10^{-2}$	23.3
Benzene hydrogenation	$1.2 \times 10^{-1}$	14.2
Sulfur dioxide oxidation	$1.2 \times 10^{-2}$	14.8

A useful asymptotic method has been developed by Petersen [E.E. Petersen, *Chem. Eng. Sci.*, 17, 987 (1962)] for the estimation of  $\eta$  for large values of  $\phi_S$ . When  $\phi_S \gg 1$  we may write the mass conservation equation in the form

$$\frac{d^2 f}{d\mu^2} + (-r') = 0 \quad (7-30)$$

where

$$\mu = (1 - \zeta)\phi_S; \quad \zeta = \frac{r}{R_p} \quad (\text{spherical geometry})$$

$$f = \frac{C}{C_0}; \quad (-r') = \frac{-r(\zeta)}{-r(1)}$$

with the boundary conditions that  $\mu = 0$  for  $f = 1$  and  $\mu \rightarrow \infty$  for  $(df/d\mu) = 0$ ,  $f = 0$ . The second condition here reflects that, under conditions of strong diffusional limitation, the reactant will be totally consumed in the outer layers of the particle. If we make the substitution  $p = df/d\mu$ , equation (7-30) may be directly integrated to

$$\frac{df}{d\mu} = -\sqrt{2} \left[ \int_0^{f(\mu)} (-r') df \right]^{1/2} \quad (7-31)$$

Normally one is interested in  $(df/d\mu)$  at the surface, since this is required for the evaluation of surface flux and hence effectiveness. It can be shown that

$$\eta = \frac{1}{\phi_S^2} \left( \frac{df}{d\mu} \right)_{\mu=0}$$

so that

$$\eta = \frac{\sqrt{2}}{\phi_S} \left[ \int_0^1 (-r') df \right]^{1/2} \quad (7-32)$$

This approximation may be used for either isothermal or nonisothermal systems. The dashed lines on Figure 7.8 are solutions obtained by this method; applications are detailed further by Petersen [E.E. Petersen, *Chemical Reaction Analysis*, p. 70, Prentice-Hall, Englewood Cliffs, NJ, (1965)].

We mentioned earlier that it is possible to simplify somewhat the nonisothermal analysis by the use of a combined thermal parameter,  $\beta\gamma$ , and reported the result presented by Liu in equation (7-28). Now, having examined the anatomy of the results presented in Figure 7.8, we can benefit from looking at these mapping functions in more detail. For our favorite Academic Reaction #1 (second-order kinetics can also be managed this way), we have the function given by equation (7-28) but now must add that certain regions of the  $\eta - \phi_S$  plot are excluded. The full story is

$$\eta = (1/\phi_S) \exp(\delta/5)$$

for  $\phi_S > 2.5$  and where  $\delta = \beta\gamma$ . The following ranges of parametric values are excluded.

$$\delta > 2.5 \quad \phi_S < 1.235 - 0.94\delta$$

$$\delta \leq 2.5 \quad \phi_S < 1.820 - 0.32\delta$$

In this region

$$\eta = \exp(0.14\phi_S\delta^{1.6}) - 1 + \frac{\tanh \phi_S}{\phi_S} \quad (7-33a)$$

For endothermic reactions,

$$\eta = \frac{\tanh \phi_S^*}{\phi_S^*} \quad (7-33b)$$

with  $\phi_S^* = \phi_S(1 - \delta)^{0.3}$ .

We should not completely rule out multiplicity in individual catalyst particles as being only of laboratory interest, however, further detail is beyond our present interest. A good background on this in both experiment and analysis is given by Harold et al. [M.P. Harold, M. Sheinfuch and D. Luss, *Ind. Eng. Chem. Research*, 26, 786 (1987)].

### Illustration 7.3

Much of the discussion and the illustrations so far have employed power-law kinetic forms as the vehicle to build the analysis, because these are used the most often and best understood. However, too much reliance on these can get us into a lot of trouble. A well-known reaction in this regard is the oxidation of carbon monoxide over a supported Pt catalyst. The intrinsic kinetics of this reaction in excess oxygen are given by

$$(-r_{\text{CO}}) = \frac{k[\text{CO}]}{(1 + K[\text{CO}])^2} \quad (\text{i})$$

This reaction has very widely different behavior<sup>3</sup> dependent upon the level of [CO]. For  $K[\text{CO}] \ll 1$  we have a well-behaved first-order reaction

$$(-r_{\infty}) = k[\text{CO}] \quad (\text{ii})$$

but, for  $K[\text{CO}] \gg 1$  there develops an inverse dependence of rate on [CO].

$$(-r_{\text{CO}}) = k'([\text{CO}])^{-1} \quad (\text{iii})$$

The value of  $K$  is such that even at low CO concentrations the conditions of equation (iii) can govern kinetics. Parametric values have been determined for this reaction by Voltz et al. [S.E. Voltz, C.R. Morgan, D. Liederman and S M. Jacob, *Ind. Eng. Chem. Design Devel.*, 12, 294 (1973)].

$$k = (1.83 \times 10^{12}) \exp(-45,000/RT) \text{ s}^{-1} \quad (\text{iv})$$

$$K = (0.655) \exp(3460/RT) \text{ mol \%}^{-1} \quad (\text{v})$$

$$(-\Delta H) = 67,000 \text{ cal/gmol}$$

$$T = ^\circ\text{C} \quad (\text{vi})$$

Develop a computational model describing the coupling between diffusion and reaction and solve the equations to demonstrate the behavior of  $\eta$  versus  $\phi_S$  for

<sup>3</sup>“It went this way, then the other way, then back. Man, was I confused!”—Anonymous (The X-Files)

isothermal conditions and spherical geometry. [See T.G. Smith, J. Zahradnik and J.J. Carberry, *Chem. Eng. Sci.*, 30, 763 (1975)].

### Solution

Let us start by formulating the basic mass balance in spherical coordinates. The spherical cousin of equation (7-2) is

$$D_{eff} \left( \frac{1}{r^2} \right) \frac{d}{dr} \left( r^2 \frac{d[\text{CO}]}{dr} \right) - (-r_\infty) = 0 \quad (\text{vii})$$

where  $r$  is the spherical radius. In nondimensional form the mass balance is

$$\frac{d^2 C}{dr'^2} + \left( \frac{2}{r'} \right) \frac{dC}{dr'} = \phi_0^2 \left[ \frac{C}{(1 + K' C)^2} \right] \quad (\text{viii})$$

where  $K' = K[\text{CO}]_S$ ,  $C = [\text{CO}]/[\text{CO}]_S$ ,  $[\text{CO}]_S$  is the concentration of CO at the particle surface, and  $r' = (r/R_p)$ . Boundary conditions follow equation (7-3).

$$C = 1, r' = 1; \quad (dC/dr') = 0, r' = 0 \quad (\text{ix})$$

This equation may be solved by any of the several methods discussed in Chapter 6 (see Illustration 6.4), with the result as shown in Figure 7.9. Now, this is an *isothermal* calculation, but it shows both of the prominent features of the *nonisothermal* results of Figure 7.8, i.e., effectiveness  $> 1$  for some ranges of  $\phi_S$  and multiplicity for high values of the parameter  $K'$ . We have not said much in the text discussions to this point about negative-order kinetics; this example should help us to keep in mind that reaction order  $< 0$  is a world away from  $> 0$ .

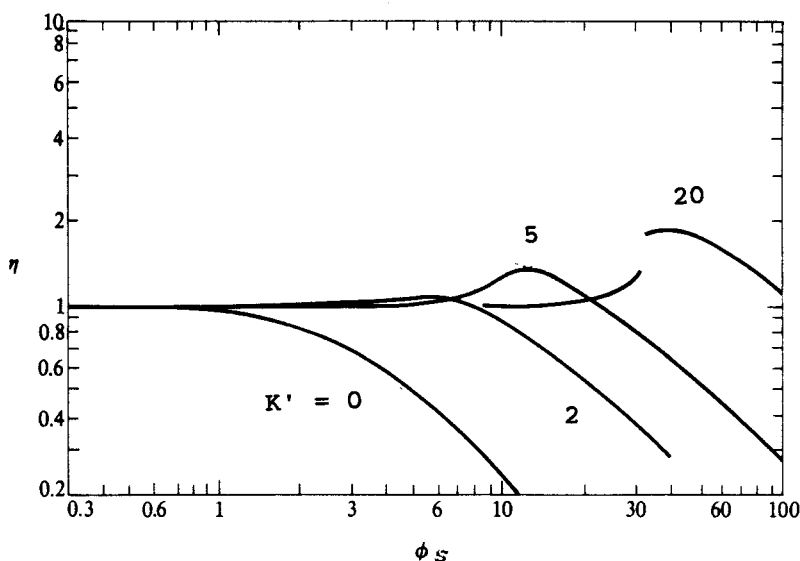


**Figure 7.9** Isothermal effectiveness (spherical coordinates) for the CO oxidation reaction. [After T.G. Smith, J. Zahradnik and J.J. Carberry, *Chem. Eng. Sci.*, 30, 763, with permission of Pergamon Press, Ltd., London, England, (1975).]

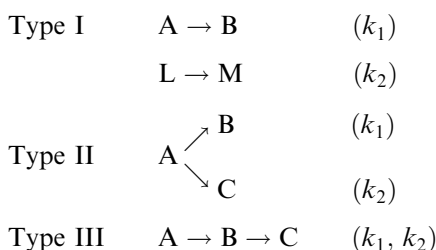


HORATIO SAYS

If the isothermal results shown here are any indication of what's what, the nonisothermal case must be a real show-stopper. Hang on for more exciting developments!

### 7.1.4 Some Intrapphase Selectivity Problems

The effect of transport limitations on selectivity is in many instances far more pronounced than on activity. Important early work in this area for isothermal systems was conducted by Wheeler [A. Wheeler, *Catalysis*, vol. (P.H. Emmett, ed.), Reinhold, New York, NY, (1955)] using the Types I, II, and III selectivity models we have employed in previous chapters here. To review, these are



The following analysis is presented for a given condition of reactant concentration (a point or differential selectivity), so that in reactor modeling the effects illustrated will change according to the conversion level.

*Type I.* In the absence of diffusion we may write

$$r_A = -k_1 C_{A_0}$$

$$r_L = -k_2 C_{L_0}$$

and a differential selectivity, slightly modified from equation (1-73), is

$$\frac{r_A}{r_A + r_L} = \frac{1}{1 + R/S_i} = \Delta \quad (7-34)$$

where  $S_i$  is the intrinsic selectivity,  $k_1/k_2$ , and  $R = (C_{L_0}/C_{A_0})$ . In the presence of an intraphase transport limit,

$$r_A = -\eta_A k_1 C_{A_0} \quad r_L = -\eta_L k_2 C_{L_0}$$

and

$$\frac{r_A}{r_A + r_L} = \frac{1}{1 + \eta_L k_2 C_{L_0} / \eta_A k_1 C_{A_0}} = \Delta_{diff} \quad (7-35)$$

Under strong diffusion conditions for isothermal reactions we have  $\eta \rightarrow 1/\phi$ , so equation (7-35) becomes

$$\Delta_{diff} = \frac{1}{1 + (k_2 C_{L_0} / \phi_L)(\phi_A / k_1 C_{A_0})} \quad (7-36)$$

$$\frac{\Delta_{diff}}{\Delta} = \frac{1 + (R/S_i)}{1 + R\phi_A / S_i\phi_L} \quad (7-37)$$

In this case  $(\Delta_{diff}/\Delta)$  can be greater or less than unity, depending on the value of  $(\phi_A/\phi_L)$ . For nearly equal effective diffusivities of the reactants A and L,  $(\phi_A/\phi_L) \approx S_i^{1/2}$  and equation (7-37) becomes

$$\frac{\Delta_{diff}}{\Delta} = \frac{1 + R/S_i}{1 + R/S_i^{1/2}}$$

and the value of  $(\Delta_{diff}/\Delta)$  depends on whether  $S_i$  is greater or less than unity. This is illustrated in Figure 7.10; for intrinsic selectivities greater than unity  $(\Delta_{diff}/\Delta) < 1$  but not greatly so, particularly for small values of  $R$ ; for  $S_i$  less than unity, point selectivity is considerably increased in the presence of strong diffusion.

*Type II.* In this case, assuming equal-order kinetics for the two reaction paths, there can be no influence of diffusion on selectivity, since a common reactant is involved.

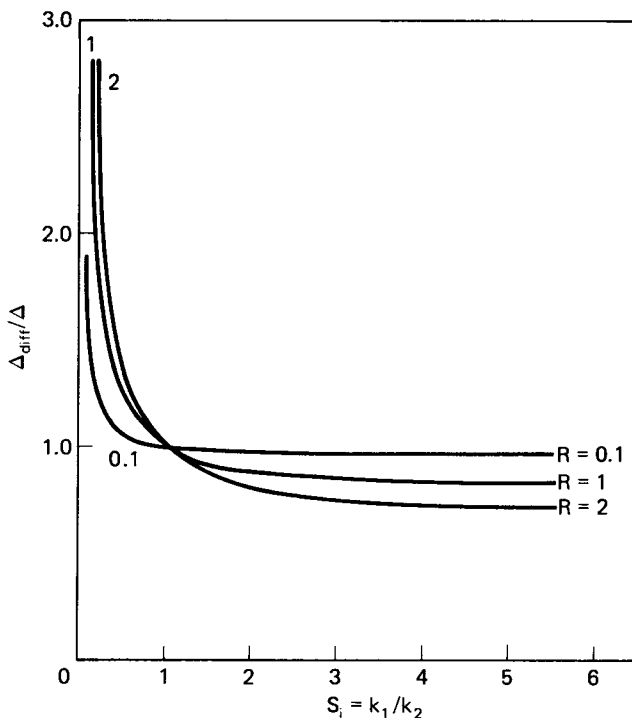


**Figure 7.10** Influence of diffusion on selectivity in a Type I reaction system.



*Type III.* The first step in this sequence yields for reactant A, from equation (7-4)

$$C_A = C_{A_0} \left[ \frac{\cosh(\sqrt{k_1/D_{eff,A}z})}{\cosh \phi} \right] \quad (7-38)$$

and for B

$$D_{eff,B} \frac{d^2 C_B}{dz^2} - k_2 C_B = -k_1 C_A \quad (7-39)$$

where  $C_A$  in equation (7-39) is given by equation (7-38). The differential selectivity, defined as the ratio of the rate of production of the intermediate to the rate of consumption of reactant, is

$$\Delta_{diff} = \frac{r_B}{r_A} = \frac{D_{eff,B}(dC_B/dz)_W}{D_{eff,A}(dC_A/dz)_W} \quad (7-40)$$

Solving equation (7-39) for  $C_B = f(z)$  and obtaining the derivatives involved in equation (7-40) gives, for conditions of large diffusional effects

$$\Delta_{diff} = \frac{R}{\sqrt{S_i}} - \frac{\sqrt{S_i}}{1 + \sqrt{S_i}} \quad (7-41)$$

where the ratio of effective diffusivities has been taken as unity and  $R = C_{B_0}/C_{A_0}$ . In the absence of diffusional influence

$$\Delta = -1 + \frac{R}{S_i} \quad (7-42)$$

so that

$$\frac{\Delta_{diff}}{\Delta} = \frac{\sqrt{S_i}[R(1 + \sqrt{S_i}) - S_i]}{(R - S_i)(1 + \sqrt{S_i})} \quad (7-43)$$

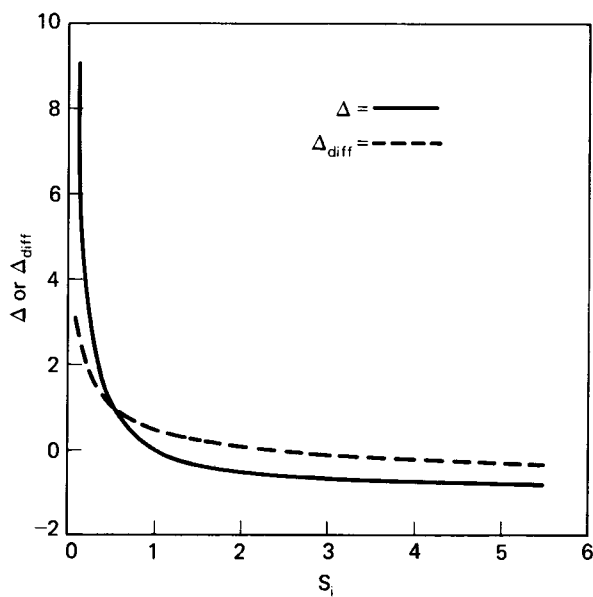
The differential selectivity varies with conversion as represented by the value of  $R$ , so to obtain a complete picture we would have to compare the behavior of diffusionally and nondiffusionally limited systems as the reaction proceeds. The Type III selectivity problem is of particular interest in this regard, and has been treated in the original work by Wheeler. If we integrate equation (7-42) (no diffusional limitation) over a range of conversions

$$f_B = \frac{S_i}{S_i - 1} (1 - f_A)[(1 - f_A)^{(1-S_i)/S_i} - 1] \quad (7-44)$$

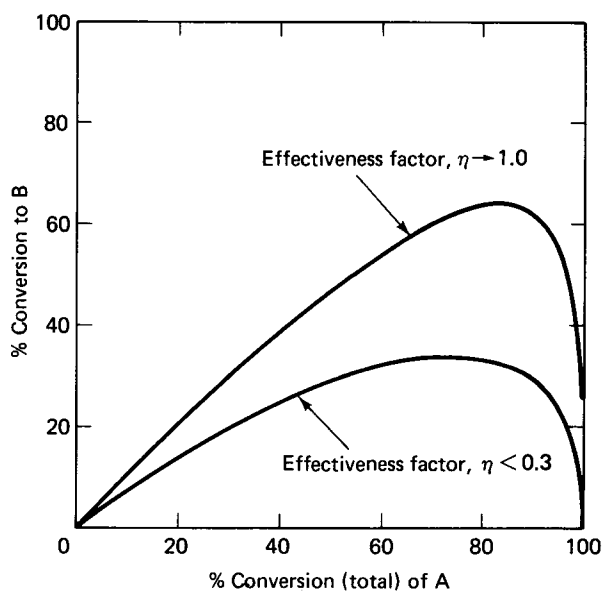
where  $f_B$  is the fraction of initial A reacted to B and  $f_A$  is the total fraction of A reacted. For the diffusion limited case, similar integration of equation (7-41) gives

$$f_B = \frac{S_i}{S_i - 1} (1 - f_A)[(1 - f_A)^{(1-\sqrt{S_i})/\sqrt{S_i}} - 1] \quad (7-45)$$

Plots of the comparative differential selectivities [equations (7-41) and (7-42)] and the overall selectivities [equations (7-44) and (7-45)] are given in Figure 7.11. In the region of primary interest, for  $S_i > 1$ , both  $\Delta$  and  $\Delta_{diff}$  assume negative values, indicative of a net production of the intermediate B. The negative sign arises from the difference in the direction of the fluxes of A and B at the catalyst surface. When



(a)



(b)

**Figure 7.11** (a) Variation of  $\Delta$  and  $\Delta_{diff}$  with intrinsic selectivity, Type III reaction,  $R = 1$ ; (b) variation of overall selectivity with conversion, Type III reaction,  $S_i = 4$ . [From *Catalysis*, P.H. Emmett, ed., reprinted by permission of Van Nostrand Reinhold Co., New York, NY, (1955).]

$S_i > 1$ , the effectiveness factor for A is less than that for B, assuming equal diffusivities, so that both point and overall selectivities for production of intermediate are adversely affected. In both illustrations of Figure 7.11, the loss in point selectivity or in maximum yield of intermediate is in the order of 50%, so these selectivity problems are not trivial.

For nonisothermal systems a point selectivity analysis has been given by Østergaard [K. Østergaard, *Proc. III Int. Cong. Catalysis*, North-Holland, Amsterdam, The Netherlands (1965)], and for Type III reactions by Butt [J.B. Butt, *Chem. Eng. Sci.*, 21, 275 (1966)]. In both instances the selectivity is computed from equation (7-40), where the concentration derivatives are evaluated by numerical solution of the corresponding conservation equations. For example, the Type III equations to be solved are

$$\begin{aligned} D_{eff,A} \frac{d^2 C_A}{dz^2} - (-r_A) &= 0 \\ D_{eff,B} \frac{d^2 C_B}{dz^2} + (-r_A) - (-r_B) &= 0 \\ k_{eff} \frac{d^2 T}{dz^2} + (-\Delta H_A)(-r_A) + (-\Delta H_B)(-r_B) &= 0 \end{aligned} \quad (7-46)$$

with corresponding parameters  $\beta_1$ ,  $\beta_2$ ,  $\gamma_1$ , and  $\gamma_2$  pertaining to the individual reaction steps. Some results for the Type III reaction are illustrated in Figure 7.12. This selectivity problem becomes so highly parameterized for the nonisothermal reaction that it is difficult to get a good overall picture of what is going on. Figure 7.12, then, really just gives a snapshot of Type III behavior for various values of the thermicity parameter  $\beta$  of the two reaction steps for intrinsic selectivities of 1 and 4 (referred to the particle surface conditions) and for  $\gamma_1 = \gamma_2$ . The effectiveness factor behavior is shown in Figure 7.12a (corresponding to Figure 7.8 for a single reaction step), overall selectivity for the two  $S_i$  is shown in Figure 7.12b, and the variation in selectivity for a range of  $S_i$  is shown in Figure 7.12c.

The catalytic effectiveness shown in Figure 7.12a behaves in much the same manner as that for simple reactions, except in those cases where there is a difference in the thermicity of the reaction between the two steps (i.e., exothermic-endothermic or vice versa). In this event, the reaction behavior can apparently be dominated by the action of one of the reaction steps, then shift abruptly to dominance by the other step, as shown in Case F. Also, if one reaction is thermally neutral and the other is not, the region of parametric sensitivity can be shifted to ranges of the diffusion modulus not characteristic for single reactions, as shown in case D.

Selectivity as shown in Figure 7.12b is affected very strongly by both the heat- and mass-transport parameters. The shift from net negative to net positive values of  $\Delta_{diff}$  illustrated indicates that the intermediate is reacting as fast as it is produced, and whatever intrinsic selectivity for the formation of intermediate that existed has been annihilated. Only for Cases A, B, D, and F is there any net production of intermediate, that is,  $\Delta_{diff} > 0$ .

A further look at selectivity behavior is provided by Figure 7.12c, where we fix the activation energies and diffusional modulus and examine the net selectivity as a function of intrinsic selectivity at the catalyst surface temperature (reference

Reaction System	$\beta_1$	$\beta_2$
A	0.80	0.80
B	0.80	0.00
C	0.80	-0.40
D	0.00	0.80
E	0.00	-0.40
F	-0.40	0.80
G	-0.40	0.00
H	-0.40	-0.40
J	0.00	0.00

Thermal parameters of the two reaction steps

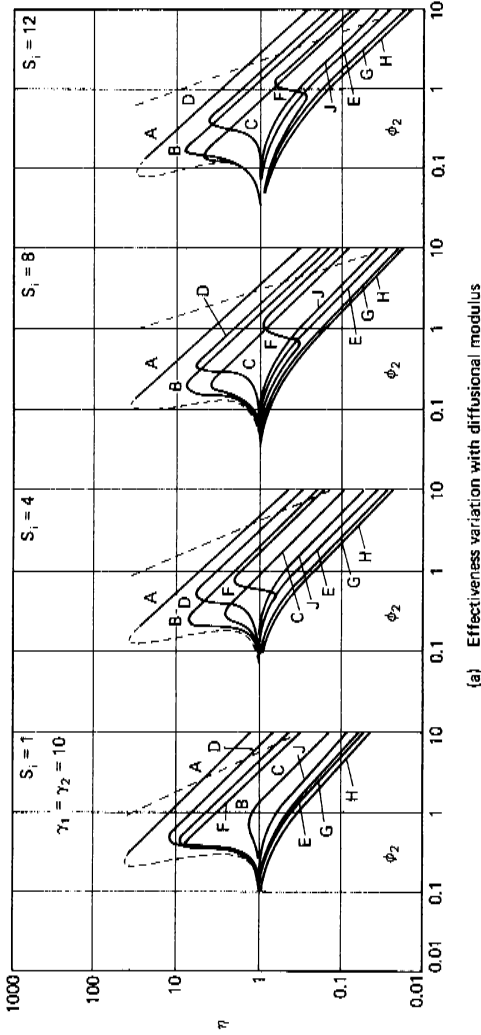


**Figure 7.12** Heat and mass diffusion effects on a Type III reaction: (a) catalytic effectiveness; (b) overall selectivity; and (c) selectivity for a range of  $S_f$ . [After J.B. Butt, *Chem. Eng. Sci.*, 21, 275, with permission of Pergamon Press, Ltd., London, England, (1966).]

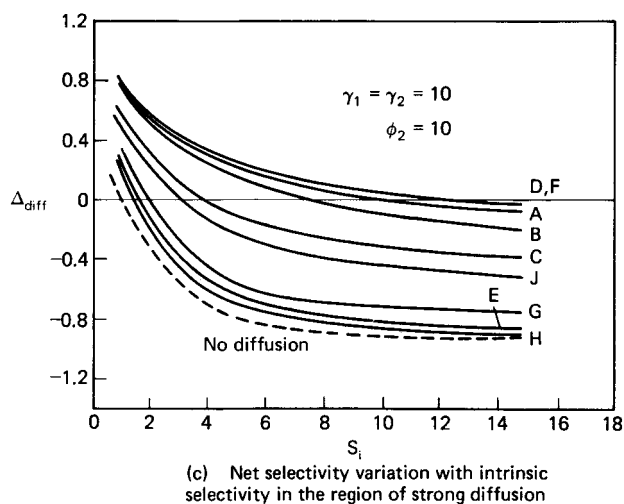
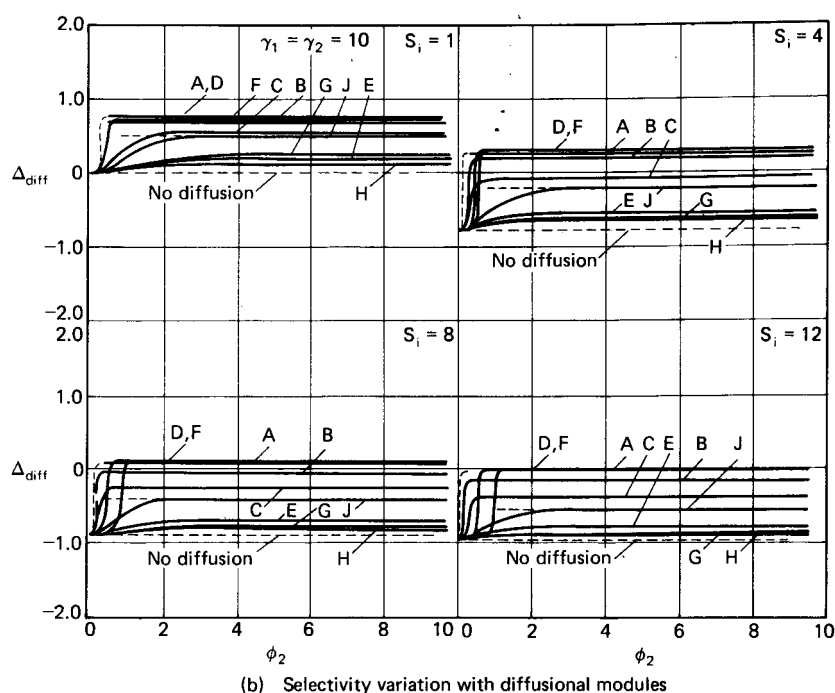


Figure 7.12 Continued.

temperature). Again, we see a large region of parameter space where the intrinsic selectivity is distorted, particularly for higher values of  $(k_1/k_2)$ . This reflects the physical picture which considers that for  $k_1 \gg k_2$  the intermediate, rapidly formed, is slower to react away to product, so the net selectivity actually is improved, although one would still see only net production of intermediate for the range  $\Delta_{diff} > 1$ .

We might conclude this section by reminding ourselves that the activity-selectivity behavior shown in Figure 7.12 is purposely taken to illustrate extreme, limiting cases. Given the tabulation of values given in Table 7.1, it is extremely unlikely that one would encounter a Type II system of, for example,  $\beta_1 = 0.8$  and  $\beta_2 = -0.4$  (Case C). Thus one might disregard these results as computational curiosities; the real justification here is to sense the trends illustrated and their relationship to the parameters under investigation.<sup>4</sup>

### 7.1.5 Diffusion and Chemical Reactions: The Interphase/Intraphase Problem

To this point we have dealt only with transport effects within the porous catalyst matrix (intraphase), and the mathematics have been worked out for boundary conditions that specify concentration and temperature at the catalyst surface. In actual fact, external boundaries often exist that offer “resistance” to heat and mass transport, as shown in Figure 7.1, and the surface conditions of temperature and concentration may differ substantially from those measured in the bulk fluid. Indeed, if internal gradients of temperature exist, interphase gradients in the boundary layer must also exist because of the relative values of the pertinent thermal conductivities [J.J. Carberry, *Ind. Eng. Chem.*, 58(10), 40 (1966)].

Reformulation of the problems previously explained to account for interphase gradients essentially requires only the change of the surface boundary conditions. Assuming that we may see traditional mass- and heat-transfer coefficients as the rate constants characteristic of interphase transport, the boundary conditions for mass and energy conservation equations become

$$\begin{aligned} z = 0 \quad \frac{dC}{dz} = 0; \quad z = W \quad D_{eff} \left( \frac{dC}{dz} \right) &= k_m(C_0 - C_S) \\ z = 0 \quad \frac{dT}{dz} = 0; \quad z = W \quad k_{eff} \left( \frac{dT}{dz} \right) &= h(T_0 - T_S) \end{aligned} \quad (7-47)$$

where  $C_0$  and  $T_0$  refer to bulk conditions and  $C_S$  and  $T_S$  to surface conditions.

In the isothermal case we may solve the problem without having to deal with the mass balance with the new boundary conditions if the kinetics are simple. Let us equate the rate of mass transport at the external surface to the rate of reaction.

$$k_m S_A (C_0 - C_S) = (-r) \bar{V} \quad (7-48)$$

where  $(-r)$  is the observed rate of reaction per unit volume of catalyst,  $\bar{V}$  the catalyst volume, and  $S_A$  external surface area. For first-order reactions,

$$k_m S_A (C_0 - C_S) = \eta k C_S \bar{V} \quad (7-49)$$

Solving equation (7-49) for the unknown surface concentration and resubstituting into the expression for the rate of reaction yields

$$(-r) = \frac{\eta k C_0}{1 + (\eta k / k_m)(\bar{V} / S_A)} \quad (7-50)$$

<sup>4</sup> “It is a thing of no great difficulty to raise objections against another man’s oration . . . but to produce a better in its place is a work extremely troublesome.”—*Plutarch*

where the effectiveness factor  $\eta$  is that determined previously (intrapphase). The quantity  $(k/k_m)(V/S_A)$  in equation (7-50) is called the *Damköhler number* ( $N_{Da}$ ) and expresses the relative rates of the intraphase reaction to external mass transport.

A little clearer physical interpretation is obtained, however, if we write equation (7-50) in terms of the ratio of the inter- to intraphase transport coefficients, a quantity called the *mass Biot number*,  $N_{Bi_m}$ . We define

$$N_{Bi_m} = \left( \frac{k_m}{D_{eff}} \right) \left( \frac{\bar{V}}{S_A} \right) \quad (7-51)$$

Then

$$\eta N_{Da} = \eta \frac{k(\bar{V}/S_A)^2}{(D_{eff})(N_{Bi_m})}$$

which is

$$\begin{aligned} \eta N_{Da} &= \phi \frac{\tanh \phi}{N_{Bi_m}} \quad (slab) \\ \eta N_{Da} &= \frac{\phi_S \coth \phi_S - 1}{3N_{Bi_m}} \quad (sphere) \end{aligned} \quad (7-52)$$

This gives, for the global rate of reaction in equation (7-50)

$$(-r) = \frac{\eta k C_0}{1 + [(\phi \tanh \phi)/N_{Bi_m}]} \quad (slab) \quad (7-53)$$

An extensive discussion of various limiting forms of equation (7-53) has been given by Carberry [J.J. Carberry, *Catalysis Reviews*, 3, 61 (1969)], and we shall have the opportunity to revisit some of these forms in Chapter 8.

Alternative to the derivation of equation (7-53), the isothermal mass balance may be solved analytically with the boundary conditions of equation (7-47). This gives us, for spherical geometry

$$\eta_0 = \left( \frac{3N_{Bi_m}}{\phi_S^2} \right) \frac{\phi_S \cosh \phi_S - \sinh \phi_S}{\phi_S \cosh \phi_S + (N_{Bi_m} - 1) \sinh \phi_S} \quad (7-54)$$

The effectiveness factor of equation (7-54) is an overall value and is *not* the same as the intraphase effectiveness factor used in the derivation of equation (7-53). The Biot number used above is defined as  $(k_m R_p/D_{eff})$ , where  $R_p$  is the particle radius.

Interphase/intrapphase selectivity problems under isothermal conditions have also been treated by Carberry. For the important Type III system, the differential selectivity corresponding to equation (7-41) is

$$\Delta_{diff} = \frac{m_1 \phi_2 \tanh \phi_2}{m_2 \phi_1 \tanh \phi_1} \left( R + \frac{S_i}{S_i - 1} \right) + \frac{S_i}{S_i - 1} \quad (7-55)$$

where the effective diffusivities of A and B are the same, and reaction transport parameters are defined on the basis of  $(V/S_A)$  as the characteristic dimension. The quantities  $m_1$  and  $m_2$  are defined as

$$m_i = 1 + \frac{\phi_i \tanh \phi_i}{N_{Bi_m}} = 1 + \frac{\phi_i^2 \eta_i}{N_{Bi_m}} \quad (7-56)$$

Integration of equation (7-55) over a range of conversions gives the analog of equation (7-45)

$$f_B = \frac{S_i}{S_i - 1} [(1 - f_A)^\Psi - (1 - f_A)] + R_1(1 - f_A)^\Psi \quad (7-57)$$

where  $\Psi$  is

$$\Psi = \frac{m_1 \phi_2 \tanh \phi_2}{m_2 \phi_1 \tanh \phi_1} = \frac{m_1 \phi_2^2 \eta_2}{m_2 \phi_1^2 \eta_1}$$

and  $R_1$  is the initial concentration ratio,  $(C_{A_0}/C_{B_0})$ . The results of some calculations with equations (7-55) and (7-57) are given in Figure 7.13.

The two other major types of selectivity are more easily analyzed. For Type II it may be shown, as previously, that if reaction orders are the same, diffusion has no effect on selectivity (or, more precisely, influences both reactions equivalently). For Type I reactions, the differential selectivity is determined directly from the ratio of the rates of the two reactions as computed from equation (7-53).

The analysis of activity and selectivity in nonisothermal reactions, of course, requires the numerical solution to the mass- and energy-balance equations with the boundary conditions of equation (7-47). In nondimensional form, and for first-order kinetics, these are

$$\begin{aligned} \nabla^2 \tau + \beta \phi^2 f \exp\left(\frac{-\gamma + \gamma \tau}{\tau}\right) &= 0 \\ \nabla^2 f - \phi^2 f \exp\left(\frac{-\gamma + \gamma \tau}{\tau}\right) &= 0 \end{aligned} \quad (7-58)$$

with

$$\begin{aligned} \frac{\partial f}{\partial \zeta} &= \frac{\partial \tau}{\partial \zeta} = 0 & \zeta &= 0 \\ \frac{\partial f}{\partial \zeta} &= N_{Bi_m}(1 - f_S) & \zeta &= 1 \\ \frac{\partial \tau}{\partial \zeta} &= N_{Bi_m}(1 - \tau_S) & \zeta &= 1 \end{aligned}$$

The normalization in the above equations is with respect to bulk conditions, and  $N_{Bi_h}$  is a Biot number for heat transfer,  $(hR_p/k_{eff})$ . The effectiveness factor may be written as

$$\eta = \frac{3N_{Bi_m}}{\phi^2} (1 - f_S) \quad (7-59)$$

and from the Prater relationship we have

$$\tau = \tau_S + \beta(f_S - f) \quad (7-60)$$

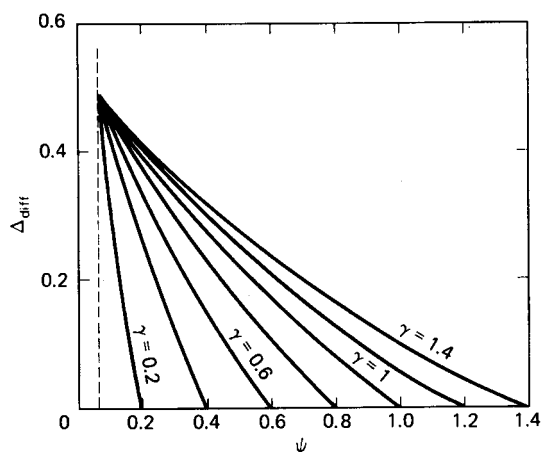
so

$$\frac{\partial \tau}{\partial \zeta} = -\beta \frac{\partial f}{\partial \zeta}$$

which can be employed to show, in the end, that

$$\tau = 1 + \beta\mu(1 - f_S) + \beta(f_S - f) \quad (7-61)$$



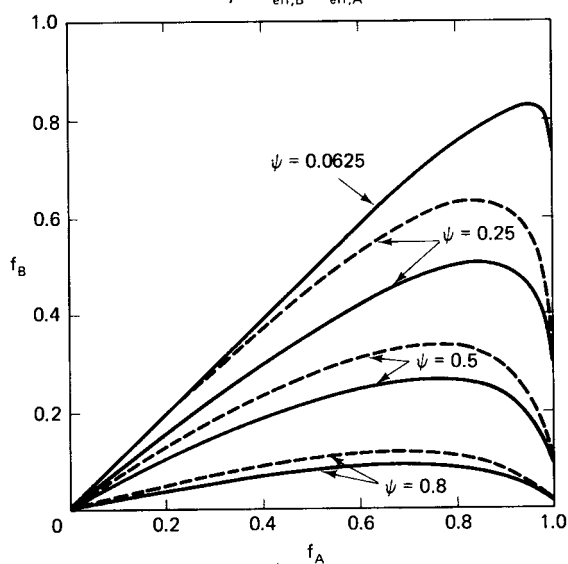


(a) Differential selectivity, type III

$$R = 0.5$$

$$S_i = 16$$

$$\gamma = D_{\text{eff},B}/D_{\text{eff},A}$$



(b) Overall selectivity, type III

$$\gamma = 1$$

$$C_{B0} \text{ (initial)} = 0$$

$$S_i = 16 \text{ —}$$

$$S_i = 4 \text{ - -}$$

**Figure 7.13** Differential and overall selectivities in an isothermal Type III reaction with both interphase and intraphase gradients. [After J.J. Carberry, *Chem. Eng. Sci.*, 17, 675, with permission of Pergamon Press, Ltd., London, England, (1962).]

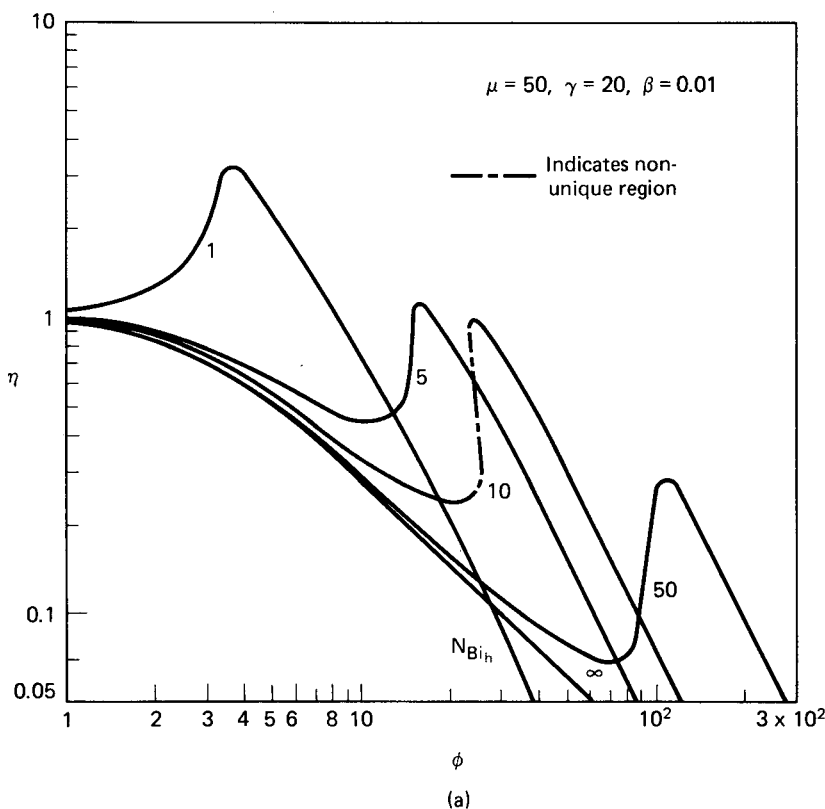


**Figure 7.14** Two examples of nonisothermal effectiveness factor results on inter- and intra-phase gradients. [After D.L. Cresswell, *Chem. Eng. Sci.*, 25, 267, with permission of Pergamon Press, Ltd., London, England, (1970).]

with

$$\mu = \frac{N_{Bi_m}}{N_{Bi_h}}$$

Equation (7-61), expressing  $\tau$  as a function of  $f$ , allows one to reduce the pair of equations (7-58) to a single equation for numerical solution, as described by Weisz and Hicks for the intraphase problem.<sup>5</sup> Some results of effectiveness factor calculations for first-order reactions are given in Figure 7.14. These indicate clearly the significant effects that boundary-layer resistances have on catalytic activity and behavior. Both the locus and the magnitude of the region of multiplicity are altered with changing heat and mass Biot numbers. Illustrated is the variation in effectiveness with the thermal Biot number at a fixed ratio,  $\mu = 10$ , which is a reasonable value in view of practice. Particularly striking are the apparent minima in effectiveness factor occurring at intermediate values of the Thiele modulus. This is associated with the magnitude of the external thermal gradient and it corresponds to a rapid

<sup>5</sup> "You're either in the loop, or you're out of the loop. But more likely you don't know where the loop is or even if there is a loop."—R. Reich

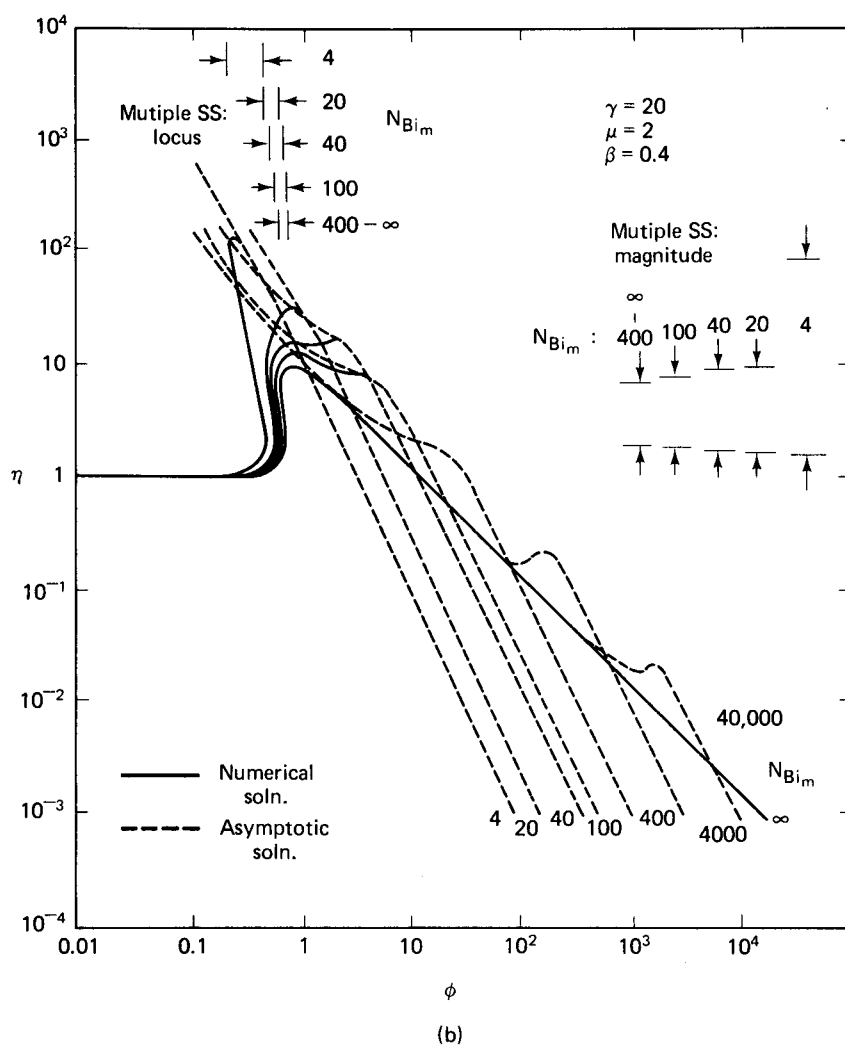


Figure 7.14 Continued.

increase in  $\tau_S$  over a small change in  $\phi$ . The higher temperature increases the overall reaction rate and hence the overall effectiveness.

An asymptotic solution to equation (7-58) based on the method of Petersen has also been developed [J.P. Kehoe and J.B. Butt, *Chem. Eng. Sci.*, 25, 345 (1970)]. The result is

$$\frac{N_{Bi_m}}{\phi} = \frac{e^{\gamma/2}}{\beta(1-f_S)} \left[ A(A+\gamma)e^{-\gamma/A} - (A-\beta f_S)(A+\beta f_S+\gamma) \cdot \exp\left(\frac{-\gamma}{A-\beta f_S}\right) - \gamma(2A+\gamma) \int_{\gamma/A}^{\gamma/(A-\beta f_S)} \frac{e^{-t}}{t} dt \right]^{1/2} \quad (7-62)$$

where  $A = 1 + \beta\mu - \beta\mu f_S + \beta f_S$ . The integral of equation (7-62) is a tabulated

function. The asymptotic solution is given by the combination of equations (7-62) with (7-59). For set  $\gamma$ ,  $\beta$ , and  $\mu$ , the value of the RHS of equation (7-62) is determined as a function of  $f_S$  and  $\eta$  computed from (7-59).

Further discussion of the effects of internal and external gradients on effectiveness are given by Hatfield and Aris [B. Hatfield and R. Aris, *Chem. Eng. Sci.*, 24, 1213 (1969)]; Smith et al. [T.G. Smith, J. Zahradnik, and J.J. Carberry, *Chem. Eng. Sci.*, 30, 763 (1975)]; and McGreavy and Cresswell [C. McGreavy and D.L. Cresswell, *Chem. Eng. Sci.*, 24, 608 (1969); *Can. J. Chem. Eng.*, 47, 583 (1969)].

Since the major thermal resistances in nonisothermal reaction systems are encountered in the boundary layer, while the major mass transfer resistances occur within the particle, we can entertain some simplification of the overall effectiveness factor problem we have been considering. This simplified model envisions *interphase* temperature gradients and *intraphase* concentration gradients only. For this case

$$\eta = \frac{3N_{Bi_m}}{\phi_S^2} \left[ \frac{\lambda - \tanh \lambda}{(N_{Bi_m} - 1) \tanh \lambda + \lambda} \right] \quad (7-63)$$

where

$$\begin{aligned} \phi_S &= \phi_S^\circ \exp \left( \frac{-\gamma}{2} \right) \\ \lambda &= \phi_S^\circ \exp \left( \frac{-\gamma}{2\tau} \right) \\ \tau &= 1 + \frac{\beta\eta}{3N_{Bi_h}} (\phi_S^\circ)^2 e^{-\gamma} \end{aligned}$$

Calculation of the effectiveness factor in this case requires an iterative procedure, since  $\eta$  is required to obtain the value of  $\tau$  which appears in equation (7-63) via  $\lambda$ .

#### Illustration 7.4

The analysis we have been working with has considered the case where the areas involved are the external surface,  $a$ , and internal area,  $s$ , for transport and reaction, respectively. Consider now the case [W. Goldstein and J.J. Carberry, *J. Catal.*, 28, 33 (1973)] where the contribution of the external surface (which is also catalytic) to the overall reaction is not negligible compared to the internal surface,  $s$ . This can be quite possible when the catalyst supplied is very active and is finely divided to minimize transport effects. We would like to know what the isothermal effectiveness and the point selectivity of intermediate for Type III reaction in such a situation is. Recall that the point or differential selectivity is defined as (rate of production of  $j$ )/(rate of reaction of  $i$ ).

#### Solution

Generally for first-order reactions we define the rate constant,  $k$ , in terms of reciprocal time. Here, though, to make the distinction between an internal and external surface, let us write a new constant,  $k'$ , in terms of the area involved such that

$$k' \times (\text{area/volume}) = k \quad (i)$$

Further, define  $f$  as the ratio

$$f = a/(a + s) \quad (ii)$$

so that we may specify the following gradients

$$\left(\frac{dC_A}{dt}\right)_i = \eta_i(1-f)k'C_{A_0} \quad (\text{internal}) \quad (\text{iii})$$

$$\left(\frac{dC_A}{dt}\right)_x = \eta_x f k' C_{A_0} \quad (\text{external}) \quad (\text{iv})$$

and so

$$\left(\frac{dC_B}{dC_A}\right)_i = S_i \quad (\text{internal point selectivity}) \quad (\text{v})$$

$$\left(\frac{dC_B}{dC_A}\right)_x = S_x \quad (\text{external point selectivity}) \quad (\text{vi})$$

Here  $\eta_i$  and  $\eta_x$ , are internal and external effectiveness factors. The overall effectiveness,  $\eta_0$ , can be obtained from these as

$$\eta_0 = (1-f)\eta_i + f\eta_x \quad (\text{vii})$$

Now we have to evaluate yields and selectivities. The overall point yield is

$$Y_p = \frac{[(dC_A/dt)(dC_B/dC_A)]_i}{(dC_A/dt)_i + (dC_A/dt)_x} + \frac{[(dC_A/dt)(dC_B/dC_A)]_x}{(dC_A/dt)_i + (dC_A/dt)_x}$$

Substituting from the definitions of equations (ii)-(vii),

$$Y_p = \frac{(1-f)\eta_i S_i + f\eta_x S_x}{(1-f)\eta_i + f\eta_x} \quad (\text{viii})$$

Now, from equation (7-53) we have

$$\eta_i = \frac{\tanh \phi}{\phi[1 + (\phi \tanh \phi)/N_{Bi_m}]} \quad (\text{ix})$$

where

$$\phi = \Lambda \left[ \frac{(1-f)k'}{D_{eff}} \right]^{1/2}$$

$$N_{Bi_m} = \left( \frac{k_m}{D_{eff}} \right) \Lambda$$

Following the development of equation (7-51), the external effectiveness is

$$\eta_x = \frac{1}{1 + N_{Da}} \quad (\text{x})$$

$$N_{Da} = \frac{\phi^2}{N_{Bi_m}} \left( \frac{f}{1-f} \right)$$

We are now in a position to calculate the overall effectiveness. From equation (vii)

$$\eta_0 = \frac{(1-f) \tanh \phi}{\phi[1 + (\phi \tanh \phi)/N_{Bi_m}]} + \frac{f}{1 + [(\phi^2/N_{Bi_m})f/(1-f)]} \quad (\text{xi})$$

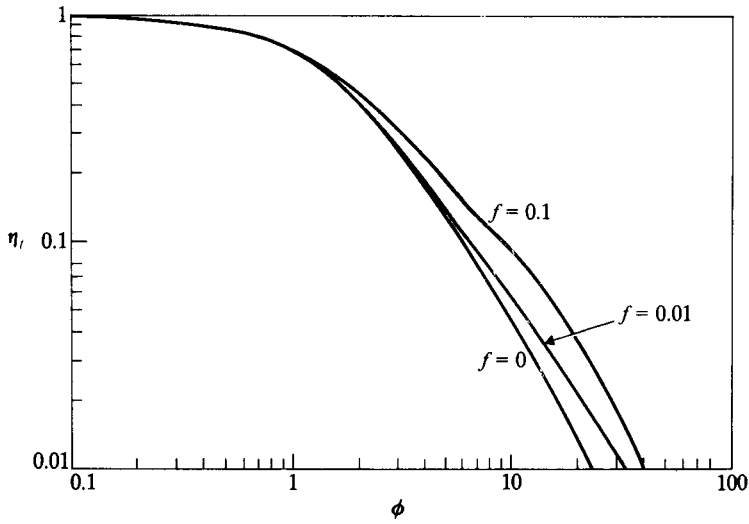


**Figure 7.15** Combined inter-intraphase effectiveness factor,  $\eta_i$ , for a finite external surface area with mass Biot number equal to 10.

The internal point selectivity,  $S_i$ , is what we have called  $\Delta_{diff}$  in the text. Thus,

$$S_i = \frac{m_1 \phi_2 \tanh \phi_2}{m_2 \phi_1 \tanh \phi_1} \left( R + \frac{S_i}{S_i - 1} \right) + \frac{S_i}{S_i - 1}$$

where  $R = (C_{B_0}/C_{A_0})$ , the effective diffusivities of A and B are the same,  $S_i$  is the intrinsic selectivity  $= (k'_1/k'_2)$ , and  $m_i$  is as defined in equation (7-56). The corresponding external selectivity can be found as

$$S_x = \frac{1}{1 + N_{Da_2}} - S_i^{-1} \left( \frac{1 + N_{Da_1}}{1 + N_{Da_2}} \right) \left( \frac{C_{B_0}}{C_{A_0}} \right) \quad (\text{xii})$$

Combination of equations (7-55) and (xii) according to equation (viii) will give the desired point yield.

As might be expected, the influence of the external area contribution dominates for high values of  $\phi$ . Figure 7.15 demonstrates the effect for a moderate value of the mass Biot number equal to 10.



HORATIO SAYS

Illustration 7.4 is not quite as illustrative as it might be. Go further and derive the expression for external selectivity given by (xii). Do boundary layers interfere here?

### 7.1.6 Criteria for the Estimation of Transport Effects

It is desirable to have some means to ascertain the effects of transport on reaction rates, *a priori*, both from the experimental measurement of catalytic reaction kinetics and for the design of catalytic reactors. Such criteria, to be of use, must then be based upon what can be measured or directly observed, nothing else. We can approach this problem in two different ways.

1. Development of means for the determination of catalytic effectiveness on the basis of observable quantities in a given situation.
2. Development of *a priori* criteria to ensure the absence of significant concentration/temperature gradients.

It is probably not necessary to be reminded that this problem is very important, since transport disguises such as those discussed in Section 7.12 will not be seen unless we look for them in a rather determined manner.

An analysis of Point 1 above has been given in the work of Weisz and Hicks, previously cited, and a summary of results reported for Point 2 is also available [J.B. Butt and V.W. Weekman, Jr., *Amer. Inst. Chem. Engr. Symp. Ser.*, 70(143), 27 (1975)]. To examine the first point, let us look at means that might be available for estimation of the effectiveness factor from observable quantities. Now, normally the experimentalist has at hand information concerning observed rates of reaction, concentrations, catalyst dimension, and temperature—but no values for intrinsic kinetic parameters. Let us define, for reasons that will be seen in a moment, a new parameter,  $\Phi_S$

$$\Phi_S = \frac{R_p^2}{D_{eff}} (-r) \left( \frac{1}{C_0} \right) \quad (7-64)$$

where  $(-r)$  is the observed rate of reaction per unit volume of catalyst,  $R_p$  is particle radius (spherical), and  $C_0$  is the reactant concentration. For integral-order kinetics,

$$(-r) = kC_0^n \eta = \frac{C_0 D_{eff}}{R_p^2} \phi_s^2 \eta \quad (7-65)$$

Combining equations (7-64) and (7-65), we obtain

$$\Phi_S = \phi_s^2 \eta \quad (7-66)$$

Now each of the quantities in  $\phi_s$  is experimentally observable, while the RHS of equation (7-66) can be computed from results such as those given in Figure 7.8. Hence a set of graphs such as those given in Figure 7.16 can be prepared relating  $\Phi_S$  to  $\eta$  and the effectiveness estimated directly from experimental results.

A substantial number of *a priori* criteria for the estimation of transport effects on catalytic reaction rates has been reported by a number of workers. These criteria are generally derived on the premise that one does not desire the net transport effect to alter the true rate by more than some arbitrarily specified amount, normally 5%. Because of the uncertainty involved in knowing some of the parameters, the philosophy in applying these criteria should be conservative; one does not look to marginal satisfaction of their requirements, but perhaps to be an order of magnitude better.

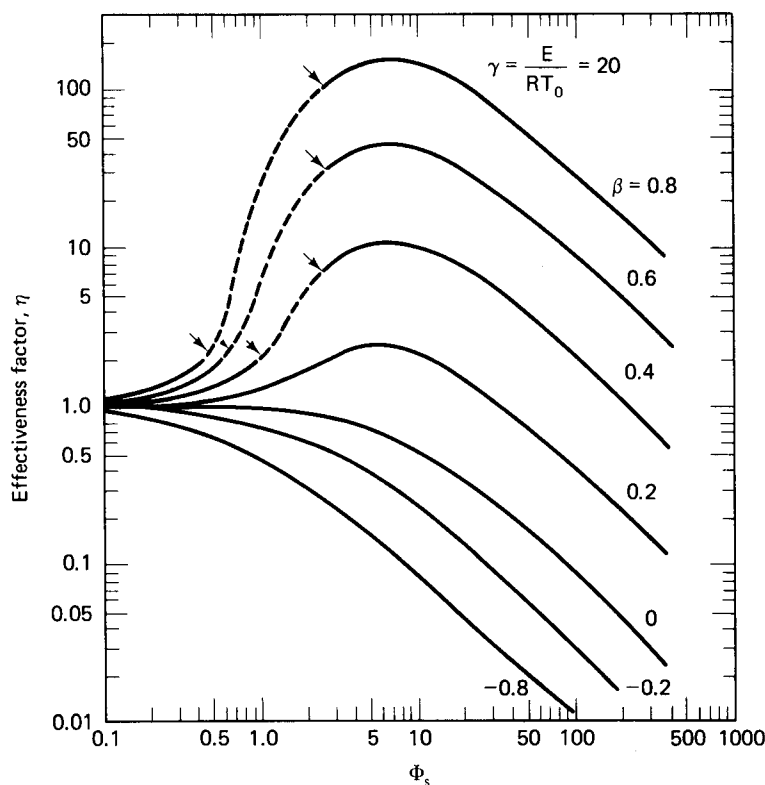


**Figure 7.16** Catalytic effectiveness in terms of the experimentally observable parameter  $\Phi_s$ . First-order reaction, spherical geometry. [After P.B. Weisz and J.S. Hicks, *Chem. Eng. Sci.*, 17, 265, with permission of Pergamon Press, Inc., London, England, (1962).]

A summary of intraparticle transport criteria is given in Table 7.2. The most general of the criteria, 5(a) of Table 7.2, ensures the absence of any net effects (combined) of temperature and concentration gradients but does not guarantee that this may not be due to a compensation between heat- and mass-transport rates. (In fact, this is the case when  $\gamma/\beta \approx n$ ). It may therefore be the most conservative general policy to see that the separate criteria for isothermality are met, for example, by the combination of 3 and 5(c), or of 3 and 4 in Table 7.2. The presentations of Table 7.2 deal with power-law kinetics only; more complicated issues, such as what to do with complex kinetics or reactions involving volume change, have also been treated in the literature and are summarized by Mears [reference 5(b) in Table 7.2].

A disturbing question may be just how successful these criteria are in utilizing only observable quantities. For example, if we follow the letter of the statements above, the true activation energy is apparently defined as an experimentally observable quantity in the nonisothermal criteria. This would presumably be an experimental value resulting from studies in which intraparticle transport effects were absent, but this is precisely what one is trying to determine. What can we say? Sometimes an active imagination plus iteration is the best course.



**Table 7.2** Intraparticle Transport Criteria\*

1. For the absence of concentration gradients in an isothermal spherical particle ( $\eta \geq 0.95$ ), first-order reaction:

$$\frac{rR_p^2}{C_0 D_{eff}} < 1 \quad \text{Weisz and Prater}$$

2. For the absence of concentration gradients in an isothermal spherical particle ( $< 5\%$  deviation from a flat concentration gradient), power-law kinetics:

$$\left. \begin{array}{l} \frac{rR_p^2}{C_0 D_{eff}} \end{array} \right\} \begin{array}{l} < 6.0 \text{ zero order} \\ < 0.6 \text{ first order} \\ < 0.3 \text{ second order} \end{array} \quad \text{Weisz}$$

3. For the absence of concentration gradients in an isothermal particle ( $\eta > 0.95$ ), power-law kinetics:

$$\frac{rR_p^2}{C_0 D_{eff}} < \frac{1}{|n|} \quad \text{Hudgins}$$

$$r_0 = kC_0^n \quad n \neq 0, n > 0$$

4. For the absence of temperature gradients (rate does not differ by more than 5% of isothermal rate):

$$\frac{|\Delta H| r R_p^2}{k_{eff} T_0} < \frac{T_0 R}{E} \quad \text{Anderson}$$

5. (a) For the absence of combined effect of temperature and concentration gradients ( $\eta = 1 \pm 0.05$ ), power-law kinetics:

$$\frac{rR_p^2}{C_0 D_{eff}} < \frac{1}{|n - \gamma\beta|} \quad \text{Kubota and Yamanaka}$$

$$\gamma = \frac{E}{RT_0} \quad \beta = \frac{(-\Delta H) D_{eff} C_0}{\lambda T_0}$$

- (b) Modification when  $n \approx \gamma\beta$

$$\frac{rR_p^2}{C_0 D_{eff}} < 13 \quad \text{Mears and Petersen}$$

- (c) For isothermal operation, compare 5(a) and 3:

$$|\gamma\beta| < 0.05n \quad \text{Mears}$$

(a)  $r$  is the observed rate of reaction per unit particle volume.

(b) For other geometries the spherical particle radius can be approximated by a characteristic dimension given by the volume/external surface ratio.

(c) Since these criteria refer exclusively to intraparticle transport,  $C_0$  and  $T_0$  refer to surface temperature and concentrations.

$\gamma, \beta$  = parameters defined in 5(a);  $\eta$  = effectiveness factor.

\*References: 1. P.B. Weisz and C.D. Prater, *Advan. Catalysis*, 6, 143 (1954).

2. P.H. Weisz, *Z. Physik. Chem.*, N.F., 11, 1 (1957).

3. R.R. Hudgins, *Chem. Eng. Sci.*, 23, 93 (1968).

4. J.B. Anderson, *Chem. Eng. Sci.*, 18, 147 (1963).

5(a). H. Kubota and Y. Yamanaka, *J. Chem. Eng. (Japan)*, 2, 238 (1969).

5(b). D.E. Mears, *Ind. Eng. Chem. Proc. Design Devel.*, 10(4), 541 (1971); E.E. Petersen, *Chemical Reaction Analysis*, Prentice-Hall, Englewood Cliffs, NJ., 1965.

5(c). D.E. Mears, *Ind. Eng. Chem. Proc. Design Devel.*, 10(4), 541 (1971).

Source: From J.B. Butt and V.W. Weekman, Jr. *Amer. Inst. Chem. Eng. Symp. Ser.*, 70, (143), 27, with permission of the American Institute of Chemical Engineers, (1975).

**Table 7.3** Interphase Transport Criteria\*

1. For the absence of interphase concentration gradients in isothermal systems ( $\eta > 0.95$ ); first-order reaction:

$$\frac{\eta k}{k_m A} < 0.1 \quad \text{Carberry}$$

2. For the absence of interphase concentration gradients in isothermal systems ( $\eta > 0.95$ ); power-law kinetics:

$$\frac{r R_p}{C_0 k_m} < \frac{0.15}{n} \quad \text{Mears}$$

3. For a less than 5% deviation in the rate of reaction due to interphase temperature gradients alone (criterion independent of whether intraparticle gradients exist or not):

$$|\chi| = \frac{(-\Delta H) r R_p}{h T_0} < \frac{0.15 R T_0}{E} \quad \text{Mears}$$

4. For the absence of combined intraparticle/interphase gradients ( $\eta = 1 \pm 0.05$ ):

$$\frac{r R_p^2}{C_0 D_{eff}} < \frac{1 + 0.33 \gamma \chi}{|n - \gamma \beta| (1 + 0.33 n w)} \quad \text{Mears}$$

where  $\eta$ ,  $\gamma$ , and  $\beta$  are defined as in Table 7.1, 5(a), with  $C_0$  and  $T_0$  as bulk rather than surface values.

$$w = \frac{r R_p}{C_0 k_m}$$

5. For isothermal operation:

$$|\gamma \beta + 0.3 n \gamma \chi| < 0.05 n \quad k = \text{first-order rate constant per unit particle volume;} \quad \text{Mears}$$

$A = \text{external surface to volume ratio of particle.}$

\*References: 1. J.J. Carberry, *Amer. Inst. Chem. Eng. J.*, 7, 350 (1961).

2. D.E. Mears, *Ind. Eng. Chem. Proc. Design Devel.*, 10, 4, 541 (1971).

3. D.E. Mears, *J. Catalysis*, 20, 127 (1971).

4. D.E. Mears, *Ibid.*

5. D.E. Mears, *Ind. Eng. Chem. Proc. Design Devel.*, 10, 4, 541 (1971).

Source: From J.B. Butt and V.W. Weekman, Jr., *Amer. Inst. Chem. Eng. Symp. Ser.*, 70, 143, 27, with permission of the American Institute of Chemical Engineers, (1975).

In Table 7.3 are interphase transport criteria for both isothermal and non-isothermal reactions. The most general expression is given in Case 4; if condition 5 is satisfied, the influence in intraparticle mass transport can be examined via 1 or by the criteria of Table 7.2. It has been shown that interphase thermal resistance is dominant over intraparticle resistance if the heat Biot number,  $(h R_p / k_{eff})$ , is  $< 5$ . In such cases, equation (7-63) can be used directly to estimate effectiveness. Some further discussion of the criteria of Table 7.3 has also been given by Dogu and Dogu [T. Dogu and G. Dogu, *Amer. Inst. Chem. Eng. J.*, 30, 1002 (1984)].

It would be useful to have some experimental diagnostics available that will give an indication as to whether internal or external gradients are important in a given situation. By and large we would also like to have these diagnostics be independent of any calculation based on transport or rate parameters so that they

may be used in addition to the criteria set forth in Tables 7.2 and 7.3, as a kind of cross check.

The procedure is quite simple in the case of intraparticle effects, since the diffusional modulus is directly proportional to the characteristic particle dimension. Thus the very practical idea of “chop ’em up and run ’em again” is very sound. If there is any influence of intraparticle transport, it should be manifested by a change (normally an increase) in the rate or conversion observed, with all other factors being the same. In principle, one should always be able to minimize intraparticle transport effects by working with catalyst particles of sufficiently small size. There are, however, practical limits associated with doing this, such as high pressure drops in fixed beds or elution in slurry or fluid beds that employ very fine particles (as we will see later).

For interphase limitations (boundary layer effects) the situation seems, at first glance, as simple as that for internal gradients, since most correlations for heat- and mass-transfer coefficients show a proportionality to the flow velocity of the surrounding fluid,  $v^n$ , where normally  $0.6 < n < 1$ . At the lower velocities associated in particular with laboratory reactor operation, however,  $n$  tends to be closer to 0.6 than to 1, and the transport coefficients become insensitive to flow velocity and changing flow velocity is not an effective diagnostic.

A way around this was proposed by Koros and Nowak [R.M. Koros and E.J. Nowak, *Chem. Eng. Sci.*, 22, 470 (1967)]; see also [R.J. Madon and M. Boudart, *Ind. Eng. Chem. Fundls.*, 21, 438 (1982)]. This procedure requires that the catalyst be crushed to a fine mesh size and then be diluted with an inert of the same mesh size and pore structure to form a set of samples with varying ratios,  $p$ , of active and inert ingredients. These are then reformed into pellets of the same dimension as the original catalyst. Reaction experiments are now run on the original catalyst and the diluted samples. If the observed rate versus  $p$ , is linear over the entire range to  $p \approx 1$ , then the intrinsic kinetics are being observed for the conditions under investigation. Deviations from linearity indicate intrusion of heat- and/or mass-transport rates. It is probably not a bad idea in practice to combine the Koros-Nowak diagnostic procedure with a series of runs at varying flow velocities if interphase gradient intrusions are suspect.

### Illustration 7.5

Give a quantitative description of how and why the Koros-Nowak procedure works. Use an irreversible first-order reaction under isothermal conditions as an example.

#### Solution

Recall the general expression for the rate of reaction in an isothermal system given by equation (7-50)

$$(-r) = \frac{\eta k C_0}{1 + \left( \frac{\eta k}{k_m} \right) \left( \frac{\bar{V}}{S_A} \right)} \quad (\text{i})$$

For the catalyst dilution experiment

$$k = k_i p \quad (\text{ii})$$

Thus,

$$(-r) = \frac{\eta k_i p C_0}{1 + \left( \frac{\eta k_i p}{k_m} \right) \left( \frac{\bar{V}}{S_A} \right)} \quad (\text{iii})$$

(1) For no internal gradients

$$(-r) = \frac{k_i p C_0}{1 + \left( \frac{k_i p}{k_m} \right) \left( \frac{\bar{V}}{S_A} \right)} \quad (\text{iv})$$

(2) For no external gradients

$$(-r) = \eta k_i p C_0 \quad (\text{v})$$

(3) For no gradients of any kind

$$(-r) = k_i p C_0 \quad (\text{vi})$$

In either case, (v) or (vi), there is direct proportionality between  $(-r)$  and  $p$ .



HORATIO SAYS

What would you expect the temperature dependence to be for a reaction that is completely controlled by the external mass transfer rates over the temperature range under consideration?

### 7.1.7 Parametric Quantities

In addition to the kinetic parameters such as rate constant and activation energy that we have become accustomed to dealing with, the analysis of this section has introduced some very important newcomers. Two of these, the effective transport properties within the porous matrix of the catalyst,  $D_{eff}$  and  $k_{eff}$ , differ in substance from the transport coefficients in homogeneous phases with which we are familiar, and warrant some special discussion.

As indicated in Figure 7.1, diffusion of reactants to and products from the site of chemical transformation occurs through the pore structure of the catalyst. Many words have been written about this; Petersen [E.E. Petersen, *Chemical Reaction Analysis*, Prentice-Hall, Inc., Englewood Cliffs, NJ, (1965)] says it best in a few. For effective mass-transport parameters one may separately identify factors dealing with the transport rates and with structural effects. Following this we may write for an effective diffusivity,

$$D_{eff} = D_i \cdot f(\text{structure}) \quad (7-67)$$

where  $D_i$  is some intrinsic transport coefficient. Unfortunately, the situation is not simple as far as  $k_{eff}$  is concerned, since the open pore structure is not the only pathway for energy transport. For now, though, let us concentrate on  $D_{eff}$ . The following type

of correlation for effective diffusivity is the most convenient and is widely employed.

$$D_{eff} = D_i \left( \frac{\epsilon}{\tau} \right) \quad (7-68)$$

where  $\epsilon$  is the volume fraction voids in the particle and  $\tau$ , the *tortuosity*, is a structural factor accounting for increased diffusional path length and irregular and varying channel cross section seen by individual diffusing molecules. There seems to be no reliable method for the precise estimation of  $\tau$  aside from separate experiments,<sup>6</sup> since theoretical approaches that have been proposed require information on pore sizes and their distribution [G.R. Youngquist, *Ind. Eng. Chem.*, 62, 8, 53 (1970)]. A useful, simple approach leading to equation (7-68) has been detailed by Johnson and Stewart [M.F.L. Johnson and W.E. Stewart, *J. Catalysis*, 4, 248 (1965)]. Values of  $\tau$  and  $\epsilon$  from this are given in Table 7.4. Although these range over a wide spectrum of values, a reasonable order-of-magnitude estimation might propose

$$D_{eff} \approx (0.1) D_i \quad (7-69)$$

Equations (7-67) to (7-69) also pose the question of what to use for  $D_i$ . This seems simple at first, but further thought brings difficulties. Typical catalyst structures may consist of widely varying pore-size distributions such that the smallest pores may be of diameter much less than the mean free path of the diffusing molecules and the largest pores much greater than this. Thus, possible modes of diffusion range from Knudsen diffusion in the smallest pores to bulk diffusion in the largest, with some “transition” mechanism between Knudsen and bulk being important in the midrange. (Zeolite structures are an exception to this rule of thumb and are not included in Table 7.4. For further information on this see Satterfield or Bhatia [S. Bhatia, *Zeolite Catalysis: Principles and Applications*, CRC Press, Inc., Boca Raton, FL, (1990)]. In order to determine what mechanism of diffusion is operative, we must have a comparison of the mean free path under the conditions of interest and a measure of the characteristic pore dimension. The former is given to us by kinetic theory, while the latter is provided either via experimental data or by one of numerous estimation methods. Wheeler has suggested that an effective average value may be defined by analogy to cylindrical geometry, since the radius of a cylinder is equal to twice the volume divided by the external surface. For a porous material of surface  $S_q$  (area/wt), void volume  $V_q$  (volume/wt), and bulk density of  $\rho_b$  (wt/volume) we may write

$$\bar{R} = \frac{2V_q}{S_q} = \frac{2\epsilon}{S_g \rho_b} \quad (7-70)$$

The following procedures may then be used to obtain  $D_i$  pertinent to the type of diffusion mechanism that predominates:

1. *Bulk diffusion*—independent of  $R$ . Values obtained from tabulated data, interaction theory [J.O. Hirschfelder, C.F. Curtiss, and R.B. Bird, *Molecular Theory of Gases and Liquids*, Wiley, New York, NY, (1954)]; or semitheoretical calculations [J.C. Slattery and R.B. Bird, *Amer. Inst. Chem. Eng. J.*, 4, 137 (1958)].

<sup>6</sup> Alas, the reliable elements of “Earth, Air, Fire and Water” do not always work.

**Table 7.4** Tortuosity Factors for Diffusion in Catalysts

Catalyst	Technique	$\epsilon$	$\tau$	Reference <sup>a</sup>
Ag/8.5% Ca alloy pelletized from powder	Gas diffusion, 1 atm	0.3 0.04	6.0 $\infty$	1
Ag pelletized from above powder after removal of Ca by leaching	Gas diffusion, 1 atm	0.6 0.3 0.1	7.5 10 $\infty$	1
Ni pelleted from commercial powder	Gas diffusion, 1 atm	0.26	6	1
Ag pelleted from powder	Gas diffusion, 1 atm	0.7 0.3	1.7 3.3	2
Sprayed Ag-alloy catalyst after activation	Gas diffusion, 1 atm	0.68 0.41	2–3.5 16	3
Pelletized boehmite alumina	Gas diffusion, 1 atm	0.34 0.31	2.7 1.8	4
Pelleted Cr <sub>2</sub> O <sub>3</sub> /Al <sub>2</sub> O <sub>3</sub> catalyst	Gas diffusion, 1 atm	0.22	2.5	5
1% Pd on alumina spheres; commercial support	From reaction (liquid phase)	0.5	7.5	6
0.5% Pd on alumina; commercial type catalyst pellets	From reaction (liquid phase)	0.59	3.9	7
Pelletized from 1 to 8- $\mu$ iron powder	Gas diffusion, 1 atm	0.22–0.32	2.6–2.9	8
Harshaw commercial MeOH synthesis catalyst, prereduced	Gas diffusion, 65 atm	0.49	6.9	9
Haldor-Topsøe commercial MeOH synthesis catalyst, prereduced	Gas diffusion, 65 atm	0.43	3.3	9
BASF commercial MeOH synthesis catalyst, prereduced	Gas diffusion, 65 atm	0.50	7.5	9
Girdler G-52 commercial catalyst, 33% Ni on refractory oxide support	Gas diffusion, 65 atm	0.44	4.5	9
Girdler G-58 commercial catalyst, Pd on alumina	Gas diffusion, 6 atm	0.39	2.8	9

<sup>a</sup> 1. C.M. Amberg and E. Echigoya, *Can. J. Chem. Engr.*, 39, 215 (1961).

2. S. Masamune and J.M. Smith, *Amer. Inst. Chem. Eng. J.*, 8, 217 (1962).

3. G. L. Osberg, A. Tweddle, and W.C. Brennan, *Can. J. Chem. Engr.*, 41, 260 (1963).

4. N. Wakao and J.M. Smith, *Chem. Eng. Sci.*, 17, 825 (1962).

5. C.N. Satterfield and S.K. Saraf, *Ind. Eng. Chem. Fundls.*, 4, 451 (1965).

6. C.N. Satterfield, A.A. Pelossof and T.K. Sherwood, *Amer. Inst. Chem. Eng. J.*, 15, 226 (1969).

7. C.N. Satterfield, Y.H. Ma and T.K. Sherwood, cited in C.N. Satterfield, *Mass Transfer in Heterogeneous Catalysis*, MIT Press Cambridge, Mass., 1970.

8. J. Hoogschagen, *Ind. Eng. Chem.*, 47, 906 (1955).

9. C.N. Satterfield and P.J. Cadle, *Ind. Chem. Fundls.*, 7, 202 (1968).

Source: After C.N. Satterfield, *Mass Transfer in Heterogeneous Catalysis*, with permission of MIT Press, Cambridge, MA, (1970).

2. *Knudsen diffusion*. For diffusion of a molecule A, an analog to the result for regular cylindrical capillaries is

$$D_{K_A} = \left( \frac{2\bar{R}}{3} \right) \left( \frac{8kT}{m_A} \right)^{1/2} \quad (\text{molecular units})$$

or

$$D_{K_A} = 9700\bar{R} \left( \frac{T}{M_A} \right)^{1/2} \text{ cm}^2/\text{s} \quad (7-71)$$

where  $T = \text{K}$ ,  $M_A$  is the molecular weight, and  $R$  is in cm.

3. *Transition diffusion*. This a bit more complicated than the two limits, since the theoretical result for  $D_i$  does not fit into the form of equation (7-67). For binary diffusion of A in B, the following has been shown to apply [R.B. Evans, G.M. Watson, and E.A. Mason, *J. Chem. Phys.*, 33, 2076 (1961)].

$$D_i(\text{transition}) = \left( \frac{1 - \alpha x_A}{C\mathcal{D}_{AB}} + \frac{1}{CD_{K_A}} \right)^{-1} \quad (7-72)$$

where  $C$  is total concentration,  $x_A$  the mol fraction of A,  $\mathcal{D}_{AB}$  and  $D_{K_A}$  bulk and Knudsen diffusion coefficients, respectively, and  $\alpha$  a quantity related to the ratio of fluxes of B to A,  $(N_B/N_A)$ , as

$$\alpha = 1 + \frac{N_B}{N_A} \quad (7-73)$$

The diffusivity is thus dependent upon concentration and flux ratio, and strictly speaking we should not see a theory of catalyst effectiveness based on constant diffusivity. However, this is more detail than it is worth; a good approximation is obtained from the limit of equation (7-72) for constant pressure conditions and  $N_B = -N_A$ . Then

$$D_i(\text{transition}) = \left( \frac{1}{\mathcal{D}_{AB}} + \frac{1}{D_{K_A}} \right)^{-1}$$

and a working form for effective diffusivity would be<sup>7</sup>

$$D_{eff} = \left( \frac{\tau}{\mathcal{D}_{AB}\epsilon} + \frac{\tau'}{D_{K_A}\epsilon'} \right)^{-1} \quad (7-74)$$

The geometric parameters  $\tau'$  and  $\epsilon'$  for the Knudsen mechanism may, in general, differ from those for the bulk mechanism due to the nature of the pore radius distribution. Again, however, it is doubtful in practice whether this amount of detail is necessary.

The problem of estimating or correlating effective thermal conductivities,  $k_{eff}$ , for porous media is much more difficult than the corresponding mass transport problem. However, it turns out that this is a very important parameter. One reason for the difficulty is that, while for mass diffusion the solid forms a barrier between the

<sup>7</sup> "Form follows function," or is it the other way around?

**Table 7.5** Thermal Conductivities of Some Porous Catalysts

Catalyst	Temp. (°C)	Density (g/cm <sup>3</sup> )	$k_{\text{eff}}$ (cal/sec-cm-°C)		Reference <sup>a</sup>
			1 atm	Vacuum	
1. Chromia/Al <sub>2</sub> O <sub>3</sub> (reforming)	90	1.4	$0.7 \times 10^{-3}$	—	1
2. SiO <sub>2</sub> /Al <sub>2</sub> O <sub>3</sub> (cracking)	90	1.25	$0.86 \times 10^{-3}$	—	1
3. Pt/Al <sub>2</sub> O <sub>3</sub> (reforming)	90	1.15	$0.53 \times 10^{-3}$	—	1
4. Activated carbon	90	0.65	$0.64 \times 10^{-3}$	—	1
5. Al <sub>2</sub> O <sub>3</sub> (boehmite)	50	1.12	$0.52 \times 10^{-3}$	$0.39 \times 10^{-3}$	2
6. Pelleted Ag	34	2.96	$1.7 \times 10^{-3}$	$0.15 \times 10^{-3}$	3
7. Cu/MgO	25	0.70	$0.18 \times 10^{-3}$	—	4
8. Pt/Al <sub>2</sub> O <sub>3</sub> (reforming)	—	1.34	$0.35 \times 10^{-3}$	—	5
9. Ni/kieselguhr, 58% (hydrogenation)	40	1.88	$0.36 \times 10^{-3}$	—	6
10. Ni/kieselguhr, 25% graphite	40	1.56	$3.5 \times 10^{-3}$	—	6

<sup>a</sup>1. R.A. Sehr, *Chem. Eng. Sci.*, 9, 145 (1958).

2. R.A. Mischke and J.M. Smith, *Ind. Eng. Chem. Fundls.*, 1, 288 (1962).

3. S. Masamune and J.M. Smith, *J. Chem. Eng. Data*, 8, 54 (1963).

4. R.E. Cunningham, J.J. Carberry, and J.M. Smith, *Amer. Inst. Chem. Eng. J.*, 11, 636 (1965).

5. F.W. Miller and H.A. Deans, *Amer. Inst. Chem. Eng. J.*, 13, 45 (1967).

6. J.P.G. Kehoe and J.B. Butt, *Amer. Inst. Chem. Eng. J.*, 18, 347 (1972).

portions of the structure (voids) in which transport occurs, this is not so for thermal diffusion. One has heat transport through the internal (fluid-filled) voids and through the surrounding solid structure as well. Experimental data are scarce; some typical values are given in Table 7.5 for a number of materials. One notable feature is that the range of values for  $k_{\text{eff}}$  is small for the porosities of a given class of materials, and does not seem to be very dependent upon the thermal conductivity of the solid material itself. If one is pressed for a value of  $k_{\text{eff}}$  and has no data available, a guess of  $0.5 \times 10^{-3}$  cal/s-cm-K can not be terribly off the mark.

For reactions in which thermal effects are important, we have seen the emergence of the parameters  $\beta$  and  $\gamma$ . Now  $\beta$  is a measure of the thermicity of the reaction of interest, but unfortunately it is also proportional to the ratio of the effective transport coefficients, ( $D_{\text{eff}}/k_{\text{eff}}$ ). Since it is difficult to make good *a priori* estimates of  $D_{\text{eff}}$  and  $k_{\text{eff}}$ , particularly the latter, it is then also difficult to estimate  $\beta$ , and we just have to live with some uncertainty here. The activation energy parameter,  $\gamma$ , may be tied down a little better than  $\beta$ , since one is probably not going to do any serious reaction engineering without a value of the activation energy in hand. Always keep in mind, however, that uncertainties in the activation energy, hence in  $\gamma$ , are going to be exponentially amplified in any calculations using the Arrhenius equation. For our purposes the precise numbers themselves are not as important as the norms that they establish for representative ranges of  $\beta$  and  $\gamma$ , and the corresponding results as shown in Figures 7.8 and 7.12. We will also keep in mind that in most cases  $N_{Bi_m} \gg N_{Bi_h}$ , reflecting the fact that major thermal resistances reside in the boundary



layer external to the catalyst particle, while the major mass resistances reside within the porous matrix of the catalyst particle.

This leaves us with the external transport parameters for heat and mass transfer,  $k_m$  and  $h$ , to examine. The discussion here will be somewhat particular to the very important case of particles in fixed beds, since the correlations that have been developed depend in certain instances on the physical configuration involved. Correlations as required for other types of reactors will be presented in Chapter 8. The heat- and mass-transfer coefficients already presented in this chapter are set in terms of the corresponding fluxes, thus

$$h = \frac{Q}{(T_0 - T_S)} \quad (7-75)$$

$$k_m = \frac{N}{(C_0 - C_S)} \quad (7-76)$$

where  $Q$  is a heat flux in kJ/area-°C (or equivalent), and  $k_m$  is in mass or mols/area-time-ΔC. The study of these transport coefficients has a long and venerable history, dating to the beginning of what we identify as chemical engineering, since these are central factors in any process design involving mass or heat transfer, in addition to any applications here. We have correlations of the general form,

$$N_{Bi_m} = f_1[(N_{Re})^p, (N_{Sc})^q] \quad (7-77)$$

$$N_{Bi_h} = f_2[(N_{Re})^p, (N_{Pr})^q] \quad (7-78)$$

where the Reynolds, Schmidt, and Prandtl numbers are defined in terms of the properties of the fluid phase, so that

$$\begin{aligned} N_{Pr} &= \frac{C_p \mu}{k} \\ N_{Sc} &= \frac{\mu}{\rho \mathcal{D}} \\ N_{Re} &= \frac{R_p G}{\mu} \end{aligned} \quad (7-79)$$

with  $G$ , the mass flow rate;  $\mu$ , fluid viscosity;  $\mathcal{D}$ , bulk diffusivity;  $C_p$ , heat capacity; and  $k$ , thermal conductivity. Heat- and mass-transfer coefficients traditionally have been correlated in terms of the  $j_H$  and  $j_D$  factors, defined as

$$j_H = \frac{h}{C_p G} (N_{Pr})^{2/3} = f_2(N_{Re}) \quad (7-80)$$

$$j_D = \frac{k_m M_m}{G} (N_{Sc})^{2/3} = f_1(N_{Re}) \quad (7-81)$$

Correlations for  $j_H$  and  $j_D$ , in a general form, are shown in Figure 7.17. A detailed discussion of such correlations has been given by Schlünder [E.U. Schlünder, *ACS Symp. Series*, 72, 110 (1978)]. A convenient numerical form is provided by Petrovic and Thodos [L.J. Petrovic and G. Thodos, *Ind. Eng. Chem. Fundls.*, 1, 274 (1968)];

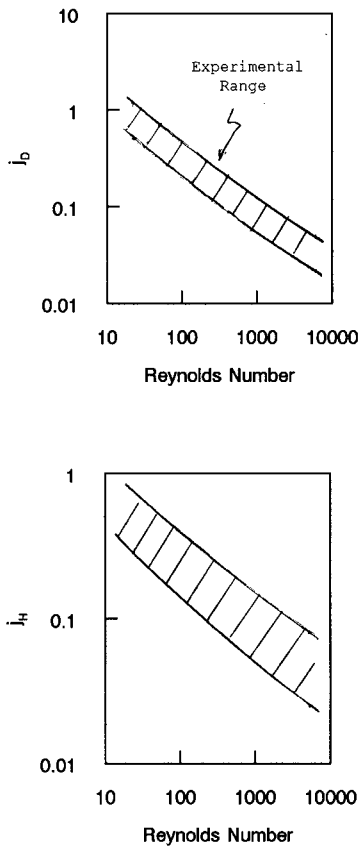


**Figure 7.17** Correlations of  $j_D$  and  $j_H$  for fixed beds of spherical particles. (Void fraction = 0.37.)

see also [F. Yoshida, D. Ramaswamy, and O.A. Hougen, *Amer. Inst. Chem. Eng. J.*, 8, 5 (1962)].

$$N_{Bi_m} = \left( \frac{a}{2\epsilon} \right) \left( \frac{\mathcal{D}}{D_{eff}} \right) (N_{Re})^{1+b} (N_{Sc})^{1/3} \quad (7-82)$$

$$N_{Bi_h} = \left( \frac{a}{2\epsilon} \right) \left( \frac{k}{k_{eff}} \right) (N_{Re})^{1+b} (N_{Pr})^{1/3} \quad (7-83)$$

where  $a = 0.357$  and  $b = -0.359$  for  $3 < N_{Re} < 2000$ ,  $\epsilon$  is bed porosity,  $\mathcal{D}$  the diffusion coefficient of the reactant in the bed,  $D_{eff}$  the effective diffusivity of the reactant in the catalyst,  $k$  the thermal conductivity of the fluid phase, and  $k_{eff}$  the effective thermal conductivity of the catalyst. Note that the equations here are written in a somewhat different form than many  $j_H$  correlations. Mercer and Aris [M.C. Mercer and R. Aris, *Rev. Lat. Amer. Quim. Apl*, 2, 149 (1971)] have summarized the range of values for the two Biot numbers to be expected in fixed beds, based on  $(k/k_{eff}) = 0.1$ ,  $(\mathcal{D}/D_{eff}) = 10$ ,  $N_{Pr} = N_{Sc} = 1$  and  $\epsilon = 0.45$ . These range from 4 to 530 for mass Biot number and 0.04 to 5.3 for heat Biot number as the Reynolds number varies from 1

to 2000. A summary for extreme ranges for the parameters involved in very exothermic reactions given by Mercer and Aris would increase the range of Biot numbers by an order of magnitude; also,  $1 < (N_{Bi_m}/N_{Bi_h}) < 2000$ ,  $0 < \beta < 1$ , and  $0 < \gamma < 60$  in such reactions.

Additional discussions of parameter values involved in transport effects on chemical reactor behavior are given by Carberry [J.J. Carberry, *Ind. Eng. Chem. Fundls.*, 14, 123 (1975)]; Carberry and White [J.J. Carberry and D. White, *Ind. Eng. Chem.*, 61, 27 (1969)]; Creswell and Patterson [D.L. Cresswell and W.R. Patterson, *Chem. Eng. Sci.*, 25, 1405 (1970)]; and Dumez and Froment [F.J. Dumez and G.F. Froment, *Ind. Eng. Chem. Proc. Design Devel.*, 15, 291 (1976)]. We will have more to say about interphase transport in fixed beds later in this chapter.

### 7.1.8 Gas-Solid Noncatalytic Reactions

Gas-solid reactions between a fluid and a solid are important in a number of applications such as coal gasification, metallic ore processing, and catalyst regeneration. They are related in many aspects to the gas-solid catalytic reactions we have treated in developing the concepts of catalytic effectiveness, but differ in the very important aspect that the solid itself (in the form of a porous matrix) is one of the reactants. Since the solid phase itself is involved in reaction, often conditions of diffusion/reaction change with time of reaction and the overall process is an unsteady-state one. As with effectiveness factors, many variants on a theme can be envisioned, i.e., is the reaction fast or slow, does the particle porosity (hence  $D_{eff}$ ) change with reaction, are boundary layer transport effects of importance, etc.? We will present in some detail the developments of Wen concerning these questions [C.Y. Wen, *Ind. Eng. Chem.*, 60, 34 (1968); H. Ishida and C.Y. Wen, *Amer. Inst. Chem. Eng. J.*, 14, 311 (1968)].

Let us start by considering a gaseous component A reacting with a porous solid particle under isothermal conditions. For spherical geometry the mass, conservation equation is

$$\frac{\partial(\epsilon_S C_{A_S})}{\partial t} = \left(\frac{1}{r^2}\right) \frac{\partial}{\partial r} \left(D_{eff} r^2 \frac{\partial C_{A_S}}{\partial r}\right) - (-r_A) \quad (7-84)$$

where  $\epsilon_S$  is the porosity of the solid particle,  $C_{A_S}$  the concentration of A within the porous matrix, and  $(-r_A)$  the volumetric rate of reaction of A. It is understood that, as written in equation (7-84), both  $\epsilon_S$  and  $D_{eff}$  can be variant with time or position. For the solid

$$(-r_S) = \left(\frac{\partial C}{\partial t}\right) \quad (7-85)$$

and the whole process is at an unsteady state, as indicated by the time derivatives in equations (7-84) and (7-85). The initial conditions here are

$$C_{A_S} = C_{A_{S,0}}; \quad C_S = C_{S,0}; \quad t = 0$$

and the boundary conditions,

$$\begin{aligned} \left(\frac{\partial C_{A_S}}{\partial r}\right)_0 &= 0 \\ D_{eff} \left(\frac{\partial C_{A_S}}{\partial r}\right)_R &= k_m [C_A - (C_{A_S})^S] \end{aligned} \quad (7-86)$$

where  $C_{A_{S,0}}$  is the initial concentration of A at the particle surface,  $(C_{A_S})^S$  the surface concentration of A for  $t > 0$ ,  $C_{S,0}$ , and the surface concentration of solid at  $t = 0$ . A reasonable assumption is that  $\epsilon_S$  is a linear function of the conversion of solids.

$$\epsilon_S = (\epsilon_S)_0 + C_{S,0}(V_S - V_p) \left( 1 - \frac{C_S}{C_{S,0}} \right) \quad (7-78)$$

where  $V_S$  and  $V_p$  are solids and product molar volumes, respectively, and  $(\epsilon_S)_0$  is the initial porosity. If the porosity does change with the conversion of the solid, one would expect a change in  $D_{eff}$  as well, so we have the additional problem of describing  $D_{eff}$  as a function of  $\epsilon_S$ . A menu of possibilities is available, but the one normally selected is

$$\frac{D_{eff}}{(D_{eff})_0} = \left[ \frac{\epsilon_S}{(\epsilon_S)_0} \right]^\gamma \quad (7-88)$$

If we take a moment to review what has been written in the mathematics of this problem so far, well, it's discouragingly complex.<sup>8</sup> Indeed, at this point, one might look for a way out. Fortunately, there is: frequently  $(C_{A_S}/C_S) < 10^{-3}$ , in which case the time derivative for  $C_{A_S}$  in equation (7-84) can be neglected and we have another version of the pssh pertaining to the diffusion/reaction system. In the analysis of Wen, we are given numerical solutions for the following power-law kinetics.

$$\begin{aligned} (-r_A) &= k[C_{A_S}]^n[C_S]^m \\ (-r_S) &= (k/\nu)[C_{A_S}]^n[C_S]^m \end{aligned} \quad (7-89)$$

where  $\nu$  is a stoichiometric coefficient (mols A reacted per mols S). Since we are dealing with a fluid–solid reaction here, it is necessary to be a little careful with units. The rates of reaction are per unit volume of solid, the concentration  $C_{A_S}$  is in mols/volume-fluid, and  $C_S$  in mols solid/volume-particle (assuming all the solid, not just a component, reacts).

As in the case of the more complicated effectiveness factor problems, the mathematical description is highly parameterized and it is hard to obtain an overall picture of what is occurring without a number of plots prepared for individual cases. For the present, let us select an example in which  $n = 2$ ,  $m = 1$  (by Wen),  $C_A = (C_{A_S})^S$ , and the diffusional modulus  $\phi$  is

$$\phi = R \left[ \frac{k(C_{A_S})^S C_{S,0}}{(D_{eff})_0} \right] = 70 \quad (7-90)$$

Computational results for  $C_S$  and  $C_{A_S}$  are shown in Figure 7.18. Here we can see that the concentration profiles, given for parametric values of a reduced time  $\theta = (k/\nu)(C_{A_S,0})^2 t$ , are established rather rapidly, particularly for the solid phase, and progress with a nearly constant sigmoid shape through the matrix. Note that for values of  $\theta > 4.88$  in this example there is an outer region with  $C_S = 0$ , so beyond this point there is diffusion only through part of the matrix, and diffusion and reaction in the inner region. This, then, divides the reaction into two stages, depending upon whether the surface concentration of the solid reactant is zero or not. This

<sup>8</sup> "... he had been puzzled so long by at least four-fifths of the phenomena of existence that he no longer made any effort to comprehend them."—*T. Wolfe*

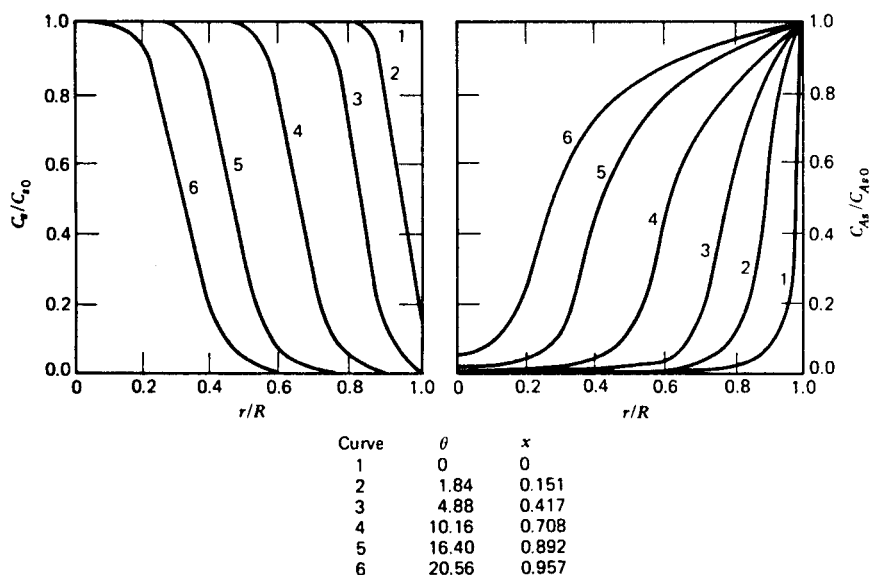


**Figure 7.18** Solids and reactant concentration profiles for gas–solid reaction with a large value of the diffusional modulus. No interphase transport limits. [After C.Y. Wen, *Ind. Eng. Chem.*, 60, 34, with permission of the American Chemical Society, (1968).]

situation can be treated by considering a two-zone particle, each with its characteristic value of  $D_{eff}$ , and with boundary conditions between the two zones expressed as

$$C'_{As} = C_{As} \quad D'_{eff} \left( \frac{\partial C'_{As}}{\partial r} \right) = D_{eff} \left( \frac{\partial C_{As}}{\partial r} \right) \quad (7-91)$$

Results for this two-zone model are given in the paper by Ishida and Wen.

A very important particular case of gas–solid reactions is that in which a component of the solid phase reacts with the reactant gas phase very rapidly and the particle size remains constant. This establishes a reaction interface between the two zones; in one zone there is diffusion (but no reaction) to the interface, and in the other there is only reaction at the interface. This is usually called the *shrinking core* model. If again we make the pseudo-steady-state assumption, then from equation (7-84)

$$\left( \frac{1}{r^2} \right) \frac{\partial}{\partial r} \left( D_{eff} r^2 \frac{\partial C_{As}}{\partial r} \right) = 0 \quad (7-92)$$

where now the rate of reaction will be expressed in the interface boundary condition for equation (7-92). Let us consider the point at which the reaction interface has penetrated a distance  $\lambda$  along the particle radius. Here

$$D_{eff} \left( \frac{\partial C_{As}}{\partial r} \right)_{\lambda} = \nu k_S C_{As} C_{S,0} \quad (7-93)$$

where the rate constant,  $k_S$ , is based on the interfacial (reactive) area, and  $\nu$  is the stoichiometric coefficient employed before. The concentration in the diffusion zone,

$C_{A_s}$  can be found as

$$\left( \frac{C_{A_s}}{C_A} \right)_r = \frac{(1 + P_1)(1/\lambda) - (1/r)}{(1 + P_2)(1/\lambda) - (1 - P_3)(1/R)} \quad (7-94)$$

where:

$$P_1 = 1 + (D_{eff}/k_S C_{S,0} \lambda)$$

$$P_2 = 1 + (D_{eff}/\nu C_{S,0} \lambda)$$

$$P_3 = 1 - (D_{eff}/k_S R)$$

and the concentration at the reaction interface is given by equation (7-94) with  $r = \lambda$ . The time required for the reaction interface to move from  $R$  to  $\lambda$  is

$$t_\lambda = \frac{\nu R C_{S,0}}{C_A} \left[ \left( \frac{1}{3} \right) \left( \frac{1}{k_S} - \frac{R}{D_{eff}} \right) \left( 1 - \frac{\lambda^3}{R^3} \right) + \frac{R}{2D_{eff}} \left( 1 - \frac{\lambda^2}{R^2} \right) + \frac{1}{\nu k_S C_{S,0}} \left( 1 - \frac{\lambda}{R} \right) \right] \quad (7-95)$$

At complete conversion,  $\lambda = 0$ , and the time required is

$$t_R = \frac{\nu R C_{S,0}}{C_A} \left( \frac{1}{3k_S} + \frac{R}{6D_{eff}} + \frac{1}{\nu k_S C_{S,0}} \right) \quad (7-96)$$

The sum involved in equation (7-96) reminds us that we are dealing with a resistance-in-series model, so that we can identify various relationships for  $t_R$  corresponding to different controlling resistances.

### Illustration 7.6

Consider the gas-solid reaction



conducted between a gaseous component and a spherical solid particle of initial radius  $R_0$ . Derive an expression that will allow one to predict whether the sphere will contract, expand, or remain unchanged upon reaction. You may assume that data for the density and the molecular weight of the reactant and product solids are available.

*Solution*

After a given time of reaction,  $t$ , the number of mols of **B** reacted will be

$$N_B = \frac{\rho_B (4\pi/3) (R_0^3 - \lambda^3)}{M_B} \quad (ii)$$

where  $\rho_B$  is the density of the solid **B**,  $M_B$  the molecular weight, and  $\lambda$  the unreacted core radius. The mols of **C** formed correspondingly are

$$N_C = \frac{\rho_C (4\pi/3) (R^3 - \lambda^3)}{M_C} \quad (iii)$$

with  $R$  the radius at  $t$  and  $M_C$  the molecular weight of C. From stoichiometry we also have

$$N_B = (b/c)N_C \quad (\text{iv})$$

Thus, equating the expressions for  $N_B$  and  $N_C$  according to equation (iv)

$$\frac{\rho_B(R_0^3 - \lambda^3)}{M_B} = \left(\frac{b}{c}\right) \frac{\rho_C(R^3 - \lambda^3)}{M_C} \quad (\text{v})$$

Thus,

$$R^3 = R_0^3 \left[ \frac{\rho_B M_C c}{\rho_C M_B b} + \left(1 - \frac{\rho_B M_C c}{\rho_C M_B b}\right) \left(\frac{\lambda}{R_0}\right)^3 \right] \quad (\text{vi})$$

Now let

$$P = \frac{\rho_B M_C c}{\rho_C M_B b} \quad Q = \frac{\lambda}{R_0} \quad (\text{vii})$$

and the particle dimension can be written as

$$R = R_0 [P + (1 - P)Q^3]^{1/3} \quad (\text{viii})$$

The particle dimension is seen to be governed by the numerical value of the parameter  $P$ .

$P > 1$  – expansion

$P = 1$  – no change

$P < 1$  – contraction



HORATIO SAYS

Help! Show me how to get from equations (7-92) and (7-93) to (7-94). (See exercises.)

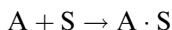
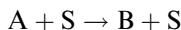
As stated in the beginning of this section, there have been quite a number of versions of the gas-solid reaction analysis. Further detail has been provided by Bischoff, Luss, and Yoshida, et al. [K.B. Bischoff, *Chem. Eng. Sci.*, 46, 7111 (1963); D. Luss, *Can. J. Chem. Eng.*, 46, 154 (1968); R. Yoshida, D. Kunii and F.J. Shimizu, *Chem. Eng. Japan*, 8, 417 (1976)]. A more detailed model, considering the granular nature of most porous solids, has been given by Szekely and coworkers [H.Y. Sohn and J. Szekely, *Chem. Eng. Sci.*, 25, 1091 (1970); J. Szekely and J.W. Evans, *Chem. Eng. Sci.*, 27, 763 (1972); 29, 630 (1974); J. Szekely, J.W. Evans, and H.Y. Sohn, *Gas-Solid Reactions*, Academic Press, New York, NY, (1976)]. Some more studies of a similar nature, but with application to catalyst regeneration, will be given in the next section.

### 7.1.9 The Influence of Catalyst Deactivation

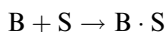
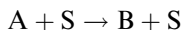
In the discussion of the deactivation of active surfaces in Chapter 3, we made the point that the existence of deactivation changed an entire class of steady-state phenomena into unsteady-state phenomena. This is well illustrated by extending the analysis of diffusion and chemical reaction in heterogeneous catalysis to include deactivation. On a quantitative level a precise analysis can become intricate and difficult, so we will confine the presentation here to a more qualitative level (and it's tough enough at that).

We will start by considering the simple case of diffusion and reaction described by equation (7-2). Let us further assume that the catalytic surface is being deactivated by some type of coking mechanism, with the reaction scheme corresponding to (XXIII) of Chapter 3. We will consider two limiting cases of that scheme.

*Parallel fouling*



*Series fouling*



The conservation equation for (XXIIIa), for example, then becomes

$$D_{eff} \frac{\partial^2 C_A}{\partial z^2} - \epsilon \frac{\partial C_A}{\partial t} - (k + k_{da})sC_A = 0 \quad (7-97)$$

Several factors and assumptions are built into equation (7-97). The most noticeable is the time variation of this term will be important if the rate of the deactivation is rapid compared to the rate of the main reaction, that is if  $k_{da} \gg k$ . The most important assumption in equation (7-97), however, is that the deactivation kinetics are separable; hence the activity factor  $s$  in the reaction rate term. Finally, since  $A$  disappears in both of the reactions in the parallel scheme, the overall rate constant is given by the sum shown above. For the series scheme, of course, some changes will have to be made that, by now, one hopes will be obvious.

Going further with the parallel scheme, we couple with the conservation equation the following kinetics of the deactivation

$$\frac{ds}{dt} = -k_{da}sC_A \quad (7-98)$$

In many instances the rate of deactivation is relatively slow compared to the rate of the main reaction, so the following simplification may be used,

$$D_{eff} \left( \frac{d^2 C_A}{dz^2} \right) - ksC_A = 0 \quad (7-99)$$

In this case the coupling of equations (7-98) and (7-99) represents a quasi-steady-state model for the overall reaction. This does not imply steady-state behavior of the system at all, only that the time scale of the deactivation is long and to a reactant molecule within the catalyst at any given time the active surface is in a steady state compared to



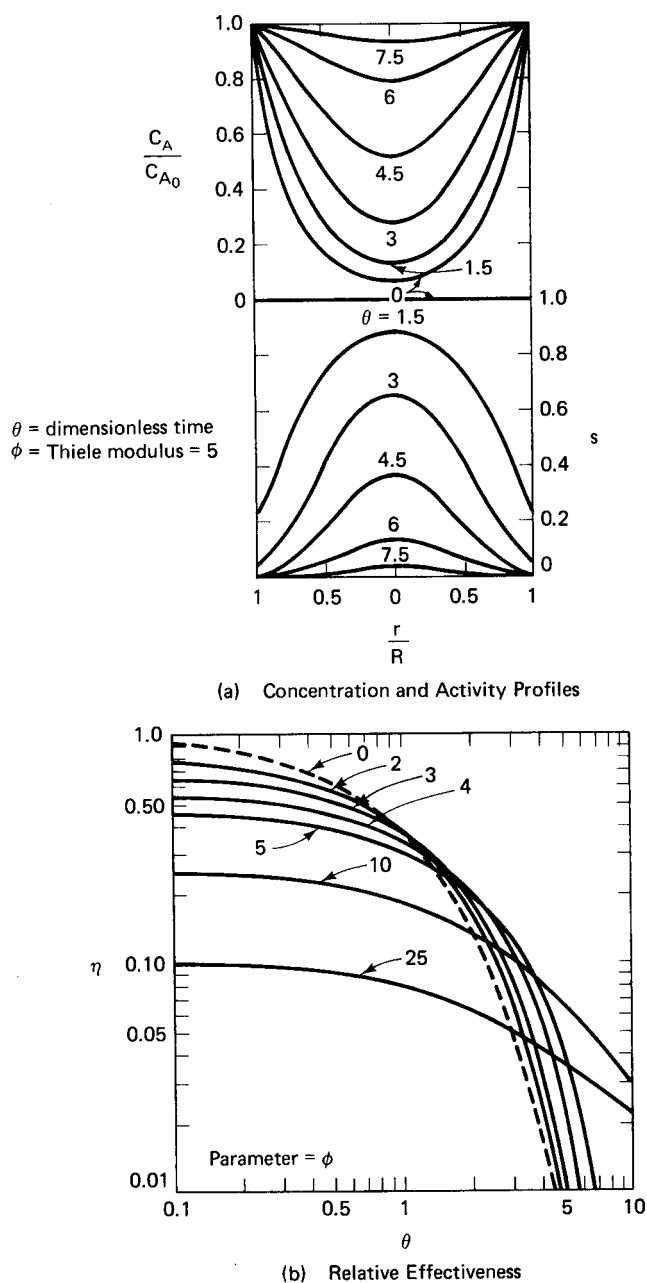


**Figure 7.19** Catalyst particle behavior with parallel deactivation (a) Profiles; (b) relative effectiveness. [After S. Masamune and J.M. Smith, *Amer. Inst. Chem. Eng. J.*, 12, 384, with permission of the American Institute of Chemical Engineers, (1966).]

the characteristic reaction time. Obviously, a similar development can be applied to the series scheme, requiring an additional conservation equation for B.

Some typical solutions for equations (7-98) and (7-99) (but in cylindrical coordinates) are shown in Figure 7.19. These have the boundary conditions of equation (7-3) and the initial condition  $s(z, t = 0) = 1$ . What do we learn from this? It is truly a bit tricky to get through it all, but have patience. The research was done by Masamune and Smith [S. Masamune and J.M. Smith, *Amer. Inst. Chem. Eng. J.*, 12, 384 (1966)], and what they show are, first, the concentration profiles of the reactant, and, second, the activity profiles of the catalyst as a function of time of reaction. The profiles move a lot. Where they go is even more interesting. Look at the shapes of the concentration and activity profiles and their change with time of reaction. Since A is responsible for fouling in the parallel scheme, the point rate of deactivation will be greatest where A is present in greatest concentration; hence this catalyst particle is fouled from the outside to the inside. Note also the shapes of the relative effectiveness factor curves, where initially more active catalysts (smaller influence of diffusion) are deactivated more rapidly than those with severe diffusion limits. This is again the result of the parallel fouling mechanism; easier access of A to the interior of the particle promotes deactivation as well as the rate of the main reaction. In this case the existence of deactivation suggests a strategy in catalyst

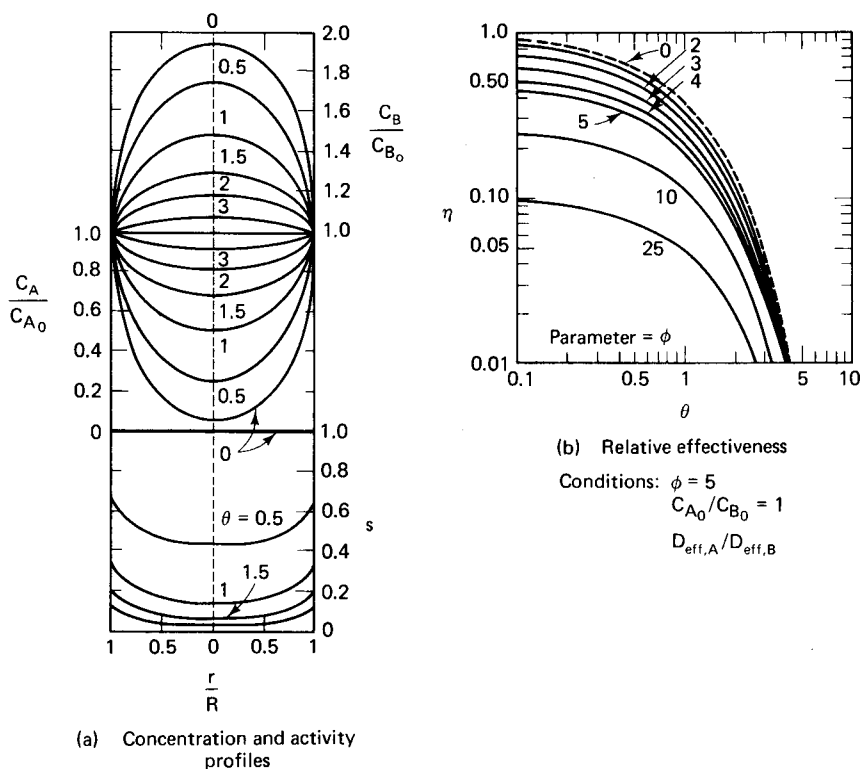
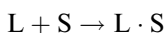
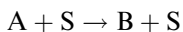


**Figure 7.20** Catalyst particle behavior with series deactivation. [After S. Masamune and J.M. Smith, *Amer. Inst. Chem. Eng. J.*, 12, 384, with permission of the American Institute of Chemical Engineers, (1966).]

formulation that would probably never be considered if the kinetics of the main reaction were the sole concern, that is, *to build in a certain diffusion limitation to retard fouling*.

Corresponding results for the series fouling scheme (XXIIIb) are shown in Figure 7.20. Now, the product of the reaction is the fouling agent and the point rate of deactivation is greatest where the concentration of B is the greatest. As a consequence of this, the particle must foul from the inside outward. Further, since it is the product of the reaction that is responsible for deactivation, there is no advantage of diffusional limitation here, and the relative effectiveness factors decrease monotonically in regular fashion.

The results obtained by Masamune and Smith, particularly for the case of parallel fouling, suggest a simple strategy to cope with this form of deactivation. It is simply to move the active catalytic ingredient away from the zone of fouling, if this makes sense chemically. Nonuniform distributions of active ingredients have been investigated theoretically by several investigators, with some of the principal early contributions by Shadman-Yazdi and Petersen [F. Shadman-Yazdi and E.E. Petersen, *Chem. Eng. Sci.*, 27, 227 (1972)], Corbett and Luss [W.E. Corbett, Jr. and D. Luss, *Chem. Eng. Sci.*, 29, 1473 (1974)], and Becker and Wei [E.R. Becker and J. Wei, *J. Catal.*, 46, 372 (1977)]. The latter is particularly informative in a qualitative way. They studied the behavior of four nonuniform catalyst distributions as shown in Figure 7.21a for the parallel deactivation scheme



where L is an impurity poison that irreversibly deactivates the catalyst via strong chemisorption on the active surface.

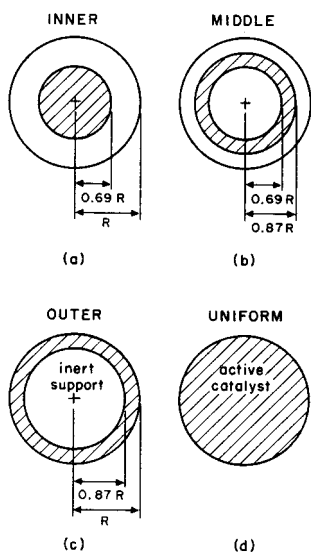


**Figure 7.21** (a) Possible nonuniform distributions of catalytic materials within a sphere. [After E.R. Becker and J. Wei, *J. Catal.*, 46, 372, with permission of Pergamon Press, Inc., London, England, (1977).]

Now let us assume that linear deposition of the poison occurs within the catalyst, and that the relationship between the amount of poison on the surface and the catalyst activity is exponential,

$$s = b \exp[-a(C_{L.S})] \quad (7-100)$$

where  $a$  and  $b$  are scaling constants. Both the main reaction and the poisoning reaction can be diffusion limited, as would be indicated by the relative values of the Thiele modulus for the two,  $\phi_m$  and  $\phi_p$ , respectively. In the study of Becker and Wei to compare catalysts, the values of  $\phi_m$  and  $\phi_p$  were held constant for each of the catalysts and the time to reach an effectiveness of 0.4 (an arbitrary but reasonable value) was determined. These results are shown in Figure 7.21b. Each of the catalyst configurations shown in Figure 7.21a has its particular “best” region. When  $\phi_m$  is small and  $\phi_p$  is large, the inner or “egg yolk” distribution is best. For small  $\phi_m$  and small  $\phi_p$ , all distributions behave in about the same way, so a uniform distribution could be used. When  $\phi_m$  is large and  $\phi_p$  is small, the catalytic ingredient is best placed close to the outer surface of the pellet, where it is available to the main reactant. (The active surface here will be available to the impurity wherever it is located within the particle because  $\phi_p$  is small.) The performance of the various pellets for intermediate values of  $\phi_m$  and  $\phi_p$  suggests that an intermediate distribution of catalytic ingredient gives the best results. This is at least in agreement with physical intuition, where one wishes to place the catalytically active materials in the interior to protect it from the poison, yet at the same time locate it near enough to the surface to be available to

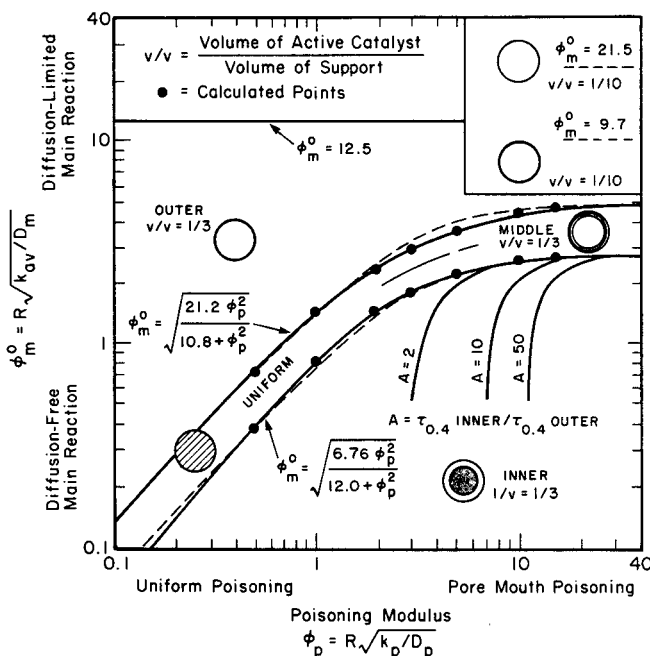


**Figure 7.21** (b) Selection chart based on maximum operating time to a specified final effectiveness. [After E.R. Becker and J. Wei, *J. Catal.*, 46, 372, with permission of Pergamon Press, Inc., London, England, (1977).]

the reaction mixture. The location of the active ingredient is thus a compromise, depending upon the specific values of  $\phi_m$  and  $\phi_p$ . There is nothing really surprising in that.<sup>9</sup> Note that in the results of Figure 7.21b both uniform and middle distributions are confined to a rather narrow range of values for both of the diffusional parameters. Preferential loading of an active catalyst ingredient within a catalyst particle is thus not just an academic exercise. This has been shown experimentally by Au, et al. [S.S. Au, J.S. Dranoff, and J.B. Butt, *Chem. Eng. Sci.*, 50, 3801 (1995)] for the hydrogenation of benzene over supported Ni, poisoned by sulfur, which is certainly a classical example of the parallel scheme that we have been discussing.

### Illustration 7.7

A little reflection on the results shown in Figure 7.19 should be enough to convince us that when the rate of deactivation is very high, the profiles of activity developed will be very sharp and the deactivated zone in the catalyst particle will proceed from the outside to the center as a growing shell (*shell progressive*) of deactivated catalyst grows with a well-defined interface between active and deactivated zones. The physical picture is not that much different from that of the zones developed in noncatalytic gas-solid reactions.

Given this speech, now let us bring down the scale to the dimension of an individual pore, and consider two cases of decay by poisoning such as in scheme XXXIIIc. In the first, the main reaction is still diffusion limited but the poisoning is relatively uniform. In the second, poisoning is very rapid so that deactivation is also diffusion limited. In both cases the main reaction is first-order, irreversible, rate constant  $k$ , and the rate constant decreases linearly with the fraction of surface poisoned,  $\alpha$ , as,

$$k = k_0(1 - \alpha)$$

What we wish to do is to derive expressions for  $F$ , the ratio of the rate of the poisoned catalyst to the rate on the fresh catalyst, for the two cases.

#### Solution

As a simplification we will assume that the reaction-diffusion results for slab geometry can be used for the individual pore, and appropriate scaling can be made for the overall result. Then, for the diffusion-limited main reaction we will have, for the first case,

$$(-r)_0 = \frac{\tanh \phi}{\phi} k_0 C_0 \quad (\text{i})$$

where  $\phi$  is  $L(k/D_{\text{eff}})^{1/2}$ ,  $L$  is pore length, and  $C_0$  is the external concentration of reactant. If we write out equation (i) for the unpoisoned catalyst, then

$$(-r)_0 = \frac{\tanh[L(k_0/D_{\text{eff}})^{1/2}]k_0 C_0}{L(k_0/D_{\text{eff}})^{1/2}} \quad (\text{ii})$$

<sup>9</sup> "Important principles may and must be flexible."—A. Lincoln

For the poisoned catalyst,  $k = k_0(1 - \alpha)$ , and we have

$$(-r)_p = \frac{\tanh\{L[k_0(1 - \alpha)/D_{eff}]^{1/2}\}}{L[k_0(1 - \alpha)/D_{eff}]^{1/2}} \quad (\text{iii})$$

The ratio,  $F$ , that we are looking for is, after some algebra,

$$F = \frac{(-r)_p}{(-r)_0} = \frac{\tanh[\phi_0(1 - \alpha)^{1/2}]}{\tanh \phi_0} (1 - \alpha)^{1/2} \quad (\text{iv})$$

where  $\phi_0 = L(k/D_{eff})^{1/2}$ . We can, further identify interesting limiting cases. For large  $\phi_0$

$$F \rightarrow (1 - \alpha)^{1/2} \quad (\text{v})$$

and for small  $\phi_0$

$$\tanh \phi_0 \rightarrow \phi_0; \quad F \rightarrow (1 - \alpha) \quad (\text{vi})$$

For reasons that will soon become apparent, these are generally referred to as “antiselective” and “nonselective”, respectively.

Now let us look at the second case, where the poisoning reaction has become very rapid itself. The picture here is shown in Figure 7.22. In this instance (often called *pore-mouth poisoning*), the fraction poisoned over length  $\alpha L$  will be inactive, while the fraction over length  $(1 - \alpha)L$  retains the original catalyst activity. We take the transport of reactant from the pore mouth through the poisoned portion to be via diffusion only, with its accompanying linear concentration gradient. Thus,

$$N = \frac{D_{eff}(C_0 - C_i)}{\alpha L} \quad (\text{vii})$$

where  $N$  is the flux of reactant. In the undeactivated portion of the pore there is both diffusional transport and reaction. If there is to be steady state, then the reactant flux in the two regions must be the same, so  $N$  is also equal to

$$N = \frac{\tanh[L(1 - \alpha)(k_0/D_{eff})^{1/2}]}{L(1 - \alpha)(k_0/D_{eff})^{1/2}} \cdot k_0(1 - \alpha)LC_i \quad (\text{viii})$$

There is a little problem here, since we do not know  $C_i$ ; however we can equate equations (vii) and (viii) and solve for the as-yet unspecified concentration  $C_i$ .

$$C_i = \frac{C_0}{1 + (\alpha\phi_0) \tanh[\phi_0(1 - \alpha)]} \quad (\text{ix})$$

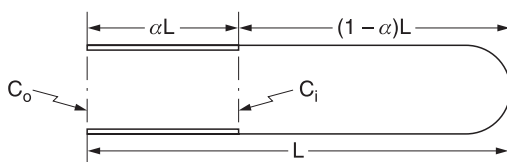


**Figure 7.22** Diagram of pore-mouth poisoning with diffusion and reaction. [After A. Wheeler, *Advan. Catal.*, 3, 249 with permission of Academic Press, New York, NY, (1951).]

Then,

$$\left(\frac{D_{eff}}{\alpha L}\right)(C_0 - C_i) = \left(\frac{D_{eff}C_0}{\alpha L}\right) \left[1 - \frac{1}{1 + (\alpha\phi_0) \tanh[\phi_0(1 - \alpha)]}\right] \quad (x)$$

and the rate for the poisoned pore is

$$(-r)_p = \frac{D_{eff}C_0}{\alpha L} \left[ \frac{(\alpha\phi_0) \tanh[\phi_0(1 - \alpha)]}{1 + (\alpha\phi_0) \tanh[\phi_0(1 - \alpha)]} \right] \quad (xi)$$

For the unpoisoned pore,

$$(-r)_0 = \frac{\tanh \phi_0}{\phi_0} (kC_0L) \quad (xii)$$

Then,

$$F = \left[ \frac{(\alpha\phi_0) \tanh[\phi_0(1 - \alpha)]}{1 + (\alpha\phi_0) \tanh[\phi_0(1 - \alpha)]} \right] \left( \frac{1}{(\alpha\phi_0) \tanh \phi_0} \right) \quad (xiii)$$

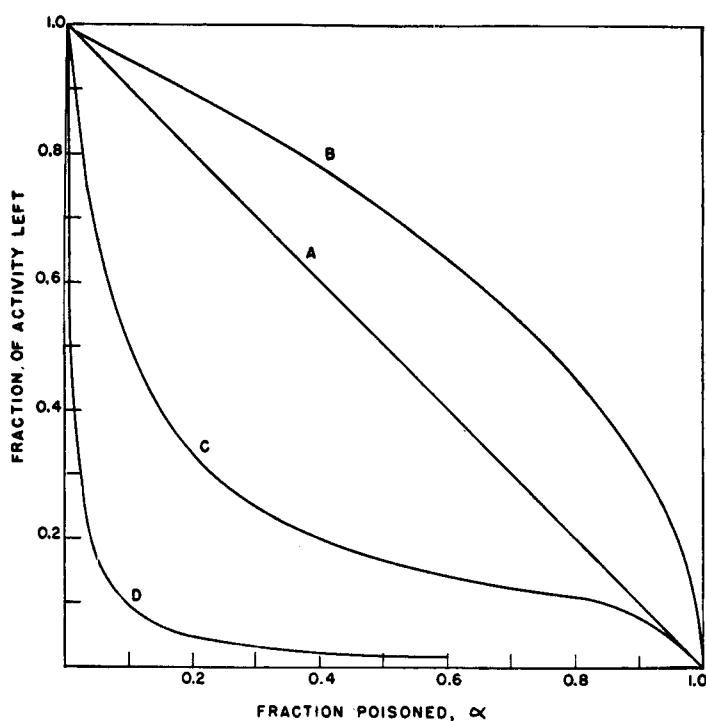


**Figure 7.23** Types of relationships encountered with porous catalysts. Curve A is the result for nonselective deactivation for equations (vi) and (xvi). Curve B is for uniform deposition of poison with  $\phi_0$  large and antiselective deactivation, equation (v). Curves C and D are for selective deactivation, equation (xiv), with  $\phi_0 = 10$  and  $100$ , respectively. [After A. Wheeler, *Advan. Catal.*, 3, 249 with permission of Academic Press, New York, NY, (1951).]

The limiting cases of interest are, for large  $\phi_0$ ,  $\tanh \phi_0 \rightarrow 1$  and

$$F = \left( \frac{\alpha\phi_0}{1 + \alpha\phi_0} \right) \left( \frac{1}{\alpha\phi_0} \right) = \frac{1}{1 + \alpha\phi_0} \quad (\text{xiv})$$

For small  $\phi_0$ ,  $\tanh \phi_0 \rightarrow \phi_0$  and

$$F = \frac{(1 - \alpha)}{1 + \alpha\phi_0^2(1 - \alpha)} \quad (\text{xv})$$

which, for small  $\phi_0$  will be

$$F = (1 - \alpha) \quad (\text{xvi})$$

The relation of equation (xvi) for large  $\phi_0$  is commonly termed *selective deactivation*, while that of equation (xv) is the same result for *nonselective deactivation* that was shown in equation (vi).

The results of all this analysis are shown in Figure 7.23, giving the relationship between the  $F$  ratio and the fraction poisoned,  $\alpha$ . These are very powerful results, as our friend Horatio will remind us in his comments.



HORATIO SAYS

Note in particular curves C and D in Figure 7.23. Selective deactivation is particularly pernicious because, as can be seen, a little bit of poison goes a long way in the deactivation.

While the title of this section is “The Influence of Deactivation,” we can now spend a little time on the happier topic of catalyst regeneration. There is not much point to talk about regeneration from poisoning, since each case is so much to itself, but the regeneration of catalysts that have been deactivated by coke formation is another matter. In general, let us be concerned with the regeneration of catalysts that have been deactivated by coke formation, either by one of the limiting examples of fouling given in schemes XXIIIa and b, or other more complex reactions that have been reported. Our treatment will be confined to the removal of carbonaceous deposits, assumed to be uniform throughout the particle, via oxidation (either  $\text{O}_2$  or air).

The oxidation of coke is a rapid reaction, for we are essentially considering a combustion process, and it resembles in many respects the gas–solid noncatalytic reactions that we have already discussed. Due to the large intrinsic rate of reaction, we often have a situation where there is diffusive transport through an outer (regenerated) zone, with the reaction localized at the interface between the regenerated and unregenerated zones. If this sounds familiar, it is—recheck the development described in equations (7-91) to (7-96). The intrinsic kinetics of carbon burning were reported by Bondi, et al. [A. Bondi, R.S. Miller, and W.G. Schlaffer, *Ind. Eng. Chem. Proc. Design Devel.*, 1, 196 (1962)] to be first-order in carbon and



first-order in oxygen according to:

$$(-r_c) = k_c(P)y_{O_2}C_c \quad (7-101)$$

where  $P$  is the total pressure,  $y_{O_2}$  the mol fraction of oxygen, and  $C_c$  the weight of coke on the catalyst. For a constant coke concentration, corresponding to the interfacial reaction condition, then,

$$(-r_c) = k'_c P y_{O_2} \quad (7-102)$$

when there is diffusion and interfacial reaction, the catalyst particle cross-section after some time of reaction will look like the “inner section” of Figure 7.21a. The locus of coke is represented by the hatched portion, and the regenerated part by the outer shell. This is commonly termed *shell-progressive*. Now, we have already derived the mathematical expression pertinent to this situation in equation (7-95), assuming that the regeneration time is the quantity of interest. If we set the rate of combustion to be rapid, and external gradients to be absent, then diffusion throughout the regenerated shell is rate determining and

$$(t)_{regen} = \frac{\nu R^2 C_{S,0}}{6D_{eff}C_A} [1 - 3(1-x)^{2/3} + 2(1-x)] \quad (7-103)$$

where  $x = 1 - (\lambda/R)$ . If the interphase resistance is rate-determining, equation (7-95) also applies but simplifies to

$$(t)_{regen} = \left( \frac{\nu R C_{S,0}}{3C_A k_S} \right) x \quad (7-104)$$

This type of analysis was employed by Weisz and Goodwin [P.B. Weisz and R.D. Goodwin, *J. Catal.*, 2, 397 (1963); 6, 425 (1966)] in the study of the regeneration of coked silica/alumina cracking catalysts. From equation (7-103) we can see that

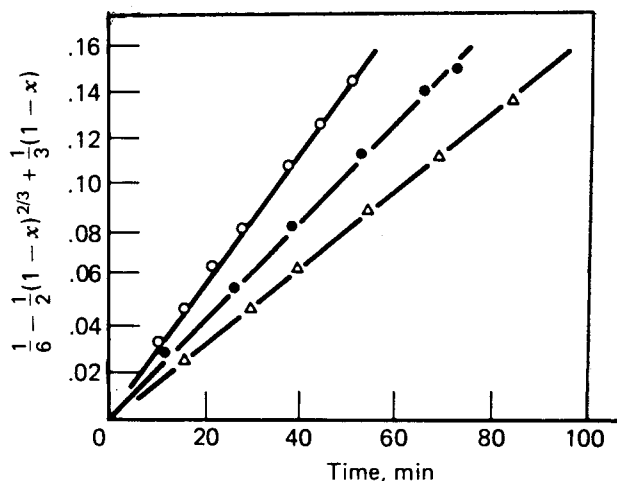


**Figure 7.24** Regeneration time as correlated by equation (7-105) for three different sizes of coked particles. [From P.B. Weisz and R.W. Goodwin, Jr., *J. Catal.*, 2, 397, with the permission of Academic Press, Inc., New York, NY, (1963).]

regeneration time is proportional to

$$(t)_{\text{regen}} = \alpha \left( \frac{1}{6} \right) - \left( \frac{1}{2} \right) (1-x)^{2/3} + \left( \frac{1}{3} \right) (1-x) \quad (7-105)$$

The results obtained for coke burning correlated in this way are shown in Figure 7.24 for three different particle sizes. One could not wish for a better agreement between theory and experiment for a wide range of both x- and y-axis values.

Other tests can also be made. In practice it is difficult to determine exactly the time required to arrive exactly at the point of complete regeneration, so Weisz and Goodwin set an arbitrary value  $t_{85}$ , the time required for removal of 85 wt% of the coke, as the measure of merit for the regeneration. For shell-progressive regeneration, then, equation (7-103) becomes

$$t_{85} = \frac{(0.0755) \nu R^2 C_{S,0}}{D_{\text{eff}} C_A} \quad (7-106)$$

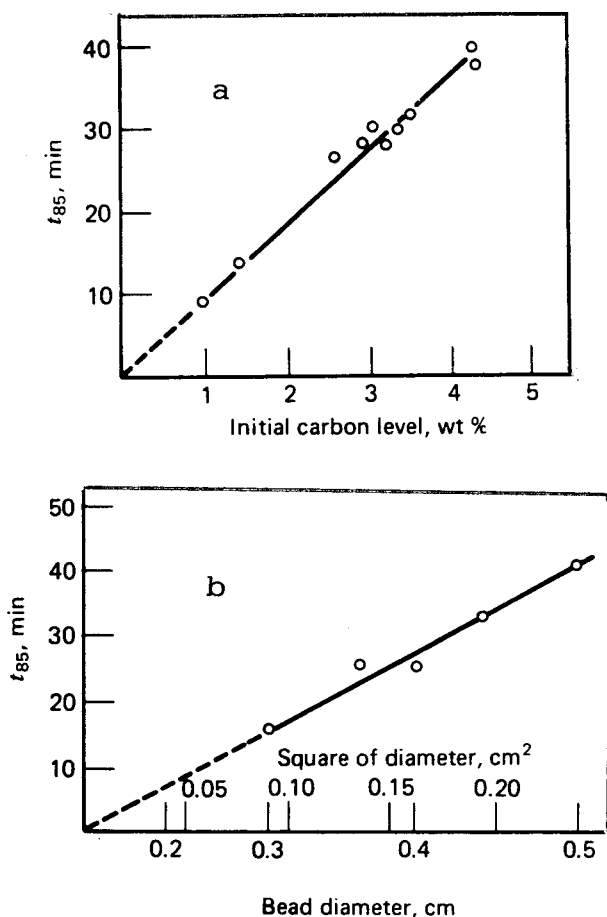


**Figure 7.25** (a) Test of  $t_{85}$  correlation for the influence of initial carbon level; (b) test of  $t_{85}$  correlation for the influence of catalyst bead diameter. [From P.B. Weisz and R.D. Goodwin, Jr., *J. Catal.*, 2, 397, with the permission of Academic Press, Inc., New York, NY, (1963).]

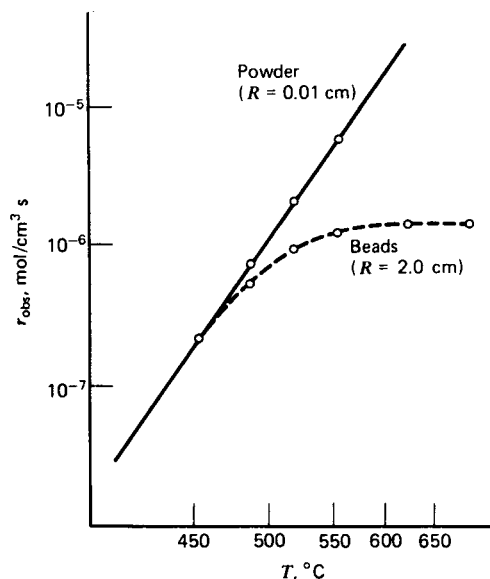


**Figure 7.26** Observed coke burning rates for a silica/alumina cracking catalyst with an initial coke content of 3.4 wt%: big beads and fine powder. [From P.B. Weisz and R.D. Goodwin, Jr., *J. Catal.*, 2, 397, with the permission of Academic Press, Inc., New York, NY, (1963).]

A test of this correlation for two of the proportionalities shown, initial carbon concentration,  $C_{S,0}$ , and the square of the particle radius,  $R^2$ , is illustrated in Figure 7.25.

Again, there is impeccable agreement of the data with the shell-progressive theory, and we are provided a working relationship central to the design of a reactor-regenerator system for cracking under the conditions employed.



HORATIO SAYS

By George, those regeneration correlations sure are good, but let's have another try. Figure 7.26 shows data on the rate of coke burning as a function of temperature for big beads and fine powder. How well would the Weisz-Prater criterion (Case 1, Table 7.3) predict the rate below which diffusion is not important if  $C_0$  were  $3 \times 10^{-6}$  mols/cm<sup>3</sup> and  $D_{eff}$   $5 \times 10^{-3}$  cm<sup>2</sup>/s?

## 7.2 Reactions in Gas/Liquid Systems

The theory of reaction and diffusion in gas/liquid systems is similar in many respects to that for gas/solid systems, but it also differs significantly in a number of important details. The most important of these differences is in the state of mixing normally existing in the liquid phase, which decreases the relative importance of thermal

gradients. Second, there are several different theoretical developments for interphase mass transfer between gas and liquid, such as the film theory and the surface renewal theory, so the analysis of diffusion/reaction is somewhat dependent on the mass-transport theory upon which it is based.

Historically, the analysis of gas/liquid systems arose from the problem of gas absorption accompanied by chemical reaction. Since the chemical reaction in this instance tends to increase the rate of absorption (mass transfer), much of the analysis is based on exploring the effects of chemical reaction on a diffusional process. This is just the opposite of the viewpoint in the theory for gas/solid systems, where we have explored the effects of appending a diffusional process to a chemical reaction. The net result of this difference in viewpoints is that most theories of gas/liquid reactions are concerned with determining enhancement factors for the mass-transfer coefficient rather than penalty functions, such as the effectiveness factor for the reaction kinetic constant. This difference in viewpoints can be rather refreshing in pointing out the various contrasts between the two approaches.

### 7.2.1 Diffusion and Reaction: Some Film Theory Results

Formal analysis of gas/liquid systems actually antedates that for gas/solid systems by about a decade, even though the two problems are very similar. The first study of this was reported by Hatta [S. Hatta, *Tôhoku Imp. Univ. Tech. Repts.*, 8, 1 (1928); for a more accessible reference see S. Hatta, *Int. Chem. Eng.*, 18, 443 (1978)] for a first-order reaction occurring in a stagnant film. Although the analysis is similar to the effectiveness factor problem, the objectives are somewhat different as explained above, and we will present it here.

Consider the idealized picture of a mass-transfer process based on the two-film theory as shown in Figure 7.27. The partial pressure profile in the gas film is linear, as called for by steady-state diffusion, but the concentration profile in the liquid film falls below a linear measure as a result of a first-order chemical reaction removing the absorbed gas. A normal mass balance over the differential segment  $dz$  (we may assume unit area normal to the direction of diffusion) produces a familiar result:

$$\frac{d^2C}{dz^2} - \frac{k}{D} C = 0 \quad (7-107)$$

where  $D$  is the diffusion coefficient in the liquid phase. The boundary conditions envisioned by Hatta specify  $C = C_i$  at  $z = 0$  and  $C = C_L$  at  $z = L$ . We thus fix the concentration at point  $L$ , rather than working with the derivative as in the effectiveness factor problem. The solution of equation (7-107) for these boundary conditions is

$$C = \frac{C_L \sinh(a_0 z) + C_i \sinh[a_0(L - z)]}{\sinh(a_0 L)} \quad (7-107a)$$

where  $a_0 = (k/D)^{1/2}$ . Evaluating the concentration gradient at the interface and substituting in Fick's law equation yields

$$N_A = Da_0 \left[ \frac{C_i \cosh(a_0 L) - C_L}{\sinh(a_0 L)} \right]$$

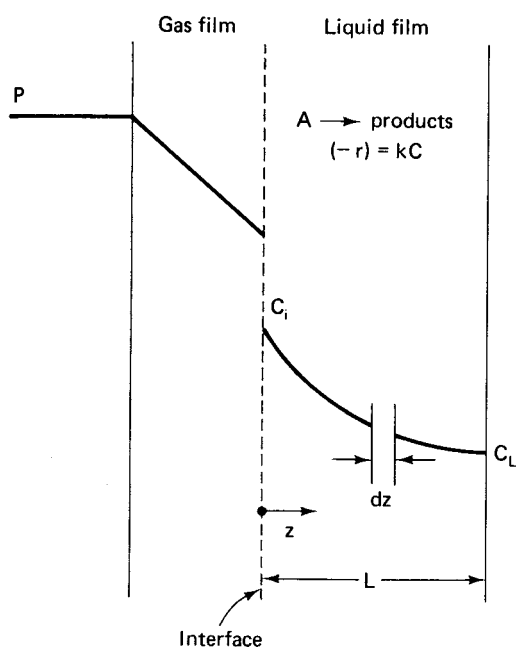


**Figure 7.27** Concentration profile for diffusion and reaction in a liquid film: two-film theory.

In order to make a comparison between this result and normal film theory, we may say that for small values of  $C_L$ ,

$$N_A \approx \frac{a_0 L}{\tanh(a_0 L)} \left( \frac{D}{L} \right) (C_i - C_L)$$

Now, the second two factors above are the results of standard film theory for diffusion through a length  $L$ , with the mass-transfer coefficient,  $k_M$ , given by

$$k_M = \left( \frac{D}{L} \right)$$

Thus, an *enhancement factor*,  $\lambda$ , for mass transfer in this instance is given by

$$\lambda = \frac{a_0 L}{\tanh(a_0 L)}$$

The limiting cases of slow reaction and very fast reaction are of interest. For slow reactions,  $a_0$  is small,  $\tanh(a_0 L)$  approaches  $(a_0 L)$ , and

$$N_A = \left( \frac{D}{L} \right) (C_i - C_L) = k_M (C_i - C_L) \quad (7-108)$$

For fast reactions,  $a_0$  is large,  $\tanh(a_0 L)$  approaches unity, and

$$N_A = (kD)^{1/2} (C_i - C_L) \quad (7-109)$$

The limit of equation (7-109) has been verified for such diverse systems as  $\text{CO}_2$  absorption into aqueous  $\text{NaOH}$  solutions and phosgene absorption in water.

If we compare this analysis of the gas-liquid reaction to that used for comparable gas-solid reactions, the difference in viewpoints is immediately apparent. The enhancement factor for gas-liquid reactions is an improvement function that tells one how much the reaction is increasing the rate of diffusion owing to the existence of gradients, while the effectiveness factor is a penalty function that tells one how much diffusion is decreasing the rate of reaction owing to the existence of gradients.<sup>10</sup>

If we wish to express these results for gas-liquid reactions in strict analogy to those for the catalytic effectiveness factor, then the solutions of equation (7-107) can be written in the form

$$\eta_L = \frac{N_A A_V}{k C_{A_i}} = \frac{1}{(a_0 L)(N_{Sh}) \tanh(a_0 L)} \cdot \left( 1 - \frac{C_{A_L}}{C_{A_i} \cosh(a_0 L)} \right) \quad (7-110)$$

where  $A_V$  is the interfacial transport area per unit volume and  $N_{Sh} = (k_M/A_V D)$ . For rapid reactions this expression reduces to

$$\eta_L = \frac{1}{(a_0 L)(N_{Sh})} \quad (7-111)$$

In many cases of gas-liquid reactions the gaseous component is transferred into the liquid phase from a pure gas phase. There is no gas-side resistance to mass transfer and equations (7-110) and (7-111) express the overall gas-liquid reaction enhancement. If we wish to include gas-phase resistance, however, a simple modification is possible. Here we will designate  $P_{Ag}$  and  $P_{Ai}$  as the partial pressures of the transferred component in the bulk gas and at the interface, respectively,  $k_G$  is the gas film mass-transfer coefficient, and  $H$  is Henry's law constant pertaining to equilibrium at the interface. Then, the overall flux relationship may be derived as

$$N_A = \frac{P_{Ag} - [H C_{A_L} / \cosh(a_0 L)]}{(1/k_G) + (H/k_M) [\tanh(a_0 L)/(a_0 L)]} \quad (7-112)$$

which, for large  $(a_0 L)$ , becomes

$$N_A = \frac{P_{Ag}}{[(1/k_G) + H/k_M(a_0 L)]} \quad (7-113)$$

The significance of equation (7-113) is that the reaction is completed in the liquid film,  $C_{A_L}$  is zero, and the overall rate expression assumes the form of an additive resistance law.

Finally, we may define a two-phase effectiveness as well, based on the bulk gas composition. This is defined as

$$\eta_G = \frac{N_A A_V H}{k P_{Ag}} \quad (7-114)$$

<sup>10</sup> "Ne'er look for birds of this year in the nests of the last."—*M. de Cervantes*

which is the ratio of the actual reaction rate per unit volume of liquid to that occurring at a liquid phase concentration of A in equilibrium with its gas-phase partial pressure. Now, since

$$N_A A_V = \eta_L k C_{A_i} \quad (7-115)$$

and

$$N_A = k_G (P_{A_g} - P_{A_i}) \quad (7-116)$$

then

$$N_A = \frac{P_{A_g}}{[(1/k_G) + (H A_V / k \eta_L)]} \quad (7-117)$$

From these relationships we obtain the combination

$$\frac{1}{\eta_G} = \frac{1}{\eta_L} + \frac{k}{H k_G A_V} \quad (7-118)$$

In terms of the Sherwood number,  $N_{Sh}$ , as defined in equation (7-110), this is

$$\frac{1}{\eta_G} = \frac{1}{\eta_L} + \left( \frac{k_M}{H k_G} \right) (a_0 L)^2 (N_{Sh}) \quad (7-119)$$

and for large values of  $(a_0 L)$ ,

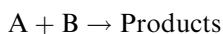
$$\frac{1}{\eta_G} = (a_0 L) (N_{Sh}) + \left( \frac{k_M}{H k_G} \right) (a_0 L)^2 (N_{Sh}) \quad (7-120)$$

With a little bit of algebra,

$$\frac{1}{\eta_G} = (N_{Sh}) (a_0 L) \left[ 1 + \frac{k_M (a_0 L)}{H k_G} \right] \quad (7-121)$$

The overall gas-liquid effectiveness factor is thus proportional to the inverse of the mass transfer Sherwood number, and we have a nice theoretical resolution for the analysis of gas-liquid reaction for the irreversible first-order kinetics considered.

The only problem in the above is that many reactions involved in gas/liquid systems are second order, where there is reaction of a dissolved component with a second species in solution (normally at low concentration). In such cases, the reaction can not even be approximated as pseudo-first-order, and if the reaction and diffusion rates are of the same order of magnitude a zone of reaction will exist as shown in Figure 7.28. In most cases these reactions are irreversible, or nearly so, and a suitable reaction is



The appropriate mass conservation relationships are

$$\begin{aligned} D_A \frac{d^2 C_A}{dz^2} - k C_A C_B &= 0 \\ D_B \frac{d^2 C_B}{dz^2} - k C_A C_B &= 0 \end{aligned} \quad (7-122)$$

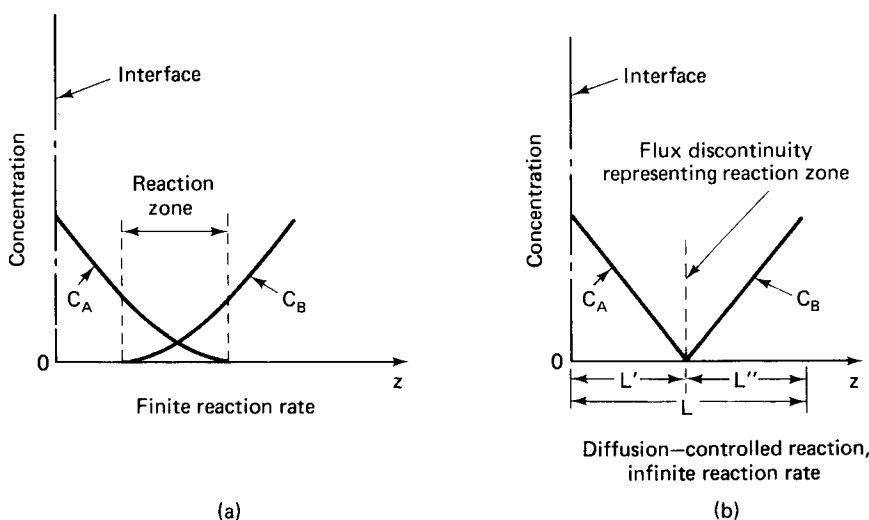


**Figure 7.28** Structure of concentration profiles and the reaction zone near the interface. [After S.K. Friedlander and K.H. Keller, *Chem. Eng. Sci.*, 18, 365, with the permission of Pergamon Press, Ltd., London, England, (1963).]

There is no general analytical solution to equations (7-122), but a very simple analysis pertains when the rate of reaction becomes very large. In this instance, species A and B cannot coexist at the same spatial location, and the reaction occurs at a plane as shown Figure 7.28b, located at point  $L'$ . Now if the total thickness of the film is given by  $L$ , then it can be divided into two regions,  $L'$  and  $L''$ , where the concentration of A is greater than zero and zero, respectively. Within the film

$$N_A = \left( \frac{D_A}{L'} \right) C_{A_i} = \left( \frac{D_B}{L''} \right) C_{B_L} = -N_B$$

For diffusion of A within the films without reaction

$$N_A = \left( \frac{D_A}{L} \right) C_{A_i}$$

so the effect of the reaction is the decrease in the apparent film thickness from  $L$  to  $L'$ . As indicated in the flux balance written above, the fluxes of the two reactants are in opposite directions, as indicated by  $N_A = -N_B$ , so

$$N_A + N_B = 0 = \left( \frac{D_A}{L'} \right) C_{A_i} - \left( \frac{D_B}{L''} \right) C_{B_L} \quad (7-123)$$

$$\frac{L'}{L''} = \left( \frac{D_A}{D_B} \right) \left( \frac{C_{A_i}}{C_{B_L}} \right)$$

Equation (7-123) may be solved simultaneously with

$$L = L' + L'' \quad (7-124)$$



giving the enhancement factor  $\lambda$  as

$$\lambda = \left( \frac{D_B}{D_A} \right) \left( \frac{C_{B_L}}{C_{A_i}} \right) + 1 \quad (7-125)$$

Thus

$$k_M^* = \lambda k_M$$

in which  $k_M^*$  is the mass-transfer coefficient in the presence of infinitely rapid chemical reaction.

The more general case is illustrated in Figure 7.28a. The reactions are of finite velocity and it is possible for A and B to coexist in a zone of reaction as shown. This was first analyzed by Van Krevelen and Hoftijzer [D.W. Van Krevelen and P.J. Hoftijzer, *Rec. Trav. Chim.*, 67, 563 (1948)], who showed that the film theory solution with concentration boundary conditions specified as  $C_A = C_{A_i}$  at the interface and  $C_A = C_{A_L}$ ,  $C_B = C_{B_L}$  at  $L$  (in effect, a bulk phase concentration) was well approximated by

$$\lambda = \frac{\sqrt{M} \sqrt{1 - (\lambda - 1)/rq}}{\tanh[\sqrt{M} \sqrt{1 - (\lambda - 1)/rq}]} \quad (7-126)$$

where

$$\sqrt{M} = \sqrt{\frac{k D_A C_{B_L}}{k_M}} \quad r = \frac{D_B}{D_A}$$

$$q = \nu \frac{C_{B_L}}{C_{A_i}} \quad \nu = \frac{\text{mols B reacted}}{\text{mol A}}$$

A graph of the solution to equation (7-126) is given in Figure 7.29, in which  $\lambda$  is obtained as a function of  $(M)^{1/2}$  in terms of the parametric values of  $rq$ . For small values of  $(M)^{1/2}$ , that is when  $k$  is small, the process approaches the limit of pure physical diffusion and  $\lambda = 1$  for all values of  $rq$ . At high values of  $(M)^{1/2}$  an asymptotic limit is approached, the value dependent on  $rq$ , which is the solution given by equation (7-125). Finally, for  $rq = \infty$ , the solution becomes that for a pseudo-first-order reaction, essentially the result of Hatta. Note that some independent estimation of parameters is required in the application of these results, notably values for the diffusivities, the stoichiometric coefficient, and  $(M)^{1/2}$  requires a value for the mass-transfer coefficient in the absence of chemical reaction.

## 7.2.2 Diffusion and Reaction: Penetration Theory

The penetration theory presents a somewhat more sophisticated alternative to the film theory of mass transfer in that the absorption into the liquid phase is viewed as an unsteady-state process [R. Higbie, *Trans. Amer. Inst. Chem. Eng.*, 31, 365 (1935)]. The transferred component diffuses into an element of fluid which is periodically removed from the interface and replaced by a fresh element in a process of *surface renewal*. If no chemical reaction occurs, the average rate of mass transfer over a given contact time,  $\theta$ , is

$$N_A = 2 \sqrt{\frac{D_A}{\pi \theta}} (C_{A_i} - C_{A_L}) \quad (7-127)$$

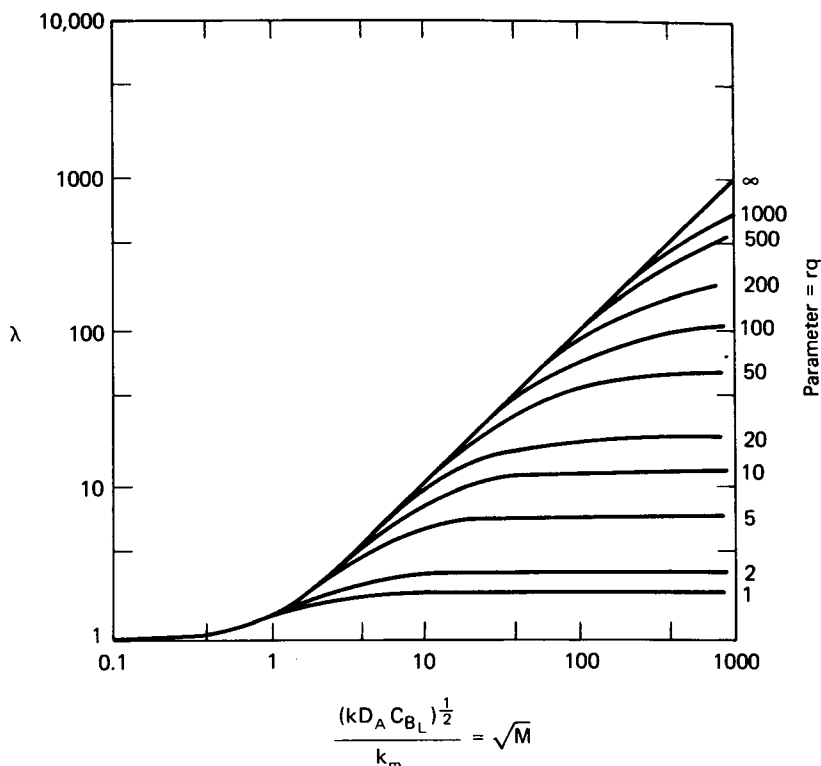


**Figure 7.29** Film theory solution for general second-order reaction. [After D.W. Van Krevelen and P.J. Hoftijzer, *Rec. Trav. Chim.*, 67, 563, with permission of the Royal Netherlands Chemical Society, (1948).]

so the mass-transfer coefficient according to the penetration theory is

$$k_M = 2\sqrt{\frac{D_A}{\pi\theta}}$$

In effect, this approach swaps the arbitrary thickness,  $L$ , of the film theory for the arbitrary contact time,  $\theta$ . Enhancement factors for a number of cases have been determined in terms of this theory. For a first-order reaction we have [P.V. Danckwerts, *Trans. Faraday Soc.*, 46, 300 (1950)]

$$\lambda = \frac{1}{2} \left[ \sqrt{\frac{\pi}{k\theta}} \left( \frac{1}{2} + k\theta \right) \right] \operatorname{erf} \sqrt{k\theta} + \exp(-k\theta) \quad (7-128)$$

where  $k$  is the first-order rate constant and  $\operatorname{erf}$  is defined in the usual way.

For second-order reactions, the asymptotic solution for infinitely rapid reaction [P.V. Danckwerts, *Trans. Faraday Soc.*, 46, 701 (1950)] is given by the awkward parametric form

$$\lambda = \frac{1}{\operatorname{erf}(\sigma)} \quad (7-129)$$

where  $\sigma$  is obtained from the solution of

$$q\sqrt{r} = \frac{1 - \operatorname{erf}(\sigma/\sqrt{r})}{\operatorname{erf}(\sigma) \exp[\sigma^2(1 - 1/r)]} \quad (7-130)$$

Finally, when finite rates of reaction are involved in the second-order case, Gilliland et al. [E.R. Gilliland, R.F. Baddour, and P.L.T. Brian, *Amer. Inst. Chem. Eng. J.*, 4, 223 (1958)] proposed that the following correlation, modeled on equation (7-126), could be used as an approximation to results obtained numerically

$$\lambda' = \frac{\sqrt{M} \sqrt{1 - (\lambda' - 1)/(\lambda - 1)}}{\tanh[\sqrt{M} \sqrt{1 - (\lambda' - 1)/(\lambda - 1)}]} \quad (7-131)$$

where  $\lambda$  is determined from equations (7-129) and (7-130) and  $(M)^{1/2}$  is as defined previously. Brian et al. [P.L.T. Brian, J.F. Hurley, and E.H. Hasseltine, *Amer. Inst. Chem. Eng. J.*, 7, 226 (1961)] found that the approximation provided by equation (7-131) becomes only fair for certain ranges of  $(M)^{1/2}$  and  $\lambda$ , and give correction factors for the approximation in terms of these parameters.

In general, penetration theory results differ significantly from film theory results only when the diffusivity ratio,  $r$ , differs significantly from unity, so the additional complexity involved in the solutions of equations (7-129) to (7-131) should reasonably restrict their use to this situation. For extensive discussions of the theory of diffusion and reaction in gas/liquid systems (in terms of both film and penetration models), the reader is referred to the works of Astarita [(G. Astarita, *Mass Transfer with Chemical Reaction*, Elsevier, Amsterdam, (1967)] and Danckwerts [P.V. Danckwerts, *Gas-Liquid Reactions*, McGraw-Hill, New York, (1970)]. See also the discussion in Chapter 8.

### Illustration 7.8

Derive an expression for the fraction  $F$  of a solute A entering the boundary layer that reaches the bulk phase without reacting. From your results define a characteristic parameter that may be used to indicate the magnitude of diffusional effects. Give the value of the parameter for the following two cases.

- (a)  $F > 0.95$  (reaction rate controlling)
- (b)  $F < 0.05$  (diffusion rate controlling)

Consider that the bulk concentration is a small (about 10%) portion of the interfacial value for the calculation.

#### Solution

The concentration profile in the boundary layer is given by equation (7-107a).

$$C_A = \frac{C_L \sinh(a_0 z) + C_i \sinh[a_0(L - z)]}{\sinh(a_0 L)} \quad (i)$$

and the flux of A at the interface is

$$(N_A)_{z=0} = -D \left( \frac{dC}{dz} \right)_{z=0} \quad (ii)$$

and at  $L$

$$(N_A)_{z=L} = -D \left( \frac{dC}{dz} \right)_{z=L} \quad (\text{iii})$$

Now,  $F$  is defined in terms of these fluxes

$$F = \frac{(N_A)_{z=L}}{(N_A)_{z=0}} \quad (\text{iv})$$

Taking the derivative of equation (i)

$$\frac{dC}{dz} = \frac{C_L a_0 \cosh(a_0 z) - C_i a_0 \cosh[a_0(L - z)]}{\sinh(a_0 L)} \quad (\text{v})$$

Evaluating this derivative at  $z = 0$  and  $L$  and substituting into equation (iv) gives

$$F = \frac{C_L \cosh(a_0 L) - C_i}{C_L - C_i \cosh(a_0 L)} \quad (\text{vi})$$

Recall now that  $a_0 = (k/D)^{1/2}$  and that  $(a_0 L)$  is the characteristic parameter (similar to the Thiele modulus for catalytic reactions), indicating the magnitude of diffusional effects. Here we wish to define the values of this parameter for  $F > 0.95$  and  $< 0.05$  corresponding to the kinetic regimes indicated in the problem statement. If we let  $\cosh(a_0 L) = M$ , then

$$F = \frac{C_L M - C_i}{C_L - C_i M} = \frac{0.1M - 1}{0.1 - M} \quad (\text{vii})$$

for the conditions specified. Solving for  $M$

$$M = \frac{0.1F + 1}{F + 0.1} \quad (\text{viii})$$

Case (a):  $F > 0.95$

$$\cosh(a_0 L) = (1.0950)/(1.05) = 1.042$$

$$(a_0 L) > 0.29$$

Case (b):  $F < 0.05$

$$\cosh(a_0 L) = (1.0050/90.15) = 6.700$$

$$(a_0 L) > 2.59$$



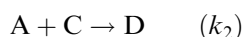
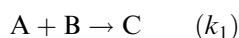
HORATIO SAYS

Suppose the above analysis were applied to a gas-liquid system with  $D \approx 10^{-5} \text{ cm}^2/\text{s}$  and  $k \sim 0.1 \text{ s}^{-1}$ . What would this imply for the range of the corresponding values of film thickness  $L$ ?

### 7.2.3 Selectivity Factors in Gas/Liquid Reactions

The alteration of selectivity due to transport in gas/liquid reactions is less commonly encountered than for gas/solid reactions. The reason for this is basically that the reaction essentially must occur completely in the film for transport to alter selectivity. If the reaction occurs predominately in the (mixed) bulk phase, concentrations of reactants and products are observable and the selectivity is simply determined by the reaction kinetics in the homogeneous phase.

Selectivity in gas/liquid systems was examined in detail by van de Vusse [J.G. van de Vusse, *Chem. Eng. Sci.*, 21, 631, 645 (1966)] for the consecutive reactions



which reduces to a Type III scheme when A (from the gas phase) is present in considerable excess. Sequences such as the above are typical of successive substitution reactions, for example the chlorination of paraffins (*n*-decane was studied by van de Vusse) or aromatics such as benzene. The individual reaction steps are second order and may be analyzed in terms of the general theory given above.

In terms of the reaction parameter  $(M)^{1/2}$ , two limiting regions of behavior may be identified. For  $(M)^{1/2} < 0.5$ , the reaction takes place in the bulk liquid phase and, while the rate of reaction may be affected by the mass transport, the selectivity is unaffected. For  $(M)^{1/2} > 2$ , the concentration of A is essentially depleted within the film and no reaction occurs in the bulk liquid phase. Whether there is a significant gradient of B within the film, and hence whether there is a significant effect on selectivity, depends entirely on the relative concentrations of A and B. For large values of the ratio,  $(C_{B_L}/C_{A_i}) \gg (M)^{1/2}$ , the concentrations of B and C in the film are nearly constant; the rate is affected but the selectivity is not changed. In this case the rate is given by

$$(-r_A) = N_A a = a C_{A_i} \sqrt{k_1 D C_{B_L}} \quad (7-132)$$

where  $D$  is a diffusion coefficient and  $a$  is the gas/liquid specific interfacial area. For values of the ratio  $(C_{B_L}/C_{A_i}) \approx (M)^{1/2}$  and smaller, reactant B is significantly depleted in the film and both rate and selectivity are affected. A summary of this analysis is given in Table 7.6.

**Table 7.6** Mass-Transport Effects on Rate and Selectivity

	$\sqrt{M} > 2$	$\sqrt{M} < 0.5$
$\frac{C_{B_L}}{C_{A_i}} \gg \sqrt{M}$	Effect on rate; none on selectivity	No effects on selectivity
$\frac{C_{B_L}}{C_{A_i}} \approx \sqrt{M}$	Effect on rate and selectivity (A and B profiles in film)	If $k_1 C_{B_L} \ll \frac{D}{L}$ ( $a$ ), the chemical reaction rate is $(-r_A) = k_1 C_{A_i} C_{B_L}$
$\frac{C_{B_L}}{C_{A_i}} \ll \sqrt{M}$	Effect on rate and selectivity (location of reaction plane)	If $k_1 C_{B_L} \ll \frac{D}{L}$ ( $a$ ), physical transfer rate is $(-r_A) = a \left( \frac{D}{L} \right) C_{A_i}$

In the instances where selectivity is affected, this will be expressed in the ratio  $(C_{C_L}/C_{B_L})$ , which will vary with the extent of the reaction. van de Vusse found that a satisfactory correlation between the variation of  $C_{C_L}$  and  $C_{B_L}$  was given by

$$\frac{dC_{C_L}}{dC_{B_L}} = \alpha \frac{C_{C_L}}{C_{B_L}} - \beta \quad (7-133)$$

With the initial condition that  $C_{C_L} = 0$  for  $C_{B_L} = C_{B_L}^0$ , this may be integrated to

$$\left(\frac{1-\alpha}{\beta}\right) C_{C_L} = (C_{B_L})^\alpha - C_{B_L} \quad (7-134)$$

Now, either in the case that the kinetics of the sequence do not depend upon the concentration of A or that  $C_{A_i} \gg C_{B_L}$ , the mass conservation equations may be integrated analytically to obtain the following values for  $\alpha$  and  $\beta$ .

$$\alpha = \left(\frac{k_2}{k_1}\right)^{1/2} \frac{\tanh \sqrt{M_2}}{\tanh \sqrt{M_1}} \quad (7-135)$$

where

$$\sqrt{M_1} = \frac{\sqrt{k_1 D C_{A_i}}}{k_M} \quad \sqrt{M_2} = \sqrt{\frac{k_2 D C_{A_i}}{k_M}}$$

and

$$\beta = \frac{k_1}{k_1 - k_2} (1 - \alpha) \quad (7-136)$$

Without diffusion limitation  $(M_i)^{1/2} < 0.3$  and  $\alpha$  and  $\beta$  are given by

$$\alpha = \frac{k_1}{k_1} \quad \beta = 1 \quad (7-137)$$

For strong diffusion limitation  $(M_1)^{1/2} > 2$ , the corresponding values of  $\alpha$  and  $\beta$  are [note that all of this is controlled by  $(M_1)^{1/2}$ ]

$$\alpha = \sqrt{\frac{k_2}{k_1}} \quad \beta = \frac{1}{1 + \sqrt{k_2/k_1}} \quad (7-138)$$

For values of  $(M_1)^{1/2}$  intermediate between these limits, the mass conservation equations must be solved numerically as is also required if  $C_{A_i} < C_{B_L}$ . The results of a typical calculation for this system are given in Figure 7.30 for a reaction system with strong diffusion control,  $(M_1)^{1/2} = 6.3$ . Here the maximum yield  $(C_{C_{max}}/C_{B_L}^0)$  is plotted as a function of the concentration ratio  $(C_{B_L}^0/C_{A_i})$ . The limiting value of yield for  $(C_{B_L}^0/C_{A_i}) = 0.1$  is computed from equations (7-134) and (7-138) for flat A profile and strong diffusion, while the limit of no diffusion effect is computed from equation (7-134) with  $\alpha$  and  $\beta$  given by equation (7-137). It can be seen that the no-diffusion limit is approached as  $(C_{B_L}^0/C_{A_i})$  becomes much larger than  $(M_1)^{1/2}$  as indicated in the previous qualitative discussion and as shown in Table 7.6.

The dependence of selectivity and yield on concentrations is typical of reactions in gas/liquid systems, and makes generalization of the results quite difficult. The

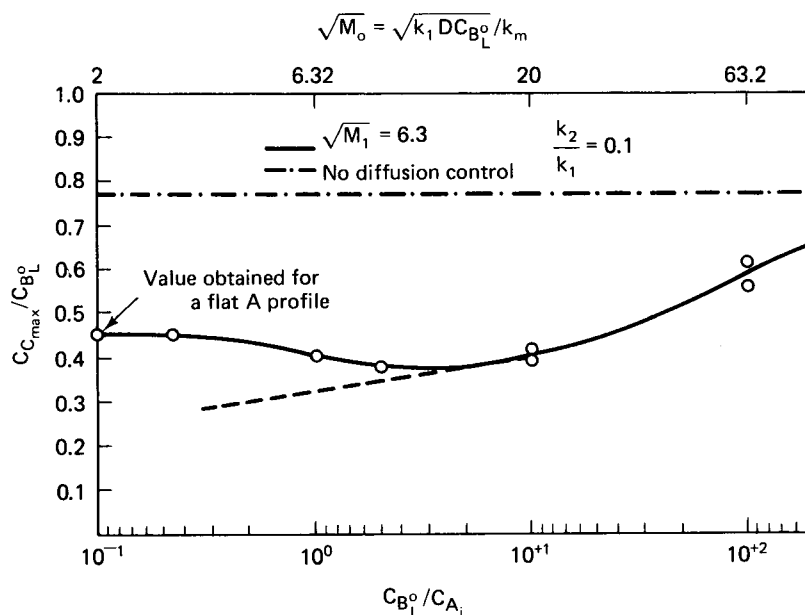


**Figure 7.30** Influence of diffusion on the yield in a consecutive second-order gas/liquid reaction. [After J.G. van de Vusse, *Chem. Eng. Sci.*, 21, 631, with permission of Pergamon Press, Ltd., London, England, (1966).]

particular case treated here, rapid bimolecular reaction, is, however, the most important instance in which selectivity alteration may occur in gas/liquid reactions.

Studies of selectivity in gas/liquid reactions directly concerned with the Type III scheme were reported by Bridgewater [J. Bridgewater, *Chem. Eng. Sci.*, 22, 185 (1967)] using the film theory for mass transfer, and by Szekely and Bridgewater [J. Szekely and J. Bridgewater, *Chem. Eng. Sci.*, 22, 711 (1967)] using a penetration theory analysis. Interestingly, it was shown in these two papers that some difference was obtained in the results for selectivity provided by these two approaches for the Type III reaction. In the simpler case of a single direct reaction, where one is concerned only with conversion (or rate of mass transfer), there is little difference in the film or penetration theory results.

### Illustration 7.9

Kramers and Westerterp [H. Kramers and K.R. Westerterp, *Elements of Chemical Reactor Design and Operation*, Academic Press, Inc., New York, NY, (1963)] developed a variant<sup>11</sup> of the gas-liquid theory we discussed above. They considered the pseudo-first-order-reaction



in which the concentration of B was taken to be constant at a bulk value  $\bar{C}_B$ . The film thickness was set at  $L$ , and  $A_V$  was the interfacial area per unit volume of mixture,  $V$ .

<sup>11</sup> "... how, among so many millions of faces, there should be none alike."—Anonymous

We then have two equations corresponding to (7-122), but the boundary conditions employed differ from those used before. Here

$$z = 0; \quad C_A = C_{A_i}; \quad \left( \frac{dC_B}{dz} \right) = 0 \quad (\text{B nonvolatile}) \quad (\text{ii})$$

$$z = L; \quad C_B = \bar{C}_B; \quad -A_V D \left( \frac{dC_A}{dz} \right) = k \bar{C}_B C_A (V - A_V L) \quad (\text{iii})$$

The difference in formulation is seen in (iii), in which the diffusive flux of A into the bulk phase is set by reaction, rather than by specifying a value of  $C_A$  at  $L$ . Using this approach, derive an expression for  $\eta_L$ , the phase effectiveness.

### Solution

It is convenient to use the following nondimensional form for the variables.

$$f = \frac{C_A}{C_{A_i}} \quad y = \frac{z}{L}$$

so that

$$\frac{d^2 f}{dy^2} = L^2 \left( \frac{k C_B}{D} \right) f \quad (\text{iv})$$

while

$$f = 1 \quad \text{at} \quad y = 0, \quad (\text{v})$$

$$-\frac{df}{dy} = \frac{L k \bar{C}_B f}{A_V D} (V - A_V L) \quad (\text{vi})$$

We can define  $a'_0 = \{[L(k\bar{C}_B/D)^{1/2}]/k_M\}$  where  $k_M$  is the mass transfer coefficient in the absence of chemical reaction. Then we have

$$\frac{d^2 f}{dy^2} = (a'_0)^2 f \quad (\text{vii})$$

with  $y = 0$  for  $f = 1$ , then

$$y = 1; \quad -\frac{df}{dy} = (a'_0) f (\alpha - 1) \quad (\text{viii})$$

where  $\alpha = (V/A_V L)$ . The general form of solution for this equation is

$$f = C_1 e^{(a'_0)y} + C_2 e^{-(a'_0)y} \quad (\text{ix})$$

Evaluation of the constants  $C_1$  and  $C_2$  from the boundary conditions (viii) gives the following very simple relation between them.

$$C_1 = 1 - C_2$$

and

$$C_2 = \frac{[(a'_0)(\alpha - 1) + 1]e^{(a'_0)}}{(e^{(a'_0)} + e^{-(a'_0)}) + (a'_0)(\alpha - 1)(e^{(a'_0)} - e^{-(a'_0)})}$$



Substituting these values for  $C_1$  and  $C_2$  into equation (ix) and writing the exponential terms as hyperbolic trigonometric functions gives

$$f = \frac{\cosh[(a'_0)(1-y)] + (a'_0)(\alpha-1) \sinh[(a'_0)(1-y)]}{\cosh(a'_0) + (a'_0)(\alpha-1) \sinh(a'_0)} \quad (\text{x})$$

The flux of A is obtained from

$$N_A = -\frac{DC_{A_i}}{L} \left( \frac{df}{dy} \right)_{y=0} \quad (\text{xi})$$

and the phase effectiveness,  $\eta_L$ , is defined as

$$\eta_L = \frac{N_A}{(-r_A)_0}$$

where  $(-r_A)_0$  is the intrinsic rate of reaction in the absence of diffusion,  $(k\bar{C}_B C_{A_i} V/A_V)$ . Combining this with equations (x) and (xi) gives the desired expression for phase effectiveness

$$\eta_L = \frac{[(a'_0)(\alpha-1)] + \tanh(a'_0)}{\alpha(a'_0)[(\alpha-1)(a'_0 \tanh a'_0) + 1]} \quad (\text{xii})$$



HORATIO SAYS

I can do even better than this, I think. Let's see if I can derive an "observable criterion" for the gas-liquid system corresponding to that of Weisz and Hicks for catalytic reactions (see Figure 7.16). I already have the phase effectiveness from (xii) above, and I know too that I can write the expression for the observable rate of reaction,  $(-r_A)$ , as

$$(-r_A) = \eta_L k C_{A_i} \bar{C}_B \quad (\text{xiii})$$

Now, if I multiply both sides of this rate expression by

$$\frac{(a'_0)^2}{DC_{A_i}} = \frac{D}{k_M^2 C_{A_i}}$$

then

$$\frac{N_A}{k_M^2 C_{A_i}} = \eta_L \frac{k \bar{C}_B D}{k_M^2} = \eta_L (a'_0)^2 \quad (\text{xiv})$$

and this is what I'm looking for.  $N_A$  would be the measured rate,  $k_M$  I should be able to obtain from correlation; I should also be able to determine  $C_{A_i}$ , and somebody, somewhere, is going to tell me about  $D$ .

Since I have come this far, I might as well show a graph of the results. Note that the volume ratio  $\alpha$ , as might be expected, is quite important in the determination of phase effectiveness. Shown in Figure 7.31 is a range of results for  $\alpha$  from 1 to 1000, encompassing a range of  $10^5$  for  $\eta_L(a_0')^2$ . It is important also to realize that  $\eta_L$  is involved on both axes of Figure 7.31, not usually desirable but unavoidable here, so a trial process is required for solution.

Actually, one point is swept under the rug in the discussion above. The value of  $C_{A_i}$  is really not a directly (or at least easily) measured quantity, and normally would be determined from measurement of  $C_A$  and use of a Henry's law equilibrium constant  $H$ . Thus, the overall analysis will depend on correlations or reported data for the diffusion coefficient,  $D$ , the mass transfer coefficient,  $k_M$ , and the Henry's law constant,  $H$ . As we have pointed out in many other cases, the individual uncertainties involved in determination of each of these constants can accrue a considerable uncertainty in the final evaluation of  $\eta_1$ .

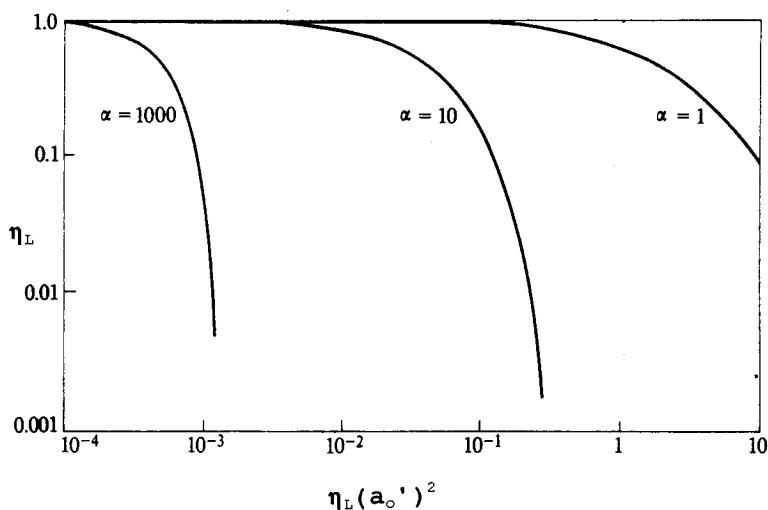


**Figure 7.31** Liquid-phase effectiveness as a function of observable quantities for a pseudo-first-order reaction following the theory of Kramers and Westerterp. [After J.J. Carberry, *Chemical and Catalytic Reaction Engineering*, with permission of McGraw-Hill Book Co., New York, NY, (1976).]

### 7.3 Two-Phase Reactor Models: The Dispersion Approach

It is without question that most instances of reactor design or analysis that are likely to be encountered in practice involve more than one phase. Almost everything up to this point can be thought of as leading up to the capabilities required to look at multiphase problems, and much of the remainder of this chapter and the next two chapters are devoted to this.

However, a fundamental question presents itself right at the onset of the development. This is briefly posed as “how heterogeneous must the models be?” Shall we retain the models we have developed to date and use them in pseudo-homogeneous approximation, or shall we expand them into separate balances for each of the two phases? How do we handle catalytic effectiveness, via curve-fit effectiveness factor correlations or by formulation of the intraparticle diffusion/reaction step as one possibly involving yet another phase? The list goes on and on, unfortunately. Certainly in terms of the esthetics of physicochemical modeling the more complete the model, the fewer (perhaps limiting) assumptions there will be. Just as certainly, though, there is a definite point of diminishing returns; there is no need to put more detail into models than is necessary to obtain the necessary design or analysis objectives [for an example see (V.W. Weekman, Jr., *Ind. Eng. Chem. Proc. Design Devel.*, 7, 90 (1968)]. Since there is probably an order of magnitude more effort involved in the implementation of even two-phase reactor models, the pseudo-homogeneous approach is an attractive first step for more detailed reactor modeling. It is nice to know, of course, when this approach is not going to be adequate for the task at hand, as we have discussed to some extent already in Chapters 5 and 6. The incorporation of transport effects in reactor models using the pseudo-homogeneous approach can be accomplished on the basis of the theories detailed in this chapter. We can view this overall as sort of a first-level approximation to reality, which may be entirely sufficient for some types of design problems and useful in the construction of exploratory models for other situations.

Application of the theory in this case is quite simple, in fact, since we have been careful to define quantities such as the effectiveness factor or the enhancement factor in terms of the rate under observable conditions. Consider as an example a PFR catalytic reactor model in which we wish to include possible diffusion limitations on the catalyst activity. This becomes, *de facto*, a two phase model since the inclusion of an effectiveness factor means that we are considering the catalyst as a separate phase. We start with the design equation written in the following form

$$-\frac{u}{\epsilon} \frac{dC}{dz} = (-r)_0$$

in which  $u$  is the linear velocity based on the empty tube cross section,  $\epsilon$  the bed porosity, and  $(-r)_0$  the observed rate of reaction. Now we have available a model for the intrinsic kinetics of the reaction, say  $(-r) = kC$ , and the observed rate may be determined from this using an effectiveness factor appropriate for the situation. For example, if the reactor is isothermal and we are concerned with both intra- and interphase mass-transport limitations,

$$\eta = \left( \frac{3N_{Bi_m}}{\phi_S^2} \right) \frac{\phi_S \cosh \phi_S - \sinh \phi_S}{\phi_S \cosh \phi_S + (N_{Bi_m} - 1) \sinh \phi_S} \quad (7-54)$$

for spherical catalyst geometry, and the reactor model is

$$-\frac{u}{\epsilon} \frac{dC}{dz} = \eta k C \quad (7-139)$$

Writing the problem out in this manner seems almost too easy, but one has to remember that a lot of prior effort has been invested to make it so, particularly in the development of the effectiveness factor for gas/solid systems.

Now, what would be a model following that of equation (7-139), but expressing the two-phase nature of the reactor more directly? We would first write a mass balance for the gas phase

$$-\left(\frac{u}{\epsilon}\right) \frac{dC}{dz} = k_M a (C - C'_0) \quad (7-140)$$

where  $k_M$  is an interphase (gas-solid) mass-transfer coefficient per unit volume,  $C$  is the bulk gas phase concentration in the reactor, and  $C'_0$  is the reactant concentration at the catalyst surface. This balance, then, accounts for everything that is happening to the reactant in the gas phase, i.e., convective transport and transport to the catalyst surface. For the catalyst phase we have

$$D_{eff} \left[ \frac{1}{r^2} \cdot \frac{d}{dr} \left( r^2 \frac{dC'}{dr} \right) \right] - k C' = 0 \quad (7-141)$$

where  $C'$  is the concentration within the spherical catalyst particle of radial dimension  $r$ , and  $k$  is the appropriate first-order reaction rate constant. The corresponding initial and boundary conditions are

$$C = C_0 \quad z = 0$$

$$C' = C'_0 \quad r = R_p$$

$$\frac{dC'}{dr} = 0 \quad r = 0$$

Note that we have used a pseudo-homogeneous model for the diffusion/reaction process in the catalyst particle.

In spite of this enticing come-on, we will not solve this problem for the moment, being content with its illustration of a typical two-phase reactor balance formulation using the PFR model. We hasten to add, however, that the solution to the set of equations (7-140) and (7-141) with the initial and boundary conditions given is identical to that for the much simpler set of (7-54) and (7-139).<sup>12</sup> In the following sections we shall pursue in detail the developments using the by-now familiar dispersion model for tubular reactors, and in Chapter 8 will treat a number of other multiphase reactor models.

### 7.3.1 The Pseudo Homogeneous Radial Dispersion Model and Its Derivatives

In Chapter 5 we went at the development of axial dispersion models in more detail than was probably needed at that point. A firm grounding in that topic was required however, to understand the origin of the axial dispersion model as a simpler substitute for the radial dispersion model, having its basis in the description of the fluid

<sup>12</sup> "Make it simple, make it smart."—H. Bliss

mechanics of dispersed flows described in Chapter 4. Having said that, we can get to the essential point: the simplification allowed by the axial dispersion approach is considerable and very useful, *as long as one does not forget where it came from*. We are now in position to build up much more detail in reactor models, and the question is whether we still wish to use an axial model for a radial effect. The answer is generally no, particularly for nonisothermal reactors. It has been shown in many studies that axial dispersion, *per se*, is not really important except for very shallow beds and, more importantly, that the axial dispersion coefficient is not a very good way to represent radial gradients, which normally are the important ones. The large literature of the 1960s through the 1980s on axial dispersion models can probably be traced back to concerns with the cost of computer time on the large main-frame computers of that era. This is much less difficult today.

All of this translates into the pseudo-homogeneous model that has radial dispersion and axial convection as the driving components. Given the extensive treatment in Chapter 5, we will not rederive these equations. For a reaction component A, the mass balance is

$$\epsilon D_r \left( \frac{\partial^2 C}{\partial r^2} + \frac{1}{r} \cdot \frac{\partial C}{\partial r} \right) - u \frac{\partial C}{\partial z} - (-r_A) = 0 \quad (7-142)$$

where  $\epsilon$  is bed porosity, and  $D_r$  the radial dispersion coefficient,  $u$  the superficial velocity in the axial direction, and  $(-r_A)$  is the rate of reaction of A per unit volume. An accompanying heat balance is

$$\lambda_r \left( \frac{\partial^2 T}{\partial r^2} + \frac{1}{r} \cdot \frac{\partial T}{\partial r} \right) - u \rho C_p \frac{\partial T}{\partial z} + (-\Delta H)(-r_A) = 0 \quad (7-143)$$

where  $\lambda_r$  is the bed radial effective thermal conductivity,  $\rho C_p$  the gas-phase heat capacity, and  $(-\Delta H)$  is the heat of reaction. The immediate and unpleasant fact that one notices in equations (7-142) and (7-143) is that they are by necessity partial differential equations and for most practical purposes we are once again in the land of numerical solutions. The boundary conditions that would normally be specified are

$$z = 0 \quad C = C_0; \quad T = T_0 \quad (0 \leq r \leq R) \quad (7-144)$$

$$r = 0 \quad \frac{\partial C}{\partial r} = \frac{\partial T}{\partial r} = 0 \quad (7-145)$$

$$r = R \quad \frac{\partial C}{\partial r} = 0; \quad \frac{\partial T}{\partial r} = -\frac{\alpha_w}{\lambda_r} (T_R - T_w) \quad (7-146)$$

In particular, equation (7-146) expresses that there is no mass transfer at the wall, since the concentration derivative is zero, and that heat transfer occurs with a constant wall temperature,  $T_w$ , and a local heat-transfer coefficient,  $\alpha_w$ . This heat-transfer coefficient is now appearing in a boundary condition and is not equivalent to the overall heat-transfer coefficient used in nonisothermal axial dispersion models. The radial dispersion coefficient,  $D_r$ , is, as the name implies, the radial counterpart to the axial dispersion coefficient, and while we expect a different correlation for it there are no new conceptual boundaries set here. The effective bed thermal conductivity,  $\lambda_r$ , however, is another matter altogether and we will worry about it more later.

Since it is apparent from the form of equations (7-142) and (7-143) that numerical solutions will be required, let us first turn our attention to the “new” parameters involved, i.e.,  $\alpha_W$ ,  $D_r$ , and  $\lambda_r$ . These must, obviously, be determined from independent correlation.

1. The wall heat-transfer coefficient,  $\alpha_W$ , has been the subject of quite a bit of investigation over the years and, as one might expect, a number of correlations exist that sometimes do not agree with each other. Many early studies were evaluated by Beek [J. Beek, *Adv. Chem. Eng.*, 3, 203 (1962)], who resolved some of the discrepancies by proposing two correlations based on whether the packing (catalyst) was cylindrical or spherical. For particles that pack like cylinders

$$N_{Nu} = (2.58)N_{Re}^{1/3}N_{Pr}^{1/3} + (0.094)N_{Re}^{0.8}N_{Pr}^{0.4} \quad (7-147)$$

For particles that pack like spheres

$$N_{Nu} = (0.203)N_{Re}^{1/3}N_{Pr}^{1/3} + (0.22)N_{Re}^{0.8}N_{Pr}^{0.4} \quad (7-148)$$

where

$$N_{Nu} = \alpha_W d_p / K \quad N_{Pr} = C_p \mu / K \quad N_{Re} = d_p G / \mu$$

with  $K$  the fluid thermal conductivity and  $G$  the mass velocity. These forms in large part follow those suggested originally by Thoenes and Kramers [D. Thoenes, Jr. and H. Kramers, *Chem. Eng. Sci.*, 8, 271 (1958)] for the corresponding mass transfer case. Stagnant conduction effects were ignored ( $N_{Re} > 40$ ). Additional correlations for  $\alpha_W$  were proposed by Yagi and Wakao [S. Yagi and N. Wakao, *Amer. Inst. Chem. Eng., Jl.*, 5, 79 (1959)] and Calderbank and Pogorski [P.H. Calderbank and L.A. Pogoreki, *Trans. Inst. Chem. Engrs.*, 35, 195 (1957)]. In the former

$$N_{Nu} = (0.20)N_{Re}^{0.8}N_{Pr}^{0.33} \quad (7-149)$$

and in the latter

$$N_{Nu} = (3.6)N_{Re}^{0.37} \quad (7-150)$$

A comparison of the proposals of Beek and of Yagi and Wakao is shown in Figure 7.32 and gives some idea as to the range of uncertainty involved in estimates of  $\alpha_W$ . We must keep in mind that these correlations for  $\alpha_W$  are based on point temperature at the wall, not some averaged reactor temperature. The best-known correlation of the latter type is that of Leva [M. Leva, *Ind. Eng. Chem.*, 39, 857 (1947); M. Leva and M. Grummer, *Ind. Eng. Chem.*, 40, 415 (1948)]. In this case the mixing patterns resulting in the average temperature seem to eliminate the distinction according to particle geometry, however, two correlations are still necessary, one for heating and one for cooling. In that order,

$$N_{Nu} = (0.9)N_{Re}^{0.9}N_{Pr}^{0.33} \left( \frac{d_p}{d_i} \right) e^{-6d_p/d_i} \quad (7-151)$$

$$N_{Nu} = (3.9)N_{Re}^{0.7}N_{Pr}^{0.33} \left( \frac{d_p}{d_i} \right) e^{-4.6d_p/d_i} \quad (7-152)$$

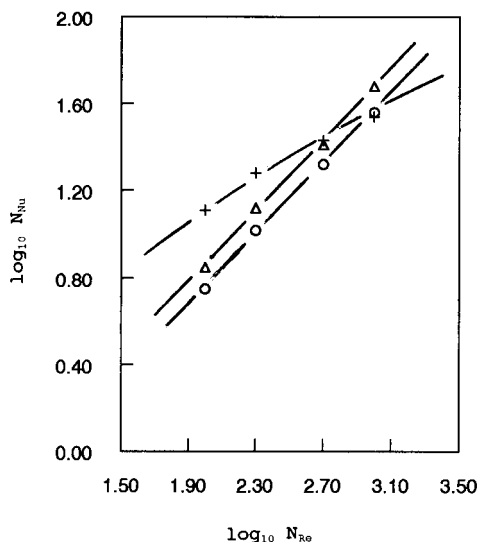


**Figure 7.32** Some correlations for wall heat-transfer in fixed-bed reactors: +, Beek, cylinders;  $\Delta$ , Beek, spheres;  $\circ$ , Yagi and Wakao.  $N_{Pr} = 0.7$  in all cases.

where  $d_p$  is the particle diameter and  $d_t$  the tube diameter. One cannot help but note that all this work is quite old by now and surely better correlations must exist. Indeed they do, but in the writer's experience almost all are proprietary<sup>13</sup>; the study of wall heat-transfer coefficients ceased to exist as a fashionable area of research many years ago.

2. The radial dispersion coefficient,  $D_r$ , we might expect to be correlated in terms of the Reynolds number and a radial Peclet number,  $(d_p u / D_r)$ , with  $u$  the flow velocity in the axial direction. This parameter was also the subject of intense study some time ago, as indicated in the works of Beek [see also the very important works of E. Singer and R.H. Wilhelm, *Ind. Eng. Chem.*, 46, 343 (1950); W.B. Argo and J.M. Smith, *Chem. Eng. Prog.*, 49, 443 (1953); R.W. Fahien and J.M. Smith *Amer. Inst. Chem. Eng. Jl.*, 1, 25 (1955)]. These are also old references. Figure 5.10 gave a composite of the results obtained over the years in terms of the radial Peclet number. It was shown that the value approaches 10 in a fashion similar to the asymptotic value of 2 for the axial Peclet number shown in Figure 5.9. For convenience, we repeat the correlating equations. For liquids,

$$(N_{Pe})_r = \frac{17.5}{N_{Re}^{0.75}} + 11.4 \quad (5-52)$$

For gases,

$$\frac{1}{(N_{Pe})_r} = \frac{0.4}{(N_{Pe} N_{Sc})^{0.8}} + \frac{0.09}{1 + (10 / N_{Re} N_{Sc})} \quad (5-53)$$

<sup>13</sup> "There is no secret so close as that between a rider and his horse."—R.S. Surtees

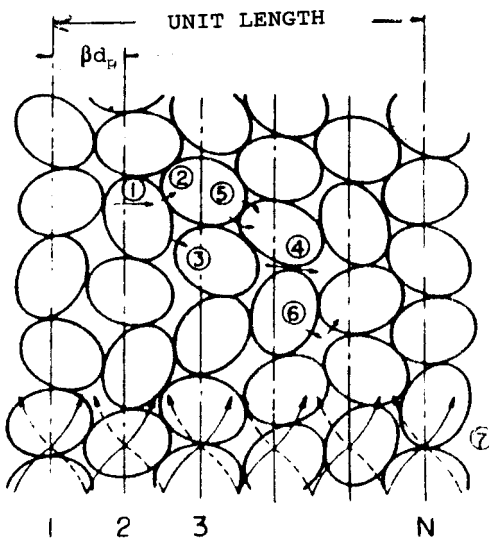


**Figure 7.33** Conceptual model for heat transfer in a packed bed. [After S. Yagi and D. Kunii, *Amer. Inst. Chem. Eng. Jl.*, 3, 375, with permission of the American Institute of Chemical Engineers, (1957).]

3. The third parameter is the thermal conductivity of the bed,  $\lambda_r$ . This is a much more complicated problem than mass dispersion, since thermal energy has more pathways for transport available. Mass dispersion is effectively confined to the void area of the bed, but heat transport can occur in the voids and in the solids. Two of the best known correlations are those of Argo and Smith (reference above) and of Yagi and Kunii [S. Yagi and D. Kunii, *Amer. Inst. Chem. Eng. Jl.*, 3, 375 (1957); see also D. Kunii and J.M. Smith, *Amer. Inst. Chem. Eng. Jl.*, 6, 71 (1960)]. Both approaches visualize the heat transfer process within the bed as depicted in Figure 7.33, and both have a common ancestor in the work of Bruggeman [D.A. Bruggeman, *Ann. Phys.*, 24, 636 (1935); see also R. Kamiuto, *J. Nuc. Sci. Tech.*, 27, 473 (1990)]. Quite a number of things occur at the same time, as indicated by the numbers on the figure. In brief, we have
  1. Heat transfer through the solid.
  2. Heat transfer through the contact surface of the solid.
  3. Radiant heat transfer between surfaces of the solid (gas phase).
  4. Radiant heat transfer between adjacent voids (gas phase).
  5. Heat transfer through the fluid film near the contact surface.
  6. Heat transfer by convection: solid-fluid-solid.
  7. Heat transfer by lateral mixing.

The result of Argo and Smith for gas-solid systems, negligible molecular conduction effects, and particle Reynolds numbers  $> 40$  is

$$\lambda_r = \left[ \frac{d_p C_p G}{N_{Pe_m} \epsilon} + \frac{(0.346)}{(10^6) \epsilon} f d_p T^3 \right] \epsilon + \frac{(0.6) h d_p K_S}{2 K_S + (0.7) h d_p} \quad (7-153)$$



Here the numerical constants employed are consistent with  $\lambda_r$  in BTU/h  $-\circ\text{R}$ ,  $T$  is in  $\circ\text{R}$ ,  $h$  is the solid-gas heat transfer coefficient [c.f. equation (7-83)],  $K_S$  the thermal conductivity of the solid phase,  $N_{Pe_m}$  the mass Peclet number,  $G$  the mass velocity,  $C_p$  the heat capacity,  $d_p$  the particle diameter, and  $\epsilon$  is the bed porosity. The second term in brackets represents the radiative heat transfer contribution to the apparent thermal conductivity; this is normally negligible for operation at less than 300–350  $\circ\text{C}$ . The quantity  $f$  is a surface emissivity factor that normally can be estimated as  $0 < f < 0.1$  (see Argo and Smith). Keep in mind that equation (7-153) is for gas flow in packed beds with  $N_{Re} < 40$ . Other situations are discussed by both Beek, and Argo and Smith. Note also that, with the possible exception of  $f$ , there are no adjustable parameters in equation (7-153). Since the radiative contribution is normally quite small except at very elevated temperatures, a typical working form of equation (7-153) is

$$\lambda_r = \frac{d_p C_p G}{N_{Pe_{m,r}}} + \frac{(0.6)h d_p K_S}{2K_S + (0.7)h d_p} \quad (7-154)$$

The approach of Yagi and Kunii yields the following expression for gas-solid systems with no radiative contribution (notation as given by Yagi and Kunii).

$$\frac{\lambda_r^\circ}{K_g} = \frac{\beta(1 - \epsilon)}{\gamma(K_g/K_S) + \phi} \quad (7-155)$$

and

$$\frac{\lambda_r}{K_g} = \frac{\lambda_r^\circ}{K_g} + (\alpha\beta)N_{Pe_m} \quad (7-156)$$

where  $K_g$  and  $K_S$  are the thermal conductivities of the gas and solid phases,  $\lambda_r^\circ$  is the effective thermal conductivity of the bed in the absence of flow,  $\alpha$  the mass velocity of fluid flowing in the direction of heat transfer,  $\beta = l_p/d_p$  is the ratio of the average length between centers of adjacent particles in the direction of heat flow ( $l_p$ ) to particle diameter ( $d_p$ ),  $\gamma = l_s/d_p$  is the ratio of the effective length of solid relating to heat conduction ( $l_s$ ) to particle diameter (normally  $\approx 1$ ), and  $\phi = l_v/d_p$  is the ratio of the effective thickness of the fluid film adjacent to two contact surfaces ( $l_v$ ) to particle diameter.

Although the quantities  $\alpha$ , and  $\phi$  have physical significance as described above, they cannot (as one might suspect) be determined on an *a priori* basis. Background data for their evaluation are shown in Figure 7.34.

It is probably a reasonable exercise at this point to review all the dimensionless numbers that have increased in density as this discussion has progressed. First revisit the material in Section 7.1. Then,

1.  $N_{Pe,a}$  is the axial Peclet number,

$$\frac{d_p u}{D_a} = \frac{\text{axial convection}}{\text{axial dispersion}}$$

2.  $N_{Pe,r}$  is the radial Peclet number,

$$\frac{d_p u}{D_r} = \frac{\text{axial convection}}{\text{radial dispersion}}$$

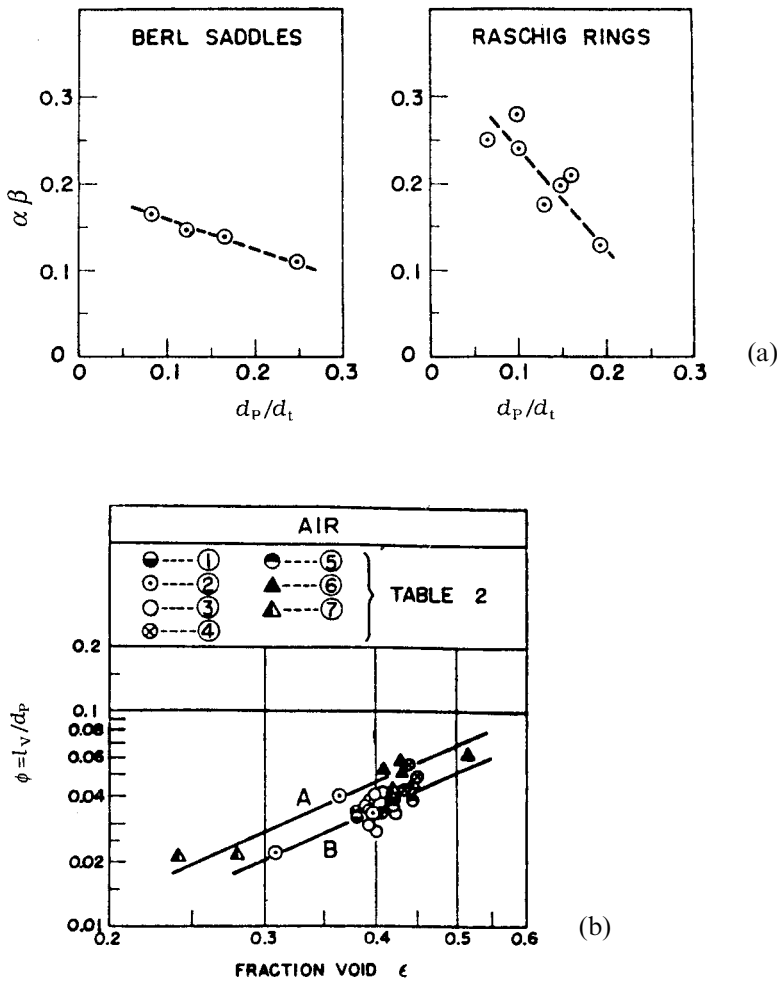


**Figure 7.34** (a) Typical values of  $\alpha\beta$  as a function of relative particle diameter. (b) Values of  $\phi$  calculated for air-solid systems. Plot is referred to Table 2 in the paper of Yagi and Kunii. (c) Ratio of  $(\phi/\phi_{air})$  for various fluids correlated versus fluid thermal conductivity. [After S. Yagi and D. Kunii, *Amer. Inst. Chem. Eng. Jl.*, 3, 375, with permission of the American Institute of Chemical Engineers, (1957).]

3.  $N_{Bi,W}$  is the wall Biot number,

$$\frac{\alpha_W R_0}{\rho c_p \lambda_r} = \frac{\text{temperature gradient (bed core)}}{\text{temperature gradient (wall film)}}$$

4.  $N_{Bi,m}$  is the local mass Biot number,

$$\frac{k_M \Lambda}{D} = \frac{\text{interphase mass transfer}}{\text{intraphase mass transfer}}$$

See also equation (7-51)

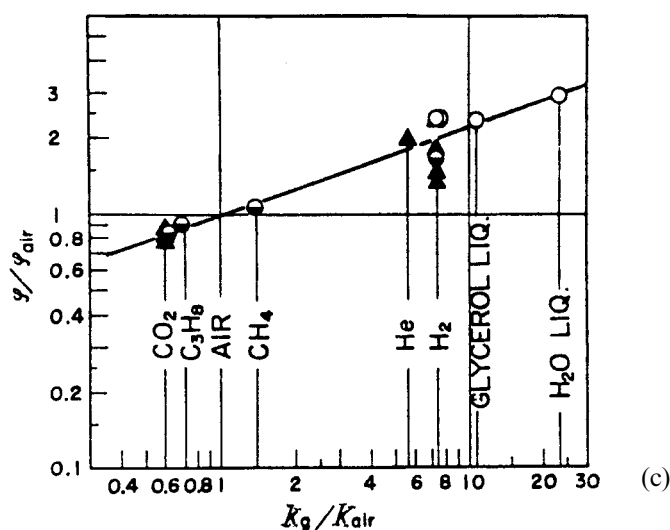


Figure 7.34 Continued.

5.  $N_{Bi,h}$  is the local thermal Biot number,

$$\frac{h\Delta}{K} = \frac{\text{interphase heat transfer}}{\text{intraphase heat transfer}}$$

6.  $N_{Nu,W}$  is the wall Nusselt number,

$$\frac{\alpha_W d_p}{K_r} = \frac{\text{interphase heat transfer}}{\text{intraphase heat transfer}}$$

And, of course,

7.  $N_{Re}$  is the Reynolds number,

$$\frac{d_p u \rho}{\mu} = \frac{d_p G}{\mu} = \frac{\text{convective flow}}{\text{viscous flow}}$$

8.  $N_{Pr}$  is the Prandtl number,

$$\frac{\mu}{\rho K} = \frac{\text{momentum diffusion}}{\text{thermal diffusion}}$$

9.  $N_{Sc}$  is the Schmidt number,

$$\frac{\mu}{\rho D} = \frac{\text{momentum diffusion}}{\text{mass diffusion}}$$

The individual quantities appearing in the above are defined (in order of their appearance) as

- $d_p$  particle or packing diameter  
 $u$  axial velocity  
 $D_a$  axial dispersion coefficient  
 $D_r$  radial dispersion coefficient

$R_0$	reactor radius
$\rho$	fluid density
$C_p$	fluid heat capacity
$K_r$	radial thermal conductivity
$K$	fluid thermal conductivity
$k_M$	mass transfer coefficient
$l$	characteristic dimension
$D$	molecular diffusion coefficient
$h$	local heat transfer coefficient
$k$	thermal conductivity
$\alpha_W$	wall heat transfer coefficient
$\mu$	viscosity

### Illustration 7.10

Expand upon the radial dispersion model of equations (7-142) and (7-143) to include axial dispersion effects as well. Reduce this model to nondimensional form and express the characteristic parameters in terms of the dimensionless numbers described above, as far as possible. Start with the unsteady-state forms of the model equations.<sup>14</sup>

#### Solution

By now we should almost be able to write such conservation equations down from memory. We consider that we have a fixed-bed tubular reactor of length  $L$  and radius  $R$ , and a reaction species with concentration  $C$  and rate of reaction  $(-r)$ . Then, for the mass balance

$$\frac{\partial C}{\partial t} - D_a \frac{\partial^2 C}{\partial z^2} - D_r \left( \frac{\partial^2 C}{\partial r^2} + \frac{1}{r} \frac{\partial C}{\partial r} \right) + u \frac{\partial C}{\partial z} = (-r) \quad (\text{i})$$

and the heat balance,

$$\rho C_p \frac{\partial T}{\partial z} - \rho C_p \lambda_a \frac{\partial^2 T}{\partial z^2} - \rho C_p \lambda_r \left( \frac{\partial^2 T}{\partial r^2} + \frac{1}{r} \frac{\partial T}{\partial r} \right) + \rho C_p u \frac{\partial T}{\partial z} = (-r)(-\Delta H) \quad (\text{ii})$$

Here a distinction has been made between the two bed effective thermal conductivities,  $\lambda_r$  and  $\lambda_a$ , although it is probably not unreasonable to consider them equal to each other. Now, we can define a small herd of nondimensional quantities.

$$\begin{aligned} n &= \left( \frac{L}{d_p} \right); & m &= \left( \frac{R_0}{d_p} \right); & a &= \left( \frac{L}{R_0} \right); & \theta &= \left( \frac{L}{u} \right) \\ f &= \left( \frac{C}{C_0} \right); & v &= \left( \frac{T}{T_0} \right); & w &= \left( \frac{r}{R_0} \right); & \xi &= \left( \frac{z}{L} \right); & \tau &= \left( \frac{t}{\theta} \right) \end{aligned}$$

<sup>14</sup> The development here follows, in general outline, that given by J.J. Carberry, *Chemical and Catalytic Reaction Engineering*, Chapter 10, McGraw-Hill Book Co., New York, NY, (1976). See this reference for additional detail of this approach.

These definitions give the following forms for the continuity equations.

$$\frac{\partial f}{\partial \tau} - \left( \frac{D_a}{Lu} \right) \frac{\partial^2 f}{\partial \xi^2} - \left( \frac{D_r}{R_0 u} \right) \left( \frac{L}{R_0} \right) \left( \frac{\partial^2 f}{\partial w^2} + \frac{1}{w} \frac{\partial f}{\partial w} \right) + \frac{\partial f}{\partial \xi} = \frac{(-r)\theta}{C_0} \quad (\text{i-a})$$

$$\frac{\partial v}{\partial \tau} - \left( \frac{\lambda_a}{Lu} \right) \frac{\partial^2 v}{\partial \xi^2} - \left( \frac{\lambda_r}{R_0 u} \right) \left( \frac{L}{R_0} \right) \left( \frac{\partial^2 v}{\partial w^2} + \frac{1}{w} \frac{\partial v}{\partial w} \right) + \frac{\partial v}{\partial \xi} = \frac{(-r)(-\Delta H)\theta}{\rho C_p T_0} \quad (\text{ii-a})$$

Now if we compare some of the parametric groupings in the above with the non-dimensional numbers we have discussed, we can recognize that

$$N_{Pe,a} = \frac{d_p u}{D_a}; \quad N_{Pe,r} = \frac{d_p u}{D_r}$$

so

$$\left( \frac{Lu}{D_a} \right) = (N_{Pe,a})(n); \quad \left( \frac{R_0 u}{D_r} \right) \left( \frac{R_0}{L} \right) = (N_{Pe,a})(m/a)$$

The fully reduced equations that we finally obtain are

$$\frac{\partial f}{\partial \tau} - \frac{1}{N_{Pe,a}(n)} \frac{\partial^2 f}{\partial \xi^2} - \frac{a}{N_{Pe,r}(m)} \left( \frac{\partial^2 f}{\partial w^2} + \frac{1}{w} \frac{\partial f}{\partial w} \right) + \frac{\partial f}{\partial \xi} = \frac{(-r)\theta}{C_0} \quad (\text{iii})$$

$$\frac{\partial v}{\partial \tau} - \frac{1}{N_{Pe,ha}(n)} \frac{\partial^2 v}{\partial \xi^2} - \frac{a}{N_{Pe,hr}(m)} \left( \frac{\partial^2 v}{\partial w^2} + \frac{1}{w} \frac{\partial v}{\partial w} \right) + \frac{\partial v}{\partial \xi} = \frac{(-r)(-\Delta H)\theta}{\rho C_p T_0} \quad (\text{iv})$$

We have had to invent two new Peclet numbers.

$$N_{Pe,ha} = \text{axial heat dispersion} = \left( \frac{d_p u}{\lambda_a} \right)$$

$$N_{Pe,hr} = \text{radial heat dispersion} = \left( \frac{d_p \mu}{\lambda_r} \right)$$

The boundary condition in the axial direction should be familiar from the discussion in Chapter 5, so

$$\begin{aligned} \xi = 0 \quad f &= 1 + \frac{1}{N_{Pe,a}(n)} \left( \frac{\partial f}{\partial \xi} \right)_{\xi=0} \\ v &= 1 + \frac{1}{N_{Pe,ha}(n)} \left( \frac{\partial v}{\partial \xi} \right)_{\xi=0} \\ \xi = 1 \quad \left( \frac{\partial f}{\partial \xi} \right)_{\xi=1} &= \left( \frac{\partial v}{\partial \xi} \right)_{\xi=1} = 0 \end{aligned}$$

The radial conditions are perhaps a bit more complicated.

$$w = 0 \quad \left( \frac{\partial f}{\partial w} \right)_{w=0} = \left( \frac{\partial v}{\partial w} \right)_{w=0} = 0$$

Now, at  $w = 1$ , for mass transfer (there is no mass transfer through the wall),

$$w = 1 \quad \left( \frac{\partial f}{\partial w} \right)_{w=1} = 0$$

However, for heat transfer

$$\left( \frac{\partial v}{\partial w} \right)_{w=1} = \frac{\alpha_w R_0}{\rho C_p \lambda_r} (v - v_W)$$

The astute observer will recognize that the first grouping on the right of the equation is the wall Biot number,  $N_{Bi,W}$ . This is often written as the product of a Peclet number and (ugh, yet another one) a Stanton number,  $N_{St}$ , so

$$N_{Bi,W} = \frac{\alpha_w R_0}{\rho C_p \lambda_r} = \left( \frac{\alpha_w}{\rho u C_p} \right) \left( \frac{R_0}{d_p} \right) N_{Pe,hr} = N_{St} N_{Pe,hr}(m)$$

So far we have done nothing except manipulate equations to show that the development is another pseudo-homogeneous model. However, where we go from here depends, in large part, on how the reaction rate term,  $(-r)$ , is handled. So far, we have made no specification for this. To be comfortable, recall an isothermal reaction, first-order with respect to  $C$ . We recall that the rate term may be written as

$$(-r) = \frac{\eta k C}{1 + \left( \frac{\eta k}{k_m} \right) \left( \frac{\bar{V}}{S} \right)} \quad (7-50)$$

where  $\bar{V}$  is the catalyst particle volume,  $S$  the external surface area, and  $\eta$  the intraparticle effectiveness factor. If an approximation for slab geometry of the particle is allowed, then

$$(-r) = \frac{\eta k C}{1 + [(\phi \tanh \phi)/N_{Bi,m}]} \quad (7-53)$$

or

$$(-r) = \frac{k C \tanh \phi}{\phi \{1 + [(\phi \tanh \phi)/N_{Bi,m}]\}} \quad (7-53a)$$

Substitution of equation (7-53a) into equation (iii) then completes the model for radial dispersion and isothermal first-order reaction. A corresponding nonisothermal model may be built up in the same way, using the approach of McGreavy and Cresswell shown in equation (7-63).

Another approach, which requires a bit of foreknowledge concerning the magnitude of the Thiele modulus likely to be encountered, employs the direct analysis of Liu given in equations (7-28) and (7-33). For example, if we have a first-order nonisothermal reaction system that fits the restrictions accompanying equation (7-33), then

$$(-r) = \left\{ [\exp(0.14\phi\delta^{1.6})] - 1 + \frac{\tanh \phi}{\phi} \right\} \quad (v)$$

Substitution of equation (v) into (iii) and (iv) completes this version of the model.

All of these approaches end up as two-phase reactor models by the way in which the reaction kinetics are handled, but are also sort of “back door” methods in that the diffusion/reaction results are added on to the reactor model. We hasten to say that there is nothing wrong with this (indeed, why is the effectiveness factor defined in the way that it is), but separate analytical expressions will not always be available for the effectiveness factor. In such a case one has to solve the intra-particle diffusion reaction problem along with the reactor continuity equations. If one wishes a lesson in humility, this is a good place to start.

So, let's take a look at what this looks like, aside from trouble. In the steady state the rates of reaction and of heat generation (assuming exothermic reactions for the moment) are balanced first by the rates of interphase transport between the fluid phase and the catalyst. Thus,

$$\begin{aligned}(-r) &= k_m S(C - C_S) \\ (-r)(-\Delta H) &= hS(T - T_S)\end{aligned}$$

where  $C_S$  and  $T_S$  are conditions at the catalyst surface. Casting these into nondimensional form,

$$\begin{aligned}\frac{(-r)\theta}{C_0} &= k_m S\theta(f - f_S) \\ \frac{(-r)(-\Delta H)\theta}{\rho C_p T_0} &= \left(\frac{hS}{\rho C_p}\right)\theta(v - v_S)\end{aligned}\quad (\text{vi})$$

These are the basic relationships that connect the fluid phase (reaction mixture) to the solid phase (catalyst). Following this we can now write the conservation equations for the catalyst. Assuming slab geometry for the moment as a reasonable approximation, then, for general power-law kinetics,

$$\begin{aligned}D_{eff} \frac{d^2 C}{dl^2} &= kC^q \\ K_{eff} \frac{d^2 T}{dl^2} &= (-\Delta H)kC^q\end{aligned}$$

It is convenient to write the equations in nondimensional form as well, normalizing with respect to particle dimension,  $\Lambda$ , and bulk fluid conditions of temperature and concentration,  $T_b$  and  $C_b$ .

$$\frac{d^2 f}{dy^2} = \frac{\Lambda^2 k_b (C_b)^{q-1}}{D_{eff}} f^q \exp[-\gamma(1/v - 1)] \quad (\text{vii})$$

$$\frac{d^2 v}{dy^2} = \frac{(-\Delta H)D_{eff}C_b}{K_{eff}T_b} \cdot \frac{\Lambda^2 k_b (C_b)^{q-1}}{D_{eff}} f^q \exp[-\gamma(1/v - 1)] \quad (\text{viii})$$

where  $y = (1/\Lambda)$  and  $\gamma = (E/RT_0)$ . The boundary conditions for solution of the intraphase (particle) problem are

$$\begin{aligned} y = 0; \quad \left(\frac{df}{dy}\right)_{y=0} &= 0; \quad \left(\frac{dv}{dy}\right)_{y=0} = 0 \\ y = 1; \quad v_S &= v_b - \frac{1}{N_{Bi,h}} \left(\frac{dv}{dy}\right)_{y=1} \\ f_S &= f_b - \frac{1}{N_{Bi,m}} \left(\frac{df}{dy}\right)_{y=1} \end{aligned} \quad (ix)$$

Now we may substitute from (ix) the expressions for the interphase gradients into equations (iii) and (iv). These substitutions end up more or less as might be expected.

$$\frac{(-r)\theta}{C_0} = -\frac{k_m S \theta}{N_{Bi,m}} \left(\frac{df}{dy}\right)_{y=1} = -\frac{\theta D_{eff}}{\Lambda^2} \left(\frac{df}{dy}\right)_{y=1}$$

and

$$\frac{(-r)(-\Delta H)\theta}{\rho C_p T_0} = -\frac{h S \theta}{\rho C_p N_{Bi,h}} \left(\frac{dv}{dy}\right)_{y=1} = -\frac{\theta K_{eff}}{\Lambda^2} \left(\frac{dv}{dy}\right)_{y=1}$$

It is seen clearly that the heterogeneous part of the problem (i.e., kinetics and effectiveness factor) shows up in the overall reactor balance in terms of the gradients of concentration and temperature at the catalyst surface,  $y = 1$ .

The question is whether there are any ways out of such a complicated formulation, because solution of the above will surely be a rather involved numerical problem. There are probably no general ways to simplify the problem, but perhaps some of the things we have done before can help. Our friend Horatio will pose the question in a very direct manner.



HORATIO SAYS

Are there any relationships among the variables here (of which there seems an enormous number) that might make the problem a little less formidable? What can we do about the effectiveness of the catalyst phase, if anything?

Well, yes, Horatio. We finally got you, because you are obviously forgetting the analysis given in Chapter 6, Section 3! For example, the two continuity equations for the catalyst are coupled through the reaction rate term,  $kC^q$ . In nondimensional form this results in the following working relationship.

$$v = 1 + \beta(f_s - f_c)$$

where  $\beta$  is the thermicity parameter

$$\beta = \frac{(-\Delta H) D_{eff} C_b}{K_{eff} T_b}$$



and  $f_c$  is the dimensionless concentration at  $y = 0$ . For strong diffusion limits  $f_c \rightarrow 0$  and there is a simple linear relationship between  $v$  and  $f_s$ . This can be used to reduce the number of equations to be solved by one, but does not eliminate the need for a numerical solution to obtain the gradients at  $y = 1$ . [See also equation 6-108].

Fortunately, in many cases such as the above, there are at least some simplifications that can be employed for the equations appearing in Illustration 7.10. Two that are implied (by the way that the equations were written) are that  $\rho C_p$  and  $(-\Delta H)$  are temperature-independent, or at least that their temperature dependence is small compared to that of the Arrhenius dependence of the reaction rate constant.

The Peclet numbers also bear further scrutiny. At several points we have said, without much justification, that axial dispersion is a factor that is physically important only in shallow beds. We should be a little more quantitative about this. In Chapter 5 the relationship between axial dispersion and CSTR models was discussed. For a packed bed of length  $L$  and packing of diameter  $d_p$ , the effective number of CSTR mixing stages,  $n'$ , is

$$n' = \frac{d_p u}{2D_a} \left( \frac{L}{d_p} \right) = \frac{N_{Pe,a}}{2} \left( \frac{L}{d_p} \right) \quad (7-157)$$

However, for particle Reynolds numbers greater than about 10,  $N_{Pe,a} \rightarrow 2$ , thus

$$n' = \left( \frac{L}{d_p} \right) = n \quad (7-158)$$

Reference to the residence-time distribution curves in Chapter 5 shows that  $n$  does not have to be a large number before the CSTR sequence approaches PFR behavior. A safe approximation, for  $N_{Re} > 10$  is to assume axial dispersion negligible if  $(L/d_p) > 105$  [J.J. Carberry, *Can. J. Chem. Eng.*, 36, 207 (1958)]. The question of what to do about radial dispersion is not so easily disposed. Certainly in reactors with significant thermal effects and heat transfer at the wall, there should exist some level of radial gradients, particularly thermal. Now, for the results shown in Figure 5.10,  $N_{Pe,r}$  approaches 10 at high  $N_{Re}$ , so that if we define a number of radial mixing stages by analogy to the axial case,

$$m' = \frac{R_0 u}{2D_r} = \frac{N_{Pe,r}}{2} \left( \frac{R_0}{d_p} \right) \quad (7-159)$$

and for the limiting  $N_{Pe,r} \rightarrow 10$

$$m' = 5 \left( \frac{R_0}{d_p} \right) = 5m \quad (7-160)$$

If there were *no* gradients in the radial direction, one CSTR would be all that is required, i.e.,  $m'$  should approach unity. Obviously, on the basis of equation (7-160), this cannot be obtained in practice; however, we can approach this condition by

reducing the radial  $m$  ratio (minimizing the number of particles in the radial direction). In practice this means an  $m$  of 2 to 4, as is the norm for the tube-bundle reactors commonly employed in hydrocarbon oxidation. Keep in mind, though, that the total temperature gradient from the reactor center-line to the tube wall will also be strongly influenced by the magnitude of the wall heat-transfer coefficient as contained in  $N_{Bi,W}$ .

The basic message in all of the above is essentially that one may avoid axial dispersion effects if it is possible to design with the necessary axial aspect ratio,  $n$ , but there is no way in general to avoid radial dispersion effects.

Two final questions arise concerning i) the nature of velocity profiles across the bed and ii) the pressure drop along the length of the reactor. With regard to the first question, it is probably reasonable to assume that there will be a velocity profile of some sort regardless of the conditions of operation—but of what type? Small particle to tube diameter ratios,  $m$ , encourage relatively flat velocity profiles, but for a fixed tube dimension, decreasing the particle size decreases the corresponding particle Reynolds number. A generalized sketch of a typical velocity profile at the particle Reynolds numbers corresponding to  $N_{Pe,a} \rightarrow 2$  is shown in Figure 7.35. A number of studies of velocity profiles in fixed beds can be found in older literature [see, for example, V.P. Dorweiler and R.W. Fahien, *Amer. Inst. Chem. Eng. Jl.*, 5, 139 (1959)] and are summarized in the review by Beek, who presents an horribly complex empirical curve-fit expression for data up to 1960 (which does not fit the data anyway).

The most prominent feature of Figure 7.35 is the two local maxima located near the tube walls. A probable reason for this is that the random orientation is disturbed in the vicinity of the wall and the void fraction at this point is somewhat greater than in the bed as a whole. This annular volume of decreased resistance to flow then allows a higher velocity. This may also be an important factor in the differences in correlations of wall heat-transfer coefficients for various packing materials, as shown in Figure 7.32.

Pressure drop in fixed beds is normally interpreted in terms of the Ergun equation [S. Ergun, *Chem. Eng. Prog.*, 48, 89 (1952)].

$$\frac{\Delta P}{\Delta z} = \frac{G}{\rho g_c d_p} \left( \frac{1 - \epsilon}{\epsilon^3} \right) \left[ \frac{150(1 - \epsilon)\mu}{d_p + 7.75G} \right] \quad (7-161)$$

where  $G$  is the superficial mass velocity,  $\epsilon$  bed void fraction,  $\rho$  fluid density, and  $g_c$  the gravitational constant. For the numerical values appearing in equation (7-161), a consistent value for the latter is 16 ft/lb (force)-h<sup>2</sup>. Some idea of the fit this

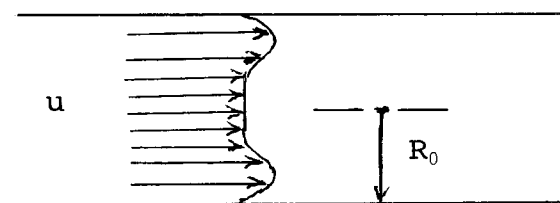


**Figure 7.35** Generalized representation of the velocity profile in a fixed bed for  $N_{Pe,a} \rightarrow 2$ .

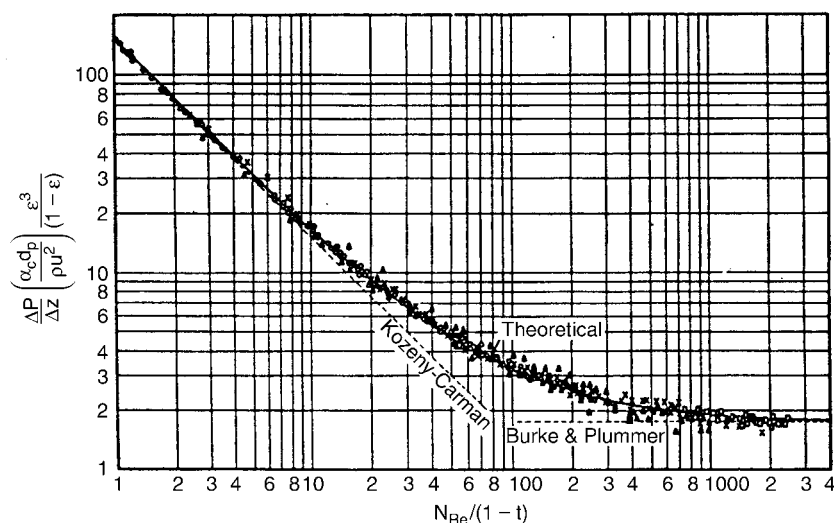


**Figure 7.36** Correlation of pressure drop in fixed beds according to the Ergun equation;  $N_{Re} = (d_p u \rho / \mu)$ . [From S. Ergun, *Chem. Eng. Prog.*, 48, 89, with permission of the American Institute of Chemical Engineers, (1952).]

correlation provides is shown in Figure 7.36; as can be seen, the equation does very well. There are two points of caution, however. First is that the bed void fraction appears as a cubed term, with the result that the correlation is very sensitive to this quantity and  $\epsilon$  should be determined as precisely as possible before any attempts to estimate  $(\Delta P / \Delta z)$ . The second caution derives from the fact that the original work was not based on very much data pertaining to beds with fine grain-size powders. For fine mesh material, the observed  $\Delta P$  is often substantially greater than that estimated from equation (7-161)<sup>15</sup>. If there is a substantial pressure drop indicated for a given reactor-catalyst system, it may be necessary to reformulate the conservation equations to reflect changes in  $\rho$  and  $u$  with axial position, but we will not do that here.

### 7.3.2 Summary

If one were to attempt to determine any communality in the discussion of models given in this chapter, about the best would be to say that the parameters invoked are derivatives of the model, as would be inferred from the titles of the previous sections. For example, there is the overall heat-transfer coefficient,  $h$ , that appears in the nonisothermal, one-dimensional axial dispersion model, which is not to be confused with the wall heat transfer coefficient,  $\alpha_w$ , that belongs to the radial dispersion model. Similarly, would the bed thermal conductivity be the same in an axial dispersion model as in a radial dispersion model? What is the difference between a mass Peclet number and a thermal Peclet number? and so on. In fact, let us take a moment

<sup>15</sup> However, the Ergun equation is used as the basis for defining minimum fluidization velocity in fluid beds, as will be seen in Chapter 8. "Let's do something, even if it's wrong."—Anonymous

to survey what we have done in a rather general way. This “big picture” could possibly be written as

### Mass balance (fluid)

$$-\nabla \cdot (-D\nabla C) - \nabla \cdot [f(r)C] - \Psi(C) + [-r(C)] = 0 \quad (7-162)$$

Boundary conditions would specify something about the inlet concentration  $[C(z=0) = C_0]$ , the radial behavior of concentration  $[(\partial C/\partial r) = 0 \text{ at the tube wall}]$ , and the exit concentration  $[(\partial C/\partial z) = 0 \text{ at } L]$ .

### Thermal balance

$$-\nabla \cdot (-\lambda\nabla T) - \nabla \cdot [f(r)\rho C_p T] + \xi(T) + (-\Delta H)[-r(C)] = 0 \quad (7-163)$$

with boundary conditions, except at the tube wall, generally of the same form as for the mass balance.

These equations are written for the steady-state reactor, with  $f(r)$  the velocity as a function of radius,  $\Psi(C)$  mass transfer from fluid to solid phase,  $[-r(C)]$  reaction rate, and  $\xi(T)$  heat transfer to surroundings. Note that either  $\Psi(C)$  or  $[-r(C)]$  can appear in mass balance, but not both. Looking back, we can see that many of the concerns of this chapter have been with parameters or functions such as  $D_a$ ,  $D_r$ ,  $\lambda$ ,  $f(r)$ ,  $\Psi(C)$ , and  $\xi(T)$ . Now the overall balances above implicitly assume that the fluid- and solid-phase temperatures are the same. It is, of course, possible to write balances for the individual phases, fluid and solid. Not all of these will be independent equations, normally, but the procedure is desirable in many cases, as will be seen in Chapters 8 and 9. One may write the heat balance, for example, as

### Solid Phase

$$-\nabla \cdot (-\lambda_S \nabla T_S) - \mu(T_S, T) + (-\Delta H)[-r(C, T_S)] = 0 \quad (7-164)$$

### Fluid Phase

$$-\nabla \cdot (-K_f \nabla T) - \nabla \cdot [f(r)C] + \mu(T_S, T) = 0 \quad (7-165)$$

where  $\lambda_S$  is the solids effective thermal conductivity,  $K_f$  fluid effective thermal conductivity, and  $\mu(T_S, T)$  is the heat transfer from solid to fluid. The effective thermal conductivities will differ from that of equation (7-163), but by now we should be able to handle this distinction. The intraparticle effectiveness is also not included explicitly but can easily be done so by incorporation of the appropriate effectiveness factor with  $[-r(C, T_S)]$ ; similarly for catalyst deactivation influences as shown in Chapters 5 and 6.

So, in summary, what is the menu of parameters that must be known or evaluated before one may commence a design? Try this list.

1. Dispersion coefficients in the fluid phase.
2. Effective thermal conductivities, either of the bed as a whole or of individual fluid and solid phases.
3. Velocity distribution.

4. Bed porosity.
5. Mass-transfer coefficient between fluid and solid phases.
6. Heat-transfer coefficient between fluid and solid phases.
7. Heat-transfer coefficient between reactor and surroundings (if there is a flat temperature profile or if a radial average temperature is used).
8. Heat-transfer coefficient at the wall (if there is a radial temperature gradient).
9. Heat of reaction.
10. Densities and specific heats.
11. Form of rate equation, rate constants, and activation energies.
12. Pressure variation within the bed.
13. Effective thermal conductivity and effective diffusivity of the solid (catalyst) phase.
14. Particle size.

Horatio would ask if we have forgotten anything. Whether so or not, the point is that this is a formidable list, to say the least, but one must remember that almost every case of reactor design is going to be an individual, since each reaction has its own personality. Over-generalization can be unrewarding in simple cases; oversimplification dangerous in complex ones. In spite of all the work that has been done over the years, one cannot avoid being struck by how large our uncertainty concerning many of these reactor design parameters is, and yet at the same time see that many of the references are pretty old. Even in 1962 Beek observed that "... in view of the large experimental effort which has gone into this field, it does not seem to be an inviting one to enter, but serious questions remain that are worthy of attention..."

Finally, let us review thoughts concerning model building and parameterization. Some of the points below are perhaps self-evident, but we include them anyway.

1. Elimination of the heat balance is valid if the heat of reaction is very small, or if the extent of conversion is low.
2. If the heat-transfer coefficient between solid and a fluid is large, then the temperatures of fluid and solids can be considered equal, even if the overall process is nonisothermal.
3. For conditions in which the axial Peclet number approaches 2 and the radial Peclet number approaches 10, it is reasonable to assume plug flow with a velocity based on the average mass-flow velocity across the reactor cross section.
4. Theory exists for determination of overall bed thermal conductivity, or for splitting it into separate fluid and solids contributions, as discussed above. Radiative contributions to effective thermal conductivity are generally negligible below temperatures of  $\sim 300^\circ\text{C}$ .
5. Except for very shallow beds the axial dispersion of mass is normally small and the effort required to account for it is large.
6. Thermal axial dispersion must be treated with care. Even if axial dispersion of mass is negligible, the same may not be true for heat transport. The "dispersion" coefficient that appears in the thermal Peclet number is very different from the dispersion coefficient of the mass Peclet number. The combination of a plug-flow model for the mass balance and a dispersion

model for the energy balance is useful in many cases [see for example C.E. Megiris and J.B. Butt, *Ind. Eng. Chem. Research*, 29, 1065, 1073 (1990)].

7. The location of interphase and intraphase gradients depends on the relative magnitudes of the pertinent transport parameters. Examination of typical heat-transfer coefficients and catalyst effective thermal conductivities versus corresponding mass-transfer coefficients and catalyst effective diffusivities leads to the conclusion that when catalytic effectiveness is a factor in design the major thermal gradients reside in the external boundary layer (film) and the major concentration gradients within the particle. Effective diffusivities can vary widely according to the details of catalyst pore structure, while effective thermal conductivities have been found to vary only to a small extent even for widely differing materials. Do not forget the usefulness of criteria such as that of Weisz and Prater, based on observables, in preliminary evaluation work.
8. Catalyst particle size is a very important factor in possible pressure variation. While catalyst effectiveness normally improved upon the use of smaller particles, it is often at the expense of higher pressure drops along the reactor length, so a design compromise is sometimes necessary.

As in previous lists, it seems that this one can also go on and on. One has to stop somewhere, however, in the spirit that each case is its own self and it has to be the responsibility of the analyst or designer at some point to fill in the blanks.

It also seems reasonable to end this discussion of reactor modeling with an illustration showing some of the nuts and bolts (and warts) associated with setting up these models for numerical solution. Some software programs are available, but there is nothing like a bit of practical experience to gain an understanding of what may be involved. A large variety of approaches are possible, such as the tridiagonalization method discussed previously, but since our concerns are primarily with reactor design and not numerical analysis, only a couple of approaches are illustrated below.

### Illustration 7.11

Devise a scheme for the numerical solution of the nonisothermal radial dispersion model as set forth below

$$u \frac{\partial C}{\partial z} - D_r \left( \frac{\partial^2 C}{\partial r^2} + \frac{1}{r} \frac{\partial C}{\partial r} \right) = \bar{R} \quad (\text{i})$$

$$u \frac{\partial T}{\partial z} - \lambda_r \left( \frac{\partial^2 T}{\partial r^2} + \frac{1}{r} \frac{\partial T}{\partial r} \right) = \frac{(-\Delta H)}{\rho C_p} \bar{R} \quad (\text{ii})$$

$$z = 0; \quad T(0, r) = T_0(r); \quad C(0, r) = C_0(r) \quad (\text{iii}) \quad (\text{iv})$$

$$r = 0; \quad \frac{\partial T}{\partial r} = \frac{\partial C}{\partial r} = 0 \quad (\text{v})$$

$$r = R_0; \quad \frac{\partial C}{\partial r} = 0; \quad \alpha_w (T - T_w) = -\rho C_p \lambda_r \left( \frac{\partial T}{\partial r} \right) \quad (\text{vi})$$

We will assume that an analytical expression for  $\eta$ , such as that of Liu, is available, thus the flux terms at the interface between the catalyst (solid) phase and the reactor (fluid) phase may be written as

$$\bar{R} = \eta(-r) \quad (\text{vii})$$

so

$$\frac{D_{eff}}{\Lambda} \left( \frac{\partial C}{\partial l} \right)_{l=\Lambda} = \eta(-r) \quad (\text{viii})$$

and

$$\frac{h}{\Lambda} (T_S - T) = (-\Delta H)\eta(-r) \quad (\text{ix})$$

### Solution

Let us first determine the overall strategic approach to the problem. Since only the first derivatives of concentration and temperature with respect to axial position are involved, we can think of this as a kind of initial value problem with respect to  $z$ , so that the problem can proceed step-by-step down the bed. There, for each axial increment, the radial part of the problem is solved before proceeding to the next axial point. We can picture a grid as below, and set the sequence of calculations as follows.

1. Start at  $z = 0$ , where we know the values of  $T$  and  $C$  from the inlet boundary conditions as  $f(r)$ .
2. We then calculate  $\bar{R}$  from (vii) and  $T_S$  from (ix). This presumes that a kinetic correlation,  $(-r)$ , is available in terms of  $T$  and  $C$ . In fact,  $(-r)$  is a function of  $T_S$ , not  $T$ , so if the two differ an iterative solution (starting with  $T_S = T$ ) will be necessary.
3. If iteration in step 2 is necessary, one suggestion is to start with  $T_S = T$ , solve (vii) for  $\bar{R}$ , then use this value of  $\bar{R}$  in (ix) to solve for an updated value of  $T_S$ . Use this for an updated value of  $\bar{R}$  and continue the cycle via (vii) and (ix) until a converged solution for  $T_S$  is obtained.
4. When steps 1 to 3 are completed, we then have  $C(0, r)$ ,  $T(0, r)$  and  $T_S(0, r)$ , which are all that are needed to calculate other quantities such as wall heat transfer, catalytic effectiveness, etc.
5. Now we have to move down one grid step in the  $z$  direction, and in order to do this we must use the finite difference versions of conservation equations (i) and (ii). There are two ways to do this, using either the so-called "explicit" or "implicit" approximations. We will use the explicit method for illustration here.
6. For explicit solution we replace the axial derivatives with a forward-difference approximation, and the radial derivatives with central differences. Consider Figure 7.37, where the closed circles represent the grid points with known values of everything that will be used to determine the new point, shown as the open circle. The numerical setup is as follows

Normalize dimensions such that  $z$  is divided into  $(1/p)$  increments, and  $r$  into  $(1/m)$ . Then  $J$  at tube wall is  $(1/M)$ , and the finite-difference approximation is for values of the index  $j$  for 1 to  $J - 1$ . Then, for any

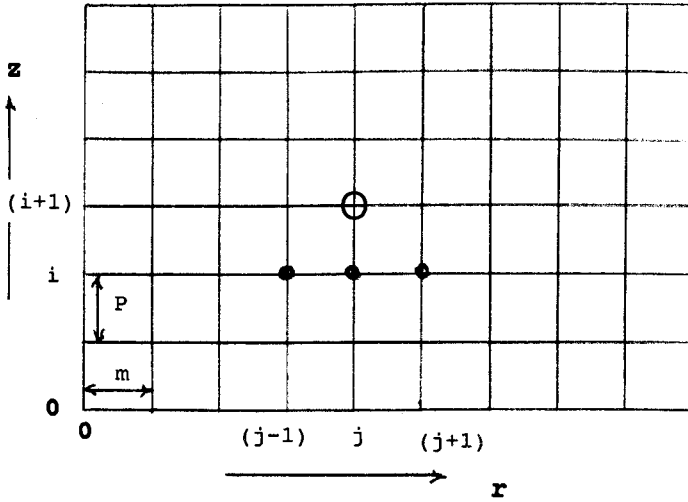


**Figure 7.37** Grid system for explicit method of solution of the nonisothermal radial dispersion model.

independent variable, we can write the variation with distance,  $z$ , as

$$\frac{\partial w}{\partial z} = \left( \frac{1}{p} \right) [w(i+1, j) - w(i, j)] \quad (\text{x})$$

$$\left( \frac{1}{r} \right) \frac{\partial w}{\partial r} = \left( \frac{1}{2jm^2} \right) [w(i, j+1) - w(i, j-1)] \quad (\text{xi})$$

$$\frac{\partial^2 w}{\partial r^2} = \left( \frac{1}{m^2} \right) [w(i, j+1) - 2w(i, j) + w(i, j-1)] \quad (\text{xii})$$

7. Upon substitution of these general forms into equations (i) and (ii), one finds that it is then possible to solve for  $w(i+1, j)$  in terms of  $(i, j)$  values. Then increment by one and repeat.

The method of solution proposed uses rate evaluations at  $(i, j)$  to determine new profiles at  $(i+1, j)$ . For a fine  $z$  grid this will present no problem since only small changes in the dependent variables with  $\Delta z$  are involved. However, problems with the stability of the solution may arise if the grid is too coarse. It has been shown that this explicit method is stable so long as

$$\left( \frac{1}{m^2} \right) = \left( \frac{1}{2\alpha} \right) \quad (\text{xiii})$$

where

$$\alpha = \frac{LD_r}{R_0^2 u} \text{ (mass);} \quad \alpha = \frac{L\lambda_r}{R_0^2 u} \text{ (heat)}$$

8. The procedures 1 to 7 correspond to any  $j = 1$  to  $j = J - 1$ . At  $j = 0$  and  $j = J$ , the boundary conditions must be used to obtain  $T$  and  $C$  at the wall and at the center. In order to see clearly how this is done, let us rewrite the



conservation equations in general form as

$$\frac{\partial w}{\partial z} + A \left( \frac{\partial^2 w}{\partial r^2} + \frac{1}{r} \frac{\partial w}{\partial r} \right) = B\bar{R} \quad (\text{xiv})$$

where  $w$  is either  $(C/C_0)$  or  $(T/T_0)$ , and  $A$  and  $B$  are constants. For  $w(i+1, 0)$  use a Taylor series expansion about  $r = 0$

$$w(i+1, 1) - w(i+1, 0) + \left( \frac{\partial w}{\partial r} \right)_{i+1,0} (m) + \left( \frac{\partial^2 w}{\partial r^2} \right)_{i+1,0} (m^2/2!) + \dots$$

The first derivative at this point now disappears because of the symmetry conditions of equation (v), so we have

$$\left( \frac{\partial^2 w}{\partial r^2} \right)_{i+1,0} = \left( \frac{2}{m^2} \right) [w(i+1, 1) - w(i+1, 0)] \quad (\text{xv})$$

We can substitute this for the second derivative in equation (xiv). However, we still have troubles with the  $(1/r)(\partial w/\partial r)$  term, which is intermediate at  $r = 0$ . If we use L'Hopital's rule, this becomes

$$\left( \frac{1}{r} \right) \left( \frac{\partial w}{\partial r} \right)_{r=0} \rightarrow \left( \frac{\partial^2 w}{\partial r^2} \right)_{i=0}$$

and then

$$\frac{w(i+1, 0) - w(i, 0)}{p} + \frac{4A}{m^2} [w(i+1, 1) - w(i+1, 0)] = B\bar{R}(i, 0) \quad (\text{xvi})$$

which can be solved directly for  $w(i+1, 0)$ . A similar procedure can be employed at  $j = J$  for  $w(i+1, J)$ .

The particular method employed here was treated in detail by Hlavacek and Votruba [V. Hlavacek and J. Votruba in *Chemical Reactor Theory*, (L. Lapidus and N.R. Amundson, eds.), Ch. 6, McGraw-Hill Book Co., New York, NY, (1977)]. An alternative explicit procedure was also proposed by Liu [S.L. Liu, *Amer. Inst. Chem. Eng. Jl.*, 16, 501 (1970)].

Various claims for computational efficiency have been made for different approaches. All, however, require a large number of repetitive numerical calculations, so computer speed rather than the specific algorithm employed seems more important. By now, though, all these approaches are within the capabilities of modern PC systems.



HORATIO SAYS

Remember that the algorithm given above includes the assumption that an analytical expression for  $\eta(C, T)$  is easily available. If this is not so, matters would be considerably more complex. How would the modeling and computational procedure be altered in this event? As usual, I have the last word.

## Exercises

## Section 7.1.1

1. Compare the shapes of the concentration profiles within a porous catalyst (slab geometry) for values of the Thiele modulus of 0.1, 0.5, 1 and 3 for a first-order irreversible reaction. What are the ratios of the corresponding effectiveness factors?
2. Write out the analog of equation (7-4) in spherical coordinates, with appropriate boundary conditions, and derive the result given in equation (7-10).
3. Kehoe and Butt [J.P. Kehoe and J.B. Butt, *Amer. Inst. Chem. Eng. Jl.*, 18, 347 (1972)] studied the kinetics of benzene hydrogenation on a supported, partially reduced Ni/kieselguhr catalyst. In the presence of a large excess of hydrogen (90 mol%) the reaction is pseudo-first-order at temperatures below 200 °C with the rate given by

$$(-r) = (P_H^\circ k_1^\circ K^\circ) \exp \left[ \frac{-Q - E}{RT} \right] P_B$$

where

$P_H^\circ$  = hydrogen partial pressure, torr

$k_1^\circ$  = 4.22 mol/g cat.-s-torr

$K^\circ$  =  $4.22 \times 10^{-11}$  torr<sup>-1</sup>

$-Q - E$  = 2.7 kcal/mol

For the case of  $P_H^\circ = 685$  torr,  $P_B = 75$  torr, and  $T = 150$  °C, estimate the effectiveness factor for this reaction as carried out using spherical catalyst particles of density 1.88 g/cm<sup>3</sup>,  $D_{eff} = 0.052$  cm<sup>2</sup>/s, and  $R_p = 0.3$  cm.

4. Equation (vii) of Illustration 7.1 defined a generalized modulus as

$$\phi = \left( \frac{\bar{V}}{S} \right) \left[ \frac{(-r)_w}{\sqrt{2}} \right] = \left[ \int_{C_{A_{e,0}}}^{C_{A_0}} D_{eff}(C_A)(-r) dC_A \right]^{1/2}$$

Show that this reduces to the form of equation (7-5) for a first-order reaction with constant  $D_{eff}$ .

5. A reaction carried out in the laboratory employed spherical catalyst pellets of approximate total volume = 1.5 cm<sup>3</sup>. The observed rate was  $5 \times 10^{-9}$  mol/cm<sup>3</sup> cat-s. It is known from other data that the intrinsic rate constant (first order) is  $2.75 \times 10^{-7}$  s<sup>-1</sup>. What would be the dimension of a spherical particle that would yield the same observed rate?  $D_{eff} = 0.02$  cm<sup>2</sup>/s.
6. Suppose that you have made activation energy measurements on a reaction-catalyst system that you suspect to be severely diffusion-limited, and obtained a value of  $E_a = 10.5$  kcal/mol. What would be the difference in the rate constants projected from 100 °C to 125 °C for the diffusion-limited and the diffusion-free reaction?

## Section 7.1.3

7. Using whatever information you may find appropriate in the sources below, estimate the order of magnitude of the maximum temperature increase that might be encountered within a 1/4-inch cylindrical platinum on alumina pellet employed in the catalysis of benzene hydrogenation at 150 °C, 10 mol% benzene and 10 atm. total pressure (assume reaction is first-order in benzene under these conditions) [R.A. Sehr, *Chem. Eng. Sci.*, 9, 145 (1958); C.D. Prater, *Chem. Eng. Sci.*, 8, 284 (1958); P.B. Weisz and J.S. Hicks, *Chem. Eng. Sci.*, 17, 265 (1962)).
8. In Figure 7.38 are some experimentally measured temperature profiles within a catalyst pellet used for benzene hydrogenation. Reaction

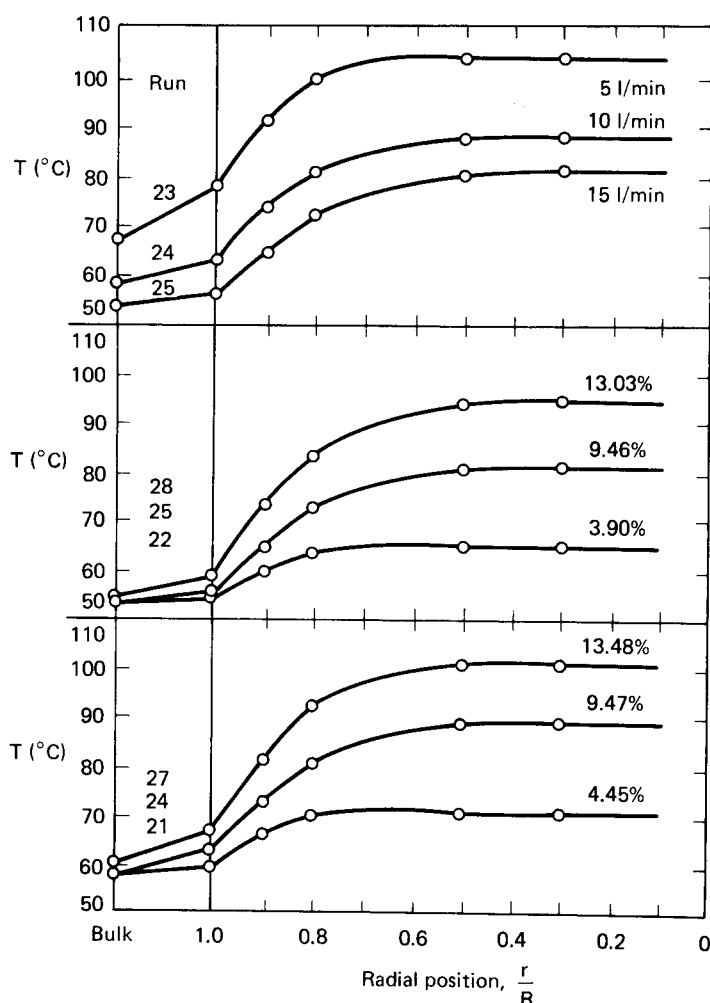


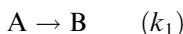
**Figure 7.38** Experimental intraparticle temperature profiles for benzene hydrogenation on Ni/kieselguhr. [After J.P. Kehoe and J.B. Butt, *Amer. Inst. Chem. Eng. Jl.*, 18, 347, with permission of the American Institute of Chemical Engineers, (1972).]

conditions were 52 °C bulk gas-phase temperature and 1 atm total pressure. The runs shown at the top of the figure were carried out with a benzene concentration of 10 mol%. The runs on the lower portion of the figure were carried out at the benzene concentration indicated and a flow of 15 l/min. For  $D_{eff} = 0.052 \text{ cm}^2/\text{s}$ , estimate the thermal conductivity of the catalyst from this data. Compare these values for internal consistency and for variations in reaction conditions. How do the results compare with the values tabulated in Table 7.6?

9. (a) Problem 8 may have illustrated the fact that some of the parameters involved in the analysis of diffusion and reaction in nonisothermal systems are subject to considerable uncertainty. For a reaction of  $\phi_S = 5.0$ ,  $\gamma = 20$ , and  $\beta = 0.3$ , what would be the changes in effectiveness if the thermal conductivity of the catalyst were subject to an uncertainty of  $\pm 20\%$ ?
- (b) Define the region of uncertainty in effectiveness if both  $D_{eff}$  and  $k_{eff}$  are subject to  $\pm 20\%$  uncertainty.

#### Section 7.1.4

10. Derive the relationship for  $(\Delta_{diff}/\Delta)$  for the reactions



where order corresponds to stoichiometry and B is the desired product. What is this value for  $C_A^0 = 3.5 \times 10^{-2}$  mols/liter and  $S_i = 4$ ? Does the existence of strong diffusional effects increase or decrease selectivity in this case?

11. Following the procedure suggested in the text, derive equation (7-41).
12. In the analysis and discussion of the selectivity as a function of conversion in the Type III reaction scheme, attention was confined to values of  $S_i > 1$ . Would the same conclusions hold for  $S_i < 1$ ? Verify your answer by demonstrating the nature of  $f_B$  versus  $f_A$  for  $S_i = 0.2$ .
13. Contrast the temperature dependence of  $f_B$  in a Type III reaction with  $E_2 > E_1$ , to that for  $E_1 > E_2$ .

#### Section 7.1.5

14. Mercer and Aris detailed some ranges of  $N_{Bi,m}$  to be expected for ranges of  $N_{Re}$  and likely to be encountered in practice. Compare the effect of interphase mass transfer on the effectiveness of a spherical catalyst particle with the intraparticle value for  $2 \leq N_{Bi,m} \leq 50$ . Under what conditions would you deem this to be a significant effect in the sense of the criteria set forth in Table 7.4?
15. How does the range obtained in problem 14 compare with a similar magnitude of effect in a Type II selectivity  $(\Delta_{diff})$  for  $S_i = 10$ ?
16. Consider the isothermal effectiveness expression for a spherical catalyst particle. For finite values of  $N_{Bi,m}$ , what does this imply as to the apparent activation energy of a given reaction for very large values of  $\phi_S$ ?

17. Price [T.H. Price, M.S. Thesis, Northwestern University, (1975)] reports values of  $N_{Bi,m} = 10$  and  $N_{Bi,h} = 0.81$  for the hydrogenation of benzene in a fixed bed of 1.1 mm diameter nickel/kieselguhr catalyst particles. Experimental conditions were  $N_{Re} = 1.85$ ,  $T = 150^\circ\text{C}$ , and a benzene concentration of  $6.4 \times 10^{-4} \text{ kg mol/m}^3$ . Transport and kinetic parameters were  $D_{eff} = 0.034 \times 10^{-4} \text{ m}^2/\text{s}$ ,  $k_{eff} = 3.52 \times 10^{-4} \text{ kcal/m-s-K}$ , and  $k = 3.28 \times 10^2 \text{ s}^{-1}$ . Determine the catalytic effectiveness factor under these conditions.

### Section 7.1.6

18. Consider the following data on ethylene hydrogenation in a batch system.

$T = 100^\circ\text{C}$       Initial  $P(\text{C}_2\text{H}_4) = 350 \text{ torr}$

Initial  $P(\text{H}_2) = 612 \text{ torr}$

Wt catalyst = 0.43 g

Vol. catalyst =  $0.21 \text{ cm}^3$

The gas phase reaction mixture is recirculated through the catalyst bed, so that overall mixing is similar to that of a batch reactor.

Time (min)	g mols ( $\text{C}_2\text{H}_6$ in product)
0	0.00008
1	0.0008
5	0.00289
10	0.00516

The catalyst particles were  $0.3 \times 0.3\text{-cm}$  cylinders, 10% Ni on alumina. Surface area was  $30 \text{ m}^2/\text{g}$ , and the diffusivity of hydrogen within the catalyst at  $25^\circ\text{C}$  was  $0.07 \text{ cm}^2/\text{s}$ . Is there evidence that diffusion was important? Assume Knudsen diffusion in the catalyst pore structure.

19. The rate of addition of deuterium to 2-butyne at  $25^\circ\text{C}$  over a 0.03% Pd/ $\text{Al}_2\text{O}_3$  catalyst was reported to be  $0.11 \text{ g mol/h-cm}^3$  (catalyst). Experimental conditions were: feed,  $\text{D}_2$  saturated with 2-butyne at  $25^\circ\text{C}$ ; catalyst dimension, 40 mesh;  $D_{eff} \approx 0.15$  of the bulk diffusivity of 2-butyne in hydrogen at  $25^\circ\text{C}$ . Was intraparticle diffusion important in this experiment? (*Note:* Persevere in obtaining all the exact numbers you need to do this calculation. They come from various sources, and it takes some time. After all, this is real life).
20. What particle dimension would be required in the case of problem 17 to eliminate the net effects of inter- and intraphase gradients?

### Section 7.1.7

21. The hydrogenation of cyclopropane is to be carried out on a Pt/ $\text{SiO}_2$  catalyst at  $0^\circ\text{C}$ . This is a prototype study for control of some higher molecular weight atmospheric pollutants in which the cyclopropane ring is thought to control both reactivity and transport properties. The porosity of the proposed catalyst is 0.45, its bulk density is  $1.2 \text{ g/cm}^3$ , and

specific surface area (BET) is  $265 \text{ m}^2/\text{g}$ . Estimate a value for  $D_{eff}$  in this catalyst under the conditions of the experiment. Hydrogen is expected to be present in about tenfold excess.

22. Using equivalent values of 3 for  $\tau$  and  $\tau'$ , and 0.5 for  $\epsilon$  and  $\epsilon'$ , determine the range of pore radius for which transition-region diffusion will exist in the following systems at room temperature and 1 atm.
  - a)  $\text{H}_2/\text{CO}_2$
  - b)  $\text{H}_2/1\text{-butene}$
  - c)  $\text{O}_2/\text{propylene}$

The following criteria may be used to define the transition region.

- a) Lower limit:  $D_{eff} = 0.9D_{KA}$
  - b) Upper limit:  $D_{eff} = 0.9D_{AB}$
23. Data for porosity and tortuosity of a  $\text{Pd}/\text{Al}_2\text{O}_3$  catalyst are presented in Table 7.4. Using these data and the value of effective thermal conductivity of boehmite given in Table 7.5, estimate a value of the parameter  $\beta$  for the hydrogenation of ethylene at  $50^\circ\text{C}$ , 1 atm total pressure, and an ethylene/hydrogen (molar) ratio of 1:2. How does this compare with the values given in Table 7.1 for this reaction?
  24. The rate of hydrogenation of propylene on a test catalyst has been measured as  $0.2 \text{ mol}/\text{cm}^3 \text{ cat.}\cdot\text{h}$  in an experiment conducted in a fixed bed at a particle Reynolds number of 1000 and an isothermal fluid temperature of  $120^\circ\text{C}$ . What was the temperature of the catalyst?

### Section 7.1.8

25. Demonstrate for typical values of the parameters  $P_1$ ,  $P_2$ , and  $P_3$ , in equation (7-94) the behavior to be expected for  $(C_{As}/C_A)_r$ . The value of  $D_{eff}$  can be taken to  $0.05 \text{ cm}^2/\text{s}$ , the intrinsic rate constant is 0.1 in consistent units,  $\nu$  is unity, and the average particle radius is 3-mm.
26. Show Horatio how to get from equations (7-92) and (7-93) to equation (7-94).

### Section 7.1.9

27. A certain industrial reactor is well modeled by a sequence of  $N$  CSTRs with equivalent holding times,  $\bar{t}$ . The catalyst in this reactor is subject to deactivation, so that the rate constant of the first-order irreversible reaction being carried out decreases with time according to

$$k = k_i - 0.001(t)$$

where  $k_i$  = initial value of the rate constant  $= k_0 \exp(-E/RT_0)$ ,  $k$  = rate constant at time  $t = k_0 \exp(-E/RT)$ , with  $t$  the time in days and  $T_0$  the initial temperature. It is necessary to maintain a constant conversion in this reactor even though the catalyst is decaying. This is accomplished by increasing the temperature according to a time schedule such that the net activity remains the same. Derive an equation for the necessary time schedule

$$\text{temperature} = f(\text{time-on-stream})$$

28. In many cases the effect of poisoning on catalytic surfaces can be represented as a linear function of the fraction of total surface poisoned ("non-selective" poisoning).

$$k_{actual} = ks = k(1 - \alpha)$$

where  $\alpha$  is the fraction of surface poisoned. For a strongly diffusion-limited first-order irreversible reaction, what is the apparent rate constant when poisoning occurs, assuming that the above relation holds? Would this deactivation model have any effect on the apparent order or activation energy of the reaction?

### Section 7.2.1.

29. From the solution of Illustration 7.8, we found that  $(a_0L) \approx 0.3$  corresponded to 95% unreacted solute A entering the bulk liquid phase, while  $(a_0L) \approx 2.6$  corresponded to 5%. Now follow up this analysis with the question posed by Horatio with  $D = 10^{-5} \text{ cm}^2/\text{s}$  and  $k = 0.1 \text{ s}^{-1}$ . What order of magnitude does this imply for the corresponding film thickness  $L$ ?
30. Consider the absorption of  $\text{CO}_2$  into an aqueous NaOH solution. The rate-limiting step of the reaction is



Using the analysis of van Krevelen and Hoftijzer, determine the rate of absorption of  $\text{CO}_2$  into a NaOH solution under the following conditions.

- Bulk partial pressure of  $\text{CO}_2 = 1.4 \times 10^{-2} \text{ atm}$
- Bulk concentration of NaOH = 0.8 M
- Henry's law constant ( $20^\circ\text{C}$ ) =  $35.8 \text{ m}^3\text{-atm/kmol}$
- $k_M = 7.75 \times 10^{-5} \text{ m/s}$
- $\text{CO}_2$  diffusivity in  $\text{H}_2\text{O}$  at  $20^\circ\text{C} = 1.2 \times 10^{-5} \text{ cm}^2/\text{s}$
- Rate constant at  $20^\circ\text{C} = 7.75 \times 10^6 \text{ cm}^3/\text{gmol-s}$
- Overall stoichiometric coefficient = 2

### Section 7.2.2

31. Compare the film theory result obtained in Problem 30 with that for the penetration theory.

### Section 7.3.1

32. Predict the effective thermal conductivity of a fixed-bed reactor to be used for  $\text{SO}_2$  oxidation with the following conditions: reactor is a 2.06-in i.d. tube through which a mixture of air (93.5 mol%) and  $\text{SO}_2$  (6.5 mol%) flow at a superficial velocity of  $350 \text{ lb/ft}^2\text{-h}$ . The catalyst pellets, egg-shell Pt/ $\text{Al}_2\text{O}_3$ , (0.2 wt%), are in the form of 1/8-in spheres. Additional data:
- Total pressure = 1.04 atm
  - Solid thermal conductivity =  $0.5 \text{ Btu/h-ft-}^\circ\text{F}$
  - Emissivity = 0.5
  - Bed porosity = 0.4
  - Average bed temperature =  $450^\circ\text{C}$

Compare the values predicted by the Argo-Smith analysis with those obtained from the Yagi-Kunii correlation. Also, determine the sensitivity of the Argo-Smith analysis to a typical  $\pm 15\%$  precision of the  $j$ -factor correlations. If you have to pick between the Argo-Smith and the Yagi-Kunii values, which would you choose, and why? (There is probably no “correct” answer to this last question).

### Section 7.3.2

33. The Crank-Nicholson technique is a widely applied method for solving partial differential equations such as those for the radial dispersion model. However, it is implicit in approach and thus a little balky sometimes. Use this approach to develop an algorithm for the solution of the equations of Illustration 7.11. You will see that, if the method is developed properly, it will result in equations leading to a tridiagonal matrix similar to those treated in Illustration 6.4.

### Notation

$A$	constant $= (1 + \beta\mu - \beta\mu f_S + \beta f_S)$
$A_v$	interfacial transport area/volume, $\text{length}^{-1}$
$a$	gas/liquid specific interfacial area; gas/solid, interfacial area/volume
$a, b$	correlation constants; see equations (7-82) and (7-83); activity scaling constants in equation (7-100)
$a, f, m, n, v, w$	nondimensional quantities; see after equation (ii), Illustration 7.10
$a_0$	liquid diffusion-reaction modulus $= (k/D)^{1/2}$
$a'_0$	constant $= (kC_B D)^{1/2}/k_M$ , Illustration 7.9
$C$	reactant concentration, mols/volume
$C_A$	concentration of A, mols/volume
$C_B$	concentration of B, mols/volume
$C_b$	bulk concentration, mols/volume
$C_c$	wt% coke on catalyst
$C_i$	interfacial concentration of reactant, mols/volume
$C_L, C_{L_0}$	concentration at position L, mols/volume; surface concentration of L, mols/volume
$C_0$	surface concentration of reactant; inlet concentration, mols/volume
$C_p$	heat capacity, kcal/mol-°C, K or kcal/volume-°C, K
$C_S$	surface concentration, mole/volume
$C_{A_0}$	equilibrium concentration of A, mols/volume
$C_{A_i}$	concentration of A at gas-liquid interface, mols/volume
$C_{A_0}$	bulk or surface concentration of A, mols/volume
$C_{A_s}, C_{A_{s,0}}$	concentration of A within porous matrix; see equation (7-84); initial concentration of A within porous matrix, mols/volume
$C_{A_w}$	centerline concentration of A, mols/volume
$C_{B_L}$	concentration of B in bulk liquid, mols/volume
$C_{S,0}$	initial concentration of solid matrix
$C_{A,s}$	concentration of A in the second zone of the porous matrix, mols/volume; see equation (7-91)
$C'_0$	reactant concentration at catalyst surface, mols/volume



- $D$  Diffusion coefficient in the liquid phase, length<sup>2</sup>/time  
 $D_A, D_B$  liquid-phase diffusion coefficients for A and B, cm<sup>2</sup>/s  
 $D_i$  intrinsic transport coefficient, cm<sup>2</sup>/s  
 $D_r$  radial dispersion coefficient, cm<sup>2</sup>/s  
 $D_{AB}$  bulk diffusion coefficient for AB, cm<sup>2</sup>/s  
 $D_{KA}$  Knudsen diffusion coefficient for A, cm<sup>2</sup>/s  
 $D_{eff}$  effective diffusivity, typically cm<sup>2</sup>/s  
 $D_{eff}^\circ$  preexponential factor for  $D_{eff}$ , cm<sup>2</sup>/s  
 $D_{eff,i}$  effective diffusivities for  $i$ , cm<sup>2</sup>/s  
 $(D_{eff})_0$  initial value of  $D_{eff}$ , cm<sup>2</sup>/s  
 $d_p$  particle diameter, length  
 $d_t$  tube diameter, length  
 $E_a$  apparent activation energy, kJ or kcal/mol  
 $E_0$  activation energy for diffusion, kJ or kcal/mol  
 $f$  nondimensional concentration,  $(C_A/C_{A0})$ ;  $(C_A/C_{A_i})$  in Illustration 7.4; surface emissivity, see equation (7-153)  
 $f_A$  total fraction A reacted  
 $f_B$  fraction initial A reacted to B  
 $f_S$  nondimensional concentration =  $(C_S/C_0)$   
 $f_S, f_b$  surface and bulk values of  $f$ , Illustration 7.10  
 $f(T_0, C_0)$  form of rate expression under gradientless conditions  
 $f'(C_0)$  derivative of rate expression with respect to  $T$   
 $f_1(N_{Re}), f_2(N_{Re})$   $j_D$  and  $j_H$  functions; see equations (7-80) and (7-81)  
 $G$  superficial mass velocity; mass flow rate, mass/time  
 $g_c$  gravitational constant  
 $H$  Henry's law constant, mols/volume-atm  
 $(-\Delta H)$  heat of reaction, kJ or kcal/mol  
 $(-\Delta H_A), (-\Delta H_B)$  heat of reaction for A or B, kcal/mol  
 $h$  heat-transfer coefficient; solid heat transfer coefficient, see equation (7-153); kcal/area-time-°C, K  
 $I_0, I_1$  modified Bessel functions of the first kind  
 $j_D, j_H$  mass- and heat-transfer factors; see equations (7-80) and (7-81)  
 $K$  equilibrium constant, adsorption equilibrium constant; fluid thermal conductivity, energy/time-length °C, K; see equation (7-147)  
 $K_g$  thermal conductivity of gas, energy/time-length °C, K  
 $K_s$  thermal conductivity of solid, energy/time-length °C, K; see equation (7-153)  
 $k$  rate constant, time<sup>-1</sup>; thermal conductivity, kcal/s-cm-°C  
 $k_c$  coke burning rate constant, time<sup>-1</sup>  
 $k_f, k_r$  forward and reverse rate constants, time<sup>-1</sup>  
 $k_G$  gas film mass-transfer coefficient, mols/area-ΔP-time  
 $k_M, k_m$  mass-transfer coefficient =  $(D/L)$ , cm/s; mass transfer coefficient, mols or mass/area-time-ΔC  
 $k_s$  rate constant at surface conditions, time<sup>-1</sup>  
 $k_{da}$  deactivation rate constant, time<sup>-1</sup>  
 $k_{eff}$  effective thermal conductivity, typically cal/s-cm-°C  
 $k_1, k_2$  rate constants in Type I, II, III schemes, time<sup>-1</sup>  
 $k^\circ$  pre-exponential factor, time<sup>-1</sup>  
 $k'$  modified rate constant, equation (iii), illustration 7.3

$k'_c$	coke burning rate constant at constant $C_c$ , $\text{time}^{-1}$
$k_m^*$	mass-transfer coefficient in the presence of rapid reaction, $\text{cm/s}$
$L$	liquid film thickness, length
$L', L''$	liquid film diffusion zones for A and B, length
$l$	length dimension, rectangular coordinates
$M$	parameter of equation (7-126); $\cosh(a_0 L)$ in Illustration 7.8
$M_A$	molecular weight of A
$M_m$	molecular weight of $m$
$m$	kinetic power-law exponent; constant = $(R_0/d_p)$
$m_A$	mass/molecule A
$m_1, m_2$	constants defined in equation (7-56)
$m'$	constant = $(R_0 u / 2 D_r)$
$N$	flux, mole/area-time
$N_A, N_B$	flux of A or B, mols/area-time
$N_{Bi,h}$	heat Biot number = $(h/k_{eff})R_p$
$N_{Bi,m}$	mass Biot number = $(k_m/D_{eff})(\bar{V}/S_A)$
$N_{Bi,w}$	wall Biot number = $(\alpha_w R_0 / \rho C_p \lambda_r)$
$D_{Da}$	Damkohler number = $(k/k_m)(\bar{V}/S_A)$
$N_{Nu}$	Nusselt number = $(\alpha_w d_p / K)$
$N_{Pr}$	Prandtl number = $(C_p \mu / k)$
$N_{Re}$	Reynolds number = $(d_p G / \mu)$
$N_{Sc}$	Schmidt number = $(\mu / \rho \mathcal{D})$
$N_{Sh}$	Sherwood number = $(k_m / A_V \mathcal{D})$
$N_{St}$	Stanton Number = $(\alpha_w / \rho u C_p)$
$N_{Pe,m}$	mass Peclet number = $(d_p u / \mathcal{D})$
$N_{Pe,ha}$	axial heat dispersion Peclet number = $(d_p u / \lambda_a)$
$N_{Pe,hr}$	radial heat dispersion Peclet number = $(d_p u / \lambda_r)$
$n$	reaction order; power constant for $k_m$ and $h$ as a function of $(v)^n$
$n_a$	apparent reaction order
$n'$	effective number of mixing stages
$P$	pressure, normally atm
$P_{Ag}, P_{Ai}$	partial pressures of A in bulk and at interface, atm
$P_1, P_2, P_3$	constants defined after equation (7-94)
$p$	ratio of active to inert ingredients
$p, q$	correlation exponents in equations (7-77) and 7-78
$Q$	heat flux, kJ or kcal/area-°C
$q$	concentration ratio = $(\nu C_{B_L} / C_{A_i})$ ; reaction order, Illustration 7.10
$R$	gas constant, normally kJ or kcal/mol-K; concentration ratio = $(C_{L_0} / C_{A_0})$ ; radius, length
$R_p$	particle radius, length
$R$	effective average radius, length
$r$	diffusivity ratio = $(D_B / D_A)$ ; radial position, length
$(-r)$	rate of reaction, mols/volume-time
$(-r_A), (-r_B)$	rate of reaction of A or B, mols/volume-time
$r_L$	rate of reaction of L, mole/volume-time
$(-r)_{net}$	net reaction rate, mols/volume-time
$(-r)_0$	observed rate of reaction, mols/volume-time
$(-r)_W$	reaction rate at $W$ , mols/volume-time

$(-r_c)$	rate of carbon burning, wt/volume-time
$(-r_s)$	rate of reaction of solid matrix
$(-r')$	nondimensional rate = $-r(\mathcal{L})/ -r(1)$
$S$	interfacial surface area, equation (vi), Illustration 7.10
$S_A$	external surface area
$S_i$	intrinsic selectivity = $(k_1/k_2)$
$S_i$	surface area of porous solid, area/wt
$s$	activity variable for deactivation
$T$	temperature, normally °C or °K
$T_0$	bulk or surface temperature; inlet temperature, °C
$T_s$	bulk temperature, °C
$T_s$	surface temperature, °C
$\Delta T$	temperature difference = $(T - T_0)$
$(\Delta T)_{\max}$	maximum $\Delta T$
$t$	time
$t_R$	time required for complete conversion
$t_{\text{regen}}$	time required for regeneration
$t_\lambda$	time required for interface to move from $R_p$ to $\lambda$
$u$	linear velocity based on empty cross section, length/time
$V$	volume of liquid mixture
$V_q$	void volume, volume/wt
$V_p$	product molar volume, volume/mol
$V_s$	solids molar volume, volume/mol
$V$	particle volume
$v$	flow velocity, length/time; reduced temperature, Illustration 7.10
$v_s, v_b$	surface and bulk values of $v$ , Illustration 7.10
$v_W$	reduced wall temperature, Illustration 7.10
$W$	slab half-thickness, length
$x$	distance factor = $1 - (\lambda/R)^3$
$Y_p$	point yield, Illustration 7.4
$y$	constant = $(1/\Lambda)$ , Illustration 7.10
$y_{O_2}$	mol fraction oxygen
$z$	length dimension

*Greek*

$\alpha$	parameter of equation (7-134); constant = $(V/A_V L)$ in Illustration 7.9; mass velocity of fluid flow in direction of heat transfer; flux ratio = $(1 + N_B/N_A)$
$\alpha_W$	local wall-heat transfer coefficient, energy/cm <sup>2</sup> -time-°C
$\beta$	heat of reaction parameter; parameter of equation (7-134)
$\beta, \gamma, \phi$	length ratios; see equation (7-155)
$\gamma$	activation energy parameter = $(E/RT_0)$
$\Delta$	selectivity factor under diffusion-limited conditions
$\delta$	constant = $\beta\gamma$
$\epsilon$	volume fraction voids; porosity for Knudsen diffusion; porosity of bed
$\epsilon_s$	porosity of solid particle; see equation (7-84)
$(\epsilon_s)_0$	initial porosity of solid particle
$\zeta$	nondimensional length variable = $(z/W)$ or $(r/R_p)$
$\eta$	effectiveness factor

$\eta_0$	overall effectiveness factor
$\eta_L$	liquid phase effectiveness factor
$\eta_G$	overall effectiveness factor
$\eta_{LG}$	two-phase effectiveness factor; see equation (7-114)
$\eta_1, \eta_2$	effectiveness factors for reaction steps 1, 2
$\theta$	dimensionless time; contact time in penetration theory
$\theta, \zeta, \tau$	nondimensional quantities; see after equation (ii), Illustration 7.10
$\Lambda$	characteristic dimension $= (V/S_A)$ ; particle dimension in Illustration 7.10
$\lambda$	diffusion/rate term $= \phi_s^0 \exp(-\gamma/2\tau)$ ; see equation (7-63); reaction interface location inside particle, length; enhancement factor for gas-liquid reaction
$\lambda_G$	effective bed thermal conductivity in axial direction, kcal/s-cm-°C
$\lambda_r$	radial effective bed thermal conductivity, kcal/s-cm-°C
$\lambda_r^\circ$	effective bed thermal conductivity in absence of flow, kcal/s-cm-°C
$\mu$	variable $= (1 - \xi)\phi_S$ ; see equation (7-30); constant $= (N_{Bi,m}/N_{Bi,h})$ ; fluid viscosity, cp
$\nu$	stoichiometric coefficient; see equation (7-89); stoichiometric ratio, mols B reacted/mol A; constant $= (\mu/\rho)$
$\rho_b$	bulk density, wt/volume
$\rho C_p$	volumetric gas-phase heat capacity, energy/volume-°C
$\sigma$	function defined by equation (7-130)
$\tau$	nondimensional temperature $= (T/T_0)$ ; function defined in equation (7-63); tortuosity
$\tau_S$	nondimensional surface temperature $= (T_S/T_0)$
$\tau'$	tortuosity for Knudsen diffusion
$\Phi_S$	experimental parameter; see equation (7-64)
$\phi$	Thiele modulus
$\phi_A, \phi_L$	Thiele modulus for A and L
$\phi_0$	Thiele modulus, equation (viii), Illustration 7.3
$\phi_p, \phi_m$	Thiele modulus for poisoning and main reactions
$\phi_s$	Thiele modulus at surface conditions; see equation (7-63)
$\phi_s^*$	modified Thiele modulus; see equation (7-33b)
$\Psi$	constant defined after equation (7-57)

*Note:* Additional notation is self-contained in Illustration 7.4, 7.6, 7.7, and 7.11.

# 8

---

## Multiphase Reactors

Music, to create harmony,  
must investigate discord

— *Plutarch*

The first part of this text was concerned with chemical reaction kinetics and reactor design-analysis procedures that showed the common features pertaining to homogeneous or pseudo-homogeneous systems. In fact, we got rather far along with the latter approach in the last chapter, extending to some rather advanced problems in reactor analysis. There comes a time<sup>1</sup>, though, when we have to acknowledge the existence of more than one phase, and we *really* can't get around it. Some of this we have even tried to cope with in Chapter 7 regarding catalytic effectiveness, for example.

In this chapter we shall look at the analysis of multiphase reactors, typically gas-liquid-solid, that are found in diverse applications throughout the reaction engineering world. The reaction/reactor models that we have presented, at least up to Chapter 7, had some pretense of generality. As we go forward, any hope of that is gone. Our abilities in design and scale-up are not yet developed to the point where we can develop a general correlation of, for example mass transfer, that can be applied to any three-phase reactor that comes along. Thus, we will see in this chapter the development and presentation of much material that is specific to well-defined subsystems, and our basic task will be to assemble a number of these in a rational way to define the overall. This is fun, but one will quite soon see what is meant by “conservative design”.

### 8.1 Fluidized-Bed Reactors

Fluidized-bed reactors are used in a number of applications ranging from catalytic cracking in the petroleum industry to oxidation reactions in the chemical industry. A number of advantages and disadvantages may be tabulated for this type of reactor, but we can shorten this somewhat by saying that most applications involve reactions in which catalyst decay is prominent and a continuous circuit is required for catalyst regeneration, or reactions where close control of operating conditions, particularly

---

<sup>1</sup>“... when the fat lady sings ...”—*Anonymous*

temperature, is required. We will see that the high level of mixing in most fluidized beds leads to behavior similar in some aspects to that of CSTRs. We will first describe qualitatively some simple fluid mechanics associated with fluidized beds, and then proceed to reactor applications. The treatment here is limited to some of the simpler models; much more detail is available in the work of Kunii and Levenspiel [D. Kunii and O. Levenspiel, *Fluidization Engineering*, 2 ed, Butterworth-Heinemann, Boston, MA, (1991)].

### 8.1.1 Simple Fluid Mechanics: Minimum Fluidization and Entrainment

Most discussions of fluidized beds begin with a discussion of some fluid mechanics, and we will follow suit. Figure 8.1 depicts what one might observe upon passing a gas upward through an initially fixed bed with increasing gas velocity. At lower velocities, in region (a), the bed of particles retains its fixed-bed configuration, and the pressure drop across the bed increases linearly with the flow velocity. At a particular point, mainly dependent upon the size and shape of the particles, there will be a slight expansion of the bed and some limited particle movement will be observed. This point is termed *incipient fluidization*, and the corresponding gas velocity is  $u_{mf}$ . Since the changes in bed configuration are still quite small at this point, it is difficult to observe visually, however, it is characteristic that above the point of incipient fluidization the pressure drop remains constant with increasing flow velocity. The configuration of the bed, though, changes considerably. Region (b) corresponds to a free bubbling behavior in which the fluidizing gas forms discrete bubbles

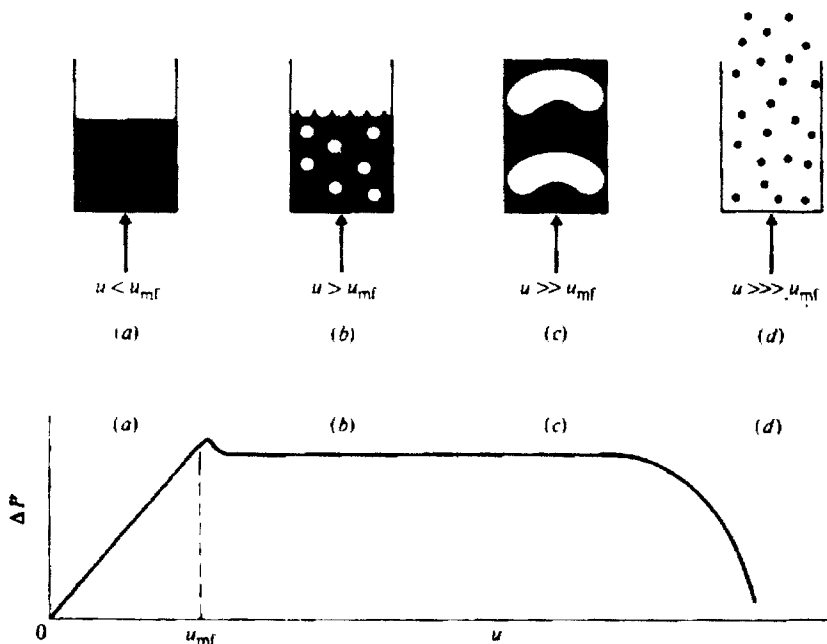


**Figure 8.1** Gas transport through a bed of particulate solids regions of operation. [After J.J. Carberry, *Chemical and Catalytic Reaction Engineering*, with permission of McGraw-Hill Book Co., New York, NY, (1976).]

that pass through the now fluidized bed without interacting with each other. Region (c) is that in which bubble agglomeration is sufficient that coalescing bubbles can grow to a size on the order of the containing vessel. Finally, region (d) corresponds to fluid velocities that are sufficiently large that individual particles are entrained in the gas phase and possibly transported out of the vessel. The two quantities that we would like to know from a simple, practical point of view are this entrainment velocity,  $u_t$ , which sets a limit on the operable region of fluidization at the high end of the velocity scale, and the incipient fluidization velocity,  $u_{mf}$ , which does the same thing at the lower end of the scale. We will also see that many of the correlations used in fluid-bed design are based on  $u_{mf}$ , making knowledge of that quantity essential.

For the determination of the entrainment velocity, assuming that there is no particle-particle interaction, we may use a force balance based on Stoke's law

$$(\rho_s - \rho)gV_p = 3\pi\mu d_p u_t \quad (8-1)$$

where  $d_p$  and  $V_p$  are the particle diameter and volume, respectively,  $\mu$  and  $\rho$  are gas-phase properties, and  $\rho_s$  is the density of the particles. Using spherical geometry as an example

$$V_p = \left(\frac{4}{3}\right)\pi\left(\frac{d_p^3}{2}\right) \quad (8-2)$$

and

$$u_t = \frac{(d_p)^2(\rho_s - \rho)g}{18\mu} \quad (8-3)$$

Practical operating conditions for fluidized beds must obviously be lower than this value, often about one-half of  $u_t$ . The entrainment velocity is strongly dependent upon particle diameter so that in a given operation if a range of  $d_p$  is involved and there is to be no elution of solid from the bed, then the size distribution must be taken into account.

Determination of the minimum fluidization velocity is a little more complicated, but still straightforward. The well-accepted correlation for pressure drop of a fluid flowing through a packed bed, from Ergun, we repeat here, but written in terms of the minimum fluidization velocity,

$$\frac{\Delta P}{L} = \frac{150(1 - \epsilon)^2}{d_p^2 \epsilon^3} \mu u_{mf} + \frac{1.75 \rho (u_{mf})^2 (1 - \epsilon)}{d_p \epsilon^3} \quad (8-4)$$

We have already stated in the previous chapter reservations about the applicability of this equation to pressure drop with small particles but it seems a visible basis for much work on fluid beds—thus, if it works, don't fix it.

The  $\Delta P$  is balanced by the gravitational force at the point of incipient fluidization,

$$(\rho_s - \rho)AL(1 - \epsilon)g = (\Delta P)A \quad (8-5)$$

where  $A$  is the cross-sectional area,  $\epsilon$  the bed void fraction,  $L$  the length of the bed, and  $\rho_s$  and  $\rho$  densities of the solid and fluid, respectively. The minimum

fluidization velocity is given implicitly by equating the pressure drops in equations (8-4) and (8-5):

$$(-\epsilon)(\rho_s - \rho)g = \frac{150(1 - \epsilon)^2}{d_p^2 \epsilon^3} \mu u_{mf} + \frac{1.75\rho(u_{mf})^2(1 - \epsilon)}{d_p \epsilon^3} \quad (8-6)$$

Again, if there is a distribution of particle sizes this must be taken into account and there will be no unique  $u_{mf}$  for the bed as a whole.

### 8.1.2 A Two-Phase Reactor Model

If we look at the picture of fluidization given for  $u > u_{mf}$  (case b of Figure 8.1), a two-phase model is suggested in which there is a dilute or bubble phase (consisting mostly of gas but perhaps some entrained particles as well) and a dense phase which is mostly particulate but with a porosity  $\epsilon$  somewhat greater than that of the fixed bed (i.e., gas “entrained” in the particulate phase, if one wishes to push the analogy with the dilute phase). We can further picture that such a condition of fluidization will produce an isothermal reaction due to the mixing and agitation of the dense phase produced by bubble motion. This, indeed, is the visualization of the two-phase model proposed by Davidson and Harrison [J.F. Davidson and D. Harrison, *Fluidized Solids*, Cambridge University Press, London, England (1963)].

The two phases of the Davidson-Harrison model are a *bubble phase* of the gas passing throughout the reactor (with no catalyst entrainment), and an *emulsion phase* containing all of the catalyst particles and some gas. The bubble phase is normally considered to pass through the reactor in plug flow, while the emulsion phase can be either well mixed or in plug flow itself. Since all of the catalyst is contained within the emulsion phase, that is where all of the reaction occurs. Communication between the bubble and emulsion phases occurs by cross-flow and diffusion across the interphase boundary. Finally, any increase in bed height upon fluidization is considered to be due to the volume of the bubbles in the bed. The emulsion phase moves at a velocity equal to the minimum fluidization velocity,  $u_{mf}$ , and the bubble phase at a kind of slip velocity,  $u_0 - u_{mf}$ , where  $u_0$  is an entering gas velocity.

This description gives a formidable laundry list of requirements that are embedded in the model, and in any given system some may not be valid. We do have to start somewhere, however, and the Davidson-Harrison list of specifications is as reasonable as any at this point. Figure 8.2 presents a schematic of what is envisioned in the two-phase model. Some of the requirements can be written immediately in mathematical form. For height, we have

$$\pi R^2 L = \pi R^2 L_0 + \pi R^2 LNV$$

or

$$L = \frac{L_0}{(1 - NV)} \quad (8-7)$$

where  $L$  and  $L_0$  are the heights of the fluid bed and the unexpanded bed, respectively,  $N$  is the number of bubbles per unit volume of bed,  $V$  the average volume per bubble, and  $R$  is the bed radius. For the mass transfer between the bubble and emulsion phases we can define a mass exchange coefficient as the sum of individual



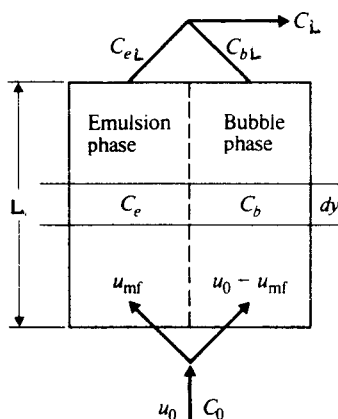


**Figure 8.2** Schematic of the two-phase model of a fluidized bed according to Davidson and Harrison. [After J.J. Carberry, *Chemical and Catalytic Reaction Engineering*, with permission of McGraw-Hill Book Company, New York, NY, (1976).]

coefficients relating to diffusional transport and cross-flow

$$Q = q + k_d S \quad (8-8)$$

where  $Q$  is an overall coefficient, volume/time,  $q$  the cross-flow coefficient,  $k_d$  the normal mass-transfer coefficient (but in volumetric units), and  $S$  an interphase area. Since there is no reaction in the bubble phase, then concentration changes of position are possible only via interphase transport and the mass balance in the reactor at any point is

$$(q + k_d S)(C_e - C_b) = u_b V \left( \frac{dC_b}{dy} \right) \quad (8-9)$$

where  $C_e$  and  $C_b$  are, the concentrations of reactant in the two phases and  $u_b = u_0 - u_{mf}$ .

To proceed further we must make an assumption concerning the nature of the flow in the emulsion phase. Taking this to be plug flow at the velocity  $u_{mf}$ , we may now set forth an overall balance for the two phases as

$$u_{mf} \left( \frac{dC_e}{dy} \right) + (u_0 - u_{mf}) \left( \frac{dC_b}{dy} \right) + k C_e (1 - NV) = 0 \quad (8-10)$$

where the rate constant  $k$  is for Academic Reaction #1. Alternatively, if it is assumed that the emulsion phase is well mixed, we obtain

$$NV u_b (C_0 - C_e) [1 - \exp(-QL/u_b V)] + u_0 (C_b - C_e) = \chi \quad (8-11)$$

with  $\chi = k L C_e (1 - NV)$ . The reactor model is expressed overall, then, as the combination of equations (8-9) and (8-10), or as (8-9) and (8-11). Proceeding with the

first pair, with the emulsion in plug flow, the equations (in terms of grouped coefficients) are

$$\left(\frac{dC_b}{dy}\right) + \left(\frac{\gamma}{L}\right)(C_b - C_e) = 0 \quad (8-12)$$

$$(1 - \beta)\left(\frac{dC_e}{dy}\right) + \beta\left(\frac{dC_b}{dy}\right) + \left(\frac{\alpha}{L}\right)C_e = 0 \quad (8-13)$$

where

$$\alpha = \frac{kL_0}{u_0}; \quad \beta = 1 - \frac{u_{mf}}{u_0}; \quad \gamma = \frac{QL}{u_b V}$$

The boundary conditions for equations (8-12) and (8-13) are

$$y = 0; \quad C_b = C_0; \quad \left(\frac{dC_b}{dy}\right) = 0 \quad (8-14)$$

These two equations can be combined to give the following expression with  $C_b$  as the dependent variable

$$L^2(1 - \beta)\left(\frac{d^2C_b}{dy^2}\right) + L(\gamma + \alpha)\left(\frac{dC_b}{dy}\right) + \alpha\gamma C_b = 0 \quad (8-15)$$

Two boundary conditions at the same point are normally to be avoided, however, the nature of what we look at here does not permit the exit derivative condition so useful in dispersion model analysis. As indicated in Figure 8.2, the overall exit concentration is determined by the combination of the expressions for  $C_{bL}$  and  $C_{eL}$ , as

$$u_0 C_L = (u_o - u_{mf})C_{bL} + u_{mf}C_{eL} \quad (8-16)$$

and, at any point, from equation (8-12)

$$C_e = C_b + \left(\frac{L}{\gamma}\right)\left(\frac{dC_b}{dy}\right) \quad (8-17)$$

The overall result for plug flow in both bubble and emulsion phases is

$$\left(\frac{C_L}{C_0}\right) = \frac{1}{(a_1 - a_2)} \left[ a_1 \left(1 - \frac{u_{mf}La_2}{\gamma u_0}\right) \exp(-a_2L) - a_2 \left(1 - \frac{u_{mf}La_1}{\gamma u_0}\right) \exp(-a_1L) \right] \quad (8-18)$$

where

$$a_1, a_2 = \frac{(\gamma + \alpha) \pm [(\gamma + \alpha)^2 - 4(1 - \beta)\alpha\gamma]^{1/2}}{2L(1 - \beta)}$$

We will discuss the evaluation of some of these model parameters subsequently, but let us first examine a second example of modeling of fluidized beds.

### 8.1.3 A Three-Phase Model

In the two-phase model above it was assumed that the bubble phase contained no solids (no catalyst), and that the bubbles were spherical. In fact, both of these assumptions are wrong in most cases. We need in particular to address the question of bubble geometry. Figure 8.3 illustrates what a bubble traversing a bed of particulate solids is more likely to look like. The shape is more that of a distorted hemisphere, or the dome of a mushroom, than that of a sphere. Moreover, there is a phase immediately surrounding the bubble that contains a concentration of solids different from both the bubble and emulsion phases. This is shown in the figure as a “cloud” or “wake” phase. This view of the bubble in passage through the bed is not one made up for the sake of proposing a new model, but is based on a large amount of experimental data, much of it photographic. Obviously, such evidence would call for some restructuring of the Davidson-Harrison approach to account for actual bubble geometry and, more importantly, to account for the existence of three phases. To a considerable extent these factors depend on the types of particles that are being fluidized, which in turn determine the type of fluidization to be expected. A widely used classification is that of Geldhart [D. Geldhart, *Powder Technol.*, 7, 285 (1973); 19, 133 (1978)] which divides particulates into four different types of behavior. These are

- A Materials with small mean particle size and/or low particle density ( $< 1.4 \text{ g/cm}^3$ ). These are easily fluidized and give small bubbles at higher velocities.

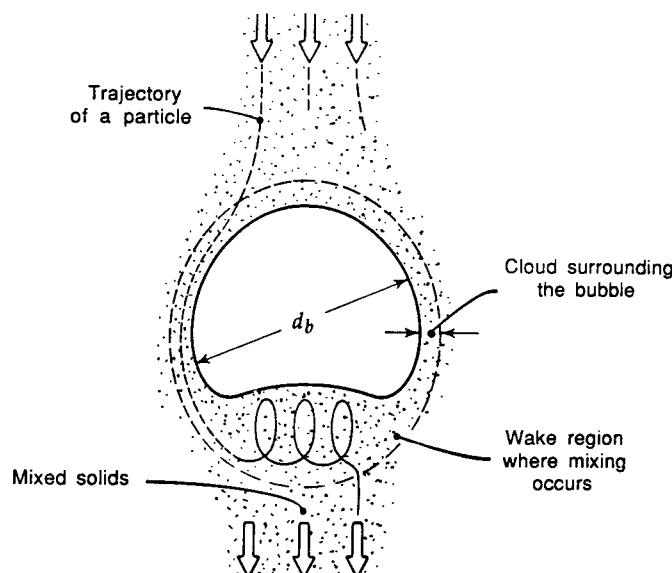


**Figure 8.3** A more precise view of bubble geometry. [After D. Kunii and O. Levenspiel, *Fluidization Engineering*, with permission of Butterworth-Heinemann, Boston, MA, (1991).]

- B** Sand-like materials with particles 40-500  $\mu\text{m}$  in diameter and density of 1.4-4.0  $\text{g}/\text{cm}^3$ . These also fluidize well but demonstrate bubble coalescence and growth.
- C** Very fine powders that are cohesive due to interparticle attraction. Difficult to fluidize; flour and starch are examples.
- D** These are large and/or dense particles that are difficult to fluidize and give erratic fluidization patterns with channeling and spouting behavior. Drying grains, roasting coffee, and coal gusification are examples.

Each of these groups can be classified generally as to the particle size/density as a generic measure of the nature of fluidization. This is shown in Figure 8.4. As indicated in the figure, group **A** (and sub-group **A'**) are the most likely to be associated with reactor design, and the data leading to the visualization of Figure 8.3 has been obtained in large part from fluidized solids belonging to this group.

The Kunii-Levenspiel model [D. Kunii and O. Levenspiel, *Ind. Eng. Chem. Fundls.*, 7, 446 (1968); *Ind. Eng. Chem. Proc. Design Devel.*, 7, 481 (1968); *Fluidization Engineering*, 2 ed., Butterworth-Heinemann, Boston, MA, (1991)] envisions a solid-free bubble phase, generally corresponding to operations where  $u_0 \geq 2u_{mf}$ , is surrounded by the cloud-wake phase which, in turn is surrounded by the emulsion phase. In general the flow of all three phases is in the same upward direction, although in some ranges of bubble velocity the emulsion phase may flow in the opposite direction. In any event, at a given point in the reaction three rate processes occur simultaneously:

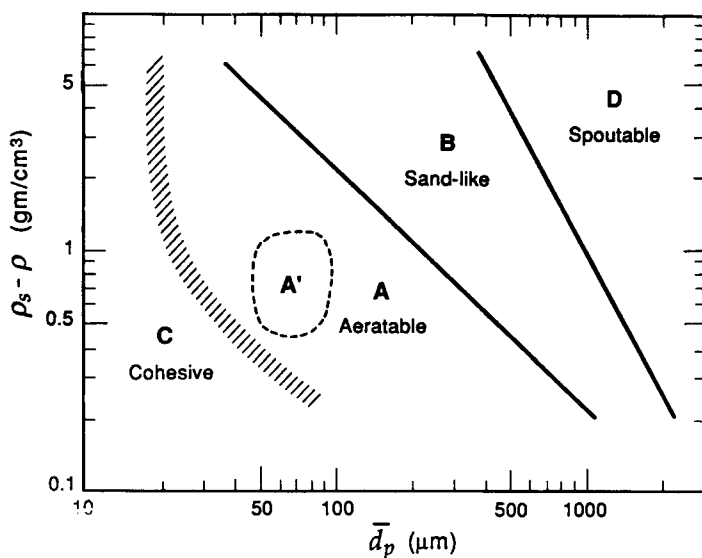


**Figure 8.4** Geldhart classification of particles for fluidization by air at ambient temperature. Region **A'** corresponds to the properties of well-behaved fluid cracking catalysts. [After D. Kunii and O. Levenspiel, *Fluidization Engineering*, with permission of Butterworth-Heinemann, Boston, MA, (1991).]

1. Mass transfer from the bubble to the cloud-wake phase. There is a possible chemical reaction in the bubble phase, but this will be small since the amount of catalyst in the bubble phase is also small.
2. Mass transfer of reactant into the cloud-wake phase from the bubble phase, and from there into the emulsion phase. There is chemical reaction in the cloud-wake phase.
3. Mass transfer of reactant from the cloud-wake phase into the emulsion phase. There is chemical reaction in the emulsion phase.

This sequence of events is depicted schematically in Figure 8.5, following the reactant. More precisely, we may write the balances for reactant as

$$\text{Disappearance in bubble} = \text{reaction in bubble} + \text{transfer to cloud-wake}$$

$$\text{Transfer to cloud-wake} = \text{reaction in cloud-wake} + \text{transfer to emulsion}$$

$$\text{Transfer to emulsion} = \text{reaction in emulsion}$$

Using the notation given in Figure 8.5, we have

$$-\left(\frac{dC_b}{dt}\right) = -u_b \left(\frac{dC_b}{dy}\right) = \gamma_b k_r C_b + K_{bc}(C_b - C_c) \quad (8-22)$$

$$K_{bc}(C_b - C_c) = \gamma_c k_r C_c + K_{ce}(C_c - C_e) \quad (8-23)$$

$$K_{ce}(C_c - C_e) \approx \gamma_e k_r C_e \quad (8-24)$$

If we allow ourselves the latitude to replace  $\approx$  with  $=$  in the above, then combination of (8-22) to (8-24) to eliminate the concentrations  $C_c$ , and  $C_e$  gives

$$-u_b \frac{dC_b}{dy} = K_f C_b \quad (8-25)$$

where  $u_b = (u_0 - u_{mf})$ , and  $K_f$ , the composite rate constant, is given by

$$K_f = \gamma_b k_r + \frac{1}{\beta} \quad (8-26)$$

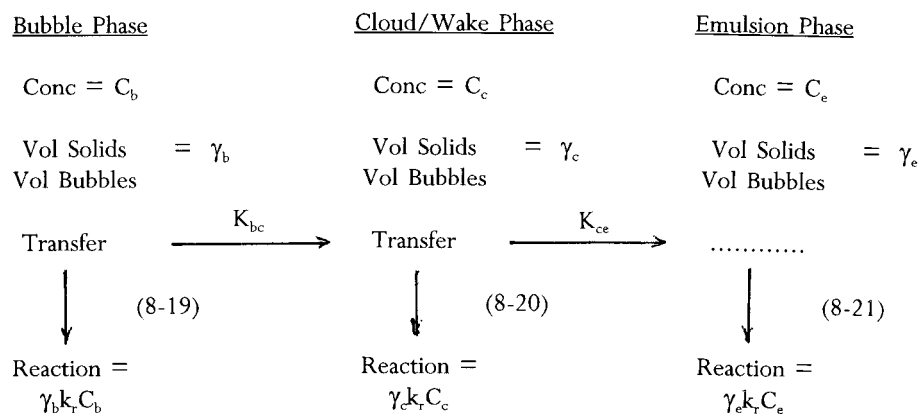


**Figure 8.5** Mass transfer and reaction steps in the three-phase model.

with

$$\beta = \frac{1}{K_{bc}} + \frac{1}{\gamma_c k_r + 1/\alpha}$$

and

$$\alpha = \frac{1}{K_{ce}} + \frac{1}{\gamma_e k_r}$$

Integrating equation (8-25) gives the bubble concentration at height  $y$  as

$$\left( \frac{C_b}{C_0} \right) = \exp \left[ -K_f \left( \frac{y}{u_b} \right) \right] \quad (8-27)$$

and overall

$$1 - X = \left( \frac{C_{bL}}{C_0} \right) \exp(-K_f L / u_b) \quad (8-28)$$

where  $X$  is the conversion of reactant. In beds where the bubble motion is quite vigorous, then  $u_0 \gg u_{mf}$ , and a good approximation of equation (8-28) is

$$1 - X = \exp \left( -\frac{k_f \gamma_b \delta L}{u_0} \right) \quad (8-29)$$

with  $\delta = (u_0 / u_b)$ .

Some study of the structure of equation (8-26) provides support for the advice that all parameters are (can be) equal, but some are more equal than others. For a fast reaction,  $k_r$  is large and the early steps dominate. Inversely, for slow reactions  $k_r$  is small and the latter steps prevail. For a *very fast reaction* transport rates limit, and the value of  $K_{bc}$  is approached by  $k_r \gamma_b$ , even though  $\gamma_b$  is generally very small. This results in

$$K_f = (\gamma_b k_r - K_{bc}) \quad (8-30)$$

and

$$1 - X = \exp \left[ -(\gamma_b k_r + K_{bc}) \left( \frac{\gamma L}{u_0} \right) \right] \quad (8-31)$$

For a *very slow reaction*,  $k_r \ll K_{bc}$  and  $K_{ce}$ , thus,

$$K_f = (\gamma_b + \gamma_c + \gamma_e) k_r = k_r \left( \frac{1 - \epsilon_f}{\delta} \right) \quad (8-32)$$

This will give us an expression for the overall conversion of reactant as

$$1 - X = \exp \left[ \frac{-k_r (1 - \epsilon_f) L}{u_0} \right] \quad (8-33)$$

where  $\epsilon_f$  is the porosity of the fluidized bed.

It is of interest to compare the efficiency of a fluidized bed in terms of the Kunii-Levenspiel model to that of a corresponding plug-flow reactor. We can do this by comparing the catalyst requirement in a PFR to that in the fluid-bed reactor (FBR) for the same conversion, which in general is the ratio of the effective

overall rate constant (first-order, remember) in the FBR to the intrinsic rate constant, so

$$E = \frac{k_e \delta}{(1 - \epsilon_f)} = \frac{K_f \delta}{k_r (1 - \epsilon_f)} \quad (8-34)$$

where  $k_e = (K_f/k_f)$  and  $E$  is an efficiency in terms of (PFR/FBR). For a slow reaction  $E \rightarrow 1$ , and for a fast reaction  $E \rightarrow [\gamma_b \delta / (1 - \epsilon_p)]$ .

An alternative development of the three-phase model, in terms of nondimensional parameters, is very good for those who like to think in terms of numbers. We define the reaction-transport parameters using the corresponding Damköhler numbers,

$$N_{Da,c} = \frac{k_r}{K_{bc}}; \quad N_{Da,e} = \frac{k_r}{K_{ce}} \quad (8-35)$$

and phase effectiveness factors,

$$\eta_i = \frac{\gamma_i}{1 + \gamma_i N_{Da,i}} \quad (8-36)$$

The fluid-bed effectiveness has the physical significance that for small  $N_{Da,i}$ ,  $\eta_i \rightarrow \gamma$  and there is total utilization of catalyst in that phase, while for large  $N_{Da,i}$ ,  $\eta_i \rightarrow 0$  and the phase is not utilized for chemical reaction. Thus, the effectiveness definitions for the three phases are

$$\begin{aligned} \eta_b &= \gamma_b \\ \eta_c &= \frac{\gamma_c}{1 + \gamma_c N_{Da,c}} \end{aligned} \quad (8-37)$$

We also define the overall fluid-bed efficiency as

$$E = \left( \frac{K_f}{K_r} \right) \left( \frac{V_b}{V_s} \right) = \eta_0 \left( \frac{V_b}{V_s} \right) \quad (8-38)$$

where  $V_b$  is the volume of the bubble phase and  $V_s$  the volume of solids. For the three-phase model this is given by

$$E = \left( \frac{V_b}{V_s} \right) \left[ \gamma_b + \frac{1}{N_{Da,c} + 1/(\gamma_c + \eta_e)} \right] \quad (8-39)$$

For large  $N_{Da}$  and fast reaction,

$$\eta_e = 0; \quad \eta_c = 0; \quad E = \left( \frac{V_b}{V_s} \right) \gamma_b \ll 1 \quad (8-40)$$

For large  $N_{De}$  and intermediate reaction,

$$\eta_e = 0; \quad E = \left( \frac{V_b}{V_s} \right) (\gamma_b + \eta_c) < 1 \quad (8-41)$$

For small  $N_{Da}$  and slow reaction,

$$E = \left( \frac{V_b}{V_s} \right) (\gamma_b + \gamma_c + \gamma_e) \rightarrow 1 \quad (8-42)$$

### 8.1.4 The Parameters of Fluidized-Bed Reactors

While building up mathematical models for reactor design and performance is fun, the day of reckoning must come sooner or later when we have to determine if the model parameters are experimentally visible, or how they may be correlated to reaction conditions or properties of the reaction system.<sup>2</sup> An important aspect of the Kunii-Levenspiel model is that, building upon the insights provided by Davidson and Harrison, a substantial amount of information has been accumulated over the years concerning the parameters involved. We focus attention to fluid beds with discrete, noninteracting bubbles in the bed, generally corresponding to operation in region **A** (or more particularly **A'**) in the diagram of Figure 8.4. To a large extent these parameters are concerned with bubbles, bubbles, and even more bubbles.

For mass transfer from the bubble to the cloud-wake phase, we can go back to the form of equations (8-22) and (8-23), where

$$K_{bc} = (q + k_{bc}S_{bc}) \quad (8-43)$$

In this,  $q$  is the cross-flow coefficient and  $S_{bc}$  the interfacial area. From the work of Davidson and Harrison, the value of  $q$  is expressed in terms of the bubble diameter,  $d_b$ , as

$$q = (3\pi/4)u_{mf}(d_b)^2 \quad (8-44)$$

For spherical-cap bubbles and a penetration theory model, the mass-transfer coefficient is given by

$$k_{bc} = (0.975)(\mathcal{D})^{1/2} \left( \frac{g}{d_b} \right)^{1/4} \quad (8-45)$$

so that overall we have

$$K_{bc} = (4.5) \left( \frac{u_{mf}}{d_b} \right) + (5.85) \left( \frac{\mathcal{D}^{1/2} g^{1/4}}{d_b^{5/4}} \right) \quad (8-46)$$

For transport between the cloud-phase there is no net flow of gas, so that diffusion is the only mechanism of transport. This is similar to a problem worked out by Higbie [R. Higbie, *Trans. Amer. Inst. Chem. Eng.*, 31, 365 (1935)] in terms of the penetration theory.

$$k_{ce} \approx \left( \frac{4\mathcal{D}\epsilon_{mf}}{\pi t} \right) \quad (8-47)$$

For bubbles with thin clouds, generally corresponding to the Geldhart region **A'**,

$$d_c \approx d_b; \quad \frac{S_{bc}}{V_b} \approx \frac{6}{d_b} \quad (8-48)$$

<sup>2</sup> “Lots of models, lots of shining stars, lots of days. The models and the stars go away, but the days don’t.”—Ascribed to *B. Hope*



The exposure time for an element of bubble surface in contact with the emulsion phase,  $t$ , is approximated as

$$t = \left( \frac{d_b}{u_{br}} \right) \quad (8-49)$$

Now if we set the results of equations (8-48) and (8-49) into (8-47)

$$K_{ce} = \left( \frac{S_{ce}}{V_b} \right) k_{ce} = \left[ \left( \frac{4D\epsilon_{mf}}{\pi} \right) \left( \frac{u_{br}}{d_b} \right) \right]^{1/2} \left( \frac{S_c}{V_b} \right) \quad (8-50)$$

or

$$K_{ce} = (6.77) \left( \frac{D\epsilon_{mf}u_{br}}{d_b^3} \right)^{1/2} \quad (8-51)$$

The velocity term,  $u_{br}$ , appearing in these equations is the rise velocity of the bubble with respect to the emulsion phase, and is given by

$$u_{br} = (0.711)(gd_b)^{1/2} \quad (8-52)$$

and the bubble velocity,  $u_b$ , is

$$u_b = u_o - u_{mf} + u_{br} \quad (8-53)$$

The particle distribution among the three phases of course determines the relative magnitude of chemical reaction. The  $\gamma$  values appearing in equations (8-22) to (8-24) are defined as (volume of solids)/(volume of bubble). If  $\delta$  is the volume fraction of a bed occupied by bubbles, we have the balance,

$$\delta(\gamma_b + \gamma_e + \gamma_c) = (1 - \epsilon_f) = (1 - \epsilon_{mf})(1 - \delta) \quad (8-54)$$

and

$$\gamma_e = \frac{(1 - \epsilon_{mf})(1 - \delta)}{\delta} - \gamma_b - \gamma_c \quad (8-55)$$

For the cloud-wake phase

$$\gamma_c = \frac{(1 - \epsilon_{mf})}{(f_c + f_w)} = (1 - \epsilon_{mf}) \left[ \frac{3}{(u_{br}\epsilon_{mf}/u_{mf}) - 1} + f_w \right] \quad (8-56)$$

where  $f_c$  and  $f_w$  are factors for the cloud volume and wake, respectively. The value of  $f_c$  is given by

$$f_c = \frac{3}{(u_{br}\epsilon_{mf}/u_{mf}) - 1} \quad (8-57)$$

while the value of  $f_w$  is best estimated from the correlation of experimental data in terms of  $d_p$  shown in Figure 8.6. From this we go forward by combining equations (8-56) and (8-57) to obtain

$$\gamma_c = (1 - \epsilon_{mf}) \left[ \frac{3}{(u_{br}\epsilon_{mf})/u_{mf} - 1} + f_w \right]$$

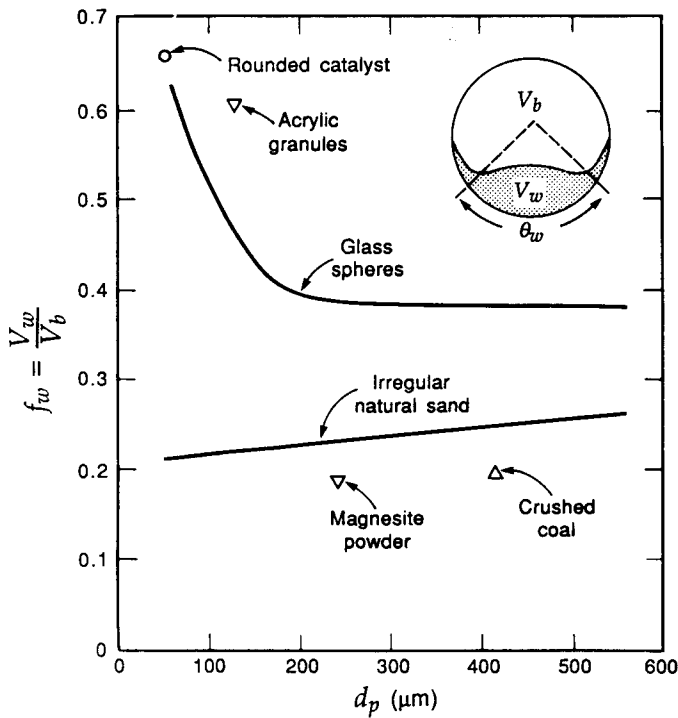


**Figure 8.6** Wake fraction of three-dimensional bubbles. [After D. Kunii and O. Levenspiel, *Fluidization Engineering*, 2 ed., with permission of Butterworth-Heinemann, Boston, MA, (1991).]

and, inserting the correlations for  $u_{br}$ ,

$$\gamma_c = (1 - \epsilon_{mf}) \left[ \frac{(3u_{mf}/\epsilon_{mf})}{(0.711)(gd_b)^{1/2} - u_{mf}/\epsilon_{mf}} + f_w \right] \quad (8-58)$$

This leaves the value of  $\gamma_b$ , which we know to be quite small, but not necessarily zero. Kunii and Levenspiel cite values on the order of  $10^{-2}$  to  $10^{-3}$  based on experimental results of questionable accuracy, and suggest a rule-of-thumb value of 0.005 for  $\gamma_b$ .

Finally, there is the value of  $\delta$  to be considered. This quantity, the fraction of the bed in bubbles, can vary significantly depending upon velocity. For *slow bubbles* ( $u_b < u_e$ ),

$$\delta = \frac{u_0 - u_{mf}}{u_b + 2u_{mf}} \quad (8-59)$$

where  $u_e$  is the upward superficial velocity of the gas through the emulsion phase, defined by

$$\left( \frac{\epsilon_e}{\epsilon_{mf}} \right)^3 \frac{(1 - \epsilon_{mf})}{(1 - \epsilon_e)} = \frac{u_e}{u_{mf}} \quad (8-60)$$

For *fast bubbles* ( $u_b > 5u_{mf}/\epsilon_{mf}$ ),

$$\delta = \frac{u_0 - u_{mf}}{u_b - u_{mf}} \quad (8-61)$$

and in the limit where  $u_0 \gg u_{mf}$

$$\delta = \left( \frac{u_0}{u_b} \right) \quad (8-62)$$

Equations (8-43) to (8-62) have now taken us through a full tour of the parameters of the three-phase model. Our interests here are primarily for vigorously-bubbling beds that exhibit behavior characteristic of the  $\mathbf{A}'$  region of the Geldhart diagram, or at least close to it. One sees in review of these equations the very important role that  $d_b$  and  $u_{mf}$  play in determining fluid bed behavior.

### Illustration 8.1<sup>3</sup>

Estimate the conversion for a first-order irreversible reaction with rate constant  $k_f$  of  $10 \text{ m}^3\text{-gas/m}^3\text{-cat-s}$  taking place in a fluidized bed, given the following data.

$$\begin{aligned} \text{Gas} \quad \quad \quad \mathcal{D} &= 2 \times 10^{-5} \text{ m}^2/\text{s} \\ \text{Particles} \quad \quad (d_p) &= 68 \mu\text{m}, (\rho_s - \rho_q) = 0.8 \\ \text{Bed} \quad \quad \quad \epsilon_m &= 0.50 \text{ (fixed bed)}, \gamma_b = 0.005 \\ &\epsilon_{mf} = 0.55; u_{mf} = 0.006 \text{ m/s}; d_b = 0.04 \text{ m} \\ &L_0 = 7 \text{ m}; u_0 = 0.1 \text{ m/s}; d_{bed} = 0.26 \text{ m} \end{aligned}$$

#### Solution

Let us first check where we are with respect to the Geldhart classification of Figure 8.4. The values of  $d_p$  and  $(\rho_s - \rho_q)$  given as data land us well into the  $\mathbf{A}'$  region of Geldhart  $\mathbf{A}$  particles, so the parameter correlations presented above should be valid. Further  $u_0 = 16u_{mf}$ , and  $u_b \approx 90u_{mf}$  (shown subsequently), so that we are dealing with a fine-particle bed, fast bubbles, and a thin cloud phase. From equation (8-52),

$$u_{br} = (0.711)(gd_b)^{1/2} = (0.711)[(9.8)(0.04)]^{1/2} = 0.445$$

from equation (8-53),

$$\begin{aligned} u_b &= u_0 - u_{mf} + u_{br} = 0.1 - 0.006 + 0.445 \\ u_b &= 0.539 \text{ m/s} \end{aligned}$$

<sup>3</sup> Adapted from [D. Kunii and O. Levenspiel, *Fluidization Engineering*, 2 ed., with permission of Butterworth-Heinemann, Boston, MA, (1991).]

From equation (8-54),

$$K_{bc} = \frac{(4.5)(0.006)}{0.04} + \frac{(5.85)(2 \times 10^{-5})^{1/2}(9.8)^{1/4}}{(0.04)^{5/4}}$$

$$K_{bc} = 3.26 \text{ s}^{-1}$$

From equation (8-51),

$$K_{ce} = (6.77) \left[ \frac{(2 \times 10^5)(0.55)(0.445)}{(0.04)^3} \right]^{1/2}$$

$$K_{ce} = 1.87 \text{ s}^{-1}$$

Since  $(u_b/u_{mf}) \gg 1$ , we may use equation (8-62) for  $\delta$ .

$$\delta = (0.1/0.539) = 0.186$$

For the values of the various  $\gamma$ s, we have

$$\gamma_b = 0.005$$

From equation (8-57a),

$$\gamma_c = (1 - 0.55) \left[ \frac{3}{(0.445)(0.55)/(0.006) - 1} + 0.60 \right]$$

where the value of  $f_w$  is obtained from the correlation of Figure 8.6 for glass spheres,  $d_p = 68 \mu\text{m}$ . Thus,

$$\gamma_c = 0.304$$

From equation (8-55),

$$\gamma_e = \frac{(1 - 0.55)(1 - 0.186)}{0.186} - 0.005$$

$$\gamma_e = 1.668$$

The data give us a value for  $L_0$ , the height of the fixed (unfluidized) bed, so we must determine  $L$  for this operation. An overall mass balance for bed solids is

$$L_o(1 - \epsilon_m) = L_{mf}(1 - \epsilon_{mf}) = L(1 - \epsilon_f) \quad (\text{i})$$

thus

$$L = \frac{L_o(1 - \epsilon_m)}{(1 - \epsilon_f)} \quad (\text{ii})$$

The fluid bed voidage,  $\epsilon_f$ , is related to the total fraction of bubbles in the bed,  $\delta$ , and the voidage of the emulsion phase,  $\epsilon_e$ , by

$$(1 - \epsilon_f) = (1 - \delta)(1 - \epsilon_e) \quad (\text{iii})$$

However, we have no value for  $\epsilon_e$ ; a reasonable approximation in this case is that

$$\epsilon_e \approx \epsilon_{mf} \quad (\text{iv})$$

and then

$$(1 - \epsilon_f) = (1 - \delta)(1 - \epsilon_{mf}) \quad (v)$$

so, finally

$$(1 - \epsilon_f) = (1 - 0.186)(1 - 0.55)$$

$$(1 - \epsilon_f) = 0.366$$

From equation (ii),

$$L = \frac{(0.7)(1 - 0.50)}{0.366}$$

$$L = 0.956 \text{ m}$$

We may now consider the rate of chemical reaction. We can determine  $K_f$  from equation (8-26) using the quantities detailed above. The result is

$$K_f = 1.98 \text{ s}^{-1}$$

Then, using equation (8-28)

$$(1 - X) = \exp\left(-\frac{K_f L}{u_b}\right)$$

$$(1 - X) = \exp\left[-\frac{(1.98)(0.956)}{0.539}\right]$$

$$(1 - X) = 0.030$$

### Illustration 8.2

Develop a measure of reaction-reactor performance that can be used directly from fluid-bed operation to compare PFR and CSTR conversion limits.

*Solution*

This sounds formidable, but it really is not. For a feed rate  $v$  ( $\text{m}^3/\text{s}$ ) of reactant gas at concentration  $C_{A,i}$  ( $\text{mols}/\text{m}^3$ ) to a catalyst bed containing solids of volume  $V_s$  ( $\text{m}^3$ ), the outlet concentration,  $C_{A,o}$ , or the outlet fractional conversion,  $X_A$ , are given by familiar forms.

$$\text{PFR} \quad 1 - X_A = (C_{A,o}/C_{A,i}) = \exp(-k_r \tau) \quad (i)$$

$$\text{CSTR} \quad 1 - X_A = (C_{A,o}/C_{A,i}) = (1 + k_r \tau)^{-1} \quad (ii)$$

However, rather than thinking of  $\tau$  as just a contact time, let us define it as

$$\tau = \left( \frac{\text{volume catalyst}}{\text{volumetric flow rate}} \right) = \left( \frac{V_s}{v} \right) \quad (iii)$$

For illustration, this value of  $\tau$  would be in units of ( $\text{m}^3 \text{ cat}/\text{m}^3 \text{ feed-s}$ ). For the fluid bed, the dimensionless rate group is given by

$$k_r \tau = \frac{k_r L(1 - \epsilon)}{u_0} \quad (iv)$$

for isothermal flow with no density changes.



HORATIO SAYS

We have worried previously about basing the minimum fluidization velocity on the Ergun equation. How would the results of Illustration 8.1 be affected by a  $\pm 10\%$  uncertainty in  $u_{mf}$ ?

Partially because of the backmixing behavior and partially because of the efficiency of contact between fluid- and catalyst-phases, fluidized beds are less efficient than fixed beds, at least in terms of the amount of catalyst required to attain a given conversion. Although plug flow seems reasonable for the motion of the bubbles, particularly in the Geldhart A–A' regions, bubble-emulsion interchange,

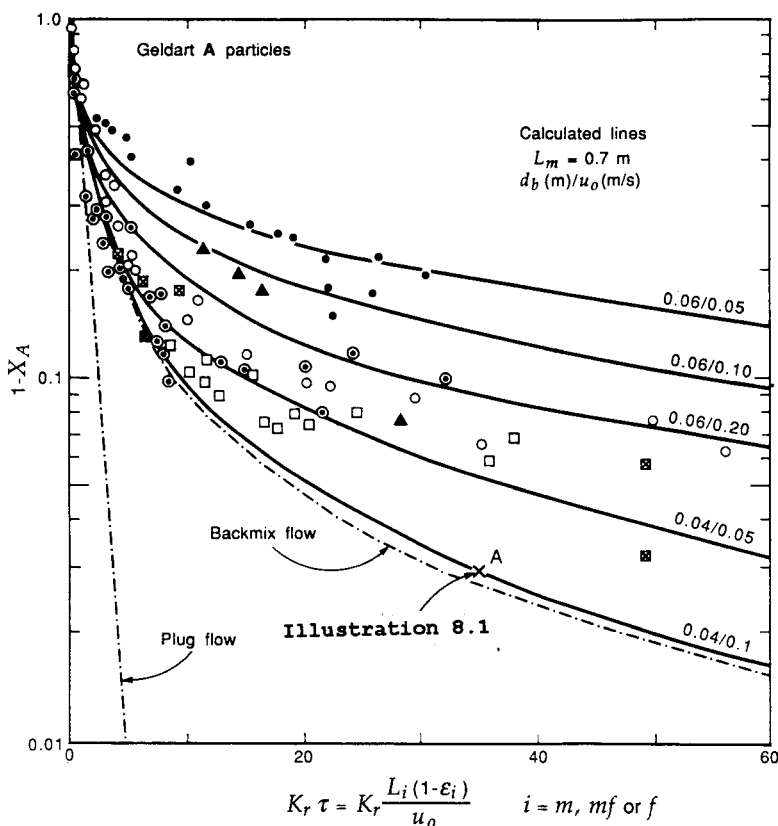
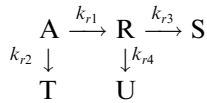


**Figure 8.7** Conversion in fluid beds of very fine Geldhart A catalysts. Lines calculated with equations (8-26) and (8-27),  $u_{mf} = 0.006 \text{ m/s}$ ,  $(d_p/u_0)$  as the parameter; see Illustration 8.1. [After D. Kunii and O. Levenspiel, *Ind. Eng. Chem. Research*, 29, 1226, with permission of the American Chemical Society, (1960).]

bypass flow, and other mass-transfer resistances are not accounted for and can make serious deviations from the PFR model. At the same time, though, such deviations do not approach the limits of the CSTR model. Figure 8.7 gives a summary of results for a number of experimental studies on reactions conducted on fine Geldhart A catalysts, together with the predictions from PFR and CSTR models. The results shown are calculated as in Illustration 8.1; the lines follow in general trend the data presented, if  $(d_b/u_0)$  is used as a parameter. We really cannot say however, that this resolves the problem of fluid-bed design, since there are still a couple of adjustable parameters lurking.

### 8.1.5 Selectivity Factors in Fluidized-Bed Reactors

The three-phase model is readily extended to more complex reaction systems if one is willing to endure the algebraic complications. This was worked out [O. Levenspiel, N. Baden and B.D. Kulkarni, *Ind. Eng. Chem. Process Design Devel.*, 17, 478 (1978)] for the classical Denbigh reaction sequence.



with  $k_{r12} = k_{r1} + k_{r2}$  and  $K_{r34} = k_{r3} + k_{r4}$ . The key equations are the material balances for A and R. Thus, for A,

$$-u_b \left( \frac{dC_{Ab}}{dy} \right) = \gamma_b k_{r12} C_{Ab} + K_{bc,A} (C_{Ab} - C_{Ac}) \quad (8-63)$$

$$K_{bc,A} (C_{Ab} - C_{Ac}) = \gamma_c k_{r12} C_{Ac} + K_{ce,A} (C_{Ac} - C_{Ae}) \quad (8-64)$$

$$K_{ce,A} (C_{Ac} - C_{Ae}) = \gamma_e k_{r12} C_{Ae} \quad (8-65)$$

and for R,

$$-u_b \left( \frac{dC_{Rb}}{dy} \right) = \gamma_b k_{r34} C_{Rb} - \gamma_b k_{r1} C_{Ab} + K_{bc,R} (C_{Rb} - C_{Rc}) \quad (8-66)$$

$$K_{bc,R} (C_{Rb} - C_{Rc}) = \gamma_c k_{r34} C_{Rc} - \gamma_c k_{r1} C_{Ac} + K_{ce,R} (C_{Rc} - C_{Re}) \quad (8-67)$$

$$K_{ce,R} (C_{Rc} - C_{Re}) = \gamma_e k_{r34} C_{Re} - \gamma_e k_{r1} C_{Ao} \quad (8-68)$$

For no intermediate in the feed the initial conditions are

$$C_{Ab} = C_A; \quad C_{Rb} = 0; \quad y = 0$$

As in the case for a single reaction we eliminate the intermediate concentrations  $C_{Ac}$ ,  $C_{Ae}$ ,  $C_{Rc}$ , and  $C_{Re}$  in the equations above. Integration and considerable algebraic manipulation produces the following results.

$$\frac{C_{A0}}{C_{Ai}} = \frac{C_{Ab0}}{C_{Abi}} = \exp(-K_{f12}\tau) \quad (8-69)$$

$$\frac{C_{R0}}{C_{Ai}} = \left( \frac{K_{fAR}}{K_{f34} - K_{f12}} \right) [\exp(-K_{f12}\tau) - \exp(-K_{f34}\tau)] \quad (8-70)$$

where

$$\tau = \frac{V_s}{v} = \frac{L(1 - \epsilon_f)}{u_0} = \frac{L(1 - \epsilon_f)}{u_b \delta} \quad (8-71)$$

This gives a cumbersome but straightforward result for  $K_{f12}$ ,

$$K_{f12} = \left[ \gamma_b k_{r12} + \frac{1}{(\alpha + \zeta)} \right] \frac{\delta}{(1 - \epsilon_f)} \quad (8-72)$$

where

$$\begin{aligned} \alpha &= 1/K_{bc,A} \\ \zeta &= [\gamma + 1/(\lambda + \omega)] \\ \gamma &= \gamma_e k_{r12} \end{aligned}$$

and

$$\lambda = 1/K_{ce,A}; \quad \omega = 1/(\gamma_e k_{r12})$$

Similarly, for  $K_{f34}$

$$K_{f34} = \left[ \gamma_b k_{r34} + \frac{1}{(\alpha' + \zeta')} \right] \frac{\delta}{(1 - \epsilon_f)} \quad (8-73)$$

where

$$\begin{aligned} \alpha' &= 1/K_{bc,R} \\ \zeta' &= [\gamma' + 1/(\lambda' + \omega')] \\ \gamma' &= \gamma_e k_{r34} \end{aligned}$$

and

$$\begin{aligned} \lambda' &= 1/K_{ce,R}; \quad \omega' = 1/(\gamma_e k_{r34}) \\ K_{fAr} &= \left( \frac{k_{r1}}{k_{r12}} \right) K_{f12} - K_{fA} \end{aligned} \quad (8-74)$$

Finally,  $K_{fA}$  is given by equation (8-75), which is sufficiently awkward to warrant its own space on the following page.

Now while those equations seem to go on and on, they essentially represent the simple combinations of reaction and mass transfer parameters that will either be known for the system (various  $k_r$ ) or that can be calculated (mass-transfer coefficients). Overall there are 22 separate reaction and mass-transfer steps represented in this



$$\begin{aligned}
 K_{fA} &= \frac{[A + (B)(C)](D)}{[(E)(F) + G][(H)(L) + M]} \\
 A &= (K_{bc,R}K_{ce,A})/\gamma_c^2 \\
 B &= k_{r12} + K_{ce,A}/\gamma_c + K_{ce,A}/\gamma_e \\
 C &= k_{r34} + K_{ce,R}/\gamma_c + K_{ce,R}/\gamma_e \\
 D &= (\delta K_{bc,A}k_{r1}k_{r34})/(1 - \epsilon_f) \\
 E &= k_{r12} + K_{bc,A}/\gamma_c \\
 F &= k_{r12} + K_{ce,A}/\gamma_e \\
 G &= (k_{r12}K_{ce,A})/\gamma_c \\
 H &= k_{r34} + K_{bc,R}/\gamma_c \\
 L &= k_{r34} + K_{ce,R}/\gamma_e \\
 M &= (k_{r34}K_{ce,R})/\gamma_c
 \end{aligned} \tag{8-75}$$

analysis of the Denbigh sequence as shown in Figure 8.8. The concentrations of other components involved in the reaction are obtained by a sequence of material balances as,

$$C_{S_0} = \frac{k_{r1}k_{r3}}{k_{r12}k_{r34}(C_{A_i} - C_{A_0})} \tag{8-76}$$

$$C_{T_0} = \frac{k_{r2}}{k_{r12}} (C_{A_i} - C_{A_0}) \tag{8-77}$$

$$C_{u_0} = \frac{k_{r1}k_{r4}}{K_{r12}k_{r34}} (C_{A_i} - C_{A_0}) \tag{8-78}$$

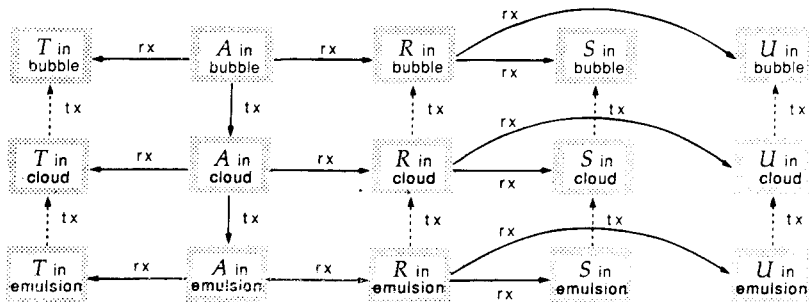


**Figure 8.8** Reaction and mass transfer steps for the Denbigh reaction sequence–three-phase model. [After D. Kunii and O. Levenspiel, *Fluidization Engineering*, with permission of Butterworth-Heinemann, Boston, MA, (1991).]

As might be expected, numerous simplifications of this analysis are possible for special cases. Two of particular interest are

1.  $k_{r34} \ll k_{r1}$

In this case  $k_{fA}$  in equation (8-74) is small and as an approximate result

$$k_{fAR} = \left( \frac{k_{r1}}{k_{r12}} \right) K_{f12} \quad (8-79)$$

2.  $K_{bc}$  and  $K_{ce} \rightarrow \infty$

Here the balance equations can be simplified to

$$\begin{aligned} \left( \frac{C_{A_0}}{C_{A_i}} \right) &= \exp(-k_{r12}\tau) \\ \left( \frac{C_{R_0}}{C_{A_0}} \right) &= \frac{k_{r1}}{k_{r34} - k_{r12}} [\exp(-k_{r12}\tau) - \exp(-k_{r34}\tau)] \end{aligned} \quad (8-80)$$

Finally, the maximum amount of intermediate is often a quantity of interest. If we consider that R is a desired product, then

$$\frac{C_R(max)}{C_{A_i}} = \left( \frac{K_{fAR}}{K_{f12}} \right) \left( \frac{K_{f12}}{K_{f34}} \right)^{K_{f34}/(K_{f34}-K_{f12})} \quad (8-81)$$

with  $\tau$  at  $C_R(max)$  as

$$\tau(max) = \frac{V_s}{v} = \frac{\ln(K_{f34}/K_{f12})}{(K_{f34} - K_{f12})} \quad (8-82)$$

As a final word on this development of selectivity, and indeed the developments and illustrations provided throughout this discussion of fluidized beds, we must remember that good old Academic Reaction #1 was employed throughout. However, one should be able to insert any form of reaction kinetics desired with the expectation that the equations will become nonlinear. The concept of rate processes occurring in a series of steps is a core of these models, even though there is no strong *a priori* evidence to support this view.<sup>4</sup> A different viewpoint, picturing mass transport from a solids-lean phase to a solids-rich, cloud-emulsion phase was reported to be superior in some respects to series models such as that of Kunii and Levenspiel [see J.J. Carberry, *Trans. Inst. Chem. Eng.*, 59, 15 (1981) and A.A. Shaikh, *Chem. Eng. Technol.*, 13, 273 (1990)].

## 8.2 Slurry Reactors

As can be envisioned by the name, slurry reactors are normally three-phase reactors that involve gas and liquid phases with a catalyst solid phase. Normally the catalyst particulate phase is finely divided with motion-mixing largely governed by the motion of the liquid phase. We will also see in the following that the bubbles of the fluidized bed apply to slurries, although the correlations are somewhat different. In general, we will consider the slurry to be a continuous phase with the gas well-dispersed within the reactor.

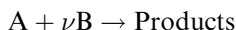
<sup>4</sup>“Stick close to your desks and never go to sea.”—*W.S. Gilbert*

There are many applications of slurry reactors in industrial processes, see for example, Y.T. Shah, *Gas-Liquid-Solid Reactor Design*, McGraw-Hill Book Co., New York, NY, (1979). Examples include hydrogenation of unsaturated oils, oxidation of olefins, and various polymerization reactions. Advantages over competing three-phase reactors such as trickle beds include improved catalytic effectiveness (small catalyst size), better mass transfer between phases, and better heat transfer (i.e., better temperature control). However, on the negative side it will be seen that a well-agitated slurry reactor is first cousin to a classical CSTR<sup>5</sup> and high conversions are best achieved by staging since the rate of chemical transformation is dictated by the exit concentration of the reactants.

In slurry systems, similar to fluidized beds, the overall rate of chemical transformation is governed by a series of reaction and mass-transfer steps that proceed simultaneously. Thus, we have mass transfer from the bubble phase to the gas-liquid interface, transport of the reactant into the bulk liquid and then to the catalyst, possible diffusion within the catalyst pore structure, adsorption and finally reaction. Then all of this goes the other way for product. Similar steps are to be considered for heat transfer, but because of small particle sizes and the heat capacity of the liquid phase, significant temperature gradients are not often encountered in slurry reactors. The most important factors in analysis and design are fluid holdups, interfacial area, bubble and catalyst particle sizes and size distribution, and the state of mixing of the liquid phase.<sup>6</sup>

### 8.2.1 An Analysis of Mass Transfer

A typical three-phase slurry reaction is



where A and B are the reactants in the gas or liquid phases. Generally we will refer to A as a reactant in the gas phase and B as a nonvolatile reactant in the liquid phase. This is typical of hydrogenation and oxidation reactions [R.V. Chaudhari and P.A. Ramachandran, *Amer. Inst. Chem. Eng. J.*, 26, 177 (1980)]. The intrinsic rate of reaction per unit weight of catalyst can be represented with a power-law kinetic model,

$$(-r) = k_{(m+n)}[A]^m[B]^n \quad (8-83)$$

or, since we are generally dealing with catalytic reactions, a Langmuir-Hinshelwood expression such as

$$(-r) = \frac{k[A][B]}{1 + K_A[A] + K_B[B]} \quad (8-84)$$

where  $(-r)$  is the local rate of reaction at a point within the catalyst where the concentrations are  $[A]$  and  $[B]$ . Often the liquid-phase reactant is present in large concentration excess. In such case, the variation in  $[B]$  in the reactor (or with time of

<sup>5</sup> Slurry-phase reactions are also sometimes carried out in bubble-column reactors, where mixing of the slurry phase is promoted by bubble motion in the column. We will not, however, consider this case explicitly here.

<sup>6</sup> After the tribulations of analyzing the Denbigh sequence in fluidized beds, a reasonable reaction might be "Worth seeing? yes; but . . . worth going to see?"—S. Johnson

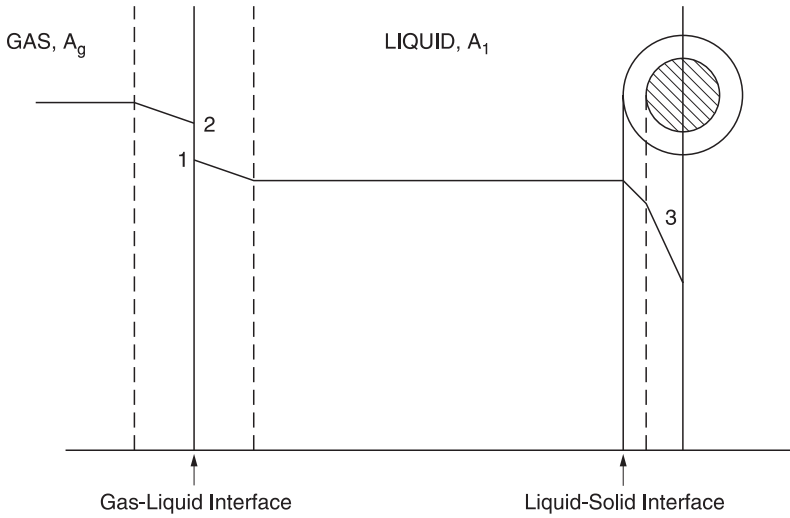


**Figure 8.9** Concentration profiles for a reactant, A, in a slurry reactor. Point 1 =  $A_{lg}$ , Point 2 =  $A_{gl}$ , Point 3 =  $A_g$ .

reaction) is not significant, the intraparticle concentration of B is constant equal to that in the bulk liquid phase, and consequently the reaction is pseudo-first-order,

$$(-r_A) = k_m[A]^m \quad (8-85)$$

where  $k_m = k_{(m+n)}\{[B]_l\}^n$ . The overall mass transfer/reaction in a slurry reactor is illustrated in Figure 8.9 in terms of the concentration profiles characteristic of the gas-phase reactant A.

For steady-state conditions and the assumptions of plug flow in the gas phase and complete mixing in the liquid phase, one can write the mass balance for reactant at any point in the reactor as

$$-u_g \left( \frac{dA_g}{dy} \right) - (k_g S)_A (A_g - A_{gl}) = 0 \quad (8-86)$$

where  $y$  is a measure of position in the reactor (we are tacitly assuming that the bubbles will flow upwards through the reactor),  $u_g$  is bubble velocity and  $S$  is an area for mass transfer. The brackets denoting concentration have been removed for simplicity. For mass transfer we have further,

$$(k_g S)_A (A_g - A_{gl}) = (k_l S)_A (A_{lg} - A_l) \quad (8-87)$$

Now, assuming that Henry's law is valid for the gas-liquid interface,

$$A_{gl} = H_A A_{lg} \quad (8-88)$$

Combining equations (8-86) to (8-88) gives

$$-u_g \left( \frac{dA_g}{dy} \right) = (K_L S)_A \left[ \left( \frac{A_g}{H_A} \right) - A_l \right] \quad (8-89)$$

where  $K_L S$  is the overall mass-transfer coefficient for the transport of A from bulk-gas to bulk-liquid phase, and  $H_A$  is Henry's law constant for A. The overall mass-transfer coefficient is related to the individual coefficients by direct application of the film theory of resistances in series.

$$\frac{1}{(K_L S)_A} = \frac{1}{H_A(k_g S)_A} + \frac{1}{(k_l S)_A} \quad (8-90)$$

which, so far, is not yet anything to get particularly excited about. Let us integrate equation (8-89) over the reactor height,  $y$ , to get

$$\frac{A_g - H_A A_l}{A_{gi} - H_A A_l} = \exp(-\alpha_A y) \quad (8-91)$$

where

$$\alpha_A = \frac{(K_L S)_A}{u_g H_A}$$

The concentration of reactant A leaving the reactor is

$$A_{go} = A_{gi} [\exp(-\alpha_A L)] + H_A A_l [1 - \exp(-\alpha_A L)] \quad (8-92)$$

The rate of reactant consumption per unit volume of the slurry phase is

$$R_A = \frac{H_A v}{V_L} (A_{go} - A_{gi}) \quad (8-93)$$

where subscripts  $o$  and  $i$  refer to outlet and inlet conditions, respectively,  $v$  is the volumetric flow rate of gas, and  $V_L$  is the volume of the slurry. The rate of mass transfer from the liquid to the surfaces of the catalytic phase is also  $R_A$  at steady state,

$$R_A = (k_s S_p)_A (A_l - A_s) \quad (8-94)$$

with  $(k_s S_p)_A$  an appropriate mass-transfer coefficient and  $A_s$  the reactant concentration at the external surface of the catalyst particles. Combining equations (8-93) and (8-94)

$$R_A = M_A \left[ \left( \frac{A_{gi}}{H_A} \right) - A_s \right] \quad (8-95)$$

with

$$M_A = \left\{ \frac{1}{(H_A v / V_L) [1 - \exp(-\alpha_A L)]} + \frac{1}{(k_s S_p)_A} \right\}^{-1} \quad (8-96)$$

Before equations (8-95) and (8-96) can be used to estimate the overall rate of mass transfer for A, we must eliminate the surface concentration,  $A_s$ . The rate of chemical reaction, written for the power-law expression of equation (8-85), is

$$(-\gamma_A) = R_A = \eta_o W k_m A_s^m \quad (8-97)$$

where  $W$  is the mass of catalyst per unit volume of slurry and  $k_m$  is the pseudo- $m$ th-order rate constant in  $(\text{cm}^3/\text{g})(\text{cm}^3/\text{mol})^{m-1}\text{s}^{-1}$ . The catalyst effectiveness factor, for

spherical geometry, can be approximated by

$$\eta_c = \frac{1}{\phi} \left[ \coth(3\phi) - \frac{1}{3\phi} \right] \quad (8-98)$$

where  $\phi$  is the generalized Thiele modulus as defined by Bischoff [K.B. Bischoff, *Amer. Inst. Chem. Eng. J.*, 11, 351 (1965)].

$$\phi = \left( \frac{R}{3} \right) \rho_p (-r_A)_s \left[ \int_0^{A_s} 2D_e \rho_p (-r_A) dA \right]^{-1/2} \quad (8-99)$$

where  $(-r_A)$  is the local rate of reaction. For an  $m$ th-order irreversible reaction this reduces to

$$\phi = \left( \frac{R}{3} \right) \left[ \frac{(m+1)\rho_p k_m A_s^{m-1}}{2D_e} \right]^{1/2} \quad (8-100)$$

with  $D_e$ , the effective diffusivity of the reactant in the catalyst pore structure and  $\rho_p$  the catalyst particle density. Since the Thiele modulus is a function of  $A_s$ , except for  $m = 1$ , a trial procedure is required to calculate  $R_A$  for the general power-law case.

Ramachandran and Chaudhari [P.A. Ramachandran and R.V. Chaudhari, *Can. J. Chem. Eng.*, 58, 412 (1980); *Chem. Eng., J.*, 20, 75 (1980)] have shown that it is advantageous to define an overall effectiveness for the reactor in such cases. This is defined as the ratio of the actual rate of chemical reaction per unit volume of the slurry to the rate that would have prevailed if the liquid phase were in equilibrium with the inlet gas phase. Following this,

$$\eta = \frac{R_A}{W[-r(A^*)]}; \quad A^* = \left( \frac{A_{gi}}{H_A} \right) \quad (8-101)$$

For reaction of order  $m$

$$\eta = \frac{R_A}{W k_m (A^*)^m} \quad (8-102)$$

The effectiveness factor defined by equation (8-101) is for the entire reactor and thus, in principle, takes into account any variation of the concentration of A in the gas phase along the height of the reactor. To obtain an analytical solution for effectiveness we eliminate the surface concentration by expressing it in terms of the overall effectiveness itself. From equations (8-95) and (8-101) we get

$$a_s = \left( \frac{A_s}{A^*} \right) = 1 - \frac{\eta}{\alpha_A} \quad (8-103)$$

where

$$\sigma_A = \frac{M_A A^*}{W[-r(A^*)]}$$

Combining equations (8-103) and (8-97), the overall effectiveness factor for an  $m$ th-order reaction in a slurry reactor can be obtained as

$$\eta = \frac{1}{\phi} \left[ \coth(3\phi) - \frac{1}{3\phi} \right] \left[ 1 - \frac{\eta}{\sigma_A} \right]^m \quad (8-104)$$

From equation (8-100) it is clear that the modulus is a function of  $A_s$  and, in turn,  $A_s$  is a function of  $\eta$ . Using equation (8-103), and eliminating  $A_s$  from equation (8-100), we obtain

$$\phi = \left( \frac{R}{3} \right) \left[ \frac{(m+1)\rho_p k_m (A^*)^{m-1}}{2D_e} \left( 1 - \frac{\eta}{\sigma_A} \right)^{m-1} \right] \quad (8-105)$$

Equation (8-105) is an implicit expression for  $\eta$ , since  $\eta$  is a function of  $\phi$ , and  $\phi$  also a function of  $\eta$ , so a trial procedure is necessary to determine a final value for  $\eta$ . The overall rate for  $m$ th-order kinetics can be obtained from equation (8-102) once a value of  $\eta$  has been determined. This approach, using the overall effectiveness, incorporates all the transport resistances and thus simplifies the calculation required to obtain an overall rate of reaction.

For a first-order reaction the problem is less taxing, since

$$\phi = \left( \frac{R}{3} \right) \left[ \frac{\rho_p k_1}{D_e} \right]^{1/2} \quad (8-106)$$

which is independent of  $A_s$ . Hence the rate of reaction is

$$R_A = \left( \frac{A_{gi}}{H_A} \right) \left\{ \frac{1}{(H_A v/V_L)[1 - \exp(-\alpha_A L)]} + \frac{1}{(k_s S_p)_A} + \frac{1}{Wk_1[\coth(3\phi)/\phi - (1/3\phi^2)]} \right\}^{-1} \quad (8-107)$$

Equations for the overall effectiveness factor and the modified Thiele modulus are shown in Table 8.1 for several types of rate equations (but all dependent upon  $A$  alone). Figure 8.10 gives some idea as to the nature of the overall effectiveness factor for the first-order case treated above.

### 8.2.2 Gas Mixing and Semi-Batch Operation

If the gas phase does not move in plug flow, and the gas phase is perfectly mixed for whatever reason, the mass balance for gas  $A$  is

$$v(A_{gi} - A_{go}) = (K_L S)_L \left[ \left( \frac{A_{go}}{H_A} \right) - A_l \right] \quad (8-108)$$

Solving for  $A_{go}$ , the concentration of  $A$  leaving the reactor, gives

$$A_{go} = \frac{A_{gi}}{(1 + \alpha_A L)} + H_A A_l \left( 1 - \frac{1}{(1 + \alpha_A L)} \right) \quad (8-109)$$

If we compare equation (8-109) with the corresponding balance for plug flow, equation (8-92), it can be seen that the only difference is that the term  $\exp(-\alpha_A L)$  in (8-92) is replaced by  $[1/(1 + \alpha_A L)]$  in (8-109).

Slurry reactors are also sometimes used in the semi-batch or batch-filling mode, and we should look at an analysis of this type of operation. These are most often used in situations where a gas phase is passed through an agitated slurry phase with

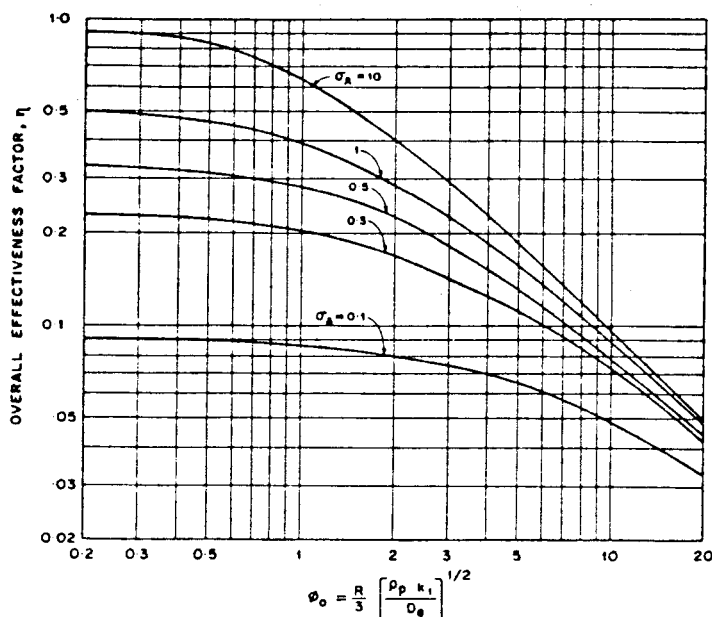
**Table 8.1a** Equations for Overall Effectiveness for a Slurry Reactor with Various Rate Equations

Kinetic model	Overall effectiveness factor, $\eta^2$	Generalized Thiele modulus definition, $\phi$
mole/gm/sec		
$k_m A^m$	$\eta_c \left(1 - \frac{\eta}{\sigma_A}\right)^m$	$\frac{R}{3} \left[ \frac{(m+1)}{2} \frac{\rho_p k_m A^{*m-1}}{D_{eA}} \left(1 - \frac{\eta}{\sigma_A}\right)^{m-1} \right]^{1/2}$
$k_1 A$	See equation (8-107)	$\frac{R}{3} \left( \frac{k_1 \rho_p}{D_{eA}} \right)^{1/2}$
$k_0$	$\sigma_A \left[ 1 - \frac{\phi^2}{6} \{1 - 3(1 - \eta)^{2/3} + 2(1 - \eta)\} \right]$	$\frac{R}{3} \left[ \frac{\rho_p k_0}{D_{eA} A_0} \right]^{1/2}$
$\frac{k_1 A}{1 + K_A A}$	$\eta_c \left[ \frac{(1 + K_A A_0)(1 - \eta/\sigma_A)}{[1 + K_A A_0(1 - \eta/\sigma_A)]} \right]$	$\frac{R}{3} \left[ \frac{\rho_p k_1}{D_{eA}} \right]^{1/2} \cdot \frac{K_A A_0(1 - \eta/\sigma_A)}{\{1 + K_A A_0(1 - \eta/\sigma_A)\} \sqrt{2[K_A A_0(1 - \eta/\sigma_A) - \ln\{1 + K_A A_0(1 - \eta/\sigma_A)\}]}}$
$\frac{k_1 A}{(1 + K_A A)^2}$	$\eta_0 \left[ \frac{(1 + K_A A_0)^2(1 - \eta/\sigma_A)}{[1 + K_A A_0(1 - \eta/\sigma_A)]^2} \right]$	$\frac{R}{3} \left[ \frac{\rho_p k_1}{D_{eA}} \right]^{1/2} \cdot \frac{K_A A_0(1 - \eta/\sigma_A)}{\{1 + K_A A_0(1 - \eta/\sigma_A)\}^2 \sqrt{2 \ln \left[ \{1 + K_A A_0(1 - \eta/\sigma_A)\} - \frac{K_A A_0(1 - \eta/\sigma_A)}{1 + K_A A_0(1 - \eta/\sigma_A)} \right]}}$



**Table 8.1b** Overall Rate of Reaction in a Slurry Reactor without Intraparticle Diffusional Effects

Reaction type	Kinetic model (mols/gm/s)	Rate of reaction ( $R_A$ mols/cm <sup>3</sup> /s)
First-order	$k_1 A$	$A_0 \left[ \frac{1}{M_A} + \frac{1}{wk_1} \right]^{-1}$
Second-order	$k_2 A^2$	$\frac{M_A^2}{2k_2 w} \left[ \left( 1 + \frac{2wk_2 A_0}{M_A} \right) - \left( 1 + \frac{4wk_2 A_0}{M_A} \right)^{1/2} \right]$
Half-order	$k_{1/2} \sqrt{A}$	$\frac{(wk_{1/2})^2}{2M_A} \left[ \left( 1 + \frac{4A_0 M_A^2}{(wk_{1/2})^2} \right)^{1/2} - 1 \right]$
Langmuir-Hinselwood [single site]	$\frac{k_1 A}{(1 + K_A A)}$	$\frac{M_A}{2K_A} \left\{ \left( 1 + K_A A_0 + \frac{wk_1}{M_A} \right) - \left[ \left( 1 + K_A A_0 + \frac{wk_1}{M_A} \right)^2 - \frac{4wkK_A A_0}{M_A} \right]^{1/2} \right\}$


**Figure 8.10** Overall effectiveness factor for a first-order reaction in a slurry reactor. [After R.V. Chaudhari and P.A. Ramachandran, *Amer. Inst. Chem. Eng., JI.*, 26, 177, with permission of the American Institute of Chemical Engineers, (1980).]

no net flow of the slurry. Normally, then, we wish to determine the conversion of liquid-phase reactant B as a function of time. The previous analysis is modified, because  $[B] \gg [A]$  does not apply here. In the semibatch operation the concentration of B is changing continuously, just as in any batch reactor (sort of) and simplifying assumptions about kinetics are not likely to be good.

Consider a reaction that is first-order in A, and zero-order in B. The batch time,  $t_B$ , required for a given conversion,  $x$ , of the liquid phase reactant B is

$$t_B = \frac{B_{l_0} x}{\nu A^*} \left( \frac{1}{M_A} + \frac{1}{\eta_c W K_1} \right) \quad (8-110)$$

where the effectiveness factor  $\eta_c$  is given by equation (8-98) and  $\phi$  is defined by equation (8-106).

In a more realistic case we may have the reaction first-order in both A and B, where the analysis is complicated by the fact that the Thiele modulus becomes a function of  $B_1$ , which is changing with time. This complication is tractable, however, and the final time-conversion relationship is

$$t_B = \frac{B_{l_0} x}{\nu A^* M_A} + \frac{B_{l_0} R^2 \rho_p I}{3 \nu A^* W D_e} \quad (8-111)$$

where  $I$  is an integral function defined as

$$I = \int_{1-x}^1 \frac{dx}{\phi_0 x^{1/2} \coth(\phi_0 x^{1/2}) - 1} \quad (8-112)$$

In equation (8-111)  $B_{l_0}$  is the initial concentration of B, and  $t_B$  is the batch time required to reach a conversion of  $x$ . The quantity  $\phi_0$  is the Thiele modulus at  $t = 0$ , that based on the initial concentration of B

$$\phi_0 = R \left( \frac{\rho_p k_2 B_{l_0}}{D_e} \right)^{1/2} \quad (8-113)$$

A plot of  $I$  versus  $(1 - x)$  convenient for calculation is given in Figure 8.11. For  $\phi_0 < 0.2$ , the effectiveness factor  $\eta_c$  approaches unity and equation (8-111) simplifies to

$$t_B = \frac{B_{l_0} x}{\nu A^* M_A} - \frac{\ln(1 - x)}{\nu A^* W K_2} \quad (8-114)$$

For a general  $m, n$ th order reaction (power-law form) the rate of reaction of B per unit volume of slurry is obtained from the expression

$$\frac{dB_1}{dt} = \nu R_A = \nu W K_2 \eta \left( \frac{A_{g_i}}{H_A} \right)^m (B_1)^n \quad (8-115)$$

The effectiveness factor is a function of  $B_1$ , thus numerical solution will be required to obtain the  $B_1$  versus  $t$  relationship.

### 8.2.3 Another Approach

The slurry reactor analysis given above employed the concept of an overall effectiveness factor. It is informative to break down the problem into analysis of individual phase effectiveness factors assembled together as was done for the three-phase fluid-bed model. Equating the rates of the individual steps in a manner similar to

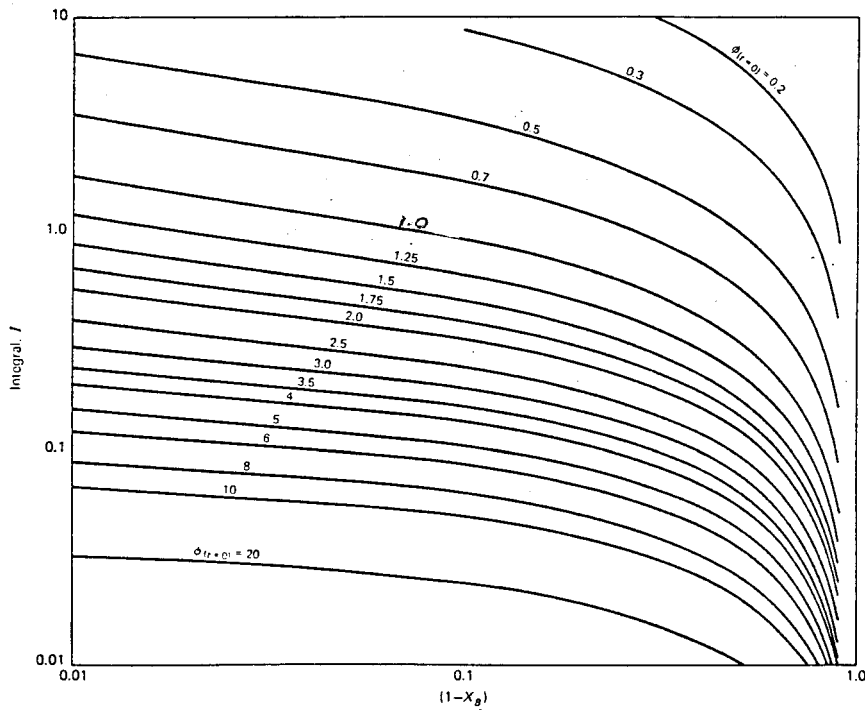


**Figure 8.11** Design chart for equation (8-112). Semi-batch slurry reactor with reaction first-order in both A and B. Parameter is  $\phi$  at  $r = 0$ .

equation (8-87) gives,

$$\begin{aligned}
 R_A &= (k_g S_b)(A_g - A_{g1}) \\
 &= (k_1 S_b)(A_{1g} - A_1) \\
 &= (k_s S_p)(A_1 - A_s) \\
 &= \eta k S_p A_s
 \end{aligned} \tag{8-116}$$

for our example first-order reaction. We wish to combine all these factors into an over-all expression that will allow a determining rate via the measurable quantity,  $A_g$ , i.e.,

$$(-\gamma_A) = R_A = K_0 A_g \tag{8-117}$$

Eliminating intermediate concentrations in equation (8-116),

$$\frac{A_g}{R_A} = \frac{1}{K_0} = \left( \frac{1}{\eta k} + \frac{1}{k_s} \right) \left( \frac{1}{S_p} \right) + \left( \frac{1}{k_1} + \frac{1}{k_g H_A} \right) \left( \frac{1}{S_b} \right) \tag{8-118}$$

where  $H_A$  is the Henry's law constant. Now, let us define phase effectiveness as

$$\eta_b = \frac{1}{1 + (N_{Da})_b} \tag{8-119}$$

$$\eta_l = \frac{1}{1 + (N_{Da})_l} \tag{8-120}$$

where

$$(N_{Da})_b = \frac{k_1}{K_g H_A}; \quad (N_{Da})_1 = \frac{\eta k}{k_s}$$

Substitution in equation (8-118) and rearrangement gives

$$K_0 = \frac{\eta_1 \eta k S_p}{1 + (\eta_1 \eta k S_p / \eta_b k_1 S_b)} = \frac{\eta_1 \eta k S_p}{1 + (N_{Da})_0} \quad (8-121)$$

where

$$(N_{Da})_0 = \frac{\eta_1 \eta k S_p}{\eta_b k_1 S_b}$$

Now  $\eta_0$  can be defined as an overall effectiveness

$$\eta_0 = \frac{1}{1 + (N_{Da})_0} \quad (8-122)$$

Then,  $\eta_0 = 1 - \eta_0 (N_{Da})_0$ , and dividing by  $\eta_0 k_1 S_b$ ,

$$\frac{(N_{Da})_0}{1 + (N_{Da})_0} = \eta_0 (N_{Da})_0 = \frac{K_0}{\eta_b k_1 S_b} \quad (8-123)$$

$$(8-124)$$

This is about as far as we can go with the individual phase effectiveness; however, it should suffice if  $\eta_0$  is available from observation and correlations are available for the mass-transfer and area parameters. This brings us to exactly the same point addressed in Section 8.14 for fluidized beds. How can we estimate the parameters involved?

## 8.2.4 The Parameters of Slurry Reactor Design

At issue here are the determination of values for the mass-transfer coefficients  $k_g$ ,  $k_1$ , and  $k_s$ , and the interfacial areas  $S_b$  and  $S_p$ .

Mass transfer between spheres and surrounding fluids has been a topic of extensive study through the years. The most comprehensive situation is when the relative velocity between the solid and liquid phases is small, which is approximately the case in slurries of small particles. The general results are represented by the curve in Figure 8.12, showing the relationship between the Sherwood number,  $(k_s d_p / \mathcal{D})$ , and a Peclet number  $(g d_p^3 \Delta \rho / 18 \mu \mathcal{D})$ . The solid curve is given by [P.L.T. Brian and H.B. Hales, *Amer. Inst. Chem. Eng. Jl.*, 15, 419 (1969)]

$$\left( \frac{k_s d_p}{\mathcal{D}} \right)^2 = 4 + 1.2 \left( \frac{g d_p^3 \Delta \rho}{18 \mu \mathcal{D}} \right)^{2/3} \quad (8-125)$$

and the dotted line is that of an asymptotic solution obtained by Levich [V.G. Levich, *Physicochemical Hydrodynamics*, Prentice-Hall, Englewood Cliffs, NJ, (1962)].<sup>7</sup> This gives us the relationship

$$N_{Sh} = \left( \frac{k_s d_p}{\mathcal{D}} \right) = 0.997 (N_{Pe})^{1/3} \quad (8-126)$$

<sup>7</sup> In practice, working values of  $k_s$  appear to be about twice the value that would be computed from this correlation. "A miss is as good as a mile."—Anonymous

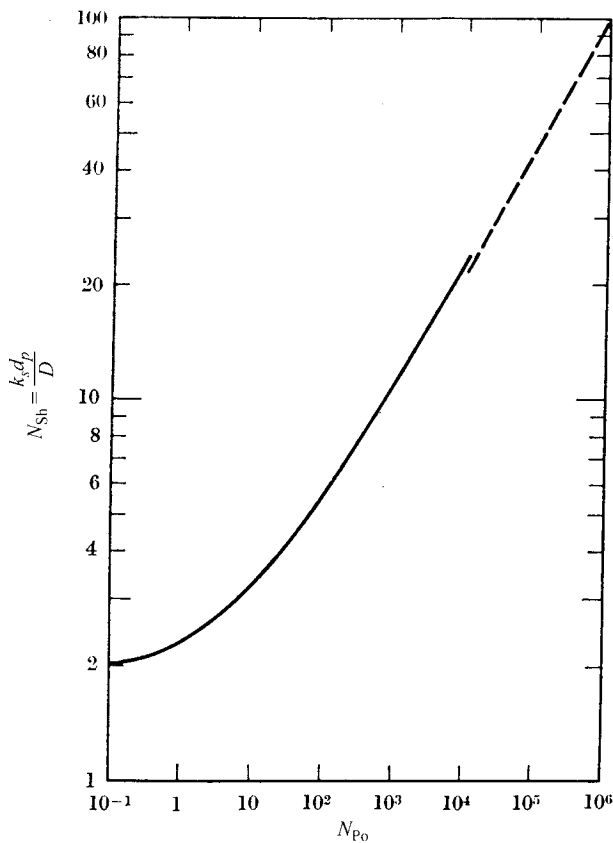


**Figure 8.12** Correlation of mass transfer to a single sphere in a liquid for low relative velocities. [After C.N. Satterfield, *Mass Transfer in Heterogeneous Catalysis*, with permission of MIT Press, Cambridge, MA, (1970).]

where  $N_{Pe}$  (Figure 8.12, x-axis) is

$$N_{Pe} = \left( \frac{g d_p^3 \Delta \rho}{18 \mu D} \right)$$

Considerable work has been reported also for the case of bubble-liquid mass transfer and its associated coefficient  $k_1$ . A general review of much of this was given by Calderbank [P.H. Calderbank in *Mixing, Vol. II* (V.W. Uhl and J.B. Gray, eds.), Academic Press, New York, NY, (1967)], and a correlation reported there has passed the test of time rather well,

$$k_1 (N_{Sc})^{1/2} = 0.42 \left( \frac{g \mu \Delta \rho}{\rho_1^2} \right) \quad (8-127)$$

where  $N_{Sc}$  is for the liquid phase. Equations (8-125) and (8-127), then, provide at least a good initial estimate for the transport coefficients  $k_s$  and  $k_1$ . Further detail on these correlations is given by Satterfield [C.N. Satterfield, *Mass Transfer in Heterogeneous Catalysis*, MIT Press, Cambridge, MA, (1970)].

The quantity  $k_q$  is sort of the “odd-man-out” in most work on slurry reactors (and even also for fluid-bed and gas-liquid reactors). If the bubble (gas) phase consists of pure reactant only, then a mass-transfer resistance in a film inside the bubble loses its meaning and  $k_q$  drops out of the problem. Even in the case of mixed gas-phase components, gas phase mass-transfer coefficients are so much larger than their liquid-phase counterparts that the gas-phase transport rate would seldom be of importance in determining the overall rate of chemical reaction.

The interfacial areas do not appear explicitly in the correlations of equations (8-125) and (8-127), but they present another correlation problem in themselves. One is easy; one is more difficult. The easy one is  $a_p$ , the interfacial area between the catalyst particles and the liquid making up the slurry phase. Here, if the particle size (or average particle size) is known and the weight loading of catalyst is known,

$$S_p = \left( \frac{6m}{\rho_p d_p} \right) \quad (8-128)$$

where  $m$  is the loading (in g cat/volume expanded slurry). The estimate of  $S_b$  is a little more tricky. The expression

$$S_b = \left( \frac{6h}{d_p} \right) \quad (8-129)$$

where  $h$  is the gas holdup and  $d_p$  the bubble diameter, was suggested by both Carberry [J.J. Carberry, *Chemical and Catalytic Reaction Engineering*, McGraw-Hill Book Company, New York, NY, (1976)] and Fan [L-S. Fan, *Gas-Liquid-Solid Fluidization Engineering*, Butterworths, Boston, MA, (1989)]. However, this would appear to change one estimation problem into another, since the holdup (or the bubble diameter for that matter) may not be known *a priori*. If the number of bubbles per volume,  $N$ , and the volume per bubble,  $V$ , are known, then holdup can be calculated as shown previously for gas-solid fluidized beds, and  $d_b$  also comes from the estimate. Slurry reactors, however, seem to be reluctant to yield to correlations of  $S_b$  that have any generality. In Figure 8.13a is a generalized diagram of interfacial area versus holdup resulting from a correlation of data for both bubble- and slurry-bubble columns [M. Fukuma, K. Muroyama and A. Yasunishi, *J. Chem. Eng. Japan*, 20, 321 (1987)]. These results seem to arrange themselves along a diagonal, as they are plotted, but with a very generous  $\pm$  range. Note particularly in this regard that the correlation is given on a log-log plot. Attempts at correlation of  $S_b$  versus gas bubble velocity are of about the same dubious quality (as per Figure 8.13b).

The high and low ranges of results shown in Figure 8.13b are the result of special circumstances and can be ignored in non-foaming systems that do not have high catalyst loadings. Then, once again, we have a diagonal portion of the figure reporting  $S_b$  with a generous  $\pm$  variation. Aside from the graphical correlation, Chang et al. [S.K. Chang, Y. Kang and S.D. Kim, *J. Chem. Eng. Japan*, 19, 524 (1986)] reported more quantitative results.

$$S_b = (2.08 \times 10^6)(u_g)^{0.35}(u_1)^{0.85}(d_p)^{0.85} \quad (8-130)$$

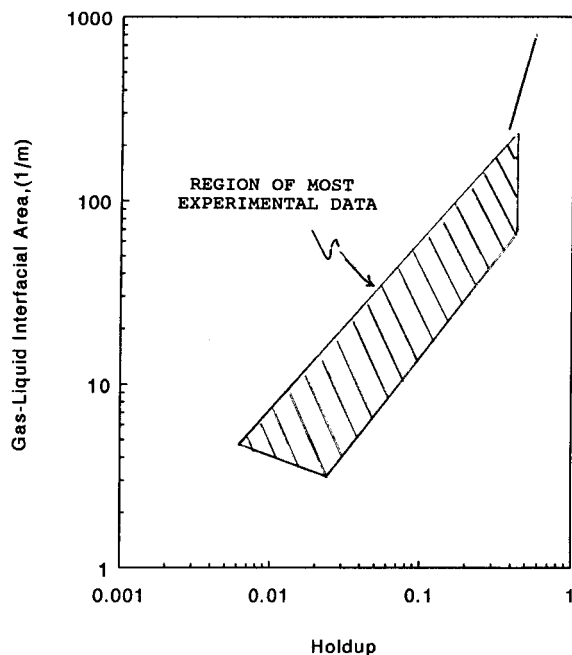


**Figure 8.13** (a) Correlation of interfacial area (gas-liquid) with holdup in slurry bubble columns. [After M. Fukuma, K. Muroyama and A. Yashnishi, *J. Chem. Eng. Japan*, 20, 321, with permission of the Japanese Society of Chemical Engineers, (1987).]

and

$$k_1 S_b = (1597)(u_g)^{0.68}(u_1)^{0.63}(d_p)^{1.12} \quad (8-131)$$

where the numerical values given are consistent with SI units, m, ( $\text{m}^2/\text{m}^3$ ), and ( $\text{mol/s}$ ).

If we substitute the parameter correlations of equations (8-125), (8-127), (8-128), and (8-129) into the expression for the overall rate constant,  $K_0$ , given by equation (8-118), then

$$\frac{1}{K_0} = \left( \frac{\rho_p d_p}{6\eta_1 \eta k} \right) \left( \frac{1}{m} \right) + \frac{d_b}{6\eta_b k_1 h} \quad (8-132)$$

Recalling that  $K_0^{-1}$  (as defined) is equal to the ratio of the observed global rate of reaction to the exit concentration of reactant in the gas phase, then a series of experiments in which rate is measured as a function of catalyst loading,  $m$ , can yield information on the magnitude of various parameters (or groups of parameters). Then plots of  $(1/R_A)$  versus  $(1/m)$  should be straight lines (always a fervent hope), with a slope of  $(\rho_p d_p / 6\eta_1 \eta k)$  and intercept  $(d_b / 6\eta_b k_1 h)$ . We must keep in mind that the graphical correlation of equations (8-130) and (8-131) are based on data from slurry bubble-columns and should be used gingerly for reactors of other geometry.<sup>8</sup>

<sup>8</sup> "We know to tell many fictions like to truths."—Hesiod

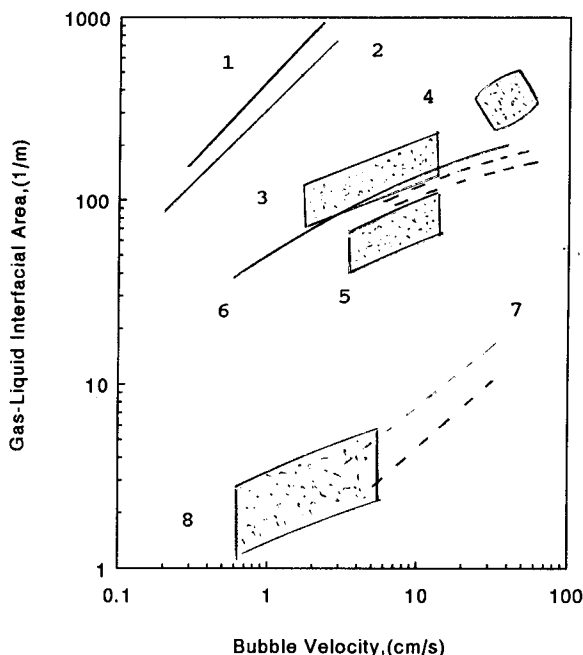


**Figure 8.13** (b) Correlation of interfacial area (gas-liquid) with bubble velocity in slurry bubble columns. 1. Deckwer et al. (1980); CO-paraffin-alumina slurry. 2. Sakai and Ohi (1977); Hydrogen-methylstyrene-Pd black slurry. 3. Quicker et al., (1984); Air-sulfite-activated carbon slurry. 4. Sada et al., (1987); Sulfite-alumina slurry. 5. Capuder and Koloni (1984); CO<sub>2</sub>-calcium hydroxide slurry. 6. Sada et al. (1987); water. 7. Godbole et al. (1983); Air-sulfite-polystyrene slurry. 8. Fukuma et al. (1987); Air-water-glass beads slurry. Citations from [L-S. Fan, *Gas-Liquid-Solid Fluidization Engineering*, Butterworths, Boston, MA (1989).]

### Illustration 8.3<sup>9</sup>

An unsaturated hydrocarbon oil is to be hydrogenated at 316 °C and 54.5 atm using a slurry reactor with a catalyst loading of 8 g-cat per liter of oil. Assuming that the oil can be maintained at hydrogen saturation what space velocity would be required if the reaction consumes 89 m<sup>3</sup> (15 °C, 1 atm) per m<sup>3</sup> liquid feed? We may assume that the catalyst is very active and that the overall rate of hydrogenation is controlled by the rate of mass transfer of hydrogen from the liquid phase to the catalyst particle surfaces. Data:

Mol. wt. Oil = 170

Specific gravity = 0.51 at 316 °C

Viscosity = 0.07 cP

$H$  = Henry's law coefficient = 5.0 (mol fraction in gas/mol fraction in liquid)

$D$  = Hydrogen in oil at 316 °C =  $5 \times 10^{-4}$  cm<sup>2</sup>/s

$d_p$  (spherical) = 0.001 cm

$\rho_p$  = 3.0 g/cm<sup>3</sup>

<sup>9</sup>[After C.N. Satterfield, *Mass Transfer in Heterogeneous Catalysis*, with permission of MIT Press, Cambridge, MA, (1970).]



*Solution*

We will consider, as an estimate from the given data, that the catalyst particles can be considered as small spheres in the limit of Stoke's settling law, where

$$N_{Pe} = \frac{d_p^3 g \Delta \rho}{18 \mu \dot{D}} = \frac{(0.001)^3 (981) (3.0 - 0.51)}{(18)(0.0007)(5 \times 10^{-4})} = 0.39$$

The corresponding  $N_{Sh}$  from Figure 8.12 is about 2.0. Now, since this is a value based on the terminal settling velocity of small spheres in liquids, it has been shown to give values that are low compared to practical situations where turbulence arising from various factors may exist. Harriott [P. Harriott, *Amer. Inst. Chem. Eng. J.*, 8, 93 (1962)] suggested that actual  $k_s$  values might range from 2 to 4 times those estimated from the figure [or from equation (8-125)]. Thus, we estimate  $k_s$  for this case as

$$k_s = \frac{(2)(2)(5 \times 10^{-4})}{0.001} = 2 \text{ cm/s}$$

The particle surface area is estimated from equation (8-125) as

$$S_p = \frac{6m}{\rho_p d_d} = \frac{(6)(8.0 \times 10^{-3})}{(3)(0.001)} = 16 \text{ cm}^2/\text{cm}^3 \text{ slurry}$$

The hydrogen concentration in the oil (pure hydrogen in the gas phase) is  $(1.0/5.0) = 0.2$  mol fraction, and for this concentration the average molecular weight of the liquid phase is 136. Assuming that the specific gravity of the saturated oil is somewhat lower than that of the pure material, say 0.15, then the hydrogen concentration in the liquid phase is about  $0.00066 \text{ gmol/cm}^3$ . Then

$$\text{Hydrogen transfer} = (2)(16)(1000)(0.00066) = 21.2 \text{ gm}$$

This gives a (LHSV) liquid hourly space velocity requirement for the feed as

$$LHSV = \frac{(21.2)(22.4)(288)(3600)}{(89)(273)}$$

or

$$LHSV = 20,200 \text{ m}^3/\text{h-m}^3$$

What happens if some things were changed around, such as hydrogen consumption, or if the rate constant (poor catalyst), was much lower?



HORATIO SAYS

Let's try to develop a profile on the case above. What happens, in addition to the problem statement, if

- The reaction consumes  $40 \text{ m}^3/\text{m}^3$  of feed?
- The reaction consumes  $120 \text{ m}^3/\text{m}^2$  feed?

All the other assumptions used in the Illustration are valid.

### 8.3 Gas-Liquid Reactors

At first glance gas-liquid reactors might appear to be easier to analyze than slurry reactors since they both involve gas and liquid phases, but the solid phase is not present in the former. On the other hand, the fluid mechanics and transport behavior have been investigated in more detail in gas-liquid systems than in gas-liquid-solid systems, so it is possible to include a little more detail in analysis if desired. The analysis and design equations can also be applied to liquid-liquid systems, as described below.

In Chapter 7 we discussed the basics of the theory concerned with the influence of diffusion on gas-liquid reactions via the Hatta theory for first-order irreversible reactions, the case for rapid second-order reactions, and the generalization of the second-order theory by Van Krevelen and Hofitjzer. Those results were presented in terms of classical two-film theory, employing an “enhancement factor” to account for reaction effects on diffusion via a simple multiple of the mass-transfer coefficient in the absence of reaction. By and large this approach will be continued here however, alternative and more descriptive mass transfer theories such as the penetration model of Higbie and the surface-renewal theory of Danckwerts merit some attention as was done in Chapter 7.

Gas-liquid reactions are most often conducted in stirred-tank systems with flow of both gas and liquid through the reactors, or in bubble columns, or in packed columns—with countercurrent flow typical in the last two. For the most part the analysis given is independent of the specific configuration of the reactor (bubbles are still with us and still important in design), but correlations for transport coefficients may vary with the individual reactor and type of operation.

#### 8.3.1 Diffusion and Reaction Considerations

If we return to the Hatta picture of reaction and diffusion, recall that reaction and diffusion occur *only* in the film. Reaction also occurs in the bulk liquid phase, of course, but there the concentration of reactants as a function of position is determined by the nature of mixing in that phase. Let us reformulate the problem so that the fraction of liquid phase occupied by the film,  $\alpha$ , is defined explicitly. If  $L$  is film thickness and  $S_L$  interfacial area, then

$$\alpha = (V/S_L L) \quad (8-133)$$

where  $V$  is the total liquid volume per volume of reactor. For diffusion and reaction in the film we have

$$\frac{d^2 f}{dy^2} = \phi^2 f \quad (8-134)$$

where the boundary conditions are

$$\begin{aligned} y = 0; \quad f &= 1 \\ y = 1; \quad -\frac{df}{dy} &= \phi^2(\alpha - 1) \end{aligned} \quad (8-135)$$

and

$$f = \left( \frac{A}{A_0} \right); \quad y = \left( \frac{1}{L} \right); \quad B = \text{constant}$$

$$\phi = K \sqrt{\frac{kB}{D}} = \frac{\sqrt{kBD}}{k_{1_o}}$$

with  $k_{1_o}$  the mass-transfer coefficient in the absence of reaction. The diffusional modulus,  $\phi$  is a first cousin of the  $a_0$  defined in Chapter 7, but the boundary condition at  $y = 1$  differs. The solution of equation (8-134) with the boundary conditions of (8-135) is

$$f = \frac{\cosh[\phi(1-y)] + \phi(\alpha-1) \sinh[\phi(1-y)]}{\cosh \phi + \phi(\alpha-1) \sinh \phi} \quad (8-136)$$

For the flux, mols/area-time,

$$(-R_A) = - \left( \frac{DA_0}{L} \right) \left( \frac{df}{dy} \right)_{y=0} = \left( \frac{DA_0}{L} \right) \frac{\phi[\phi(\alpha-1) + \tanh \phi]}{(\alpha-1)\phi \tanh \phi + 1} \quad (8-137)$$

$$(-R_A) = k_1 A_0 \quad (8-138)$$

where  $k_1$  is the mass-transfer coefficient in the presence of reaction. The enhancement factor,  $\lambda$ , defined by this result is

$$\lambda = \frac{k_1}{k_{1_o}} = \phi \left[ \frac{\phi(\alpha-1) + \tanh \phi}{(\alpha-1)\phi \tanh \phi + 1} \right] \quad (8-139)$$

We may also define a *phase utilization factor* as the ratio of observed rate to the intrinsic rate ( $kBA_0V/S_L$ )

$$\eta = \frac{\phi(\alpha-1) + \tanh \phi}{\alpha\phi[(\alpha-1)\phi \tanh \phi + 1]} \quad (8-140)$$

Limiting cases of this analysis turn out similarly to those identified in Chapter 7, so that

1.  $kB$  is large

$$\tanh \phi \rightarrow 1; \quad (k_1/k_{1_o}) = \phi; \quad \eta \rightarrow \left( \frac{1}{\phi} \right)$$

$$k_1 = \sqrt{kBD} : \quad \text{reaction within the film}$$

2.  $kB$  is small

$$\left( \frac{k_1}{k_{1_o}} \right) = \frac{\alpha\phi^2}{\alpha\phi^2 - \phi^2 + 1} \quad (8-141)$$

$$\eta = \frac{1}{\alpha\phi^2 - \phi^2 + 1} \quad (8-142)$$

The analysis for  $kB$  small may further be divided into two situations.

(a)  $\phi$  is small and  $\alpha\phi^2$  large

$$\left(\frac{k_1}{k_{1_o}}\right) \rightarrow 1; \quad k_1 \rightarrow k_{1_o}$$

$$\eta \rightarrow \frac{1}{\alpha\phi^2}$$

(b)  $\phi$  is small and  $\alpha\phi^2$  small

$$\left(\frac{k_1}{k_{1_o}}\right) < 1$$

$$\eta \rightarrow 1$$

Note that in this case the reaction occurs throughout the liquid phase and the rate is determined by the intrinsic kinetics of the chemical reaction.

The results obtained in equations (8-136) to (8-142) assume constant  $B$ , i.e., the reaction is pseudo-first-order in  $A$ . Another limiting case that yields to analytical solution is that in which the rate of reaction is very rapid and the reaction occurs wholly within the film. Here we consider the reaction  $A + \nu B \rightarrow P$  to occur very rapidly compared to mass-transfer/diffusion rates. The profiles look as in Figure 7.17b, and the overall flux and enhancement factor are given by

$$(-R_A) = k_1 A_g H_A \quad (8-143)$$

where  $H_A$  is Henry's law constant and  $A_g$  is the concentration of reactant in the gas phase. The enhancement factor is

$$\lambda = \left(\frac{D_B}{D_A}\right) \left(\frac{B}{A_g}\right) + 1$$

For the intermediate region encompassed by a finite reaction rate, in between equations (8-139) and (7-82) we have the solution of Van Krevelen and Hoftijzer [D.W. Van Krevelen and P.J. Hoftijzer, *Rec. Trav. Chim.*, 67, 563 (1984)] given in Chapter 7 by equation (7-83) and Figure 7.18.

We can summarize the major results of this section in terms of the three enhancement factor equations—(8-139), (7-82) and (7-83) for the pseudo-first-order reaction, the infinitely rapid second-order reaction, and the true second-order reaction, respectively. Via  $\lambda$  all mass-transfer coefficients under reaction conditions can be expressed in terms of their pure mass-transfer relatives, so correlations developed for the mass-transfer coefficient  $k_{1_o}$  can be used for estimation of  $k_1$ . These three cases probably constitute the large majority of gas-liquid reactions one is likely to encounter. Some additional cases are discussed by Fromont and Bischoff [G.F. Fromont and K.B. Bischoff, *Chemical Reactor Analysis and Design*, 2 ed., John Wiley and Sons, New York, NY (1990)].

### 8.3.2 Overall Analysis for Batch or Counter-Current Contactors

Here we consider a batch case with a reaction, first-order irreversible once again, with the reaction  $A \rightarrow B$  occurring in the liquid phase. The components of the liquid

phase are considered to be nonvolatile.<sup>10</sup> For the mass-transfer rate we have the normal film theory expression overall

$$N_A = k_1 S_1 (A^* - A_1) \quad (8-144)$$

with  $A^* = H_A A_g$ . Individual balances in gas and liquid phases are

$$-V_g \left( \frac{dA_g}{dt} \right) = k_1 S_1 (H_A A_g - A_1) V \quad (8-145)$$

$$-V_l \left( \frac{dA_1}{dt} \right) = k A_1 V_1 - k_1 S_1 (H_A A_g - A_1) V \quad (8-146)$$

where  $V$  is the reactor total volume. Combination of the two individual mass balance gives,

$$\left( \frac{V_g}{V k_1 S_1} \right) \frac{d^2 A_g}{dt^2} + \left( H_A + \frac{k V_g}{V k_1 S_1} + \frac{V_g}{V_1} \right) \frac{dA_g}{dt} + k H_A A_g = 0 \quad (8-147)$$

with solution of the general form

$$A_g = G_1 e^{\rho_1 t} + G_2 e^{\rho_2 t} \quad (8-148)$$

and

$$A_1 = G_1 \left( H_A + \frac{V_g \rho_1}{V k_1 S_1} \right) e^{\rho_1 t} + G_2 \left( H_A + \frac{V_g \rho_2}{V k_1 S_1} \right) e^{\rho_2 t} \quad (8-149)$$

From the initial conditions of the system,

$$G_1 + G_2 = A_{g_0} \quad (8-150)$$

and

$$G_1 \left( H_A + \frac{V_g}{V k_1 S_1} \rho_1 \right) + G_2 \left( H_A + \frac{V_g}{V k_1 S_1} \rho_2 \right) = A_{1_0} \quad (8-151)$$

For B, assuming equimolal reaction with A, we have from stoichiometry

$$B_1 = (A_{g_0} - A_g) \left( \frac{V_g}{V_1} \right) + (A_{1_0} - A_1) \quad (8-152)$$

Now, for nonvolatile reactant B,  $B_g = 0$ . If we are dealing with a liquid-liquid system, however, another balance can be written for B (assuming here and above that  $B_{1_0} = 0$ ).

$$\left[ \frac{V_1}{V(k_1 S_1)_B} \right] \frac{d^2 B_1}{dt^2} + \left( \frac{V_1}{V_2} + H_B \right) \frac{dB_1}{dt} = k A_2 \quad (8-153)$$

where 1 and 2 refer to the two liquid phases involved. Thus,

$$B_1 = H_0 + H_1 e^{\sigma t} + A_1 e^{\rho_1 t} + A_2 e^{\rho_2 t} \quad (8-154)$$

<sup>10</sup> The analysis here is sufficiently general that it can be applied to liquid-liquid reactions as well, with only minor modifications [See P. Trambouze, M.T. Trambouze and E.L. Piret, *Am. Soc. Chem. Eng. Jl.*, 7, 138 (1961).]

where

$$A_1 = \frac{kG_1[H_A + \rho_1 V_1/(k_1 S_1)_A V]}{\rho_1[\rho_1 V_1/(k_1 S_1)_B V + (V_1/V_2) + H_B]}$$

$$A_2 = \frac{kG_2[H_A + \rho_1 V_1/(k_1 S_1)_A V]}{\rho_1[\rho_1 V_1/(k_1 S_1)_B V + (V_1/V_2) + H_B]}$$

and

$$B_2 = H_B H_0 + H_1 \left[ \frac{V_1 \sigma}{V(k_1 S_1)_B} + H_B \right] e^{\sigma t} + A_1 \left[ \frac{V_1 \rho_1}{V(k_1 S_1)_B + H_B} \right] e^{\rho_1 t}$$

$$+ A_2 \left[ \frac{V_1 \rho_2}{V(k_1 S_1)_B + H_B} \right] e^{\rho_2 t} \quad (8-155)$$

The constants  $H_0$  and  $H_1$  are also determined from initial conditions. For  $\rho_1$  and  $\rho_2$  we start with (8-147) again, now in operator notation

$$(AD^2 + ND + R)A_1 = 0$$

Then,

$$D = \frac{-N \pm \sqrt{N^2 - 4AR}}{2A}$$

where  $A$ ,  $N$  and  $R$  are identified with the corresponding coefficient terms in equation (8-147). Thus,  $A = V_1/V(k_1 S_1)_A$ , and so on. The result is,

$$\rho_1, \rho_2 = \frac{-[H_A + kV_1/Vk_1 S_1)_A + (V_1/V_2)]}{2V_1/V(k_1 S_1)_A}$$

$$\pm \frac{\{[H_A + kV_1/V(k_1 S_1)_A + (V_1/V_2)]^2 - 4H_A(k_1 S_1)_A V_1/V(k_1 S_1)_B\}^{1/2}}{2V_1/V(k_1 S_1)_A}$$

This analysis gives the general result for a batch reaction (both phases) for either gas-liquid or liquid-liquid reactions—in the latter case for reactant B distributed between both phases (but reaction in phase 2 only). Determination of the constants ( $G$  and  $H$ ) is left as an algebraic exercise for those with sufficient patience.

For the case of a *countercurrent contactor*, we envision the arrangement as shown in Figure 8.14. We will consider that both phases are in plug flow, and again we have the irreversible reaction that occurs in phase 2. Since we have the possibility of either gas-liquid or liquid-liquid reaction, we will just number the phases 1 and 2. Now, over  $dy$ , we can write the mass balances as

$$d(F_1 A_1) - K_A(A_2^* - A_2)S_c dy = 0 \quad (8-156)$$

$$d(F_2 A_2) - K_A(A_2^* - A_2)S_c dy = kA_2 S_c \epsilon dy \quad (8-157)$$

where  $S_c$  is a contact area defined such that  $\epsilon S_c dy = dV_2$ . The equilibrium will be

$$A_2^* = \alpha_A A_1 + \beta_A$$

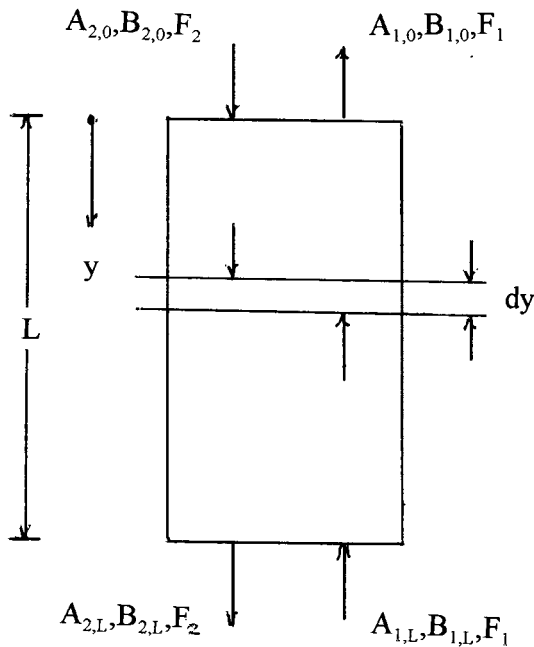


**Figure 8.14** A countercurrent reactor; gas-liquid or liquid-liquid.

This is a linear relationship, but more complex than Henry's law, so

$$\frac{F_1}{S_c} \left( \frac{dA_1}{dy} \right) - K_A \beta_A + K_A A_2 - K_A \alpha_A A_1 = 0 \quad (8-158)$$

and

$$-\frac{F_2}{S_c} \left( \frac{dA_2}{dy} \right) + K_A \beta_A - K_A \alpha_A A_1 - k \epsilon A_2 = 0 \quad (8-159)$$

where  $k$  is the rate constant for the first-order reaction, here assuming pseudo-first order in the transferred component A. Combining by eliminating  $A_1$

$$\left( \frac{F_1 F_2}{K_A S_c^2 \alpha_A} \right) \frac{d^2 A_2}{dy^2} + \frac{1}{S_c} \left[ \frac{F_1}{\alpha_A} \left( 1 + \frac{k \epsilon}{K_A} \right) - F_2 \right] \frac{dA_2}{dy} - k \epsilon A_2 = 0 \quad (8-160)$$

so

$$A_2 = G_1 e^{\rho_1 y} + G_2 e^{\rho_2 y}$$

This really gets a lot worse, but since an analytical solution in terms of the reactor/reaction parameters is available, one can't dodge it. For the exponential constants

$\rho_1$ , and  $\rho_2$  we have

$$\rho_1, \rho_2 = - \left\{ \frac{F_1}{\alpha_A} \left[ 1 + \left( \frac{k\epsilon}{K_A} \right) \right] - F_2 \left( \frac{1}{2F_1F_2/K_A S_c \alpha_A} \right) \right. \\ \left. \pm \frac{\left\{ \left[ \frac{F_1}{\alpha_A} \left( 1 + \frac{k\epsilon}{K_A} \right) - F_2 \right]^2 + \frac{4k\epsilon F_1 F_2}{K_A \alpha_A} \right\}^{1/2}}{(2F_1F_2/K_A S_c \alpha_A)} \right\}$$

The concentration  $A_1$  may be evaluated from equation (8-156), similarly indigestible but unavoidable,

$$\beta_A + \alpha_A A_1 = G_1 \left( \frac{F_2}{K_A S_c} \rho_1 + \frac{K_A + k\epsilon}{K_A} \right) e^{\rho_1 y} + G_2 \left( \frac{F_2}{K_A S_c} \rho_2 + \frac{K_A + k\epsilon}{K_A} \right) e^{\rho_2 y} \quad (8-161)$$

Similarly for  $B_1$  and  $B_2$

$$B_2 = H_0 + H_1 e^{\sigma y} + A_1 e^{\rho_2 y} + A_2 e^{\rho_2 y} \quad (8-162)$$

where

$$\sigma = \frac{S_c K_B \alpha_B}{F_1 F_2} \left( F_2 - \frac{F_1}{\alpha_B} \right) \\ D_1 = \frac{2k\epsilon G_1}{\rho_1} + \frac{F_1 \rho_1 - S_c K_B \alpha_B}{(F_1 F_2 \rho_1 / S_c) + F_1 K_B - F_2 K_B \alpha_B} \\ D_2 = \frac{2k\epsilon G_2}{\rho_2} + \frac{F_1 \rho_2 - S_c K_B \alpha_B}{(F_1 F_2 \rho_2 / S_c) + F_1 K_B - F_2 K_B \alpha_B}$$

and

$$B_1 = \frac{1}{\alpha_B} \left[ H_0 - \beta_B + H_1 \left( \frac{F_2 \sigma}{S_c K_B} + 1 \right) e^{\sigma y} + D_1 \left( \frac{F_2 \rho_1}{S_c K_B} + 1 \right) e^{\rho_1 y} \right. \\ \left. + D_2 \left( \frac{F_2 \rho_2}{S_c K_B} + 1 \right) e^{\rho_2 y} - \frac{2k\epsilon}{K_B} (G_1 e^{\rho_1 y} + G_2 e^{\rho_2 y}) \right] \quad (8-163)$$

As for the batch case,  $H_0$  and  $H_1$  are determined from the feed compositions. In these analyses, whenever we can write two mass balances with only the first derivative of concentration, they may be combined into a single second-order equation for one concentration.

### 8.3.3 Another Approach

The basic equations for these gas-liquid reactors are, to start with, not terribly complicated or difficult to understand conceptually, but the analysis of the section above shows that we are left with cumbersome solutions with many terms—enough so that one might reasonably feel somewhat uncomfortable working with them.

Another way to approach the topic of gas-liquid reactor design is just to state the basic phase balances in very general form, and then simplify according to the particular situation. A possible drawback is that there is a seemingly endless number of these individual situations, e.g., is there plug flow or CSTR behavior (in one or both phases), is bubble size constant, is the equilibrium according to Henry's law,



and so on. We seek some reasonable classification scheme to order these various possibilities. One such scheme is to divide the treatment into analysis of systems either involving gas-liquid "tank-type" reactors or systems involving "tubular" reactors (normally vertical, but not always), and then proceed with subdivisions in the pertinent area. This approach was established by Russell et al. [R.W. Schaftelein and T.W.F. Russell, *Ind. Eng. Chem.*, 60, 12 (1968); P.T. Cichy, J.S. Ultman and T.W.F. Russell, *Ind. Eng. Chem.*, 61, 6 (1969)] and will be followed.

### *Tank-type reactors*

These are generally classified as either CSTRs, semiflow batch reactors (SFBR), or plain batch reactors, which we treated in the previous section. If the reactor is well-mixed, the liquid-phase mass balance is the same general form for all. For component  $j$ ,

$$vC_{oj} - vC_j + K_G a' P V_b N V_L \left( y_j - C_j \frac{H}{P} \right) - r_j V_L = \frac{d}{dt} (V_L C_j) \quad (8-164)$$

where  $a'$  is the ratio of surface area to single bubble volume ( $\lambda$ ),  $V_b$  the volume of a single bubble ( $\lambda^3$ ),  $N$  the number of bubbles per unit volume of liquid,  $r_j$  the rate of reaction for component  $j$ ,  $V_L$  volume of the liquid phase, and  $v$  is the volumetric flow rate of the liquid phase.

One can see immediately that this approach will be a little more detailed than the previous section, since the bubble mechanics are contained in the basic material balance. Various simplifications of equation (8-164) are possible according to the reactor type by deleting terms; for a steady-state CSTR the time derivative is zero, for a batch reactor the flow rate terms are zero, etc. For the gas phase the situation is complicated by the fact that the configuration (and concentration) of bubbles can be a function of both time and position; that is, the total mass of  $j$  in a given bubble,  $(P V_b y_j / RT)$ , can depend on both position  $z$  and time  $t$ .

If the bubbles are passed through the liquid phase in the absence of mechanical agitation it is possible to approach plug flow behavior, and the gas (bubble) mass balance is

$$-K_G a' P V_b \left( y_j - C_j \frac{H}{P} \right) - v_b \frac{\partial}{\partial z} \left( \frac{P V_b}{RT} y_j \right) = \frac{\partial}{\partial t} \left( \frac{P V_b}{RT} y_j \right) \quad (8-165)$$

where  $H$  is Henry's law constant and  $v_b$  is the bubble velocity. If there is mechanical agitation, or other factors that promote mixing in the liquid phase, then the well-mixed bubble mass balance is

$$G_1 y_{oj} - G_2 y_j - K_G a V_L P \left( y_j - C_j \frac{H}{P} \right) = \frac{d}{dt} \left[ (N V_L V_b) \left( \frac{P y_j}{RT} \right) \right] \quad (8-166)$$

with  $G_1$ ,  $G_2$  the molar gas flow into and out of the reactor,  $a V_L$  the total area for mass transfer,  $N V_L V_b$  the total gas volume, and  $a$  the mass-transfer area per unit volume of continuous phase. From the above we can also define the average liquid residence time,

$$t_L = V_L / v$$

and the total surface area per volume of liquid

$$a = a' V_L N$$

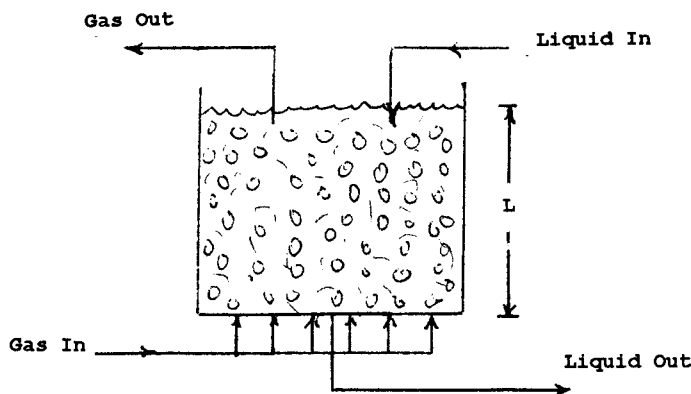


**Figure 8.15** A CFTR with plug-flow gas and well-mixed liquid phases.

Now, on the basis of equations (8-164) to (8-166) we can break down the analysis into simplified forms that apply to very specific situations. The most obvious place to start is with the continuous flow case with both gas and liquid passing through the reactor [termed *continuous flow tank reactors* (CFTR) by Russell et al.], as shown in Figure 8.15. Let us look at some of the specific situations.

*Plug-flow gas and well-mixed liquid CFTR.* From the general balance of equations (8-164) and (8-165), for the gas phase in steady state

$$-K_G a' P V_b \left( y_j - C_j \frac{H}{P} \right) - v_b \frac{d}{dz} \left( \frac{P V_b}{RT} y_j \right) = 0 \quad (8-167)$$

and for the liquid phase

$$v C_{oj} - v C_j + K_G \bar{a}' P \bar{V}_b N V_L \left( \bar{y}_j - C_j \frac{H}{P} \right) - r_j V_L = 0 \quad (8-168)$$

where the overlined quantities represent suitable average values for the liquid phase. The gas-phase concentration is a function of position if the gas feed is not composed of pure reactant, so averages such as

$$\bar{y}_j = \left( \frac{1}{L} \right) \int_0^L y_j(z) dz \quad (8-169)$$

must be computed in the most general case.

Now we have written the balance in some detail as to the properties and behavior of the gas (bubble) phase, so we must establish further subclassifications according to this. Consider  $V_b$  constant, which will be true if  $y_j$  is small or mass transfer is slow. In this case  $a'$  and  $V_b$  are both constant, and equation (8-167) can be integrated directly as

$$y_j = C_j \left( \frac{H}{P} \right) + \left( y_{oj} - C_j \frac{H}{P} \right) \exp(-K_G a' R T L / v_b) \quad (8-170)$$

and from equation (8-169)

$$\bar{y}_j = C_j \left( 1 - \frac{1 - e^{-n}}{n} \right) \left( \frac{H}{P} \right) + y_{oj} \left( \frac{1 - e^{-n}}{n} \right) \quad (8-171)$$

with  $n = (K_G a' RTL / v_b)$ . For the liquid-phase concentration, the best we can do is an implicit equation for  $C_j$  obtained by substituting  $y_j$  in equation (8-168),

$$C_j = C_{oj} + \left[ y_{oj} - C_j \left( \frac{H}{P} \right) \right] \left( \frac{P V_b N V_L v_b}{RT v_L} \right) \cdot \left[ 1 - \exp \left( - \frac{K_G a' RTL}{v_b} \right) \right] - r_j \left( \frac{V_L}{v} \right) \quad (8-172)$$

Another important case is that for  $V_b = \text{constant}$  but  $y_j = 1$  (pure gas phase). Here the bubble volume changes because of the transfer of reactant into the liquid (reaction) phase, and both  $a'$  and  $V_b$  are functions of position. We have to have some detail on the bubbles. If it is assumed that all bubbles are spherical, then

$$S = (6)^{2/3} \pi^{1/3} = 4.84 \quad (8-173)$$

$$a' = S V_b^{-1/3}$$

where  $S$  is a bubble shape factor. An expression for the bubble rise velocity, borrowed from Davidson and Harrison, is

$$v_b = W V_b^{1/6} \quad (8-174)$$

with

$$W = (0.711) g^{1/2} (6/\pi)^{1/6}$$

The gas-phase balance can now be integrated to give us  $V_b$  as a function of  $z$

$$V_b(z) = \left\{ V_{0b}^{1/2} - \frac{K_G RTS}{2W} \left[ 1 - C_j \left( \frac{H}{P} \right) \right] z \right\}^2 \quad (8-175)$$

and

$$\bar{V}_b = V_{0b} + \left( \frac{L^2 F^2}{3} - V_{0b}^{1/2} L F \right) \quad (8-176)$$

$$F = \frac{K_G RTS}{2W} \left[ 1 - C_j \left( \frac{H}{P} \right) \right] \quad (8-177)$$

and from equation (8-173)

$$\bar{a}' = S \bar{V}_b^{1/3} \quad (8-178)$$

Again we obtain an implicit equation for  $C_j$ , this time in terms of  $a'$  and  $V_b$ ,

$$C_j = C_{oj} + K_G \bar{a}' \bar{V}_b N P \left( \frac{V_L}{v} \right) \left[ 1 - C_j \left( \frac{H}{P} \right) \right] - r_j \left( \frac{V_L}{v} \right) \quad (8-179)$$

Keep in mind for later calculation via equations (8-172) and (8-179) that all the odds and ends are still not tidied up, because we still need numbers for quantities such as  $V_{0b}$  and  $N$ .

The most general case is for CFTRs in which  $V_b \neq \text{constant}$  and  $y_j \neq 1$ . The overall gas-phase balance is now

$$-K_G a' P V_b \left[ y_j - C_j \left( \frac{H}{P} \right) \right] - v_b \frac{d}{dz} \left( \frac{P V_b}{RT} \right) = 0$$

which we can rewrite as

$$K_G a' R T \left[ y_j - C_j \left( \frac{H}{P} \right) \right] + \frac{v_b}{(1 - y_j)} \left( \frac{dy_j}{dz} \right) = 0 \quad (8-180)$$

This equation requires expressions for  $a'$  and  $v_b$  as related to  $y_j$  in order to be solved. The path to solution is sort of convoluted:  $a'$  and  $v_b$  are functions of  $V_b$ , as shown in equations (8-173) and (8-174). Then we can obtain  $a'$  and  $v_b$  via

$$\int_{a'_o}^{a'} da' = \int_{y_{oj}}^{y_j} \left( \frac{da'}{dV_b} \right) \frac{v_b}{(1 - y_j)} dy_j$$

and  $V_b$  is related to  $y_j$  via

$$V_b = V_{0b} \left( \frac{1 - y_{oj}}{1 - y_j} \right)$$

Step by step, then, with  $a'$  and  $v_b$  as functions of  $y_j$ , equation (8-180b) can be integrated and  $\bar{y}_j$  determined. The value of  $V_b$  is then obtained from the overall mass balance using  $y_j$  as obtained from (8-180b). With  $\bar{V}_b$  known, then  $\bar{a}'$  can be determined.

*Well-mixed gas and liquid phases in the CFTR.* In this case, under steady-state conditions, there is no variation of concentration with position. Although it is possible to obtain some degree of mixing in the gas phase through bubble motion alone, normally tank-type reactors fitting this description are agitated via externally powered impellers of various designs. The following were obtained directly from equations (8-164) and (8-166). For the gas,

$$G_1 y_{oj} - G_2 y_j - K_G a V_L P \left[ y_j - C_j \left( \frac{H}{P} \right) \right] = 0 \quad (8-181)$$

and for the liquid,

$$\left( \frac{v}{V_L} \right) (C_{oj} - C_j) + K_G a P \left[ y_j - C_j \left( \frac{H}{P} \right) \right] - r_j = 0 \quad (8-182)$$

These form an algebraic pair, and the overall two-phase model is obtained by determining  $y_j$  from equation (8-181) and substituting it into (8-182).

The second important configuration is that of the *semiflow batch reactor (SFBR)*, in which the liquid phase is contained and only the gas flows through. This is also envisioned in Figure 8.15, but with no liquid flow. Again, we will take the liquid phase to be well-mixed, with limiting gas-phase behavior either plug flow or well mixed.

*Plug-flow gas, well-mixed liquid SFBR.* Here, from the general phase balance, for the gas

$$K_G a' P V_b \left[ y_j - C_j \left( \frac{H}{P} \right) \right] + v_b \frac{d}{dz} \left( \frac{P V_b}{RT} y_j \right) = 0 \quad (8-183)$$

and for the liquid,

$$K_G a' P V_b N V_L \left[ \bar{y}_j - C_j \left( \frac{H}{P} \right) \right] - r_j V_L = \frac{d}{dt} (V_L C_j) \quad (8-184)$$

An important point in analysis is that even though the batch liquid-phase concentration is time dependent, this is not important if changes (within one bubble rise-time in the reactor) are small compared to changes with respect to position. For  $V_b = \text{constant}$  and first-order reaction in the liquid phase, we first obtain  $y_j$  as in equation (8-169) to (8-171). For the liquid phase the balance is

$$\frac{dC_j}{dt} = -C_j (H K_G a' V_b N + k) + K_G a' P V_b N \bar{y}_j \quad (8-185)$$

Substituting for  $y_j$  and simplifying gives

$$\frac{dC_j}{dt} + k_1 C_j = k_2 \quad (8-186)$$

$$C_j = \left( \frac{k_2}{k_1} \right) + (C_{oj} - k_2/k_1) e^{-k_1 t} \quad (8-187)$$

where

$$k_1 = k + (1 - e^{-n}) H V_b N v_b / R T L$$

$$k_2 = y_{oj} (1 - e^{-n}) V_b N v_b P / R T L$$

and  $k$  is the reaction rate constant.

For  $V_b \neq \text{constant}$  but  $y_j = 1$ , the general equations yield, for the gas phase, equation (8-183) again, and for variable bubble volume equations (8-176) to (8-178) again. Substituting into the liquid-phase model, (8-184), gives

$$\frac{dC_j}{dt} = -C_j (H K_G \bar{a}' \bar{V}_b N + k) + K_G \bar{a}' \bar{V}_b N P \quad (8-188)$$

Solution of this set of equations is best accomplished numerically. Horatio may ask a question about this later.

*Well-mixed gas, well-mixed liquid SFBR.* In this case the concentrations are spatially invariant, but do depend on time because of the batch liquid phase. For the gas

$$G_1 y_{oj} - K_G a V_L P \left[ y_j - C_j \left( \frac{H}{P} \right) \right] = 0 \quad (8-189)$$

and for the liquid,

$$K_G a P \left[ y_j - C_j \left( \frac{H}{P} \right) \right] - k C_j = \frac{dC_j}{dt} \quad (8-190)$$

Here the gas-phase equation may be solved for  $y_j$ ; this is substituted into the liquid-phase equation which can then be integrated to obtain  $C_j(t)$ . The results are of the same form as equations (8-187a) end (8-187b).

#### *Tubular or Column Reactors*

The approach to analysis of reactors of this type depends to a large extent on the nature of the flow patterns. (Is this news?) In bubble-column reactors, which are of

primary interest, such patterns can be described in a way similar to those used for fluidized beds. A general description would include the following:

1. Dispersed flow. Liquid flows as individual droplets in a high-velocity turbulent gas stream.
2. Annular-flow. Liquid flows as a thin film around the inner surface of the column. The film thickness is not usually a function of position within the column, but the gas-liquid interface is not smooth.
3. Slug flow. Here we have alternating flows of gas and liquid slugs that are of the same size as the column diameter.
4. Bubble flow. The gas travels in discrete volumes with a distribution of sizes and shapes, ranging from single bubbles moving separately to bubble swarms or clouds.

An analysis of flow patterns in vertical countercurrent contactors was reported by Govier et al. [G. Govier, B.A. Rodford, and J.S.C. Dunn, *Can. J. Chem. Eng.*, 38, 58 (1957)] and a generalized flow regime chart based on their findings is given in Figure 8.16.

In fact, the flow patterns are even more complex than appear in the figure. Russell and co-workers identified no less than 26 regions of flow behavior, including both horizontal and vertical configurations [P.T. Cichy, J.B. Ultman, and T.W.F. Russell, *Ind. Eng. Chem.*, 61, 6 (1968)]. The most basic divisions, as far as reactor modeling is concerned, are those systems in which both gas and liquid phases are continuous versus those in which the two phases are discrete. Those are treated accordingly below.

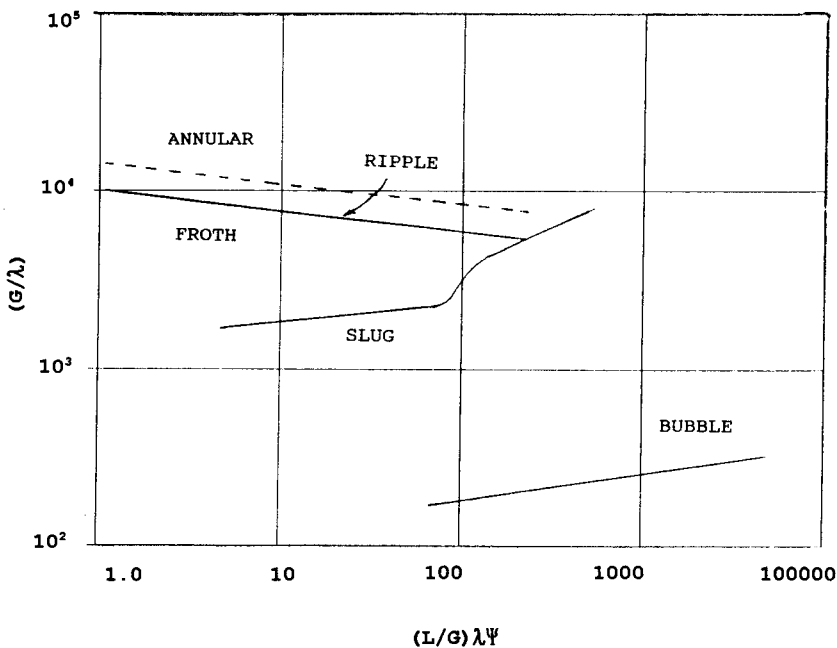


**Figure 8.16** Govier chart for bubble-liquid flow in vertical columns.  $\lambda = (\rho_G/0.075)(\rho_L/62.3)^{1/2}$ ;  $\psi = (73/\gamma_L)[\mu_L(63.2/\rho_L)^2]^{1/3}$ . [O. Baker, *Oil Gas J.*, 56, 256 (1958).]

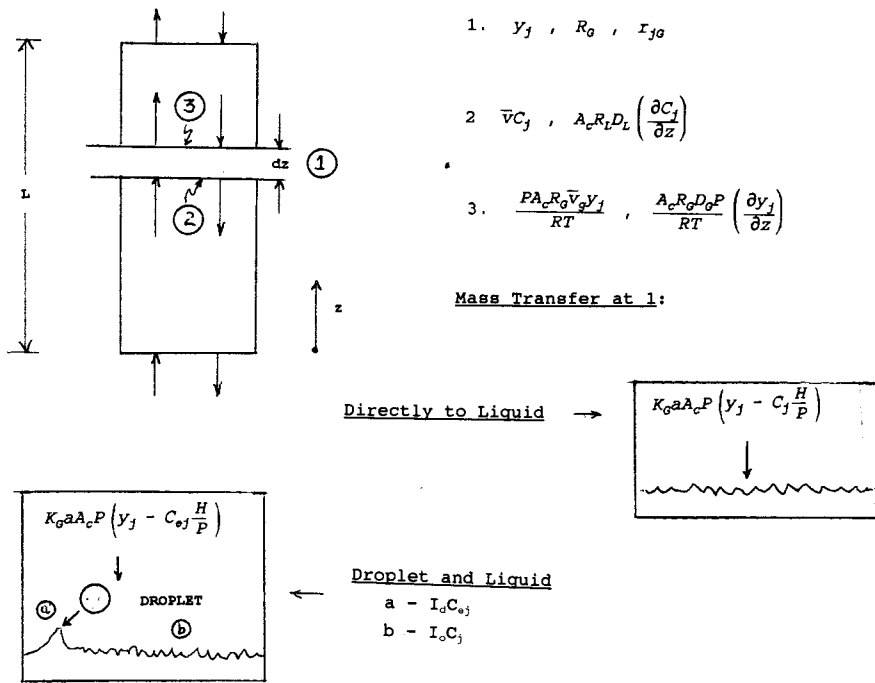


Figure 8.17 A two-phase mass transfer model for gas-liquid reactors.

When the two phases may be considered as continuous, we can envision the transport and reaction process as shown in Figure 8.17. This two-phase model, as written for a length,  $dz$ , and a column cross sectional area,  $A_c$ , comprises both the familiar term for interphase transfer plus the addition of mass transfer from the gas phase to entrained liquid droplets, given by  $(I_o C_j / \rho_0)$  and  $(I_d \bar{C}_{ej} / \rho_d)$  to account for convective transport to and from the droplets. The quantity  $I_d$  is the rate of deposition of the dispersed droplet phase on the liquid film ( $m/tz$ ) and  $I_o$  is a corresponding rate of entrainment from the liquid phase into droplets. The very general mass balances below will consider both types of mass transfer, will also consider the possibility of reaction in both gas and liquid phases, and will include a dispersion factor to model deviations from actual plug flow if necessary. Now this is a little like diving off the 10 meter board, but here we go with the continuous gas-phase balance.

$$\begin{aligned} \frac{\partial}{\partial t} \left( \frac{Py_j R_G A_c}{RT} \right) = & - \frac{\partial}{\partial z} \left( \frac{\bar{v}_b Py_j R_G A_c}{RT} \right) - K_G a A_c P \left[ y_j - C_j \left( \frac{H}{P} \right) \right] \\ & - \frac{\partial}{\partial z} \left( \frac{PR_G A_c D_G}{RT} \frac{\partial y_j}{\partial z} \right) - r_G R_G A_c \\ & - (K_G a)' A_c P \left[ y_j - \left( \frac{\bar{C}_{oj} H}{P} \right) \right] \end{aligned} \quad (8-191)$$

where  $R_L$  is the liquid-phase holdup and  $R_G = (1 - R_L)$ ,  $r_G$  is the gas-phase rate of reaction in mols/time-volume, and  $\bar{C}_{oj}$  is the average concentration of species  $j$  in the

entrained liquid phase. The two mass-transfer coefficients  $(K_G a)'$  and  $K_G a$  are included to account for differences between direct transfer from the gas phase and transfer via dispersed droplets. Now, continuing with the liquid-phase balance,

$$\begin{aligned} \frac{\partial}{\partial t} (R_L A_c C_j) = & -\frac{\partial}{\partial z} (\bar{v} R_L A_c C_j) + K_G a A_c P \left[ y_j - C_j \left( \frac{H}{P} \right) \right] \\ & - \frac{\partial}{\partial z} \left( A_c R_L D_L \frac{\partial C_j}{\partial z} \right) - r_L R_L A_c - \frac{I_0 C_j}{\rho_0} + \frac{I_d \bar{C}_{oj}}{\rho_d} \end{aligned} \quad (8-192)$$

The dispersion coefficients  $D_G$  and  $D_L$  are included to account for deviations from plug flow in both gas and liquid phases, as mentioned above. Equations (8-191) and (8-192) include all possibilities (or at least as many as we are willing to consider at this point), so we can now look at individual cases of interest by chipping away the particular parts that do not apply.

*Continuous fluid phases with a well-defined interface.* This case, not particularly the most important, is nonetheless convenient to start with since the interface between phases formed by vertical annular flow without droplets gives us an area for mass transport that is easy to determine.<sup>11</sup>

Other important assumptions for this example consist of operation in the steady state, liquid holdup constant (or represented by an appropriate average value), reaction in the liquid phase only, first-order irreversible kinetics (yet again), constant temperature and total pressure, and  $H$  independent of concentration. These assumptions allow some considerable simplifications to the general balance equations given above. First, we will define gas and liquid flow rates as

$$G = \frac{P R_G A_c \bar{v}_b}{RT}; \quad q = R_L A_c \bar{v}$$

For the gas phase,

$$\frac{d}{dz} (G y_j) = -K_G a A_c P \left[ y_j - C_j \left( \frac{H}{P} \right) \right] - \frac{R_G A_c D_G P}{RT} \left( \frac{d^2 y_j}{dz^2} \right) \quad (8-193)$$

and for the liquid phase,

$$q \left( \frac{dC_j}{dz} \right) = K_G a A_c P \left[ y_j - C_j \left( \frac{H}{P} \right) \right] - A_c R_L D_L \left( \frac{d^2 C_j}{dz^2} \right) - k R_L A_c C_j \quad (8-194)$$

In addition, we can write an overall gas-phase balance

$$\left( \frac{dG}{dz} \right) = -K_G a A_c P \left[ y_j - C_j \left( \frac{H}{P} \right) \right] \quad (8-195)$$

in the event that there are significant changes in the gas flow rate through the contactor.

This model bears a familial resemblance to some that were discussed earlier in this chapter. When the dispersion terms are discarded and appropriate changes in the names and significance of some of the parameters are recognized, then we end up basically at the Davidson-Harrison model for fluidized beds.

<sup>11</sup> We deviate from the wise advice to “do the most important thing first ...” to “do the easiest thing first ...”



The first consideration is the very general one where both the gas-phase flow rate,  $G$ , and the solute concentration,  $C_j$ , are functions of axial position, but plug flow prevails. This is roughly the situation when the solute is transferred from a concentrated gas stream. The following governing equations can be written.

*Gas phase*

$$\frac{G(z)}{(1-y_j)} \left( \frac{dy_j}{dz} \right) = -K_G a A_c P \left[ y_j - C_j \left( \frac{H}{P} \right) \right] \quad (8-196)$$

*Liquid phase*

$$q \left( \frac{dC_j}{dz} \right) = K_G a A_c P \left[ y_j - C_j \left( \frac{H}{P} \right) \right] - k R_L A_c C_j \quad (8-197)$$

where

$$G(z) = G_0 - \int_0^z K_G a A_c P \left[ y_j - C_j \left( \frac{H}{P} \right) \right] dz$$

After evaluation of  $G(z)$ , the concentration profile can be obtained using a procedure similar to that suggested for equations (8-180a) and (8-180b).

When dispersion is not important and  $G$  is constant, we have a much simpler situation.

$$\left( \frac{dy_j}{dz} \right) = -\frac{K_G a A_c P}{G} \left[ y_j - C_j \left( \frac{H}{P} \right) \right] \quad (8-198)$$

$$\left( \frac{dC_j}{dz} \right) = \frac{K_G a A_c P}{G} \left( \frac{G}{q} \right) \left[ y_j - C_j \left( \frac{H}{P} \right) \right] - \frac{k R_L A_c C_j}{q} \quad (8-199)$$

This can be solved directly for the liquid concentration profile,

$$\begin{aligned} C_j(z) = C_0 & \left[ \frac{(1-r_1)}{(r_2-r_1)} \exp \left( -\frac{K_G a A_c P}{G} r_1 z \right) - \frac{(1-r_1)}{(r_2-r_1)} \exp \left( -\frac{K_G a A_c P}{G} r_2 z \right) \right] \\ & + \frac{y_0 G}{q} \left[ \left( \frac{1}{(r_2-r_1)} \right) \exp \left( -\frac{K_G a A_c P}{G} r_1 z \right) \right] \\ & - \left( \frac{1}{(r_2-r_1)} \right) \exp \left( -\frac{K_G a A_c P}{G} r_2 z \right) \end{aligned} \quad (8-200)$$

where

$$\begin{aligned} -r_1 &= \left( \frac{1}{2\alpha} \right) [-(1+\beta+\alpha) + (1+2\beta+\beta^2+2\alpha-2\alpha\beta+\alpha^2)^{1/2}] \\ -r_2 &= \left( \frac{1}{2\alpha} \right) [-(1+\beta+\alpha) - (1+2\beta+\beta^2+2\alpha-2\alpha\beta+\alpha^2)^{1/2}] \end{aligned}$$

where

$$\alpha = \frac{Pq}{(1+G)}; \quad \beta = \frac{k R_L}{K_G a H}$$

When dispersion is not important and there is a pure gas phase, then

$$y_j = 1$$

$$C_j = C_0 \exp \left[ - \left( \frac{A_c}{q} \right) (HK_G a + kR_L) z \right] + \frac{K_G a P}{HK_G a + kR_L} \left\{ 1 - \exp \left[ - \left( \frac{A_c}{q} \right) (HK_G a + kR_L) z \right] \right\} \quad (8-201)$$

*One continuous and one discrete fluid phase.* Most often this will be a discrete (bubble) phase and a continuous liquid phase. The simplifying assumptions made above will be retained for this case as well. For the general model equations (8-191) and (8-192), with negligible dispersion and constant bubble size and velocity in the gas phase,

$$\left( \frac{dy_j}{dz} \right) = - \frac{K_G a' RT}{\bar{v}_b} \left[ y_j - C_j \left( \frac{H}{P} \right) \right] \quad (8-202)$$

where  $\bar{v}_b$  is the average velocity of bubble phase rise. For the liquid phase,

$$\left( \frac{dC_j}{dz} \right) = \frac{N_B V_{DG} K_G a' A_c P}{q} \left[ y_j - C_j \left( \frac{H}{P} \right) \right] - \frac{kR_L A_c}{q} C_j \quad (8-203)$$

with  $N_B$  the number of bubbles per reactor volume,  $V_{DG}$  the volume of bubble, and  $K_G a'$  the mass-transfer coefficient based upon the area per unit volume ( $a'$ ) of discrete phase.

Finally, assuming no dispersion and pure gas phase,

$$\left( \frac{dC_j}{dz} \right) = \frac{N_B A_c K_G a' P}{q} \left[ y_j - C_j \left( \frac{H}{P} \right) \right] - \frac{kR_L A_c}{q} C_j \quad (8-204)$$

with initial conditions for both (8-203) and (8-204) of  $C_0$  at  $z = 0$ .

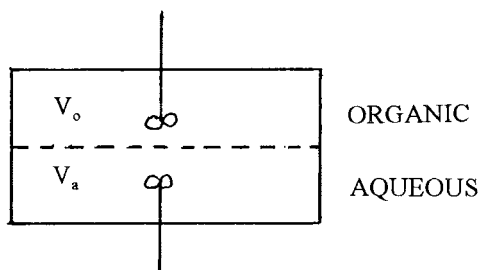
Well, the idea was to try to simplify some of the equations we started with, but the temptation was too much, and we included all the bubble interactions. The equations become large; so much for that good intention.<sup>12</sup>

Now, our quest for knowledge concerning gas-liquid reactors, if we look at it, began with equation (8-164); so we should feel nearly saturated at this point. In fact, though, there are many other cases considered in the work of Russell et al., that may be of use in certain applications. We have taken what might be considered the most important, or most frequently encountered for presentation. As in the case for fluid-bed or slurry reactors, we must now determine where the many parameters appearing in the reactor equations for gas-liquid systems originated. But first, an example.

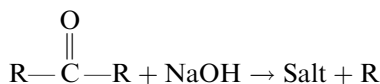
#### Illustration 8.4

Consider the batch liquid-liquid contractor illustrated below, in which the two largely nonmiscible phases are agitated sufficiently to be homogeneous in concentration, but not sufficiently to disperse one of the phases into the other. (We note that this is a liquid-liquid reactor, not gas-liquid, but the flexibility of the gas-liquid theory will be seen here. Some of the correlations may be different.)

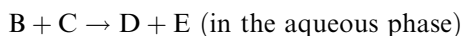
<sup>12</sup>“The road to Hell is paved with good intentions.”—*W. J. Butt*



An example of this type of reactor/reaction would be



that is,



The mass transfer occurs from the organic to the aqueous phase only, and it may be assumed that  $V_o$  and  $V_a$ , do not change as the reaction progresses. We define the concentration of reactant as A in the organic phase and B in the aqueous (reaction) phase.

Determine the concentrations  $B(t)$  and  $D(t)$  in the aqueous phase. The interfacial equilibrium is given by a distribution coefficient  $K$ , where  $A_i = KB_i$ . The overall mass-transfer coefficient is  $K_D S$ , and the reaction rate constant is  $k$ .

### Solution

It is reasonable to assume that the concentration of B in the reaction phase is  $\ll$  than that of C, hence  $k$  is a pseudo-first-order rate constant. We may also assume that C, D and E are not transferred into the organic phase to any extent. The pertinent balance equations are then,

$$-V_o \left( \frac{dA}{dt} \right) = K_D S (A - KB) \quad (\text{i})$$

and

$$V_a \left( \frac{dB}{dt} \right) = K_D S (A - KB) - k V_a B \quad (\text{ii})$$

Now, if we look at the second derivative of B,

$$\frac{d^2 B}{dt^2} = \left( \frac{K_D S}{V_a} \right) \left[ \left( \frac{dA}{dt} \right) - K \left( \frac{dB}{dt} \right) \right] - k \left( \frac{dB}{dt} \right) \quad (\text{iii})$$

Substitution of  $(dA/dt)$  from equation (i) into (iii) and rearranging gives

$$\frac{d^2 B}{dt^2} = M \left( \frac{dB}{dt} \right) + NB = 0 \quad (\text{iv})$$

with

$$M = \left( \frac{K_D S}{V_o} + k + \frac{K_D S K}{V_a} \right); \quad N = \frac{K_D S k}{V_o}$$

The solution comes fairly directly as

$$B = C_1 \exp\left(\frac{-M + \sqrt{M^2 - 4N}}{2} t\right) + C_2 \exp\left(\frac{-M - \sqrt{M^2 - 4N}}{2} t\right) \quad (\text{v})$$

When,

$$t = 0; \quad B = 0$$

and

$$C_1 + C_2 = 0$$

Then,

$$B = 2C_1 \exp\left(-\frac{Mt}{2}\right) \sinh\left(\frac{\sqrt{M^2 - 4N}}{2} t\right) \quad (\text{vi})$$

For the constant  $C_1$ ,

$$\frac{dB}{dt} = \left(\frac{K_D S}{V_a}\right) A_0$$

at  $t = 0$ . Then,

$$B(t) = \frac{2K_D S A_0}{V_0 \sqrt{M^2 - 4N}} \exp\left(-\frac{Mt}{2}\right) \sinh\left(\frac{\sqrt{M^2 - 4N}}{2} t\right) \quad (\text{vii})$$

For the product  $D$ ,

$$D - D_0 = \int_0^t k B(t) dt$$

Let

$$\alpha = \frac{\sqrt{M^2 - 4N}}{2}; \quad \beta = \frac{K_D S A_0}{V_a}$$

then,

$$D(t) = D_0 + \left(\frac{k\beta}{2\alpha}\right) \left[ \frac{e^{(-M/2+\alpha)t} - 1}{\alpha - (M/2)} + \frac{e^{(-M/2-\alpha)t} - 1}{\alpha + (M/2)} \right] \quad (\text{viii})$$



HORATIO SAYS

All this seems tiresome but not very difficult. I worry about mass-transfer correlations for liquid-liquid phases. Go through the literature and see how many experimental studies you can find that report mass-transfer data (or any correlation) for liquid-liquid phases. Do you think that it is possible to use  $K_D S$ , from gas-liquid to liquid-liquid, only by making density corrections?

Our chief interest is concerned with the quantities required for analysis of an existing reactor or one that, for design purposes, is to be compared with other

possibilities. Certain parameters are either known or are variables that may be adjusted to obtain the design objectives; these are normally the liquid volume,  $V_L$ , the liquid flow rate,  $q$ , the pressure,  $P$ , temperature,  $T$ , initial concentrations,  $C_{oj}$  (liquid phase) and  $y_{oj}$  (gas phase), the gas phase flow rate,  $G$ , and the required conversion. We would also assume that if one is serious enough to contemplate the design of a reactor, separate information concerning phase equilibria (treated here in terms of Henry's law constant,  $H$ ), and reaction kinetics  $r_j$  is available as well.

In reviewing this list it becomes clear that the remaining parameters have to do with *bubbles*.<sup>13</sup> This second list would include the mass-transfer coefficient  $K_G$ , and the individual bubble parameters  $a'$ ,  $V_b$ ,  $v_b$ , and  $N$ . There is some difference in the correlations pertaining to tank-type and columnar reactors, so we consider them separately below.

### 8.3.4 The Parameters of Tank-Type Reactors

The overall coefficient  $K_G$  employed in the design equations is related to individual coefficients for liquid and gas phases by the inverse addition law for systems that follow Henry's law.

$$\frac{1}{K_G} = \frac{H}{k_L} + \frac{1}{k_G} \quad (8-205)$$

In most of the cases involved in design for gas-liquid systems, the gas-phase resistance to mass transfer,  $1/k_G$ , is small compared to the liquid-phase term,  $(H/k_L)$ , unless there is a very fast liquid-phase reaction. Thus, correlations for  $k_L$  are the ones we seek for design purposes. We have seen in Section 8.3.1 the analysis of the effect of reaction on the mass-transfer coefficient for several types of reactions. These were reported via the values of an enhancement factor applied to the magnitude of the liquid-phase mass-transfer coefficient in the absence of reaction, which we will term here  $k_L^o$ . There are numerous correlations available for  $k_L^o$  in bubbling systems, summarized in the work of Russell et al. A reasonable and typical correlation is that of Hughmark [G.A. Hughmark, *Ind. Eng. Chem. Proc. Design Devel.*, 6, 218 (1967)], claimed to fit experimental data to about  $\pm 15\%$ .

$$N_{Sh} = \frac{k_L^o d_b}{D} = 2 \pm \left[ N_{Re}^{0.48} N_{Sc}^{0.34} \left( \frac{d_b g^{1/3}}{D^{2/3}} \right)^{0.072} \right]^b \quad (a) \quad (8-206)$$

where

$$N_{Re} = \frac{u d_b}{\mu}; \quad N_{Sc} = \frac{\nu}{D}$$

For single bubbles  $u$  is the bubble velocity, for bubble swarms  $u$  is the bubble/(slip velocity),  $\nu$  is the kinematic viscosity (length)<sup>2</sup>/t, and  $D$  the molecular diffusivity (length)<sup>2</sup>/t.

For single bubbles  $a = 0.061$  and  $b = 1.61$ ; for bubble swarms  $a = 0.019$  and  $b = 1.61$ . When  $N_{Re}$ ,  $N_{Sc}$  and  $(d_b g^{1/3}/D^{2/3})$  are all  $\ll 2$  then there is an apparent

<sup>13</sup> "A harbor, even if it is a little harbor, is a good thing."—S.O. Jewett

relationship between single bubbles and bubble swarms given by

$$\frac{(k_L^\circ)_{BS}}{(k_L^\circ)_{SB}} \approx 0.31$$

which signals the interesting fact that the mass-transfer coefficient for single bubbles is greater than that for bubble swarms. In the event of mechanical agitation of the liquid phase, the reported correlations become highly specific as to power input and configuration, as discussed by Hughmark.

In order to convert these values of  $k_L^\circ$  into useful mass-transfer coefficients it is convenient to use the classification of Astarita (G. Astarita, *Mass Transfer with Chemical Reaction*, Elsevier, Amsterdam, (1967)]. Let us define two characteristic times,

$$t_D = \frac{D}{(k_L^\circ)^2} \quad (8-207)$$

$$t_R = \frac{C_{ej} - C_{ej}}{r_j} \quad (8-208)$$

where  $C_{ej}$  is the interfacial (equilibrium) concentration determined by Henry's law and  $C_{ej}$  is an equilibrium value for  $j$  in cases of reversible reaction (and thus zero for irreversible reaction). The physical interpretation of these times is:  $t_D$  is a diffusion time characteristic of the life of a surface fluid element exposed to the gas phase and  $t_R$  is a reaction time representative of the time required for the chemical reaction in the liquid phase to go to an appreciable extent of conversion. This would be taken, for example, for a first-order irreversible reaction, as  $t_R = 1/k$ . For bubbling systems the situation is a little more complicated, and

$$0.005 < t_D < 0.04 \text{ s}$$

and for typical values of  $D$  in the liquid phase this translates to

$$0.015 < k_L^\circ < 0.04 \text{ cm/s}$$

If the liquid-phase reaction is slow ( $t_D \ll t_R$ ), then we can identify three differing situations as follows:

1. Diffusion subregime The overall driving force is dominated by diffusional transport. Here

$$\frac{D}{k_L} \ll \frac{1}{a}$$

and

$$(1/a)(r_j)(C_{ej} - C_{ej}) > k_L^\circ(C_{ej} - C_{ej})$$

For typical values of  $D$  and  $k_L^\circ$  this gives an  $a$  range as

$$(1/a) \gg 2.5 \times 10^{-4} \text{ cm}$$

Further,  $K_G$  is just  $(H/k_L^\circ)$  in this subregime, and since the entire rate process is diffusion-driven,  $k_L = k_L^\circ$ .

2. Kinetic subregime The chemical reaction in the liquid phase is very slow and diffusional transport effects are not important. Then

$$(1/a)(r_j)(C_{ej} - C_{ej}) \ll k_L^\circ(C_{ej} - C_{ej})$$

In this case mass-transfer terms in the reactor model equations may be neglected.

3. Intermediate subregime As expected, this is intermediate between the limits of (1) and (2). Here

$$(1/a)(r_j)(C_{ej} - C_{ej}) = k_L^\circ(C_{ej} - C_{ej})$$

and for a first-order irreversible reaction

$$k_L = \left( \frac{1}{k_L^\circ} + \frac{a}{k} \right)^{-1}$$

One must remember that all three of the subregimes above are subject to  $t_D \ll t_R$ .

If the liquid-phase reaction is fast ( $t_D \gg t_R$ ), for a first-order example once again,

$$k_L = (Dk)^{1/2}$$

Finally, if the liquid phase reaction is very, very fast, corresponding to the physical picture envisioned in the derivation of equation (7-82),

$$\frac{t_D}{t_R} \gg \frac{C_{ol}}{\alpha C_{ej}}$$

where  $C_{ol}$  is the initial bulk concentration of liquid-phase reactant,  $C_{ej}$  the interfacial concentration of gaseous reactant in the liquid phase, and  $\alpha$  is a stoichiometric coefficient, mols liquid-phase reactant/mol absorbed reactant. This regime is typical of acid-base reactions in the liquid phase. Further details concerning the analysis of this regime are given in the text by Astarita.

*Gas phase properties* As stated before, all the model equations involve parameters that are determined by the behavior of bubbles, either alone or in groupings, and the analysis becomes more of an exercise in bubble fluid mechanics than in reactor design. For *plug-flow* gas phase reactors there are a number of correlations that relate in-reactor bubble properties as a function of the inlet conditions. These are available for the bubble volume  $V_b$ , the bubble rise velocity  $v_b$ , the surface to volume ratio  $a'$ , and the number of bubbles per unit volume  $N$ . In addition, if bubbles are spherical (or approximately so), information on  $d_b$  allows determination of  $a'$  and  $V_b$ . However, these correlations are subdivided by the gross characteristics of bubble formation, namely whether there is a gas phase consisting of discrete bubbles, or whether there is interaction among bubbles with some coalescence, commonly termed a swarm bubble phase.

For a *discrete bubble phase* we borrow heavily from work done with single bubbles for correlations. Many of those are posed in terms of the initial bubble diameter as the gas is introduced into the liquid phase via an orifice or other type of dispersion device. For low flow rates, where single bubbles are emitted at some fixed frequency,  $f$ , a force balance yields

$$(d_{ob})^3 = \frac{6D_0\sigma}{g(\rho_L - \rho_G)} \quad (8-209)$$

where  $D_0$  is the orifice diameter and  $\sigma$  the interfacial tension of the gas-liquid interface. For spherical bubbles the frequency  $f$  is also easily calculated as

$$f = \frac{Qg(\rho_L - \rho_G)}{\pi D_0 \sigma} \quad (8-210)$$

where  $Q$  is the gas volumetric flow rate. For somewhat higher flow rates (orifice  $N_{Re}$  to 2000) an, empirical correlation was proposed,

$$d_{ob} = (0.18)D_o^{0.5}N_{Re}^{0.33} \quad (8-211)$$

There are not much data available for the region of “jet flow” (higher velocities still), but some assistance can be found in handbook correlations. For bubble velocity we have used the expression presented by Davidson and Harrison,

$$v_b = (0.711)(gd_b)^{1/2} \quad (8-212)$$

where  $d_b$  is some equivalent spherical bubble diameter if the bubbles are not spherical. If we have a value for the bubble rise velocity we can calculate the number of bubbles per unit volume as

$$N = \frac{QL}{V_{ob}v_bV_L} \quad (8-213)$$

where  $V_{ob}$  is the initial bubble volume and  $V_L$  the volume of the liquid phase. Remember that the indicated relationship of  $N$  to  $(v_b)^{-1}$  means that the number of bubbles may vary with position in the liquid phase, depending upon the value of  $d_b$  in equation (8-212).

The correlations for the *swarm bubble phase*, still for the gas in plug flow, are rather equipment-specific. For example, for bubble swarms issuing from porous plates, the bubble diameter may be estimated from the correlation of Koide et al., [K. Koide, T. Hirahara and H. Kubata, *Chem. Eng. (Japan)*, 30, 712 (1966)],

$$d_{ob} = 1.35(N_{Fr}/N_{We}^{1/2})^{0.28}(g\rho/\sigma\delta) \quad (8-214)$$

where  $N_{Fr}$  (Froude number) is  $(u^2/g\delta)$ ,  $N_{We}$  (Weber number) is  $(\delta u^2\rho/\sigma)$ ,  $\delta$  is the orifice diameter in the gas-phase distributor,  $\sigma$  is the liquid surface tension, and  $\rho$  is liquid density. From this point on there are a number of different procedures suggested in the literature to obtain bubble velocity, the number per unit volume, and the gas holdup for the swarm. Approaches are suggested in the review of Cichy et al., who also give a number of references to some of the basic work on parameters of the swarm bubble phase. As mentioned above, these tend to be very specific to particular operating situations, and it is probably more fruitful to consider the original work rather than report the litany here.

### 8.3.5 The Parameters of Column Reactors

Our primary interests here are directed toward vertical-flow contacting devices, generally referred to as bubble-column reactors. These can be empty, with stage-wise placing of porous plates for bubble redispersion, or filled with a commercial packing such as Raschig rings. These two types have received full attention in work directed toward mass-transfer/separation processes, and will not be considered further here. What we will examine now is the case in which there are discrete



gas-phase bubbles passing through a continuous liquid phase. This puts us generally in the southeast corner of the Govier chart of Figure 8.16.

As in the situation for tank-type reactors, we need first to define the characteristic time quantities associated with the reactor design. The characteristic diffusion time,  $t_D$ , is given in equation (8-207), and the extent-of-reaction time,  $t_R$ , is given in equation (8-208). The third time here is  $t_p$ , the length of time an element of fluid remains in the reactor. This is reminiscent of the exit-age distribution function developed for homogeneous tubular-flow reactors, but the development of the theory for multiphase reactors has been different.<sup>14</sup>

We may estimate  $t_p$  from a knowledge of the liquid holdup in the reactor,  $R_L$ , via

$$(t_p)_L = \frac{R_L A_c L}{q} \quad (8-215)$$

$$(t_p)_G = \frac{(1 - R_L)(A_c L P)}{GRT} \quad (8-216)$$

where  $R_L$  is the liquid-phase holdup (ratio of cross sectional area of column occupied by liquid to the total cross sectional area),  $q$  is the volumetric flow rate of liquid,  $A_c$  the total cross sectional area, and  $G$  is a molar gas flow rate. A number of correlations for holdup are available, some with a semi-theoretical basis and others more or less completely empirical. Two that have passed the test of time rather well are those of Hughmark [G.A. Hughmark, *Chem. Eng. Prog.*, 58, 62 (1964)] and Lockhart and Martinelli [R.W. Lockhart and R.C. Martinelli, *Chem. Eng. Prog.*, 45, 39 (1949)].

The interfacial area, based on a unit volume of reactor, is given by the general relation

$$a = Na'V_{DG} \quad (8-217)$$

where  $V_{DG}$  is the average bubble volume. If the bubbles are spherical  $V_{DG}$  is easily estimated if there is some information concerning the size distribution. The value of  $N$  can also be estimated from inlet conditions,

$$N = \frac{(1 - R_L)}{(V_{DG})_0} \quad (8-218)$$

This value would not be expected to change much with position for the discrete bubble regime that we are considering. The initial bubble volume,  $(V_{DG})_0$ , is estimated from

$$(V_{DG})_0 = \frac{G_0 RT}{P\nu} \quad (8-219)$$

where  $\nu$  is a bubble formation frequency that must be known from other data, or may be roughly estimated from the average bubble volume and the gas volumetric flow rate.

The bubble rise velocity, important in determining gas-phase residence time, is estimated by a correlation reminiscent of fluidized beds.

$$\bar{v}_B = \bar{v}_L + 0.711g^{1/2} \left( \frac{6}{\pi} \right)^{1/8} (V_{DG})^{1/6} \quad (8-220)$$

<sup>14</sup>“That great dust-heap called ‘history’.”—A. Birrell

where  $\bar{v}_L$  is the average velocity of the liquid phase. All of these expressions offer ways of approximating interfacial areas, most often through the assumption of spherical geometry, determination of  $V_{DG}$ , and then area from equation (8-217). A direct correlation for  $a$  was reported by Scott and Hayduk [D.S. Scott and W. Hayduk, *Can. J. Chem. Eng.*, 44, 130 (1966)],

$$a = \left( \frac{A}{LA_c} \right) \left( \frac{\alpha}{LA_c} \right) \left[ \frac{G_0}{G_0 + (qRT/P)} \right]^m \quad (8-221)$$

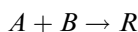
where  $\alpha = (qP/HG)$ ,  $A$  is the total surface area in the reactor, and  $q$  and  $G_0$  are as defined before. The exponent  $m$  is a value obtained from curve-fit that can vary from 0.66 to 1.0. One wonders how useful this correlation may be, since the estimate of  $A$  required would seem no less of a task than simply estimating a value for  $a$  based on intuition or experience. The whole business seems fairly insecure, if we remember the fluid-bed studies that have shown that bubbles in multiphase reactors are anything but spherical. There isn't much else to go on, however.

Estimation of the mass-transfer coefficients associated with columnar operation, at least for the discrete bubble phase we are considering, is the same in practice as for tank-type reactors. Thus, one determines the value of the diffusion time by equation (8-207) and goes on to the calculation of  $k_L$  for the appropriate conditions as defined in the classification of Astarita.

Two final comments are appropriate here. First is reminder that if one gets "stuck" among the intricacies of all the correlations and sub-classifications described, an unhurried perusal of the procedure given in Perry's Handbook is always a good place to start.<sup>15</sup> The second comment has to do with some straw men that have been set up in the general derivations, then not mentioned again (aside from spherical bubbles). In particular these include the droplet-liquid model of Figure 8.17, and the possible use of axial dispersion models to describe deviations from ideal plug flow or completely mixed phase behavior. These approaches may be appropriate in specific instances, but are beyond what we need here. So, we depart from the topic of gas-liquid reactors secure with the knowledge that such insecure methods exist.<sup>16</sup>

### Illustration 8.5<sup>17</sup>

The reaction of ethylene oxide with water to produce monoethylene glycol can be represented by



where the aqueous liquid phase is A, the pure gas of ethylene oxide is B, and the monoglycol product is R. Experimental data on this reaction were obtained under isothermal conditions at 90°C in a semi-flow reactor with a volume of 445 cm<sup>3</sup>, with cylindrical geometry, 1-inch i.d. and length 32.4 in. A summary of experimental conditions is given below. What reactor subregime would apply here?

<sup>15</sup> Maybe some more Debussy will help. Definitely not Wagner.

<sup>16</sup> "The most difficult of all musical instruments to learn to play is second fiddle."—Anonymous

<sup>17</sup> After R.W. Schaflein and T.W.F. Russell, *Ind. Eng. Chem.*, 60, 12, with permission of the American Chemical Society, (1968).

$$C_{eB} = 0.01838 \text{ lb mol/ft}^3$$

$$D_0 = 0.0825 \text{ in}$$

$$d_{ob} = 0.4 \text{ cm (observed experimentally)}$$

$$H = 0.0498 \text{ lb mol/ft}^3\text{-atm}$$

$$k = 0.789 \text{ h}^{-1}$$

$$L = 2.7 \text{ ft}$$

$$P = 1 \text{ atm}$$

$$Q_1 = 40 \text{ cm}^3/\text{min}$$

$$T = 90^\circ\text{C}$$

$$V_L = 445 \text{ cm}^3$$

### Solution

The experimental measurements produced concentration-time plots of ethylene oxide and ethylene glycol in the liquid phase, as shown in Figure 8.18. The physical picture of this reaction/reactor system is most closely approximated by the plug-flow gas phase, well-mixed batch liquid phase. The appropriate relationships to model this system are given in equations (8-176) to (8-178), (8-183), and (8-188). The bubble volume is variable, and the nature of the variation changes with the extent of conversion (i.e., concentration of glycol in the liquid phase), however, the pure oxide gas phase allows  $y_B = 1$ . The modified equations specific to this reactor are then

$$\frac{dC_B}{dt} = (\bar{a}' \bar{V}_b N) k_L C_{eB} - [(\bar{a}' \bar{V}_b N) k_L + k] C_B \quad (\text{i})$$

$$a = \bar{a}' \bar{V}_b N = NS[V_{ob} + (L^2 F^2 / 3 - V_{ob}^{1/2} L F)^{2/3}] \quad (\text{ii})$$

and

$$F = \frac{k_L R T S}{2 P W} \quad (\text{iii})$$

$$C_R(t) = k \int_0^t C_B(t) dt \quad (\text{iv})$$

The boundary conditions for equations (i) and (iv) are,

$$\begin{aligned} t = 0, \quad C_A = 0; \quad C_B = 0 \\ t = t; \quad C_B = C_B; \quad C_R = C_R \end{aligned} \quad (\text{v})$$

We now need to determine the reaction regime (classification of Astarita) for this operation. From equation (8-208) for an irreversible reaction, together with

$$r_j = k C_{ej}$$

$$k = (2.2 \times 10^{-4}) \text{ s}^{-1}$$

then

$$t_R = (1/k) = (4.55 \times 10^4) \text{ s} \quad (\text{vi})$$

The typical range of  $t_D$  for bubbling systems is from 0.005 to 0.04 s, thus  $t_R \gg t_D$  and

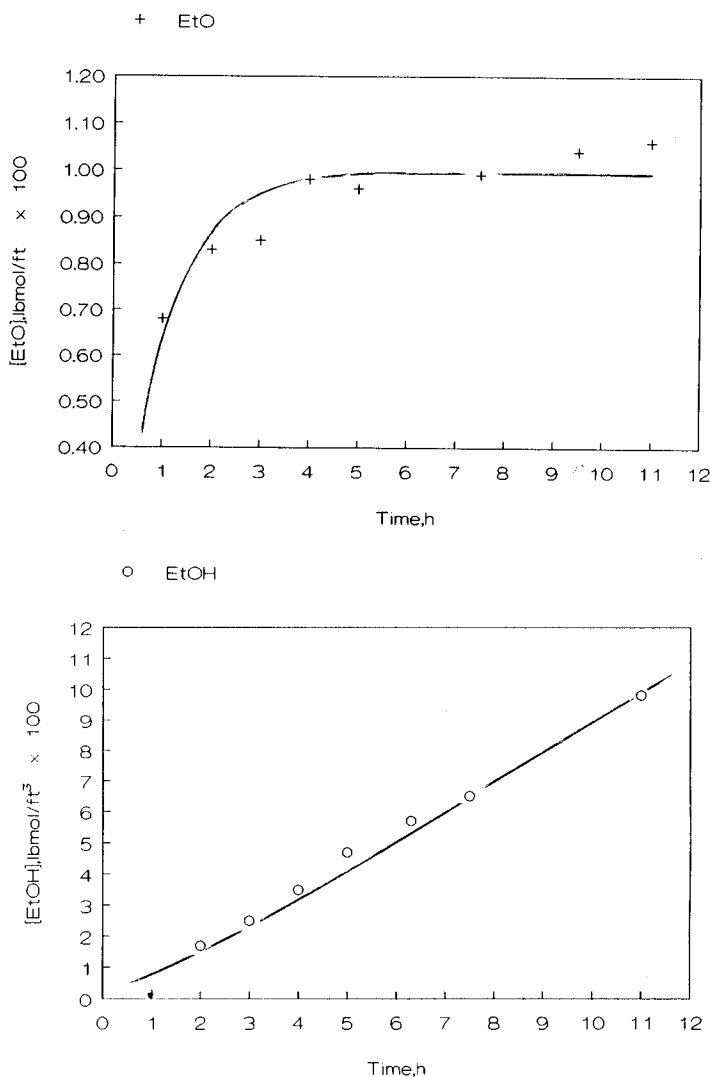


**Figure 8.18** Concentration-time profiles for the reaction of ethylene oxide with water. Solid lines are model predictions.

the reaction belongs to the “slow reaction” regime, and we have to determine which of the reaction subregimes (diffusion, kinetic, or intermediate) is applicable. For the conditions given, this ends up in terms of the following criteria.

$$\left(\frac{k}{a}\right) >; \quad =; \quad < k_L^\circ? \quad (\text{vii})$$

The value of  $k_L^\circ$  is determined from equation (8-206) to be 8.21 ft/h. From equation (8-209) we estimate  $d_{ob}$  as 0.43 cm. Thus, from equation (ii), using

$$\bar{a}' \approx \frac{6}{d_{ob}}; \quad \bar{V}_b = \frac{\pi(d_{ob})^3}{6}$$

$N$  from equation (8-213), and  $v_b$  from equation (8-212), we obtain

$$k_L^\circ = 8.21 \text{ ft/h}; \quad N = 5940 \text{ ft}^{-3}; \quad a \approx 3.64 \text{ ft}^{-1}$$

Using these values one obtains numbers for the comparison of equation (vii) as

$$(k/a) = 0.22$$

$$k_L^\circ = 8.21$$

which puts us into the “intermediate” subregime, where kinetic and diffusion rates are of the same order of magnitude, and

$$k_L = \left( \frac{1}{k_L^\circ} + \frac{a}{k} \right)^{-1} \quad (\text{viii})$$

Equations (i) to (viii) comprise the reactor model.

A test of this model is reported by Schaftlein and Russell, in which best-fit values for  $k_L$  and  $N$  were determined from the data in Figure 8.18, using an observed value of 0.4 cm for  $d_{ob}$ . These calculations are represented by the solid lines in Figure 8.18, with best-fit parameter values of

$$k_1 = 0.56 \text{ ft/h}; \quad N = 5900 \text{ ft}^{-3}; \quad a = 1.40 \text{ ft}^{-1}$$

This should be considered a reasonable agreement between correlation and best-fit values, as such things go.



HORATIO SAYS

Here I go again with my favorite question. Suppose there is a doubt of  $\pm 20\%$  in such estimation used above. Where would this put us as far as the answer is concerned? We must *always* remember that correlations do not descend from Higher Powers. Unpleasant results can, and do happen from time to time.

## 8.4 Trickle-Bed Reactors

The name “trickle-bed reactor” is usually applied in reference to a fixed bed in which a liquid phase and a gas phase flow concurrently throughout a bed of catalyst. By far the most important application, and hence much of the work, on these reactors has been in the hydrotreating of heavy feedstocks in the petroleum industry (hydrocracking, hydrodesulfurization, hydrodenitrogenation). However, this seems a very versatile processing method, and has not been exploited nearly to its potential in other areas such as waste water treatment—at least as the scientific literature would indicate.

The hydrodynamics of trickle beds are complex, to say the least, and although an enormous amount of time and effort has been expended on research in this area, it is probably true to say that design and scale-up procedures are somewhat more tenuous than for fixed- or even fluid-bed reactors. Fortunately, there are relevant reviews that give some insight [C.N. Satterfield, *Amer. Inst. Chem. Eng. Jl.*, 21, 209

(1975); H. Hofmann, *Catal. Rev. Sci. Engr.*, 17, 71 (1978); A. Gianetto, G. Baldi, V. Speccina, and S. Sicardi, *Amer. Inst. Chem. Eng. Jl.*, 24, 1087 (1978)], as well as a book devoted to the topic [Y.T. Shah, *Gas-Liquid-Solid Reactor Design*, McGraw-Hill Book Co., New York, NY, (1979)].

As in the case of other multiphase reactors discussed in this chapter, topical material divides itself rather naturally into three major aspects: hydrodynamics, transport, and reaction processes. We will stay with fairly simple approaches, particularly in the area of hydrodynamics and correlations. An extensive amount of research continues to this day on trickle beds, so we cannot attempt to present the latest word.

### 8.4.1 Hydrodynamics in Trickle Beds

The areas concerned with hydrodynamics in trickle beds include flow regimes, liquid distribution on the solid (catalyst) packing, pressure drop, liquid holdup, and, more generally, the effect of the physical properties of the liquid and gas phases on all hydrodynamic properties.

The basic “trickle-flow regime” is most often associated with low liquid and gas flow rates (often termed “gas-continuous regime”), in which the liquid flows over the packing in the form of films, and rivulets or drops that essentially can be considered to be in laminar flow and not affected much by the gas phase flow, be it either laminar or turbulent. As the gas rate is increased a larger liquid phase velocity is induced via increased drag on the liquid, and eventually turbulence will result, with some liquid even becoming separated from the liquid film as slugs or droplets, eventually to reform over the packing.<sup>18</sup> This is commonly called “ripple” or “pulsating” flow and is probably most characteristic of the hydrodynamics encountered in commercial operation. At high liquid rates and low gas rates, however, the liquid phase can become the continuous phase and the gas passes through the reactor in a bubble (dispersed bubble) flow. Various flow maps—somewhat reminiscent of the Geldhart correlation for fluid beds—have been reported. One of the most easily visualized is that of Satterfield given in Figure 8.19. This is presented together with a tabulation of limiting flow conditions encountered in typical petroleum processing applications in Table 8.2. Large differences in behavior are seen between foaming and nonfoaming systems. Our discussion is limited to the former.

A somewhat more quantitative approach to the designation of flow regimes was attempted by Gianetto et al. in correlation of the results of several investigations. In particular the correlation recognizes that a large portion of flow research on trickle-beds, at least that which had been published, had employed the air-water system and required an act of deep faith to be extended to non-aqueous systems. In order to cope with this, one can devise some system-scaling parameters, of which the most useful are

$$\lambda = [(\rho_o/\rho_{air})(\rho_L/\rho_{H_2O})]^{1/2} \quad (8-222)$$

<sup>18</sup> For more on this and other aspects, the reader is referred to J.M. deSantos, T.R. Mell, and L. E. Scriven, *An. Rev. Fluid Mach.*, 23, 233 (1991).



and

$$\psi = (\sigma_{H_2O}/\sigma_L)(\mu_L/\mu_{H_2O})^{1/3}(\rho_{H_2O}/\rho_L)^{2/3} \quad (8-223)$$

Use of these in a flow-rate correlation provides a somewhat clearer picture of the transition between flow regimes, as shown in Figure 8.20. While there are undoubtedly some exceptions to the generalized correlation here, it can be considered fairly reliable for the majority of systems. Our specific interests in this section are limited for the most part to the region of "gas-continuous trickling flow". For a more recent attempt at defining the shaded transition region in Figure 8.20, the reader is referred to the paper of Dimenstein and Ng [D.M. Dimenstein and K.M. Ng, *Chem. Eng. Commun.*, 41, 215 (1986)].

Pressure drop is a factor that we have not considered in this chapter, for it is only of secondary importance in the design or analysis of fluidized beds, slurry reactors, or gas-liquid contactors. However, for trickle beds the situation is more complex and there is no generally accepted correlation such as the Ergun equation for fixed beds. A summary of a number of these can be found in the review of Gianetto et al. [A. Gianetto, G. Baldi, V. Specchia and S. Sicardi, *Amer. Inst. Chem. Eng. Jl.*, 24, 1087 (1978)]. One possibility in the absence of any other information is to use the single-phase pressure drop correlation with the void fraction reduced to account for liquid holdup in the bed, treating the liquid phase as an extension of the solid phase, which is very conservative. There is no lack of ideas in between for determining trickle-bed pressure drop, however. Many of these propose what are basically combining rules for liquid-phase and gas-phase pressure drops determined individually. One well-known correlation is that of Larkins et al. [R.P. Larkins, A.R. White and D.W. Jeffrey, *Amer. Inst. Chem. Eng. Jl.*, 7, 231 (1961)],

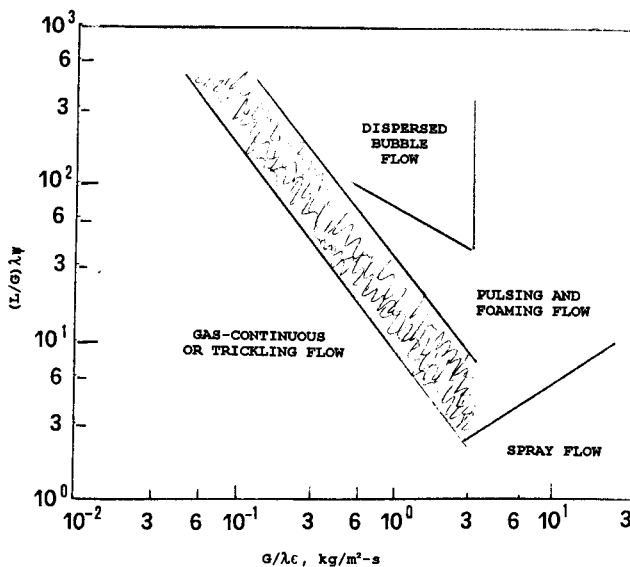


**Figure 8.20** Generalized flow map for trickle-bed reactors. The shaded area is the transition region from gas-continuous to gas-dispersed flow.



which proposes

$$\log \left( \frac{\Delta P_{LG}}{\Delta P_L + \Delta P_G} \right) = \frac{0.42}{\log(\chi)^2 + 0.67} \quad (8-224)$$

where  $\chi = (\Delta P_L / \Delta P_G)^{1/2}$  is in the range 0.05 to 30. Equation (8-224) was derived from results with various packing materials, with dimensions on the order of 10 mm, for all of the flow regimes shown in Figure 8.20. Later modifications of this approach, offering perhaps better correlation (at the expense of additional complexity), were offered by Sato and Hashiguchi [Y. Sato and Y. Hashiguchi, *J. Chem. Eng. Japan*, 6, 315 (1973)] and Midoux et al. [N. Midoux, M. Favier and J.C. Charpentier, *J. Chem. Eng. Japan*, 9, 350 (1976)]. In terms of simplicity, the latter is particularly attractive.

$$\left( \frac{\Delta P_{LG}}{\Delta P_L} \right)^{0.5} = 1 + \left( \frac{\Delta P_L}{\Delta P_G} \right)^{-0.5} + (1.14) \left( \frac{\Delta P_L}{\Delta P_G} \right)^{-0.27} \quad (8-225)$$

One caution that applies to the use of these pressure-drop correlations has to do with the possible buildup of deposits in the trickle bed with increasing time-on-stream, particularly in the case of hydrotreating. Here the buildup of carbonaceous or metallic deposits on the catalyst may possibly block a portion of the bed void present initially, and  $\Delta P_{LG}$  will be much greater than expected on the basis of equation (8-224) or (8-225).

Liquid holdup is another factor that is important in the design and analysis of trickle beds that we have not been concerned with in any detail in earlier sections of this chapter. The effect of liquid holdup on performance depends upon the nature of the reaction occurring. In some hydrotreating reactions such as hydrosulfurization or demetallation, the liquid holdups encountered are sufficiently high that all the solid phase surfaces are wetted. In other reactions requiring less demanding conditions, this may or may not be so. In the latter case the effective reaction rate will then decrease with an increase in liquid holdup, since the mass-transfer resistance is greater in the liquid phase than in the gas phase.

The liquid-phase holdup is expressed as a fraction of bed volume, i.e., volume of liquid present per volume of empty reactor. This is then subdivided into *external holdup*, liquid contained in the void fraction of the bed outside of the catalyst particles, and *internal holdup*, liquid within the pore volume of the catalyst. There is an even further subdivision of the external holdup into a “*static holdup*”—the amount of liquid in the bed that remains after the bed has been allowed to drain freely—and “*dynamic holdup*” which depends on a number of factors but is most simply defined as the difference between total holdup and static holdup.<sup>19</sup>

The maximum internal holdup is determined primarily by the pore structure/volume of the catalyst, and can range from about 0.1 to 0.4 for typical materials. Static holdups in the range of 0.02 to 0.05 are characteristic of most packed beds of porous catalyst. Summaries of such correlations for work done up to about 1980 are found in the reviews of Gianetto et al., and Satterfield, as cited. These seem fairly

<sup>19</sup> Related measures may have external holdup divided into “free-draining” and “residual” fractions. The latter is related to the static holdup, but be careful. The names sound the same but result in entirely different numbers. “. . . and a cast of thousands.”—*Anonymous*

well established figures, and not much work directly on this point has been done in recent years.

The static holdup,  $\beta_r$ , depends primarily on the physical properties of the liquid phase, and particle size, shape and wetting. This is often correlated in terms of yet another nondimensional parameter, the Eötvös number,

$$N_{Eo} = \left( \frac{\rho_L g d_p^2}{\sigma_L} \right) \quad (8-226)$$

which expresses the ratio of gravity to surface forces. Smaller particle diameters and fluid density, and larger surface tension, thus give larger static liquid holdups. As indicated by its name, static holdup is not particularly sensitive to operating conditions and, as stated above, we can select some number on the order of 0.05 as representative ( $N_{Eo} < 4$  for  $\epsilon\beta_r \sim 0.05$ , decreasing with increasing  $N_{Eo}$ ). Workable correlations for dynamic holdup,  $\beta_f$ , and total holdup,  $\beta_t$ , have been proposed in a number of studies. From Larkin et al.,

$$\log(\beta_f) = (0.525) \log \chi - (0.11)(\log \chi)^2 - 0.774 \quad (8-227)$$

for  $0.05 < \chi < 30$  [see equation (8-224)]. Midoux et al. give one correlation for all hydrodynamic regimes for nonfoaming systems

$$\beta_t = \frac{0.66(\chi)^{0.81}}{1 + 0.66(\chi)^{0.81}} \quad (8-228)$$

for  $0.1 < \chi < 80$ . Speccia et al. [V. Speccia, G. Baldi and A. Gianetto, *Chem. Eng. Sci.*, 32, 515 (1977)] propose, for the low interaction regime

$$\beta_f = 3.86(N_{Re})_L^{0.545} (N_{Ga})_L^{-0.42} \left( \frac{a_v d_p}{\epsilon} \right) \quad (8-229)$$

where

$$(N_{Ga})_L = \frac{d_p^3 \rho_L (\rho_L g + \Delta P_{LG})}{\mu_L^2}$$

and  $3 < (N_{Re})_L < 470$ . Shah has recommended the use of equation (8-229) for the low interaction range for trickle-flow conditions in calculation of dynamic liquid holdup, and the correlation of Midoux et al. for calculation of total liquid holdup in all flow regimes. In the above equations  $\epsilon$  is the void fraction of the bed and  $a_v$ , the area per unit volume of the catalyst external surface.

It is hard to find out much about internal holdup. Presumably this will be determined by the internal void fraction of the catalyst, which one may assume is totally filled with liquid phase—at least for reactions in which no phase change to vapor occurs.

In the above we have seen only a few of the many correlations that exist for hydrodynamic factors in trickle-bed flow reactors, and more specifically those dealing with aqueous- or hydrocarbon-based reactions. Once again we are faced with the question of how to select the particular correlation to be used from a rich menu available. Again, also, there is no fixed procedure, but the most important general rule is never to extrapolate a correlation beyond reasonable limits corresponding to

its database. Unfortunately, this may not always be possible and one is left to pick the most conservative value among several possibilities.

### 8.4.2 Mass-Transfer Correlations

As one might expect, these are conveniently subdivided into correlations for gas-liquid coefficients and for liquid-solid coefficients. The overall structure of these correlations is not much different from those we have seen for other multiphase reactors, but the correlation coefficients, of course, are very-specific to the application.

*Gas-liquid.* Charpentier [J.C. Charpentier, *Chem. Eng. Jl.*, 11, 161 (1976)] presented a thorough summary of literature on gas-liquid mass transfer in trickle beds some time ago. The liquid phase mass-transfer coefficient is affected by both gas and liquid flow rates. At very high gas- and liquid-flow rates values of  $k_L a_L$  may exceed  $1 \text{ s}^{-1}$ , a value normally not achieved in any other type of gas-liquid conductor. In the trickle-flow regime, however,  $k_L a_L$  values are more consistent with those expected on the basis of experience with other contactors. Trends in the gas-phase coefficient,  $k_G a_L$ , also follow in general order expectations based on experience with gas-liquid slurry reactors. For  $k_L a_L$  a modified correlation following the earlier suggestions of Reiss [L.P. Reiss *Ind. Eng. Chem. Proc. Design Devel.*, 6, 486 (1967)] is recommended by both Satterfield and Charpentier.

$$(k_L)_1 a_L = (0.0011)(E_L) \left( \frac{D_{AL}}{2.4 \times 10^{-9}} \right) s^{-1} \quad (8-230)$$

where  $D_{AL}$  is the diffusivity of reactant A in the liquid phase, and  $E_L$  is an energy dissipation factor for liquid-phase flow, given by

$$E_L = \left( \frac{\Delta P_{LG}}{\Delta z} \right) u_{SL} \quad (8-231)$$

where  $u_{SL}$  is the superficial liquid-phase velocity and  $E_L$  is in  $\text{W/m}^3$ . This is shown in Figure 8.21a. Goto et al. [S. Goto, J. Levec and J.M. Smith, *Catal. Rev. Sci. Eng.*, 15, 187 (1977)] gave a summary of results on  $k_L a_L$  in both cocurrent and countercurrent contractors as a function of liquid velocity, shown in Figure 8.21b. The results of Gianetto et al. are much lower than those of other reports, however, they establish a norm for conservative design.

The gas phase mass-transfer coefficient can also be correlated with an equation in the form of equation (8-230). In this case,

$$k_G a_L = 2.0 + C_1 (E_G)^{0.66} \quad (8-232)$$

where the energy dissipation term is

$$E_G \left( \frac{\Delta P_{LG}}{\Delta z} \right) u_{SG}$$

and  $C_1 = 0.10$  for  $E_G$  in  $\text{W/m}^3$ . Alternative correlations to be considered are given in the papers of Gianetto et al. (Figure 8.21c) or Shende and Sharma [B.W. Shende and M.M. Sharma, *Chem. Eng. Sci.*, 29, 1763 (1974)]. As was shown previously for fluidized bed and slurry reactors, the gas phase mass-transfer resistance is most often smaller than that of the liquid phase in the overall transport process, and disappears altogether in the case of a pure component gas feed.

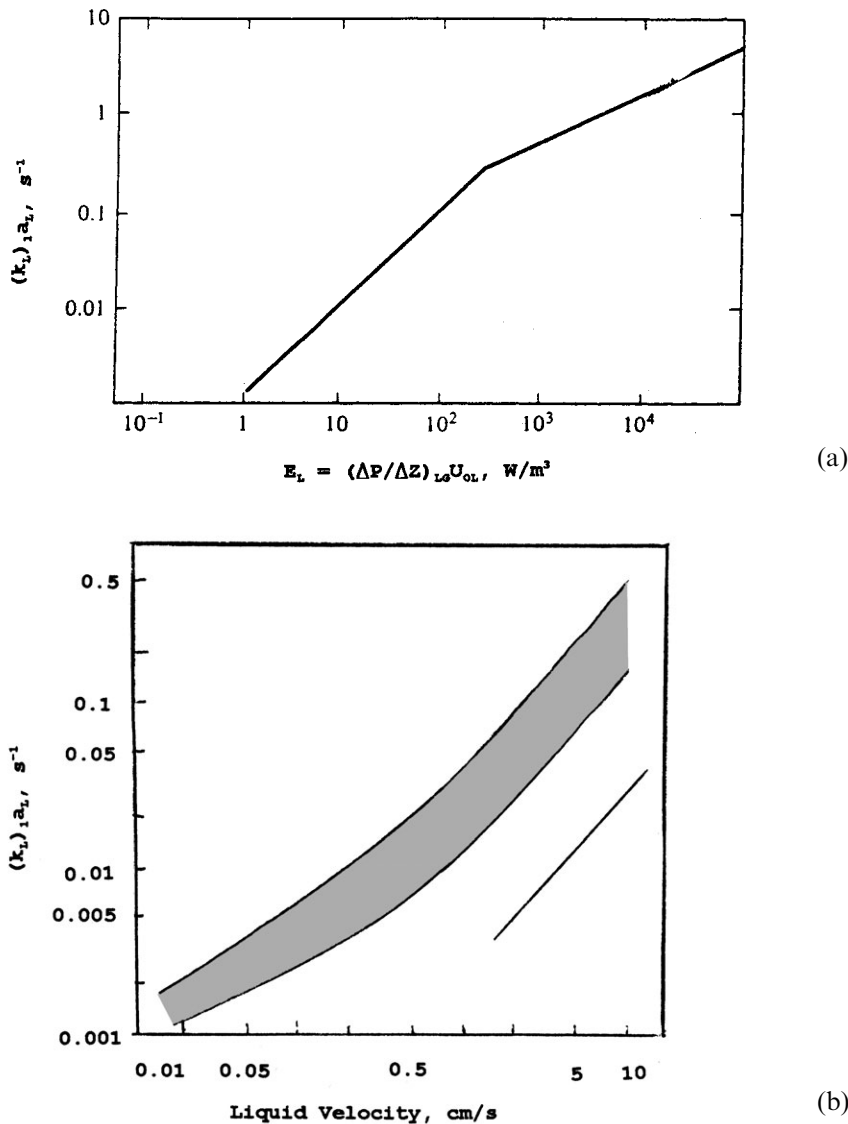
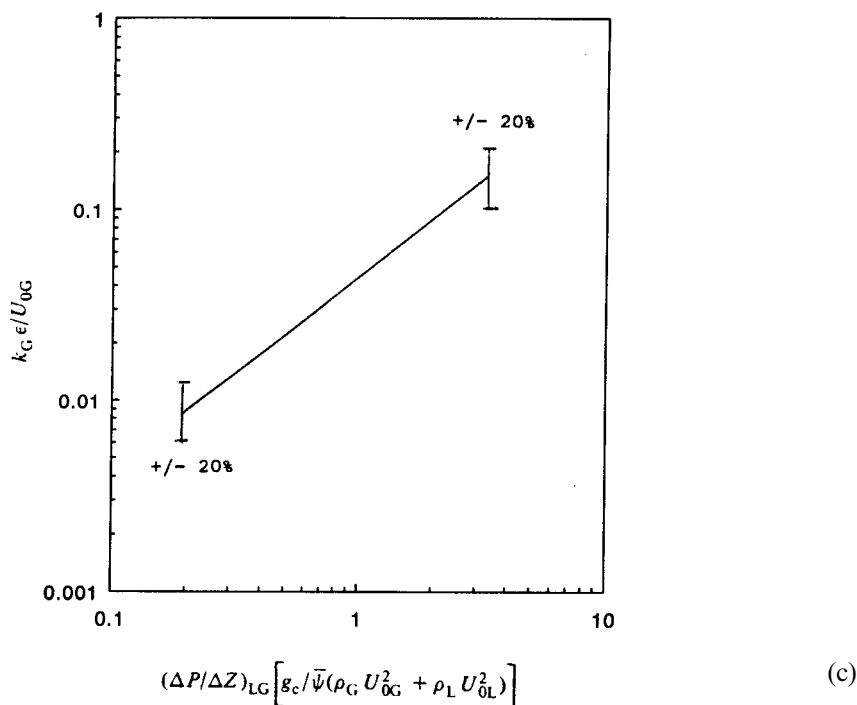


**Figure 8.21** (a) Energy dissipation correlation for  $k_L a_L$  in cocurrent downflow trickle beds. (b) Correlation of  $k_L a_L$  with liquid velocity in cocurrent and countercurrent contactors. Line: countercurrent,  $0.001 < k_L a_L < 0.03 s^{-1}$ ; shaded, cocurrent,  $0.003 < k_L a_L < 0.5 s^{-1}$ . [After A. Gianetto, G. Baldi and V. Specchia, *Quad. Eng. Chim. Ital.*, 6, 125 (1970); *Amer. Inst. Chem. Eng. Jl.*, 19, 916, with permission of the American Institute of Chemical Engineers, (1973).] (c) Energy dissipation correlation for  $K_G$  in cocurrent downflow trickle beds.

Packing	$\Psi, m^{-1}$
6 mm glass spheres	24.5
6 mm Berl saddles	18.4
6 mm ceramic rings	36.5
6 mm glass rings	17.1



*Liquid-solid.* Transport between the liquid and solid (catalyst) phases in trickle-bed reactors is at least a first cousin to transport in more conventional fixed beds, and our understanding of the liquid phase mass-transfer coefficient here benefits from the decades of research devoted to that topic. A good correlation was reported as far back as 1948 by Van Krevelen and Krekels [D.W. Van Krevelen and J.T.C. Krekels, *Rec. Trav. Chim. Pays-Bas*, 67, 512 (1948)], who proposed

$$N_{Sh} = 1.8(N_{Re})_L^{0.5} (N_{Sc})^{0.33} \quad (8-233)$$

with

$$N_{Sh} = \left( \frac{k_{L2}}{a_S D_{AL}} \right); \quad N_{Re} = \left( \frac{\rho_L L}{A_c a_s \mu_L} \right)$$

where  $a_S$  is the liquid-solid interfacial area per unit volume,  $A_c$  the column cross-sectional area, and  $L$  the volumetric liquid flow rate. The data on which equation (8-233) is based indicated that the liquid-solid mass-transfer coefficient is greater in the trickle bed than in a comparable bed with a continuous liquid phase for large catalyst particle size (presumably via turbulence induced by gas-phase flow), although for smaller particles ( $d_p < 2$  mm) Goto and Smith [S. Goto and J.M. Smith, *Amer. Inst. Chem. Eng. Jl.*, 21, 706 (1975)] reported a reverse effect, which is a reasonable result.

Other correlations reported for  $k_L$  generally follow the same form. Reasonable alternatives to equation (8-233) are the correlations reported by Dharwadkar and Sylvester [A. Dharwadkar and N.D. Sylvester, *Amer. Inst. Chem. Eng. Jl.*, 23, 376

(1977)] and by Ruether et al. [J.A. Ruether, C.S. Yang and W. Hayduk, *Ind. Eng. Chem. Proc. Design Devel.*, 19, 103 (1980)]. From the former,

$$j_D = \left( \frac{k_{L_2}}{a_S D_{AL}} \right) (N_{Sc})^{0.67} = 1.64 (N_{Re})_L^{0.33} \quad (8-234)$$

for  $0.2 < (N_{Re})_L < 2400$ . From Ruether et al.,

$$\theta \epsilon \left( \frac{k_{L_2}}{a_S D_{AL}} \right) = s [(N'_{Re})_L]^q (N_{Sc})^{0.33} \quad (8-235)$$

where  $\theta$  is the catalyst porosity and  $\epsilon$  is the bed void fraction. The correlation constants  $s$  and  $q$  depend upon the flow regime defined in terms of the modified Reynolds number  $(N'_{Re})_L$

$$s = 0.842; \quad q = 0.78 \quad \text{for } (N'_{Re})_L < 55 \text{ (trickle flow)}$$

$$s = 0.044; \quad q = 1.52 \quad \text{for } 55 < (N'_{Re})_L < 100$$

$$s = 0.680; \quad q = 0.42 \quad \text{for } (N'_{Re})_L > 100 \text{ (pulse flow)}$$

where  $(N'_{Re})_L = (\rho_L u_L / a_s \mu_L \beta_t)$ , and the total  $\beta_t$  can be determined from equation (8-228).

Finally, some experimental results from the work of Hirose et al. [T. Hirose, M. Toda and Y. Sato, *J. Chem. Eng. Japan*, 7, 187 (1974)] are shown in Figure 8.21d.

**Intraparticle diffusion.** Contrary to fluid beds or slurry reactors, which normally employ finely divided catalyst particles, trickle beds normally are employed with catalyst particles of similar dimension to those of conventional fixed beds, and intraparticle diffusion can become an important factor in the overall rate of reaction and/or selectivity to various products in complex reactions. Indeed, both Satterfield [C.N. Satterfield, *Amer. Inst. Chem. Eng. Jl.*, 21, 209 (1975)] and Speccia et al., [V. Speccia, G. Baldi and A. Gianetto, *Chem. Eng. Sci.*, 32, 515 (1977)] pointed

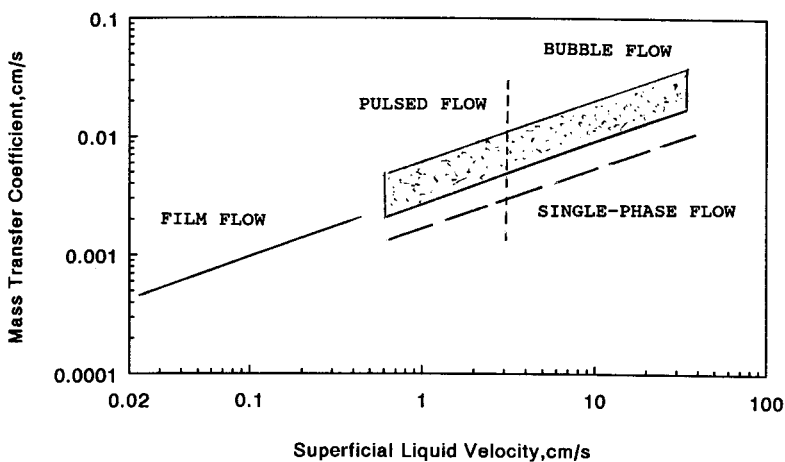


**Figure 8.21** (d) Experimental results for the liquid-solid mass-transfer coefficient in a down-flow trickle bed; liquid velocity range from 1 to 100 cm<sup>3</sup>/s. For film flow  $d_p = 9 - 12$  mm; for other regimes  $d_p = 12$  mm.

out that gas-liquid and liquid-solid mass transfer resistances can be neglected if the diffusional (Thiele) modulus for the catalytic reaction is  $> 1$ .

Normal procedures for estimation of the effectiveness factor,  $\eta$ , in reaction with single-phase flow were discussed in Chapter 7, and if the pores in the catalyst particles are completely filled with liquid, then similar methods can be used with appropriately modified diffusivities for trickle-bed reactors. Since diffusion coefficients in the liquid phase are considerably smaller than those in the gas phase, catalyst effectiveness can be low for trickle-bed reactors, even for relatively small particle sizes. Following the development in Chapter 7 we can still say that,

$$\eta = \frac{\tanh \phi}{\phi} \quad (8-236)$$

in the region of strong diffusion, with the Thiele modulus defined for arbitrarily shaped particles as

$$\begin{aligned} \phi &= \Lambda(k/D_{eff})^{1/2} \\ \Lambda &= \left( \frac{V_p}{S_p} \right) \end{aligned} \quad (8-237)$$

for our Academic Reaction #1. In Chapter 7 we discussed the nature of  $D_{eff}$  in some detail; here let us follow the simplest defining relationship,

$$D_{eff} = \left( \frac{\mathcal{D}\epsilon_p}{\tau} \right) \quad (8-238)$$

where  $\epsilon_p$  is the particle void fraction,  $\tau$  the tortuosity factor (normally about 3 to 5), and  $\mathcal{D}$  the liquid-phase diffusion coefficient (normally of reactant).

If the catalyst particles are not completely wetted by the liquid phase and the pores consequently not completely filled with liquid phase (static holdup gives some indication of whether this is the case or not), the situation is considerably more complex. In addition to being a function of the Thiele modulus, the catalytic effectiveness will now depend on the fraction of external wetting,  $\eta_{CE}$ , and the fraction of pore volume filled with liquid,  $\eta_i$ . Dudokovic [M.P. Dudokovic, *Amer. Inst. Chem. Eng. Jl.*, 23, 940 (1977)] proposed a reasonable approach that accounts for all three factors. If the reaction proceeds only on the catalyst surface effectively wetted by the liquid phase and components of the reaction mixture are nonvolatile, then one can in principle modify the definition of the Thiele modulus to

$$\phi_{TB} = \left( \frac{\eta_i}{\eta_{CE}} \right) \phi \quad (8-239)$$

The effectiveness factor in the trickle bed would then be defined as

$$\eta_{TB} = (\eta_{CE}/\phi) \tanh \left( \frac{\eta_i \phi}{\eta_{CE}} \right) \quad (8-240)$$

For small values of  $\phi$  (slow reaction),

$$\eta_{TB} \rightarrow \eta_i \quad (8-241)$$

and for large  $\phi$ ,

$$\eta_{TB} = (\eta_{CE}/\phi) = (\eta_{CE})\eta \quad (8-242)$$

The general results accord with common sense. For example, for large diffusional resistances ( $\phi \gg 1$ ) the reaction occurs in a narrow zone close to the external surface of the particle, and the utilization of the catalyst then becomes proportional to the fraction of external surface wetted,  $\eta_{CE}$ . Via similar reasoning, in the kinetically controlled regime ( $\phi \ll 1$ ) the reaction rate is proportional to the internal volume wetted,  $\eta_i$ . Now, all of this sounds fine and the dedicated would undoubtedly scurry off immediately in search of appropriate correlations for the parameters  $\eta_{CE}$  and  $\eta_i$ . Unfortunately, they are doomed to return empty-handed, or nearly so, since there are essentially no correlations available for  $\eta_i$ , and those for  $\eta_{CE}$  are unreliable [J.G. Schwartz, E. Weger and M.P. Dudokovic, *Amer. Inst. Chem. Eng. Jl.*, 22, 894 (1976)]. A rather detailed study of wetting efficiency was reported by Mills and Dudokovic [P.L. Mills and M.P. Dudokovic, *Amer. Inst. Chem. Jl.* 22, 894 (1981)] who gave a correlation in terms of nondimensional quantities. However, it is difficult to estimate the reliability of that correlation because of the few reliable experimental data available—then or now. One can always make an estimate, at risk, of  $\eta_i$  and  $\eta_{CE}$  from static holdup data.<sup>20</sup>

If the reaction is gas-reactant limited, Ramachandran and Smith [P.A. Ramachandran and J.M. Smith, *Amer. Inst. Chem. Eng. Jl.*, 25, 538 (1978)] suggested that the overall effectiveness factor can be obtained as the weighted average of the wetted and unwetted parts of the catalysts. Hence,

$$\eta_0 = \frac{(\eta_{CE}/\phi) \tanh \phi}{1 + \frac{\phi \tanh \phi}{(N_{Sh})_L}} + \frac{(1 - \eta_{CE})[(\tanh \phi)/\phi]}{1 + \frac{\phi \tanh \phi}{(N_{Sh})_G}} \quad (8-243)$$

but even this still leaves the dedicated in search of a correlation. If the catalyst is completely wetted by the liquid phase one can retreat to the basic definitions of equations (8-236) to (8-238). The rate constant  $k$  must, of course, be available from other sources, but  $\Lambda$  is directly measurable, as well as the particle porosity  $\epsilon$ . The tortuosity  $\tau$  may cause a bit more difficulty, but as discussed after equation (8-238) the general range of expected values is known, and values of this parameter have been measured for quite a number of typical porous materials including catalysts and catalyst supports (see Table 7.4, Chapter 7). Problems may come from an unexpected direction, which is the evaluation of a proper value for the effective diffusivity,  $D_{eff}$ . Many applications of trickle beds involve heavy molecular weight materials, in which the molecular size is significant compared to catalyst pore dimension. In such cases, the effective diffusivity decreases because of the proximity of the pore wall and estimates based on liquid-phase diffusivities will be too large. There is not a lot of fundamental information concerning this, but some approaches were suggested by Pitcher et al. [W.H. Pitcher, C.K. Colton and C.N. Satterfield, *Amer. Inst. Chem. Eng. Jl.*, 19, 628 (1973)] and by Tamm et al. [P.W. Tamm, H.F. Harnsberger and A.G. Bridge, *Ind. Eng. Chem. Proc. Design Devel.*, 20, 262 (1981)].

<sup>20</sup> "Any old port in a storm."—Anonymous



**Illustration 8.6**<sup>21</sup>

Satterfield defined an “ideal” trickle-bed reactor as one that obeys the following conditions.

1. Plug flow of liquid.
2. No mass- or heat-transfer limitations between gas and liquid, between liquid and solid, or intraparticle within the catalyst.
3. First-order, isothermal, irreversible reaction with respect to reactant in the liquid phase; gaseous reactant present in great excess.
4. Catalyst pellets completely wetted.
5. Reaction occurs only at the catalyst-liquid interface.
6. No vaporization or condensation.

Derive a workable set of equations, in accord with the restrictions above, to determine the reactant conversion in such an ideal trickle-bed reactor. What is the relationship of this to reality?

*Solution*

The answer to the question above is probably “very little” (see Section 8.3), however, let us take a closer look at the situation. From a mass balance across a differential volume element,  $d\bar{V}$ , of the reactor, we have

$$FC_0 dx = (-r) d\bar{V} \quad (\text{i})$$

where  $C_0$  is the reactant concentration in the entering liquid phase in, say, mols/cm<sup>3</sup>,  $x$  fractional conversion of reactant, and  $d\bar{V}$  is the differential volume element under consideration. For first-order reaction,

$$(-r) = kC(1 - \epsilon) \quad (\text{ii})$$

where the rate constant is in units of (cm<sup>3</sup> liquid/cm<sup>3</sup> pellet-s). Combining (i) and (ii),

$$FC_0 dx = k(1 - \epsilon)C d\bar{V} \quad (\text{iii})$$

$$C = C_0(1 - x)$$

and

$$F \int \frac{dx}{1 - x} = k(1 - \epsilon) \int d\bar{V} \quad (\text{iv})$$

Thence,

$$\ln\left(\frac{C_0}{C_{out}}\right) = \left(\frac{\bar{V}}{F}\right)k(1 - \epsilon) = \frac{k(1 - \epsilon)}{(L_v/h)} \quad (\text{v})$$

or, in terms of the liquid hourly space velocity (LHSV),

$$\ln\left(\frac{C_0}{C_{out}}\right) = \frac{3600 k(1 - \epsilon)}{LHSV} \quad (\text{vi})$$

<sup>21</sup> After C.N. Satterfield, *Amer. Inst. Chem. Eng. JI.*, 21, 209, with permission of the American Institute of Chemical Engineers, (1975).

where  $L_v$  is the liquid superficial flow rate in cm/s, and  $h$  is the depth of the packed bed.

*Comparison with slurry reactor measurements*

If the simplifying assumptions above also hold for a slurry reactor, one should be able to obtain values for the rate constant  $k$  in an autoclave experiment. One would measure changes in concentration with time (i.e., batch reactor procedure) rather than changes with position as in a trickle bed, but the two measures should be proportional to each other. For the slurry reactor,

$$\left(\frac{dC}{dt}\right) = \frac{(-r)(v_{cat} - v_L)}{v_L} \quad (\text{vii})$$

where  $(-r)$  is the rate in [mols/(cm<sup>3</sup> cat + cm<sup>3</sup> liquid)-s],  $v_{cat}$  is the volume of catalyst in the reactor in cm<sup>3</sup>, and  $v_L$  is the volume of liquid in the reactor, also in cm<sup>3</sup>. Now, using equation (ii) in equation (vii) we have

$$\left(\frac{dC}{dt}\right) \left(\frac{v_L}{v_{cat}}\right) = kC(1 - \epsilon) \quad (\text{viii})$$

where  $(1 - \epsilon)$  is the volume fraction of catalyst in the slurry. Integrating,

$$\ln\left(\frac{C_0}{C_t}\right) = \left(\frac{v_{cat}}{v_L}\right)kt(1 - \epsilon) \quad (\text{ix})$$

where, for the slurry reactor,  $C_0$  refers to the initial concentration. We may then evaluate  $k$  in the normal manner from  $C_t$  versus  $t$  data; the only thing to remember is that the slope of a plot of  $\ln(C_0/C_t)$  versus  $t$  contains the factor  $(v_{cat}/v_L)$ .



HORATIO SAYS

How much does all of this differ from the analysis of a typical plug-flow reactor? What are the corresponding terms between the two reactor models?

### 8.4.3 Axial Dispersion Considerations

We might wonder about the necessity of giving the illustration above, since the ideal trickle-bed reactor is nothing more than a glorified PFR with a couple of additional parameters. Such criticism is, in fact, hard to rebut. Possibly the best justification is that the ideal model gives us a place to start. The discussion of hydrodynamic factors in Section 8.1 suggests that nonidealities in the liquid flow are of potential importance, and indeed this is so. Here we can return to an old friend from Chapter 5, the axial dispersion coefficient  $D_L$ . In general Pellet numbers are significantly lower for trickle-flow conditions than for single-phase flow through conventional packed beds

under similar circumstances. There is no lack of proposed correlations. A simple and reasonably reliable one is that Mitchell and Furzer [R.W. Mitchell and I.A. Furzer, *Chem. Eng. Jl.*, 4, 531 (1972)].

$$(N_{Pe})_L = (N_{Re})_L^{0.7} (N_{Ga})_L^{-0.32} \quad (8-244)$$

where

$$(N_{Pe})_L = \frac{u_L d_p}{D_L}; \quad (N_{Re})_L = \frac{d_p \rho_L u_L}{\mu_L}; \quad (N_{Ga})_L = \frac{d_p^3 g \rho_L^2}{\mu_L^2}$$

with  $u_L$  the interstitial velocity and  $D_L$  the axial dispersion coefficient. Early on Van Swaaij et al. [W.P.M. Van Swaaij, J. C. Charpentier and J. Villermux, *Chem. Sci. Eng. Sci.*, 24, 1083 (1969)] suggested that the Peclet number could be correlated with liquid holdup. Furzer and Mitchell [I.A. Furzer and R.W. Mitchell, *Amer. Inst. Chem. Eng. Jl.*, 2, 380 (1970)] thus provided us with

$$(N'_{Pe})_L = 4.3[(N'_{Re})_L / \beta_f]^{1/2} (N_{Ga})_L \quad (8-245)$$

where the primed quantities are defined using the superficial liquid velocity instead of the interstitial value, and  $\beta_f$  is the dynamic holdup. The only difficulty found is that such correlations are for air-water systems. Some variety is provided by Hochman and Effron [J.M. Hochman and E. Effron, *Ind. Eng. Chem. Fundls.*, 8, 63 (1969)], who studied the  $N_2$ -methanol system and proposed

$$(N_{Pe})_L = 0.042(N_{Re})_L^{0.5} \quad (8-246)$$

where  $(N_{Re})_L$  was defined as

$$(N_{Re})_L = [u_{OL} \rho_L d_p / \mu_L (1 - \epsilon)]$$

with  $u_{OL}$  the superficial velocity. The three correlations for Peclet number above are really quite similar; the role of the Galileo number is somewhat tenuous in these correlations and equation (8-246) is recommended for hydrocarbon systems in the book by Shah.

#### 8.4.4 Some Combined Models

A long time ago,<sup>22</sup> in Chapter 5, we presented some combinations of PFR and CSTR as a means of modeling nonideal flow patterns—particularly when large deviations (short-circuiting, dead volume, etc.) were encountered. However, to this point we really have not done much to exploit such models. They do have a home, to some extent, in modeling flow patterns in trickle-bed reactors when the axial dispersion model is not up to the task. A number of those, classified as to the number of parameters involved (nothing in this life is completely free), were discussed in the text by Shah. It is not clear that any of these have ever been used as the basis for a design, but they are fun anyway. Table 8.3 gives an overview of some of these. The question as when to stop in Table 8.3 is arbitrary, since there are other four-parameter models around, and even some with five parameters. However, remember the little morality tale concerning the number of parameters involved in physico/chemical models that was set forth in Chapter 3.

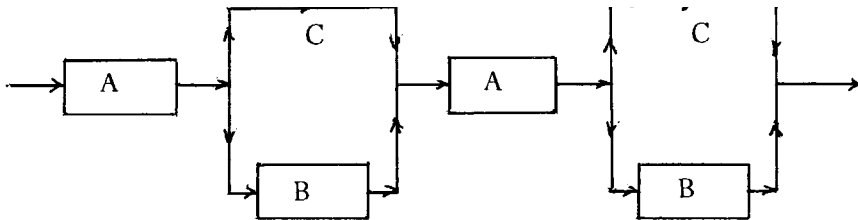
<sup>22</sup> "... in a galaxy far, far away..."—G. Lucas (Star Wars).

**Table 8.3** Some Combined Models Proposed for Trickle-Bed Flow1. *Simple Bypass*

Parameters: One: fraction of flow to perfect mixing.

Reference: R.W. Mitchell and I.A. Furzer, *Trans. Inst. Chem. Eng.*, 50, 334 (1972).

Picture:



A: Laminar film region

B: Perfectly mixed static holdup region

C: Instantaneous bypass

2. *Deans and Lapidus Mixing Cells in Series*

Parameters: Two: fraction of liquid that is stagnant and the mass-transfer coefficient between stagnant and flowing liquid.

References: H.A. Deans and L. Lapidus, *Amer. Inst. Chem. Eng. Jl.*, 6, 656 (196); H.A. Deans, *Soc. Pet. Eng. Jl.*, 3, 49 (1963).

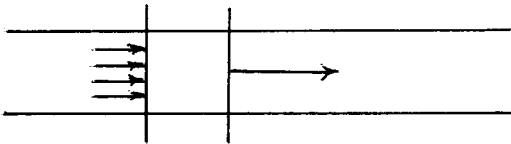
Picture: See Chapter 6.

3. *Axial Dispersion*

Parameters: Two: fractional liquid holdup and the axial dispersion coefficient.

Reference: See Chapter 5.

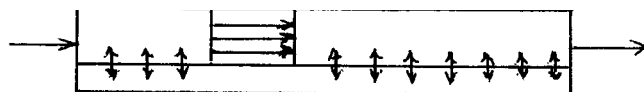
Picture:

4. *Cross Flow*

Parameters: Two: fraction of liquid in plug flow and the mass-transfer coefficient between stagnant and flowing liquid.

References: J.M. Hochman and E. Effron, *Ind. Eng. Chem. Fundls.*, 8, 63 (1969); C.J. Hoogendoorn and J. Lips, *Can. J. Chem. Eng.*, 43, 125 (1965).

Picture: Main plug flow channel flowing and stagnant liquid

5. *Time delay*

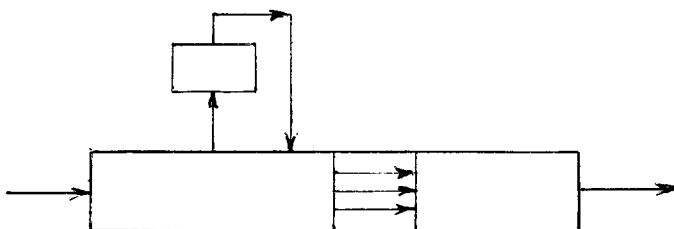
Parameters: Three: time for initial breakthrough of tracer in an  $E(t)$  experiment, mean delay time, and total number of delays per element of fluid during its residence time. The delay times are exponentially distributed about a mean value.

Table 8.3 Continued.

## 5. Time Delay

References: B.A. Buffham, *Chem. Eng. Jl.*, 1, 31 (1971); B.A. Buffham and L.G. Gibilaro, *Chem. Eng. Jl.*, 1, 31 (1970); B.A. Buffham, L.G. Gibilaro and M.N. Rathor, *Amer. Inst. Chem. Eng. Jl.*, 16, 218 (1970).

Picture: Main plug flow with lateral streams delayed at different points the bed (perfectly mixed).



## 6. Modified Cross Flow

Parameters: As for cross flow, plus axial dispersion in the flowing liquid.

References: W.P.M. Van Swaaij, J.C. Charpentier and J. Villiermaux, *Chem. Eng. Sci.*, 24, 1083 (1969).

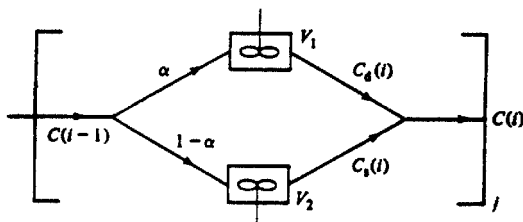
Picture: See 4 above.

## 7. Staged Backmixing

Parameters: Three: fraction of liquids in the mobile zone and relative volumes of mobile and stagnant zones, plus the number of stages.

Reference: See 6 above; also J. Villiermaux and W.P.M. Van Swaaij, *Chem. Eng. Sci.*, 24, 1097 (1969).

Picture: Split of feed into fractions  $\alpha$  and  $(1 - \alpha)$  into stagnant,  $V_i$ , and mobile,  $V_s$ , zones. Figure is for the  $i$ th stage in the sequence.

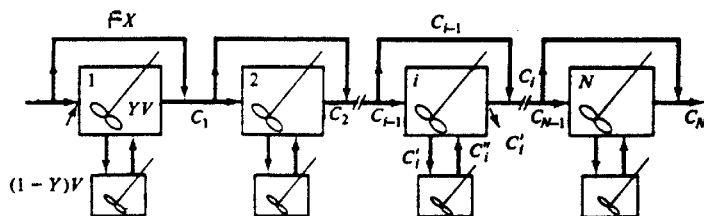


## 8. Staged Mixing with Bypassing

Parameters: Four: fraction bypass flow, relative volumes of stagnant and mobile zones, and number of stages.

Reference: J. Raghuraman and Y.B.G. Varma, *Amer. Inst. Chem. Eng. Jl.*, 22, 612 (1976).

Picture:



### 8.4.5 Trickle-Bed Reactor Models

It is very interesting, after all this discussion of hydrodynamics, mass transfer, and other properties of trickle beds, to see what people have actually done when they get down to the task of trickle-bed reactor design.<sup>23</sup> Things get fairly basic quite rapidly, and while we don't retreat all the way to the ideal trickle-bed reactor model, neither do we attempt the presumption of three or four parameters. Some have proposed simplified heterogeneous models, others consider only the degree of contact between the liquid and solid phases, and still others base the approach on the mass-transfer factors appearing in the three-phase reactor/reaction system. Finally, there are some approaches based on the directly-determined residence time distribution function. We will take a brief look at each.

*Plug flow.* This is a small modification of the ideal model, including the catalyst effectiveness factor. Then,

$$\frac{dC}{d\xi} = -\frac{k(1-\epsilon)\eta C^m}{(LHSV)} \quad (8-244)$$

where  $\epsilon$  is the bed void fraction,  $m$  the order of reaction with rate constant  $k$ , and  $\xi$  a nondimensional distance (position within the reactor). In most applications  $m$  is either 1 or 2, with the result

$$\ln\left(\frac{C_0}{C_{out}}\right) = \frac{\eta k(1-\epsilon)}{(LHSV)}; \quad m = 1 \quad (8-245)$$

$$\frac{1}{C_{out}} - \frac{1}{C_0} = \frac{\eta k(1-\epsilon)}{(LHSV)}; \quad m = 2 \quad (8-246)$$

The effectiveness can be determined from the appropriate procedure in Section 8.4.2 for the case at issue. A consistent set of units would be  $k(m=1)$  in  $\text{cm}^3 \text{ liquid}/\text{cm}^3 \text{ solid-h}$  or  $k(m=2)$  in  $(\text{cm}^3 \text{ liquid})^2/\text{g-cm}^3 \text{ solid-h}$ , LHSV in  $\text{cm}^3 \text{ liquid}/\text{cm}^3 \text{ solid-h}$ , and  $C$  in  $\text{g}/\text{cm}^3$ . Aside from Satterfield, this model has appeared in reports by Reiss [L.P. Reiss, *Ind. Eng. Chem. Proc. Design Devel.*, 6, 486 (1967)] and Henry and Gilbert [G.H. Henry and J.B. Gilbert, *Ind. Eng. Chem. Proc. Design Devel.*, 12, 328 (1973)].

*Liquid holdup.* This approach derives from the observation that at low flow rates (typical of many pilot-plant studies), the apparent rate of reaction is dependent upon liquid flow rate. This was investigated by Henry and Gilbert using a correlation proposed by Satterfield for the external holdup,

$$\beta_{te} = \beta_r + \beta_f = a(N_{Re})_L^{1/3} (N_{Ga})_L^{-1/3} \quad (8-247)$$

where

$$(N_{Re})_L = \frac{G_L d_p}{\mu_L}; \quad (N_{Ga})_L = \frac{d_p^3 g \rho_L^2}{\mu_L^2}$$

where  $G_L$  is the mass flow rate of liquid per unit area, and  $a$  is a proportionality constant [C.N. Satterfield, A.A. Pelossof and T.K. Sherwood, *Amer. Inst. Chem.*

<sup>23</sup> As one might say, "... where the rubber meets the road ..."—Advertising copy, ca. 1970-1990).

Eng. Jl., 15, 226 (1969)]. Thus, for a first-order reaction,

$$\ln\left(\frac{C_{out}}{C_0}\right) \propto -\frac{k\beta_{te}}{(LHSV)^n} \quad (8-248)$$

Combining equations (8-247) and (8-248) gives

$$\ln\left(\frac{C_{out}}{C_0}\right) \propto -\frac{k\beta_{te}}{(LHSV)^{2/3}} \quad (8-249)$$

or, in more detail,

$$\ln\left(\frac{C_{out}}{C_0}\right) = (Z)^{1/3}(LHSV)^{-2/3}(d_p)^{-2/3}\nu^{1/3} \quad (8-250)$$

where  $\nu = \mu/\rho$  for the liquid, and  $Z$  is bed length.

There is no *a priori* justification for assuming that the reaction rate is proportional to holdup, however, the experimental evidence is there (at least according to Henry and Gilbert). According to this view, a certain minimum amount of holdup is required for full catalyst utilization. The correlating parameter in terms of the hydrodynamics is the ratio  $[(N_{Fr})_L/(N_{Re})_L]^{1/3}$ , where  $(N_{Fr})_L$  is given by  $(G_L^2/\rho_L d_p g)$  and  $(N_{Re})_L$  is as defined above. The general situation is shown in Figure 8.22. The particular holdup correlation used by Henry and Gilbert has been criticized as lacking in generality. This is probably so, and more recent work has expanded the range of variables considered. However, one would like to use some of the more general approaches for holdup given previously in this chapter, but this apparently has not been done. There is disagreement about the critical value of  $[(N_{Fr})_L/(N_{Re})_L]$  yielding 100% catalyst utilization, and the matter has not been resolved.

**Catalyst wetting.** As indicated by its name, this model is based on the assumption that the fraction of the outer surface of the catalyst wetted by the liquid phase is the critical factor in determining the overall reaction rate [D.E. Mears,

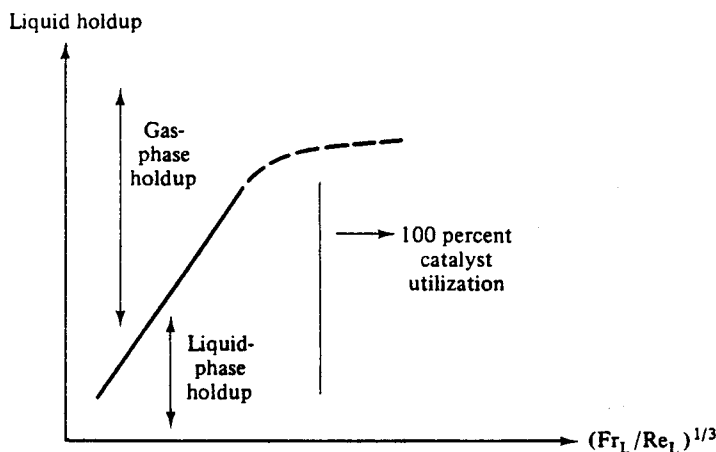


**Figure 8.22** Liquid holdup regimes in downflow trickle-bed operation.

*Advan. Chem.*, 133, 218 (1974)]. In this case we modify equation (8-244) to

$$\frac{dC}{d\xi} = -\frac{k(1-\epsilon)\eta a_W C}{(LHSV)} \quad (8-251)$$

where  $a_W$  is the ratio of wetted external area to total external area. It is thus an adjustable parameter, but the suggestion is to use the correlation of Purinak and Volelpohl [S.S. Purinak and A. Voelpohl, *Chem. Eng. Sci.*, 29, 501 (1974)]

$$a_W = 1.05(N_{Re})_L^{0.047}(N_{We})_L^{0.135}\left(\frac{\sigma_c}{\sigma_L}\right) \quad (8-252)$$

where  $(N_{We})_L$ , the Weber number for the liquid phase, is  $(G_L^2 d_p / \sigma_L \rho_L)$ ,  $\sigma_L$  is the liquid surface tension, and  $\sigma_c$  is a critical surface tension for a contact angle between liquid and packing. Combining equations (8-251) and (8-252) and integrating gives

$$\ln\left(\frac{C_0}{C_{out}}\right) = \frac{(Z)^{0.32}(d_p)^{0.18}(\sigma_c/\sigma_L)^{0.21}\eta}{(LHSV)^{0.6}(\nu_L)^{0.05}} \quad (8-253)$$

Comparison of the  $a_W$  correlation with experiment, however, indicates that the results lie above the predictions of equation (8-252) at higher liquid rates ( $\sim 500$  g/cm<sup>2</sup>-h), and in this region the correlation of Onda et al. [K. Onda, H. Takeuchi and H. Koyama, *Kagaku*, 31, 121 (1976)] should be used.

$$a_W = 1 - \exp[-1.36G_L^{0.05}(N_{We})_L^{0.2}(\sigma_c/\sigma_L)^{0.75}] \quad (8-254)$$

Combining this with equation (8-251) gives

$$\ln\left(\frac{C_0}{C_{out}}\right) = \frac{k(1-\epsilon)\eta}{(LHSV)} \{1 - \exp[-\gamma(Z)^{0.4}(LHSV)^{0.4}]\} \quad (8-255)$$

where dependencies on viscosity, surface tension, density, and particle size have been lumped into the factor  $\gamma$ . Since we are wandering away from the textbook to the handbook here, we will conclude this discussion of catalyst wetting now. Much more is available elsewhere.

**External mass transfer.** The method of moments applied to the pulse response of fixed-bed reactors [M. Suzuki and J.M. Smith, *Amer. Inst. Chem. Eng. Jl.*, 16, 882 (1970); *Chem. Eng. Sci.*, 26, 221, (1971)] was adapted to the consideration of reaction/mass-transfer effects in trickle beds [N.D. Sylvester and P. Pitayagulsarn, *Amer. Inst. Chem. Eng. Jl.*, 19, 640 (1973); *Can. Jl. Chem. Eng.*, 52, 539 (1974)]. In this latter work it was shown that the zeroth, first and second moments of the response to a pulse input can be divided rather neatly into several factors, each associated with a particular step in the overall reaction-transport process. The zeroth moment of the output is related to a series of parameters given by

$$1 - x = \exp(-\lambda_3 W) \quad (8-256)$$

where

$$W = (2Z/d_p); \quad \lambda_1 = \left(\frac{3}{F}\right)[(\lambda_0 F)^{1/2} \coth(\lambda_0 F)^{1/2} - 1]$$

$$\lambda_2 = \frac{1}{(1/\lambda_1 + 1/S)}; \quad \lambda_3 = \left(\frac{N_{Pe}}{2}\right)\{[1 + 4\lambda_2/(N_{Pe})]^{1/2} - 1\}$$



The significance of the factors above is as follows.

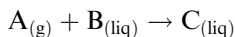
1.  $F = u_{OL}d_p/2D_{eff}(1 - \epsilon_p)$  considers the effect of intraparticle diffusion;  $u_{OL}$  is the superficial liquid velocity and  $\epsilon_p$  is the particle void fraction.
2.  $(N_{Pe}) = u_{OL}d_p/2D_L$  is the axial dispersion parameter.
3.  $S = 3(1 - \epsilon)K_T/u_{OL}$  is the external mass-transfer factor;  $K_T$  is the overall external mass-transfer coefficient.
4.  $\lambda_0 = k(1 - \epsilon)^2d_p/2u_{OL}$  is the surface reaction factor. The overall mass-transfer coefficient,  $K_r$ , is defined as

$$\frac{1}{K_r} = \frac{1}{k_G H \beta_G} + \frac{1}{k_L} + \frac{1}{K_s} \quad (8-257)$$

where  $\beta_G$  is the gas holdup based on the total volume of the reactor and  $K_s$  is the liquid-solid mass-transfer coefficient. Overall, the term  $\lambda_3$  can be considered as a reaction rate; when axial dispersion is negligible,  $\lambda_3 = \lambda_2$ , and when external diffusion is negligible,  $\lambda_3 = \lambda_1$ .

Note that this work of Sylvester and Pitayagulsarn does not present a design model per se; the moments analysis allows one to apply an experimental approach that is convenient for parameter evaluation in the reaction/reactor system when both transport and catalyst wetting are important in affecting overall conversion. We repeat a word of warning here. The evaluation of moments depends upon the numerical evaluation of a time-response versus time from 0 to  $\infty$ . Long tails on the response (often experimental artefact) can lead to very large  $\pm$  estimates of parameters. Despite the theoretical appeal, moments analysis is hazardous [see W.E. Munro, S. Delgado-Diaz and J.B. Butt, *J. Catal.*, 37, 158 (1975)].

*General approach.* It is interesting, as stated before, that when we get around to discussing the realities of reactor design we find simple models.<sup>24</sup> These are normally based on one particular factor, such as holdup, catalyst wetting, etc., and as a consequence have little value to more general design considerations. For this reason it is a good exercise to sit down and, at least, write out the mathematical relationships that are appropriate based on what we know about reactor analysis and design. So, here goes, considering the reaction to be



with intrinsic kinetics

$$(-r_A) = kA_S B_S \quad (8-258)$$

For isothermal reaction conditions, the mass balances are

A – Gas

$$D_G \frac{d^2 A_G}{dz^2} - u_{OG} \frac{dA_G}{dz} - K_L a_L (A_G - A_L) = 0 \quad (8-259)$$

<sup>24</sup>“The ugliest of trades have their moment of pleasure.”—*D. Jerrold*

A – Liquid

$$D_L \frac{d^2 A_L}{dz^2} - u_{OL} \frac{dA_L}{dz} + K_L a_L (A_G - A_L) - K_{SA} a_S (A_L - A_S) = 0 \quad (8-260)$$

$$K_{SA} a_S (A_L - A_S) = k a_S \eta A_S B_S \quad (8-261)$$

B – Liquid

$$D_L \frac{d^2 B_L}{dz^2} - u_{OL} \frac{dB_L}{dz} - K_{SB} a_S S (B_L - B_S) = 0 \quad (8-262)$$

$$K_{SB} a_S (B_L - B_S) = k a_S \eta A_S B_S \quad (8-263)$$

C – Liquid

$$D_L \frac{d^2 C_L}{dz^2} - u_{OL} \frac{dC_L}{dz} + K_{SC} a_S (C_S - C_L) = 0 \quad (8-264)$$

$$K_{SC} a_S (C_S - C_L) = k a_S \eta A_S B_S \quad (8-265)$$

Also, with many boundary conditions

$$D_L \frac{dA_G}{dz} = u_{OG} (A_G - A_{Gi}); \quad z = 0^+ \quad (8-266)$$

$$D_L \frac{dA_L}{dz} = u_{OL} (A_L - A_{Li}); \quad z = 0^+$$

$$D_L \frac{dB_L}{dz} = u_{OL} (B_L - B_{Li}); \quad z = 0^+ \quad (8-267)$$

$$D_L \frac{dC_L}{dz} = u_{OL} (C_L - C_{Li}); \quad z = 0^+$$

and

$$\frac{dA_G}{dz} = \frac{dA_L}{dz} = \frac{dB_L}{dz} = \frac{dC_L}{dz} = 0; \quad z = Z$$

Now one recognizes this instantly as an axial dispersion model, both gas and liquid phases, and by now we ought to be able to write it down from memory. Nonetheless, let us take one last look to make *sure* that we know what everything means. An important point, not explicit in the equations, is that the liquid holdup (or the catalyst wetting) does not vary through the bed. The individual terms are then [see Figure (8.23)],

$D_G, D_L$  axial dispersion coefficients in gas and liquid phases; taken the same for A, B, C.

$k_L a_L$  overall gas-liquid volumetric mass-transfer coefficient (includes both gas- and liquid-side resistances for A).

$K_{Si} a_S$  liquid-solid mass-transfer coefficients ( $i = A, B, C$ ), normally the same for all species.

$z, Z$  axial coordinate and reactor length.

$\eta$  effectiveness factor.

$u_{OG}, u_{OL}$  superficial gas and liquid velocities.

$G, L, S$  subscripts for gas, liquid, and solid surface.

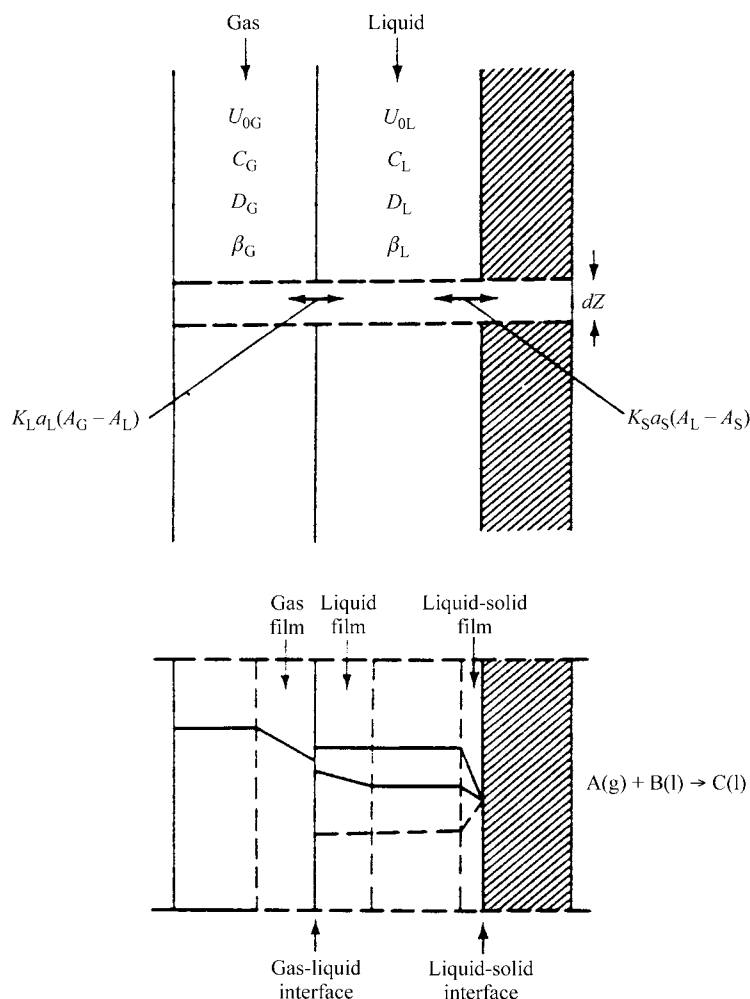


**Figure 8.23** Schematic diagram of a trickle-bed system for a second-order reaction.[After Y-T. Shah, *Gas-Liquid-Solid Reactor Design*, with permission of McGraw-Hill Book Co., New York, NY, (1979).]

At this point we can also play the game of DOP (“drop the parameter”). Although this seems like something lighthearted, DOP is fairly serious. If the gas moves in plug flow, which is often the case, then the term with  $D_G$  in equation (8-259), disappears. If the concentration of B in the liquid phase is very large, which is often the case, then terms involving  $B_L$  are nearly constant and equations (8-262), (8-263) and the condition on  $(dB_L/dz)$  will disappear. If the liquid-solid mass-transfer resistances are small, then  $A_L = A_S$ ,  $B_L = B_S$ , and  $C_L = C_S$ . If the feed gas is pure A, and B and C are nonvolatile, the  $A_G = A_L$ . Various limiting forms of the governing equations for this situation have been given in the literature [K. Ostergaard, *Advan. Chem.*, 26, 1361 (1971); H. Hofmann, *Int. Chem. Eng.*, 17, 19 (1977); S. Goto, S. Watabe and M. Matsubara, *Can. J. Chem. Eng.*, 54, 531 (1976)].

We probably don't have to, at this point, say that the overall model here, or even considerable simplifications of it, are best left to numerical solution. The axial dispersion model seems to work pretty well, at least for cases where the holdup/wetting does not vary much with position in the reactor. For large changes in this factor, or for nonideal flows involving stagnant zones or liquid/gas bypassing, some version of one of the combined models will be required. It will be understood that these will be *very specific* to the particular design under consideration.

### Illustration 8.7<sup>25</sup>

A new catalyst for the desulfurization of a heavy feedstock is to be evaluated. Some experimental results for operation at LHSV = 1 h<sup>-1</sup>, 136 atm, 400°C, and a hydrogen circulation rate of 1.4 × 10<sup>8</sup> cm<sup>3</sup>/bbl (STP), are available. The reactor was a 6.35 cm i.d. stainless steel tube provided with a 0.635 cm o.d thermowell mounted along the center-axis of the reactor. The catalyst size was 8-14 mesh.

The percentage desulfurization versus liquid flow rate data obtained with this catalyst are shown in Figure 8.24. As one explanation for the results shown in this figure it was proposed that axial dispersion in shorter beds caused their poor performance. Is this a viable explanation? Look at it. Based on the criterion of Mears, what is the maximum length required to eliminate axial dispersion as a factor important in reactor performance? Assume that the desulfurization reaction is pseudo-first-order, and that the reactor operation was isothermal. The relevant liquid properties are  $\rho_L = 0.93$  g/cm<sup>3</sup> and  $\mu_L = 0.15$  cP.

*Additional notes:*

1. The plot given, versus liquid flow rate, is equivalent to a plot versus length of reactor, since the LHSV was kept constant.
2. For analysis of dispersion effects see Montagna and Shah [A.A. Montagna and Y.T. Shah, *Ind. Eng. Chem. Proc. Design Devel.*, 14, 479 (1975)].
3. According to the Mears criterion [D.E. Mears, *Chem. Eng. Sci.*, 26, 1361 (1971)], the minimum ( $Z/d_p$ ) required to hold the isothermal reactor length to within 5% of that of the plug-flow case is

$$\left(\frac{Z}{d_p}\right) \leq \frac{20m}{(N_{Pe})_L} \ln\left(\frac{C_0}{C_{out}}\right) \quad (i)$$

where  $m$  is the reaction order and  $N_{Pe}$  the Peclet number based on the particle diameter.

### Solution

Montagna and Shah show that in cases where axial dispersion effects are important, a plot of  $\ln [C_{out}(\text{DISP})/C_{out}(\text{PFR})]$ , outlet concentration with dispersion divided by outlet concentration for plug flow, values of the  $\ln$  term versus  $Z$  should be a straight line with slope  $< -1$ . Values of this quantity as a function of  $Z$  obtained from Figure 8.24 are shown in Figure 8.25. Here the results from the longest bed, 80 cm, are taken to represent the plug-flow case. the results shown in the figure

<sup>25</sup> After Y-T. Shah, *Gas-Liquid-Solid Reactor Design*, with permission of McGraw-Hill Book Co., New York, NY, (1979).]

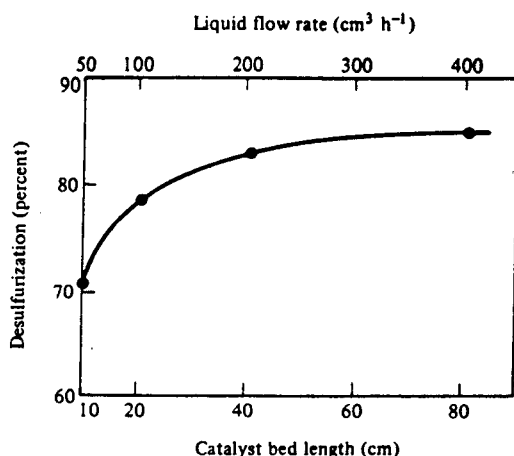


**Figure 8.24** Percentage desulfurization as a function of bed length and flow rate.

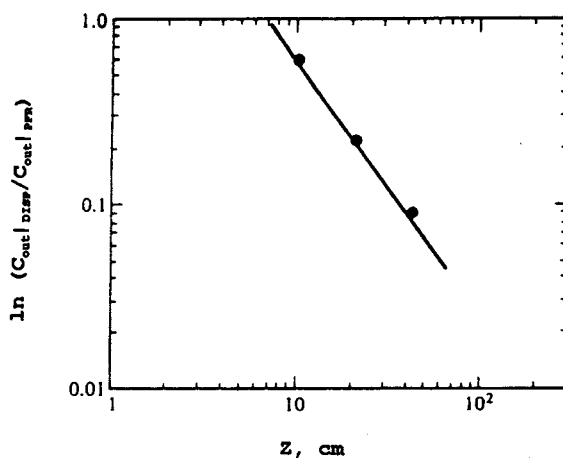


**Figure 8.25** Test of trickle-bed HDS data for axial dispersion using the proposal of Montagna and Shah.

show a strong influence of axial dispersion, which we have not seen in homogeneous, tubular-flow reactors, or even in fixed-bed catalytic reactors with reactants and products in the gas phase.

If we set  $C_0$  and  $C_{out}$  in the criterion of equation (i) as the inlet and outlet concentrations of sulfur, the effect of axial dispersion can be evaluated quantitatively. We will employ the correlation of Hochman and Effron [J.M. Hochman and E. Effron, *Ind. Eng. Chem. Fundls.*, 8, 63 (1969)] for Peclet number

$$(N_{Pe})_L = 0.042(N_{Re})_L^{0.5} \quad (ii)$$

where  $N_{Re}$  is also based on particle diameter, and on the superficial liquid velocity. Now  $Z_{min}$  can be determined from equations (i) and (ii) for various bed lengths, with

**Table 8.4** Minimum Bed Length to Eliminate Axial Dispersion Effects

Length, cm	$(N_{Pe})_L$	$Z_{min}$ , cm
10	0.023	189
20	0.033	172
40	0.047	147
80	0.066	93

Note:  $L_{min}$  varies with bed length since at constant LHSV as the bed length is varied the liquid flow is also varied.

the results shown in Table 8.4. These show that the minimum bed length to eliminate axial dispersion effects is  $\sim 80$  cm. Given uncertainties, let us call this  $\sim 100$  cm.



HORATIO SAYS

Does the approach used above include pore diffusion effects, which seem to be of great possible import in the operation of trickle beds? if not, how can we modify the analysis?

## Exercises

### Section 8.1

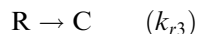
- Equation (8-11) expresses the behavior of the emulsion phase in the two-phase model when it is considered to be well-mixed. Derive this equation.
- A decomposition reaction is carried out in a fluidized-bed reactor with the following parameters specified.

$$\begin{array}{ll}
 L = 38 \text{ cm} & u_0 = 17 \text{ cm/s} \\
 \epsilon_m = 0.45 & \gamma_b = 0 \\
 \epsilon_{mf} = 0.50 & D = 0.19 \text{ m}^2/\text{s} \\
 k_r = 3 \text{ s}^{-1} & d_p = 4 \text{ cm} \\
 u_{mf} = 2.1 \text{ cm/s} & D_r = 25 \text{ cm} \\
 g = 980 \text{ cm/s}^2 &
 \end{array}$$

Using the three-phase model, compute the conversion to be expected assuming operation in the Geldhart A' region. Compare this with the equivalent PFR and CSTR results.

- Given the extreme parametric sensitivity of some oxidation reactions carried out in PFRs, as shown in Chapters 4 and 6, it could be considered more desirable to utilize the closer control of temperature provided by a

fluidized bed. Again, naphthalene oxidation is a good example reaction, where the sequence is



where A is naphthalene, R is phthalic anhydride, and C are the oxidation products. The following data are available:

$$d_p(50\%) = 50\text{--}70 \mu\text{m}; \quad (25\text{--}35\%) < 44 \mu\text{m}$$

$$u_{mf} = 0.005 \text{ m/s}; \quad \gamma_b = 0.005$$

$$\epsilon_m = 0.52; \quad \epsilon_{mf} = 0.57$$

Feed composition = 2.27 mol% A in air

$$D_A = 8.1 \times 10^{-6} \text{ m}^2/\text{s}; \quad D_R = 8.4 \times 10^{-6} \text{ m}^2/\text{s}$$

$$T = 350^\circ\text{C}; \quad P = 2.52 \text{ bar}; \quad u_0 = 0.45 \text{ m/s}$$

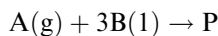
$$L = 5 \text{ m}; \quad D_R = 0.5 \text{ m}$$

$$k_{r1} = 1.5, \quad k_{r3} = 0.01 \text{ m}^3(\text{g})/\text{m}^3(\text{cat})\text{-s}$$

It is also estimated from correlation that  $d_b$  is 0.05 m and  $u_b = 1.5 \text{ m/s}$ . Calculate the conversion to desired product, and the selectivity, defined as  $[R/(A_0 - A)]$ .

## Section 8.2

4. For the case of irreversible first-order kinetics, show how the result of equation (8-107) can be reduced to the form for rate of reaction given in Table 8.1b.
5. The hydrogenation of  $\alpha$ -methylstyrene to cumene was studied in an agitated slurry reactor at 70–100°C using as a catalyst powdered 0.5 wt% Pd/ $\text{Al}_2\text{O}_3$ . The catalyst loading,  $W$ , was  $4 \times 10^{-3} \text{ g/cm}^3$  slurry, and the catalyst had a density,  $\rho_p$ , of  $1.58 \text{ g/cm}^3$  and an average particle diameter,  $d_p$ , of 0.005 cm. At 100°C the density of  $\alpha$ -methylstyrene is  $0.84 \text{ g/cm}^3$ , the viscosity is 0.47 cP, and the diffusivity of  $\text{H}_2$  in the liquid is  $3.6 \times 10^{-6} \text{ cm}^2/\text{s}$ . Determine if the rate of mass transfer is an important factor in the observed rate of reaction, which at 100°C was about  $4.3 \times 10^{-8} \text{ gmol/cm}^3$  slurry-s.
- 6.<sup>26</sup> Determine the liquid volume of a slurry reactor, which is well agitated, that will be required to convert 60% of the liquid reactant in an addition reaction at 525°K for



The gaseous reactant is present in excess for saturation at  $10^{-4} \text{ mol/cm}^3$ , with a Henry's law constant of 3  $[(\text{mol/cm}^3)_g/(\text{mol/cm}^3)_1]$ . The inlet concentration of B in aqueous solution is  $10^{-5} \text{ mol/cm}^3$ , and is introduced at

<sup>26</sup> After H.H. Lee, *Heterogeneous Reactor Design*, with the permission of Butterworth Publishers, Boston, MA, (1985).

a volumetric flow rate of  $1 \text{ cm}^3/\text{s}$ . The liquid-solid mass-transfer coefficient,  $k_S S_p$ , is  $2 \text{ s}^{-1}$  for both A and B. The intrinsic rate of reaction has been determined separately and is given by

$$(-r_A) = 10^{10} [\exp(-20/RT)] C_B C_A^{1/2}$$

where the activation energy is in kcal/mol and the rate in  $\text{mol}/\text{cm}^3 \text{ catalyst-s}$ . It may be assumed that the fraction of the liquid volume occupied by the catalyst is 0.02.

7. (a) Suppose oxygen is supplied from air into a well-dispersed suspension of bacteria in a mixed reactor. Oxygen transfer from the bubbles of air to the suspension liquor is usually the rate-limiting step in the overall aerobic process. Using the parameters below, find the apparent maximum rate of oxygen transfer from the suspension to the bacterial surface.

$D_0$  = diffusivity of  $\text{O}_2$  in the suspension =  $10^{-5} \text{ cm}^2/\text{s}$

$d_p$  = average cell diameter =  $2 \times 10^{-4} \text{ cm}$

$C_0$  = cell density =  $10^8 \text{ cm}^{-3}$

$C_1$  = bulk liquid  $\text{O}_2$  concentration = 6 ppm

$T = 25^\circ\text{C}$

It may be assumed that the relative velocity between the bacteria and the suspension medium is very small.

- (b) The observed rate of  $\text{O}_2$  uptake under the conditions stated above actually turns out to be some orders of magnitude less than that calculated in (a). Can you propose an explanation?
- (c) Do a little research and find out how the parameters described above are determined.
8. We are most accustomed to the generic problem of “given the parameters, how is something (often the conversion) determined?” However, it sometimes occurs that the conversion required is a specified design requirement, and we must determine a permissible feed concentration (or corresponding range). In this case let us consider a first-order irreversible reaction taking place in a given slurry reactor. All of the mass-transfer coefficients, the mass of the catalyst, the gas velocity, the Henry’s law constant, etc., are known. The required exit concentration is specified. What should be the inlet concentration of the reactant?
- (a) To have fun with this problem, consider that the reaction is actually second-order in reactant.
- (b) For further fun assume that the catalyst (either case of kinetics) diminishes in activity in a linear fashion by  $1/2$  over one day (dependent only upon time-on-stream), and you must design for operation to final specifications over a three-day period.
9. Consider a slurry reactor with a well-mixed slurry phase in which the reaction of Problem 6 is taking place. The gas-phase concentration of A is  $C_{A_0} = 10^{-4} \text{ mol}/\text{cm}^3$ , and the inlet liquid-phase concentration of B is  $C_{B_0} = 10^{-5} \text{ mol}/\text{cm}^3$ . It is assumed that the products have no effect on



the system, and it is required that 60% of B is to be converted to products. Further details are

$$D_0 = 10^{-5} \text{ cm}^2/\text{s}$$

$$\rho_p = 3.0 \text{ g/cm}^3 \text{ (catalyst particles)}$$

$$d_p = 10^{-3} \text{ cm (catalyst particles)}$$

$$k_s S_p = 2 \text{ s}^{-1} \text{ (for B)}$$

$$k_m = k_0 \exp(E_A/RT) C_A^{1/2}$$

$$k_0 = 10^{10} \text{ (cm}^3/\text{mol)}^{1/2}/\text{s}$$

$$E_A = 20 \text{ kcal/mol}$$

$$H_A = 3[\text{cm}^3/\text{mol}]_1/(\text{cm}^3/\text{mol})_g]$$

$$\rho_B = 0.5 \text{ g/cm}^3$$

*Additional information:* All the parameters may be taken as independent of temperature. The liquid feed contains 2 vol% of catalyst, and it was determined that the rate of mass-transfer of A to the catalyst surface is much greater than that of B. The intrinsic rate of reaction of B is

$$(-r_B) = k_0 \exp(-E_A/RT) [C_B]^m [C_A]^{1/2}; \quad m = 1$$

(a) Calculate the effectiveness factor for reaction temperatures of 350, 750 and 950°K (nonvolatile liquid phase). Determine from this whether the overall conversion is reaction limited, mass-transfer limited, or a mixture of the two, for each temperature level.

(b) Repeat part (a) for different kinetics:  $m = 0.5$  and  $2.0$ . Demonstrate the effect of apparent reaction order in B on the relative rate-controlling steps.

### Section 8.3

10. As promised in the text, derive the expressions for the constants  $G_1$ ,  $G_2$ ,  $H_0$ , and  $H_1$  appearing in the analysis of Section 8.3.2 for both batch and countercurrent cases.
11. Outline an experimental procedure and a method of data analysis that will enable one to determine the constants  $K_D S$ ,  $K$  and  $k$  of Illustration 8.4 with a minimum of experimental effort. Assume that  $D(t)$  measurements were taken at equal time increments (i.e., 0.1, 0.2, 0.3... h.)
12. Benzene is to be nitrated in a batch reactor with acid composed of 15 mol%  $\text{HNO}_3$ , 25 mol%  $\text{H}_2\text{SO}_4$ , and 60 mol%  $\text{H}_2\text{O}$ . The amount of this acid is to be 10% in excess of the theoretical amount required for 100% conversion, although only 96% conversion is required. The reaction temperature is 40°C, at which the densities are 0.87, 1.20 and 1.60 g/cm<sup>3</sup> for benzene, nitrobenzene, and the acid mixture, respectively.

The changes in density with composition may be neglected, but volume changes upon reaction should be considered. The solubility of organics in the acid phase, and water and sulfuric acid in the organic phase, may be

neglected, but the distribution of nitric acid between the two phases is important and should be accounted for (the volume of nitric acid in the organic phase, however, can be neglected). The simplification of solubilities here is for material balance purposes, since the reaction actually occurs in both phases.

We must calculate the time required for 96% conversion. The rate information of Biggs and White [M. Biggs and R.R. White, *Amer. Inst. Chem. Eng. Jl.*, 2, 321 91956)] can be used, and one may assume that the volume of benzene and nitrobenzene are additive. Note that the equation in the title of Figure 11 of that reference is in error. (Optional question: What does one do with the reaction mixture at the end—both to recover product and minimize environmental problems?)

13. Below are two sets of data on the hydrogenation of benzene and of phenol. Determine a means for the interpretation of the lowest and highest pressure data, and use your correlation to predict the middle-pressure results. Note that the original charge was apparently partially hydrogenated. Temperature in both cases was 120°C.

Percentage of Benzene Hydrogenated			
Time, h	30 atm	169 atm	323 atm
0	17	29	34
0.5	40	68	75
1.0	61	90	93
1.5	76	98	100
2.0	87	100	—
2.5	96	—	—

Percentage of Phenol Hydrogenated			
Time, h	40 atm	150 atm	330 atm
0	5	27	20
1	27	49	49
2	41	63	62
3	50	73	70
4	59	81	—
5	67	85	—
6	72	87	—
7	76	—	—

14. Let us now re-examine the data and your interpretation for the benzene hydrogenation data of Problem 13. We now need to design a suitable hydrogenation reactor system. It was proposed to charge an autoclave with 75 liters of pure benzene at operating temperature (120°C) under conditions such that at the end of the charging period there is negligible free space in the reactor. The pressure of the operation, though, must be maintained at 30 atm.
- (a) Estimate the intake volume of the hydrogen compressor (liters/time at SC) required to duplicate the time cycle of the laboratory run.

(b) What is the time required to attain 99% conversion with a compressor with only half the capacity of (a).

Neglect any inerts in the hydrogen and the benzene vapor. The density of benzene at these conditions is  $0.76 \text{ g/cm}^3$ .

15. The heat of reaction for the nitration of benzene with the mixed acid of the composition considered in problem 12 is about 38 (kcal/gmol-benzene) at the start of the reaction. Calculate the rate of heat evolution under these conditions. This will be found to be a dangerously high value. What manner of reactor operation would you suggest to get around this difficulty?

Further, plan a process in which the reaction is to be carried out with a charge of 5000 pounds of benzene in a vessel equipped with internal heat-transfer coils and with sufficient surface area to satisfy an allowable temperature rise of  $10^\circ\text{C}$ . Cooling water is available at  $20^\circ\text{C}$ . In the reactor the heat-transfer area is  $300 \text{ ft}^2$ , and an overall heat-transfer coefficient of  $200 \text{ Btu/ft}^2\text{-h-}^\circ\text{F}$  can be maintained. The reaction is to be carried out at  $40^\circ\text{C}$ , and under these conditions the nitric acid dissolved in the organic layer may be neglected. The acid is to be fed at a constant rate such that if it were all converted the limiting heat-removal rate would not be exceeded.

Now, calculate the rate and the conversion at the end of the feed period. Again, the total acid used should be 10% in excess of that theoretically required. Remember that after all the acid has been fed (after the feed period is over), the remaining time for the desired final conversion can be calculated in the usual way for a batch reaction.

#### Section 4.4

16. What system parameters are important in the scale-up of a trickle-bed reactor to be used for a gas-liquid-solid catalytic reaction if the reaction occurs in the liquid phase only and is controlled by
- (a) the gas-liquid mass transfer?
  - (b) the liquid-solid mass transfer?
  - (c) the intrinsic reaction kinetics.
17. Consider a fixed-bed column with downward cocurrent flow of liquid and gas phases. The column is packed with 0.3 cm diameter catalyst particles, with bed void fraction of 0.48, bed diameter of 5 cm, and bed length of 150 cm. Gas and liquid fluxes (both superficial) are  $10^3$  and  $10^4 \text{ kg/m}^2\text{-h}$ , respectively. Under reaction conditions the relevant gas properties are: average molecular weight = 10, density  $0.06 \text{ g/cm}^3$ , viscosity =  $0.6 \text{ cP}$ , surface tension =  $10 \text{ dynes-cm}$ , specific gravity = 0.9, and the molecular diffusivity of reactant =  $10^{-3} \text{ ft}^2/\text{h}$ . From these data estimate
- (a) Flow regime.
  - (b) Pressure drop.
  - (c) Gas and liquid holdups.
  - (d) Axial dispersion coefficient (liquid).
  - (e) Gas-liquid mass-transfer coefficient.
  - (f) Liquid-solid mass-transfer coefficient.

18. Figure 8.21d presents some experimental data on liquid-solid mass-transfer coefficients. How well do these agree with values predicted by the correlations of equations (8-233), (8-234), and (8-235)?

### Notation

$A$	bed cross-sectional area, length <sup>2</sup> ; total surface area in reactor, length <sup>2</sup>
$A_c$	cross-sectional area, length <sup>2</sup>
$A_G$	concentration of A in gas phase, mols/volume
$A_g$	concentration of A in gas phase, mols/volume
$A_L$	concentration of A in liquid phase, mols/volume
$A_1, B_1$	bulk liquid concentrations of A and B, mols/volume
$A_0$	concentration of A at gas-liquid interface, mols/volume
$A_{g1}, A_{1g}$	concentration of A (gas) or (liquid) at gas-liquid interface, mols/volume
$A_{go}, A_{gi}$	outlet and inlet concentrations of A in slurry reactor, mols/volume
$A_{g0}, A_{l0}$	inlet concentration of A in gas and liquid phases, mols/volume
$A_{Li}, B_{Li}, C_{Li}$	inlet concentrations of A, B and C, mols/volume
$A_S, B_S, C_S$	concentrations of A, B and C at external surface of catalyst particle, mols/volume
$A_1, A_2$	constants in equation (8-154); concentration of A in phases 1 and 2, mols/volume
$A_1, A_2, D_1, D_2, G_1, G_2, H_0, H_1$	constants in equations (8-160)-(8-163)
$A^*$	modified concentration = $(A_{gi}/H_A)$ ; modified concentration = $(H_A A_g)$
$A_2^*$	equilibrated concentration of A in phase 2, mols/volume
$a$	surface area per unit volume of continuous phase; proportionality constant in equation (8-247)
$a, b$	Constants in correlation of equation (8-206)
$a_s$	nondimensional concentration of A, see equation (8-103); liquid-solid interfacial area per volume
$a_v$	catalyst external surface area per volume of catalyst
$a_w$	ratio of wetted external area to total external area
$a'$	constant = $(a/V_L N)$ ; $(SV_b^{-1/3})$ in equation (8-173)
$a'_0$	initial value of $a'$
$\bar{a}', \bar{V}_b, \bar{y}$	average values of $a'$ , $V_b$ and $y$ ; see equation (8-169)
$a_1, a_2$	constants defined after equation (8-18)
$B_1$	concentration of B in liquid phase, mols/volume
$B_{l0}$	initial concentration of B in liquid phase; see equation (8-111)
$B_1, B_2$	concentration of B in phases 1 and 2, mols/volume
$C_b$	concentration of reactant in bubble phase; mols/volume
$C_c$	concentration of reactant in cloud/wake phase, mols/volume
$C_e$	concentration of reactant in emulsion phase, mols/volume
$C_j$	concentration of component j in liquid phase, mols/volume
$C_L$	$C_{eL} + C_{bL}$
$C_0$	inlet concentration of pure reactant, mols/volume
$C_{Ai}, C_{Ao}$	inlet and outlet concentration of A in Denbigh sequence, mols/volume
$C_{bL}$	bubble phase concentration at L, mols/volume
$C_{ib}, C_{ic}, C_{ie}$	concentration of A in bubble, cloud and emulsion phases, mols/volume

- $C_{oj}$  inlet concentration of j in liquid phase, mols/volume  
 $C_{ol}$  initial bulk concentration of liquid phase reactant, mols/volume  
 $C_{ej}$  equilibrium concentration of j with reversible reaction, mols/volume  
 $C_{S_o}, C_{T_o}, C_{U_o}$  outlet concentrations of S, T and U, Denbigh sequence, mols/volume  
 $C_{in}, C_{out}$  reactant concentration in and out of reactor, mols/volume  
 $C_R(max)$  maximum concentration of R, mols/volume  
 $C_1$  constant in equation (8-232)  
 $D$  molecular diffusivity, length<sup>2</sup>/time, typically cm<sup>2</sup>/s  
 $D_A, D_B$  diffusivities of A and B in liquid phase, cm<sup>2</sup>/s  
 $D_G, D_L$  axial dispersion coefficients for gas and liquid phases, cm<sup>2</sup>/s  
 $D_e$  effective diffusivity, cm<sup>2</sup>/s  
 $D_o$  orifice diameter, length  
 $D_{AL}$  diffusivity of reactant A in liquid phase, length<sup>2</sup>/time  
 $D_{eff}$  effective diffusivity, cm<sup>2</sup>/s  
 $\bar{D}$  bulk diffusivity; diffusivity in liquid; see equation (8-238), cm<sup>2</sup>/s  
 $d_b$  bubble diameter, length  
 $d_c$  diameter of cloud/wake phase, length  
 $d_p$  particle diameter, length  
 $d_{ob}$  initial bubble diameter, length  
 $E$  efficiency at same conversion, (PFR/FBR); see equation (8-34)  
 $E_G, E_L$  energy dissipation factor for gas and liquid phases, equations (8-231) and (8-232), W/m<sup>3</sup>  
 $F$  factor defined in equation (8-177)  
 $F_1, F_2$  flow rates of phases 1 and 2, volume/time  
 $f$  nondimensional concentration of A = (A/A<sub>0</sub>); frequency of bubble formation, time<sup>-1</sup>; bed void fraction  
 $f_c$  cloud volume factor; see equations (8-56) and (8-57)  
 $f_w$  wake volume factor; see equations (8-56) and (8-57)  
 $G$  gas phase flow rate, mols/time  
 $G_L$  liquid mass flow rate, mass/area-time  
 $G_0$  inlet gas phase flow rate, mols/time  
 $G_1, G_2$  constants in equation (8-151); gas flow rate into and out of reactor, mols/time  
 $g$  gravitational constant, length/time<sup>2</sup>  
 $H$  Henrys law constant, typically atm/(mol/volume)  
 $H_A, H_B$  Henrys law constant for A and B, atm/(mol/volume)  
 $H_0, H_1$  constants in equation (8-154)  
 $h$  gas phase holdup  
 $I$  integral function defined in equation (8-112)  
 $j_D$  mass transfer factor  
 $K_A$  mass transfer coefficient, time<sup>-1</sup>  
 $K_A, K_B$  absorption equilibrium constants in Langmuir-Hinshelwood rate equation, volume/mol  
 $K_s, K_{si}$  liquid-solid mass transfer coefficient for i, length/time  
 $K_T$  overall external mass transfer coefficient, length/time  
 $K_f$  composite rate constant; see equation (8-26), time<sup>-1</sup>  
 $K_o$  overall rate constant; see equation (8-117), time<sup>-1</sup>

- $K_r$  rate constant,  $\text{time}^{-1}$ ; see Figure 8.7  
 $K_{bc}, K_{ce}$  overall mass transfer coefficients, bubble to cloud/wake phase and cloud/wake to emulsion phase, respectively,  $\text{time}^{-1}$   
 $K_{fA}$  rate constant defined in equation (8-75)  
 $K_{fAR}$  rate constant defined in equation (8-74)  
 $K_{f12}, K_{f34}$  overall rate constants in equations (8-72) and (8-73)  
 $K_{bc,i}, K_{ce,i}$  mass transfer coefficients for i, bubble to cloud/wake phase and cloud/wake to emulsion phase, respectively,  $\text{time}^{-1}$   
 $K_{Ga}, K_{Ga}'$  overall gas phase mass transfer coefficients, mols/time-volume-atm  
 $(K_L S)_A$  overall mass transfer coefficient for A,  $\text{time}^{-1}$   
 $K_2$  rate constant in Langmuir-Hinshelwood scheme, typically (volume/mol)/time-wt; see equation (8-84)  
 $k$  rate constant,  $\text{time}^{-1}$   
 $k_L, k_G$  individual liquid and gas phase mass transfer coefficients, length/time  
 $k_d$  mass transfer coefficient, length/time; see equation (8-8)  
 $k_e$  rate constant ratio =  $(K_f/k_r)$   
 $k_g$  gas phase mass transfer coefficient, length/time  
 $k_1$  liquid phase mass-transfer coefficient, length/time; mass-transfer coefficient in presence of reaction; see equation (8-138), length/time  
 $k_m$  pseudo first-order rate constant,  $\text{time}^{-1}$   
 $k_{(m+n)}$  rate constant,  $\text{time}^{-1}$ ; see equation (8-83)  
 $k_r$  rate constant,  $\text{time}^{-1}$   
 $k_s$  liquid-solid mass transfer coefficient, length/time  
 $k_{bc}, k_{ce}$  mass-transfer coefficients, bubble to cloud/wake phase and cloud/wake to emulsion phase, respectively,  $(\text{time-area})^{-1}$   
 $k_{r1}, k_{r2}, k_{r3}, k_{r4}$  rate constants in Denbigh sequence,  $\text{time}^{-1}$   
 $k_{L2}$  mass-transfer coefficient in liquid phase; see equation (8-233), length/time  
 $k_{lo} k_L^\circ$  liquid phase mass-transfer coefficient in absence of reaction, length/time  
 $k_{r12}, k_{r34}$  combined constants =  $(k_{r1} + k_{r2}), (k_{r3} + k_{r4})$   
 $k_{GaL}, k_{LaL}$  gas and liquid phase mass-transfer coefficients in trickle bed,  $\text{time}^{-1}$   
 $(k_g S_b)$  gas phase mass-transfer coefficient,  $\text{time}^1$   
 $(k_1 S_b)$  liquid phase mass-transfer coefficient,  $\text{time}^{-1}$   
 $(k_s S_b)$  liquid-catalyst surface mass-transfer coefficient,  $\text{time}^1$   
 $(k_g S)_A$  gas phase mass-transfer coefficient for A in slurry reactor,  $\text{time}^{-1}$   
 $(k_1 S_1)_B$  liquid phase mass-transfer coefficient for B,  $\text{time}^{-1}$   
 $(k_L^\circ)_{SB}, (k_L^\circ)_{BS}$  values of  $k_L^\circ$  for single bubbles and bubble swarms  
 $k_1, k_2$  constants defined in equation (8-187b),  $\text{time}^{-1}$   
 $L$  bed length or height (expanded); liquid film thickness, length  
 $L_0$  height of unexpanded bed, length  
 $l$  distance variable in liquid film, length  
 $LHSV$  liquid hourly space velocity,  $\text{time}^{-1}$   
 $M_A$  constant defined in equation (8-96)  
 $m$  catalyst loading, wt catalyst/volume slurry; fitting constant in equation (8-221)  
 $m, n$  reaction orders  
 $N$  number of bubbles/volume of bed; number of bubbles/volumes of liquid  
 $N_B$  number of bubbles/reactor volume  
 $N_{Eo}$  Eötvös number =  $(\rho_L g d_p^2 / \sigma_L)$

- $N_{Fr}$  Froude number =  $(u^2 g / \delta)$   
 $N_{Ga}$  Galileo number =  $[d_p^3 \rho_L (\rho_L q + \Delta P_{LG})] / \mu_L^2$   
 $N_{Sc}$  Schmidt number =  $(\nu / D)$   
 $N_{Sh}$  Sherwood number =  $(k_s d_p / D)$ ;  $(k_{L2} / a_s D_{AL})$   
 $N_{Re}$  Reynolds number =  $(\rho_L L / A_c a_s \mu_L)$ ; see equation (8-233);  $(g d_b / \mu)$   
 $N_{We}$  Weber number =  $(\delta \rho u^2 / \sigma)$   
 $(N_{Da})_b$  gas phase Damköhler number =  $(k_1 / k_g H_A)$   
 $(N_{Da})_c$  Damköhler number for cloud/wake phase =  $(k_r / K_{bc})$   
 $(N_{Da})_e$  Damköhler number for emulsion phase =  $(k_r / K_{ce})$   
 $(N_{Da})_l$  liquid phase Damköhler number =  $(\eta k / k_s)$   
 $(N_{Da})_o$  overall Damköhler number; see equation (8-124)  
 $(N_{Fr})_L$  Froude number =  $(G_L^2 / \rho_L^2 d_p G)$   
 $(N_{Pe})_L, (N_{Re})_L, (N_{Ga})_L$  Peclet, Reynolds and Galileo numbers defined on the basis of interstitial velocity; see equation (8-244)  
 $(N_{Re})_L$  Reynolds number =  $(G_L d_p / \mu_W)$ ; see equation (8-247)  
 $(N_{Sh})_G, (N_{Sh})_L$  Sherwood numbers for gas and liquid phases  
 $(N_{We})_L$  Weber number =  $(G_L^2 d_p / \sigma_L \rho_L)$   
 $(N_{Re'})_L$  modified Reynolds number =  $(\rho_L u_L / a_s \mu_L \beta_i)$   
 $n$  constant in equation (8-171); reaction order  
 $P$  pressure, atm  
 $\Delta P_G, \Delta P_L$  pressure drop in gas and liquid phases, atm  
 $\Delta P_{LG}$  pressure drop of liquid-gas phase, atm  
 $Q$  gas flow rate, volume/time; overall mass exchange coefficient  
 $q$  cross flow mass transfer coefficient in fluid bed, volume/time; liquid phase flow rate, volume/time  
 $R$  bed radius, length, catalyst particle radius, length; gas constant, kcal/mol-K  
 $R_A$  rate of reactant consumption, mols/volume slurry-time; rate of reaction of A, mols/volume-time; flux of A, equation (8-137)  
 $R_G$  gas holdup =  $(1 - R_L)$   
 $R_L$  liquid phase holdup  
 $(-r)$  rate of reaction, mols/wt-time; see equation (8-83)  
 $(-r_A)$  rate of reaction of A, mols/volume-time  
 $r_j$  rate of reaction for component j, mols/volume-time  
 $[-r(A^*)]$  rate in terms of A\*, mols/volume-time  
 $r_1, r_2$  constants defined after equation (8-200)  
 $S$  interphase area; interphase area for mass transfer, typically area/volume; bubble shape factor; see equation (8-173); external mass-transfer factor; see after equation (8-256)  
 $S_c$  interfacial area; see equations (8-156) and (8-157)  
 $S_L$  interfacial area; see equation (8-133)  
 $S_1$  gas-liquid interfacial area; see equation (8-144),  $\text{cm}^2/\text{cm}^3$   
 $S_p$  particle external surface area,  $\text{length}^2$   
 $S_p, S_b$  interfacial areas for liquid-solid and gas-liquid in slurry reactor, area/volume  
 $S_{bc}, S_{ce}$  interfacial area, bubble to cloud/wake phase and cloud/wake phase to emulsion phase  
 $s, q$  correlation constants; see equation (8-235)  
 $T$  temperature, °C, K

- $t$  time; exposure time for element of bubble surface in contact with emulsion phase  
 $t_B$  batch time required for conversion  $x$   
 $t_D, t_R$  characteristic times for diffusion and extent of reaction; see equations (8-207) and (8-208)  
 $t_L$  average liquid residence time  $= (V_L/v)$   
 $(t_p)_L, (t_p)_G$  residence time for liquid and gas phases, respectively  
 $t_p$  length of time that an element of fluid remains in reactor  
 $U_{oG}, U_{oL}$  superficial gas and liquid velocities; see equation (8-256), length/time  
 $u$  fluid velocity, length/time  
 $u_b$  bubble phase velocity  $= (u_o - u_{mf})$ , length/time  
 $u_o$  superficial velocity of gas through emulsion phase, length/time  
 $u_g$  bubble velocity in slurry reactor, length/time  
 $u_L$  interstitial liquid velocity, length/time  
 $u_1, u_g$  liquid and gas velocity; see equations (8-130) and (8-131), m/s  
 $u_0$  inlet fluid velocity, length/time  
 $u_t$  entrainment velocity, length/time  
 $u_{br}$  bubble rise velocity, length/time  
 $u_{mf}$  minimum fluidization velocity, length/time  
 $u_{SL}$  superficial velocity of liquid phase, length/time  
 $V$  average volume per bubble; liquid volume per volume of reactor; total reactor volume  
 $V_b$  volume of bubble phase; volume of a single bubble  
 $V_g$  gas phase volume  
 $V_1$  liquid phase volume  
 $V_L$  slurry volume; volume of liquid phase  
 $V_p$  particle volume  
 $V_s$  volume of solids  
 $V_{DG}$  volume of a bubble; see equation (8-203)  
 $V_{oG}, (V_{oG})_0$  average bubble volume; initial average bubble volume  
 $V_{ob}$  initial bubble volume  
 $V_1, V_2$  volume of phases 1 and 2  
 $v$  volumetric flow rate, volume/time  
 $v_b$  bubble velocity, length/time  
 $v_B$  average bubble rise velocity, length/time  
 $v_L$  average velocity of liquid phase, length/time  
 $W$  mass of catalyst/volume of slurry; constant  $= 0.711 \text{ g}^{1/2} (6/\pi)^{1/6}$   
 $X$  reactant conversion  $= [1 - C_{(outlet)}/C_{(inlet)}]$   
 $x$  reactant conversion  
 $y$  distance (reactor length) variable; nondimensional length  $= (1/L)$   
 $y_j$  mol fraction of component  $j$  in gas phase  
 $y_{oj}$  inlet mol fraction of  $j$   
 $Z$  bed length  
 $z$  length variable  
  
*Greek*  
 $\alpha$  fraction of liquid phase occupied by liquid film; stoichiometric coefficient; constant in equation (8-221)  $= (qP/HG)$   
 $\alpha, \beta$  constants in  $r_1, r_2$ , defined after equation (8-200)



- $\alpha, \beta, \gamma$  constants in equations (8-21) and (8-13)  
 $\alpha_A$  constant =  $(K_L S)_A / u_g H_A$   
 $\alpha_A, \beta_A$  constants in equilibrium relationship for  $A_2^*$   
 $\beta_L, \beta_G$  liquid and gas holdup based on total reactor volume  
 $\beta_f, \beta_t$  dynamic holdup; total holdup  
 $\beta_{te}$  external holdup  
 $\gamma$  correlation factor in equation (8-255)  
 $\gamma_b, \gamma_c, \gamma_e$  volume solids/volume fluid in bubble cloud/wake, and emulsion phases, respectively  
 $\delta$  velocity ratio =  $(u_0/u_b)$ ; volume fraction of bubbles in bed; see equation (8-59); stoichiometric coefficient; distributor orifice diameter, length  
 $\epsilon$  bed porosity; fraction of volume in phase 2  
 $\epsilon_f$  fluidized bed porosity  
 $\epsilon_{mf}$  bed porosity at  $u_{mf}$   
 $\eta$  overall effectiveness factor; see equation (8-101); effectiveness factor for catalyst  
 $\eta_{CE}$  fraction of external catalyst particle surface wetted  
 $\eta_{TB}$  effectiveness factor in trickle bed  
 $\eta_b, \eta_l$  phase effectiveness factors; see equations (8-119) and (8-120)  
 $\eta_o$  catalyst effectiveness factor; see equation (8-97)  
 $\eta_i$  phase  $i$  effectiveness =  $[\gamma_i / (1 + \gamma_i N_{Da_i})]$ ; fraction of catalyst pore volume filled with liquid  
 $\eta_0$  overall effectiveness; see equation (8-122)  
 $\theta$  catalyst porosity  
 $\lambda$  enhancement factor; see equation (8-139); trickle bed scaling parameter; see equation (8-222)  
 $\Lambda$  generalized dimension =  $(V_p/S_p)$   
 $\Lambda_1, \Lambda_2, \Lambda_3$  parameters in equation (8-256)  
 $\mu$  gas viscosity, typically cP; viscosity, cP  
 $\mu_L$  liquid viscosity, cP  
 $\mu_{H_2O}$  viscosity of water, cP  
 $\nu$  stoichiometric coefficient; kinematic viscosity =  $(\mu/\rho)$ ; bubble formation frequency,  $\text{time}^{-1}$   
 $\xi$  nondimensional distance =  $(z/Z)$   
 $\rho$  gas density, mass or mols/volume  
 $\rho_L, \rho_G$  gas and liquid densities, mass or mols/volume  
 $\rho_l$  liquid density, mass or mols/volume  
 $\rho_p$  catalyst particle density, mass/volume; solids density, mass/volume  
 $\rho_s$  solids density, mass/volume  
 $\rho_{air}, \rho_{H_2O}$  densities of air and water, mass/volume  
 $\rho_1, \rho_2$  constants in equations (8-154) and (8-160)  
 $\sigma$  constant in equation (8-154); surface tension of gas-liquid interface, mass/ $\text{time}^2$   
 $\sigma_A$  constant in equation (8-103)  
 $\sigma_L$  liquid surface tension; see equation (8-252), mass/ $\text{time}^2$   
 $\sigma_{H_2O}$  surface tension of water, mass/ $\text{time}^2$   
 $\tau$  ratio =  $(V_s/v)$   
 $\tau(max)$   $\tau$  corresponding to  $C(max)$

$\phi$	generalized Thiele Modulus; see equations (8-100) and (8-135)
$\phi_0$	Thiele Modulus = $L(k/D)^{1/2}$
$\phi_{TB}$	modified Thiele Modulus; see equation (8-239)
$\chi$	pressure drop ratio
$\Psi$	trickle bed scaling parameter; see equation (8-223)

*Note:* Additional notation is given in Tables 8.1 and 8.3, in Figures 8.16 and 8.17, equations (8-191) and (8-192), and in Illustrations 8.4 and 8.6.

---

## Some More Unsteady-State Problems

Great science nobly labored  
to increase the people's joys,  
But every invention seemed  
to add another noise

— *A.P. Herbert*

For the most part we have labored over the analysis of steady-state problems, although there have been some important side trips into the unsteady state. Principal among these were the analysis of CSTR startup, visits to fixed-bed and CSTR dynamics arising from catalyst deactivation, and some discussion on adsorption variations. The purpose of this chapter is to pursue some of these topics in more detail; the range of interests here is rather broad, but all can be linked through a common concern with fixed-bed dynamics.

### 9.1 The Adsorption Wave

The title of this section is taken from an important early work of Klotz [I.M. Klotz, *Chem. Rev.*, 39, 241 (1946)] which had a basic objective "... to obtain an understanding of the various factors which determine the variation in the concentration of a gas effluent from a bed of adsorbent ...". We do not necessarily deal with chemical reactions here, but we have already had some introduction to the topic in Chapter 4, Section 7. There is more to add to the story, and much of what we say here is applicable to ion exchange as well as adsorption [see also, D.M. Ruthven, *Principles of Adsorption and Adsorption Processes*, Wiley-Interscience, New York, NY, (1984)].

A good deal of information about the basic interaction between the adsorbate and the adsorbent can be inferred from the shape of an effluent concentration-time (breakthrough) curve. Consider the cases shown in Figure 9.1.

If the interaction were instantaneous and without mass-transfer rate limitations, then we would have a simple transmission of whatever input of adsorbate that was admitted to the bed, with the input function at the exit of the bed at a time equal to the residence time in the bed. A step-function input is shown in Curve A. More commonly, we have breakthrough curves such as B in Figure 9.1, where the mass transport and/or adsorption processes are not infinitely rapid, or C in the figure, where rates are slow and even some reversible reaction may occur.

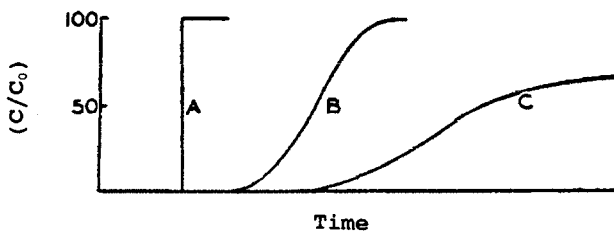


**Figure 9.1** Typical adsorbate breakthrough curves.

The similarity of these breakthrough curves to residence-time distribution curves is apparent, and in fact we can think of them as a kind of residence-time distribution for the adsorbate, although the processes occurring within the bed and leading to the observed breakthrough are much more complex than those occurring in a simple tracer experiment.

There are a number of steps that are involved in the adsorption process.

1. Mass transfer of the adsorbate from the fluid phase to the exterior surface of the adsorbent.
2. Pore diffusion of the adsorbate within the adsorbent pore structure.
3. Adsorption on the internal surface of the adsorbent.
4. Possible catalytic reaction of the adsorbate.

This sequence of steps should be familiar, since they are the same as those developed in Chapter 7 for the derivation of the catalytic effectiveness factor. Here we are interested primarily in steps 1–3, although there is one more case of chemical reaction to be considered. This one requires more analysis than before. To this point we have been sailing along; not much more.

It is convenient here to identify the analysis of the rate-controlling step and the type of equilibrium involved. In Chapter 4, Section 7, we presented one case corresponding to a “favorable” (or “very favorable” according to some) equilibrium. If we enlarge on this terminology, there are three principal types of equilibrium to be dealt with in adsorption/ion exchange, as shown in Figure 9.2.

As long as the equilibrium relationship is linear, one may obtain a rigorous mathematical solution to the problem, although the cure may be worse than the disease. For nonlinear cases there are a number of linearization approximations that can be used with success, as will be shown.

### 9.1.1 Favorable Equilibrium with Interphase Mass Transport Rate-Controlling

Actually, we have already discussed this case in Chapter 4, although the emphasis there was more as an example of an unsteady-state problem (i.e., nature of the problem) than as an example of the class of problems associated with adsorption and ion exchange. The important result of that analysis was the Klotz equation

$$\ln\left(\frac{C}{C_0}\right) = \left(\frac{k_D S C_0}{q_\infty v}\right)y - \left(\frac{k_D S}{v}\right)x - 1$$

The derivation in Chapter 4 was made using the constant bandwidth assumption, and thus strictly applied only to that particular situation. Here we wish to be a little

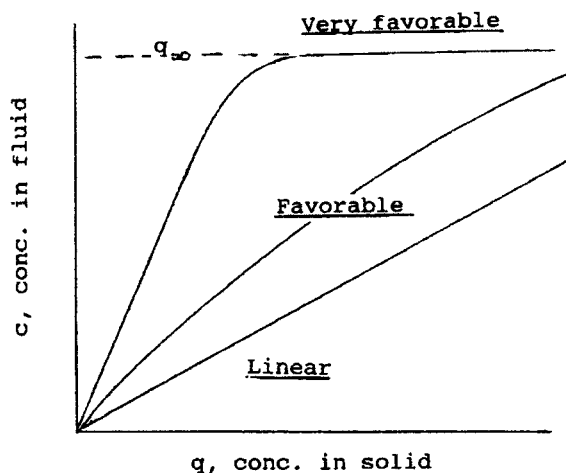


Figure 9.2 Typical equilibrium relationships for adsorption/ion exchange.

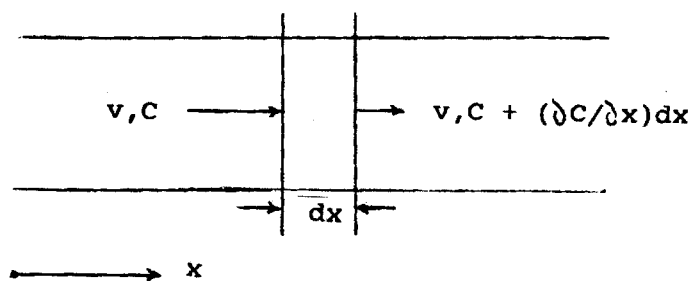


Figure 9.3 Schematic of adsorption system.

more fussy about the derivation, and will rework the case in a more formal manner. Consider the flow-system schematic of Figure 9.3. As in Chapter 4, the  $dx$  segment represents the active bandlength. Upstream of  $dx$  the adsorbant is saturated with adsorbate ( $q_\infty$  corresponding to favorable equilibrium), and downstream the adsorbent is empty ( $q = 0$ ). A material balance over the bed for a time interval  $dt$  is

$$wC dt = w \left[ C + \left( \frac{\partial C}{\partial x} \right) dx \right] dt + \left( \frac{\partial q}{\partial t} \right) dx dt + m(dx) \left( \frac{\partial C}{\partial t} \right) dt \quad (9-1)$$

where the first term is input by convection, the second is output by convection, the third term is accumulation by adsorbent, and the fourth term is accumulation by adsorbate. Here  $w$  is the volumetric flow rate of adsorbate (fluid phase), and  $m$  the bed void volume in volume per unit weight of bed.<sup>1</sup> We can not excuse the changing of symbols for things that are familiar from before, other than to say that here we follow the conventions of the literature in this area to make reference somewhat easier.

<sup>1</sup> Sorry for the change in notation. "I should be dead of joy."—*J. Lee*

If we simplify equation (9-1), then

$$\left(\frac{\partial C}{\partial x}\right)_t + \frac{m}{w} \left(\frac{\partial C}{\partial t}\right)_x + \frac{1}{w} \left(\frac{\partial q}{\partial t}\right)_x = 0 \quad (9-2)$$

Let us now make the variables change

$$\begin{aligned} x &= x \\ y &= wt - mx \end{aligned} \quad (9-3)$$

where  $y$  can be thought of as a downstream (wave front) volume equal to the volumetric flow up to time  $t$ , minus the volume of voids. Using the rules for changes of variables with partial derivatives, we have

$$\left(\frac{\partial C}{\partial x}\right)_t = \left(\frac{\partial C}{\partial x}\right)_y \left(\frac{\partial x}{\partial x}\right)_t + \left(\frac{\partial C}{\partial y}\right)_x \left(\frac{\partial y}{\partial x}\right)_t$$

or

$$\left(\frac{\partial C}{\partial x}\right)_t = \left(\frac{\partial C}{\partial x}\right)_y - m \left(\frac{\partial C}{\partial y}\right)_x \quad (9-4)$$

and

$$\begin{aligned} \left(\frac{\partial C}{\partial t}\right)_x &= \left(\frac{\partial C}{\partial y}\right)_x \left(\frac{\partial y}{\partial t}\right)_x = w \left(\frac{\partial C}{\partial y}\right)_x \\ \left(\frac{\partial q}{\partial t}\right)_x &= \left(\frac{\partial q}{\partial x}\right)_t \left(\frac{\partial x}{\partial t}\right)_x + \left(\frac{\partial q}{\partial y}\right)_x \left(\frac{\partial y}{\partial t}\right)_x \end{aligned} \quad (9-5)$$

The end of all this exercise in writing is

$$\left(\frac{\partial q}{\partial t}\right)_x = w \left(\frac{\partial q}{\partial y}\right)_x \quad (9-6)$$

If we now go back to the mass balance, we will obtain

$$\left(\frac{\partial C}{\partial x}\right)_y + \left(\frac{\partial q}{\partial y}\right)_x = 0 \quad (9-7)$$

As we progress in this section we will see that equation (9-7) is a standard form of mass balance for almost all of the problems we are involved with here.

Now we must consider more detail on the mass-transfer processes that go along with the intraphase adsorption/ion exchange

$$\left(\frac{\partial q}{\partial t}\right)_x = K_D S [C - f(q)]$$

or

$$\left(\frac{\partial q}{\partial y}\right)_x = \left(\frac{K_D S}{w}\right) [C - f(q)] \quad (9-8)$$

Initial and boundary conditions for equations (9-7) and (9-8) are

$$\begin{aligned} C(x=0, y) &= C_0; & q(x, y=0) &= 0 \\ f(q) &= 0; & q < q_\infty; & f(q) = C_0; & q &= q_\infty \end{aligned} \quad (9-9)$$

Now, recall the mass balance for the band

$$q_\infty x = C_0 y \quad (9-10)$$

At this point we have to worry a little bit about the nature of the input to the bed, which is given as a step-function from 0 to  $C_0$  in equation (9-9), and how it relates to what happens in the band. We will assume that the sharp front of the step-function is translated to the entrance to the band unchanged—as far as the fluid mechanics are concerned, then, there is plug flow. Now we have to have some way to tell this to equations (9-7) and (9-8). To do this, let us define two more new variables<sup>2</sup>, whose values will be *equal* in the band. This is done by finding a pair of constant multipliers for  $x$  and  $y$ , that we will term  $A$  and  $B$ , such that the

$$\begin{aligned} \text{New variable } u &= Ay & \text{and} \\ \text{New variable } v &= Bx \end{aligned} \quad (9-11)$$

so that  $u = v$  in the band in order to introduce the step-function relationship. Then, from equation (9-10),

$$x = \left( \frac{C_0}{q_\infty} \right) y$$

Multiplying by  $(K_D S/w)$ ,

$$\left( \frac{K_D S C_0}{q_\infty w} \right) y = \left( \frac{K_D S}{w} \right) x \quad (9-12)$$

A quick check on the units (remember from Chapter 4 that  $K_D S$  is a *volumetric* mass-transfer coefficient) reveals that these are dimensionless quantities, so

$$u = Ay = \left( \frac{K_D S C_0}{q_\infty W} \right) y \quad (9-13)$$

$$v = Bx = \left( \frac{K_D S}{W} \right) x \quad (9-14)$$

with  $A$  in dimensions of reciprocal volume and  $B$  in reciprocal mass. With these new variables, the working equations become

$$B \left( \frac{\partial C}{\partial v} \right) + A \left( \frac{\partial q}{\partial u} \right) = 0 \quad (9-15)$$

$$\left( \frac{\partial q}{\partial u} \right) = \left( \frac{B}{A} \right) [C - f(q)] \quad (9-16)$$

where we have dropped the subscripts from the partial derivatives for simplicity. In

<sup>2</sup>“Some play poker, some play bridge; others like to define variables.”—*C. Walker*

the band the relationship  $u = v$  holds, and we can treat  $f(q)$  as a step function,  $s_K$ ,

$$\begin{aligned} s_k &= 0; & u < v \\ s_K &= 1; & u > v \end{aligned} \quad (9-17)$$

with boundary conditions

$$\begin{aligned} C(v=0, u) &= C_0 \\ q(v, u=0) &= 0 \end{aligned} \quad (9-18)$$

The set of equations (9-15) to (9-18) can be solved directly by Laplace transforms. In view of the boundary conditions above, it is convenient to transform with respect to the variable  $u$ . Let us define

$$\begin{aligned} \mathcal{L}[C] &= \mathbf{C}; & \mathcal{L}[q] &= \mathbf{R} \\ \mathcal{L}[\partial C / \partial v] &= (d\mathbf{C} / dv) \\ \mathcal{L}[\partial q / \partial u] &= s\mathbf{R} - q(u=0) = s\mathbf{R} \end{aligned} \quad (9-19)$$

and

$$\mathcal{L}[s_k] = \left( \frac{e^{-sv}}{s} \right) C_0 \quad (9-20)$$

Hence the transformed equations are

$$B \left( \frac{d\mathbf{C}}{dv} \right) + As\mathbf{R} = 0 \quad (9-21)$$

$$s\mathbf{R} = \left( \frac{B}{A} \right) [\mathbf{C} - (e^{-sv}/s) C_0] \quad (9-22)$$

Combining (9-21) and (9-22) and simplifying

$$\left( \frac{d\mathbf{C}}{dv} \right) + \mathbf{C} = \left( \frac{e^{-sv}}{s} \right) C_0 \quad (9-23)$$

This is solved readily enough, with integrating factor  $e^v$ , as

$$d(\mathbf{C}e^v) = \left[ \frac{e^{v(1-s)}}{s} \right] C_0 dv \quad (9-24)$$

with limits

$$\mathbf{C}e^v[v=0]; \quad \mathbf{C} = (C_0/s) \rightarrow \mathbf{C}, v = \frac{C_0 e^{v(1-s)}}{s(1-s)} \quad (0 \rightarrow v)$$

Then

$$\mathbf{C} = \left[ \frac{C_0}{(s-1)} \right] e^{-v} - \left[ \frac{C_0}{s(s-1)} \right] e^{-sv} \quad (9-25)$$



Upon inversion of equation (9-25) we obtain the complete solution

$$C = C_0 e^{(u-v)}; \quad 0 < u < v \quad (9-26)$$

$$C = C_0 e^{(u-v)} + C_0 [1 - e^{(u-v)}] = C_0; \quad u > v \quad (9-27)$$

If we return to the original variables of the problem, we find

$$\ln\left(\frac{C}{C_0}\right) = \left(\frac{K_D S C_0}{q_\infty w}\right)y - \left(\frac{K_D S}{w}\right)x \quad (9-28)$$

This is the same as the Klotz equation of Chapter 4, equation (4-168), with the exception of the  $(-1)$  term. This discrepancy is the result of the fact that in order to use the step-function we had to neglect the material in the band in writing the material balance.

### 9.1.2 Linear Equilibrium with Mass-Transfer Rates Controlling

The origins of this analysis go back a long way, in fact, to the related heat-transfer problem [C.C. Furnas, *Trans. Amer. Inst. Chem. Eng.*, 24, 1942 (1930)], with subsequent adaptation to adsorption/ion exchange problems as discussed by Thomas [H.C. Thomas in *Ion Exchange*, (F.C. Nachod, ed.), Academic Press, New York, NY, (1949)]. The pair of starting equations are the same as (9-7) and (9-8), with the exception that  $f(q)$  now represents the linear equilibrium rather than a step-function. Then

$$f(q) = \left(\frac{C_0}{q_\infty}\right)q \quad (9-29)$$

so

$$\left(\frac{\partial q}{\partial y}\right) = \left(\frac{K_D S}{w}\right)C - \left(\frac{K_D S C_0}{q_\infty w}\right)q \quad (9-30)$$

Making the same variable substitutions in terms of  $u$  and  $v$  we obtain

$$B\left(\frac{\partial C}{\partial v}\right) + A\left(\frac{\partial q}{\partial u}\right) = 0 \quad (9-31)$$

$$\left(\frac{\partial q}{\partial u}\right) = \left(\frac{B}{A}\right)C - q \quad (9-32)$$

where  $A$  and  $B$  are the same as defined in equations (9-13) and (9-14). The boundary conditions are also as defined previously, equation (9-18), and we can again solve the equations via Laplace transforms. The transformed equations are

$$B\left(\frac{dC}{dv}\right) + AsR = 0 \quad (9-33)$$

and

$$R = \frac{(B/A)C}{(1+s)} \quad (9-34)$$

Substituting (9-34) into (9-33) for  $\mathbf{R}$ ,

$$\left(\frac{d\mathbf{C}}{dv}\right) + \left(\frac{s}{1+s}\right)\mathbf{C} = 0 \quad (9-35)$$

The solution to (9-35) is

$$\mathbf{C} = C_0 e^{-v} \left[ \frac{1}{(s+1)} + \frac{1}{s(s+1)} \right] e^{v/(1+s)} \quad (9-36)$$

and the inverse is obtained as

$$C = C_0 e^{-(u+v)} I_o(2\sqrt{uv}) + C_0 e^{-v} \int_0^u e^{-u} I_o(2\sqrt{uv}) du \quad (9-37)$$

For convenience we define

$$\phi(u, v) = e^u \int_0^u e^{-u} I_o(2\sqrt{uv}) du$$

then

$$\left(\frac{C}{C_0}\right) = e^{-(u+v)} [I_o(2\sqrt{uv}) + \phi(u, v)] \quad (9-38)$$

and

$$\left(\frac{q}{q_\infty}\right) = e^{-(u+v)} [\phi(u, v)] \quad (9-39)$$

The  $\phi(u, v)$  function arises in a number of problems involving linear equilibrium; some of the properties of this function are given in Table 9.1.

The solutions to equations (9-38) and (9-39) are given in Figures 9.4 and 9.5, and their arrangement is largely self-explanatory. For a given design one would presumably know the values of the parameters  $K_D S$  and  $q_\infty$ , and the operating conditions  $C_0$ ,  $w$ , and  $x$ . Then  $Bx$  can be determined directly and the corresponding pair  $(C/C_0)$  and  $A_y$  estimated from Figure 9.4, corresponding  $(q/q_\infty)$  from Figure 9.5.

**Table 9.1** Some Properties of the Functions  $\phi(u, v)$

---


$$\phi(u, v) + \phi(v, u) = e^{u+v} - I_o(2\sqrt{uv})$$

Thus,

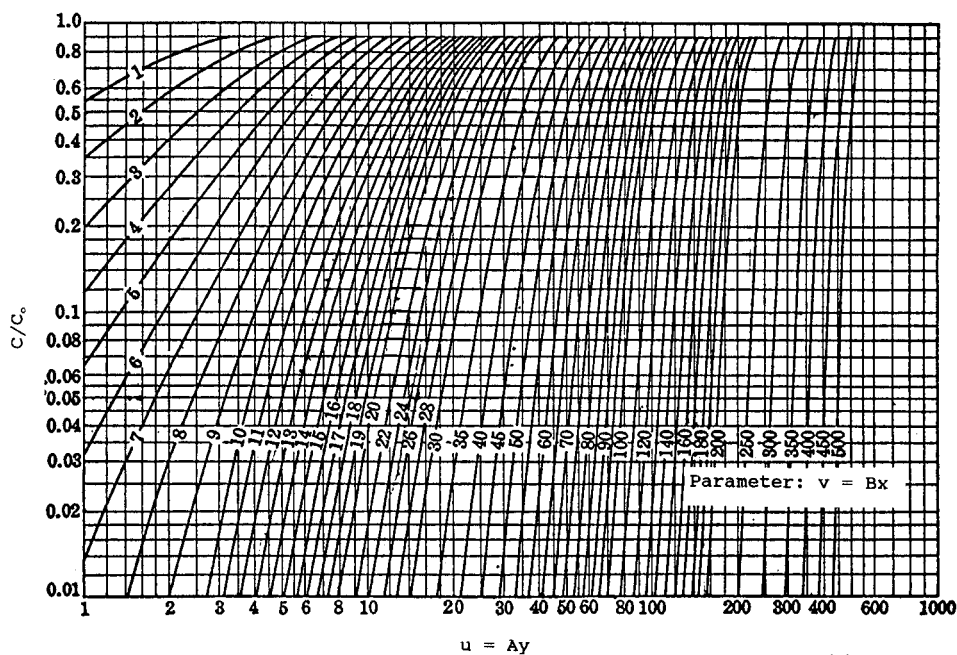
$$\phi(u, v) \neq \phi(v, u)$$

$$\frac{\partial \phi(u, v)}{\partial u} = \phi(u, v) + I_o(2\sqrt{uv})$$

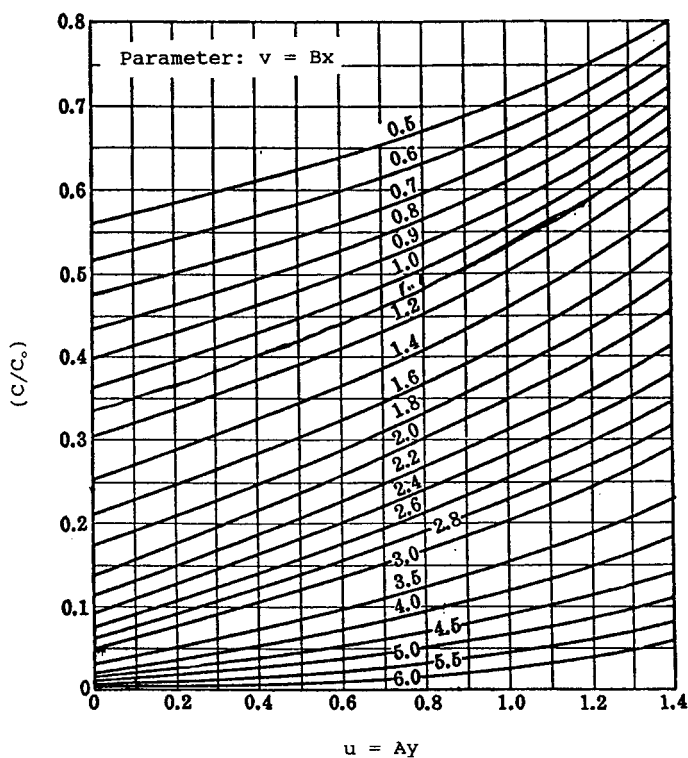
$$\frac{\partial \phi(u, v)}{\partial v} = \phi(u, v) - \frac{\partial}{\partial v} [I_o(2\sqrt{uv})]$$

$I_o = \text{modified Bessel function}$

---



(a)



(b)

**Figure 9.4** (a) Solution to  $\exp(-u-v)\{\phi(u,v) + I_0[2(uv)^{1/2}]\}$ ; fraction of the adsorbate remaining in the fluid phase—linear equilibrium. (b) Fraction of adsorbate remaining in fluid phase—low time range. [From O.A. Hougen, C.C. Watson and R.A. Ragatz, *Chemical Process Principles, Vol. III*, with permission of John Wiley and Sons, New York, (NY), (1957).]

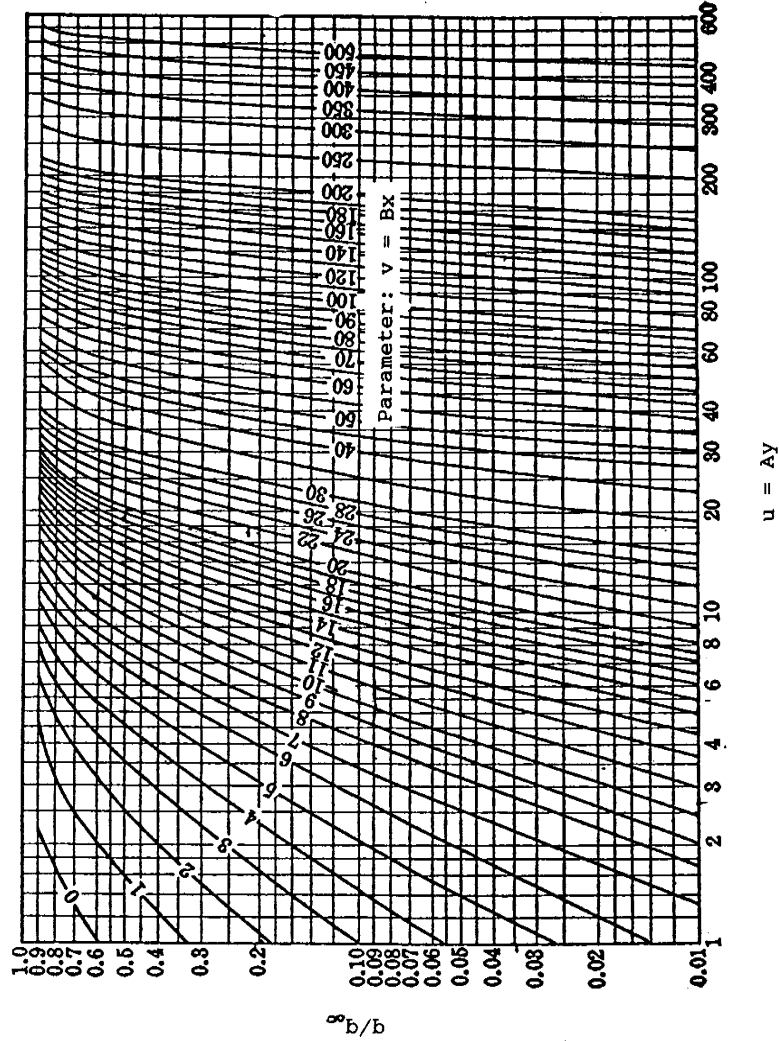


**Figure 9.5** Solution to  $\exp(-u - v)[\phi(u, v)]$ . [From O.A. Hougen, C.C. Watson and R.A. Ragatz, *Chemical Process Principles, Vol. III*, with permission of John Wiley and Sons, New York, (NY), (1957).]

The estimation of parameters (normally  $K_D S$  and  $q_\infty$ ) from breakthrough data can also be accomplished, although the procedure is a little more complicated. Figure 9.6 presents values of the derivatives of the breakthrough

$$\frac{d[\log(C/C_0)]}{d[\log(Ay)]} \quad \text{vs.} \quad Bx$$

evaluated using the derivative properties given in Table 9.1 and plotted as a function of  $C/C_0$ . Breakthrough data are normally obtained as  $(C/C_0)$  versus  $y$ , so that from experiment we may obtain the equivalent form of the above derivative,

$$\frac{d[\log(C/C_0)]}{d[\log(y)]}$$

Thus, we can evaluate the slope from experimental data at various values of  $(C/C_0)$  on the breakthrough curve and obtain the corresponding value of  $Bx$  from Figure 9.6. Then, using  $(C/C_0) - Bx$  pairs we obtain the corresponding  $Ay$  values. Both  $x$  and  $y$  are known from experiment, so that  $K_D S$  and  $q_\infty$  can be obtained.

Some useful approximations have been reported for this problem. If we write the mass-transfer rate as

$$\left( \frac{\partial q}{\partial t} \right) = k(q^* - q) = kK(C - C^*) \quad (9-8a)$$

where  $q^*$  is the interfacial equilibrium value of  $q$ , corresponding to  $C^*$ , then

$$\left( \frac{C}{C_0} \right) = (0.5) \operatorname{erfc}[(\xi)^{1/2} - (\tau)^{1/2} - (1/8)(\xi)^{1/2} - (1/8)(\tau)^{1/2}] \quad (9-38a)$$

for  $\xi > 2$  with error  $< 0.6\%$ , or

$$\left( \frac{C}{C_0} \right) = (0.5) \operatorname{erfc}[(\xi)^{1/2} - (\tau)^{1/2}] \quad (9-38b)$$

for large  $\xi$ . In these last two equations,

$$\tau = k(t - x/v)$$

$$\xi = \frac{kKx}{v} \left( \frac{1 - \epsilon}{\epsilon} \right)$$

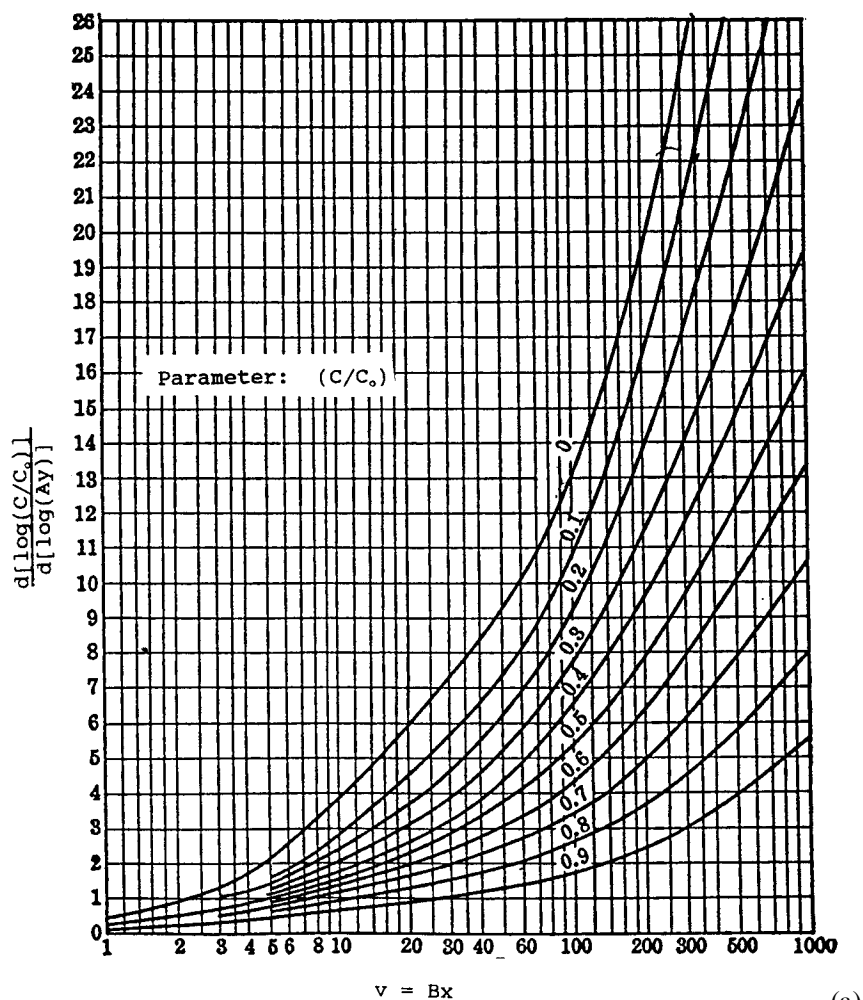
For this notation, equation (9-38) becomes

$$\left( \frac{C}{C_0} \right) = e^{-\xi} \int_0^\tau e^{-u} I_0(2\sqrt{\xi u}) du + e^{-(\tau+\xi)} I_0(2\sqrt{\tau\xi}) \quad (9-38c)$$

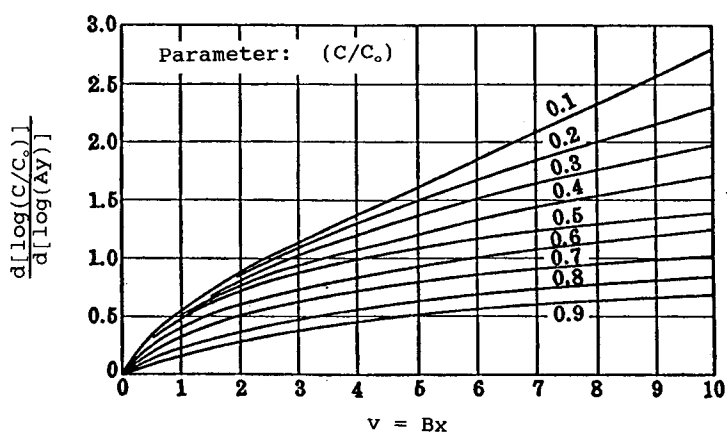
### 9.1.3 Adsorption with a Langmuir Isotherm

Once again we have the material balance of equation (9-7), but to incorporate the Langmuir isotherm we must modify the adsorption rate expression. The rate of adsorption will be taken proportional to the unoccupied surface, and desorption is first-order with respect to the concentration of adsorbed material. Thus,

$$\left( \frac{\partial q}{\partial t} \right) = k[C(q_\infty - q) - \beta q(C_0 - C)] \quad (9-40)$$



(a)



(b)

**Figure 9.6** (a) Rate of fluid phase composition change at exit. (b) Rate of fluid phase composition change at exit for small values of  $x$ . [From O.A. Hougen, C.C. Watson and R.A. Ragatz, *Chemical Process Principles, Vol. III*, with permission of John Wiley and Sons, New York, (NY), (1957).]

At equilibrium,

$$\left(\frac{q}{q_\infty}\right) = \frac{kC}{kC + \beta(C_0 - C)} \quad (9-41)$$

The solution to this case was first reported by Thomas [H.C. Thomas, *J. Am. Chem. Soc.*, 66, 1664 (1944); *Ann. N.Y. Acad. Sci.*, 49, 161 (1948)]

$$\left(\frac{C}{C_0}\right) = \frac{\phi(\beta\xi, \tau)}{\phi(\beta\xi, \tau) + [1 - \phi(\xi, \beta\tau)] \exp[(\beta - 1)(\tau - \xi)]} \quad (9-42)$$

with

$$\phi(\alpha, \beta) = 1 - \int_0^\alpha \exp(-\beta - \alpha) I_0(2\sqrt{\beta\xi}) d\xi$$

$$\tau = (kC_0)(t - z/v)$$

$$\xi = \left(\frac{kq_\infty z}{v}\right) \left(\frac{1 - \epsilon}{\epsilon}\right)$$

where  $v$  is the interstitial velocity of fluid,  $z$  is the axial distance, and  $\epsilon$  is the bed void fraction. This solution reduces to the findings of Furnas when  $\beta = 1$ .

#### 9.1.4 Irreversible Adsorption

Bohart and Adams [G. Bohart and E. Adams, *J. Am. Chem. Soc.*, 42, 523 (1920)], in what was probably the first detailed mathematical analysis of the adsorption wave problem, considered that irreversible adsorption occurred on surface, so that

$$\left(\frac{\partial q}{\partial t}\right) = kC(q^* - q) \quad (9-43)$$

The solution for a bed with  $q = 0$  initially is

$$\left(\frac{C}{C_0}\right) = \frac{1 + \exp(\tau)}{\exp(\tau) + \exp(\xi) - 1} \quad (9-44)$$

with notation the same as that for equation (9-42). Note that this result is also obtained from equation (9-42) with  $\beta = 0$ .

#### 9.1.5 Other Cases

It has already been pointed out that the forms of solution to the adsorption wave problem are similar to those representing the elution of tracer in a residence-time distribution experiment. Closest to what we considered in Chapter 5 are solutions of Levenspiel and Bischoff [O. Levenspiel and K.B. Bischoff, *Adv. Chem. Eng.*, 4, 95 (1963)] and Lapidus and Amundson [L. Lapidus and N.R. Amundson, *J. Phys. Chem.*, 56, 984 (1952)]. With the rate equation written as in equation (9-8a), these are

$$\left(\frac{C}{C_0}\right) = (1/2) \operatorname{erfc} \left\{ \frac{1 - (t/t_R)}{2[(D_L/vz)(t/t_R)]^{1/2}} \right\} \quad (9-45)$$

Also from Levenspiel and Bischoff [see equation (5-26) in Chapter 5], and

$$\left(\frac{C}{C_0}\right) = \exp\left(\frac{vz}{2D_L}\right) \left[ F(t) + k \int_0^t F(t) dt \right] \quad (9-46)$$

where

$$F(t) = e^{-kt} \int_0^t I_0 \{ 2k[(K/\epsilon)(1-\epsilon)u(t-u)]^{1/2} \} \cdot \left( \frac{z}{2\sqrt{\pi D_L u^3}} \right) \\ \times \exp \left[ \frac{-z^2}{4D_L u} - \frac{v^2 u}{4D_L} - \frac{kKu(1-\epsilon)}{\epsilon} - ku \right] du \quad (9-47)$$

as per Lapidus and Amundson.<sup>3</sup>

Finally, Rosen [J.B. Rosen, *J. Chem. Phys.*, 20, 387 (1952); *Ind. Eng. Chem.*, 46, 1590 (1954)] presented the solution for linear equilibrium and intraparticle diffusion-controlled adsorption (no external mass-transfer resistance). In this case

$$\left( \frac{\partial q}{\partial t} \right) = \frac{1}{r^2} \cdot \frac{\partial}{\partial r} \left( D_{eff} \frac{\partial q}{\partial r} \right) \quad (9-48)$$

with

$$q(R_p, t - z/v) = q^* = KC \quad (9-49)$$

$$q(avg) = \left( \frac{3}{R_p^3} \right) \int_0^{R_p} q r^2 dr \quad (9-50)$$

and

$$\left( \frac{\partial q}{\partial r} \right) (0, t - z/v) = 0 \quad (9-51)$$

From these, we have

$$\left( \frac{C}{C_0} \right) = \frac{1}{2} + \left( \frac{2}{\pi} \right) \int_0^\infty \exp[-\xi H_1(\lambda)/5] \sin[2\lambda^2 \tau/15] - \xi H_2(\lambda)/5 \quad (9-52)$$

where

$$H_1(\lambda) = \frac{\lambda[\sinh(2\lambda) + \sin(2\lambda)]}{\cosh(2\lambda) - \cos(2\lambda)} - 1$$

$$H_2(\lambda) = \frac{\lambda[\sinh(2\lambda) - \sin(2\lambda)]}{\cosh(2\lambda) - \cos(2\lambda)}$$

$$\xi = \frac{(15)D_{eff}}{r^2} \left( \frac{kz}{v\epsilon} \right) (1-\epsilon); \quad \tau = \frac{(15)D_{eff}}{r^2} (t - z/v)$$

An asymptotic form for long beds is

$$\left( \frac{C}{C_0} \right) = \left( \frac{1}{2} \right) \operatorname{erfc} \left( \frac{\xi - \tau}{2\sqrt{2}} \right) \quad (9-53)$$

A lot more is available from Rosen, but this is probably about as far as we want to go with this problem.

<sup>3</sup> Note that these are dispersed-flow models; all others treated here assume plug flow of the fluid. "A few honest men are better than numbers."—O. Cromwell



Another type of analysis is based on the pattern of the concentration front in the bed, essentially the reverse image of the breakthrough curve, particularly when this front passes through the bed with a constant velocity. Some of this we mentioned in Chapter 4. Such *constant pattern waves* are not limited to ion exchange or adsorption, for they are often encountered in the poisoning of fixed-bed reactors, in either isothermal [A. Wheeler and A.J. Robell, *J. Catal.*, 13, 299 (1969); H.W. Haynes, Jr., *Chem. Eng. Sci.*, 25, 1615 (1970)] or nonisothermal operation [H.S. Weng, G. Eigenberger and J.B. Butt, *Chem. Eng. Sci.*, 30, 1341 (1975); T.H. Price and J.B. Butt, *Chem. Eng. Sci.*, 32, 393 (1977)].

The constant pattern approximation is a very useful design-estimation method, since the computation of the adsorption wave under such conditions is straightforward. As shown in Chapter 4, the constant pattern condition is expressed in the material balance as

$$\left(\frac{C}{C_0}\right) = \left(\frac{q}{q_\infty}\right) \quad (9-54)$$

For our present purposes, let us consider a plug-flow system with a Langmuir adsorption isotherm, where the adsorption rate is given by a linearized equation,

$$\left(\frac{\partial q}{\partial t}\right) = k(q^* - q) \quad (9-55)$$

with equilibrium

$$\begin{aligned} \frac{q^*}{q_\infty} &= \frac{bC}{1 + bC} \\ \beta &= 1 - \frac{q_0}{q_\infty} \end{aligned} \quad (9-56)$$

where  $q_\infty$  is the saturation capacity of the adsorbent and  $q_0$  is the equilibrium capacity of the adsorbent for the inlet concentration of adsorbate,  $C_0$ . Writing the adsorption rate equation in terms of the constant pattern condition, together with the adsorption isotherm, gives

$$\left(\frac{\partial q}{\partial t}\right) = kq_\infty \left[ \frac{bC_0(q/q_0)}{1 + b(q/q_0)} \right] - \left(\frac{q}{q_\infty}\right) \quad (9-57)$$

The corresponding constant pattern is given by

$$k(t_2 - t_1) = \left(\frac{1}{1 - \beta}\right) \ln \left[ \frac{\phi_2(1 - \phi_1)}{\phi_1(1 - \phi_2)} \right] + \ln \left(\frac{\phi_1}{\phi_2}\right) \quad (9-58)$$

where

$$\phi_1 = \left(\frac{C_1}{C_0}\right); \quad \phi_2 = \left(\frac{C_2}{C_0}\right)$$

As we mentioned before, with the exception of the results of Levenspiel and Bischoff, and Lapidus and Amundson, all the results presented in this section are based on plug-flow models. Some idea of the magnitude of dispersion effects can be

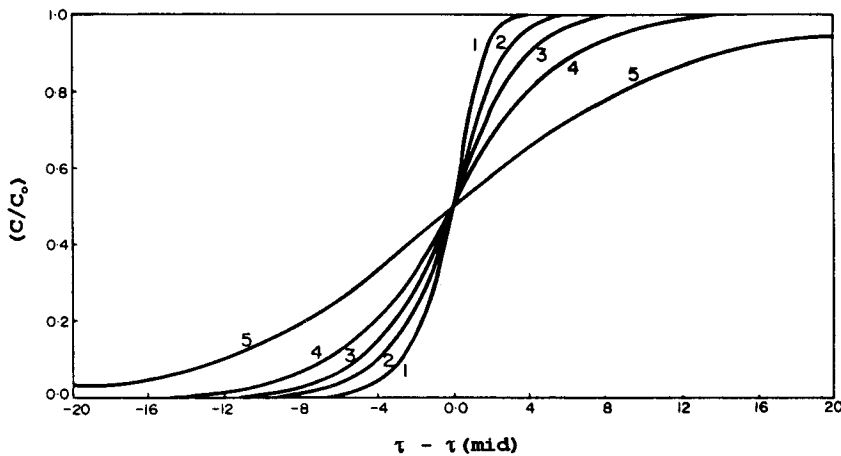


**Figure 9.7** Combined effects of axial dispersion and mass-transfer resistance for a Langmuir system with  $\beta = 0.33$ . The curves are normalized to the point  $\tau(\text{mid})$ ,  $(C/C_0) = 0.5$ ;  $\delta$  is the parameter. [After D.M. Ruthven, *Principles of Adsorption and Adsorption Processes*, reprinted with permission of John Wiley and Sons, New York, (NY), (1984).]

obtained by defining the parameter

$$\delta = \left( \frac{1 - \epsilon}{\epsilon} \right) \left( \frac{3k_f}{R_p} \right) \left( \frac{D_L}{v^2} \right) \quad (9-59)$$

where  $k_f$  is a fluid film mass-transfer coefficient. A comparison of the constant pattern breakthrough curves for a fixed value of  $\beta$  [equation (9-40)] with  $\delta$  as the parameter is shown in Figure 9.7 for a favorable Langmuir equilibrium system. A value of  $\delta = 0$  gives the constant pattern of the Thomas solution given in Section 3. Again, note the similarity of these curves to the residence-time distribution results shown in Chapter 5. Further detail on dispersion effects can be found in papers by Garg and Ruthven [D.R. Garg and D.M. Ruthven, *Chem. Eng. Sci.*, 30, 1192 (1975)] and Acrivos [A. Acrivos, *Chem. Eng. Sci.*, 13, 1 (1960)].

### Illustration 9.1

The original work of Bohart and Adams was concerned with the adsorption of chlorine on activated charcoal. They wrote balance and rate equations in terms of a residual capacity of the adsorbate,  $a = (q^* - q)$ , such that the rate of adsorption was as shown in equation (9-43). The mass balance corresponding could then be written as

$$-v \left( \frac{\partial C}{\partial x} \right) = k(a)(C)$$

where  $v$  is the volumetric flow rate and  $k$  the adsorption rate constant. Derive equation (9-44) from this model. As usual,  $C = C_0$  and  $a = a_0$  at  $t = 0$ . It will be convenient to work with nondimensional variables;  $a' = (a/a_0)$ ,  $C' = (C/C_0)$ ,  $x' = (ka_0x/v)$ , and  $t' = kC_0t$  are suggested.

*Solution*

For the mass balance and rate equations we have

$$\left(\frac{\partial a}{\partial t}\right) = -kaC \quad (\text{i})$$

$$-v\left(\frac{\partial C}{\partial x}\right) = kaC \quad (\text{ii})$$

with

$$t = 0; \quad a = a_0; \quad \text{for all } x$$

$$x = 0; \quad C = C_0; \quad \text{for all } t$$

If we make the variables nondimensional as suggested

$$\left(\frac{\partial C'}{\partial x'}\right) = -a'C' \quad (\text{iii})$$

$$\left(\frac{\partial a'}{\partial t'}\right) = -a'C' \quad (\text{iv})$$

or, more conveniently

$$\left[\frac{\partial \ln(C')}{\partial x'}\right] = -a' \quad (\text{v})$$

$$\left[\frac{\partial \ln(a')}{\partial t'}\right] = -C' \quad (\text{vi})$$

Now,  $t' = 0$  for  $a' = 1$ , and equation (v) integrates directly to

$$C' = \exp(-x') \quad (\text{vii})$$

Also,  $x' = 0$  for  $C' = 1$ , and equation (vi) integrates directly to

$$a' = \exp(-t') \quad (\text{viii})$$

The derivatives of equations (v) and (vi) are

$$\frac{\partial^2 \ln(C')}{\partial t' \partial x'} = -\left(\frac{\partial a'}{\partial t'}\right) = a'C' \quad (\text{ix})$$

$$\frac{\partial^2 \ln(a')}{\partial x' \partial t'} = -\left(\frac{\partial C'}{\partial x'}\right) = a'C' \quad (\text{x})$$

Subtracting (x) from (ix),

$$\frac{\partial^2 \ln(C'/a')}{\partial t' \partial x'} = 0 \quad (\text{xi})$$

or

$$\ln(C'/a') = f(x') + f(t') \quad \text{in general} \quad (\text{xii})$$

Starting with equation (ix), we can go either of two ways. If we integrate with respect to  $x'$  first, we will have

$$\frac{\partial \ln(C'/a')}{\partial t'} = B_1(t')$$

and

$$\ln(C'/a') = B_1(t')t' + B_2(x') \quad (\text{ia})$$

Similarly, if we integrate with respect to  $t'$  first,

$$\ln(C'/a') = B_3(x')x' + B_4(t') \quad (\text{iaa})$$

The RHS of both (ia) and (iaa) =  $\ln(C'/a')$ , so

$$B_1(t') + B_2(x') = B_3(x')x' + B_4(t') \quad (\text{iiia})$$

From the initial condition on  $t$ , at  $t = 0$ ,  $a = a_0$ ,  $a' = 1$ , so equation (ia) is

$$\ln(C') = B_2(x')$$

But we know from equation (vii) that  $C' = \exp(-t')$  at  $t' = 0$ , so

$$\ln(C') = -x' = B_2(x') \quad (\text{iva})$$

Similarly, from the initial condition on  $x$ , at  $x = 0$ ,  $C = C_0$  and  $C' = 1$ , so equation (iaa) is

$$\ln(1/a') = B_4(t') = (t'); \quad a' = \exp(-t')$$

and

$$\ln(1/a') = B_4(t') = t' \quad (\text{va})$$

Now, with  $B_3(x')$  and  $B_4(t')$  in hand, we can go back to equation (vii)

$$\ln(C'/a') = t' - x'$$

Remembering the restriction imposed by equation (iiia), then

$$B_1(t')t' + B_2(x') = B_3(x')x' + B_4(t')$$

or

$$B_1(t')t' - x' = B_3(x')x' + t'$$

This must require that

$$B_1(t') = 1; \quad B_3(x') = -1$$

or

$$t' - x' = t' - x'$$

Then, back to equation (ia),

$$\ln(C'/a') = t' - x' \quad (\text{via})$$

If we still remember equations (iii) and (iv) at this point, we can rewrite them as

$$-\frac{\partial(C'/C^2)}{\partial x'} = \frac{a'}{C'} = \exp(x' - t') \quad (\text{xiii})$$

$$-\frac{\partial(a'/a^2)}{\partial t'} = \frac{C'}{a'} = \exp(t' - x') \quad (\text{xiv})$$

Integrating,

$$\frac{1}{C'} = e^{x'-t'} - f(t')$$

$$\frac{1}{a'} = e^{t'-x'} - f(x')$$

The constants in these two equations can be evaluated from equations (vii) and (viii). For example, for  $C'$

$$x = 0; \quad C = C; \quad C' = 1$$

$$1 = \exp(-t') - f(t')$$

so

$$f(t') = \exp(-t') - 1$$

and

$$\frac{1}{C'} = e^{x'-t'} - e^{-t'} + 1 \quad (\text{xv})$$

In a similar manner

$$\frac{1}{a'} = e^{-t'-x'} - e^{-x'} + 1 \quad (\text{xvi})$$

or, in final form

$$C' = \frac{e^{t'}}{e^{x'} + e^{t'} - 1} \quad (\text{xvii})$$

$$a' = \frac{e^{x'}}{e^{x'} + e^{t'} - 1}$$

which are forms of the Bohart-Adams equation corresponding to equation (9-41) of the text.



HORATIO SAYS

It would help me out some if someone could show me that equations (xvii) and (9-41) are really the same. Besides, the derivation of Illustration 9.1 seems very convoluted. Isn't there some easier way?

### 9.1.6 A Heat-Transfer Problem

A number of years ago, “pebble bed” heaters were often encountered in process systems, normally as a means of recovering potential heat loss. As design methods became more sophisticated and process integration became tighter, these units became an endangered species. Now, however, a number of new uses such as in

solar energy systems, seem to be on the horizon and an excursion into the analysis is appropriate.

The background here shares a common origin with the background on the adsorption wave through the old work of Anzelius [A. Anzelius, *Zeits. für Ang. Math. und Mech.*, 6, 291 (1926)], Schumann [T.B. Schumann, *J. Frank. Inst.*, 208, 405 (1929)] and Furnas [C.C. Furnas, *U.S. Bureau of Mines Bull.*, 361, (1932)], so we can legitimately slip in this analysis of thermal waves.

The equilibrium relationship in heat transfer is always linear; in fact it is simply

$$(T_{solid})_{eq} = (T_{fluid})_{eq} \quad (9-60)$$

The model here assumes no radial variation of fluid velocity or temperature, physical properties independent of temperature, and no axial conduction of heat in the bed. This last assumption is not always justified, but we will worry about that later.

The energy balance over a differential length of bed,  $dx$ , is

$$vc_f\rho_f\left(\frac{\partial T_f}{\partial x}\right) + \epsilon c_f\rho_f\left(\frac{\partial T_f}{\partial t}\right) + (1-\epsilon)c_s\rho_s\left(\frac{\partial T_s}{\partial t}\right) = 0 \quad (9-61)$$

where  $c_i\rho_i$  is the heat capacity and density of the solid and fluid phases,  $\epsilon$  is bed void fraction,  $T_f$  fluid phase and  $T_s$  is the solid phase temperature. The rate equation for heat transfer between solids and fluid is

$$(1-\epsilon)c_s\rho_s\left(\frac{\partial T_s}{\partial t}\right) = h(T_f - T_s) \quad (9-62)$$

where  $h$  is a volumetric heat-transfer coefficient (i.e., J/s-cm<sup>3</sup>-°C, etc). Now we can make the familiar variables change for the problem,

$$y = \frac{h}{c_s\rho_s(1-\epsilon)}\left(t - \frac{L\epsilon}{v}\right)$$

$$z = \left(\frac{h}{c_f\rho_f v}\right)x$$

where  $L$  is total bed length. Equations (9-61) and (9-62) now become

$$\left(\frac{\partial T_f}{\partial z}\right) + \left(\frac{\partial T_s}{\partial y}\right) = 0 \quad (9-63)$$

$$\left(\frac{\partial T_s}{\partial y}\right) = T_f - T_s \quad (9-64)$$

with boundary conditions

$$T_f = (T_f)_0 \quad (y, z = 0)$$

$$T_s = 0 \quad (y = 0, z)$$
(9-65)

The second of these boundary conditions requires some explanation, since this situation obviously is not often encountered in practice. The set of conditions (9-65) corresponds to those of (9-18), which is the convenient form for solution of problems using Laplace transforms. All temperatures, thus, are scaled with respect to an initial solids temperature of zero. The heat-transfer problem is now mathematically

identical to that in Section 9.1.2, so

$$\frac{T_f}{(T_f)_0} = e^{-(y+z)} [I_0(2\sqrt{yz}) + \phi(y, z)] \quad (9-66)$$

with  $\phi(y, z)$  the same function as described before. The interpretation of data or solution for various cases is also carried out exactly as before, except the parameters  $y$  and  $z$  replace  $Ay$  and  $Bx$ , respectively. Following this,

$$\frac{T_s}{(T_f)_0} \quad \text{replaces} \quad \left( \frac{q}{q_\infty} \right) \quad (9-67)$$

$$\frac{T_f}{(T_f)_0} \quad \text{replaces} \quad \left( \frac{C}{C_0} \right) \quad (9-68)$$

The corresponding equation for the solids temperature is

$$\frac{T_s}{(T_0)_0} = e^{-(y+z)} [\phi(y, z)] \quad (9-69)$$

An important variant on this problem is one in which there is an initial distribution of temperature in the bed. This case was worked out by Reilly [P.M. Reilly, *Amer. Inst. Chem. Eng. Jl.*, 3, 513 (1957)], where we allow arbitrary boundary conditions of the form

$$\begin{aligned} T_s &= F_1(y); & z &= 0 \\ T_f &= F_2(z); & y &= 0 \end{aligned} \quad (9-70)$$

Following the development of Reilly,

$$\left( \frac{\partial T_f}{\partial y} \right) = T_s - T_f \quad (9-71)$$

$$\left( \frac{\partial T_s}{\partial z} \right) = T_f - T_s \quad (9-72)$$

with

$$z = \left( \frac{h_s}{\rho_s c_s} \right) \left( t - \frac{\rho_f \epsilon L}{g} \right); \quad y = \left( \frac{h_s}{g c_f} \right) x$$

where  $h_s = h/(1 - \epsilon)$  and  $g$  is a mass flow rate in g/h-m<sup>2</sup> (or other compatible units). The arbitrary initial temperature profile of the solids,  $F_1(y)$ , can be expressed as

$$\begin{aligned} T_s(y, 0) &= 0; & y &< 0 \\ T_s(y, 0) &= F_1(y); & 0 &< y < Y \\ T_s(y, 0) &= 0; & Y &< y \end{aligned} \quad (9-73)$$

where the bed under consideration is split into three parts *a la* Wehner and Wilhelm (as discussed in Chapter 5), and  $Y$  is defined as

$$y = \left( \frac{h_s L}{g c_s} \right) \quad (9-74)$$

A general solution for these boundary conditions is

$$T_s = \left[ a \cos \left( y - \frac{z}{1+c^2} \right) + b \sin \left( y - \frac{z}{1+c^2} \right) \right] \exp \left( \frac{-c^2 z}{1+c^2} \right)$$

The mathematicians among us will recognize that the constants  $a$ ,  $b$ , and  $c$  that fit the boundary conditions can be found in terms of the Fourier integral form

$$T_s = \left( \frac{1}{\pi} \right) \int_0^\infty \left[ g(\alpha) \cos \left( y\alpha - \frac{z\alpha}{1+\alpha^2} \right) + h(\alpha) \sin \left( y\alpha - \frac{z\alpha}{1+\alpha^2} \right) \right] \times \exp \left( \frac{-z\alpha^2}{1+\alpha^2} \right) d\alpha \quad (9-75)$$

where

$$g(\alpha) = \int_0^Y F_1(w) \cos(\alpha w) dw$$

$$h(\alpha) = \int_0^Y F_1(w) \sin(\alpha w) dw \quad (9-76)$$

Substituting the derivative of equation (9-75) into (9-72) gives

$$T_f = \left( \frac{1}{\pi} \right) \int_0^\infty \left[ \frac{g(\alpha) - \alpha h(\alpha)}{1+\alpha^2} \cos \left( y\alpha - \frac{z\alpha}{1+\alpha^2} \right) + \frac{h(\alpha) + \alpha g(\alpha)}{1+\alpha^2} \times \sin \left( y\alpha - \frac{z\alpha}{1+\alpha^2} \right) \right] \exp \left( -\frac{z\alpha^2}{1+\alpha^2} \right) d\alpha \quad (9-77)$$

which is the solution for an arbitrary initial distribution of  $F_1(y)$  for the solids temperature, with  $T_f$  at  $y = 0$  specified. The procedure can be expanded to handle both of the conditions of equation (9-70) for any datum temperature, and the Fourier integral solutions are tabulated in the paper by Reilly. It was claimed there that a more convenient form for computation is afforded by a Fourier series approximation (also reported), but the resulting equations are large enough to choke a very large horse, and not worth the space here.

For additional analysis of various versions of the heat-transfer problem, see Klinkenberg and Harmes [A. Klinkenberg and H. Harmes, *Chem. Eng. Sci.*, 11, 260, (1960)] and Brinkley [S.R. Brinkley, *J. App. Phys.*, 18, 582 (1947)]. All this rather elderly work results in very elegant analytical solutions, although the equation/results are very, very complex, and one must pray for the accuracy of those old-time typesetters. Keep this work in mind, however, in the sense that even with modern computation it is still easier to work from an analytical solution than to start off on a numerical simulation.

A reminder: *neither* of the two heat-transport models considered in this section account for thermal conduction in the bed. If gradients are substantial, this can be a miserable assumption as shown by the discussion of nonisothermal reactors in Chapter 7. It is probably fair to say that if any conduction effects are included, axial or radial, the problem formulation is not complicated very much (just the addition of a second derivative term with respect to temperature), but the solution to the problem becomes a numerical one and sufficiently complicated to be a subject



for nightmares (re: the horse alluded to above). Whether these sorts of heat-transfer applications will re-emerge to prominence is still a question of developing technology.



HORATIO SAYS

Pay attention to units. They will finish you if care is not taken. In particular, in Sections 1–3 of this chapter, the mass-transfer coefficient is written on a volumetric basis, and must be consistent with the units of  $w$  and  $x$ . Hence, if  $w$  is expressed in liters/min and  $x$  in grams, then the proper units for  $K_D S$  are liters/g-min, and so on. Also, in ion-exchange applications of these equations, the concentrations are often expressed as meq/liter in the fluid phase and meq/g in the solid. A corresponding consistent set of units would be  $\text{cm}^3/\text{min}$  for velocity, g for the weight of the solid phase, and  $\text{cm}^3$  for volume. This gives  $K_D S$  in  $\text{cm}^3/\text{g-min}$ . A good self-consistency is afforded by remembering that the groupings

$$(K_D S C_0 / q_\infty w) y$$

and

$$(K_D D / w) x$$

are dimensionless. A similar comment applies to the heat-transfer coefficient in Section 9.1.6.

## 9.2 Chromatography

Much of the basic theory of chromatography has been set forth in the preceding section, although perhaps under some camouflage. Indeed, the conservation equations and, in most cases, the equilibrium relationships (linear) are the same. For chromatographic separations that we recognize from laboratory experience, we need only replace the inlet step function with a pulse function (or, in reality, perhaps a square wave). Before doing this, however, let us fashion a simple analysis of chromatography from what we already know.

### 9.2.1 A Basic Theory

Let us assume that we have a binary mixture of components in the fluid phase, each characterized by its own favorable equilibrium adsorption isotherm on the solid adsorbent, and with the rate of mass transfer from the fluid to the solid phases determined by the fluid film mass-transfer coefficients. These are often nearly the same for similar chemical species, but for the sake of some generality we will assume that there are different values of  $K_D S$  for the two components. The solid phase can be considered to be either an intimate mixture of two adsorbents, each specific for

one of the two fluid-phase components, or a single adsorbent capable of noninter-active adsorption of both. Either of these two is common in chromatography. All of this sets the stage such that the Klotz equation, (4-168), applies independently to the adsorption wave of each of the components.

What we need to do first is define an index of separation that will describe the difference in the breakthrough curves at any specific (and equal) value of  $(C/C_0)_i$ . Further, if we assume that the adsorbate consists of an intimate mixture of two separate materials, how is the separation of breakthrough curves affected by changing the relative amounts of the two? We will define the total bed weight as  $x_T$ , with the relationship between the amounts of adsorbent for components 1 and 2 as

$$x_2 = ax_1 \quad (9-78)$$

so that

$$x_1 = x_T(1 + a) \quad (9-79)$$

$$x_2 = ax_T/(1 + a) \quad (9-80)$$

We will specify the separation requirement to correspond to an arbitrary value of  $(C/C_0)_i$

$$\ln(C/C_0)_1 = \ln(C/C_0)_2 = D \quad (9-81)$$

with the Klotz equation

$$\ln\left(\frac{C}{C_0}\right)_i = \left[\frac{(K_D S)_i (C_0)_i}{(q_\infty)_i w}\right] y_i - \left[\frac{(K_D S)_i}{w}\right] x_i - 1 \quad (9-82)$$

Thus, for two components being adsorbed, we have

$$D = A_1 y_1 - B_1 x_1 - 1 \quad (9-83)$$

$$D = A_2 y_2 - B_2 x_2 - 1 \quad (9-84)$$

As the separation factor we will use the individual values of  $y$  corresponding to  $D$ , so that

$$\Delta y = |y_1 - y_2| = (D + B_1 x_1)/A_1 - \dots - (D + B_2 x_2)/A_2 \quad (9-85)$$

thus we have

$$\Delta y = \frac{A_2 B_1 x_1 - (D)A_2 + aA_1 B_2 x_1 - (D)A_1}{(A_1 A_2)} \quad (9-86)$$

If the separation is specified in this way, with individual components set as 1 and 2, then, more generally,

$$\Delta y = |y_1 - y_2| = \frac{D + B_1 x_1}{A_1} - \frac{D + B_2 x_2}{A_2} + \frac{1}{A_1} - \frac{1}{A_2} \quad (9-87)$$

$$\Delta y = \frac{x_T}{(1 + a)} \left( \frac{B_1}{A_1} - \frac{aB_2}{A_2} \right) + \left( \frac{D + 1}{A_1} - \frac{D + 1}{A_2} \right) \quad (9-88)$$

with limiting cases of  $a \rightarrow 0$

$$\text{Lim}(\Delta y) = \left( \frac{B_1}{A_1} \right) x_T + \left( \frac{D+1}{A_1} - \frac{D+1}{A_2} \right) \quad (9-89)$$

and  $a \rightarrow \infty$ ,

$$\text{Lim}(\Delta y) = - \left( \frac{B_2}{A_2} \right) x_T + \left( \frac{D+1}{A_1} + \frac{D+1}{A_2} \right) \quad (9-90)$$

Now, since there is not much that we can do about the factors  $(D+1)/A_i$ —they will compensate each other to some extent—the major thing to look at in separation is the first term in equation (9-88). Let us then define more precisely a separation factor,  $S_f$ , as,

$$S_f = \frac{x_T}{(1+a)} \left( \frac{B_1}{A_1} - \frac{aB_2}{A_2} \right) \quad (9-91)$$

If we are interested in the relative amounts of  $x_1$  and  $x_2$  with respect to the separation (i.e.,  $a$ ) then

$$\left( \frac{dS_f}{da} \right) = 0 \text{ at maximum, so } \left( \frac{B_1}{A_1} \right) = \left( \frac{B_2}{A_2} \right) \quad (9-92)$$

To a certain level of insight this is a useful approach; however there is not much more to be obtained following this approach, since it is bounded by questionable assumptions on every side. It is not really misleading, but so far as we have gone it is quite possible to say that it will be more rewarding to return to a more fundamental development. There may be more arithmetic, but what is surprising about that?

## 9.2.2 A Continuum Theory

Since the applications of chromatography were nurtured to a large extent by use in the field of separation processes, much early work was couched in terms arising from the concepts of equilibrium-stage separation units. Indeed, some of these ideas go back quite some time [A.J.P. Martin and R.L.M. Singe, *Biochem. J.*, 35, 1359 (1941)]. However, our approach throughout the text has been in terms of continuum balances (with the possible exception of CSTR sequences), and we will continue that approach. As in previous sections of this chapter, there is more than a superficial resemblance in the analysis to earlier considerations of residence-time distribution in flow reactors. This presentation will largely follow the classical work of Lapidus and Amundson [L. Lapidus and N.R. Amundson, *J. Phys. Chem.*, 56, 984 (1952)].

Consider, then, a section of a chromatographic column (pseudo-homogeneous fixed bed) as shown in Figure 9.8. Here  $F_I$  and  $F_{II}$  represent volume fractions of the moving (fluid) phase and the stationary (adsorbent/adsorbate) phase, respectively,  $\alpha$  is an appropriate mass-transfer coefficient between phases, and  $K$  is a Henrys law constant. One can see that this is not too removed from several models we have considered before, such as that of Section 9.2. Here, though, our interest is in the separation of two or more fluid-phase components, not just the adsorption wave of a single species. Nonetheless, let us look at the balances referred to an individual component with concentration  $C_i$ . We will write separate balances for phases I

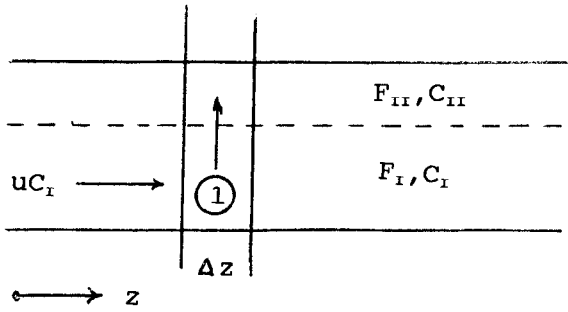


**Figure 9.8** Section of a chromatographic column.

and II as

$$F_I \left( \frac{\partial C_I}{\partial t} \right) = F_I D \left( \frac{\partial^2 C_I}{\partial z^2} \right) - F_I u \left( \frac{\partial C_I}{\partial z} \right) + \alpha (K C_{II} - C_I) \quad (9-93)$$

and

$$F_{II} \left( \frac{\partial C_{II}}{\partial t} \right) = \alpha (C_I - K C_{II}) \quad (9-94)$$

Now, in chromatography as actually applied, we are not able to use the most commonly employed initial conditions of a step or pulse input, rather we must be concerned with the response to some “square wave” input, say with a concentration of component I,  $C_0$ , and for a short time,  $t_0$ . In this case the solution of the paired equations (9-93) and (9-94) is

$$\begin{aligned} \left( \frac{C_I}{C_0} \right) &= \frac{z t_0}{2t(\pi D t)^{1/2}} \exp \left[ -\frac{(z - ut)^2}{4Dt} - \frac{\alpha t}{F_I} \right] \\ &+ \int_0^t \left[ \frac{z t_0}{2t'(\pi D t')^{1/2}} \right] \exp \left[ -\frac{(z - ut')^2}{4Dt'} \right] F(t') dt' \end{aligned} \quad (9-95)$$

where

$$\begin{aligned} F(t') &= \left[ \frac{\alpha^2 K t'}{F_I F_{II} (t - t')} \right]^{1/2} \exp \left[ -\left( \frac{\alpha K}{F_{II}} \right) (t - t') - \left( \frac{\alpha t'}{F_I} \right) \right] \\ &\cdot 2F_I \left[ \frac{\alpha^2 K t' (t - t')}{F_I F_{II}} \right]^{1/2} \end{aligned} \quad (9-96)$$

For conditions often applicable in practice we will have

$$z > \left( \frac{2D}{u} \right), \quad z > \left( \frac{F_I u}{\alpha} \right)$$

then a nice simplification of the above is afforded:

$$\left( \frac{C_I}{C_0} \right) = \frac{\beta t_0}{[2\pi(\sigma_1^2 + \sigma_2^2)]^{1/2}} \exp \left[ -\frac{(z/u - \beta t)^2}{2(\sigma_1^2 + \sigma_2^2)} \right] \quad (9-97)$$

with

$$\sigma_1^2 = \left( \frac{2Dz}{u^3} \right), \quad \sigma_2^2 = \left( \frac{2\beta^2 F_{II}^2 z}{\alpha F_I K^2 u} \right) \quad (9-98)$$

$$\frac{1}{\beta} = 1 + \left( \frac{F_{II}}{F_I K} \right)$$

This essentially completes the mathematical part of the problem for the continuum approach.

It is useful, though, to express these results also in equilibrium-stage terminology. From that approach, the result corresponding to equation (9-97) is

$$(C_I)_{inlet} = \frac{AC_0}{v(2\pi n)^{1/2}} \exp \left[ -\frac{(s/v - n)}{2n} \right] \quad (9-99)$$

where  $A$  is the volume of input feed of concentration  $C_0$ ,  $v$  is an effective stage volume defined as

$$v = v_I + (v_{II}/K) \quad (9-100)$$

with  $v_I$ ,  $v_{II}$  the volumes of individual moving and fixed phases, respectively,  $n$  the number of equilibrium stages, and

$$C_I = KC_{II} \quad (9-101)$$

For comparison of the staged equilibrium approach and the continuum approach, we first define the equilibrium stage volume following equation (9-100) as

$$v = HF_I + \left( \frac{HF_{II}}{K} \right) = \left( \frac{HF_I}{\beta} \right) \quad (9-102)$$

and

$$s = F_I ut, \quad z = nH \quad (9-103)$$

Here  $H$  is most often referred to as the HETP for the separation. Comparison of equations (9-97) and (9-99) in terms of the definitions above gives,

$$H = \frac{2D}{u} + \frac{(2uF_I/\alpha)}{(1 + KF_I/F_{II})^2} = L + \frac{2h}{(1 + KF_I/F_{II})^2} \quad (9-104)$$

in which

$$L = \text{Height of a mixing stage} = \left( \frac{2D}{u} \right)$$

$$h = \text{Height of a transfer unit} = \left( \frac{uF_I}{\alpha} \right)$$

## Illustration 9.2

How would the theory above give any insight as to the efficiency of separation of components in particular instances?

### Solution

A reasonable example is provided by some data for the adsorption of *n*-butane and *i*-butane on celite. The particular data employed were obtained from experi-

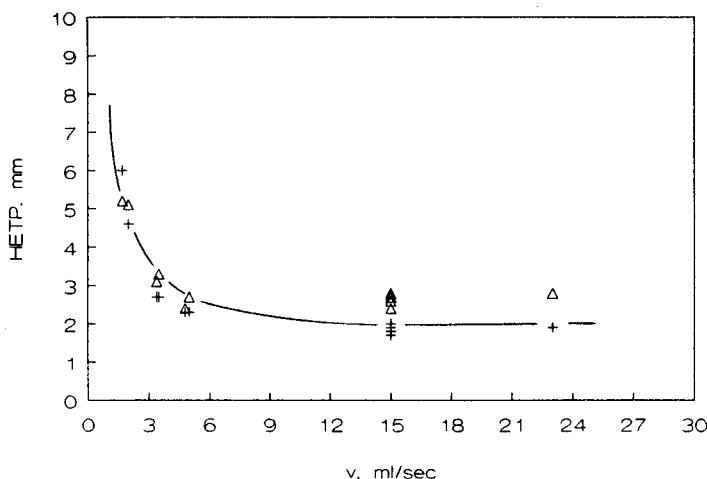


**Figure 9.9** HETP for  $n$ - and  $i$ -butane separation on celite;  $\Delta = n - C_4$ ,  $+ = i - C_4$ .

ments at room temperature, feed 90 mol%  $n$ - $C_4$ , in a carrier of nitrogen at one atmosphere total pressure. The celite particles were small ( $< 30\mu$ ), so that intraparticle diffusion was not a factor.

The analysis of experimental results, in terms of HETP from the equilibrium-stage theory, is shown in Figure 9.9. One sees that there is little difference between the trends for the two, thus the separation on this adsorbent is not well-resolved. We will revisit this question of separation efficiency in the Exercises for this chapter.



HORATIO SAYS

Aside from changing the adsorbent, what can we do to improve the separation shown in Figure 9.9? If we increased the velocity through the column, would this help? What, if we increased the temperature to say  $100^\circ\text{C}$ ? What sort of other information would we need to know if any of these ideas would work?

### 9.2.3 Determination of Parameters Via Chromatography

Sometimes Nature smiles upon us or maybe Nature cannot subvert mathematics (or the other way around). Chromatography is a promising method for the determination of some of the difficult parameters that we have worried about that appear in continuum model simulations of fixed-bed reactors or adsorbers. The approach is not without its difficulties but, properly used, would appear to be very useful.

Let us now think particularly of the adsorption of some gas component, A, in a fixed bed.<sup>4</sup> The general model below considers axial dispersion, interphase and

<sup>4</sup>“The trouble is not in going there ... the trouble is to stay there after you get there.”—E.P. Alexander

intraphase mass transport, and the adsorption-desorption kinetics of the component of interest. This is about as general as one can get in the absence of thermal effects. In general we follow the work of Schneider and Smith, Kubin, and Kucera, which is admirably summarized in a review by Haynes [P. Schneider and J.M. Smith, *Amer. Inst. Chem. Eng., J.*, 14, 762, 886 (1968); M. Kubin, *Coll. Czech. Chem. Commun.*, 30, 1104, 2900 (1965); E. Kucera, *J. Chromotog.*, 19, 237 (1965); H.W. Haynes, Jr., *Catal. Rev. Sci. Eng.*, 30, 563 (1988)]. The mass balances according to the continuum model are

*Column*

$$\left(\frac{D_L}{\epsilon_B}\right)\left(\frac{\partial^2 C}{\partial z^2}\right) - u\left(\frac{\partial C}{\partial z}\right) - \left(\frac{3D_{eff}}{R}\right)\frac{(1 - \epsilon_B)}{\epsilon_B}\left(\frac{\partial C_i}{\partial r}\right)_{r=R} - \left(\frac{\partial C}{\partial t}\right) = 0 \quad (9-105)$$

with boundary conditions

$$\begin{aligned} C(z, 0) &= 0; & z > 0 \\ C(0, t) &= C_0; & 0 \leq t \leq t_0 \\ C(0, t) &= 0; & t > 0 \end{aligned} \quad (9-106)$$

*Catalyst particle*

$$\frac{D_{eff}}{\epsilon_p} \left( \frac{\partial^2 C_i}{\partial r^2} + \frac{2}{r} \frac{\partial C_i}{\partial r} \right) - \frac{\partial C_i}{\partial t} - \frac{\rho_p}{\epsilon_p} \left( \frac{\partial C_{ads}}{\partial t} \right) = 0 \quad (9-107)$$

with initial condition

$$C_i(r, 0) = 0; \quad r \geq 0$$

and boundary conditions

$$D_{eff} \left( \frac{\partial C_i}{\partial r} \right)_{r=R} = k_f (C - C_i) \quad (9-108)$$

with

$$\frac{\partial C_i(0, t)}{\partial r} = 0$$

Finally, we have the expression for the linear adsorption isotherm as

$$\frac{\partial C_{ads}}{\partial t} = k_{ads} (C_i - C_{ads}/K_A) \quad (9-109)$$

Notice that in the set of equations above there are no less than three distinct concentration values. First is the concentration in the bulk fluid phase, given by  $C$  in equation (9-105); second is the concentration within the individual catalyst pores,  $C_i$ , in equation (9-107); finally the concentration of material adsorbed on the internal surface,  $C_{ads}$ , in equation (9-109).

This is about as detailed as a model can get before the individual parameters begin to disappear into the sunset. However, here some operational mathematics [see equations (9-15) to (9-28)] come to our rescue. Most importantly we recognize that

the Laplace transformation of the measurable concentration  $C$  and the moments of the output distribution of  $C$  are related by

$$\mathbf{C}(z, p) = \int_0^\infty e^{-pt} C(z, t) dt \quad (9-110)$$

This serves to simplify the set of equations above to a linear set in terms of the transformed variable  $\mathbf{C}$  as

$$\mathbf{C}(z, p) = \left( \frac{C_0}{p} \right) [1 - \exp(-pt_0)] \exp(-\gamma z) \quad (9-111)$$

where  $0 < p < 1$ , and with

$$\mathbf{C}(L, p) = \left( \frac{C_0}{p} \right) [1 - \exp(-pt_0)] \exp(-\gamma L) \quad (9-112)$$

$$\begin{aligned} \gamma &= -\frac{\epsilon_B v}{2D_L} + \left[ \left( \frac{\epsilon_B v}{2D_L} \right)^2 + \frac{p\epsilon_B}{D_L} [1 + h(p)] \right]^{1/2} \\ h(p) &= \frac{3k_f}{R} \left( \frac{1 - \epsilon_B}{\epsilon_B} \right) \left[ \frac{\sinh(R/\bar{\lambda})}{(pD_{eff}/\bar{\lambda}k_f) \cosh(R/\bar{\lambda})} + \frac{\sinh(R/\bar{\lambda})}{p(1 - D_{eff}/Rk_f) \sinh(R/\bar{\lambda})} \right] \end{aligned} \quad (9-113)$$

and

$$\bar{\lambda} = \frac{p\epsilon_p}{D_{eff}} \left[ \frac{1 + (\rho_p/\epsilon_p)K_A k_{ads}}{K_A p + k_{ads}} \right] \quad (9-114)$$

Now let us examine the moments of the eluted peak. The  $n$ th moment is defined as

$$m_n = \int_0^\infty t^n \cdot C(L, t) dt$$

the  $n$ th absolute moment by

$$\mu_n = \frac{\int_0^\infty t^n \cdot C(L, t) dt}{\int_0^\infty C(L, t) dt} = \frac{m_n}{m_0}$$

and the  $n$ th central moment by

$$\mu'_n = \frac{\int_0^\infty (t - \mu_1)^n C(L, t) dt}{\int_0^\infty C(L, t) dt}$$

These, of course, are experimentally measurable quantities from the output  $C(L, t)$  measurements. The heart of the analysis is to recognize that such moments are related to the Laplace transform as

$$m_n = (-1)^n \lim_{p \rightarrow 0} \left\{ \frac{d^n}{dp^n} [\mathbf{C}(L, p)] \right\} \quad (9-115)$$



so from equations (9-112) and (9-115) we can get explicit expressions for the moments in terms of model parameters. Of particular interest is the first absolute moment,  $\mu_1$ , and the second central moment (or variance),  $\mu_2'$ . These are

$$\mu_1 = \left(\frac{L}{v}\right)(1 + \delta_0) + \left(\frac{t_0}{2}\right) \quad (9-116)$$

where  $t_0$  is the time duration of the input function, and

$$\mu_2' = \left(\frac{2L}{v}\right) \left[ \delta_1 + \frac{D_L}{\epsilon_B} (1 + \delta_0) \cdot \frac{1}{v^2} \right] + \frac{t_0^2}{12} \quad (9-117)$$

where

$$\delta_0 = \frac{(1 - \epsilon_B)}{\epsilon_B} \epsilon_p (1 + \rho_p K_A / \epsilon_p) \quad (9-118)$$

and

$$\delta_1 = \frac{(1 - \epsilon_B)}{\epsilon_B} \epsilon_p \left[ \frac{\rho_p K_A^2}{\epsilon_p k_{ads}} + \frac{R^2 \epsilon_p}{15} \left( 1 + \frac{\rho_p K_A}{\epsilon_p} \right)^2 \cdot \left( \frac{1}{D_{eff}} + \frac{5}{k_f R} \right) \right] \quad (9-119)$$

Physically the first absolute moment represents the average residence time, while the variance represents the relative spread around the mean of the output peak.

The other bit of information that we can use, together with the above, is that for the elution of a nonadsorbed gas introduced under similar conditions. In this case,  $K_A = 0$ , and

$$\delta_1(inert) = \frac{(1 - \epsilon_B)}{\epsilon_B} \epsilon_p \left[ \frac{R^2 \epsilon_p}{15} \left( \frac{1}{D_{eff}} + \frac{5}{k_f R} \right) \right] \quad (9-120)$$

$$\mu_1(inert) = \left(\frac{L}{v}\right) \left[ 1 + \frac{(1 - \epsilon_B)}{\epsilon_B} \cdot \epsilon_p \right] + \frac{t_0}{2} + \mu_{1D} \quad (9-121)$$

where

$$\mu_{1D} = \mu_{1t} - (t_0/2)$$

and  $\mu_{1t}$  is the moment measured with the active component but with no column (i.e., inlet and outlet effects). For a well-designed experiment the value of  $\mu_{1t}$ , which is essentially a correction factor, will be small in comparison to other quantities. One additional datum is provided by the variance of the inert, here assuming blank corrections to be negligible,

$$\mu_2'(inert) = \left(\frac{2L}{v}\right) \left[ \delta_1(inert) + \frac{D_L}{\epsilon_B} \left( 1 + \frac{(1 - \epsilon_B)}{\epsilon_B} \cdot \epsilon_p \right)^2 \left( \frac{1}{v^2} \right) \right] \quad (9-122)$$

We are now in a position to determine some of the parameters of the system from these moment values. Normally the quantities of interest are  $K_A$  and  $D_{eff}$  (since we are using only two moments, only two parameters can be determined independently). The value of  $k_{ads}$  is normally very large and terms containing this factor in the denominator become small. Values for the dispersion coefficient,  $D_L$ , and the mass-transfer coefficient,  $k_f$ , are available from independent correlations. Thus, let

us examine the difference in first moments between the experimental system and the inert system. This is

$$\mu_1(exp) - \mu_1(inert) = \Delta\mu_1 = \frac{(1 - \epsilon_B)}{\epsilon_B} \rho_p K_A (L/v) \quad (9-123)$$

Thus the adsorption coefficient  $K_A$  can be determined from the slope of a plot of  $\Delta\mu_1$ , versus  $(L/v)$  if  $\epsilon_B$  is known (which is usually the case).

The second moment expressions contain  $k_{ads}$ ,  $D_L$ ,  $D_{eff}$ , and  $k_f$ . For the axial dispersion coefficient in columns typical of chromatography, a correlation such as that of Smith and Suzuki [J.M. Smith and M. Suzuki, *Chem. Eng. Jl.*, 3, 256 (1972)] can be used

$$D_L = \eta \mathcal{D}_{AB} + \rho(\epsilon_B v) \quad (9-124)$$

where  $\eta$  is a fitting constant, and  $\rho$  is a mixing-length parameter. The correlation here applies to particle Reynolds numbers from about 0.001 to 10. For the mass-transfer coefficient many correlations are available. Again, one suited to chromatographic conditions is that of Wakao, et al., [N. Wakao, T. Oshima and S. Yagi, *Chem. Eng. Japan*, 22, 780 (1958)],

$$\frac{2Rk_f}{\mathcal{D}_{AB}} = 2 + (1.45)(N_{Sc})^{1/2}(N_{Re_p})^{1/2} \quad (9-125)$$

where

$$N_{Re_p} = \frac{u_0(2R)\rho}{\mu} < 100, \quad N_{Sc} = \frac{\mu}{\rho \mathcal{D}_{AB}}$$

with  $u_0$  the superficial velocity in the column.

### 9.2.4 A Chromatographic Reactor

There is really no reason that chemical reactors employing simultaneous chromatography cannot be employed as a useful tool, at least for laboratory investigations, as well as for the chromatograph alone. Let us rewrite equation (9-93) in a slightly modified form

$$F_I \left( \frac{\partial C_I}{\partial t} \right) + F_{II} \left( \frac{\partial C_{II}}{\partial t} \right) = F_I D \left( \frac{\partial^2 C_I}{\partial z^2} \right) + F_{II} u \left( \frac{\partial C_I}{\partial z} \right) - F_I r_I - F_{II} r_{II} \quad (9-126)$$

where  $r_I$  and  $r_{II}$  are reaction rate terms for the moving and stationary phases, respectively. Also, for the stationary phase

$$\left( \frac{\partial C_{II}}{\partial t} \right) = k_f (KC_I - C_{II}) - r_{II} \quad (9-127)$$

where  $k_f$  is a mass-transfer coefficient between phases I and II, and  $K$  is a phase partition coefficient (Henry's law constant) for the chromatographic reactant. We may take these equations as the basis for an *ideal chromatographic reactor* [see S.H. Langer and J.E. Patton, *New Developments in Gas Chromatography*, (J.H. Purnell, ed.), John Wiley and Sons, New York, NY, (1973)]. This reactor will have chemical control of reaction rates, will be isothermal and without dispersion

effects, and as shown in equation (9-127), will have a concentration distribution between moving and stationary phases such that

$$\left(\frac{C_{II}}{C_I}\right) = K \quad (9-128)$$

Let us presume further that we have a first-order reaction in both phases

$$r_I = k_I C_I; \quad r_{II} = k_{II} C_{II} \quad (9-129)$$

Then, the more general expression (9-126) now becomes

$$(F_I + F_{II}K) \left( \frac{\partial C_I}{\partial t} \right) = -F_I U \left( \frac{\partial C_I}{\partial z} \right) - (F_I k_I + F_{II} k_{II} K) C_I \quad (9-130)$$

The inlet/boundary conditions are

$$C_I(0, t) = \phi(t); \quad C_I(z, 0) = 0 \quad (9-131)$$

where  $\phi(t)$  is an arbitrary input function. The solution, in the absence of significant dispersion effects, is simply

$$C_I(z, t) = \phi(t - \alpha\tau) \exp(-\beta\tau) \quad (9-132)$$

where

$$\tau = (z/u); \quad \alpha = \frac{F_I + F_{II}K}{F_I}$$

$$\beta = \frac{F_I k_I + F_{II} k_{II} K}{F_I}$$

The first term in equation (9-132) represents the time displacement of the input function  $\phi(t)$ , and the second is the amplitude attenuation of the input. As can be seen, the amplitude term contains all of the kinetic and phase-distribution parameters. The exit concentration is also given by equation (9-132), but now with

$$\tau = t_R = (L/u) \quad (9-133)$$

Now let us in addition write a mass balance for the reactant entering and leaving the column. Entering,

$$W_{inlet} = AuM \int_0^\infty C_I(0, t) dt = AuM \int_0^\infty \phi(t) dt \quad (9-134)$$

where  $A$  is the void cross section,  $u$  the velocity, and  $M$  is the molecular weight. Leaving,

$$W_{out} = AuM \int_0^\infty C(L, t) dt = AuM \exp(-\beta t_R) \int_0^\infty \phi(t - \alpha t_R) dt \quad (9-135)$$

Since there is no dispersion considered for the ideal chromatographic reactor, changes in the  $\phi$  function are due only to the reactor residence time,  $t_R$ , so that

$$\int_0^\infty \phi(t) dt = \int_0^\infty \phi(t - \alpha t_R) dt \quad (9-136)$$

hence

$$\left( \frac{W_{inlet}}{W_{out}} \right) = \exp(\beta t_R) \quad (9-137)$$

Let us define some phase residence times as follows,

$$\left( \frac{t_{II}}{t_R} \right) = \left( \frac{KF_{II}}{F_I} \right) \quad (9-138)$$

$$t_R = \left( \frac{L}{u} \right) = \left( \frac{t_{II}F_I}{KF_{II}} \right) \quad (9-139)$$

This gives

$$\beta = \frac{F_I k_I}{F_{II}} + \frac{KF_{II} k_{II}}{F_I}$$

or

$$\beta = \frac{k_I t_R + k_{II} t_{II}}{t_R} \quad (9-140)$$

Substituting this result for  $\beta$  back in equation (9-137) gives

$$\left( \frac{W_{out}}{W_{inlet}} \right) = \exp[-(k_I t_R + k_{II} t_{II})] \quad (9-141)$$

In most cases of interest it would be expected that there would be reaction only in the stationary phase (II), so that an appropriate working equation for this case is

$$\left( \frac{W_{out}}{W_{inlet}} \right) = \exp(-k_{II} t_{II}) \quad (9-142)$$

which is a result that follows the PFR form and is hardly surprising. In application of equation (9-142), the stationary phase residence time is given via equation (9-138) as

$$t_{II} = \frac{t_R KF_{II}}{F_I} \quad (9-143)$$

so that we must still have some measure of the partition coefficient  $K$  to utilize the chromatographic reactor.

The analysis is readily extended to nonlinear kinetics of the power-law form. For example,

$$r = kC^n$$

and

$$(F_I + KF_{II}) \left( \frac{\partial C_I}{\partial t} \right) = -uF_I \left( \frac{\partial C_I}{\partial z} \right) - (F_I k_I + F_{II} k_{II} K^n) C_I^n \quad (9-144)$$

This can be simplified to

$$\alpha \left( \frac{\partial C_I}{\partial t} \right) + u \left( \frac{\partial C_I}{\partial z} \right) + \beta_n C_I^n = 0 \quad (9-145)$$

where

$$\alpha = \frac{F_I + KF_{II}}{F_I}; \quad \beta_n = \frac{F_I + F_{II}k_{II}K^n}{F_I}$$

Now, as before, we have the relationship between the residence times

$$\left(\frac{t_{II}}{t_R}\right) = \left(\frac{KF_{II}}{F_I}\right)$$

so

(9-146)–(9-148)

$$\alpha = \frac{T_R + t_{II}}{t_I}; \quad \beta_n = \frac{k_I t_R + k_{II} t_{II} K^{n-1}}{t_I}; \quad \tau_n(z) = (z/u^n)$$

The solution, with the same boundary and initial conditions as before, is

$$C_I(z, t) = \frac{u\phi[t - \alpha\tau_1(z)]}{u^{n-1} \sqrt{1 + (n-1)\beta_n\tau_n(z)\{u\phi[t - \alpha\tau_1(z)]\}^{n-1}}} \quad (9-149)$$

An in-out balance for a second-order irreversible reaction would be, for example

$$W_{out} = AuM \int_0^\infty \frac{\phi[t - \alpha\tau_1(L)]}{1 + \beta_2\tau_2(L)u\phi[t - \alpha\tau_1(L)]} dt \quad (9-150)$$

which may be written as

$$W_{out} = AuM \int_0^\infty \frac{\phi(t)}{1 + \beta_2\tau_2(L)u\phi(t)} dt \quad (9-151)$$

using the same reasoning as that for equation (9-136). For the input, we have as before

$$W_{inlet} = AuM \int_0^\infty \phi(t) dt \quad (9-152)$$

Because of the nonlinear reaction kinetics, however, we must now evaluate equations (9-151) and (9-152) in terms of the specific nature of the input function  $\phi(t)$ . For a square wave input,

$$\begin{aligned} \phi(t) &= C_0; & 0 \leq t \leq t_0 \\ \phi(t) &= 0; & t > t_0 \end{aligned} \quad (9-153)$$

After doing this, though, the procedure is the same in general as for first-order kinetics.

We still have not exhausted the supply of information available from the chromatographic reactor, since there are yet data available from product appearance. The material balance on product is

$$F_I \left( \frac{\partial C_{I,p}}{\partial t} \right) + F_{II} \left( \frac{\partial C_{II,p}}{\partial t} \right) = -F_I u \left( \frac{\partial C_{I,p}}{\partial z} \right) + F_I r_I + F_{II} r_{II}$$

Again we assume Henry's law partition, so that

$$K_p = \left( \frac{C_{II,p}}{C_{I,p}} \right); \quad K_A = \left( \frac{C_{II}}{C_I} \right) \quad (9-155)$$

with initial and boundary conditions combining equations

$$C_{I,p}(z, 0) = 0$$

$$C_{I,p}(0, t) = 0$$

Combining equations (9-154) and (9-155) gives

$$(F_I + K_p F_{II}) \left( \frac{\partial C_{I,p}}{\partial t} \right) + F_{II} u \left( \frac{\partial C_{I,p}}{\partial z} \right) = \eta_p (F_I k_I + F_{II} k_{II} K_R) C_I \quad (9-156)$$

with  $\eta_p$  a stoichiometric coefficient, mols product per mols reactant (rate constants are defined on a per mol basis). Now, as before

$$C_I = \phi[t - \alpha\tau(z)] \exp[-\beta\tau(z)]$$

and we define

$$\alpha_R = 1 + (F_{II} K_R / F_I)$$

$$\alpha_p = 1 + (F_{II} K_p / F_I)$$

$$\beta = k_I + (k_{II} F_{II} K_R / F_I)$$

Substituting these into equation (9-156) gives

$$\alpha_p \left( \frac{\partial C_{I,p}}{\partial t} \right) + u \left( \frac{\partial C_{I,p}}{\partial z} \right) = \eta_p \beta [t - \alpha_R \tau(z)] \exp[-\beta\tau(z)] \quad (9-157)$$

Again, assume a square wave input as per equation (9-153). The solution for product is

$$C_{I,p}(L, t) = (\eta C_0) [\exp(k'_{app} t_0) - 1] \exp[-k'_{app}(t - t_p)] \quad (9-158)$$

with

$$t_p + t_0 < t < t_R$$

$$t_p = t_{II,p} + t_g \quad (9-159)$$

$$k'_{app} = k_{II} + (t_g / t_{II}) k_I$$

The characteristic time,  $t_p$ , is normally measured as the retention time for an inert gas such as air or helium under the same conditions of temperature and pressure as the reaction experiment.

### 9.2.5 Snakes in the Grass

We have tried to be careful so far to talk about plus or minus limits on data and what these may mean in the interpretation of data. Here, it is probably more important than ever. One notes in much of the interpretation of chromatographic data (and fixed bed adsorption/ion exchange as well), integrals of the form

$$\int_0^\infty f(t) dt$$

where  $f(t)$  is often a concentration as a function of time. The problem is strictly an experimental and practical problem, since the difficulty is to define exactly where  $t = \infty$  is. Even the best electronics may drift a little, particularly if the elution time is

long, so where is  $t$  at  $\infty = t_\infty$ ? The result of this is that parameter values determined from moments analysis, or reaction values determined from chromatographic reactors, must be given pretty wide plus or minus latitude until one becomes very experienced with the method.

For further details on the moments analysis, the reader is again referred to the review by Haynes; and for the chromatographic reactor, to Langer and coworkers [J. Coca and S.H. Langer, *Chemtech*, 682, November, (1983); C-Y. Jeng and S.H. Langer, *J. Chromatography*, 1, 589 (1992)].

### 9.3 Deactivation Waves

In Chapter 5 we had the opportunity to look at some transients associated with fixed-bed operation that arose because of catalyst deactivation. At this point, we have been through a lot of reactor analysis, and in line with the title of this chapter, it is now fitting to further investigate the behavior of reactors with these sorts of transients.<sup>5</sup>

The particular cases we want to examine here are transients caused by catalyst decay in fixed-bed reactors. What we will do is essentially pick up where we left off in Chapter 5.

As a reminder, the isothermal deactivation wave model discussed there was based upon the quasi-steady state assumption with respect to the relative rates of deactivation and of the main reaction, where deactivation was slow. A partial consequence of this was that coke profiles, and hence activity profiles, extended throughout the length of the reactor during most of the process. Now let us take a look at the opposite end of the spectrum, where we have poisoning, rather than coking, and the uptake of the poison is rapid and irreversible. Here, after a period of initial operation, an activity profile develops such that the inlet to the bed will be completely deactivated, the exit portion will retain initial activity, and a central portion (moving) will display a sharp change from no activity to full activity. This sounds like the adsorption wave all over again, and it is. We return to the basic idea, somewhat in the thought of Bohart and Adams, put forward by Wheeler and Robell [A. Wheeler and A.J. Robell, *J. Catal.*, 13, 299 (1969)] for Type I poisoning (reactant and poison in parallel competition for the catalytic surface) of an irreversible reaction in a fixed-bed reactor. The poison is assumed to be distributed in the bed according to Bohart-Adams results, and for the present development we can write for the adsorption of poison,

$$\frac{\partial C_p}{\partial \theta} = r_{ads} + k_{ads} C_{p,g} (1 - C_p / C_{p\infty}) \quad (9-160)$$

$$\frac{\partial C_{p,g}}{\partial z} = r_{ads} \quad (9-161)$$

where  $k_{ads}$  is the adsorption rate constant and  $C_{p,g}$  the concentration of poison in the fluid phase. The solution for a bed with no poison adsorption under initial

<sup>5</sup> In real time things can go very fast or very slow. In reference to the residence-time in the reactor, we take it easy here. Fast? "Beam me up, Scotty."—G. Roddenberry

conditions is

$$\left(\frac{C_p}{C_{p\infty}}\right) = \frac{1 + \exp(-N_t\theta/\theta_\infty)}{1 + \exp(-N_t\theta/\theta_\infty)[\exp(N_t z/L) - 1]} \quad (9-162)$$

where  $N_t = (k_{ads}L/v)$  is the number of adsorption transfer units in the reactor and  $\theta_\infty$  is the ratio of the total capacity of the catalyst bed for poison adsorption to the rate at which poison is introduced into the reactor.

$$\theta_\infty = (\rho_B C_{p\infty} L / M v C_{p,g}^o) \quad (9-163)$$

Here  $\rho_B$  is the bulk density of the catalyst,  $M$  the molecular weight of the poison, and  $C_{p,g}^o$  the inlet concentration of the poison. Now, turning to the chemical reaction part of the analysis, for Academic Reaction #1, we have

$$\ln\left(\frac{C_L}{C_0}\right) = \frac{1}{v} \int_0^L k \, dz \quad (9-164)$$

where  $k$  is the reaction rate constant,  $C_0$  and  $C_L$  the inlet and outlet concentrations of reactant,  $v$  the superficial velocity, and  $L$  is the reactor length. The rate constant is a function of poison concentration, which in turn is a function of position and time. We have an option as to how the value of the rate constant (and therefore activity) is related to poison concentration. (In real life, we do not have an option; Mother Nature tells us so). In the most simple case we will have a linear function (*nonselective poisoning*) such that

$$\left(\frac{k}{k_0}\right) = s = 1 - \left(\frac{C_p}{C_{p\infty}}\right) \quad (9-165)$$

A generalization of this is the *selective poisoning* model, as described in Illustration 7.7. We can write this here as,

$$\left(\frac{k}{k_0}\right) = s = \frac{1}{1 + \phi_0 C_p / C_{p\infty}} - \frac{(C_p / C_{p\infty})}{1 + \phi_0} \quad (9-166)$$

where  $\phi_0$  is the Thiele modulus for the unpoisoned catalyst and, in the context of equation (9-166), is also the parameter that determines the degree of selectivity. The value of  $C_p$  determines the poison concentration, and  $C_{p\infty}$  the saturation poison concentration ( $s = 0$ ). Equation (9-165) is just the limiting value of (9-166) as  $\phi_0 \rightarrow 0$ .

Equations (9-162) and (9-166) can be combined and the integral of equation (9-164) evaluated to give the following general solution for exit concentration as a function of time:

$$\begin{aligned} \ln\left(\frac{C_L}{C_0}\right) = \frac{k_0/k_{ads}}{1 + \phi_0} \left\{ \ln\left[1 + \exp\left(\frac{-N_t\theta}{\theta_\infty}\right)(\exp(N_t) - 1)\right] \right. \\ \left. + \phi_0 \ln\left[1 + \frac{\exp(-N_t\theta/\theta_\infty)(\exp(N_t) - 1)}{1 + \phi_0[1 - \exp(-N_t\theta/\theta_\infty)]}\right] \right\} \end{aligned} \quad (9-167)$$

For nonselective poisoning

$$\ln\left(\frac{C_L}{C_0}\right) = -\left(\frac{k_0}{K_{ads}}\right) \ln\{1 - \exp(-N_t\theta/\theta_\infty) + \exp[N_t(1 - \theta/\theta_\infty)]\} \quad (9-168)$$



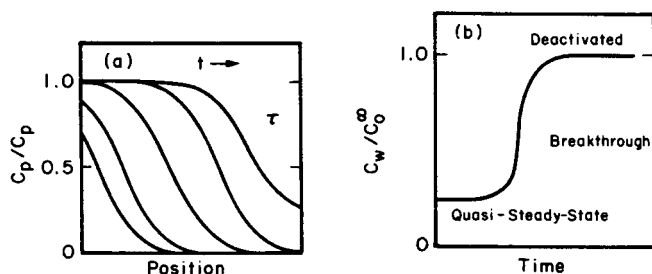


**Figure 9.10** (a) Bohart-Adams generalized poisoning wave profiles. The parameter  $\tau = N_t\theta/\theta_\infty$ . (b) Conversion-time behavior for a very sharp poisoning wave.

The solutions of equations (9-167) and (9-168) can be used to evaluate the parameters  $\theta_\infty$ ,  $N_t$ ,  $(k_0/k_{ads})$  and  $\phi_0$  from various limiting cases. The most reasonable limits are at  $t = 0$ , conversion before breakthrough of poison, conversion at long time ( $\theta/\theta_\infty \gg 1$ ), and conversion at  $\theta = \theta_\infty$ . Some typical profiles obtained from the Bohart-Adams equation are shown in Figure 9.10a. It is clear that after an initial period of operation the transients disappear and a wave, or front, of poison concentration is established, invariant in shape, that passes through the bed at essentially constant velocity. This wave can be diffuse or sharp, depending upon the parametric value, of course. Sharp poisoning fronts are associated with small values of  $(k_0/k_{ads})$ ; in such cases one would observe a very dramatic decrease in conversion with time-on-stream as the poison breakthrough from the bed occurs. This is shown qualitatively in Figure 9.10b.

The Wheeler-Robell analysis envisions the main reaction to be diffusion-controlled, but not the poisoning reaction. Whether or not this is so is a question of relative dimensions of molecules, but dual diffusion control would seem more typical. The analysis has been extended to diffusion-controlled poisoning by Haynes [H.W. Haynes, Jr., *Chem. Eng. Sci.*, 25, 1615 (1970)], who used a shell model as an approximation for rapid poisoning in a Type I system. The Thiele modulus for the poisoning reaction is  $\phi_p$ , and  $\phi_p \gg \phi_0$  for the shell model assumption to be valid. For a spherical catalyst particle the fraction of original activity,  $s$ , is related to the radius of the poison-free zone by

$$s = 1 - \zeta^3 \quad (9-169)$$

where  $\zeta$  is the ratio,  $r_1/R$ , of the poison-free zone to the total radius. The effectiveness factor as a function of the degree of poisoning is obtained by mass balances on the poisoned and poison-free zone as

$$\eta_p = \frac{3}{\phi_p^2 \zeta^2} \left[ \frac{\phi_p \zeta \coth(\phi_p \zeta) - 1}{\phi_p (1 - \zeta) \coth(\phi_p \zeta) + 1} \right] \quad (9-170)$$

The equation for poisoning kinetics and the conservation equation giving the poison distribution in the bed are

$$\frac{\partial(C_{p,g}/C_{p,g}^\circ)}{\partial z} = \frac{3N_t(C_{p,g}/C_{p,g}^\circ)}{\phi_p^2} \left[ \frac{\phi_p \zeta \coth(\phi_p \zeta) - 1}{\phi_p (1 - \zeta) \coth(\phi_p \zeta) + 1} \right] \quad (9-171)$$

and

$$\frac{\partial \zeta}{p\tau} = \frac{(C_{p,g}/C_{p,g}^{\circ})}{\phi_p^2} \left[ \frac{\phi_p \zeta \coth(\phi_p \zeta) - 1}{\phi_p (1 - \zeta) \coth(\phi_p \zeta) + 1} \right] \quad (9-172)$$

where  $N_t$  is the number of adsorption transfer units as defined before,  $z$  the dimensionless reactor length, and  $\tau$  a dimensionless time defined by

$$\tau = \frac{k_{ads} C_{p,g}^{\circ}}{C_{p,\infty}}$$

Analytical solution in terms of the diffusion-free forms is possible as  $\phi_p \rightarrow 0$ , but in general numerical solution will be required. If the poison distribution is determined as a function of time and position in the bed from equations (9-171) and (9-172), then the corresponding bed activity is

$$(s)_{bed} = \left[ \frac{\phi_0 \zeta \coth(\phi_0 \zeta) - 1}{\phi_0 (1 - \zeta) \coth(\phi_0 \zeta) + 1} \right] \left( \frac{1}{\phi_0 \coth \phi_0 - 1} \right) \quad (9-173)$$

and the conversion relationship for first-order kinetics is

$$\ln \left( \frac{C_L}{C_0} \right) = -k' \left( \frac{L}{V} \right) \int_0^1 (s)_{bed} dz \quad (9-174)$$

with

$$k' = k[(3/\phi_0^2)(\phi_0 \coth \phi_0 - 1)] \quad (9-175)$$

which can be considered the rate constant for the unpoisoned catalyst. Generalized graphical plots of the solutions to equations (9-171) to (9-174) are given in the original reference. The properties of the system that must be known are  $k$ ,  $k_{ads}$ ,  $\phi_0$ ,  $\phi_p$ , and the limiting poison adsorption capacity,  $C_{p,\infty}$ , which is enough for an afternoon in the laboratory.



HORATIO SAYS

Help! Show me the way out of all this! Well, yes:  
“There’s something in the parting hour, will chill  
the warmest heart.”—*E. Pollock*

Good bye, Horatio, I’m sad to see you go (I think).  
—*JBB*

## Exercises

### Section 9.1

1. (Note that this is an expansion on the development of Section 9.2a.) Consider the adsorption of two components, 1 and 2, in a bed consisting of an intimate mixture of two adsorbents, each specific for one of the components. For each of the two it may be assumed that the Klotz equation applies, and that there is no interaction between components.

Let us define the total bed weight as  $x_T$ , and describe the relationship between the amounts of adsorbent for 1 and 2 as

$$x_2 = ax_1$$

so

$$x_1 = x_T/(1+a); \quad x_2 = ax_T/(1+a)$$

(a) Derive a criterion that defines whether the separation in the breakthrough curves at any specified (and equal) values of  $(C/C_0)_i$  for 1 and 2 will increase or decrease as one increases  $x_2$  (i.e.  $a$ ) relative to  $x_1$ .

(b) Assuming that  $(K_D S)_1$  and  $(K_D S)_2$  have the same dependence on velocity of the form

$$(K_D S)_i = b_i v^n$$

would it be possible to maximize the separation in the breakthrough curves by manipulation of the velocity? All of the parameters, including  $a$ , are fixed. Discuss the reason for your answer (See also Problem 6).

2. On the basis of the results in Illustration 4.8, establish the weight of resin necessary to ensure 98% utilization at a breakthrough of 0.01. The flow is to be  $30 \text{ cm}^3/\text{min}$ , the column diameter the same, and the inlet concentration  $10 \text{ meq/l}$ . Note that a full-scale bed can be designed in this manner; one would change only the diameter to keep the same linear velocity.
3. Benzene vapor is to be removed from a waste gas (air) stream in a solvent recovery plant by passage through a bed of 4-6 mesh silica gel,  $d_p$  0.013 ft, at  $70^\circ\text{F}$  and atmospheric pressure. The mass velocity,  $G$ , on a solvent-free basis is  $7.5 \text{ lb/ft}^2\text{-min}$  based on total cross sectional area. Design requirements call for operation for three hours until breakthrough to  $(C/C_0) = 0.1$ . The entering composition is 0.90 mol% benzene.

A correlation for the mass-transfer coefficient in this system is given by

$$H_T = (1.42/a_v)(d_p G/\mu)^{0.51}$$

where  $H_T$  is the height of a transfer unit in ft., and is defined as

$$H_T = G/(k_d a_v)(M_m)(P_T)$$

with

$M_m$  = mean molecular weight of gas stream

$G$  = solvent-free gas mass velocity

$P_T$  = total pressure, atm

$k_d a_v$  = volumetric mass-transfer coefficient

$\mu$  = viscosity =  $74.5 \times 10^{-5} \text{ lb/ft-min}$

$a_v$  = interfacial area/volume =  $202 \text{ ft}^{-1}$

$\rho_b$  = bulk density of solid =  $39 \text{ lb/ft}^3$

Equilibrium in this system is given by

$$q = (13.36)P_B \quad (70^\circ\text{F})$$

with

$q$  = lb benzene/lb silica

$P_B$  = partial pressure of benzene, atm

Determine the depth of bed required for this application. Also determine the benzene concentration in the bed at the end-of-run condition.

4. A bed of hot, coked catalyst 20 ft high, originally at 800°C, is to be dry-quenched with nitrogen entering the bed at 25°C. The flow rate of nitrogen is to be 0.2 liters(SC)/cm<sup>2</sup>-s. The bed has a porosity of 0.5 and the particles in the bed average 6 cm in diameter. Solids heat capacity is 0.22 cal/g-°C and the density is 1 g/cm<sup>3</sup>. The following equation has been used for the correlation of heat-transfer coefficients in this application:

$$h = \frac{Au^{0.7}T^{0.3}(10)^{(1.7f-3.56f^2)}}{d_p^{1.3}}$$

where  $h$  is in cal/s-cm<sup>3</sup>-°C,  $u$  is the flow rate in liters(SC)/cm<sup>2</sup>-s,  $T$  is in °K,  $f$  is porosity,  $d_p$  is particle diameter in cm, and  $A$  is an empirical fitting constant = 0.012 for the coked catalyst. The data on which this equation was based was interpreted on the condition that the volume-based heat capacity and the volumetric flow rate of the gas were taken at standard conditions, so no temperature corrections are required.

What is the exit temperature of the quench gas, in 5 min increments, for the first 30 min of operation?

What increase in the gas velocity would be required to cut the quenching time in half, if it is assumed that quenching time is measured from the initial conditions to a gas exit temperature of 100°C?

Which of the two procedures above uses less total quench gas?

## Section 9.2

5. On the following pages are some data on the adsorption of CO on an unsupported Cu catalyst using a chromatographic technique. The pertinent properties of the catalyst used were  $\rho_p = 1.394$  g/cm<sup>3</sup>,  $\epsilon_p = 0.823$ , and  $R(\text{average}) = 0.65$  mm. Properties of the columns used in the investigation were:

	Column 4	Column 6
Total length, cm	40.0	28.0
Packed length, cm	31.4	25.8
Internal diameter, cm	0.47	0.395
Void fraction	0.398	0.360
Mass of catalyst, g	4.580	2.817
Temperature, °C	150; 175	140

Determine values of the adsorption equilibrium constant for CO on Cu, the heat of adsorption, and the effective diffusivity of CO within the Cu structure under these conditions. You may assume that  $k_{ads}$  is very large. The carrier gas in all runs with CO was He, however, inert runs, as shown, were conducted with Ar.

$y, \text{ft}^3$	$C_1/(C_0)_1$	$C_2/(C_0)_2$
2.5	0.05	0.0
5.0	0.08	0.0
7.5	0.11	0.0
12.0	0.31	0.0
15.0	0.64	0.01
17.0	0.91	0.02
17.5	0.98	0.02
20.0	1.0	0.03
28.0	1.0	0.08
30.0	1.0	0.11
35.0	1.0	0.25
40.0	1.0	0.55
42.5	1.0	0.82
44.0	1.0	0.98
46.0	1.0	1.0

CO-Cu and Ar-Cu (Column 4)						
Gas	$T, ^\circ\text{C}$	$(L/v), \text{sec}$	$t_0, \text{sec}$	$\mu_1, \text{sec}$	$\Delta\mu'_2, \text{sec}^2$	$v, \text{cm/s}$
Ar	150	5.43	3.38	36.37	1.64	5.77
Ar	150	6.22	3.88	41.46	2.37	5.04
Ar	150	7.21	4.49	47.88	9.00	4.35
Ar	150	8.78	5.48	58.00	12.34	3.57
Ar	150	10.76	6.71	70.77	23.98	2.91
Ar	150	12.86	8.02	84.40	38.30	2.44
Ar	150	14.40	8.99	95.15	58.75	2.17
Ar	150	16.28	10.15	106.21	79.78	1.92
CO	150	5.14	3.29	37.68		6.11
CO	150	8.74	5.76	63.86		3.58
CO	150	6.25	3.99	46.27		5.02
CO	150	13.15	8.37	97.66		7.38
CO	150	7.30	4.66	53.08		9.30
CO	150	10.85	6.92	80.48		2.89
CO	150	16.57	10.57	123.96		1.89
CO	150	11.90	7.60	90.74		2.63
CO	150	16.49	10.52	122.56		1.90
CO	150	11.88	7.58	90.08		2.64
CO	175	5.33	3.61	39.41	24.83	5.88
CO	175	8.65	5.86	63.34	70.30	3.63
CO	175	6.17	4.18	47.60	42.15	5.09
CO	175	13.30	8.99	94.68	198.74	2.36
CO	175	7.40	5.01	53.42	51.93	4.24
CO	175	14.60	9.84	105.44	255.03	2.15
CO	175	10.98	7.44	79.17	138.85	2.86
CO	175	16.47	11.12	117.15	324.51	1.90
CO	175	11.94	8.08	84.71	145.08	2.63

Gas	$T, ^\circ\text{C}$	CO-Cu and Ar-Cu (Column 6)				$v, \text{cm/s}$
		$(L/v), \text{sec}$	$t_0, \text{sec}$	$\mu_1, \text{sec}$	$\Delta\mu'_2, \text{sec}^2$	
Ar	140	2.60	3.09	24.25		9.89
Ar	140	3.19	3.79	29.25		8.07
Ar	140	3.76	4.47	33.95		6.86
Ar	140	4.35	5.17	38.95		5.93
Ar	140	5.71	6.79	50.56		4.51
Ar	140	6.71	7.98	60.07		3.84
Ar	140	7.60	9.05	68.31		3.39
Ar	140	7.58	9.00	67.64		3.40
Ar	140	2.83	3.37	26.00		9.10
Ar	140	3.16	3.76	29.03		8.15
Ar	140	4.33	5.16	39.11		5.94
Ar	140	8.54	10.12	79.06		3.02
CO	140	5.65	6.71	56.88	60.57	4.56
CO	140	6.16	7.32	62.32	94.66	4.18
CO	140	4.61	5.45	47.17	48.57	5.59
CO	140	6.76	8.02	67.92	96.23	3.81
CO	140	7.57	8.98	76.20	120.12	3.40
CO	140	2.85	3.37	29.82	22.41	9.06
CO	140	8.47	10.05	86.13	170.19	3.04
CO	140	3.16	3.75	33.20	25.31	8.14
CO	140	3.13	3.71	33.17	25.81	8.23
CO	140	3.72	4.42	38.77	30.17	6.93
CO	140	8.41	9.99	84.40	143.92	3.06

6. The following data were obtained for the adsorption, in a mixed bed, of two components from a third, inert gas.

The bed was composed of 5 lb granulated carbon, active for component 1, and 30 lb silica gel, active for component 2, compounded into an intimate mixture. A total gas flow of  $10 \text{ ft}^3/\text{h}$  was used and the adsorber operation was isothermal at  $343^\circ\text{K}$ . The initial concentration of component 1,  $C_1/(C_0)_1$ , was  $0.12 \text{ lb}/\text{ft}^3$ , and for component 2,  $C_2/(C_0)_2$ , was  $0.08 \text{ lb}/\text{ft}^3$ .

Analyze these data with respect to the following points.

1. The type of equilibrium involved.
2. The values of the pertinent equilibrium parameters.
3. Possible importance of diffusional transport and the values of the corresponding parameters.

It may be assumed that there were no significant interaction effects between the two components.

### Notation

- $A$  constant =  $(K_D S/w)$ ,  $\text{volume}^{-1}$ ; total volume of input feed of concentration  $C_0$ ; column void cross section
- $A_i$  constant =  $[(K_D S)_i(C_0)_i/(q_\infty)_i w]$ ; see equations (9-83) and (9-84)
- $a$  proportionality constant =  $(x_2/x_1)$
- $a, b, c$  constants in solution for  $T_s$ ; see after equation (9-74)

- $B$  constant =  $(K_D S/w)$ , mass<sup>-1</sup>  
 $B_i$   $[(K_D S)_i/w]$  see equations (9-83) and (9-84)  
 $b$  adsorption constant; see equation (9-56)  
 $C$  concentration, mass, mols or meq/volume  
 $C_i$  intraparticle concentration, mols/volume  
 $C_L$  concentration of reactant at L, mols/volume  
 $C_0$  inlet concentration of reactant, mass, mols or meq/volume  
 $C_p$  concentration of poison, mass or mols/volume  
 $C_{ads}$  concentration of adsorbate on surface, mols/volume  
 $C_I, C_{II}$  concentrations in phases I and II, mols/volume  
 $C^*$  interfacial equilibrium concentration, mols meq/volume  
 $C_{p,g}$  concentration of poison in gas phase, mass or mols/volume  
 $C_{p\infty}$  saturation capacity for poison, mass or mols/volume  
 $C_{I,p}, C_{II,p}$  product concentrations in phases I and II, mols/volume  
 $(C/C_0)_1, (C/C_0)_2$  specified breakthrough; see equation (9-81)  
 $(C_I)_n$  concentration of component in phase I, stage  $n$   
 $C_{p,q}$  inlet concentration of poison, mass or mols/volume  
 $c_f \rho_f$  fluid volumetric heat capacity, kcal/volume-K  
 $c_s \rho_s$  solids volumetric heat capacity, kcal/volume-K  
 $D$  index of separation (specified breakthrough); see equation (9-81); axial dispersion coefficient, length<sup>2</sup>/time  
 $D_L$  axial dispersion coefficient, cm<sup>2</sup>/s  
 $D_{eff}$  effective diffusivity, cm<sup>2</sup>/s  
 $D_{AB}$  bulk diffusion coefficient for A-B, cm<sup>2</sup>/s  
 $F(t)$  function defined in equation (9-47)  
 $F_1(y), F_2(z)$  arbitrary temperature boundary conditions; see equation (9-70)  
 $F_I, F_{II}$  volume fractions of moving and stationary phases, I and II  
 $F'(t)$  function defined in equation (9-96)  
 $f$  bed void fraction  
 $f(q)$  function of  $q$  in equation (9-9); see also equation (9-29)  
 $G$  mass flow rate, mass/area-time  
 $g$  mass flow rate, g/m<sup>2</sup>-h  
 $g(\alpha), h(\alpha)$  integral functions defined in equation (9-76)  
 $H$  HETP for separation, length  
 $H_1(\lambda), H_2(\lambda)$  functions defined after equation (9-52)  
 $h$  volumetric heat-transfer coefficient, kcal/s-cm<sup>3</sup>-°C; height of a transfer unit =  $(uF_I/\alpha)$ , length  
 $h(p)$  parameter defined in equation (9-113)  
 $h_s$  modified heat-transfer coefficient =  $h/(1 - \epsilon)$ , kcal/s-cm<sup>3</sup>-°C  
 $I_o(\omega)$  Bessel function of general variable  $\omega$   
 $i$  index for component  $i$   
 $K$  interfacial coefficient =  $(q^*/C^*)$ ; see equation (9-8a); interfacial equilibrium constant =  $(q^*/C)$ ; see equation (9-49); Henry's law constant, units of  $C_{II}/C_I$ ; distribution coefficient =  $(C_I/C_{II})$ ; see equation (9-101); phase partition coefficient =  $(C_{II}/C_I)$ ; see equation (9-127)  
 $K_A$  adsorption constant for linear isotherm; see, equation (9-109)  
 $K_R$  partition coefficient; see equation (9-155)  
 $K_p$  product partition coefficient =  $(C_{II,p}/C_{I,p})$

$K_D S$	mass-transfer coefficient, normally $\text{cm}^3/\text{g-min}$
$k$	mass-transfer coefficient, $\text{time}^{-1}$ ; see equation (9-8a); adsorption rate constant, volume/mol-time; reaction rate constant for $n$ th-order reaction
$k_f$	fluid film mass-transfer coefficient, $\text{time}^{-1}$
$k_0$	initial (unpoisoned catalyst) rate constant, $\text{time}^{-1}$
$k_{ads}$	adsorption rate constant, $\text{time}^{-1}$
$k_I, k_{II}$	rate constants in phases I and II, $\text{time}^{-1}$
$k'$	modified rate constant; see after equation (9-174)
$k'_{app}$	apparent rate constant $= k_{II} + (t_g/t_{II})k_I$
$L$	bed length; height of a mixing stage $= (2D/u)$
$\mathcal{L}(\omega)$	Laplace transform of general variable $\omega$ ; $\mathbf{C}$ is the transform of $C$ , $\mathbf{R}$ is the transform of $q$
$M$	molecular weight
$m$	bed void fraction
$m_n$	$n$ th moment of eluted peak
$N_{Re}$	Reynolds number; see equation (9-125)
$N_{Sc}$	Schmidt number; see equation (9-125)
$N_t$	number of adsorption transfer units $= (k_{ads}L/v)$
$n$	number of equilibrium stages; reaction order
$p, s$	Laplace transform parameter
$q$	concentration of component transferred to solid phase, mass or meq/volume
$q_0$	capacity of solid corresponding to $C_0$ , mass or meq/volume
$q$	equilibrium concentration of transferred component in solid phase, mass or meq/volume
$q(avg)$	average value of $q$
$q^*$	interfacial equilibrium value of $q$ , mass or meq/volume
$R, R_p$	particle radius, length
$r$	radial distance variable, length
$r_{ads}$	adsorption rate, mass or mols/volume-time
$r_1$	radius of poison-free zone in catalyst, length
$r_I, r_{II}$	reaction rates in moving and stationary phases, mols/volume-time
$s$	modified time variable $= (F_I u t)$ ; activity variable $= (k/k_0)$
$s_k$	step function; see equation (9-17)
$(s)_{bed}$	overall bed activity
$T_f$	fluid temperature, $^{\circ}\text{C}$
$T_s$	solids temperature, $^{\circ}\text{C}$
$(T_f)_o$	inlet fluid temperature, scaled according to $T_s = 0$ ; see equation (9-65)
$t$	time
$t_g$	retention time for inert gas
$t_0$	time duration of square wave input
$t_p$	product retention time $= (t_{II,p} + t_g)$
$t_R$	residence time in bed $= L/u$
$t'$	variable of integration in equation (9-95)
$t_1, t_2$	times specified for $C_1, C_2$
$t_I$	residence time in phase I
$t_{II}$	residence time in phase II $= t_R(KF_{II}/F_I)$
$t_{II,p}$	product retention time in phase II
$u$	variable $= Ay$ ; axial velocity, length/time



- $v$  variable =  $Bx$ ; interstitial velocity of fluid, length/time; effective stage volume; see equation (9-100); superficial velocity of fluid, volume/time; see equation (9-164)
- $v_I, v_{II}$  volumes of moving and stationary phases
- $W_{inlet}, W_{out}$  weight of component into and leaving column
- $w$  flow rate, volume/time
- $x$  weight of bed; bed length variable
- $x_T$  total bed weight
- $x_1, x_2$  amount of adsorbent for components 1 and 2, weight
- $Y$  constant =  $(h_s L / g c_f)$
- $y$  downstream volume =  $(wt - mx)$ ; modified time variable in heat transfer; see after equation (9-62)
- $\Delta y$  increment in  $y = |y_1 - y_2|$ , volume
- $y_1, y_2$  downstream volumes for components 1 and 2
- $z$  axial distance variable, length; scaled length variable; see after equation (9-62); bed length variable; see equation (9-93); length variable =  $nH$ ; dimensionless reactor length; see equation (9-171)

*Greek*

- $\alpha$  variable of integration in equations (9-75) and (9-77); mass-transfer coefficient,  $\text{time}^{-1}$ , constant =  $(F_I + KF_{II})/F_I$ ; see after equation (9-145)
- $\alpha, \beta$  parameters in equation (9-132); see also equation (9-140); constant =  $(1 - q_0/q_\infty)$ ; constant defined in equation (9-98); constant defined as =  $[k_I + (k_{II} F_{II} K_R / F_I)]$  in equation (9-157)
- $\beta_n$  constant =  $[(F_I k_I + F_{II} K_{II} K^n) / F_I]$ ; see after equation (9-145)
- $\gamma$  parameter defined in equation (9-113)
- $\delta$  parameter defined in equation (9-59)
- $\delta_0, \delta_1$  constants defined in equations (9-118) and (9-119)
- $\epsilon, \epsilon_B$  bed void fraction
- $\epsilon_p$  particle porosity
- $\zeta$  ratio  $(r_1/R)$  of poison-free zone to total radius
- $\eta$  correlation coefficient; see equation (9-124)
- $\eta_p$  stoichiometric coefficient, mole product/mols reactant
- $\theta$  nondimensional time; see equation (9-162)
- $\theta_\infty$  poison capacity/rate ratio =  $(\rho_B C_{p,\infty} L / M v C_{p,q}^0)$
- $\lambda$  variable of integration in equation (9-52); parameter defined in equation (9-114)
- $\mu_n$   $n$ th absolute moment =  $(m_n/m_0)$
- $\mu'_n$   $n$ th central moment
- $\mu_{lo}$  correction factor for  $\mu_1(\text{inert})$  in equation (9-121)
- $\mu_{lt}$  first absolute moment corresponding to column inlet and outlet effects
- $\Delta\mu_1$  difference in moments =  $[\mu_1(\text{exp}) - \mu_1(\text{inert})]$
- $\xi$  nondimensional variable =  $(Kkx/v)[1 - \epsilon]/\epsilon$ ; see after equation (9-38); radial variable =  $(15D_{eff}/r^2)(Kz/v)[(1 - \epsilon)/\epsilon]$ ; see after equation (9-52)
- $\rho_B$  bulk density of catalyst, mass/volume
- $\rho_f$  fluid density, mass or mols/volume
- $\rho_p$  density of particle, mass/volume
- $\rho$  mixing length parameter

- $\sigma_1, \sigma_2$  constants defined in equation (9-98)  
 $\tau$  nondimensional variable =  $[k(t - x/v)]$ ; see after equation (9-38b); time variable =  $[(15D_{eff}/r^2) \cdot (t - z/v)]$ ; see after equation (9-52); modified distance variable =  $(z/u)$ ; nondimensional time =  $[k_{ads}(C_{p,g}^0)t/C_{p,\infty}]$   
 $\tau_n(z)$  modified distance variable =  $(z/u^n)$   
 $\phi(t)$  arbitrary pulse input function  
 $\phi(u, v)$  integral function defined after equation (9-87)  
 $\phi_0$  Thiele modulus for unpoisoned catalyst  
 $\phi_p$  Thiele modulus for poisoning reaction  
 $\phi_1, \phi_2$  nondimensional concentrations =  $(C_i/C_0)$

*Note:* Some additional notation is given and described in Illustration 9.1.

---

## Index

- Accumulation, 5
- Activated complex (*see also* Transition state theory), 133
- vibration of, 141
- Activation energy (*see also* Apparent activation energy), 9, 12
- Active center (*see also* Active intermediate; Chain carrier; Surface intermediate), 14, 170
- Active intermediate (*see also* Active center; Chain carrier; Surface intermediate), 35–36
- Activity coefficient (*see also* Nonideal systems), 148
- Activity variable (*see also* Deactivation), 216
- Adiabatic reactor, axial dispersion model (*see also* Dispersion models, nonideal reactors), 430–431
- Adiabatic or nonisothermal CSTRs, 295–301
- hysteresis of, 301
- operating states, 297–300
- ignited, 300
- multiple, 300–301
- quenched, 300
- self-regulating, 300
- temperature level, steady-state, 295–296
- Adiabatic or nonisothermal PFRs, 289–293
- constant activity policy (illustration), 293–294
- numerical calculations of, 291
- parametric sensitivity, 293
- Adsorption (*see also* Isotherm, Surfaces), 170–176
- characteristics of, 181
- competitive, 174
- dissociative, 173–174
- equilibrium, 172
- [Adsorption (*see also* Isotherm, Surfaces)]
- heat of, 172
- interpretation of, 174–177
- isobar, 173
- isotherms for, 173–179
- rates of, 171
- sites, 171
- fraction occupied, 173
- number of, 172
- Adsorption inhibition (*see also* Langmuir-Hinshelwood rate equations), 189
- Adsorption wave, the (*see also* Ion exchange and adsorption), 673–688
- adsorption process steps, 674
- analysis, favorable equilibrium with
- interphase mass transport, 674–679
- boundary conditions, 677
- definition of variables, 677
- material balance, 675
- solution of, 679
- analysis, Langmuir isotherm with
- interphase mass transport, 683–685
- Bohart-Adams result, 685
- solution of, 685
- analysis, linear equilibrium with interphase
- mass transport, 679–683
- functions, properties of, 680
- functions, special, 680
- solution of, 680
- analysis, linear equilibrium with
- intraparticle diffusion, 686
- axial dispersion effects, 688
- breakthrough curves, 674
- constant pattern, 687
- equilibrium relationships, 675
- favorable equilibrium, 674
- Klotz equation, 674

- Ammonia synthesis, 195
- Apparent activation energy (*see also* Activation energy), 43–44
- Arrhenius equation (*see also* Temperature dependence approximations), 9, 12
- Barkelew diagram, 441
- BET theory (*see also* Physical adsorption), 182–186
- Bimolecular rate constant, hard spheres:  
like molecules, 119  
unlike molecules, 119
- Boudart, Mears, Vannice criteria (*see also* Interpretation, kinetics of surface reactions), 209–210
- Boundary conditions, axial dispersion model (*see* Axial dispersion model, nonideal reactors)
- Breakthrough curves (*see* Adsorption wave, the; Ion exchange and adsorption)
- Bypassing (*see* Ideal flows, deviations from)
- Catalysis (*see* Surface reactions)
- Chain carrier (*see also* Active center, Active intermediate; Surface intermediate)  
35–36, 38, 46
- Chain length (*see also* Long-chain approximation; Polymerization), 39
- Chains:  
branching, 48  
polymerization, 46
- Channeling (*see* Ideal flows, deviations from)
- Chemisorption (*see also* Adsorption), 170–171  
heat of, 178–179
- Chemostat, 261
- Chromatographic determination of  
parameters, 700–704  
boundary conditions, 701  
correlations, axial dispersion and mass transfer, 704  
model, concentrations in, 701  
model, general, 700–701  
moments of eluted peak, 702–704  
application to parameter determination, 703–704  
correction factor for, 703  
first absolute, 703  
*n*th, 702  
*n*th absolute, 702  
*n*th central, 702  
relation to the Laplace transform, 702  
second central (variance), 703
- Chromatographic reactor, 704–708  
balances, moving and stationary phases, 704  
determination of rate constants, 706  
phase residence times, 706  
product appearance, 707–708  
balance for, 707  
solution for, 708  
solution for, 705–707  
first-order reaction, 705–706  
power-law kinetics, 706–707
- Chromatography, 695–699  
basic theory, 695–697  
favorable equilibrium, 696–696  
index of separation, 696–697  
Klotz equation in, 696  
continuum theory, 697–699  
height, mixing stage, 699  
height, transfer unit, 699  
HETP for separation, 699  
moving phase balance, 698  
simplifications of, 698–699  
solution of, 698  
stationary phase balance, 698
- Clausius-Clapeyron equation, 178
- Closed sequence, 170
- Coking or fouling (*see also* Deactivation), 212  
detailed scheme for, 216–218  
example, 213  
reaction pathways, 214  
regeneration, 213
- Collision models, detailed, 132–133  
bimolecular association, 133  
isomerization, 132
- Collision number:  
bimolecular, Maxwellian populations, 113–114  
per molecule, Maxwellian gas, 113  
with surfaces, 115  
termolecular, 120  
typical, 115
- Collision theory:  
rate constants from, 116–119  
binary, hard-sphere, 116  
effect of relative velocity, 117  
energy dependence, 118
- Collisional activation and deactivation (*see also* Lindemann theory; Unimolecular reactions), 123–124
- Combined models, 382–383  
solutions to example models, 383

- [Combined models]
  - unsteady state solutions, 388
- Combined models, mixing, 356–361
  - basic combinations, 356
  - channeling, model for, 359
  - comparisons, in terms of Peclet number, 376
  - criterion, negligible dispersion effects, 373
  - design equation, 370
    - nondimensional form of, 372
  - solutions to (first-order kinetics), 372–373
    - differences in, 374–375
    - general (Wehner and Wilhelm), 377–379
    - Type A (Danckwerts), 372
    - Types B and C, 375
  - solutions to (non-first-order kinetics), 379–382
  - typical models, 358–359
  - unsteady state solutions, 387
- Compensation effect (*see also* Interpretation, kinetics of surface reactions), 208–209
- Everett correlation, 208–209
- Conversion (*see also* Conversion and selectivity, ideal reactors; Extent of reaction), 17–18
- Conversion and selectivity, ideal reactors (*see also* Reactions, Selectivity), 279–286
  - conversion at same residence time, PFR and CSTR, 281
  - maximum of intermediate, CSTR, 284–286
  - residence times for equal conversion, PFR and CSTR, 279–280
  - selectivity comparisons, PFR and CSTR, 283–286
    - Type II reaction, 283
    - Type III reaction, 283–286
- Coverage:
  - fractional, 173
  - monolayer, 174
  - multilayer, 183
- CSTR (*see* Perfect mixing, reactor model)
- CSTR sequences (*see also* Thermal effects, mixing-cell sequences) 263–271
  - conversion illustration, first- and second-order reactions, 267–268
  - first-order irreversible reactions, 263–264
  - graphical analysis for, 269–270
  - maximum of intermediate in, 284–286
  - recursion formulae for, 265
  - second-order irreversible reactions, 264
- Deactivation (*see also* Deactivation, in flow reactors; influence on diffusion/reaction), 169, 212–219
  - by coking or fouling, 212, 510, 518–521
  - correlations, 216, 218
  - detoxification, 213
  - examples of, 213
  - kinetics of, 215–216, 510
  - by poisoning, 212
    - pore-mouth, 516
    - selective, 516
  - redispersion, 213
  - regeneration, 213, 518–521
  - separable, 216
  - shell-progressive, 515
  - by sintering, 212
- Deactivation, in flow reactors (*see also* Deactivation; Deactivation waves), 301–308
- CSTRs, 306–307
  - time-on-stream correlation, 307
- PFTs, 301–305
  - parallel reaction pathways (coking) in, 305–306
  - series reaction pathways (coking) in, 306
- reaction zones, 304
- temperature forcing of reactors (constant conversion), 445–451
- Deactivation, influence on diffusion/reaction (*see also* Deactivation), 510–521
  - active ingredients, nonuniform distribution of, 513–514
  - parallel deactivation sequence, 513–514
  - selection chart, 514
- coking, 510, 518–521
  - burning rates, 518–521
  - oxidation of, 518
- kinetics of, 510
- poisoning, 515–516
  - illustration of, 517
  - nonselective, selective, antiselective, 516
  - pore-mouth, 516
- profiles, intraparticle, 511–512
  - parallel deactivation, 511
  - series deactivation, 512
- reaction schemes, parallel and series, 510
- regeneration, 518–521
  - correlations of  $t_{85}$ , 520
  - kinetics of, 519
  - oxidation of coke, 518
  - parameter,  $t_{85}$ , 520
  - shell-progressive, 519

- [Deactivation]
  - time of, 519
  - shell-progressive, 515
- Deactivation waves (*see also* Deactivation, in flow reactors), 709–712
  - diffusion-controlled poisoning, 711–712
    - bed activity, 712
    - conversion, first-order reaction, 712
    - distribution of poison, 711
    - effectiveness factor, 711
  - Wheeler-Robell analysis, 709–711
    - distribution of poison, 709
    - model, solutions for, 710–711
    - nonselective poisoning, 710
    - parallel (Type I) poisoning, 709–710
    - selective poisoning, 710
- Dead volume (*see* Ideal flows, deviations from)
- Dehydrogenation:
  - butene, 191–194
    - rate equations for, 193
    - reaction schemes for, 193
  - methylcyclohexane, 210–212
- Denbigh sequence, 33, 71
- Desorption, 170–172
  - energy of, 171
  - rates of, 172
- Diethyl ether, 12
- Differential reactor, 255
- Diffusion and catalytic reaction, interphase/
  - intraphase, 484–492
    - boundary conditions, 484
    - gradients, relative importance of, 490
    - isothermal systems, first-order reaction, 484–487, 490–492
      - Damköhler number, 485
      - with finite external surface, 490–492
      - mass Biot number, 485
      - selectivity, Type III, 485–487
      - slab geometry, 485
      - spherical geometry, 485
    - nonisothermal systems, first-order reaction, 486–490
      - asymptotic solution, 489–490
      - balance equations, 486
      - effectiveness factors, 488–489
      - thermal Biot number 486
- Diffusion and catalytic reaction, isothermal (*see also* Parametric quantities, diffusion and reaction; Transport effects, estimation of), 460–465
  - complex kinetics, 475–476
  - [Diffusion and catalytic reaction, isothermal]
    - Fick's law in, 461
    - generalized modules for, 465
    - mass balance for, 460
    - overall rate, 461–463
      - effectiveness factor for various geometries, 461–462
      - no gradients, 461
      - power-law kinetics, 463
      - reversible reaction, 463
      - strong diffusion, 462
      - Thiele (diffusional) modulus, 461
    - in slurry reactors, 596, 600
    - in trickle-bed reactors, 644–646
- Diffusion and catalytic reaction,
  - nonisothermal (*see also* Parametric quantities, diffusion and reaction; Transport effects, estimation of), 470–474
    - activation energy parameter, 471, 502
    - effectiveness factor, nonisothermal, 472–474
      - asymptotic solution for, 474
      - greater than unity, 472
      - multiplicity of, 472
      - parametric sensitivity of, 472
    - mapping functions, 472, 474
    - Prater relationship, 471
    - thermicity (heat of reaction) parameter, 471, 473, 502
      - values of, 473
- Diffusion, mass, 11
- Dilution rate, 261
  - maximum, 262
- Dimensionless numbers in heterogeneous reaction systems (review), 543–551
- Dispersion (*see also* Dispersion models, mixing; Dispersion models, reactors), 332
- Dispersion model, nonideal reactors, 370–382
  - boundary conditions, 370–371
    - inlet/outlet configurations, 370
    - Types A (Danckwerts, B and C), 371
  - uniqueness of, 432–440
- Dispersion models, mixing, 341–348
  - comparison with mixing-cell model, 346–348
  - criteria from, 345–346
    - Aris, 346
    - Taylor, 345
  - dispersion coefficient, axial, 342

- [Dispersion models]
  - exit-age distribution, 343
  - Peclet number, axial, 342
  - residence-time distribution, 342
  - response experiment, equation for, 341
- Distributions (*see also* Macromixing):
  - exit-age, 235, 238–239
  - internal-age, 235, 238–239
  - residence-time, 235, 238–239
  - speed, 111
  - translational energy, 112
  - velocity, 110
- Dusty gas, 113
- Effectiveness factors (*see* Diffusion and catalytic reaction, isothermal; ... nonisothermal; Diffusion and catalytic reaction, interphase/intraphase; Multiphase reactors)
- Effective transport coefficients (*see* Parametric quantities, diffusion and reaction)
- Elementary step, 8, 13
- Elephants, 194, 197
- Ely-Rideal mechanism, 189, 203
- Energy-conservation relationships, 62–63
- Enhancement factor (*see* Gas-liquid systems, reactions in) velocity profiles, 552
- Enthalpy and entropy of activation (*see also* Transition state theory), 146
- Enzyme kinetics, 197–200
  - Michaelis constant, 198
  - Michaelis-Menton equation, 198
  - multisubstrate reactions, 199
  - pssh in, 197
  - substrate in, 197
- Equilibrium, chemical:
  - equilibrium constants, 52, 55–56
  - single-phase systems, 49
- Estimation methods, 155, 160
  - activation energies, 155–157
    - Hirschfelder correlation, 155
    - Semenov correlation, 155–156
  - linear free-energy relationships, 157–160
    - Hammett correlation, 157–159
    - Taft correlation, 159–160
  - rate parameters, 160
- Exit-age distribution (*see* Macromixing)
- Experimental results:
  - kinetic parameters of various reactions, 151–155
- Extent of reaction (*see also* Conversion), 18, 54–55
- Extrapolation, 83, 194–197, 258, 640
- Falsification of kinetics by diffusion, 465–468
  - activation energy, 466
  - order of reaction, 466–468
  - regimes of diffusion in, 467
- Fluidized bed reactors, 571–592
  - efficiency of, 580–581, 588–589
  - fluid mechanics in, 572–574
    - entrainment velocity, 573
  - Ergun equation, 573
  - incipient fluidization, 572–573
  - minimum fluidization velocity, 573–574
  - pressure drop, 573
  - selectivity factors (Denbigh sequence) in, 589–592
    - limiting cases, 592
  - mass transfer-reaction coefficients, 590–591
  - mass transfer-reaction steps, 591
  - reactions and balances, 589
- three-phase model (Yagi-Kunii), 577–585
  - A' regime, 582, 585
  - bubble geometry, 577
  - bubble rise velocity, 583
  - efficiency, comparison with PFR, 580–581
  - exposure time, bubble/emulsion, 583
  - fast reaction in, 580–581
  - fraction of bubbles, fast, 585
  - fraction of bubbles, slow, 584
  - Geldhart classification, 577–578
  - intermediate reaction in, 581
  - mass transfer, bubble to cloud-wake phase, 582
  - mass transfer, cloud-wake to emulsion phase, 582–583
  - mass transfer and reaction balances, 579–580
  - mass transfer and reaction steps, 579
  - particle distributions among phases, 583–584
  - phases in, 578
  - phase effectiveness factors, 581
- two-phase model (Davidson and Harrison), 574–576
  - boundary conditions, 576
  - bubble phase of, 574
  - bubble phase velocity, 574
  - cross-flow, 575

- [Fluidized bed reactors]
  - emulsion phase of, 574
  - emulsion phase, plug flow balance, 575
  - emulsion phase, well-mixed balance, 575
  - emulsion phase velocity height, 574
  - mass-exchange coefficient, 574–575
  - mass transfer in, 574–575
  - overall balances, 576
  - solution for, 576
- Fouling (*see* Coking)
- Free energy:
  - of formation, 52, 54
  - minimum, 50
  - partial molar, 49
  - total, 50
- Free-energy of activation (*see also* Transition state theory), 146
- Freundlich isotherm (*see also* Adsorption), 178, 194
- Fugacity, 51
- Gas-liquid reactors, 608–635
  - batch reactor, 610–612
    - first-order reaction, 610
    - overall balance, 611
    - solution for, 612
  - countercurrent contactor, 612–614
    - balance equation, 613
    - solution for, 614
  - diffusion and reaction in, 608–610
    - enhancement factor, 609
    - Hatta theory, first-order reaction, 608
    - limiting cases, 609–610
    - phase utilization factor, 609
    - rapid second-order reaction, 610
  - tank-type reactor, 615–619
    - classification of Astarita, 628–629
    - continuous flow tank reactor (CFTR), 616
      - general balances, 615
      - parameters of, 627–630
    - plug flow gas, well-mixed liquid CFTR, 616
    - plug flow gas, well-mixed liquid SFBR, 618
    - semi-flow batch reactor (SFBR), 618
    - well-mixed as well-mixed liquid, CFTR, 618
  - tubular and column reactors, 619–632
    - bubble column flow patterns, 620
    - continuous fluid phases in, 622–624
    - discrete-continuous phases in, 624
- [Gas-liquid reactors]
  - general balances for, 621–622
  - parameters of, 630–632
  - two-phase mass-transfer model, 621
- Gas-liquid systems, reaction in (*see also* Gas-liquid reactors), 521–537
  - effectiveness in terms of observables, 535–536
  - Hatta theory, first-order reaction, 522–525
    - concentration profiles from, 523
    - effectiveness factor, analogy, 524
    - enhancement factor from, 523
    - mass balance, 522
  - sherwood number, 525
    - two-film theory, application in, 522
  - Kramers-Westerterp approach, first-order reaction, 533–536
  - penetration theory, 528–529
  - rate and selectivity, mass transport effects on, 531
  - second-order reactions, 525–528
    - conservation equations for, 525
    - enhancement factors for, 527
    - finite rate of reaction, 527–528
    - infinite rate of reaction, 526–527
  - selectivity factors, Type III, 531–533
- Gas-solid noncatalytic reactions, 505–510
  - diffusional modulus for, 506
  - interface motion, time of, 508
  - mass conservation equation, 505
  - shrinking-core model, 507–508
  - solutions for, power-law kinetics, 506–507
- Gas-solid systems, reactions in, 457–460
  - catalytic reaction, sequential steps for, 458
  - concentration profiles, 459
  - effectiveness factor, 459
  - transport limitations, 459
    - interphase, 459
    - intrapphase, 459
- Gaussian distribution (*see also* Distributions), 112
- Growth (*see also* Growth rate, specific, Microbial kinetics, Product formation), 200–201
  - definition, 200
  - product inhibition of, 201
- Growth rate, specific (*see also* Microbial kinetics):
  - definition, 200
  - maximum, 200



- Half-life (*see also* Interpretation of kinetics), 17
- Hard sphere model, 107–108
- Hatta theory (*see* Gas-liquid systems, reactions in; Gas-liquid reactors)
- Heat of formation, 53
- Heat of reaction, standard state, 12
- Heat transfer in fixed beds, 691–694  
  boundary conditions, 692  
  energy balance, 692  
  equilibrium relationship, 692  
  pebble-bed heaters, 691  
  solution for, 693–694
- Herbert model (*see also* Microbial kinetics), 200
- Hyperbolic correlation (*see also* Deactivation), 218
- Ideal flows, deviation from, 332  
  bypassing, 332  
  channeling, 332  
  dead volume, 332  
  dispersion, 332
- Ideal flows, reactors with (*see* Laminar flow reactors, Perfect mixing reactor model, Plug flow reactor model, Semibatch reactors)
- Impact parameter, 117
- Integral reactor, 254
- Internal-age distribution (*see* Macromixing)
- Interpretation, kinetics of surface reactions, 202–212  
  bimolecular reaction (example), 203–204  
  constants, 206–210  
    Boudart, Mears, Vannice criteria for, 209–210  
    consistency of, 207–210  
    evaluation of, 206–207  
  Eley-Rideal mechanism, 203  
  Hougen and Watson procedure, 203  
  initial rate, 203–204  
  statistical techniques, 202
- Interpretation of kinetics:  
  graphical methods, 77–82  
  general discussion of, 74  
  half-life, 88  
  initial rates, 86  
  maxima of intermediates, 87  
  pseudo-order, 85
- Ion exchange and adsorption (*see also* Adsorption wave, the)  
  breakthrough, 310  
  [Ion exchange and adsorption]  
    curves for, 310–311  
    downstream volume, 309–310  
    elution, constant-pattern, 311  
    equilibrium, favorable, 308  
    Klotz equation, 311  
    zone (band) of activity, 308–309
- Isomerization, 3
- Isomerization, cyclopropane (*see also* Unimolecular reactions), 124
- Isotherm (*see also* Adsorption), 173–179  
  Freundlich, 178, 194  
  Langmuir, 173, 189  
  physical adsorption, 181  
  Temkin, 179
- Kinetic theory, 107–115
- Klotz equation (*see also* Adsorption wave, the; Ion exchange and adsorption), 311, 674, 696
- Langmuir isotherm (*see also* Adsorption), 173, 189
- Laminar flow reactors, 250–252, 277–278  
  applications, 277–278  
    first-order irreversible reaction, 277  
    second-order irreversible reactions, 278  
  design equation for, 251–252  
  exit-age distribution for, 251  
  residence-time distribution for, 251
- Langmuir-Hinshelwood rate equations (*see also* Isotherm; surface reactions), 189, 193–195, 207, 209, 217, 593  
  comparison with power-law equations, 195–196  
  constants of, 206–210  
  consistency of, 207–210  
  evaluation of, 207–210
- Lewis-Randall rule, 56
- Lindemann theory (*see also* Unimolecular reactions), 78, 123–124, 126–131  
  basic, 123–124  
  modifications of, 126  
    decomposition, 128  
    equilibrium of first step, 128  
    Hinshelwood model, 127  
    internal degrees of freedom, 126  
    overall rate constant, 130  
    Rice, Ramsperger, Kassel (RRK) model, 129
- Lineweaver-Burke plot (*see also* Michaelis-Menton equation), 205

- Liquid-liquid reactor (illustration), 624–626
- Long-chain approximation, 39
- Luediking-Piret model (*see also* Microbial kinetics; Product formation), 201
- Macromixing, 231, 235–245  
   age, average, 239  
   C-diagram, 239, 331  
   combinations with micromixing, 243  
   distributions in, 235–245  
     exit age 235, 238–239, 331, 334, 339, 343  
     internal-age, 235, 238–239, 331  
     life-expectancy, 235  
     relationships among, 238–239  
     residence-time, 235, 238–239, 337, 339, 342  
   F-diagram, 236, 331  
   residence-time, mean, 236, 239  
   response experiment for, 236, 239, 241
- Maintenance (*see also* Microbial kinetics):  
   definition, 200  
   Herbert model for, 200
- Marr, Nilson, Clark model (*see also* Microbial kinetics), 201
- Mass action law, 6, 8, 12
- Mass-conservation relationships, 1, 2, 62
- Maxwellian distribution (*see also* Distributions), 112
- Michaelis constant (*see also* Enzyme kinetics; Michaelis-Menton equation), 198–199
- Michaelis-Menton equation (*see also* Enzyme kinetics), 198  
   derivation of, 198–199  
   interpretation of, 204  
   review of, 201
- Microbial kinetics, 200–202  
   definition of terms in, 200  
   Herbert model, 200  
   Monod model, 200, 261–262  
   Marr, Nilson, Clark model, 201  
   yield coefficient, 200, 262
- Micromixing, 231–235  
   ages in, 232–233  
   combinations with macromixing, 243  
   importance of, 232–234  
      $n$ th-order reaction, 233–234  
     second-order reaction, 232–233  
   maximum-mixedness, 232  
   segregation in, 232–234
- Microscopic reversibility, 9
- Mixing-cell sequence models, mixing,  
   337–341, 346–348
- [Mixing-cell sequence models, mixing]  
   backmixing in, 340  
   comparison with dispersion model,  
     346–348  
   exit-age distribution, 339  
   mixing parameter,  $n$ , 339  
   recirculation in, 340  
   residence-time distribution, 337, 339
- Mixing-cell sequence models, nonideal  
   reactors, 362–370  
   effect on conversion, 363  
   first-order kinetics, 362  
   Type II reaction, 367–369  
     comparisons, conversion and yield, 369  
     effect on conversion, 367  
     effect on yield, 368  
   Type III reaction, 363–366  
     comparisons, selectivity and yield, 366  
     effect on selectivity, 363–364  
     effect on yield, 365  
   unsteady state solutions, 385–386
- Molecule, ideal gas, 107
- Moments (*see also* Chromatographic determination of parameters),  
   702–704, 708–709  
   applications in chromatography, 703–704  
   definitions of, 702  
   precautions with, 708–709  
   relation to the Laplace transform, 702
- Monod model (*see also* Microbial kinetics),  
   200
- Multiphase reactors (*see* Fluidized Bed Reactors, Gas-liquid reactors, Slurry reactors, Trickle-bed reactors)
- Multiplicity (*see* Adiabatic or nonisothermal CSTRs)
- Nonideal systems, reactions in, 147–148  
   activity coefficient, 148  
   rate equation example, 148
- Nonideal flows, models for effect on reactor  
   performance, 332–361  
   combined, 356–361  
   dispersion/plug-flow, 332  
   mixing-cell approximations, 332, 337–341  
   recycle, 352–355  
   residence-time distribution (RTD), 332,  
     333–336
- Nonideal reactors, models for, 361
- Order of reaction:  
   isothermal systems, 15–23

- [Order of reaction]
  - integral, 15–21
  - nonintegral, 16, 18, 21
  - reversible reactions, 22–23
  - nonisothermal systems, 62–65
- Parametric quantities, diffusion and reaction
  - (*see also* Diffusion and catalytic reaction, isothermal, ... nonisothermal), 498–505
- activation energy, 471, 502
- effective diffusivity, 499–501
  - bulk diffusivity, estimation of, 499
  - Knudsen diffusivity, estimation of, 501
  - pore dimension, characteristic, 499
  - tortuosity, 499–500
  - transition diffusivity, estimation of, 501
- effective thermal conductivity, 501–502
- external transport, 503–505
  - Biot (heat and mass) numbers, 504–505
  - $j_D$  and  $j_H$  factors, 503–504
  - Prandtl number, 503
  - Schmidt number, 503
- Parametric sensitivity of a PFR (*see also* Plug flow, reactor model), 440–445
  - balance equations, nonisothermal model, 440
  - Barkelew diagram, 441
  - conditions leading to, 441
  - hot spot temperature, 442–443
  - inlet conditions, critical, 444
  - maxima curves, 443
- Partition functions, 138–140
  - translation, rotation, vibration and electronic, 139–140
  - approximate, 140
  - exact, 139
- Pattern analysis of kinetics, 90–93
- Peclet number (*see also* Dispersion models, mixing; Dispersion models, nonideal reactors), 348–352
  - axial, definition of, 342
  - for laminar flow (axial), 348–350
    - fluids in empty tubes, 348–349
    - gas phase in fixed beds, 350
    - liquid phase in fixed and fluidized beds, 350
  - radial, definition of, 351
    - for liquids and gases in fixed beds, 351–352
  - for turbulent flow (radial), 348–350
    - fluids in empty tubes, 348–349
    - gas phase in fixed beds, 350
- [Peclet number]
  - liquid phase in fixed and fluidized beds, 350
- Perfect mixing, reactor model (CSTR) (*see also* Stability of a CSTR; Uniqueness of a CSTR), 250
  - applications, 258–263
    - biochemical reactions, 262
    - conversion/residence time relationships, 259
    - first-order irreversible reaction, 258
    - laboratory use, 269
    - polymerization reactions, 259–261
    - second-order irreversible reactions, 259
  - design equation for, 250
  - stability of, 410, 414
  - uniqueness of, 414–424
- Perfect mixing, model for, 249–250
  - residence-time distribution of, 250
- Perfect mixing (*see also* Perfect mixing model; Perfect mixing reactor model), 243
- PFR (*see* Plug flow, reactor model)
- Physical adsorption (*see also* BET theory), 179–182
  - characteristics of, 181
  - isotherms for, 181
- Plug flow (*see also* Plug flow, mixing model; Plug flow, reactor model), 242
- Plug flow, mixing model, 245
  - residence-time distribution of, 245
- Plug flow, reactor model (PFR), 246–248
  - applications of, 252–255
    - conversion/residence time relationships, 254
    - first-order irreversible reaction, 252
    - laboratory use, 254–255
    - second order irreversible reaction, 253
    - volume changes, 253
  - design equation for, 247
  - differential operation, 255
  - integral operation, 254
  - parametric sensitivity of, 440–445
  - residence time, 248
  - space time, 248
  - space velocity, 248
  - uniqueness of, 431–432
    - unsteady-state solution, 384–385
- Poisoning (*see also* Deactivation), 212
  - bifunctional reaction, 214–215
  - detoxification, 213
  - example, 213
  - reaction pathways, 214

- Polymer characterization:
  - number-average, 47
  - weight-average, 48
- Pore-mouth poisoning (*see* Deactivation, influence on diffusion/reaction)
- Potential energy surfaces (*see also* Transition state theory), 135–137
- Power-law equations (*see also* Isotherm), 178
  - comparison with Langmuir-Hinshelwood equations, 195–196
- Precision of measurements, 74–77
- Preexponential factor, 9
- Processes:
  - chemical reaction, 2
  - separation, 1
  - steady-state, 4
  - unsteady-state, 4
- Product formation (*see also* Microbial kinetics), 201
  - growth-associated, 201
  - nongrowth-associated, 201
  - Luedeking-Piret model for, 201
- Pseudo-steady-state-hypothesis (pssh), 35–36
  
- Rate of reaction, transition state theory (TST), 140–141
  - example result for reaction  $AB + C$ , 140–141
  - generalized rate constant, 141
- Rate-controlling steps:
  - surface reaction, 187–189
    - first-order reaction, 187–188
    - second-order reaction, 188–189
- Reactions (*see also* Selectivity):
  - adiabatic, 63–65
  - autocatalytic, 24
  - chain, 13, 35–45
    - efficiency of, 43
    - general treatment of, 37
  - essential feature of, 14
  - heterogeneous, 13
  - homogeneous batch, 15, 63
  - independence of, 58
  - initiation, 35–39
  - nearly complex, 24–33
  - nonisothermal, 62
  - parallel (Type I), 26–27
  - parallel (Type II), 26–27
  - propagation, 35–39
  - rate of, 3–4, 26
  - reversible, 22–24
  - series (Type III), 27–29
- [Reactions]
  - temperature-scheduled, 69–70
  - termination (breaking), 35, 39
- Reactor models, applications of (*see also* Laminar flow reactors; Perfect mixing, reactor model; Plug flow, reactor model):
  - Laminar flow, 277–278
  - perfect mixing (CSTR), 258–263
  - plug flow (PFR), 252–255
- Reactor/heat exchanger systems, 424–430
  - autothermal reactors, 424–430
    - adiabatic balances, (CSTR), 424 (PFR), 424–425
    - multiplicity of, (CSTR), 424, (PFR) 426–427
  - countercurrent operation, 427–430
    - balances in, 428
    - temperature crossover in, 429
    - temperature maximum in, 429
- Reactors:
  - chromatographic, 704–708
  - fluidized bed, 571–592
  - gas-liquid, 608–635
  - homogeneous batch, 5, 231, 250
  - ideal flows in, 245
  - laminar flow, 250, 277–279
  - nonisothermal or adiabatic, 289–301
  - plug flow (PFR), 246–248
  - recycle, 352–355
  - semibatch, 274–277
  - slurry, 592–607
  - stirred tank (perfectly mixed CSTR), 250
  - trickle-bed, 635–660
- Recycle flow reactors, 352–355
  - design equations for, 354
  - mixing parameter, recycle ratio, 353
- Regeneration (*see* Deactivation, influence on diffusion/reaction)
- Residence-time distribution (*see* Macromixing)
- Rice-Herzfeld mechanism, 42
  
- Schultz-Flory distribution, 48
- Segregated flow (RTD) model, mixing/
  - nonideal reactor, 333–336, 361
  - conversion, effect of order on, 336
  - discrete approach, 336
  - laminar flow reactor, 336
  - reaction kinetics, results for various, 334–336
  - comparison of, 335

- [Segregated flow (RTD) model, mixing/
  - nonideal reactor]
    - first-order irreversible reaction, 334
    - half-order irreversible reaction, 335
    - second-order irreversible reaction, 334
- Segregation (*see also* Micromixing), 232–234
- Selective poisoning (*see* Deactivation, influence on diffusion/reaction)
- Selectivity, diffusional effects on (*see also* Selectivity), 477–484
  - isothermal reactions, 477–481
    - Type I, 477–478
    - Type II, 478
    - Type III, 479–480
  - nonisothermal reactions, 481–484
  - conservation equations, 481
  - Type III, effectiveness and selectivity, 482–483
- Selectivity (*see also* Conversion and selectivity, ideal reactors; Mixing-cell sequence models, nonideal reactors; Reactions; Selectivity, diffusional effects on), 26–30
  - differential, 26–27, 29
  - intrinsic, 27, 29
  - overall, 26, 29
  - Type I, 477–478
  - Type II, 478
  - Type III, 30, 363–366, 479–480, 482–487, 531–533
- Semibatch reactors, 274–277
  - numerical calculations for, 277
  - second-order reactions in, 274–276
    - irreversible, 274–275
    - reversible, 276
- Separable forms, 9
- Separable kinetics (*see also* Deactivation), 216
- Sequences, open and closed (*see also* Chains; Polymerization), 14
- Shell-progressive mechanisms (*see* Deactivation, influence on diffusion/reaction)
- Shrinking-core model (*see* Gas-solid noncatalytic reactions)
- Sintering (*see also* Deactivation), 212
  - example, 213
  - redispersion, 213
- Slurry reactors, 592–607
  - flow operation, 592–597
    - concentration profiles in, 594
    - first-order reaction, 597
- [Slurry reactors]
  - generalized Thiele (diffusional) modulus, 596, 600
  - Henry's law, 594
  - Langmuir-Hinshelwood kinetics, 593
  - mass balance, 594
  - mass-transfer coefficient, 595
  - overall effectiveness in, 596, 598–599
  - overall rate of mass transfer in, 595
  - overall rate of reaction in, 599
  - power-law kinetics, 598
- semibatch operation, 587–600
  - batch time, 600
  - design chart, 601
  - phase effectiveness approach, 600
- parameters of, 602–606
  - holdup, 604
  - interfacial area, 604–605
  - mass-transfer correlation, 603
  - overall rate constant, 605
  - Peclet number, 602
  - Sherwood number, 602
- Space velocity, 248
- Speed:
  - average, 112
  - median, 112
  - most probable, 110
  - typical, 115
- Stability of a CSTR (*see also* Perfect mixing, reactor model), 410–414
  - conditions for, 412
  - heat generation/removal factors in, 414
  - mass and energy balances, unsteady-state, 410
    - eigenvalues of, 411–412
    - linearization of, 410–411
  - startup, 412
    - phase-plane diagram for, 413
- Standard state, 51–52
- Steric factor, 119, 145, 147
- Sterile feed, 261
- Sticking probability, 171
- Stoichiometric coefficient, 3, 7, 26
- Stoichiometry, 2
- Strong diffusion, 462
- Surface intermediate (*see also* Active center, Active intermediate, Chain carrier), 36
- Surface reactions (*see also* Langmuir-Hinshelwood rate equations), 187–197
  - ideal surfaces, 187–194
  - nonideal surfaces, 194–197

- Surfaces, activity of (*see also* Deactivation), 212–219
- Surfaces, ideal (*see also* Adsorption), 170–171
  - comparison with nonideal (rate equation), 195–197
- Surfaces, nonideal (*see also* Adsorption), 177–179
  - comparison with ideal (rate equation), 195–197
- Temkin isotherm (*see also* Adsorption), 179
- Temperature effects, non-elementary reactions:
  - overall, 68
  - selectivity, 68
- Temperature forcing, reactors with
  - deactivation (*see also* Deactivation, in flow reactors), 445–451
  - constant conversion, 445
  - temperature increase required (TIR), 445–451
    - adiabatic conditions, 446–448
    - for deactivation dependent upon activity alone, 449–451
    - isothermal conditions, 446
    - reactor behavior, characteristics of, 445–449
- Temperature-dependence approximations (*see also* Apparent activation energy), 67
- Thermal decomposition, 42
- Thermal effects, mixing-cell (CSTR)
  - sequences (*see also* CSTR sequences), 399–410
  - hysteresis, 401
  - mass and energy balances for, 399
  - operating diagram for, 400–401
  - two-dimensional model, 402–410
    - energy balance, 405
    - geometrical formulation, 403–404
    - mass balance, 402
    - overall model, 405
    - Peclet number, radial, 403
    - solution procedure, 406–407
    - step-function response of, 407–410
- Thiele (diffusional) modulus (*see* Diffusion and catalytic reaction, isothermal, . . . nonisothermal)
- Tortuosity, 350, 499–500
- Transition state theory (TST),
  - thermodynamic analysis of, (*see also* Transition state theory, applications of; Transition state theory, development of), 146–147
  - enthalpy and entropy of activation, 146
  - free-energy of activation, 146
  - relation between activation energy and enthalpy, 146–147
  - volume of activation, 150
- Transition state theory (TST), applications of (*see also* Transition state theory, development of; Transition state theory, thermodynamic analysis of), 143–145
- Transition state theory (TST), development of, (*see also* Transition state theory, applications of; Transition state theory, thermodynamic analysis of), 133–137
  - activated complex, 133
  - equilibrium of, 137–138
  - potential energy surfaces, 135–137
  - reaction coordinate, 134
  - reaction pathways, 135–137
- Transport effects, estimation of (*see also* Diffusion and catalytic reaction, isothermal, . . . nonisothermal), 493–498
  - diffusional modulus, observable, 493–494
  - experimental methods, 496
    - interphase limitations, 496
    - intrapphase limitations, 496
  - interphase transport criteria, 496
  - intrapphase transport criteria, 495
  - Koros-Nowak analysis, 496
- Trickle-bed reactors, 635–660
  - axial dispersion in, 648–649
  - combined models for, 649–651
  - design, approaches for, 652–658
    - catalyst wetting, 653–654
    - liquid holdup, 652–653
    - mass transfer, 654–655
    - plug flow, 652
  - general model for, 655–658
    - balances, 655–656
    - boundary conditions, 656
    - simplifications of, 657–658
  - hydrodynamics in, 636–641
    - dispersed bubble flow, 636
    - gas-continuous regime, 636
    - gas and liquid flow rate ranges, 637–638

- [Trickle-bed reactors]
  - pressure drop, 638
  - ripple (pulsating) flow, 636
  - scaling parameters, 636
- ideal reactor, 647–648
- internal holdup, 639–640
  - dynamic, 640
- intraparticle diffusion, 644–646
  - complete wetting, 645
  - partial wetting, 645–646
- TST (*see also* Transition state theory), 143–145
- Two-phase reactor models, 537–543, 551–559
  - axial and radial dispersion, criteria for, 551
  - plug flow reactor (PFR), 537–538
  - pressure drop, Ergun equation for, 552–553
  - radial dispersion, 539–543, 556–559
    - balances for, 539
    - coefficient of, 541
    - numerical solution of model, 556–559
    - thermal conductivity, 542–543
    - wall heat-transfer coefficient, 540
  - summary of, 553–556
    - equations, 553–554
    - parameters, 554–556
- Type II isotherm, 186
- Unimolecular reactions (*see also* Lindemann theory), 122–126
  - collisional activation and deactivation, 123–124
  - internal energy modes, 122
  - rate, 124
    - high and low concentration limits, 124
    - reaction pathway, 124
    - “soft” collisions, energy exchange in, 123
- Uniqueness of a PFR (*see also* Plug flow, reactor model), 431–432
  - operating diagrams, steady-state, 432
- Uniqueness of a CSTR (*see also* Perfect mixing, reactor model), 414–424
  - application to fluidized bed, 421–424
  - balances, sum of, 414
  - criteria for, 415–424
    - alternative analysis, 420–424
    - first-order kinetics, 415
    - first-order kinetics (more precise), 416
    - multiple reactions, 418–420
    - n*th-order kinetics
- Uniqueness, axial dispersion model (*see also* Dispersion models, nonideal reactors), 432–440
  - balance equations, nonisothermal model, 432
  - computational procedure, 434–440
  - multiplicity, 433
  - operating diagrams, 433
- Van’t Hoff relationship, 11
- Vibration, transition state complex, 141
- Virtual pressure (*see also* Langmuir-Hinshelwood rate equations), 189
- Volume change, 4, 17, 20
- Voorhies correlation (*see also* Deactivation), 216
- Washout, 262
- Waves (*see* Adsorption wave, the; Chromatography; Ion exchange and adsorption)
- Yield (*see also* Mixing-cell sequence models, nonideal reactors):
  - Type II, 368
  - Type III, 26, 30, 36, 365
- Yield coefficient (*see also* Microbial kinetics), 200